The International Antarctic Weather Forecasting Handbook

J Turner and S Pendlebury (Eds.)

The International Antarctic Weather Forecasting Handbook

Editors:

John Turner
Physical Sciences Division
British Antarctic Survey

Stephen Pendlebury
Regional Forecasting Centre, Hobart
Australian Bureau of Meteorology

Version 1.3, 12 June 2001

CONTENTS

FOREWORD

The highly successful International Geophysical Year of 1957–58 gave rise to the formulation of the Antarctic Treaty in 1959 and its ratification in 1961. The Treaty was given considerable impetus for the investigation of major scientific problems in Antarctica and encouraged cooperation between nations. The Antarctic Treaty is unique in the field of international relations in that it guarantees freedom of scientific research and exchange of data.

The Antarctic continent and its surrounding Southern Ocean, south of the Antarctic convergence, are probably the least known regions of the world. There are 44 stations operated by 18 Scientific Committee on Antarctic Research (SCAR) nations. Technology has developed at such a rapid pace that a new standard of meteorological services in Antarctica can be specified. Representation of Antarctica in global numerical weather prediction models has improved; remote sensing of atmospheric variables and sea ice from polar orbiting satellites has become more sophisticated.

Weather forecasting is one of those rare activities that unite nations in a common endeavour from which people worldwide benefit daily. Most of the SCAR stations provide routine coded surface synoptic weather reports to the Global Telecommunications System operated by the World Meteorological Organization (WMO). In addition, there are 70 Automatic Weather Stations separate from the staffed stations that provide extensions to the surface weather–reporting network. Fourteen of the staffed stations are also providing upper–air soundings of meteorological variables with vertical profiles from the surface to altitudes of frequently around 25 km and occasionally 35 km (the lower stratosphere). Through weather satellites and the combined efforts of nations, we can track the forces that control our weather and forecast their behaviour up to a week or more ahead.

Despite the hostile conditions and the problem of logistics, the Antarctic Basic Synoptic Network is well implemented. The percentage of Antarctic reports received at the main centres of WMO's telecommunication network is close to the global average. Weather observations reported in real time are archived in the climate database. Most of the staffed surface observation stations in Antarctica are included in the upper–air and surface networks of the Global Climate Observing System (GCOS). They provide a significant contribution to GCOS data sets.

Substantial meteorological activity is required to support human operations in the Antarctica and the Southern Ocean. The surface weather observing and upper–air–sounding networks organized by WMO are examples of scientific work of practical and economic importance. The consequential historical data bank is fundamental to our understanding of contemporary processes of global relevance such as ozone depletion, atmospheric pollution, climate change, melting of ice shelves and glaciers, sea level rise, all require Antarctic data to ensure true global perspective.

This handbook looks at Antarctic weather from the perspective of one of the most challenging sciences as well as the application of meteorology in providing operational weather services in Antarctica to support national Antarctic research programs. It should provide a valuable reference book for operational meteorologists and students of atmospheric science. If subject to continuous review and improvement, it could be long lived. The main contributions of in kind support came from the Australian Bureau of Meteorology and British Antarctic Survey. However, the great scope and substance of the publication depends on the quality of input material from 15 nations. The contents clearly indicate that wholehearted effort went into gaining the knowledge in the first place and then synthesizing it into a clear account. The meteorological expertise and English expression of the editors John Turner (British Antarctic Survey) and Steve Pendlebury (Australian Bureau of Meteorology) were vital to its success. Acknowledgment is made of the national contributions that were arranged through the national representatives who are Members of the WMO Executive Council Working Group on Antarctic Meteorology. Dr John Zillman, Director of Meteorology, Australian Bureau of Meteorology, and President of WMO, encouraged participation in the development of this quality publication, which makes is a significant contribution to our understanding of Antarctic Meteorology.

Hugh A. Hutchinson
Chairman, Working Group on Antarctic Meteorology
WMO Executive Council
4 July 2000

DISCLAIMER

The contributors and editors have made all reasonable endeavours to ensure that the information and material provided is accurate. The publication is, however, intended as a guide only. The science of forecasting is by its nature imprecise. No warranty of accuracy or reliability as to such material or information is accordingly implied or given by this publication. The user utilises it at his/her own risk, and no responsibility for loss arising in any way from or in connection with errors or omissions in any information or material provided, (including responsibility to any person by reason of negligence), is accepted by the contributors, editors or any person or organisation endorsing the publication or any of their agents or employees.

EDITORIAL REQUEST FOR FEEDBACK

The editors plan to keep revising this handbook, as appropriate, and would be grateful for advice of any changes or additions to the handbook which contributors, or readers, might consider appropriate. The editors' addresses for communicating any such feedback are:

John Turner
British Antarctic Survey
High Cross
Madingley Road
Cambridge CB3 OET
United Kingdom
Fax: +44 1223 221 279
E–mail: JTU@BAS.AC.UK

Stephen Pendlebury
Bureau of Meteorology
GPO Box 727
Hobart Tasmania Australia 7001
Fax: +61 3 6221 2080
E–mail: s.pendlebury@bom.gov.au

ACKNOWLEDGEMENTS and DEDICATION

There have been many contributors to this handbook: needless to say, without these contributions the handbook would not exist in the comprehensive form that it has taken. The editors wish to thank all who contributed directly or indirectly, and in summarising the known contributions below, hope that any person who was been inadvertently missed from the acknowledgments will accept the editors' apologies.

The countries from which contributions have been received are:

- Argentina (Arg);
- Australia (Aus);
- Belgium (Bel);
- China (PRC);
- Chile (Chi)
- France (Fra);
- Germany (Ger);
- India (Ind);
- Italy (Ita);
- Japan (Jap);
- Russia (Rus);
- South Africa (SA);
- Ukraine (Ukr);
- United Kingdom (UK);
- United States of America (USA).

The table in Appendix 5 below lists in detail the sections to which the various contributions were made by the following people: N. Adams (Aus); I. Barnes–Keoghan (Aus); V. Belyazo (Rus); R. Bernstein (USA); L. (Lingen) Bian (PRC); R. Brauner (Ger); J. Brimelow (UK); de Broy Brooks (SA); W. Budd (Aus); J. Callaghan (Aus); J. Carrasco (Chi); J. Cassano (USA); A. Cayette (USA); B. Clavier (Fra); S. Colwell (UK); F. Coppola (Ita); L. Cowled (Aus); M. De Keyser (Bel); J. Evans (UK); S. Harangozo (UK); T. Hart (Aus); I. Hunter (SA); H. Hutchinson (Aus); K. Jacka (Aus); R. Jardine (Aus); M. Jones (Aus); G. König–Langlo (Ger); A. Korotkov (Rus); S. Krakovaskaja (Ukr); J. Kramer (USA); A. Kuznetsov (Rus); T. Lachlan–Cope (UK); V. Lagun (Rus); Lakshmanaswamy (Ind); M. Lazzara (USA); R. Leighton (Aus); E. Loutsenko (Rus); D. Lubin (USA); R. Massom (Aus); G. Mills (Aus); J. Nairn (Aus); S. Pendlebury (Aus); P. Pettré (Fra); M. Pook (Aus); M. Romain (Arg); L. Ryzhakov (Rus); P. Salter (UK); W. Seifert (Ger); J. Shanklin (UK); I. Simmonds (Aus); B. Southern (Aus); C. Stearns (USA); T. Takao (Jap); J. Turner (UK); S. Wattam (UK); G. Weidner (USA) ; T. Yamanouchi (Jap); A. Yates (Aus).

The editors are also very grateful to:

- The staff of the British Antarctic Survey and the Tasmanian and Antarctic Regional Office of the Australian Bureau of Meteorology who assisted with computing, mapping, and production of the front cover. Particular thanks go to N. Adams (Aus) for the production of the regional scale maps in Chapter 7; S. Dixon

and B. Atkinson (Aus) for computing support; and to C. Rumble of the British Antarctic Survey for the design of the front cover.

- P. Chang, R. Ferraro and N. Grody (all of NOAA NESDIS ORA), T. Lee (US Naval Research Lab.), S. Tremble (Remote Sensing Systems, USA), and C. Kummerow (NASA Goddard Space Flight Center) for providing excellent information and guidance on the section of passive microwave data (Section 4.3.3).

- The South African Weather Bureau (SAWB) Climate Division for providing the climate data; I Hunter and J. van der Merwe (SAWB) for providing information on SANAE IV; and N. Sharp for reviewing the drafts of SAWB material. (Section 7.5.5).

- The material relating to Frei in Section 7.3.2 is based on internal reports by meteorologists of the Dirección Meteorológica de Chile. To all of them goes the recognition and appreciation of the authors of Section 7.3.2.

- B. Lunnon (Head of Aviation Applications, UK Meteorological Office (UKMO) and A. Skomina and D. Thomas (both of the Australian Bureau of Meteorology) for providing feedback on Section 6.6.10; S. Bauguitte for the translation (French to English) of Section 7.2.7; J. Smith (Palmer Station Science Technician) for feedback on aspects of Section 7.3.6; Moyher (Manager Laboratory Science Raytheon Polar Services Company) for co–ordinating aspects of Sections 7.3.6; 7.12.5, 7.12.6, and 7.13.2; J Wilson (Australian Bureau of Meteorology) for providing comprehensive suggestions on Appendix 4.

The editors wish to dedicate this handbook:

- to all the weather observers and technicians who year–round make measurements and observations, and maintain the observing equipment, in the hostile environment of the Antarctic, without which forecasts and knowledge of the climate of the Antarctic would be guesswork;

- to all the researchers and modelers who seek to make sense of these observations and who seek to provide the scientific infrastructure upon which sound forecasts are made;

- to the authors of the various Antarctic forecasting handbooks or manuals which have assisted the Antarctic weather forecasters of individual nations. It is known that S. Allen, A. Stark and H. R. Phillpot were primarily responsible for the Australian Antarctic Forecasters' Handbook (Australian Bureau of Meteorology, 1991) (H.R. Phillpot followed this work with, *inter alia,* a comprehensive study of weather in East Antarctica with operational forecasters in mind (Phillpot (1997)); J. Turner, T. Lachlan–Cope and R. Ladkin authored the British Antarctic Survey Forecasting Manual (British Antarctic Survey, 1997); while R. W. Sallee and A.W. Snell were the original major contributors to the US Navy's Antarctic Forecasters Handbook (US Navy (1970)). It is also known that many Soviet/Russian forecasters (for example, V. Belyazo, A. Kuznetsov, E. Lutsenko and L. Ryzhakov) have made a significant contribution to the weather forecasting programme for the Russian Antarctic stations. The editors would appreciate advice on similar contributors to these or other Antarctic weather forecasting handbooks or manuals that they might be acknowledged here in future revisions of this handbook.

- and finally, to all weather forecasters who have dared to, or who will yet dare to predict the future state of the Antarctic atmosphere.

A HINT TO NAVIGATING THIS HANDBOOK

The document map features of Word and Adobe PDF, where appropriate, may be used to quickly navigate one's way around the electronic versions of the handbook. Moreover, generally speaking, where a figure, table, or piece of text are referred to as being "above" or "below": by left–clicking on the "above" or "below" the reader is taken directly to the relevant figure, table or text. The reader may then return their original place by using the "go back" facility appropriate to the text viewer being used.

1   INTRODUCTION

Forecasts of the weather over the Antarctic have been made since the first expeditions to the continent, although in the early years the success of these predictions was poor since few observations were available and there was only a rudimentary understanding of the workings of the high latitude climate. This situation changed little until the International Geophysical Year (IGY) of 1957–58 when a number of research stations were established across the Antarctic, with many of these making routine radiosonde ascents. These additional data allowed more reliable surface and upper–air analyses to be prepared, although there were still few observations over the ocean areas. Since IGY there have been a number of major advances that have greatly aided weather prediction over the continent. Since the 1960s satellite imagery has been an extremely important tool in identifying the locations of synoptic and mesoscale weather systems over the ocean areas and the continent itself. Although the early imagery was poor with a coarse resolution and few grey–scales, today many stations have digital receivers capable of providing high resolution images at several wavelengths. These images can provide early warning of approaching weather systems, fronts and isolated cloud banks, as well as supplementary information on sea ice extent. Figure 1.1 is an example of satellite infra–red imagery coverage of Antarctica overlaid with a surface pressure analysis.

   Objective information on upper–level temperature and humidity have also been produced from satellite sounder data since the late 1970s and these data have been essential for the computer analysis of atmospheric conditions at high southern latitudes. Such data allowed the implementation of global numerical weather prediction (NWP) systems that could provide forecasts out to about a week ahead. During the 1980s the accuracy of Antarctic forecasts from such NWP systems was much lower than those for tropical and mid–latitude areas, but during the 1990s there have been marked improvements as a result of better analysis techniques, higher model resolution and additional data from new satellite instruments, such as the wind scatterometer.

   As Antarctic weather forecasting techniques were developed by the various nations involved in operations on the continent, so a number of forecasting manuals and handbooks were developed. These were often used to train new forecasters going South and to build up information and knowledge gained by successive generations of forecasters. These books were often concerned with specific areas of the Antarctic and were usually focussed on the forecasting needs of the particular nation, whether it be aviation or marine forecasting. Such volumes had a limited circulation and there was little interchange of information on forecasting between nations. However, today Antarctic logistics are very complex with scientists working in remote parts of the continent, flights taking place throughout the year and thousands of tourists visiting the continent each summer. There is therefore a pressing need for accurate weather forecasts for the continent and good exchange of information between forecasters working in the Antarctic.
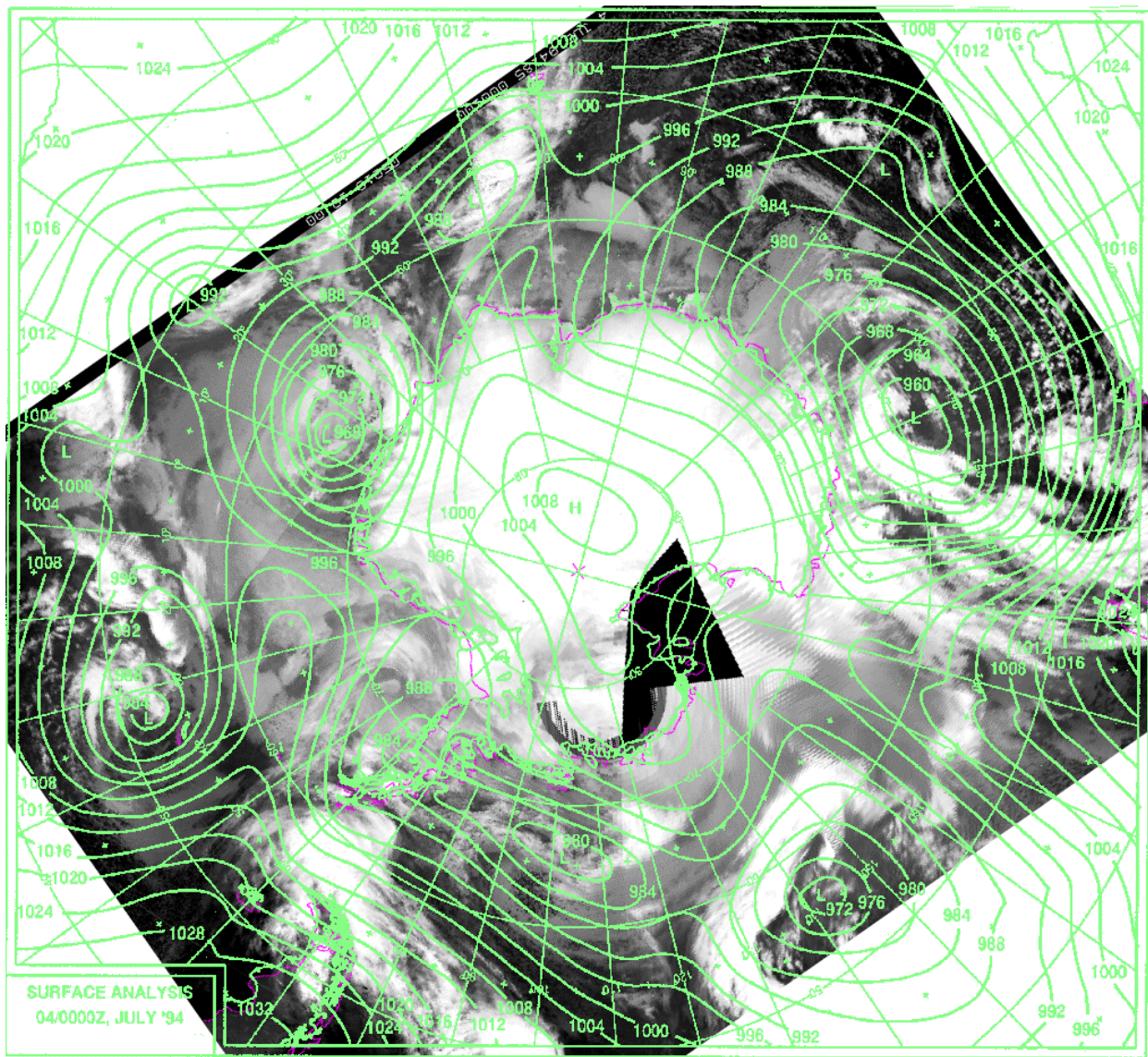
Figure 1.1 Composite of geostationary and polar orbiting infra–red satellite imagery for the nominal time of 0000UTC 4 July 1994. (The imagery is courtesy the University of Wisconsin–Madison's Space Science and Engineering Center. The analysis overlay was produced during the First Regional Observing Study of (the Antarctic) Troposphere Project).

This handbook has been written following the successful First International Symposium on Operational Weather Forecasting in the Antarctic, which was held in Hobart, Australia between 31 August and 3 September 1998 (Turner *et al.,* 2000a). This meeting brought together practicing forecasters with Antarctic experience, administrators responsible for providing forecasting services for Antarctic operations, developers of numerical models and researchers with a close interest in weather forecasting. The attendees came from Australia, Belgium, Brazil, China, France, Italy, Russia and the UK so that a great deal was learnt about the forecasting operations taking place in the Antarctic and the techniques used at the various stations. A major outcome of the symposium was the decision to prepare this handbook to aid the interchange of forecasting techniques, to provide information for use when forecasting for an unfamiliar area and for training purposes.

The handbook splits into two main sections. Chapters 1 to 6 provide general background on the meteorology and climatology of the continent, the requirement for

forecasts, data availability and characteristics, and general information on the analysis and forecasting techniques applicable to the Antarctic. Chapter 7 gives details information on the meteorology of all the main areas of the continent for which weather forecasts are issued, along with local forecasting techniques used. Data are also provided for many of the sub–Antarctic islands. Figure 1.2 shows the geographical area of interest considered in the handbook.

Figure 1.2 A map of the Antarctic showing the principal regions and a selection of the research stations.

2   AN OVERVIEW OF THE METEOROLOGY AND CLIMATOLOGY OF THE ANTARCTIC

2.1   The physical environment of the Antarctic

2.1.1   The polar cell in the three cell structure of the Earth's atmosphere

The location of the Antarctic continent corresponds somewhat fortuitously to the region of the southern polar cell in the three cell structure of the meridional circulation of the Earth's atmosphere. The factors which influence the meridional cell structure include the scale of the planet, the rotation rate, and the depth and differential meridional heat balance of the atmosphere.

Numerical modeling has been used to show that even without the high surface orography of the Antarctic continent (i.e. if it were replaced by a snow surface at sea level) a high surface pressure region would develop, in the mean, over the south polar domain approximately corresponding to the region south of the Antarctic circle. The cold air at the surface flowing outwards from the polar cell turns towards the west, from the Coriolis acceleration, to form strong south easterly to easterly surface winds by the edge of the domain around the Antarctic circle. With strong westerly winds prevailing north of 60º S, from the general circulation in the three cell structure of the Earth's atmosphere, a strong cyclonic vorticity at the surface naturally occurs between the polar cell and the prevailing westerlies around the Antarctic domain.

As the cold air from the south moves over the warmer, oceanic surface to the north strong baroclinic instabilities and convection occur, which together with the high cyclonic vorticity result in the formation of numerous mesoscale and synoptic scale cyclonic systems around the edge of the Antarctic domain. These synoptic low–pressure centres tend to move with the westerlies around the Antarctic region and also drift southwards into the edge of the polar cell region.

The general outflow of cold air at the surface from the polar cell is balanced by the spiraling southwards of the upper–air westerlies to give subsidence over the central south polar region. The advective heat transport of the atmospheric circulation largely balances the heat loss from the negative net radiative balance, with a strong seasonal cycle, over the south polar region.

This simple picture of the atmospheric circulation around the Antarctic is strongly modified by the orography of the Antarctic continent and also by the way in which the sub–marine orography influences the ocean and sea ice patterns around Antarctica.

2.1.2   Radiation and heat balances

At the top of the Earth's atmosphere there is a net radiation loss of heat, in the annual mean, for the domain south of about the latitude of 40º S. There is a strong seasonal cycle in the zone of net radiation loss associated with the tilt of the Earth's axis. This domain of net

radiation loss varies from south of about 12º S in winter to south of about 70º S in summer. This means that the region covering most of the Antarctic continent experiences a net loss of heat from the atmosphere all year round. Near the South Pole this net radiation loss has an annual mean of about 80 Wm^{-2}, varying from about 50 Wm^{-2} in summer to about 130 Wm^{-2} in winter.

The net radiative heat loss through the year is balanced by the heat transport of the atmosphere, with net inflow at upper levels, subsidence over the continent and net flow outwards near the surface. In addition to this general circulation pattern, the synoptic scale eddies which move around the continent giving rise to horizontal advection through the troposphere with flow inwards to the Antarctic on the eastern side of the low–pressure centres and outflow on the western sides, with intense mixing of heat and moisture. The greater radiation loss in winter is associated with greater cooling over the continent, with larger horizontal temperature gradients around the continent and more intense circulation with stronger winds.

The snow surface which covers all but about 3% of the Antarctic continent has a number of important influences on the heat balance. The high albedo, averaging about 0.85, means that most of the solar radiation in summer is reflected with relatively little absorbed. On the other hand the high emissivity (~0.97) relative to that of the atmosphere means that the strong radiation loss, along with the low snow thermal conductivity, tends to keep the surface temperature low allowing strong surface inversions to develop in the boundary layer over the interior, particularly during winter and when it is calm. The mean inversion strength in the central zone of the high East Antarctic plateau averages about 25ºC in winter and is mostly concentrated in the lowest few tens of meters of the atmosphere. The cold surface air tends to flow downslope, as a density current, towards the coast increasing in mean speed with the surface slope and the channeling of the flow by the surface orography. The katabatic flow is also strongly influenced by the synoptic scale pressure systems. At the coast the combination of strong katabatic flow with favourable synoptic gradients give rise to the blizzards which are characterized by gale–force winds and turbulent snow transport reaching several hundred meters above the surface.

Although some loss of moisture occurs with the drift snow transport most moisture loss occurs in summer from evaporation and outward transport in the boundary layer. As a whole the moisture budget for the continent is positive with a net latent heat transport to the continental domain associated with the net precipitation gain over the Antarctic ice sheet. The net snow accumulation varies from about 1000 mm per year water equivalent near the coast, to about 20 mm per year over the high interior of East Antarctica, with a mean over the continent of about 150 mm per year. The latent heat contribution from the moisture budget, while averaging about 12 Wm^{-2}, only contributes about 1/6 of the input to compensate for the radiative heat loss. The remainder is contributed primarily from the atmospheric sensible heat advection which comes from a combination of the mean flow and most importantly the transient eddies.

2.1.3   Orography

The Antarctic continent has a profound influence on the atmospheric circulation over the south polar region. Although the area of the continent is contained largely within the 60º S latitude circle, its high orography has a marked asymmetric character (see Figure 1.2). The Antarctic Peninsula forms a narrow protrusion northwards to about 57º S near 57º W but with the rest of the West Antarctic region of the continent as a whole being much less extensive

than that of the eastern region. The mean elevation of the whole continents is about 2,000 m but West Antarctica has most of its area below 2,000 m, although high mountain regions above 3,000 m are common. Outside the Antarctic Peninsula and Queen Maud Land (0–10º W) the West Antarctic coastline is primarily south of 73º S with the coast of the large ice shelf embayments of the Weddell and Ross Seas reaching about 77º S. In these regions the low, flat ice shelves extend much further south with the 100 m elevation contour inland of the Ronne Filchner Ice Shelf reaching to about 83º S and that inland of the Ross Ice Shelf reaching to about 86º S. Nevertheless, the high coastal regions of Marie Byrd Land (~ 140 – 100º W) and the Antarctic Peninsula act as strong barriers to the prevailing westerly winds of the lower troposphere and to the movement of the low–pressure cyclonic systems.

The East Antarctic Ice Sheet has its highest central dome of over 4,000 m elevation (Dome A) located at about 81º S, 79º E. The coast line in Enderby Land (~55º E) reaches as far north as about 66º S, as does the coast in Queen Mary Land (~102º E) and Wilkes Land (~112º E). From 0º to 170º E the ice sheet surface tends to rise steeply from the coast reaching to near 2,000 m elevation within about 400 km from the coast in most regions. The one exception is in the Amery Ice Shelf–Lambert Glacier region where Prydz Bay represents an embayment reaching near to 69º S and the 100 m elevation contour extends inland to about 72º S.

This asymmetry of the Antarctic continent combines with the asymmetry of the locations of the three major continents further north, together with the climatological patterns of the ocean surface, such as the sea surface temperature and sea ice distribution, to give strong orographic and surface forcing to the atmospheric circulation around the south polar region.

The prevailing mean westerly winds in the lower troposphere of the mid–latitudes extend southwards to the minimum in the mean surface pressure distribution, which occurs around the Antarctic as a feature referred to as the Antarctic circumpolar trough (CPT). The CPT is located at about 63º S around East Antarctica and closer to about 68–70º S around West Antarctica but with a break associated with the Antarctic Peninsula. Several dominant low–pressure centres within the CPT tend to be associated with the Antarctic orography and sea surface temperature pattern. These separate centres in the mean surface pressure field (see Section 2.6) contribute to the mean 3 to 5 wave number character of the lower troposphere circulation around Antarctica. In winter the dominant centres tend to be located near 20º E, 90º E and in the Ross Sea (~170º W) with a weaker centre over the Bellingshausen Sea (~100º W). This results in a predominant 3–4 wave pattern. In summer, with the reduction in sea ice, the Bellingshausen Sea centre usually deepens and a further centre tends to form in the Weddell Sea near 20º W. This results in an approach more towards a 4 – 5 wave number pattern. However, there is very high variability in the mean patterns on inter–annual as well as seasonal time scales.

The high orography has a strong influence on surface temperature with the mean temperatures decreasing inland with elevation as well as increasing latitude. This places the central coldest region around the Dome A vicinity in East Antarctica where the annual mean surface temperature reaches about –60ºC. Immediately inland of the coast where the ice cap rises steeply the surface temperature tends to decrease at a rate close to the dry adiabatic lapse rate around 1ºC/100m. Further inland where the plateau slope is smaller this rate may become much higher. This is a feature associated with the reduction in katabatic wind speeds with the reduction in slope. The katabatic winds tend to break down the strong inversions due to mixing. As a result the flatter regions tend to have lower mean temperatures, which is also a common feature of the large, flat ice shelves. Further inland again the mean surface temperature lapse rate reduces more towards the moist adiabatic lapse rate associated with the continual subsidence over the high interior.

The elevation of the ice sheet surface also has a dominant influence on the distribution of precipitation. The annual mean total column moisture decreases from about 2 to 3 mm of water near the coast to less than 0.1 mm over the high interior of East Antarctica. The net accumulation rate tends to follow this smooth distribution of the column moisture but is distorted from it primarily by the pattern of the mean wind transport of the lower and mid troposphere.

The mean cloud climatology is similarly influenced by the elevation and moisture transport. The Antarctic coastal region is characterised as being one of the most cloudy regions of the world with mean total cloud cover typically around 80%. Inland over the continent the low and mid level cloud are greatly reduced by the high orography with much thinner high cloud prevailing.

In a similar way the large concentration of cyclones moving around the coast of Antarctica are obstructed by the high and steep orography of the ice sheet. Occasionally some of the deeper cyclonic systems penetrate inland over the high plateau, but the most frequent penetration occurs over the lower elevation regions such as those of the large ice shelves. The low amounts of cloud and air moisture over the interior are important factors contributing to the radiation loss from the surface. On the other hand the high variability in the moisture and cloud cover plays an important role in the radiation balance and the generation of anomalous temperature and pressure episodes over the interior plateau, which may change relatively quickly with changing synoptic events.

2.2   The Ocean Areas

2.2.1   The surface ocean circulation pattern

The most striking feature of the ocean area around Antarctic is the strong seasonal cycle of sea ice and surface temperature change. The sea ice pack is dynamic being subject to the variable wind stress and ocean currents and plays an interactive role in the heat exchange between the atmosphere and the ocean.

The ocean circulation is primarily influenced by the submarine orography, the oceanic density gradients and the wind stress. The location of the Antarctic ocean surface divergence (AD) follows the atmospheric CPT closely around the Antarctic continent. South of the divergence the mean ocean surface currents flow from east to west (the East Wind Drift) over the continental shelf with a strong influence of the submarine orography and also the mean easterly winds. The current speeds tend to be greatest near the edge of the continental shelf. Further north from the AD the prevailing currents are towards the east forming the Antarctic Circumpolar Current (ACC). Typical current speeds are of the order of 0.1 m s^{-1} (~9 km per day) but can be very much higher as a result of higher wind speeds.

At a number of locations around the continent where the orography develops a north–south trend the east wind drift tends to turn the flow northwards and connect with the ACC. These occur in the large gyres of the Weddell and Ross Seas but also in a smaller way near the Balleny Islands (~162º E), the 90º E ridge, and near the Riiser–Larsen shelf (~33º E). At other locations the submarine orography contributes to turning the ACC southwards towards the continental shelf, such as the region west of the Antarctic Peninsula (near Marguerite Bay, ~70º W) and west of the Balleny Islands (~157º E). This broad picture of Antarctic ocean

mean surface currents shows considerable similarity to the surface geostrophic wind directions from the mean sea level pressure patterns. Although the mean winds contribute to the mean ocean current patterns, the submarine orography also has a strong influence. This raises the question as to why the mean sea level pressure field has its observed pattern. The answer is that it is partly influenced by the continental orography and the large–scale circulation, but is also influenced by the surface heat balance over the ocean and sea ice.

In addition to the smooth pattern of ocean surface currents as depicted above there is high variability generated by the continual change in winds associated with the continual development and movement of low–pressure systems around Antarctica. In a similar way there is a continual development and movement of oceanic eddies which have spatial scales of typically several tens of kilometres diameter. These are very common near the Antarctic Divergence, particularly in high shear regions and also often in association with submarine orographic features.

2.2.2   The sea ice and its annual changes

In late summer (February to March) only about 3 million km^2 of the sea ice extent remains from the maximum extent of almost 20 million km^2 reached in September to October. This remaining sea ice is primarily concentrated in the western Weddell Sea along the Antarctic Peninsula and from the Bellingshausen and Amundsen Seas to the eastern Ross Sea. This sea ice extends about 500 km from the coast near the front of the Ronne Ice Shelf and in the eastern Ross Sea, and about several hundred kilometres from the coast east of the Antarctic Peninsula and in the Bellingshausen and Amundsen Seas. Around the rest of the coastline, mainly East Antarctica, on average only patches of sea ice, generally less than a few tens of kilometres in extent, tend to remain. Figure 2.2.2.1 shows 20–year (1979–98) averages of sea ice concentrations from Special Sensor Microwave/Imager (SSM/I) data derived using the "Bootstrap Algorithm" (Comiso *et al.*, 1997).

Over the period of open water, mainly from January to March, the surface mixed layer of the ocean (to about 200 m depth) tends to warm by about 1 to 2ºC above the ocean surface freezing point (~ −1.8ºC). This warming results primarily from the absorption of solar radiation with the low albedo of the water, compared with that of the sea ice and the mixing to deeper levels by the strong winds.

After the period of the maximum surface temperature, usually reached in January to February, the ocean surface mixed layer tends to cool until freezing point is reached. Starting with the high latitude regions first, most notably in the Ross and Weddell Seas, the sea ice cover gradually spreads outwards. In some locations fast ice attached to the coast extends several tens of kilometres to seaward while in other locations strong offshore winds maintain coastal polynyas with low ice concentration for some time. Beyond the fast ice the pack drifts with the wind and currents primarily towards the east, but with considerable temporal and spatial variation, until the ice extends to the region beyond the Antarctic Divergence where the eastwards flowing Antarctic Circumpolar Current prevails. In the outer pack, mean sea ice drift rates of 0.2 m s^{-1} (~18 km per day) are not uncommon. This means that over a six month winter period the sea ice movement in the outer pack could exceed 3,000 km. There is also a tendency for the ice drift to be directed to the left of the wind (~ an average of 25º). This tends to drive the sea ice northwards in the circumpolar current spreading the ice outwards in a divergent manner.

Similarly around the climatological mean low–pressure centres within the Antarctic Circumpolar Trough the mean outwards divergence tends to make the ice more open and

thinner there than in the surrounding sea ice area. The increased heat flux through the thinner more open ice tends to enhance the mean low–pressure centre. This gives a positive feedback to the strong coupling between the ocean currents, the submarine orography, the sea ice drift and concentration, and the mean wind and pressure fields.
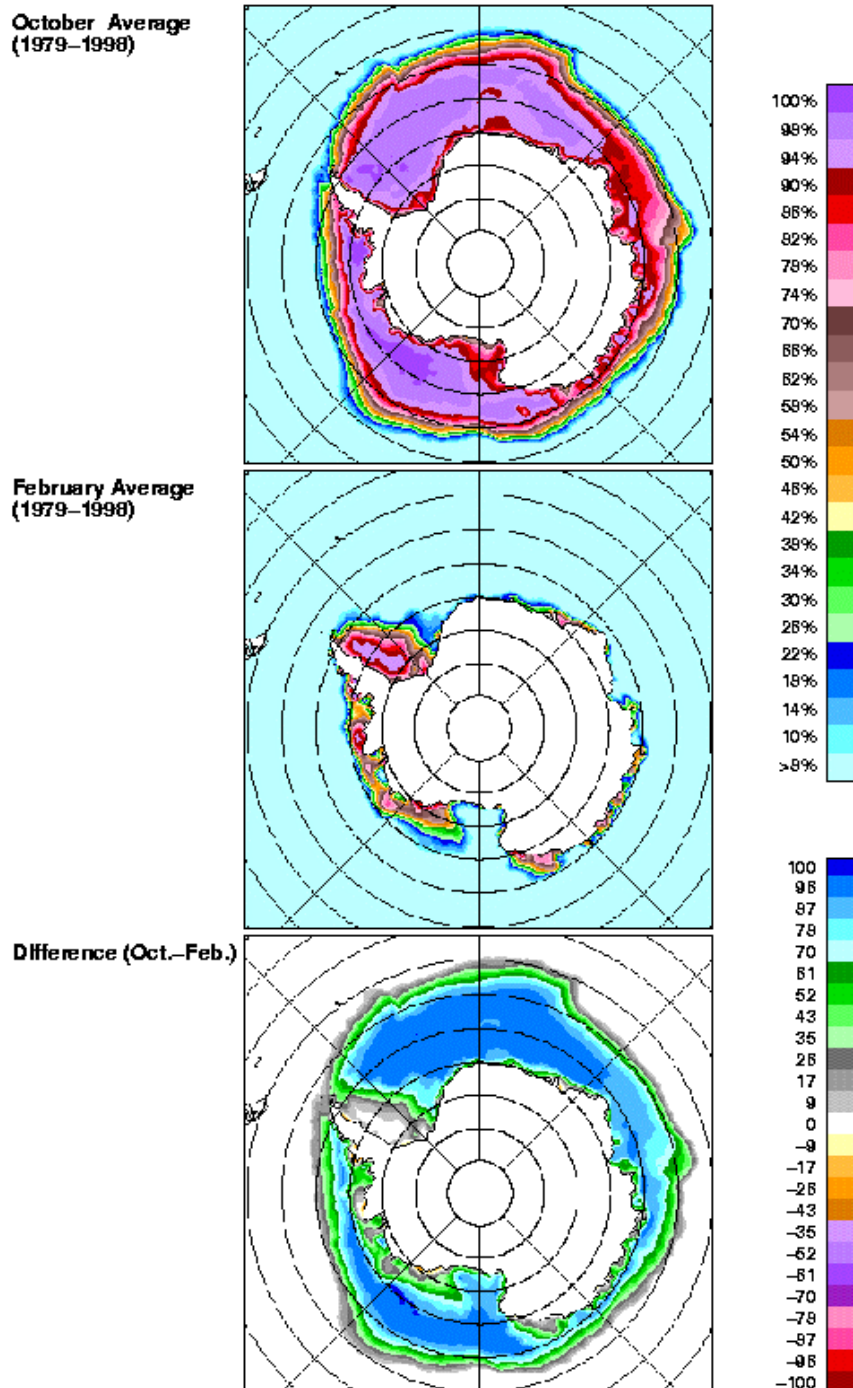
Figure 2.2.2.1   20–year (1979–98) averages of sea ice concentrations from SSM/I data. The top panel shows concentrations in October, the middle panel in February, and the difference (October minus February) is shown in the bottom panel. (The mapping technique used is polar stereographic with the mapping plane at 70º S. The key SSM/I channels used in the algorithm are the 37 GHz and 19 GHz channels. These channels have different resolutions but the data are all mapped onto the SSM/I grid which has a fix resolution of 25 km). (Figure

courtesy of J. Comiso, Laboratory for Hydrospheric Processes, NASA Goddard Space Flight Center).

Similarly for the transient low–pressure systems there is strong feedback between the opening and closing of the pack by the winds and the heat fluxes from the ocean to the atmosphere. In the mean, the generally divergent movement of the pack, tends to maintain the regions north of the divergence at average ice concentrations of around 80% during winter. This results in continual freezing and relatively thin, dynamic ice. A feedback with a self–regulating tendency, acts to maintain the ice concentration in the pack near to the observed mean values. If the pack opens too much, both the heat fluxes from the ocean and freezing increase, reducing the open water fraction. When the pack closes, or freezing of new ice covers the leads, the mean surface temperature decreases and the direction of the mean sensible heat flux can change to be directed from the atmosphere to the sea ice surface.

Snow cover over the sea ice acts as a strong insulating factor for Antarctic sea ice. In East Antarctica the winter sea ice typically accumulates about 0.3 m of snow thickness. The snow conductivity is ordinarily about an order of magnitude lower than that of the sea ice so that the snow thickness therefore has a disproportionate influence on the heat flux through the pack compared with the ice thickness alone. In some regions, such as the Bellingshausen and Amundsen Seas the snow thickness on average is much greater, but as a consequence, flooding and freezing can take place, reducing the low conductivity snow thickness to a buoyancy limit.

In many locations around the coast persistent polynyas with lower ice concentration occur. These locations tend to be associated with coastal obstructions to the ocean currents in the East Wind Drift, and also with strong offshore winds from the continent. These polynyas tend to provide high levels of heat flux to the atmosphere along with high freezing rates which can reach about an order of magnitude above that of the mean in the surrounding pack. In some of these locations the possibility of increased atmospheric cyclonicity has been proposed. Because of the high variability of the atmospheric systems and the pack ice dynamics in the sea ice zone it is difficult to establish clear mean associations. Nevertheless, modeling simulations indicate an enhancement of the depth of Antarctic low–pressure systems over the sea ice zone with interactive dynamic sea ice or an increased open water fraction.

2.3   The role of the Antarctic in the Global Climate System

The Antarctic region plays an important role in the global climate system in two main areas. Firstly, in the global heat balance the Antarctic and the Arctic represent the main regions of net heat loss of the Earth to space. Secondly, the Antarctic plays a particularly important role in the net water budget which is then redistributed by the ocean circulation but for part of which the Antarctic Ice Sheet acts as a long term storage system. Since the moisture transport also forms part of the heat balance these two main roles are closely connected. Each are also involved in the atmosphere and ocean circulation and dynamics which form part of the global circulations of the atmosphere and ocean both of which have particularly strong interactions in the Southern Hemisphere mid–latitudes.

2.3.1   The heat balance

The mean net radiative heat loss to space of the Earth's domain south of about 40º S needs to be compensated by the atmospheric and oceanic transport from the net gain regions further north. Most of the total transport is provided by the atmosphere (about 3/4) and by the edge of the Antarctic continent the atmosphere is responsible for all of the net heat transport further south. All of the ocean heat transport into the Antarctic domain is released as heat flux at the surface into the atmosphere. The sea ice not only plays a pivotal role in the heat exchange between the atmosphere and ocean through the annual cycle, but also, through the ice movement, plays a key role in the annual net surface heat flux and the north–south heat transport. If the sea ice just grew in winter and melted in summer without movement there would be an annual cycle of heat storage by the ice but no net heat transport. The ice dynamics transports sea ice from the generally more southerly regions of net freezing to the outer pack regions of net melting. This results in vertical net fluxes to the atmosphere and an effective net latent heat transport directed towards the south. Of a total of about 60 Wm^{-2} net annual heat loss through the top of the atmosphere over the domain of the sea ice about 15 Wm^{-2} comes from the net heat flux from the ocean surface and about 5 Wm^{-2} from the net sea ice transport.

For the atmospheric heat transport the synoptic scale eddies play a dominant role. Due to the Earth's rotation, and the north–south temperature gradient in the atmosphere, the mean troposphere winds in mid–latitudes become westerlies. This means that it is difficult to obtain very much north–south heat flux from the mean flow. Consequently the bulk of the net meridional heat flux results from a combination of the stationary and transient long waves in the flow and the synoptic and smaller scale eddies right down to the scales of atmospheric diffusion. Of these systems the synoptic scale eddies are the most important. The mean tropospheric winds have a maximum in the westerlies around 45º S. North of this region, on average, anticyclonic eddies are dominant whereas southwards of the mid–latitudes the cyclonic eddies dominate the latitude band around the Antarctic maximum sea ice zone represents the most concentrated domain of cyclonic systems on the globe. These systems generally extend through a large part of the troposphere and provide a dominant part of the meridional heat transport via the horizontal air movement. Once the Antarctic continent is reached, the high and steep orography of the continent impairs much of the lower tropospheric air flow, except for the large embayments and the ice shelves. As a consequence the synoptic scale eddies play a very important role around the coast of Antarctica but not so strongly in the interior. The upper level flow into Antarctica is not so restricted and supplies a continual transport of air inwards to the continent to compensate for the net outflow at lower levels due to the katabatic winds. This means that there is a strong net vertical circulation also involved in the net meridional heat transport of the atmosphere to the Antarctic. The larger part of the net atmospheric heat transport to the Antarctic is from the sensible heat, but part also comes from the moisture transport contributing the net positive accumulation of snow over the region.

2.3.2   The moisture and water balance

South of about 45º S there is a net positive balance of precipitation over evaporation (P–E). This net positive P–E is compensated (as a long term balance) by the ocean flow and the flow

of the Antarctic ice sheet, with some basal melting, and the calving of ice bergs at the margins.

Part of the oceanic net transport is accomplished by the horizontal circulation of the surface ocean. In the regions around the Antarctic where the large gyres direct the ocean flow to the north, fresher water is transported to the lower latitudes. In the Antarctic Circumpolar Current, Ekman drift also plays a role in the northward surface transport. In addition, the mixing due to ocean eddies provides an effective mean diffusion of ocean properties resulting in a meridional northward net flux of fresh water.

The most important role of the Antarctic region in the ocean circulation concerns the vertical meridional thermohaline circulation. Saltier water is brought to the Antarctic Ocean from the ocean basins further north, particularly the Atlantic Ocean. As this water circulates around the Antarctic continent and impinges on the continental shelf, it becomes capped by the fresher water from the positive P–E balance. Even with the lower surface temperature, decreasing to freezing point in winter, this surface water would still be too fresh and light to sink. The freezing of sea ice over the continental shelf can increase the surface water density enough to produce deep mixing below the warmer saltier Circum–Polar Deep Water (CPDW). In some locations this densification is sufficient to form Antarctic Bottom Water (AABW). The AABW then spreads around the Antarctic in the deep layers and mixes northwards to replenish bottom water in the other major ocean basins. This deep circulation is also important for the transport of dissolved gases (e.g. O_2 and CO_2) and nutrients around the global oceans.

At the surface, the melting of the sea ice, adds to the positive P–E and ice flux from the Antarctic to produce the fresh upper ocean water mass which spreads around the Antarctic ocean and drifts northwards to the Antarctic convergence (near 50º–55º S) where it sinks below the warmer saltier water from the other ocean basins drifting south. This flow of ocean water tends to maintain the strong meridional sea surface temperature gradients in the Southern Ocean.

The longer transport and storage times of the ocean and Antarctic ice sheet compared to that of the atmosphere means that climatic changes can result in significant imbalances over shorter time scales. These imbalances can also occur with inter–annual climatic fluctuations. For the Antarctic region one of the most prominent of these internal changes is the Antarctic Circumpolar Wave (ACW). This involves interaction between the atmosphere, ocean and sea ice with large anomalies of the scale of wave number 2 to 3 moving around the Antarctic continent with about the speed of the mean ocean flow. The ACW can therefore interact with the similar large inter–annual atmosphere–ocean anomalies associated with the other large ocean basins such as the El Niño in the Pacific Ocean. As a result, over longer periods, occasions occur where these interactions make significant contributions to the inter–annual variability of the atmosphere–ocean sea ice system around Antarctica.

2.4   Synoptic–scale weather systems in the Antarctic

One of the most remarkable features of the sub–Antarctic latitudes is the high frequency of cyclonic storms, many of which are intense. These systems have a large impact on weather in the region and particularly at coastal locations, where most Antarctic stations are located (Simmonds, 1998). It is clearly important for a number of reasons that the behaviour of these systems be understood and that they be forecast with acceptable accuracy. These transient systems are also significant in a climatological sense in that they effect most of the poleward energy transport in the region (van Loon, 1979; Peixoto and Oort, 1992).

The study of cyclones and cyclogenesis has experienced a remarkable renewal of interest in recent times due to the emergence of new theoretical problems and new approaches to diagnose these phenomena (Mass, 1991; Joly *et al.*, 1997; Turner *et al.*, 1998). There have been a number of significant papers which have examined the behaviour of cyclones over the Southern Hemisphere. Taken chronologically, these reflect a steady improvement in our fundamental understanding of these systems, the quality of the analyses from which they were obtained, and the techniques which have been used to identify systems. Amongst the literature we confine ourselves to citing the works of Lamb and Britton (1955), Taljaard (1967), Streten and Troup (1973), Carleton (1979, 1983), Kep (1984), Leighton (1992), Jones and Simmonds (1993a), Sinclair (1994, 1995, 1997), Simmonds and Murray (1999), and Simmonds *et al.* (1999).

In attempting to understand and document the characteristics of cyclones in the high southern latitudes, it is important to bear in mind that this is a region of great temporal variability of the synoptic environment (seen on a broad range of time scales) and is also presently displaying significant change (e.g., Jones and Simmonds, 1993b; King, 1994; Simmonds *et al.,* 1998; Simmonds and Keay, 2000). Hence consideration of only short epochs may lead to an incomplete understanding of the behaviour of these important transient features.

2.4.1   Depression occurrence

Among the most important developments to have taken place in recent decades in terms of our understanding of the behaviour of cyclonic systems has been the evolution of high quality digital analyses, and the development of automatic algorithms to find and track systems in them. One of these is the Melbourne University automatic cyclone tracking scheme (Simmonds and Murray,1999; Simmonds *et al.*, 1999). This scheme has been applied to the six–hourly global re–analyses produced by the National Centers for Environmental Prediction (NCEP) (Kalnay *et al.*, 1996) (which cover the period 1958–97) and some of the results are shown below.

The density of systems (D) (the mean number per analysis found in a 10^3 (deg. lat.)^2 area) in summer (December to February) and winter (June to August) over the 40–year period is presented in Figure 2.4.1.1. In summer (panel a) in the Atlantic and Indian Ocean sectors the greatest cyclone densities exceed 4×10^{-3} cyclones (deg. lat.)$^{-2}$ near 60° S, while in the Pacific the axis of the maxima lies somewhat further south. In winter (panel b) local maxima are also seen in the Bellingshausen Sea and in Prydz Bay. For the most part, the frequency is higher in this season, although this is not true everywhere (e.g., northern parts of the Weddell Sea).

It is important that these densities be compared with those obtained with more traditional techniques. Figure 2.4.1.1 (c) displays the July distribution of 'cyclonicity' derived manually by Leighton from the Australian operational analyses for the 22–year period 1973–94. Cyclonicity is defined as the total time (in hours) per month during which cyclone centres occupy a given 5×5 degree latitude–longitude cell. This method of counting can be understood to give values which are related to the 'density' measure used above, except for the fact that the counting base area becomes smaller as latitude increases. One can see that the overall structure of the plot is similar to that produced by the automatic scheme, with both showing maxima just to the south of 60° S in the Indian Ocean and to the south of Australia. However, it is important to be clear on the relationship between these measures of cyclone frequency.

To quantify this relationship in general let the cyclonicity in a box of longitudinal range $\delta\lambda$ and bordered by latitudes θ_1 and θ_2 (for an N–day period) be denoted by C. Then the mean number of cyclones to be found in that box per analysis is $C / (24\, N)$. To allow comparison between the two measures of cyclone density we need to compare the two base areas. It can be easily shown that the area of the box considered above is given by Equation 2.4.1.1:

$$A_C = 2a^2 \delta\lambda \, \sin\left(\frac{\delta\theta}{2}\right) \cos\theta \qquad\qquad \text{Equation 2.4.1.1}$$

where a is the radius of the Earth, $\delta\theta = (\theta_1 - \theta_2) / 2$, and $\theta = (\theta_1 + \theta_2) / 2$. The area of 10^3 (degree latitude)^2 is given simply by Equation 2.4.1.2:

$$A_D = 10^3 \left(\frac{2\pi a}{360}\right)^2 \qquad\qquad \text{Equation 2.4.1.2}$$

It follows from the above that the general relationship between system density of cyclonicity is given by Equation 2.4.1.3:

$$D = F \, \frac{C}{\cos\theta} \qquad\qquad \text{Equation 2.4.1.3}$$

where the conversion factor, F, is a given by:

$$F = \frac{10^3 \pi^2}{360^2 \, 2 \, \delta\lambda \, \sin\left(\frac{\delta\theta}{2}\right) 24\, N} \qquad\qquad \text{Equation 2.4.1.4}$$

For the box size used by Leighton and taking $N = 31$ (the case for January and July) this reduces to $D = 0.107 \times C$ at 60° S, and $D = 0.084 \times C$ at 50° S.

It will be seen from Figures 2.4.1.1 (b and c) that the cyclonicity in the manual analysis is about one third to one half that which would be implied by the automatic algorithm. Or, put another way, the computer scheme finds considerably more systems in the sub–Antarctic region, in agreement with the findings of Simmonds *et al.* (1999). To convince ourselves that this difference in cyclone numbers is not simply due to the different periods of analysis used in the two schemes, the mean July system density from the automatic scheme has been drawn for the same period used by Leighton (i.e., 1973–94). The mean system density for this period (Figure 2.4.1.1 (d)) can be seen to be somewhat smaller than that for the 40–year period, but not by an amount to explain the discrepancy referred to above. The reason for the difference is resolved when we confine our system density compilation to consider only closed systems. The resulting system density distribution and values produced by the automatic scheme (Figure 2.4.1.1 (e)) can be seen to be similar to that obtained by the manual process (once the correction above has been applied). That the difference can be explained in this way should not come as a surprise, because it will be appreciated that in regions of strong background pressure gradients and frequent systems the manual analyst will probably be biased toward the counting of 'closed' systems. It can be argued that open depressions are of similar importance to closed systems, and the automatic scheme will find these more easily that would the manual analyst. All the points raised here serve to indicate that when discussing cyclone occurrence and behaviour, there must be a clear definition of these features, and that the comparison of various compilations must be undertaken with the difference in definition in mind.
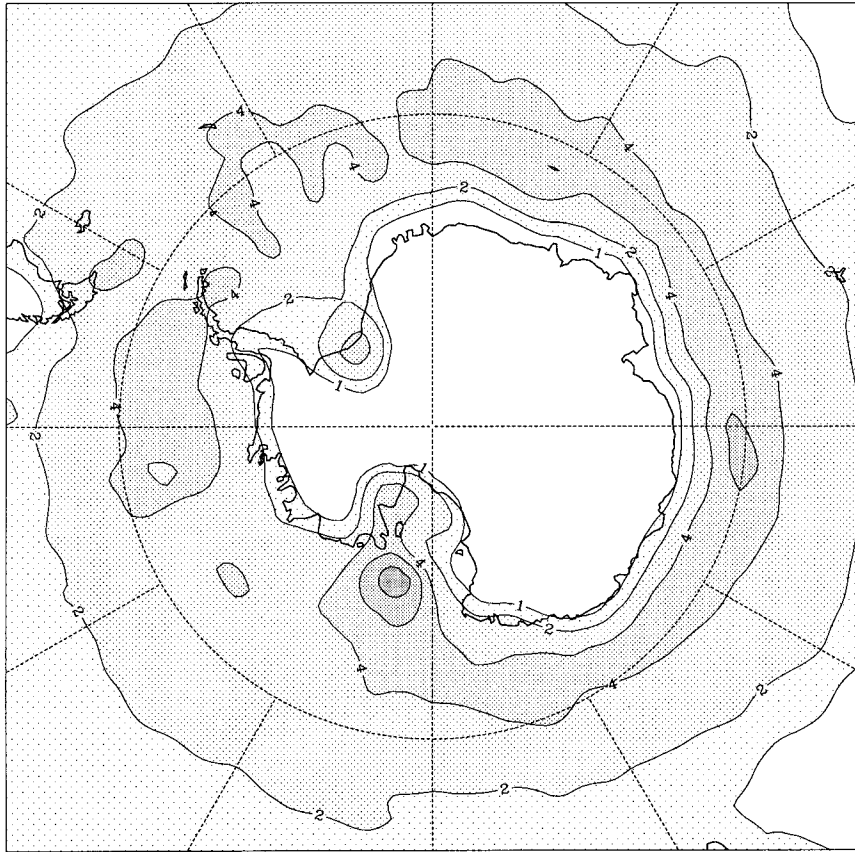
(a)
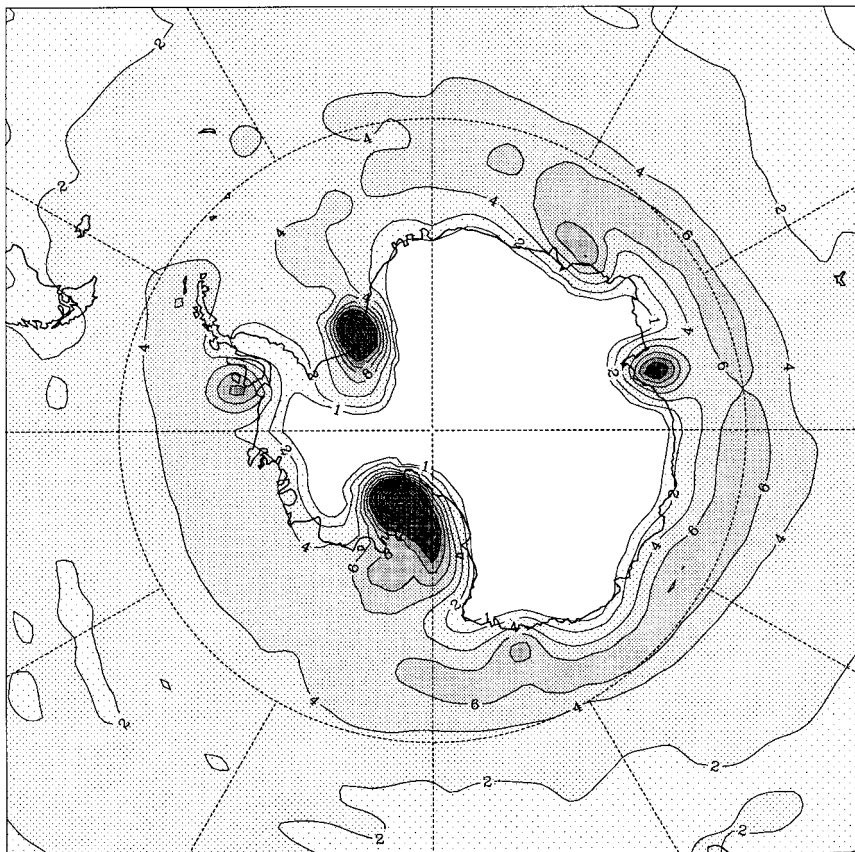
(b)
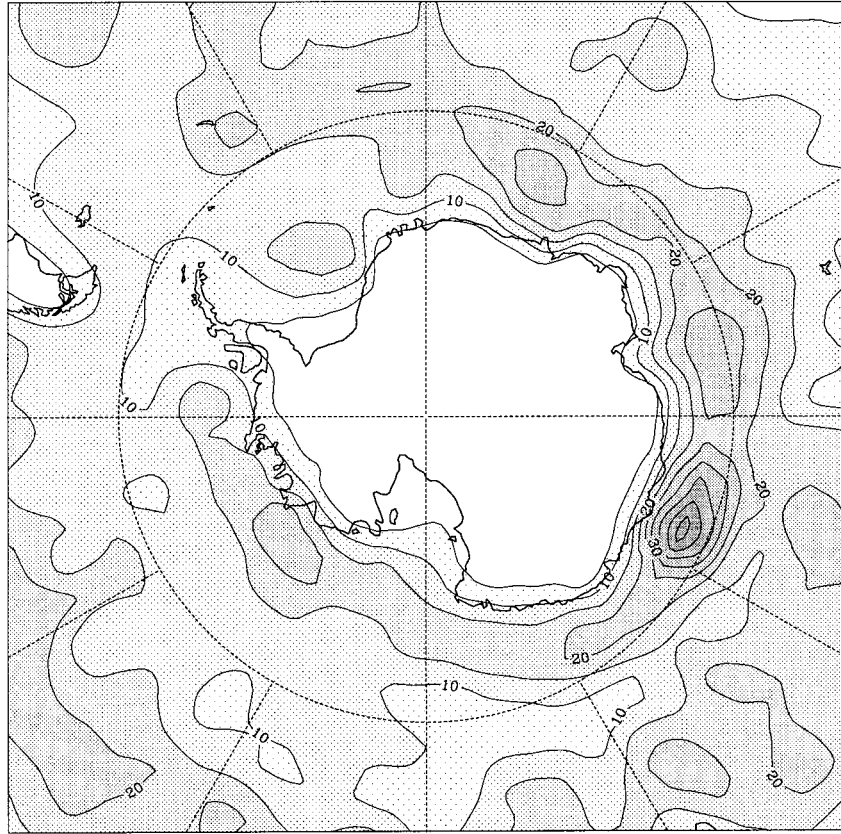
(c)
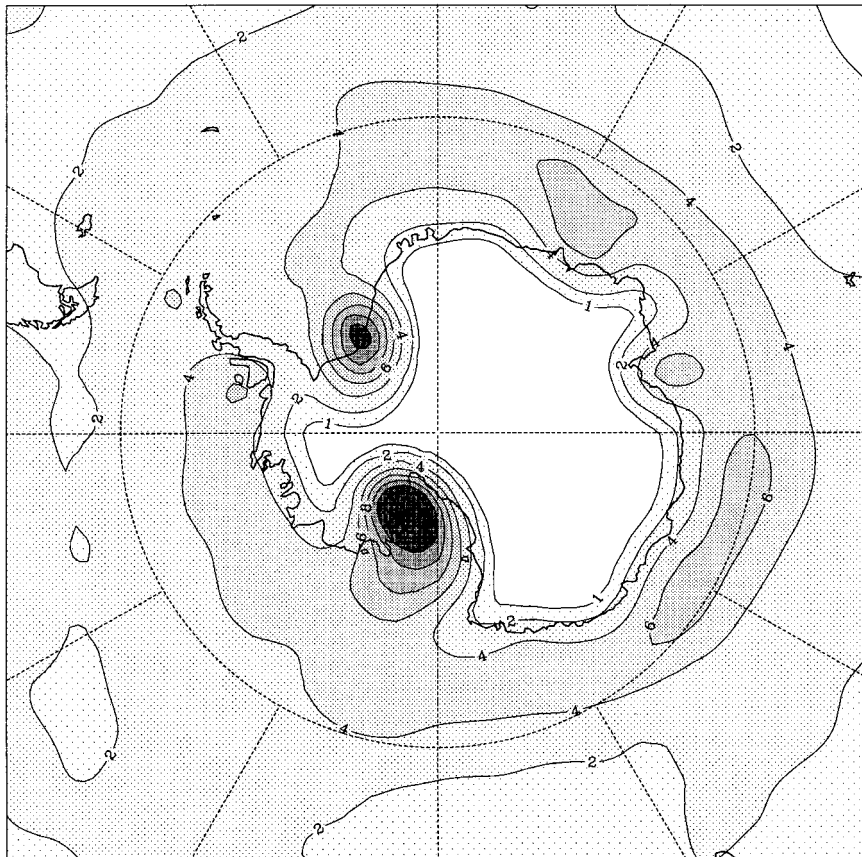
(d)
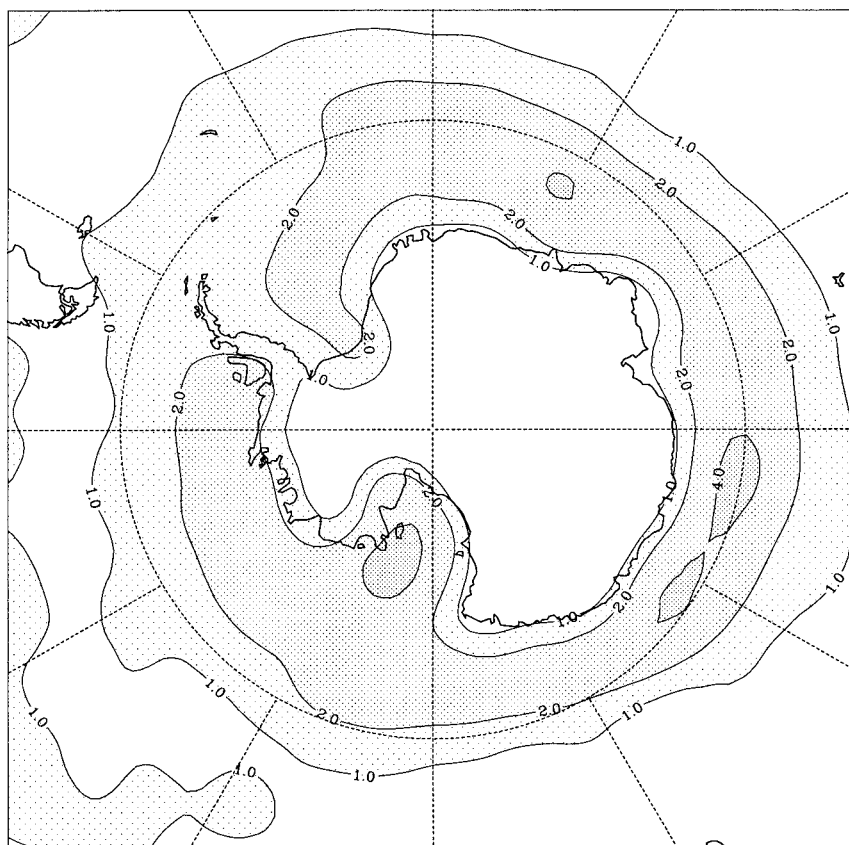
(e)

Figure 2.4.1.1   (a) System density in DJF identified in the automatic algorithm for the period 1958–97; (b) as part (a) but for JJA; (c) July distribution of manually–derived cyclonicity for the period 1973–94; (d) System density in July identified in the automatic algorithm for the period 1973–94; and (e) when only systems with closed centres are considered. The contour intervals in (a), (b), and (d) are 2×10^{-3} (deg. lat.)$^{-2}$ (with an extra contour at 1×10^{-3} (deg. lat.)$^{-2}$). In (c) the contour interval is 5 hours per month per 5✕5 latitude–longitude cell. In (e) the contour interval is 1×10^{-3} (deg. lat.)$^{-2}$.

2.4.1.1   Trends in depression occurrence

We saw above that the July sub–Antarctic system density during the period 1973–94 was somewhat less than that diagnosed over the 1958–97 epoch. For forecasting it is important to have an appreciation of the background level of cyclone activity, and the extent to which this may be changing. Prompted by the above observation, we have calculated the linear trend displayed by July cyclone density over the four decade period of the reanalysis, and present this in Figure 2.4.1.1 1 (a).

There has been a general reduction, much of which is statistically significant, in cyclone numbers over most of the domain. The greatest reductions occur near the 60° S latitude circle. (Immediately on the coast there are several 'bull's–eyes' of increases in the number of cyclones. Simmonds and Keay (1999a) noted similar features in their analysis of the annual totals of cyclone and offered reasons for the existence.) It is interesting to note that the

reduction appears not to be dominated by changes in a given sub period. As support for this statement, we see that the July trends calculated over the 1973–94 epoch (Figure 2.4.1.1.1 (b)) are very similar.

Leighton and Deslandes (1991), Leighton (1997), and Leighton et al. (1997). have also identified regional trends in manually–derived cyclonicity. When Leighton's analysis of 22 years of July cyclonicity in the sub–Antarctic region is subject to trend analysis (Figure 2.4.1.1.1 (c)) there are a number of features in common with those revealed by the automatic scheme over the period. Among these are the reductions in much of the eastern Pacific and to the north of the Weddell Sea, and the changes to the south of Australia. However, the sign of the change in the central Indian Ocean to the north of 60° S is opposite in the two compilations. In light of our discussion above it would seem fruitful to determine the trends for the automatic scheme when consideration is restricted to closed systems. Figure 2.4.1.1.1 (d) shows that in this case is diagnosed positive trends in the central Indian Ocean, in broad agreement with the sign of the change revealed in the manual analysis. Following on from our point raised above, it is clear that the definition of a cyclone must be clearly expressed before we can speak sensibly of secular changes in their behaviour.

2.4.2   Cyclogenesis

Here we consider the mean genesis of cyclonic systems in the Antarctic region as revealed in the automatic algorithm's analysis of the 40 years of NCEP data. In summer (Figure 2.4.2.1 (a)) most of the domain experiences genesis rates in excess of 0.5×10^-3 cyclones (deg. lat.)$^{-2}$ day^{-1}. The axis of maxima is found on, or to the south of, 60° S and extrema are found over Graham Land, in the embayment to the north of Tierra del Fiego, off Victoria Land and the Siple Coast, as well as in the southern part of the Weddell Sea. Figure 2.4.2.1 (b) shows that the pattern in winter is rather similar, but the level of cyclogenetic activity is increased. A minimum of cyclogenesis is apparent at about 45° S across much of the Pacific and Atlantic Oceans while a maximum is observed in the Indian Ocean.

2.4.3   Depression tracks

To obtain a general appreciation of the behaviour of individual cyclones in the sub–Antarctic region we have plotted, as examples, the paths of all cyclones which appear in 1996 and 1997 in the months of January (Figure 2.4.3.1 (a)) and July (Figure 2.4.3.1 (b)). One can see that while these systems have a predominant eastward motion, there is a significant poleward translation of most systems, particularly in the region north of about 60° S. In both months there is a very dense network of tracks just off the Antarctic coast, particularly in the Indian and western Pacific Oceans. We had alluded to this aspect in our earlier discussion on the system density.
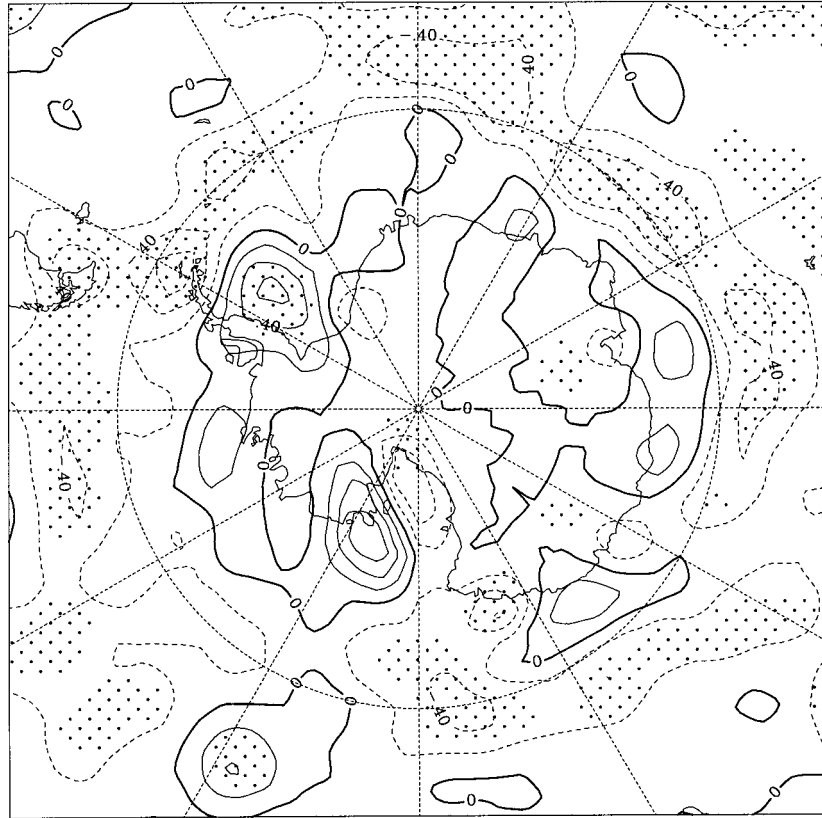
(a)
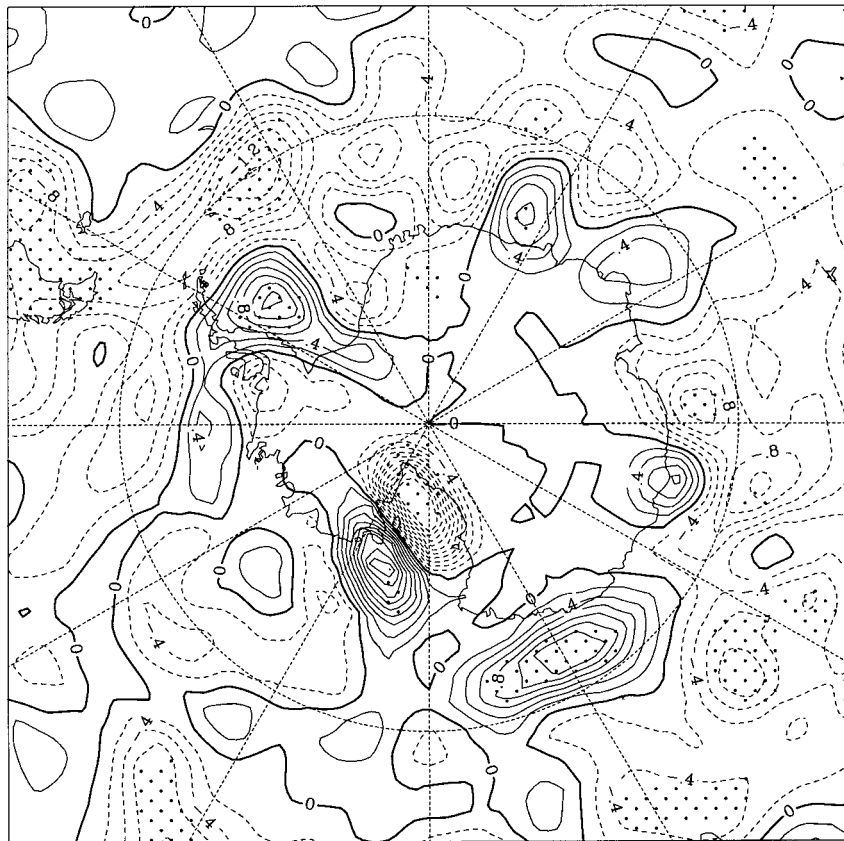
(b)
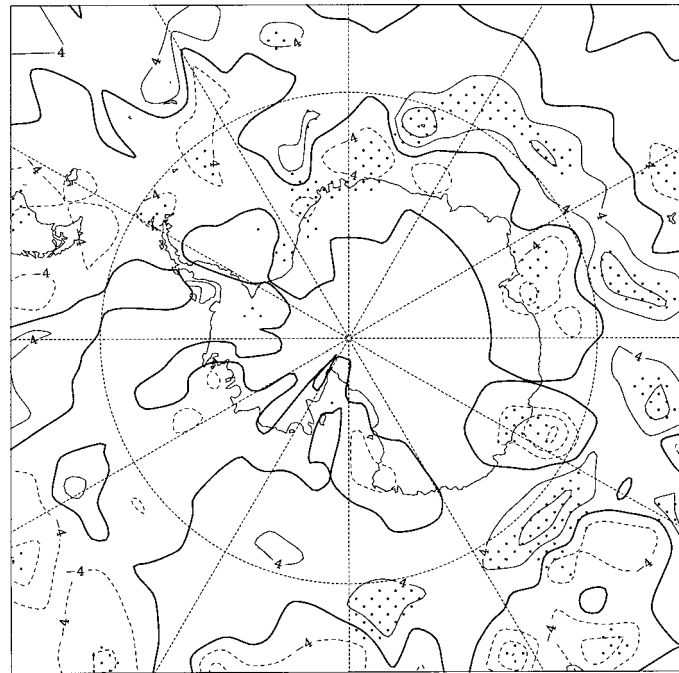
(c)
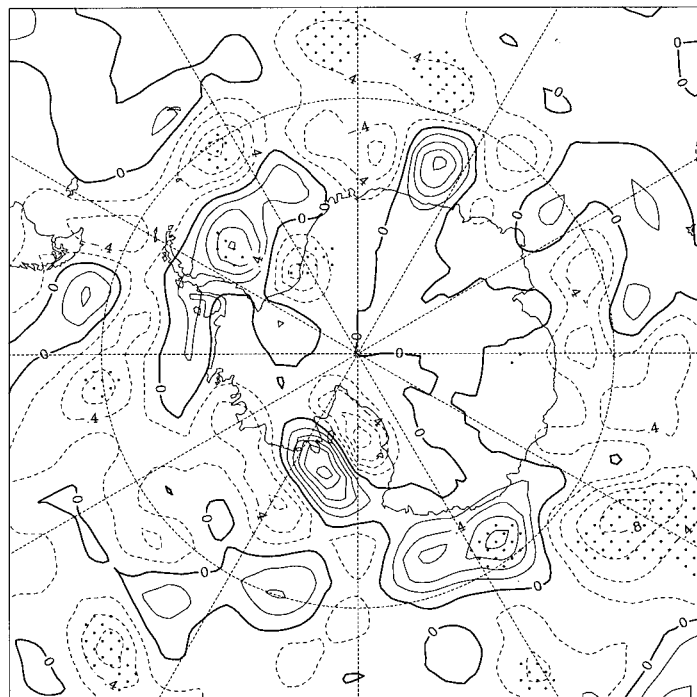
(d)

Figure 2.4.1.1.1 (a) Linear trend in July system density identified in the automatic algorithm for the period 1958–97. (b) Linear trend in July system density identified in the automatic algorithm for the period 1973–94. (c) Linear trend in July manually–derived cyclonicity for the period 1973–94. (d) as for part (b) but when only systems with closed centres are considered. Stippling denotes regions over which the trends differ significantly (95% confidence level) from zero. The contour interval is 0.2×10^{-3} (deg. lat.)$^{-2}$decade^{-1}, except in part (c) where it is 2 hours per month per 5 × 5 latitude–longitude cell per decade.
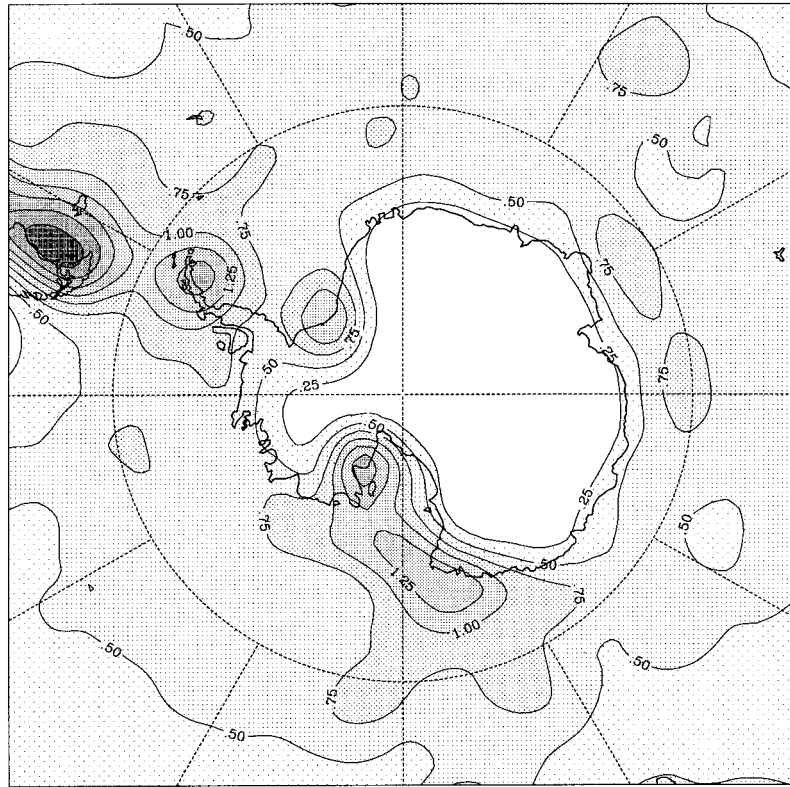
(a)
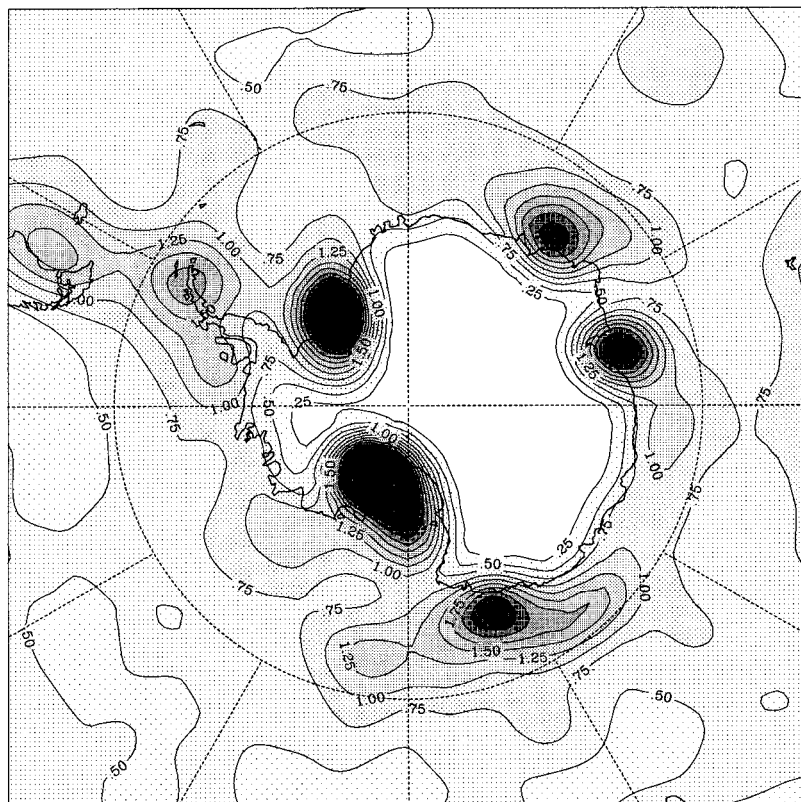
(b)

Figure 2.4.2.1   Cyclogenesis identified in the automatic algorithm for the period 1958–97 for (a) DJF and (b) JJA. The contour interval is 0.25×10^{-3} cyclones (deg. lat.)$^{-2}$ day^{-1}.
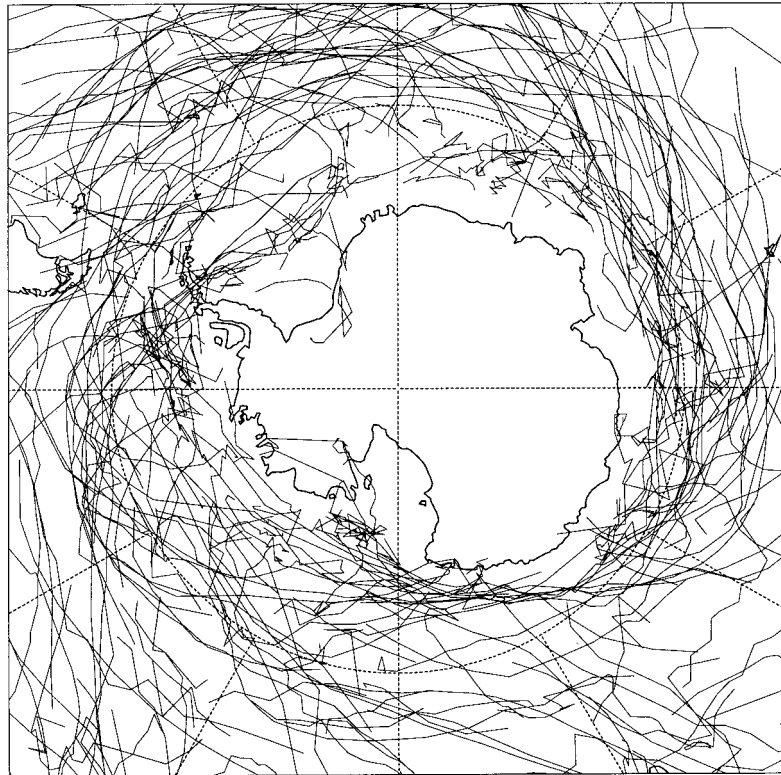
(a)
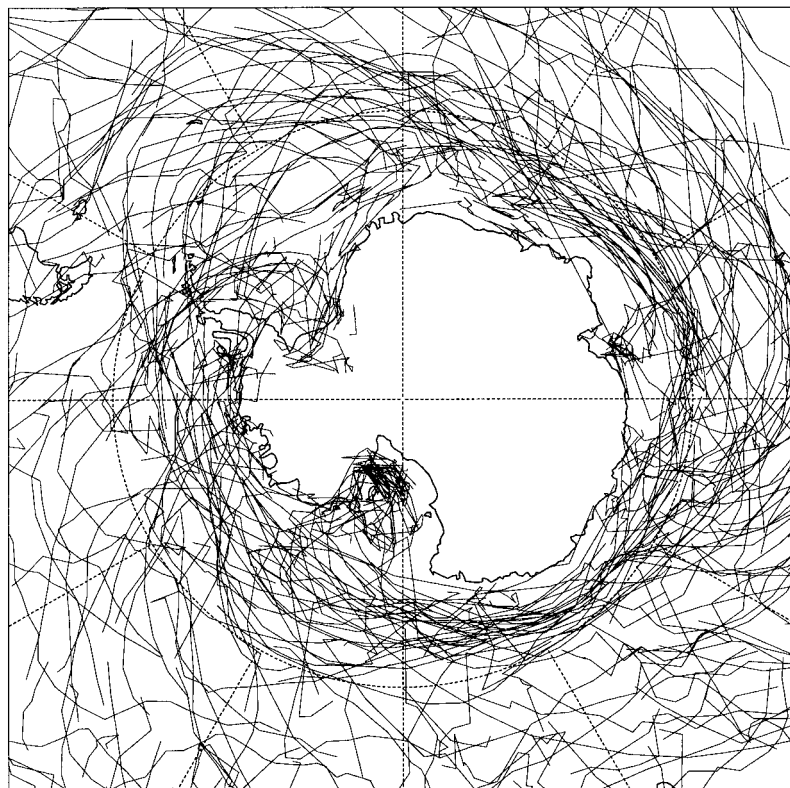
(b)

Figure 2.4.3.1   Tracks of all cyclones identified in the automatic algorithm in 1996 and 1997 in (a) January and (b) July.

2.4.4   Cyclolysis

Regarding the distribution of summer cyclolysis (i.e., termination of systems) Figure 2.4.4.1(a) shows very large values just north of the Antarctic coast, particularly off much of East Antarctica, and in the Ross and Bellingshausen Seas. While the pattern bears some resemblance to that of the cyclogenesis (Figure 2.4.2.1 (a)) it can be seen that for the most part the rates of lysis exceed those of genesis. (Maxima are seen near 20° E and 120° E, and these are areas of only modest cyclogenesis.) Given that a significant proportion of the systems that are generated in the lower latitudes finish their days near the Antarctic coast (Figure 2.4.3.1 (a)) this enhancement is not surprising. Overall, similar remarks may be made in connection with the cyclolysis in winter (Figure 2.4.4.1 (b)), except that the overall level of cyclolytic activity is greater in the winter season.

2.4.5   Difference between rates of cyclogenesis and cyclolysis

The relationship between the geographical distributions of cyclogenesis and cyclolysis can be appreciated more readily by considering the difference between the two. The patterns of difference are very similar in summer and winter (Figure 2.4.5.1) (although it will be noticed that the excess of lysis is greater in winter around most of West Antarctica, particularly in the Ross and Bellingshausen Seas). Over most of the domain of interest here cyclolysis rates exceed those of cyclogenesis. The only exceptions to this of note is that genesis greatly exceeds lysis off the east coast of the southern tip of South America, through the Drake Passage and down the eastern side of the Antarctic Peninsula. This indicates, among other things, that a significant portion of the systems that are born in these regions are mobile and end their days elsewhere. Genesis also exceeds lysis in both seasons in the region around Oates Land.

Hence, with these regional exceptions, over the high southern latitudes cyclolysis exceeds cyclogenesis and hence this domain is a cyclone 'graveyards' in this mean sense. having said this, it is important to bear in mind that there is significant levels of genesis in the sub–Antarctic regions.

2.4.6   Weather systems over the interior

From what we have shown above it will be realised that few systems have been represented at mean sea level (MSL) over the main part of the Antarctic continent. Part of the reason for this is that the value of 'MSL pressure' (MSLP) chart in weather analysis is diminished when that level is far beneath the surface. In fact, to circumvent misleading deductions the automatic cyclone tracking scheme ignores any system identified at a location where the height of the orography exceeds 1 km (Simmonds and Murray, 1999). There are many theoretical reasons for believing that very few systems will penetrate inland (e.g., potential vorticity considerations, weakening of baroclinicity).

Notwithstanding these points, it is not unknown for weather systems to be detected over the interior of the Antarctic continent (e.g., Pook and Cowled, 1999). The difficulties associated with the identification of atmospheric pressure systems over the Antarctic interior
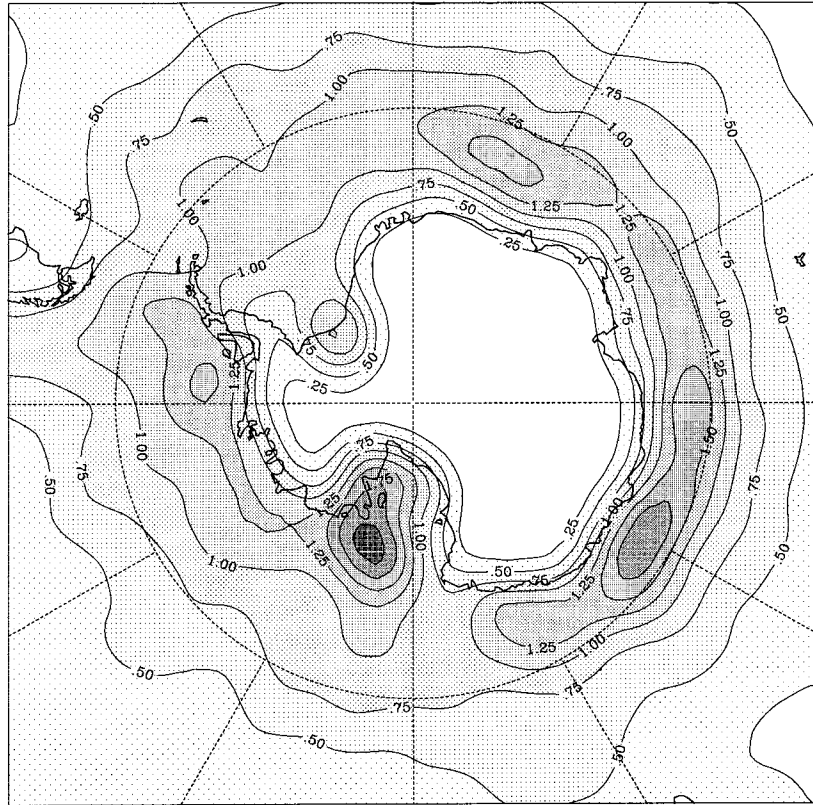
(a)
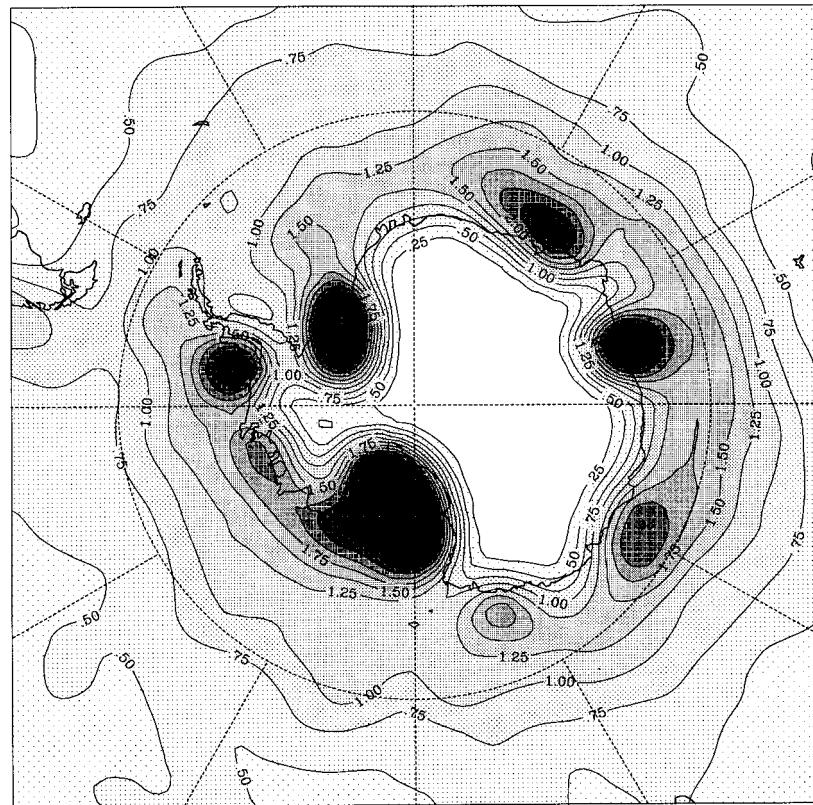
(b)

Figure 2.4.4.1   Cyclolysis identified in the automatic algorithm for the period 1958–97 for (a) DJF and (b) JJA. The contour interval is 0.25×10^{-3} cyclones (deg. lat.)$^{-2}$ day^{-1}.
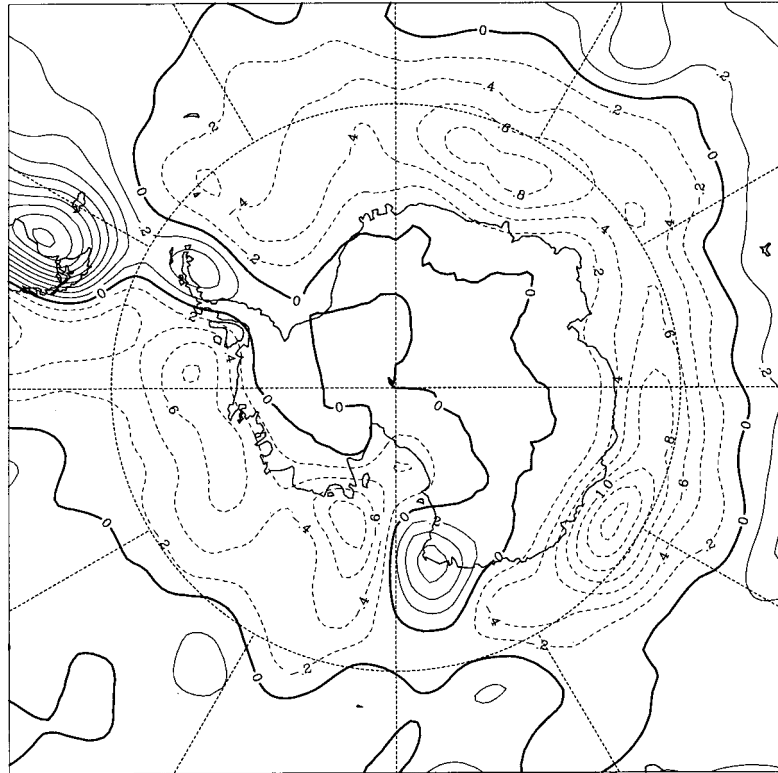
(a)
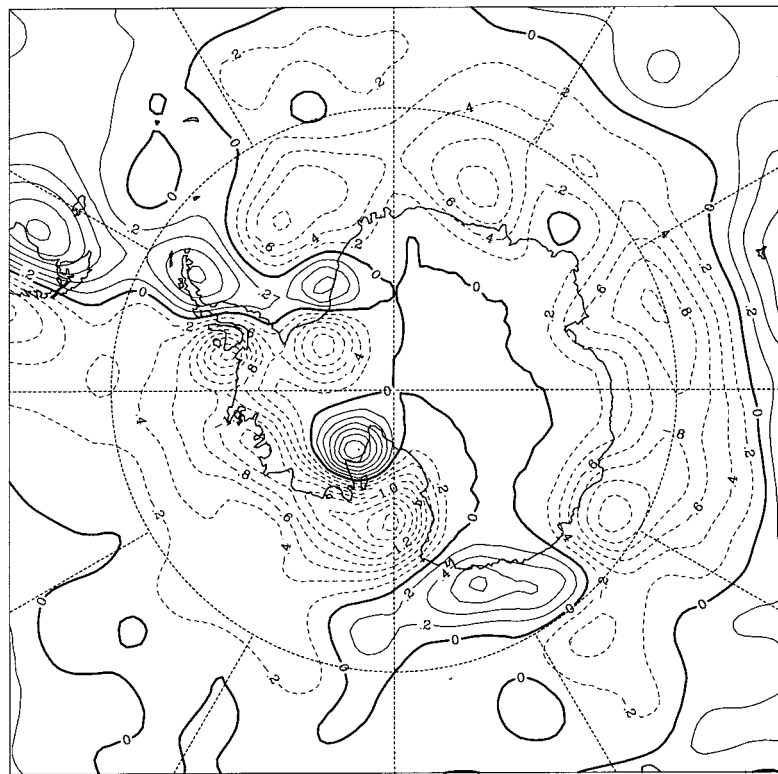
(b)

Figure 2.4.5.1   Difference between cyclogenesis and cyclolysis identified in the automatic algorithm for the period 1958–97 for (a) DJF and (b) JJA. The contour interval is 0.2×10^{-3} cyclones (deg. lat.)$^{-2}$ day^{-1}.

are well known to analysts and have been discussed by, *inter alia*, Schwerdtfeger (1984) and Phillpot (1997). As well, identifiable weather systems moving inland from the Antarctic coast have proved very difficult to track. Apart from the obvious limitations of the observational network, cloud signatures of systems are difficult to identify over the underlying very cold ice surface. Furthermore, the elevation of the Antarctic Plateau which rises from approximately 2 km close to the coast to over 4 km at its highest point requires that synoptic and mesoscale systems moving inland have well defined vertical structures in order to survive.

Early inferences about pressure systems over Antarctica were influenced by charts of equivalent mean sea level pressure. However, the method of constructing MSL charts requires the reduction of station barometric pressures to sea level by assuming that a column of air of known mean virtual temperature exists between the station and the datum. Errors introduced by this process make the practice of producing MSLP analyses over the Antarctic interior unreliable. This means that the regular appearance of very high pressure over Antarctica on MSL synoptic charts cannot be given a physical significance, a point emphasized by Schwerdtfeger (1984).

Analysts are faced with the difficulty of selecting a pressure level which is not significantly affected by the orography of Antarctica but which is sufficiently close to the surface to be linked dynamically to the surface wind field. Phillpot (1991, 1997) selected the 500–hPa surface as the most suitable level for analysis over East Antarctica. The problem with working at this level is then to obtain sufficient data to complete the analysis. There has been a reduction of upper–air observations in the interior of the continent in recent years. In 1994, South Pole Station was the only inland station still conducting an upper–air programme of observations throughout the year. This contrasts with the situation during the International Geophysical Year of 1957–58 when there were nine staffed scientific stations providing meteorological data from elevations of 1500 m or more (Dalrymple, 1966). This lack of rawinsonde stations makes conventional upper–air analysis impossible without the input of other data. At this stage remote sensing has not provided a satisfactory solution. Whereas TIROS Operational Vertical Sounder (TOVS) data provide good agreement with radiosonde data over the Southern Ocean their accuracy over the elevated Antarctic continent is problematic and evidence of strong seasonal bias has been detected (Adams *et al.*, 1999). Improvements in the retrieval schemes employed to invert the TOVS data into geophysical quantities may ultimately lead to improvements in the quality of the data over the continent.

To some extent the problem has been eased by the gradual expansion in the network of surface observations that has been achieved in recent years by the installation of automatic weather stations (AWSs). Phillpot (1991) devised a method for estimating 500–hPa geopotential heights from station level observations of pressure and temperature at AWSs with elevations exceeding 2500 m. His analyses of the 500–hPa geopotential field over East Antarctica were incorporated in a set of analyses covering the region south of 50° S for the month of July 1994 (Phillpot, 1997; see his Figure 7.5). These analyses form part of a project known as the Antarctic First Regional Observing Study of the Troposphere (FROST) which provided an opportunity to investigate pressure systems over the interior of Antarctica. The FROST Project (Turner *et al.*, 1996a) was designed to study the effects of all sources of 'late' data on meteorological analyses over the Southern Ocean and Antarctic region and the probable impacts of these data on the performance of numerical weather prediction models. A detailed description of the FROST analysis programme is given in Hutchinson *et al.* (1999).

Phillpot (1997) also contributed analyses for a period in January 1995. The analyses for this period (see his Figure 16) were constructed by modifying the Australian Global Assimilation Prediction system (GASP) analyses with the addition of estimated geopotential heights from AWS observations and some 'late' observations from staffed stations. Monthly means for the months of July 1994 and January 1995 were modified by Phillpot (1997) in a similar manner (see his Figure 7.7).

2.4.6.1   Anticyclones over continental Antarctica

The over–emphasized strength of the anticyclone over the Antarctic continent, that appears on some MSLP analyses, has little significance and arises from attempts to estimate equivalent MSLP from station level pressures at elevations generally exceeding 1 km. Saucier (1955, (1972 reprint), p 56) discusses difficulties with pressure reduction to levels below the Earth's surface. For practical purposes, 450 m (~ 1500 ft) is regarded as about the altitude limit for which accurate pressure reductions may be made to MSL (see, for example, Meteorological Office (1971, p. 13). However, the 500–hPa surface does not intersect the Antarctic terrain and can be regarded as a useful level at which to investigate the presence of significant anticyclonic systems in the free atmosphere above Antarctica (Schwerdtfeger, 1984; Phillpot, 1997).
          Phillpot (1997) has demonstrated the relative complexity of the atmospheric circulation over Antarctica in a sequence of 500–hPa contour fields during the first Special Observing Period (SOP–1) of the FROST Project in July 1994. The analyses contrast the steady west to east movement of the major troughs and ridges north of the continent with the sluggish movement observed over Antarctica. It is notable that the range of pressure readings at surface stations over the Antarctic Plateau during periods of days or weeks are comparable to those observed at mid–latitude stations. As discussed in Turner *et al.* (1996a) significant variations of surface pressure were found to occur over East Antarctica during SOP–1. At 500 hPa the increase in geopotential over Victoria Land during the period 22 to 28 July 1994 was in excess of 250 m. Parish and Bromwich (1998) have demonstrated how a similar synoptic configuration in late June and early July of 1988 was associated with drainage of air from Antarctica through the Ross Sea, resulting in pressure decreases of 20 hPa or more across a large portion of Antarctica.
          The FROST analysis exercise also revealed how a high over the continent can merge into an intense ridge extending from a blocking anticyclone in the southwest Pacific Ocean (Pook and Cowled, 1999). In this case the Pacific ridge appeared to propagate from the east across the plateau. Time series of pressure anomalies at AWSs at elevated locations showed pressure increasing at the easternmost stations first. Surface pressure variations for a selection of Australian AWSs on the Antarctic continent throughout SOP–1 have previously been shown by Turner *et al.* (1996a) in their Figure 10.
          The monthly mean of the 500–hPa geopotential height over East Antarctica from SOP–1 (Turner *et al.*, 1996a; their Figure 11) identified three maxima (centres exceeding 5,000 gpm) over the high plateau of East Antarctica; near 50° E, 90° E and 120° E. This degree of detail was achieved by incorporating estimated geopotential heights from AWSs (see Section 5.4.3 and in particular Figure 5.4.3.1.1 below) and contrasts with the published 500–hPa climatologies of Schwerdtfeger (1970) and Le Marshall *et al.* (1985).

2.4.6.2   Cyclones over continental Antarctica

Broad regions of relatively low geopotential height are detectable over the Antarctic continent on the mean (e.g. 500–hPa) contour charts. Drawing on data from the IGY, Dalrymple (1966) identified four main features of the mean circulation in the middle troposphere over Antarctica. Regions of relatively high geopotential were found to occur over central East Antarctica and over Marie Byrd Land in West Antarctica with minima over the Ross and Weddell seas. Schwerdtfeger (1970) demonstrated that these features are preserved in the seasonal cycle for the most part but there is a decrease of total mass over Antarctica in winter

and the region of lowest geopotential height tends to be more centred near the pole in summer.

Pook and Cowled (1999) produced a set of analyses of the 500–hPa surface south of 50° S for the period 22 to 28 July 1994 in the FROST SOP–1. These analyses followed the previous set of 500–hPa contour fields prepared for the period 1 to 15 July 1994 (Phillpot, 1997; his Figure 7.5) which incorporated AWS and 'late' station data. For this 'special' week of analyses, high quality visible and infra–red imagery from the US Defense Meteorological Satellite Program (DMSP) satellites was employed in addition to initial fields analysed by Phillpot and other members of the FROST analysis team. In their Figure 3, Pook and Cowled (1999) demonstrated that closed cyclonic circulations were in evidence over the continent in the daily analyses and underwent significant evolution with time. In the Indian Ocean sector the trough was oriented parallel to the coast throughout the period with individual centres over the ocean and, on some occasions, just inland.

Variations in station level pressure experienced at AWSs on the high plateau during the FROST experiment were similar to ranges experienced at lower latitudes of the Southern Hemisphere and suggest that the atmospheric circulation is complex, even at these high latitudes and elevations.

2.4.6.3   Cyclones Migrating Inland from the Southern Ocean

According to published climatologies of cyclones over the Southern Hemisphere, lows over the Antarctic continent are extremely rare, particularly over East Antarctica south of 70°S (Sinclair, 1994; Jones and Simmonds, 1993a; Simmonds and Keay, 2000b). Similarly, studies of polar air vortices, or 'polar lows' have shown an almost total absence of these systems over the continental interior (Carleton and Carpenter, 1990). While the effects of maritime lows can be felt inland (see, for example, Section 7.10.2 (Vostok) below) cyclones rarely move over East Antarctica as a discrete entity because of the 'so–called' barrier effect of the elevated ice sheet (Bromwich, 1988). In any case, it is not a trivial problem to track cyclonic vortices over the Antarctic continent. Firstly, it is difficult to discriminate cloud from the ice surface on satellite imagery because of the similar brightness temperatures observed in the thermal infra–red channels and the similar albedos of the two surfaces in the visible channels (Turner and Row, 1995). Analysts normally find it necessary to compare and contrast Advanced Very High Resolution Radiometer (AVHRR) channels and to use techniques as basic as detecting cloud shadows on visible channel imagery. Secondly, the limited nature of the conventional observational network makes it very difficult to follow the progress of synoptic and mesoscale systems, although recent improvements in the network of AWSs over East Antarctica have helped analysts.

Although cyclonic systems generally remain offshore, moisture from these systems is regularly transported inland resulting in cloudiness and precipitation. Sinclair (1981) carried out a case study into a situation in December 1978 in which strong positive temperature anomalies and precipitation occurred over the Antarctic Plateau. Facquet (1982) used a compositing technique to develop a conceptual model of moist air advection across the Antarctic coast.

There are few published studies of the identification and tracking of weather systems over the Antarctic interior. Pook and Cowled (1999) have reported a situation in July 1994 during which two vortices were observed to move across the coast of Antarctica and migrate inland over Wilkes Land (see Fig. 2.4.6.3.1). These vortices were apparent in the DMSP satellite thermal infra–red cloud imagery and were steered across the Antarctic by an intense blocking anticyclone which developed in the southwest Pacific. An atmospheric pressure peak associated with the intensification of this ridge appeared to propagate across East Antarctica

28

from the Pacific sector of the Southern Ocean. The easternmost vortex was detectable at the surface from observations reported by the AWS at Dome C (74.5° S, 123° E, 3280 m elevation above mean sea level (AMSL)). This station had indicated a steadily rising barometric pressure over several days but experienced a fall in pressure of approximately 3 hPa as the vortex passed the station and the anemometer recorded a rapid increase in wind speed from approximately 2 m s^{-1} at 0000 UTC to 7.1 m s^{-1} at 1200 UTC and back to zero m s^{-1} by 0000 UTC on the following day. The wind changed direction from easterly to northerly and back to easterly within 24 h. It is important to note that the diameter of this system was probably never more than 2.5° latitude (275 km) and remained in the mesocyclone scale length throughout its lifetime.
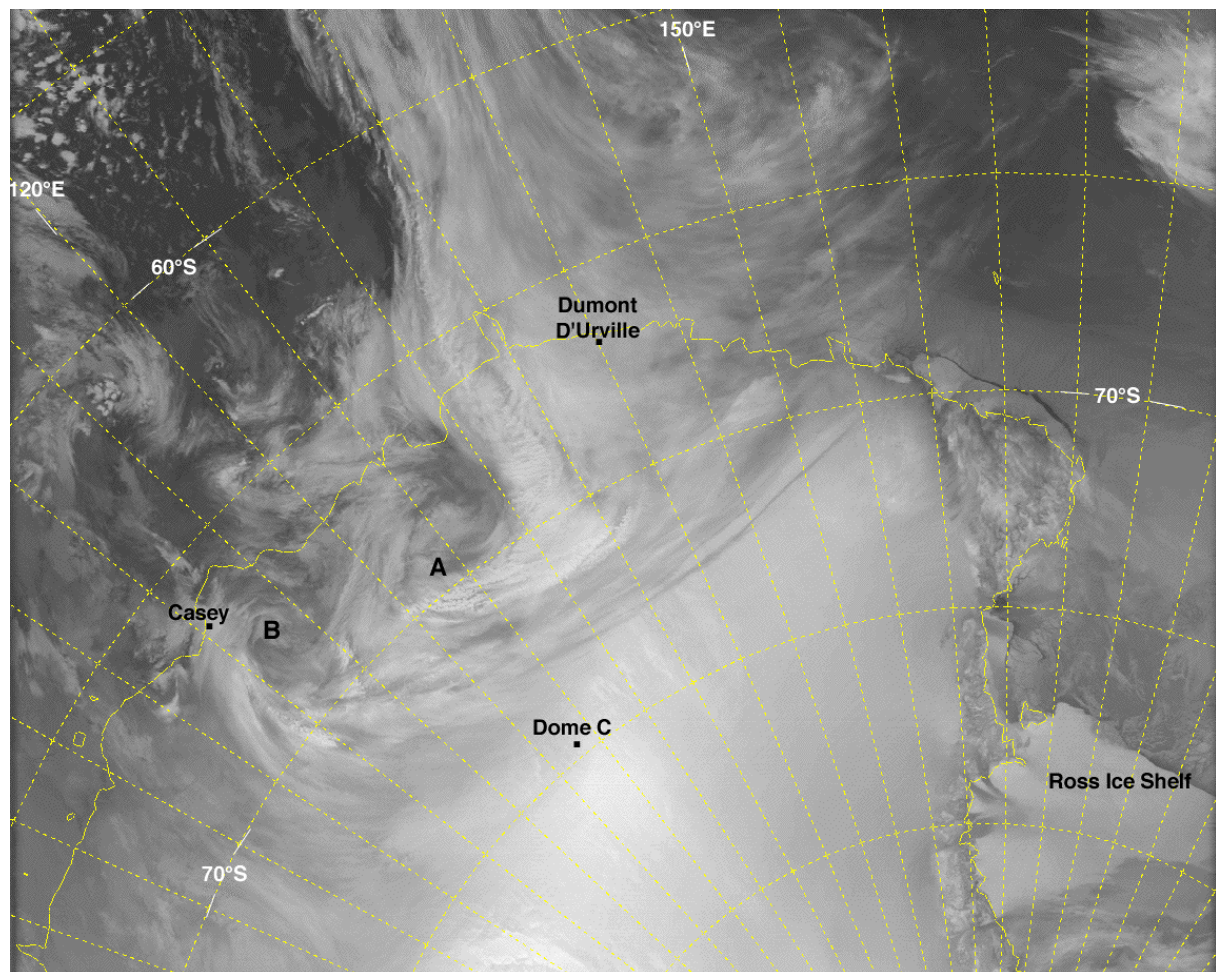
Figure 2.4.6.3.1 A DMSP image of cyclonic vortices over East Antarctica at approximately 2300 UTC 26 July 1994. (from Pook and Cowled (1999) – their Fig. 7a).

This study within FROST demonstrated that vortices originating over the Southern Ocean can penetrate the high plateau of East Antarctica and move well inland before decaying. The development of an intense blocking anticyclone in the Tasman Sea sector appears to have been a critical factor in this case. Although these events are relatively rare, occurrences of this type have the potential to influence precipitation events over the Antarctic interior in a significant way and further study is required to attempt to quantify the effects of these cyclones.

Numerical models currently in operational use do not have the necessary resolution to identify the relatively small cyclonic systems with their comparatively short lifetimes which penetrated inland during this study. Nor was it possible to locate them using traditional methods of manual analysis as the density of observations in Antarctica is too low. (In contrast to the Phillpot method discussed previously where there was a clearly enough data to at least analyse the 500–hPa level). The new generation of mesoscale models nesting within global models may provide the possibility for modeling these systems over the Antarctic in future.

Now that good climatologies exist for many AWSs in Antarctica the technique employed in this paper to detect cyclonic systems over the Antarctic Plateau using AWS anomaly fields and high resolution satellite imagery appears capable of adaptation to operational use. The possibility exists for analysis of AWS pressure anomalies from high frequency observations (possibly at 1–hourly intervals) with the addition of other parameters such as temperature, dew point and wind. In addition, the derivation of similar anomaly fields from numerical prognoses, especially in the next generation of high resolution models, could provide a useful predictive capability.

2.5   Mesocyclones

Mesocyclones are high latitude, sub–synoptic–scale depressions that have a horizontal length scale of less than about 1000 km and generally exist for less than 24 h. With their limited horizontal scale they can often pass undetected between synoptic reporting stations and are usually identified via visible or infra–red satellite imagery. In fact these lows were hardly known in the pre–satellite era and have only been studied since about the early 1980s. Despite their small scale, these lows can be very important in the forecasting process in some sectors of the Antarctic since they can have winds of greater than gale–force and can bring moderate or heavy snowfall to coastal locations. In this section we provide a brief introduction to mesocyclones. Further information on these systems can be found in the meteorological literature (Turner and Row, 1989; Turner *et al.*, 1993; Turner *et al.*, 1991; Heinemann and Claud, 1997) and in Section 6.5 below, which deals with the specific problems involved in forecasting these vortices. There is a bewildering variety of names applied to these systems in the two polar regions including polar lows, Arctic hurricanes, polar depression, mesocyclones and cold air vortices. However, these terms all refer to mesoscale depressions in the polar regions and we will refer to them here simply as mesocyclones. It should be noted that the term polar low is often used to refer to the more intense vortices that have surface wind speeds of greater than gale–force.

2.5.1   The general characteristics of mesocyclones

Mesocyclones are cold air vortices that are usually found south of the main polar front and well away from the main frontal cloud bands. Since they tend to form in cold air outbreaks they are often found to the west of large synoptic–scale lows when very cold continental air pushes northwards over the Southern Ocean. A typical example of a mesocyclone–synoptic scale low passing through the Drake Passage to the north of the Antarctic Peninsula is shown in Figure 2.5.1.1.

As discussed above, most mesocyclones have a horizontal length scale of less than 1000 km, although some vortices can be as large as 1500 km, since there is really a spectrum of low-pressure systems around the Antarctic and it is not possible to specify any firm boundary separating the different types of lows. However, satellite studies (Turner and Thomas, 1994) have shown that the vast majority of mesocyclones are less than 500 km in horizontal extent. The satellite imagery has also shown that most mesocyclones are quite short lived with most existing for less than 12 h (Heinemann, 1990).

The satellite imagery has also provided much useful information on the cloud patterns associated with mesocyclones. What distinguishes mesocyclones from frontal cyclones is that they tend to have a single band of cloud around the low centre, rather than the warm, cold and occluded fronts of a classic baroclinic wave. This cloud can take the form of a single comma or can be wrapped two or more times around the low centre in the form of a spiral cloud band. Although many papers refer to comma and spiral systems it is not clear whether there is any fundamental differences in the mechanisms involved in their development. However, spiraliform systems tend to be found in synoptically quiet regions while comma–type lows are more usually found when the background flow is stronger, such as to the west of a deep depression. A third type of mesocyclone that has been noted is the 'merry–go–round' type of development discussed below.

New forms of satellite data, such as passive microwave imagery and winds from the scatterometers, have provided information on the surface wind field associated with mesocyclones. These data have shown that most mesocyclones are quite weak and often have no more than a trough in the surface pressure field. When *in situ* data have been available they have suggested that most mesocyclones have a surface pressure perturbation of less than 5 hPa. However, a number of deep systems with winds at gale–force or stronger have been observed.

As with other types of depression, mesocyclones are local maxima of cyclonic vorticity. This vorticity can increase for a number of reasons associated with the formation and development of the low's circulation. Our understanding of the formation of mesocyclones is far from complete but the following factors seem to be important in the development of some systems:

- *Baroclinic instability*. Small scale lows with the appearance of classic baroclinic waves have been observed to form on some frontal bands, for example near the ice edge where a significant horizontal thermal contrast can be found, especially when the flow is parallel to the ice edge. It has been suggested that the small horizontal scale of the lows is a result of the shallow depth of the baroclinic zone.

- *Barotropic instability*. This is a shearing instability that can be responsible for the development of some vortices were there is a pronounced horizontal wind shear without any major thermal gradient. An example of this type of development occurs in Prydz Bay, at the mouth of the Lambert Glacier, where the phenomenon has become known locally as the 'Prydz Bay Low'. Figure 2.5.1.2 is an example of this type of low: in this image the structure of the pack ice north of the Amery Ice Shelf reflects the strong south to southwest continental outflow from the Lambert Glacier with a small low having formed on the eastern shear zone of the outflow. Low–level convergence (see below) may also play a role here.

- *Upper level troughs and cold pools*. Upper troughs can be responsible for significant cyclonic vorticity advection into an area resulting in the spin–up of mesocyclones. This can take place to the west of synoptic–scale lows where the mesocyclone can be associated with minor surface and upper–air troughs. In addition, the presence of an upper cold pool can be an important factor in generating

instability through a layer of the atmosphere.

- *The decay of large synoptic–scale lows*. As large lows decline and become slow–moving they can often decay into a number of mesoscale centres of circulation that rotate around a common centre (Figure 2.5.1.3). Such systems tend to be rather rare around the Antarctic.
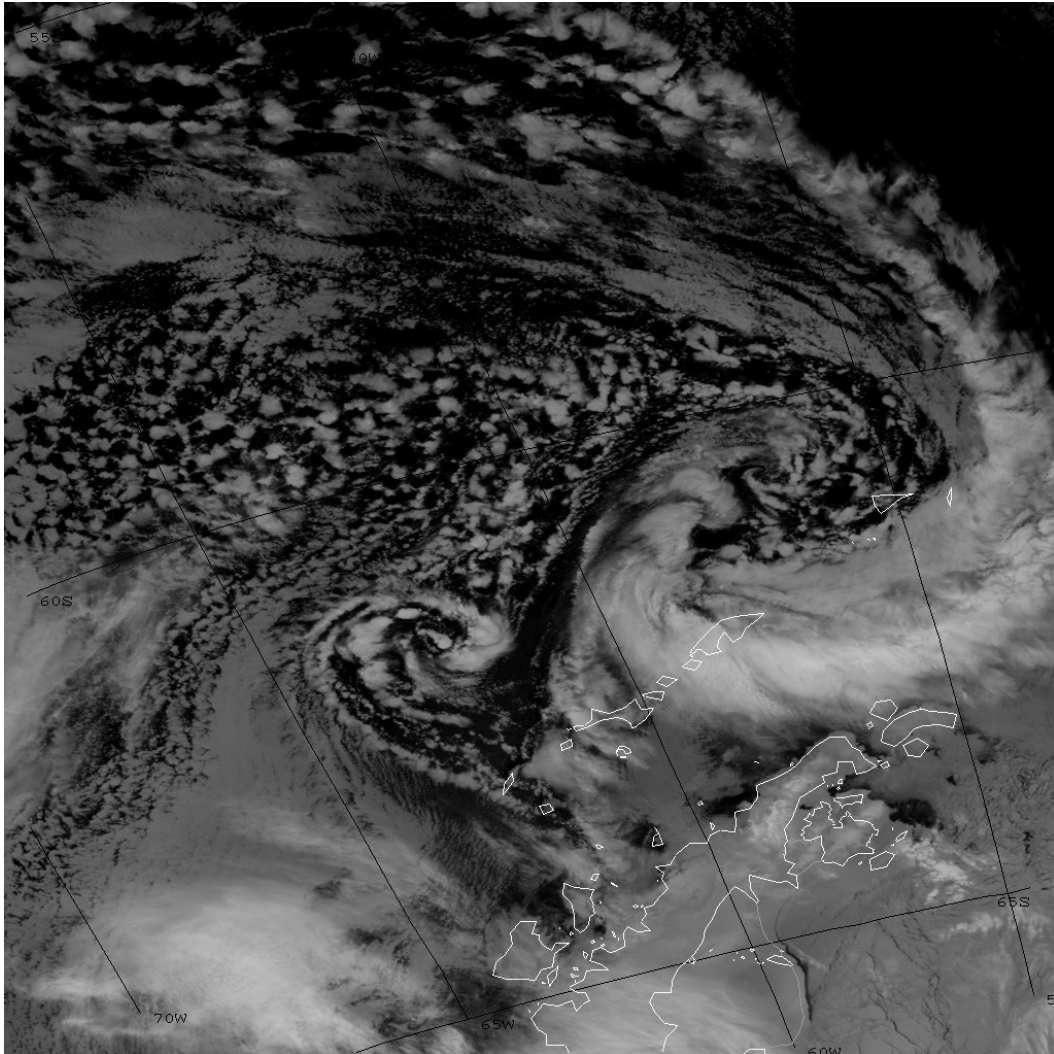
Figure 2.5.1.1   A typical example of a mesocyclone–synoptic scale low passing through the Drake Passage to the north of the Antarctic Peninsula.
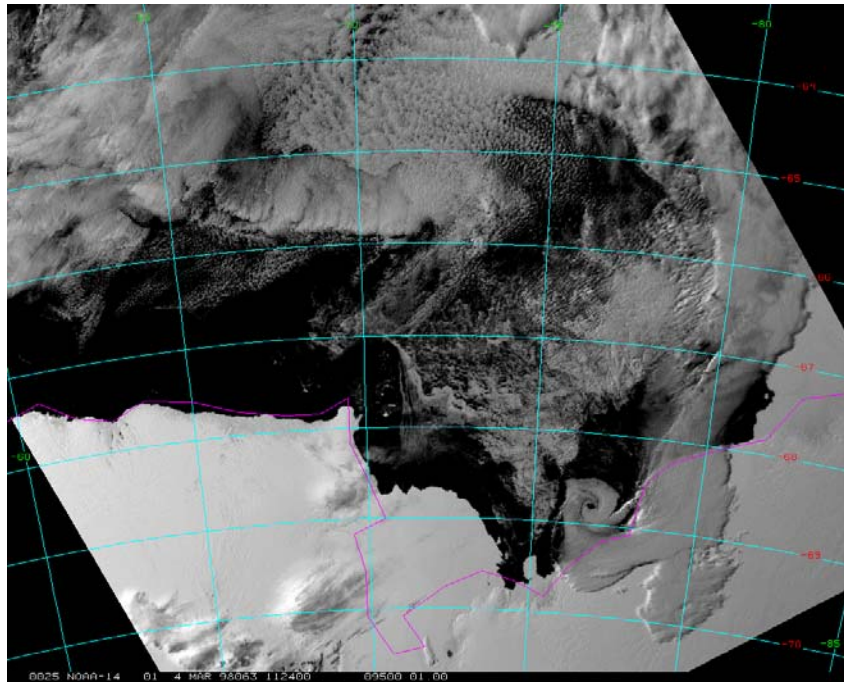
Figure 2.5.1.2 An example of a coastal mesoscale low formed as a result of shear in a continental outflow. (The image is from the US National Oceanographic and Aeronautical Administration (NOAA) 14 satellite at 1124 UTC 4 March 1998).
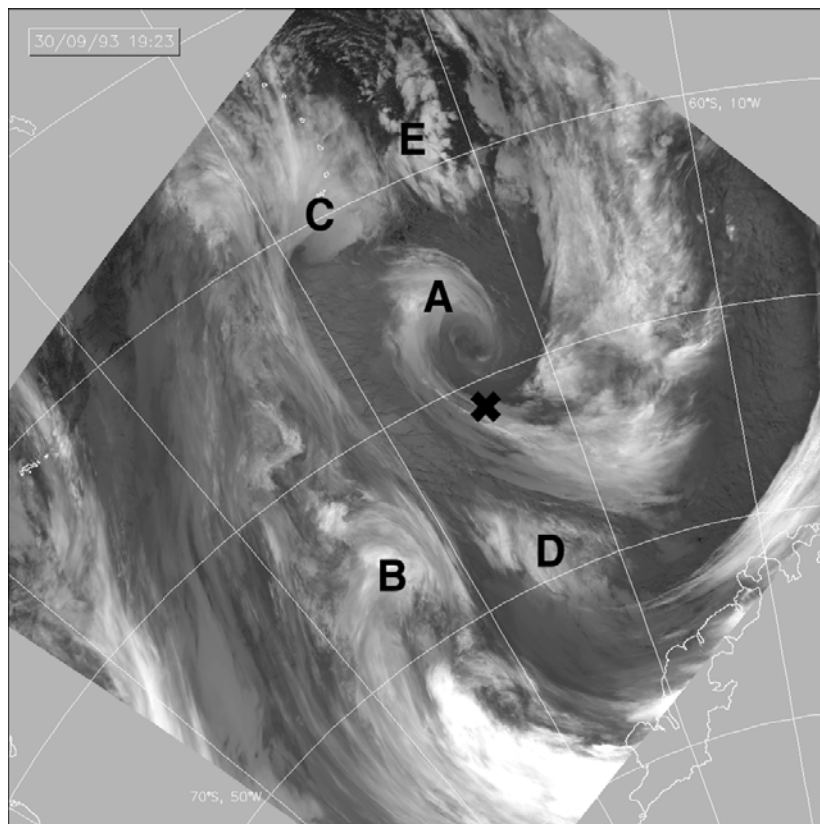
Figure 2.5.1.3 A 'merry–go–round' group of mesocyclones (indicated by the letters A to E) over the northern Weddell Sea that formed from a disintegrating synoptic–scale low.

- *Surface fluxes of heat and moisture*. The ocean currents around the Antarctic tend to be quite zonal and warm, mid–latitude water is rarely carried to high latitudes. The flux of heat into the atmosphere therefore tends to be quite small, although it is important for triggering low–level convection and large fields of convective cloud can be observed during cold air outbreaks over the ocean. Mesocyclones can be observed to form in some of these cumulus fields on occasions. In contrast to the Northern Hemisphere, the layer of instability thus generated is usually quite shallow, and so vigorous convection does not occur. This limits the vertical development of such systems and so the associated weather conditions are not generally severe. Although not severe, conditions may be hazardous, particularly to aviation operations, with winds up to 35 knots, sustained heavy snowfall and low cloud. Heavy icing may be encountered.
- *Low–level convergence*. Some parts of the Antarctic are prone to frequent convergence at low level, such as on the large Ronne and Ross Ice Shelves where flow down from the surrounding mountains takes place. This flow pattern can result in the spin–up of mesocyclones, especially during the winter when the katabatic flow is most pronounced.

Of course more than one of these factors can be responsible for the development of an individual mesocyclone. For example, over a coastal polynya there may be strong fluxes of heat and moisture into the lowest layers destabilising the atmosphere, with the arrival of an upper level trough triggering the spin–up of a mesocyclone.

2.5.2   Spatial distribution

Most mesocyclones are found over the ocean areas around the Antarctic and there are very few vortices over the high plateau areas of the continent. Since many mesocyclones develop in cold air outbreaks and there is an almost continuous band of frequent depression activity around the continent it is not surprising that mesocyclones are found in all sectors of the Southern Ocean. In some areas where depressions become slow–moving, such as the Bellingshausen Sea, mesocyclone developments are particularly common. Similarly, when there is frequent off–shore flow over open water caused by katabatic winds (for example near Terra Nova Bay) or the broad–scalecirculation (the eastern Weddell Sea) then mesocyclones are commonly found.

The low–lying ice shelves also have many mesocyclone developments because of the low–level convergence and supply of moist air from passing synoptic depressions. Studies on the Ross Ice Shelves based on AWS data have shown that vortices can occur that have no cloud present.

Although mesocyclones are rare on the plateau some systems do occur here and these lows can be a problem for fieldwork in the interior. Such lows move with the broad–scaleflow and can be quite long–lived because of the lack of synoptic activity to cause their dissipation. An example of this type of development is shown in Figure 2.5.2.1.
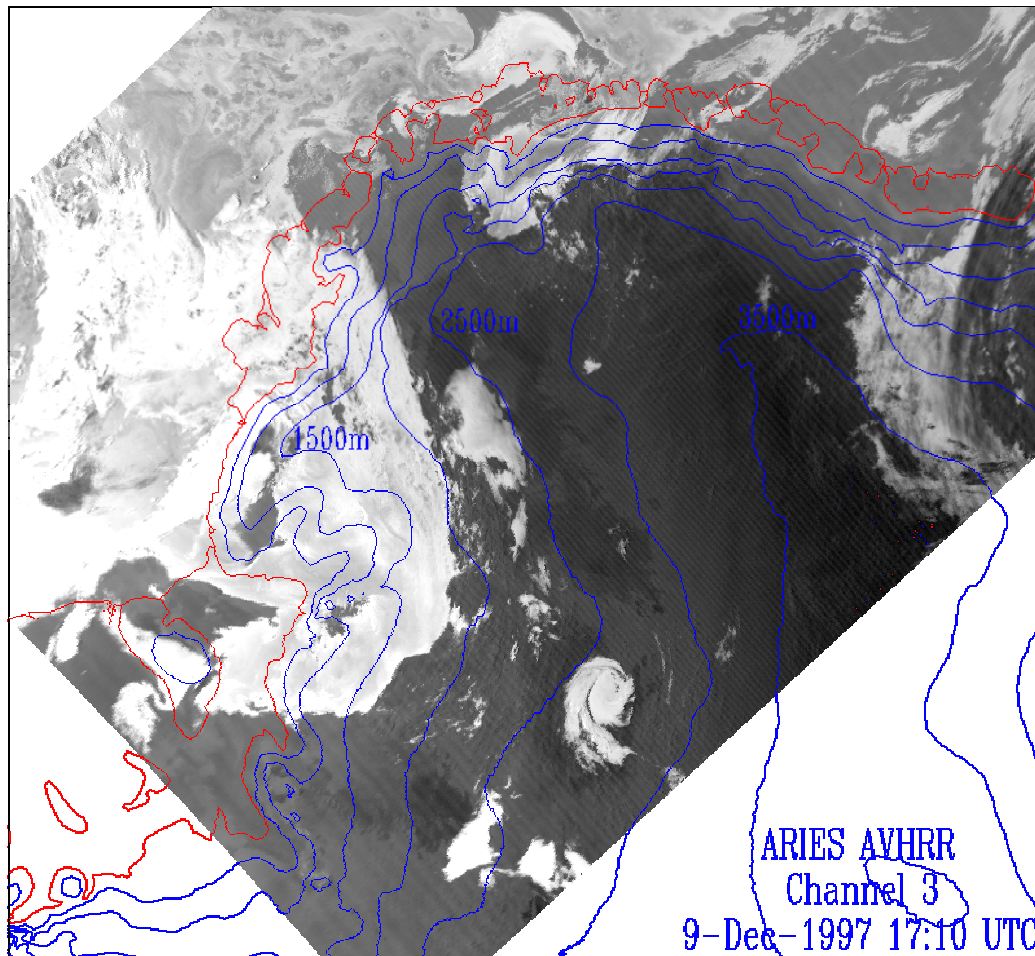
Figure 2.5.2.1   A mesocyclone over Dronning Maud land high on the Antarctic plateau as observed in AVHRR channel 3 imagery. The ice surface appears black and the cloud composed of supercooled water droplets white.

2.5.3   Temporal variability

Mesocyclones are a feature of all seasons but year–round investigations in the Antarctic Peninsula region (Turner *et al.,* 1996b) have shown a peak of activity during the summer months when more open water is present and there is a greater supply of moisture. However, many systems also occur in winter when the lows can be seen over the sea ice in the coastal zone. Since the development of mesocyclones is so closely associated with synoptic–scale activity we can expect a link with the semi–annual oscillation and longer period climatic cycles, although such considerations are not of importance in forecasting these lows.

2.6   Mean values of the main meteorological elements

2.6.1   Pressure at Mean Sea Level

The lack of observations over the Southern Ocean and across much of the interior of the Antarctic makes the production of accurate, mean climatological fields rather difficult and there are quite large differences between the data sets that have been produced over the last few decades. Nevertheless, the modern NWP systems are capable of assimilating the many forms of satellite and *in situ* data that are available and can be regarded as producing reasonable analyses. However, there is still a problem with the derivation of MSLP fields under the high orography of the continent, which is over 4 km in height in places and where the surface pressure is less than 600 hPa. Therefore, although MSLP is plotted across the whole of the Antarctic on many meteorological charts, it should not be regarded as meaningful where the orography is higher than about 1 km.

Figure 2.6.1.1 shows the mean fields of MSLP (1969–98) for the four seasons as produced from the US NCEP re–analysis project (see, for example, Kalnay, 1996). Key features apparent on these charts are:

- The circumpolar trough that rings the Antarctic between the latitudes of 60–70° S. This feature is present because of the large number of depressions in this zone that have either developed at these latitudes or moved south from the extra–polar regions.
- Within the circumpolar trough there are three climatological low–pressure centres throughout the year located close to 30° E, 90° E and 150° E.
- Generally high pressure over the continent, although as noted above, because of the reduction of pressures to sea level, the fields over the interior should be regarded as no more than a qualitative indicator of conditions.

The circumpolar trough exhibits a semi–annual oscillation in both its position and strength (Simmonds and Jones, 1998), a signal that can be observed in the observations from the coastal stations. As can be seen in Figure 2.6.1.1 the trough is deepest and at its most southerly position in the spring and autumn and further to the north and weaker in the summer and winter. To the north of the circumpolar trough, in the mid–latitude regions the phase of the semi–annual oscillation is reversed, with pressure maxima in the spring and autumn.

2.6.2   The upper–air height field

Mean fields of geopotential height (1969–98) at the 500–hPa and 300–hPa levels for the four seasons as produced from the US NCEP re–analysis project are shown in Figures 2.6.2.1 and 2.6.2.2 respectively. The 500–hPa surface is everywhere above the orography of the Antarctic and is therefore useful for forecasting for sites on the high plateau. At this level the mean flow (Figure 2.6.2.1) consists of a weak cyclonic vortex centred over the Ross Ice Shelf/South Pole region. The flow over the Southern Ocean is generally zonal, but with a weak wave number three pattern with troughs close to 20° E, 90° E and 90° W. At the 300–hPa level (Figure

2.6.2.2) the vortex is stronger and centred closer to the pole and there is a weak trough/ridge structure that varies throughout the year. Of course on a day–to–day basis the height fields at both these levels show a marked trough/ridge structure and the zonal symmetry only becomes apparent when mean fields are produced.
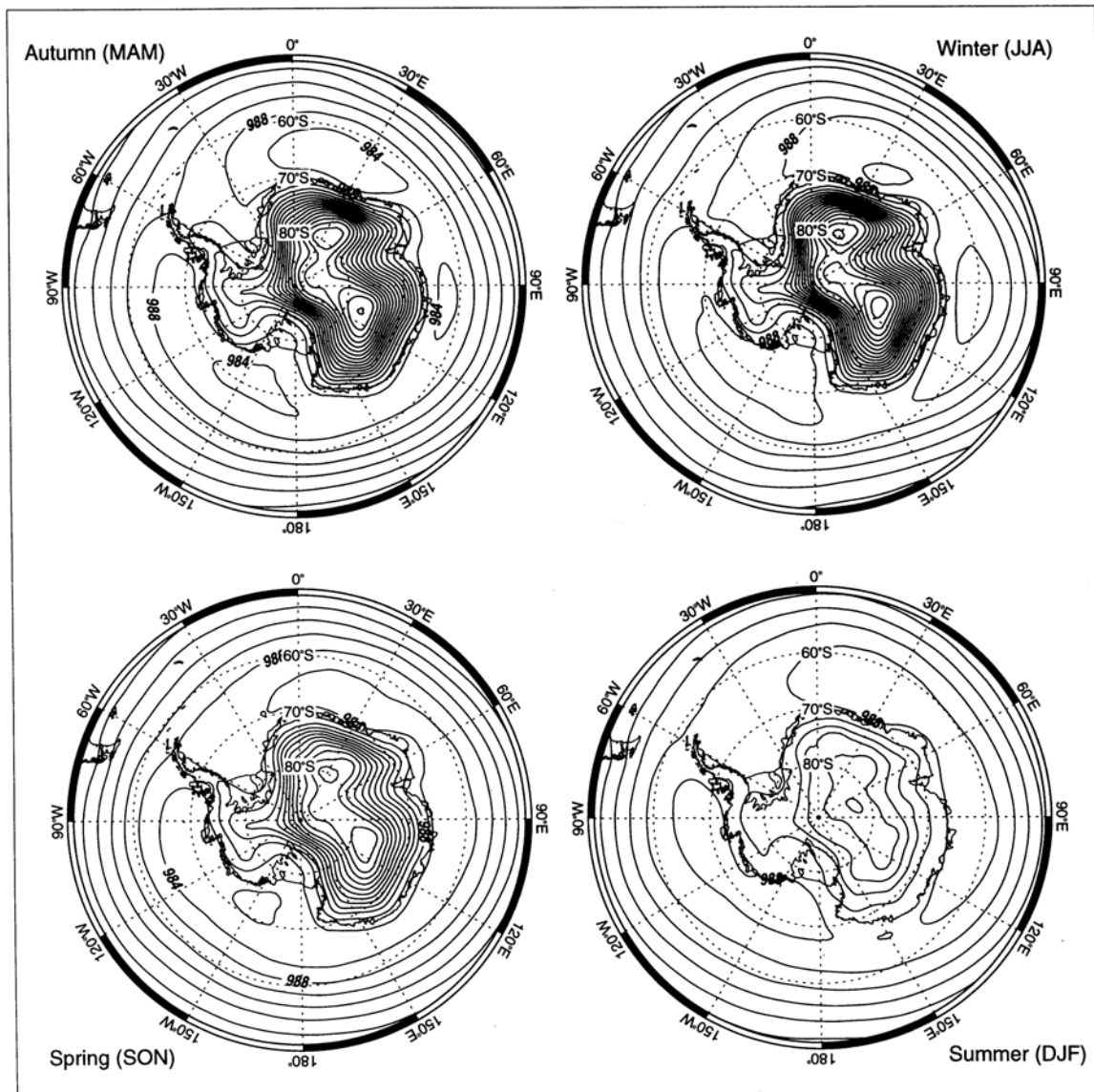
Figure 2.6.1.1   Mean (1969–98) fields of MSL air pressure (hPa) for the four seasons as produced from the US NCEP re–analysis project.

For an appreciation of the mean vertical temperature structure and wind flow the reader is referred to Appendix 3 below in which mean January and July vertical temperature profiles and wind rose data are presented.
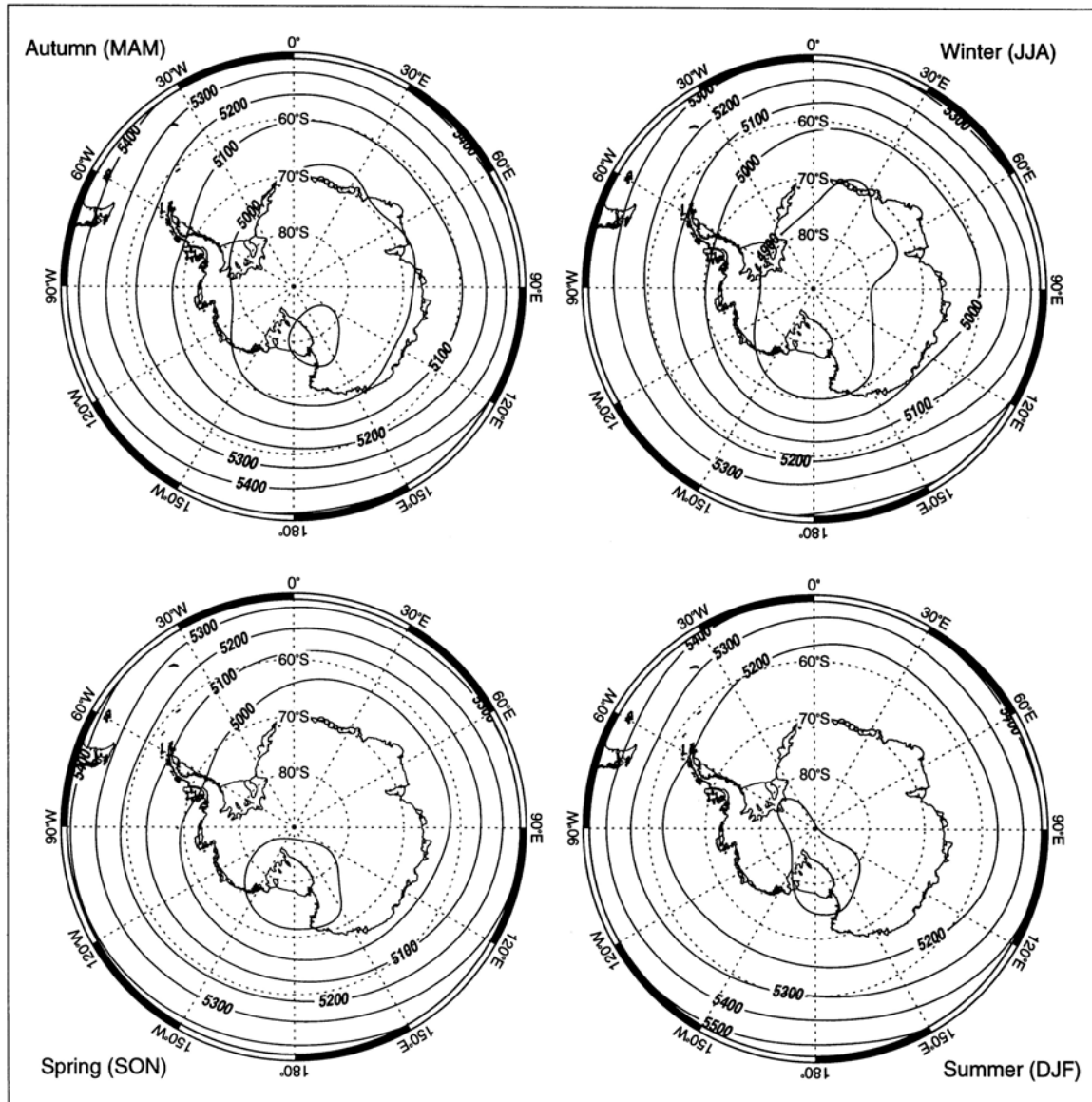
Figure 2.6.2.1 Mean (1969–98) fields of geopotential height (m) at the 500–hPa level for the four seasons as produced from the US NCEP re–analysis.
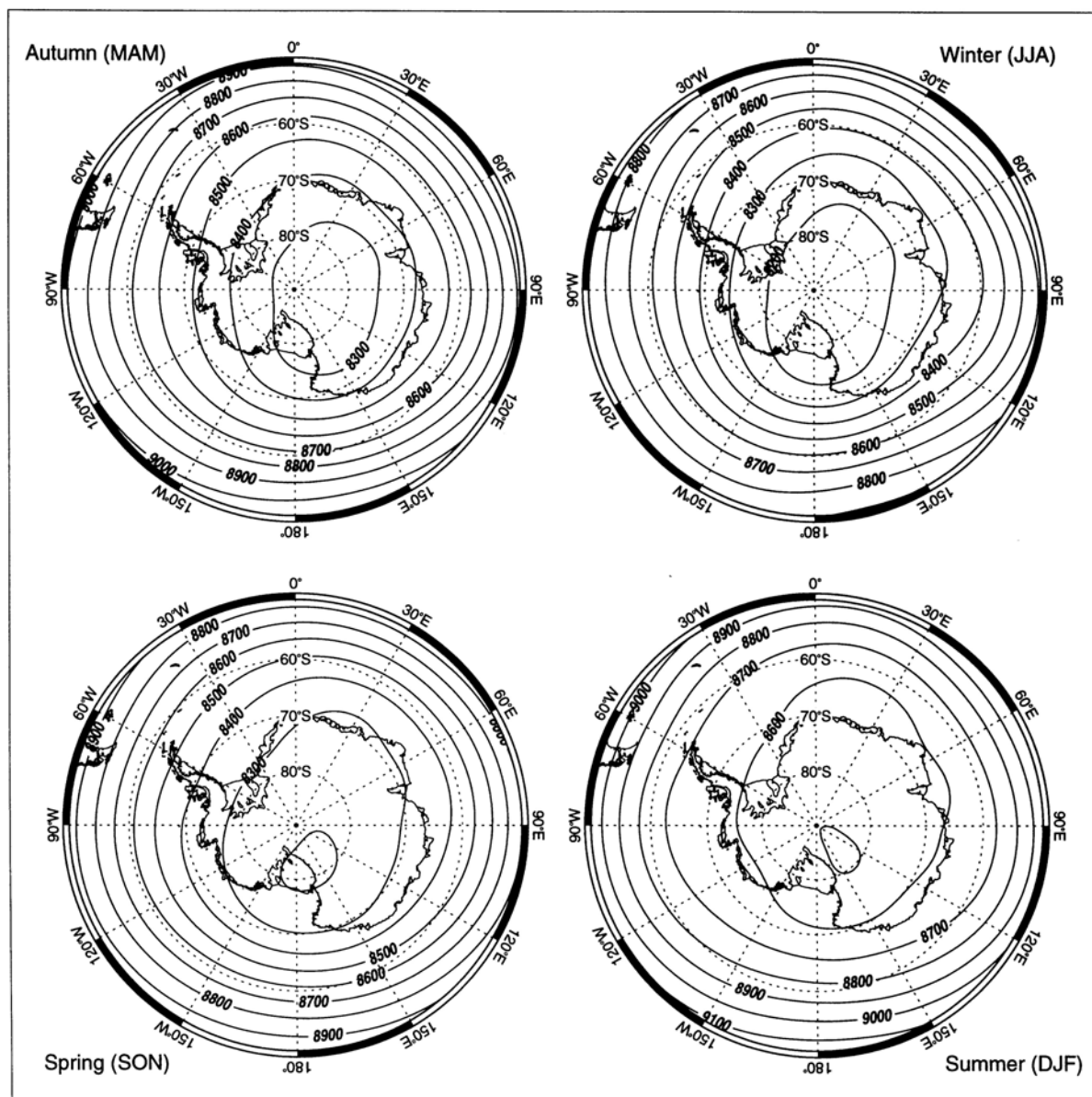
Figure 2.6.2.2 Mean (1969–98) fields of geopotential height (m) at the 300–hPa level for the four seasons as produced from the US NCEP re–analysis

2.6.3 Surface air temperature

The air near the surface over continental Antarctica is intensely chilled as heat is lost to the ice surface by conduction, then, in turn, through long wave radiation from the ice surface to space. This chilling of the surface air flow continues as it drains towards the coast.

On the dome–shaped ice cap of Antarctica, temperatures drop steadily away from the coast. This is due in large part to the higher elevation, but also to the higher latitude and hence less intense insolation of the continental interior. In most coastal regions the mean annual temperature is around –10 to –15ºC, at 1,000 m –20ºC, and in the highest parts near 4,000 m it falls to near –60ºC. Figure 2.6.3.1 shows estimated surface (10 m) air temperature across the

Antarctic: these have been computed from the 10 m mean temperatures in ice cores, which approximates to the annual surface air temperature.
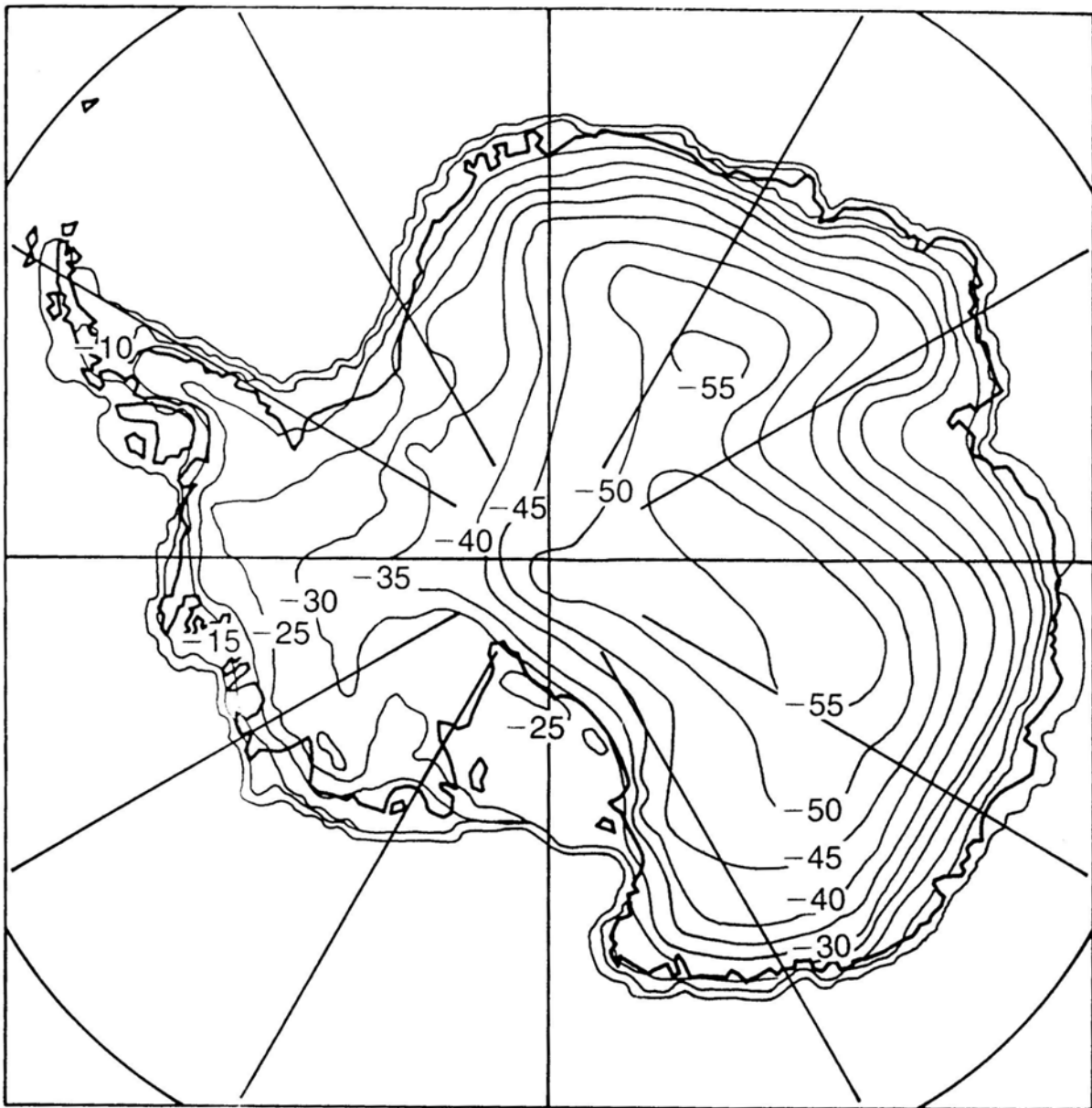
Figure 2.6.3.1   Annual mean surface temperatures over Antarctica, deduced from 10 m snow temperature measurements. (After King and Turner, 1997, p. 82).

On top of this general pattern there are many variations. In some coastal regions, especially the Antarctic Peninsula during mid–summer, temperatures occasionally rise to around +10ºC, while in winter they fall into the minus forties and fifties, depending on latitude. High on the polar plateau of East Antarctica, the temperature in summer rises to around –30ºC before the cold of winter returns with extremes in the minus eighties. Unlike annual surface air temperature estimates, seasonal equivalents are not as readily estimated. At present the only reasonably accurate (to within about 5ºC) way of obtaining such estimates is through a numerical model. Figure 2.6.3.2 shows the European Centre for Medium–range Weather Forecasts (ECMWF) seasonal temperatures from the ECMWF 15–year re–analysis (Gibson *et al.*,1996).
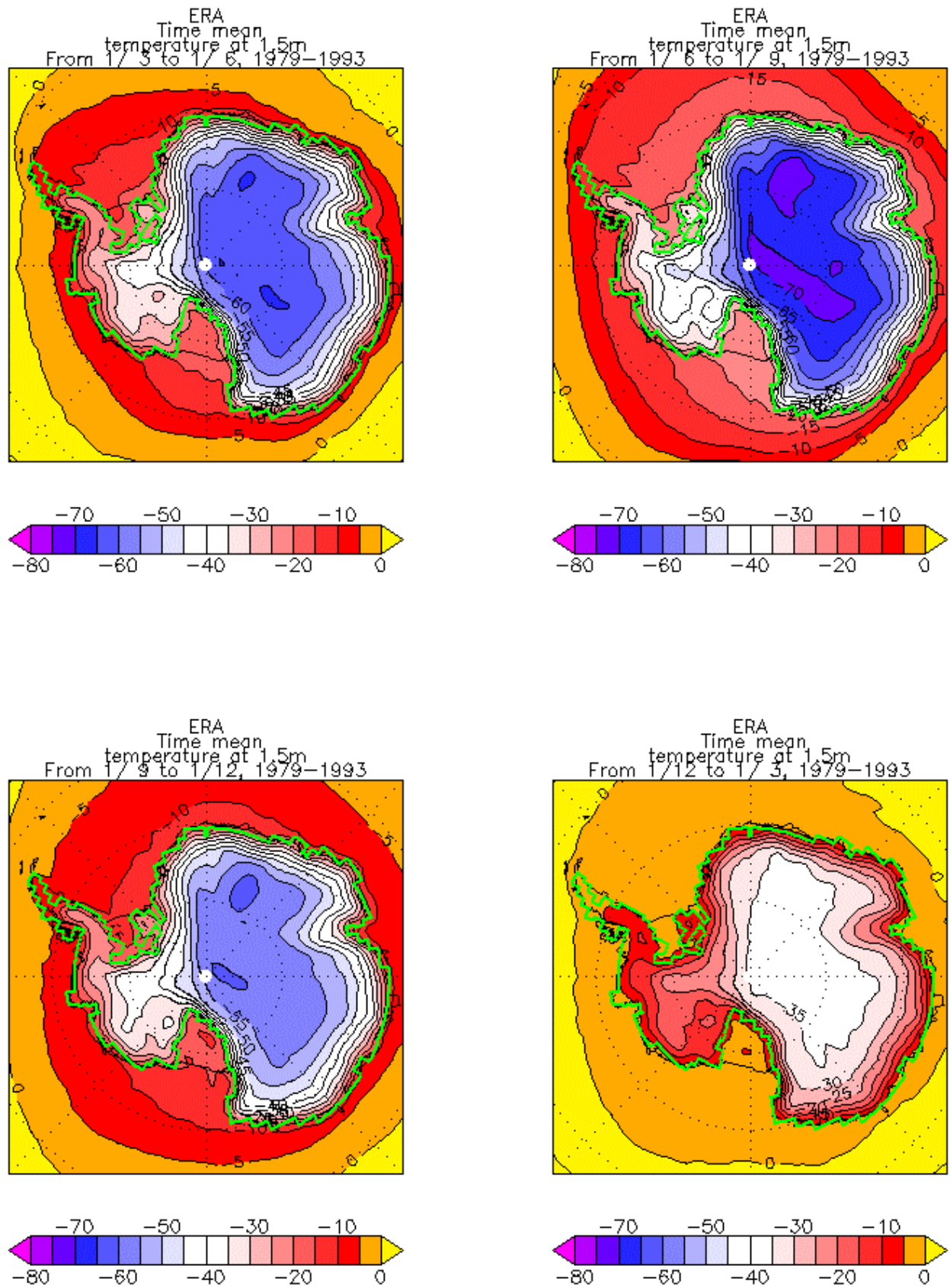
Figure 2.6.3.2   Estimates of seasonal surface air temperature over the Antarctic: top left –
"autumn"; top right – "winter"; bottom left "spring"; bottom right – "summer" (from the
ECMWF 15–year re–analysis programme)

On average, many Antarctic stations, in particular those on the continent, experience little variation in temperature during the winter months which has lead to the notation that the Antarctic has a "coreless" winter. Figure 2.6.3.3, for example, shows the annual temperature variation at four stations located in the Antarctic interior. The shape of each graph shows a well defined temperature peak in the summer but a relatively flat section for the winter ("coreless winter"). (See also Figure 7.12.2.4.1 in Appendix 2 below as an example for a more coastal station, Terra Nova Bay in this case). Part of the reason for the rapid summer temperature rise is the increase in solar radiation, but also the surface of the ice is a little less reflective after the winter. The winter onset is rapid; a small accumulation of fresh snow restores the surface albedo. The "coreless" nature of the winter is due to an approximate equilibrium state being reached in the near surface heat budget after an initial rapid loss of heat through radiation induced losses from the near surface at the onset of darkness (Schwerdtfeger, 1970, p. 276–277).
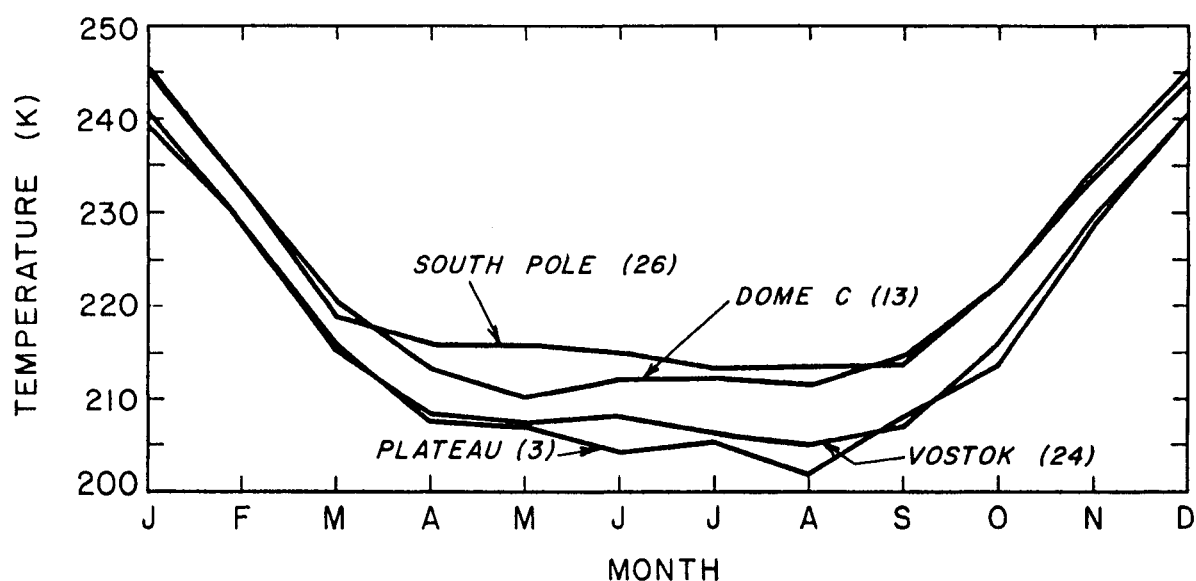
Figure 2.6.3.3   Mean monthly temperatures at interior stations South Pole (Amundsen–Scott), Dome C, Vostok and Plateau. The numbers in parentheses indicate the number of years in each record. (From Bromwich and Parish (1998, p. 177)).

The world's lowest surface temperature yet recorded was –89.2°C at Vostok Station (on 21 July 1983), 1,300 km from the coast at an elevation of 3,488 m, in East Antarctica. The South Pole area is generally much colder than its northern counterpart primarily because of its elevation (2,800 m above sea level) but also because the continental ice cap reflects 80 to 90% of incoming solar radiation back to space. Moreover, relatively few maritime air masses reach this location. There is a marked surface temperature inversion of up to 40°C in the lowest 600 m of the atmosphere over the continental interior in mid–winter, that is the temperature above this atmospheric boundary layer is much warmer than at the ice surface.

2.6.4   The continental surface temperature inversion

Temperatures vary markedly in the lowest few hundred metres of the atmosphere over the continent. There is a close correspondence between surface temperature and inversion strength, both for individual stations on a day–to–day or month–to–month basis; and for all stations for the winter season.

The surface temperature inversion over the Antarctic continent results from the radiative heat loss from the ice surface, particularly during the polar night of winter. Phillpot and Zillman (1970) found (see Fig 2.6.4.1) that the average strength of the surface temperature inversion over the Antarctic continent in winter was about 25°C on the high plateau area of East Antarctica decreasing to about 5°C near the coast. Winter mean inversion depths of 500–700 m are found at high plateau stations while the depth at McMurdo it is in the range 400–500 m. At coastal stations that are not on ice shelves, such as Mawson and Davis, have a depth of 300–400 m in winter. There is also a definite seasonal variation of inversion strength and depth. In some cases the surface temperature occasionally falls to near –80°C at Vostok in winter and the strength of the surface temperature inversion exceeds 30°C. Then the depth of the boundary layer (as defined by the height above the ice surface of the highest temperature in the troposphere) may be 1.5 km.

Schwerdtfeger (1984) noted that acoustic soundings at Amundsen–Scott indicated a well–defined ground–based shear zone of some 40–300 m deep, well below the height of the highest tropospheric temperature. Radiosonde measurements leave no doubt that above this pronounced surface inversion layer in the interior, normally there is a rather thick layer between say 500 and 1500 m above the ice surface in which the temperature changes little with height.
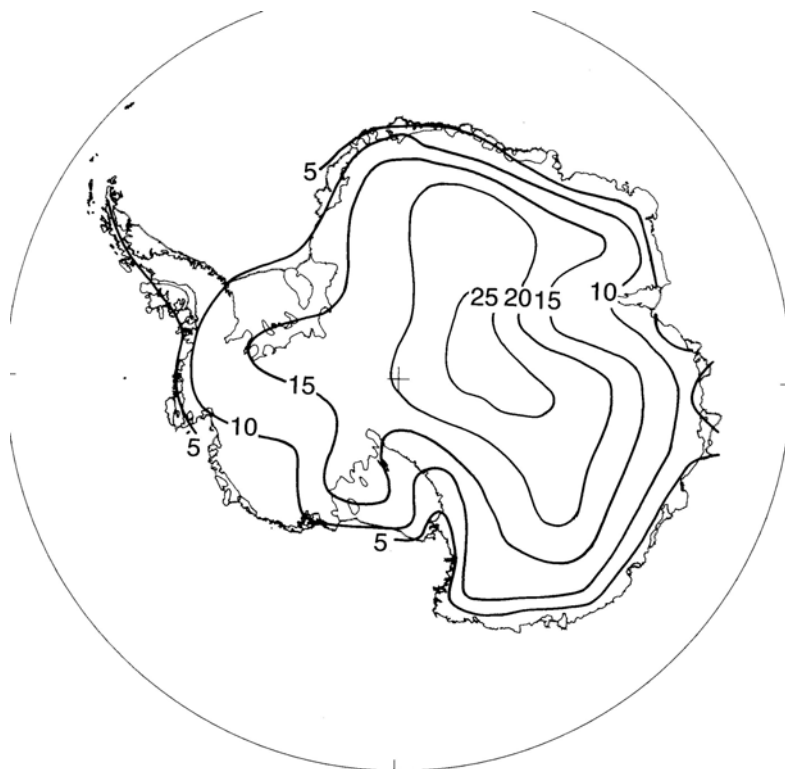
Figure 2.6.4.1   Isopleths of the average strength (ºC) of the surface inversion in winter (June–August). After Schwerdtfeger (1970, p. 275).

2.6.5   Cloud, white–out and surface and horizon definition

2.6.5.1   Distribution of cloud amount

Schwerdtfeger (1970, p. 298) outlines some of the difficulties with surface cloud observations in the Antarctic; for example: blowing snow and a lack of light during winter. More recently the role of satellites has contributed significantly to the monitoring of, among other parameters, cloud characteristics. In 1982 the International Satellite Cloud Climatology Project (ISCCP) was established as part of the World Climate Research Programme (WCRP) to collect and analyze satellite radiance measurements (collected from the suite of weather satellites operated by several nations) to infer the global distribution of clouds, their properties, their diurnal, seasonal, and inter–annual variations. However, satellite observations also have limitations: for example, King and Turner (1997, p. 104) note that the ISCCP data underestimate the cloudiness at the South Pole when compared to conventional surface observations taken at the South Pole Station and attribute the discrepancy to poor cloud detection algorithms particularly for thin ice clouds at high southern latitudes.

Referring to Figures 2.6.5.1.1 and 2.6.5.1.2, which show mean summer and winter cloud cover isopleths from ISCCP data for the area south of about 50º S, one might infer that there is less cloud over the Antarctic continent in summer than in winter. This seems at odds with the observational/climatological study of Warren *et al.*(1986) which indicated increased cloudiness over the continent in summer when compared to winter and yet the ISCCP data for winter agree very well with the Warren data for winter. (See for example, King and Turner (1997, p. 102–104, their Figures 3.25 and 3.26). Perhaps the area of doubt lies with the ISCCP summer data. Intuitively one would expect increased cloudiness in summer/autumn, at least over the Antarctic coast and near inland, due to the greater availability of moisture from open sea water after the sea ice has reached a minimum due to melt.

This certainly seems to be the case for stations in East Antarctica. Figure 2.6.5.1.3 shows mean total cloudiness for the sub–Antarctic Macquarie Island and for the East Antarctic coastal stations of Casey, Davis, and Mawson (I. Barnes–Keoghan and D. Shepherd, personal communication). It may be seen that while there is little variation in cloud amount in the marine environment of Macquarie Island there are clear summer/early autumn maxima in cloud amounts at Casey, Davis and Mawson which correspond with minimum sea ice coverage in the neighbouring seas. However, even with these three stations the maximum in cloudiness appears to occur early to mid summer at Mawson and late summer to early autumn at Casey and Davis. In other words, as with most other parameters, it is important to obtain data specific to a site or area when trying to specify mean cloud amounts.

2.6.5.2   Distribution of cloud type

King and Turner (1997, p. 105) report on the work of Warren *et al.* (1986) in summarising the zonal distribution of cloud types. As noted by these workers stratiform cloud (stratus/nimbostratus/altostratus/cirrus) is the most common cloud type although cumuliform clouds do occur as reported, for example, by Schwerdtfeger (1970, p 299). Moreover, in some cases localised instability can be quite severe and lead to mammatus and small cumulonimbus development (see, for example, the comments on cloud near Davis Station in Section 7.8.4.4 below) particularly where local convergence occurs in coastal environments or where cold air flows over relatively warm water or rock.

2.6.5.3   White–out and surface and horizon definition

In the context of practical weather forecasting for the Antarctic, cloud amount is arguably more important than cloud type because one particularly insidious Antarctic hazard that deserves special comment is white–out. This is an optical phenomenon that occurs in uniformly overcast conditions over a snow–covered surface. It is associated with diffuse (uniform), shadowless illumination which causes a lack of surface definition/contrast (the ease with which features on a snow surface can be) and reduced horizon definition (the ease with which the horizon can be defined) (defined: see Table 2.6.5.3.1). A person's ability to perceive snow–covered orographic features depends on the shadows that they cast, such forms become indistinguishable under white–out conditions. Without any visual stimulation it is common to incorrectly evaluate an incline: one may walk up and down hills without realising it. Furthermore, it is known that an individual attempting to follow a straight path unaided will veer. Judgments of the distance and orientation of objects in the field of view is severely handicapped. Such spatial disorientation is enhanced inside a moving vehicle. White–out conditions can occur while visibility (i.e. transparency of the air) remains good.

　　　While total white–out results from nil surface and horizon definition there are degrees of this effect, for example, partially reduced horizon and surface definition can occur under a broken cloud layer. Thus figures such as Figures 2.6.5.1.1 and 2.6.5.1.2 (summer and winter mean cloud amounts) are a defacto measure of the occurrence of white–out.
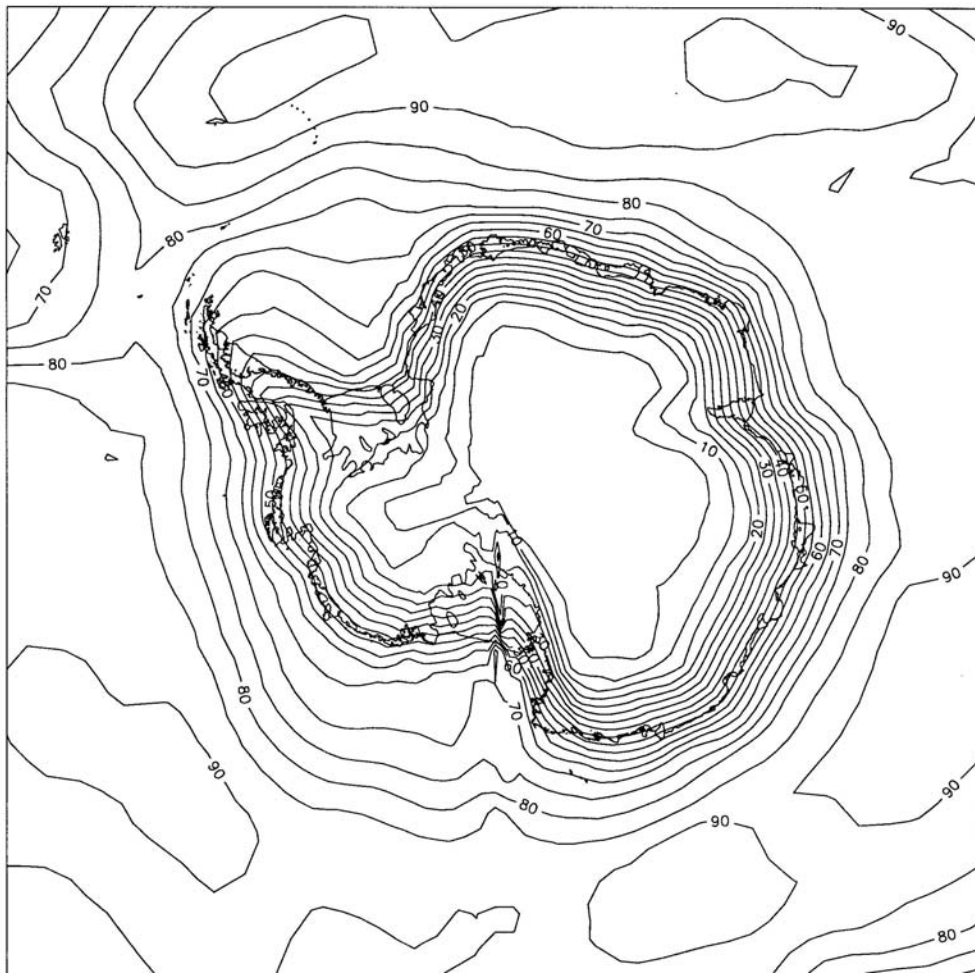
Figure 2.6.5.1.1 Mean summer cloud amount (%) from ISCCP data.
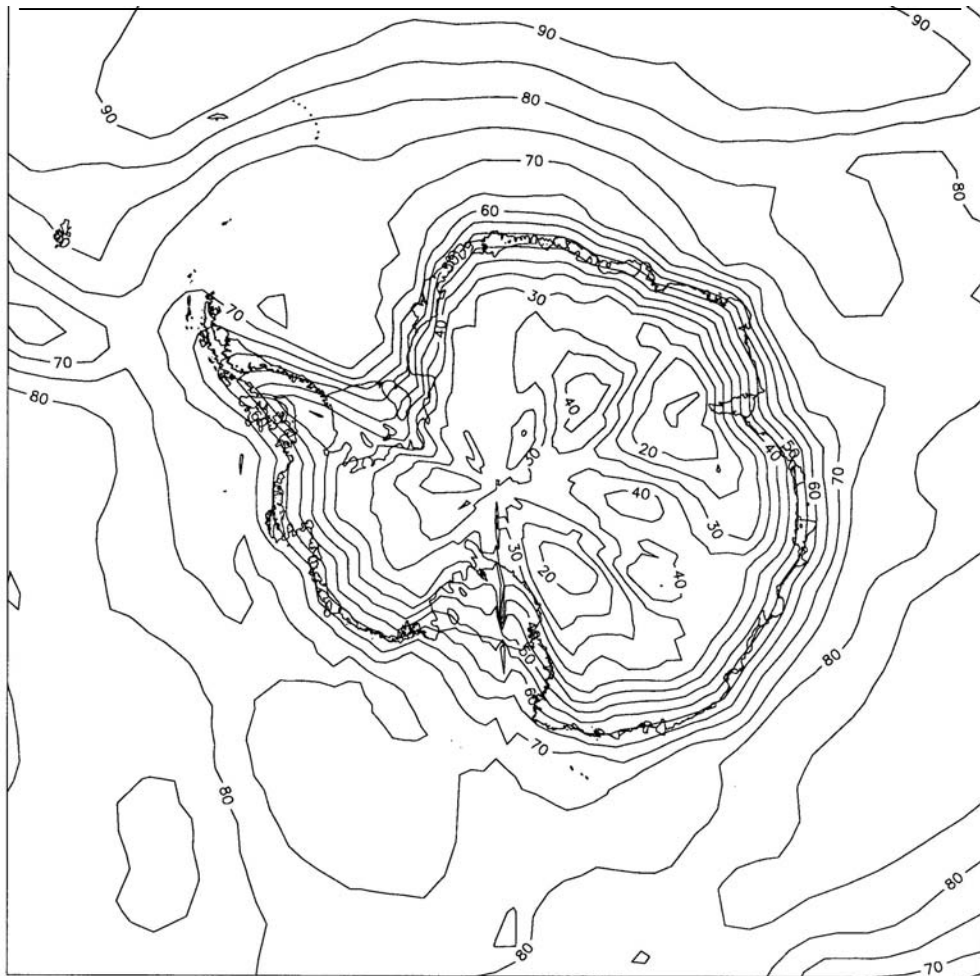
Figure 2.6.5.1.2 Mean winter cloud amount (%) from ISCCP data
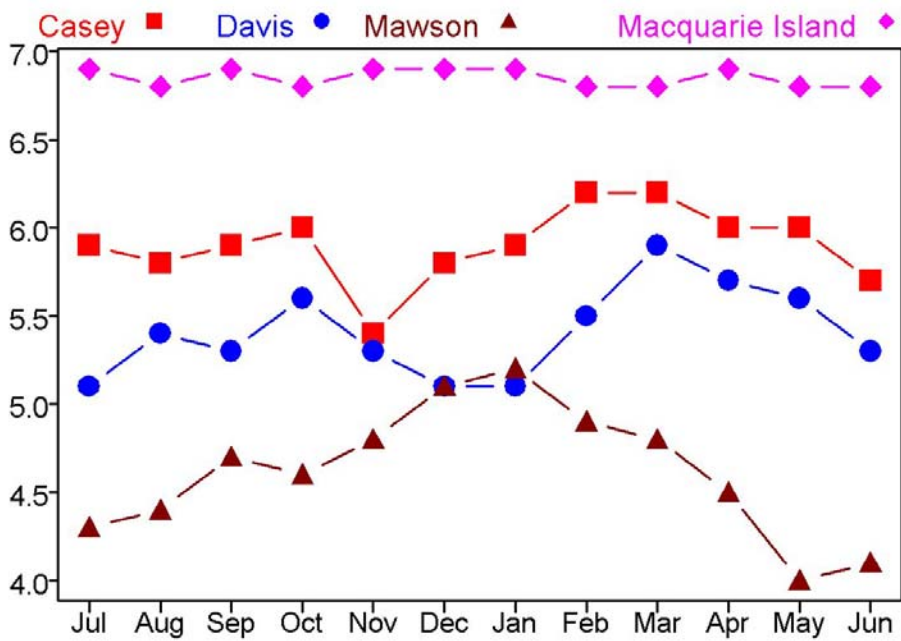
Figure 2.6.5.1.3 Mean cloud amounts (oktas) for Casey, Davis, Mawson, and Macquarie Island. (Data from 1969–97 synoptic observations).

2.6.6   Precipitation/Accumulation

Schwerdtfeger (1970, p. 294) notes "With reference to Antarctica, the term "cryometeors" might be more appropriate than "hydrometeors, but it is not used".

Over the continent of the Antarctic air is extremely dry, (although more moist over the marginal sea ice zone and further north). Air in the upper levels of the atmosphere circulates towards Antarctica from more northern latitudes. By the time the air descends over the polar central plateau to reach the boundary layer of the atmosphere, which is immediately above the dome shaped ice cap, most of the moisture has been removed.

Although precipitation falls mainly as snow, some coastal areas, especially the Antarctic Peninsula can receive rain at any time of the year. Synoptic scale lows, mesoscale lows, and their associated frontal systems are responsible for much of the near coastal precipitation. The high plateau of Antarctica receives little precipitation and is the world's largest and driest desert: much of the precipitation which does occur results from clear sky deposition of ice crystals.

The measurement of precipitation over the Antarctic is, however, an issue in itself: how can falling snow be separated from that snow which has already been precipitated and is being blown along by the wind? Scientists currently prefer to report snow accumulation, that is the snow cover which results from the balance of precipitation and "evaporation", where "evaporation" includes the removal of snow by the wind (ablation).

For the continent as a whole, annual snow accumulation is equivalent to about 150 mm of water. Figure 2.6.6.1 shows estimates of the mean annual accumulation of snow and it may be seen that the 50 mm water equivalent isopleth over central Antarctica accords well with the estimate of mean annual precipitation there of around 50 mm of water equivalent, given that wind speeds, and thus ablation, are relatively low over central Antarctica. On the other hand the accumulation rate on the eastern slopes of Law Dome (120 km from Casey), for example, is in excess of 700 mm water equivalent per year; making it second only to the northwest Antarctic Peninsula in accumulation rates measured at specific sites. In general there is a rapid drop in accumulation away from the coast.
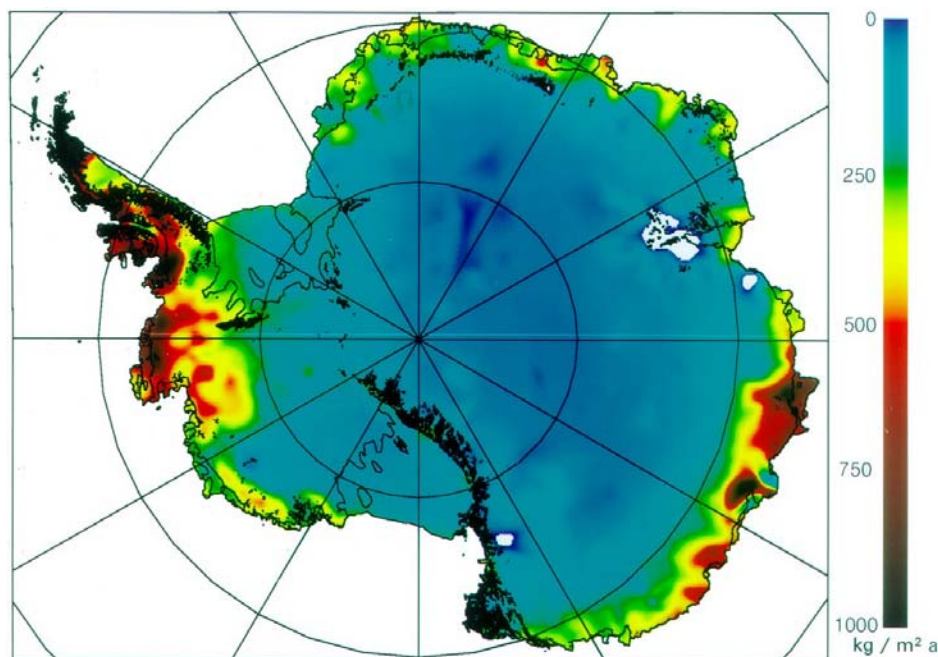
Figure 2.6.6.1   Annual net accumulation (P–E) (in kg m^{-2} a^{-1} (mm water equivalent)) over the Antarctic continent. After Vaughan *et al.* (1999).

Qualitative term	Surface definition or contrast	Horizon definition	White–out
Good	Snow surface features such as sastrugi, drifts and gullies are easily identified by shadow. The sun is usually un–obscured. Surface features are clearly defined for as far as the eye can see.	The horizon is sharply defined by shadow or contrast. The horizon is distinct with an obvious difference between land (snow) and sky.	Nil
Fair or moderate	Snow features can be identified by contrast. No definite shadows exist. The sun is usually totally obscured. Surface features become indistinct at distances of more than a few kilometres.	The horizon may be identified, although the contrast between sky and snow is not sharply defined.	Perhaps slight effect.
Poor	Snow surface features (e.g. skidoo tracks) cannot readily be identified except from close up (within 50 metres). The sun is usually totally obscured.	The horizon is barely discernable: in other words, the sky can be discriminated from land but no distinct horizon is visible.	Partial – may be more noticeable in some directions, or at a distance.
Nil	Snow surfaces cannot be identified. No shadows or contrast exist. Dark coloured objects appear to float in the air. The sun is totally obscured, although the overcast sky may exhibit considerable glare. The glare appears to be equally bright from surface reflection and from all directions.	Total loss of horizon: the snow surface merges with the whiteness of the sky.	100%

Table 2.6.5.3.1 White–out (and surface and horizon definition) defined in terms of the obscurity of the sun.

2.6.7   The wind field

The surface wind regime is one of the most characteristic features of Antarctic climatology. Nowhere on any other continent has one single element such an overwhelming influence on the climate of the continent as a whole. The model of the Antarctic wind regime described below requires validation, and certainly the relevance of this scale of motion to the general circulation of the atmosphere is still open to debate. For example, researchers are trying to

determine the interrelationship, if any, between the katabatic flow and the circumpolar vortex found during winter and spring in the upper levels of the troposphere and in the lower stratosphere. More information on the nature of surface winds in the Antarctic is given in Section 6.6.1 below.

2.6.7.1   Katabatic winds

The Antarctic surface winds are significantly influenced by the strong radiative cooling of the ice sheet; the very cold (dense), high velocity airflow is confined to a layer about 600 m thick, with the highest speed winds at a height of about 200 m above the ice surface. The gravity driven flow moves very slowly at first away from high elevation areas of the ice cap, accelerating as it moves towards the coast. The configuration of the ice orography provides an extensive elevated cold air source and lower lying glacial basins which cause strong confluence of airflows. (See Figure 2.6.7.1.1).

   These katabatic winds blow with remarkable constancy in direction, forced to the left of the line of maximum ice slope as a result of the Earth's rotation (the Coriolis force). The wind slowly accelerates over more than a thousand kilometres in some areas, reaching a mean speed of about 11 m s^{-1} (22 kt) perhaps 200 km from the coast. In some glacial valleys where confluence is particularly strong, katabatic winds can reach around 40 m s^{-1} (~75 kt) for hundreds of kilometres as the airflow makes its way towards the coast. There is often, however, a slight decrease in speed, due to ice surface roughness, within 100 km of the coastal escarpment. The flow of air down the ice slopes brings about a compensatory downward movement of dry air from the atmosphere above the katabatic wind level.

   Once katabatic winds reach the Antarctic coast their downslope driving force has been lost. Rapid deceleration and dissipation occurs within a short distance offshore because glacial valley convergence in the airflow is replaced by divergence of the shallow air–stream which was once katabatic. However, it should be noted that katabatic flow has been measured at some offshore islands. Figure 2.6.7.1.2 is a schematic of the variation of wind speed radially northwards from the continental interior.

2.6.7.2   Pressure gradient winds

The simple conceptual model of katabatic winds given above is, in reality, complicated by the existence of migratory low–pressuresystems over the seasonal sea ice zone. Low–pressuresystems, which bring bad weather to the coastal regions of Antarctica, are generally born over the Southern Ocean and move on a south–eastward course toward the Antarctic low–pressuretrough, which is located off the Antarctic coast. On the other hand, there are numerous instances of cyclogenesis over the seasonal sea ice zone, the smaller scale cases being described as "polar lows", often with life times of less than 24 h. Whatever their origin, low–pressure systems can add considerable influence to the coastal katabatic winds, producing some of the strongest winds on the face of the earth. Wind speeds often exceed hurricane force (33 m s^{-1} (~64 kt)) for several days at a time, with maximum gusts of more than 70 m s^{-1} (~140 kt). This is equivalent in force to Tropical Cyclone Tracy which destroyed Darwin, Australia, in 1975. The winds from that storm, however, affected Darwin for only a few hours. Over most of the interior of the Antarctic continent, where the slope is slight and low–pressure systems normally are less frequent and less intense, the wind speed is often less than 4 m s^{-1} (~8 kt).
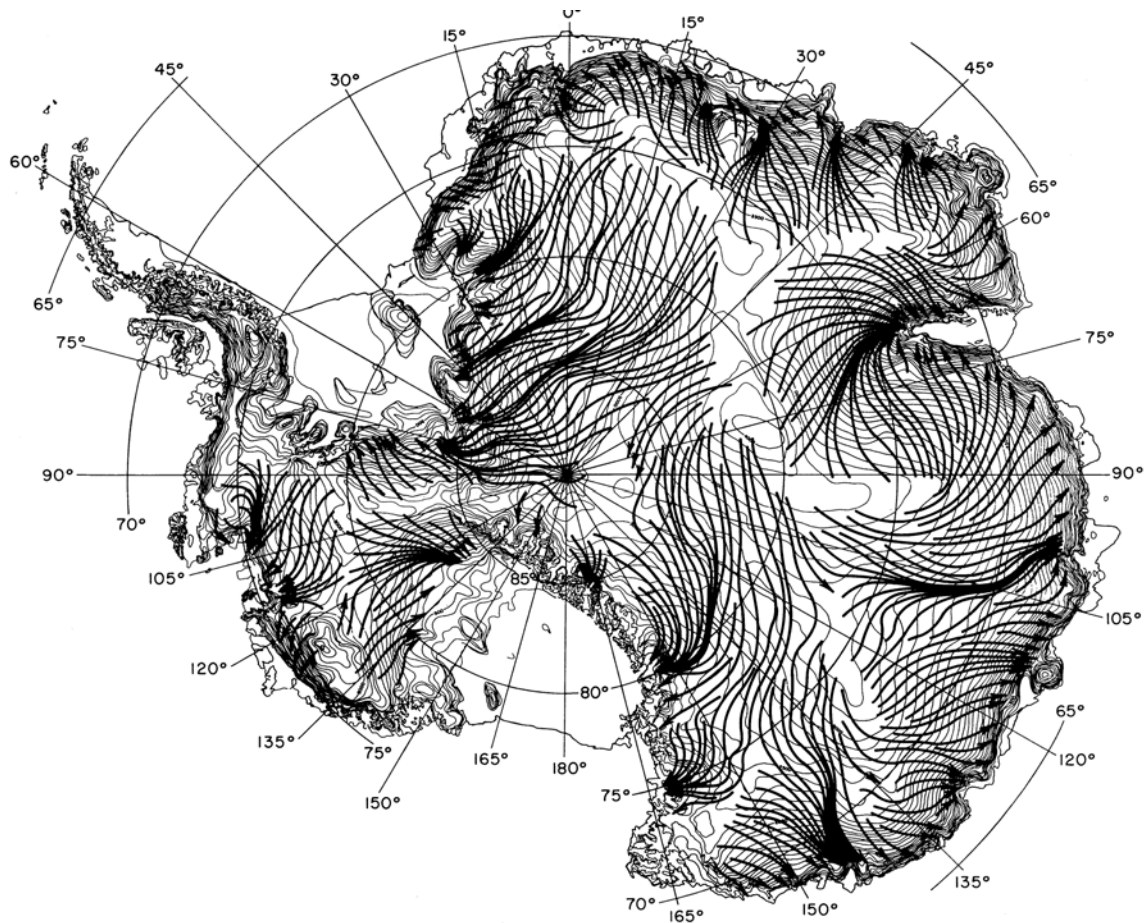
Figure 2.6.7.1.1 Idealised katabatic streamlines for average winter conditions. From Parish and Bromwich (1987).
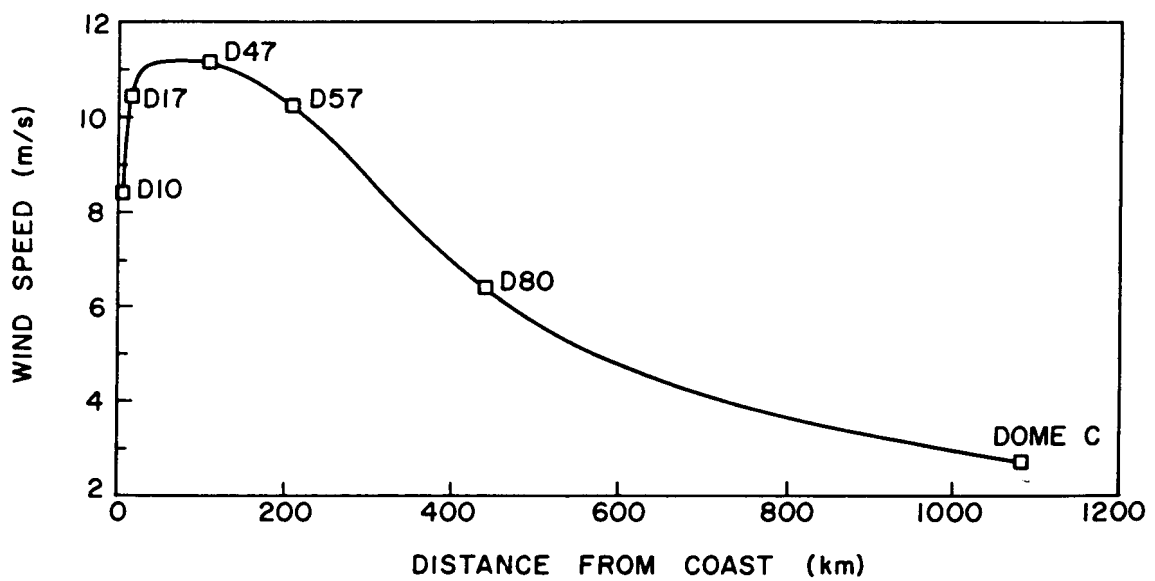
Figure 2.6.7.1.2 Variation of mean wind speed from Dome C to coast. From Parish and Wendler (1991). (See Figure 6.6.13.1 below for the locations of most of these AWSs).

2.6.7.3   Barrier winds

Ironically, one of the calmest places on Earth is believed to be in the Antarctic, in the area of Windless Bight which delineates the Ross Ice Shelf just south east of Mt Erebus. O'Connor and Bromwich (1988) describe how the interaction between synoptic scale flow and the Antarctic environment cause a stagnation region over Windless Bight as "barrier winds" are deflected around Ross Island.

The barrier winds themselves are formed by synoptically driven boundary layer air with strong static stability impinging on high orography. And not being able to ascend the orography the winds are forced parallel to the barrier (O'Connor and Bromwich, 1988, p. 921). In the case described by O'Connor and Bromwich (see also O'Connor *et al.,* 1994) the high orographic barrier is caused by the Transantarctic Mountains which are west of the Ross Ice Shelf. The Ice Shelf plays a role in allowing strong low level temperature inversions to develop thus giving rise to the high static stability. After a period of time if no other meteorological event has occurred in the area the cold air has dammed against the high barrier. In the case of the Ross Ice Shelf–Transantarctic Mountains situation with a synoptic easterly pressure gradient, the depth of the cold air boundary layer increases from east to west, that is towards the mountains. A geostrophic balance is then set up between the Coriolis force and the pressure gradient force generated by the relatively high–pressure area in the cold air dammed against the mountains and the relatively low pressure further east over the ice shelf. Thus south to southwest winds, often quite strong, are generated below the height of the orographic barrier.

Schwerdtfeger (1975) was the first to describe this phenomenon in the Antarctic context when he discussed a possible mechanism for the strong south and southwesterly surface winds along the east coast of the Antarctic Peninsula in the absence of significant low–pressure systems over the Weddell Sea. In a very similar manner to the Ross Ice Shelf–Transantarctic Mountain situation described above, cold air masses may move westwards over the frozen Weddell Sea, particularly in winter, and dam against the mountains of the Antarctic Peninsula.

2.6.8   Visibility including blizzards/blowing snow

2.6.8.1   Blowing snow

As winds increase in speed to above about 8 m s^{-1} (~15 kt) they can cause any loose snow on the surface to begin to drift. If winds strengthen to exceed about 11 m s^{-1} (~21 kt) and loose snow is present, then drifting snow may be raised above eye level thus disrupting outdoor activity and being defined as blowing snow for the purpose of international reporting of weather observations. Winds stronger than about 17 m s^{-1} (~33 kt) can reduce visibility to only a few hundred metres, if there is sufficient loose snow in the vicinity. In coastal Antarctica, blowing snow is slightly less of a problem during the warmest part of the summer because some melting and consolidation of the surface layer of snow occurs.

2.6.8.2   Blizzards

Occasionally, blizzards bring all activity to a halt, often for several days at a time. They are said to occur with the combination of freezing temperatures, gale–force winds (or stronger), with blowing snow causing the visibility to be reduced to 100 m or less. Blizzards are usually, but not always, associated with a deep low–pressure systems hundreds of kilometres off the coast of Antarctica. Blizzards may or may not be accompanied by precipitation, although the difference between falling and blowing snow is difficult to discern.

2.7   Recent change in the Antarctic

2.7.1   Trends in the surface observations

The relatively short length of many of the series of observations from the Antarctic research stations makes the assessment of trends in the meteorological conditions across the continent very difficult and it is not usually possible to find trends that are statistically significant. However, an examination of the longest series of data is instructive and in Figure 2.7.1.1 the series of annual mean surface air temperature values from a number of stations are shown, along with trend lines determined from least–squares regression. These stations are located across the continent from the South Pole (Amundsen–Scott), to the high interior plateau (Vostok), coastal stations (Mirny and Halley) to Orcadas in the South Orkney Islands. It can be seen that all the stations show a high degree of inter–annual variability, which is a feature of stations in both polar regions, but that the variability is largest on the western side of the Antarctic Peninsula at Faraday/Vernadsky Station. This station is located close to the northern limit of the Bellingshausen Sea sea ice and small variations in the ice extent are amplified into much larger surface temperature variations depending on whether the ocean west of the station is ice–covered or ice–free in a particular winter. Most of the stations show a small warming trend; the exception being Amundsen–Scott Station, where there has been a slight cooling since the late 1950s. The warming on the western side of the Antarctic Peninsula is larger than elsewhere in the Antarctic and even though the record is not long by the standards of stations outside the Antarctic, the warming trend is statistically significant at the 99% level (King, 1994). In parallel with the warming trend there has also been a statistically significant increase in the number of precipitation reports at the stations on the western side of the Peninsula (Turner *et al.*, 1997). At the moment we do not know whether the climatic changes observed in this area are the result of local factors or because of broader scale circulation changes across the Pacific region. However, there is no evidence that the warming is taking place because of any 'global warming' associated with the increased anthropogenic emission of greenhouse gases.

Antarctic–wide temperature trends were considered in an earlier investigation (Raper *et al.*, 1984) within which seasonal and annual average temperatures for Antarctica were calculated by computing areally weighted means of all available station data. The annual mean Antarctic temperature showed a warming trend of 0.029ºC per year for the period 1957–82, which was significant at the 95% level. However, the greatest contribution from this temperature rise came from the stations on the western side of the Antarctic Peninsula.
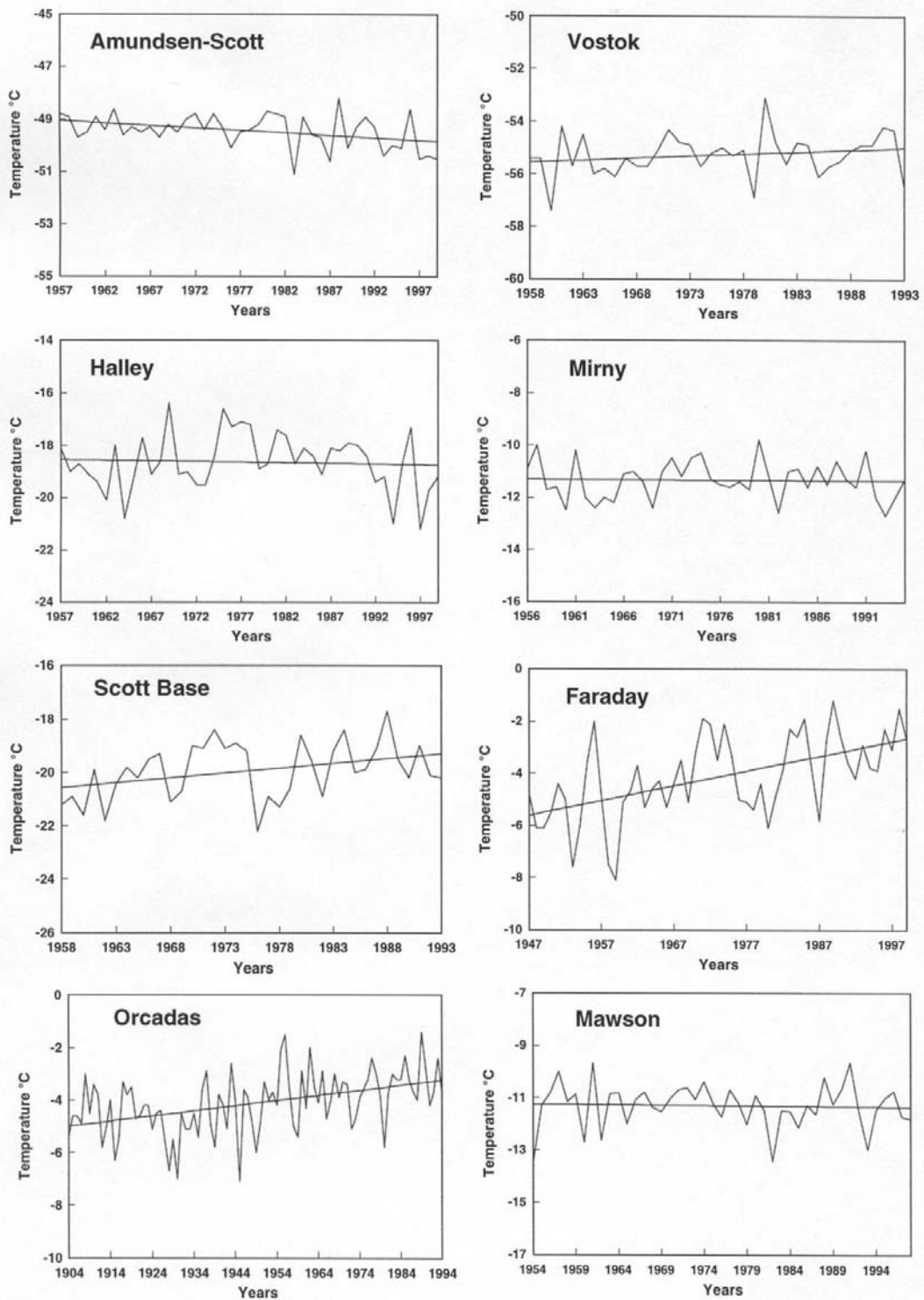
Figure 2.7.1.1   Time series of annual mean surface air temperature at a number of Antarctic stations. Data are from Jones and Limbert (1987), updated from recent reports in some cases.

2.7.2   Ozone over Antarctica

Ozone is one of the key radiatively active gasses in the stratosphere. Where there is less ozone the stratosphere tends to be colder and at any one location there is a good correlation between the 100 or 70–hPa temperature and the total column ozone. Ozone also absorbs solar uv light and where there is less ozone more uv will reach the surface, posing risks to human health.

The total column ozone was first measured in Antarctica during the International Geophysical Year of 1957–58. The instrument used to make the measurements was the Dobson ozone spectrophotometer, designed by Professor G. M. B. Dobson in the 1920s and still the standard instrument today. A typical value for the total ozone column is around 300 Dobson Units (DU), or 300 milli–atmosphere–centimetres, which corresponds to a layer of ozone 3 mm thick at the surface. This 3 mm is in reality spread through a column, the bulk of which lies between the tropopause and 40 km altitude, with a maximum at around 17 km altitude.

The seasonal pattern of the total ozone column in Antarctica is linked to the development and breakdown of the winter circumpolar vortex. Historically ozone values were around 300 DU at the beginning of the winter, and similar at the end. During the winter, ozone amounts build up in a circumpolar belt just outside the vortex, due to transport of ozone from source regions in the tropics. Very high values, occasionally exceeding 500 DU may be seen in this belt, which typically lies between about 60° S and 40° S. When the polar vortex breaks down in the spring, this belt of high ozone column air sweeps across Antarctica, typically reaching the area around the central Pacific sector first and the Atlantic sector last. Peak values used to exceed 450 DU, and then slowly declined back to 300 DU during the summer and autumn.

Since the mid 1970s an increasingly different pattern of behaviour is seen – the Antarctic Ozone Hole. At the end of the winter, values are around 10% lower than they were in the 1970s and drop at around 1% per day to reach around 100 DU at the end of September. Values then slowly begin to recover, but the spring warming in the stratosphere is often delayed to the end of November or into December. During this spring period Antarctic personnel should be advised to use high factor blocking creams, even during cloudy weather as the increase in surface uv radiation can lead to severe sun–burn. Peak values in the spring warming are now substantially lower than in pre–Ozone Hole times. Figure 2.7.2.1 shows the seasonal variation of total ozone at Halley for the period 1957 to 1998 and the decline in late spring and early summer values since about the early seventies is very evident as is the presence of very low October values since about the 1980s. Figure 2.7.2.2 shows the total October ozone at Halley since records began: the decrease from about 1975, and certainly from 1980 onwards, is very marked.

The mechanism which controls the development of the Antarctic ozone hole is linked to the dynamics of the winter polar vortex. During the winter, lower stratospheric temperatures drop below –80°C and at these temperatures stratospheric clouds can form. (Figure 2.7.2.3). Observers at stations along the Antarctic Peninsula regularly see these during the late winter as nacreous or Mother of Pearl clouds, created by lee–waves off the mountains of the Peninsula. More southerly stations sometimes report them as 'ultra–cirrus', which may cover the entire sky in a faint milky veil. Occasionally there are reports of clouds which resemble noctilucent clouds and it is just possible that such mesospheric clouds are seen in the Antarctic winter; these reports need further investigation. Once the clouds have formed, chemical reactions take place on the cloud surfaces which lock up nitrogen oxides and water and liberate chlorine and bromine (from CFCs, halons and other similar chemicals) in an active form. When exposed to sunlight, photochemical catalytic reactions take place which rapidly destroy ozone.
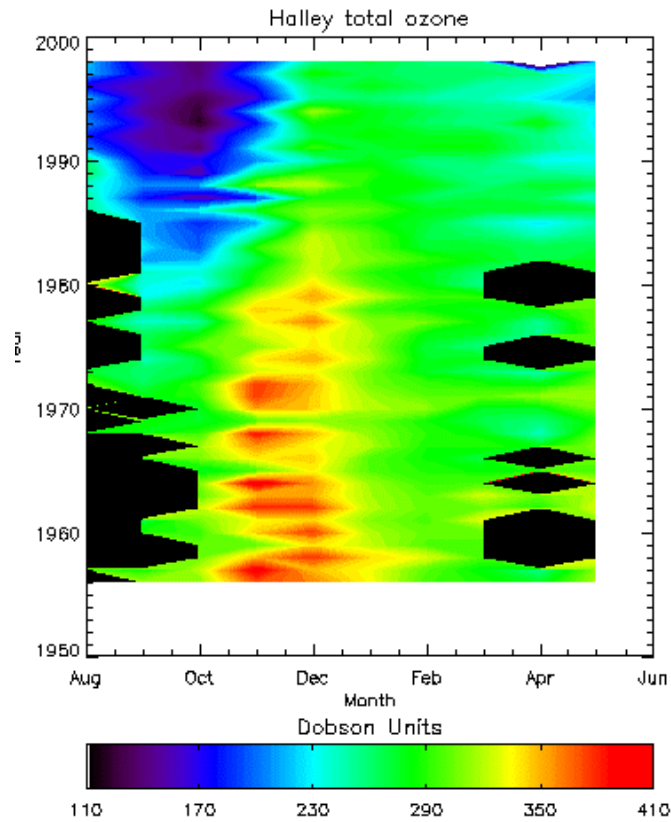
Figure 2.7.2.1   The seasonal variation of total ozone at Halley for the period 1957 to 1998.
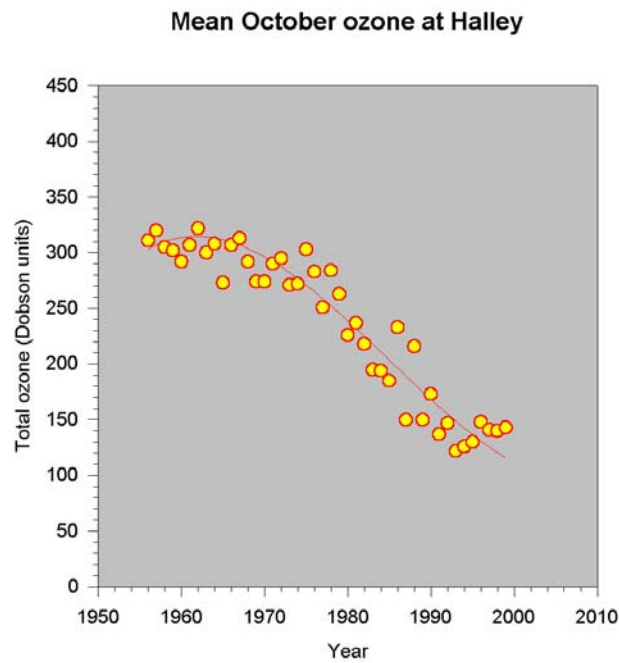
Figure 2.7.2.2   Mean total ozone for October as measured at Halley since the 1950s.
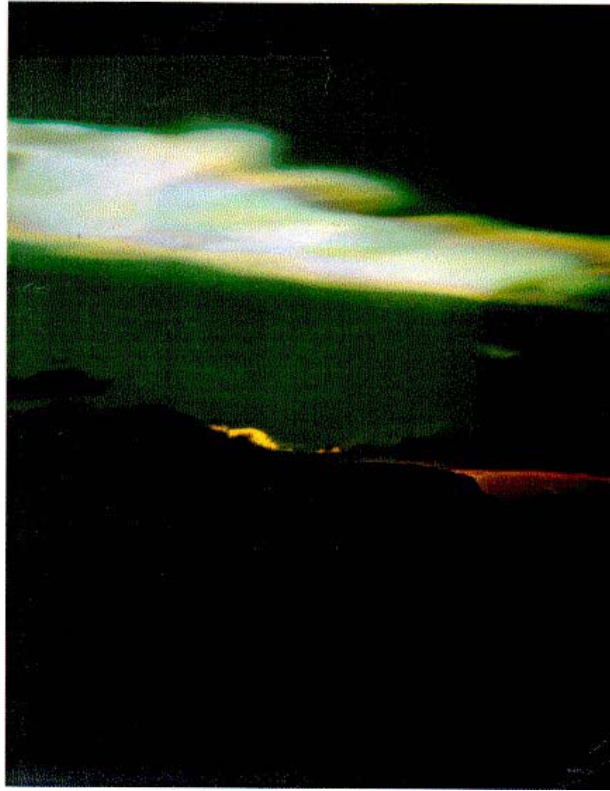
Figure 2.7.2.3   Stratospheric clouds viewed
from Faraday.

When the circumpolar vortex is at its strongest the ozone hole tends to be roughly circular, (see, for example, Figure 2.7.2.4) but as it weakens the vortex often becomes strongly elliptical (Figure 2.7.2.5) and often offset from the pole towards the Atlantic. At these times the northern edge of the vortex can reach as far north as 50° S, posing a risk of increased uv exposure for the inhabitants of southern South America and the sub–Antarctic islands. The wave rotation period of the vortex is typically around a month and this can be used to give rough forecasts of the period when such areas are most at risk. Further guidance can be given from the forecast 100 or 70 hPa temperature fields: the –70ºC temperature on the 100–hPa-surface gives a rough indication of the edge of the vortex and the –65ºC contour can be used for conservative forecasting.

The mean 100–hPa temperature during October to December is now significantly lower than it was 30 years ago. This is due to a combination of the delayed spring warming and the lower amount of ozone in the stratosphere. (Figure 2.7.2.6 is a comparison of recent measurements of the total ozone at Halley compared to 1957–72 values). This potentially has implications for the surface climate, though the coupling between stratosphere and troposphere is weak.

The size and depth of the ozone hole at its maximum extent now seem to be near their peak. The size of the hole is constrained by the circumpolar vortex, which in turn is constrained by the size of the Antarctic continent. The depth of the hole is constrained by the height range where temperatures are cold enough for the stratospheric clouds to form. We should see a very slow return to the pre–1970 situation, provided that the Montreal Protocol is adhered to, and that there are no other changes to the atmosphere. Greenhouse warming is one such change, and although this warms the lower troposphere it cools the lower stratosphere, making the occurrence of stratospheric clouds more likely. This may delay the recovery of the Ozone Hole past the middle of the 21st century.
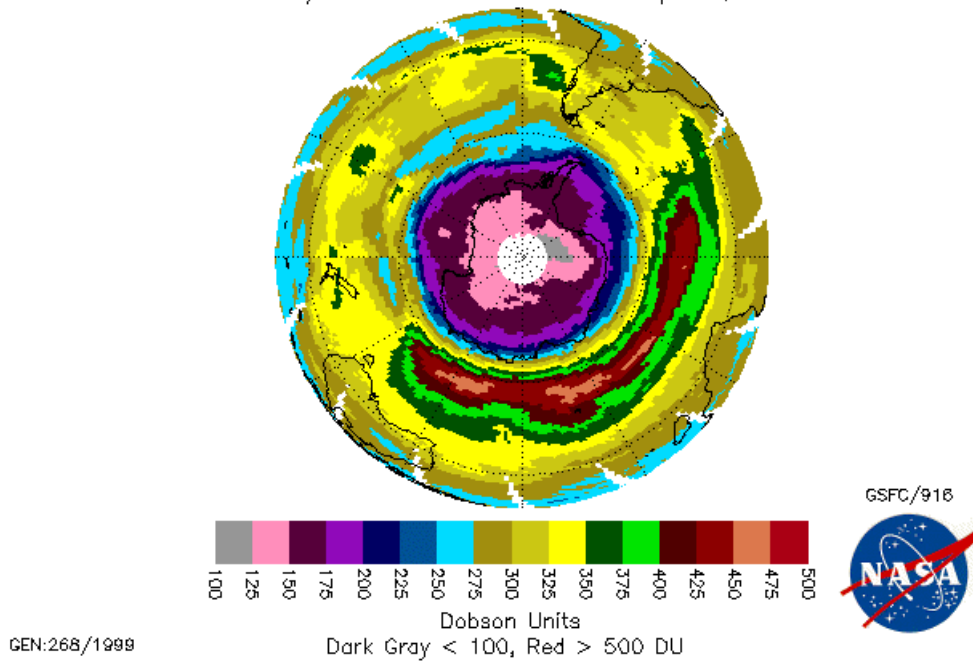
Figure 2.7.2.4   Total ozone for 23 September 1999: an example of the circular nature of the ozone hole when at its greatest depth.
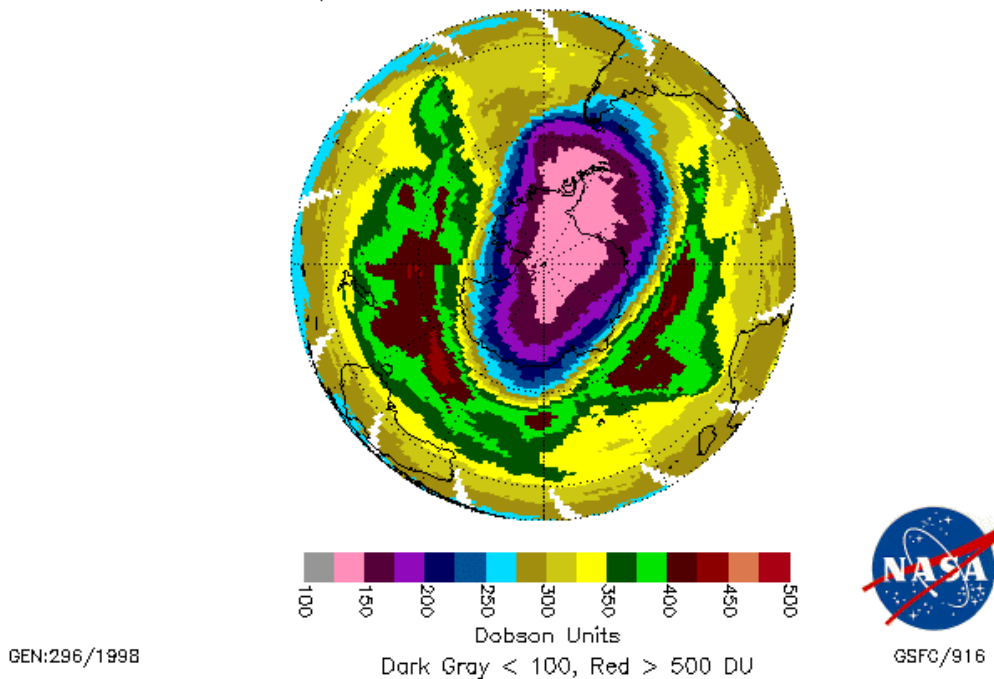
Figure 2.7.2.5   Total ozone for 21 October 1998: an example of the elliptical nature of the ozone hole during the weakening phase (compare with Figure 2.7.2.4).
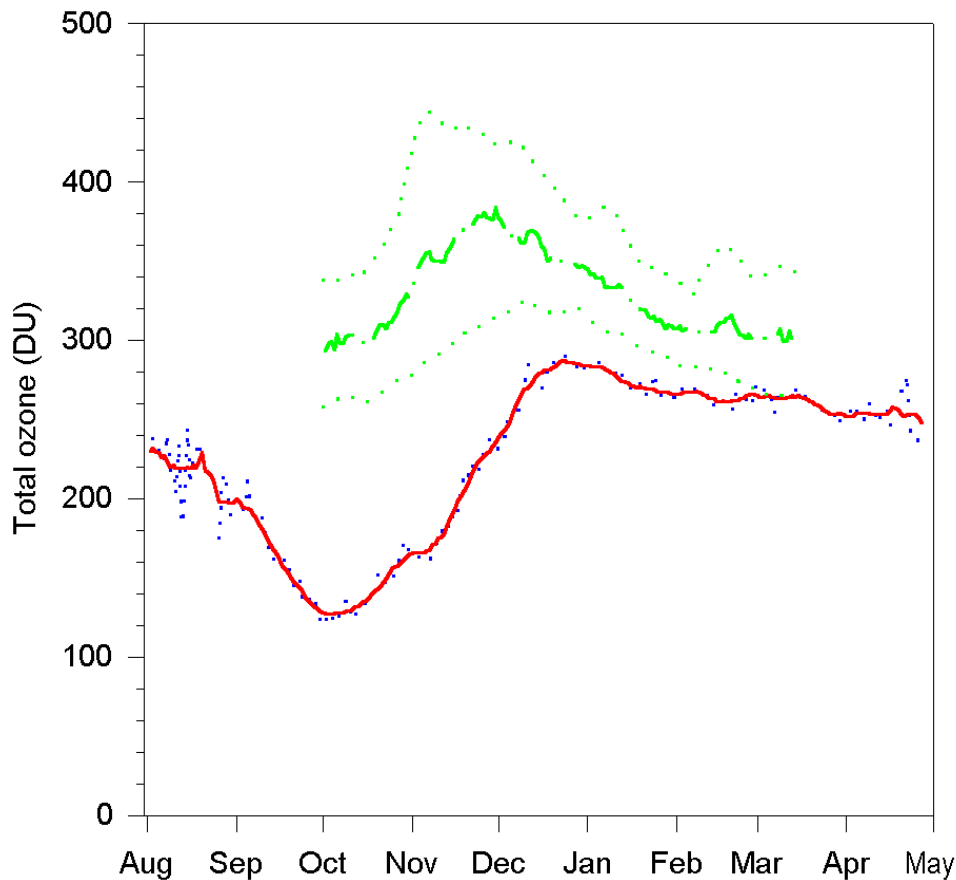
Figure 2.7.2.6   Daily mean total ozone (red line) and 11 day running mean for the 1990s. The solid green line is the 11 day running mean for 1957–72 with the dotted green lines showing the smoothed extremes during this latter period.

2.7.3   Recent changes to Antarctic ice shelves

Recently researcher Dr. Rob Massom of the Antarctic Co–operative Research Centre, Hobart has noted the disintigration of the Ninnis Glacier tongue (Massom, in preparation): see http://www.antcrc.utas.edu.au/antcrc/research/polar/seaice/Rob_Massom//Rob_Ninnis_Text.html. As will be discussed below it is not yet clear if the recent changes to Antarctic ice shelves and glaciers is indicative of anthropogenic induced climate change or is due to normal long–term cycles in ice–sheet variability.

2.7.3.1   On the relationship between polar ice sheets, climate and sea–level

In a recent summary of the relationship between polar ice sheets, climate and sea–level rise the Antarctic Co–operative Research Centre, Hobart, Australia issued a position statement on 10 February 2000 (see: http://www.antcrc.utas.edu.au/antcrc/) as follows:

"At the end of the last ice age the melting of the ice–sheets on North America and Europe caused sea level to rise by 120 m. (The last great ice–age had its peak about 18 thousand years ago and retreated to roughly the present situation by about 11 thousand years ago. It is thought that the process was triggered by slight changes in the orbit and inclination of the Earth, which in turn altered the ratio of summer to winter solar heating at high latitudes).

There is popular speculation that greenhouse warming of two or three degrees over the next century might trigger a similarly large change in association with melting of the two remaining ice–sheets of Greenland and Antarctica. (One scenario of global warming in the context of the 'enhanced greenhouse effect' involves a tripling of the concentration of atmospheric carbon dioxide over the next hundred years and, as a consequence, a rise of two or three degrees in the world's average surface temperature. The scenario assumes that the increase of carbon dioxide will level out after a hundred years).

The Greenland ice–sheet is the smaller of the two. It contains an amount of ice which, if melted completely, would raise the level of the world's oceans by 6 m. Calculations suggest a warming of a few degrees might trigger the melting of much of the Greenland ice–sheet. The process would take perhaps one or two thousand years.

The Antarctic ice–sheet is much larger. Its effective volume is equivalent to 55 m of global sea level. It is not expected that it would melt as a result of a warming of two or three degrees. This is because temperatures in most of Antarctica are well below the melting point of ice.

In many places around Antarctica, outward flowing glaciers fan out into vast ice shelves floating on the ocean. They may disappear quite quickly with global warming of a few degrees. Since they are floating, the process would not directly affect sea level. However it may allow grounded ice behind the shelves to flow faster into the ocean. Calculations suggest this extra flow could contribute one or two metres to sea level over the next one or two thousand years.

In the shorter term – that is, over the next century or two – it is expected that there will be relatively little melting of the ice–sheets. Indeed it is expected that the volume of Antarctic ice will increase slightly because greater snowfall caused by higher evaporation from the warmer oceans will outweigh any increase in melting.

Thus for the next century or two the rise of world–wide sea level will be determined mainly by thermal expansion of the oceans and the melting of non–polar glaciers. (Another possible contributor to sea level change is variation in the volume of water in artesian basins and in the storage of water by people. The uncertainties are large, but it is believed that any contribution to sea level (which might be positive or negative) will be small). The best estimate is a rise at the rate of 'several tens of centimeters per century'. (Thermal expansion is likely to continue for at least several centuries until all the world's ocean takes up the increase of surface temperature). It is difficult to be more precise because, among other things, it is hard to estimate how quickly the warming of the surface will penetrate into the deeper ocean. The relevant processes in the Southern Ocean and in the northern Atlantic are not sufficiently well understood.

Certain regions of the modern world already have experience of rates of sea level change of this order. (Parts of the coastline of Scandinavia are rising about 80 cm per century. Much of the east coast of Japan is falling at 80 or more cm per century. Parts of coastal Holland are falling at about 20 cm per century. Some Pacific islands are rising and some are

falling at rates of the order of 10 cm per century, as are parts of the east coast of the United States and Canada. These are regions where the land is rising or falling relative to the sea surface because of geological processes). "

2.7.3.2   <u>Changes in the Larsen Ice Shelf</u>

Most of the information in Section 2.7.3.2 is reproduced (with permission) from Hulbe (1997), from the "articles" link at the "**naturalSCIENCE**" web–site at: http://www.naturalscience.com/. In her article Hulbe (1997) writes: "There is clearly a connection between warming around the Antarctic Peninsula and the collapse of Peninsula ice shelves. Profound ecological changes are also occurring in response to local climate change. However, temperatures in the interior of the continent have remained fairly constant (Mosely–Thompson, 1992) and it is not yet known whether the observed warming is part of a global trend or is simply a normal fluctuation in local climate. Moreover, warming may actually increase the volume of ice stored in the large Antarctic ice sheets. Dramatic as the retreat of Peninsula ice has been, that ice is less than 1% of the total Antarctic ice volume (Swithinbank 1988) and its maximum possible contribution to global sea level is less than 50 cm……Ice shelves around the northern coasts of the Antarctic Peninsula have been retreating for the last few decades." Hulbe (1997) goes on to point out that an "event to gain attention occurred on the Larsen Ice Shelf, a series of small shelves fringing the eastern coast of the Peninsula from about 71º S to 64º S (Figure 2.7.3.2.1). The seaward front of the northernmost Larsen Ice Shelf (Larsen–A) began a gradual retreat in the late 1940s that ended dramatically in January of 1995, when almost 2000 km^2 of ice disintegrated into hundreds of small icebergs during a storm (Rott *et al*., 1996). At the same time, a 70 km by 25 km iceberg broke off the ice front of Larsen–B, between the Jason Peninsula and Robertson Island (Figure 2.7.3.2.2). The settings and styles in which this and other Peninsula ice shelves (for example, the Wordie and Müller Ice Shelves on the western side of the Peninsula (Doake and Vaughn, 1991; Vaughn and Doake, 1996) have retreated are different but the events all coincide with an observed 2.5ºC warming around the Antarctic Peninsula over the last 50 years."

Hulbe (1997) further explains: "Ice shelves are thick (hundreds of metres) platforms of floating ice that today comprise about 2% of the volume of Antarctic ice. They form where inland glaciers and ice sheets discharge into the ocean. Once afloat, the ice flows by gravity–driven horizontal spreading. Resistance to flow is provided by lateral shear where the shelf flows past bay walls and islands, and by compression upstream of sea–floor rises and islands. The rises and islands are often called "pinning points," a name which belies their importance to the stability of an ice shelf. Ice shelves gain mass by flow from inland ice, by snow accumulation on the upper surface of the shelf, and in some areas by freezing of seawater onto the lower surface. The relative importance of those contributions depends on the size and location of the shelf. Small Peninsula shelves are composed almost entirely of meteoric (snowfall–derived) ice, whereas the bulk of larger shelves, such as the Ross Ice Shelf in West Antarctica, derives from inland ice. Mass is lost primarily by iceberg calving at the seaward ice cliff and secondarily by melting at the lower surface. Except in the northern Peninsula, surface melting makes a trivial contribution to mass loss. Recent estimates of the proportion of ice loss due to calving for all of Antarctica range from 75% to 90% (van der Veen, 1991). The uncertainty is due to the difficulty of measuring melting rates beneath ice shelves. Small iceberg calving (less than 28 km^2) is common, whereas larger events occur less frequently. The shelf front may advance for tens of years before an iceberg the size of the 1995 Larsen–B iceberg breaks off. Indeed, the current (1997) Larsen–B front position is similar to its 1960 position on the American Geographical Society map of Antarctica (1981). In the absence of

external forcing, the cycle of ice advance and calving maintains a stable shelf front position over time.
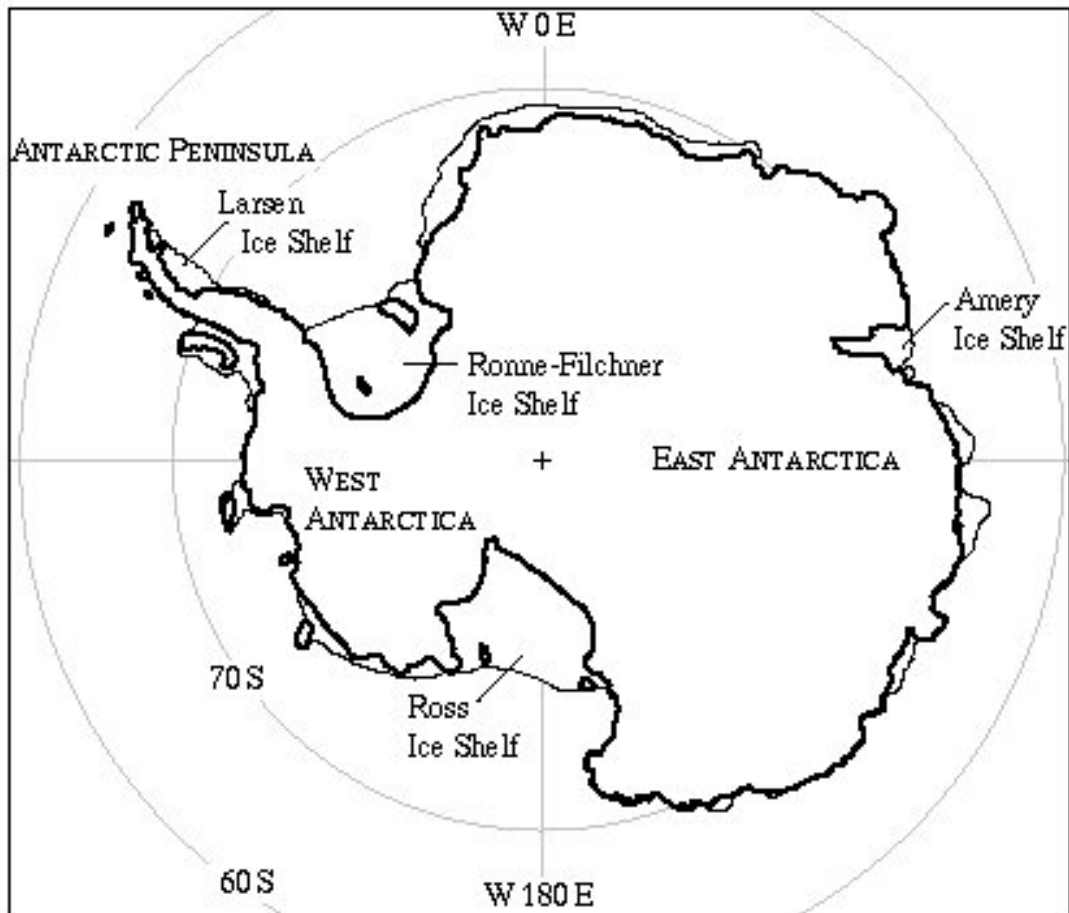
Figure 2.7.3.2.1 A sketch map of Antarctica showing the major ice shelves. The heavy line traces the outline of the continent, including grounded ice and bare rock, and the light lines trace the approximate extent of floating ice shelves. (The total volume of ice on Antarctica is 30,109,800 cubic km, about 2.4% of which is in the form of ice shelves (11% of the surface area). The West Antarctic and East Antarctic Ice Sheets contain 11 and 86% of the total, respectively. Melted, Antarctic ice would contribute 66 meters to global sea level (that figure accounts for changes in salinity and for back–filling of the Antarctic continent with water once the ice is removed). Note that melting ice shelves does not increase sea level because the shelves are floating and thus displace a mass of water equivalent to their own mass.)
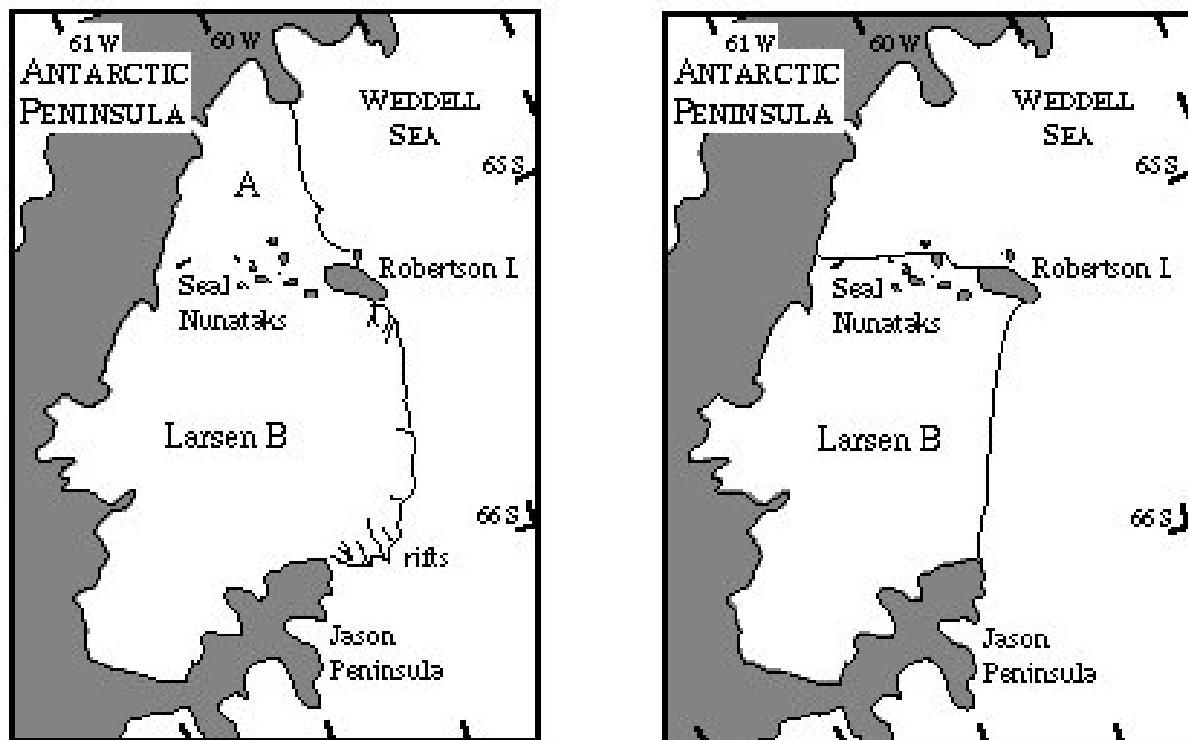
Figure 2.7.3.2.2 The northern Larsen Ice Shelf before (left) and after (right) late January 1995. The Antarctic Peninsula and pinning–point islands are shaded (both ice–covered and bare rock). The shelf maintains contact with the Seal Nunataks and Robertson Island at present (1997) but new large shelf–front rifts have been observed (Greenpeace, 1997) and summertime surface melt ponds appear in many satellite images of Larsen–B. (Scambos and Hulbe, 1996).

Changes in local climate affect ice shelf mass balance (the accounting between the mass of ice gained and the mass of ice lost by the shelf) and thus, the size of the shelf and the location of its calving front. An increase in snowfall, either on the shelf itself or on the inland ice which feeds it, will cause the ice shelf to gain mass. A decrease in snowfall will have the opposite effect. Variations in snow accumulation on the shelf itself are felt quickly, whereas changes in the inland ice may take decades or centuries to be felt. An increase in atmospheric temperature, if large enough to push summer temperatures above the freezing point, will increase mass loss directly by increasing melting at the upper surface. Warmer sea surface temperature (SST) that may accompany warmer air temperature could also increase the rate of ice shelf melting. The indirect effects of warmer air temperature are important as well. Melt water collecting in surface crevasses (wedge–shaped cracks in the ice that normally close by about 50 m depth) allows the cracks to open to greater depth because water exerts a larger outward pressure on crevasse walls than does air. Water–filled crevasses may penetrate to the bottom of the ice, possibly weakening the ice shelf and hastening its decay. Warmer air and sea surface temperatures could produce a positive effect on mass balance by promoting evaporation, which in turn increases snow accumulation over inland ice and the mass of ice flowing into the shelf. Simple comparison between mean summer air temperatures and the locations of extant ice shelves led Mercer (1978) to propose a climatic limit for ice shelf stability: North of the –4°C mean annual isotherm, ice shelves should be unstable. The present–day warming and retreat of ice shelves around the northern Antarctic Peninsula seem to confirm that hypothesis.

The effects of CO2–induced climate warming on Antarctica have been studied using numerical models that simulate ice flow and changes in ice sheet and ice shelf size over time (Huybrechts and Oerlemans, 1990; Budd *et al*., 1994). The model predictions can be summarized in three main points. First, the glaciers and ice shelves of the Peninsula are lost. Second, the large Ross and Ronne–Filchner Ice Shelves, into which the West Antarctic Ice Sheet drains, are lost to basal melting assumed to be caused by increased SST. Third, the volume of ice in both the West Antarctic and East Antarctic ice sheets increases as a result of increased snow accumulation. This somewhat surprising result arises because CO2–induced climate warming increases SST, which decreases sea ice cover around Antarctica. As sea ice-coverage decreases, available moisture, and in turn, precipitation, increase. In one 2 × ambient CO2–induced climate warming scenario, net precipitation over Antarctica nearly doubles. Thus, while some spatial redistribution of ice occurs, there is no dramatic change in total ice volume.

Despite its small role in the mass balance of Antarctic ice as a whole, the recent collapse of Larsen–A and the ongoing changes on Larsen–B and other Peninsula ice shelves offer an exciting opportunity to learn about poorly–understood ice shelf processes such as iceberg calving, ice shelf rift (crevasses that penetrate the full ice thickness) evolution, and pinning–point dynamics.

Although large iceberg calving events occur routinely with ice shelves, sudden disintegration is not. The unusual breakup of Larsen–A may have been the consequence of weakening caused by extreme surface melting during several consecutive warm summer seasons in the 1990s. Water–filled crevasses could have penetrated the entire thickness of the shelf, creating a network of wounds, held together by remaining bridges between crevasses and by frozen sea water within the crevasses. The importance of sea ice crevasse–filling was first suggested by a study of shelf–front dynamics at the Hemmen Ice Rise, near the northeast corner of the Ronne–Filchner Ice Shelf (MacAyeal *et al*., 1998). The study used a combination of satellite radar interferometry and numerical models of ice shelf flow. By comparing observed and model–derived interferograms, we found that the layer of sea ice and in–blown snow that fills many shelf–front rifts acts as a structurally cohesive unit, capable of transmitting stress across the rift, essentially gluing the rift walls together. However, rift–filling "glue" may be more vulnerable to warming and more likely to fail during large storm events than the thicker ice shelf ice.

The dynamical effects of the 1995 disintegration and calving events were studied using a numerical model that simulates pre–and post–calving ice shelf flow (Hulbe, unpublished report). Neither event changed significantly the stress regime or seaward flow of the remaining ice shelf. That result is due to two circumstances. First, the ice in most of the pre–calving Larsen–B iceberg was already spreading near the rate predicted for a freely–floating iceberg of equivalent thickness (Weertman, 1957). Thus, to the interior of the ice shelf, the ice extending beyond the post–calving shelf front was dynamically equivalent to the sea water that replaced it. Second, the shelf maintained contact with the chain of islands along its northern boundary (the Seal Nunataks and Robertson Island). The resistance to flow provided by those pinning points stabilized the shelf front position. In a model experiment where the shelf maintained contact with Robertson Island but not with the Seal Nunataks, flow across the northern edge of the ice shelf increased by about 50%, on average, and the ice shelf thinned rapidly. The time required for complete decay cannot be computed because the volume of ice flowing into the shelf from Peninsula glaciers is not well known. However, it is clear that the support provided by a small group of nunataks is key to the survival of the remaining ice.

Ice at the boundary where the shelf flows past a pinning point may be vulnerable to climate warming, although little is currently (1997) known about this subject. The ice in such shear margins is typically crevassed, is often broken into rubble, and in some instances,

contains large sea–water filled voids (MacAyeal *et al.*, 1986). Warmer sea water in the boundary voids will warm the ice internally, softening it and increasing the rate at which it can flow past the pinning point. Crevasses filled with melt water may penetrate to the base of the shelf, thereby weakening contact between the shelf and the small islands that stabilize it. New rifts discovered during the recent Greenpeace (1997) cruise around the Antarctic Peninsula may be such sources of instability. These proposals are speculative at best and require studies, like the combined interferometry–modeling work described above, to be confirmed or denied.

Hulbe (1997) poses the question: "What does the future hold for Antarctic ice?" and asserts "Unless there is a change in the observed warming trend, further retreats of fringing ice shelves along the Antarctic Peninsula are likely. This seems dramatic on the human scale but is less so on the geologic scale. The present incarnations of Antarctic Peninsula ice shelves have existed for only the last several thousand years and have, in that time, experienced cycles of advance and retreat(Clapperton, 1990; Domack *et al.*, 1995). The present glaciological events may be part of a normal long–term cycle. How ongoing changes to global climate affect the interior of Antarctica remains to be seen. The most sophisticated models available predict an increase, not a decrease, in the volume of ice in the West and East Antarctic ice sheets in future warming scenarios".

2.7.3.3   <u>Changes in the Ross Ice Shelf</u>

Of more recent interest is the calving of an immense iceberg (B–15) from the Ross Ice Shelf during March 2000. The following information is via the Antarctic Co–operative Research Centre, Hobart, Australia's web home page. An image of the iceberg (and several others) is given in Figure 2.7.3.3.1, courtesy of the Antarctic Meteorological Research Center at the University of Wisconsin – Madison. The approximate dimensions of B–15 have been assessed using AVHRR images as 295 km (~ 170 nm) long, 37 km (~ 25 nm) wide (on average). The area of B–15 is estimated to be about 11,000 km^2. This is certainly the longest iceberg on record and probably the largest iceberg by area in the modern, satellite era where images from satellites are used to monitor the distribution of icebergs. The previous largest iceberg was A20 (~95 km by 95 km) that calved from southern Larsen Ice Shelf in early 1986.

The thickness of B15 is estimated to range between about 200 m toward the old front and 350 m on the inland margin. Thickness immediately at the old front is probably less than 200 m. Height above sea level of the old front of the Ross Ice Shelf, which now forms one of the long sides of B–15, has been measured to be between 20 m and 40 m. The other long side of B15, which was along the rift in the interior of the shelf, could be as much as 40 to 60 m in height above the ocean surface.
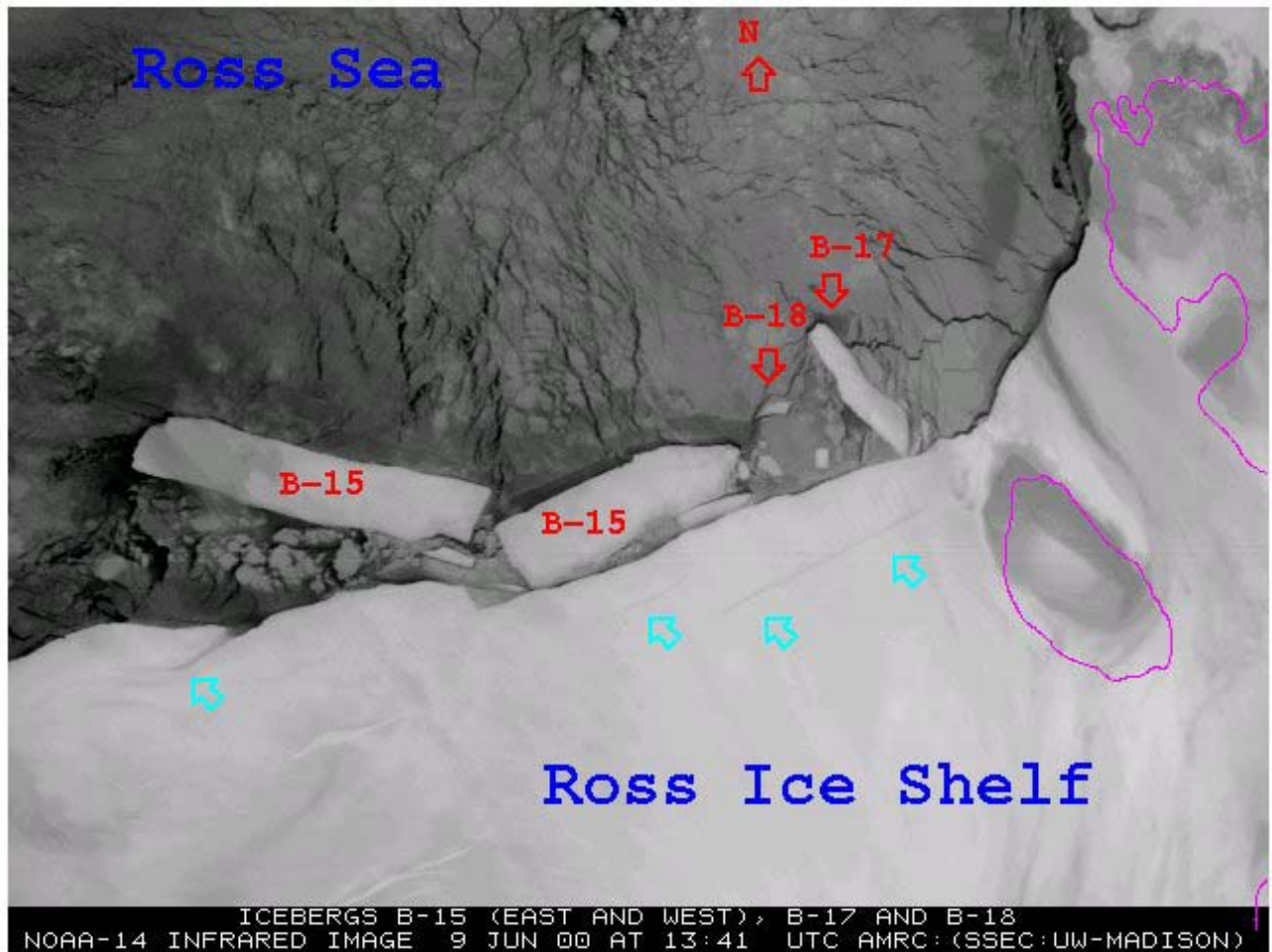
Figure 2.7.3.3.1 A NOAA–14 infra–red image of B–15, taken 1341 UTC 9 June 2000. (Courtesy Matt Lazzara, Antarctic Meteorological Research Center at the University of Wisconsin – Madison). (See also Figure 4.3.4.5.2 below).

Ross Ice Shelf front and previous calving events

The front of the Ross Ice Shelf, the seaward margin of the ice shelf, is currently (June 2000) at its most advanced state for any time this past century, and, except for the more easterly section, the most advanced since 1841. A review of this information can be found in Keys *et al*. (1998). In the sector where B–15 is calving, the front is advancing outwards with the flow and spreading of the ice at a rate of about 900 m/year. So, the 37 km width is equivalent to about 40–45 years of advance of the ice shelf front.

　　The most recent major calving was of iceberg B–9, 154 km by 35 km, from the sector east of Roosevelt Island, neighbouring the Bay of Whales, and immediately east of the calving site of B–15. B9 calved in 1987, and took 20 months to drift away from the front of the ice shelf, and then across the Ross Sea (Keys *et al.,* 1990).

The cause of the calving of B–15

The calving of B–15 is a natural consequence of the development of an ice shelf. Snow which has fallen on the surface of the ice cover, compacts and forms ice as further snow accumulates on top. The ice gradually flows outwards till it crosses the margins of the grounded ice cover. In many areas this ice flows into ice shelves which are the floating parts of the ice cover. Ice is lost from the ice sheet by calving of icebergs from the outer margins and by melting from the basal surface. The rate of loss from the margins roughly balances the input of snow to the surface.

In satellite images it is possible to see rifts forming in the Ross Ice Shelf many kilometres inland from the margin, and running parallel to the margin. These rifts typically develop and extend over time till an iceberg breaks off. The rifts which form the "calving front" for B–15 could be clearly seen in images acquired in September 1997 over a length of about 240 km. The precursors to these rifts were identifiable many years before this. The calving of B–15 could thus be anticipated, but the exact timing is very difficult if not impossible to predict.

The calving of B–15 is the consequence of a natural progression of events that occur in ice shelves, and is quite unrelated to "Global warming" or "Greenhouse" effects. Calving events on ice shelves and glacier tongues may occur frequently and produce a few or many small icebergs, or occur rarely and produce one or a few very large icebergs. It is common for many smaller fragments to be produced in a calving event.

2.8   Some aspects of Antarctic ice

Since the physics of ice are not directly meteorological and generally forecasters do not have extensive background in this subject, this section covers some of the basics of the subject. The relevance of sea ice to weather forecasting may not always be entirely obvious. An example of the need to consider sea ice formation occurs when, in light wind conditions, moist air from open water areas moves over the sea ice resulting in low stratus and fog (see Section 6.6.4.1 below). This can prevent helicopter reconnaissance and limit satellite interpretation of sea ice conditions and thus strand operations.

2.8.1   Ice terminology and classification

For an excellent overview on the observing of Antarctic sea ice the reader is referred to Worby (1999) which is a CD based practical guide for conducting sea ice observations from vessels operating in the Antarctic ice pack. WMO (2000) is also another very relevant source. The primary division of ice is into sea ice and freshwater ice. Sea ice may be classified by age as follows:

- *New ice* is a general term for recently formed sea ice. These types of ice are composed of ice crystals which are only weakly frozen together and have a definite form only while they are afloat.
- *Frazil ice* is fine spicules or plates of ice suspended in water.

- *Grease ice* is at a later stage of freezing when the crystals have coagulated to form a soupy layer on the surface. It reflects little light, giving the sea a matt *appearance.*
- *Slush* is snow which is saturated and mixed with water on land or ice surfaces, or as a viscous floating mass in water after a heavy snowfall.
- *Shuga* is an accumulation of spongy white ice lumps, a few centimetres across; *they are formed from grease, ice or slush.*
- *Nilas* is a thin elastic crust of ice, easily bending on waves and swell and under pressure, thrusting in a pattern of interlocking fingers.
- *Young ice* is in the transition between nilas and first–year ice, (10 cm to 2 m). May be subdivided into thin first–year/white ice (30 – 70 cm), medium first–year ice (70 – 120 cm) and thick first–year ice (over 120 cm).
- *Pancake ice* is floating ice predominantly circular from 30 cm to 3 m in diameter and may be divided into grey ice – 10–15 cm thick less elastic than nilas and breaks on swell – and grey–white ice – 15–30 cm thick so when under pressure more likely to ridge than to raft. It may be formed on a slight swell from grease ice, as a result of breaking of ice rind etc.
- *First–year ice* is of not more than one winter's growth, developing from young ice; thickness 30 cm –2 m. May be subdivided into thin first–year/white ice (30 – 70 cm), medium first–year ice (70 – 120 cm) and thick first–year ice (over 120 cm).
- *Old ice* is sea ice which has survived at least one summer's melt. Because it is thicker and less dense than first–year ice, it stands higher out of the water. Summer melting produces a regular pattern of numerous small puddles which develop into smooth hammocks. Bare patches and puddles are usually greenish–blue.

Other relevant terminology also includes:

- *Glaciology* is the study of frozen water in any of its forms or locations. Sometimes the term is used in the restricted sense for the study of glaciers.
- *Fast ice* is sea ice which forms and remains fast along the coast, where it is attached to the shore, to an ice wall, to an ice front, between shoals or grounded icebergs. Vertical fluctuations may be observed during sea level changes. Fast ice may be formed *in situ* from sea water or freezing of pack ice of any age to the shore, and it may extend a few metres or several hundred kilometres from the coast. Fast ice may be more than one year old. If it is thicker than about 2 m and above sea level it is called an ice shelf.
- *Pack ice* is a term used in a wide sense to include any areas of sea ice, other than fast ice, no matter what form it takes or how it is disposed. The concentration is generally expressed in terms of the areal density of ice in a given area. An average thickness of Antarctic pack ice is about 1.0 m.
- *A lead* in the ice is any fracture or passageway through the sea ice that is navigable by surface vessels.
- *A polynya* is any non–linear shaped opening enclosed in the ice. Polynyas may contain brash ice and/or be covered with new ice, nilas or young ice; submariners refer to these as "skylights". Sometimes the polynya is limited on one side by the coast and is called "shore or coastal polynya" or by fast ice and is called "flaw polynya". If it recurs in the same position every year, it is called a "recurring polynya". Polynyas can occur throughout the year around the coast due to persistent offshore winds. During periods of light winds, the sea surface may be covered over with new and young ice or for onshore winds a packing occurs which closes

the polynyas.

- _Frost smoke_ is a fog–like cloud due to contact of cold air with relatively warm water, which can appear over openings in the ice.
- For ice of land origin:

  –_Ice Cap:_ Ninety–five percent of the continent is covered by ice sheets which range in typical thickness from 100 m at the coast to over 40 km over parts of the plateau. The average thickness of the ice sheets is about 2500 m: this weight of ice has caused an ice static depression which has resulted in parts of the continental ground surface being 600 m below sea level. The pressure of ice also results in a constant flow towards the coast, the rate of movement varying between 1 to 6 m per day.

  –_A glacier_ is a mass of snow and ice continuously moving from higher to lower ground or, if afloat, continuously spreading.

  –_An iceberg_ is a massive piece of ice of greatly varying shape, more than 5 m above sea–level, which has broken away from a glacier, and which may be afloat or aground. A tubular berg is flat–topped usually formed by calving from an ice shelf and with horizontal banding.

  –_A "bergy bit"_ is a large piece of floating glacier ice, generally showing less than 5m above sea–level but more than 1 m and normally about 100–300 m^2 in area.

  –_Growlers_ are smaller pieces of thin bergy bits, often transparent but appearing green or almost black in colour, extending less than 1 m above sea–level and normally occupying an area of about 20 m^2.

  –_Surface Snow Layer_: The formation of the surface snow layer is a complex process involving both the existence of a glazed surface and the deposition–erosion process depending on snow surface conditions such as micro–relief, undulations, texture and structure and meteorological conditions. Snow deposition and erosion are primarily dependent on the roughness of the surface, so occur least when the surface is wind–packed smooth or glazed. In light winds, snow particles settle behind obstacles taking forms, such as barchans, tails and dunes.

  –_Sastrugi_ are an erosional form of the surface layer caused by katabatic winds carving pre–existing dunes (dunes are orientated at an acute angle of about 30º). Cyclonic winds usually last for a short time so sastrugi are not modified by them. Sastrugi generally occur in elongated forms parallel to the persistent wind.

  firn is old snow which has crystallised into a dense material. Unlike snow, the particles are to some extent joined together; but unlike ice, the air spaces in it still connect with each other.

  –_The firn line_: On the lower steeper slopes up to 500 m (the firn line) the surface is usually exposed ice. There is surface leveling in summer with an ice crust; such a flat surface is called a summer surface.

  –_The dry snow line_: The area of summer melting extends up to 700 to 1000 m (the dry snow line) depending on the local geography.

  –Above 1800 m are found the areas with a glazed surface and they are usually well inland, so away from most cyclonic influences.

  –Snow deposition is most common during the "winter", generally from February to September.

2.8.2   Freezing of sea water

If an aqueous salt solution is frozen extremely slowly, the foreign ions remain in the melt and perfectly pure ice is formed. The freezing rate in nature is usually too rapid for the rejection process to approach completion and the growing ice crystals trap a certain amount of brine. Over time the brine may slowly drain through the ice under the influence of gravity or migrate along the direction of higher temperatures (usually down). If a block of ice is removed from contact with the sea, as by being pushed up on the shore, it loses salt very rapidly during the warmer months of spring and summer. Much Antarctic ice is polar (that is continental) ice which is several years old and when without a snow cover is pale blue in colour, in contrast to the greyish–white of annual sea ice. Polar ice has a low salinity.

The concentration of salts in sea water is sufficiently uniform to be described by a single parameter, the salinity S, which is defined as the total amount of solid material contained in unit mass of sea water. It is usually quoted as a ratio in g per kg of sea water, that is, in parts per thousand (ppt). A value of S=35 ppt is typical of the oceans.

Pure water freezes at 0^0C at normal atmospheric surface pressures but expands by about 9% on freezing. It has a maximum density at 4^0C. For a salinity of S, the freezing point is – 0.053*S (i.e. ~–1.9^0C for a typical salinity of 35 ppt). In still pure water, as the surface layer cools, it becomes denser and sinks setting up a vertical circulation until the water reaches a uniform 4^0C. Further cooling to 0^0C results in ice forming on the surface. In sea water this circulation is not set up and the entire body of water must cool to its freezing point before ice can form, hence sea ice only forms at high latitudes. Ice is usually described as a visco–elastic solid, that is, it can be subjected to deformations and it can flow.

2.8.3   Formation and dissipation of sea ice

As implied in Section 2.2.2 the melting of the Antarctic floating ice occurs from the latter part of October through to the early March. Solar heat absorption is more intensive in ice of high salinity i.e. first year ice. There are accumulations of diatoms on the underside of the ice and there is a vigorous absorption of radiant energy and melting is initially greatest from below. In November the numbers of polynyas and leads begin to increase, accelerating the southward retreat of the ice edge. Refreezing occurs quickly in early summer where snow laden and brashy sea water forms a favourable aggregate in calm conditions and temperatures as high as –3 ^0C. The final disintegration of the sea ice is due to swell and wind induced breakup. The polynyas act as solar heat accumulators, on account of the relatively low albedo present on the dark water surface and young ice. Consequently, the surface waters are warmed more with an increased rate of ice melting.

Steady ice formation starts approximately in mid–March, first in narrow bays and at the southern shores of marginal seas, such as Ross Sea. As a rule of thumb it requires calm days of –12^0C. New ice could possibly appear in other regions, especially in the presence of residual ice and grounded icebergs, as well as along the eastern shore of ice shelves which interfere with the general ice drift from east to west in the coastal zone.

2.8.4   Ice Drift

In the Antarctic beyond the shore–fast ice lies the pack ice which is a mixture of sea ice, fragments broken off from the shore–fast ice, and pieces of disintegrated land ice. The averaged wind flow around the coast is easterly and there is a easterly weak current causing the pack ice to drift to the west. This ice drift is a diverging flow since the ice is being moved towards an ever–increasing area of ocean. Consequently the pack ice is open with wide leads and channels between the floes. If it were not for this fortunate fact, marine navigation would be extraordinarily difficult. When the drifting ice reaches 60º S, or further north, it encounters the region of the westerlies and of the Antarctic Convergence Zone.

An iceberg will move under the same forces but the effect of the current is the dominant one since 90% of its mass is below the surface. It is sometimes observed that icebergs will move through the pack ice in a separate general direction reflecting the effect of sub–surface currents. Some of the Antarctic icebergs are over 500 m thick and tens of kilometres in width. Since one of these vast icebergs may take up to 10 years to melt, it can travel great distances and there are recorded cases of icebergs being sighted in the tropical zone.

Typically at the time of maximum sea ice extent the percentage of open water within the sea ice zone appears to decrease from about 50% near the edge to about 10% near the fast ice which is generally within about 50 km of the coast of Antarctica. The ice concentration or the amount of open water is highly variable in both space and time and is the dominant factor in the exchange of heat from ocean to atmosphere.

Similarly the average sea ice thickness is highly variable, and dynamic as the winds and currents move the ice together to form thick pressure ice regions, or apart, to form leads and open water regions. A large part of the Antarctic sea ice zone is young ice with an average ice thickness in the range of 0.5 to 1 m. This relatively low thickness is partly a feature of the general movement and divergence of the sea ice. The drift of the ocean and icebergs generally provides an indication of the general drift motion of the sea ice. In the short term there is a strong correlation between the wind and the movements of the pack ice (order cm s^{-1}) with the sea ice moving at about 2% of the wind speed) while the correlation in the longer term favours sea ice movement in accord with the ocean currents (i.e. persistent wind anomaly pattern). Figures 2.8.4.1 and 2.8.4.2 show, respectively, NOAA 12 visible band images for 29 and 30 October 1992. On these days strong to galeforce southeasterly katabatic winds were believed to be noticeably moving the sea ice in Vincennes Bay near Casey Station. Note, for example, the movement of the ice floe located northeast of Casey between the two images which are almost 24 h apart.

2.8.5   Icebreakers

The icebreaker is the brute force approach to making a channel in unwanted ice. Typically they have two screws aft capable of driving the ship at 8 m s^{-1} (~16 kt). The bow is narrow and sharply raked to provide a good cutting edge. The hull below the water line is very rounded so that if the ship is trapped in a converging ice area, the pressure will tend to lift the vessel without punching the sides. To resist ice damage, the part of the hull that may come in contact with ice is made of 4 cm steel plates.

A peculiar feature is a system of heeling tanks. These are symmetrically placed sets of tanks down either side of the vessel which allow water to be rapidly pumped from one side of the vessel to the other. If this heeling action is carried out with the engines running full astern,

it is extremely effective. As a last resort the ship is sometimes backed slowly into the ice barrier so that the propeller may chop the ice to pieces. However, this technique is rather hard on the propeller blades.
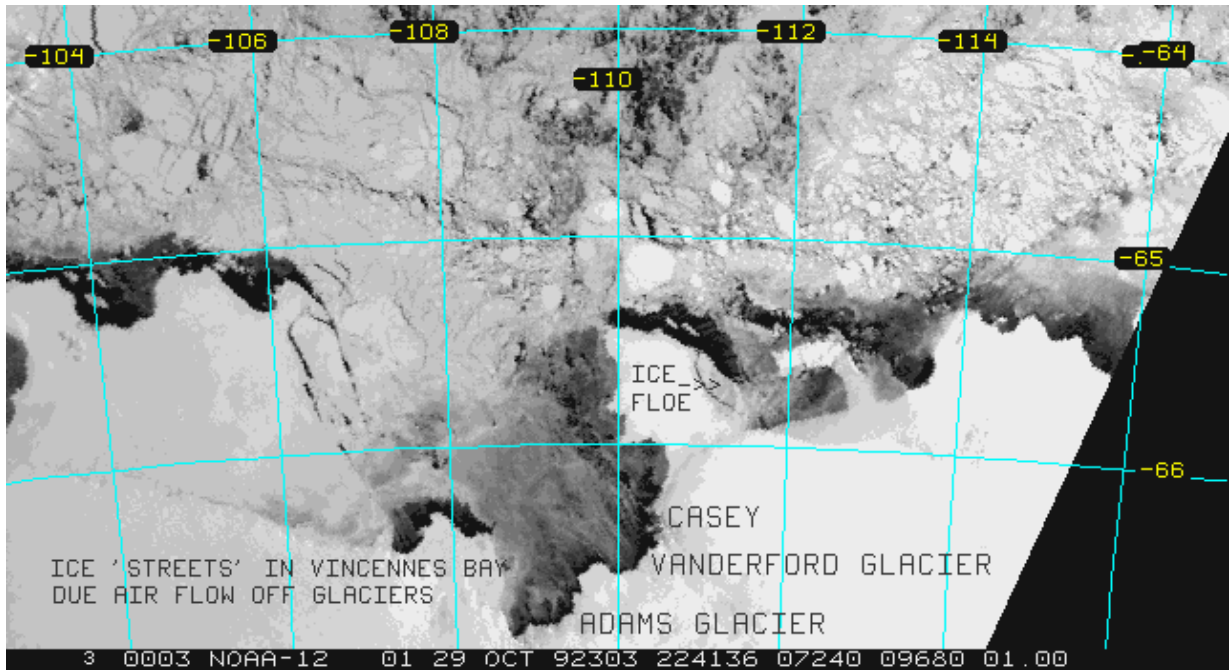
Figure 2.8.4.1   NOAA−12 visible image at 2242 UTC 29 October 1992.
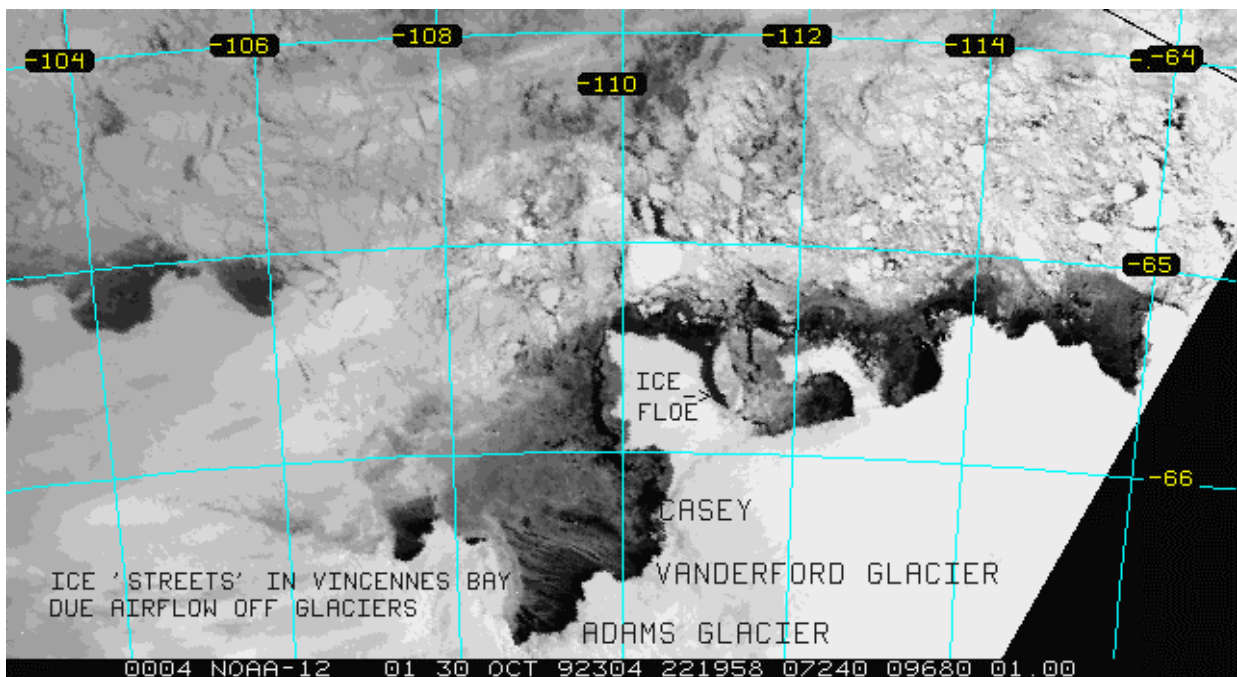
Figure 2.8.4.2   NOAA−12 visible image at 2220 UTC 30 October 1992

71

2.8.6   Sea ice information services

Since the establishment of satellite imagery, it has been possible to regularly monitor sea ice extent on a large-scale. WMO (2000) provides an overview of the sea ice information services which are available world-wide. The most well-known service, which has operated from 1973 to the present, is the US Navy Fleet Weather Facility's Ice Forecasting Group, now called the National Ice Center (NIC). NIC provides analyses of the Antarctic sea ice extent and concentrations during the southern summer and occasionally the location of the larger icebergs. As one may learn from http://www.natice.noaa.gov/ the NIC mission is "to provide worldwide operational sea ice analyses and forecasts for the armed forces of the US and allied nations, the Departments of Commerce and Transportation, and other U S Government and international agencies, and the civil sector. The NIC produces these analyses and forecasts of Arctic, Antarctic, Great Lakes and Chesapeake Bay ice conditions to support customers with global, regional and tactical scale interests. The NIC regularly deploys NAVICECEN Ice Reconnaissance personnel to the Arctic and Antarctica in order to perform aerial ice observation and analysis in support of NIC customers. NIC ice data are a key part of the US contribution to international global climate and ocean observing systems".

Other centres, particularly those with High Resolution Picture Transmission (HRPT) or DMSP facilities can also provide sea ice information. For example, the Antarctic Meteorological Centre at Casey provides AHVRR sea ice imagery (in GIF file format) upon request and routinely through the world-wide web at:

http://www.bom.gov.au/weather/tas/inside/amc/satindex.shtml

2.8.6.1   Egg code

At http://www.natice.noaa.gov/egg.htm a brief description of the WMO's system for sea ice symbolism is given. The key symbol used is known as the "Egg Code" due its the oval shape. Referring to Figure 2.8.6.1.1 the following explanation of the Egg code is to be found at the above web address.

Total Concentration

The total concentration (C) is reported in tenths and is the uppermost group. Concentration may be expressed as a single number or as a range, not to exceed two tenths (i.e., 3-5, 5-7)

Partial Concentrations

Partial concentration (Ca, Cb, Cc) are also reported in tenths, but must be reported as a single digit. These are reported in order of decreasing thickness. That is, Ca is the concentration of the thickness ice and Cc is the concentration of the thinnest ice.
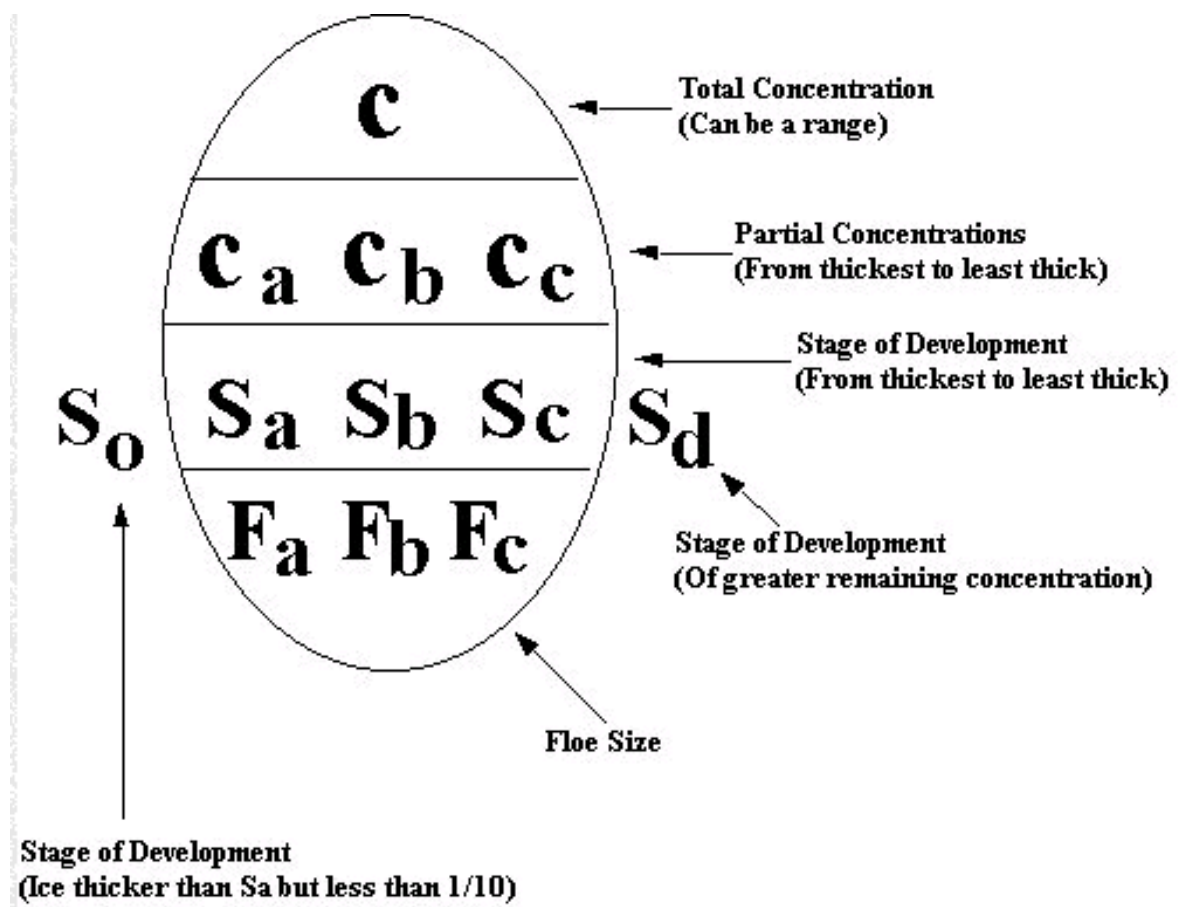
Figure 2.8.6.1.1   The Egg Code symbol. (From http://www.natice.noaa.gov/egg.htm

Stages of Development

Stages of development (Sa, Sb, Sc, So, Sd) are listed using the following code in decreasing order of thickness. These codes are directly correlated with the partial concentrations above. Ca is the concentration of stage Sa, Cb is the concentration of stage Sb, and Cc is the concentration of Sc. "So" is used to report a development with the greatest remaining concentration that will not fit into the egg. If all particle concentrations equal the total concentration and there is a Sd, Sd is considered to be present in a trace amount. The codes which are used to denote stages of development for sea ice are given in Table 2.8.6.1.1.

Forms of Sea Ice

Forms of sea ice (Fa, Fb, Fc) indicate the floe size corresponding to the stages identified in Sa, Sb, and Sc respectively. The codes used to denote forms of sea ice are shown in Table 2.8.6.1.2

Stage of Development	Code Figure
New Ice-Frazil, Grease, Slush, Shuga (0-10 cm)	1
Nilas, Ice Rind (0-10 cm)	2
Young (10-30 cm)	3
Grey (10-15 cm)	4
Grey-White (15-30 cm)	5
First Year (30-120 cm)	6
First Year Thin (30-70 cm)	7
First Year Thin- First Stage (30-70 cm)	8
First Year Thin- Second Stage (30-70 cm)	9
Med First Year (70-120 cm)	1.
Thick First Year (>120 cm) Old-Survived at least one seasons melt (>2 m)	4.
Old-Survived at least one seasons melt (>2 m)	7.
Second Year (>2 m)	8.
Multi-Year (>2 m)	9.
Ice of Land Origin	▲

Table 2.8.6.1.1   Egg code figures for stages of development of sea ice.

Form of sea ice	Code Figure
New Ice (0 cm - 10 cm)	X
Pancake Ice (30 cm - 3 m)	0
Brash Ice (less than 2 m)	1
Ice Cake (3 m - 20 m)	2
Small Ice Floe (20 m - 100 m)	3
Medium Ice Floe (100 m - 500 m)	4
Big Ice Floe (500 m - 2 km)	5
Vast Ice Floe (2 km - 10 km)	6
Giant Ice Floe (greater than 10 km)	7
Fast Ice	8
Ice of Land Origin	9
Undetermined or Unknown (Iceberg, Growlers, Bergy Bits) (Used for Fa, Fb, Fc, only)	/

Table 2.8.6.1.2   Egg code figures for forms of sea ice.

3   THE FORECASTING REQUIREMENT

3.1   Introduction

In recent years there has been a huge increase in the number of people visiting the Antarctic continent for scientific research activities, on vessels re–supplying the research stations, as part of private expeditions, on tourist vessels and even on aircraft conducting tourist over–flights. For example, at the International Symposium on Operational Weather Forecasting in Antarctica held in Hobart, during September 1998, M. Betts (see Turner *et al.,* 2000a) described the rapidly increasing number of tourist operations working in the Antarctic and the large number of private expeditions arriving on the continent. For the first time in recent years the number of tourists has exceeded the number of government sponsored expeditioners with there currently being about 10,000 tourists per year. Tourism operators expect the number of Antarctic tourists to reach 14,000 per annum very shortly and demand for meteorological forecasting support in the future will be increasingly from the tourism operators rather than from the government sponsored expeditions.

Now although weather forecasts have been attempted since the very first voyages to Antarctica took place, the increasing complexity of modern logistical activities on the continent means that ever more specialised and accurate forecasts are required. For example, many operators use small fixed–wing aircraft equipped with both skis and wheels to deploy and recover field parties at isolated locations in the interior of the continent. The fuel for such flights has to be brought into the Antarctic via ship and for flights well away from the research stations has to be placed in depots at more southerly locations. With accurate forecasts of upper winds and the weather at the destination, the timing of such flights and the route/flight level used can be optimised to conserve the fuel required. Of particular importance is the need to avoid fights that are aborted close to the destination because of bad weather, since the cost in wasted fuel will be considerable.

The consideration of weather analyses and forecasts is therefore an important part of planning field activities in the Antarctic. And more generally, most outdoor Antarctic activities require weather forecasts to ensure that they are conducted in a safe manner in what is a harsh and dangerous environment, even in the summer months when most visits occur. The following sections concentrate mostly on aviation forecast requirements as this sector is arguably the most weather sensitive.

3.2   Overview of general meteorological and forecasting requirements

The history of the activities of the various national Antarctic forecasting services will vary from country to country as will their current requirements. For an excellent overview of the infrastructure of many of the stations which are operating in the Antarctic the reader is referred to the web site of the Council of Managers of National Antarctic Programs (COMNAP) at http://www.comnap.aq/comnap/comnap.nsf. Here the visitor will gain an overview of the extent of the international effort in Antarctica.

In some cases (e.g.: Australia) a government–based national weather agency is recognised as the national lead agency for Antarctic weather programmes. In other cases semi–government research institutions (e.g.: British Antarctic Survey (BAS)) or private interests provide the services on contract to the national government concerned. In general though, collectively the major objectives of the weather services/agencies of many nations which operate in Antarctica are, among others, to:

- maintain, if not improve, the present quality of surface and upper–air observing programmes;
- ensure efficient real–time transmission of meteorological data as contributions to the international network agreed to by the World Meteorological Organization (WMO), Antarctic Treaty Consultative Meeting (ATCM) and the Scientific Committee on Antarctic Research (SCAR);
- develop the application of data received by satellite remote sensing of the atmosphere over Antarctica and the Southern Ocean;
- provide sea ice images and analyses in support of shipping operations and climate research;
- improve assimilation of high latitude data in global and limited area weather prediction models of the atmosphere;
- improve understanding of Antarctic meteorology, with the aim of providing, improved weather forecasts;
- collaborate with other agencies in improving the coupled ice–ocean–atmosphere climate models;
- continue to monitor atmospheric trace gases and particles (aerosols) as indicators of the impact of human activities.

3.3   Meteorological Services

Meteorological services in the Antarctic generally have components which include a basic monitoring or climate focus; forecasting facilities such as the reception of satellite data; and then the forecasting services themselves. This section provides a brief overview of aspects of each of these.

3.3.1   Environmental Conditions and Climatological Study

An important component of planning operations to Antarctica is a climatological study of the area in question. For example, as the economics of operating flights to Antarctica are often heavily dependent on the ability to predict the best operating windows for landings and take–offs, a climatological study of the airstrip conditions is essential to maximize mission success. These type of studies can include a statistical analysis, based on historical meteorological data, of the amount and height of low cloud, surface horizontal visibility, and surface wind direction and speed. With these data, comparisons can be made between potential sites as to their suitability for aircraft operations. Estimates can be made of the

percentage of time that meteorological conditions would be safe for landing or take–off. An example of such an approach applied to conditions at Casey is given in Section 7.10.1 **below**.

3.3.2   Forecasting facilities

The following equipment is considered important in providing meteorological information for forecasting purposes:

3.3.2.1   High Resolution Picture Transmission (HRPT)

Images of nominally 1.1 km horizontal resolution, obtained from the Advanced Very High Resolution Radiometer instruments on board the NOAA series of polar orbiting satellites are available to provide meteorological information. The HRPT station at McMurdo, for example, provides coverage of much of Antarctica. A similar facility at Rothera provides coverage of the Antarctic Peninsula while the HRPT station at Casey provides data for all of East Antarctica. Even the HRPT facility at Melbourne provides data as far south as the Antarctic coast near Dumont d'Urville.

Increasingly re–supply and research vessels: for example, the Chinese Antarctic Research Expedition (CHINARE) and the BAS vessels are equipped with HRPT facilities.

3.3.2.2   Automatic Picture Transmission (APT) data

NOAA satellite imagery at 4 km horizontal resolution may be available at some stations, on some ships, and at some remote locations using APT equipment which is a simpler system than HRPT, for example, needing only an omni–directional antenna.

3.3.2.3   Geostationary Meteorological Satellite (GMS) data

Hourly satellite imagery from the geostationary meteorological satellites is available to provide useful information between low latitudes and the Antarctic coastal regions.

3.3.2.4   DMSP

The US Defense Meteorological Satellite Program series of satellites are monitored in real time by McMurdo and Palmer Stations. In the case of McMurdo the NOAA, DMSP, and Meteor satellite data are received and processed providing McMurdo Station and the Ross Ice Shelf area with nearly continuous coverage. The TeraScan processor enables overlay, and still animation for the DMSP and NOAA images.

3.3.2.5   Numerical weather prediction

As will be seen in Chapter 7 output from numerical weather prediction models is widely used in many aspects of weather forecasting and provides the main means of producing forecasts for the next few days ahead.

3.3.2.6   Global Telecommunications System (GTS), HF radio–facsimile, File Transfer Protocol (FTP) and the World Wide Web (WWW)

The GTS is the prime source of weather observations in real-time. However, in a personal communication, Ian Hunter, Deputy Director, Marine Meteorological Services for the South African Weather Bureau cautions "Forecasters must realise that the data on the GTS have to be requested. For example, we missed very valuable data from the vessel *Polarstern* because the data were going via Meteosat to Darmstadt and were never routed to Pretoria. We have had similar problems with the *Marion Dufresne's* VOS data. In other words, forecasters must find out what data they should be getting on the GTS."
      Increasingly the above data, plus many other data types, can be provided point to point using facilities such as FTP and can be made available on the WWW. Conventional fax may also be used where appropriate. HF radio–facsimile is another valuable source of data, particularly chart-based information. A comprehensive list of global radio–facsimile (and other information) may be found at: http://www.nws.noaa.gov/om/marine/rfax.pdf .

3.3.2.7   Automatic Weather Stations (AWSs)

Tables in Appendix 1 **below** includes many of the AWSs which are in operation in the Antarctic and notes which of these are available on the GTS. Local readout of AWSs for the entire Antarctic continent is usually available at stations with HRPT facilities.

3.3.2.8   Forecast dissemination

There are several methods by which forecasts are disseminated to the user:

- E-mail and the Word Wide Web;
- Point to point via satellite transmission;
- Broadcast by satellite, for example, all the South African Weather Bureau forecasts are broadcast via Inmarsat's Atlantic Ocean Region -East or Indian Ocean Region satellites;
- High Frequency (HF) broadcasts.

3.3.3   Forecast services

Typically, Antarctic weather forecasting services and meteorological advices are provided by the various nations/agencies to support/provide:

- national re–supply and research vessels en–route to and from Antarctica;
- ship–shore–ship helicopter operations;
- helicopter operations within the local area (about 400 km range) from stations or field base as well as the so called "long range" helicopter operations between stations;
- weather forecast and sea ice analysis assistance to other nations/agencies, if requested;
- public style weather forecasts and warnings for the various stations and their immediate environs, especially the issuing of prior advice of impending blizzards;
- weather sensitive activities during summer field (mostly scientific) programmes;
- fixed–winged aircraft operations within the Antarctic, or to and from the continent;
- tourist activities (mostly inter and intra–continental flights and ship voyages).

3.3.3.1   Aviation specific services

Area or Forecasts of Route Conditions (ROFOR)

Route forecasts of wind velocities and temperatures at standard flight levels over a specific flight path for a specified period of validity are provided by many forecasting services.

Significant Weather Prognosis (SiG WHR PROG)

Significant weather prognoses are a useful pictorial means of portraying the forecast weather elements.

Terminal Aerodrome Forecasts (TAFs)

Terminal aerodrome forecasts for the destination, alternate landing strips and the place of departure are prepared by relevant forecasting offices.

Weather watch

Most forecast services will maintain a close watch on the forecasts that they have issued and provide an amendment service if specified error criteria are met or exceeded.

3.4   Forecasting requirements for aircraft operations

Arguably the most weather sensitive of all Antarctic based logistical operations are those concerned with aviation. Although often an inconvenience, and occasionally costly in money terms, most marine and land based activities have the benefit of being able to wait out adverse weather. Aircraft, on the other hand, have a relatively limited operating range before they must land. Even in the case of the long–range aircraft operations where weather is considered to be less of a risk to life, the purpose of the aircraft flight might be compromised by inclement weather. In the following sections some of the requirements of inter and intra continental aircraft operations are considered in the Antarctic context.

3.4.1   Intercontinental operations

There is an increasing number of aircraft flights to and from and over Antarctica. For example, the great circle route from Australia to South America includes a flight path over the Antarctic sea ice. The US has been flying personnel into its station at McMurdo, from New Zealand, since the mid–1950s, while flights from South American countries to the Antarctic Peninsula are common place.

3.4.1.1   Intercontinental operations at minimal weather risk

At the recent International Symposium on Operational Weather Forecasting in Antarctica, (Turner *et al.,* 2000a), Captain Dennis described the tourist over–flights of the Antarctic that the Australian airline QANTAS operate. These start at Melbourne, Sydney, Adelaide, or Perth, pass over various parts of the continent, including Dumont d'Urville, the McMurdo area, the Transantarctic Mountains, Casey or Davis and then return to Australia. The aircraft used are Boeing 747–400 series aircraft and the primary aim is to maximise time over the continent in clear sky conditions. Operating procedures dictate that the aircraft must, at all times, be able to return to an airport (in Australia, New Zealand or South Africa) if simultaneous failure of two engines and loss of cabin pressure occur.

Upper winds and the choice of route are critically important for these flights so as to maximise the tail wind for as much of the journey as possible. Meteorological analyses and forecasts are obviously very important in the pre–flight planning of these journeys and during the flights the pilots are in radio contact with meteorological personnel who are located in Australia and at the Antarctic research stations. In the future pilots hope to be able to receive, in flight, satellite imagery for themselves to aid the identification of cloud–free areas of the continent.

It will be inferred that this type of operation is virtually "weather" risk free provided that the aircraft always maintain a safe cruising altitude. The weather related penalties are mostly related to economic loss due to fuel burnt unnecessarily and to loss of viewing conditions when cloud obscures the Antarctic features of interest from fee paying tourists.

3.4.1.2   <u>Intercontinental operations with some weather risk</u>

In contrast to flights which only fly over the Antarctic, aircraft operations which have the prime purpose of ferrying people to and from the Antarctic face an increased risk by virtue of having to land in the Antarctic. Here we do not want to overstate the risk: for example the US has never lost a life during its many years of flying fixed–winged aircraft into McMurdo on an almost daily basis. However, generally speaking, the meteorological support/infrastructure for flights which must land in the Antarctic is substantial.

While each nation/agency will approach this task differently there are some common requirements. At the International Symposium on Operational Weather Forecasting in Antarctica, Mr. Jack Sayers (Executive Secretary of the Council of Managers of National Antarctic Programs) gave a summary (Turner *et al.* 2000a) of the requirements of inter and intra–continental flights and discussed the need for aviation forecasts for flights such as those undertaken by both national and commercial operators.

Mr. Sayers noted that COMNAP plays an important part in developing procedures for aircraft operations in Antarctica and has published an Antarctic Flight Information Manual (AFIM) plus an Antarctic Telecommunications Operators Manual (ATOM). During his talk Mr. Sayers dealt in particular with the possible development of an East Antarctic Air Network (EAAN) which would air–link various countries with the Antarctic via appropriate embarkation/disembarkation airports/runways. Mr. Sayers indicated that such an enterprise would obviously require accurate weather forecasts including information such as:

- an outlook two to three days prior to flight;
- a further outlook including route winds and Terminal Airfield Forecasts (TAFs) 24 h prior to takeoff;
- detailed route forecast and diversion route forecasts, satellite pictures, TAFs and alternate TAFs two to five hours prior to flight;
- continual weather watch and phone contact with meteorological personnel during flight, plus hourly Meteorological Aerodrome Reports (METARs), aerodrome reports when special (adverse) criteria are met (SPECIs) and Trend Type Forecasts (TTFs) (or landing forecasts);
- updated METAR and TTF 30 min before the point of safe return (PSR).

3.4.2   Aircraft requirements with the Antarctic

Aircraft operate within the Antarctic for a variety of reasons including: transport of supplies and personnel between stations, field camps and re–supply ships; sea ice reconnaissance flights from vessels; science purposes such as magnetometer and ground penetrating ice radar transverses; and for mapping. The actual weather limitations on aircraft operating parameters will be aircraft type dependent: rotary winged aircraft (helicopters) can, for example, land in very small spaces, and, can land in very strong surface winds which would otherwise prevent a fixed winged aircraft from safely touching down. On the other hand a fixed winged aircraft is somewhat safer to operate in white–out conditions in that such an aircraft can approach the landing site with a very shallow flight path. A helicopter, on the other hand, tends to blow up loose snow which exacerbates the surface definition problem and is prone to tipping on the slightest incline.

The following notes are an overview of how various elements might affect aircraft in a general sense. They are based on information supplied by V. Barkell for the Australian Antarctic Forecaster Handbook and have a bias towards helicopter operations. Nonetheless the information is of general interest to aviation activities in the Antarctic. Lied (1968) also provides useful information. A more detailed account of forecasting methods for these elements is given in Section 6.6 **below** while site specific information is given in Chapter 7.

3.4.2.1   Visual Flight Rules

While aircraft operate under various jurisdictions in so far as operational rules are concerned, it is generally accepted that intra–Antarctic flights are conducted under "Visual Flight Rules" (VFR), that is under Visual Meteorological Conditions (VMC).

3.4.2.2   White–out and cloud

White–out is the most potentially dangerous weather condition that a pilot in flight over unrelieved horizon to horizon might face. As a consequence the presence or likelihood of cloud developing in such areas must be forecast as accurately as possible: this requirement cannot be too heavily emphasised.

3.4.2.3   Wind velocity

Surface

Surface wind speed and direction can affect aircraft operations in several ways including:

- on landing and take off: in common with other areas of the world, aircraft are operated most safely when landing and taking off into the wind. Moreover, aircraft will have specific cross wind thresholds above which they cannot operate.
- Rotary winged aircraft (helicopters) blades generate lift at quite low rotational speeds during engine start or engine run–down: in strong winds the blades will tend to sail and there is a risk of damage to the tail boom as a result of a blade strike or damage to the rotor head. On the other hand helicopters can operate (hover) in quite high surface wind speeds as long as there is no attempt to switch off. Fixed winged aircraft would not generally be able to land at these high wind speeds (say 25 to 30 m s^{-1} (~50–60 kt)).
- At high surface wind speeds both types of aircraft are susceptible to mechanical damage if parked. Fixed wing aircraft are likely to be affected at lower speeds.
- Strong winds can cause drift snow to rise to such a degree that take–off or landing becomes hazardous or impossible.
- Above about 25 m s^{-1} (~50 kt) winds will cause problems for sling loading operations.

Upper

Turbulence aside, the main direct effects of upper winds on aircraft are that they are needed to be taken into account in navigation and they can affect aircraft speed relative to the ground and impact on fuel usage.

3.4.2.4   Turbulence

Due to the general smoothness of the ice surface, mechanical turbulence is mostly confined to areas near mountains or nunataks. Clear Air Turbulence (CAT) is occasionally encountered. In some coastal areas after the fast ice has broken out, roll or rotor cloud has been frequently encountered together with associated very strong vertical air movements. Almost invariably lenticular cloud is associated with the roll or rotor cloud. Cloud level is often about 300 to 600 m (~1000 to 2000 ft) above the surface.

In general, fixed winged aircraft are more susceptible in flight to turbulence than are helicopters.

3.4.2.5   Drift snow

Particles of drift snow are extremely fine and a wind speed of approximately 5–8 m s^{-1} (~10–15 kt) is enough to move them in a bouncing motion called "saltation". As the wind speed increases, drift snow travelling at wind speed, rises above the general surface. At about 10 m s^{-1} (~20 kt) drift will rise to approximately 1 m while wind speeds of about 17 m s^{-1} (~33 kt) causes the sky to be obscured to a standing human observer. During blizzards with wind speeds in excess of about 40 m s^{-1} (~80 kt) drift snow may rise to 30 to 40 m (~100 to 150 ft).

Whilst in flight (under VMC) drift snow can be readily seen blowing over the snow surface. It is, however, somewhat harder to estimate the height to which the drift rises although the above rule of thumb may be used if the surface wind speed is known.

It is dangerous for aircraft to attempt to land in blowing drift snow conditions without some ground reference – a building; cane marker; fuel drum etc. (Without a reference a helicopter may easily come onto the surface with an appreciable rearward speed, so that the aircraft will inevitably tip backwards onto its tail rotor or perhaps roll if there is lateral travel in addition to rearward travel on surface contact.

If blowing snow has risen to a height much in excess of 2 m above the surface, a helicopter pilot attempting to land may lose all visibility before touch down and increasing the risk of an accident.

3.4.2.6   Icing

In the early part of each summer when fast ice may extend many kilometres seaward from the coast, the possibility of airframe icing in VMC over the continent is much reduced because the air is almost devoid of moisture. When operating inland from the coast in VMC the same generally applies regardless of the fast ice disposition.

When the fast ice breaks out from the coast, moisture laden maritime air is present in coastal areas. When the dew–point and air temperature are within a couple of degrees of each other, rime icing occurs in clear air and may cover windscreens etc. As the airframes are at a

temperature below freezing, the rime ice impacts and builds an opaque mass assuming that there is no de–icing equipment available.

Landing becomes hazardous as the pilot has very restricted vision ahead. There is the possibility of rotor blades and engine air intake icing leading to severe airframe vibration on the one hand and possible engine failure on the other (again technological solutions notwithstanding).

3.4.2.7   QNH

The diurnal and semi–diurnal surface pressure variations over the Antarctic are small, the amplitudes of both these waves being about 0.2 hPa, and so most significant variations in air pressure will be due to weather systems. In calculating the QNH (the pressure value used on altimeters to give altitude) allowance needs to be made for the cold Antarctic environment.

Altimeters are normally calibrated according to a standard atmosphere (see Appendix 3 **below**) with a fixed lapse rate of 0.65ºC per 100 m and a MSL temperature of 15ºC (288 K). To adjust for the real atmosphere's departure from 15ºC the following equation may be used (Meteorological Office (1971, p15)):

$$Z \; = \; Z_{ind}(1 + (T_s – 15)/288)$$ Equation 3.4.2.7.1

It may be seen that when the surface air temperature (T_s (in ºC)) is below 15ºC the altimeter readings (Z_{ind}) will be higher than the estimated "true" height Z. For example, if the surface air temperature is –20ºC the indicated height (Z_{ind}) has to be multiplied by 0.88 to give a more accurate (lower) estimate of altitude.

3.5   Forecasting requirements for marine, station/field and research activities

3.5.1   Forecasting requirements for marine activities in Antarctic

Although the actual number of vessels operating in Antarctic and Southern Ocean waters is unknown, it is likely that, over the Austral summer at least, there is a significant amount of marine activity covering a wide variety of purposes. These include:

- re–supply of Antarctic stations using ships due to the volume and weight of cargo and the number of personnel involved;
- marine science voyages;
- resource exploration;
- fishing;
- monitoring illegal activity;
- and inshore small boat activity, for example, biological surveys.

While generally less sensitive to inclement weather than aviation, the marine sector nevertheless benefits from the provision of timely and accurate weather forecasting services. In most cases a text–based general high seas forecast would be obtained which covers wind velocity and sea state (sea and swell).

For the high seas the WMO Marine Programme co-ordinates the dissemination of warnings and weather and sea bulletins according to a broadcast schedule, in conformity with procedures laid down under the Global Maritime Distress and Safety System (GMDSS) protocols within the Safety of Life at Sea convention (SOLAS). For broadcast purposes, the world's oceans are divided into a number of areas of responsibility called Metareas (see Figure 3.5.1.1). South Africa, for example, has METAREA VII which includes the Southern Ocean down to the Antarctic coast, from 20º W to 80º E. Because this is such a large area of responsibility the South African Weather Bureau (SAWB) does not routinely issue forecasts for the areas south of 40º S - vessels have to request for these areas to be included.
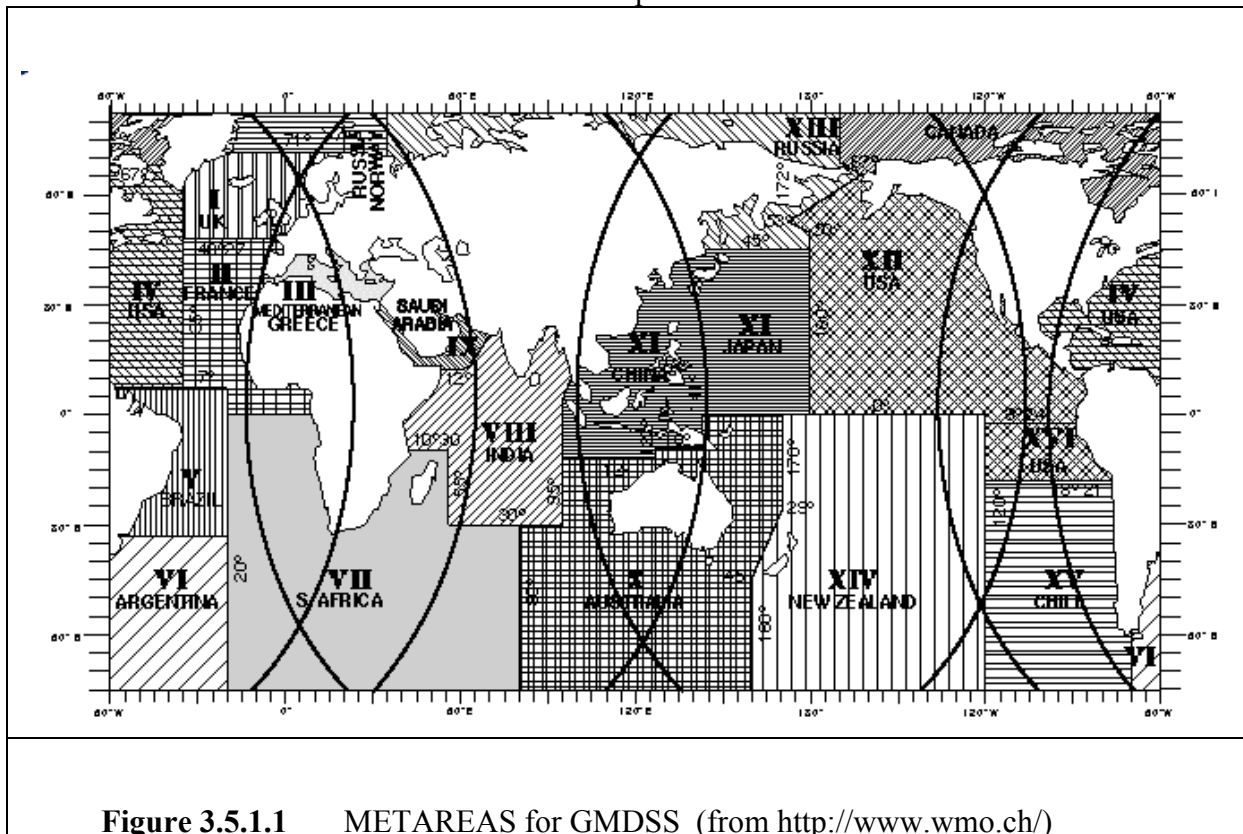
Figure 3.5.1.1   METAREAS for GMDSS (from http://www.wmo.ch/)

Similarly, over recent years the Antarctic Meteorological Centre (AMC) at Casey has been issuing graphical representations of the high seas forecasts for the area south of 50º S between 80º E and 160º E. Recently this service has been replaced by a text based service from the Australian National Meteorological Operations Centre in Melbourne. However, Figure 3.5.1.2 is a trial graphic that this centre is considering using to replace the text–based forecast.

For ships operating near the coast, sea ice information is of importance. Direct read out satellite imagery is of most use: these data might be obtained from onboard APT or HRPT/DMSP receiving equipment. Also of value are sea ice analyses which might be obtainable from sources such as the US National Ice Center.

Marine science cruises are often supported by their own onboard meteorologists who use the various fax–based; web–based; and/or onboard satellite imaging systems, together with single station forecasting techniques to provide a forecast service. This service may include an aviation component where aircraft (usually helicopters) are used to provide additional logistical and navigational support to the cruise.

3.5.2   Forecasting requirements for station/field and research activities in Antarctica

For most Antarctic stations there is no dedicated weather forecasting service available on a year round basis. Occasionally, a station might request an *ad hoc* forecast service for a winter traverse or a similar venture. Usually, however, station activities proceed on the basis of "hoping for the best but preparing for the worst", in other words, station management insist on expeditioners taking all possible care when going about their outdoor tasks, and in particular keep a close watch on the weather.

On the other hand, during the Austral summer, many stations have their numbers increased due to scientific and maintenance personnel, and field camps are established from which scientists conduct their research. It is during this period, when aircraft might be ferrying people and cargo between stations/ships/field camps, or when aircraft are deploying scientific personnel in the field, or when there is an increase recreational activity by staff who leave the station for a break, that a routine forecast service is often requested.

The style of such a service will vary according to the need, but in general it would include reference to wind and precipitation, and perhaps include a wind–chill and a statement on the risk of blizzards. Usually such forecasts are less detailed than the aviation service due to less stringent requirements.
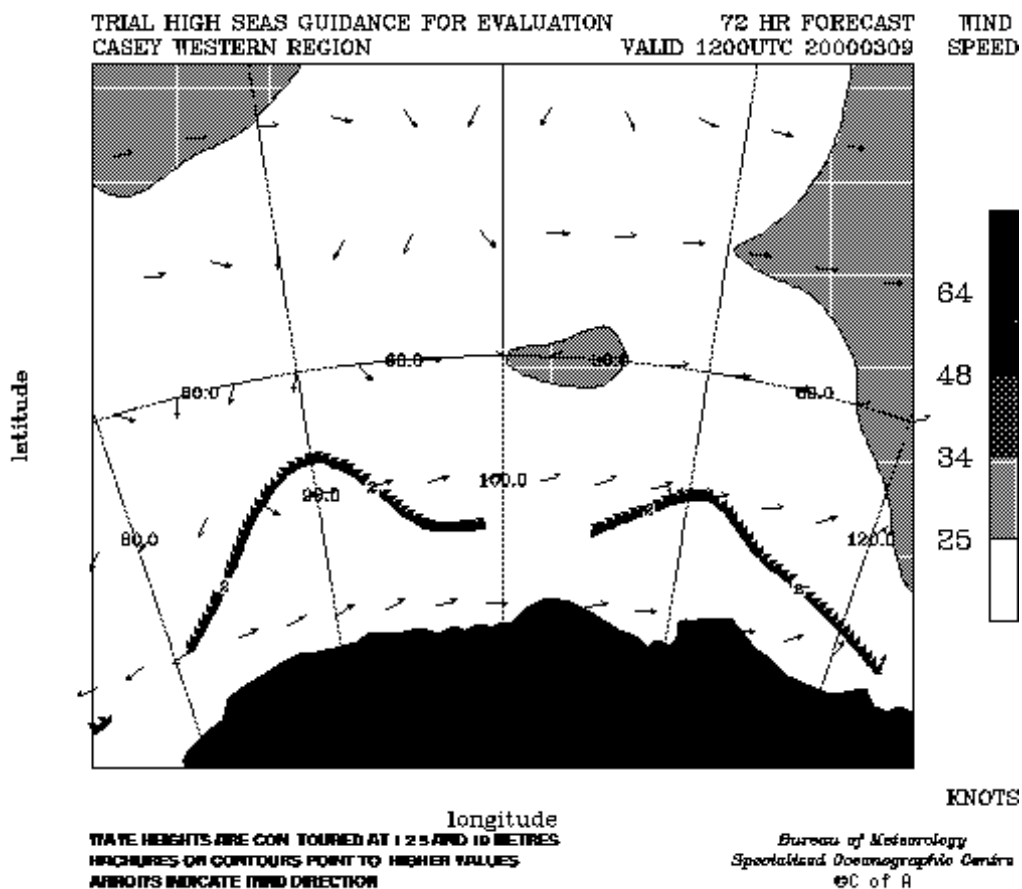
Fig 3.5.1.2   A trial graphical high seas product.

4   DATA AVAILABILITY AND CHARACTERISTICS

4.1   *In situ* observations

4.1.1   Conventional reporting stations

Most Antarctic stations and a few Antarctic supply ships make surface synoptic observations which are reported on the Global Telecommunications System (GTS). Fewer stations and ships make radiosonde observations, with perhaps a dozen covering the entire Antarctic continent.

Surface meteorological measurements are often the easiest to carry out, and for this reason most Antarctic staffed stations do make them. The personnel making the observations may be trained meteorologists, observers specifically trained for the task, or untrained support staff. Some stations use simple instrumentation, others use computer sensed electronic instruments in an AWS linked to manual input of observed parameters. The degree of quality control is variable, but most stations strive to provide precise, timely observations. Typical problems with measurements include incorrect calibration, particularly for electronic instrumentation, poor instructions and poor exposure (particularly for temperature which can be subject to severe radiation effects in Antarctica, and may also be affected by snowdrift filling Stevenson screens). High altitude stations may not have their height correctly determined and this will give errors in the pressure reduction to a standard level.

Once the observations are made there is no guarantee that they will get to the outside world. HF transmissions are subject to the state of the ionosphere and to the availability of the transmission equipment, which may be in use for other purposes such as flight following. Antarctic stations are usually near the edge of the footprint of geostationary satellites and Data Collection Platform (DCP) transmissions are often subject to errors and outages. In the future, improved communication of observations may be realised through the introduction of satellite telephone systems.

Ship reports are normally only available during the summer season when they re–supply the Antarctic stations. Reports are normally sent via Inmarsat to the designated marine reporting centres and insertion on the GTS is good. Rothera Station also collects reports from the UK ships and includes them in their ARQ HF telex broadcast for local use in the Antarctic Peninsula area. Some ships make meteorological measurements for research purposes and do not report them on the GTS. The majority of supply ships and all tourist ships are not selected as supplementary or auxiliary reporting ships and do not make meteorological observations. All Parties to the Antarctic Treaty who have vessels operating in Antarctic waters are encouraged to recruit them into the Voluntary Observing Fleet.

Ship reports are usually made according to the dictates of navigation duties and are often made away from the nominal synoptic hour. UK practice is not to report the time of the observation, although this can be done using the group 9GGgg. The computer program supplied by the Koninklijk Nederlands Meteorologisch Instituut (KNMI) and in use on some

selected ships assumes the use of a whirling frame psychrometer, rather than the more traditional wet and dry bulb psychrometry and this can lead to slightly inaccurate dew–points.

Radiosonde stations in the Antarctic use either the Global Positioning System (GPS) or radio theodolite tracking for wind determination. The GPS systems tend to have problems in the boundary layer, due to poor acquisition of the signal and occasional gaps in satellite coverage. The theodolite stations also have problems of locking on to side lobes. Most stations now use the WMO code to report details of radiation corrections to temperature measurements. A few radiosonde stations carry out flights for research or aviation support and these are often not available on the GTS. Some stations carry out a programme that is seasonally dependent, either linked to studies of the ozone hole, or to summer aircraft operations.

Data availability in the Antarctic is often limited, with fewer stations now making their observations directly available within Antarctica than in the 1980s. Those countries which can afford direct computer links to centres outside Antarctica can retrieve observations from the GTS, however the data availability varies a little from centre to centre depending on the efficiency of bulletin forwarding. Computer outages at varies stages of the links can further affect data availability, however in general around 85% of the observations that are made will be available through the GTS.

4.1.2   Automatic Weather Stations

Allison (1986) reported on automatic weather station systems and sites installed by the United States Antarctic Program (USAP), Australian National Antarctic Research Expedition (ANARE), Norway, Chile, Brazil, Japan, and the USSR. Since 1986 the number of AWS sites in Antarctica has more than doubled. Italy and Germany have added several AWS sites that are given here and probably other countries have added sites that are not known to the authors at this time.

An automatic weather station is a stand–alone system that typically measures surface meteorological variables such as wind speed and direction, air temperature, and air pressure and may measure additional variables such as relative humidity, or vertical air temperature difference. Most Antarctic AWSs transmit data in the blind for reception by the ARGOS System on board the polar–orbiting satellites of the NOAA series (Schwalb, 1979) or stored on a memory module for retrieval at a later date.

The technological developments that were essential for practical AWS units in Antarctica were low power (CMOS) electronics and polar orbiting satellites equipped with the ARGOS System. The low power electronics enabled the development of simple computers that control the sampling, processing, and transmission of the meteorological variables. The ARGOS System on board the NOAA series of polar orbiting satellites receive the transmitted data from platforms and delivered the data to a data centre for distribution to the users. In addition the NOAA satellites transmit the ARGOS data in the data collection system (DCS) on a beacon transmitter and imbedded in the high resolution picture transmissions. The DCS data can be collected when the satellite is in view of a ground receiver and used for local forecasting. Holmes, et al. 2000 gives an example of the use of the data for forecasting high wind speeds at McMurdo, Antarctica. The ARGOS data received at the ground stations can be entered into the Global Telecommunications System (GTS) at specific times and used in synoptic charts and for use in forecasting models. Tables 4.1.2.1 to 4.1.2.5 in Appendix 1 below give the WMO numbers for the sites that have data on the GTS. It is known that the

European Centre for Medium–range Weather Forecasts and the Australian Bureau of Meteorology (ABOM) actively use the data.

The AWS sites may be temporary, remote, and seldom visited and the elevations of the AWS sites are not necessarily well known. In the case of the USAP AWS sites the units are often installed using helicopters (from ice breakers and McMurdo, Antarctica), twin otter, and LC–130 aircraft to and from remote sites and the result is that the elevations of the sites are not well known. Most site elevations were based on the aircraft altimeter. If the flight is over several hundred kilometers there can be a considerable change in the horizontal pressure field and there will be a considerable error in the elevation based on the aircraft altimeter. Currently, USAP is getting new site elevations using the UNAVCO recording GPS units. The typical ground time at an AWS site is between one and two hours. The recording GPS unit can determine the site elevation with an error of one or two meters in that time span. This corresponds to a pressure error of 0.1 to 0.2 hPa which is about the accuracy of the pressure measurement by the AWS unit. Table 4.1.2.1 in Appendix 1 below gives the USAP sites that have new elevations based on the GPS. Some of the elevation corrections were more than 50 m.

The AWS on Bouvetoya (54º 24' S, 3º 25' E), is an example of the usefulness of AWSs on remote sub-Antarctic Islands (see Section 7.2.4 below).

Tables 4.1.2.1 to 4.1.2.5 in Appendix 1 below indicate that at least 62 sites have WMO numbers and should be going into the GTS. Figure 4.1.21 shows the locations of the USAP AWS and AGO sites, ANARE AWS sites, and one Antartide (Italian) site. Thirty–seven AWS sites and six AGO sites have WMO numbers. The sixteen sites in Table 4.1.2.2 have WMO numbers and cover the sector between D–10 and Relay Station. About two thirds of Antarctica is now covered with GTS sites. The sectors with a paucity of data are between 30° E to 30° W and 120° W to 75° W.

The GTS data are delivered every three hours to the major meteorological centres preparing Antarctic synoptic charts and medium range forecasts. We know that the Australian Bureau of Meteorology has been using the US AWS data for at least 10 years. One way to find out if anybody is using one's data is to remove an AWS unit from South Pole, which has a WMO number tied to the ARGOS ID, ship the unit to Japan where it is put on ice breaker which reaches Antarctica two years later. The unit is then shipped overland in a tractor train to Dome Fuji where it is installed and put on the air. In a few days the ABOM will contact you and tell you that they know the site is not at South Pole because there is a diurnal air temperature cycle and the site is higher because the pressure is lower. The European Centre for Medium–range Forecasts has contacted us about an error in the location of Siple Dome site. The US National Center for Environmental Prediction has never contacted us about our AWS sites or data so we are fairly certain that they are not using our data in their synoptic charts and models. Having two out of three major meteorological centres using the USAP AWS data makes it worth while to get the data into the GTS. The USAP AWS data are being used by the ECMWF in the re–analysis of past data. If the AWS data makes a difference by improving their models then we will have had an impact on worldwide meteorology.

The AWS units transmit to the ARGOS System at 401.650 MHz. At McMurdo, Antarctica there is a system currently installed that receives the AWS transmissions in line of sight at 401.650 mHz from sites south of Ross Island to Minna Bluff and can convert the transmission to meteorological units for real–time display. This system is independent of the satellite. The USAP AWS unit updates the data every 10 minutes and the result is the data from the received AWS sites is at 10–minute intervals. The data are used for fog forecasts for aircraft flights and have shown an improvement in the fog forecasts and a better understanding of the processes causing the fog to develop.
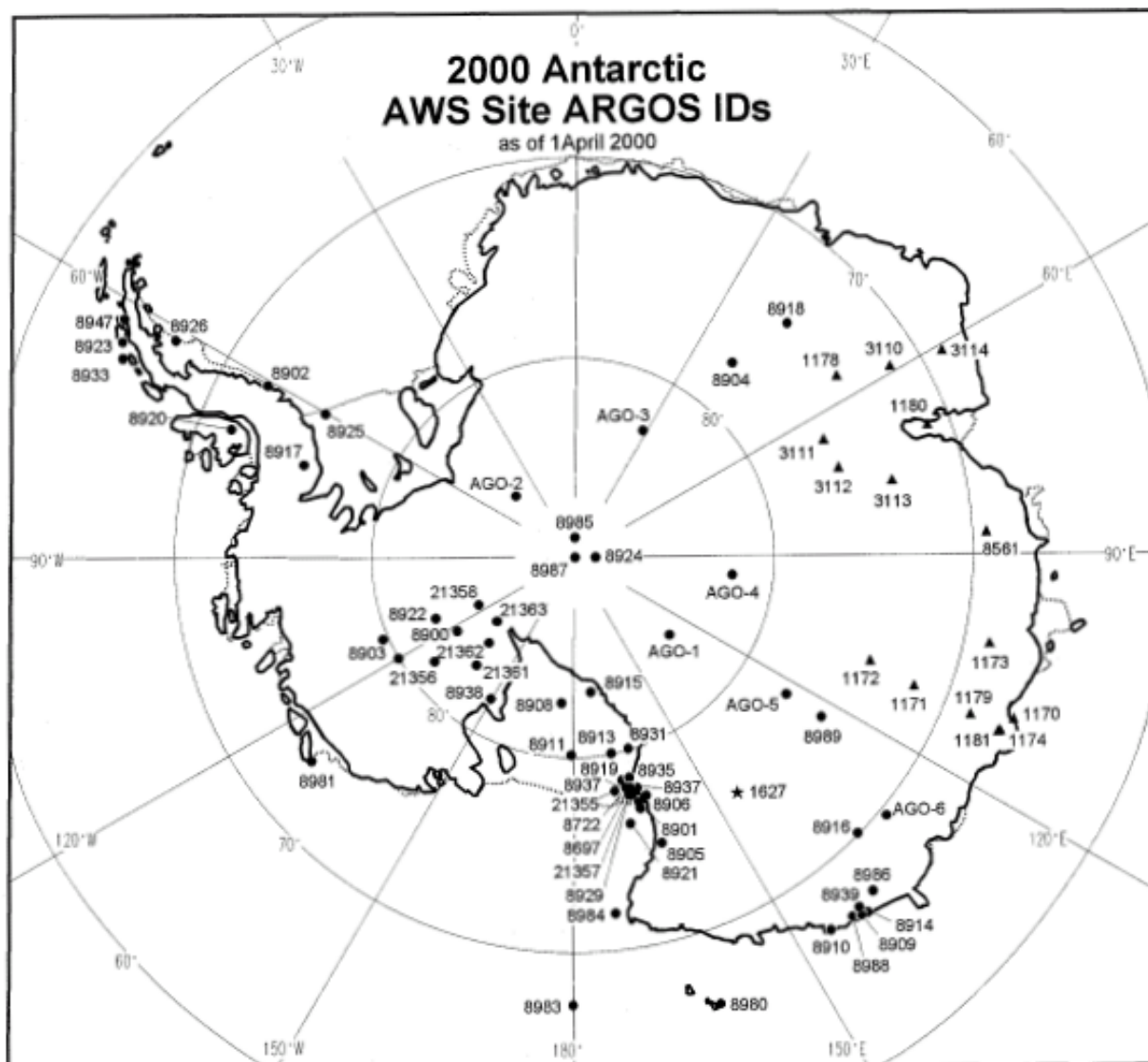
Figure 4.1.2.1.　USAP AWS and AGO sites (filled circle), ANARE sites (filled triangle) and one Antartide site (filled star) for 2000.　The remaining sites in Table 4.1.2.3 are in the vicinity of Terra Nova Bay inland from Manuela site on Inexpressible Island.　The two sites in Table 4.1.2.4 are not shown.

The AWS sites further south of Minna Bluff and on the Ross Ice Shelf are useful for forecasting high wind speeds and blowing snow at the runways in the vicinity of Ross Island (Holmes, *et al.*, 2000). Data from these sites cannot be collected directly from the unit but must be collected from the satellite HRPT transmission at McMurdo, Antarctica. The system used to process the AWS data may not get updated on an annual basis. The result is that some of the data are lost and some data are incorrect in location and are not processed correctly. Thus the value of the AWS data for forecasting may not be fully realized.

The Antarctic AWS sites can have an impact on the synoptic maps and the development of medium range forecast models. Getting the data into the GTS for worldwide distribution does not guarantee that the synoptic centres will actually use the data. It has taken roughly 10 years for the ECMWF to try to use the data in their meteorological analysis of Antarctica. The ABOM took less time but they are more interested in Antarctic meteorology than the Northern Hemisphere meteorologists. The AWS data are not the same as the usual meteorological station data. The elevation problem has been mentioned. The units stop from

90

time to time and the units may be moved to another site or removed altogether as the primary purpose may be for research or research support.   There are problems with maintaining a specific site. For example, Young Island and Scott Island (Table 4.1.2.1 in Appendix 2 below) are located in a data sparse region (Figure 4.1.2.1). The only way to reach the sites is by helicopter from a United States Coast Guard icebreaker. The units operate for two to three years after installation and then require replacement because clouds or snow prevent the solar panels from charging the batteries. This may take several years due to the distribution of sea ice or the availability of the icebreaker. The groups maintaining the AWS sites may have two to four people doing the work. They may get only one chance each year to visit the site. An established meteorological station will have people that can repair or replace equipment rather quickly. Automated stations are replacing some of the manned meteorological stations. Experience is showing that these automated stations need constant attention by someone. The AWS groups in Antarctica are doing very well considering the extreme climate, short field season, and limited transportation resources. The AWS groups will continue to try to fill in the data voids in Antarctica.
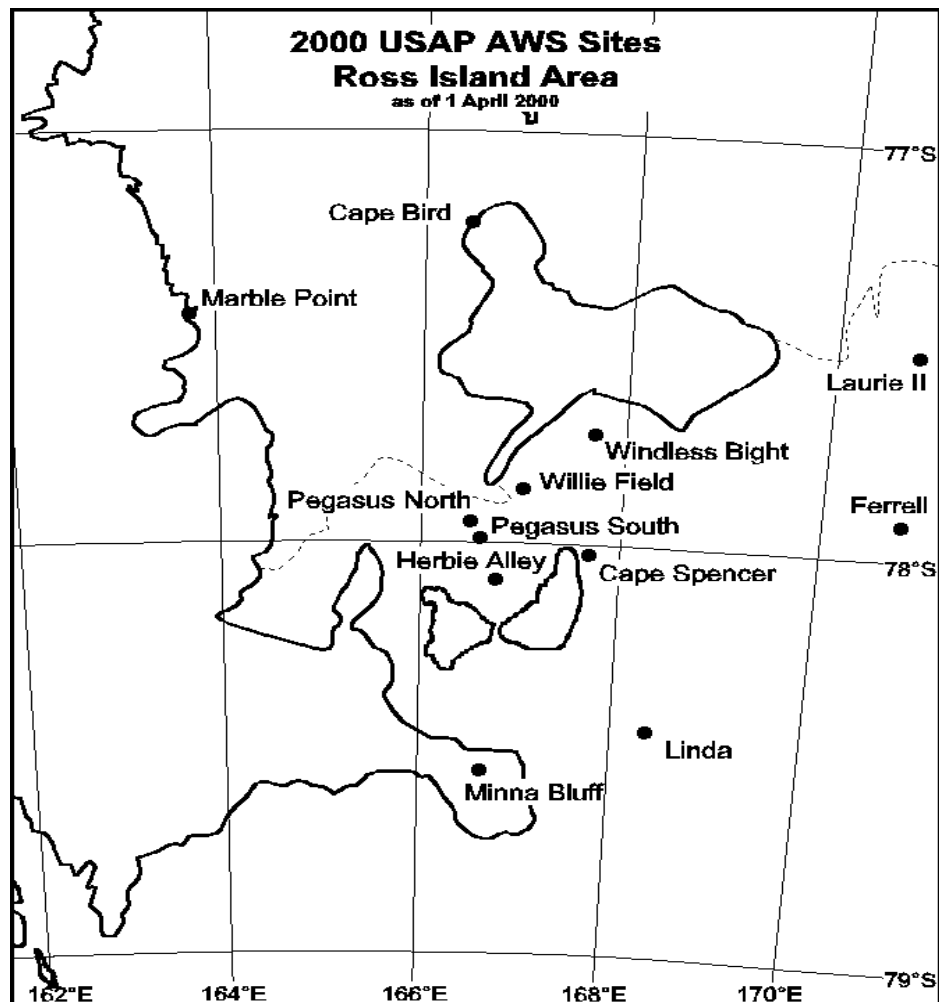
Figure 4.1.2.2 USAP automatic weather station sites in the vicinity of Ross Island, Antarctica. The sites south of Ross Island are received in real time at the McMurdo, Antarctica meteorology office and the data are used for making fog forecasts for aircraft flights.

4.1.3   Drifting Buoys

Much of the material in this section follows the lead of King and Turner (1997, pp. 29–36). These authors note that the major advance in the development and deployment of drifting buoys came with the First GARP (Global Atmospheric Research Project) Global Experiment (FGGE) when over 300 systems were deployed in the Southern Ocean as part of this very large scientific project to investigate atmospheric predictability and the requirements for an optimum observing system. These buoys were contributed by eight different countries with the goal of having no point in the ocean more than 500 km from a buoy. Also noted was that while recent advances in satellite technology have provide surface data such as wind vectors over the ice free Southern Ocean, drifting buoys still play a vital role in the specification of surface air pressure, and near–surface air temperature and humidity. Thus buoys continue to be deployed in the open ocean and in the Antarctic sea ice to provide data for operational forecasting and research into the atmosphere and sea ice.

4.1.3.1   Buoy design and data collection

Buoy design

King and Turner (1997, p. 30) report that "Many different types of drifting buoy have been deployed in recent years and currently a number of commercial companies and research institutes manufacture buoys. These are of varying degrees of sophistication, from low–cost ocean drifters with no meteorological sensors to very advanced systems making a wide range of atmospheric and oceanographic measurements.
          Various instrumentation can be attached to the basic buoy platform, depending on the data requirements and the experiments that are to be carried out. Measurements made by buoys in recent years have included atmospheric pressure, wind speed and direction, air temperature and humidity at various levels above the surface and, in the case of buoys on ice floes, the surface temperature of the snow or ice and snow thickness". As an actual example of buoy deployment G. Ball (personal communication) advises that the Australian Bureau of Meteorology deploy two types of buoys: the FGGE type and SVP type. The FGGE, or spar type buoy is available as either:

- *standard*: with air pressure, air temperature and sea surface temperature, or
- *wind buoy*: with air pressure, air temperature, sea surface temperature, wind speed and wind direction, and comes either:
  –drogued with a weighted line attached to the base, so that the buoy drifts with the sub–surface currents, or
  –undrogued, which drifts with the surface wind and waves.

Figure 4.1.3.1.1 shows the deployment of a standard FGGE drogued buoy from M.V. *Anro Australia* on 28 April 1991. The red markings on the pallet indicate the location of holding bolts removed immediately prior to the deployment and replaced with salt tablets. As the buoy and pallet enter the water, the salt tablets dissolve, releasing the holding straps and allowing the buoy to drift away from the sinking pallet. Figure 4.1.3.1.2 is a schematic of a FGGE wind speed and direction buoy.

The SVP (Surface Velocity Program) buoy was originally developed for oceanography and consists of a surface float, a smaller sub–surface float and a holey sock drogue as shown in the schematic in Figure 4.1.3.1.3. An SVP buoy fitted with a barometer (SVP–B) is a lower cost alternative to the FGGE buoy for meteorological purposes.

Buoys in the ice–free ocean can measure sea surface temperature and salinity and also make measurements of the temperature profile in the ocean to a depth of 200 m or more. A number of buoys have recently carried GPS receivers, which provide a more accurate alternative to the ARGOS Doppler method for determining the location of the buoy.

Because of the very harsh environment experienced around the Antarctic the sensors on a buoy are often duplicated in an attempt to extend its lifetime and to ensure high data quality. Nevertheless, despite the poor conditions, many buoys deployed on sea ice do survive for long periods and eventually, when the sea ice melts, float northwards to joint the main eastward–flowing ocean currents. Some buoys, however, can enter areas of very heavy ice and be crushed between the floes with the loss of the buoy being indicated by the cessation of the transmitted data. Other reasons for buoys being lost include exhaustion of the battery and failure of the transmitter.

The accuracy of data collected by a drifting buoy will clearly not be as good as that of data from a staffed station where the instrumentation can be checked periodically and cleared of rime or other deposition. Nevertheless, improvements in systems over recent years have produced data that are acceptable for most investigations. The accuracy of data collected by the sensors on a group of five buoys deployed in the Weddell Sea during 1990–93, as reported by Launiainen and Vihma (1994) is given in Table 4.1.3.1.1

Parameter	Number of sensors on each buoy	Accuracy
Atmospheric pressure	1	1 hPa
Air temperature	4	$0.05^{o}C$
Relative humidity	2	2%
Buoy hull temperature	1	$0.2^{o}C$
Water temperature	10 or 20	0.1 or $0.05^{o}C$
Wind speed	2	0.3 m s^{-1}
Wind direction	1	5°
Snow depth	1	2 cm

Table 4.1.3.1.1. Meteorological parameters measured by a series of five buoys deployed in the Weddell Sea during 1990–93. Also included are the number of sensors mounted on the buoys and the accuracy of the measurements. From Launiainen and Vihma (1994).

Figure 4.1.3.1.1 Deployment of a FGGE type buoy
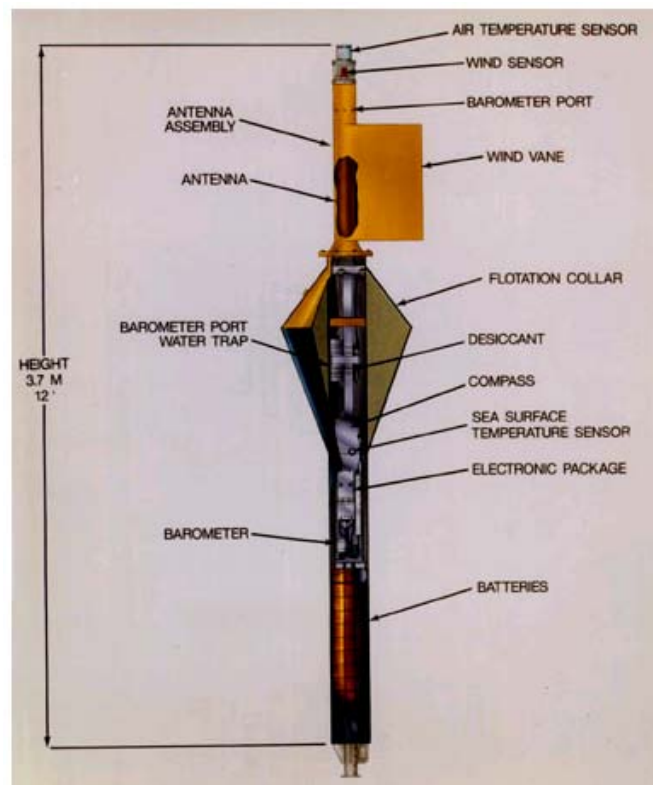
Figure 4.1.3.1.2 Schematic of a FGGE wind speed and direction buoy
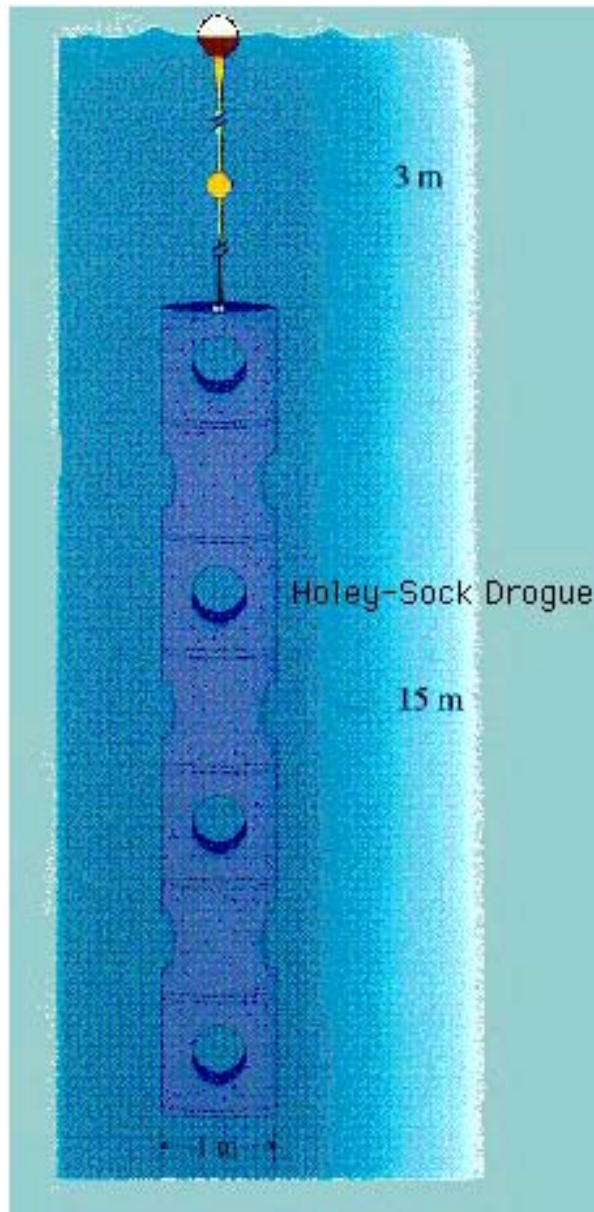
Figure 4.1.3.1.3 Schematic of a SVP type buoy
(Courtesy Meteo–France)

Although the values in Table 4.1.3.1.1 appear acceptable for most applications, a number of major problems can befall sensors on buoys. In common with many humidity sensors used at manned stations, those on buoys perform poorly at low temperatures and are often very inaccurate at temperatures below about –10ºC. Radiation errors are also a major problem with the temperature sensors on many buoys. Ice accretion on the anemometer can be a major problem and, under severe conditions, can stop collection of data or lead to very poor results. A further problem, especially at more northerly latitudes, is that, if the snow accumulation is particularly heavy then the anemometers may become buried and stop working. The experiences of Launiainen and Vihma (1994) suggest that cup anemometers perform less well than do systems based on propellers if ice accretion is heavy.

Data collection

The primary means of collecting data from drifting buoys is via the ARGOS Data Collection System (DCS) on the USA's NOAA polar orbiting meteorological satellites (Schwalb, 1982). Most buoys transmit data every few minutes with data being collected at every satellite pass. As NOAA aim to maintain two polar orbiting satellites in operation at all times and since the satellites have an orbital period of about 100 min, the frequent passes over the polar regions result in buoy data being collected about every hour from all platforms. In an area such as the Weddell Sea, which is at a relatively high latitude, about 20 satellite passes per day can collect data when two satellites are in orbit. This gives a mean interval between passes of 1.2 hr (Launiainen and Vihma, 1994).

The transmissions from the buoys are collected at ground stations after being downloaded from the polar orbiting satellites when they pass over North America or Europe. Here the buoy data are processed to convert the raw observations into geophysical measurements and various quality control checks are carried out. A very important step is to compute the location of each buoy using a knowledge of the location of the satellite that collected the data and the characteristics of the signal from the buoy. Once this has been completed the data are usually coded according to the WMO standard drifting buoy code (FM 18–X BUOY) and input to the GTS at a suitable node.

4.1.3.2   The deployment of drifting buoys in the marginal ice zone

Drifting buoys have been deployed both in association with limited experiments organised within national research programmes and as part of major international projects. Experiments such as the Winter Weddell Sea Project have involved the deployment of buoys by a number of nations and have provided extensive data sets for atmospheric and sea ice research.

An International Programme for Antarctic Buoys (IPAB) has recently been established (http://www.antcrc.utas.edu.au/antcrc/buoys/buoys.html) within the World Climate Research Programme . The goal of this initiative is to coordinate and develop the buoy network to an acceptable density over the coming years. To get a spacing of 500 km between buoys in the sea ice zone would require around 50 buoys to be in place at any time.

At present, a number of nations are involved in the deployment of drifting buoys around the Antarctic, including Australia, Brazil, Finland, Germany, Italy, Japan, South Africa, the UK and the USA. The actual deployment of the buoys on the sea ice or in the ocean usually takes place from research vessels during the austral summer or autumn when they are often engaged in combined research and logistical re–supply operations. Although buoys to be used to study sea ice are usually deployed on suitable ice floes, they can initially be placed in open water and allowed to become frozen into the ice and be carried forward within the advancing pack. Despite the pressure exerted on the buoys during the freezing process, it is usually possible for them to operate successfully under such conditions (Allison, 1989).

Buoys can also be deployed from aircraft, although there is a much greater risk of damage to the instrumentation when this is done. However, the advantages are that many systems can be dropped within a short period of time and the work is not dependent on the tight logistical programmes of research vessels.

Because of the divergent flow of the sea ice around the Antarctic, most buoys drift northwards and emerge into the open water within several months. This means that Antarctic buoys have a much shorter useful life in the ice than do those in the Arctic, although they can provide useful ocean data.

4.1.3.3   Operational applications of drifting buoy data

From the experiences of using data from drifting buoys during the FGGE experiment it became clear that the data gave a significant improvement in the operational forecasts produced by the main meteorological centres (Fitt *et al*., 1979). This was not only in terms of improving the numerical analyses which were able to use the objective measurements but also in the manual analysis process, in which it was found that depression centres could be identified more accurately. More recently Seaman (1994, p.48) has shown "the confirmation of the disproportionately influential role of the drifting buoy network as an argument for its continuance and extension". And even more recently Jacka (1997) has cited examples of the combined effect of high latitude buoys and scatterometer data on GASP analyses and prognoses over the Australian mainland.

Today, buoy observations continue to be an important element of the World Weather Watch system and make a major contribution to analysis and forecasting over the Southern Ocean. For example, in a personal communication Ian Hunter, Deputy Director, Marine Meteorological Services for the South African Weather Bureau advises that "Vessels sailing into high southern latitudes during the Austral summer provide ideal platforms for the deployment of drifting buoys in the Southern Ocean. The importance of these observations in an area where there may be no other surface measurements for over a thousand nautical miles, cannot be overemphasised. NWP models are thus very much dependent on these input data for an accurate analysis and subsequently, accurate forecasts. Whereas it is possible to *estimate* the central pressure of mid-latitude cyclones from satellite imagery, only an *in situ* pressure observation will truly capture a case of rapid intensification, for input into the prediction models.

The SAWB thus places a high priority on the purchase and deployment of drifting buoys. Most are deployed on annual relief voyages to Gough (Section 7.2.3 below) and Marion Islands (Section 7.2.5 below - and SANAE (Section 7.5.5 below). Deployment positions are based on (a) current positions of all barometer drifters in the area (b) drift climatology and (c) preferred areas of development at different times of the year.

Those having to produce forecasts for the Southern Ocean and Antarctica are urged to encourage their respective agencies to invest in the deployment of more 'barometer' drifters - and they themselves should keep a look out for faulty buoy pressures. These should be reported as soon as possible as they may adversely effect global model analysis and predictions."

Unfortunately, at the present time, a number of the observations made by the buoys are still not disseminated on the GTS and a high priority for the future must be to ensure that the observations are made available to the main forecast centres within several hours so that they can be assimilated into the numerical models. Figure 4.1.3.3.1 shows the areal divisions from which drifting buoys and other platforms report through Argos. Countries will monitor drifting buoys which are of prime interest to the particular country. For example, Figure 4.1.3.3.2 shows the buoys which the Australian Bureau of Meteorology monitored on 29 February 2000. A full list of buoys and other platforms is available through the WMO/Argos Cross Reference List at : http://dbcp.nos.noaa.gov/dbcp/wmolist.html.
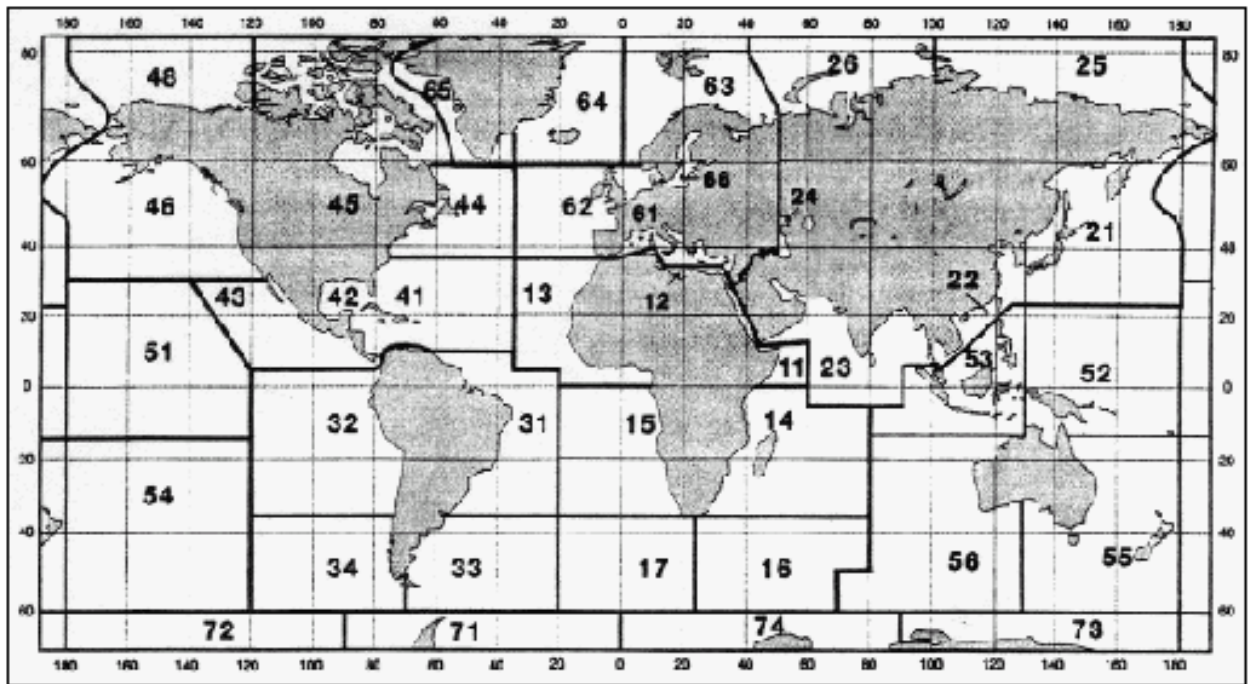
Figure 4.1.3.3.1 Reporting areas for various data platforms including drifting buoys. (The first digit indicates the WMO Regional Association area in which the platform was deployed. The second digit indicates the sub–area of the WMO Regional Association area. (from WMO–No. 306, Manual on Codes, code table 0161)).
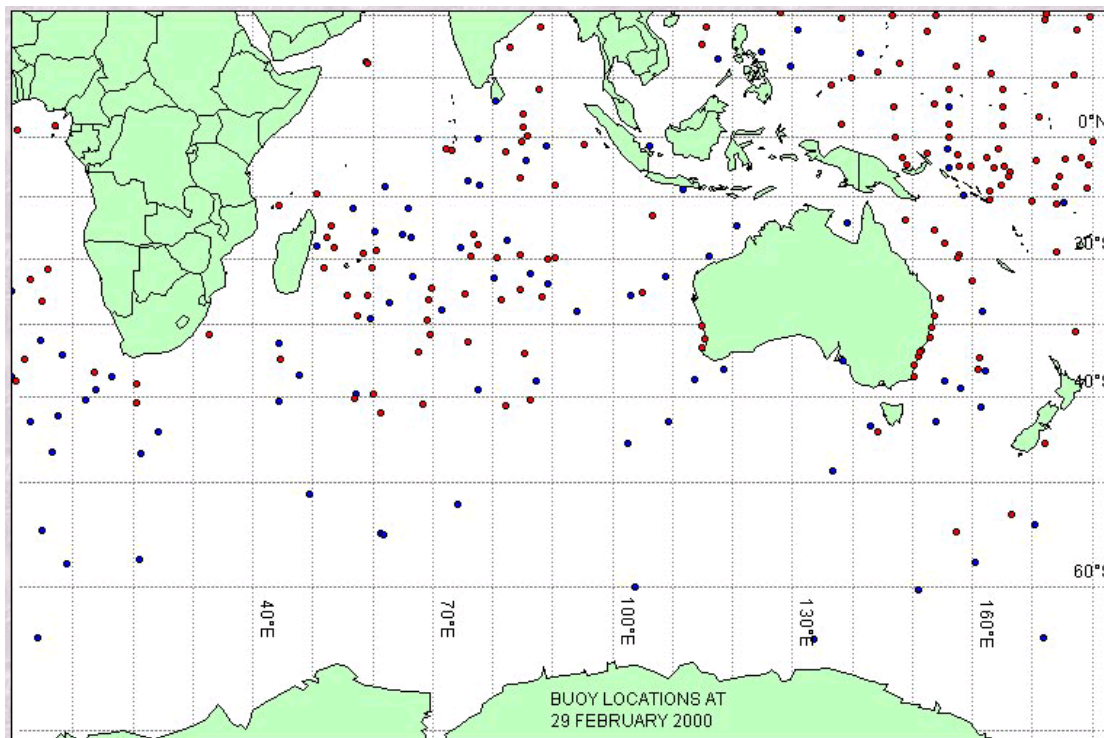
Figure 4.1.3.3.2 A snapshot of drifting buoys which were monitored by the Australian Bureau of Meteorology on 29 February 2000. (Red dots indicated buoys without air pressure sensors, the blue dots represent buoys with air pressure sensors).

4.2   NWP Model fields

4.2.1   Introduction

Numerical weather prediction model output is available for high southern latitude forecast guidance from a wide variety of global forecast models, and will increasingly be available from limited area and mesoscale models. Indeed some of the global models are now approaching the horizontal resolutions that were the domain of mesoscale models only a few years ago. Figure 4.2.1.1 illustrates for example, the domain grid of the Australian Global Assimilation Prediction system model: although the GASP model is not the highest resolution global model available, the present ~75 km grid resolution is approaching the higher end of mesoscale model grid spacings. It has been widely recognised in the mid–latitudes that these models are becoming increasingly accurate and sophisticated and are an essential component of the forecast process. However, in the Antarctic, users have to be aware that the output from the NWP systems cannot be used in the same way as in mid–latitudes. Over the ocean areas around the continent the performance of the models is slightly poorer than in mid–latitudes because of the lack of *in situ* data and the high reliance on satellite sounder data. However, in the interior of the continent the output of the models is of very limited use and the forecaster has to adopt a nowcasting approach. This comes about because of the difficulties in representing the orography of the Antarctic in the models, the fact that satellite sounder data are not used at tropospheric levels and the small number of AWS observations on the GTS. In the Antarctic coastal region therefore the performance of the models drops away very rapidly. These ideas will be discussed further in the following. However, over the ocean there is no intrinsic reason why NWP model forecasts should not be as essential a tool for the Antarctic forecaster as for his/her colleagues in other regions, as shown by studies such as those of Hines *et al.*(1995) and Parish and Bromwich (1998).
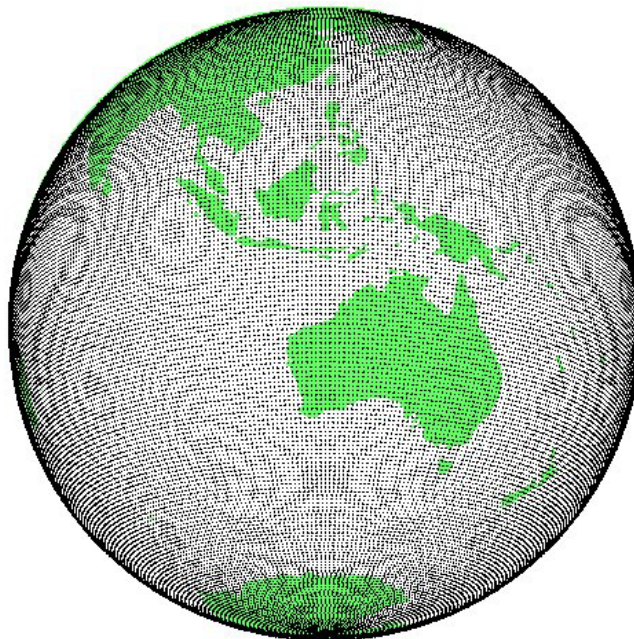
Figure 4.2.1.1   Model domain for the Australian Global Assimilation Prediction system 0.75º (T239) model.

NWP model forecasts can be used by a forecaster as direct guidance, with little interpretation, or can be used to understand why a model may be forecasting, or not forecasting, a particular event. In order to use the models in the latter way, the forecaster should understand the components of the NWP system, the scales resolved, and the physical processes represented. In this way there can be a greater understanding of the strengths and weaknesses of the model's performance. Brief descriptions of the components of a NWP system follow in the next section.

A particular strength of NWP models is that their fields are internally dynamically consistent. Further, all such operational NWP systems include as an essential component a data assimilation system whereby observational data are incorporated into the model so as to provide the most accurate possible initial state for the next forecast. These analyses and model fields can be used as dynamically consistent data sets to diagnose the current and future kinematics and dynamics of the atmosphere. Suggested techniques where the numerical analyses and forecasts can be used to enhance the forecaster's understanding of the numerical guidance follow Section 4.2.2.

4.2.2   Components of an NWP system

The essential components of a NWP system comprise:

- Forecast model
- Data
- Assimilation/initialisation phase

A NWP model numerically integrates the momentum, thermodynamic, and moisture equations to produce a forecast of temperature, humidity, pressure, and the wind field, at a future time. Most models include what are termed the "dynamics" – that component of the model which integrates the equations – and the "physics" in which those processes not explicitly included in the forecast equations are "parameterised" in order to include their effects. These parameterised processes include radiation and its interaction with the Earth and atmosphere, convection, surface processes, and turbulent processes (see Haltiner and Williams, 1980). Moist processes (stratiform rainfall and convection) have been included in the physical parameterisations for many years, but explicit prognostic equations for moisture substance are increasingly being used.

In order for a NWP model to produce an accurate forecast, not only do the model numerics need to be well formulated, and the physical parameterisations represent as accurately as possible the processes occurring in the atmosphere, but also the initial state must be accurately specified. This requires not only that the three dimensional state of the momentum and thermodynamics of the atmosphere be specified, but also an accurate depiction the Earth's orography, surface characteristics (roughness, snow cover, sea ice extent and lead fraction) and sea surface temperature consistent with the model formulation.

The data input typically comprise surface observations from land, and ocean–based platforms, rawindsonde profiles, temperature, humidity and wind data observed or diagnosed from sensors on board orbiting and geostationary satellites, and observations from aircraft. During the assimilation process the model state is corrected to "fit" the observations to within their observational error, so that the resulting fields retain the balance and information content of a short–term forecast based on previous information, but also reflects the information

content of the most recent observations. (In this context, the short–term forecast used to provide the guess field can also be regarded as data.) Observations are subject to complex quality control procedures, usually including gross error checks followed by some form of "buddy checking". The systems also include techniques for elimination of redundant data (highly correlated observations) and complex data selection algorithms so that dense observations of one type do not overwhelm complementary data of another type.

Unfortunately, the data available for use in the Antarctic is inhomogeneously distributed in space and time. The density of surface observations varies from land to sea and is highest around the coast of the continent. Typical data distributions available to an operational NWP system are shown in Puri *et al.* (1998). As the distribution of data, and types of data, are so inhomogeneous, it is necessary to include mass–wind coupling in the analysis so that the mass field is adjusted in the presence of wind only data and vice–versa so that information is inserted in a balanced way into the forecast model, and thus retained during the model's integration. The appropriate statistics for background error correlations and observational error characteristics must also be included. Daley (1991) provides a comprehensive review of the topic. It should be noted that satellite sounder data are not generally used at tropospheric levels across the Antarctic because of the high orography of the continent and the problems of deriving sounding over an ice surface. In addition, the only part of the surface messages from staffed stations and AWSs that is used is the surface pressure data. This is because the wind and temperature data tend to be representative of the local area rather than the synoptic–scale environment.

Until recently, most major NWP centres used forms of multivariate statistical interpolation (Lorenc, 1981) to correct the short–term forecasts (also known as the background field), with data insertion typically every six hours (intermittent data insertion). Recently, though, there has been a trend towards 4–dimensional variational analysis (e.g. : Derber, 1989, Rabier et al, 1998). In such a system, the model state is variationally adjusted to minimise its difference from the observations, subject to the strong constraint that the adjusted state is consistent with the model equations. Some of the advantages of variational data assimilation are that variables such as radiance in a given spectral band, as measured by satellite, can be treated as an observation, rather than needing to first have a temperature "retrieved" from these data, and the addition of the time dimension allows the time–tendency of the model state to match the implicit time tendency of data observed at through the assimilation period.

Initialisation schemes are used after the intermittent data insertion phase to "balance" the analysis fields – that is, to remove dynamic inconsistencies between the mass and the wind fields which may lead to spurious gravity waves (see in Figure 4 of Puri *et al.* 1998) being generated early in the model forecasts. Their removal is desirable so that subsequent data insertions are not adversely affected, and to reduce the spurious prediction of rainfall early in the forecast period. Such schemes can be normal mode initialisation schemes (e.g. Ballish *et al.* 1992), digital filter schemes (Lynch and Huang 1992) or use some form of Newtonian relaxation (eg Davidson and Puri 1992). The variational assimilation schemes include constraints based on the model equations, and so initialisation is implicit in these schemes.

4.2.3   Use of primary model output variables

Forecasters have for many years based their subjective forecasts on analyses of mean–sea level pressure and tropospheric height and wind analyses in pressure coordinates. Implicit in

this thinking are the simple geostrophic relations that result from this choice. The forecast is then based on the knowledge and experience, and on conceptual models of the relations between the isobaric patterns and observed and expected weather elements. The use of NWP model output has tended to follow the same path, with a model forecast MSLP pattern being used as a basis for a subjective forecast of weather elements. With the improving quality of operational NWP systems over the last 20 years, more direct use of model output is advantageous. The precipitation forecasts from NWP models are an example of direct model guidance of a critical forecast parameter, and while further improvement in the skill of these forecasts is needed, the forecasts do contain very useful information (Ebert and McBride, 1997).

The primary variables carried in an NWP model are pressure, temperature, wind components, and humidity. Further, most operational NWP models are formulated with some form of terrain–following vertical coordinate system. Thus it is more direct to use the forecast models' low level wind fields as direct guidance, rather than first use what may be an extrapolation of the model data to a constant pressure or height surface, and then make subjective estimates of wind based on geostrophic relations and knowledge of local effects. (Antarctic forecasters are perhaps less subject to this behaviour than forecasters who habitually deal with areas of lesser relief, as they are well acquainted with the problems of pressure reduction over regions of high orography.) It must also be remembered that many of the significant weather producing systems are highly ageostrophic, and so using geostrophic assumptions is most likely to lead to mis–interpretation of model guidance in the most critical weather situations.

NWP models usually perform reasonably well over the Southern Ocean (although the fine–scale detail can often be in error (Turner *et al.*, 1996a), but the forecaster should not expect them to out–perform their design. For example, global models of the 1980s did not have sufficient resolution to adequately resolve the orographic slopes of the Antarctic plateau. Therefore the forecast fields from these models did not resolve the distortion of the wind fields by these orographic barriers. As the resolution of the models and the sophistication of their physical parameterisations have increased, so the representation of the smaller–scale effects in these models has become more realistic. Forecasters should ensure that changes to operational models are communicated to them so that they can account for changes in the character of the forecast fields.

A simple but very powerful example of the direct use of the model fields is in the identification of cold and warm fronts over the ocean areas around the Antarctic. The MSLP field can be used to diagnose the locations of fronts from the position of pressure troughs in the forecast fields. However, the primary characteristic of a cold or warm front is a zone of enhanced temperature gradient in the atmosphere. Therefore it is far simpler to inspect fields of temperature near the surface to determine the location of fronts than to use the pattern of MSLP contours to infer their location. The wind field shows a cyclonic curvature at a frontal "discontinuity", and so this field can be used to supplement the information from the thermal field. Figure 4.2.3.1 shows a MSLP forecast from the Australian LAPS model over the Southern Ocean. This should be compared with the fields of equivalent potential temperature (θe) and streamlines on the model's lowest sigma (ρ/ρ_{surf}) surface (~ 70 m) in Figures 4.2.3.2 and 4.2.3.3 respectively. The zone of enhanced gradient of θe marking the position of the cold front and wind shear at the front mark the cold front more precisely than does the MSLP field.

A further benefit of this type of approach is to then use the model information about cold frontal structure to understand the patterns of cloud shown (independently) in the satellite imagery (Figure 4.2.3.4), rather than use the cloud imagery to attempt to diagnose the position of the surface front.
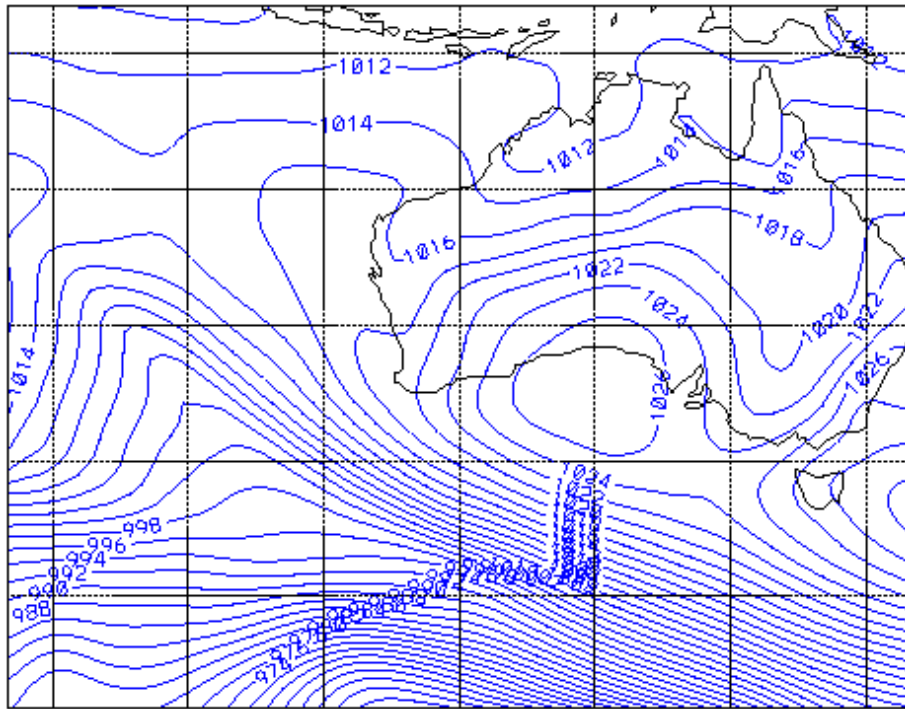
Figure 4.2.3.1   NWP MSLP forecast for 1100 UTC 25 August 1998.
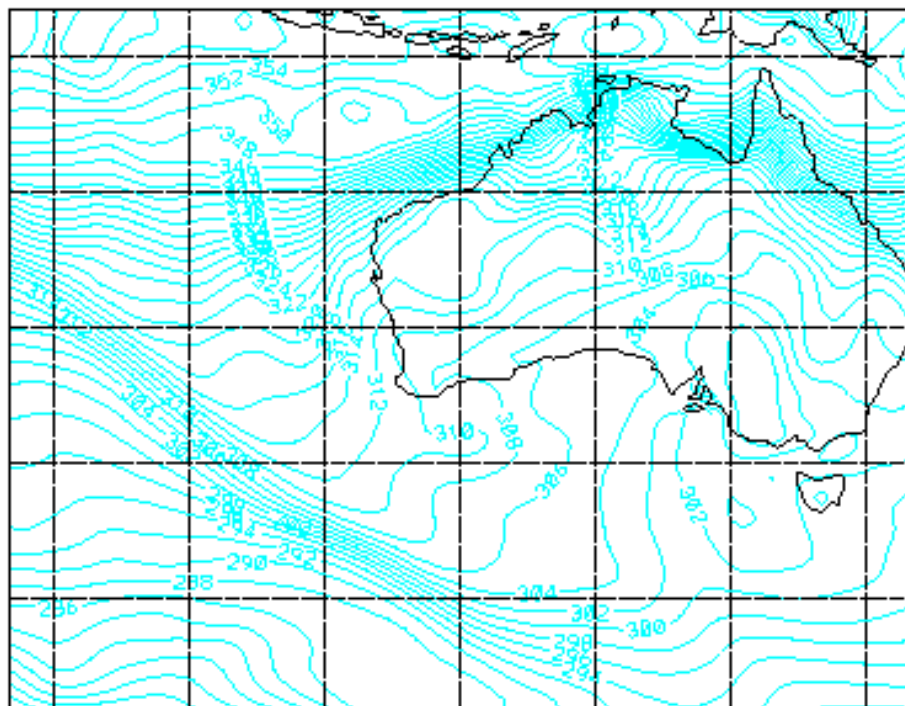
Figure 4.2.3.2   NWP equivalent potential temperature (θe) forecast
for 1100 UTC 25 August 1998 on the model's lowest sigma surface (~ 70 m).
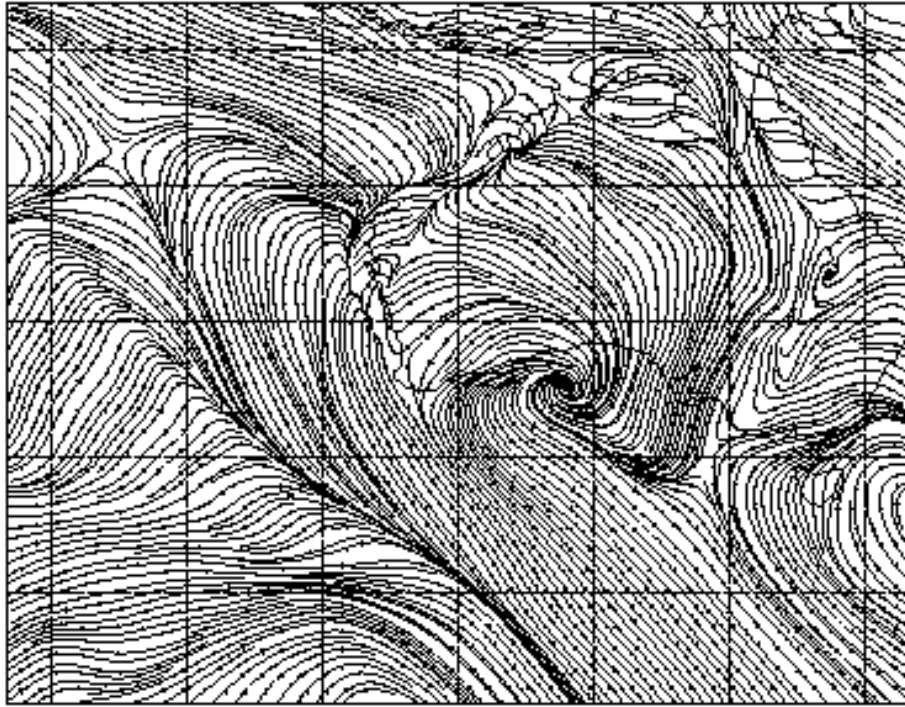
Figure 4.2.3.3   NWP streamline forecast for 1100 UTC 25 August 1998 on the model's lowest sigma surface (~70 m).
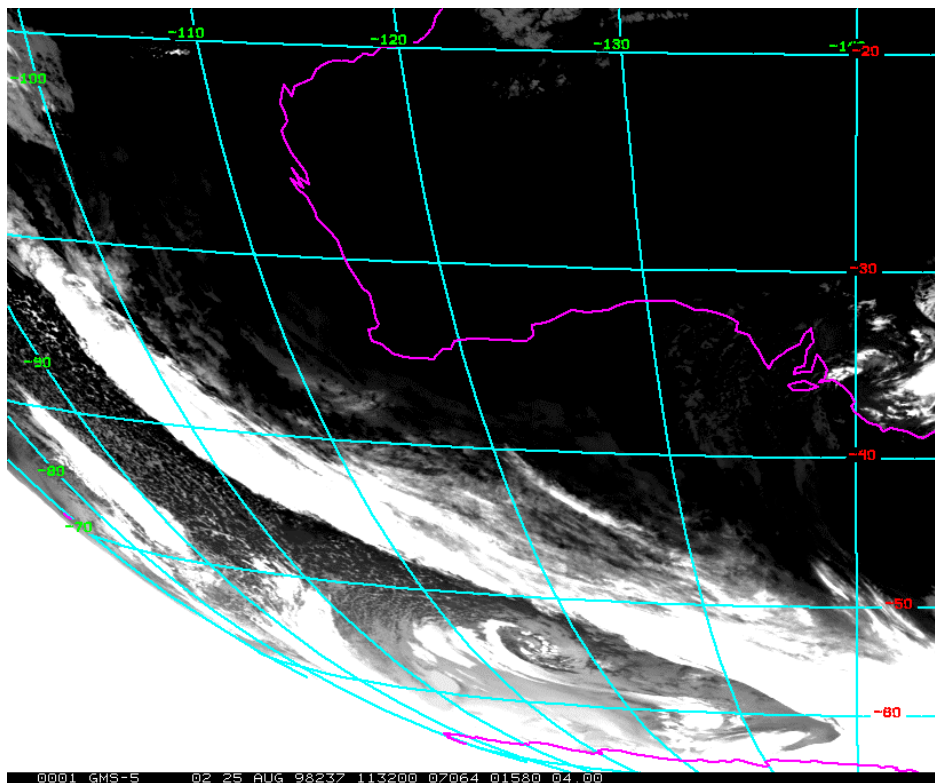
Figure 4.2.3.4   GMS imagery for 1130 UTC 25 August 1998.

4.2.4   Use of conceptual models

Conceptual models of atmospheric systems are widely used to encapsulate the space–time–parameter evolution of weather systems. Perhaps the best known is the polar front theory of Bjerknes and Solberg (1922), but many others exist in the literature. These include isentropic relative flow theory (Green *et al.*1966) and its applications (eg Browning and Harrold, 1970 and Carlson, 1980), and isentropic potential vorticity (IPV) thinking as espoused by Hoskins *et al.*(1985).

The advantage of a good conceptual model is that it enables a meteorologist to visualise a complex atmospheric state. Such conceptual models, when applied to numerical model data, can aid the forecaster's understanding of "why" the model is predicting a certain evolution of the atmosphere. However, forecasters should have a strong understanding of the assumptions or basis of the conceptual model they are using. For example, the conceptual model of cyclogenesis shown by Hoskins *et al.*(1985) (see their Fig 21) has implicit in it that the amplitude and horizontal scale of the "induced circulation" is dependent on the static stability of the atmosphere. Thus the forecaster should be aware of this additional parameter.

Forecasters should also be cautious in applying a conceptual model developed in one geographical area, based on what might have been a relatively small sample of events, to a wider sample of situations than is warranted. While the Norwegian cyclone model has been widely applied, and very successfully, for some 70 years, recent field experiments, such as the Genesis of Atlantic Lows Experiment (GALE) have revealed some distinct differences from this classic model (see Shapiro and Keyser, 1990). Although these conceptual models may be applicable over the Southern Ocean they are rarely of value over the interior of the Antarctic where few 'classic' depressions are found. In addition, recent research has shown that many of the low–pressure systems found within the circumpolar trough have non–standard frontal structure and the conceptual models used in mid–latitudes may not be applicable here.

Conceptual models should not be used to "second guess" the NWP model. An example of such a process would be for a forecaster to subjectively assess the location of vertical circulations in the model using quasi–geostrophic concepts (Bluestein 1993) or by use of jet entrance circulation concepts (Keyser and Shapiro 1986) and then decide that the model has forecast the vertical motion to be misplaced relative to its wind and temperature fields. The model may be in error, but its fields will be internally consistent, and so this form of thinking is flawed. A forecaster can, however, use conceptual models to understand which features resolved by the model are associated with the forecast vertical circulations. Qualitative techniques for separating the forcing of vertical motion in numerical model output into that associated with wave–scale (curvature) and jet streaks (linear acceleration) are described in Keyser and Shapiro (1986), and examples applied to real situations are described in Velden and Mills (1990) and Mills and Russell (1992). Such techniques can enhance the understanding of particular model developments.

4.2.5   Use of independent data – assessing whether the model is "on track"

If the forecast is in error due to deficiencies in initial state specification, there is little a forecaster can do to compensate, due to the non–linearity of the models. There are cases where large errors in the analysis, due to quality control errors, result in imperceptible changes in the subsequent forecast. On the other hand, Rabier *et al.*(1996) describe a case where very small changes in the analysis over North America produced very large changes in

the forecast over Europe in a medium range forecast. This will be especially the case in the Antarctic/Southern Ocean where the lack of data will produce analyses that are poorer than in mid–latitudes. The ensemble forecast approach (see Sivillo *et al.,* 1997 and references therein) is being actively explored to account for uncertainty in initial conditions, but how to use this information to best assist the preparation of a forecast is yet to be determined. Therefore, if forecasters have valid doubts about the quality of the initial conditions, then their subsequent forecasts should represent this uncertainty. However, it may be very difficult to reliably assess the "quality" of the initial analysis.

One means by which the quality of a model forecast can be assessed is to compare the early fields (say up to six hours) against the locations of weather systems in satellite imagery. This will show whether the timing of the developments is essentially on track.

A numerical system will objectively produce a consistent product given the same input data. It can sometimes be difficult for forecasters to reconcile their subjective manual analysis with the numerical product, particularly with somewhere like the Antarctic where there are many local wind systems and mesoscale disturbances. However, it should be remembered that the NWP systems essentially produce synoptic–scale analyses and that few mesoscale features will be represented. This does not mean that the objective analysis is "wrong" – it has been deliberately designed this way to initialise a forecast model. The fact that an objective analysis has not directly taken into account a particular observation may be because an observation was rejected by quality control procedures, not selected, or because the three–dimensional multivariate nature of the analysis has affected the way in which that observation was treated. Clearly a univariate analysis will fit observations more closely than a multivariate system. In addition, the background field will also affect the pattern of the analysis.

Some confidence in the quality of the analysis can be gained if the distribution of data available to the analysis is presented to the forecaster, and if those data rejected by the analysis during quality control are also flagged. This can assist a forecaster to understand why a feature is present or not present in a particular analysis. These products may not be operationally available in the Antarctic, but can and should be. Further, it is almost self–evident that if a significant component of the observational data–base is missing from a given analysis, then the forecast based on that analysis is less likely to be accurate.

A powerful way in which conceptual models can be used to infer whether a NWP model is "on track" is by developing an understanding of what atmospheric features should be present in a given situation. Mills (1997) shows that a small region of enhanced cumulus cloud which could be tracked over the Southern Ocean for some 48 h was related to a region of cyclonic vorticity advection resolved in the assimilated analyses of the Australian Bureau of Meteorology's limited area data assimilation system. The relation between such cloud systems and "cva maxima" has long been known (see Anderson *et al.*1969, Zillman and Price, 1972), and forecasters use them as surrogates for the differential vorticity advection term in the quasi–geostrophic omega equation (Bluestein 1993). Using NWP models, this methodology can be inverted, and the cva patterns in the NWP model can be compared with the "cva clouds" in the satellite imagery. If the independent evidence of the satellite imagery confirms the NWP fields, as was the case in Mills (1997), then there can be some reasonable confidence in the subsequent evolution of the forecast. Another example of this type of technique is described by Mansfield (1994), where water–vapour imagery was used to qualitatively validate the IPV structure of the model atmosphere in the early stages of a forecast. In this case, correctly or incorrectly located jet streaks, as identified by the dry slots in the water–vapour imagery, were reflected in the accuracy of the later stages of medium–range forecasts. Weldon and Holmes (1991) and Bader *et al.* (1995) contain many more examples comparing NWP data with satellite and radar imagery.

These two cases quoted above are only examples of this technique – all independent data can be used to validate the model in this way, and it is a powerful technique for gaining confidence in and understanding of the reasons for a NWP model's prediction.

4.2.6   NWP systems and the Antarctic

From the above it will be realised that while NWP systems have made great advances in recent years the emphasis has often been on improving their performance in the tropics and mid–latitude areas where most of the large centres of population are located. Indeed while there are a huge number of verification statistics on model performance in the extra–polar regions the data available for the Antarctic is relatively limited. Projects such as FROST (Turner *et al.* 1996a), which examined the quality of Antarctic analyses and forecasts, found that the models were fairly good over the ocean areas but lacked the mesoscale and small synoptic–scale detail that is often what concerns the forecaster. Other studies, for example Leonard *et al.*(1997) who examined the performance of the UK Met. Office model over the Antarctic, found that temperatures over the interior were too cold resulting in the katabatic winds being too strong. However, as models are developed and new parameterisation schemes introduced the nature of the errors can change since the model developers tend to check the results of their changes most carefully in the extra–polar regions.

While small, rapid developments in the Antarctic can easily be missed by the NWP systems it should not be forgotten that they can successfully predict some major storms up to a week in advance. For example, Pendlebury and Reader (1993) described the forecasting several days in advance by the ECMWF model of a very deep storm that affected Casey Station giving wind gusts up to 66.9 m s^{-1} (130 kt).

In summary, a forecaster should always be aware of the strengths and weaknesses of NWP model output in the Antarctic. It can be extremely valuable in giving guidance on the broad–scalesynoptic environment but should be used in conjunction with satellite imagery and *in situ* data within the forecasting process.

4.3   Satellite data

4.3.1   Visible and infra–red satellite imagery

Visible and infra–red satellite imagery is one of the most powerful tools available to the forecaster since it allows the preparation of analyses in areas where no *in situ* observations are available, it can be used to determine whether NWP forecasts are developing according to plan and can be used to extrapolate the movement of cloud features in the production of short–period forecasts (nowcasts). In the early days of forecasting in the Antarctic only low resolution hardcopy imagery was available but today many stations have receivers for high resolution, digital imagery that can be viewed and manipulated on a computer.

The most commonly used imagery for forecasting in the Antarctic is that from the Advanced Very High Resolution Radiometer on the USA's NOAA series of weather

satellites. These platforms are the operational civilian polar orbiting satellites operated by the National Oceanographic and Atmospheric Administration, who usually maintain two spacecraft in orbit at all times. The satellites are in a low–altitude (approximately 800 km) altitude orbit and make just over 14 orbits of the Earth each day, so they provide frequent coverage of the polar regions. The AVHRR is a useful instrument for forecasting since it has such a good data coverage by virtue of its medium horizontal resolution of 1 km and a wide, 3000 km swathe of data. With the five visible and infra–red channels available (Table 4.3.1.1) the AVHRR is a very valuable source of data for monitoring cloud, the oceans, sea ice and land ice. Data from the instrument are broadcast continuously by the satellites in real time in two forms. First, the full resolution five–channel data are broadcast as part of the High Resolution Picture Transmission data stream at a rate of 665 kbps for collection by stations with a steerable antenna. Secondly, a reduced resolution (4 km) Automatic Picture Transmission broadcast is made of one visible and one infra–red channel at a data rate that can be taken by very simple receivers with only an omni–directional, helical antenna.

Channel Number	Central wavelength	Applications
1	0.6 μm	Monitoring cloud and sea ice during the day.
2	0.9 μm	Similar to channel 1. The difference between channels 1 and 2 is valuable for minimising the effect of cloud in sea ice observation.
3	3.7 μm	Detection of water droplet clouds over ice during the day. Used in night–time sea surface temperature (SST) algorithms.
4	11 μm	Year–round observing of cloud. Computation of SST, ice surface temperature and cloud top temperature.
5	12 μm	Similar to channel 4. The difference between channels 4 and 5 is useful in detecting semi–transparent cirrus. Used with channel 4 in SST algorithms.

Table 4.3.1.1   AVHRR channels on the USA's NOAA series of satellites and typical applications in Antarctic meteorology.

The Defense Meteorological Satellite Program series of satellites are the military equivalent of the NOAA spacecraft and are operated by the USA Department of Defense. As with the NOAA series, there are usually two spacecraft operational at any time at an orbital height of about 800 km. The imager on these spacecraft is the Operational Linescan System (OLS), which has a horizontal resolution of about 0.5 km and a swathe width of over 3000 km. The OLS differs from the AVHRR in having only two channels – a broadband visible channel and a thermal infra–red channel (Table 4.3.1.2).

Satellites of the Russian Meteor series of polar orbiting weather satellites began to be launched in the 1970s by the USSR and provide a useful supplement to the data from the USA's spacecraft. They are at a relatively high altitude of approximately 1200 km and there are usually two spacecraft in orbit at any time. Although the spacecraft carry a high–resolution (1.5 km) radiometer and, occasionally, an Earth resources instrument, it is the APT transmissions, which are in a similar format to the American broadcasts, that are usually received in the Antarctic.

Channel Number	Wavelength (μm)	Applications
1	0.4 – 1.1	A broadband visible channel for observing cloud, sea ice and land ice.
2	10.5 – 12.6	A thermal infra–red channel for monitoring of cloud and the surface.

Table 4.3.1.2   OLS channels on the DMSP satellites.

In some sectors of the Antarctic the imagery from the geostationary satellites, which are located around the Equator, can be used as an aid to analysis and forecasting, even though the Antarctic continent is at the extreme limits of the imagery. The data can be used as far south as about 70º S at the longitudes where the satellites are located, which means that the GMS imagery is useful near Casey and Mawson and the Meteosat data shows the area around Neumayer. Even though the imagery is stretched in the north–south direction the high frequency with which the imagery is provided make it a useful tool, allowing movie–loops to be created. The geostationary satellites also provide 'water vapour imagery' from around 6.7 μm in the infra–red, which can provide information on the air flow in the mid– to upper–troposphere.

The primary application of satellite imagery is to provide information on the location of synoptic and mesoscale weather systems, frontal bands and areas of cloud over the continent and surrounding sea areas. A typical example of visible–wavelength (AVHRR channel 1) imagery is shown in Figure 4.3.1.1. Here a major depression can be seen over the Bellingshausen Sea, revealed by the swirl of frontal cloud that extends from the centre of the low towards lower latitudes. Because the unfrozen ocean has a very low albedo and the cloud much higher values, the details of the cloud band are very clearly revealed and an analyst can easily determine the centre of the depression and the location of the front. Similarly, the difference between the albedo of the ocean and that of sea ice allows the accurate determination of the extent of the ice, provided that it is not covered by thick cloud. Such albedo differences can also be exploited for routine monitoring of iceberg calving, the extent of the ice shelves and the opening of ice–free areas near the coast (polynyas).

At night and during the winter months when there is no solar illumination, use must be made of the thermal infra–red (TIR) imagery which provides data on the temperature of the surface and cloud tops. An example of 11 μm TIR imagery for the situation shown in Figure 4.3.1.1(a) is illustrated in Figure 4.3.1.1(b). Here the sea surface temperatures over the Bellingshausen Sea are relatively high while the cloud top temperatures of the frontal band are much lower, providing good resolution of the structure of the cloud associated with the depression. Infra–red imagery is excellent for observing the major weather systems which have high, cold cloud associated with them but is less useful for detecting areas of cloud that have a similar temperature to the surface. Under these conditions it may be impossible to differentiate the cloud from the surface and multi–spectral techniques, have to be employed. Nevertheless, TIR imagery has found many applications in the Antarctic and some that have emerged recently are the investigation of the katabatic drainage flow via warm signatures on the ice shelves, the study of mesocyclones and the determination of the motion of sea ice.
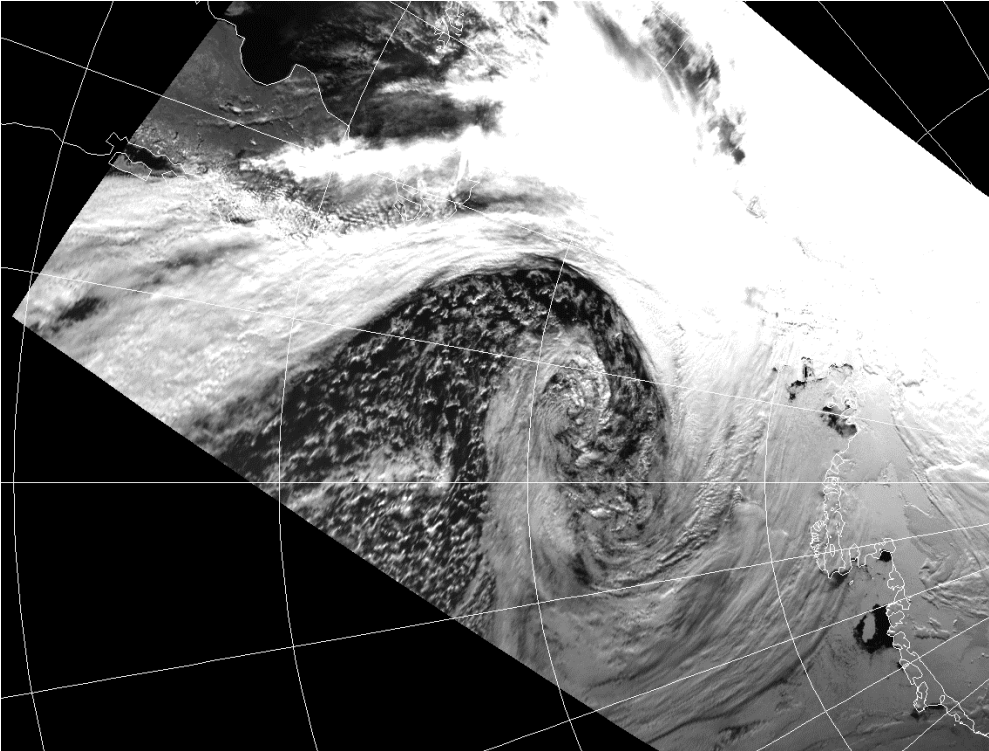
(a)
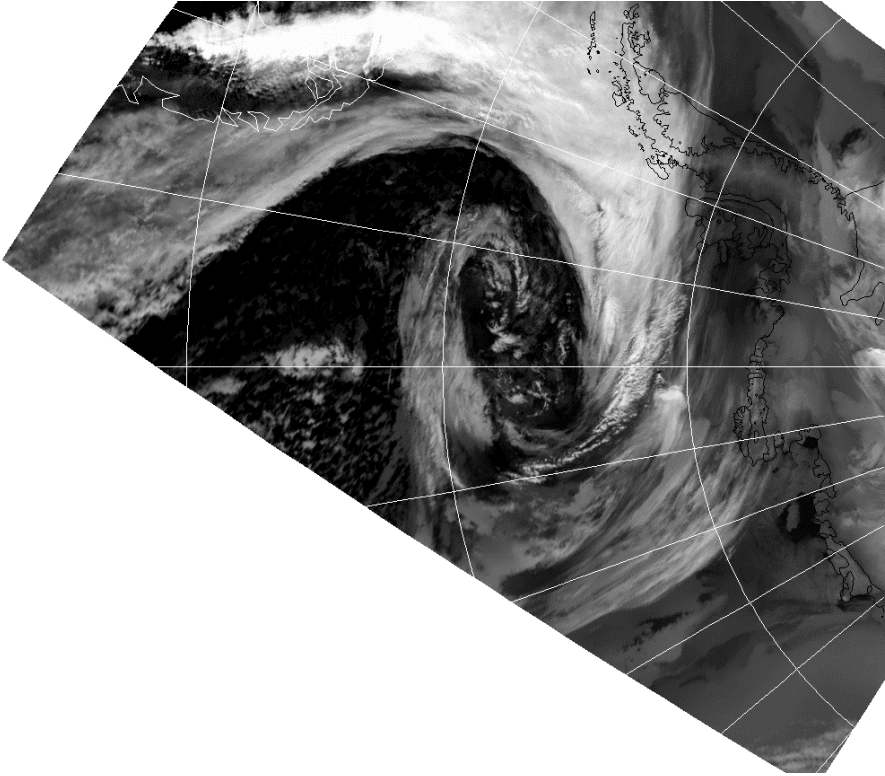
(b)
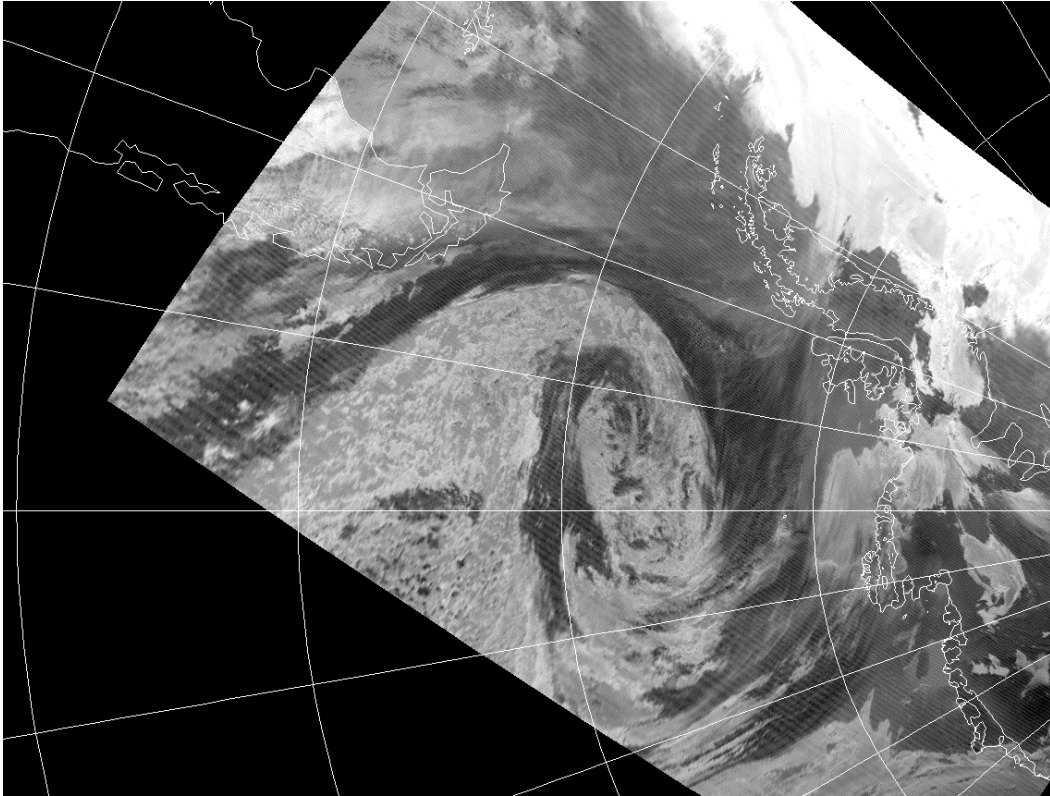
(c)

Figure 4.3.1.1 A major depression over the Bellingshausen Sea observed with
a) visible (0.6μm), b) 11 μm and c) thermal infra–red (3.7 μm) AVHRR imagery.

Over the last few years other wavelengths in the infra–red part of the spectrum have been
used in addition to the TIR data. In particular, imagery at 3.7 μm has proved to be of great
value for separating different types of cloud. The 3.7 μm data for the case already discussed
above are shown in Figure 4.3.1.1(c). During the day, imagery at this wavelength contains a
combination of emitted terrestrial radiation and reflected solar radiation, which complicates
the interpretation of the data. At night, with no solar component, the imagery is very similar
to TIR data and can be interpreted in much the same way. During the day, the reflected
component is dominant and the imagery primarily contains information on the albedo of the
cloud and surface at this wavelength. At first glance the image in Figure 4.3.1.1(c) appears
rather strange because the reflectivity of some of the surfaces is very different from that in the
visible part of the spectrum. For example, while the unfrozen ocean appears dark and clouds
composed of water droplets have a high albedo, all ice, whether it is in the form of land ice,
sea ice or ice crystal clouds, has a very low albedo and appears black. This results in the low
cloud associated with the depression appearing white, while the higher cloud composed of ice
crystals looks black. It can be seen in Figure 4.3.1.1(c) that the snow and ice on the surface of
the continent appear black and resemble the ocean, which makes it difficult to detect the
coastline. However, because clouds composed of water droplets appear white, even when they
are supercooled, it is very easy to detect them over the continent during the day. Imagery at
this wavelength is therefore very useful as an aid to forecasting cloud movement over the
continent, in the detection of fog, and in cloud analysis within research investigations.

4.3.2 **Synthetic Aperture Radar imagery**

A limitation of AVHRR sensors is that the wavelengths used are affected by cloud. In recent years Synthetic Aperture Radar (SAR) imagery has become available. The SAR is a powerful microwave instrument that transmits and receives signals to "see" through clouds, haze, smoke, and darkness, and obtains high quality images of the Earth in all weather, day or night. This provides significant advantages in viewing the Earth under conditions that preclude observation by aircraft or optical satellites. As an example, using a single frequency, C-Band, the Canadian Space Agency RADARSAT SAR has the unique ability to shape and steer its radar beam over a 500 km range. Users have access to a wide variety of beam selections that can image swaths from 45 to 500 km width, with resolutions from 8 to 100 m and at incidence angles from 10 to 60 degrees. (See http://radarsat.space.gc.ca/)
Although the satellite's orbit path is repeated every 24 days, RADARSAT can provide daily coverage of the Antarctic, view any part of Canada, for example, within three days, and achieve complete coverage at equatorial latitudes every six days using the 500 km swathe. RADARSAT provides complete global coverage with the flexibility to support specific requirements: for example, operators of relief vessels negotiating heavy pack ice might find it cost-effective to have SAR imagery available for navigation purposes. As an example of the detail provided by SAR imagery Figures 4.3.2.1 and 4.3.2.2 are from the Antarctic Mapping Mission page at http://radarsat.space.gc.ca/ . Figure 4.3.2.1 is a low-resolution version of the first seamless mosaic of Antarctica, which was compiled from RADARSAT SAR images acquired in September and October 1997. They were acquired as part of the RADARSAT Antarctic Mapping Project which is a collaboration between the U.S. National Aeronautics and Space Administration and the Canadian Space Agency to completely map the Antarctic with RADARSAT-1. (The mosaic was created at the Byrd Polar Research Center using a mapping system developed by Vexcel Corporation. The Alaska SAR Facility processed all of the raw signal data to images. The Jet Propulsion Laboratory developed the mission acquisition plan. In addition, the project received assistance from the National Science Foundation and the National Imagery and Mapping Agency). Figure 4.3.2.2, a view of the Lambert Glacier, is one of the high resolution images (available at http://radarsat.space.gc.ca/)
For another excellent example of the imagery from SAR instruments see:
http://www.antcrc.utas.edu.au/antcrc/research/polar/seaice/Rob_Massom//Rob_Ninnis_Text.html

4.3.3 **Antarctic Composite Satellite Images**

In late October, 1992, the Antarctic Meteorological Research Center (AMRC), at the Space Science and Engineering Center (SSEC) University of Wisconsin–Madison began the generation of a composite satellite image over Antarctica and the Southern Ocean (for examples see Figures 1.2 and 4.3.3.1). These mosaics combined infra–red (~11.0 μm) window channel imagery from both geostationary and polar orbiting satellite platforms. The AMRC employed the collection of real–time data located at the SSEC data centre and from the AMRC office in the Crary Science and Engineering Center at McMurdo Station to fuse GOES, METEOSAT, GMS, NOAA and later DMSP imagery. The composite is generated every three hours with imagery from the various satellites. Data are only included if they are within 50 min either side of the top of the synoptic hour for which the composite is generated. This ensures that older data are not included into the composite images. The composite is

produced at 10 km resolution in polar stereographic projection centred at South Pole with standard latitude of 60º S and standard longitude of 140º W. The image is purposely not orientated grid north, as most maps and charts of Antarctica are referenced. This allows all of New Zealand to be included in the composite image to support the United States Antarctic Programs (USAP) intercontinental flights between Christchurch, New Zealand and McMurdo Station, Antarctica.

The composite images offer a unique perspective of the Antarctic and the Southern Oceans. Animations of the composite images reveal the evolution of weather systems on the synoptic and even sub–synoptic scale. The applications of the composite towards forecasting include:

- Diagnose of the current synoptic weather situation (satellite implied long wave pattern, short wave features, low–pressuresystems and cloud patterns).
- Monitoring of synoptic and sub–synoptic weather features for development trends (low–pressure systems, even some mesolow–pressure systems, etc.)
- Verification of numerical weather prediction model analysis

These and other important meteorological phenomena (such as exchange and transport of air masses around the Antarctic and Southern Ocean, evidence of blocking patterns, etc.) are important for Antarctic weather forecasting.
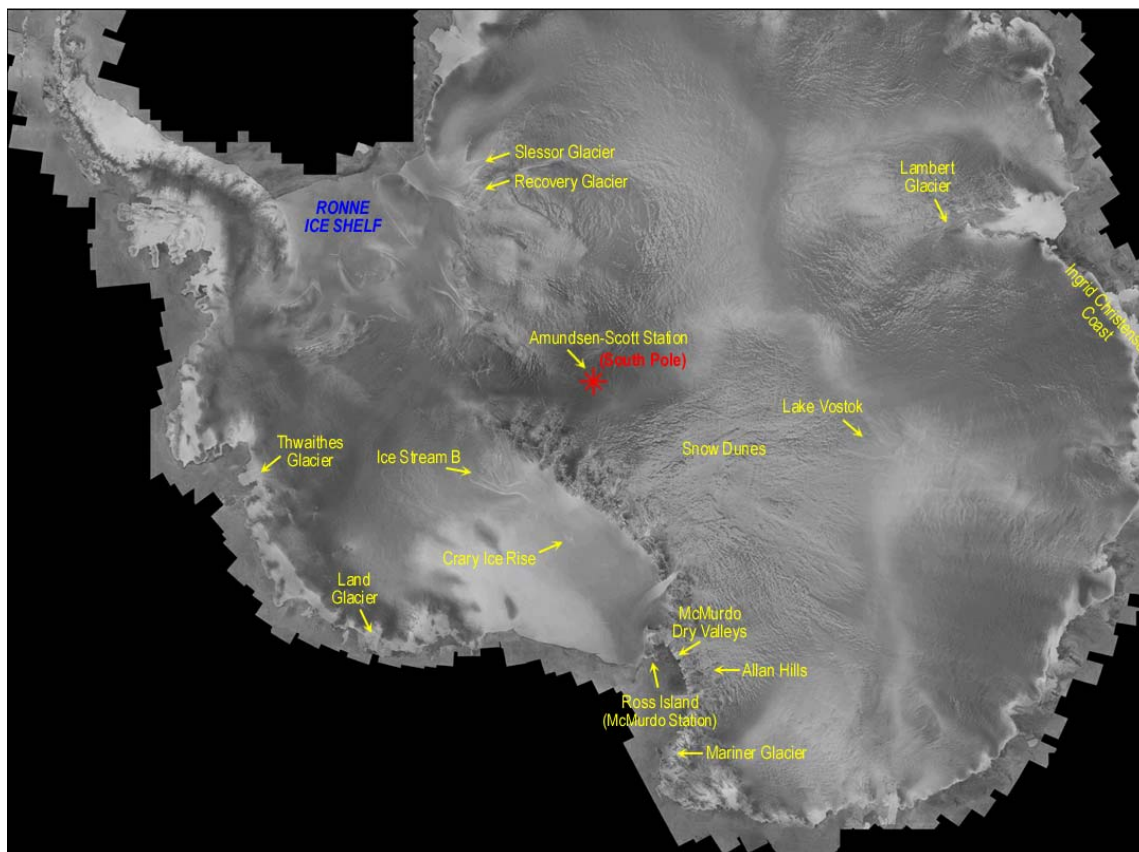
Figure 4.3.2.1   A low-resolution version of part of the first seamless mosaic of Antarctica, which was compiled from RADARSAT SAR images acquired in September and October 1997. The places labeled in yellow may be seen in higher resolution, for example See Figure 4.3.2.2. (Image © Canadian Space Agency http://radarsat.space.gc.ca/)

Figure 4.3.2.2   A high resolution SAR image of the Lambert Glacier. (See Figure 4.3.2.1 for location). Image © Canadian Space Agency

4.3.4   Scatterometer winds

The lack of meteorological data over the Southern Ocean presents a serious problem to the Antarctic meteorologist, both for weather forecasting and for numerical prediction models. Arguably this lack of data represents the primary limiting factor in our ability to forecast Antarctic and Southern Ocean weather. However, with the advent of satellites, the task has become somewhat easier. Sections 4.3.4.1 to 4.3.4.4 examine briefly the data from the scatterometer instrument on the European Space Agency's (ESA) Earth Resources Satellites ERS–1 and ERS–2 while Section 4.3.4.5 briefly discusses data from the QuikSCAT satellite.

The scatterometer is an active microwave instrument capable of detecting small ocean–surface ripples formed by the surface wind thus allowing the determination of surface wind speed and direction. Variations of the scatterometer were flown on Seasat (1978), ERS–1 and ERS–2 (1991–present) and ADEOS (1996–97). Several future missions are proposed. The systems on–board the ERS–1 and ERS–2 satellites are depicted in Figures 4.3.4.1 and 4.3.4.2.

ANTARCTIC COMPOSITE INFRARED IMAGE FROM GOES-8, GOES-10, GMS-5, METEOSAT-7, NOAA-12, NOAA-14, DMSP 5 NOV 98 AT 21:00 UTC (AMRC:SSEC:UW-MADISON)
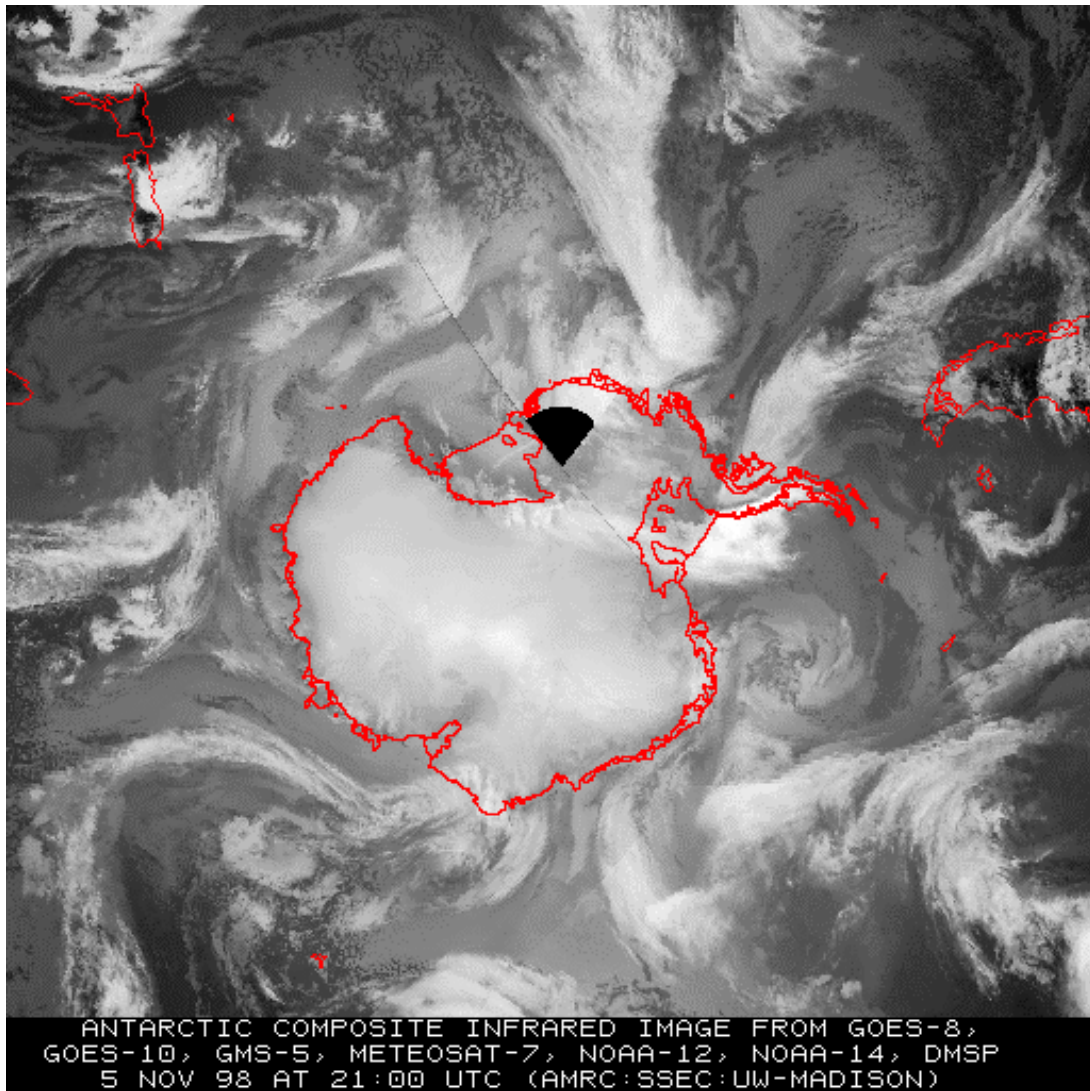
Figure 4.3.3.1   A sample Antarctic composite infra–red image from 21 UTC on 5 November 1998 depicting the storms that circulate around Antarctica.

4.3.4.1   <u>Brief overview of the data type</u>

The scatterometer instrument transmits a microwave pulse towards the Earth's surface. The emitted pulse is broad and aligned out to the right–hand side of the satellite track. The illuminated area of the ocean surface is 500 km wide, the closest edge 200 km from the sub–satellite track.

A calm, glassy ocean surface will reflect the microwave pulse out to space with negligible scattering back in the direction of the satellite. An ocean surface roughened by

strong winds will scatter the microwave pulse in all directions, including back towards the satellite. There is a close relationship between backscatter and 10 m wind speed over the ice–free ocean. However, there are problems: the backscatter patterns from up–wind and down–wind directions are often too similar for an unambiguous solution. Experimental studies have shown that more information is required before perfect quality wind data can be obtained.

Figure 4.3.4.1.1 shows an example of scatterometer data from the ERS–1 satellite superimposed on the overlaid with forecast 75 m wind barbs from the Australian GASP system. The scatterometer winds represent estimates at 10 m above the ocean surface. They are shown in this diagram alongside 75 m wind estimates from the Australian GASP model. An example of erroneous wind direction in the scatterometer data can be seen in this figure. Most meteorological centres now use a NWP background field to verify scatterometer wind direction.

4.3.4.2   Data uses

Several NWP systems now assimilate scatterometer data in real time. Most published studies report a small positive impact on analysis and forecast quality with the inclusion of scatterometer winds. In data sparse areas, the Southern Ocean in particular, a clear improvement in numerical analyses has been identified with the inclusion of scatterometer data.

Although there is no direct read out of scatterometer data available in the Antarctic, the data are assimilated routinely into the ECMWF global model. Trials have been conducted in the US (NCEP global model) and Australia (GASP global model). Scatterometer winds can assist greatly with manual, subjective mean sea–level pressure analysis of the Southern Ocean. They are most valuable for the exact identification of fronts, low–pressure centres, and, in particular, multi–centred lows. They are useful for forecasting for ships at sea and give an accurate estimate of wind speed for that purpose.

4.3.4.3   Data quality

Real time ERS–2 data from ESA are accurate to ±2.0 m s^{-1} or 10%, whichever is greater, for wind speeds in the range 1 to 28 m s^{-1} (~2 to 54 kt). (At high wind speed the signal becomes saturated). Wind direction accuracy is $\pm20º$. Wind data processed off–line at the French Research Institute for the Exploitation of the Sea (IFREMER) are claimed to have a similar accuracy.

4.3.4.4   Data availability

Near real–time scatterometer data from ERS–2 are sent to meteorological agencies world–wide via the Global Telecommunications System. See http://www.esa.int for details. IFREMER data are re–processed data and are available on CD–ROM. See http://www.ifremer.fr/anglais for details. Data from NSCATT, the NASA instrument flown on–board the ADEOS satellite, can be obtained from NASA. See http://sapient.jpl.nasa.gov for details.
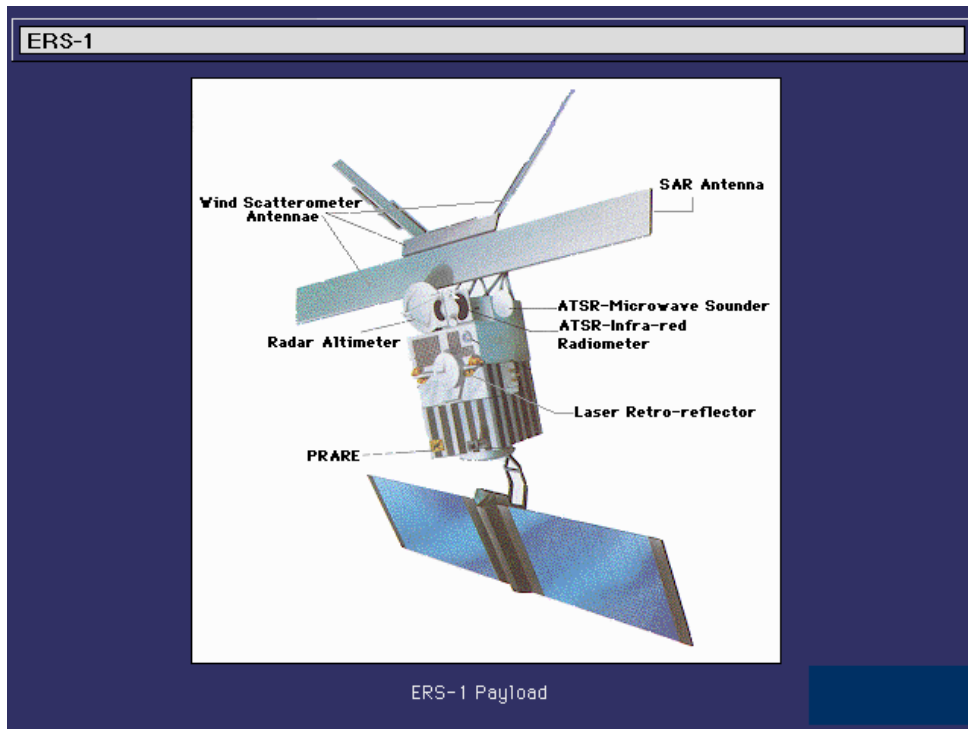
Figure 4.3.4.1 The ERS–1 payload (similar to ERS–2). Reproduced from the ESA world wide web page http://www.esa.int.
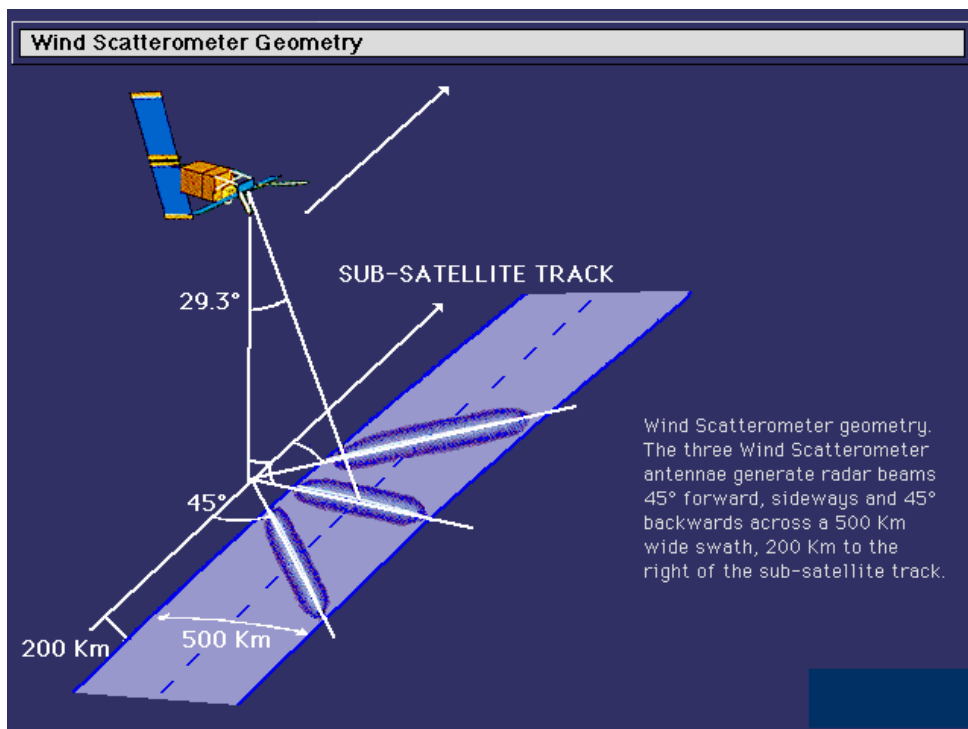
Figure 4.3.4.2 Schematic diagram of the scatterometer instrument geometry on the ERS–2 satellite. Reproduced from the ESA world wide web page http://www.esa.int.
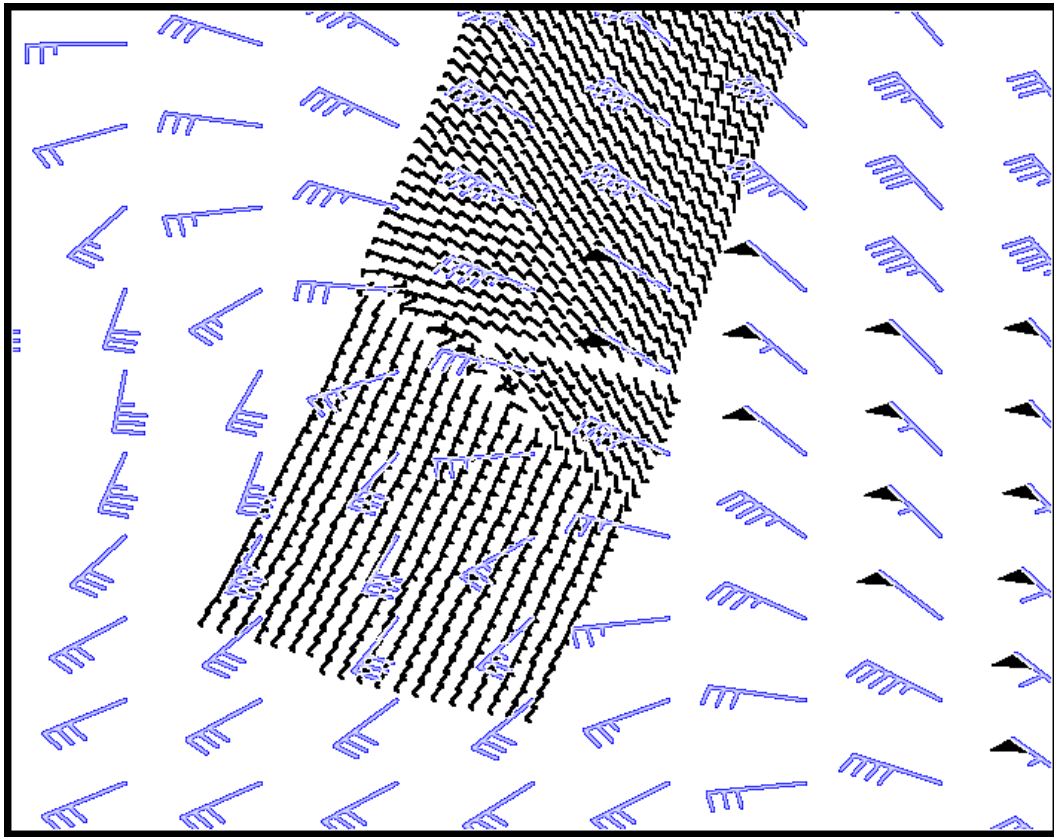
Figure 4.3.4.1.1 An example of a swathe of ERS–1 Scatterometer wind data, over the South Atlantic Ocean, overlaid with forecast 75m wind barbs from the Australian GASP system. The scatterometer swathe is 500km wide. A wind front can be easily identified in the scatterometer data. An example of erroneous wind direction in the scatterometer data can also be seen near the centre of the figure.

4.3.4.5   QuickSCAT data

The QuikSCAT mission, launched on 19 June 1999, is a "quick recovery" mission to fill the gap created by the loss of data from the NASA Scatterometer (NSCAT). For an excellent overview of this mission the reader is referred to the NASA/Jet Propulsion Laboratory (JPL) web site at: http://winds.jpl.nasa.gov/news/newsindex.html. .

From the above web site we learn that "The SeaWinds instrument on the QuikSCAT satellite is a specialized microwave radar that measures near–surface wind speed and direction under all weather and cloud conditions over the Earth's oceans. SeaWinds uses a rotating dish antenna with two spot beams that sweep in a circular pattern. The antenna radiates microwave pulses at a frequency of 13.4 GHz across broad regions of the Earth's surface. The instrument collects data over ocean, land, and ice in a continuous, 1,800 km–wide band, making approximately 400,000 measurements and covering 90% of the Earth's surface in one day". Wind speed measurements in the range 3 to 20 m s^{-1} have an accuracy of 2 m s^{-1} while wind direction has an accuracy of 20 degrees. Wind vectors are retrieved with a resolution of 25 km.

Figure   4.3.4.5.1   (from   http://winds.jpl.nasa.gov/news/wind_ice_fig_6.html) demonstrates the capability of the SeaWinds instrument on the QuikSCAT satellite in monitoring both sea ice and ocean surface wind. The grey–scale image of normalized radar back scatter shows various kinds of ice in Antarctica. The map (including both ice and wind) is produced from one day, July 21, 1999, of QuikSCAT observations.
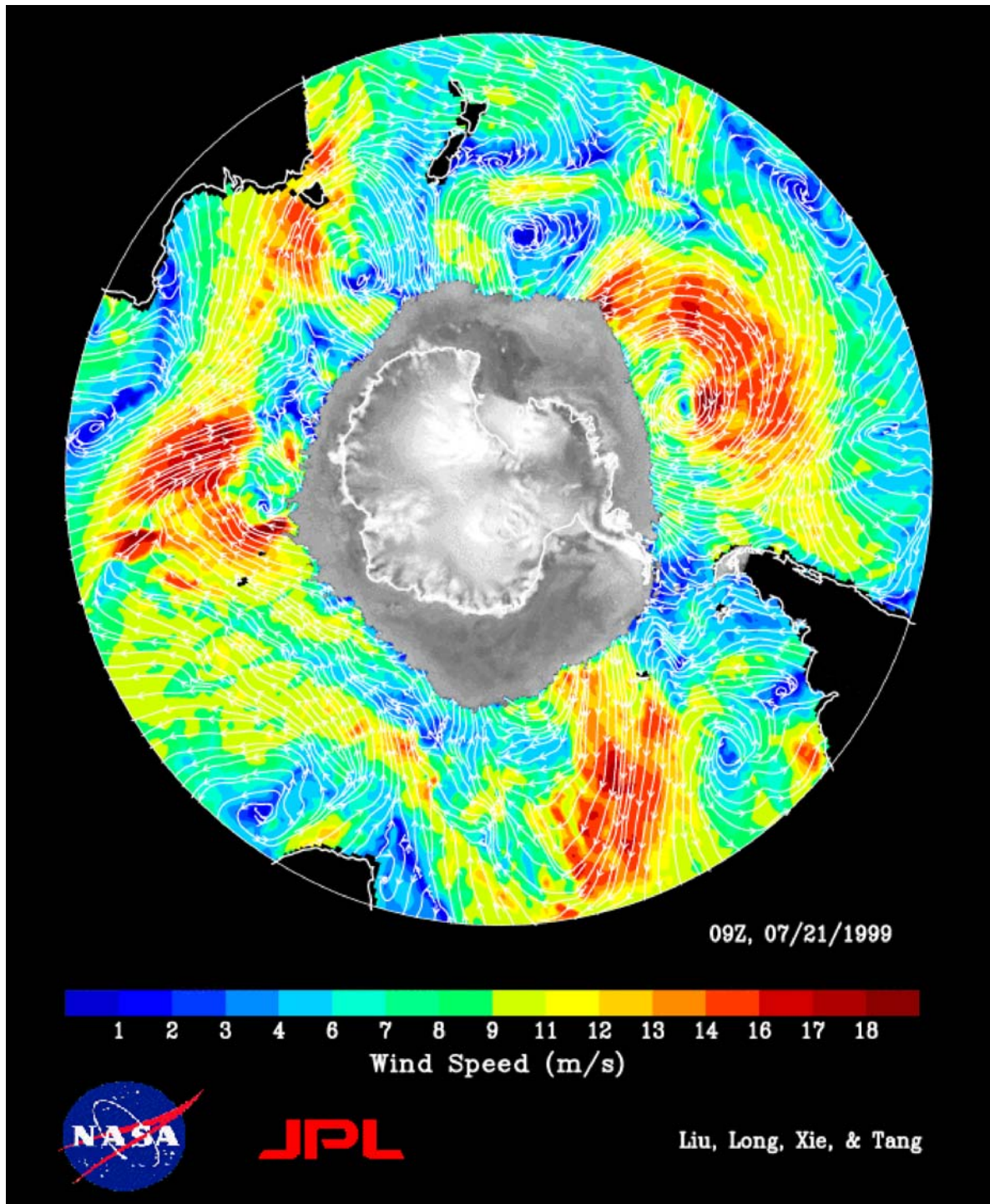
Figure 4.3.4.5.1   One day, July 21, 1999, of QuikSCAT interim observations. The Antarctic continental mass is outlined in white. The grey area outside the land mass is occupied by sea ice. Outside of the ice, white streamlines representing wind direction are overlaid onto the color image of wind speed distribution.

Figure 4.3.4.5.2 (via http://winds.jpl.nasa.gov/news/antarctica.html) shows the utility of QuikSCAT to monitor the formation and life cycle of large icebergs. Note that B–15 has only recently formed and is discussed in Section 2.7.3.3 above.
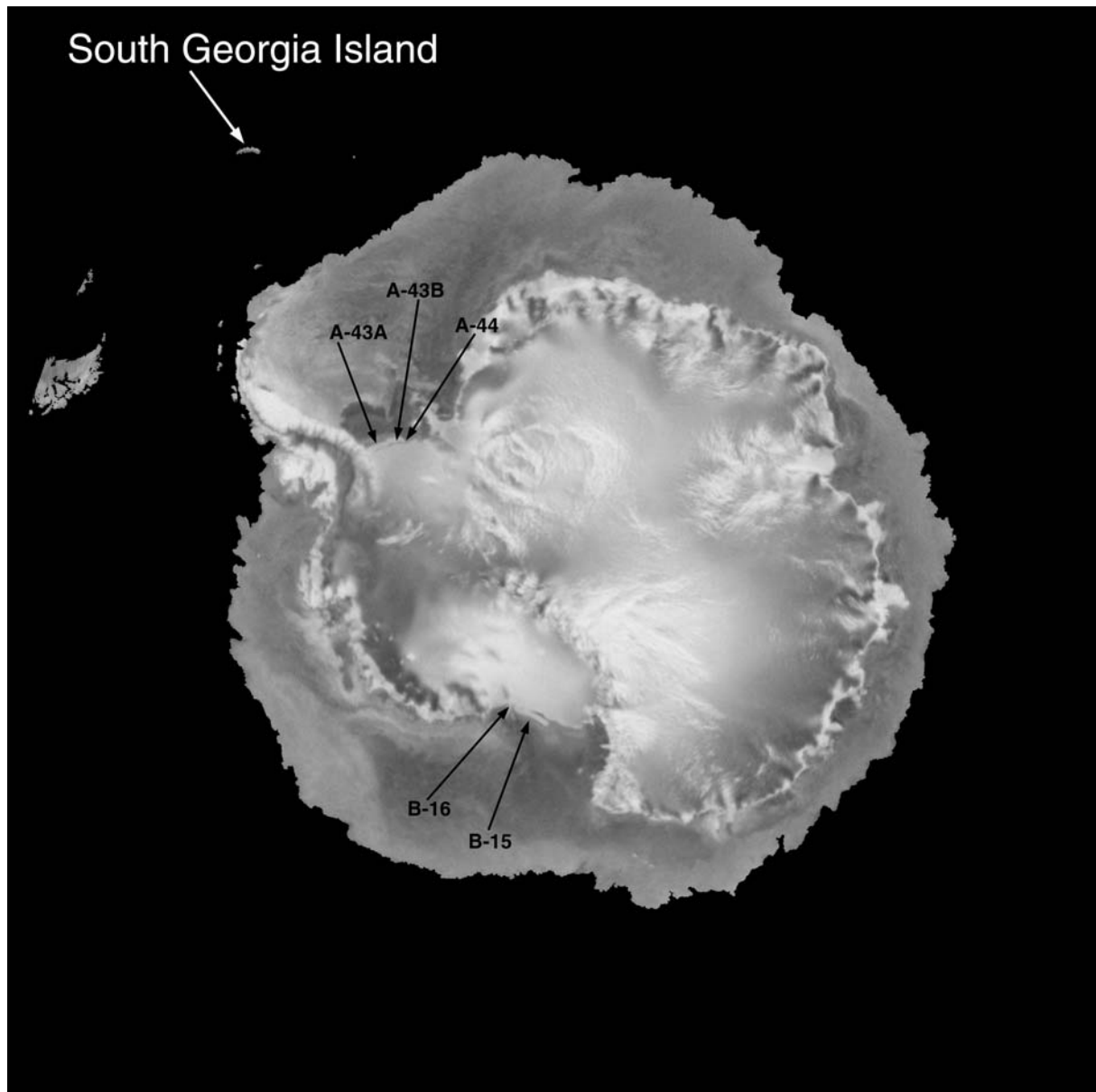
Figure 4.3.4.5.2   An image formed from SeaWifs sigma–0 (radar backscatter) measurements around Antarctica helps demonstrate the wealth of information contained in the scatterometer data. This image was constructed from a single day of scatterometer data (May 24, 2000). The brighter central area in the image is the Antarctic continent. It is bright due to high radar return echoes from glacial snow and ice. The darker outer area in the centre of the image is the sea icepack surrounding the continent. The variations in sea ice show the circulation patterns in the sea ice and are due to the snow cover, thickness, and history of the ice since formation. The alpha–numeric symbols and arrows point to large icebergs. For a close look at B–15, for example, see Figure 2.7.3.3.1 above.

Of more direct interest to weather analysis and forecasting Figure 4.3.4.5.3 demonstrates the utility of QuikSCAT's SeaWinds instrument in observing mesoscale winds systems. This

figure (from http://winds.jpl.nasa.gov/news/so_georgia_island_fig_2.html) shows the disturbed wind flow around South Georgia Island. This island, which is in the South Atlantic Ocean (~1,500 km, east of the Falkland Islands), is only 170 km long (~106 nm) and 30 km (~19 nm) wide, but contains 13 peaks exceeding 2,000 m (more than 6,500 ft) in height (see also Figure 4.3.4.5.2, and Section 7.2.2 below). The graphic is from QuikSCAT measurements of wind speed and direction during a single pass over the island on September 13, 1999. South Georgia island itself is shown as black for heights less than 750 m; green for heights between 750 and 1,500 m; and red for regions higher than 1,500 m. The white area surrounding the island represents the region where land contamination does not allow wind measurements to be made. The horizontal and vertical coordinates are in kilometers, with origin on the island at latitude 54.5º S and longitude 30º W.

Figure 4.3.4.5.3 shows regions of high wind speed off both the eastern and western ends of island, corresponding to "corner accelerations" as the winds stream by the steep island orography. The lowest wind speeds are seen to be in the lee of the highest island orography. Note that the winds are blocked by the island's mountain barrier that produces a long "shadow" of low winds on the downwind side of the island stretching for hundreds of kilometers (about 500 nm long).
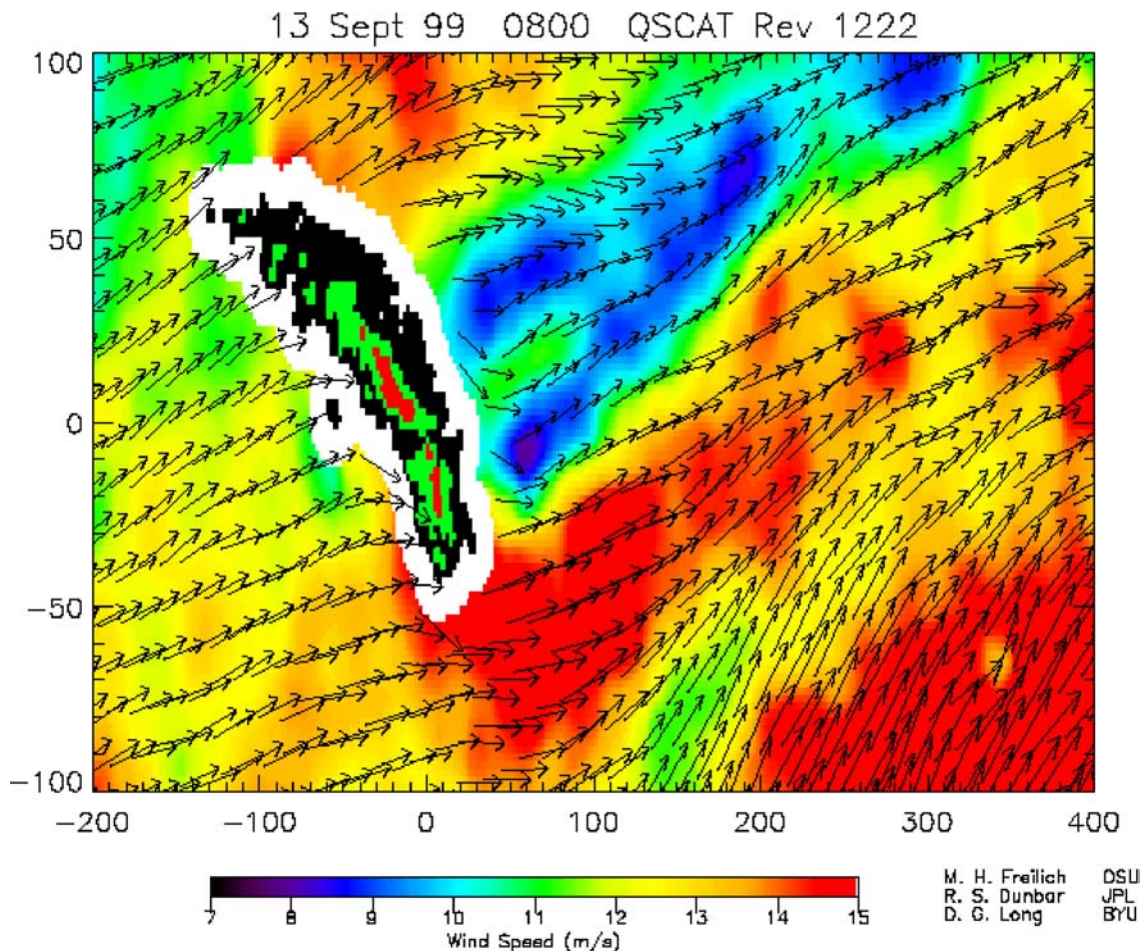
Figure 4.3.4.5.3   A graphic from QuikSCAT measurements of wind speed and direction during a single pass on September 13, 1999 over South Georgia Island. The island is shown as black for heights less than 750 m; green for heights between 750 and 1,500 m; and red for regions higher than 1,500 m. The white area surrounding the island represents the region where land contamination does not allow wind measurements to be made. The horizontal and vertical coordinates are in kilometres, with origin on the island at latitude 54.5º S and longitude 30º W.

4.3.5   Passive microwave products

Passive microwave instruments are important in Antarctic weather forecasting because they can provide a number of important fields of the high latitude environment, including rain rate, cloud liquid water, surface wind speed and total precipitable water over the ice–free ocean as well as sea ice extent. The unique ability to produce surface data under cloud is particularly valuable around the Antarctic where cloud cover is extensive and persistent.

The atmospheric sounding instruments also have passive microwave channels and Section 4.3.6 TOVS/ATOVS (below) should also be consulted.

For the most part, the algorithms used to convert the satellite measurements into atmospheric parameters are tuned for open–ocean conditions in the tropics and mid–latitude areas. Care should therefore to taken in using passive microwave products in high latitudes.

Excellent background information on passive microwave instruments can be found in Ferraro *et al.* (1998), Grody (1993), Janssen (1993), Kidder and Vonder Haar (1995).

4.3.5.1   <u>The passive microwave instruments</u>

The Special Sensor Microwave/Imager (SSM/I), first launched in 1987 onboard the US Defense Meteorological Satellite Program (DMSP) series of satellites, has six channels in atmospheric "window" regions (19, 37 and 85 GHz, all dual–frequency), operating over a ~1,400–km wide swath. A seventh channel is centred on the 22.23 GHz water–vapour line (vertical polarization only). The footprint size varies from 60 km at 19 GHz to 15 km at 85 GHz. Two SSM/Is are in orbit (currently on satellites F–13 and F–14), having overpass times ~four hours apart (06:00 and 10:00, and 18:00 and 22:00 LST). Global operational products include cloud liquid water (CLW), water vapour or total precipitable water (TPW), and ocean–surface winds (OSW) [Ferraro *et al.*, 1996]. SSM/I products are generated by the US Navy and distributed to both the US Air Force and NOAA.

4.3.5.2   <u>Derived products</u>

Total Precipitable Water (TPW)

Total precipitable water (TPW) over the open ocean, often called the integrated water vapour, is retrieved from data collected near the centre of a weak water–vapour absorption line at 22 GHz (Alishouse *et al.*, 1990; Ferraro *et al.*, 1998). The TPW mainly corresponds to low level water vapour (i.e., 700–hPa and below). The error is ~10% when compared with radiosonde measurements. In mid–latitudes this product is one of the most accurate and useful of the SSM/I products. It is generally considered to be as accurate as radiosonde values of integrated vapour. Accordingly, it is assimilated into numerical models routinely, including the US Navy Operational Global Atmospheric Prediction System (NOGAPS). Since it shows gradients of low–level moisture well, it can provide an excellent marker of marine cold fronts. To locate fronts using this parameter, forecasters should look for a rapid decrease in integrated values in the vicinity of frontal systems. The strongest gradient marks the boundary between deep moisture in the pre–frontal airmass and shallower, drier air in the post–frontal air mass. An example of integrated water vapour values derived around the Antarctic is shown in Figure 4.3.5.2.1.

Integrated Water Vapour [kg/m²]

6.1.95 0:00 GMT +/- 3h

Scale (for 60°S) 1:70000000
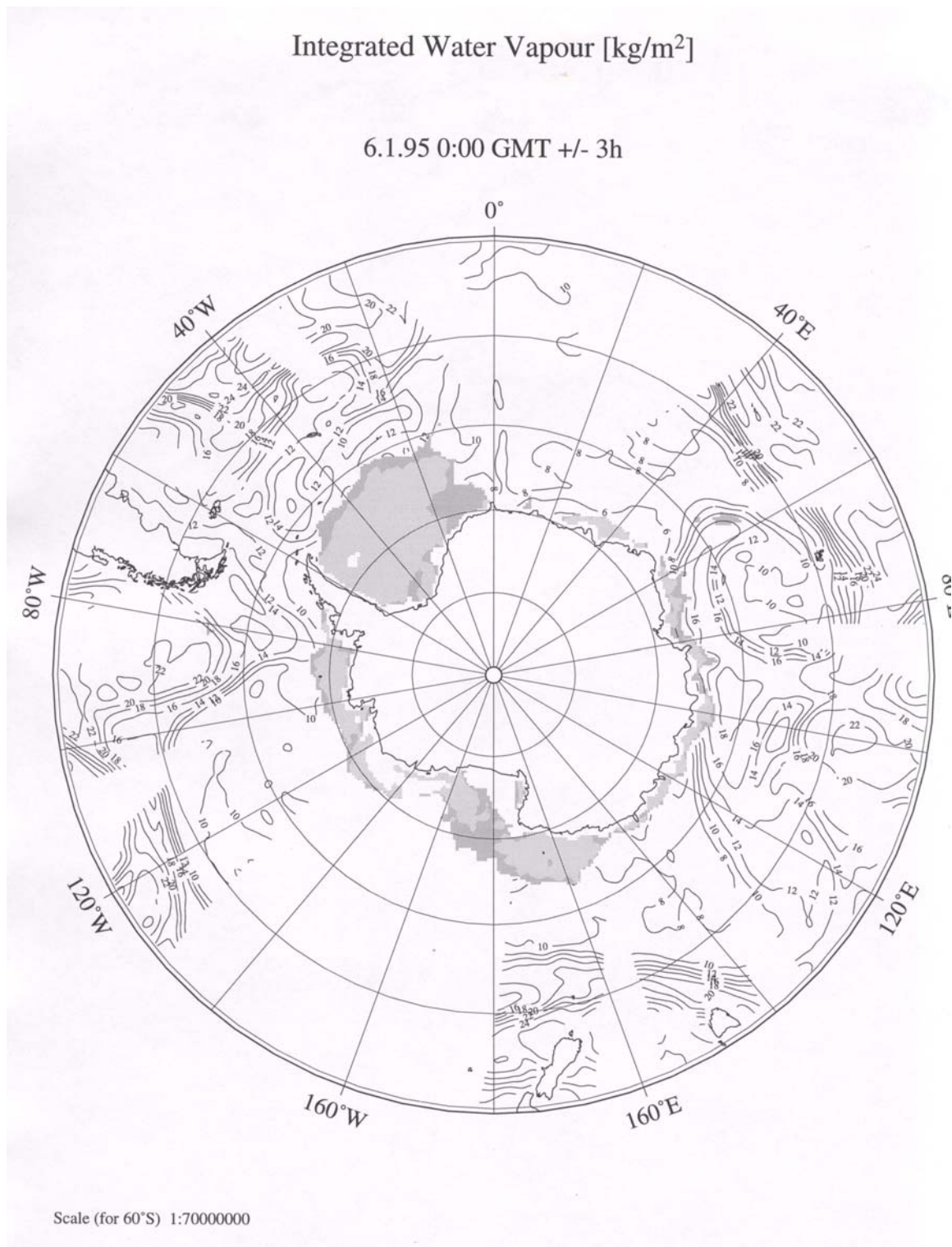
Figure 4.3.5.2.1 An example of SSM/I integrated water vapour values derived for around the Antarctic. (Figure courtesy Günther Heinemann, Meteorologisches Institut der Universitat Bonn)

Rain Rate (RR)

At frequencies between ~20 and 40 GHz, absorption by liquid drops of rain and by clouds can be used to derive information about their horizontal extent and water content [Grody, 1993]. Rainfall has a dual effect on Earth–emitted radiation (Ferraro *et al.*, 1998): scattering by ice

particles, and absorption by rain drops. The absorption/emission signature of rain drops is easily detected against the low emissivity of the ice–free open ocean surface, but not against a land or ice surface. Little is known about how the low rain rates found around the Antarctic affect the performance of the processing algorithm as no major validation programmes have been carried out at high latitudes.

Ocean–Surface Wind Speed (OSWS)

Winds blowing across an ice–free ocean surface locally generate capillary waves, small–scale gravity waves, and foam. These act to roughen the ocean surface at the millimetre– and centimetre–scale wavelengths that the microwave remote sensing instruments used for ocean surface retrieval are sensitive to. For the SSM/I, the changes in the ocean surface are measured by the 37 GHz channel. Since this frequency channel is also sensitive to water vapour and liquid water in the atmosphere, other channels are used to help determine accuracy limits to place on the wind retrievals (Ferraro *et al.*, 1998). The SSM/I data are flagged for sea ice using the data themselves, although some data may periodically occur in the vicinity of the ice edge. The current operational SSM/I wind retrieval algorithm is a version of the Goodberlet *et al.* (1989) algorithm (modified for high TPW values), and uses the 19V, 22V, 37V and 37H channels. The accuracy of the SSM/I wind speed retrievals will degrade considerably as the level of water vapour and liquid water in the atmosphere increases. An example of surface wind speed data is shown in Figure 4.3.5.2.2.

Cloud Liquid Water (CLW)

Integrated cloud liquid water (CLW) can be retrieved over the open ocean due to the low microwave emissivity of the background ocean surface. The NOAA algorithm for retrieving oceanic CLW uses SSM/I data collected at 19, 37, and 85 GHz. Use of the 85 GHz data enables the retrieval of extremely low amounts of CLW. This product differs from TPW (integrated water vapour), since it measures water in its liquid form. Integrated liquid water has magnitudes one or two orders of magnitude less than integrated water vapour. An example of cloud liquid water values is shown in Figure 4.3.5.2.3.

4.3.6   Temperature sounding instruments

Temperature soundings from polar–orbiting satellites are a key component of the global observing system. In particular, they underpin the analysis of the three–dimensional structure of the troposphere and stratosphere by operational numerical analysis and prediction systems from centres such as ECMWF.

Satellite soundings utilise the strong absorption bands in terrestrial wavelengths of some atmospheric gases, where the absorption varies strongly with wavelength. At wavelengths in the centre of such bands, radiation from the atmosphere is absorbed and re–emitted over relatively short distances; radiation emerging from the top of the atmosphere will have originated from the upper atmosphere and will represent the temperature of that region. In the

wings of the bands the absorption is much less and the emerging radiation will, on average, have originated from lower in the atmosphere
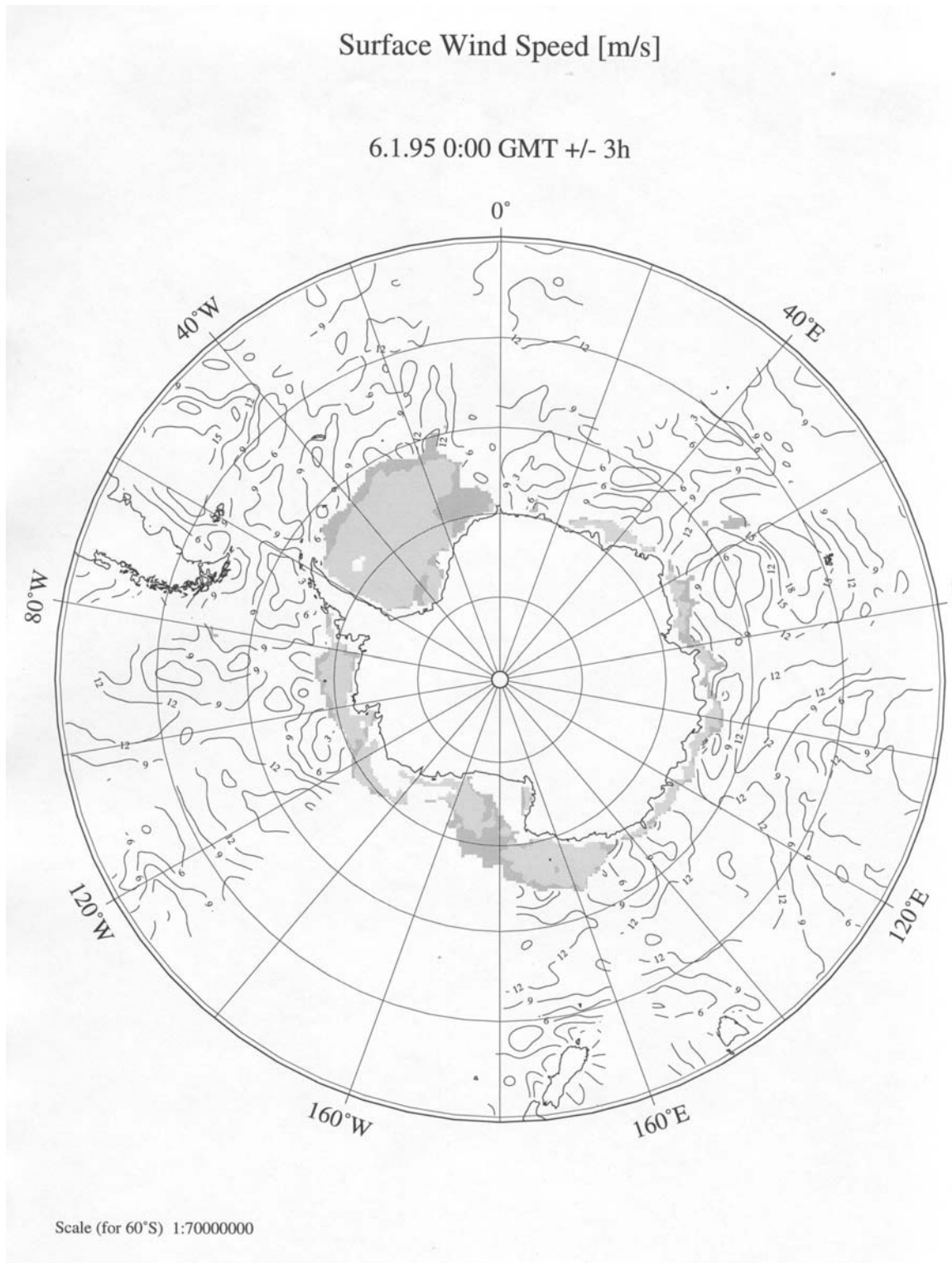
Figure 4.3.5.2.2 An example of SSM/I surface wind speed values derived for around the Antarctic. (Figure courtesy Günther Heinemann, Meteorologisches Institut der Universitat Bonn)

Cloud Liquid Water [kg/m²]

6.1.95 0:00 GMT +/- 3h

Scale (for 60°S) 1:70000000

0.00 0.05 0.10 0.15 0.20 0.25 0.30 0.35 0.40 0.45 0.50
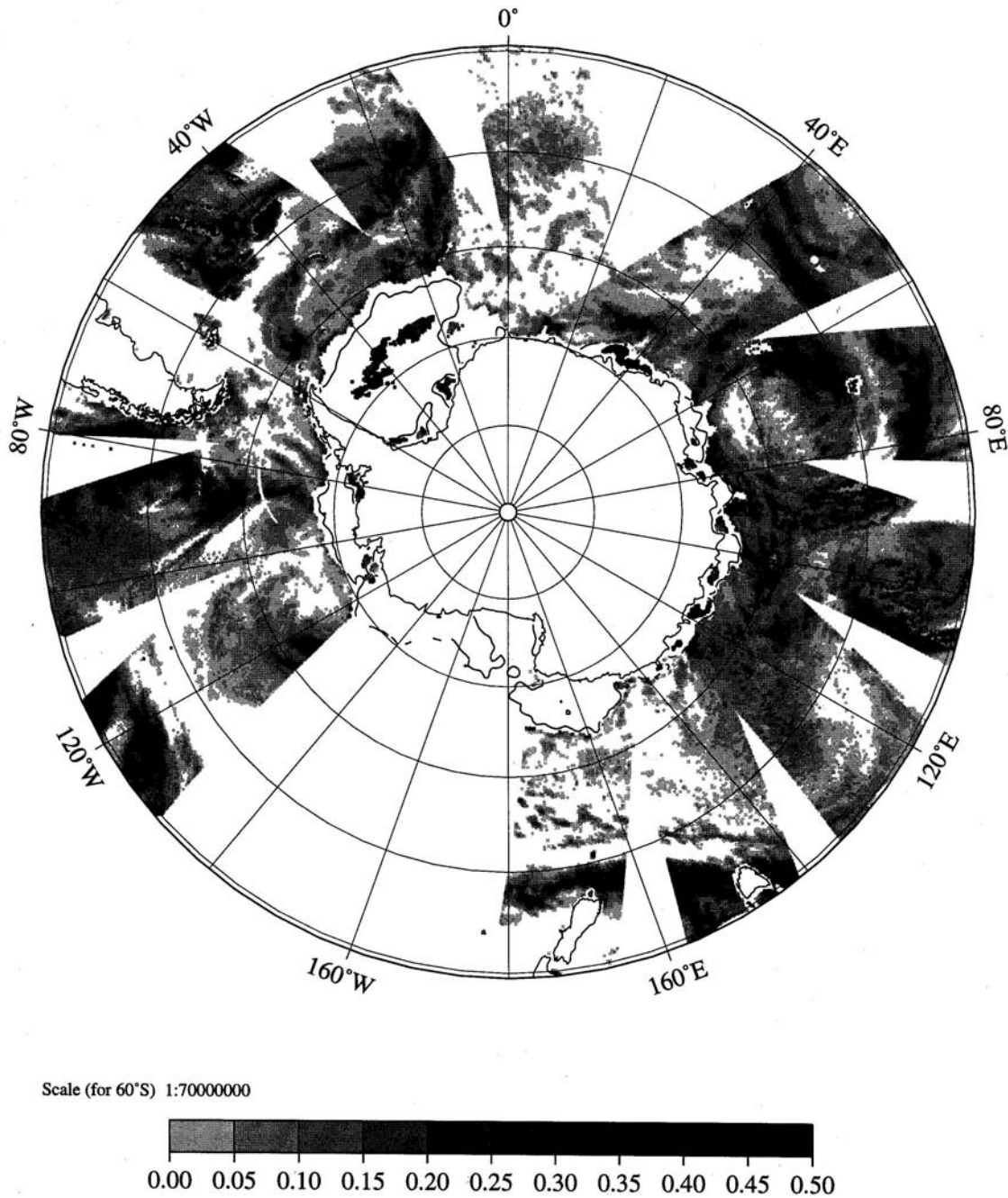
Figure 4.3.5.2.3 An example of cloud liquid water values derived for around the Antarctic. (Figure courtesy Günther Heinemann, Meteorologisches Institut der Universitat Bonn)

4.3.6.1   The TOVS Package

The major operational group of instruments for many years was the TIROS Operational Vertical Sounder (TOVS) flying on the NOAA satellites. However, in the late 1990s the TOVS began to be replaced by the ATOVS (see below). Soundings are calculated from measurements taken by a combination of instruments, collectively known as TOVS, comprising the 20–channel High Resolution Infra–red Sounder (HIRS), a 4–channel Microwave Sounding Unit (MSU) and a three–channel infra–red Stratospheric Sounding Instrument (SSU). HIRS measures upwelling radiation at several wavelengths in the carbon dioxide 15 μm infra–red absorption band, while the Microwave Sounding Unit (MSU) uses the oxygen absorption band at 50 GHz (between 50.3 and 57.05). HIRS also makes measurements in water vapour absorption and ozone bands to provide information on these properties. There are also an infra–red and a microwave channel at wavelengths where the atmosphere is transparent to provide surface information.

Although their nadir fields of view differ (HIRS 17 km, MSU 110 km, SSU 147 km) all have comparable scan widths and the measurements can be merged before soundings are computed. TOVS processing registers the varying pixel sizes to produce soundings from the measurements in about 30 channels relating to a single pixel location. Pre–processing steps must also determine surface temperature and the presence of cloud or aerosol contamination in the column.

To derive vertical profiles of atmospheric temperature and water vapour from the measurements is not straightforward. The radiation received by the sensor comprises radiation from the surface, and the emissions from gases along the path, reduced by the absorption of intervening gases. The absorption also depends to some extent on temperature, whose values are being sought. In the infra–red region clouds are a major limitation, as to a lesser extent are aerosols. In the microwave region variations of surface emissivity complicate the problem, although over the sea the emissivity is constant. Apart from areas of heavy rainfall which can contaminate microwave emissions, clouds are generally transparent at 50 GHz. An additional complication is that the mathematical problem or inversion of the measured radiances to soundings of temperature and moisture is not well–posed and there are many possible solutions. Good summaries of the process of atmospheric sounding and the common solution techniques are given in Liou (1980) and Twomey (1977).

A variety of techniques are used to detect problems in the observations and to give physically realistic profiles. The latter include statistical techniques based on regression between observed radiances and radiosonde measurements, or variational solutions starting from a physically realistic first guess and adjusting the temperature and moisture (and perhaps cloud cover) through a radiative transfer scheme, until the best fit is obtained. Operational numerical analysis systems at centres such as ECMWF and NCEP extend this approach to actually making their three–dimensional analyses of the state of the atmosphere using the radiances directly without making explicit retrievals.

The vertical resolution of the retrieved profiles is related to the number of channels in the instrument. The weighting functions for some of the TOVS channels, shown in Fig 4.3.6.1.1, indicate the sensitivity of the measurements to the temperature at any level. It can be seen that the retrievals are representative of deep layers in the vertical and cannot be expected to depict small–scale vertical structure. The microwave channels permit almost all–weather soundings, because microwaves penetrate most clouds, but with only three channels, apart from the surface channel, the vertical resolution of soundings derived from MSU measurements alone is very coarse.

The accuracy of the retrievals is typically regarded as an average of about 2 K through most of the troposphere based on comparisons with collocated radiosondes. However, errors

are considerably larger where there are sharp vertical discontinuities such as inversions and the tropopause.
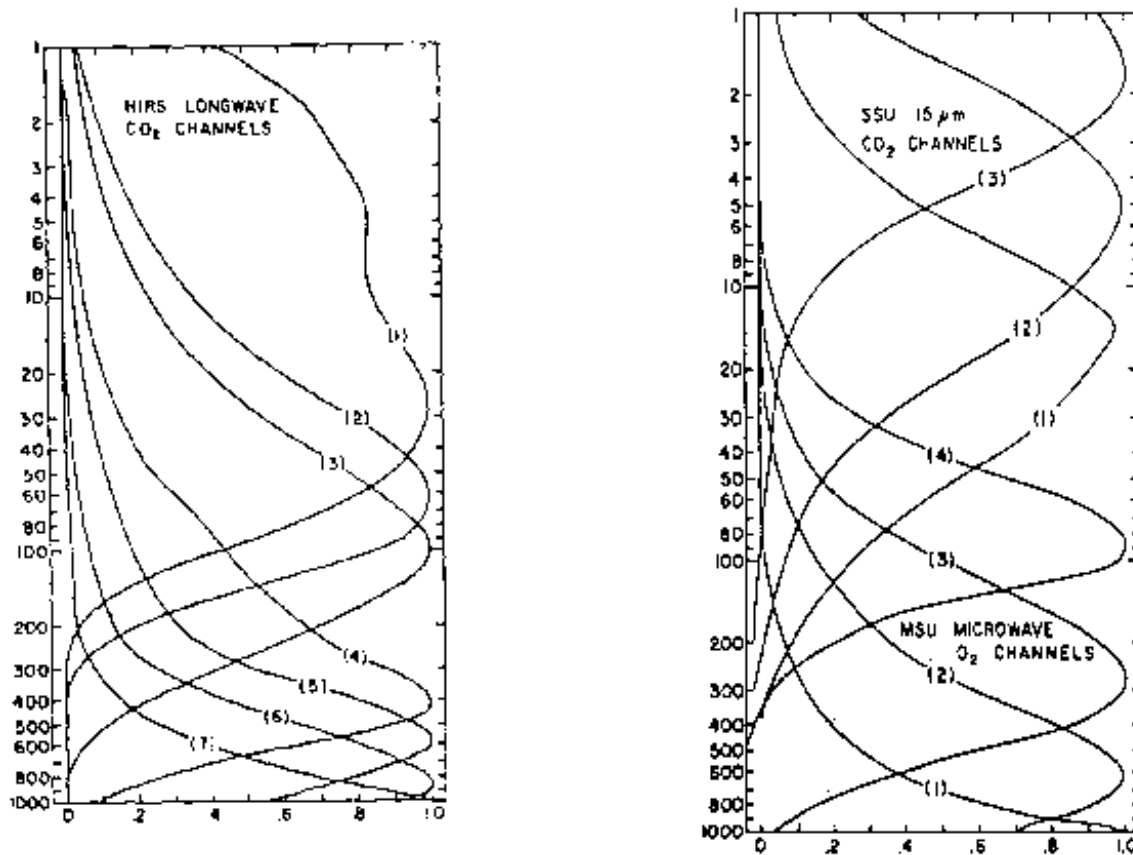
Figure 4.3.6.1.1 TOVS weighting functions showing the sensitivity of channels to temperature through the depth of the atmosphere (from Smith *et al.* ,1979).

4.3.6.2   The ATOVS

An improved version of the MSU, the Advanced Microwave Sounding Unit (AMSU), was launched by NOAA on NOAA–15 (NOAA–K) in May 1998. The 20–channel AMSU (consisting of three modules: –A1, A2 and –B), which is part of the Advanced TOVS (ATOVS) sensor package, was designed to improve the accuracy of temperature soundings compared to the 4–channel MSU. AMSU–A has 15 channels ranging from 23.8 to 89.0 GHz providing atmospheric temperature soundings even under cloudy conditions at vertical resolutions comparable with that from HIRS. AMSU–B has 5 channels from 89.0 to 183.31 GHz aimed at deriving humidity profiles. Window channels at 31.4 and 89 GHz are used to monitor precipitation, while total precipitable water (TPW) is derived from a channel centred on 23.8 GHz. The AMSU units have better horizontal resolution (45 km at nadir for AMSU–A and 15 km for AMSU–B). On later satellites there will be further upgrades but the main effect will be to extend the upper limits of the sounding altitude from 45 to 73 km. Within ATOVS the HIRS instrument will continue, but not SSU.

Earlier indications are that the soundings from ATOVS are producing significant improvements in the NWP forecasts when assimilated into the numerical analyses.

4.3.6.3   The DMSP sounders

The DMSP satellites carry an atmospheric temperature sounder (the Special Sensor Microwave/Temperature sounder, or SSM/T) and a water–vapour sounder (SSM/T2). First launched in 1979, the SSM/T consists of seven channels in the 50–60 GHz oxygen band, which measure temperature profiles from the surface to about 5 hPa. One channel acts as a surface window channel. The sub–track spatial resolution is an approximate circle of 174 km diameter at nadir. At the far end of each scan, resolution degrades to an ellipse of 213 × 304 km size. The SSM/T data swath is ~1500 km.

The SSM/T2 was first flown on the F–11 satellite in 1991, and continues to be launched on DMSP satellites. In addition to window channels at 91 and 150 GHz, it contains three channels operating around the strong water vapour line at 183.31 GHz, which are used to derive moisture profiles from the surface to ~300 hPa, and to identify precipitation (over ocean and land). There are 28 observations (beam positions) per scan for each channel, with each observation having a spatial resolution of ~48 km. The total swath width is ~1400 km. The SSM/T2 scan mechanism is synchronized with SSM/T scan motion so that beam cell patterns coincide.

4.3.6.4   Availability of sounding products:

Processing of a global coverage is carried out by NOAA/NESDIS and the results circulated to meteorological centres on the GTS. The soundings and clear sky radiances are available separately in character format (WMO codes SATEM and SARAD) at a horizontal resolution of 500 km or combined in the WMO binary BUFR format at a horizontal resolution of about 120 km (i.e. about 50,000 retrievals globally from each satellite per day). Alternatively, the signal from the satellite can be received locally and the soundings computed from publicly available software, the International TOVS Processing Package. The soundings then can be made at the full resolution of the HIRS instrument.

The TOVS processing aims to produce clear sky retrievals where possible based mainly on the HIRS measurements. Where partial cloud cover is detected the processing uses the small–scale spatial variations to estimate the radiances from clear sky conditions, the so–called N* retrievals. If the cloud cover is too dense the retrieval may be made down to the cloud top or a microwave only retrieval made. In the messages transmitted on the GTS the type of retrieval is indicated to provide users with an estimate of the data quality.

The output products include layer mean virtual temperatures (at 15 standard layers) or equivalently the geopotential thickness between selected standard pressure levels, layer precipitable water, cloud amount and cloud top pressure, vertically integrated ozone amount and the clear sky radiances (expressed as equivalent blackbody temperatures). The information on ozone has proved useful for monitoring the ozone distribution over Antarctica in the absence of other measurements such as TOMS.

4.3.6.5   Particular problems for soundings near and over Antarctica

The Antarctic region has the potential benefit of frequent soundings due to the significant overlap of orbits near the poles. However, several studies have shown that the particular properties of Antarctica and high southern latitudes require particular attention to be paid to the retrieval process in these regions. These include:

- contamination of the channels by surface radiation from the elevated continent region
- the sharp surface temperature inversion
- variable surface emissivity over sea ice affecting microwave measurements
- atypical temperature structures in the polar vortex, especially in the spring
- problems of calibration at the low temperatures encountered over the continent.

Consequently, the major operational centres restrict their usage of TOVS retrievals in the Antarctic region, most confining retrievals over the continent to above the 100–hPa level, although using all levels over the ocean and sea ice.

Several studies have shown that with care, useful information on the vertical temperature structure can be derived. (e.g.: Lachlan–Cope, 1992; Lutz *et al.,* 1990; and Francis, 1994). However, the retrievals are probably more useful in depicting horizontal gradients in layer thickness fields to identify baroclinicity (Carleton *et al.*, 1995).

Adams *et al.* (1999) show a comparison of TOVS soundings and radiosonde measurements for the Antarctic region during the FROST experiment. While the comparisons show good agreement for oceanic and coastal locations, there are continuing problems over the elevated continental area. A comparison of collocated soundings for the South Pole showed particular problems in the spring period of FROST, but suggested reasonable agreement for the 500–250 hPa geopotential thickness at other times.

Hirschberg *et al.* (1997) advocate the use of the MSU–3 imagery as a forecasting aid in analysing and forecasting baroclinic waves related to upper–level potential vorticity anomalies. This technique may have particular application for the Antarctic region, especially over the storm–track region over the ocean. Over the very elevated areas of Antarctica surface contamination of the MSU–3 channels could be a problem.

A similar problem may exist with water vapour imagery, which relies on the properties of water vapour to absorb 6.7 μm wavelength radiation and which is useful in low to mid–latitudes for definition of the moisture distribution and circulation patterns in the upper atmosphere. In the Antarctic context, however, the dryness of the Antarctic atmosphere means that the satellite can detect radiation re–emitted from moisture layers down to quite low levels. The height of the Antarctic therefore intrudes into the imagery taken over the higher parts of the continent thus compromising interpretation of the data (Turner and Ellrott, 1992).

4.3.6.6   Operational contact and documentation:

An useful Web address is the NOAA/NESDIS Office of Satellite Processing and Distribution accessible from: http://ns.noaa.gov/NESDIS/NESDIS_Home.html.

4.3.7   Some aspects of future satellite systems

4.3.7.1   Future developments in US environmental satellite systems

A succinct view of the future developments in the US–based environmental satellite systems may be found at http://www-bprc.mps.ohio-state.edu/ (through the "Antarctic Weather Forecasting Workshop, May 17-19 2000, link). The following information is obtained from

this source. "NASA's flagship series of Earth Observing System (EOS) satellites AM (Terra) and PM (Aqua) will operate until mid-decade 2000s. At that point, their sensing capabilities will effectively transfer into the operational NPOESS (National Polar Orbiting Environmental Satellite System) satellites, beginning with the NPP (NPOESS Preparatory Platform) satellite, scheduled for launch in 2005. Figure 4.3.7.1.1 illustrates this decade-long transition. Focusing on the Antarctic, it then becomes natural to begin making full use of the EOS (and other) research satellites now, for both research and operational purposes."

Figure 4.3.7.1.1   The proposed transition from the Polar Orbiting Environmental Satellite type systems to the National Polar Orbiting Environmental Satellite System. (From http://www-bprc.mps.ohio-state.edu/   )
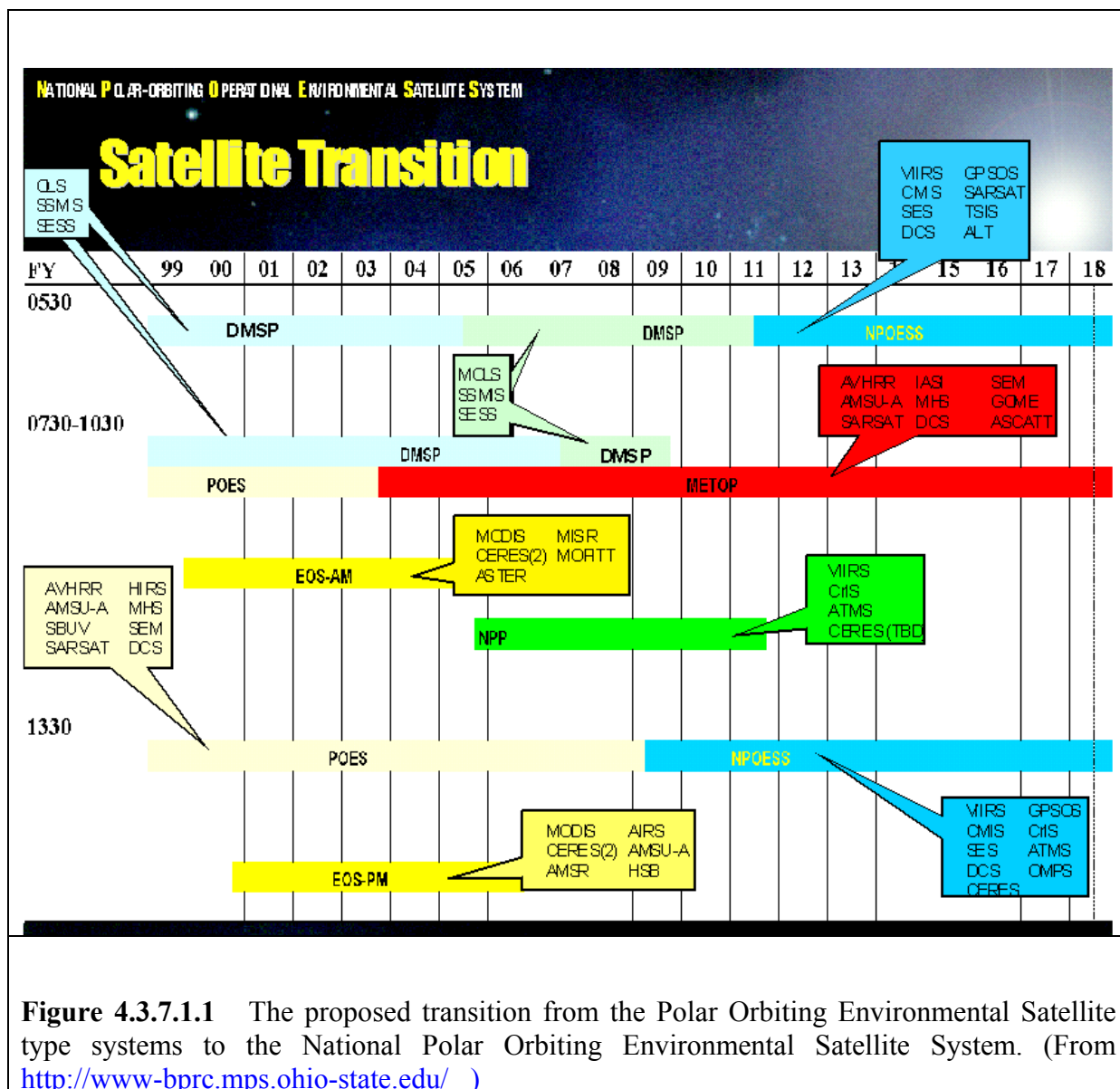
As may be inferred from Figure 4.3.7.1.1, currently (2000), and continuing for the next five to ten years, there will be a series of new polar orbiting meteorological satellites that have been or will be launched. These new data sources will be vital to:

- Minimize the satellite data gap for Antarctic stations (see Section 4.3.7.2)
- Provide new satellite products to aid forecasters
- Provide new inputs for NWP modeling

In the short term, plans could be profitably made and infrastructure developed to acquire EOS Terra and Aqua data for use in the field. It is unanimously recognized that EOS sensors such as the Moderate Resolution Imaging Spectroradiometer (MODIS) potentially offer vast improvements in not only basic aspects of satellite imagery, such as spatial resolution, but also in the multispectral capability to retrieve a host of atmospheric properties immediately relevant to forecasting and numerical simulation.

The COSMIC (Constellation Observing System for Meteorology, Ionosphere and Climate) programme, a unique application of the radio occultation technique for atmospheric profiling, should add considerably to modeling and forecasting capabilities throughout the sparsely sampled Antarctic continent. The spacecraft launch is anticipated for December 2003. Throughout the first half of 2004, validation studies should be carried out in Antarctica by means of such techniques as frost-point hygrometer sondes or differential absorption LIDAR. (For an overview of the COSMIC project see, for example, http://www.cosmic.ucar.edu/cosmic/internal/acmc/ACMC.html

In late 2001 or 2002, NASA's Triana spacecraft will be launched, for deployment at the L1 Lagrange point between the Earth and the Sun. At the L1 point, Triana will view the entire sunlit part of the Earth, and will return imagery every fifteen minutes. Triana's Earth Polychromatic Imaging Camera (EPIC) will provide solar ultraviolet and visible wavelength imagery during the austral summer, with a spatial resolution of approximately 14 km at Antarctic latitudes. This imagery can in some respects assist with the satellite data gap problem. However, the Triana is a NASA pathfinder mission, the first of its kind, and useful geographic coverage of the Antarctic by EPIC cannot presently be guaranteed with the same level of confidence as a low-earth-orbit AVHRR sensor

In the long term, countries operating weather services for the Antarctic should continually evaluate new satellite remote sensing capabilities (e.g., Japanese ADEOS-2, U.S. NPOESS program, etc.), and maintain flexibility to take advantage of them. Ways should also be explored to provide complete geographical coverage of the Antarctic continent and surrounding Southern Ocean; this is not presently available with current satellite data collection facilities in Antarctica.

4.3.7.2   Satellite Data Gap

Weather forecasters in the Antarctic will have noted one important problem in their use of the presently available operational satellites: a persistent time gap in the daily cycle of the NOAA and DMSP satellites that provide imaging and sounding over the Antarctic. This gap, which occurs between about 1030 and 1700 local time, generally coincides with the period of greatest human activity, including, where applicable, air traffic. Figure 4.3.7.2.1, for example, depicts the daily NOAA/DMSP schedule of overpasses that cover McMurdo Station from which this coverage gap is immediately apparent.

The gap in coverage is due to the fact that these are sun-synchronous orbit satellites, and the orbit time is determined by the governmental satellite organizations. The selected orbit times have been optimized for considerations other than Antarctic operations. To some extent then, such gaps in coverage are inevitable. Certain new and upcoming launches may help reduce (but not eliminate) the size of the diurnal coverage gap. For example, NASA launched its first EOS satellite, Terra, into a 2130 UTC (1030 local time) orbit in December 1999, and will launch the second EOS satellite, named Aqua, in December 2000, into an 0030 UTC (1330 local time) orbit. The next NOAA and DMSP satellites will be launched late in 2000. With these four additional satellites (two for research, two for operations), the daily coverage of McMurdo is improved as indicated in Figure 4.3.7.2.2. Moreover, the Sea-viewing Wide Field-of-view Sensor (SeaWiFS) has recently offered new operational and scientific

capabilities, and could be further exploited. SeaWiFS data have provided some help in spanning the gap of missing data during, for example, McMurdo Station's operational day.
    Recapping the next few years' of development:

- NASA will be deploying its Triana whole-Earth observatory satellite at the L1 Lagrange point in late 2001 or 2002;
- Japan will launch its ADEOS-2 also in 2002;
- and the European community will launch the first of its polar orbiting environmental satellites in 2003;
- In 2004 a Taiwan-led initiative, with support from the U.S. (NSF, NASA, NOAA, Navy, and Air Force) will launch COSMIC.

So to a considerable extent, the diurnal gap in coverage over Antarctica will be ameliorated (but not completely removed) in the next few years, along with the addition of very significant new sensing capabilities.
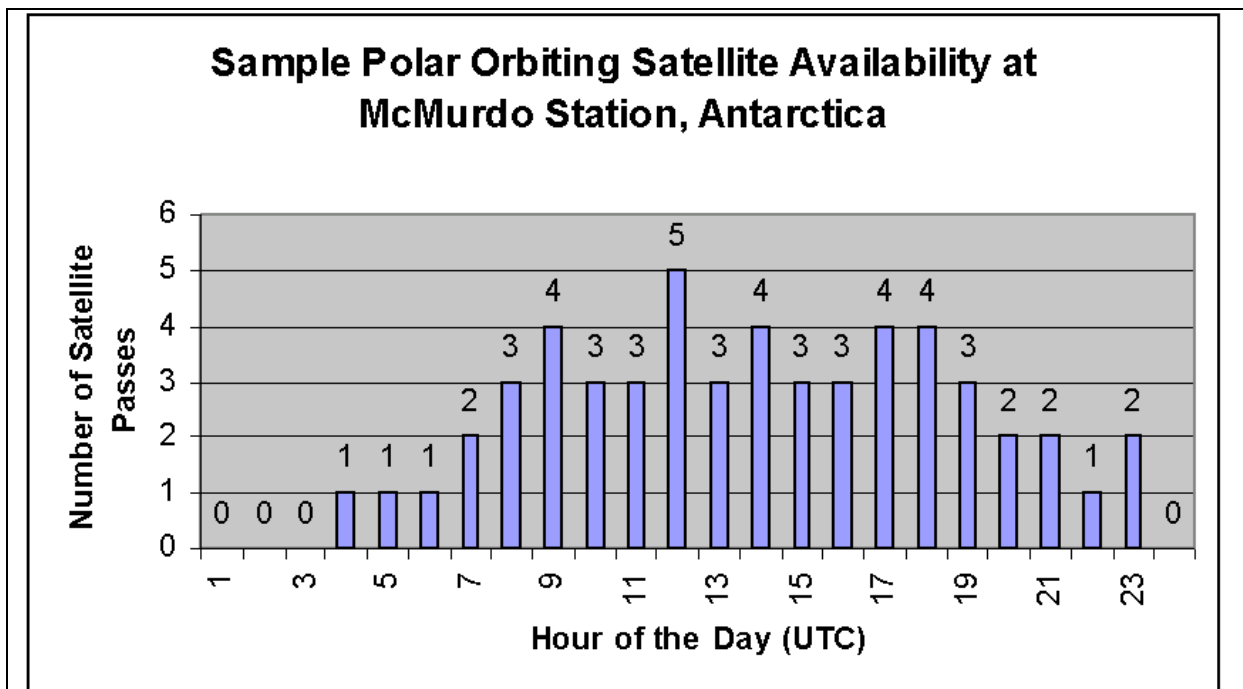
Figure 4.3.7.2.1   The daily NOAA/DMSP schedule of overpasses
                that cover McMurdo Station .

Flyover of DMSP F-15, Terra, and FY-1C   23:00 to 2:59 UTC

Figure 4.3.7.2.2   Example orbital tracks for DMSP-15, Terra, and FY-1C satellites during the data gap times at McMurdo Station. Although DMSP F-15 and FY-1C will not help with the data gap, Terra may be of help
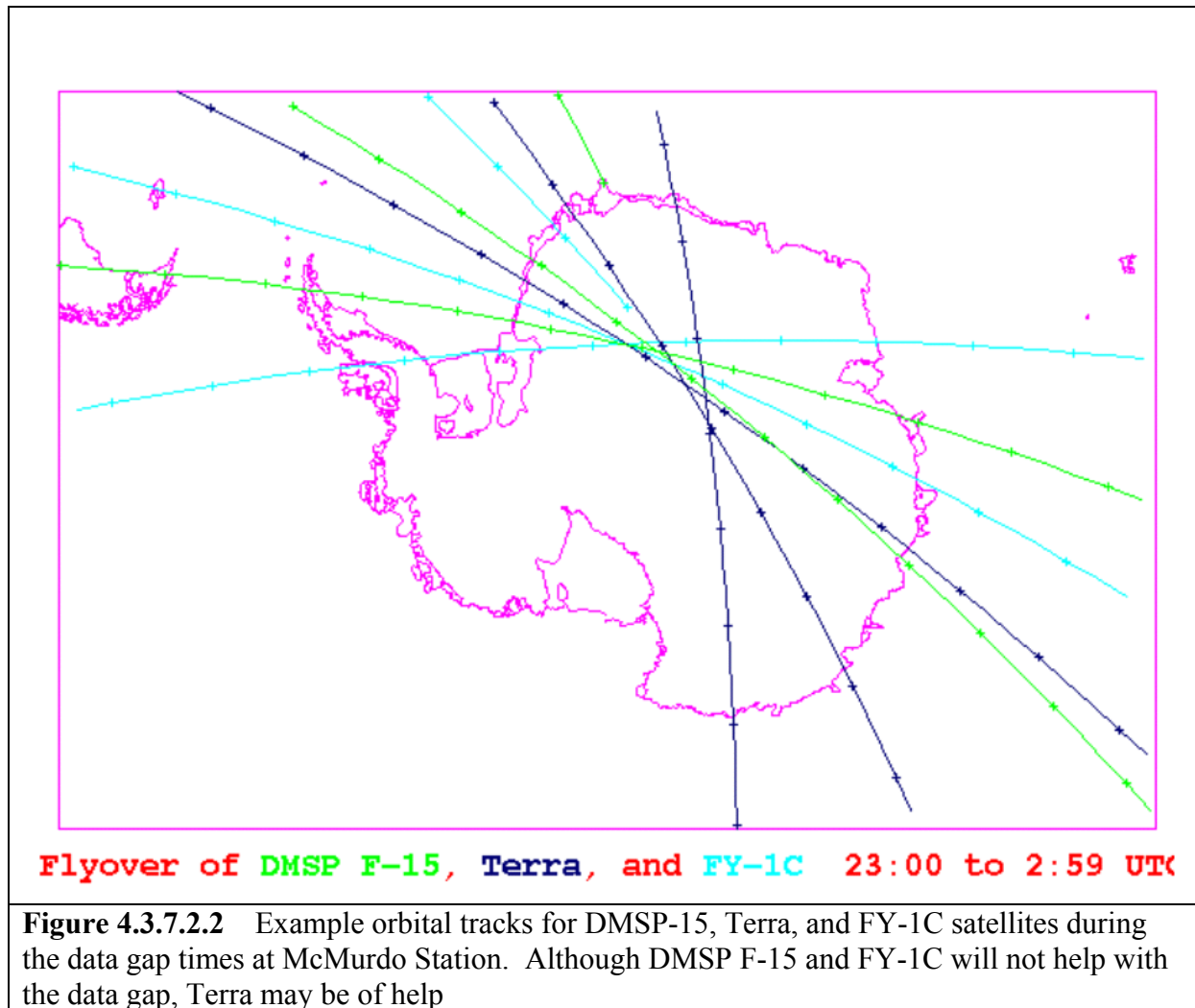
4.3.7.3   Data acquisition considerations

As may be inferred from the above, a wide array of satellite data are already available for Antarctic latitudes. The approach to obtaining these data in a timely fashion, and making the data available to Antarctic forecasters, follows two parallel routes. One is via direct reception at a particular station (for Antarctic stations with satellite reception see Table 7.1.1 in Appendix 1 below), which has proven over the years to be very effective. The other route is via storage on–board the satellite for one or more orbits, at which point the data are "dumped" to one or more special sites elsewhere on the globe, from whence they are forwarded to central processing locations. The results are then disseminated to recipients around the world.

The store and forward approach is sometimes the only method available. For example, Japanese GMS (Geostationary Meteorological Satellite) data cannot be received via direct broadcast at McMurdo, since the satellite is never in view from the station. Instead the data are received elsewhere, processed to an appropriate level and sent via the Internet to McMurdo. In general, however, when timeliness, reliability, and communications bandwidth limitations are taken into account, direct broadcast is almost always the preferred route, with store and forward used as a backup or supplement. In the specific case of the NASA EOS satellites Terra and Aqua, they both have direct broadcast capability. The data rates [approximately 15 megabits per second (Mbps)] from these satellites are 15 times greater than the current generation of NOAA and DMSP satellites (1 Mbps). The only practical way to

provide access to EOS data in the field, for flexible use by forecasters, is to track the EOS spacecraft and collect the telemetry in the field, as is presently done with the NOAA and DMSP spacecraft. Without a tracking facility at the Antarctic forecast centre/station, there will be unacceptably long delays and omissions associated with long–distance access to EOS Data and Information System (EOSDIS) via finite communications bandwidths: the EOS data sets are simply too large (tens of gigabytes per day) to access remotely.

5   ANALYSIS TECHNIQUES

5.1   Analysis and diagnosis fundamentals

5.1.1   Overview

A primary objective of meteorological analysis is to develop a coherent picture of existing atmospheric patterns, building up a model of the atmosphere. There are many components to the analysis phase. The basic observations as plotted on the weather chart may be interpreted to form initial impressions of atmospheric patterns. The two–dimensional quasi–horizontal representations of the atmosphere (at mean sea level and at upper levels), vertical representations and, as appropriate, other forms of analysis which will be discussed later, complement the observations.

Traditionally observations and analyses have been done at fixed time intervals, particularly for hand drawn analysis; however the increasing availability of asynoptic data (e.g. satellite soundings) is tending to modify the fixed–time analysis approach. The forecaster must assimilate the new data as it comes to hand to confirm his/her expectations or modify his/her picture of the atmosphere.

Several texts deal exclusively or in part with meteorological analysis and prognosis. For example, a comprehensive summary of manual analysis methods is given by Saucier (1955) and this is recommended as reference study for all forecasters. Many other texts have sections on analysis and prognosis, perhaps the most convenient being in Berry *et al.* (1945), Malone (1951) and Wickham (1970). Oliver and Oliver (1945) give useful guidance on analysis of single station data, while Fujita (1963) and Williams (1963) deal with mesoscale analysis techniques. Miller (1972), Crisp (1979) and Matley (1981) contain some good practical hints on secondary analysis of externally prepared products, and of course the literature is full of synoptic case–studies that demonstrate the advantage of various analysis techniques.

In this handbook basic competence in isobaric, streamline and contour analysis is assumed; also, the interpretation of the present weather identifications and standard clouds types, in terms of their value for analysis and short–term prognosis, is not discussed. For mid–latitude meteorology these matters can be found in texts such as Petterssen (1956) and Wickham (1970) or often in–house training notes (e.g. Bureau of Meteorology, 1983). This chapter is concerned with broad principles which may be applicable to a particular situation. It should be noted that analysis in the Antarctic is not fundamentally different from that carried out for other parts of the world. However, a number of factors need to be taken into account. These include:

- the lack of data;
- the variations in orography from near seal level to above 4 km requiring differing analysis techniques to be followed;
- the lack of weather systems with the standard frontal characteristics.

5.1.2   Basic observations

The basic observations plotted on a mean sea level chart usually provide strong clues to the physical processes taking place in the atmosphere and form an integral part of the forecaster's analysis and prognosis. Some examples of the value of individual observations in the short–term forecasting context are given below.

- An observation of strong winds at a station must be carefully assessed from a geographic and climatological viewpoint, as well as in the overall meteorological context. The strong winds may be, for example, a normal katabatic which will ease as insolation increases; or may be due to a passing low–pressure system. Winds in katabatic prone areas may not be representative of the synoptic scale flow.
- An AVHRR channel 3 cloud observation of supercooled water cloud near the coast might indicate a risk of airframe icing should aircraft unwisely venture into the cloud.
- Relatively large corrected pressure tendency falls often indicate the approach of a large–scale low–pressure system and the possible eventual onset of strong winds. Again though, the overall meteorological context of the pressure falls is important: it may be that there is a general pressure fall over an area not necessarily linked to a discrete low.

Competent visual weather observations taken at more frequent intervals than the normal three–hourly time space may reveal aspects of the meso–structure of the atmosphere. Certain changes in visibility, cloud growth rates, cloud structure and movement provide critical indications of ongoing change.

5.1.3   Mean sea level pressure analysis and satellite data

The mean sea level pressure field provides the basic integrated representation of wind flow near the ground. As will be discussed later (see Section 5.4 below) mean sea analyses have limited usefulness over the Antarctic continent itself above a height of 0.5 to 1 km, but remain a core resource for coastal Antarctic forecasting. Isobaric analysis enables weather systems such as highs, lows and fronts to be identified and tracked over time.

A primary concern of the short–term forecaster is to determine, where possible, small–scale or mesoscale perturbations in the larger scale flow. At most Antarctic stations weather watch radar is not available and sequences (or loops) of hourly and three–hourly satellite imagery from geostationary satellites, although inadequate for mesoscale forecasting, does provide a useful temporal perspective of such development. While the less frequent AVHRR data from the polar orbiting satellites often gives information which is very useful but in the context of short term forecasting, has a limited span of useful currency. On the other hand, the AVHRR and APT data have a role in the more medium term forecast time frame in identifying the main cloud features in the absence of geostationary satellite data.

The mesoscale features must be integrated with the larger–scale features on the MSLP charts to identify the various components that are causing the current weather.

5.1.4   Upper–air analysis

The most practical way of displaying the patterns of circulation in the free atmosphere is by the construction of contour charts for selected pressure levels (850, 700 hPa etc.). Contour analysis enables systems such as upper–air lows, ridges and troughs, to be identified. The degree to which a mean sea level pressure system is reflected throughout the troposphere can be readily discerned. In certain circumstances the drawing of streamlines may be preferable to contours.

The thickness of a layer refers to the difference between the contour heights of two pressure levels, and it depends on the mean virtual temperature of the layer – the greater the mean virtual temperature, the greater the thickness. Thickness analysis then represents the integrated temperature pattern between two constant pressure analyses and features such as warm or cold pools of air can be identified.

Charts of atmospheric parameters, such as humidity, vorticity and vertical motion complement the standard layer charts and enhance the forecaster's three–dimensional picture of the atmosphere and assist in diagnosis of phenomena such as snowfall. Similarly, wet–bulb potential temperature charts on isobaric surfaces (e.g. 850 hPa, 500 hPa) may be a valuable aid in analysis and forecasting frontal movement and precipitation (see Bradbury, 1977).

5.1.5   Meteograms or time series

Meteograms effectively display the magnitude of a number of elements on a common time base (timeline) so that their interaction can be seen. Figure 5.1.5.1 is, for example, a time series of observed surface data from Mawson for 1 March to 14 April 2000 and at about 21 March the surface wind has peaked at about the time of minimum surface pressure, presumably as the apex of a low–pressure trough moved past the station.

NWP may be used to produce time series for prediction or case study diagnosis Figure 5.1.5.2 shows a time cross section of upper winds, potential temperature and height for a GASP model grid point near Mawson for a period similar to that shown in Figure 5.1.5.1. It may be seen that shortly after 21 March mid–tropospheric winds veered in a manner consistent with a low–pressure system passing close to Mawson.

5.1.6   Quantitative values

Analysis involves calculations of quantitative values of appropriate parameters which are useful for short–term forecasting: usually these values would be assessed through examination of NWP output. The parameters calculated clearly depend on the particular meteorological situation and could include:

- directions and speeds of movement of key features, such as fronts, or lows;
- gradient and geostrophic wind;
- rates of advection of temperature, moisture, vorticity, etc.;
- changes in cloud top temperature or areal extent of cloud features;
- vertical and/or horizontal wind shear;
- vertical motion.
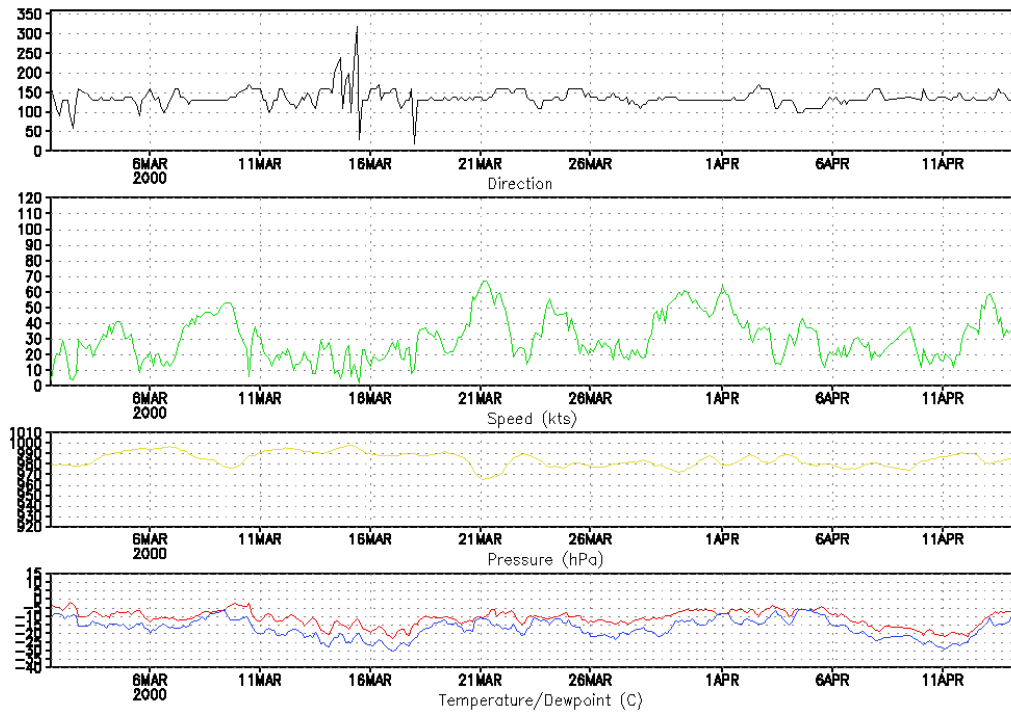
Figure 5.1.5.1   Time series of observed surface data from Mawson for
1 Mar. to 14 Apr. 2000.
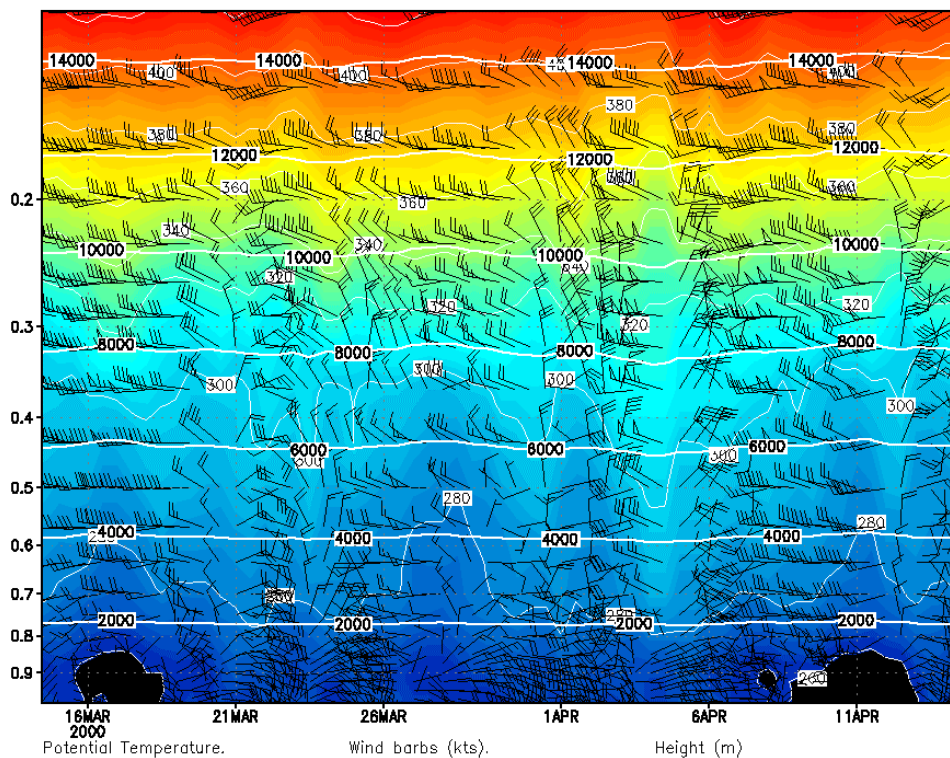
Figure 5.1.5.2   Time series of GASP model analysis of upper winds, potential
temperature and geopotential height for a grid point near Mawson for the period
16 March to 14 April 2000.

5.2   More on conventional surface and frontal analysis

The synoptic scale may be viewed as a link between the over–arching broad–scaleflow and the meso/micro–scale through which the weather actually directly affects the particular area of interest. It may be argued, for example, that, gust fronts or sea breeze fronts aside, fronts characterise this link. On the one hand fronts are mesoscale across their usual direction of travel but are synoptic–scale along their length. Also typically the mesoscale structure of fronts is determined to a large extent by the synoptic–scale environment.

5.2.1   Fronts near the Antarctic continent

It is of interest to note that there is a dearth of information in the literature on atmospheric frontal characteristics at high southern latitudes let alone the forecasting of such features. (Ironically, there are far more references to oceanic fronts). On the one hand this is surprising given that the Norwegian polar–front theory became the basis for atmospheric frontal analysis pretty much world–wide (Saucier, 1955, p 268). On the other hand, even today the Antarctic may be regarded as data sparse. And one suspects that the liberties in the application of frontal analysis in the early days of aviation reported by Beckworth (1976, p. 329) might equally apply today in the Antarctic context due to a lack of a consistent approach. It would be interesting to examine, for example, if the Norwegian cyclone model was the most appropriate model for all, or even many, cases in the Southern Hemisphere. As Shultz *et al.* (1998, pp. 1767–68) have pointed out the Norwegian model is not without its critics and may be most appropriate for the area for which it was developed. Shultz and his colleagues compare the Norwegian model with the relatively new Shapiro–Keyser cyclone–frontal model (see Shultz *et al.*,1998, p. 1770) for a brief description of this model and Shultz *et al.* (1998, p. 1787, Figure 15) for sketches of the two conceptual models in the Northern Hemisphere context.

Figure 5.2.1.1 below has adapted the Shultz *et al.* sketch (their Figure 15) of these models to the Southern Hemisphere context. *A priori*, fronts which impact on the Antarctic coast may arguably have more in common with the Shapiro–Keyser model, particularly the last stage, than they do the Norwegian model. It may well be that both the above models are applicable in the mid–latitudes of the Southern Hemisphere, where many of the high–latitude storms originate, according to the background flow in which each cyclone is embedded. (by analogy see Shultz *et al.* (1998, p. 1787). However, if either frontal type reaches the Antarctic coast it becomes more like the Shapiro–Keyser model. However, this speculation would need to be tested against numerical and observational data. In view of the doubt about the characterisation of fronts near the Antarctic continent this section will deal primarily with the forecasting of synoptic scale low depressions and anticyclones.

5.2.2   Conventional analysis over the oceans

The term "conventional" here refers to the analysts' normal use of MSLP observations and satellite interpretation along with the analysis cycles of NWP models to derive a MSLP analysis. For oceanic areas of the Antarctic there appears little difference in approach when

compared to the oceans elsewhere in the world, the above comments regarding frontal/cyclone models notwithstanding.
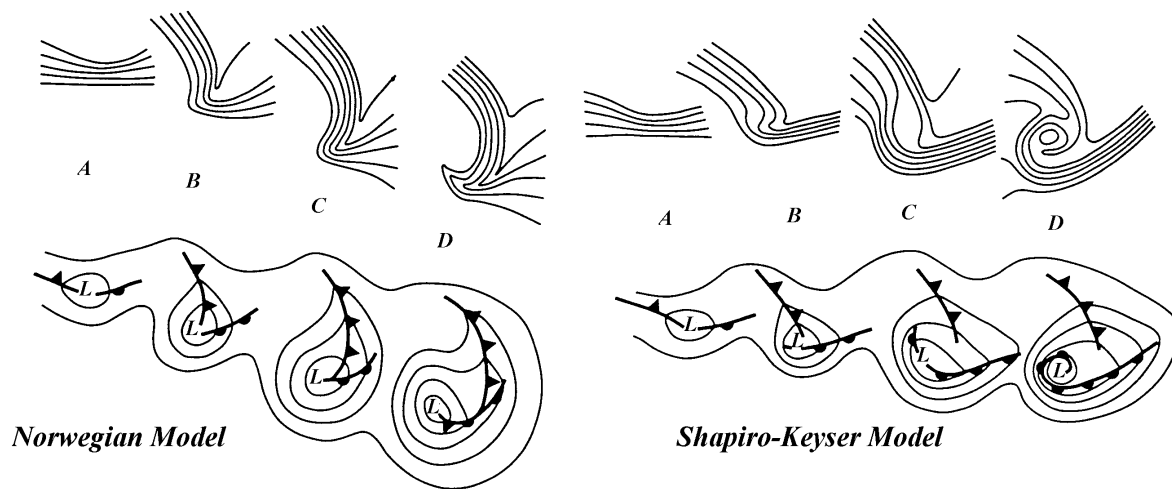
Figure 5.2.1.1   Conceptual models of cyclone evolution showing lower–tropospheric (e.g. 850 hPa) geopotential heights and fronts (bottom) and lower–tropospheric potential temperature (top). At left is the Norwegian Model showing the evolution from the incipient frontal cyclone (A) through stages B and C in which the cold front moves faster than the warm front causing the warm sector to narrow and eventually lead to an occlusion (D). At right is the Shapiro–Keyser model in which the incipient frontal cyclone is (A) with (B) depicting the cold front fracturing from the warm section leading to (C) in which the cold front is the stem of an inverted "T"–bone and the left–hand part of the warm front is bent. The final part (D) comprises the inverted "T"–bone with the left–hand part of the warm front wrapping around the low in a "seclusion". (The figure is adapted from Shultz *et al.* (1998) to reflect a Southern Hemisphere perspective: the "T"–bone shapes are not "inverted" in the Northern Hemisphere.)

5.3   Additional aids to analysis over the ocean

One additional difference with respect to the Southern Ocean and the Antarctic region is that their vast expanse has long been recognised as the most significant data void in the world. Within that region the South Pacific Ocean sector qualifies as the most deficient of all (Streten and Zillman, 1984). Increasingly satellite–derived numerical estimates of sea surface wind speed and direction and of atmospheric layer thicknesses, as well as drifting buoy data, are assisting in overcoming the shortfall. However, these data are not always available and so the specific meteorological analysis techniques which have evolved to deal with the data sparsities of the seventies and eighties still have relevance.

The Junker, and Guymer analysis techniques discussed below offer sound methods of analysis when conventional upper–air and ATOVS/TOVS data are not available in a given time frame. They also provide good training for an analyst in the identification of the key meteorological factors in a satellite image.

5.3.1   Techniques for estimating MSLP

Although numerical models are indispensable in forecasting cyclones, the sparsity of meteorological data over ocean regions may cause problems in accurate analysis and lead to incorrect forecasts especially in the Antarctic. It is helpful, therefore, to identify cyclones at an early stage of development, using satellite imagery to estimate the core or central pressure associated with their cloud patterns. King and Turner (1997, p 190–193) provide a succinct overview of the Streten–Troup (1973) method for such estimation.

Similarly, Junker (1977) has developed a technique of cloud–based interpretation following the studies of Rogers and Sherr (1965). Pictures with characteristic cloud patterns of developing or intensifying cyclones were compared with the lowest observed pressure. They are grouped into six groups of 10–hPa–increments between 1000 and 960 hPa with the typical cloud band structure.

When a wave starts to develop, the cloud band becomes bright with an anticyclonic bulge and core pressure of more than 1000 hPa. With increasing development, the pressure falls below 990 hPa and a dry slot begins to form on the rear edge of the solid bright clouds. If the intensification continues, the pressure falls to 980 hPa while the cloud band wraps itself nearly 3/4 of the way around the cyclone centre. If the central pressure reaches 970 hPa, the cloud band has completely surrounded the centre. Below 970 hPa, the cloud band wraps itself 1–1/2 times around the centre while a circular cloud pattern around the centre indicates still lower pressure.

For the data–sparse regions of the southern Atlantic between South Africa and South America and also during expeditions in the polar North Atlantic, a regression analysis has been carried out by the German maritime meteorology department (DWD) which relates parameters of the cloud band with typical core pressures of intensive cyclones.

As Figure 5.3.1.1 shows, a typical cyclonic cloud band was associated to the distance from core position to the first inner cloud band, called outer radius (OR), to the diameter of the core (ID) and to the core pressure which could be measured sometimes by buoy data or by observation through the German ship "*Polarstern*" near the centre of the low. Figure 5.3.1.2 is the MSLP analysis corresponding to the satellite image.

The relation between central pressure and the cloud structure parameters in the sub–Antarctic waters of the South Atlantic during the season from October to December was found as:

$$P = 0.0683 * OR - 0.172932 * ID - 0.03752 * PHI + 974.76231 \qquad \text{Equation 5.3.1.1}$$

where
P   = pressure in hPa;
PHI   = geographical latitude (without sign);
OR   = "outer radius" in km;
ID   = "inner diameter" in km.
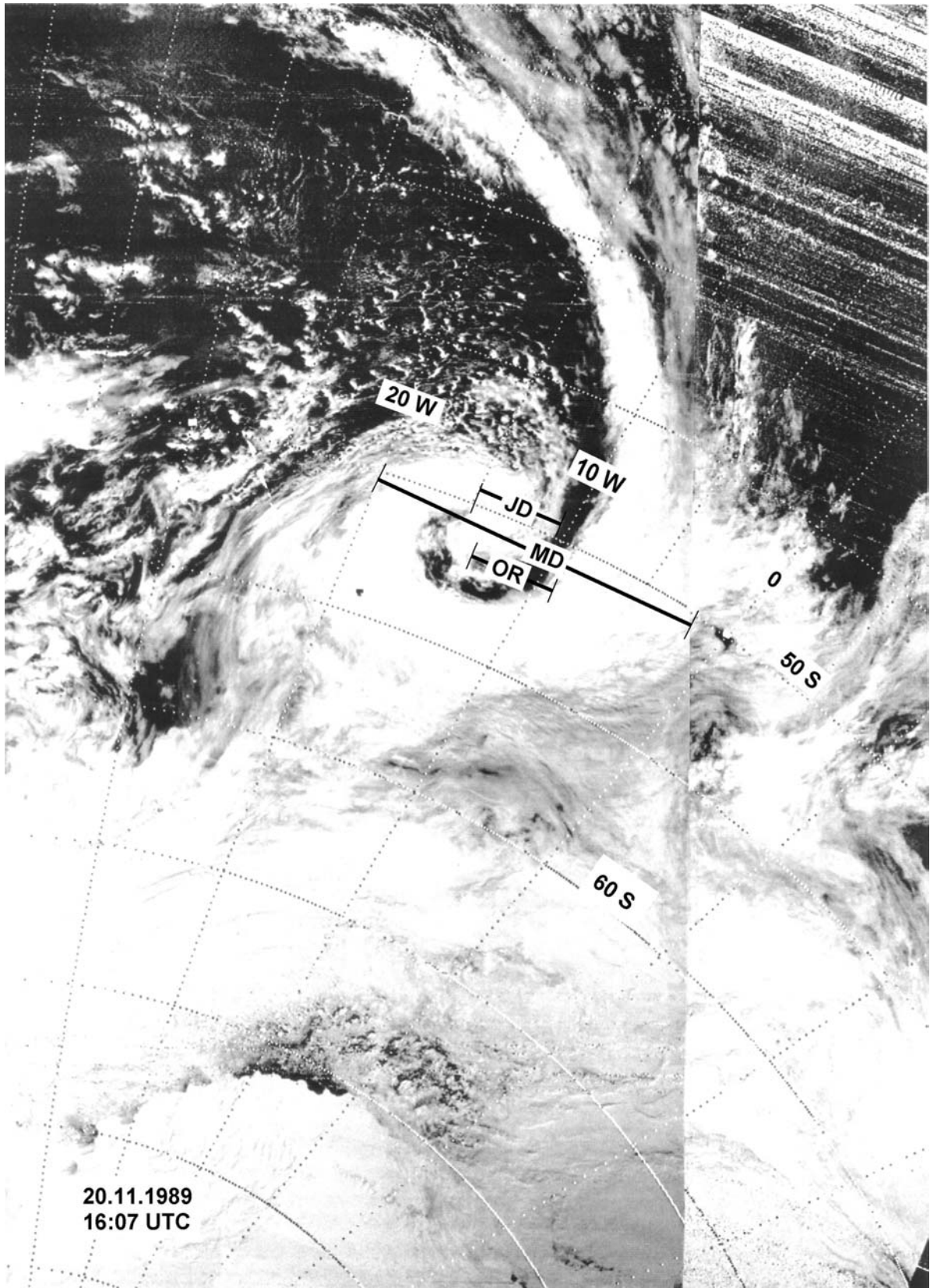
Figure 5.3.1.1   Satellite picture of a typical low centre over the Weddell Sea, with plotted parameters
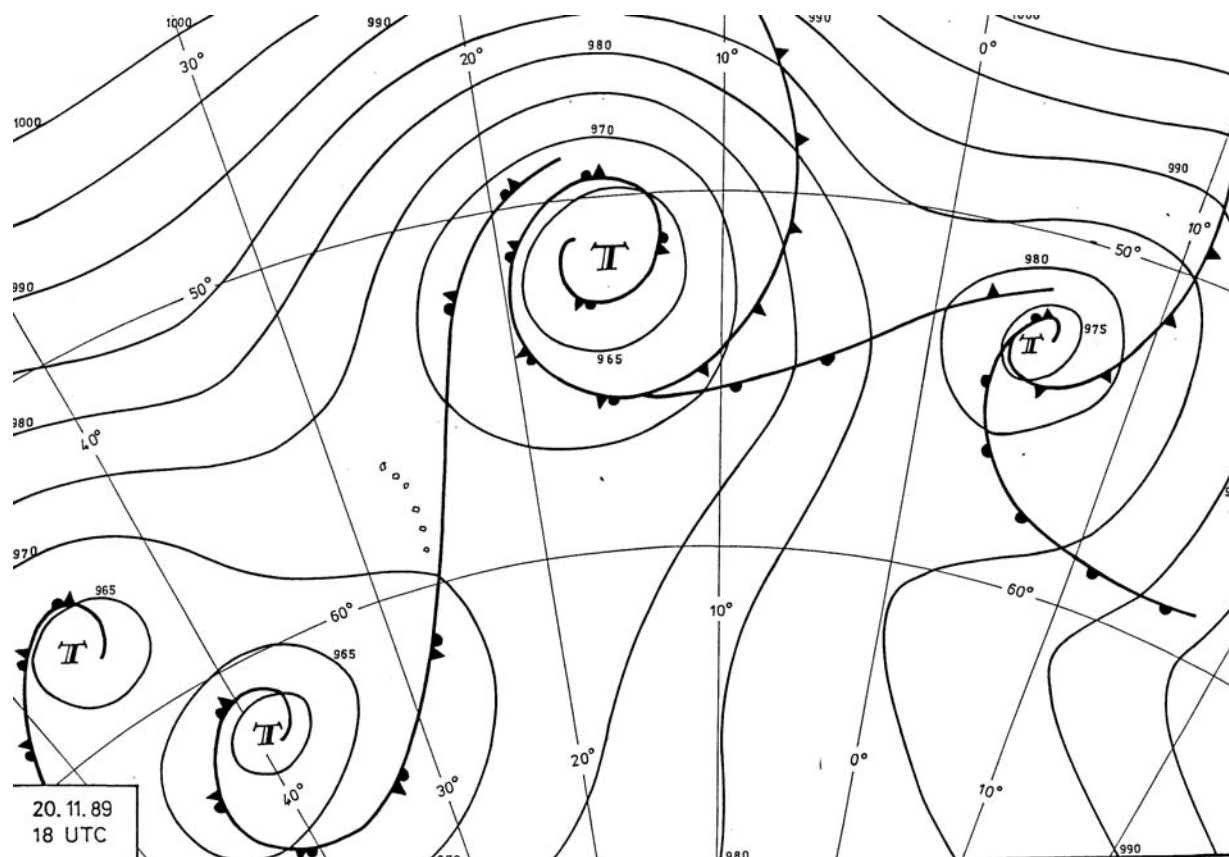
Figure 5.3.1.2   MSLP analysis corresponding to Figure 5.3.1.1

The results are in good accordance with the results of Junker (1997), with errors in pressure estimates of less than +/– 10 hPa. Using the pressure value 12 h before at the location of the low–pressure centre instead of the constant value of 974.76231 yields even better results.

A similar classification of various stages of cyclonic development by characteristic cloud patterns was made by Guymer (1978). The structure and the centre of the vortex are arranged relative to the anomaly pattern of each type of the cyclone stage. These anomaly patterns were developed and used over a 10–year period at the World Weather Centre in Melbourne. One of the decision–laws is that the sea–level–pressure–anomaly, which refers to the seasonal mean pressure for a regularly shaped vortex in mid–latitudes, is 1.5 times its east–west diameter.

5.3.2   Techniques for upper–air analysis

Although the period since the IGY has been one of steady improvement in the availability of observations and the quality of analyses for the Southern Hemisphere, the lack of upper–air observations is still a problem. Several investigations (e.g.: Trenberth, 1979; van Loon and Shea, 1988; Karoly, 1989; Pook, 1992) have shown that the data are satisfactory for the analysis of large–scale features, but the paucity of observations from conventional observing systems has been an impediment to more detailed analysis. In situations where only limited upper–air observations are available alternative analysis techniques can be employed to determine atmospheric thickness. Fronts and low–pressure systems located close to the

144

Antarctic may arguably not always, or even often, exhibit "classical" features and so the models discussed here may have less applicability near the Antarctic coast than at lower latitudes.

Guymer (1978) developed a system of analysis whereby an experienced analyst could combine interpretation of satellite imagery with mean thickness and MSLP fields to construct a 1000–500–hPa thickness chart. Using ESSA visible light imagery and extending the pioneering work of Martin (1968), Zillman (1969), Zillman and Price (1972), Troup and Streten (1972), Streten and Troup (1973) and Streten and Kellas (1973), he produced thickness anomalies which could be tied to recognisable features of the cloud field. With the increased availability of TIROS Operational Vertical Sounder data, this method has fallen out of favour but the technique can still provide a semi–objective means of employing satellite imagery (IR and VIS) to complete an analysis and to assist with pseudo observations for numerical models (Guymer 1978, Appendix). It is also instructive for analysts operating in remote environments such as Antarctica to use the technique as a means of improving their interpretation of satellite imagery.

In order to apply the 'Guymer Technique' it is necessary to adopt a realistic model of Southern Ocean depressions. The main features of the model employed by Guymer (1978) are shown in Figure 5.3.2.1. Guymer (1978) found that the frontal cloud shown as (D) in Figure 5.3.2.1 is a region of above average 1000–500–hPa geopotential thickness whereas the region on the western flank of the vortex (E) is characterised by air with 1000–500–hPa thickness well below average values for a given latitude and time of year. The critical change from above–average to below–average thickness is delineated by a 'line of zero departure" which is shown in Figure 5.3.2.2. The thickness ridge (point of maximum positive departure and thickness trough (region of greatest negative departure) are also shown in Figure 5.3.2.2.

Once the 1000–500 hPa thickness field was established, then by simple addition to the 1000 hPa field (derived from the mean sea level field through the hypsometric equation) then the 500–hPa field can be defined, as can the 850 and 700 hPa levels using regression (Guymer 1978, page 2 of his appendix).

A more recent model of a typical extra–tropical depression has been given by Bell *et al.* (1988) in which they argue that the position of the upper tropospheric wind maximum or jet stream can be inferred from the characteristic cloud pattern which occurs on the warm (equatorial) side of a baroclinic zone. Bell *et al.* (1988) identify the three principal components of this model as the jet associated cloud, the vorticity comma cloud, and the vortex deformation cloud.

Guymer (1978) has argued that the maximum thickness gradient, indicating the approximate position of the polar front jet stream, will be found between 536 and 544 dam when the curvature of the contours is cyclonic, and between 536 and 528 dam when the curvature is anticyclonic, the latter case resulting in a super geostrophic wind. Similarly, Gibson (1989) has used thickness criteria to identify a higher latitude wind maximum which he calls the Antarctic Jet.

5.3.2.1   Climatologies

The construction of a realistic thickness or MSLP anomaly field depends on the choice of climatological data sets. Initially, average fields were available from the work of Taljaard *et al.* (1969) and Taljaard (1972) but later climatologies have been developed from the Australian Bureau of Meteorology Southern Hemisphere Analyses (Le Marshall *et al.*, 1985), the NCEP reanalysis programme and the ECMWF reanalysis programme.

Ⓐ	Area of OPEN CONVECTIVE CELLS
Ⓑ	Area of CLOSED CONVECTIVE CELLS
Ⓒ	PVA MASSES
Ⓓ	FRONTAL CLOUD BAND
Ⓔ	FRONTAL VORTEX
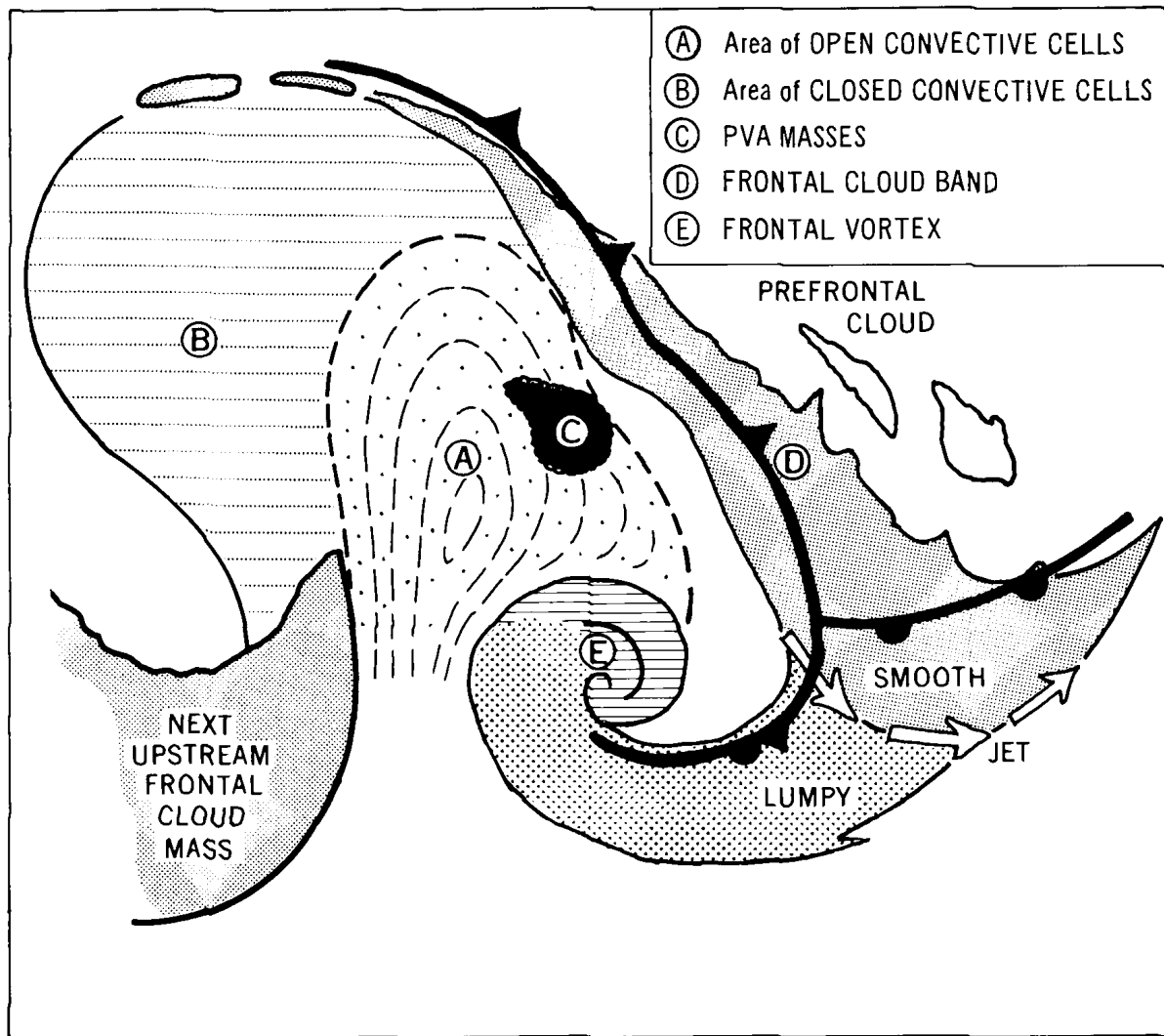
Figure 5.3.2.1   The main features of a typical extra–tropical depression (from Guymer, 1978, p 4).

5.4   Analysis over the interior

Preparing meaningful analyses over the continent is a difficult task. Apart from the fact that there is very little in the way of data upon which to base the analysis, almost the entire continent is above 2000 m, with significant portions rising over 4000 m. Reducing pressures reported from the AWSs to a mean sea level value is simply not a valid thing to do given the extent of the altitude reduction and the problems in defining a mean virtual temperature for the layer from the surface down through several kilometres of ice. Because of this, the surface layer of the atmosphere over the continent requires a different form of analysis; one that accurately and meaningfully defines the surface layer and one that can be merged with the more standard MSLP analysis performed over the oceanic and coastal regions. Three differing approaches have been used.
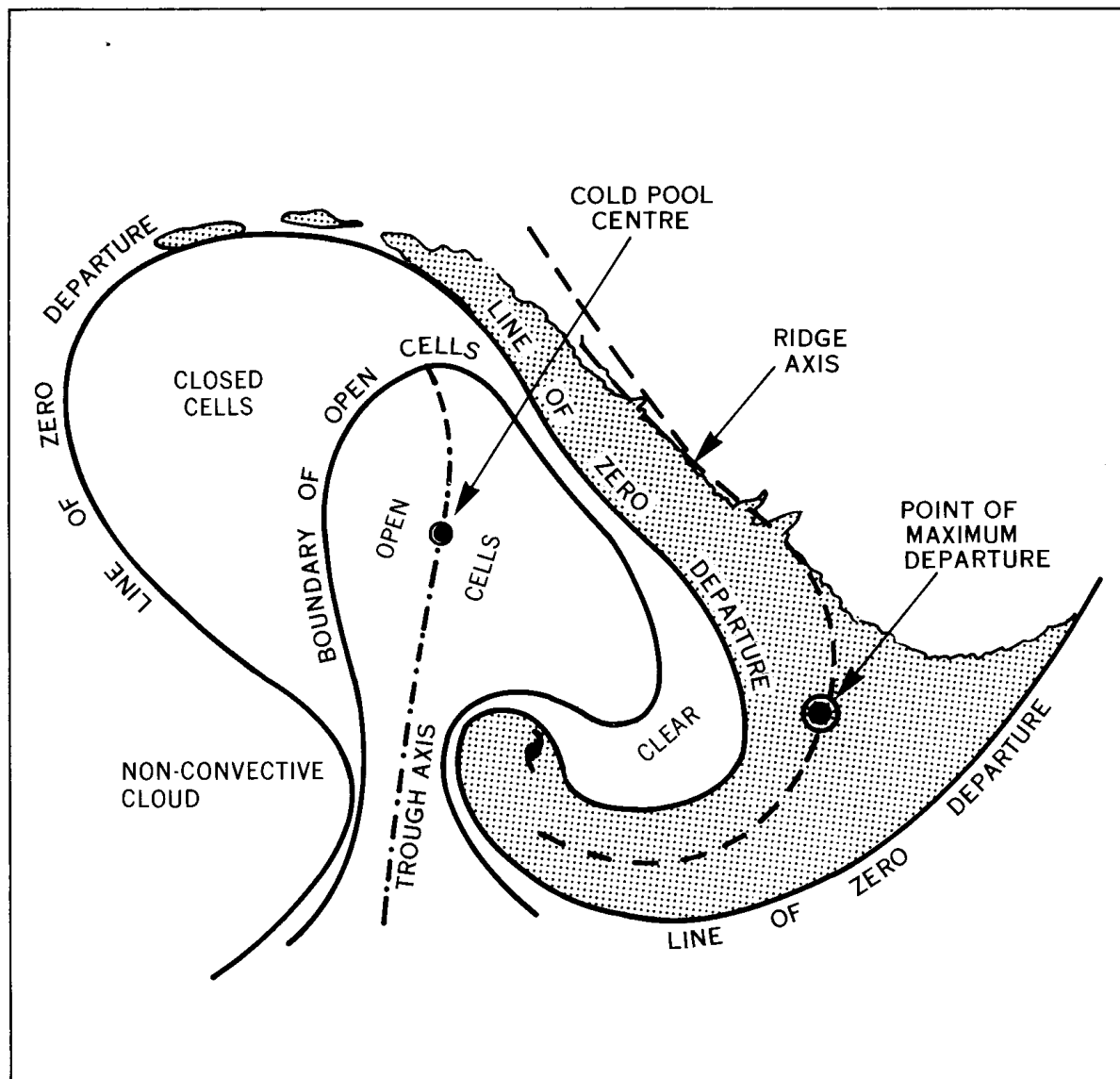
Figure 5.3.2.2   Key regions where anomalies of 1000–500–hPa thickness are likely to be located (from Guymer, 1978, p. 41).

The first of these is to use a standard reduction technique and simply analyse MSLP over the continent. This is still performed in some analysis centres but the product does not provide any useful meteorological information. The observed wind field is certainly not geostrophic and as such the flow defined by the MSLP chart highly inaccurate.

The second technique involves performing a geopotential height analysis at the first standard pressure level that does not intersect the continent. The 500–hPa surface meets this requirement and has been a standard level analysed in Antarctica for some time. Unfortunately, it suffers some of the same problems as the MSLP field in that the inferred wind regime from the analysis bears little resemblance to the surface wind field defined by the AWS data. Strong decoupling between the surface layer and the free atmosphere can make this form of analysis difficult to interpret and the amount of data provided from upper–air reporting stations is even more limited than the amount of AWS data available.

5.4.1   Streamline analysis

The third style of analysis that has, for example, been in use at Casey throughout most of the 1990s, involves merging MSLP analyses over the ocean and coastal regions with a streamline analyses of the surface wind over the continent (Figure 5.4.1.1). This style of analysis provides a meaningful assessment of surface conditions as the MSLP analysis provides marine users with a good estimate of likely wind conditions in those areas devoid of observations and the streamline analysis over the continent provides a useful assessment of likely wind conditions inland. The streamline analysis is superior to the MSLP analysis in that it not only defines the wind flow over the continent but centres of anticyclonicity/cyclonicity are also defined by the flow such that weather systems may be tracked across the continent.

The scarcity of surface data inland continues to compromise the accuracy of the analyses. However, the requirements for forecasting in these regions is also quite low. In order to better analyse conditions over data sparse areas of the Southern Hemisphere numerical model data are frequently used. The very short term forecasts from the models provide a good starting point for the analysis, as they are dynamically consistent and the short term nature of the forecast provides a reliable first guess. For the surface wind field the best model data are the first sigma level wind values. These data are typically at around 70 m above the surface and provide a good approximation to the surface 10 m flow. Figure 5.4.1.2 is an example of the surface flow from the high resolution Australian global model (GASP) displayed in the same style as used on the manual analysis.
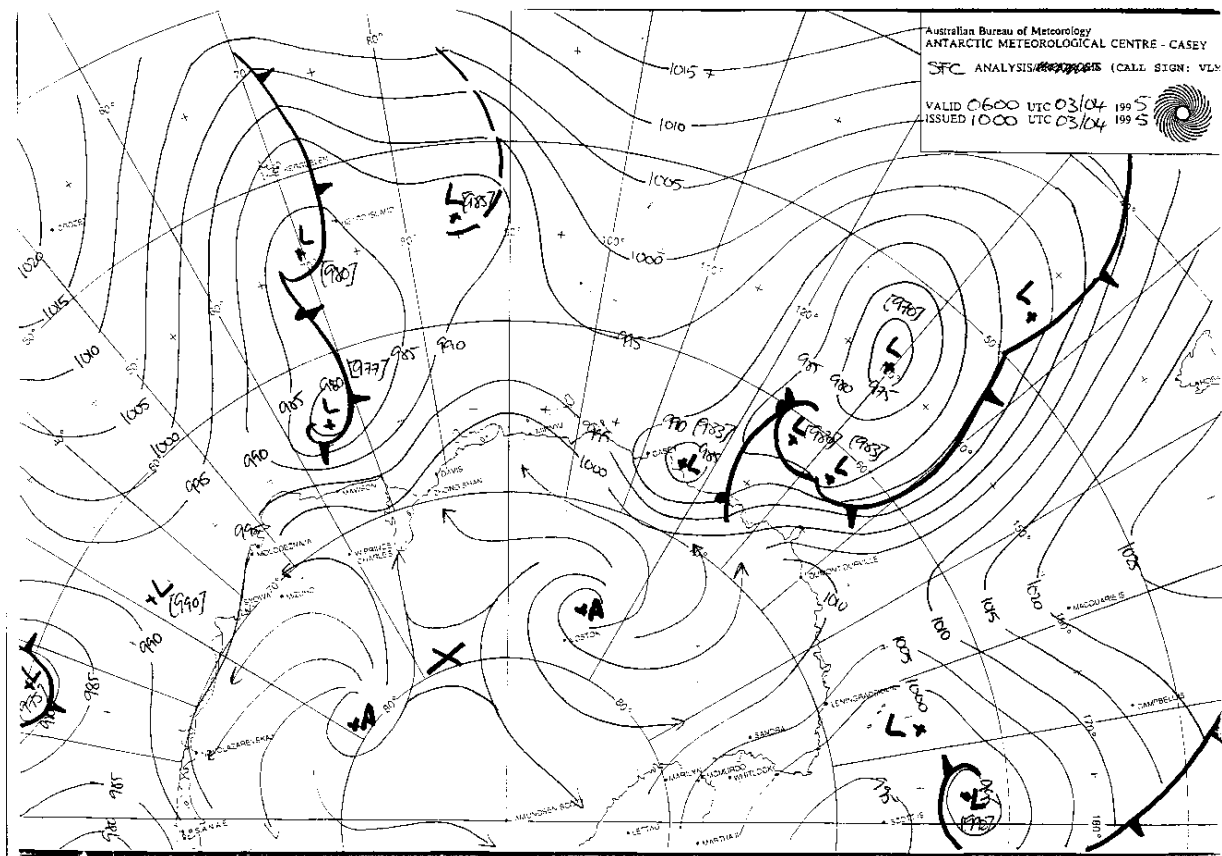
Figure 5.4.1.1 An example of streamline analysis over the Antarctic Continent
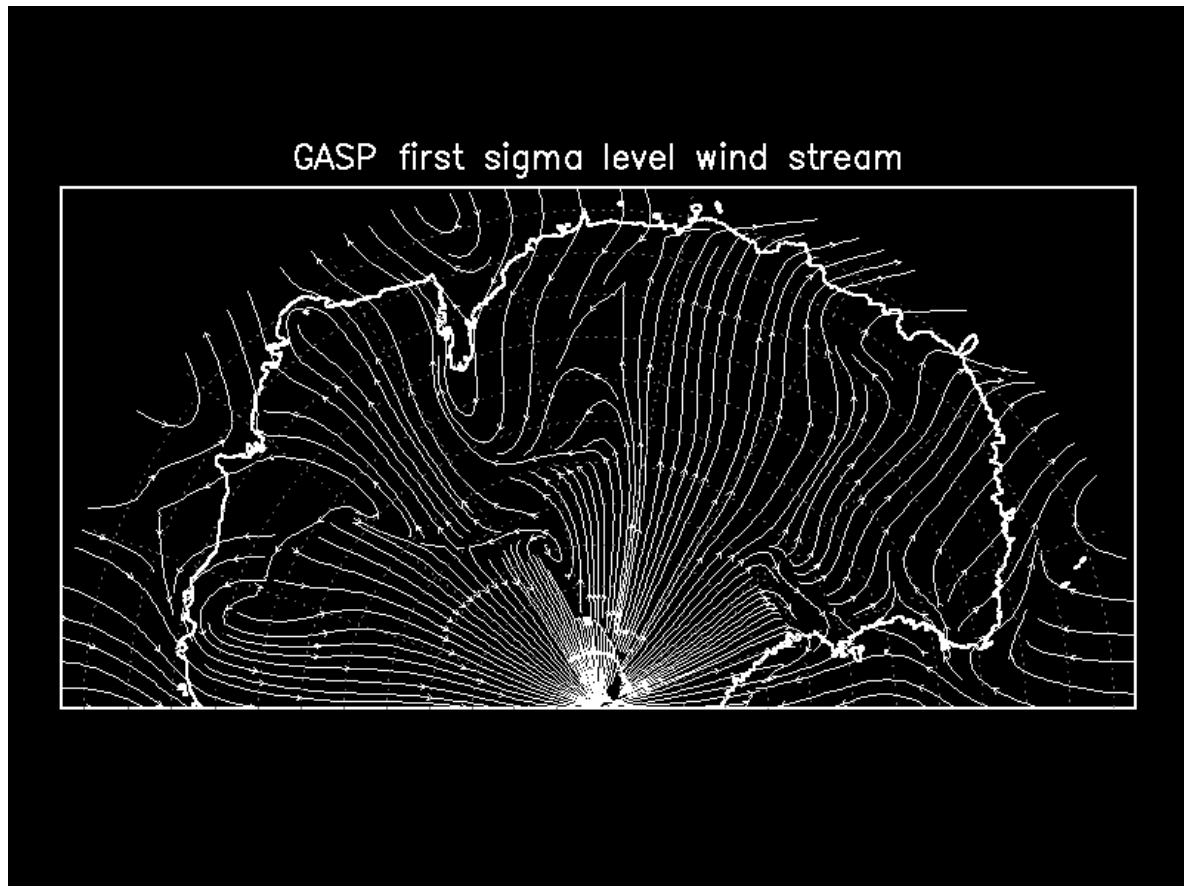
Figure 5.4.1.2   An example of the surface flow from the high resolution Australian global model (GASP) displayed in the same style as used on the manual analysis.

One deficiency in the numerical models is the poor representation of orography and the synoptic pressure gradients tend to be too weak. However, as may be seen in the following section, these model fields are still of considerable use.

5.4.2   Use of model sigma surface data

The MSLP chart remains the primary field for analysis although it has limited use in contributing to the forecast process. Pressure as a meteorological parameter provides users with no useful information, per se, but traditionally has been used to infer surface wind fields, frontal positions and associated cloud. The global models from which the MSLP charts are now obtained provide all these data anyway, rendering the MSLP chart somewhat obsolete. The most useful field in Antarctic operations is the surface wind field and the first sigma level wind data out of the numerical models provides the best guess for this. Figure 5.4.2.1 shows an example first sigma level wind forecast from the GASP model where the first sigma level is set at 0.9910. This places the data at each gridpoint at a pressure of 0.9910 times the surface pressure, resulting in the sigma surface data always remaining above ground. For example, if the surface pressure was 970 hPa then the first sigma level would be at a pressure of 965.15 hPa, which is about 70 m above the surface. In all respects these data provide the most useful guidance for wind forecasting, even over ocean areas where MSLP is typically a reliable field.

As the wind is dynamically calculated, strong ageostrophic flows associated with rapidly developing systems, along with corrections for system speed of movement, are fully defined in the model field providing far more accurate wind information than could possibly be inferred by studying an MSLP prognostic chart.
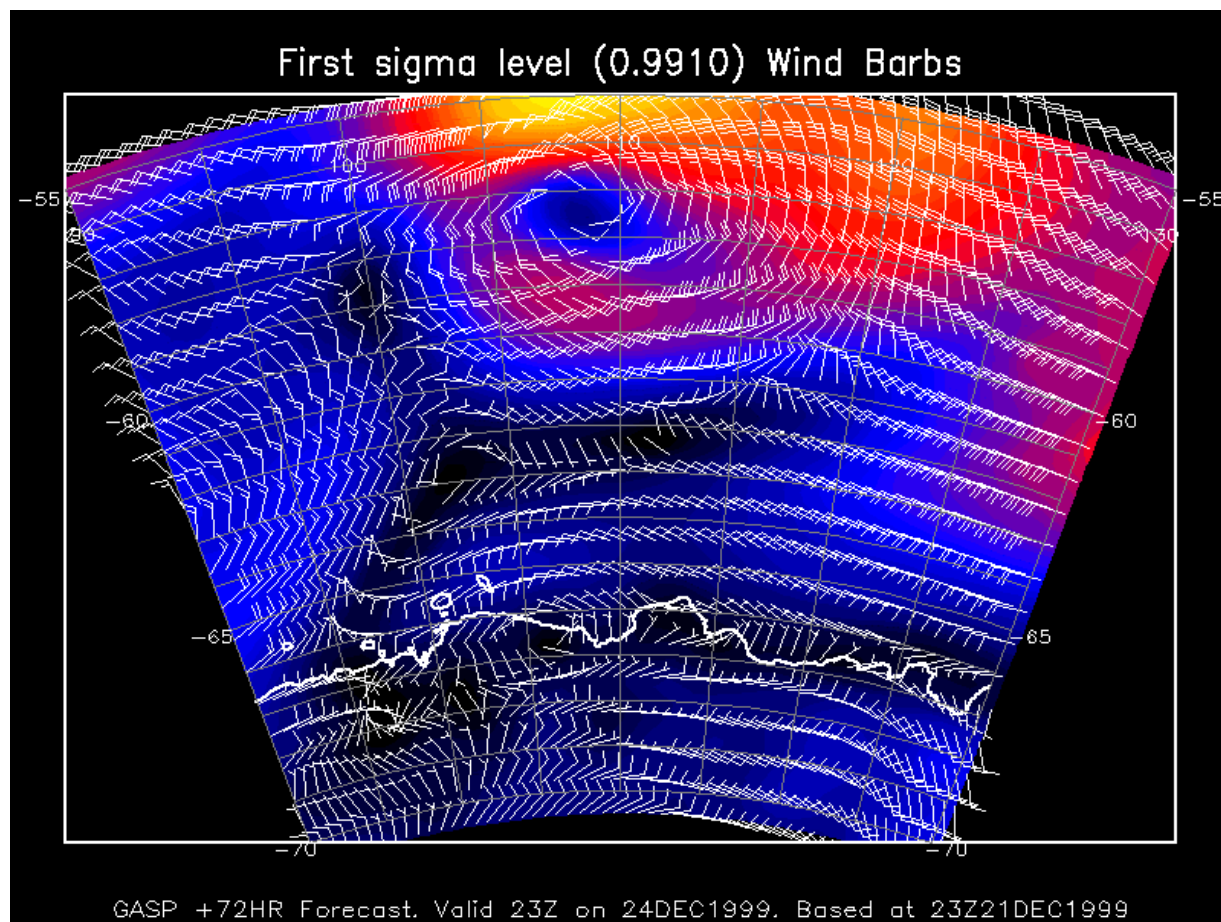
Figure 5.4.2.1   An example of a 0.9910 sigma level wind forecast from the GASP model

5.4.3   Estimating 500–hPa or 700–hPa geopotential heights from AWS observations

5.4.3.1   The Phillpot Technique for 500–hPa heights

Phillpot (1991) argued for the adoption of the 500–hPa level as relevant for Antarctic analysis. In view of the lack of upper–air observations from the interior of Antarctica, he devised a technique for the derivation of 500–hPa height from AWS surface observations in the Antarctic continental interior. This technique employed a calculation of surface to 500–hPa layer thickness based on a mean virtual temperature of 0ºC and then adding a thickness correction $\Delta Z(T_s)$ to allow for the departure of the true layer mean virtual temperature from 0ºC. (Radok and Brown (1996) refer to this as the 'thinning' of the surface to 500–hPa layer). The technique relies upon the correlation between surface temperature and the surface to 500–hPa layer mean temperature, so it is to be expected that the shallower the layer the more

150

accurate the estimated heights. Phillpot described his results as encouraging for stations above 2.5 km, but not below. The basis of the technique is as follows:

- Calculate the geopotential height of the 500–hPa level hydrostatically, assuming the surface to 500–hPa layer has a mean virtual temperature of zero. We define this as $Z_{500}(0)$.
- Apply a surface temperature dependent correction to this height to derive the actual height of the 500–hPa level. We define this correction as $\Delta Z(T_s)$ where T_s is the surface temperature.
- Thus the actual height of the 500–hPa level, here defined as $Z_{500}(T)$, is estimated from the equation:

$$Z_{500}(T) = Z_{500}(0) - \Delta Z(T_s) \qquad \text{Equation 5.4.3.1.1}$$

where Figure 5.4.3.1.1 shows the simple relationship between these variables.

Phillpot used IGY data to develop regression equations for individual sites, relating the surface temperature T_s to $\Delta Z(T_s)$. He found a relationship of the form:

$$\Delta Z(T_s) = mT_s + c \qquad \text{Equation 5.4.3.1.2}$$

where T_s is in °C, m is given in gpdm °C^{-1} and c is given in gpdm.
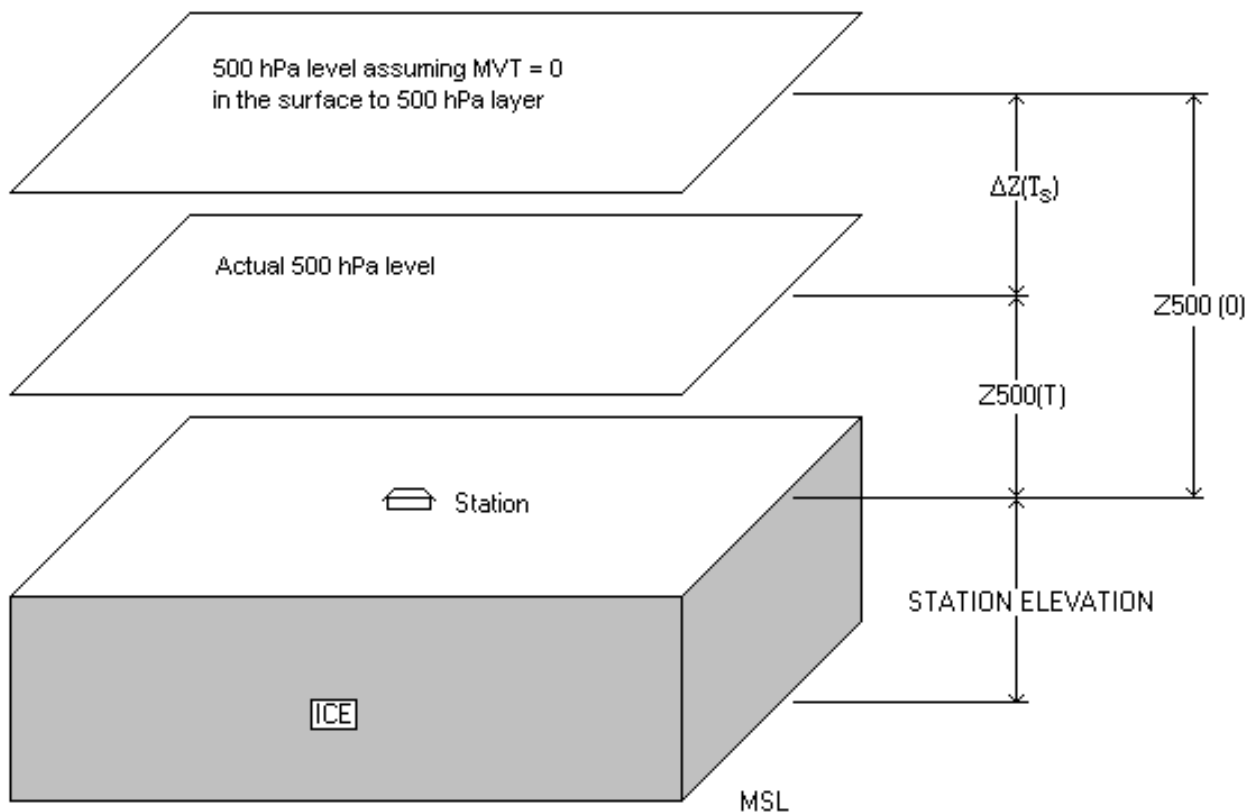
Figure 5.4.3.1.1   Relationship between $\Delta Z(T)$, $Z_{500}(0)$ and $Z_{500}(T)$

Phillpot tabulatedd values of m and c for Byrd, Pionerskaya, Amundsen–Scott, Vostok and Sovietskaya, and appears to have used stations Byrd and Sovietskaya to estimate the variation

of m and c with height. (His Figure 3 shows a straight line connecting plots for these two stations and Phillpot reported that he estimated his best fit for the stations available by eye). Assuming a linear variation of m and c between Byrd and Sovietskaya, the following relationship is found:

$$m = -0.00015h + 0.739 \qquad \text{Equation 5.4.3.1.3}$$

$$c = 0.052h - 33.8 \qquad \text{Equation 5.4.3.1.4}$$

where h is in gpdm.

This relationship does not quite yield the results shown in Phillpot's Table 2, since Phillpot appears to have quoted the original values derived from his study where available and the values derived from his best fit line otherwise. It might also be acceptable to use a line of best fit for stations above 2.5 km, since Phillpot believes his results to be accurate to 4 gpdm only above that level. Using the method of least squares, this yields the following values:

$$m = -0.0014h + 0.7 \qquad \text{Equation 5.4.3.1.5}$$

$$c = 0.058h - 35.5 \qquad \text{Equation 5.4.3.1.6}$$

where h is once again in gpdm. Given the limitations in accuracy of the technique, it is unclear that such a refinement would provide any improvement.

Thus to employ Phillpot's technique for a given AWS, the equations for m and c are solved using the elevation of the AWS. This needs to be done only once for any given AWS or surface observation station, of course. An estimation of $Z_{500}(T)$ then follows routinely as:

$$Z_{500}(T) = Z_{500}(0) - \Delta Z(T_s) = Z_{500}(0) - (mT_s + c) \qquad \text{Equation 5.4.3.1.7}$$

where $Z_{500}(0)$ is calculated via the usual hypsometric equation:

$$Z_{500}(0) = (RT/g)(\ln(Psfc/500)) \qquad \text{Equation 5.4.3.1.8}$$

in which: *Psfc* is the surface pressure; R is the universal gas constant 287.05; *T* is 273.16K; and *g* is 9.80665 m s^{-1}

5.4.3.2   Radok and Brown's technique for 500–hPa heights

Radok and Brown (1996) used Phillpot's IGY data to devise a similar technique for the estimation of 500–hPa heights, although their technique estimates the layer mean temperature rather than the 'thinning' of the surface to 500–hPa layer due to departure of the layer mean temperature from 0ºC. Radok and Brown's approach yields regression equations for all stations used by Phillpot but, as they show in their Figure 1, these equations can be replaced by a single equation with little loss of accuracy. Radok and Brown suggest that their approach should yield more accurate 500–hPa heights. Radok and Brown analysed 3494 soundings taken from stations ranging in elevation from near mean sea level (e.g. McMurdo) to over 3 km (Vostok) to yield a regression equation for the surface to 500–hPa layer mean temperature:

$$\overline{T}_{sfc-500} = 0.44T_s - 19.0$$
<div align="right">Equation 5.4.3.2.1</div>

where Ts is the surface temperature. In order to estimate Z_{500} it is necessary only to use T_s to estimate the mean virtual temperature between the surface and 500 hPa, then employ that temperature in the hypsometric equation.

Regardless of the method chosen to estimate Z_{500}, the estimate is only as good as the knowledge of the AWS elevation. Errors caused by incorrectly specified temperature become small compared to errors in AWS elevation as the elevation of the AWS increases.

The techniques related above are used only in manual analyses of the 500–hPa level, as for numerical analysis the surface conditions may be ingested directly.

5.4.3.3   700–hPa heights

The limitation of Phillpot's technique to stations above 2.5 km is particularly serious for the case of West Antarctic AWSs, most of which are below 2 km, leading Phillpot to apply his technique to the estimation of 700–hPa heights (Phillpot, undated, unpublished). In this case, Phillpot used data from Byrd and Little America Stations, collected during the IGY. Phillpot followed the same approach as for his 500–hPa study, thus:

$$Z_{700}(T) = Z_{700}(0) - \Delta Z(T_s)$$
<div align="right">Equation 5.4.3.3.1</div>

where the correction $\Delta Z(T_s)$ is once again estimated as:

$$\Delta Z(T_s) = mT + c$$
<div align="right">Equation 5.4.3.3.2</div>

Two sets of regression equations were derived, each including coefficients for winter, summer, intermediate seasons and for the whole year. His conclusion was that since the estimated height corrections vary little from season to season, sufficient accuracy would result from the use of whole year data. He also suggested that, while root mean square (RMS) errors in the Little America data precluded the use of his technique near sea level, a linear interpolation of his coefficients between the elevations of Byrd and Little America should lead to a reasonable estimate near 1000 m. Phillpot's results are shown in Table 5.4.3.2.1

	Elevation (gpdm)	**m**	**c**	**Rms error (gpdm)**
Little America	4	0.37	−10.70	1.65
Byrd	153	0.18	−4.90	3.70

Table 5.4.3.2.1   Regression coefficients for use in Equations 5.4.3.3.1 and 2.

Phillpot comments that because of the large RMS error in the Little America estimations, use of his technique is not advisable at low elevations. He suggests that a linear interpolation between the m, c and RMS errors at Little America and Byrd should give acceptable estimates of 700–hPa heights at or above 1 km elevation.

The linear relationships between m, c, rms error and height implied by Table 5.3.3.2.1 are:

<div align="left"> $m = 0.00128h + 0.375$</div>
<div align="right">Equation 5.4.3.3.3.</div>

c = 0.0389h – 10.86   Equation 5.4.3.3.4

rms = 0.0138h + 1.6   Equation 5.4.3.3.5

where h is given in gpdm.

700–hPa Height Estimation via Radok and Brown's Technique in the FROST project

In view of the simplicity of Radok and Brown's technique using a single regression equation for 500–hPa height over a range of elevations it would seem that their technique should be adapted for 700–hPa height estimations. Unfortunately, this is not straightforward because their regression estimated the surface to 500–hPa mean virtual temperature, which is not simply related to the surface to 700–hPa mean virtual temperature. It is simpler to use the Phillpot technique, but one possible approach (rather circuitous) is that used during the FROST project, sketched below:

In order to estimate the surface to 700–hPa layer thickness from the surface to 500–hPa mean layer temperature available via the Radok and Brown formula, a constant lapse rate in the two layer surface to 700–hPa and 700–500–hPa was assumed, i.e. lapse rate Γ was defined as:

$$\Gamma \equiv \Gamma_7 \quad for \; p_{sfc} > p > 700 \, hPa$$
$$\Gamma \equiv K\Gamma_7 \quad for \; 700 \, hPa \geq p > 500 \, hPa$$

Equation 5.4.3.3.6

where *K* is some constant. After examining mean temperatures and pressures of the surface, 700 and 500–hPa levels from the UCAR RAOB data set, *K* was assigned the value 1.3. Different values were found for the stations Halley (1.2), Marambio (1.4) and McMurdo (0.8). Since each of the AWS sites of interest for 700–hPa height estimations was over the ice sheets near Byrd, the figure for Byrd was used in the FROST project because there was no basis on which to estimate the variation of *K* with distance from Byrd.

In order to calculate Z_{700} for each T_{sfc} and P_{sfc}, a half interval search technique was then used to find the value of $\Gamma 7$ required to minimise the difference:

$$diff \;=\; Z_{\overline{T}500} \;-\; Z_{\overline{\Gamma}500}$$

Equation 5.4.3.3.7

between the 500–hPa height obtained assuming a layer mean temperature from the hypsometric equation :

$$Z_{\overline{T}500} = Zsfc + \frac{R\overline{T}_{sfc}500}{g}\ln\left(\frac{p_{sfc}}{500}\right)$$

Equation 5.4.3.3.8

and that obtained with the assumption of constant lapse rate :

$$Z_{\overline{\Gamma}500} = Z_{sfc} + \Delta Z_{sfc/700} + \Delta Z_{700/500}$$

Equation 5.4.3.3.9

where the thickness ΔZ of a layer with p0 > p > p1, temperature T_0 at the lower boundary and constant lapse rate Γ within the layer is given by :

$$\Delta Z = \frac{T_0}{\Gamma}\,[1-(\frac{p_0}{p})^{\frac{-R\Gamma}{g}}]$$

Equation 5.4.3.3.10

where R is the gas constant for dry air and g is the standard acceleration due to gravity.

Thus the final value of Γ_7 was used to calculate the 700–hPa height using the surface pressure and temperature and assuming constant lapse rate.

Generally, the results for both the Phillpot or Radok and Brown techniques were close to each other above 1 km elevation, where the Phillpot technique would be expected to be acceptable It would be simpler to use Phillpot's technique in the absence of a study similar to Radok and Brown and focusing on the 700–hPa level.

Regardless of whether the Phillpot technique or a modification of the Radok and Brown technique is used, however, results are dependent on the quality of the AWS data and especially on knowledge of the elevation of the AWS site.

6　　　　THE FORECASTING PROCESS

'The future position of any pressure system should be determined by as many means as possible .' (Petterssen 1941).

6.1　　　　The systematic approach to forecasting

Whilst the Antarctic environment is different from the climate and weather experienced by most forecasters in their home country, the same fundamental laws of physics and chemistry apply. Accordingly, Antarctic weather forecasters can approach their task in a manner similar to that which they are used to at their home locality. The systematic approach outlined here may not be followed worldwide but has proven to be successful in some countries (eg: Australian Bureau of Meteorology, 1984) and probably contains some steps which are adhered to in full or in part by most national forecasting agencies.

　　There are several time scales for which forecasts or outlooks are required depending on the purpose (usually logistical) for which the forecast is required: long; medium and short term. As noted by Golden *et al.* (1978, p.) "Many studies have shown that persons use the longer–term forecast to make plans but that decisions are usually made on the basis of shorter term (0–12 hr) forecasts." In accord with Golden *et al.*'s the focus here is to consider mainly the approach to short–term forecasting. Much of the material presented is adapted from Australian Bureau of Meteorology (1984), which notes that: "It is extremely helpful to have forecasting guidance notes for each station which briefly document the conditions under which various weather elements normally occur, as well as unusual events. Case histories which describe significant events also enable a new forecaster to quickly become familiar with local conditions and assist in the exercise of sound professional judgement in a particular situation. ". This is a primary goal of the International Antarctic Weather Forecasting Handbook and the station specific guidance notes for many stations are presented in Chapter 7 below. The present chapter deals with some of the issues concerned with the "generic" approach to forecasting.

6.1.1　　　　Getting to know the physical environment of the area for which forecasts are being prepared

Prior to commencing forecasting for a particular area, Australian Bureau of Meteorology (1984) advises that a new forecaster must have a detailed knowledge of the mesoscale climatology and geography of the forecast area. This information should be established for each relevant location and stored in a convenient integrated summary or display that is easily accessible.

The forecaster's detailed knowledge of the forecast area can initially be gained from the study of a large–scale map. Where possible he/she should also examine the significant features first–hand, through, for example, the use of familiarisation flights. The geographical features that should be noted include:

- The dimensions and orientation of any ice–domes, hills or mountains and the extent to which they form a barrier to the airflow in certain directions; the degree of forced uplift can then be gauged. These orographic features together with glacial valleys, and the continental plateau itself, may also give rise to local wind systems (e.g. katabatic winds; mesoscale lows).
- The location of any significant gaps in mountain ranges that might require special attention in the prediction of wind or cloud.
- The distribution of rock/ice/sea ice/open water. These factors may be important in determining local heat sources and sinks and mesoscale/micro–scale variations in low level moisture.
- The presence of rocky outcrops close to or on a flight path might also be crucial to ameliorating the effects of white–out in overcast conditions.

6.1.2   Getting to know an area's climatology

Basically, climatology summarises various aspects of weather (e.g. average cloud amount; days of gales; blowing snow; fog, etc.) in a convenient form (e.g. frequency tables) and consequently provides some information on the normal expectation of weather at a particular locality. Appendix 2 below contains climatological data for many of the places covered in this handbook. The value of these data for short–term forecasting varies greatly with locality and season. Frequently climate statistics only provide background information, but, where the weather is strongly linked to seasonal and diurnal patterns, climatology exercises a strong influence on the forecast. Nevertheless, climatology must not be insisted on at the expense of synoptic and dynamic reasoning.

Other types of climatological information have more definite relevance in everyday short–term forecasting. These include:

- typical diurnal behaviour of the katabatic wind at a particular station;
- mean hourly rates of change of temperature and dew–point temperature and the change under different synoptic conditions;
- typical rates of precipitation for different synoptic patterns

An additional factor often overlooked in applying geographical and climatological data is the effect of actual antecedent conditions: for example, is there more open water nearby than usual which might indicate increased cloudiness or an increased risk of fog? In marginal situations the incorporation of knowledge of these effects could make the difference between a confident (and successful) forecast or an uncertain one.

6.1.3   Major steps in short–term forecasting

In practice, the best approach to short–term forecasting will depend on the particular time–period of the forecast and the scale and life cycle of the weather phenomena that are expected in the forecast period. For example, in a blizzard situation persistence might be quite satisfactory for the next few hours to a day or so if a major low–pressure system has forced the blizzard and is slow moving. On the other hand, the onset or cessation of blizzard conditions may be more difficult to predict. Nevertheless, assuming familiarity with the forecast area and a knowledge of, or ready access to, local climatology, there are general principles that should be taken in a forecasting shift in order to develop a solid forecasting methodology. These principles are enunciated in a sequence of major steps which are recommended by Australian Bureau of Meteorology (1984), and outlined below and elaborated on in the subsequent sections.

- *Step 1:* Get a thorough briefing from the forecaster going off–duty (if there is one) or by examining observations/existing analyses/existing prognoses;
- *Step 2:* Plan task times and deadlines;
- *Step 3:* Do a comprehensive analysis of surface and upper–air conditions;
- *Step 4:* Formulate a model to explain current observations;
- *Step 5:* Make predictions;
- *Step 6:* Maintain a weather watch;
- *Step 7:* Repeat steps 3–7 if the forecast strategy is not working;
- *Step 8:* Brief the next forecaster thoroughly.

The mode of application of these steps will vary from place to place depending on such things as the specific work output requirements of the shift, observational and data processing facilities available, etc. Time will be an ever present constraint and so the efficient forecaster will learn to take a number of steps simultaneously and will be able to judge just how much time to spend on each step in various situations.

6.1.3.1   A thorough briefing

A thorough handover/takeover briefing is needed at the start and end of each shift in order to:

- maintain continuity of short–term forecasting services;
- provide the new shift forecaster with sufficient background to act immediately to revise a forecast or to issue a new forecast if required;
- convey the degree of confidence held in the current forecast strategy;
- alert the new shift forecaster to any current problems with observing systems, communications systems, etc.; and
- enable the forecaster to properly plan the task times and deadlines for the forthcoming shift.

The maximum time available for briefing will vary from forecast office to forecast office but is normally a minimum of about 15 minutes. It is important that the briefing be done systematically to ensure that the key pieces of information are passed on and understood. In situations where offices do not provide 24–h coverage or where the forecasts are undertaken

by a single person the forecaster may have to brief him/herself at the start of a shift. In either situation, the briefing principles are the same, namely:

- Immediately identify the critical operational factors that will affect the provision of short–term forecasting services during the shift. Critical factors include:
    (i) any warnings that are current or imminent;
    (ii) any adverse weather, current or imminent;
    (iii) any unusual deficiencies or variations in the observing system (e.g. apparent station dew–point errors, problems with autographic instruments, special observations being received, malfunction of satellite receiving equipment, special satellite picture enhancements in operation);
    (iv) any problems with telecommunications (e.g. inward traffic delays, telephone system malfunctions).
- Review the meteorological situation of the past six hours or so with emphasis on the trend in local observations. Identify critical or unusual aspects of local autographic records, hourly aerodrome weather reports, radar, satellite data etc. Try to relate cloud and other observations to the latest radiosonde/upper wind data. Relate significant changes in the evolutionary weather pattern quite clearly to features analysed on various charts. For example, cloud may be evident over a coast where the winds have become onshore, or a coastal polynya may have formed as the wind has changed to off–shore.
- Briefly outline the broad–scalescene starting with analyses at T–24 h and extending through to prognoses out to T+12 h. If available, sequential image display sequences (e.g. movie loops or video) of satellite data are an ideal briefing tool. Offices should also have a convenient fixed sequence wall display of imagery and analyses specifically for briefing purposes. The upper–air pattern exerts a strong control and the significant features must be identified.
- Clearly state the short–term forecast strategy and the degree of confidence in it. In particular try to identify:
    (i) the observations (location, time, type) and the specific analysis tools that are expected to be critical in the next six hours (these will vary according to the situation);
    (ii) the expected evolutionary pattern (movement, development, etc.) of key components of the analysis pattern;
    (iii) the expected influence of diurnal changes and local orographic effects;
    (iv) the 'safety factor' built into the forecast that accounts for likely scope for error;
    (v) any known special user requirement that might cause you to give particular attention to some aspect of the forecast;
    (vi) there should be an alternative strategy that could be applied if the forecast starts to go wrong, particularly if confidence in the initial forecast is not high.

6.1.3.2   <u>Task times and deadlines</u>

All forecasting offices have a work schedule that sets out the deadline times for issue of forecasts. Sometimes these schedules also suggest optimum times for analysis, briefing, etc., although these are hard to fix because of the variable nature of the forecast request work–load from day–to–day. However, the office work schedules do not necessarily allow adequate time for forecast preparation and certainly do not cater for variations in work–load caused by such

things as prolonged bad weather, observations/communication problems, or abnormal volumes of *ad hoc* requests. Therefore, to maximise the time available for scientific input to forecast preparation the forecaster must establish his/her own set of task times and deadlines at the start of each and every shift.

A critical factor is the actual and expected weather, details of which the forecaster will have obtained from the handover/takeover briefing. If the weather is good, and confidently expected to remain so, then forecast messages tend to be short and preparation time is minimal. In these situations forecasts can confidently be prepared well ahead of schedule (to spread the work–load more evenly over the shift) and the forecaster can devote more time to undertaking careful re–analysis of earlier data, to sharpen analysis skills and as an added check on the forecast.

The approach will be quite different in bad weather situations. Continuous monitoring of some weather elements will be essential and the forecaster will have to allocate extra analysis time according to the observational programme and facilities available. Forecast messages will be longer and more complicated, the detail of the forecasts will be more critical, and forecast accuracy confidence will tend to be lower than in good weather situations. In these situations it is very important to do a thorough analysis of all the data at strategic times rather than to become swamped by the mechanical aspects of physically writing or typing the forecasts and merely scanning incoming data.

In planning a 'bad weather' shift, try to set aside, in advance, at least one time–period for thorough analysis. During this period you will be able to formulate a good model of current atmospheric behaviour and develop a new forecast strategy (or extend the existing strategy). The actual preparation of a large number of final forecasts can then be done quite quickly.

Try to determine in advance precisely what data and what data sources are going to be the most critical in this weather situation and note the data receipt times so that you can schedule your other tasks around them. Set your own data input deadlines and remember that you can't afford to delay issue of a forecast because a critical observation has not arrived, otherwise you will get further and further behind in your work schedule to the detriment of your customers and perhaps also to your forecast accuracy. You have to do the very best with the data you already have, and to do justice to the data you must allow yourself time to analyse it. There is always scope for urgent amendment if some late data indicates that the forecast is seriously in error.

It is also essential for the forecaster to develop an understanding of how long certain forecasts take to prepare, what amendment/update criteria are specified, the time it takes for forecasts/amendments to reach the customer, etc. Incorporation of this information is important in developing a practical and realistic work schedule.

It is not possible to specify rigid time–scales for analysis and forecast preparation. Some forecasters work more rapidly than others; some situations are more complex and involve more data than others. However, each individual forecaster should be aware of his/her capabilities and allow for them in planning task times and deadlines.

In summarising the results of a three–year experimental programme in short–range forecasting in the USA, Scofield and Weiss (1972) found that, with all the available data at hand, operational meteorologists needed 10 to 15 minutes to integrate the information and to prepare and disseminate the short–term forecast. The more complex weather situations (e.g. an approaching squall line) usually involved more preparation time but, in almost all cases in the trial period, the forecasts were prepared and issued in less than 30 minutes.

6.1.3.3   Comprehensive analysis

Because of time constraints on data access and assimilation, the short–term forecaster has to be quite ruthless in selecting both the type of data and the extent of the geographical area to be analysed. All analysis must be directly relevant to the short–tern forecasting problem otherwise valuable time that could be used in other facets of short–term forecasting will be lost. Nevertheless, the analysis that is done must be as thorough and as comprehensive as possible because extrapolation of existing weather trends is such an important input for the first hour or so of a short–term forecast.

     Specific analysis techniques for use in the forecasting context are described in detail in Chapter 5 above and will not be discussed here. However, at this stage it is valuable to summarise some of the principles involved.

     The short–term forecaster's main concern should be 'primary analysis' of raw local data, but he/she must also incorporate what may be termed 'secondary analysis' of numerical models or of other externally prepared analyses of broader fields of data in terms of the relevance to the local area. The basic purpose of all analysis is to interpret the state of the atmosphere as a function of space and time so that the causes of current weather can be explained and thus used as a basis for prediction.

     A comprehensive analysis involves more than just constructing isobars and streamlines, or looking at satellite displays and surface autographic instruments. It also involves either calculations of quantitative values, (or assessment of numerical model data (see Section 4.2 above)) that can be used in forecasting and it involves an assessment of the main physical processes that prevail at the time. The main emphasis for short term forecasting should be on determining small–scale perturbations in the large–scale flow, and in identifying transitory features and minor changes in the atmosphere. Great attention must be paid to detail, and care should be taken not to ignore, change, or smooth data that at first may seem to be in error, until such time as the forecaster is absolutely sure that an error exists. Mesoscale numerical models are powerful analytical tools, but the forecaster must be able to monitor the quality and quantity of data input to them as well as understand their data assimilation processes. Moreover, in the Antarctic context such models are only now emerging with the main source of NWP data being the global models.

6.1.3.4   Formulating a model

A natural consequence of a comprehensive analysis is the formulation of a three–dimensional 'model' of the atmosphere that explains, as far as possible, all the current weather observations and ongoing changes. A numerical model will do this automatically although the forecaster must be aware of the model's structure and constraints (see Section 4.2 above). In a manual analysis environment the model will tend to be conceptual rather than mathematically exact (see, for example, the discussion on frontal models in Section 5.2.1 above). The important thing is that the forecaster must develop some sort of dynamic four–dimensional picture of the atmosphere, at least in his/her mind, so that it can be used as a basis for prediction. There are inherent dangers in blithely extrapolating parameters because of the complex nature of atmospheric processes.

     There are of course many generalised physical models available of atmospheric structure that can be used as a basis for formulating a conceptual model to suit the situation at hand in mid–latitudes. In the Antarctic context such models are less common. However, during their training course, or in subsequent reading of the literature, good forecasters will have become familiar with the various frontal models; models for 'air–stream weather' with

associated orographic interactive effects; models of katabatic winds and their interaction with synoptic systems; mesoscale lows, etc. Knowledge of these is important, but, for short–term forecasting applications these preconceived models provide a general guide only, because it is most unlikely in the situation at hand that the atmospheric structure will match them exactly. Therefore, the forecaster has to be flexible and adapt preconceived models or develop new ones *in situ*.

A general approach to formulating a real–time model for short–term forecasting applications is:

- Develop an 'overview' of the atmosphere within about 500 km of your station or for the area for which you have to produce a forecast.
- Develop a mental picture of the mechanics of the air flow and in particular the main areas and causes of vertical motion (subsidence as well as ascent).
- Ensure you have a good idea of the vertical structure of any discontinuities and pay special attention to the three–dimensional structure of wind maxima (make them 'tubes' not 'flat arrows') and thermal and/or moisture concentrations.
- Focus on the mesoscale aspects likely to affect your station in the next six hours. In some situations a self–contained conceptual model of a mesoscale feature (e.g. a local katabatic wind) may dominate for a few hours, but don't lose sight of how this feature fits in, and interacts with, the surrounding air masses.

6.1.3.5   <u>Making predictions</u>

There are two stages in making predictions. The first involves the scientific prognosis of the weather, that is, preparing the forecast. The second stage may be described as 'forecast message formulation' and involves putting the results of the first stage in a form that the customer can understand.

Preparing the forecast

Techniques for the scientific prognosis of individual weather elements are described in detail in Section 6.6 below but a general approach to the problem is summarised below.

- (i) Extrapolate existing trends in the observed weather, making sure to account for evidence of ongoing changes as distinct from past changes.
- (ii) Superimpose diurnal variations of the main meteorological elements and account for their interaction.
- (iii) Allow for broad–scaleinteraction.
- (iv) Take account of orographic and local features.
- (v) Apply any available objective aids or numerical model output for prediction of specific weather elements and adjust the forecast accordingly.
- (vi) Check final forecast for continuity and realism.

Forecast message formulation

This is a very important aspect and one that requires considerable skill. It is the vital cog in the total process of weather forecasting, the final link between the scientist and the customer.

Ideally the forecaster should convey his/her thoughts on the expected short–term weather directly, via personal or mass briefing. In this way the complete picture can be given, including suitability of the data base and the range and success probabilities of alternative predictions. In many instances however, the forecaster must convey his/her predictions to the user via a single, fairly brief message.

- For some users, the forecast must be coded and the meaning of the expected weather is defined uniquely by the code. For other users the forecast has the form of a narrative statement, which could give rise to different interpretations by different users. Some users receive their forecast in hard–copy form which can be examined in detail and repeatedly referred to as the need arises. Other users receive their forecast verbally (e.g. via radio) and may only have one opportunity to absorb all the detail and significance of the forecast message.

- Whatever the case there are a number of general guidelines that the short–term forecaster should follow in preparing the forecast message:

- the forecast must be tailored to give the user the best possible meteorological basis for planning and decision making. Even when standard forecast formats are prescribed there is usually an optimum user–oriented way of expressing the forecast.

- The forecast message must be as clear and concise as possible. Prime emphasis should be placed on hazardous weather or weather that has special significance for the customer, e.g. aircraft icing. State these things first (unless a rigid prescribed format prevents you) because that is what the customer will tune in to.

- Don't try to exceed reasonable limits of predictability, particularly in attempting to predict brief temporary improvements during bad weather situations, or the precise time of onset or cessation of hazardous weather. In such situations precise detailed forecasts have to be based on solid evidence, reliable techniques and very low probabilities of alternative results. (A simple forecast of "intermittent snow showers 0300–0600 UTC" may be far more effective than a four line narrative that attempts to specify the precise characteristics and timing of every temporary fluctuation.)

- Don't be too vague or make too many qualifying statements. This not only makes the message hard to understand but can also reduce user confidence in the product. Many customers are interested only in the forecaster's opinion of the most likely weather, although some customers specifically ask for probabilities or other expressions of the confidence held in the forecast.

- If probability estimates are required make sure that they are realistic. Some guidance on preparation of probability forecasts is provided by US Air Weather Service (1978).

- When the forecast message has been formulated, review it quickly before issue. This is a very important step that minimises the chances of non–technical errors that can occur when deadlines are tight. Always check the message to ensure that you have actually said what you intended to say. Check that you have used the correct date, time, etc. If the message indicates a major change in forecast conditions from the previous forecast, check that you have acknowledged this in some form or other. This checking process should not take very long and it is certainly time well invested. Careless errors in final message formulation can ruin the best scientific

input to the forecast.
- Don't stray into areas outside weather forecasting: for example, if preparing forecasts for aviation do not pre–empt the decisions or air operators reasons whether conditions are suitable for flying.

6.1.3.6   <u>Maintaining a weather watch</u>

Although this is shown as the last step in a systematic approach to shift–work forecasting, the maintenance of a weather watch is a continuous part of short–term forecasting. The meteorological situation must be monitored continuously so that the forecaster can take rapid action in response to signs of unexpected ongoing change.

The way in which a weather watch is maintained depends on the prevailing situation. If the weather is good and expected to remain so, the aim of the weather watch is to monitor a few key elements to confirm that no significant change is imminent. If a change from good to bad weather is expected, then the weather watch should be aimed primarily at detecting and confirming the approach or development of the bad weather. If the weather is bad, then the weather watch should be aimed mainly at monitoring the size, intensity and movement of the bad weather area. In all situations however, the basic objective is to avoid being surprised by new short–term developments.

An effective weather watch involves some or all of the following:

- *Monitoring trends in visual observations*. The main emphasis here should be on monitoring local station conditions but, if possible, a close check should be kept on reports from other stations in the area and from field parties. A lot of things about ongoing changes in the atmosphere can be inferred from visual observations, and often clues to changes are visually evident before they show up in instrumented observations. Changes in cloud types, cloud movement, or growth rates of individual clouds give an immediate indication of the net result of atmospheric processes that are occurring. (These changes may not be evident from instrumented observations until the next radiosonde or upper wind flight, which may not be for six hours or so). The significance of local conditions (e.g. poor visibility in a particular quadrant, persistent visible inversion layer, formation of rime etc.) should be taken into account. These things are not necessarily mentioned in conventional weather reports so the forecaster should work closely with the observer to ensure that a comprehensive observational watch is kept. Tell your observer what to watch out for in critical situations. However, care should be taken in interpretation of the information if the person making the report is not a trained observer.
- *Monitoring trends in instrumented observations*. All instrumented observations, their trends and inter–comparisons, should be noted. A close watch should be kept for any kind of discontinuities and general attention should be paid to factors such as:
- *Changes in surface dew–point depression*. Do these reflect local or broad–scaleadvection of dry/moist air, or are they indicative of vertical mixing processes?
- *Surface temperature and dew–point temperature*. Are the current values the same as have been forecast? If current trends are extrapolated, will they favour or inhibit the development of hazards such as fog? What inferences can be made about the onset of convection, cloud base etc.?
- *The anemograph trace*. Is the wind direction changing? It is consistent with the expected direction from the synoptic pattern? Does it contain a strong local

component? Is the range of gustiness usual? Are the peak gust speeds similar to the 300 m or 600 m (~1000–2000 ft) winds?

- *The barograph trace.* Is the pressure change indicative of the normal diurnal variation or does it reflect some mesoscale or synoptic scale effects (e.g. an approaching or departing trough or mesocyclone)?
- *Cloud ceiling indication.* Is the ceiling changing significantly? How does this relate to existing precipitation and the vertical wind, temperature and humidity profiles?
- *Vertical wind and temperature profiles.* Do the observed profiles properly reflect the existing local weather? (If not they should be subjectively updated.) How does the observed movement of the clouds compare with the upper winds? How do the existing or updated profiles compare with the prognostic profiles? Has vertical mixing occurred in the low levels? Is it imminent? Is excessive low level wind shear likely? Have stability indices changed? (Note: A thorough air mass analysis should be performed in preference to the mere extraction of stability indices.)
- *Monitoring diurnal variations.* The normal diurnal variation of all the weather elements at stations in your area should be known and should be readily available in either tabular or graphical form. In monitoring each element therefore, the forecaster should note any departures from the normal diurnal trend and try to determine their cause. A plot of a time–section for various observations allows trends to be more easily monitored. It is useful to have the normal diurnal variation curves permanently plotted and to plot the current observations over them on a transparent overlay for easy comparison. This method also allows for convenient extrapolation of current trends.
- *Monitoring over a larger area.* AIREPS and pilot debriefings provide valuable information on the current state of the atmosphere outside the visual range of ground stations, but the primary monitoring tools are satellites. These data are very useful for monitoring broad–scaleinteractions and smaller scale features that may be moving into the forecast area. In analysing satellite pictures of the local area, concentrate your attention on small–scale changes in cloud structure, cloud–free areas etc. Specific satellite data techniques are discussed in section 4.3. Facilities such as interactive graphics (for example the Man computer Interactive Data Access System (McIDAS) make the monitoring task much easier and more effective and permit superimposition of satellite, wind data, etc.
- *Monitoring the synoptic situation.* The key things to remember in monitoring the synoptic situation are:
  - (i) the short–term impact of each new observation should be assessed as it comes to hand. Don't wait till all the observations are plotted before looking at the chart;
  - (ii) pressure tendencies are very useful in determining short–term changes in the orientation of isobars;
  - (iii) keep informed on changes to the broad–scalesituation.

6.1.3.7   <u>Concluding remarks</u>

The approach to short–term forecasting outlined in this section has been deliberately aimed at encouraging the forecaster to develop a systematic method of working; a method that has a solid scientific basis but one which can also be applied in the real–time situation where there are heavy work loads, severe time constraints, and where the latest most sophisticated

technology is not necessarily available. Although new technology is being introduced into many operational areas, and in particular into the Antarctic forecast centres, with better forecasting methods being developed, and mesoscale numerical modeling will soon be an operational reality for some Antarctic operations, the general principles discussed in this chapter should still hold firm – but they should become easier to apply in practice.

An important practical point emphasised in this section is that effective short–term forecasting requires more than just the application of scientific and technical skill. Certainly scientific competence is the foundation for success, but to produce effective results in the short–term forecasting situation the forecaster also has to be a skilled manager. Rapid but accurate response is required in a situation where large volumes and different types of data may have to be assimilated and where uncertainty factors may be high. To cope with this the forecaster has to apply sound management principles to plan and organise his/her shift, direct and control the data flow and forecasting aids required to suit the situation, and to constantly review the quality of the final product.

Finally, every short–term forecaster should remember that his/her objective is to produce effective forecasts that give users the information they need, in a form they can understand, and in sufficient time for them to act upon it. As Golden *et al.* (1978) point out "... the best observations and forecasts are worthless unless someone benefits from them.'" We are not engaged in an academic exercise in which perfection is the sole objective and success is measured only in terms of statistical parameters. We are providing a real–time service in which the measure of our success is the effectiveness of our forecasts from the user viewpoint.

6.2   The Forecast Funnel

As alluded to in Section 6.1 above, the systematic approach to forecasting requires a "top–down" approach in which the forecaster gains an appreciation of the broad–scalefeatures of the atmosphere, then progressively focuses on shorter time and space scales. Snellman (1982) referred to this approach as the forecast funnel. Figure 6.2.1 is adapted from the University Corporation for Atmospheric Research (UCAR), Boulder, Colorado's excellent Cooperative Program for Operational Meteorology, Education and Training (COMET) module on the forecast process. (See, for example, http://www.comet.ucar.edu/). The figure schematically shows the process of refining the forecaster's focus from considering the longer atmospheric waves (planetary–hemisphere space scale and weeks/days time scale) through the shorter atmospheric wave length systems such as low–pressure systems/highs (synoptic space scale and days time scale) through the yet smaller systems such as mesocyclones (mesoscale with life span of hours to a day or so), right down to the very local environment of the station or field camp (microscale–virtually what is happening now).

The next three sections will consider aspects of the "forecast funnel" in the Antarctic context. Section 6.3 will illustrate how taking note of the long waves can assist in the forecast process; Section 6.4 will discuss synoptic scale systems and fronts; and Section 6.5 will deal with aspects of the forecasting of mesoscale lows. Many aspects of the microscale are site specific and the reader is referred to Chapter 7 below where forecasting aspects peculiar to each station are discussed.
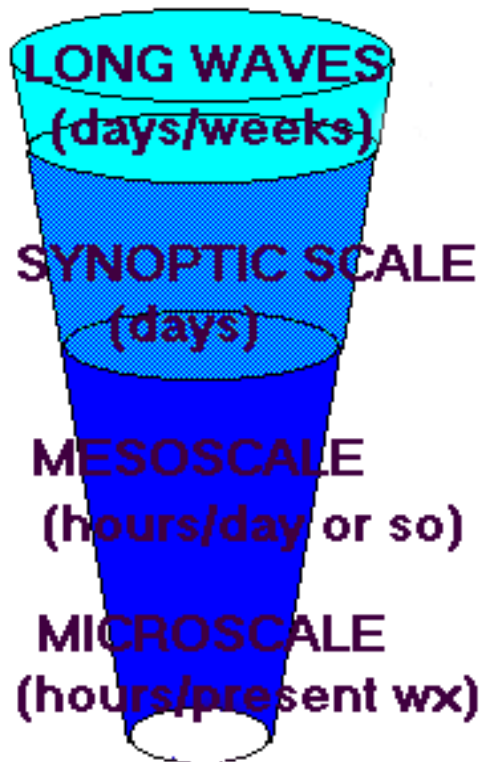
Figure 6.2.1   The Forecast Funnel (adapted from
UCAR's COMET module on the Forecast Process).

6.3   Long waves

6.3.1   Some general concepts

6.3.1.1   <u>Scale</u>

The space scale associated with "long waves" is typically considered to be in the order of 10,000 km per wave, or, typically between one (360 degrees wave–length) and five (~70 degrees wave–length) waves around the Earth. The longevity and speed of movement of these features is typically in the order of days to weeks. And in the case of some very persistent features, the effective life–span of the feature may persist for weeks to months. While outside the scope of this handbook it is noted that seasonal weather forecasting in the Antarctic may have a basis in the characteristics of Southern Hemisphere long waves (Ryzhakov, 1983; Ryzhakov *et al*., 1990; Ryabkov, 1999).

6.3.1.2   Zonal versus meridional flow

In the case where the long wave pattern has waves of small amplitude, the individual waves tend to move eastwards with relatively high speed through the pattern which is said to be of high zonal index. (Commonly, such an index might be based on the geopotential height difference at the 500–hPa level between two latitude bands). In the case of "low zonal index", the waves tend to have a much larger amplitude (that is, are greater in meridional extent) and move more slowly, may be stationary or may event retrogress (move to the west).

In very pronounced meridional situations the westerly flow may become split such that one branch of the westerly flow moves to the north, and the other branch to the south, of a "blocking pair" of a low–high–pressure system combination. Often such blocks will persists for many days if not weeks.

An excellent summary of the relationship between cyclone–frontal systems and the large–scale flow is given in Schultz *et al.* (1998, p. 1768).

6.3.1.3   Identifying and using the long wave pattern

With improvements in the global numerical models one might argue that the imperative that the long wave pattern be monitored is not quite as pressing as it used to be. Occasionally this might be the case, however, there are many instances when the various global models offer differing solutions to the extended period forecast. And so the forecaster might give extra credence to the model which offers a prognosis that is consistent with long wave theory and experience. Typically the long wave pattern has its practical use in helping to assess if the short wave features (highs/lows/fronts) will strengthen; decay; become blocked; or be steered in a particular direction, and so on.

The conventional tools used in monitoring the long wave pattern include daily and 5–day mean 500–hPa contour charts; filtered 500–hPa charts in which typically waves less than about 70 degrees wavelength are filtered out to reduce the effect of the short wave features; Hovmoller charts (for example, see Figure 6.3.1.3.1); and looped satellite imagery. In this last case, particularly where the loops span several days, the forecaster can gain an appreciation of any systematic movement of short wave features around the broader scale steering flow. Moreover, loops of water vapour imagery can be very revealing in identifying persistent areas of descent/ascent or of jet–stream location.

6.3.2   Some specific examples of long waves in the Antarctic context

It was mentioned above that systems tend to be progressive if the long wave pattern is of a high zonal index, in other words, the waves are of small amplitude and mean wind speeds are relatively high. On the other hand, if the long wave pattern is meridional then systems tend to be slow in movement or even retrogress. And in the case of blocking, low–pressure systems approaching the high–pressurepart of the block can be steered southeastwards due to the upper split flow.

In the examples (strong wind events which occurred during the early summer of 1983/1984 between Mawson and Casey) presented below it was found that when major depressions approached the East Antarctic coast, they moved closer to a station when there was long wave ridging to the east of the station. Conversely, the lows remained well offshore

when there was a long wave trough east of the station and a long wave ridge to the west. Moreover, stations lying to the west of a blocking ridge experienced prolonged periods of cloud bands crossing the coast with gale–force winds. Ridging lying to the south over the continent advected these cloud bands to the west and back towards the upstream long wave trough.
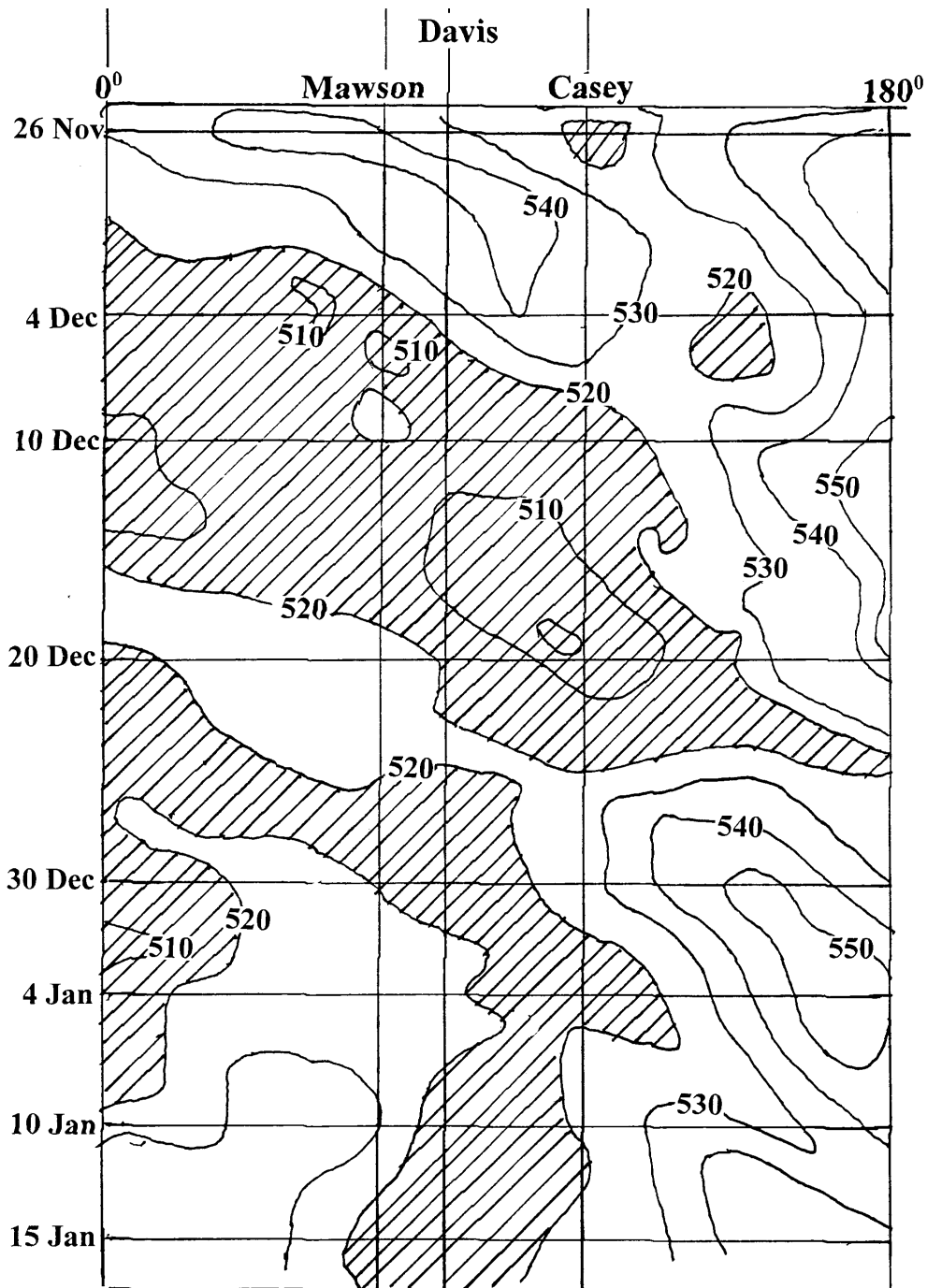
Figure 6.3.1.3.1 Hovmoller diagram showing 5–day mean heights (geopotential decametres (gpdm)) at 500 hPa for 55° S from 26 November 1983 to 15 January 1984. (The hatched areas show regions of less than 520 gpdm)

6.3.2.1   A prolonged period of bad weather at Casey

Once the blocking ridge became established east of Casey around 10 December 1983 (Figure 6.3.1.3.1) flying conditions in the area were poor. There were five events between 17 December 1983 and 12 January 1984 which produced gales at Casey Station. In each case the synoptic scale lows slowed down and weakened as they approached the long wave ridge (block) to the east. Their associated cloud bands were then steered towards the coast.
        As an example of these events the period 16 to 19 December 1983 is shown as Figure 6.3.2.1.1. In this example the depth of the approaching trough (Figure 6.3.1.3.1) was sufficient to erode the downstream block and so the short wave 500–hPa low was able to move east of Casey but the block quickly re–established itself. This example, although relevant to the Casey area, is also typical of blizzard development in the Mawson and Davis areas where ridges down–stream of the stations steer lows close by.

6.3.2.2   A major low passes harmlessly to the north

In situations where the long–wave trough is east of a station with a ridge to the west, or where the tropospheric flow is basically zonal, the major storms tend to stay away from the station. As an example an event is examined which occurred over 3 to 5 January 1984 when the long wave trough lay to the east of Mawson and Davis Stations (Figure 6.3.1.3.1). A major developing cloud vortex appeared to be moving towards Mawson and Davis on 3 January 1984 (Figure 6.3.2.2.1). However it kept on an eastward track and passed harmlessly well north of both stations during 4 and 5 January 1984.
        The 500–hPa pattern (Figure 6.3.1.3.1) shows only weak ridging associated with this event, and significantly, westerly 500–hPa flow to the east of Davis during 3 and 4 January 1984, as the cloud vortex developed.

6.3.2.3   Patterns at 500 hPa associated with winds in East Antarctica

Phillpot (1997, p. 93–163) discusses the use of 500–hPa charts in forecasting surface winds for many stations between the Molodezhnaya area and Leningradskya. In particular Phillpot presents 500–hPa composite height contour fields associated with surface winds reaching at least storm force in East Antarctica (Figures 4.23 and 4.24(d) on pages 93 and 98 of his study). Common to most situations presented by Phillpot are 500–hPa lows northwest of the station with coastal downstream ridging. This pattern is quite similar to that which is described in the specific examples above. In the absence of numerical guidance, the pattern recognition approach to be inferred from Phillpot's work provides very useful guidance.

6.3.2.4   Westward moving cloud bands

The common experience for people in mid to high latitudes is for weather systems to move from the west to the east in a basically westerly tropospheric flow. However, in situations where the long wave pattern is such that the tropospheric flow near the Antarctic coast is easterly, systems may move from the east to the west and cause significant effects as they do so (Callaghan and Betts, 1987).

200					
300					
400					
500					
600					
700					
750					
850					
900					
	1611	1623	1711	1723	1811

Three hourly surface observations at Casey from 2000 UTC 16 December 1983 to 1700 UTC 18 December 1983.
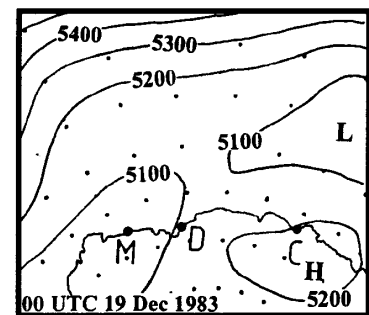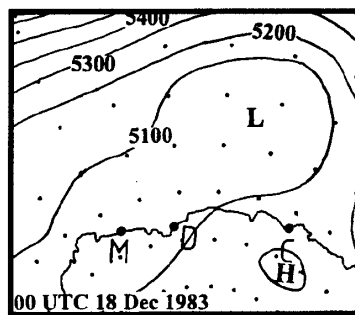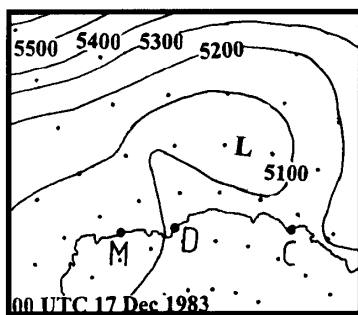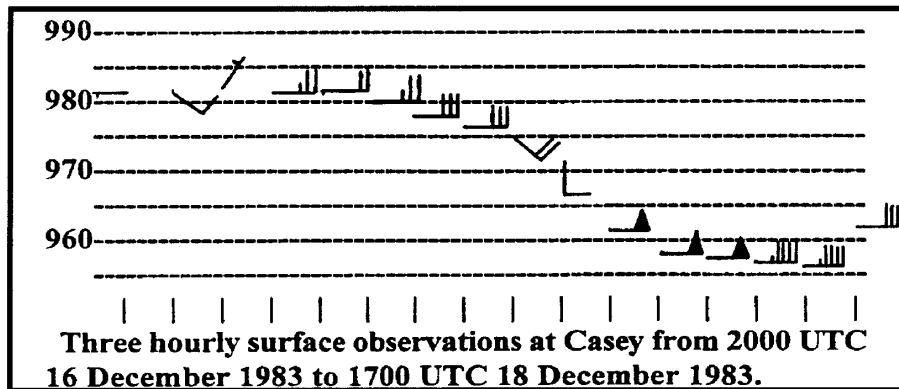
Figure 6.3.2.1.1 An example of storm force winds at Casey due to a low approaching a well defined upper ridge. (The top panel shows the upper level winds from 1100 UTC 16 December to 1100 UTC 18 December 1983; the middle panel shows the 3–hrly surface winds (knots) against surface pressure (hPa) from 2000 UTC 16 December to 1700 UTC 18 December 1983; the bottom three panels show schematic 500–hPa contour analyses (m) for 0000 UTC on 17, 18 and 19 December).
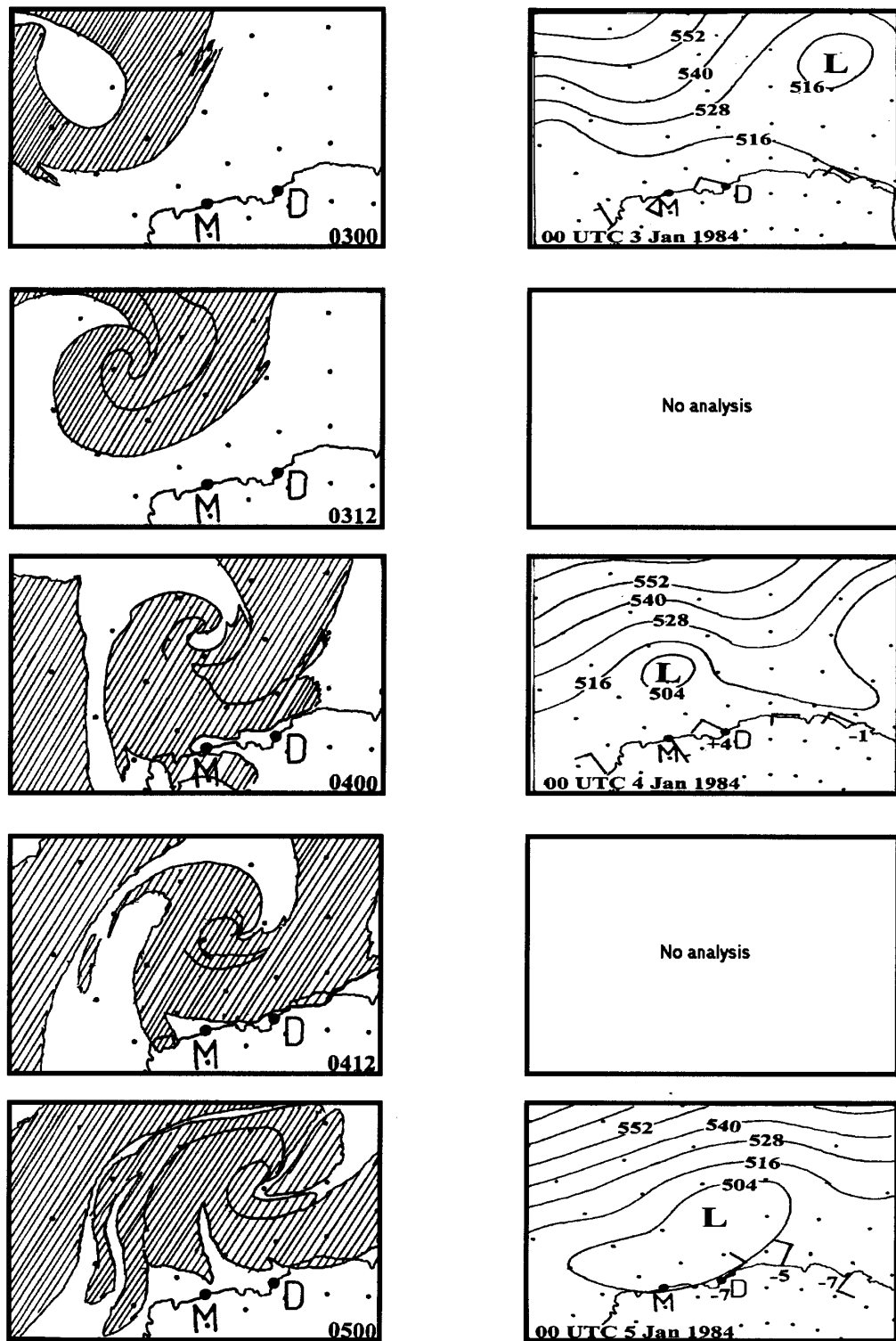
Figure 6.3.2.2.1 Example of a low keeping out to sea in the absence of a downstream long wave ridge. (The left hand panels shows nephanalyses for 0000 and 1200 UTC on 3, 4 and 5 January 1984. The right hand panels show schematic 500–hPa contour analyses (Dm) for 0000 UTC on 3, 4 and 5 January 1984. "M" indicates the location of Mawson; "D" the location of Davis. The signed (+/–) single digit numbers in the lower right hand analyses indicate the 24–hr 500–hPa height change in decametres).

6.3.2.5   Implications for planning operations

Baba (1993) reports optimism in being able to make predictions of the general trend of the weather a few weeks ahead through the prediction of the long wave pattern. It is inferred from Baba that these types of predictions can influence operational planning when he reports that, during twelve seasons of ocean bottom surveys, winds of force 4 or less occurred on about 80% of occasions in good years and only about 38% of days in bad years. Baba's results support the view in Section 6.3.2.1 that a high frequency of bad weather may occur when a long wave trough is located just west of an area, and by implication there would be a long wave ridge just east of the area.

6.4   Synoptic scale systems and fronts

Accurate prognoses of how synoptic scale systems evolve will allow the forecaster to maximise the chances of correctly predicting the individual weather elements such as wind velocity. Fraedrich and Leslie (1991) suggest that, based on the time taken for errors in the 500–hPa field to double, in areas of high baroclinicity predictability time scales might be as short as about one day. On the other hand, as mentioned in Section 6.3.2.6 above Baba (1993) suggests that at least a general trend in the local weather might be predicted well in advance in some circumstances. This section presents a brief overview of techniques which may be suitable for the prediction of synoptic scale systems and fronts in Antarctica.

6.4.1   Forecasting strategies

There are several strategies that are useful for the forecasting of synoptic scale systems and fronts. These include: climatology; monitoring the long–wave pattern; persistence; analogues; conceptual models; and numerical models. The influence of the broad–scaleon the movement of systems is discussed in Section 6.3 above and is alluded to in Section 5.2.1 above and is not developed further here. On the other hand, each of the remaining techniques will be briefly examined.

6.4.1.1   Climatology

Section 2.4 above provided a comprehensive overview of work determining, among other things, cyclone tracks and centres of persistence of synoptic features. The only other comment to be made here is that, anecdotally, no two seasons are exactly alike and so climatology provides at best, basic background information.

6.4.1.2   Persistence forecasting

In the context of forecasting synoptic scale systems persistence might be viewed as the assumption that a system will:

- · remain stationary in space or in a particular stage of development;
- · maintain its current rate of progress;
- · or in the case of a series of systems, the semi–cyclic repetition system behaviour, due perhaps to the disposition of the long wave pattern.

Persistence forecasting certainly has a place for short term forecasting in the Antarctic where the systems are evolving slowly. Satellite information will play a large role in assisting with the movement of systems under such circumstances. It is interesting to note that Fraedrich and Leslie (1991, p 8) suggest that persistence may outperform analogue models for the forecasting of the movement of systems in the Antarctic, due primarily to the absence of good analogues.

6.4.1.3   Analogue models

An example of the analogue technique is given in Fraedrich and Leslie (1991, page 5): their Figure 2 shows a pattern of 500–hPa fields for 18 to 20 July 1985 and uses these to predict what might happen for the period 6 to 8 August 1986. The limitation of this approach is mentioned above.

6.4.1.4   Conceptual models

In Section 5.2.1 above two cyclone–frontal conceptual models were discussed briefly. Section 5.3.1 above discussed the work of Junker (1977), and referred to Streten and Troup (1973), for manual methods for constructing mean sea level analyses using satellite data. Similarly, Section 5.3.2 above discusses the Guymer (1978) technique for constructing 1000–500–hPa thickness fields (and as a result, 850, 700 and 500–hPa contour fields). Section 4.2.4 above should be referred to for a suggestion as to how to get the best from a conceptual model.

6.4.1.5   Numerical models

For most forecasting purposes the Antarctic forecaster will want to access a range of numerical models. Pendlebury and Reader (1992), and Leonard *et al.* (1997), give some encouragement that, respectively, the operational numerical weather prediction systems of the European Centre for Medium–range Weather Forecasts and the UK Meteorological Office perform adequately in the Antarctic context. Adams (1997), on the other hand is less convinced. However, in a personal communication Neil Adams has more recently advised that models such as the United States' National Centers for Environmental Prediction Aviation Model have performed exceptionally well.
        Adams' (1997) study was based on the model output, for two summer seasons, from the ECMWF and from the Australian Bureau of Meteorology's Global Assimilation Prediction

System. Adams (1997) attributes the poor performance to poor initialisation analyses. Perhaps the periods studied by Adams (1997) had particular problems as Cullather *et al.* (1997) note a marked improvement in ECMWF (and NCEP) model analyses for the period 1985 to 1994.

Section 4.2 above gives an overview on how to use numerical model output and, combined with the general optimism noted above, the Antarctic forecaster should be able to use numerical guidance with some confidence (though not blindly) in the Antarctic context.

6.5   Mesoscale systems, in particular mesocyclones

6.5.1   Some general concepts

6.5.1.1   Scale

The space scale associated with the mesoscale is generally accepted to be between 2 km and 1000 km. The longevity and speed of movement of these features is typically in the order of hours to a day or so and the reliable forecast predictability is generally 24 h or less.

6.5.1.2   Models and tools.

As mentioned, numerical models are improving in their ability to provide forecasting guidance in Antarctic. However these have tended to be used in the synoptic sense given that most of the operationally available models used are global models. Nonetheless, not only are the effective spatial resolution of the grids of these models reducing to be almost considered mesoscale in their own right, there are efforts being undertaken to develop operational Antarctic regional and mesoscale numerical models (Neil Adams (personal communication)).

Where numerical guidance is unavailable the forecaster will generally rely on his or her experience combined with conceptual models built from local forecasting rules and case studies.

6.5.1.3   Mesoscale systems

In the Antarctic context the most studied mesoscale systems are probably mesoscale lows and so the main focus of this section is on forecasting this phenomenon (see Section 6.5.2 below). However, other mesoscale systems include: sea breezes; snow breezes; katabatic winds; barrier winds; lee waves/rotors/vortices; and smaller scale high–pressure systems.

Sea breeze and snow breeze circulations

While there have been no (known) sea breeze studies undertaken in the Antarctic context it is common knowledge among experienced Antarctic forecasters that sea breezes occur where

exposed rock is adjacent to open water. (Often in summer the skin temperature difference between these surfaces can be in the order of 20 to 30ºC). For example, Pendlebury *et al.*(1981) report the occasional late afternoon reversal of easterly winds at Mt King, Enderby Land: the light westerlies are thought to be the result of sea breeze type effects induced by the exposed rock of the mountain ranges of western Enderby Land and occasionally resulted in fog at the Mt King camp. (See Section 7.6.2 below)

It is very likely too that snow breeze circulations are set up in areas where exposed rock are adjacent to snow or ice. There have been some Northern Hemisphere studies (for example: Alpert and Neumann (1983); Johnson (1984); Lin and Stewart (1986) and Segal and Arritt (1992)) from which it may be inferred that similar mechanisms might exist in the Antarctic. In simple terms, where significant thermal contrasts are established then a wind circulation is likely to be set up.

Katabatic winds

Conventionally katabatic winds would be classified as a mesoscale circulation. In the Antarctic context this would still hold true, however, arguably, one might view Antarctic katabatic drainage as at least being on the synoptic scale. Parish and Bromwich (1998), for example, through a case study, examine the katabatic – troposphere circulation on a hemispheric scale. (See also, for example, Parish *et al.*(1994)). Moreover, commonly katabatic flow in the Antarctic interacts with synoptic flow to a significant amount. And so for discussion on aspects of forecasting katabatic winds see Section 6.6.1.2 below

Orographically induced mesoscale systems: barrier winds; lee waves and downslope flow.

As outlined in Section 2.6.7.3 above, high orography such as the Transantarctic Mountains and the Antarctic Peninsula may give rise to "barrier winds". These winds result from a circulation set up as cold air dams against the high ground and a geostrophic balance is established between the relatively high pressure along the mountain ridge when compared to relatively lower pressure over the adjacent flat terrain (for example, an ice sheet). It is not known whether there are forecasting methodologies established for predicting the onset of these winds but presumably knowledge of the low level atmospheric stability combined with air mass movement toward a mountain range would be key indicators.

Lee waves and lee vortices are known to occur in Antarctica and down–stream of the sub–Antarctic islands when suitable meteorological conditions exist. See for example, the disturbed flow around South Georgia Island in Figure 4.3.4.5.3 above or the lee cloud–banner blowing off Heard Island in Figure 7.2.4.7.1 below.

6.5.2   Mesocyclones

In the Antarctic, mesoscale lows can have a severe impact on research and logistical operations being carried out by both ships and aircraft through the strong winds, extensive cloud and precipitation that the systems can bring. For example, the mesocyclone described by Turner *et al.* (1993) lasted for over three days and gave very poor weather that stopped the logistical re–supply operation that was taking place at Halley Station on the eastern side of the

Weddell Sea. It is therefore essential to be able to give the best possible forecast guidance on the development of these systems.

In this section we will examine the means by which forecasters in the Antarctic attempt to predict the formation and development of mesocyclones. This task can be split into two parts. Firstly, the output from NWP forecast model predictions can be used to try and infer when mesocyclone development may take place in a particular region. Such techniques are only applicable in the period up to 12–48 h ahead. Secondly, on the day that a forecast is issued extensive use can be made of satellite imagery to try and predict the movement and development of an existing mesoscale vortex. Such a nowcasting approach is certainly valid for about six hours ahead, but can be applicable for 12 h or more in exceptional cases. In the following sections we discuss both these approaches.

6.5.2.1   Applications of model forecast fields

In recent years there has been a steady improvement in the quality of the NWP analyses and forecasts for the Antarctic. However, most mesoscale lows are missing from the analyses since such systems are only represented by a few grid points and the satellite sounder observations, which are the main form of data used to produce the analyses over the Southern Ocean, still have a coarse horizontal and vertical resolution. The forecasting of individual mesocyclones is therefore almost impossible given the poor initial conditions on the mesoscale that are used for the NWP integrations.

Although prediction of specific mesocyclones is rarely possible with the model output it is possible to try and forecast areas where such vortices may be a threat. At the most basic level, the forecast charts of MSLP can be used to determine when cold air outbreaks over the Southern Ocean will occur, suggesting the possible development of mesocyclones. In addition, minor troughs in the upper flow, deep mid–level cold pools or suitably placed upper jets can be monitored for areas were mesocyclones may occur, although specific forecasts of mesocyclone cannot be made based on such signatures.

6.5.2.2   A nowcasting approach using satellite data

In the nowcasting period of up to about 12 h ahead it is possible to use a variety of satellite tools to predict the development and movement of mesocyclones over the Antarctic continent or surrounding ocean areas. In this section we will examine how each form of data can be applied and then consider integrating the data within the forecasting process.

Visible and infra–red satellite imagery

In the tropics and mid–latitude areas the geostationary satellites provide images at hourly or more frequent intervals allowing fast–moving developments to be monitored closely. Such data cannot be employed in the high southern latitudes but the frequent overpasses of the polar orbiting satellites do allow sequences of images to be constructed that can provide guidance on the track of mesocyclones. Since the polar orbiting satellites will observe a particular location from a different viewing angle on each pass it is best to re–map the data onto a common area and map project, although this is not essential if time is not available to process the data.

Another major use of infra–red imagery in forecasting mesocyclones is in obtaining an estimate of the height of the cloud associated with a low. During winter when only infra–red imagery is available, lows that are very shallow can have cloud top temperatures that are very close to the skin temperature of the surface, making them very difficult to detect. However, the texture of the cloud is often different to that of the surface so that it is usually possible to identify the cloud, especially if the contrast of the imagery is stretched. In the more usual situation where there is a reasonable difference between the cloud top temperatures of the low and the surface the height of the system can be estimated provided that some knowledge of the lapse rate is available. This can be from a nearby radiosonde ascent, a model temperature profile or the climatological conditions. Such a height estimate is clearly not going to be very accurate but should give a reasonable indication of the general depth of a system.

The final application of satellite imagery is to try and get an estimate of the winds associated with mesocyclones. Sequences of images from geostationary satellites have been used for many years to derive cloud track winds over the tropical and mid–latitude areas and such data are used routinely in the analysis process. However, similar techniques can be used when several images from the polar orbiting satellites are available, provided that the time separation of the images is not too great. Of course only winds at the level of the cloud tops can be produced, but such data have proved to be of value in mesocyclone research (Turner *et al.*, 1993; Turner and Ellrott, 1992) and potentially has value in operational forecasting.

Surface winds from satellite scatterometers

Estimating the near–surface wind speeds associated with a mesocyclone is extremely important in order to determine whether the system is likely to disrupt air or marine operations. However, as most mesocyclones occur well away from the stations and AWSs it is necessary to use the satellite data to get some idea of the winds associated with the lows. As discussed above, sequences of images can give a general impression of the winds at upper levels, but cannot help regarding surface conditions. However, over the ice–free ocean areas surface wind vectors can be determined from the measurements from the wind scatterometers carried on a number of polar orbiting satellites.

The scatterometer winds are used in the operational assimilation schemes and also plotted onto some surface analyses. With their resolution of about 50 km the fields of scatterometer winds are able to provide information on the circulation of mesocyclones and the troughs associated with frontal bands. However, the data assimilation schemes are principally designed to produce analyses on the synoptic scale so that for forecasting of mesocyclones it is much better to use the scatterometer wind vectors directly rather than analyses that have had the vectors assimilated. For use in the Antarctic, the vectors can be sent directly to the stations for plotting or send in the form of a charts with the vectors drawn.

The scatterometer winds are useful for showing whether a particular vortex has a surface circulation and for determining the maximum surface wind speed associated with a system.

Passive microwave data

Data from passive microwave radiometers on the polar orbiting satellites can provide information on a number of geophysical parameters that are of value in forecasting mesocyclones at high southern latitudes. Instruments such as the Special Sensor Microwave/Imager on the DMSP satellites (see Section 4.3.5 above) observe the Earth at

several wavelengths and give imagery with a horizontal resolution of 12.5 or 25 km, depending on the channel. These data can then be processed to give fields of surface wind speed (Goodberlet *et al.*, 1989), integrated water vapour (Claud *et al.*, 1992) and rain rate (Dalu *et al.*, 1993) over the ice–free ocean. The wind speeds can be used in a similar way to the scatterometer observations to find the wind strength associated with particular lows, although no information is available on the circulation. Being able to determine the amount of precipitation falling from a mesoscale low is particularly valuable, although most of the algorithms used to date have been tuned for mid–latitude conditions. Nevertheless, work is underway to investigate the capabilities of passive microwave data to help in understanding the precipitation of mesocyclones (Carleton *et al.*, 1993) and further developments in this potentially very valuable tool can be expended in the future.

6.5.2.3   AWS surface data

In recent years large numbers of AWSs have been deployed in some parts of the Antarctic as part of major research programmes concerned with the meteorology of the continent, including the investigation of mesocyclones. (See for example, Table 4.1.2.1 in Appendix 1 below) In particular there have been many AWSs installed on the Ross Ice Shelf which has almost a mesoscale network of observing systems that can provide data on surface pressure, the wind field, temperature and humidity (Stearns and Wendler, 1988). Similarly, there are about 12 US and Italian AWSs in the vicinity of Terra Nova Bay, which is now well covered by observing systems. Although primarily for research, the data from these AWSs are of immense value in forecasting (see, for example, Holmes, *et al.*, 2000). Much of the data are put onto the GTS and used in the preparation of numerical analyses, but the data can be used to produce manual analyses with mesoscale detail that can be used to monitor the development of and predict the future track of mesocyclones.

6.5.2.4   Forecasting mesocyclones in particular areas of the Antarctic

Mesocyclones are found at one time or another in all parts of the Antarctic, but the prediction of such systems presents different problems depending on the area under consideration. Over the ice–free waters of the Southern Ocean, where most mesocyclones are found, the model fields are now very good and the full range of satellite observing systems can be employed. Satellite imagery from the polar orbiting satellites is not received very frequently at these more northerly latitudes, but in some areas imagery from the geostationary satellites can be employed. In this zone there is usually a good contrast between the cloud top temperatures of the mesocyclones and the sea, allowing easy detection of most lows.
    In the sea ice zone scatterometer data and products derived from passive microwave measurements are not available and there is less contrast in temperature and reflectivity between the clouds and the sea ice. Nevertheless, the lows can usually be detected against the characteristic lead pattern of the sea ice and followed in sequences of satellite imagery.
    Some areas of persistent open water close to the edge of the continent (coastal polynyas) have many mesocyclone developments and the eastern side of the Weddell Sea close to Halley Research Station and the southern part of the Ross Sea near Terra Nova Bay are particularly prone to mesocyclones. Because of the relatively ice–free conditions in these areas they have many logistical operations taking place and mesoscale lows can cause severe disruption. Although the lows can still only be predicted using a nowcasting approach, since these areas are monitored closely by forecasters on the stations, the early signs of

development, such as indications of cyclonic rotation of cloud bands can be detected at an early stage.

Although there are very few mesocyclones over the interior of the Antarctic, the ice shelves, and in particular the Ross and Ronne/Filschner Ice Shelves, do have many such developments throughout the year. As in other interior parts of the Antarctic, the models give poor predictions on the mesoscale and the systems have to be detected and their future development predicted using satellite imagery, and in the case of the Ross Ice Shelf, the AWS observations. Since the surfaces of the ice shelves are so featureless the detection of mesocyclones is very easy since the cloud vortices stand out well against the ice surface. Prediction of the movement of the lows can be carried out using sequences of images and any *in situ* measurements employed to monitor the surface pressure anomaly of the system.

6.6   Forecasting the main meteorological elements

6.6.1   Surface wind

6.6.1.1   Day to day wind forecasting: the range of considerations

Typically a forecaster is presented with the challenge of preparing a forecast for the coming day (or days) during which the wind might be forced (created) by one or more of a number of factors, for example, an approaching low–pressure system. The range of considerations which the forecaster will want to consider include:

- *Departures from persistence*: what mechanisms might operate during the forecast period to cause the wind to vary from what is happening now? Such departures would be based on the expected movement and development of synoptic and mesoscale pressure systems (and more particularly the associated pressure gradients; isobaric curvature; and isallobaric fields) and diurnal/thermal effects (for example: katabatic flow). The magnitude of the departures will also be of concern: will a strong wind event occur which might affect operations, or, conversely, will winds be light, or even calm?

- *Prognoses and wind models*: what prognoses and/or wind models (numerical and/or manual) are available and how good are they? Do they have any systematic biases? Here one would hope that studies on the reliability of numerical models (for example, Leonard *et al*. (1997) and Adams (1997) have been undertaken to assist in the assessment. *Ad hoc* assessments of numerical guidance reliability would of course be undertaken by the forecaster through comparisons of model output with analyses and observations during forecast operations.

- *Local effects*: how will the wind behaviour be affected by factors such as: orography (for example: barrier winds; lee rotor effects); and boundary layer considerations such as surface roughness; turbulence; and heat budget (net effect of insolation).

The factors mentioned above are not solely peculiar to the Antarctic environment and the forecaster will access a range of techniques that are applicable to mid–latitude forecasting. The sections below examine some key features of surface wind forecasting that might be considered in the Antarctic context.

6.6.1.2   <u>Diurnal/thermal wind systems</u>

Although most atmospheric motions (that is, wind) have as their primary cause differences in heat budgets, it is appropriate to consider wind circulations which are directly caused by diurnal or local thermal effects (for example: sea and snow breezes; inversion winds; and katabatic winds) separately from the larger scale atmospheric motions.

Sea and snow breezes

As mentioned in Section 6.5.1.3 above, sea breezes may occur in the Antarctic where exposed rock is adjacent to open water and it is probable that snow breeze circulations occur in areas where exposed rock are adjacent to snow or ice. While the Editors are not aware of any established forecasting rules for sea or snow breezes in the Antarctic, intuition suggests that, in simple terms, where significant thermal contrasts are established then a wind circulation is likely to be set up. However, these breezes are only likely to be observed when the prevailing synoptic wind velocity is suitable. For example, for a sea breeze to occur at Hobart Airport, Australia, irrespective of the land–sea thermal contrast, the opposing surface synoptic wind component can usually be no more than about 11 m s^{-1} (Whitehead 1972).

   References which might be of value in the sea/snow breeze forecasting problem for very high latitudes include: Johnson (1984); Lin and Stewart (1986), Segal and Arritt (1992); and Kozo (1982 a &b).

Katabatic winds: some definitions and clarifications in the Antarctic context

It is relevant that a clear terminology be established with respect to the Antarctic surface wind. This is important in view of the various definitions of katabatic flow which appear in the literature, and due to the more casual use of "katabatic" in the spoken word where the term is often used to refer to any sort of wind in the Antarctic. (In much the same way that the term "tidal wave" is incorrectly used to refer to a tsunami). Some examples of the various treatment of "katabatic" in the literature are as follows. Schwerdtfeger (1970, p 290) reports an earlier suggestion by H.H. Lettau that a distinction should be made between the equilibrium flow ("inversion wind": see below) that is possible over the relatively slightly inclined snow and ice slopes of the Antarctic interior and the apparently non–equilibrium downslope winds often experienced near the steep slopes of the continental margin. Schwerdtfeger (1970, p 291–292) goes on to highlight some ambiguity regarding the term "katabatic", noting that one definition allows three different types of wind: "inversion wind"; "Foehn winds"; and "bora" type katabatic flow. Murphy and Simmonds (1993, p 528), assume katabatic flow to be the deviation of the resultant wind from geostrophy, but acknowledge the difficulties of such a definition. (Phillpot (1997, p 63) reports a common definition of an Antarctic coastal katabatic wind flow being one that entails in part a speed decrease from "a fairly high surface value (~12–14 m s^{-1} (~35–30 kt) to 5 m s^{-1} (~10 kt) or less by about the 1 km or 850 hPa level". The Meteorological Glossary clearly links the term "katabatic wind" with the

downslope gravitational flow of air cooled by contact with ground which has lost heat through long wave radiation (Meteorological Office, 1991, p166).

   Parish and Waight (1987) discuss the forcing of Antarctic katabatic winds. Through the assistance of a two dimensional model these authors highlight some key differences between the characteristics of katabatic flow over the more gently orographically sloped interior when compared to the katabatic flow over the order of magnitude steeper orography near the coast. These authors show various graphs which indicate the difference, a brief summary of which is given in Table 6.6.1.2.1

Characteristic	Coast (steep slopes 10^{-1} to 10^{-2})	Near inland (intermediate)	Inland (gentle slopes 10^{-3})
Strength of katabatic flow	Strongest	Closer to "Inland"	Weakest
Onset/cessation	Most abrupt	Closer to "Inland"	Most gradual
Direction	Most downslope (less balanced by Coriolis)	Closer to "Inland"	Across slope (more balanced by Coriolis)
Forcing	Unbalanced flow resulting from strong gravitational flow of radiatively cooled air (with resulting pressure gradients across the inversion around five times the inland case), opposed by friction to some extent, but Coriolis less important. Turbulent exchange processes most important)	Intermediate, probably closer to "Inland" characteristics	Near equilibrium balance between pressure gradient, Coriolis and friction

Table 6.6.1.2.1   Inferred differences between coastal, near coastal and continental katabatic flows. (From Parish and Waight (1987, mainly pp.2224–25))

However, it is clear that both the inland downslope flow and the coastal downslope flow are "katabatic" according to the Meteorological Glossary definition and the differences are more ones of size and time to development rather than being intrinsically dissimilar. Nevertheless, it may be inferred from Parish's (1988) review of Antarctic surface winds that he subscribes to the *defacto* convention of, in cases where outward long wave radiation (radiative flux divergence) from a sloping surface is the primary forcing mechanism retaining the term "katabatic" for the coastal wind regime and "inversion winds" for the winds in the interior.

   Now, in reality of course, there is usually a synoptic (or mesoscale) pressure gradient superimposed on the pressure gradient set up by the radiative flux divergence from the orographic slope. Phillpot (1997, p 42–74) discusses surface wind behaviour in East Antarctica and refers to "enhanced katabatic" and "low level wind speed maximum" wind types (Phillpot (1997, p 66–67 and 70–73)). The latter, at least, (Phillpot (1997, p 660) clearly relates to "probable off–shore cyclonic activity". And, as is discussed in Section 6.6.1.3 below, Murphy and Simmonds (1993) relate how the synoptic pressure gradient can interact with katabatic flow to produce strong wind events.

So where does all this leave the Antarctic weather forecaster, who must, on the input side of formulating a wind forecast, understand the dynamics and thermodynamics (and related terminology) of the forces which drive the wind? Equally, however, on the output side, the forecaster must use language which portrays to the forecast recipient (client) an unambiguous forecast of wind velocity. In compiling this handbook the Editors take the view that forecasters should follow as close as possible to terminology which has developed after considerable thought by the research community provided that terminology has some meaning to the wider community.

The following terms are therefore adopted when referring to the Antarctic surface wind. On the "input" or forecast formulation side:

- *"Katabatic flow"*: we follow the Meteorological Glossary definition which relates to "downslope gravitational flow of air cooled by contact with ground which has lost heat through long wave radiation (Meteorological Office (1991, p 166)).
- *"Katabatic winds"*: we follow Parish and earlier authors (for example, Schwerdtfeger (1970, p 290)) in thinking of these winds as being largely confined to the coast, and perhaps near coast, where the relatively steep slopes in the orography allow the "katabatic flow" to be strong;
- *"Inversion winds"*: similarly, we follow Parish and earlier authors (for example, Schwerdtfeger (1970, p 290)) in thinking of these winds as being largely confined to the Antarctic interior, where the relatively shallow slopes in the orography causes the "katabatic flow" to be weak;
- *"Surface wind"*: we would recommend simply using the term "surface wind" in cases where non–katabatic forcing is a significant factor (for example, a strong synoptic pressure gradient). Here we would endorse the use of "blizzard" or "strong wind event" etc., provided that the term does not imply that "katabatic" forcing is the sole mechanism.

On the "output" or forecast dissemination side:

- "*Katabatic flow or katabatics*": are terms which most technical people would understand to be related to downslope flow in situations consistent with the "katabatic flow" definition above. (Meteorological Office (1991, p 166). In other words, when dealing with the general community, "katabatic flow" or "katabatics", should be used in both the "katabatic wind" and "inversion wind" situations described above.
- "*Surface wind*": should be used if there is any doubt about the forcing mechanism or about whether the audience would misinterpret the intent of the forecast. Again simple terms such as "blizzard" or "strong wind event" may also be used if appropriate.

Winds over the interior – "Inversion winds"

Parish (1988, p. 172) discusses the small contribution which synoptic scale maritime cyclones make to the wind climate of the Antarctic interior. The intrusion of maritime storms over the Antarctic continent does occur, however, (see for example Pook and Cowled (1997)), and a forecaster would need to use model guidance or experience built up from case studies to deal with these.

The prediction of the presumably more tractable "inversion wind" requires an assessment of the synoptic pressure gradient and the pressure gradient set up by the inversion set up by the sloping orography: from these the Coriolis force and frictional forces would be computed in some way to complete the approximate balance in the flow (see, for example, Parish and Bromwich, 1986). As may be inferred by Parish's Table 1 (Parish (1988, p 172), wind direction for most inland stations has a high degree of constancy. For example, the directional constancy at Vostok is given by Parish as 0.91. The directional constancy at the Dome C AWS is, however, much less at 0.51: this is to be expected given that this AWS, being at or near to the top of a dome would be in an area of almost no orographic slope and thus more prone to synoptic influences. However, for the most part the forecaster can use climatology to obtain at least a first guess of the inversion wind direction for many stations.

A better estimate of both direction and speed would come from an appropriate numerical model which incorporates the "inversion wind" thermodynamic and dynamic modeling. It would be the responsibility of relevant forecasters to push for the development of such models if they do not already exist operationally. Alternatively, model output statistic (MOS) type approaches, or pattern recognition – perfect prognosis approaches might also be developed.

Katabatic winds: near the Antarctic coast.

In this section we are dealing with winds generated by surface radiation flux divergence near the steep slopes of the Antarctic coast line. As mentioned, Parish and Waight (1987) discuss the forcing of Antarctic katabatic winds in general: in particular, the following is inferred as being useful in the forecasting of the katabatic flow near the coast.

- Extra strong or prolonged katabatic flow (of a NON–cyclonic storm type) might occur down–wind of a region where the inland "inversion" wind converges, thus providing a prolonged–nearly limitless supply of negatively buoyant air. (Parish and Waight, 1987, p 2226; Parish, 1984; Parish and Bromwich, 1987);
- Terrain slopes are in the order of 10^{-2} to 10^{-1} (Parish and Waight, 1987, p 2214);
- Strong radiational cooling exists (Parish and Waight, 1987, p 2225).
- Synoptic control (Gallée *et al.*,1996; Gallée and Pettré, 1998).

The first two points noted can be easily established by the forecaster by reference to the work of, for example, Parish (1984) and Parish and Bromwich (1986, 1987). (Figure 2.6.7.1.1 above is taken from the last reference and shows idealised katabatic streamlines for average winter conditions). The third point (radiational cooling) requires the forecaster to predict radiational losses which result from clear skies, usually under anti–cyclonic conditions. It would be hoped that numerical modeling, either through direct physical representation, or through model output statistic methods, would ultimately be the best forecasting tool for the coastal katabatic. However, until such models become readily available, the forecaster will need to rely on the conceptual model approach implied here or on case studies peculiar to each site.

The fourth point is partially covered in the comments on radiational cooling. However, Gallée and Pettré (1998) suggest that synoptic control has an important bearing on the cessation of katabatic flow. Through numerical modeling these authors suggest that the pooling of cold air seaward of the coast causes a pressure gradient back towards the continent.

As the radiational cooling weakens or ceases during the day, this pressure gradient may cause a reversal in the wind flow from katabatic to anabatic.

It may be inferred from the work of Gallée *et al.* (1998) that if the synoptic (or mesoscale) flow is weak then the surface warming is sufficient for generating an additional upslope buoyancy force (an effect no doubt enhanced by any sea breeze effects due to warming of exposed rock), and anabatic flow develops over the ice sheet in the afternoon. On the other hand, forecasters might note that when the large–scale wind is moderate and downslope, the piling up of cold air is enhanced and this has a dramatic impact on the flow. A sharp spatial transition is generated between downslope and the static pressure winds (antitriptic winds blowing towards the coast) over the ocean. This discontinuity moves toward the ice sheet interior in the morning and is responsible for the sudden cessation of the katabatic flow seen by static observers.

6.6.1.3   Strong Wind Events (SWEs)

Strong wind events are probably the most important winds events to be forecast in the Antarctic, as they can impact significantly on Antarctic operations and put lives at risk in some situations. Given that for blizzard conditions to exist, requires a wind speed equaling or exceeding gale–force (17.5 m s^{-1} (34 kt)) then that speed is used here to give the lower bound to the 10 minute average wind speed in a SWE. There are potentially several categories of SWE :

- the "katabatic wind" in which the prime forcing mechanism results in the "bora" type wind (for discussion see Section 6.6.1.2. above);
- the "barrier wind" (for discussion see Section 6.6.1.4 below)
- downslope winds accelerated by gravity waves (for discussion see Section 6.6.1.5 below)
- hydraulic jumps (for discussion see Section 6.6.13 below)
- events in which synoptic (or mesoscale) weather systems play an important role, with or without a contribution from katabatic flow. The last category is the focus of this current section..

It may be inferred from Streten (1968, p.52), when he refers to the work of Astapenko (1964), that the role of strengthening easterly pressure gradients between oceanic lows and continental anticyclones in coastal winds storms affecting East Antarctica was discussed at least as early as 1964. In more recent times, Murphy and Simmonds (1993) use a general circulation model to examine the role that such synoptic systems might have in SWE. The key conclusions from this recent work are that strong pressure gradients and strong katabatic flows can operate together to produce SWE, with each component in the order of three times stronger (in winter at least) than average. Moreover, it may be inferred from the work of Murphy and Simmonds that the role of the inland anticyclone is two–fold: not only does it assist with the development of above–average pressure gradients it also provides the subsidence and clear skies which are conducive to the development of the katabatic flow (Murphy and Simmonds (1993, p 533).

Figure 6.6.1.3.1 is a NOAA composite infra–red image showing, in particular, a deep low north of Casey Station and clear skies in the ridge over the continent to the south, at about the time of a SWE at the station. The surface winds at Casey were above gale–force for less than about 12 h in this event, due in part to the mobile nature of the low. As discussed in Section 6.3 above, a long wave ridge east of a station is often instrumental in blocking the

eastward movement of lows resulting in SWEs along the Antarctic coast south of the low (see also (Murphy and Simmonds (1993, p 533). On 27 December the long wave pattern was conducive to progression of the short–wave features and so the SWE event at Casey was short lived.
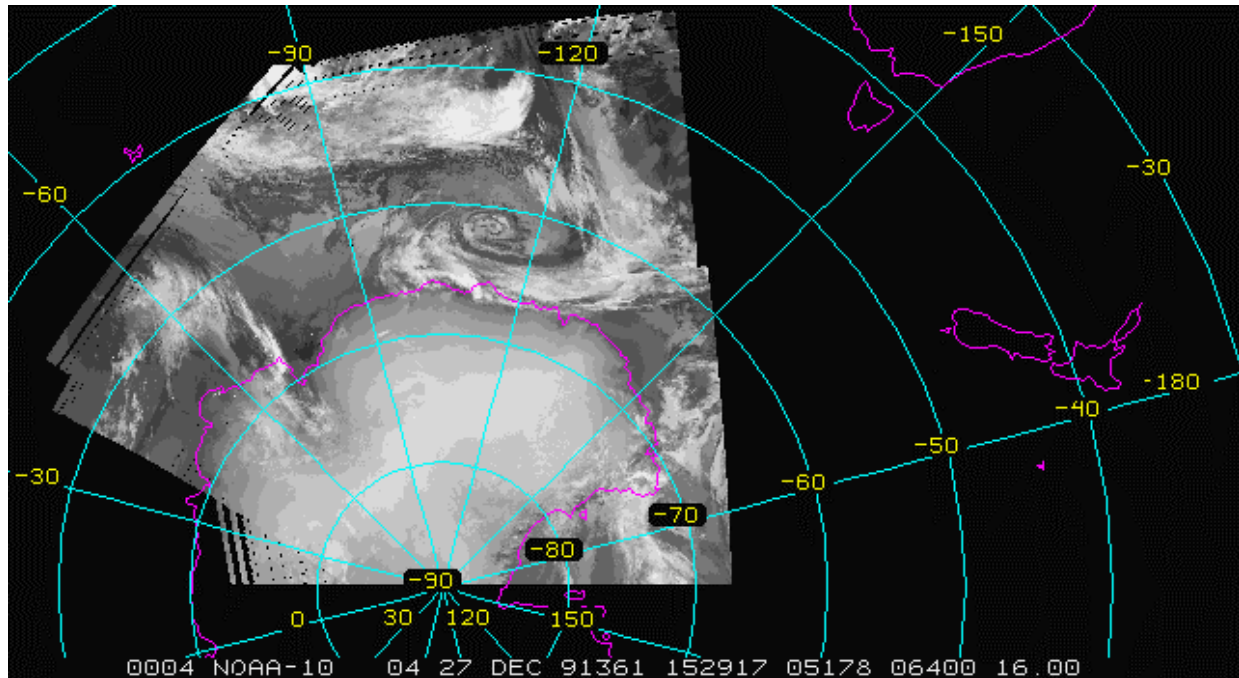
Figure 6.6.1.3.1 A NOAA infra–red composite image for 27 December 1991 (the most western segment of the image was taken nominally at 1529UTC 27 December) showing, in particular, a low–pressure system north of Casey, and clear skies to the south at the time of a strong wind event at the station.

Thus for predicting synoptically driven SWEs the forecaster will want to take into account, using, in particular, numerical model guidance and satellite data:

- pressure gradients: are they significantly (say around three times (Murphy and Simmonds, 1993) above average?
- has a high–pressure system allowed for radiative losses from the surface over the last few days to allow the formation of inversions and katabatic flow?
- local influences on the wind: for example, for stations on the north of the Antarctic Peninsula it may be enough just to consider the effects of the low, whereas, stations in the lee of ice domes may be affected by downslope flow due to gravity waves or lee waves (see Section 6.6.1.5.below).

SWEs forced by mesoscale lows need also to be considered in some circumstances. The forecast decisions will include whether such lows will form in the first place and, if so, the strength of the isobaric circulation.

6.6.1.4 Barrier winds

As discussed in Section 2.6.7.3 above, barrier winds are formed by synoptically driven boundary layer air with strong static stability impinging on high orography. In the case of the Ross Ice Shelf–Transantarctic Mountains situation, for example, with a synoptic easterly geostrophic wind, the depth of the cold air boundary layer increases from east to west, that is towards the mountains. A geostrophic balance is then set up between the Coriolis force and the pressure gradient force generated by the relatively high–pressure area in the cold air dammed against the mountains and the relatively low pressure further east over the ice shelf. Thus south to southwest winds, often quite strong, are generated below the height of the orographic barrier.

The forecaster therefore has to concern him or herself with:

- is the orography conducive to the barrier wind effect: that is to say, is there high orography adjacent to a relatively flat area?
- is the synoptic situation conducive to a prolonged (actual minimum period not known?) piling up of boundary layer air with high static stability against the high orography?
- the magnitude of the air pressure differential set up between the barrier and the nearby flat surface;
- will local orography affect the barrier wind flow in some way, by either blocking it or channeling it?

6.6.1.5 Downslope winds: lee wave/gravity wave acceleration and other thermal effects

Adams (1996) investigated a SWE at Casey and suggested that an internal atmospheric gravity wave was generated in the flow over Law Dome heralding a switch from separated flow over the Dome to a downslope wind. The strong gradient generated by the passage of a cyclone close to Casey provided the forcing for the wave over the Dome, with the downslope wind, and induced gravity wave, producing the accelerated flow in the Casey area. Turner *et al.* (in press) investigated a SWE which occurred at Casey in March 1992 and have found that the SWE evolved in a somewhat similar manner to the case presented by Adams (1996).

Turner *et al.* (in press) propose, among other things, that downslope flow in the lee of a feature such as Law Dome, might have elements which are, in part explained by the following four part conceptual model:

- *Part A*: The synoptic scale high–low–pressure system couplet of Murphy and Simmonds (1993) provides two important components. Firstly, the inland high–pressure system allows radiatively cooled air to exist in the general area. Secondly, the synoptic low–pressure system develops, moves southward, and the combined high–low couplet causes the synoptic gradient flow over Law Dome to strengthen to some critical value (possibly around 10 m s^{-1}), *and to then keep strengthening.*
- *Part B*: Following Grace and Holton (1988) entrainment of radiatively cooled air by the super critical synoptic gradient contributes to the downslope surface flow. As the storm progresses, the radiatively–cooled air is displaced by maritime airflow from which heat is lost to the ice surface, by turbulent heat flux (by analogy with Parish and Waight, 1987) thus contributing to the negative buoyancy of the boundary layer flow. However, a significant source of thermal contrast at this stage

is also provided by the lee wave system of Part C of the model.

- *Part C*: In accord with Adams (1996), the acceleration of the wind down the lee slopes of Law Dome occurs in response to a orographically induced long period vertically propagating wave with higher oscillation waves further downstream. The character of the downslope wind develops along the lines of Fig 10(b) in Miller and Durran (1991) (which is reproduced here as Figure 6.6.1.5.1) is "straight" until about Casey then "waves", but above the straight downslope surface flow is a orographically–induced vertically propagating wave (Adams (1996); Miller and Durran (1991)). This wave is another important contributor to the part that density differences play in the storm wind flow. In particular it is proposed that there is a surface wind speed acceleration down the Law Dome slope (by analogy, see for example Fig 11 (b) in Miller and Durran (1991) which is reproduced here as Figure 6.6.1.5.2) largely as a result of these differences. In other words, frictional losses aside, the wind speed at any point down the slope is largely the result of the synoptic gradient (roughly indexed by the Law Dome AWS) to which is added energy resulting from density differences due to the vertically propagating wave as well as energy resulting from boundary layer density differences.
- *Part D*: The Casey wind speed is stronger than at the nearby Airstrip AWS (89810) site (66.3^o S, 110.8^o E, 390 m elevation) at least in part because of a sudden terrain fall below the airstrip area, so that the negatively buoyant airflow increases acceleration down the steeper ice slope. Ball's (1960) theory helps to explain constancy in Casey wind direction (090 degrees) being different from the constancy of the Casey Airstrip wind direction (130 degrees).

(While not discussed by Turner *et al.* (in press), higher period wind velocity oscillations were evident in the SWE. These may have been Kármán vortices waves shed horizontally from Law Dome (or may have been due to resonance between vertical and horizontal wave motions (Scinocca and Peltier, 1989), or simply high period gravity waves (Rees and Mobbs, 1987).

There are some aspects of the above proposed conceptual model which may be of particular interest to forecasting practitioners. The reference to a threshold value of synoptic flow above which the downslope flow becomes fully established has its basis in three independent sources. Firstly, Wilson (1992, p. 124) reports that when the (synoptic) gradient increases sufficiently to produce speeds of about 15 m s^{-1} (~30 kt) in the area of the Casey Airstrip then surface winds at Casey itself will suddenly increase to 15 m s^{-1} from the east. Secondly, Barbara van Meurs (personal communication) reports on a numerical modeling study of flow around Law Dome and presents results which imply that a 3 m s^{-1} (~6 kt) north–easterly synoptic (geostrophic) wind allowed strong katabatic winds to flow down the Vanderford Glacier about 30 km to the south east of Casey, but Casey and the Airstrip itself were sheltered "being in the region of a weak eddy in the lee of Law Dome". However, when van Meurs increased the synoptic (geostrophic) flow to a 20 m s^{-1} (~40 kt) north–easterly the flow over the Casey area became easterly at 35 m s^{-1} (~68 kt). Thirdly, Grace and Holton (1988) summarise two conditions which relate to fluids flowing over obstacles. Equation 6.6.1.5.1 is the first of these conditions where D is the depth of the boundary layer; A and S$_1$ are constants, 0.002 and 0.5 respectively (Mannins and Sawford, 1979, p 622–623); α is the slope; N is the Brunt–Väisalä frequency (the angular frequency about which internal density waves oscillate) where N^2 = (g/Θ)*(dΘ/dz).

$$UA > N D ((S_1/A) * \sin\alpha)^{0.25} \qquad\qquad \text{Equation 6.6.1.5.1}$$

Taking a pre–storm value of 8 K/1366 m as representative of the stability of the synoptic flow, then N ≈ 0.015 s^{-1} and taking a typical windward slope for Law Dome of 1 in 80,
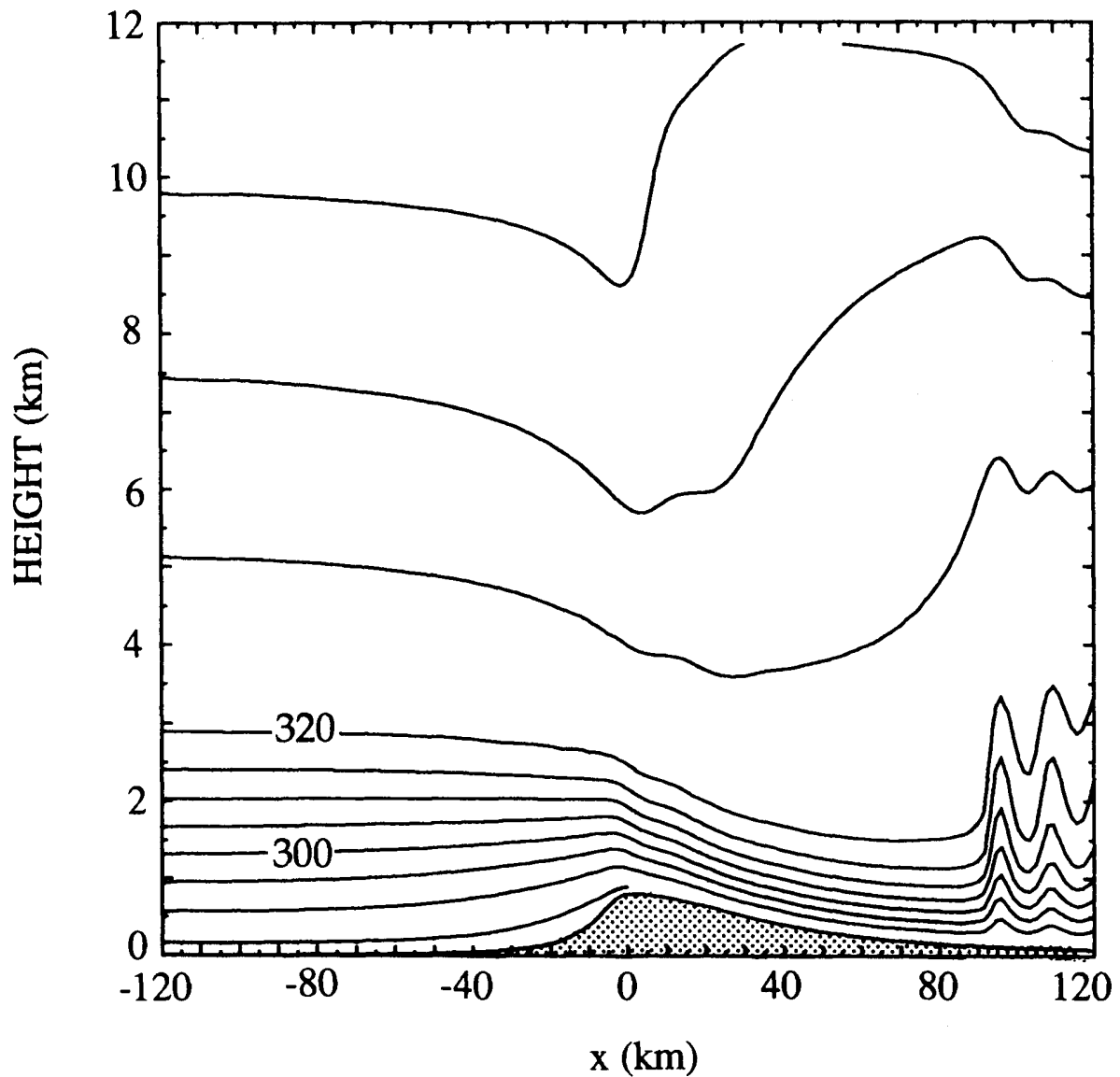
Figure 6.6.1.5.1   Steady–state isentropes (K) for a two–layer model flow over an idealised mountain (from Miller and Durran, 1991, p.1466). (The height of the idealised mountain, its shape in some air flow situations, and the distance of the peak to where the low level lee–waves are forming all closely match the Law Dome to Casey situation).
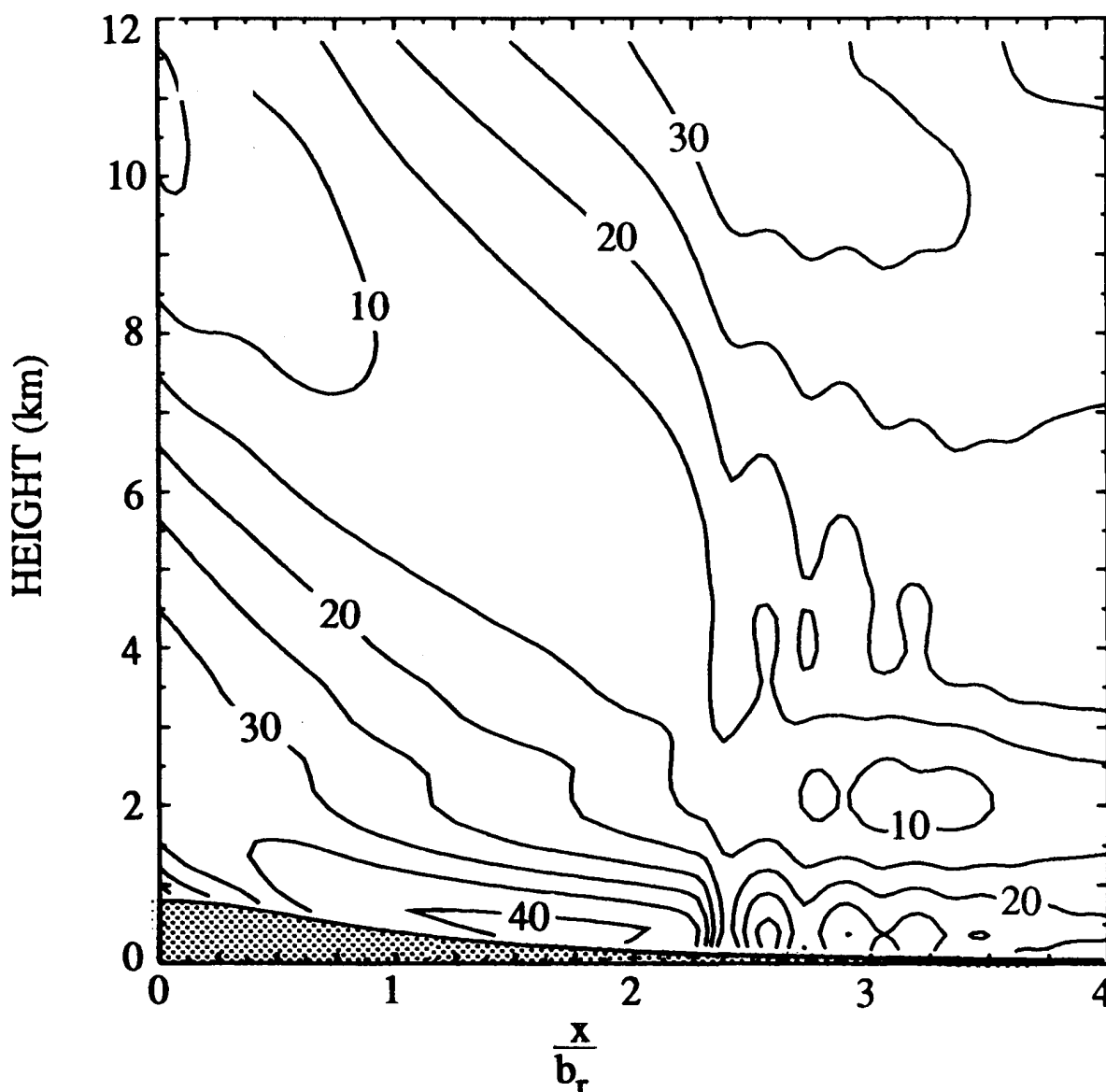
Figure 6.6.1.5.2   As in Figure 6.6.1.5.1 above except the plotted field is horizontal wind speed (m s^{-1}). (b$_r$ is the lee–slope half width (see Miller and Durran, 1991, p.1460). (from Miller and Durran, 1991, p.1467)

and a boundary layer depth of 300 m (Ohata *et al.,*1985, p10655) then for N $\approx$ 0.015 s^{-1} criterion (6.6.1.5.1) requires a synoptic flow (above the boundary layer) of about 6 m s^{-1} (~12 kt) to entrain a typical katabatic boundary layer up Law Dome. The second criteria is given by Equation 6.6.1.5.2 where H is the height of the obstacle and U is the mean flow of the fluid.

NH/U <= 2   Equation 6.6.1.5.2

For N = 0.015, and H = 1395 m (top of Law Dome), then U has to be about 10 m s^{-1} (~20 kt) for condition (6.6.1.5.2) to be met. It is of interest that, for this storm, the flow at the Law Dome AWS site exceeded 6 m s^{-1} just prior to 0000 UTC 20 March and exceeded 10 m s^{-1} in this storm at around 0100 UTC 20 March. This was about the time that the SWE event started at Casey.

Arguments for Parts B, C, and D of the model are based on the work of Grace and Holton (1988), Miller and Durran (1991), and Ball (1960). Grace and Holton (1988) present data which support their conceptual model of a mechanism effecting downslope winds which

190

are observed in the lee of a 700 m high mountain near Adelaide (34.93º S, 138.58º E, elev. 47 m AMSL), Australia. In brief these workers argue that boundary layer air is induced to ascend the windward mountain slope by the drag of the viscous shearing stress due to the geostrophic wind. The ascending boundary layer air cools adiabatically, and if the environment is stable, then the boundary air reaches the crest several degrees cooler than the environmental air at the same altitude. The boundary layer air consequently accelerates down the lee slopes as a gravity flow. These authors argue that it is the existence of the density gradient which is important, not the cause by which the density gradient is created. They also show that the difference in kinetic energies per unit mass of the downslope flow at a height H and the downslope flow at height h, further down the slope, is approximately given by Equation 6.6.1.5.3, where U is the wind speed at heights H and h; g is the acceleration due to gravity; $\Delta\theta$ is the difference in potential temperature between H, and vertically above the location where h is taken but at the same altitude as H; θ is the potential temperature averaged from H to h; R is the energy losses due to surface drag and to entrainment at the top of the boundary layer.

$$(Uh)^2 - (UH)^2 \approx 2g\,\Delta\theta\,(H{-}h)/\theta - 2R \qquad\qquad \text{Equation 6.6.1.5.3}$$

Turner *et al.* (in press) applied the above relation to the March 1992 storm and showed that it modeled the wind speed increase between the airstrip site and Casey Station quite well: it thus might be a useful diagnostic tool. And regarding the differences in wind direction at Casey and the Casey Airstrip site, Figure 6.6.1.5.3 is Ball's (1960, p. 16) Figure 7 showing the flow lines in the neighbourhood of a depression which is moving parallel to an east–west orientated coast, southward from which orographic contours steeply rise, then taper off. Ignoring any isallobaric effects, the flow lines (solid black in the figure) are the result of the nett pressure force resulting from the pressure gradient force associated with the low and from the katabatic force, the latter being strongest where the orographic slope is strongest. Following Blakers (1983), Figure 6.6.1.5.4 is Ball's Figure 7 orientated such that the idealised orographic contours are orientated (to simulate the local Casey orography) along a bearing 020º to 200 º true, that is a rotation of 70º anticlockwise from Ball's example. It may be seen then that the "Ball (1960)" flow lines in the immediate vicinity of Casey are from 090º as is generally observed in a SWE. Similarly, the local orography in the vicinity of Casey Airstrip would require Ball's Figure 7 to be orientated about 30º anticlockwise: this would lead to flow lines from about a 130º direction as is often observed at the Casey Airstrip in a SWE (Figure 6.6.1.5.5).

Blakers (1983, p. 31) notes that "It is possible for the strong winds to commence whilst the low centre is still to the northwest (of the station) such that if the low is moving more or less eastwards the station level pressure at Casey would continue to fall for some time after the onset of strong winds, then rise, with the (strong) winds continuing as the low moves further east".

The March 1992 case examined by Turner *et al.* (in press) is an example of a synoptically-induced event that had a major impact on one sector of the Antarctic coastal region, causing great disruption to logistical operations and creating extremely dangerous conditions at Casey Station. It is arguable that the downslope flow mechanism discussed above contributes to SWE at other sites, although further work is needed to verify this speculation. Some *prima facie* supporting inferences come from Streten (1968) who examined the distribution of the duration of SWE about pressure minima for Mawson, Davis and Wilkes (now Casey), arguing that if Ball's (1960) model of katabatic wind–synoptic pressure gradient interaction was realistic then there should be a bias towards a strengthening of winds after the pressure minimum, that is, when the coastal low–pressure system had moved east of a station. Streten found that for Mawson such a bias did exist but for Wilkes the strengthening of winds

was skewed towards falling pressure, the data for Davis were too limited for a conclusion to be reached. Bromwich (1989, p 693) points out that a similar increase in wind on a falling bar had been noted at Port Martin. Callaghan (1984) has updated Streten's work for Davis and found that for 47 storms examined at Davis, 61.7% of the SWE commencements were associated with rising pressure (or just prior to the pressure minimum and on the rising bar); 27.7% were associated with falling and rising barometric pressure; and 10.6% commenced on a falling bar.

Isobars 2 hPa intervals

Flow lines

Contours of z, 500m intervals

Contours of $z + P/\rho \mathring{g}$
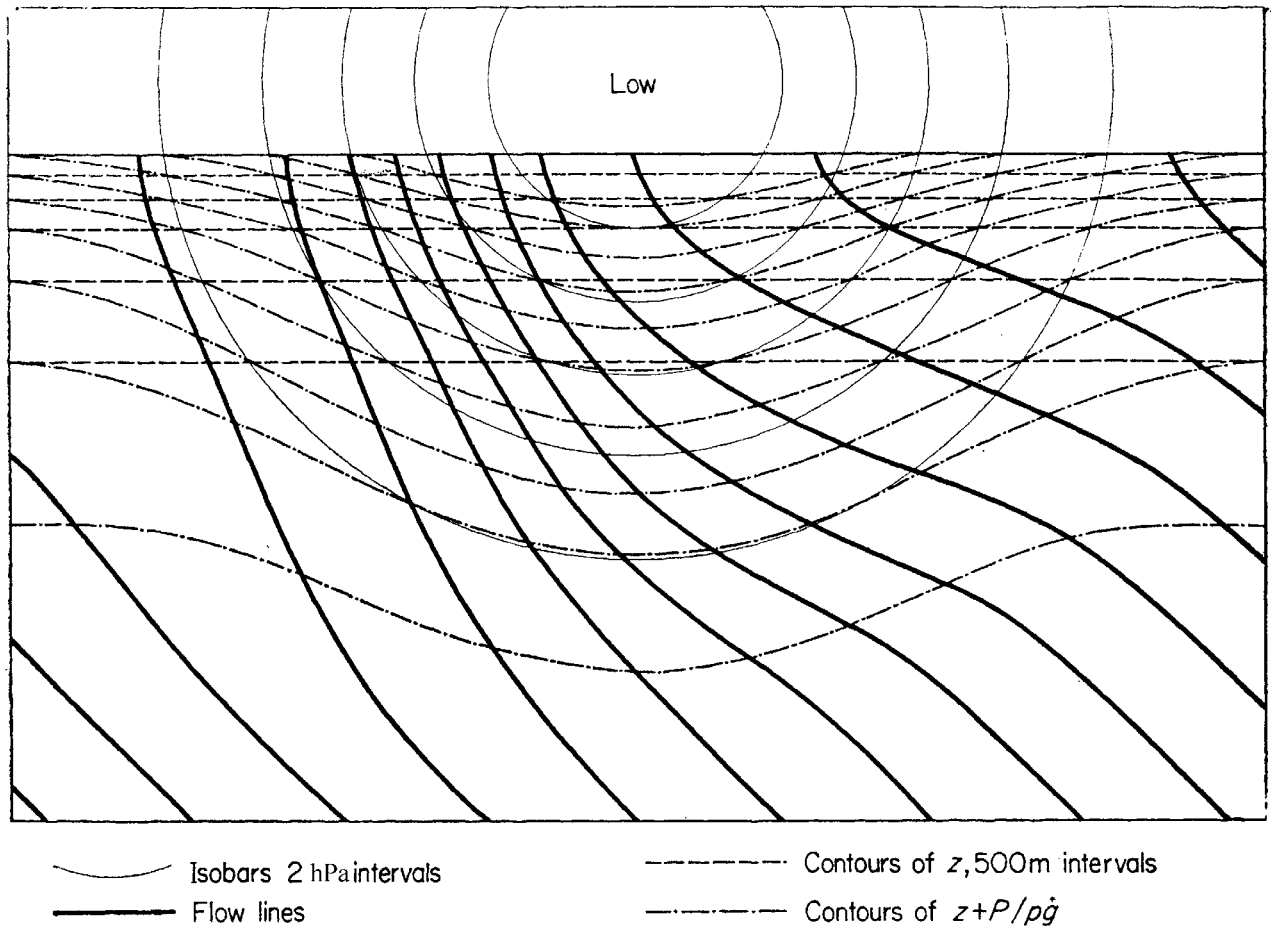
Figure 6.6.1.5.3 Flow lines in the neighbourhood of a depression, the geostrophic pressure gradient is super–imposed on a "katabatic" pressure gradient resulting from an idealised orographic gradient. (From Ball, 1960, p.16).
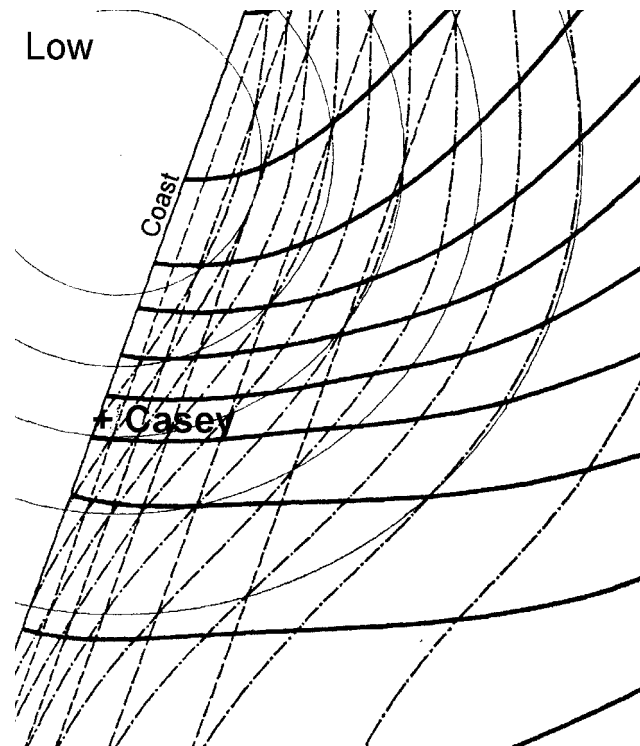
Figure 6.6.1.5.4 Similar to Figure 6.6.1.5.3 which has been rotated 70° anticlockwise to simulate the coastal terrain in the immediate Casey area. The flow lines (solid black) in the vicinity of Casey indicate an easterly wind. (After Blakers, 1983).
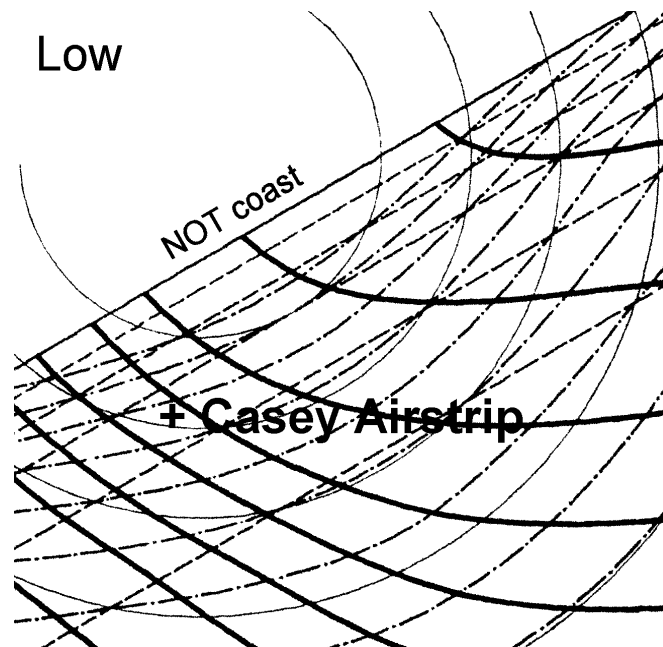
Figure 6.6.1.5.5 Similar to Figures 6.6.1.5.3 which has been rotated 30° anticlockwise to simulate the terrain in the immediate Casey Airstrip area. The flow lines (solid black) in the vicinity of Casey Airstrip indicate a southeasterly wind. Note, that unlike Figure 6.6.1.5.4 the "Not coast" indicates that we are dealing with idealised orography in the immediate area of the Airstrip but not as far east as the coast, where the contours are orientated in a more north–northeast–south–southwest direction.

It is possible to argue that while each site has its own local geographic peculiarities, the essential ingredient in the itinerant coastal wind storms of the Antarctic is the downslope nature of the flow as distinct from the radiation–katabatic flow *per se*. Here one might make the distinction between the long–lived concentrated outflow regions (such as the well known Cape Denison–Commonwealth Bay area (Parish and Wendler (1991)) or katabatic flows clearly observed in glacial valleys such as mentioned earlier in the Vanderford Glacier near Casey, and the major storms which modulate the average condition along the Antarctic coast. This would be a generalisation from the diagnosis of the March 1992 storm discussed by Turner *et al*. (in press) that the strengthening of the synoptic pressure gradient identified by early workers (for example Streten (1968)) is the catalyst in bringing a variety of site dependent factors into play, but significantly, with each factor a contributor to negative buoyancy driven downslope winds. In most coastal and near interior areas the entrainment of radiationally–turbulent heat flux cooled air will be important in providing the density differences, at least early in the storm. Some sites, such as Casey which are at the bottom of a steep moraine slope, might find that early in a storm's evolution the strong surface winds override the station, or are separated from the upstream laminar flow by hydraulic jumps or lee eddies. While other sites, such as Davis, might have a similar situation compounded by the increased friction of intervening rough orography such as the Vestfold Hills (Targett (1998)). After a while, the invasion of air of maritime origin allows the radiative and turbulent heat flux contrast to be replaced by turbulent heat losses to the ice surface from the air from warmer regions to the north. In some cases, for example Casey, the energetics of the storm are added to by gravity wave motion causing downstream low to middle level warming of the atmosphere.

Even the bias to wind storms beginning at Port Martin on a falling bar might have a contribution from this source in view of the ridge–like orography east of the port. Moreover while there is a bias for wind increases at Mawson and Davis Stations to occur on a rising bar, there are still many SWEs which commence at these stations on a falling bar and we note the presence of significant orographic ridges east of these sites.

6.6.1.6   Light winds

While there are probably no specific forecasting techniques available for the forecasting of light winds, the topic is briefly raised here simply to draw attention to the utility of such predictions. To maximise the safety of the most operations and to maximise the comfort of most people in the Antarctic (in particular to minimise the wind chill) it is usually preferable for outdoor activities to be conducted in light wind/calm situations.

In most cases the forecaster will simply be concerned with predicting situations with small pressure gradients and with reduced radiation losses to minimise katabatic effects. As noted in Section 2.6.7.3 above, light winds can also occur when strong wind streams are diverted around orographic barriers, which seems to be the case at Windless Bight.

In other situations care must be taken to interpret the synoptic/mesoscale situation carefully. For example, flow separation in the lee of orographic features can lead to light winds or reverse of flow just prior to a SWE. For example, in the 1991 situation depicted by Figure 6.6.1.3.1 above, the surface wind at Casey was southeast at 3.6 m s^{-1} (7 kt) at 1500 UTC 27 December and by 2100 UTC 27 December the wind was easterly at 23 m s^{-1} (45 kt). Following Adams (1996), it is likely that the strong winds passed over Casey (with rotor effects at the station) until the thermodynamics allowed the separation point to move downstream of the station and strong winds commenced. A similar sequence happened in the SWE described in the previous section.

6.6.2   Upper level winds

The Antarctic forecaster will have an interest in producing accurate forecasts of above surface tropospheric parameters for the following purposes:

- producing route forecasts for aviation;
- assessing synoptic and mesoscale developments;
- assessing the potential for precipitation or even just cloud (white–out).

There are few published studies which relate specifically to the analysis of the high latitude troposphere above the surface and almost none which relate to how parameters such as upper winds might be forecast. Probably the most efficient methods for such forecasts are now–casting, using any available observational upper level data, or the use of NWP output. An example of the latter is shown below. Figure 6.6.2.1 is a typical route taken by high level Antarctic tourist flights which depart Australia. Figure 6.6.2.2 is the NWP forecast cross–sectional wind, temperature, geopotential height and MSLP for the flight path shown in Figure 6.6.2.1.
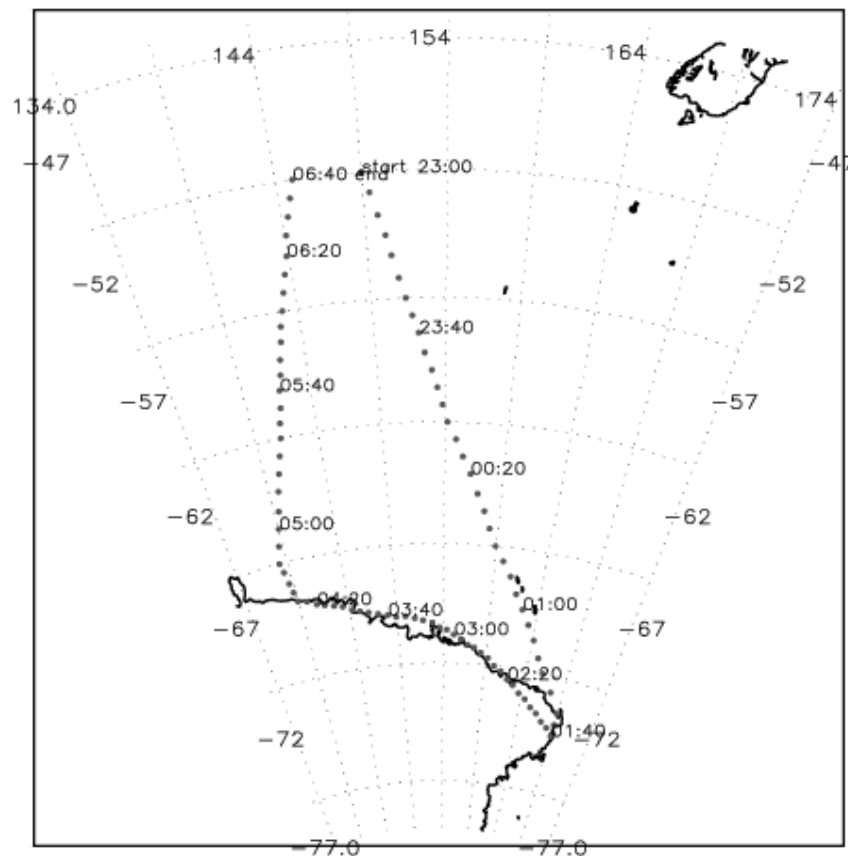
Figure 6.6.2.1   Route sector map of an Antarctic tourist flight corresponding to the flight forecast information shown in Figures 6.6.2.2.
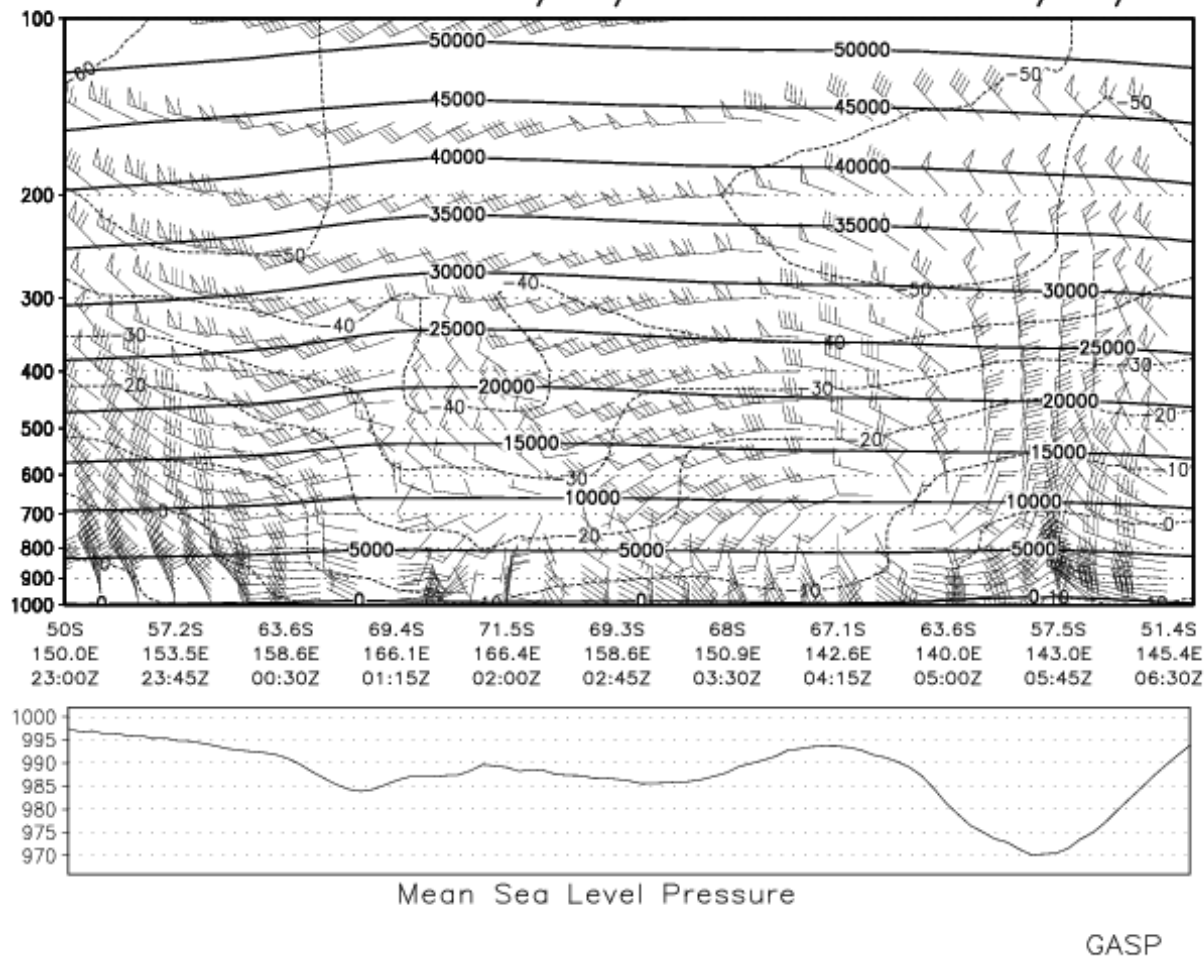
Figure 6.6.2.2   Forecast cross–sectional wind, temperature, geopotential height and MSLP for the flight path shown in Figure 6.6.2.1.

In the absence of NWP data the forecaster might be tempted to produce his/her own upper level prognoses in which case the manual analysis techniques described in Section 5.3.2 above might assist.

6.6.3   Clouds

The problem of forecasting cloud in Antarctica is similar to that in mid and low latitudes in the general approach to the problem. Namely, cloud masses need to be identified, air mass movement assessed and the likelihood of development/decay considered. However, Antarctica introduces several problems not evident in other parts of the globe. Firstly, in the process of identifying cloud masses, low, or even middle level, cloud over the continent or sea ice may be all but invisible using standard infra–red (IR) or visual channels from the AVHRR or GMS satellite systems. This problem arises from the cloud mass being at a very similar temperature to the underlying cold continental ice or sea ice surface giving rise to little or no discernible cloud signature in the IR image. Similarly, the visual characteristics of the cloud are almost identical to those of the underlying ice. The problem of assessing air–mass characteristics and movements at high latitudes is little different from other parts of the globe,

196

other than the analysis process is weaker due to a lack of observational data at high latitudes and the numerical model guidance available is of a global nature and far coarser in resolution than available in other parts of the world. The general lack of observational data and reliance on low resolution models has a necessarily adverse impact on cloud forecasting.

6.6.3.1   Cloud identification.

The number of observational sites around Antarctica providing visual observations of cloud are so small that sole reliance on these sites to identify significant areas of cloud is pointless. Satellite imagery is almost the sole tool for cloud identification. Typically, Antarctic forecasting centres have at their disposal both geostationary satellite data and imagery from polar orbiting satellites. The geostationary data includes IR data at a nominal sub–satellite resolution of 4 km (but much coarser at the latitudes of Antarctica), and visual data with a sub–satellite resolution of 1 km (e.g. GMS5). Water vapour imagery is also available, although at a coarser resolution. The primary polar orbiting data is provided by the NOAA series of satellites. These platforms have five channels of AVHRR data comprising two transmitted IR channels, one channel a combination of transmitted and reflected IR, a visual channel and a near visual channel. The sub–satellite resolution of these data are around 1 km.

Over the oceanic regions surrounding Antarctica the GMS IR and visual data provide a useful means of identifying cloud and differing airmasses. However, by far the best source of data for the broad–scaleidentification are mosaics of the AVHRR IR images remapped into a polar stereographic projection at 4 km resolution. Images such as these are routinely produced at a number of Antarctic stations with mosaicing over six–hourly time–steps. These images also allow the identification of intrusions of high level cloud over the continent such as occurs when broad–scalelow–pressure systems move inland out of the polar trough.

For aviation and field party support where cloud has a significant impact on operations, small scale local regions of cloud are just as important as the broader scale cloud masses. The areas in which cloud impinge on operations include:

- areas of low cloud below alternate minima or safe operations for the aircraft.
- cloud producing icing problems for the aircraft or snow/precipitation resulting in a significant reduction in visibility.
- uniform decks of cloud causing white–out conditions. Over–plateau operations may be significantly effected by even cirrus if the high level cloud is uniform in nature.

The most effective means of identifying such cloud areas is through the use of the 1km resolution radiometry data from the NOAA polar orbiters. Each of the five channels on the NOAA have useful information for the identification of cloud.

High cloud is most easily identified using the IR channels (bands 4 and 5) as the cloud top temperatures associated with cirrus are typically cooler than the surface temperature of the continent. In cases where the cirrus may be quite low and the temperature gradient between cloud and ground not so marked then shadowing on the visual channels (bands 1 and 2) due to a low sun angle often highlights cloud edges and gives some indication of cloud top heights.

Middle and low level cloud can often be difficult to discern on the imagery due to little or no thermal contrast between the cloud and ice surface. Under these circumstances the visual imagery (bands 1 and 2) again offer some clues through texture in the cloud tops from sun reflections and shadowing. With experience, surface ice texture, either in the sea ice zone,

or over the continent becomes familiar as does textures associated with different cloud mass types.

On some occasions low cloud masses move in over the continent or sea ice zone with little or no discernible thermal contrast or notable texture. In these cases the cloud often may go completely undetected through analysis of the transmitted IR or visual radiometry data. However, during daylight hours under certain sun angle situations significant amounts of reflected solar long–wave radiation may be evident in the band 3 channel, caused by the energy at this wavelength being reflected by the large number of water droplets. Under these circumstances, areas of low cloud or fog, that are almost undetectable on the IR and visual channels, show up clearly in band 3 imagery as high reflected energy areas over the cold ice surface. For example, Figure 6.6.3.1.1 shows three bands (1, 3, and 4) from an AVHRR image taken at about 0927 UTC (around 1500–1600 local time) on 4 March 1997 over the Amery Ice Shelf–Prydz Bay area. It is obvious from the visible band (and to a slightly lesser extent from the infra–red band) that there is a band of cloud orientated northeast–southwest over the sea just left of centre of the image. It is not clear the extent to which this cloud band crosses the coast. The band 3 image, however, clearly shows that there is an extension of the cloud over the continent. Note that the cloud appears warmer (darker in this example due to the choice of grey–scale display) than the sea in this image because of the extra energy reaching the satellite sensor from the reflected light.
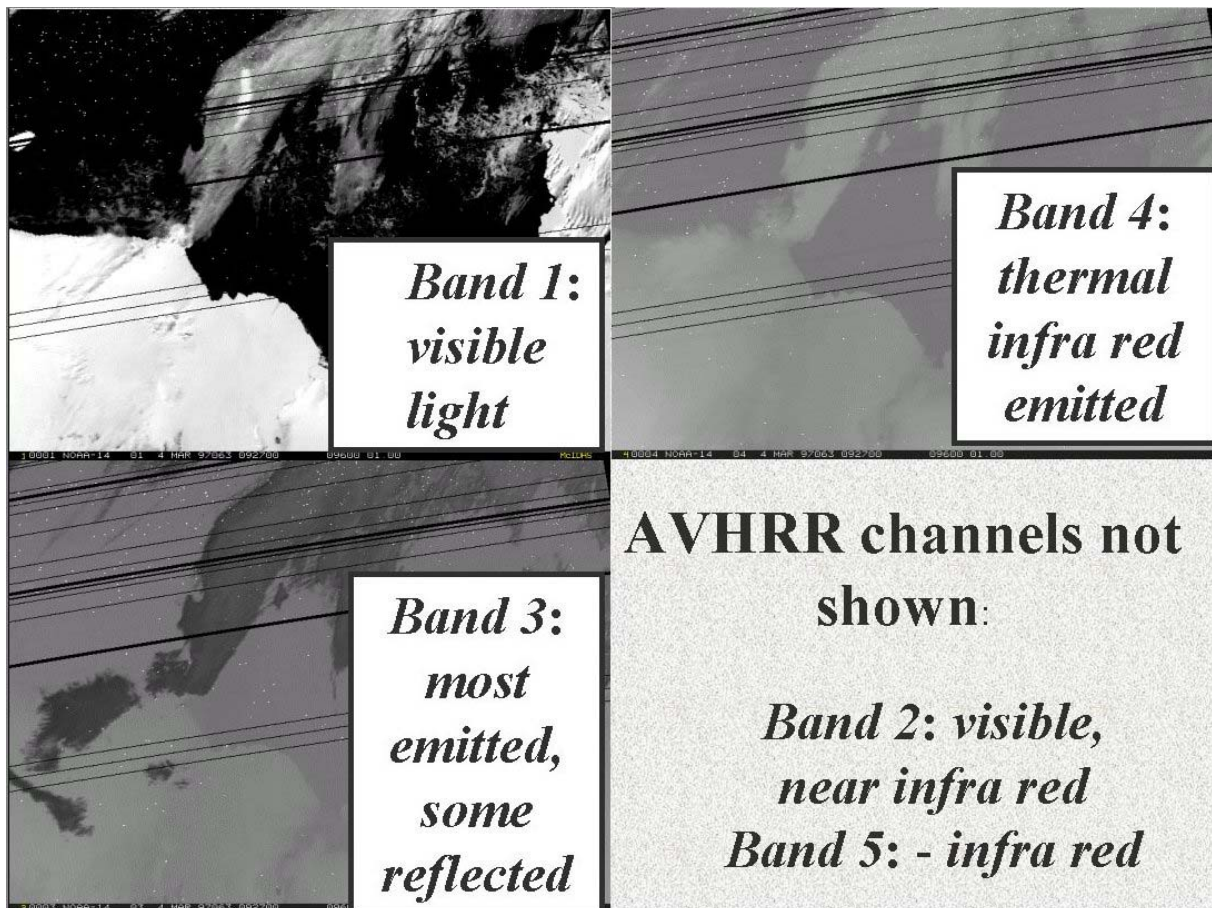
Figure 6.6.3.1.1 AVHRR images taken at about 0927 UTC 4 March 1997 over the Amery Ice Shelf–Prydz Bay area.

6.6.3.2   Cloud Forecasting

Once areas of cloud have been detected the forecaster still has the task of forecasting the movement and development of the cloud mass. Or in the case of cloud–free areas, forecasting whether cloud is likely to develop. To achieve this goal the forecaster needs knowledge of the air masses in the area and predicted movements and development of systems.

There are several key points that are particularly relevant to Antarctic cloud including the following:

- When cold dry air moves out off the continent and over the water, heat and moisture fluxes give rise to low level cloud some distance off the coast. This process may take some time to be accomplished, or may occur quickly. So even though a cold dry air mass is being forecast, if there is any open water present it is worth considering the likelihood of cloud formation. Sea smoke building into low cloud streets can form quite quickly in the sea ice zone if the wind begins to open up leads or polynyas.

- Northeasterly flow ahead of fronts and lows is the prime means of advecting moisture into coastal and inland areas. These features are generally easily identifiable on satellite imagery and normally well forecast by global numerical models. Smaller mesoscale cyclones in the coastal area may generate low level cloud and be harder to both detect and forecast. These systems typically have life cycles of less than 24 h and can cause significant forecast problems.

- Some coastal stations occasionally (around four to six days a year) develop fog or areas of very low cloud associated with a sea breeze circulation. For example, typically on a fine light wind, sunny day at Casey a northwesterly flow develops in the area and over the period of several days advects, during the afternoons, moisture into the Casey area. Radiative and conductive cooling of the moist air where it hits the steep escarpment onto the plateau leads to the formation of a narrow bank of low cloud inland form the station. During the evening and overnight, a weak southerly outflow then advects the low cloud back down the escarpment and over the station as fog which may then last through part or most of the morning until another week sea–breeze circulation begins.

- With a lot of the smaller scale features, long term forecasting techniques really do not exist and nowcasting and short term trend type forecasts are all that can be done. On the broader scale, numerical model guidance is proving to be quite useful. Most models output from their diagnostic packages a percentage figure of low, middle and high level cloud, but another technique that is proving useful is a vertically integrated model temperature product starting from the model surface temperature field and using a threshold humidity value for cloud/no cloud detection at each model level. The product that results is a model synthetic IR image assuming perfect black body radiation from model assumed cloud. Currently this product is being produced at the Casey AMC using NCEP aviation model data and has proven very useful in cloud forecasting. While only showing the humidity predictions, Figure 6.6.3.2.1 is an example of NWP humidity forecasts for the flight path shown in Figure 6.6.2.1 above. And Figure 6.6.3.2.1 is an example of a synthetic cloud forecast (unrelated to Figure 6.6.3.2.1).
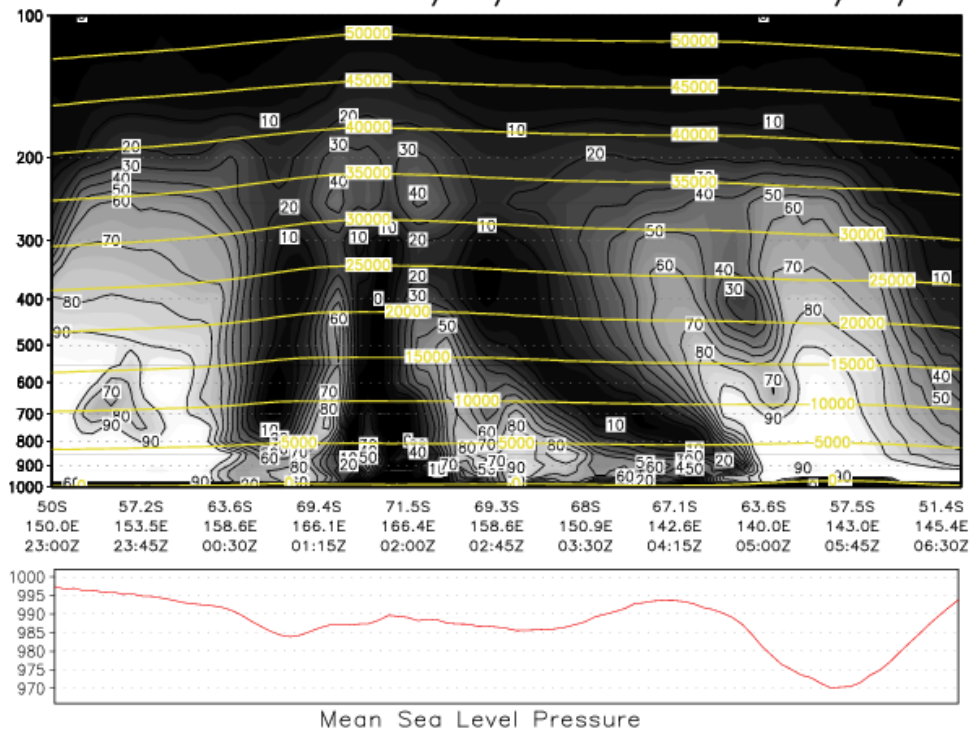
Figure 6.6.3.2.1 Forecast cross–sectional humidity and MSLP for the route shown in Figure 6.6.2.1.
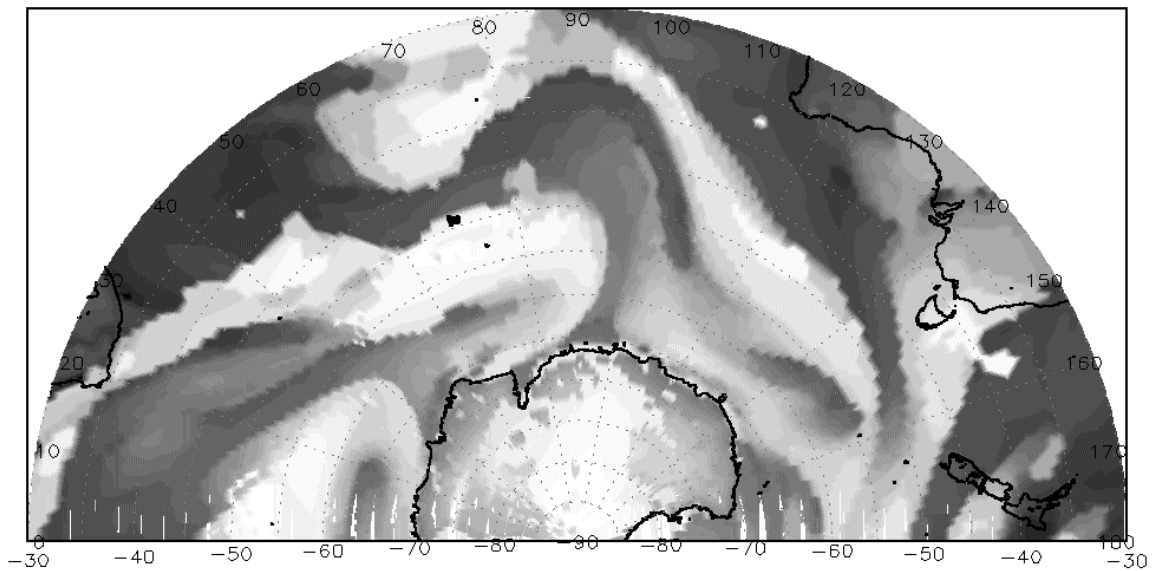
Figure 6.6.3.2.1 An example of a synthetic cloud forecast from the GASP model.

6.6.4   Visibility and fog

As in lower latitudes, fog and low stratus in the Antarctic may cause extremely dangerous conditions for aviation. Figure 6.6.4.1 shows a Pilatus Porter landing just before of a low stratus/fog bank invades the Mt King camp in Enderby Land (see Section 7.6.2 below). Arguably there are at least seven major mechanisms which relate to the formation and/or dispersal of fog and low stratus in the Antarctic region, these being:

- fog generated by air moving from open water over an ice surface;
- similarly, fog generated in the vicinity of meltpools;
- "steaming" in which fog or mist forms as very cold air flows over the sea;
- the relationship between stratus/fog and orography;
- persistent stratus layer generated by turbulent mixing;
- stratus and fog close to the Antarctic Convergence;
- fog and stratus in the warm sector of low–pressure systems.

Aspects of these mechanisms will be discussed in the following sections.

Figure 6.6.4.1   A Pilatus Porter aircraft is landing just before a low stratus/fog bank invades the Mt King camp in Enderby Land. (Photo courtesy S. Pendlebury).

6.6.4.1   <u>Fog generated by air moving from open water over an ice surface</u>

Most often this process will occur over sea ice or fast ice due to the close proximity of these surfaces to a moisture source. However, the Antarctic coastal margin might also be affected under suitable circumstances.

Seasonality

The process of fog being generated by air moving from open water over an ice surface is most likely to occur in the beginning of the summer season. At this stage the sea ice is still quite extensive. Of course this depends upon the characteristics of the previous winter. Sea ice distribution is also dependent upon the configuration of the coastline: bays are well protected locations which favour the persistence of the sea ice.

However, wherever open water is adjacent to an ice surface this process is likely to occur irrespective of season. This type of fog may form within a time span of two hours and turn a sunny and clear day, rather unexpectedly, into poor and murky conditions.

Process

Before moving over the ice surface, the air–mass is warm and moist in the lower–most levels. As the air moves from the open water to over the ice surface, cooling of the lowest atmospheric levels occurs leading to the formation of a surface inversion. The presence of a considerable amount of moisture implies that, due to the cooling, condensation will take place quite rapidly.

Fog clearance

As long as the surface air flow steers the air from the sea to over the ice, this fog type is maintained. On average the visibility ranges between 200 and 600 m whilst the depth varies between 2 and 370 m (~8 and 1200 ft). As soon as the wind changes direction so that the air is no longer blowing from the moisture source, the fog starts to disperse quite rapidly.

Locations where this process happens frequently

The above process probably happens on some occasions around the entire Antarctic marginal sea ice zone and adjacent coast. Areas of frequent occurrence are known to be:

- the Marguerite Bay–Rothera area;
- the northern part of the Larsen Ice Shelf;
- near the polynya between the Weddell Sea and the Ronne Ice Shelf;
- the Brunt Ice Shelf–Halley–area.

Forecasting considerations

Taking into account the information above, the forecaster will be mindful of the climatological predisposition for this type of process to occur in a particular area along with an assessment of the wind direction over suitable areas of adjacent open water and ice surfaces.

6.6.4.2   <u>Fog generated by melt–pools</u>

This type of process is similar to the above to the extent that relative sources of moisture and coldness are adjacent to each other, however, in this case it is more a matter of air moving from a cold, dry surface over a warmer more moist one.

Seasonality

Melt–pools are pools of liquid water on an icy surface. Usually these phenomena form during the warmer part of summer, when, for example, in the Antarctic Peninsula area, positive temperatures are observed as far south as 72–73º S

Process

The temperature of the melt–pool surface is higher than the adjacent ice surface. This temperature difference is variable but the larger the difference the more intense the following process will be:

- air moves from the ice to over the relative warmer melt–pool surface;
- as the temperature immediately above the melt–pool is higher than the adjacent ice surface evaporation from the top of the melt–pool starts;
- while over the melt–pool small scale convection occurs in the air mass;
- the resulting moisture in the air which has blown over the melt–pool is transported to the top of the surface inversion, eventually forming stratus as saturation is reached;
- as long as the temperature of the melt–pool surface is higher than the surrounding ice temperature, evaporation continues and the stratus spreads downwards, eventually reaching the surface to create fog;
- the depth of this saturated layer depends upon the height of the inversion generated by the radiational cooling of the lowest air layers over the general area. (There are likely to be more subtle inversions set up when the air flows from the melt–pool area to back over the ice surface).

Clearance of "melt–pool stratus/fog"

This feature can be very persistent, at least as long as a weak, variable wind prevails. Only a significant change within the synoptic situation is likely to lead to its clearance.

Locations where this event happens frequently

During the months of January, February and March many melt–pools are formed on the King George VI Sound ice shelf which is between Alexander Island and the southern part of the Antarctic Peninsula. As the BAS base Fossil Bluff is located in this area, BAS operations are frequently affected by this fog and stratus.

Forecasting considerations

Taking into account the information above the forecaster will be particularly mindful of synoptic situations which lead to clear skies and light winds over melt–pool regions.

6.6.4.3   "Steaming fog"

Mainly affecting marine operations, and probably not often, is the occurrence where very cold air moves quickly over the relatively warm sea. Moisture evaporates into the air, which being very cold, soon reaches saturation and fog or mist forms. This type of event may occur when southerlies sweep off the Antarctic continent over polynyas, or where a ship might force open a lead in the sea ice.

6.6.4.4   Relationship between stratus/fog and orography

A smoothly ascending slope, typically towards a ridge or a dome, over which sufficiently moist air might flow, is a prime location for stratus/fog to occur. Typically a large area of stratus ascends gently towards a ridge or a dome. When the top is reached and the downward motion starts, the stratus begins to disperse. This is clearly shown by satellite imagery which reveals the lee–edge of the stratus quite distinctively. As long as the surface flow direction is steady the lee side will remain stratus free.

Process

Cloud–free but moist air cools dry adiabatically (0.98ºC per 100 m) as it ascends the orography. Condensation occurs when the dew–point temperature is reached. The resulting stratus sheet is trapped beneath the surface inversion. Rising air continues to cool at the saturated adiabatic lapse rate, which is 0.6ºC per 100 m, due to the release of latent heat just above the cloud base.

     The often sharp edge of the lee–side clearance of stratus may have two components to the cloud evaporation. The descending air warms at the dry adiabatic lapse rate, however, at the top of the ridge the potential temperature of the air has increased compared to the value the air mass had prior to impacting on the rising orography. This increase might occur in two ways. Firstly, should precipitation occur on the windward slope then the release of latent heat through condensation will warm the air (Foehn effect). Secondly, adiabatic compression may occur by the blocking of the air at the levels below the surface inversion on the windward side.

Locations where this process takes place regularly

The slope from Alexander Island towards the ridge to the north of Sky Hi (a fuel depot of BAS in the vicinity of the Sweeney Mountains–see Section 7.3.9 below) is a favourite location as is the region around Siple Dome. The slopes of Berkner Island, on the Ronne Ice Shelf (see Section 7.4.1below) also experience stratus/fog.

        The example shown in Figure 6.6.4.1 is typical of a relatively common occurrence during summer of westerly airflow from the distant sea causing fog and low cloud at Mount King (see Section 7.6.2 below).

Forecasting considerations

The key parameters to consider appear to be the presence of a moist airflow ascending a slope. A knowledge of the upstream temperature and moisture may assist in determining the height at which the cloud might form.

6.6.4.5   <u>Persistent stratus layer generated by turbulent mixing</u>

A relatively thin layer of non–precipitating low cloud (base often varies between 250 and 400 m (~1000 and 1400 ft), may persist for two to three days without any noticeable change.

Process

An explanation for this cloud can be found in the vertical wind distribution: a directional shear, varying between 100 and 180º, between the surface wind and the wind at the level above the cloud is the main reason. On top of this, a considerable moisture content at this boundary level, should be present as well. At this boundary (level of directional shear) turbulent mixing results in a constant moisture content throughout the depth of the mixed layer. This generates a saturated layer between the mixing condensation level (base) and the top of the mixed layer (top).

Forecasting considerations

As long as the directional shear exists turbulent mixing is present. Consequently the stratus layer persists. Indications of a change in wind direction might point to the clearance of this cloud layer.

6.6.4.6   <u>Fog and stratus in the vicinity of the Antarctic Convergence and in the warm sector of lows</u>

The Antarctic Convergence is the boundary between the cold Antarctic waters to the south and the warmer sub–Antarctic waters to the north. Figure 6.6.4.6.1 shows the horizontal temperature gradient across the Antarctic Convergence while Figure 6.6.4.6.2 shows the

position of the Antarctic Convergence (or equivalently the Antarctic Polar Front) around the Antarctic Continent. Note, for example the position of the northern parts of the Antarctic Peninsula with regard to the Antarctic Convergence, constrained in location of course by South America and the Peninsula itself.
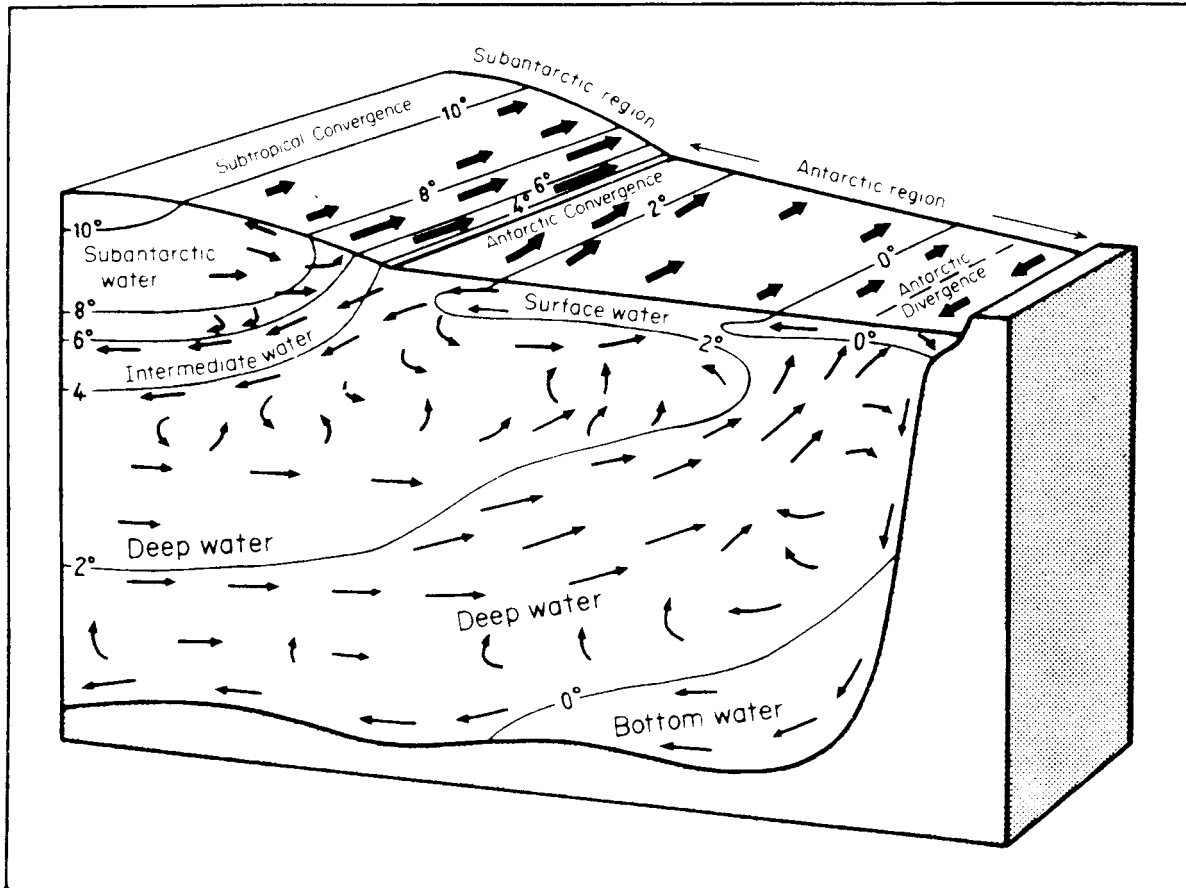
Figure 6.6.4.6.1   Movement of water masses in the Southern Ocean showing, in particular, the typical temperature variation (°C) across the Antarctic Convergence. (From King and Turner, 1997, p. 136).

Formation of fog and/or low stratus in the vicinity of the Antarctic Convergence.

This thermo–dynamic process is quite similar to the one of the water surface/ice surface case mentioned above. Air moves from north to south over the Southern Ocean and is continuously cooled in the lower–most levels. Consequently a persistent stratus layer is gradually generated. Across the Antarctic Convergence, which is characterised by a strong thermal gradient (Figure 6.6.4.6.1), the formation of fog is most likely.

Locations at which this event often affects operational activities

As the north of the Antarctic Peninsula is relatively close to the Antarctic Convergence, fog and low stratus affect frequently the weather conditions over there. Thus the impact of this phenomenon is quite significant as a lot of operational bases are positioned in that region. For

example, Marsh and Marambio, the two alternate runways for the BAS's Dash–7 aircraft are positioned in that particular location (see Sections 7.3.2 (below) and 7.3.5 (below)) Whenever the surface wind varies from westerly to northerly directions Marsh is likely to get fog. Marambio, positioned on the eastern side of the Peninsula gets fog or low stratus with a northerly to easterly surface wind.
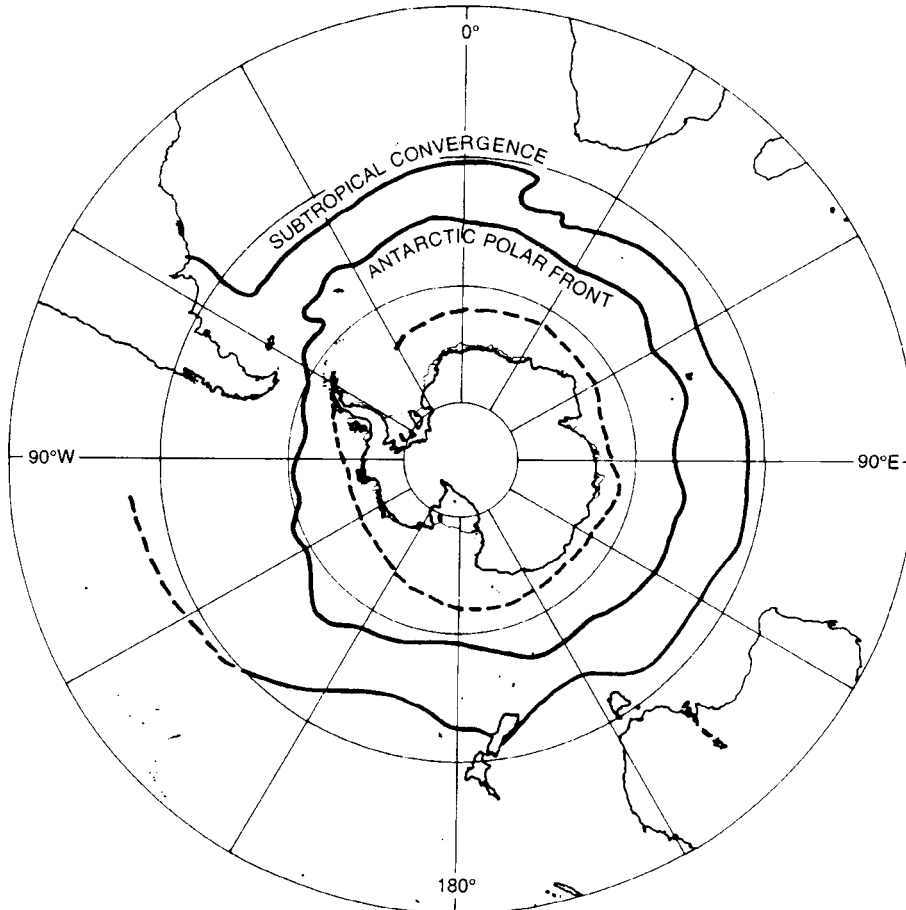
Figure 6.6.4.6.2   Mean positions of the Southern Ocean convergences (solid lines) and divergences (dotted lines). (From King and Turner, 1997, p. 135).

Warm frontal fog/low stratus

The warm sector of lows, where the warm air is moving southwards over cooler seas, is a common location for fog/low stratus.

6.6.4.7   Summary of forecasting considerations

The most important process to generate fog in the Antarctic is the advection of an airmass from a relatively warm surface onto a colder surface. This can happen within a space of time of about two hours which implies the importance of the detection of the fog in its incipient stage.

AVHRR satellite imagery is the most important information one can readily use to detect these fog patches quite rapidly. In order to obtain the most precise information both channels 2 and 3 should be checked. Channel 2 (reflected solar radiation) is less effective over a snow/ice surface. However, in channel 3 the snow/ice surface appears black so the white stratus or fog is very distinctive. To make a precise analysis of the satellite pictures a thorough knowledge of the orography is indispensable. And one should be aware of the sea ice distribution and its changes as well.

6.6.5   Surface contrast

The surface contrast is the ease with which features on a snow–covered surface can be distinguished, either from the air or by a surface observer. It is a very important element for traveling field parties who need to be able to make clear judgments about the state of the surface so as to avoid crevassed areas and large sastrugi fields. For aviation, a knowledge of surface contrast is also vital so that safe take offs and landings can be made.

Surface contrast is usually reported as good, moderate, poor or nil, although there are no internationally agreed definitions for each of these categories. The definitions used at the British Antarctic Survey are:

- *Good*: Surface features clearly defined.
- *Moderate*: Surface features visible, but become indistinct at more than a few kilometres.
- *Poor*: Surface features become indistinct at more than 50 m away.
- *Nil*: Footsteps and undulations discernible at no more than a few paces, if at all.

The surface contrast is dictated primarily by the cloud cover. In cloud–free conditions the surface contrast is usually excellent because of the small amounts of aerosol that are present in the Antarctic atmosphere and the very good visibility. When cirrus cloud is present the contrast can also be quite good. However, the greatest problems are encountered with deep, opaque layers of cloud, often in the form of featureless stratus, altostratus or nimbostratus. Under such conditions it is often not possible for a surface observer to see small mounds or crevasses on the surface when only a few metres away. When cloud with some convective elements is present, such as altocumulus or stratocumulus, the surface contrast is usually moderate or good. On the high Antarctic plateau cirrostratus can be quite near the surface and thick layers of this type of cloud can seriously reduce surface contrast.

The forecasting of surface contrast is therefore essentially one of forecasting the type and depth of cloud to be expected at a location. This subject is dealt with in depth in Section 6.5.2, however, here we will consider the aspects of cloud forecasting that are relevant to surface contrast. Forecasts of contrast are only usually required for up to about 12 h ahead so a nowcasting approach can be used with satellite imagery playing an important role. Forecasts are made on a subjective basis, with the forecaster estimating the contrast based on his assessment of the cloud type and thickness. Determining the thickness of cloud is not easy, but the visible satellite imagery can be useful for estimating cloud thickness, since some surface features can often be seen through the cloud when it is thin. Short movie loops of visible images are also useful in forecasting cloud thickness since surface features can be seen more easily against the moving cloud field.

6.6.6   Horizontal definition

The horizontal definition is the ease with which the boundary between the ground and the sky can be determined. It is a parameter most appropriate over ice shelves or areas where there are no mountains or nunataks visible, which provide visual references on the horizon. The parameter is extremely important for flying operations on the ice shelves and in featureless parts of the continent, such as over the interior plateau. As with surface contrast, horizontal definition is observed to be either good, moderate, poor or nil and at the British Antarctic Survey these are taken to be:

- *Good*: Distinct horizon with obvious difference between land and sky.
- *Moderate*: Horizon visible but with no distinct difference in appearance of land and sky.
- *Poor*: Sky can be discriminated from land but no distinct horizon visible.
- *Nil*: Sky and land appear as one, no horizon visible.

In a similar way to surface contrast, the horizontal definition is determined primarily by the type and nature of the cloud present. Horizontal definition is excellent in cloud–free conditions, but gradually reduces as the amount of featureless stratiform cloud increases. The worst conditions are experienced when there is a thick layer of stratus, altostratus or nimbostratus. Horizontal definition is reasonable when the cloud has some convective elements, such as with altocumulus or stratocumulus. At the edge of an ice shelf the presence of an ice–free lead may aid the detection of the horizon. On the high plateau cirrostratus can be found close to the surface, which may reduce horizontal definition.

As with surface contrast, the forecasting of horizontal definition is carried out once a forecast has been made of the cloud to be expected at a location. The key elements required are predictions of the type and depth of cloud, plus a knowledge of local orography, and these allow a subjective forecast of the horizontal definition to be made. As discussed under surface contrast, satellite imagery can be used successfully to estimate the type and thickness of cloud under many conditions.

6.6.7   Precipitation

The prediction of precipitation is very important for aviation and field party activities since it can reduce visibility considerably and make surface travel or work very dangerous. Moderate or heavy precipitation is almost always found in the coastal region of the Antarctic, while in the interior precipitation is usually light in intensity. These two areas also have fundamentally different types of precipitation. Near the coast most precipitation comes from frontal depressions, and to a lesser degree, mesoscale lows. In the interior most precipitation falls as clear sky precipitation or 'diamond dust', with few major synoptic scale lows reaching the area.

Near the coast the forecasts of precipitation from NWP models can be used directly to produce predictions of snow/rain amounts for several days ahead. Although we know that the current generation of NWP models have generally good representations of the large, synoptic–scale lows over the ocean areas, the precipitation forecasts should still be used with great care since the fine–scale structure, such as the locations of frontal bands, are not as good

as those for mid–latitude areas. Whenever possible the model forecasts should be compared to the most recent satellite images to correct location errors of the frontal bands.

If only the model surface pressure forecasts are available then it is still possible to make some estimation of the locations of fronts by noting the sharp troughs in the surface pressure values around low–pressure systems. It is then possible to make a prediction of the likely arrival time of a frontal band, although the degree to which the front is active and therefore the amount of precipitation to be expected has to be estimated from the thickness field.

For short range prediction of precipitation in the coastal region (up to 12 h, or exceptionally 24 h, ahead) the most useful tool is visible and infra–red satellite imagery. Using sequences of images it is possible to forecast the arrival time of fronts at particular locations and to make some estimation of the likely precipitation from the structure of the frontal cloud band and the cloud top temperatures. Determining whether non–frontal cloud is precipitating or not from satellite imagery alone is much more difficult, although the cloud top temperatures can provide information on the cloud depth. For convective cloud, which is usually found over the ocean, the atmospheric temperature profile from a model or nearby radiosonde ascent is useful for estimating the likelihood of convective precipitation.

To determine whether precipitation will be in the form of rain or snow the model 500–1000–hPa thickness values are the most useful parameter. At sea level, precipitation is usually in the form of snow (rain) when the 500–1000–hPa thickness is less (greater) than 528 dm, although consideration should also be taken of the detailed characteristics of the atmospheric temperature profile from a radiosonde ascent, if available. For example, when relatively warm air masses move over the Antarctic continent thickness values may be greater than 528 dm, but precipitation may still fall as snow because of the cold air temperatures near the surface.

Over the interior of the Antarctic prediction of precipitation is more difficult because of the lack of conventional weather systems. Diamond dust falls on many days, but because it is of such low intensity it is not a significant problem for operations. Model precipitation forecasts do not have any meaning in the interior of the Antarctic, but satellite imagery can be useful for following fronts as they penetrate inland, but any precipitation from these is usually slight once they are away from the coastal zone.

6.6.8   Temperature and windchill factor

Ironically, temperatures around the Antarctic are probably the least important parameter to forecast as all personnel will carry appropriate equipment and clothing as befits working in the Antarctic environment. Temperature forecasting in this area is performed mainly subjectively based on airmass type and knowledge of sea temperatures and ice cover. Local snow melt during the summer revealing the rocks beneath, even over a limited area, can result in a surprisingly large diurnal variation under light wind conditions; the order of 4 to 5ºC is not unusual at Rothera for instance. An assessment of the temperature at remote sites under clear sky conditions can be obtained using satellite skin temperature data. This is graphically illustrated in Figure 6.6.8.1 where one senses the dome–like nature of the orography of Law Dome which is located near 67º S, 113º E simply from the infra–red grey–scale representation.

Windchill, which was first considered by an Antarctic explorer (Paul Siple), is of course a significant factor when dealing with temperature forecasting, however local winds can be very difficult to forecast, particularly in the interior. Nevertheless, wind effects must be borne in mind, particularly when forecasting temperatures for remote sites. The approach to forecasting windchill varies from location to location: for example, the British use the

Steadman formula (Steadman 1971; 1979;1984;1994) for the relevant Antarctic Peninsula stations, while windchill is not forecast for the Australian stations. The reason for the variation probably lies in the difficulty of the task. The reader is referred to an excellent review paper on windchill by Maarouf and Bitzos (2000) which was written as a background document for the Windchill Workshop (April 3–7, 2000) – hosted on the Internet (http://windchill.ec.gc.ca/) by the Meteorological Service of Canada.

     To quote from Maarouf and Bitzos (2000), "Although windchill indices are a useful way of quantifying the various detrimental effects of chilling winds, many researchers have indicated that windchill indices used in Canada, the USA and elsewhere are overstated and should be adjusted. All windchill indices in use today or published in refereed journals are based on methods that did not involve any human experiment or experience, which is a major flaw. Recent advances in heat transfer theory as well as modern experimental facilities such as wind tunnels and controlled cold chambers offer ample support for more rigorous research to evaluate and revise, if necessary, the present windchill indices."
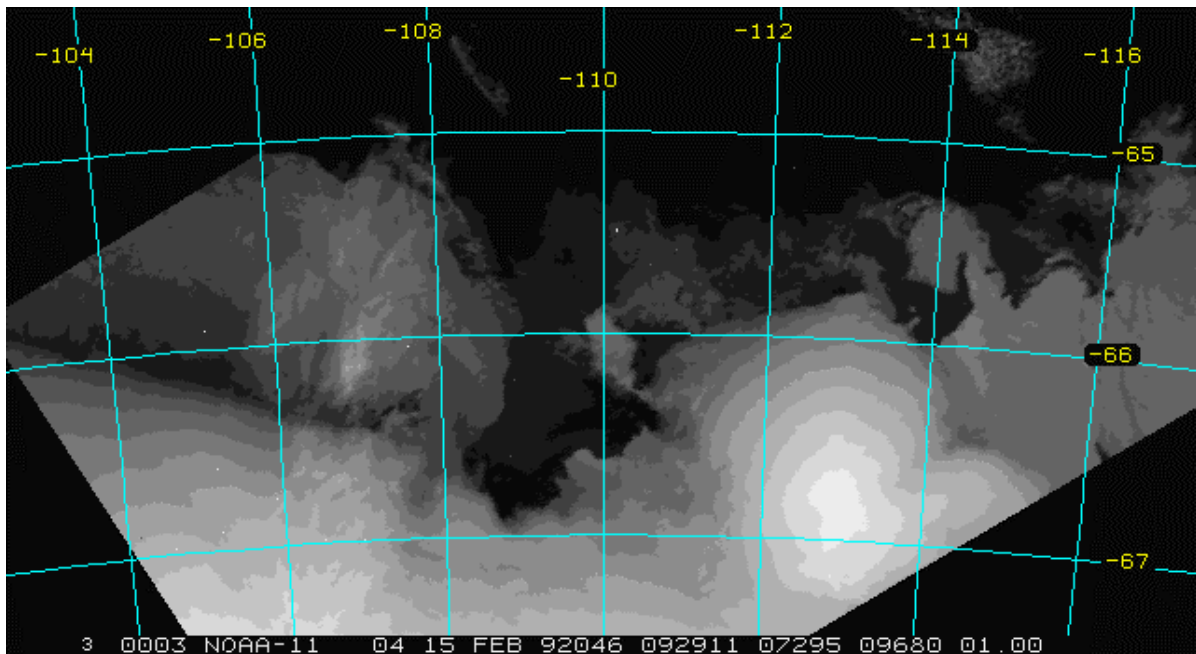
Figure 6.6.8.1   An AVHRR infra–red image taken at about 0929 UTC 15 February 1992. The circular nature of Law Dome (near 67º S 113 º E) is evident from the grey–scale contrast.

6.6.9   Aircraft icing

In Section 3.4.2.6 above a brief overview of the meteorological conditions associated with aircraft icing in the Antarctic is given, along with the effects on aircraft. Bundgaard (1951, p. 793) gives a succinct description of the physical process of aircraft icing: "For icing on aircraft in flight, the subfreezing cloud containing water in the liquid phase must be supersaturated with respect to ice. Although supercooled cloud droplets occur in air subsaturated with respect to (a plane surface of) water, sublimation starts only after the moist air attains saturation equilibrium with respect to ice. In a layer subsaturated with respect to ice, the physically unstable, supercooled fog droplets, upon striking the leading edges of the

aircraft, are induced mechanically to congeal as light rime ice which almost instantly evaporates into the air streaming very rapidly over the rime–forming surface of the aircraft."

Examination of the sections on forecasting icing at the various Antarctic station given in Chapter 7 below suggests that aircraft icing is indeed a significant risk related to the presence of supercooled water droplets. The following quote, for example, is from the relevant section on icing for Casey (see Section 7.10.1.4 below "Forecasting airframe icing in Antarctica is quite difficult as an assessment needs to be made of whether the clouds are fully glaciated or whether some supercooled liquid may still be present. Certainly helicopters operating in the Australian sector of the Antarctic have experienced icing on numerous occasions so the forecaster needs to be aware. As a matter of course if there is any cloud present where the temperatures are above –20ºC then icing is mentioned. Severe icing is considered a possibility in pre–frontal cloud near the coast where it is possible that the airflow has been strong enough to carry supercooled liquid to the Antarctic coast".

The reference here to pre–frontal cloud is supported by Bernstein *et al*. (1997) who, in a study of the relationship between aircraft icing and synoptic–scale weather conditions for North America found that the second highest threat of icing occurred 250–600 km ahead of active and stationary warm fronts. (Arctic air masses were found to be in the highest risk category). Although not strictly relevant to the Antarctic, Bernstein *et al.* (1997) is recommended as a good resource of information on aircraft icing. These authors note that "Modern in–flight icing forecasters at the (USA) Aviation Weather Center (AWC) prepare their forecasts with the help of model–based icing algorithms……." (Bernsetin *et al*. (1997, p. 742). They go on to indicate that even with these modern tools the AWC forecasters still need to hand–analyse synoptic scale weather patterns to diagnose the physical causes of icing and to interpret the NWP model data.

As an example of the state of the NWP art in this area Tremblay *et al*. (1995) have developed a technique to forecast supercooled cloud which, when coupled with NWP output of cloud water content, apparently leads to improved forecasts of aircraft icing.

6.6.9.1   The –8D method

It is not clear in the Antarctic context that the above level of sophistication available to the AWC is currently available, but with increasing access to Antarctic–focussed NWP this situation will change. At Neuymeyer (see "Icing" in Section 7.5.4.4 below) the analysis and forecasting of this parameter is prepared by using the radiosonde data processed by special software and by use of the so called "–8D–curve" method. This approach is the combination of a technique recommended half a century ago (see Bundgaard, 1951, p. 793) but using modern processing systems. In a reference quoted by Bundgaard (1951) it has been shown that supersaturation with respect to ice occurs whenever the air temperature is warmer than minus eight times the dew–point depression (D). When plotted on an aerological diagram if the "–8D" curve is located to the right of the observed temperature then icing is possible. Whereas no supercooled droplets exist when the –8D curve is left of the temperature. In Figure 6.6.9.1.1, for example, the "–8–D" curve indicates that a zone of potential supersaturation with respect to ice exists between about 800 and 700 hPa. Whether or not icing occurs will depend on the actual existence of the supercooled water droplets.

It should be pointed out that methods such as the one just described tend to be empirically based and, as indicated by Tremblay *et al*. (1995, p. 2112) "typically tend to overestimate the presence of icing regions. This causes a tendency for pilots to ignore icing forecasts…".

212

6.6.9.2   Detection of supercooled water droplets using AVHRR imagery

Sections 4.3.1 above and 6.6.3.1 above describe how to detect cloud which has supercooled water droplets in its upper levels, using, in particular, AVHRR band 3. In this band the reflected light from the supercooled droplets adds to the infra–red energy reaching the sensor thus giving a higher (than IR emission alone) count value.

6.6.9.3   Detection of supercooled water droplets using SSM/I

In Section 4.3.5.2 above products derived from the Special Sensor Microwave/Imager onboard the DMSP satellites is discussed. One of these products is cloud liquid water (see, for example, Figure 4.3.5.2.3 above). Tremblay *et al*. (1996) compare several techniques for the detection of supercooled liquid water (including the technique described in Trembley *et al*. (1995)) using SSM/I data to assist in the comparison. At a given horizontal point Tremblay *et al*. (1996, p. 70) assumed that supercooled liquid water existed if the cloud–top temperature was less than 0ºC, SSM/I retrievals of liquid water path (or cloud liquid water) exceeded 0.3 kg m^{-2} and the SSM/I radiances were assessed as not being significantly influenced by ice crystal scattering.
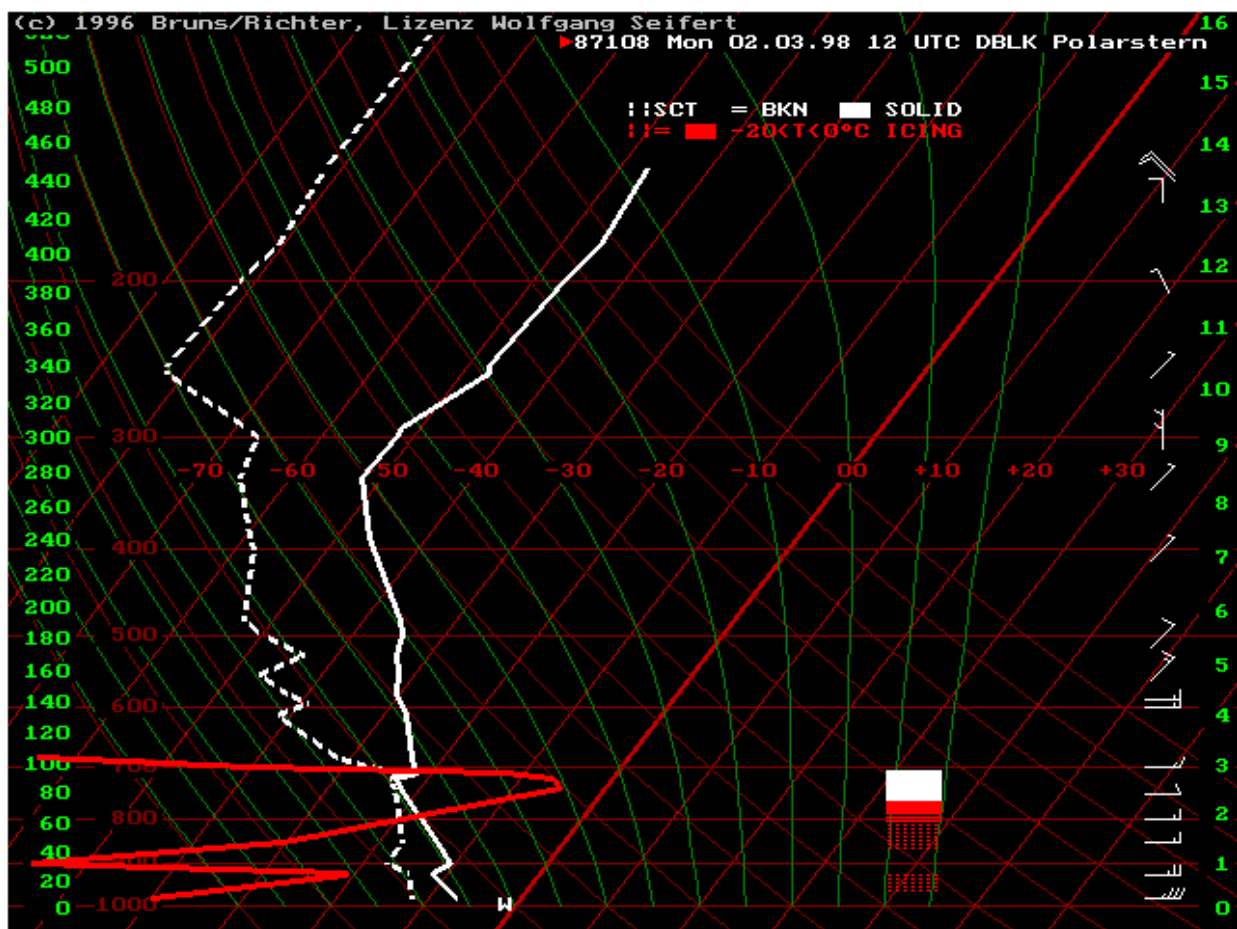
Figure 6.6.9.1.1   A temperature profile (solid white line) and dew–point temperature profile (dashed white line) together with the low level "–8D" curve (red line).

6.6.10   Turbulence

Atmospheric turbulence forecasting is primarily needed in connection with aircraft operations and so where units of speed and altitude are mentioned in this section the aviation–preferred knots (kt) and feet (ft) will be used. There are arguably at least five types of turbulence with which a forecaster has to deal. These are turbulence associated with: (a) convection/squalls; (b) "mechanical" (strong winds blowing over terrain, usually at low altitude); (c) rotor streaming and low level lee waves; (d) mountain waves (at mid to high altitudes); and (e) jet streams/curved flow. Cloud may be present with any of these turbulence categories, or the turbulence may be in clear air (CAT). Moreover, as Bob Lunnon (Head of Aviation Applications, UK Meteorological Office (UKMO) points out in a personal communication, "the distinction between wind shear and turbulence is aircraft dependent so a forecaster should consider a mechanism that causes wind shear as a possible mechanism which causes turbulence". Relevant sources of wind shear include: temperature inversions; (synoptic) fronts; katabatic flows (land breezes); sea breezes; and hydraulic jumps. Apart from the last phenomenon (hydraulic jumps) there is little in the way of direct evidence of shear–related turbulence in the Antarctic context and so turbulence associated with these wind shear phenomena are not discussed here. However, from a theoretical standpoint, turbulence should not be unexpected in these wind shear producing features.

Whilst most of the literature deals with observations, theory, and forecasting (turbulence indices) for mid to low latitudes, there is no doubt that turbulence is a major factor for Antarctic aviation. For example, Lied (1968) reports on the crash of a helicopter which was operating at the then Wilkes Station (near the present day Casey) on 13 February 1960. Lied reports that while in gale to storm force low level wind flow the aircraft experienced severe turbulence and vertical displacements of around 2500 ft per minute. Even today aircraft in Antarctica which operate near rocky out–crops in strong winds; or fly down–wind of mountain ranges; or are en route at high levels to and from lower latitudes, all face a risk of encountering turbulence.

Therefore, this section briefly examines aspects of turbulence that might assist the Antarctic weather forecaster. Most of the information and guidelines are based on non–Antarctic data/experience. Moreover, Tony Skomina, an Aviation Specialist Meteorologist and turbulence expert with the Australian Bureau of Meteorology National Meteorological Operations Centre (NMOC) cautions that, in terms of clear air turbulence " it is essentially a subgrid–scale process (microscale) and up till now we are using synoptic based predictors to isolate possible slabs of the atmosphere in which turbulence is present" (personal communication).

6.6.10.1   Categories of the strength of turbulence

It may be inferred from Meteorological Office (1993, p. 113) that moderate to severe turbulence are the benchmark categories for describing turbulence. The definitions in Table 6.6.10.1.1 are taken from that reference.

In a personal communication Bob Lunnon (UKMO) gives the following advice: "The quoted definitions (in Table 6.6.10.1.1) of turbulent severity are set in terms of the effect of the turbulence on an aircraft. The effects of turbulence on an aircraft are highly dependent on characteristics of the aircraft and the way it is flown, the most influential factors being aircraft weight and airspeed. Thus, given those quoted definitions, what might be light or moderate turbulence in a C–130 could well be severe or extreme turbulence in a Twin Otter. Thus if a forecaster is using this terminology it is important that he/she has a knowledge of what

aircraft he/she is forecasting for. Ideally the forecaster should try and set up dialogue with the pilots and establish terminology which is consistent in its use by the forecaster and the pilot. If a pilot describes turbulence as "I wouldn't ever fly in that again if I had any choice" then this can be treated as a working turbulence severity for that aircraft type. The forecaster can calibrate his/her method based on such a working turbulence severity. It should always be remembered that, ultimately, the pilot is responsible for the safety of the aircraft, but if a forecaster can say that the circumstances are similar to those in which pilot X, flying aircraft Y, said "I wouldn't ever fly in that again if I had any choice" then this can be considered to be the best type of advice that can be offered to a pilot."

Category of turbulence	Effect in/on aircraft
Light	Effects are less than those for Moderate intensity
Moderate	Moderate changes in aircraft attitude and/or height, but the aircraft remains controllable at all times. Air–speed variations are usually small. Changes in accelerometer readings of 0.5 to 1.0 g occur at the aircraft's centre of gravity. Occupants feel strain against seat belts. There is difficulty in walking. Loose objects move about.
Severe	Abrupt changes in aircraft attitude and/or height: the aircraft may be out of control for short periods. Air–speed variations are usually large. Changes in accelerometer readings of greater than 1.0 g occur at the aircraft's centre of gravity. Occupants are forced violently against seat belts. There is difficulty in walking. Loose objects are tossed about.
Extreme	Effects are more pronounced than for Severe intensity

Table 6.6.10.1.1   A categorisation of turbulence

6.6.10.2   Clear air turbulence: indices and threshold values of wind shear

Richardson number

Probably the most well known index related to atmospheric turbulence is the Richardson number (Ri) as it is related to both shear and stability. (Meteorological Office (1991, p250)). Ellrod and Knapp (1992, p150) express Ri simply as:

$$Ri = \text{static stability}(\text{vertical wind shear})^{-2} \qquad \text{Equation 6.6.10.2.1}$$

Intuitively it may be inferred from the above expression for Ri that turbulence would be associated with low values of this non–dimensional number: that is to say, one would expect turbulence to be associated with low static stability or with high vertical wind shear. According to Meteorological Office (1993, p116) turbulence is likely if Ri is less than 0.5 and is certain if Ri is less than 0.15. However, as Ellrod and Knapp (1992, p150) point out, low values of Ri are found in both turbulent and smooth regions.

Kelvin–Helmholtz instability

As described by Ellrod and Knapp (1992, p150) Kelvin–Helmholtz instability (KHI) is the principle mechanism found to be responsible for clear air turbulence: these authors liken KHI to the breaking of an ocean wave and note that KHI exists when vertical wind shear within a stable layer exceeds a critical value. Rees (1987), Kaneto (1982) and Kobayashi (1982) describe incidences of KHI in the context of strong stable stratification of the Antarctic boundary layer. Theoretical and numerical modeling discussions on KHI have been undertaken in a more general sense by authors such as: Sykes and Lewellen (1982); Fritts *et al.*(1996); and a companion paper by Palmer *et al.*(1996). Peltier and Scinocca (1990) examine the role of KHI in the pulsation of downslope wind–storms.

Recent indices for clear air turbulence are given by Ellrod and Knapp (1992):

$$TI1 = VWS* DEF \qquad\qquad\qquad \text{Equation 6.6.10.2.2a}$$

$$TI2 = VWS*(DEF + CVG) \qquad\qquad \text{Equation 6.6.10.2.2b}$$

where, TI1 and TI2 are turbulence indices (1 and 2); VWS is the vertical wind shear; DEF the deformation of the flow; and CVG, convergence of the flow. The reader is encouraged to refer to Ellrod and Knapp (1992, p 151 to 154) for an excellent description and explanation of the derivation of these indices. According to these authors "Prior research has correlated turbulence frequency to each term of the (index) equation and the three variables comprising the index (TI2) were found to contribute significantly to the turbulence potential" (Ellrod and Knapp,1992, p 163).

However, David Thomas, the Australian NMOC Supervisor cautions in a personal communication that: "NMOC uses indices which include deformation as well as sheer (for example Ellrod and Knapp's TI1) but these type of indices are very sensitive to which numerical model output is used. Thus, absolute values are quite meaningless on their own with out some historical knowledge of the performance of the index. Every time we change a model it takes some time to reassess the critical values". These remarks are supported by Bob Lunnon (UKMO) who, in a personal communication advises: "what works well over the contiguous USA may not work well in a relatively poorly observed region of the world such as Antarctica. We (the UKMO) find that American predictors perform poorly almost anywhere in the world except the US. We find that the "Brown predictor" (Brown, 1973) works as well as anything else in poorly observed parts of the world. We know that out own model (UKMO) is not particularly good at forecasting vertical wind shear, and we suspect this is the reason "Brown" works well".

It would seem prudent then for Antarctic forecasters to undertake their own evaluations of the relevance in the Antarctic context of any of the turbulence indices that may be available.

Similarly, critical values of wind shear may vary from place to place. According to Ellrod and Knapp (1992, p 153) vertical wind shear values of 6 knots per 1000 ft are considered to be the threshold for moderate or greater turbulence. This is consistent with Meteorological Office (1993, p117) which adds that the vertical wind shear lower–bound for severe clear air turbulence is around 9 knots per 1000 ft. David Thomas (NMOC) also advises that it was Australian practice to use, among a range of other considerations, this last mentioned criterion, however, experience has shown that a vertical shear criterion of around 20 knots per thousand feet seem more appropriate for predicting severe turbulence in the Australian context. So, again, the Antarctic forecaster will need to tune any such criteria listed below to suit the Antarctic experience.

Clear air turbulence: jet streams and curved flow

CAT may occur with most of the mechanisms discussed in the sections below, however, CAT is also often associated with jet streams (for example, (Shapiro, 1981)) and non–linear air–flow. The turbulence index work of Ellrod and Knapp (1992) is specifically designed to provide an objective technique for diagnosing or predicting the occurrence of CAT where wind shear, divergence and convergence are kinematic contributors.

The Meteorological Office (1993, p.116–117) provides some useful synoptic indicators of CAT which the Antarctic forecaster might also find useful. And, as pointed out by Bob Lunnon (UKMO–personal communication) Kelvin–Helmholtz instability will occur when the Richardson number is low and, in synoptic terms, the conditions under which this occurs are those described in the above reference. These are:

- CAT associated with jet streams is most probably found:
    - on the cold side, near and below the core;
    - on the warm side, above the core;
    - near exits with marked curvature and diffluence;
    - at a confluence or diffluence of two jet streams;
    - near sharp upper troughs;
    - around sharp ridges on the warm side of jets;
    - where one jet undercuts another;
    - where the tropopause fluctuates.
- CAT is also found away from jet streams, but in areas of curved flow such as:
    - in areas of anticyclonic curvature, where the actual wind speed approaches a critical value of twice the geostrophic wind speed. (Knox (1997) is an interesting reference concerning CAT and strongly anticyclonic flows);
    - within 150 nm or so of the axis of a sharp upper trough where the wind shift is over 90º;
    - occasionally, across shear lines in cols where the wind direction reverses rapidly.

6.6.10.3   Convective turbulence

Turbulence due to convection in the Antarctic will probably be generally confined to rocky outcrops during days of strong insolation and may, or may not, be visible as cumuliform cloud. According to the Australian Bureau of Meteorology (1981, p. 44), convective turbulence usually causes no serious problems for aircraft except in thunderstorms. Due to the generally high stability of the Antarctic atmosphere cumulonimbus clouds are rarely if ever seen, and if they did occur would be confined to the coastline and Southern Ocean. Prydz Bay in Eastern Antarctica is believed to be one area where cumulus congestus bordering on cumulonimbus cloud infrequently occur when cold continental air mixes in a convergent manner over the relatively warm ocean. (See the sub–section on clouds in Section 7.8.4.4 below).

Mammatus cloud is also often associated with convective instability in mid to low latitudes and may occur in the Antarctic down stream of orographic ridges/hills/domes. However, in this context the mammatus may be more indicative of KHI and rotoring/lee wave activity (see Section 6.6.10.5 below) than of convection. While not a very clear image Figure 6 presented in Adams (1996) shows an almost chaotic sky with lenticular, rotor and mammatus cloud in a strong wind and gravity wave event at Casey.

6.6.10.4   "Mechanical" type turbulence

"Mechanical" type turbulence occurs in the lowest few hundred feet of the atmosphere and results from the frictional effects which strong winds experience over terrain. According to Meteorological Office (1993, p.114) a surface wind of about 15 to 35 kt will cause moderate turbulence over flat country and severe turbulence over hilly orography while winds in excess of 35 kt will cause the turbulence to be severe and extreme respectively.

The Australian Bureau of Meteorology (1981, p.45) cautions that strong winds will produce down–currents and turbulence in the lee of mountains irrespective of whether mountain waves have formed. This references advises aircraft approaching mountains into a strong head wind to allow adequate clearance from the ground to avoid stronger winds, turbulence and down currents near and in the lee of the peak (See also Sections 6.6.10.5 and 6.6.10.6 below. Peltier and Scinocca (1990) is also recommended for aspects of downslope wind–storms in the lee of mountains).

The forecaster will therefore want to know the terrain features (smooth snow; sastrugi; rocky outcrops, etc) over which any low altitude flying might take place and will need to forecast the surface wind speed.

6.6.10.5   Rotor streaming and low altitude lee waves

Conditions in the Antarctic are probably ideal on occasions for rotor streaming in which a series of rotors form downwind of hills, ridges or mountains in a strong wind flow normal to the ridge line. According to Meteorological Office (1993, p115), and Förchtgott (1969, pp.256–257) (see also (Reece, 1979) severe turbulence due to rotor streaming can occur when:

- strong winds (20 to 25 kt) occur near the ground at ridge level;
- a sharp decrease in wind speed, accompanied by a large change in wind direction, occurs about one and a half to twice the height of the ridge;
- a stable air mass occurs above the well–mixed lowest layer.

For an Antarctic forecaster, knowledge of the vertical wind profile away from main stations presents a problem unless there are in–field wind profile measurements available. From the top panel in Figure 6.6.10.5.1 it may be inferred that severe turbulence due to rotor streaming is confined to an area relatively close to, and downstream of, the mountain/hill ridge line and spans altitudes between just below ridge height to around two ridge heights. Förchtgott (1969, p.258) also notes "besides extreme gustiness, the rotor zone is marked by local pressure deviations of several hectopascals that can easily escape the attention of pilots owing to their full occupation with the extreme effort needed to maintain the aircraft under a reasonable degree of control".

The bottom panel in Figure 6.6.10.5.1 suggests that low altitude lee wave formation is different from rotor streaming in that the lee waves can extend much further down–stream of the ridge line with the severe turbulence zones more widely separated in the vertical and horizontal. The typical vertical wind profile is also different with a peak in horizontal wind speed normal to the ridge occurring at about four times the height of the ridge.
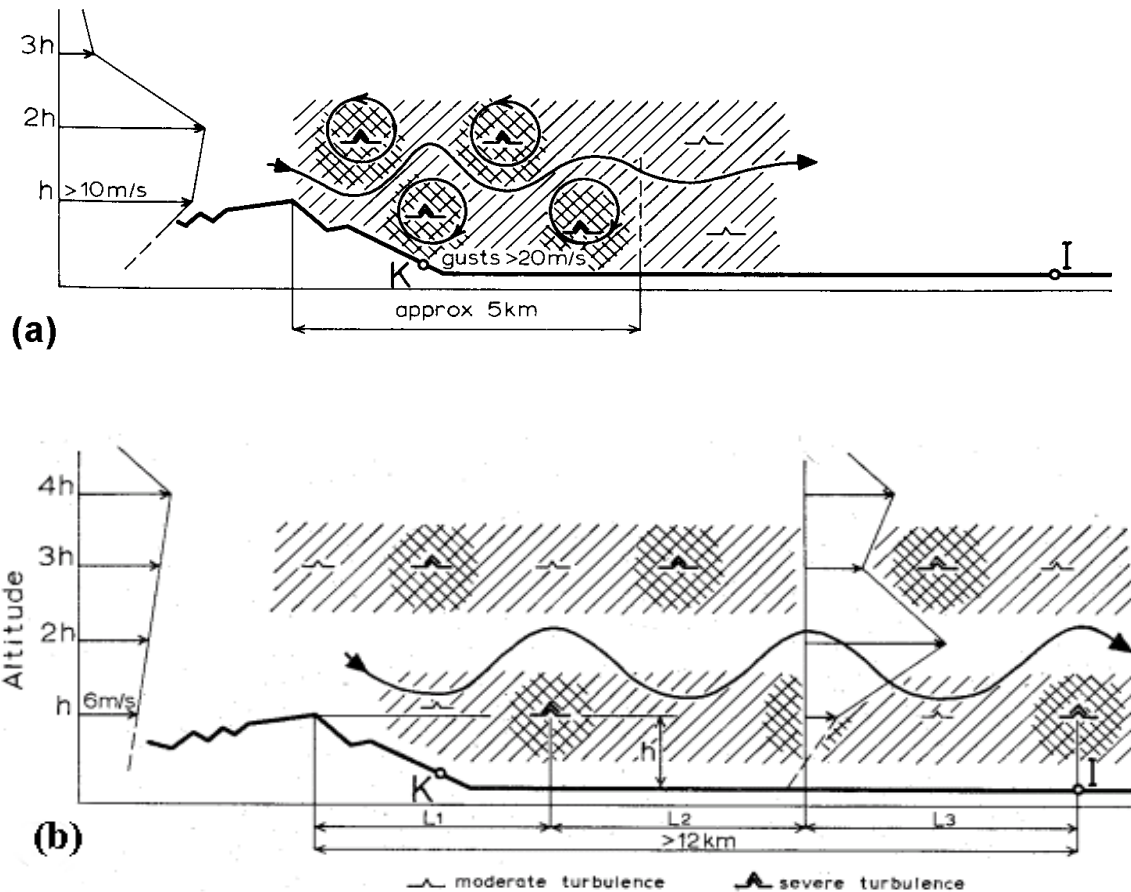
Figure 6.6.10.5.1   Schematic showing the difference between turbulence associated with rotor streaming (top panel) and low altitude lee waves (bottom panel). The figure is after Förchtgott (1969, p.257). K and I represent two towns from which data were obtained. The mountains sketched at left were about 400 m high compared to the plain at right.

6.6.10.6   Middle to high altitude turbulence associated with mountain waves.

According to Meteorological Office (1993, p 116), mountain waves are probably the major reason for turbulence in the stratosphere, and while that part of the atmosphere is well above the area of interest for the Antarctic forecaster this illustrates the vertical extent to which mountain–generated turbulence might reach.

Also according to Meteorological Office (1993, p 115), the intensity of the turbulence is proportional to the strength of the vertical motion and inversely proportional to the wavelength. The most turbulence–prone areas are likely to be near the wave crests and troughs. Check lists have been prepared for forecasting the occurrence of atmospheric turbulence, including mountain wave turbulence. The reader is referred to Ellrod (1989) for a comprehensive decision tree approach to diagnosing or predicting clear air turbulence (See Section 6.6.2.8 below) including mountain wave induced turbulence. This check list, which requires access to upper–air data and to satellite imagery (including the water vapour channel) is also available on the World Wide Web at:

http://www.met.fsu.edu/Ugrads/dwunder/prointro.html

A simpler check list which has found some utility in the Australian context is shown in Figure 6.6.10.6.1 (Australian Bureau of Meteorology, 1973).

Check:
Does the wind component normal to the ridge, near the ridge level, exceed 25 m s^{-1} (~50 kt)?
NB: follow *both* Yes/No flow paths!

Yes

No

Forecast:
MODERATE turbulence patches from the ridge level to 3000 m (~10,000 ft) above the tropopause, up to 300 nm leeward of the ridge.
SEVERE turbulence patches:
(a) at the tropopause up to 280 km (~150 nm) leeward of the ridge, and,
(b) at low levels leeward of the ridge.

Check:
Does the wind component normal to the ridge, near ridge level, exceed 13 m s^{-1} (~25 kt)?

Yes

No

Forecast:
MODERATE turbulence patches:
(i) Up to 280 km (~150 nm) from the ridge:
    (a) from 1800 m(~6000 ft) above the ridge level to the tropopause, and
    (b) from the surface to the ridge level;
(ii) from 80 to 280 km (~50-150 nm) leeward of the ridge and from the ridge level to 1800 m (~6000 ft) above.

Forecast:
Neither MODERATE nor SEVERE turbulence is likely (except if the wind profile compare with the Förchtgott profile (see Figure 6.6.10.5.1) for lee wave activity).

Check:
Does the wind component normal to the ridge exceed 13 m s^{-1} (~25 kt) to the mid-troposphere?

→ Yes →

Forecast:
SEVERE turbulence patches up to 50 nm leeward:
(a) from the ridge level to 6000 ft above, and
at the base of any relatively stable layers below the tropopause

No

Check:
Does the wind profile compare with the Förchtgott profile (see Figure 6.6.10.5.1) for rotor streaming or for lee wave activity (note the latter may have a wind speed normal to the ridge as low as around 5 m s^{-1} (~10 kt) for severe turbulence to occur).

No

Yes

Forecast:
SEVERE turbulence is unlikely.

Forecast:
SEVERE turbulence patches relevant to rotoring or lee waves.

Figure 6.6.10.6.1 A check list for turbulence associated with mountain waves.

6.6.11   Sea ice

6.6.11.1   Long–term considerations: atmosphere–ice interaction

Persistence of long wave troughs or ridges in one general area for any length of time (upwards of a week) will have an effect on the concentration and northward extent of the sea ice through the long wave modulation of synoptic features. If a long wave ridge persists over the marginal ice zone the ice pack should become more consolidated due to the formation of new ice and refreezing of old ice. This is due to more frequent periods of calm or light winds, clearer skies and colder temperatures associated with short wave features in the ridge, than if a long wave trough were located in the area.

If, on the other hand, a long wave trough does persist in the area the ice pack should be more broken with heavy rafting of floes and large fields of brash ice due to the constant motion of floes under the action of the wind. If the area is on the western side of the long wave trough then there should be a tendency for the ice edge to be further north than on the eastern side of the trough due to the winds having a greater southerly component. The ice edge on the western side of the trough will be more fragmented due to the divergent nature of this motion than that on the eastern side where the winds will be more northerly and act to concentrate the floes.

Strong winds and large amplitude swell have a great bearing on the motion of the ice in the Antarctic pack. Predictions of persistence of periods of severe or calm weather can greatly assist mariners by giving guidance on the suitability of operating in any given area and the risk of becoming trapped there for extended periods of time.

6.6.11.2   Short term considerations

Nowcasting

The sea ice analysis services (see Section 2.8.6 above) together with any available satellite imagery of sea ice conditions, may allow a very short-term forecast of ice conditions to be provided. However, the effects of wind and currents may limit the usefulness of these data, particularly very high resolution data (eg: the SAR data mentioned in Section 4.3.2 above).

Forecasts

The NIC provides a seasonal Ross Sea (90 day) forecast for the McMurdo Sound resupply: this forecast is available on 15 October of each year. (http://polar.wwb.noaa.gov/seaice/). The NCEP Ocean Modeling Branch (OMB) provides input to the NIC products as well as producing sea ice forecasts themselves. R. Grumbine (personal communication) advises that the NCEP OMP will include more general sea ice forecasts for the Antarctic in the very near future.

6.6.11.3   <u>Vessel Icing</u>

An algorithm is given by Overland *et al.,* (1986, p. 1801) relating sub–freezing air temperatures, strong winds and sea surface temperatures of less than 6^0C to superstructure icing on ships:

$$PR = V(T_f – T_a)[1+0.4(T_s – T_f)]^{-1} \qquad \text{Equation 6.6.11.3}$$

where:

V is wind speed in ms^{-1}
T_f is the freezing point of seawater (ºC)
T_a is the air temperature (ºC)
T_s is the sea surface temperature (ºC)
PR is a predictor which may be used to give ice accretion rates using Table 6.6.11.3.1

	Light	**Moderate**	**Heavy**
Predictor (PR) (m ºC s^{-1})	< 20.6	20.6 to 45.2	> 45.2
Accretion rate (cm.hr^{-1})	<0.7	0.7 to 2.0	>2.0

Table 6.6.11.3   Categorical forecast ranges for vessel icing.

6.6.12   **Waves and swell**

Forecasts of sea state are required in support of the operation of vessels of all sizes, ranging from ships on the open ocean engaged in commercial and resupply activities to small boats used in areas of open water inside the sea ice zone. The nature of this publication dictates that the treatment be extremely brief . The reader is referred to WMO (1998) from which much of this material is derived, for greater detail.

It is normal to describe the state of the sea in terms of a combination of sinusoidal wave forms. Such waves are classified according to their period and range from long period waves, such as tides and tsunamis, to extremely short period capillary waves, dominated by the surface tension of the water. The discussion here will be confined to wind generated gravity waves with periods generally ranging from 1 to 30 seconds. The derivation of the relationships regarding wave motions is beyond the scope of this publication and can be found in any standard text on wave motion (for example Crapper, 1984). Before progressing to a consideration of the state of the sea in its entirety it is useful to consider the properties of a unidirectional periodic wave.

6.6.12.1   <u>Basic Definitions and Relationships</u>

While it is beyond the scope of this handbook to explore the relationships between the following wave characteristic descriptors in detail it is considered useful to briefly list the key wave parameters:

- The wavelength (λ) is the horizontal distance between successive wave crests.
- The period (T) is the time between two successive crests passing a fixed point.
- The frequency (f) is the number of wave crests which pass a fixed point in unit time and is the inverse of the period.
- The amplitude (a) is the maximum displacement from the equilibrium position.
- Wave height (H) is the vertical distance between a wave trough and the following wave crest. In the case of a sinusoidal wave it is twice the amplitude.
- The phase speed (c) is the rate at which the wave form advances and is equal to λ/T.
- The energy propagates at the group velocity (C_g) which, in deep water, is half the phase speed.

6.6.12.2   <u>Effects of Water Depth</u>

As waves move into shallow water only the period will remain constant while the phase speed and wavelength decrease. Water depth (H) is normally classified as deep, transitional or shallow depending on the ratio of depth to wavelength. In deep water the depth exceeds one quarter of the wavelength and in shallow water the depth is less than one twenty–fifth of the wavelength.

6.6.12.3   <u>Combinations of Waves</u>

As stated earlier, the total sea state can be described in terms of a linear combination of the simple waves described above with varying amplitude, frequency, phase and direction. These waves may be generated locally by energy input due to the surface wind stress (wind waves), or propagate into the area from afar (swell waves).

It is convenient to define another parameter, the significant wave weight, which is the average height of the highest third of all waves. This quantity is one of the outputs of numerical wave models and also usually corresponds to visual observations of the sea state. It must be strongly emphasised that waves larger than the significant wave height will be encountered and the maximum wave is likely to be approximately twice the significant wave height. Even larger waves are possible.

In this spectrum of waves the variance of the surface elevation caused by each component represents the contribution to the total energy by that component, as explained above, hence the wave spectrum also represents an energy spectrum. Various functional forms for this spectrum have been proposed such as the Pierson–Moskowitz (Pierson and Moskowitz, 1964) and JONSWAP (Hasselman *et al.*, 1973).

A practical side-effect of the spectral nature of waves is that various vessel types respond differently to the wave period: as a result wave model output of the peak energy period (T_{peak} or T_p) may be more useful than the significant wave period.

6.6.12.4   Effects of sea ice

The effects of sea ice are difficult to quantify, but even the very thinnest of newly formed ice progressively removes the higher frequency, small amplitude waves as it develops and thickens. Very high concentrations of mature ice can effectively damp out all but the longest period waves. Romanov (1996) reports that the distance of swell penetration into ice cover, evaluated from satellite observations, is from 300 to 400 km and that swell waves may reach the Antarctic coast even at the time of maximum ice development.

Large recurring polynyas commence forming around the Antarctic coast about September, reach their maximum extent around January and decrease to the September level by May (Romanov, 1996). It is the presence of these large areas of quasi–open water within the sea ice zone which leads to a natural dichotomy in methods of wave forecasting. In particular, some global wave models do not include pack ice and will thus not model dampen wave motion as they should.

6.6.12.5   Numerical Wave Models

The basic principle of numerical models is to calculate the changes with time of the energy spectrum mentioned above. Models containing the region of interest to Antarctic forecasters are run on the global domain at resolutions between one and three degrees and normally in deep water mode without currents.

Without going into the specifics the total rate of change of energy equation can be written such that the energy source terms are:

- the energy input by the surface wind stress;
- non–linear transfer due to wave to wave interactions;
- and dissipation due to whitecapping.

The initial state is normally a forecast from a previous model run and the wind forcing is provided by the output from a numerical atmospheric model. The major source of error in numerical wave forecasts lies in errors in the input wind fields (Komen and Smith, 1999).

Verification data over the Southern Ocean are scarce, but preliminary results obtained in the National Meteorological Operations Centre (NMOC), Melbourne comparing the output of the GASP model (Bourke *et al*., 1990) with observations from the vessel *Aurora Australis* (Table 6.6.12.5.1) indicate an acceptable level of correlation for forecasts of up to 60 hr, with a decline for longer intervals.

Although Romeiser (1993) reported an under–estimation of wave heights in the Southern Ocean during winter by the wave model–WAM (*Hasselman et al.,* 1988) recent results obtained in NMOC Melbourne indicate a tendency for the Australian implementation of WAM to overestimate wave heights during strong wind events, resulting in a high bias over the Southern Indian Ocean.

The other major source of error in high latitudes is the presence of sea ice, the treatment of which varies between centres. The ECMWF implementation of WAM allows for a variable ice edge, based on analysed sea surface temperature which is then held fixed for the duration of the forecast, whereas the Australian implementation of WAM currently takes no account of sea ice at all.

Forecast Interval (hr)	Correlation Coefficient
0	0.89
12	0.87
24	0.84
36	0.85
48	0.82
60	0.78
72	0.61
96	0.67

Table 6.6.12.5.1. Correlation between GASP forecast wind speed and observations from *Aurora Australis*.

6.6.12.6   Manual Wave Forecasting Methods

Although manual wave forecasting methods can be applied over the open ocean, they are labour–intensive and forecasts for these regions are more conveniently derived from the output of numerical models. However, their use is mandatory in large polynyas within the sea ice.

Manual techniques rely principally on the use of nomograms to determine wave growth without consideration of the physical processes involved. They have largely been devised empirically from observed or measured wave datasets and rely on pre–determined properties of the wind field (fetch, duration and wind speed and direction). It is therefore immediately obvious that the first steps are the estimation of the wind field and ice conditions. These processes are covered elsewhere in this handbook and will not be repeated.

Having determined the likely fetch, duration and wind field it is a simple matter to determine the wave height from a nomogram. The nomogram used here (Fig 6.6.12.6.1) is derived from Groen and Dorrestein (1976) and uses characteristic wave height and period rather than the previously defined significant wave height. Although characteristic wave height is biased slightly high compared to significant wave height there is no difference for practical purposes. Two examples of the use of the nomogram are given:

- *Example 1*: Consider a wind speed of 30 m s^{-1} (~60 kt) acting over a fetch of 60 km for a duration of 12 h. Following the 30 m s^{-1} curve from the left, one first encounters the 60 km fetch line, indicating that, in this case, wave growth is limited by the fetch. A characteristic wave height of 6 m with a period of 7 sec is indicated. Maximum wave heights likely to be encountered would be approximately 12 m.
- *Example 2*: If, instead, the likely duration was 3 h, then the duration becomes the limiting factor and the nomogram yields a characteristic wave height of 5.3 m with a period of 6.5 sec.

If a functional form of the wave energy spectrum, as discussed in Section 6.6.12.3, is assumed then further information regarding the range of waves present can be calculated. However the data calculated above is the most useful for operational purposes.

As the wind field is unlikely to remain constant during the forecast period some empirical "rules of thumb" are useful in modifying the forecast wave field:

- •   (i): If the wind freshens at constant direction, subtract one quarter of the increase from the new wind speed and use this value to determine the wave height from the nomogram. For instance, if the wind speed is predicted to increase from 10 to 20 m s^{-1} over a 12 h period compute the wave height using a speed of 17.5 m s^{-1} over a duration of 12 h.
- •   (ii): Changes in wind direction at constant speed of less than 30 degrees can be ignored and the direction treated as constant. For greater changes the previous wave field should be treated as swell and it becomes necessary to perform another calculation of the newly generated sea state.
- •   (iii): Once the wind slackens swell wave heights can be reduced by 25% per 12h period.
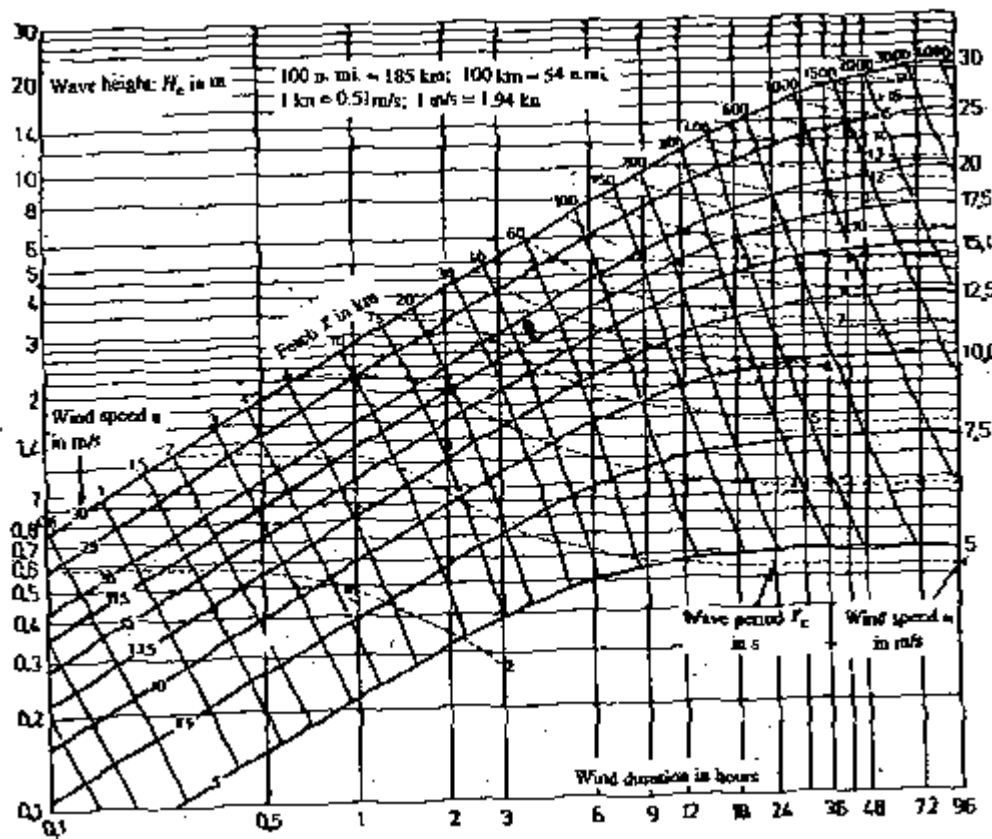
Figure 6.6.12.6.1   A nomogram for sea wave height determination. (After Groen and Dorrestein (1976).

6.6.13   Hydraulic jumps (Loewe's phenomena)

One of the most, if not the most, dramatic feature of the coastal climate of Antarctica is the very strong katabatic winds blowing frequently from the polar plateau toward the sea. Apart from the severe downslope wind itself, the most spectacular phenomenon occurring during the katabatic periods is the "Loewe's phenomenon". This type of phenomenon has been

described by Valtat (1960) as occurring at Dumont d'Urville, Adélie Land. The Loewe's phenomenon includes a sudden slowing down of the wind speed and a change in the depth of the cold air layer. This "jump" in the wind is always associated with a "jump" in the pressure so that, sometimes, the Loewe's phenomenon is just called a "pressure jump". Drifting snow is also always observed upstream of the jump, as the wind is strong. A simple theory derived from the hydraulic channel flow theory has been developed by Ball (1956), from which various characteristics of the flow can be predicted, including the conditions at a jump occurring as a transition from shooting to tranquil flow. By analogy with the hydraulic theory, the Loewe's phenomenon is then sometime called "hydraulic jump" or jump.

The IAGO (Interaction–Atmosphère–Glace–Océan) experiment was aimed at obtaining a detailed documentation of the vertical structure of the katabatic layer, and of its evolution along the slope. Two French and one American teams took simultaneous measurements of vertical profiles of atmospheric properties at three points (D57, D47 and D10) distributed over 200~km along the slope from the plateau, at about 2000~m height, toward the coast near the Dumont d'Urville (DDU) Station (Figure 6.6.13.1).
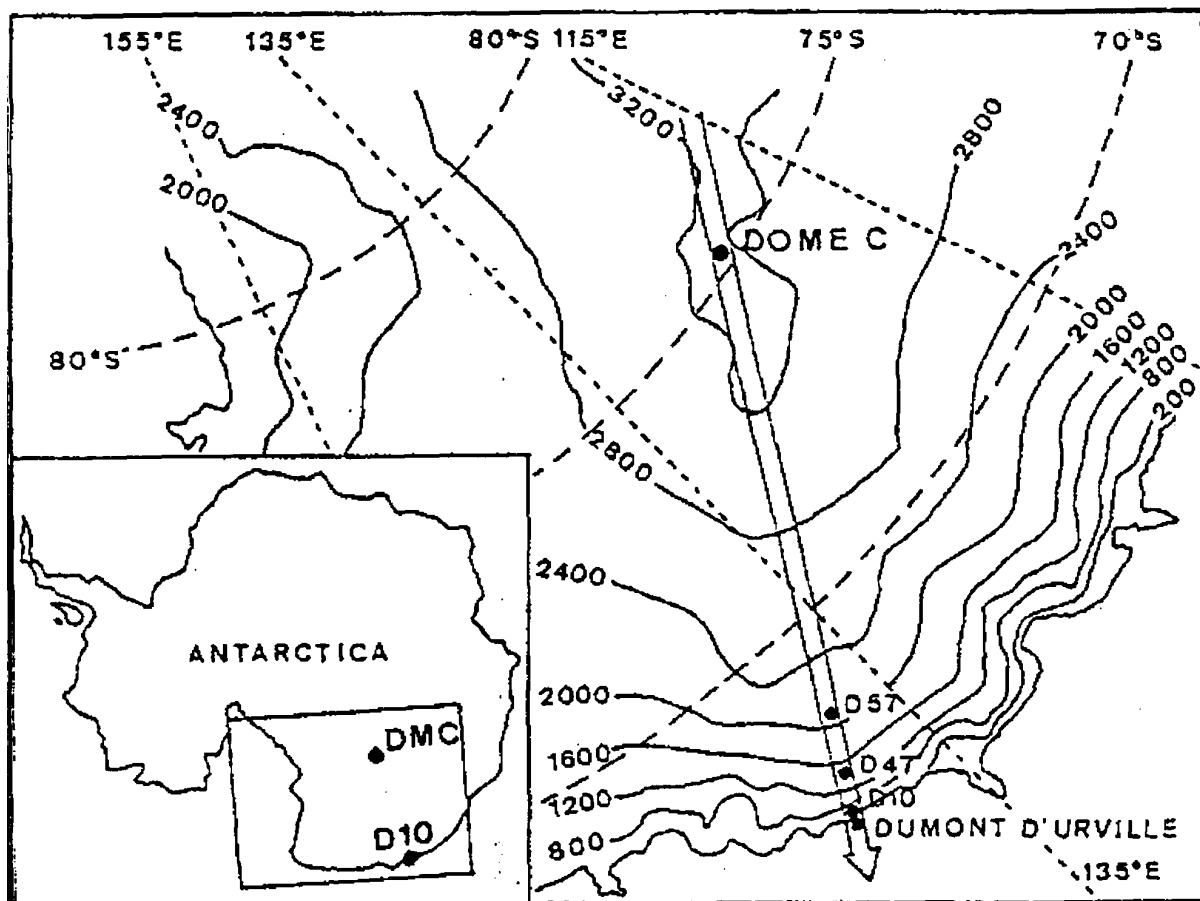
Figure 6.6.13.1   Map showing the locations of AWSs D 57, D 47 and D10 in relation to region Dumont d'Urville and Dome C.

During the IAGO–Experiment several Loewe's phenomena were observed as the terminal phase of several katabatic events. On 3 December 1985, a surprisingly large surface–pressure change (almost 6 hPa) through a jump was measured, differing very strongly from the predicted value (about 2 hPa) derived from the hydraulic theory. This case is not isolated, as

Lied (1964) reported similar observations (Lied measured 20 hPa through a jump on 12 August 1961, near Davis, Antarctica).

Although quite often quoted in reports from Antarctica explorers, relatively few Loewe's phenomena or jumps occurring through katabatic flows have been scientifically described. Obviously, Antarctica is not an ordinary experimental ground and, apart from the intense cold, the observation conditions of such phenomena are extremely severe. Nevertheless, these jumps can be considered as a common feature occurring in these regions.

Nevertheless, a typical evolution of katabatic events and of Loewe's phenomena can be drawn from the literature descriptions. The gravity flow is strengthened if the pressure in the air above the inversion decreases horizontally in the downslope direction, while it is weaker and can be completely stopped if the pressure in the overlying air increases instead. The formation of a jump happens just before a strong katabatic event and after the katabatic flow has persisted for several hours or days and generally marks the beginning and the end of the katabatic period. The jump can be defined as a narrow zone with large horizontal changes in wind speed, pressure and temperature, either stationary on the slope or slowly moving up or down. This zone separates between an upstream shallow, strong–wind layer, where the flow is said to be "shooting", and a downstream, deep, light–wind layer, where the flow is said to be "tranquil". A wall of snow often very clearly marks the downstream edge of the strong wind part of the flow.
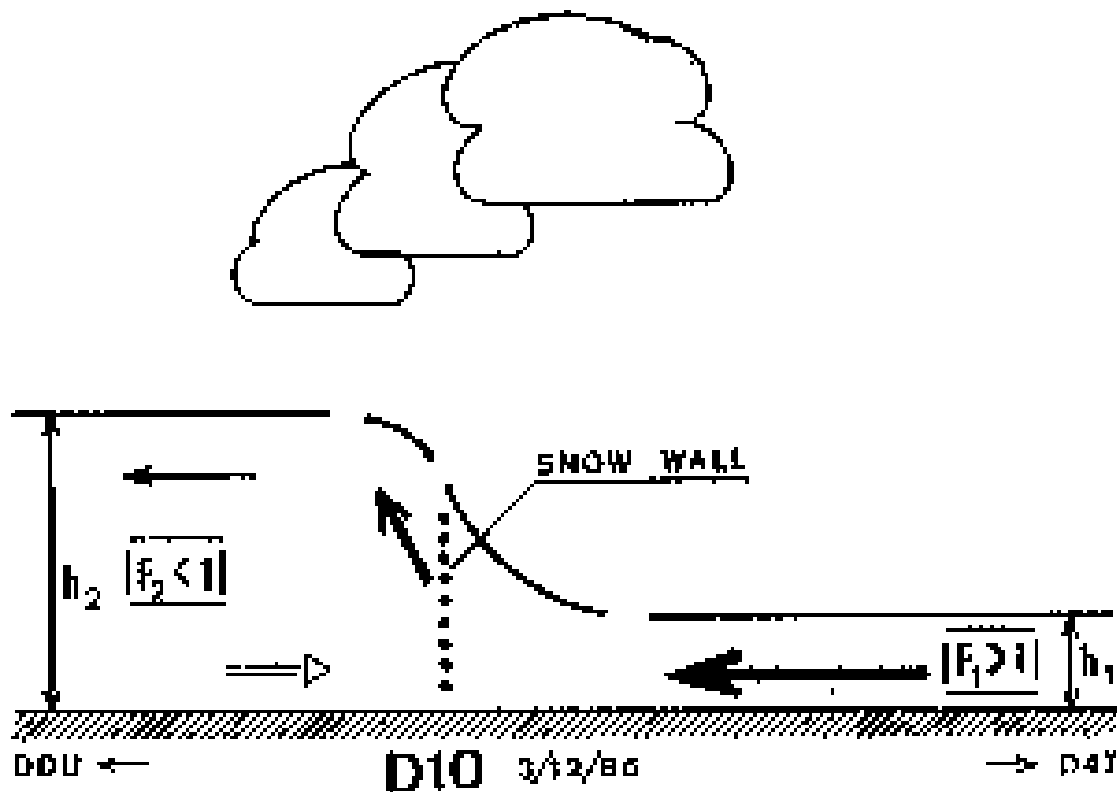
Figure 6.6.13.2   Sketch of the Loewe phenomenon which occurred on December 3, 1985, at D10 near Dumont d'Urville. (F represents the Froude number).

Figure 6.6.13.2 shows a schematic of the jump observed on December 3, 1985, at the D10 Station. A wind reversal was recorded just downstream of the wall of snow, which then

moved upslope after having passed the station. This reversal is possibly associated with a convergence effect and an updraft developing through the jump, marked by the formation of clouds situated just above, and moving with, the jump.
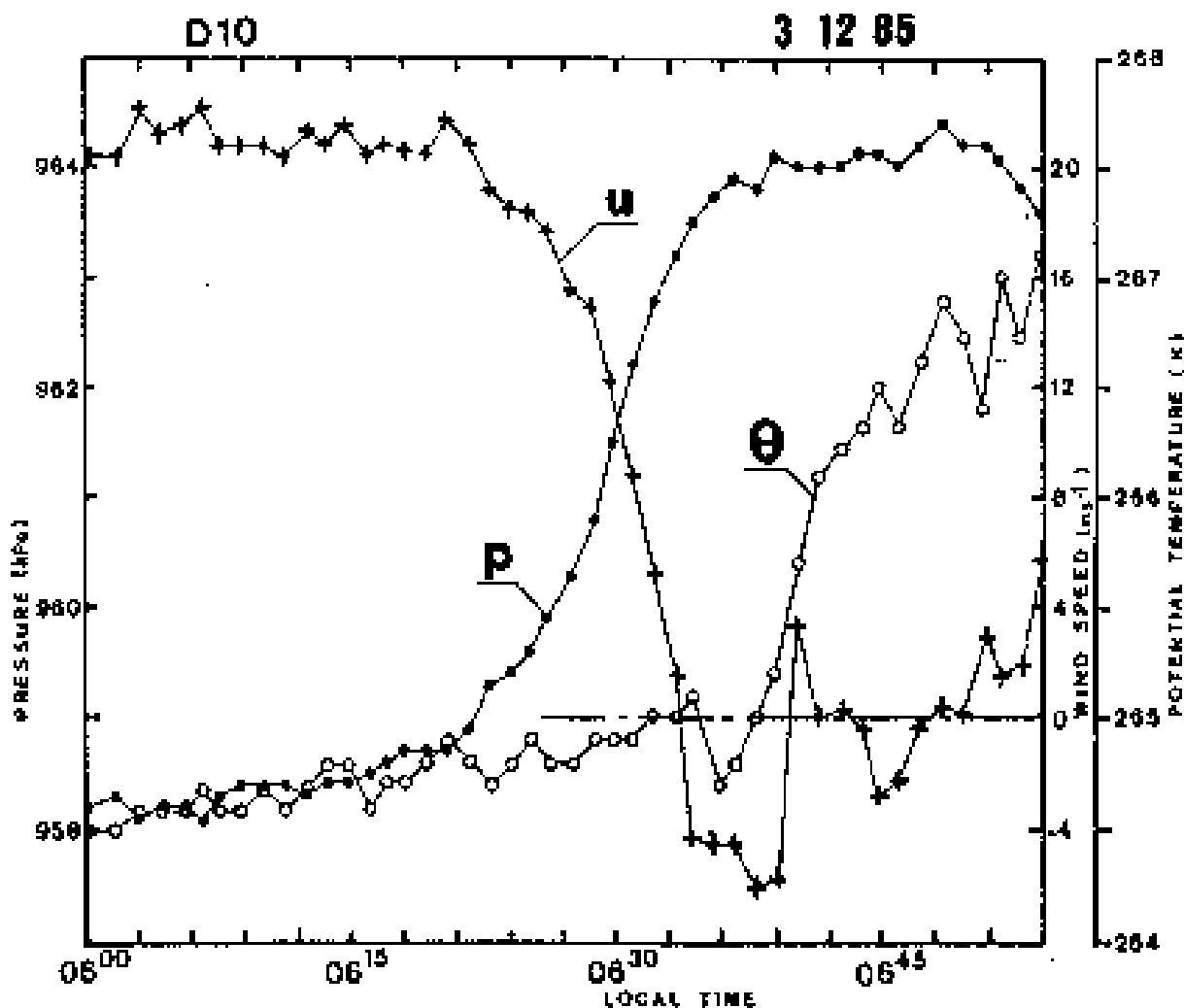
Figure 6.6.13.3 Surface measurements of pressure (solid circles), potential temperature (open circles), and downslope wind speed (crosses) as a function of local time during the phenomenon.

Figure 6.6.13.3 shows the surface measurements as the jump moved slowly upslope. The southerly surface wind suddenly dropped from 20 m s^{-1} to –5 m s^{-1} as pressure simultaneously increased from 958.5 hPa to 964.2 hPa. Some minutes later, potential temperature increased from 264.6º K to 267.0º K, probably due to turbulent mixing with upper–air associated with the jump.

Figure 6.6.13.4 shows the vertical profiles of the downslope component of the wind, before and after the jump, also interpreted as upstream and downstream conditions. The flow is vertically stratified from the surface upwards with:

- a cold–air surface–layer, either well–mixed or with a small Richardson number;

- • a very stable capping inversion layer;
- • an unstable layer thickening as the flow goes downstream;
- • a stable transition layer to the overlying free atmosphere.

The "katabatic layer" is composed of the well–mixed layer and of the capping inversion layer, where the maximum of wind speed is observed.
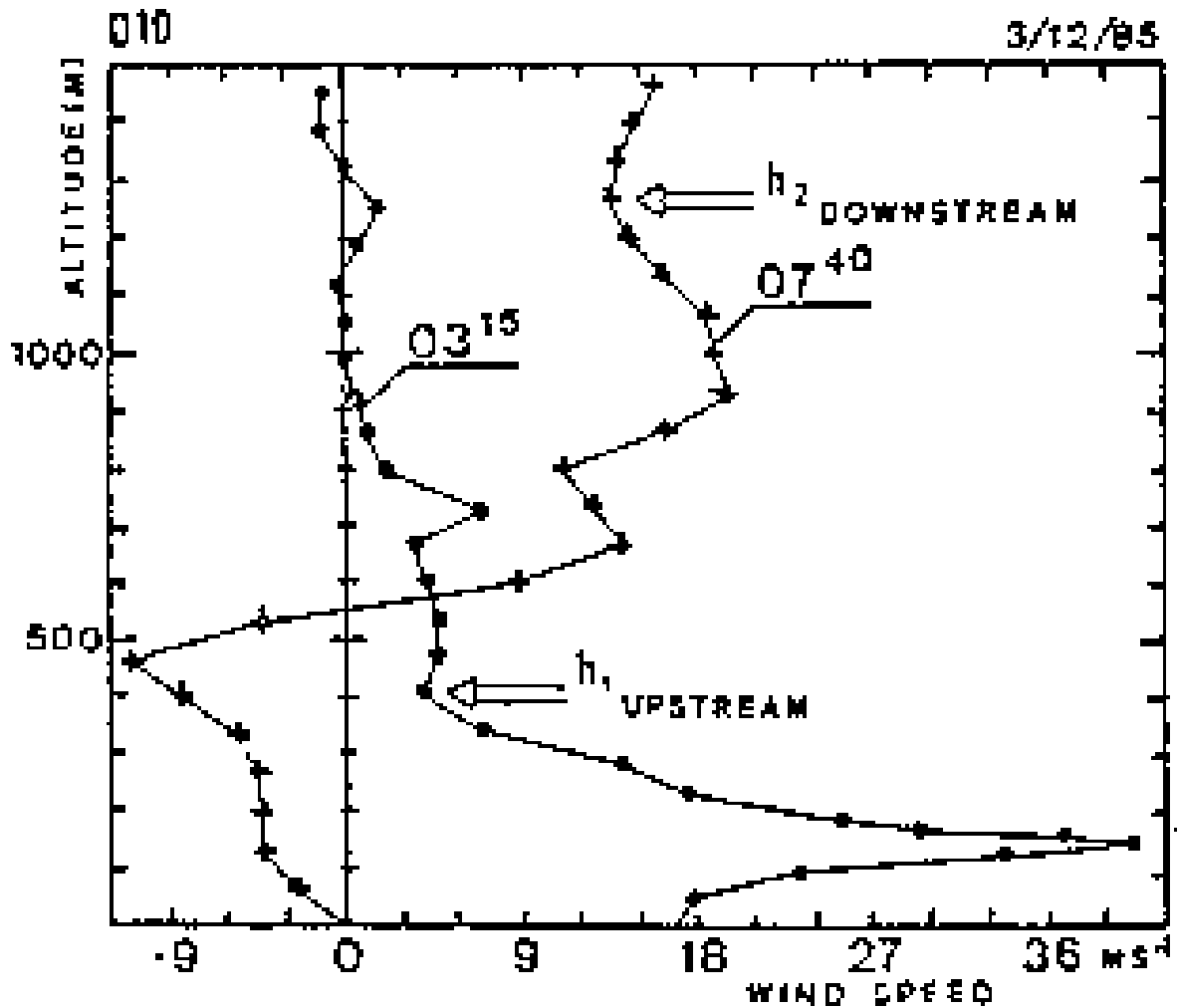
Figure 6.6.13.4 Vertical profiles of downslope wind at D10 before/upstream (0315 LT) and after/downstream (0740 LT) the December 3 jump.

6.6.13.1   Pressure change through Loewe's phenomena:

Even taking into account the perturbations associated with upstream blowing snow, the surface–pressure change mainly scales with the shear observed through the unstable layer overlying the katabatic layer. As always mentioned by people having observed Loewe's

phenomena, snow transported by strong katabatic flows can indeed be suspected to be an important factor contributing to this problem, and it can be argued safely that the largest surface–pressure changes are observed with blowing–snow conditions. An interpretation is that Antarctic katabatic flows are a perturbed state of the atmosphere, in which surface pressure is reduced in comparison to what it would be for unperturbed conditions, which are restored just downstream of the jumps whenever they occur. This reduction of pressure is mainly associated with the strong acceleration of the katabatic layer under the effect of gravity.

These conclusions are consistent with pressure changes associated with other observed Antarctic jumps. Thirty–one cases of standing katabatic jumps were reported and measured by Lied (1964) during 1961 on the slopes of the polar ice cap in Antarctica. Quoting Lied's words: "In most cases the pressure changed by 1 to 3 hPa through the jump, but on one occasion a mysteriously large change of nearly 20 hPa was measured". In fact, that surprisingly large change can be associated with a strong wind shear of 60 m s^{-1} (~ 115 kt) between the surface and the top of the well–mixed layer over the katabatic layer. Such a large pressure change is obviously exceptional, but still likely to happen considering the very strong winds occurring during katabatic events in Antarctica.

Such evidence for a layered structure of the upstream part of katabatic flows is an important feature for Antarctic katabatic flow modeling. Upstream of the jump, the vertical structure of the flow is relatively simple and exhibit, a four–layer structure, i.e. katabatic layer, inversion layer, overlying neutral or unstable layer, and above free flow. This makes it possible to use simplifying assumption, of the type used by Ball, and explains the success of Ball's hydraulic theory for describing strong katabatic flows. On the contrary, observations show that Loewe's phenomena have a frontal character and that downstream of them the flow loses its simple behaviour in such a manner that Ball's assumptions cannot be used any more, explaining then the failure of the hydraulic theory.

7   FORECASTING AT SPECIFIC LOCATIONS

7.1   The scope of this chapter

This section of the Handbook reports on the forecasting techniques, and experiences of many of the nations that provide forecasting services for stations or expeditions in the Antarctic and on the sub–Antarctic islands. Our goal has been to try and bring together local knowledge which will be of value to new forecasters joining a station and/or when forecasts have to be provided for unfamiliar areas.

In compiling the list of stations care was taken to obtain accurate data, however, there appear to be instances of conflicting information in the literature. Where data such as location, elevation and station activities were not obtained directly from a contributor of the country which operates a particular station, information was obtained from the Council of Managers of National Antarctic Programs (COMNAP) via http://www.comnap.aq.

Table 7.1.1 in Appendix 1 below is a comprehensive list of stations and AWSs in the Antarctic. The table, which is accompanied by maps showing the locations of the stations and AWS, shows the WMO number (or ARGOS number in the case of AWS reporting via the NOAA satellite system), location, elevation, name of the station or AWS, the country responsible for the station or AWS, and finally, the sub–section of this handbook where some aspects of the station are discussed. By clicking on the word "above" which is assigned to each station discussed (most of the AWSs are not discussed) the reader will be taken to the relevant section.

7.2   Representative sub–Antarctic Islands

7.2.1   The Falkland Islands

7.2.1.1   Orography and the local environment

The Falkland Islands are situated some 550 km due east of southern Argentina and are centred near 52º S, 59º W. Consisting of over 600 islands they extend some 220 km east–west and 140 km north–south. For the sake of convenience they are broadly split into West Falkland and East Falkland, separated by Falkland Sound. The area is a mixture of mountains and low moorland, and is heavily indented by sea lochs and inlets.

East Falkland is dominated by the Wickham Heights range of mountains which extend east–west across the whole of the area; there are many peaks above 400 m the highest being

Mount Usborne at 705 m. In the south, low moorland and numerous small lakes and ponds dominate the landscape.

West Falkland is generally mountainous with numerous broad valleys. There are many peaks above 400 m, the highest being Mount Robinson at 695 m. Throughout the Falkands, vegetation is mostly of white grass with areas of heather–like scrub. the mountains have large areas of bare rock.

There are numerous landing strips in the islands, but the two airports are both in East Falkland. Stanley airport, some 25 m above MSL, is situated at 51º 41´ S, 57º 46´ W. Mount Pleasant International Airport (MPIA), some 74 m above MSL, is situated at 51º 49´ S, 58º 27´ W.

7.2.1.2   Operational requirements and activities relevant to the forecasting process

The Meteorological Office's Forecasting Centre is located at MPIA (MPIAFC). The forecasting centre is staffed continuously and provides meteorological services for a wide range of activities across the Falkland Islands and more widely in the South Atlantic. Services include detailed forecasts for aircraft and ships operating out of the islands, together with general weather forecasts for the public at large as well as specialist advice for sheep farmers.

7.2.1.3   Data sources and services provided

MPIAFC is connected to the Meteorological Office's facilities at Bracknell, United Kingdom, via two satellite links. These provide routine synoptic and numerical weather prediction data as soft or hard copy and which are accessed through the recently developed NIMBUS visualisation system. NWP data are provided twice daily from The Meteorological Office's global model together with World Aviation Forecasting Centre (WAFC) products, wind wave and swell forecast data. Model data are available up to 120 h ahead. Access to the Internet is also available.

Hourly weather reports are made at MPIAFC, and at the automatic weather stations at Pebble Island, Sea Lion Island and Weddell Island. Upper–air soundings are made at MPIAFC daily at 0000 and 1200 UTC and often also at 0600 UTC and occasionally at 1800 UTC.

MPIAFC also has a satellite data reception facility which provides the downloading of line–of sight IR and visible data from NOAA polar orbiters from near 35º S to around 75º S, together with the capability to receive GOES and METEOSAT imagery. The overall coverage allows forecasters to analyse data on a fine scale, assess cloud top and sea surface temperatures, and determine the general distribution of the southern ocean sea ice in the sector from 20º W to 100º W.

7.2.1.4   Important weather phenomena and forecasting techniques used at MPIAFC

General overview

The overall weather factor at MPIA is very good and compares favourably with many northern and western parts of the United Kingdom. The weather regime in the Falkland Islands is influenced by the close proximity of the Andes to the west, the surrounding waters,

particularly the cold East Falkland current moving northwards, and the presence of the Antarctic Peninsula some 1100 km to the south. Locally the orography of the Falkland Islands, particularly the Wickham Heights, has a direct influence on wind and weather at MPIA. The predominant wind direction is westerly but the particular direction and speed on any given day will have a marked effect on the weather at MPIA. Depressions and their associated fronts frequently move east across the islands at speeds of at least 15 m s^{-1} (30 kt). Therefore frontal precipitation is relatively short–lived except when back–bent occlusions follow the preceding warm and cold frontal systems. Synoptic scale weather systems are usually well depicted on satellite imagery and are well handled by NWP model analyses.

Pacific depressions are usually held up near the Chilean coast with the Andes markedly modifying frontal structure, often leaving just cloud above around 12000 ft to move on eastwards. On a short sea track to the islands the dried out low level air produces little in the way of low cloud or precipitation at MPIA. However, a depression moving from central Argentina or from further north, and which tracks southeast towards the islands, will pick up moisture and, because of the longer time spent over the sea, extensive low cloud and precipitation are likely especially in northern parts of the islands. This will extend southwards depending on the particular track and other synoptic factors. Depressions forming near Cape Horn and tracking northeast are likely to have extensive cloud, and precipitation is likely. Dependent upon the season, and the exact track of the depression, precipitation may fall as snow even on low ground. To the rear of a v–shaped trough, or ahead of a depression tracking southeast but remaining to the north of the islands, low cloud is likely to become extensive at MPIA for a time.

Anticyclones and ridges of high pressure are usually associated with fair weather. However, when moving only slowly east and when an upstream warm frontal trough is developing and accelerating towards the Falkland Islands, this is likely to lead to very strong northerly winds especially at MPIA and lee wave activity or rotor streaming across the airfield. In winter these northerly winds are likely to advect low cloud and rain or drizzle across MPIA, but in summer cloud amounts are reduced through the effects of insolation, precipitation is unlikely in these situations unless there is medium level instability.

Surface wind and pressure field

The overall pressure distribution is routinely analysed from weather reports in the region, satellite imagery and NWP guidance; thus the general wind and pressure regime is well handled. The mean wind speed tends to be a little higher in summer than winter; nevertheless the maximum recorded gust at MPIA is less than 41 m s^{-1} (~80 kt). The effect of the Wickham Heights on a northerly airstream and an unstable south to southwesterly airstream require careful consideration, as do conditions likely to lead to the onset of sea breezes.

Northerly airstreams are generally stable, especially at the lower levels, and are generated most strongly between warm fronts to the northwest of the Falkland Islands and a slow–moving high–pressure system close to the east of the area. In addition, a low level inversion in the northerly flow increases the surface wind speed markedly at MPIA; nocturnal cooling will sharpen the inversion and hence strengthen the surface wind. When the height of the top of the inversion is close to that of Wickham Heights, northerly winds may become very strong and generate marked lee waves or rotor streaming at MPIA; this is closely linked to the degree of stability and low level wind structure. Sudden increases or decreases in wind speed, and/or in direction, are frequent in these synoptic occasions and often lead to severe low level turbulence at MPIA. This is difficult to forecast accurately but when the gradient wind speed is 20 m s^{-1} (~40 kt) or more, severe low level turbulence is likely; evidence of this can be seen on the anemogram and, when the air is sufficiently moist, by the presence of

cloud with ragged and rapidly changing edges. Sometimes such clouds can be seen to travel as slow–moving eddies over the aerodrome. With gradient wind speeds less than 15 m s^{-1} (~30 kt), the low level flow is more likely to be laminar and lee wave activity is likely to be evidenced either, by the familiar clouds, or a smooth top of low cloud spilling over Wickham Heights.

Unstable south–southwesterly airstreams are likely to produce sudden increases in wind speed associated with showers. Gusts may exceed the gradient wind speed.

Sea breezes can occur in summer under a slack pressure gradient; the wind may back to a south–southeasterly direction which, in early summer may lead to stratus being advected from the cold water offshore or developing over the warmer land surface.

Upper wind, temperature and humidity

The NWP model data are used for providing aviation forecasts and are adjusted as necessary through the analysis of sounding data and satellite imagery. The upper–air products include significant weather forecasts for aircraft operating in the region.

Cloud

The existence and nature of cloud is governed overall by the geographical location of the Falkland Islands and influenced by the proximity of the Wickham Heights to MPIA. Frontal cloud moving east across the Andes is strongly modified, the lowest layers often being completely dried out; as the low level frontal air approaches the Falklands its moisture content will have increased from travelling over the sea, nevertheless precipitation is likely to be slight. At MPIA the front may be dry with the lowest layers drying out again after crossing the islands, its passage being indicated by a shift in wind direction and the presence of cloud at medium or high levels.

Warm moist air moving south or southeast towards the colder waters of the Falklands is likely to produce a low level inversion, extensive low cloud, and sea fog and mist around the coasts. Windward coasts and upslopes will have very poor conditions with outbreaks of drizzle or rain. The resultant cloud effects of warm moist air advected south to MPIA are dependent on the particular wind direction and wind speed, together with the height of the inversion. If the wind is in the northwest quarter, MPIA is unlikely to have stratus below 200 m (~700 ft), but if the inversion is below 150 m (~500 ft) and the wind speed is at or above 15 m s^{-1} (~30 kt) then patches of low cloud below 150 m may affect the aerodrome. When the wind is in the northeast quarter, which is relatively infrequent, MPIA is very exposed to very low cloud developing as low as 60 m (~200 ft) and which, together with poor visibility and drizzle, will persist until the associated depression has moved away well to the east.

In a slack south–southwesterly airstream, upslope stratus down to 30 to 60 m (~100 to 200 ft) is likely to form from air stagnating over Lafonia and will cross the aerodrome; together with poor visibility this will persist until there is a shift in wind direction, although in summer cloud amounts should reduce through the effects of insolation.

Summer sea breezes may advect stratus from the adjacent cold waters towards MPIA, but it should disperse through insolation.

Wave clouds are common at MPIA in northwesterly wind regimes, both at relatively low and high levels, and are caused by stable air traversing the Wickham Heights and being induced to oscillate. Residual high level wave clouds from fronts moving over the Andes also can be observed occasionally at MPIA. Stratocumulus cloud in south–southwesterly

airstreams can also produce significant wave effects on the north side of the Wickham Heights and other mountains in the Falklands; short period oscillations with more than thirty waves in these types of airstreams have been observed from satellite imagery to have been set off by Wickham Heights.

Visibility: particularly precipitation and fog

Visibility in general is very good due to the lack of upstream or *in situ* sources of industrial pollution. However, haze, smoke from peat fires or volcanic ash from eruptions upwind, and precipitation, all reduce visibility to varying degrees. When the wind direction is in the northwest quarter and strong this is likely to lead in summer to haze caused by lifted dust from Patagonia.

Northerly airstreams, especially when slack, are likely to produce widespread mist or fog conditions particularly over coastal waters north of the islands and north–facing slopes and hills. MPIA is normally well sheltered from these effects, but if a slack low level flow veers to the northeast quarter then the aerodrome will be affected by poor visibility reducing to below 1000 m, especially if the fetch is persistent. A persistent south–southwesterly slack airstream is also likely to lead to poor visibility, or even fog, at the aerodrome due to the advection of moist air from Lafonia.

Radiation fog is rare at MPIA and is most likely to be caused indirectly through the advection of moist air stagnating or fog already formed over adjacent lakes.

Precipitation reduces visibility in the normal way but slight to moderate rain does not appear to lead to the same decrease as in the Northern Hemisphere; this may be due to the air being freer of pollution.

Surface contrast including white–out

No specific information on forecasting has been obtained.

Horizontal definition

No specific information on forecasting has been obtained.

Precipitation

Despite its maritime environment, rainfall in the Falkland Islands in general, and at MPIA in particular, is very low. The average annual rainfall at MPIA is around 625 mm but the station record began only in 1986. There is however a wide spread of variability with the driest month on record having less than 10 mm ranging to the wettest month recording over 120 mm. The maximum rainfall amount recorded in 24 h is over 35 mm.

As noted earlier frontal precipitation usually moves across the islands quickly so that it lasts normally no more than a maximum of two to three hours. However, a back bent occlusion of the preceding warm front will lead to heavier and more persistent precipitation particularly when the parent depression is slow–moving, or is still deepening.

Showers will occur in unstable south–southwesterly airstreams but usually move very quickly on the wind. In unstable airstreams cumulonimbus clouds, with tops no more than 1800 to 2400 m (~6000 to 8000 ft) in winter are frequent phenomena and often will produce locally heavy but short–lived showers of soft hail or snow.

Medium level instability in the form of altocumulus cloud may be detectable from satellite imagery, and is usually associated with northwesterlies with a source in South America. The associated showers are normally of soft hail or snow, but are usually short–lived.

The critical forecasting issue is whether winter precipitation will be of rain, rain and snow mixed, soft hail or snow. NWP model performance and experience point to the value of examining the 850 hPa wet bulb potential temperature (WBPT) fields together with the 1000–500–hPa thickness fields. When values of 1 to 2º C for the 850 hPa wet bulb potential temperature and 528 dm thickness values are expected then snow is more likely than not especially when ascent is forced over higher ground. Soft hail is likely if the instability extends to a depth of at least 6000 ft and local sounding data points to the instability being around 4ºC lower than the temperature indicated by the environmental lapse rate. Snow may be of granular or flake crystals, resulting in different effects in terms of whether it will lie on the ground or is blown around. Frontal snow from the northwest is unlikely to persist at MPIA before turning to rain. The exception is when a slow–moving depression passes close to the north of the Falkland Islands produces rain but this will turn to snow when there is cold undercutting air on its eastern and southern flanks. These occasions are rare but can produce very poor weather conditions and not only in terms of precipitation.

In winter it is quite common for stratocumulus cloud to be advected by a south–southwesterly airstream, and with cloud tops below 0ºC this will often produce slight or even moderate snow showers. These cloud sheets commonly follow as a ridge of high pressure moves east across the islands and thus cut off deeper convection.

Freezing rain or drizzle are rare phenomena in the Falkland Islands.

Temperature and chill factor

Temperatures are influenced by airmass characteristics, time of year, and wind direction. Recorded temperatures at MPIA range from a maximum of over 29ºC in summer to a minimum below –9ºC in winter. Temperature forecasts are required for a range of users and are predicted using techniques employed in many other forecast offices.

Underlining temperature levels in the Falkland Islands, is the constant chilling effect of the wind; this is calculated using standard techniques such as that derived by Steadman (for example, Steadman (1971)). Temperature chill factor forecasts are important not only for work outdoors but also for farmers in the sheep shearing season who, in addition, require the very significant effects of precipitation to be taken into account for sheep chill forecasts.

Icing

No specific information on forecasting has been obtained.

Turbulence

Turbulence predictions are provided on a regular basis in locally used forecasts. Whenever moderate or severe low level turbulence is expected to occur at MPIA, this is included in the routine issues of Terminal Aerodrome Forecasts (TAFs) for the aerodrome. Moderate or severe low level turbulence at the site is normally associated with a strong northerly airstream which has a marked inversion close to the height of the Wickham mountain range. Severe low turbulence occurs regularly at MPIA and can be detected through monitoring of the anemogram, and orographic cloud behaviour south of the mountains together with the varying orientation of windsocks at the aerodrome. Infrequently, the involuntary behaviour of birds in flight demonstrates the existence of sudden and strong downdraughts.

A south–southwest airstream advecting or generating a sheet of stratocumumlus across Wickham Heights may induce a low level and short period wave–train; there are few pilot reports of any associated turbulence. However, given the nature of orography of the Falkland Islands, turbulence is likely to be induced over and to the lee of high ground whenever the gradient speed is in excess of 15 m s^{-1} (~30 kt).

Hydraulic jumps

These are rare but can occur under the most severe rotor streaming events; on those occasions pressure changes as much as 3 hPa in ten minutes are possible. They are difficult to predict.

Sea ice

Falkland Island waters are not affected in general by sea ice. However, the MPIAFC monitors the extent of the sea ice and drifting icebergs associated with the Antarctic ice sheet through analysis of satellite imagery together with bulletins from specialist centres. The principal concern is the northern edge of the winter ice pack to the south and the distribution of icebergs in South Georgia waters.

Wind waves and swell

Forecasters at the MPIAFC provide forecasts for use in the Falkland Island waters which cover wind waves and swell. In the Falklands area the generation and decay of wind waves are very responsive to the wind strength, and can reach heights of 7 m (~23 ft) in a very short period of time. Swell is generally more modest, typically in the range 1 to 3 m (~3 to 10 ft) in height with a period frequently of around 10 seconds.

7.2.2   South Georgia

7.2.2.1   <u>Orography and the local environment</u>

South Georgia is situated some 1500 km east– southeast of the Falkland Islands and is centred near 54º S, 37º W. The island is south of the Antarctic Convergence Zone and lies within the maximum northern limit of sea ice associated with Antarctica. The island is around 150 km

long and roughly 30 km wide, and is orientated in a northwest–southeast direction. South Georgia has a few offshore islands but is treated here as a single land mass. It is composed mostly of steeply rising mountains and glaciers; the highest peak is Mount Paget at over 2960 m. The coastline is heavily indented with fjords and bays, the most sheltered of which are on the eastern coast. Vegetation is relatively sparse and limited to coastal fringes.

The administrative centre is at Grytviken on the east coast at the head of King Edward Cove which is an inlet from Cumberland East Bay. Nearby, at King Edward Point, synoptic observations are made several times each day.

7.2.2.2   Operational requirements and activities relevant to the forecasting process

Weather forecasts from the forecast centre in the Falkland Islands are provided in support of British military forces operating in the area.

7.2.2.3   Data sources and services provided

Surface observations are performed on South Georgia and the South African Weather Bureau operate an AWS (WMO No. 88986) on South Thule in the South Sandwich Island group.

There are no forecasting facilities on South Georgia. At the Mount Pleasant International Airport Forecasting Centre the forecasting area of responsibility and data coverage extends eastwards to include South Georgia and the South Sandwich Islands on a routine basis. Synoptic analyses, together with NWP model data and satellite imagery provide the basis for all forecasts required by personnel on the ground and British aircraft or ships in the area. Forecasts are sent via communications links with the Falkland Islands.

7.2.2.4   Important weather phenomena and forecasting techniques used at the location

General overview

Due to its location and terrain South Georgia experiences a wide range of frequently hostile weather. Prevailing winds blow from the west so that the western side of the island is particularly exposed to low cloud and severe weather conditions at all times of the year, whilst the sheltered eastern side may experience quiet and clear weather. Travelling depressions usually move east very quickly so that deteriorations in weather can be sudden; severe gales and blizzards can occur at any time of year. Depressions which engage relatively warm, low level air are likely to produce extensive low cloud, and fog, particularly when winds are light.

Sunny conditions occur most frequently on the eastern side of the island. However cloudy spells lasting several days are common across the island. Temperatures range from over 20ºC in sheltered low lying eastern areas in summer to well below –10ºC in winter.

Surface wind and the pressure field

Whenever a deep depression passes close to the island gales can be expected. The severity and direction may be markedly modified by the orography of the particular area of concern.

Local winds can be dominated by katabatic flow coming off adjacent glaciers, and thus may be contrary to the gradient direction and speed.

Katabatic winds occur in the King Edward Cove area. The predominant wind direction there is between north and west. Easterly winds are usually most common in association with a depression to the north or northeast of the island, and in general are less strong than westerlies.

Upper wind, temperature and humidity

NWP model data are used extensively for all forecasts for South Georgia. Forecast upper–air profiles are very useful tools, especially for predicting low level weather conditions important for aircraft and shipping operations. Satellite imagery interpretation provides crucial information to enhance short period model data.

Cloud

By virtue of its location, South Georgia lies close to the track of travelling depressions so the island is very exposed to cloudy systems. Warm air moving south towards the island is cooled at low levels as it travels over the cold waters; this results in extensive low cloud, and especially poor conditions when the surface gradient is northeasterly. South to southwesterly airstreams are cold and, travelling over an increasingly warm sea surface, often lead to the formation of extensive sheets of stratocumulus; on reaching the western coasts these cloud systems often thicken through forced ascent of high ground. However, the mountains act as a barrier to this direction of low level flow; satellite imagery frequently shows a dam effect with clear conditions on the eastern side of South Georgia, though cloud may spill around the extreme north and southern parts of the island.

Wave clouds are common phenomena. Satellite imagery shows wave clouds to be most frequent at or above 3000 m (~10000 ft). Occasionally, cirrus is generated by flow over the Mount Paget area, such that it appears as a long plume of dense cloud 100 km (~50 nm) or more in length with its forcing source clearly observed. Substantial wave–trains can also be induced by the South Georgia mountains, and satellite imagery shows there are occasions when there are wave–trains comprising twelve or more waves with a wavelength of around 30 km (~ 5 nm); this is close to the average width of the island.

The prediction of amounts and height of cloud is extremely difficult and forecasters rely heavily on satellite imagery and NWP model data.

Visibility: snow and fog

Visibility is governed by airmass considerations and geographical location. In active cloud systems, precipitation will reduce visibility in the normal way and, given that snow is the most common form of precipitation, this will be a frequent cause of very poor visibility. In areas sheltered from the prevailing wind, visibility is generally very good; it follows that the eastern side of the island often experiences these conditions.

Fog and poor airmass visibility arises most frequently when northeasterly winds advect moist air. Thus sea fog and hill fog can occur most readily on the eastern side of the island when it is exposed to this synoptic type.

Precipitation

Precipitation is highly variable in distribution because of the nature of the island's orography, but is most commonly of snow, though hail can occur in association with cumulonimbus clouds. Snowfall is often heavy, and frequently gives rise to blizzard conditions either from frontal systems or mesoscale features. The latter are always difficult to predict.

Temperature and chill factor

Temperatures recorded range from over 20ºC in sheltered eastern parts to extremely low values both there and elsewhere. Since most of the island is very mountainous and glaciers are numerous, frequently inland areas are likely to experience extremely low temperatures. Winds underline temperature values and will lead to dangerously low chill factors. There are no reliable methods of predicting temperatures and chill factors in South Georgia, but the Grytviken area provides perhaps one of the least hostile temperature environments due to its sheltered location.

Turbulence

Turbulence is a feature of the island, and its prediction is important for aviation forecasts. Moderate to severe turbulence may occur on the lee side of the island in an unstable airmass even when the surface gradient flow is no more than 13 m s^{-1} (~25 kt). However, a stable flow of 18 to 20 m s^{-1} (~35 to 40 kt) may not give rise to noticeable turbulence on the lee side. Forecasters rely heavily on NWP model data for assessing the airmass stability, which together with routine synoptic analysis, provide the most practical approach.

Hydraulic jumps

There is no information available on these phenomena, and it is not possible to determine their likelihood.

Sea ice

The waters surrounding South Georgia experience sea ice. In a severe winter the Antarctic ice pack may extend as far north as the island. However, the normal hazard facing shipping is one of drifting ice which has broken away from Antarctica or from the island's own glaciers. Icebergs drifting north towards the island are apparently generally largest to the west; however the eastern waters also have frequent icebergs, some of which may be large.

Forecasters rely on information from specialist ice centres and satellite imagery for determining the ice edge and the presence of any giant icebergs in the region.

Wind waves and swell

The region is very exposed to wind waves and swell but there are few observations. Both phenomena may produce mountainous seas. Forecasts of wind waves and swell are based on The UK Meteorological Office's global wave model products available to forecasters in the Falkland Islands.

7.2.3   **Gough Island**

7.2.3.1   Orography and Local Environment

Gough Island is located within the roaring forties and has a moist temperate climate. The island is orientated north–west to south–east and measures 73 km^2 in area (approximately 13 km long and 7 km at its widest). Due to the island's volcanic origin, the terrain is very rugged and rises steeply from the coast to a maximum height of 910 m (~3000 ft). Cliffs as high as 300 m (~1000 ft) and boulder beaches are found along the coastline, with few suitable spots for beaching boats. The meteorological station is located on the south–eastern portion of the island (40º 21´ S; 9º 53´ W, 54 m AMSL) and protected from the prevailing westerly wind and swell.

All climatic data provided in this section were obtained from the South African Weather Bureau climate archives for the period 1961 to 1990.

7.2.3.2   Operational Requirements

A relief vessel (SA *Agulhas*) brings fresh supplies to the base once a year (during September and October): 5-day forecasts of wind, weather, visibility and sea-state are provided for this vessel using NWP output from various models. Helicopters are used extensively to cargo sling supplies from the ship, while rafts are sometimes used to transport supplies to the coast where they are lifted ashore by a crane. The annual supply of diesel fuel is pumped ashore directly from the ship. All the aforementioned tasks are highly dependent on the weather and sea conditions in the vicinity of the base.

7.2.3.3   Data Sources and Services Provided

Dedicated forecasts are generally only issued during take–over and during voyages to and from the island. The forecasts are provided up to three days ahead to assist with the logistics and planning. When compiling a good forecast, an accurate surface analysis is crucial and surface charts for the southern Atlantic are analysed at six hour intervals. The surface pressure field is analysed using observations from land, ships and drifting weather buoys, as well as the UKMO "first guess" pressure fields and METEOSAT images. The METEOSAT imagery is particularly useful when determining the position of depressions and their corresponding

frontal systems. Surface winds are forecast using the UKMO prognostic winds out to 48 h; beyond this, winds are forecast using gradient winds inferred from the ECMWF prognostic surface pressure fields. Other forecast parameters include the expected weather and visibility. The 12–hourly ECMWF accumulated precipitation fields are used for determining the onset and duration of precipitation associated with depressions and frontal systems. *In situ* surface and upper–air data are available from the GTS and are taken into consideration when issuing short term forecasts. Sea conditions (swell period and height, as well as total sea) are forecast for days 1 and 2 using the UKMO swell model data available very 12 h (out to 120 h).

During the year several fishing vessels operate around the island, but use the high sea forecasts (available on the GTS) issued by the South African Weather Bureau.

There is also a Local User Terminal (LUT) for drifting buoy reception. Present communication limitations preclude the transfer of *raw* buoy data direct to Argos (the data processed on the island (and on Marion Island) are considered insufficiently reliable for direct inclusion on the GTS). The same equipment (there is an identical system on Marion Island) - is capable of receiving AVHRR imagery but unfortunately the limited communication bandwidth precludes its transmission to Pretoria.

7.2.3.4   Important Weather Phenomena and Forecasting Techniques

General overview

The weather is strongly influenced by the regular procession of depressions and frontal systems past the island. The formation, movement and decay of these systems are generally handled very well by the models, but due to their coarse resolution, the models can not take into account the significant impact the island's orography has on the local weather regimes. Weather conditions on Gough Island are notorious for changing rapidly and can vary significantly depending on one's location. This is particularly true for precipitation, cloud cover, wind and sea conditions. As a result, issuing forecasts for Gough Island is extremely difficult, especially if one is not familiar with the island. For the purpose of this section, we will assume the climate data and forecasting techniques are only valid for the base and Transvaal Bay where ships anchor during resupply operations.

Surface Pressure and Winds

Gough Island lies on the southern periphery of the sub–tropical high–pressure belt with a mean sea–level pressure of approximately 1015 hPa. The pressure, however, can vary over a wide range from 980 hPa to 1040 hPa.

Due to its sheltered location, winds on the south–east coast tend to be lower than over the open sea and exposed western parts of the island. The winds blow predominantly from the west, with gales observed on about 10% of days in winter and 5% in the summer. Gales at the base tend to blow from directions between north and south–west, i.e. anti–clockwise northerly through south–westerly. With the approach of each depression the wind follows a remarkably similar sequence. Ahead of the depression winds blow from the north–east or north and intensify. As the system moves closer, the winds continue to back and swing rapidly to westerly or south–westerly with the passage of the cold front. On occasions when depressions pass to the north of the island, the east coast can be buffeted by gale–force easterly or south–easterly winds.

When the wind has a westerly component, the model–derived winds are often too strong when applied to the east coast and should be used with caution. The station is relatively well exposed to winds from between north–easterly and south–easterly and under these conditions the model winds can be used with confidence. Model evaluations of the UKMO and ECMWF surface winds conducted by the authors during voyages through the South Atlantic indicate that the model winds display significant skill and can be used with confidence when forecasting winds.

A phenomenon unique to the east coast is the funneling of winds down the steep glens as strong westerly winds cross the interior. This funneling is clearly indicated by rotating columns of sea spray moving away from the coast in the vicinity of the glens: vortex shedding off the edge of major orographic features are probably also contributors to these effects.

Upper wind, temperature and humidity

No specific information on forecasting has been obtained.

Clouds

The island is often blanketed by cloud (especially on the windward slopes), with an average cloud cover of 6 oktas. The maximum cloud cover is generally observed in the late afternoon and evening. Cumulonimbus clouds are rarely observed at Gough Island, with stratocumulus, stratus and nimbostratus predominating. Warm fronts are associated with nimbostratus and stratus, with bases as low as 90 m (~300 ft). Cloud bases are higher behind cold fronts and on such occasions the clouds are typically towering cumulus, with bases higher than 450 m (~1500 ft).

Visibility: fog

The annual variation in the occurrence of fog is summarized in Table 7.2.3.4.1 in Appendix 2 below. Fog occurs most frequently during the second half of summer and early autumn (January–April), with an average of 23 days being reported at the station annually. Weak winds from the north–eastern quadrant or stagnant airflow within a moist airmass (such as in the warm sector of slow–moving depressions) are conducive for the formation of fog.

Precipitation

The precipitation statistics are summarized in Table 7.2.3.4.2 in Appendix 2 below. The meteorological station receives an average of 3154 mm of rain annually, with precipitation (>0.1 mm) observed on 293 days. July is the wettest month with an average of 28.8 days of rain, while February is the driest with 19.3 days. Snow is observed on an average of 8 days per year, and is most common between July and September. Ice pellets are frequently observed during cold outbreaks. Thunderstorms are observed an average of only 3 times per year and are most likely in May.

During the passage of frontal systems (associated with a well–defined upper–low), torrential rain (in excess of 100 mm) is possible in 24 h. It is very likely that these amounts could be substantially higher on the western side of the island and over the interior.

Temperature

The temperature statistics are summarized in Table 7.2.3.4.3 in Appendix 2 below. Temperatures at the station are mild, with a mean annual temperature of 11.7ºC and wind chill is rarely a concern when issuing forecasts. Temperatures below 0ºC have only been recorded in July and August. There is a marked seasonal variation in the mean monthly temperature, with the warmest temperatures occurring in February (14.5ºC) and the coldest in August (8.9ºC).

Wind Waves and Swell

Due to the location of the station, issuing forecasts for swell and total sea is problematic. Transvaal Bay is generally sheltered from the westerly and north–westerly swells, but any swells having a southerly component are likely to influence the conditions within the bay. The worst sea conditions are observed when the swell is running between north–easterly and south–easterly. During the winter months, 8–10 m (~26–33 ft) swells with an easterly component are occasionally observed, with swells of 4–5 m (~13–16 ft) occurring frequently. During the summer, conditions are more settled, but large south–westerly or southerly swells generated by systems far to the south occasionally reach the island.

Evaluations of the UKMO swell model have revealed that where actual wave measurements have been available, the UKMO model is seen to predict total sea (i.e. the combined effect of wind and swell waves) relatively accurately. This model, however, tends to keep the total wave energy for too long in the *wind wave component* - i.e. it will predict extreme wind waves even well after the predicted wind has dropped and a heavy swell has moved into the area. This distinction between sea and swell is important when one is trying to predict vessel motion during off-loading - or, where relevant, the likelihood of a northerly swell, needed to break up the pack ice.

7.2.4   Bouvetoya

Bouvetoya (54º 24' S, 3º 25' E), formerly known as Bouvet Island is the southern–most island of the mid–Atlantic Ridge and consists of a single volcanic cone with a wide indented crater and attaining an elevation of 780 m (2,560 ft) at Olav Peak at the centre of the island. The area of the island is 54 km^2. It was placed under Norwegian sovereignty by a Norwegian Royal Decree of 23 January 1928.

The slopes of the central cone terminate on all sides in precipitous cliffs or glaciers, descending abruptly to sea level. Glaciers cover 93% of the island and prevent landings on the south and east coasts, while steep cliffs as high as 490 m block access to the north, west and southwest.

Bouvetoya is the most isolated island on earth. The nearest substantial land mass is more than 1600 km away. And as the island is rarely visited and relevant forecasting

information unavailable the normal format used for describing other stations in this handbook has not been followed. Reference to the island is included purely because of its isolation. However, it should be noted that being so isolated the AWS on Bouvet provides a very important sea level pressure observation for input into global models. The area to the west of the island is a preferred area for explosive cyclogenesis which is largely responsible for the more severe sea/swell events in this portion of the Southern Ocean.

7.2.5   Marion Island

7.2.5.1   Orography and the local environment

Marion Island is one of the Prince Edward Islands, a pair of islands that are under the sovereignty of the Republic of South Africa. These islands are the peaks of a submerged volcano and are separated from each other by 17 km. Prince Edward Island, the more northeastern of the pair, has an area of about 100 km^2; Marion Island has an area of 210 km^2 and rises to an elevation of 1,186 m (3,890 ft) at Jan Smuts Peak.

Marion Island is bounded by rocky cliffs that are, in general, low, on the east side and high on the west side. At the northeast end Transvaal Cove is the site of the meteorological station and depot (46º 53' S, 37º 52' E; 20 m AMSL).

7.2.5.2   Operational requirements and activities relevant to the forecasting process

The station on Marion Island opened on 29 December 1947 and now supports a maximum of 24 people over the summer and an average of 12 people during winter. The following science activities are carried out on the island:

- environmental monitoring (since 1996);
- meteorological observations (since 1947);
- offshore marine biology (since 1982);
- onshore geology/geophysics (since 1965);
- terrestrial biology (since 1965).

To support these activities there are only one or two ship visits per season with no intercontinental flights possible. On the island there are around 10 helicopter flights per season. Use of wheeled vehicles is not possible on the mire conditions on the island. An outboard Zodiac is ship–based and used only during the re–supply period in April/May.

7.2.5.3   Data sources and services provided

Meteorological observations have been made on a regular basis at Marion Island since 1947. There is also a LUT for drifting buoy reception. Present communication limitations preclude the transfer of *raw* buoy data direct to Argos (the data processed on the island (and on Gough Island) are considered insufficiently reliable for direct inclusion on the GTS). The same

equipment (there is an identical system on Gough Island) - is capable of receiving AVHRR imagery but unfortunately the limited communication bandwidth precludes its transmission to Pretoria.

7.2.5.4   Important weather phenomena and forecasting techniques used at the location

General overview

The weather is generally cloudy or dull with rain or snow on most days of the year. Snow occurs in all months; varying from 2 days per month in summer to 10 days in winter. In summer the snow line varies from 300 to 900 m. Fog and very low cloud are rather common, especially on the west coasts from February to April but the frequency decreases to about three days per month for the rest of the year.

Annual means for Marion Island are: pressure 1007 hPa, temperature maximum 8ºC minimum 3ºC , wind 9 m s^{-1} (18 kt), rain–days 305.

Surface wind and the pressure field

No specific information on forecasting has been obtained on forecasting procedures. It is likely that conventional forecasting methods for mid–latitude meteorology would apply.

Upper wind, temperature and humidity

No specific information on forecasting has been obtained on forecasting procedures. It is likely that conventional forecasting methods for mid–latitude meteorology would apply.

Clouds

No specific information on forecasting has been obtained on forecast procedures but it is noted that low cloud is common. It is likely that conventional forecasting methods for mid–latitude meteorology would apply.

Visibility: precipitation and fog

No specific information on forecasting has been obtained on forecast procedures but it is noted that fog is common.

Surface contrast including white–out

No specific information on forecasting has been obtained on forecast procedures. It is noted that even in summer the snow line may be as low as 300 m and so there may be some instances where white out and surface contrast may be a problem.

Horizontal definition

No specific information available on forecast procedures.

Precipitation

Temperature and chill factor

No specific information available on forecast procedures.

Icing

No specific information available on forecast procedures.

Turbulence

No specific information available, although being in the belt of strong westerlies lee wave and mechanical turbulence should be considered.

Hydraulic jumps

Hydraulic jumps are unlikely at this location.

Sea ice

Not relevant at this location.

Wind waves and swell

No specific information on forecasting has been obtained although the numerical wave output from NWP models should be of some assistance.

7.2.6   Crozet Islands

7.2.6.1   Orography and the local environment

The Crozet Archipelago extends between the longitudes of 50º E and 53º E at a latitude of 46º S. The volcanic islands splits into two groups 100 km apart. Possession Island has an area of about 150 km². The highest point is called Pic du Mascarin and reaches 934 m (~3,060 ft).

The permanent base lies on the eastern side of a plateau at an elevation of 140 m (~450 ft).

7.2.6.2   Operational requirements and activities relevant to the forecasting process

None.

7.2.6.3   Data sources and services provided

Meteorological observations have been made on a regular basis at Crozet since 1973.

7.2.6.4   Important weather phenomena and forecasting techniques used at the location

General overview

The climate of Crozet Island is of a cold oceanic type being windy and very wet (see Tables 7.2.6.4.1 and 7.2.6.4.3 in Appendix 2 below). The precipitation is the most remarkable meteorological element; the number of days with more than 10 mm of precipitation varies between five in February and nine in August; the mean number of days in the year above this threshold is 86.

The prevailing wind direction is 220 to 340 degrees, which accounts for 75% of the observations. This percentage reaches 85% for average wind speeds greater than or equal to 16 m s^{-1} (~ 1 kt), which are observed for 317 days a year on average. Those reaching 24 m s^{-1} (47 kt) are also frequent (194 days on average) with a minimum of 10 days in February and a maximum of 20 days between June and September.

At mid–latitudes in the Indian ocean, depressions and ridges track from the west and cross the Crozet Islands and the Kerguelen Islands area. This flow regime is interrupted two or three times each month by high–pressure centres located close to the Crozet Islands.

The lows (about 10 per month on average) affecting the Crozet Islands come from:
- The Atlantic Ocean (about 50% of the systems). They appear not to be very active at Crozet. Despite the fact that they are located south of 50º S, they can lead to a strengthening of westerly winds
- The area between South Africa and Crozet (30 to 40% of lows)
- The remainder coming from the Indian Ocean south of 50º S.

Surface wind and the pressure field

Table 7.2.6.4.1 in Appendix 2 below shows monthly average wind speeds while Table 7.2.6.4.2 (also in Appendix 2 below) shows monthly mean surface pressure at Crozet. Surface values of air pressure higher than 1025 hPa are recorded every month, but the highest pressures occur in winter (the highest value measured was 1040.4 hPa).

Low–pressure systems generally do not cause the air pressure at Crozet to fall below 990 hPa. Rapid deepenings (40 to 50 hPa in 24h), as well as deep low–pressure systems, are not common (less than 10 instances per year on average, mainly between April and January (the lowest pressure recorded was 959.8 hPa).

High–pressure systems centred between 25°S and 35°S move eastwards from the Atlantic Ocean to over the Indian Ocean and the following behaviour has been noted:

- Sometimes an area of high pressure slows down at it moves eastwards and then strengthens between 40° E and 60° E.
- But sometimes a situation evolves in the following way. From a quasi-stationary anticyclone, located west of South Africa, a ridge of high pressure, generally located around 35° S, progressively extends to the Indian Ocean. In the eastern part of this high–pressure system a new anticyclone builds and can remain stationary for several days in the area between 30º S–40º S (or even further south) and 30º E–40º E.
- In summer, slow, eastward–moving anticyclones strengthen in the centre of the Indian Ocean and radiate towards the south (over the Kerguelen Island' area) or southeast (over the Crozet Islands' area.

When an anticyclone is located north of Crozet Islands the following situation occurs frequently. The cold front, associated with a low located southeast of Kerguelen Island, exhibits a strong cyclonic curvature on its leading edge and is orientated zonally south of the anticyclone, at mid–latitudes between 70°E and 40º E.)The front might then extend towards the northwest (South Africa)). In this situation the weather at Crozet can remain mild and rainy for up to 48 h with a mean westerly wind that can reach 20 m s^{-1} (~40 kt).Often a wave forms in the frontal cloud band , very close to Crozet, and the precipitation increases. At Kerguelen when the cold front has passed the weather becomes variable with westerly winds and showers.

When an anticyclone is centred close to Crozet Islands it splits the sub–Antarctic area into two zones.

- A southwest to southerly flow affects Kerguelen Islands with numerous snow showers.
- The areas just west of Crozet in the meantime benefit from an advection of warm and humid air, which has been cooled by tracking over a colder sea and characterised by advection fog and low clouds. Depressions coming from the west come up against high pressure and are deviated towards the southeast leading to the formation of a zone of strong pressure gradient, which induces strong wind gusts from the northwest to north at Crozet. It is then common to measure a mean wind speed reaching 20–25 m s^{-1} (~40–50 kt) with gusts over 40 m s^{-1} (~80 kt) from the northwest during a 12 to 24 h period, followed by weak wind from the southwest behind the depression. With a westerly flow the wind speed can be of the same order in the northwest and southwest sectors.

Different types of evolution follow this:

- The anticyclonic system shifts either towards the northeast or slowly towards the south: the westerly airflow therefore lies temporarily north of 50º S and at high latitudes the anticyclone can remain several days.
- Another type of evolution involves a shifting of the high–pressure centre

towards the east with, most frequently, a weakening of the centre.

Upper wind, temperature and humidity

No specific information on forecasting has been obtained.

Clouds

Average cloudiness is high throughout the year. Mean cloud cover is rarely lower than 2 oktas.

Visibility: blowing snow and fog

Fog is frequent at Crozet with 6–9 occurrences per month. Fog is most frequent in summer when it's frequently the base of clouds, which lower beneath the altitude of the station when storms are passing.

Surface contrast including white–out

No specific information on forecasting has been obtained.

Horizontal definition

No specific information on forecasting has been obtained.

Precipitation

Table 7.2.6.4.3 in Appendix 2 below shows the mean monthly precipitation amounts for Crozet. The monthly mean number of days of precipitation varies between 27 and 29, except for January (25) and February (22). On average 97 days with solid precipitation are recorded each year. Solid precipitation is highly likely throughout the year and a third of the precipitation events are a result of southwesterly showery airstreams behind lows.
     Satellite imagery shows that the cloudy systems which form over the Indian Ocean, west of Crozet, are large and their cold fronts sometime extend up to 20º S. Images show large cloud bands which possibly merge with groups of convective clouds or even tropical cyclones in their declining stages. The maximum amount of precipitation measured in 24 h varies between 50–70 mm, except in February, March and April when they are between 84–102 mm.

Temperature and chill factor

Table 7.2.6.4.4 in Appendix 2 below shows the mean monthly temperature at Crozet. There are, on average, 66 days of frost occurring between April and October. The temperature has varied between an extreme high of 23.1ºC to the lowest on record of –5.4 ºC.

Icing

No specific information on forecasting has been obtained.

Turbulence

No specific information on forecasting has been obtained.

Hydraulic jumps

Hydraulic jumps have not been observed in this area.

Sea ice

Sea ice is not relevant to this area.

Wind waves and swell

No specific information on forecasting has been obtained.

7.2.7   **Kerguelen Islands**

7.2.7.1   <u>Orography and the local environment</u>

The Kerguelen archipelago is located at 49º S, 70º E and is dominated by the main island, the island of Grande Terre, which has a very broken coastline, composed of numerous peninsula and fjords, extending a considerable way inland. The main island is surrounded by about 300 smaller islands. The surface area is about 7,000 km². The Cook Ice Cap extends across the western part and is reminiscent of a giant Quaternary ice sheet, with a dome reaching 1,040 m (~3400 ft) elevation. Mt. Ross, in the southern part of the island, reaches 1,850 m (~6070 ft). The permanent station, Port aux Français, is situated in the lee of the highest part of the orography, where the land is flatter.

7.2.7.2   Operational requirements and activities relevant to the forecasting process

No specific information has been obtained.

7.2.7.3   Data sources and services provided

Meteorological observations and radiosonde launches have been carried out at Kerguelen since 1951.

7.2.7.4   Important weather phenomena and forecasting techniques used at the location

General overview

Located 1,300 km east-southeast of the Crozet Islands, the Kerguelen archipelago has a windy oceanic climate, but it is slightly colder, and more importantly, drier than Crozet. The temperature variability from the long term mean is smallest in the summer, and has a maximum in June (1.6^{o}C), when there 19 days of frost, compared to 5 days at Crozet.

Surface wind and the pressure field

The prevailing direction at Kerguelen is between southwest and northwest in 80% of cases. Easterlies, on the other hand represent less than 5% of observations. The windy nature of the climate may be seen from Table 7.2.7.4.1 in Appendix 2 below where the mean annual wind speed is reported as 9.8 m s^{-1} (~19 kt). Wind speeds greater or equal to 16 m s^{-1} (~31 kt) occur on 300 days per year while speeds greater or equal to 28 ms^{-1} (~ 54 kt) occur on around 82 days per year.
     The general westerlies are interrupted during short blocking periods by high–pressure systems that may reach 1010 hPa in winter and 1025 hPa in summer. The variability in the pressure fields is discussed in the similar section on Crozet Islands above. Table 7.2.7.4.2 in Appendix 2 below shows the variation in mean monthly surface air pressure at Kerguelen.

Upper wind, temperature and humidity

No specific information on forecasting has been obtained.

Clouds

The mean cloud cover is 6 oktas but is not representative of the cloud experienced by the whole of the Kerguelen Archipelago. This is because of the Foehn winds experienced.

Visibility

The mean visibility, excluding all precipitation events, is rarely less than 30 km.

Surface contrast including white–out

No specific information on forecasting has been obtained.

Horizontal definition

No specific information on forecasting has been obtained.

Precipitation

Table 7.2.7.4.3 in Appendix 2 below shows the mean monthly precipitation totals for Kerguelen. Precipitation occurs on an average of 285 days per year, of which 23 have a total of greater than 10 mm. 103 days of snowfall are recorded for the year. Precipitation is more important on the west coast, however, the accumulation difference between Crozet and Kerguelen is important. This difference comes from the fact that advected air masses of hot and tropical origin are transported directly to Crozet, but appear indirectly at Kerguelen via a southwesterly direction. Satellite imagery allows the identification of rapidly occluding depressions during their eastward passage. When they reach the Kerguelen Island area depressions are often mature and the warm sector is then of quite limited extent and the cold front is only a narrow cloud band.

Temperature and chill factor

The average annual temperature on Kerguelen is 4.5ºC (Table 7.2.7.4.4 in Appendix 2 below). The absolute temperature extremes recorded are +23.0° C and –9.4° C. There are 116 frost days on average per year, and five days per year, on average, when the temperature does not rise above freezing point.

Icing

No specific information on forecasting has been obtained.

Turbulence

No specific information on forecasting has been obtained.

Hydraulic jumps

No specific information on forecasting has been obtained.

Sea ice

No specific information on forecasting has been obtained.

Wind waves and swell

No specific information on forecasting has been obtained.

7.2.8   Heard and McDonald Islands

7.2.8.1   <u>Orography and the local environment</u>

Heard Island is roughly circular in shape and slopes steeply upward forming an impressive and almost symmetrical mountain known as "Big Ben" at a general height of between 2,200 to 2,400 m (~7,200–7,800 ft). The mountain is of volcanic origin, and a number of cones, the highest Mawson Peak 2,827 m (~9,274 ft), project above the general level of the old crater. Subdued volcanic activity still persists and smoke and steam have been noticed issuing from fissures in Mawson Peak on many occasions. At the north end of the island, Laurens Peninsula and Rogers Head Peninsula are connected to the main body of the island by a low–lying sandy isthmus. A long narrow sand and boulder spit at the southeast end of the island extends seawards for about 6 km, ending in shoal waters. Permanent ice covers most of the island, and glaciers, descending to the sea on all sides of Big Ben, terminate in ice cliffs from 15 to 30 m high. The northern limit of the Antarctic pack–ice lies to the south of Heard Island but, during calm weather in winter pan–cake ice has been observed in Atlas Cove.

The McDonald Island group (53º 3' S, 72º 35' E), lie 37 km west–southwest of Heard Island. There are three islands in the group: McDonald Island, Flat Island, and Meyer Rock.

7.2.8.2   <u>Operational requirements and activities relevant to the forecasting process</u>

An Australian National Antarctic Research Expedition station was set up on 11 December 1947 on the Rogers Head Peninsula near the shores of Atlas Cove (53º 01' S, 72º 23' E), and operated continuously up to 1954. Synoptic observations are archived from 1 February 1948.

In more recent times there have been occasional visits for scientific work. Much of the forecast information presented here comes from an expedition held in 1980.

7.2.8.3   Data sources and services provided

Australia operates two AWS on Heard Island, one (WMO 94997) is at "The Spit" at 53º 06´ 24″ S, 73º 43´ 15″ E, at an elevation of 12 m, the other (WMO 95997) is in Atlas Cove at 53º 01´ 12″ S, 73º 23´ 24″ E, at an elevation of 3 m. Forecasting for ANARE voyages often depends on the nature of activities being undertaken, and may range from not being needed, to being provided by ship–based forecasters, or from one of Casey or Davis (if there are forecasters on station) or from Hobart, Australia.

Heard Island, Big Ben – Australian Antarctic Division photo by A.J.Graff
ⓔ Commonwealth of Australia. May be reproduced only for non-commercial educational purposes.

Figure 7.2.8.1.1   Big Ben, Heard Island.

7.2.8.4   Important weather phenomena and forecasting techniques used at the location

General overview

Table 7.2.8.4.1 in Appendix 2 below gives climate statistics for Heard Island.

Gales are frequent in all seasons and arise with astonishing rapidity. They are generally westerly, but gales from the east and north are not uncommon. Shaw (1955) has considered the representativeness of wind observations from Heard Island for broad–scaleanalysis.

Gradient winds from east–southeast to southeast observed at the station are poorly correlated with the synoptic pressure gradient.

"Big Ben" acts as a conical obstruction to the wind flow. Loewe and Radok (1955) reported on persistent downstream lenticular clouds from 700 to 7,000 m on an otherwise cloudless day of anticyclonic weather.

Cloud photographs often show lee waves and wave vortex streets near Heard Island. Brighton (1978) provided a model for strongly stratified flow past a cone with downstream waves, cowhorn eddy and vortex streets which might be applicable. So frequently is the island obscured by cloud that the first view of it from an approaching ship is of forbidding cliffs or abrupt headlands looming out of the mist. On occasions, however the icy summit of the island is visible, rising above the low cloud, from the immense distances. Big Ben's dome seems to float in the sky above the horizontal murk, making one of the most dramatic sights of the stormy southern ocean.
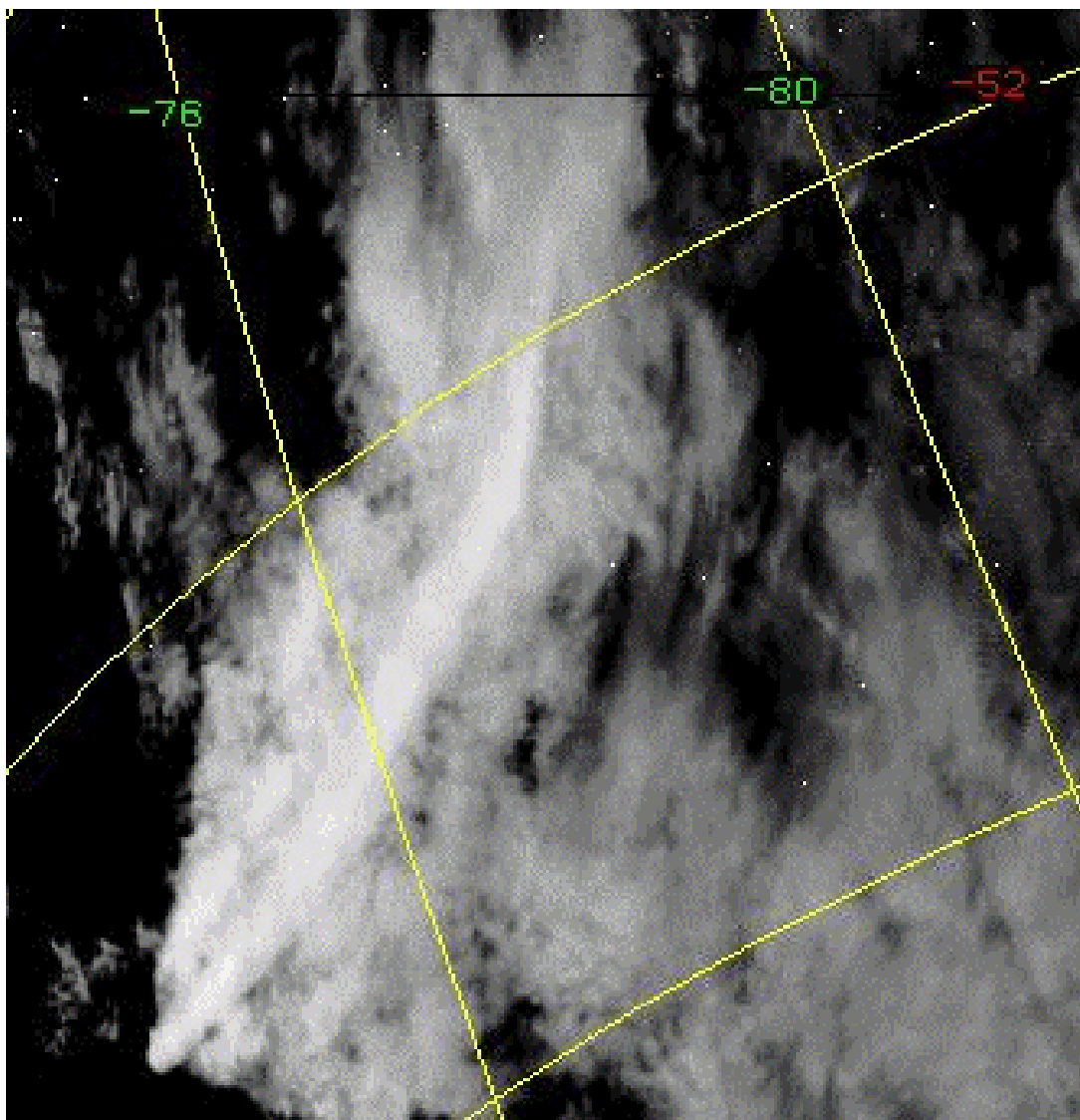
Figure 7.2.8.4.1 Banner cloud streaming from Big Ben on Heard Island.

Surface wind and the pressure field

The two main windy areas in westerly air streams are:

- firstly, the north side of the island, (the Compton and Brown Glaciers and Skua Beach area) is undoubtedly the windiest area of all with a combination of very strong squalls and a steady blast running down the mountainside and several kilometres out to sea to the northeast. These winds are turbulent and exceed 50 m s^{-1} (~100 kt) fairly frequently.
- secondly, the Fifty–one Glacier, Lambeth Bluff and Cape Lockyer area to the east of Long Beach has frequent strong winds, and being close to the cliffs, turbulent winds often above 25 m s^{-1} (~50 kt). These winds appear to sweep down the Fifty–one Glacier and divert easterly along the coast to Winston Lagoon. In the beach area blowing sand can be quite painful to the traveler.
- a third area, which also shows a great deal of squally weather is Atlas Cove. The cove is frequently whipped up by squalls descending the cliffs of the Laurens Peninsula and sweeping across the inlet of Walrus Beach. Fortunately, the full strength of these squalls rarely hits the station but when they do they can be quite devastating. Wind generated cracking and booming was reported in the Jacka Valley.

It has been often found that areas at the western end of the Laurens Peninsula (Macey Cone etc.) and the coast of the main island between the Vahsel Glacier round to Long Beach would have relatively light winds of 7 to 12 m s^{-1} (~15 to 25 kt), while a full gusty gale would affect the four bays area and particularly the Nullabor Plain. The existence of huge ventifacts at the neck between West Bay and Walrus Bay attest to this being a very windy area also. In short, weather–wise Atlas Cove is not a good place to build a base or from which to operate aircraft.

If the winds back to the south with the passage of a cyclone the compression zone appears to swing around the island to Atlas Cove, Saddle Point area on the northwest and to Spit Point on the east side. Cloud may disperse completely depending on the water vapour in the air, which is generally colder and drier.

Upper wind, temperature and humidity

No specific information on forecasting has been obtained.

Clouds

The cloud generated by the uplift of the moist air as it hits Big Ben and the Laurens Peninsula forms a spectacular and omnipresent cloud cap over the northwest/southwest side of the island extending many kilometres out to sea. This standing wave cloud is repeated at intervals of 10 to 20 km downwind and can be picked out clearly on many days on the satellite pictures as a herring bone pattern with Heard Island at its apex. As a result it is quite common for both ends of the island to have totally different weather, for example Atlas Cove could have 15 to 20 m s^{-1} (~30 to 40 kt) wind, rain and low cloud while Spit Point would be cloudless except for some lenticular or orographic cloud on the mountain, bright sunshine and calm conditions. The roll cloud generated by the mountain and rough seas off Skua, Fairchild and Compton

Glacier beaches could be clearly seen from Spit Point. Attempts to fly aircraft at Spit Point with a search and rescue (SAR) cover from Atlas Cove were frequently thwarted by those conditions of unflyable weather at Atlas Cove.

Visibility: blowing snow and fog

In the vicinity of Heard Island fog is frequent, especially with north and northwest winds, but with westerly winds visibility is often good. Fog may prevent all visual or physical ship to shore communication for several days at a time.

In 1980 it was reported that "on the couple of clear days that we experienced, flying was a real pleasure. The cold air and unlimited visibility allowed the helicopter to operate at its most efficient altitudes with power to spare".

Surface contrast including white–out

No specific information on forecasting has been obtained.

Horizontal definition

No information.

Precipitation

No specific information on forecasting has been obtained.

Temperature and chill factor

No specific information on forecasting has been obtained.

Icing

Two dangers mostly likely to cause a forced aircraft landing on the islands are bird strikes and airframe icing, which can occur with frightening speed. Rain or sleet squalls can appear suddenly around a cliff or down a valley and can make the Perspex bubble look like frosted glass in seconds.

Turbulence

Strong winds and resulting turbulence present the greatest problems for aircraft operations. During some of the vertical photography sorties in a 1980 expedition, at altitudes up to

3,000 m the winds were around 40 m s^{-1} (~80 kt) and the turbulence in the lee of Big Ben was severe.

Turbulence is created by the numerous volcanic cones like Crater and Corinth Head. Even in light winds these cones can create turbulence like "mini–cyclones". On one occasion during the 1980 expedition turbulence caused the rotors to lose speed so badly that the "engine out" warning came on momentarily.

Hydraulic jumps

There is no record of occurrence of hydraulic jumps on Heard Island.

Sea ice

No specific information on forecasting has been obtained.

Wind waves and swell

Anchorage may be obtained 1.5 km northwest of the head of Atlas Cove: it is exposed to the prevailing westerly swell rolling in from the north–northwest.

If the wind swings to the northeast a heavy swell can be expected into Atlas Cove making it a very precarious anchorage against a lee shore; at other times it is also subject to sudden and violent squalls. Compton Lagoon is much too windy and dangerous for boats, though its bar might be deep enough for some small craft and Winston Lagoon closes and opens its entrance to the sea at regular intervals.

7.2.9   Macquarie Island

7.2.9.1   <u>Orography and the local environment</u>

Macquarie Island (54º 25' S, 158º 58' E) with an area of 120 km^2 is 34 km long and up to 5 km wide, and lies in a north–south direction (Figure 7.2.9.1.1). Most of the island consists of a plateau at a general elevation of 250 to 350 m, rising in places to low rounded spurs and hills of 400 to 470 m. The edge of the plateau falls away abruptly to the sea or to narrow beaches. In the north of the island, Wireless Hill (102 m) is joined to the main mass of the island by a low, flat isthmus. The pioneer ANARE party arrived at the island on 7 March 1948 and the station was established on the isthmus near the old Australian Antarctic Expedition (1911–14) hut, which was still standing, though in poor condition. Observations are archived from April 1948. The highest point is Mount Hamilton at 433 m, 6 km north of Hurd Point, the southern most extremity.

7.2.9.2   <u>Operational requirements and activities relevant to the forecasting process</u>

Macquarie Island Station has a winter complement of staff of about 19 people: this number increases to a maximum of 40 during the summer. The following science activities are carried out at the station: environmental monitoring; human biology; ionospheric/auroral observations; terrestrial biology; and meteorological observations.

       Main re–supply of the station generally occurs during summer. Re–supply of the various huts around the island by helicopter or by small boat is another important activity which benefits from the forecasting service.

7.2.9.3   <u>Data sources and services provided</u>

The meteorological observing programme includes surface three–hourly synoptic observations. The upper–air sounding programme provides upper–air data at 12–hourly intervals, including computation of upper winds, as well as measuring pressure, temperature and moisture at upper levels of the atmosphere to a height of 22 km. Total ozone is also measured daily.

       Forecast services for the station are, in the main, provided by the Regional Forecasting Centre in Hobart, Tasmania, which provides twice daily general forecasts for the island's activities, and provides aviation forecasts when helicopters are in operation during station/hut re–supply. Forecasts are received at the station by business facsimile. The station also has access to Internet facilities through which it obtains much of its weather information from the Antarctic Division.

7.2.9.4   <u>Important weather phenomena and forecasting techniques used at the location</u>

General overview

Table 7.2.9.4.1 in Appendix 2 below shows climate statistics for Macquarie Island, which is affected by the persistent westerly belt of winds that sweep over the Southern Ocean. The island is ice–free and has no permanent snow cover, although the upper levels of the island are covered with wet snow for most of the year. The characteristic features of this island's climate are the small variation in temperature both seasonally and diurnally, and the persistent strong westerly and northwesterly prevailing winds. The windiest time of year is generally between August and October, when the north–south pressure gradient is strongest. The island's weather is also characterised by overcast skies and a large number of days with precipitation, the island often being obscured by mist. Wind chill is a major hazard for people living on the island because of the precipitation and strong winds, combined with near freezing temperatures.

       The warmer months are from December to April, and July is the coldest month. The mean relative humidity ranges between 85 and 90 percent, making it the Australian station with the highest mean relative humidity. Mean monthly rainfall is slightly higher during the warmer months.

Figure 7.2.9.1.1 A map of Macquarie Island. (Courtesy the Australian Antarctic Division)

Surface wind and the pressure field

As Macquarie Island lies in the regime of the mid–latitude westerlies, throughout the year winds are predominately from a direction between west and northwest. The mean wind speed throughout the year is 8 m s^{-1} (~16 kt). The windiest month is September with an average speed of 8.6 m s^{-1} (~16.7 kt) while the least windy month is December with an average speed of 6.9 m s^{-1} (~ 13.5 kt). The highest recorded gust occurred in September and was 51.4 m s^{-1} (~100 kt).

The wind summaries show that 70% of all wind directions blow from between west and northwest throughout the year at an average speed of about 10 m s^{-1} (~20 kt). The station winds are not always representative of the winds elsewhere around the island. In strong southwesterlies the station often reports lower wind speeds than elsewhere around the island. In a northwest airstream winds can arrive in Buckles Bay as north to northeasterlies due to flow around Wireless Hill. The elongated ridge of the island intercepts the wind flow from all directions and this results in local lee vortices particularly in the region of Buckles Bay. Here the orographic effects of the detached peak of Wireless Hill, the low lying isthmus and the northern end of the main island ridge result in variable lee wind patterns in the prevailing westerly flow. This often causes difficult conditions during ship to shore operations.

Upper wind, temperature and humidity

Forecasts of upper parameters are based on nowcasting techniques, using radiosonde data, and on NWP.

Clouds

Typical of a mid to high latitude maritime environment the average cloud amount at Macquarie Island is 7 oktas.

Visibility: mist and fog

The island is often obscured by mist and/or very low cloud. Prolonged periods of northerly air–flow, often due to slow moving highs over the Tasman Sea, bring moist warm air from lower latitudes, causing vast areas of fog over the waters surrounding the island. Fogs are also common in northerly airflow ahead of frontal changes. Fogs are observed at Macquarie Island on average about 70 days each year and are distributed fairly evenly in all months. Plateau visibility in fog is often less than 50 m.

K.C. Hines (who participated in the first ANARE in 1948) described the island's weather as: "For days on end the upper plateau would be shrouded in mist and a great wall of fog would block out the sea on all sides. A fine misty rain would be falling continuously and the inevitable wind sweeping in past the apparently impenetrable fog barrier."

Surface contrast including white–out

These are not generally a problem due to the vegetation and exposed rock.

Horizontal definition

This is not generally a problem.

Precipitation

Snowfall occurs throughout the year with a maximum frequency in spring. During September, falls can be expected on 7 days reducing to 1 day a month during summer. The upper levels of the island's plateau are covered with wet snow for most of the year, particularly from May to October, with depths in level areas between 0.5 and 1.0 m by the end of the season. The average annual rainfall total is 909 mm, varying little throughout the year. The wettest month is January (85 mm) and the driest July and August (65 mm). Rain can be expected on 305 days of the year.

Forecasting precipitation is based on airstream–weather concepts, together with satellite imagery and NWP output.

Temperature and chill factor

Mean daily maximum temperatures range from 9º C in January to 5º C in July. Mean minima range from 5º C in January to 1º C in September. This relatively small temperature range is typical of oceanic islands at these southern latitudes and is very similar to those recorded at Campbell Island, Kerguelen Island, Marion Island and the Falkland Islands. The highest temperature on record is 14º C (recorded in December), the lowest on record is –9º C (recorded in both July and August). Although temperatures seldom fall far below freezing, wind chill is a major hazard.

Icing

Forecasting icing is based on airstream–weather concepts together with satellite imagery, NWP and radiosonde data.

Turbulence

Although lee waves occur, mechanical turbulence is a main concern and is forecast on the basis of predicted low level winds.

Hydraulic jumps

Hydraulic jumps are not observed on Macquarie Island.

Sea ice

Sea ice is not relevant to Macquarie Island.

Wind waves and swell

The most important anchorage is Buckles Bay (Figure 7.298.1.1), followed by Hasselborough Bay (not shown) directly opposite a separating isthmus. Being close together, a vessel can, in the event of a complete change of wind, obtain shelter by proceeding from one to the other of these anchorages by passing round the northern most promontory.

There are short spells of east to southeast winds which reach gale–force at times and affect Buckles Bay in particular, these are generally accompanied by large waves from that direction. Swells can be critical to ship unloading, in particular on ships where the hatch covers cannot be stacked if there is a roll of more than a few degrees.

7.3 Antarctic Peninsula Sector

This section covers the Antarctic Peninsula Sector, including the South Orkney and South Shetland Island groups, the Filchner Ice Shelf and stations and other features that are on or about the Peninsula itself. For the purposes of the handbook these places have been grouped as shown below. The locations of some of these places are shown in Figure 7.3.1 which is a broad overview of the Peninsula region. Due to the great number of stations in northern parts of the Peninsula Figure 7.3.2 has been prepared to show many of these while Figure 7.3.2.1.1 should be referred to for the stations on King George Island.

Signy and Laurie Islands, South Orkney Islands   *See Section 7.3.1 below.*

All–year round station:

- Orcadas   (60º 44´ S, 44º 37´ W, 6 m AMSL).

Summer–only station:

- Signy   (60º 45´ W, 45º 56´ W, 6 m AMSL);

King George Island, South Shetland Islands   *See Section 7.3.2 below.*

All–year stations:

- Artigas (62º 11´ 04″ S, 58º 54´ 09″ W);
- Bellingshausen (62º 12´ S, 58º 58´ W, 16 m AMSL);
- Commandante Ferraz (62º 05´ 00″ S, 58º 23´ 28″ W);
- Great Wall (62º 13´ S, 58º 58´ W, 10 m AMSL);
- Jubany (62º 14´ 16″ S, 58º 39´ 52″ W, 4 m AMSL);
- King Sejong (62° 13´ 24″ S, 58° 47´ 21″ W, 10 m AMSL);
- Henryk Arctowski (62º 09´ 34″ S, 58º 28´ 15″ W);
- Presidente Eduardo Frei Montalva (62º 18.8´ S, 58º 55.5´ W, 10 m AMSL).

Summer–only stations:

- Ardley (62° 12.4´ S, 58° 53.8´ W);
- Macchu Picchu (62° 05´ 29.6″ S, 58° 28´ 16.4″ W, 10 m AMSL);.
- Juan Carlos I (62° 39´ 46″ S, 60° 23´ 20″ W).

Greenwich, Robert and Media Luna Islands, South Shetland Islands   See Section 7.3.3
                                                                   below

- Capitan Arturo Prat Station, Greenwich Island (62° 30´ S, 59° 41´ W).
- Luis Risopatron Station, Robert Island (62° 22´ S, 59° 40´ W, 40 m AMSL);
- Cámara Station, Media Luna Island (62° 36´ S, 59° 54´ W, 22 m AMSL).

Deception Island, South Shetland Islands   *See Section 7.3.4 below.*

- Decepción Station (62º 59´ S, 60º 34´ W, 7 m AMSL)

Trinity Peninsula, northern tip of the Antarctic Peninsula   *See Section 7.3.5 below.*

All–year stations:

- Marambio (64° 14´ 42″ S, 56° 39´ 25″ W, 200 m AMSL);
- Esperanza (63º 23´ 42″ S, 56º 59´ 46″ W; 25 m AMSL);
- General Bernardo O'Higgins (63° 19´ S, 57° 4´ W; 12 m AMSL).

Summer–only stations:

- St Kliment Orchridiski (62° 38´ 6″ S, 60° 21´ 7″ W);
- Petrel (63° 28´ S, 56° 17´ W; 18 m AMSL);
- Primavera (64º 09´ S, 60º 57´ 50″ W; 50 m AMSL).*The West–Central Section of the Peninsula (covers the low–lying area on the west–facing side of the Antarctic Peninsula)*   *See Section 7.3.6 below.*

All–year stations:

- Akademik Vernadasky (formerly Faraday) (65° 15´ S, 64° 16´ W; 7 m AMSL);
- Almirante Brown (64º 54´ S, 62º 52´ W, 10 m AMSL);
- Palmer (64° 46´ S, 64° 05´ W, 8 m AMSL);.Matienzo (64° 50´ S, 60° 07´ W; 32 m AMSL);Melchior (64° 20´ S, 62° 59´ W; 7 m AMSL);
- Yelcho (64° 52´ S, 63° 35´ W, 10 m AMSL).

Summer–only station:

- Presidente Gabriel Gonzalez Vidiez Station (64.8199^{o} S, 62.8633^{o} W).

Marguerite Bay/Adelaide Island western side of the Antarctic Peninsula at a location of approximately 67° S, 68° W   *See Section 7.3.7 below.*

All–year stations:

- Rothera (67° 34′ 19″ S, 68° 7′ 37″ W; 16 m AMSL);
- San Martin (68º 07′ 47″ S, 67º 06′ 12″ W; 5 m AMSL).

Summer–only station:

- Teniente Luis Carvajal (67° 45′ S, 68° 54′ W).

Fossil Bluff, King George VI Sound   *See Section 7.3.8 below.*

Summer–only forward field station:

- Fossil Bluff (71.3º S, 68.3º W).

Ski Hi/Ski Blu near the Sky–Hi Nunataks at the base of the Antarctic Peninsula
                                    See Section 7.3.9 below.

Summer–only forward field stations/blue ice runway:

- Sky–Blu blue ice runway (74º 51.14′ S, 71º 33.6′ W)
- Sky–Hi is a depot in the same general area.

The Larsen Ice Shelf, eastern side of the Antarctic Peninsula.   *See Section 7.3.10 below.*

- There are no staffed stations on the Larsen Ice Shelf so the only forecasting requirement is for flights to the area in connection with research activities or those for maintenance of the AWS at 66º 58′ S, 60º 33′ W.
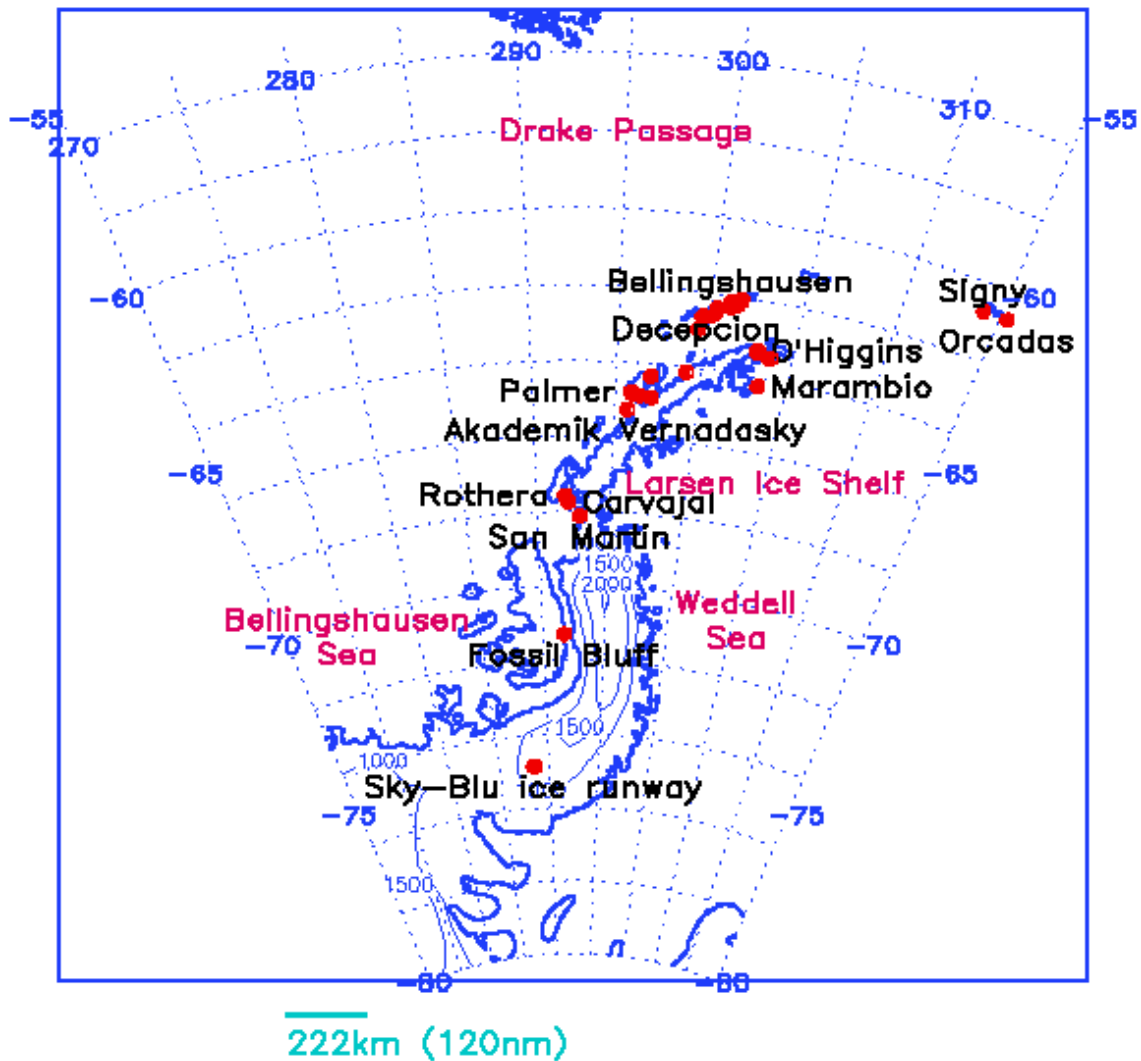
Figure 7.3.1   Sketch map showing some locations on and about the Antarctic Peninsula (contours in metres; the area is bounded by: 80º S, 55º S, 90º W and 45º W).

7.3.1   **Signy Island and Laurie Island , South Orkney Islands**

7.3.1.1   Orography and the local environment.

The South Orkney Island archipelago is located close to the tip of the Antarctic Peninsula 60° 43' S, 45° 36' W. The largest island in the group is Coronation Island and this has mountains rising to 1,278 m (~4,200 ft). Signy Island is situated a little to the south of Coronation Island and most of the rest of the islands are to the east of Coronation. The island group has two staffed stations. The Argentine station Orcadas, on Laurie Island, has been permanently occupied since 1902 and has the longest continuous meteorological record in Antarctica. The British station on Signy Island has been occupied since the 1940s and is now a summer–only station.
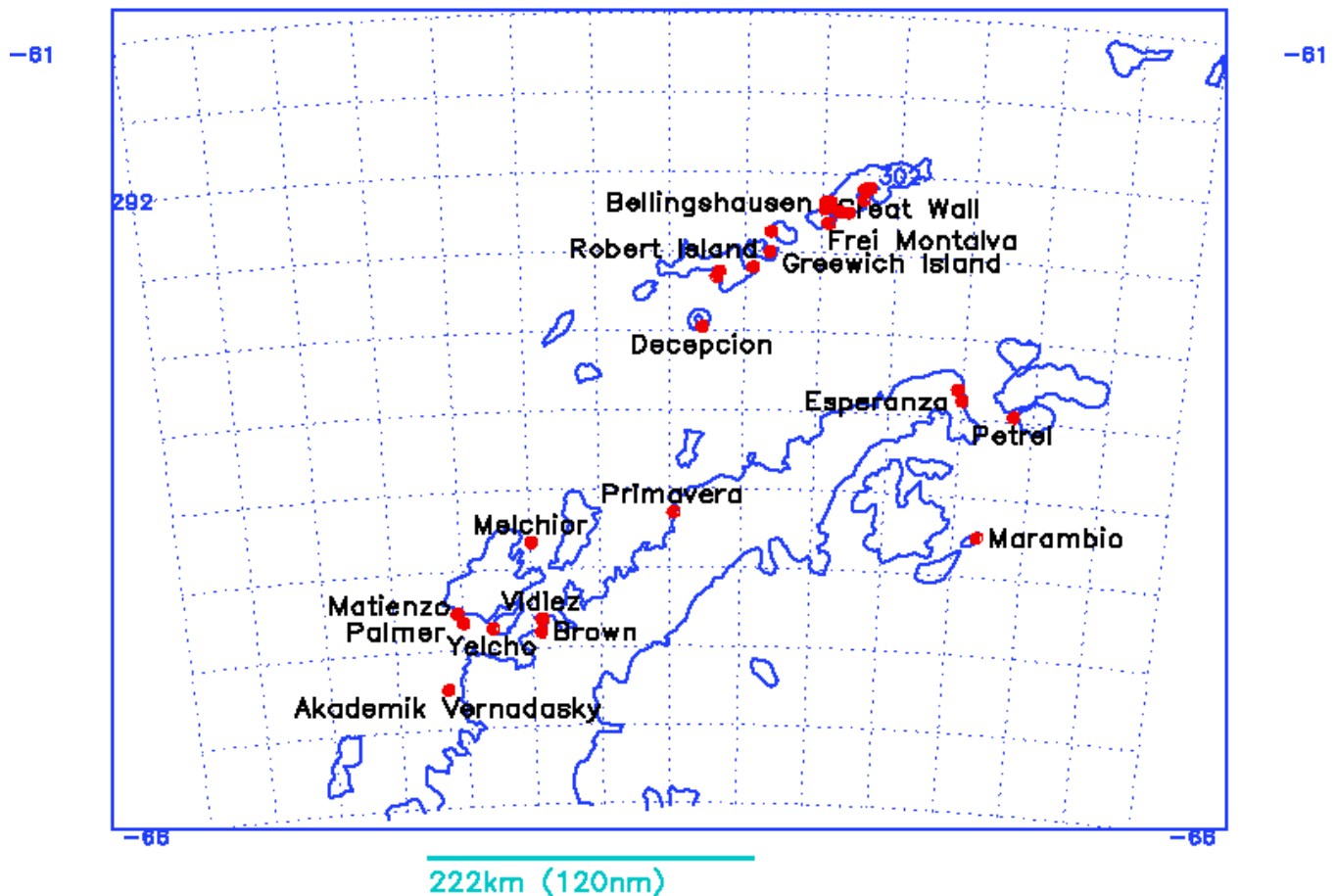
Figure 7.3.2   Sketch map showing some locations in the north of the Antarctic Peninsula (the area is bounded by: 66º S, 61º S, 68º W and 54º W).

7.3.1.2   Operational requirements and activities relevant to the forecasting process

The South Orkney group does not have any facilities for aircraft to land. The islands are on the whole too steep for an airstrip and the icecaps are too small and crevassed for an aircraft to safely land. Ships regularly call at the islands to visit and supply the two stations. The biggest problem faced by ships visiting the islands is the presence of sea ice, on at least one occasion this has meant that a station was not visited at the end of the summer season and people were left for the winter.

Forecasts for the Signy area are issued by the forecaster at Rothera Station when BAS ships are in the area

Forecasts for Orcadas are issued by the Argentine meteorological services.

7.3.1.3   Data sources and services provided

The station on Signy Island has an Inmarsat link to Cambridge and can use this to download observations from the GTS and forecast products from the UK Meteorological Office. However, as a forecaster is not based on the islands it is not normal for this information to be collected.

At Orcadas Station there is a surface meteorological observing programme.

7.3.1.4   <u>Important weather phenomena and forecasting techniques used at the location</u>

General overview

The climate in the South Orkney archipelago is strongly affected by the presence or absence of ice from the Weddell Sea. Sea ice moves in clockwise direction around the Weddell Sea and flows north past the South Orkneys. During a heavy ice year the ice edge can be well to the north of the islands during the winter and this tends to move the position of the circumpolar trough to the north of the Island and can make the winter be dominated by cold airmasses moving up from the Weddell Sea. Normally the islands are dominated by weather systems moving eastwards in the circumpolar trough making the islands one of the cloudiest places in the world.

Surface Winds and the pressure field

The stations in the South Orkneys are situated in sheltered areas and the wind observed at the stations is dominated by local orographical effects. Foehn winds are sometime experienced at Signy in northerlies flowing over Coronation Island.
        The pressure field is dominated by the large number of active depressions that cross the area and is forecast using NWP model output.

Upper wind, temperature and humidity

No radiosonde ascents are available for the islands so upper fields are predicted using the NWP model output.

Clouds

The South Orkneys are in one of the cloudiest places in the world, although this does depend on the position of the sea ice edge. When the sea ice edge is to the north of the archipelago the cloud cover tends to be lower.
        A feature of the islands is the orographic clouds that form over Coronation Island particularly in winter.
        Prediction of clouds in carried out using satellite imagery.

Visibility

No specific information on forecasting has been obtained.

Surface contrast including white–out

Surface contrast is important for travel on the islands and is predicted based on an estimate of the expected cloud cover.

Horizontal definition

Not relevant on the islands as there are no flying activities.

Precipitation

Precipitation is a frequent occurrence on the islands due to the many depressions that cross the area. It can be predicted using model rain/snowfall fields if available or from the model MSLP fields. In addition, satellite imagery can provide useful information on small–synoptic or mesoscale systems that may bring precipitation.

Temperatures and wind chill

Temperatures are also greatly effected by the position of the sea ice edge. In summer the average temperature is often above zero and the air temperature is often similar to those found on the west coast of the Antarctic Peninsula. However, during winter when the sea ice edge moves north from the Weddell Sea the temperatures drop, –40°C becoming quite common as the circumpolar trough moves north and the islands come under the influence of cold air from the Weddell Sea.

Icing

No specific information on forecasting has been obtained.

Turbulence

No specific information on forecasting has been obtained.

Hydraulic jumps

These are not reported on the islands.

Sea ice

Sea ice is highly variable around the islands and both heavy and light ice years are experienced which can cause problems for ships attempting to re–supply the stations.

Wind waves and swell

No specific information on forecasting has been obtained.

7.3.2   King George Island, South Shetland Islands

7.3.2.1   Orography and the local environment

King George Island is located in the South Shetland Islands at the tip of the Antarctic Peninsula. It is the largest island of the archipelago and had dimensions of about 80 km by 30 km. Most of the island is covered by ice but bare, rocky peaks protrude at various places. The maximal thickness of the glacier ice is 326 m (~1,070 ft). The island is not very high and the peaks are only 600–700 m (~2,000–2,300 ft) in elevation (see Figure 7.3.2.1.1) and the coast is deeply cut by many sheltered fjords and bays.

King George Island is orientated west–southwest to east–northeast and all the research stations are located on the south–facing side of the island, in the lee of the prevailing wind. The stations are generally near the coast and accessed via Admiralty Bay and Fildes Bay.

The Fildes Peninsula in the southwest corner of the island is flat and free of ice, and is where the island's only airstrip (Marsh) is located. The north–western coast is washed by the Drake Passage waters, while its southeastern shore is under the influence of the currents in the Bransfield Strait. The Fildes Peninsula is formed from igneous rocks with the relief being typically small hills rising up to 150 m and with a lot of fresh water lakes. Most of the year the lakes are covered by ice with a thickness up to 1 m. In the Ardly Bay area fast ice usually forms in the middle of March with its thickness reaches 80–100 cm towards the end of March.
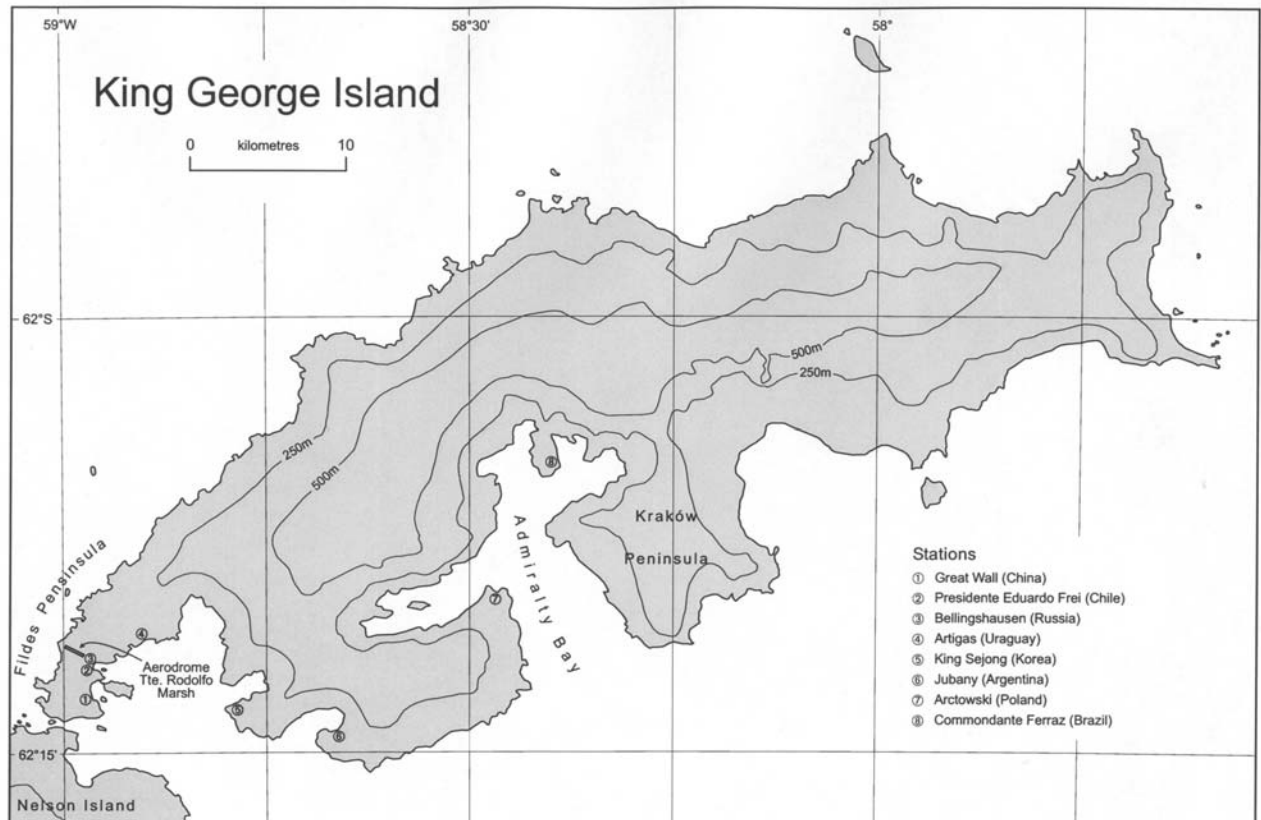
Figure 7.3.2.1.1 A map of King George Island.

7.3.2.2   Operational requirements and activities relevant to the forecasting process

King George Island is one the most densely populated parts of the Antarctic and certainly has more stations for its size than any other area of the continent. It is also visited by an increasing number of tourists.

At the time of writing (May 2001) the following stations were in use on the island:

Wintering stations:

- *Artigas* (Uraguay) (62° 11′ 04″ S, 58° 54′ 09″ W).
- *Bellingshausen* (Russia) (62° 12′ S, 58° 58′ W, 16 m AMSL). Bellingshausen Station is situated on the Fildes Peninsula in the southwestern part of the island. The station buildings are built on ice–free soil on both banks of a brook rising from the small Kiteg lake and flowing into the Ardly Bay. This bay is suitable for ship visits, with the disembarkation being executed with the help of boats and sometimes by helicopters. Bellingshausen Station was opened in February 1968 with the staff during the winter season consisting of about 20 people. The station is used as a base for field party investigations on King George island.
- *Commandante Ferraz* (Brazil) (62° 05′ 00″ S, 58° 23′ 28″ W).
- *Great Wall* (China) (62° 13′ S, 58° 58′ W, 10 m AMSL).
- *Jubany* (Argentina) (62° 14′ 16″ S, 58° 39′ 52″ W, 4 m AMSL).
- *King Sejong* (Korea), Barton Peninsula,

(62° 13′ 24″ S, 58° 47′ 21″ W, 10 m AMSL).

-     *Henryk Arctowski* (Poland) (62° 09′ 34″ S, 58° 28′ 15″ W).
-     *Presidente Eduardo Frei Montalva* (Chile), Fildes Bay.
  (62° 18.8′ S, 58° 55.5′W, 10 m AMSL).

(Note: *Teniente Rodolfo Marsh* is the 1,292 m runway next to Frei Station (see Figure 7.3.2.2.1)).

Summer–only stations:

-     *Ardley* (Chile), Fildes Bay. (62° 12.4′ S, 58° 53.8′ W).
-     *Macchu Picchu* (Peru) (62° 05′ 29.6″ S, 58° 28′ 16.4″ W, 10 m AMSL).
-     *Juan Carlos I* (Spain) (62° 39′ 46″ S, 60° 23′ 20″ W).

There are also a number of huts occupied on a short–term basis in order to conduct biological research.

The many operational and research activities on the island require accurate weather forecasts, particularly for the use of aircraft from Marsh. In addition, forecasts are required for the large number of ships that visit the stations for re–supply.
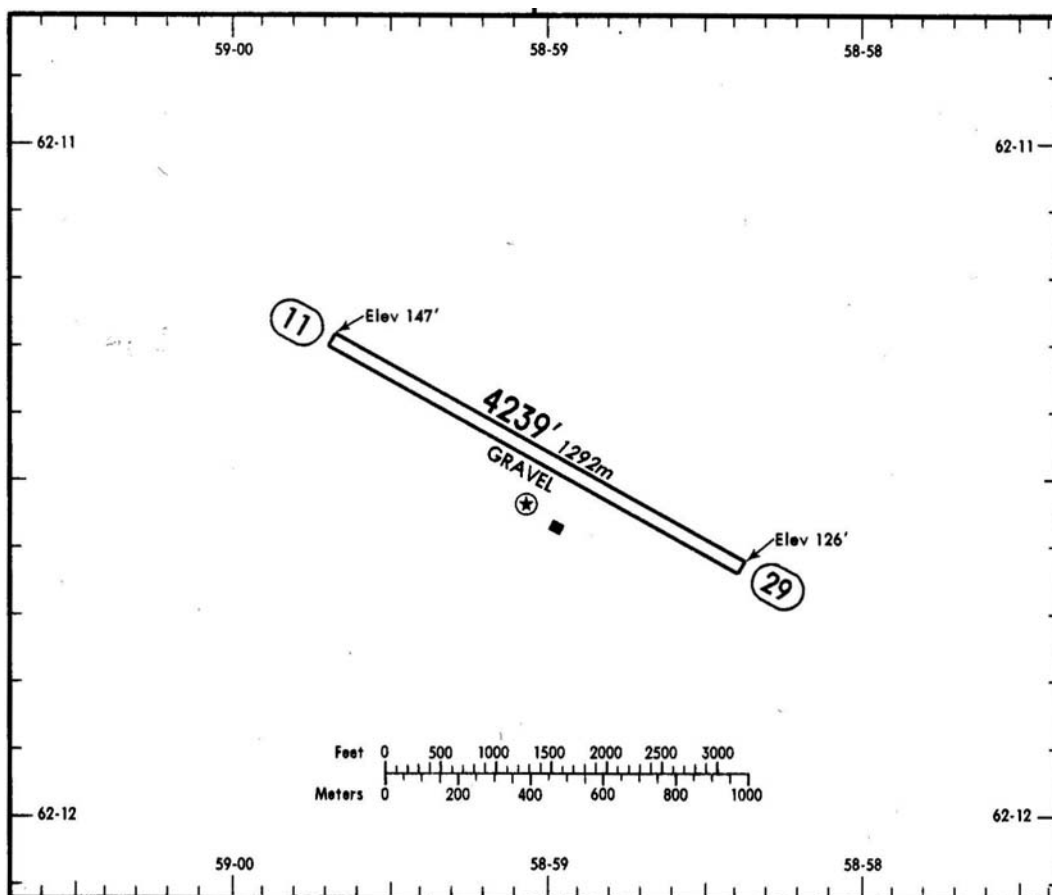
Figure 7.3.2.2.1 A map of the Marsh runway.

7.3.2.3   Data sources and services provided

In this section we consider the meteorological observing programmes and forecasting activities that take place at each of the stations:

- *Ardley* . This is a summer camp at which scientific work is undertaken but not of a meteorological nature.
- *Artigas*. The Uruguayan air operations make use of the airstrip at Marsh. There is a helipad at Artigas Station. Eight surface meteorological observations are made each day and sent to Frei Station.
- *Bellingshausen*. During the 1980s weather forecasts and ice situation information were provided for Russian marine activities for the south–western part of the Atlantic and for the south–eastern Pacific. Surface observations are available via the GTS four times a day. During summer radiosonde ascents are made at 00 UTC and provided via the GTS.
- *Commandante Ferraz*. Surface meteorological observations are collected.
- *Great Wall*. Surface observations are available via the GTS four times a day. Weather forecasts are prepared on site for the station and its vicinity, and for the Chinese research ships *Polar* and *Snowdragon*. The weather forecasts are prepared using information from the Antarctic Meteorological Centres, e.g., the Frei Meteorological Centre of Chile, and from Southern Hemisphere surface, upper–air and NWP products issued by the World Meteorological Centre, Melbourne, Australia. Other data include high–resolution imagery from polar orbiting weather satellites and analysis of station elements. Meteorological information for the operation of the research vessels is processes by ship–board meteorologists with the aid of facsimile synoptic charts, satellite data, marine and meteorological observations, and weather related ship routing suggestions sent from Beijing for consideration.
- *Jubany*. Surface observations are available via the GTS four times a day. Forecasts are obtained from Marambio.
- *King Sejong*. Surface observations are available via the GTS four times a day.
- *Henryk Arctowski*. No specific information has been obtained.
- *Presidente Eduardo Frei Montalva*. Nearby there is a small village named "Villa Las Estrellas" (The Stars Village) where 15 families winter over. This makes Eduardo Frei the second largest Antarctic station after McMurdo. The following gives an overview of this major Antarctic centre:
  - –The Antarctic Meteorological Centre at President Eduardo Frei Montalva was established as one of the three meteorological collecting centres on the Antarctic continent. This was in accord with the resolution of the First Meeting of the Working Group on Antarctic Meteorology of the Executive Council of the World Meteorological Organization held in Australia in 1966. The "Eduardo Frei" AMC technically reports to the Dirección Meteorológica de Chile (DMC) (the Chilean Bureau of Meteorology). It functions year–round with a team of meteorologists and observers who undertake national (Chile) and international meteorological requirements regarding Antarctic activities.
  - –The AMC is actually located at the nearby Teniente Rodolfo Marsh airstrip (see Figure 7.3.2.2.1) and has the responsibility of providing weather forecast to aviation and marine operations and to all other human activities carried out in the region such as research parties, tourism, etc. To

accomplish these tasks, the AMC is staffed by three meteorologists and three observers year–round.
–The AMC also carries out the function of communication centre for the collection and world–wide GTS transmission of meteorological observations from the surrounding Antarctic stations.
–Surface, 500–hPa height and 1000–500–hPa thickness charts are available to the forecasters every 12 h.
–The AMC Eduardo Frei is in communication with the DMC via a satellite link. Numerical weather forecasts from the National Centers for Environmental Prediction are received from Washington through Santiago. A satellite receiver (HRPT) workstation with TeraScan software is installed at the AMC to obtain *in situ* satellite imagery at high resolution from the NOAA polar orbiting spacecraft. Radio VHF allows exchange of weather information among Chilean stations and others located in King George Island and surroundings places.
–Routine weather observations are sent internationally every three hours through the GTS via Santiago. Routine forecast products prepare by the AMC meteorologists are broadcast on HF and distributed via the GTS to all interested users. These products include ROFOR (regional forecast for aviation), MAFOR (forecast for shipping in the Southern Ocean between 20º W and 90º W, the Drake Passage and the Bellingshausen Sea) and forecast for the general public. In addition, the AMC broadcasts the IAC (coded sea–level pressure analysis), ice report, the current and predicted (24 hrs) sea level pressure chart and predicted 500–hPa heights.
–The high variability of the atmospheric conditions over the Antarctic Peninsula and in particular on King George Island implies that the weather changes from one state to another very rapidly. Thus, forecasting for the area requires a continual evaluation of the meteorological variables and of the development of the synoptic and mesoscale perturbations in the region. Frei Station has all the facilities and human resources for providing the meteorological needs for King George Island and surrounding areas. Moreover at Punta Arenas, the southernmost large city of Chile, there is a Meteorological Regional Centre that can support this effort with weather and forecast information to any aircraft and ship that goes to the Antarctic region.

- *Macchu Picchu*. No specific information has been obtained.
- *Juan Carlos I*. No specific information has been obtained.

7.3.2.4   <u>Important weather phenomena and forecasting techniques used at the location</u>

General overview

The island is located in one of the most northerly parts of the Antarctic and has a relatively mild, maritime climate. It is also located at the latitude of the circumpolar trough and is affected my many active depressions that pass through the Drake Passage, bringing frequent gales and precipitation. The weather can generally be described as unsettled and gloomy weather with low stratus and strato–cumulus prevails. Precipitation is frequent and in the form of snow, rain, or drizzle. Around 817 mm of precipitation falls in a typical year at Bellingshausen. Cyclonic eddies move into this area on both zonal and meridional

trajectories. The zonal systems are frequently fast–moving from west to east with speeds exceeding 28 m s^{-1} (~55 kt). Those arriving on a meridional trajectory from the mid–latitude area of the Pacific tend to fill over the Bellingshausen Sea. Not all the cyclones with a zonal trajectory move over the Drake Passage. Some lows track further north or south and encounter the orographic barriers of South America or the Antarctic Peninsula. Depending on the location of the lows, the wind across the island can be either from the west or the east, with cloud lingering on the upwind side of the island.

As the Marsh runway facility is of key importance it is of interest to gain an overview of the weather that Frei Station/Marsh experience. Visibility reduced by fog and precipitation, and low cloud are the main meteorological parameters that restrict aircraft operation in Frei Station and surrounding areas. These conditions are usually associated with stable conditions. Frontal systems coming from the northwest bring warmer and moister air toward the island stabilizing the lower atmosphere. In these cases northerly winds prevail and low stratiform cloud and fog can form. Liquid precipitation events are often associated with these northwesterly fronts. In this type of meteorological situation restricted conditions can last for more that 12 hr. On the other hand, cold air masses coming from the southwest bring unstable conditions, cumulus type clouds and blizzards. Under this latter meteorological environment the runway at Frei Base can be temporarily closed for operations. Other restrictions on operations are associated with strong winds across the runway which affect aircraft performance. One synoptic–scale situation that can produce cross winds involves a high–pressure system being centreed over the Weddell Sea. In this case a southerly low–level jet (barrier wind) can develop along the east side of the mountains of the Peninsula and extend over the northern tip of the Peninsula reaching King George Island with southerly winds. Wind shear near the surface can occur with this situation

A selection of climatological data for Great Wall Station is presented in Table 7.3.2.4.1 in Appendix 2 below and gives an idea as to average conditions on King George Island.

Surface wind and the pressure field

With climatological low–pressure over the Amundsen/Bellingshausen Sea the prevailing wind direction at King George Island is from the west to northwest quadrant. However, the high frequency of major depressions passing close to the area means that the winds are rather variable on a day–to–day basis and gales are frequent – for example, Great Wall reports 36% of days with winds of more than 17 m s^{-1}(~33 kt) and a peak in gales during the months of March to October. And for Frei Table 7.3.2.4.2 in Appendix 2 below shows the monthly distribution (%) of the wind velocity for given directions while Figure 7.3.2.4.1 in Appendix 2 below displays the percentage of occurrence of wind higher than certain values. Clearly, from this figure the semi–annual oscillation of the wind speed at Frei can be seen for wind speeds higher than about 8 m s^{-1} (~ 15 kt) – two maxima may be seen, one in April and one in October. This behavior is not observed for wind speeds at Frei of less than 8 m s^{-1} – these have a maximum during the summer. In general at Frei the wind speed increases during the equinox and is, on average, higher in winter than in summer.

Anticyclones and ridges tend to be quite short–lived in the area, so that calm conditions are only reported on 1–2% of occasions, although Jubany with its sheltered location has calm in over 4% of its reports.

The local orography affects the wind as reported from the various stations and there are substantial differences in their climatological wind statistics. The group of stations on the low southwestern tip of the island tend to be more representative of the broad–scalesynoptic environment, although even here there are differences between stations. Bellingshausen has most winds between west and north with some from the southeast. Frei has the same general picture (see Figure 7.3.2.4.2 in Appendix 2 below).

Great Wall on the other hand has most winds from the north and northwest. King Sejong with its location on the Barton Peninsula is exposed to the northwesterly winds, but is sheltered from southeasterlies. The winds from Jubany should be used with great care as the station is located in an enclosed fiord and most winds come from the southwest with a secondary maximum in the northeast. They are therefore not representative of synoptic conditions.

Usually north–westerly winds bring warm, moist air to the area ahead of cyclones, with south–easterly and easterly winds, often to the west of cyclone centres, bringing cold dry air. The wind direction and speed are very variable on King George Island. Sudden wind gusts are typical.

The most persistent strong cyclonic winds occur when lows arrive from the eastern part of the Pacific Ocean along meridional trajectories. At Bellingshausen Station the number of days with wind speed exceeding 15 m s^{-1} (~30 kt) is 10–15 per month on average, the maximum being during the winter months. On the island, strong winds often cannot be explained by the pressure field alone, because there are local factors playing a role that result in changes to the pressure gradients. In some cases these effects can be explained by the presence of mesoscale disturbances.

The major NWP models are now quite successful at analysing and predicting the locations and depths of large–scale depressions, and around King George Island the analyses can be used with a fair degree of confidence because of the large number of *in situ* observations and extensive satellite data over the ice–free ocean. However, satellite imagery should also be used in conjunction with the model fields because of the large number of mesoscale weather systems that are found in this area.

Upper wind, temperature and humidity

The Russian Bellingshausen Station had a radiosonde programme for many years, but ascents stopped in 1999. So today there is no upper–air measurements taken on a routine basis anywhere on the Antarctic Peninsula. Upper–air information is therefore obtained from the NWP analyses.

Clouds

Much of the cloud that affects King George Island is frontal in origin, although some non–frontal cloud is also present. Satellite imagery allows the cloud extent and type to be assessed routinely.

When frontal systems pass the Fildes Peninsula the cloud does not change significantly, and hills are often under the cloud base if their height does not exceed 100 m above sea level. At Bellingshausen Station the mean annual cloud cover is 7.2 oktas and the seasonal and month to month variations are very small and do not exceed 1 okta. Similarly, Figure 7.3.2.4.3 in Appendix 2 below indicates that more than 70% of the time the cloud at Frei is 6 oktas or more. On about 7% of occasions at Frei cloud heights of less than 150 m combine with visibilities of less than 1500 m and thus severely restrict aviation operations.

Cloud can be predicted in the short term using satellite imagery. For longer range forecasts the cloud must be estimated from the broad–scalesynoptic environment that is expected.

Visibility: snow and fog

Visibility can be reduced considerably by the moderate or heavy snow that falls in association with the frontal cyclones. Good visibility (greater than 10 km) is recorded on more than 90% of all occasions and the frequency of low visibility (less than 2 km) is 2–6% of days per month. During the winter months poor visibility usually occurs as a result of the frequent snow–storms (up to 10–12 days), and during the summer months fog as well as precipitation (up to 8–10 days) are among main reasons for the reduction of visibility.

The probability of fog increases with the passage of a warm front with northerly winds and under such conditions the fog can occur ever in the presence of strong winds. Snow storms occur with fresh snow cover and at wind speeds exceeding 7–9 m s^{-1} (~15 kt). The probability of a snow–storm increases under dry snow conditions.

An analysis of the seasonal occurrence of visibility less than 1600 m for various wind directions has been carried out for Frei Station and Figure 7.3.2.4.4 in Appendix 2 below summarises the results. Comparing this figure with Figure 7.3.2.4.2 indicates that at Frei visibility reductions below 1,600 m occur with all wind directions. Figure 7.3.2.4.5 in Appendix 2 below shows the percentage frequency of several visibility thresholds at Frei for each season. It may be seen that between 20 and 30% of the time visibility at Frei is less than 1,600 m with a maximum during summer and a slight minimum in autumn.

Surface contrast including white–out

With the large amount of low cloud and frequent precipitation events experienced at King George Island surface contrast can be very poor. It is forecast using an estimate of the likelihood of cloud and the occurrence of precipitation.

Horizontal definition

Horizontal definition is generally moderate or good because of the large amount of open water that is found around the island and the orographic features that are visible.

Precipitation

On King George Island precipitation falls on 70% of days over the year, but with a minimum during the summer months. The precipitation is usually associated with the many frontal depressions that occur in this zone. Solid precipitation (snow, snow grains, pellets of snow) prevail during the year, but liquid and combined precipitation are found not only in summer, but also in winter. Figure 7.3.2.4.6 in Appendix 2 below shows the number of days per month when liquid and solid precipitation occur at Frei while Figure 7.3.2.4.7 in Appendix 2 below shows monthly precipitation amounts at Frei. The effect of semi–annual oscillation is quite evident in both these figures.

Also of interest is the intensity of precipitation. Figure 7.3.2.4.8 in Appendix 2 below gives an indication of precipitation rates at Frei for 24 hr periods. It may be seen from this figure that around 27% of precipitation events at Frei have 24 h rates in the range of 6 to 8.9 mm for the 24 h. Intense rainfall rates of, say, greater than 21 mm per 24 h period occur on less than 5% of occasions.

Precipitation can be forecast directly using the model output or if model precipitation fields are not available then the surface pressure fields.

Temperature and chill factor

The maritime climate of King George Island means that the annual cycle of temperatures is less extreme than at many other sites in Antarctica and at Arctowski Station over 1978–87 the mean daily temperatures varied from 2.3°C in January to –7.1°C in July. During this period the coldest temperature recorded was –32.3°C and the highest 16.7°C.

A similar range of mean temperatures occurs at Frei. The monthly average of the mean temperature at Frei Station is depicted in Figure 7.3.2.4.9 in Appendix 2 below. Positive values occur in summer (December, January and February) and near zero degrees in March. A minimum takes place in July of about – 6°C. The inter–annual variability, given by the standard deviations of mean monthly temperatures shown in Figure 7.3.2.4.9, has a winter maximum. Figure 7.3.2.4.10 in Appendix 2 below shows the monthly distribution of temperature at Frei for occasions when the temperature is above 0°C. As expected, the frequency decreases toward the winter months where only 5% of the recorded three–hourly temperatures were above freezing. In contrast, more than 70% of the temperatures are about 0°C in summer, with a maximum in January. In the range between –10°C < T° < 0°C (Figure 7.3.2.4.11 in Appendix 2 below), the frequency is higher in May and October, decreasing significantly toward the summer with a minimum in January of less than 10% in mid–afternoon, and another relative minimum in July of about 55%. Occasions (not shown) when the temperature is below –10°C reveals a maximum frequency in winter with about 40% in July during the night hours.

Temperature changes can be predicted using model fields or through the use of satellite imagery to estimate the likelihood of changes of airmass.

Icing

Icing can occur on King George Island because of the rapid variations in temperature that are experienced coupled with the availability of large amounts of cloud liquid water. Icing events at Bellingsausen Station can occur on 8–12 days per month during the period from May to September.

Turbulence

No specific information on forecasting has been obtained.

Hydraulic jumps

Hydraulic jumps have not been reported on King George Island.

Sea ice

At Bellingshausen Station regular ice observations have been carried out in Maxwell Bay, including Ardly bay and in the visible parts of the Bransfield Strait and the Drake Passage. The most reliable and complete data about the ice situation is available for Ardly bay due to the good visibility there. The results of observations, carried out since 1968 demonstrate that the ice conditions in this bay are characterized by large inter–annual variations. So, the maximum thickness of fast ice varies from 50 to 124 cm, and the number of days with stable ice (from the moment of stable ice formation to the full clearing of the ice) is from 82 to 220.

Passive microwave, visible or infra–red satellite imagery can be used to estimate the broader scale extent of the sea ice. Short period variations in sea ice position can be estimated from the forecast surface winds.

Wind waves and swell

No specific information on forecasting has been obtained.

7.3.3   Greenwich, Robert and Media Luna Islands, South Shetland Islands

7.3.3.1   Orography and the local environment.

Greenwich, Robert and Media Luna Islands are located in the South Shetland Island group close to the tip of the Antarctic Peninsula. These islands are southwest of King George Island. The stations covered in this section are:

- The Chilean *Capitan Arturo Prat Station* is on Greenwich Island (62° 30´ S, 59° 41´ W). The station was opened in 1966.
- The *Chilean Luis Risopatron Station* is on Robert Island (62° 22´ S, 59° 40´ W, 40 m AMSL). The station is located on solid rock about 150 m from the coast. Risopatron has been open since 1954. (Prat and Risopatron Stations are about 20 km apart).
- The Argentine *Cámara Station* is on Media Luna Island (62° 36´ S, 59° 54´ W, 22 m AMSL). The station is built on rock 11 km from Prat Station.

7.3.3.2   Operational requirements and activities relevant to the forecasting process

None of these station has an airstrip but forecasts are required for resupply by ship and for activities close to the stations.

- The year–round *Prat* Station has a well established meteorology programme and climatological data extend back to 1966, although the record is not complete.
- *Risopatron* is concerned with geology/geophysics and terrestrial biology.
- *Cámara* is a summer only station but does make meteorological observations.

7.3.3.3   Data sources and services provided

- *Prat* has a year–round surface meteorology programme.
- No information is available on *Risopatron*.
- *Cámara* has a surface meteorology programme.

7.3.3.4   Important weather phenomena and forecasting techniques used at the location

General overview

These islands are located in one of the most northerly parts of the Antarctic and have a relatively mild, maritime climate. They are also located at the latitude of the circumpolar trough and are affected my many active frontal depressions that pass through the Drake Passage or enter the Bellingshausen Sea, bringing frequent gales and precipitation. The weather can generally be described as unsettled and gloomy weather with low stratus and strato–cumulus prevails. Precipitation is frequent and in the form of snow, rain, or drizzle. Precipitation is around 700 mm a year.

Surface Winds and the pressure field

With climatological low–pressure over the Amundsen/Bellingshausen Sea the prevailing wind direction in the area is from the west to northwest quadrant. However, the high frequency of major depressions passing close to the area means that the winds are rather variable on a day–to–day basis and gales are frequent

The area is strongly affected by the semi–annual oscillation and surface pressures are lowest (highest) in the spring/autumn (winter and summer).

Upper wind, temperature and humidity

No radiosonde ascents are available for the islands so upper fields are predicted using the NWP model output.

Clouds

Much of the cloud that affects these islands is frontal in origin, although some non–frontal cloud is also present. Satellite imagery allows the cloud extent and type to be assessed routinely. Prediction of clouds in carried out using satellite imagery.

Visibility

No specific information on forecasting has been obtained.

Surface contrast including white–out

Surface contrast is important for surface travel on the islands and is predicted based on an estimate of the expected cloud cover.

Horizontal definition

Not relevant on the islands as there are no flying activities.

Precipitation

Precipitation is a frequent occurrence on the islands due to the many depressions that cross the area. It can be predicted using model rain/snowfall fields if available or from the model MSLP fields. In addition, satellite imagery can provide useful information on small–synoptic or mesoscale systems that may bring precipitation. In winter most of the precipitation falls as snow, although rain can fall at any time of the year. In summer rain or snow can fall.

Temperatures and wind chill

At Prat Station the annual mean temperature is usually in the range -1 to $-3^{\rm o}$C. In summer the mean temperature is one or two degrees above freezing, falling to several degrees or more before freezing in winter. During the winter the temperatures are particularly variable and are heavily dependent on the amount of sea ice present. Over the period 1966–86 the July mean temperature varied between $-2.8^{\rm o}$C to $-12.7^{\rm o}$C.

Icing

No specific information on forecasting has been obtained.

Turbulence

No specific information on forecasting has been obtained.

Hydraulic jumps

These are not reported on the islands.

Sea ice

Sea ice is highly variable around the islands and both heavy and light ice years are experienced, which can cause problems for ships attempting to re–supply the stations.

Wind waves and swell

No specific information on forecasting has been obtained.

7.3.4   Deception Island, South Shetland Islands

7.3.4.1   Orography and the local environment

Deception Island is located at the south–western end of the South Shetland group and is about 110 km (~60 nm) from the Antarctic Peninsula. The island is of volcanic origin being made up of a submerged volcanic crater. The rim of the crater has been breached and a channel 400 m wide allows ships to enter the crater, which acts as a large natural harbour called Port Foster (see Figure 7.3.4.1.1). A good anchorage is available just inside the entrance to the harbour in Whaler's Bay adjacent to the station *Decepción* (62º 59´ S, 60º 34´ W, 7 m AMSL). The hills surrounding the harbour rise up 570 m (~1,870 ft) in the east and are lowest towards the north west. The volcano is still active, the last major eruption being in 1966 when British and Argentine research stations had to be evacuated.

7.3.4.2   Operational requirements and activities relevant to the forecasting process

Scientific activities on Deception Island at present are limited to summer only work operating out of small huts. In the past, aircraft, both wheeled and float planes, have operated from Deception. The aircraft operated from a strip near the shore of Whalers Bay. Winged aircraft have landed on the strip in recent years but there has not been any operational use of Deception as a base for air operations since the 1966 eruption.

Deception Island is a favourite site for visiting tourist ships and every year many tourists parties are put ashore. The island offers a very good harbour and within Port Forster calm conditions for landing parties can be almost guaranteed.

7.3.4.3   Data sources and services provided

No meteorological observations are available from Deception on a routine basis.
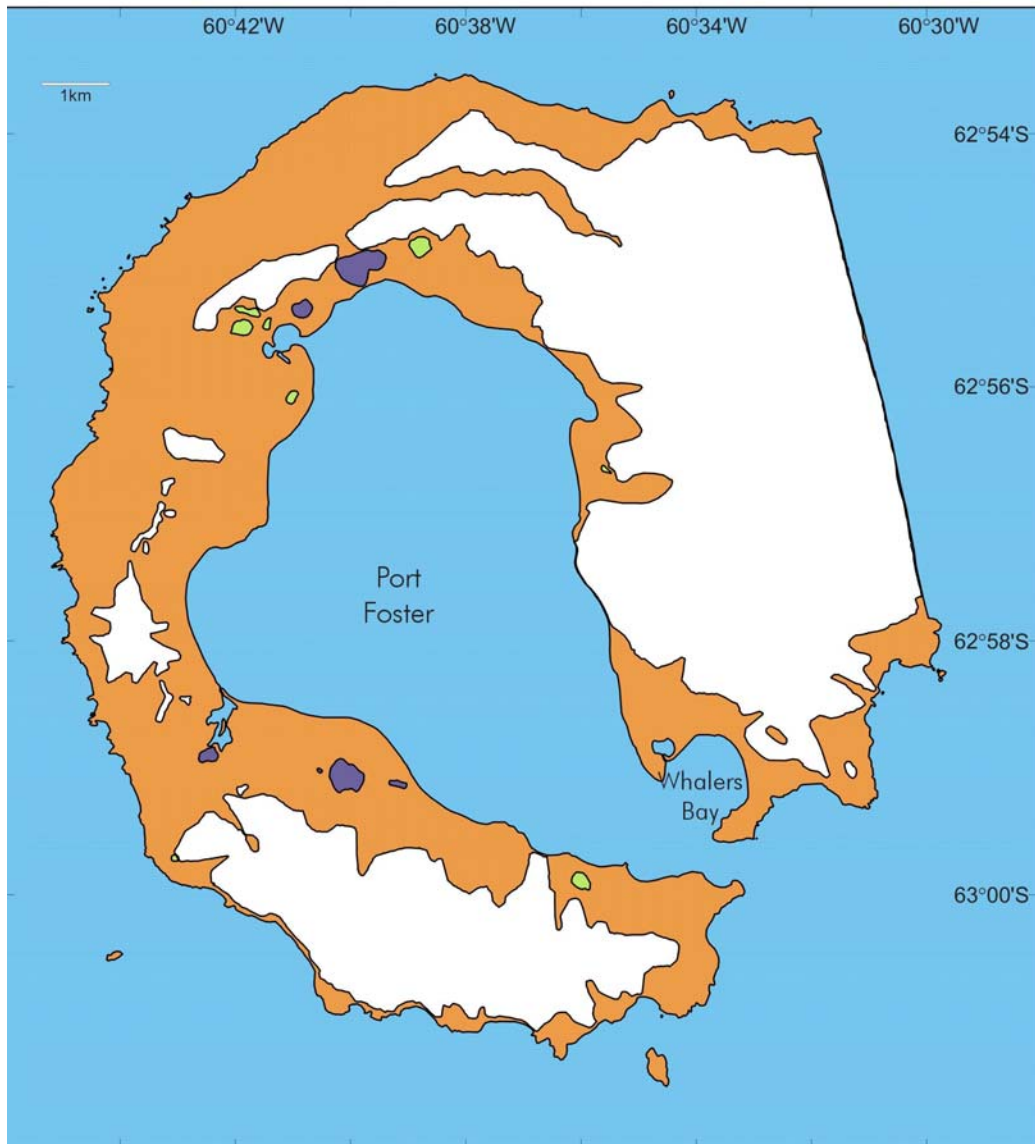
Figure 7.3.4.1.1 Location map showing Deception Island

7.3.4.4   <u>Important weather phenomena and forecasting techniques used at the location</u>

General overview

In the summer most of the island is bare loose packed volcanic ash while in the winter the ground is mostly snow–covered. The climatological conditions are similar to those found on King George Island. The island is subject to the weather systems that develop with the circumpolar trough.

Surface wind and the pressure field

The direction of the surface wind on Deception Island is predominately either westerly or northeasterly. The local hills around Port Foster will cause local variations in the wind direction and strength.

Upper wind, temperature and humidity

No radiosonde data are available for the region but upper–air conditions can be predicted using numerical weather prediction model output. These fields tend to be reasonably accurate, although errors can occur in the strength and position of the jets.

Clouds

Low stratiform clouds with heights around 300–600 m (~1,000–2,000 ft) are quite common at this location and are normally associated with synoptic scale weather systems approaching from the west. Orographic cloud is commonly observed.

Visibility: precipitation and fog

Fog is quite common and the visibility is less than 1,000 m (~3,300 ft) around 10% of the time. This low visibility is normally associated with frontal systems approaching from the north. Steam is sometimes formed by volcanic activity but rarely significantly affects the visibility.

Surface contrast including white–out

Surface contrast is usually good during the summer when the ground is clear of snow. During the winter there may be periods with poor contrast when the ground is snow covered and the cloud base low.

Horizontal definition

The presence of large areas of black volcanic ash means that the horizontal definition is normally good. It may deteriorate during periods of dense fog.

Precipitation

Precipitation is often in the form of rain during the summer, and although the amount can be very variable from year to year; monthly totals during the summer in access of 100 mm are common. During the winter the precipitation amounts are normally lower and usually falls in the form of snow, although rain can fall in any month.

Temperature and chill factor

The average annual temperature is around –4ºC with temperatures falling to a minimum of around –30ºC during the winter. The dark volcanic ash will tend to absorb radiation during the summer helping melt the winter snowfall quickly. Hot volcanic springs tend to keep a narrow band of the ocean sea ice free but these springs do not have any effect on the air temperature.

Icing

Most of the clouds observed at Deception Island are composed of water droplets and this means that icing can be a problem, especially after sudden drops in temperature.

Turbulence

Turbulence can be formed by the airflow around the steep hills of Deception Island. The presence of turbulence can sometimes be indicated by orographic clouds forming over the island.

Hydraulic jumps

Hydraulic jumps have not been observed on Deception Island.

Sea ice

Whalers Bay, and probably the greater part of Port Foster, are ice covered for most of the winter. A narrow ice–free channel near the shore of Whalers Bay is kept ice–free by hot volcanic springs.

Wind waves and swell

Port Foster and Whalers Bay are very sheltered and wind waves or swell are not a problem.

7.3.5   Trinity Peninsula

7.3.5.1   Orography and the local environment

The Trinity Peninsula is at the very tip of the Antarctic Peninsula and separates the Bransfield Strait from the waters of the Weddell Sea. The peninsula is aligned northeast to southwest and

extends for several hundred kilometres. On the Weddell Sea side, James Ross Island is separated from the peninsula by the Erebus and Terror Gulf, and the Prince Gustav Channel. For many years it was not possible to circumnavigate James Ross Island by ship, but in the late 1990s the fast ice disintegrated as a result of the warming that has taken place across the region in recent years.

There are several research stations around the Trinity Peninsula:

- The Argentine *Marambio base* (64° 14' 42" S, 56° 39' 25" W, 200 m AMSL) is located on Seymour Island, a small island just east of James Ross Island.
- The Argentine *Esperanza base* (63º 23' 42" S, 56º 59' 46" W; 25 m AMSL) is located in San Martin Land on a solid rock surface 30 m from the Antarctic coastline.
- The Chilean *General Bernardo O'Higgins Station* (63° 19' S, 57° 4' W; 12 m AMSL) is located on the western side of the Trinity Peninsula on solid rock and about 50 m from the Antarctic coastline. The station was opened in 1948.
- The Bulgarian *St Kliment Orchridiski Station* (62° 38' 6" S, 60° 21' 7" W) is located near the tip of the Trinity Peninsula.
- The Argentine *Petrel Station* (63° 28′ S, 56° 17′ W; 18 m AMSL) is located on Dundee Island about 400 m from the coast. It is 37 km from Esperanza Station.
- The Argentine *Primavera Station* (64º 09' S, 60º 57' 50' W; 50 m AMSL) is on Cape Primavera on the western coast of the Antarctic Peninsula. The station is located about 500 m from the coast and is built on rock.Operational requirements and activities relevant to the forecasting process

- At *Marambio* there is a 1,200 yard runway (see Figure 7.3.5.2.1) on a raised plateau operated by the Argentine air force that can take wheeled aircraft, including Hercules C–130 cargo planes and DHC–6, plus helicopters. The base has the only airstrip in Antarctica where planes can land year–round without skis, so it is of considerable importance within the region. Although Marambio is a military base it gives logistical support to the scientific community, with most activity taking place during the summer months. The base has about 30 staff in winter and an additional 50 temporary staff in summer, plus about 60 scientists visiting during the summer. Weather forecasts are required for flights to and from the station, base activities and scientific parties operating in the area.
- *Esperanza base* operates all year. There is an unmarked snow landing area approximately 2.8 km (~1.5 nm) from the base (see Figure 7.3.5.2.2).
- *General Bernardo O'Higgins Station* operates all year, including a year–round observations programme. There is a skyway located 2,000 m from the station at an elevation of 300 m. The station was opened in 1948.
- *St Kliment Orchridiski* Station is a summer–only station.
- *Petrel* Station is a summer–only station but has meteorological records extending back to 1967.
- *Primavera* is an another summer–only station.
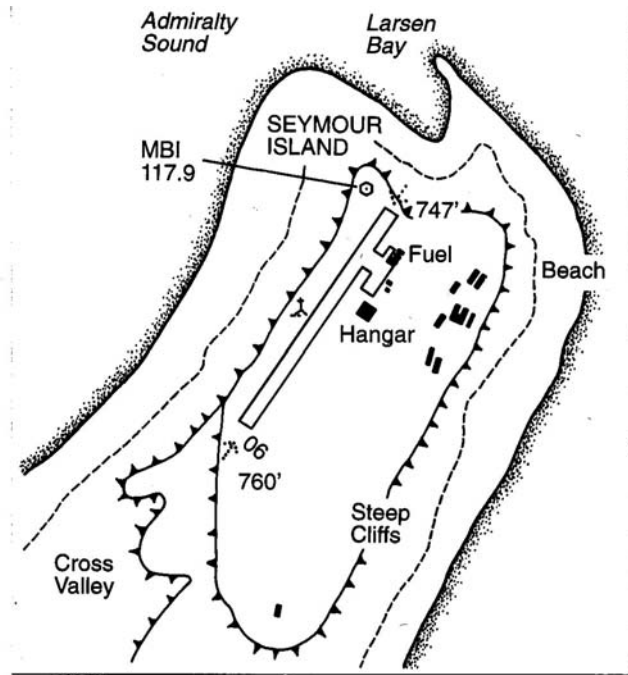
Figure 7.3.5.2.1   Map of Marambio showing the runway
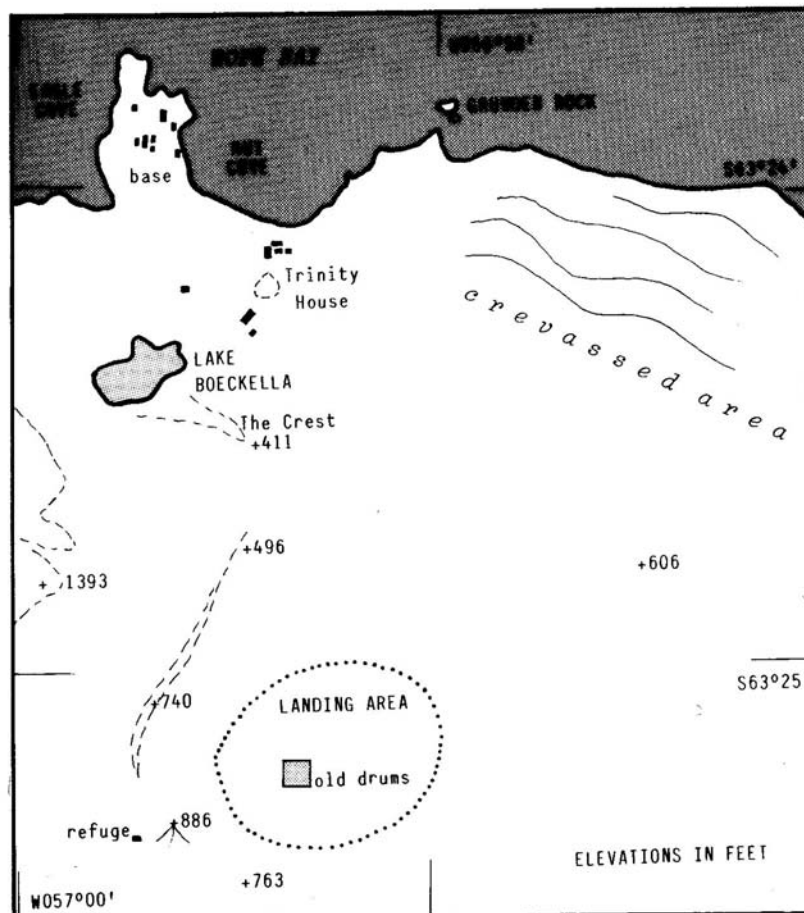
Figure 7.3.5.2.2 A Map of the snow landing area at Esperanza.

7.3.5.3   Data sources and services provided

- At Marambio there is a surface meteorological observing programme which provides 6 hourly data that are put on the GTS. The Marambio Meteorological Antarctic Center is operational year round and provides briefings for all air operations. Current weather and forecasts are also provided by HF and VHF. All information is in Spanish or English. Fax charts are obtained from the Meteorological Bureau in Buenos Aires. Satellite imagery from the NOAA polar orbiting (APT) and geostationary GOES satellites are received at the station.
- O'Higgins maintains a surface meteorological observing programme.
- Petrel maintains a surface meteorological observing programme.

7.3.5.4   Important weather phenomena and forecasting techniques used at the location

General overview

This area is close to the latitude of the circumpolar trough and is therefore affected by many active depressions throughout the year in the Bellingshausen Sea and the Drake Passage.

The western side of the area has a more maritime climate, while to the east of the Peninsula the weather is more continental and generally colder. The colder air temperatures make the region more prone to fog forming as warm air masses move south.

Stations on the western side are strongly affected by depressions in the Bellingshausen Sea and fronts that move down over the area from the northwest bringing cloud and precipitation. However, lows can also develop over the southern Bellingshausen Sea and track northeastwards over the area.

Stations on the eastern side are affected by lows passing through the Drake Passage bringing strong winds, low cloud and extensive precipitation. However, as these lows move to the east of the area they can be affected by south or south easterly winds which can bring cold, showery conditions from the Weddell Sea. Lee cyclogenesis events occur occasionally to the east of the Antarctic Peninsula

Surface wind and the pressure field

Stations on the western side are strongly affected by the climatological low–pressure in the Bellingshausen Sea and have predominantly north to northwesterly winds. Esperanza is reported to be prone to strong winds coming from the northeast that at times exceed 55 m s^{-1} (~108 kt).

The eastern side of the peninsula has winds that are predominantly from the south to southwest and reflect the barrier wind flow on the eastern side of the Peninsula. However, on a high proportion of occasions winds from the northwest are experienced as depressions enter the Drake Passage from the west. Marambio often receives strong winds which can cause problems for planes landing at the airstrip. The summer season (November – March) wind rose for Marambio is shown in Figure 7.3.5.4.1. in Appendix 2 below.

Upper wind, temperature and humidity

The nearest radiosonde station is Bellingshausen on King George Island and these observations are used in the forecasting process. Upper–air conditions are forecast using prognoses obtained from Buenos Aires or other centres.

Clouds

The tip of the Antarctic Peninsula is a very cloudy region as a result of the many depressions in the area and extensive frontal and non–frontal cloud. Marambio reports about 70% cloud cover throughout the year, which is probably typical for the region.

As indicated earlier, frontal cloud band arriving from the northwest are a major factor on the western side of the peninsula, but cloud can also arrive from the west. When a low-pressure centre is located over the Antarctic Peninsula or the western Weddell Sea a cold, showery airstream can affect the area with convective cloud being present.

At stations such as Marambio the many depressions in the Drake Passage bring extensive cloud, but less cloudy conditions are also experienced during the brief periods when anticyclones are present in the area or when drier continental air masses arrive from the south. At Marambio significant protection from low cloud in west or north–westerly winds is afforded by the high ground of the Peninsula. However, a veer to the north or north east may well bring in extensive low cloud.

Visibility: fog

Fog can be a problem at all the stations in this area since relatively warm, moist airmasses can be advected southwards over the cold ocean. The area of the strong gradient in sea surface temperature across the Antarctic Circumpolar Current is particularly prone to fog on occasions and this can affect the more northerly stations. However, the generally colder conditions on the eastern side of the Peninsula Visibility make fog a great problem in this area than to the west. Visibility is very variable at Marambio with good visibility being experienced when continental air masses arrive over the station, but also extensive fog being reported. When the station is to the south west of a depression, low cloud may produce fog on the airfield.

Surface contrast including white–out

The large amounts of cloud across the area can give poor contrast on occasions but the extensive areas of exposed rock improve matters towards the end of summer.

Horizontal definition

Not generally a problem across the area.

Precipitation

This area has some of the greatest amounts of precipitation in the Antarctic with over 1 m water equivalent being recorded. However, conditions are quite different on the eastern and western sides of the Peninsula. To the west the area is exposed to the full force of the many depressions and these bring extensive and frequent precipitation. This can be in the form of rain or snow at any season, although snow (rain) is obviously more common in winter (summer). Orographic uplift gives greater precipitation amounts at higher elevations.

   The stations on the eastern side of the Peninsula generally get less precipitation since they are in a rain/snow shadow region. However, northeasterly flow can bring relatively warm air and moderate/heavy falls to the area. Lee cyclones can also give significant falls.

Temperature and chill factor

Temperatures in this area are the highest in any part of the Antarctic and are above freezing point for extensive periods in summer. Mean January temperatures at O'Higgins are often above freezing and were $+2^{o}$C in the warm month of January 1963. On other occasions in summer they can average around -1°C.

   The colder temperatures on the eastern side are typified by Marambio where the mean monthly temperatures range from -1.9ºC in December and January to -16.3^{o}C in July, with the annual mean temperature being -9.2^{o}C. However, in summer the temperature can rise to +10 C or higher.

   Primavera has reported a maximum temperature of 13ºC giving an idea of the warm air masses that can affect the area.

Icing

The highly variable temperatures and the availability of large amounts of cloud liquid water make icing a potential problem in the area. It can be forecast using a knowledge of tropospheric temperatures from a model or radiosonde ascent and cloud information from satellite imagery.

Turbulence

The strong winds experienced on occasions at Marambio can give severe turbulence as aircraft approach the runway.

Hydraulic jumps

Hydraulic jumps have not been reported at stations in this area.

Sea ice

In summer the ocean around Marambio is covered in loose pack ice drifting northwards in the prevailing ocean current. However, sea ice is less of a problem on the western side of the peninsula.

Wind waves and swell

Wind waves and swell can be predicted using the output of wave models, which is available on the GTS.

7.3.6   The West–Central Section of the Peninsula

7.3.6.1   Orography and the local environment

The west–central region of the Peninsula covers the low–lying area on the west–facing side of the Antarctic Peninsula. The research stations are located on the many islands in the area or on the coast of the Peninsula itself. The stations covered in this section are:

- *Akademik Vernadasky* (Ukraine–formerly UK Faraday Station) (65° 15´ S, 64° 16´ W; 7 m AMSL) is located on the Argentine Islands (Galindez Is.). The Argentine Islands are a group of small islands separated from the Antarctic Peninsula by the 7 km wide Penola Strait. The Argentine Islands are ice–capped and do not rise more then 50 m above sea level. The largest Galindez Island is about 1.5 km long by 1 km wide where station Akademik Vernadsky is situated on Marina Point at the northwestern end of the island. The station area is mainly sheltered by an ice shelf from the cold southerly winds and more exposed to northerly winds from the Pacific. There are a lot of ice–free areas, pools of open water near the station and waterfalls from the rock cliffs and ice shelf during the summer.
- *Almirante Brown* (Argentina) (64º 54´ S, 62º 52´ W, 10 m AMSL). Located at Paradise Bay on the West Antarctic Peninsula.
- *Palmer* (USA) (64° 46´ S, 64° 03´ W, 15 m AMSL). Located on Anvers Island in the Palmer Archipelago slightly outside the Antarctic Circle.*Matienzo* (Argentina) (64° 50´ S, 60° 07´ W; 32 m AMSL).*Melchior* (Argentina) (64° 20´ S, 62° 59´ W; 7 m AMSL).
- *Yelcho* (Chile) (64° 52´ S, 63° 35´ W, 10 m AMSL). Located on the southern shore of South Bay on Doumer Island, Palmer Archipelago.
- *Presidente Gabriel Gonzalez Vidiez Station* (Chile) (64.8199º S, 62.8633º W), is located on the western side of the Antarctic Peninsula.

7.3.6.2   Operational requirements and activities relevant to the forecasting process

The requirements/activities at the various stations are:

- *Vernadasky* is a year–round station. The Ukrainian Antarctic Center maintains year–round scientific research programmes at the station Akademik Vernadsky, where the longest series of meteorological observations (since 1947) in the Antarctic Peninsula region have been carried out. Forecasts are required for station activities and boating operations.
- *Almirante Brown* is a summer–only station.
- *Palmer* is an all–year station. A wide range of research activities take place on the station, including meteorology and life sciences. There is an unprepared snow skiway at the station (Figure 7.3.6.2.1) which runs almost due east–west, with the western end at 101 m AMSL and the eastern end 128 m AMSL. The strip is often unusable from the end of December to March due to melt. A map of the airstrip is shown in Figure 7.3.6.2.1. There are no forecasters located at Palmer.
- *Matienzo* is a summer–only base.
- *Melchior* is a summer–only base.
- *Yelcho* is a summer–only refuge.
- *Presidente Gabriel Gonzalez Vidiez* is a summer–only station.
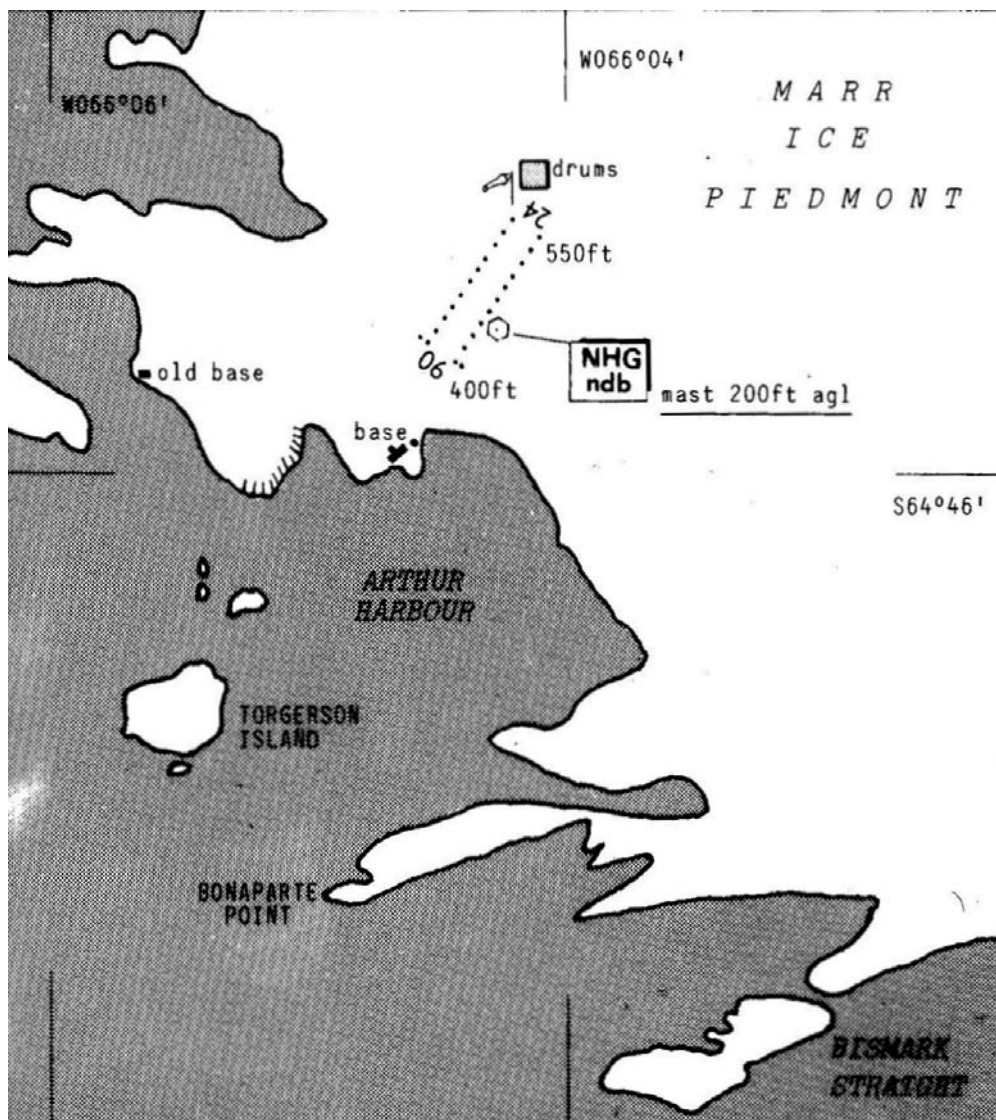
Figure 7.3.6.2.1   A map of the Palmer skiway.

7.3.6.3   Data sources and services provided

- *Vernadasky.* There are always at least two professional meteorologists over–wintering at the station. During the summer they are joined by another two meteorologists from the next expedition and a few meteorologists from the Ukrainian research ship on occasions. A Modular Automatic Weather Station (MAWS) is installed at the Akademik Vernadsky for continuous weather measurements. MAWS reads the meteorological sensors every 5 seconds and writes averaged and extreme values to a file every 5 minutes. The surface meteorological observations are taken every three hours and at 12, 18 and 00 UTC are sent by HF radio to Rothera where they are transferred to the World Meteorological Centre for use in the analysis and forecasting process. Meteorological measurements and observations for aircraft and vessels are available from Akademik Vernadsky on request. Since surface and forecast weather charts from the Chilean Weather Center are regularly received at the station via radio modem, some short–term forecasts are also available from Akademik Vernadsky.
- *Almirante Brown .* No specific information on forecasting has been obtained.
- *Palmer.* There is a meteorological observing programme at Palmer which provides 6 hourly surface observations that are put onto the GTS. The observations are collected by various base personnel, such as the doctor or communications staff. HRPT and DMSP satellite imagery is collected on the station with the data being archived and returned to the US on tape. Continent–wide isobar charts from the AMRC at the University of Wisconsin are received on a daily basis. There is no weather forecaster at the station.
- *Matienzo, Melchior,Yelcho and Presidente Gabriel Gonzalez Vidiez* are all summer–only bases/refuges.

7.3.6.4   Important weather phenomena and forecasting techniques used at the location

General overview

This area with its location on the western side of the Antarctic Peninsula has a relatively mild sub–Antarctic climate and comes under the influence of many synoptic–scale lows in the circumpolar trough. The weather here is generally overcast with frequent snow/sleet caused by west to north–westerly winds associated with depressions in the South Pacific/Bellingshausen Sea. Clear sky conditions mainly result from high–pressure ridges of the subtropical anticyclone in the summer and the Antarctic continental anticyclone in the winter. With the large amount of water present during the summer, fog can be a problem for navigation and flying operations.

Surface wind and the pressure field

Climatologically there is low pressure in the Bellingshausen Sea and winds from the Northwest, however, the complex orography of the region means that the winds experienced at the stations can be quite different. For example, because of the effects of orography, the winds at Akademik Vernadsky tend to be from the north or south. Surface winds from the NWP systems should therefore be used with care. However, changes of wind direction from

north to south and vice versa can be predicted once the evolution of the synoptic flow is estimated.

As would be expected, the prevailing northerly winds usually bring mild, moist air southwards, with southerly winds tending to bring dry, cold air northwards. However, returning maritime air on a southerly or returning continental air on a northerly can occur. Returning continental air from the north can bring improving conditions southwards down the western side of the Peninsula.

The average wind speed measured in the Argentine Islands area is about 3 m s^{-1} (~6 kt) during the summer and rises to 5–6 m s^{-1} (~10–12 kt) in winter time. But gusts can reach 20 m s^{-1} (~40 kt) in the summer and exceed 30 m s^{-1} (~60 kt) with a few hours of gale in the winter months. Usually high winds correspond to deep depressions with active atmospheric fronts rapidly moving from the west–northwest. At the same time calm weather is not rare in the region and is observed on up to 2–3 days per summer month, usually corresponding to a ridge of high pressure over the Antarctic Peninsula.

Upper wind, temperature and humidity

With no radiosonde data available for the region upper–air conditions are predicted using the output of numerical models.

Clouds

Overcast weather dominates this area with the Argentine Islands having 20–25 days per month of overcast conditions year–round with only a few days a month with clear sky. On average, about half of the sky is obscured by low cloudiness, mostly stratocumulus, stratus and nimbostratus. Due to the complex orography, quite low stratus (60–150 m (~200–500 ft)) forms over some places whilst it may be completely clear in others. Multi–layered cloud with precipitation is usual for the region when fronts arriving from the north and north–west are passing over. Sometimes fronts can cause cloudiness lowering to the surface and visibility falling to fog limits.

Cloud is forecast based on satellite imagery and a knowledge of the expected changes of airmass as determined from the NWP output.

Visibility: blowing snow and fog

As in the rest of the Peninsula, visibility is usually good, although fog does occur in the Argentine Islands 2–5 times per summer month (November–April) and can be a problem for navigation and flying activities. The formation of fog is aided by the large areas of open water, coupled with the areas of exposed ice. Fog over the Lemaire Channel, French Passage and Penola Strait tends to be rather reluctant to clear in light winds, particularly if temperatures are around zero or above and melt pools have developed on the ice shelves of the islands. Visibility can be under 1,000 m (~3,300 ft) up to 10–12 days per winter months due to snowfalls and blowing snow.

Surface contrast including white–out

Surface contrast is important mainly for field parties on the islands and the Peninsula, but is not a big problem due to many rocks free from the snow and ice all the year round. Contrast often improves as the summer progresses and more rocks are on the surface.

Horizontal definition

Mainly important for aircraft landing near to Palmer Station on Anvers Island. Predicted based on a knowledge of the forecast cloud amount and type.

Precipitation

Precipitation is produced by depressions and their associated fronts arriving from the north and north–west. The annual total at the Argentine Islands varies from 200 to more than 600 mm. Precipitation is usually in the form of snow or sleet, although rain is quite usual for the summer time and has been reported a few times for the winter. Precipitation of about 40–60 mm is usual for summer months with extreme over 100 mm. The latter mostly due to deep depressions from the South Pacific which determine the weather over the whole Peninsula for 5–7 days and bring heavy precipitation. Although large depressions west of the Peninsula often do not produce any significant precipitation at the Akademik Vernadsky, snow often occurs when the depression is filling and a relatively light pressure gradient develops with snow falling from shallow stratocumulus clouds.

Temperature and chill factor

Temperatures at Argentine Islands are usually within the range –2ºC to +3ºC during the summer months and about 10ºC colder in the winter time. Annual average temperatures are within –3ºC to –5 C with extreme maximum temperature warmer than +10º C and minimum colder than –40ºC. Actually the latter was observed in the 1950s and in the last few years minima of temperatures were much warmer and under –30ºC. Accounting for the wind chill factor above, the equivalent temperatures can be about 5ºC colder in the summer time and 10–15ºC colder in the winter due to more severe winds.

      Temperature forecasts tend to be based on continuity and a knowledge of expected changes of air mass.

Icing

With the large amounts of water droplet cloudiness over the region, icing of airframes can be a problem. The same situation can occur in fog for a vessel when supercooled water droplets collide with the surface and turn immediately to clear ice. Although when it occurs it is usually light.

Turbulence

As in other parts of the Peninsula, turbulence mostly can be regarded as being orographically induced. Orographic clouds (altocumulus lenticularis (Ac)) are observed about 4–5 times a month, which points to the presence of mountain waves over the Peninsula.

Hydraulic jumps

Hydraulic jumps have not been reported in this area.

Sea ice

During the last few years sea ice was driven from the Argentine Islands area in December–January and did not form again until April–May. But many big icebergs (20–50 m (~60–160 ft)), growlers, bergy bits and brash ice are observed around Argentine Islands in summer.

Wind waves and swell

Not relevant at this location.

7.3.7   Marguerite Bay/Adelaide Island

7.3.7.1   Orography and the local environment

The Marguerite Bay/Adelaide Island area is on the western side of the Antarctic Peninsula at a location of approximately 67º S, 68º W. Adelaide Island itself rises to a height of approximately 1,500 m (~4,900 ft) in elevation and provides significant shelter for the area to the east and the northern part of the bay (Figure 7.3.7.1.1 shows Marguerite Bay).
        Stations in this area are:

- *Teniente Luis Carvajal* (Chile) (62° 45´ S, 68° 54´ W), summer–only base which is located at the southern end of Adelaide Island.
- *Rothera* (UK) (67° 34´ 19″ S, 68° 7´ 37″ W; 16 m AMSL), all–year station and is located at Rothera Point on the southeast part of Adelaide Island.
- *San Martin* (Argentina) (68º 07´ 47″ S, 67º 06´ 12″ W; 5 m AMSL), all–year station which is located on Debbenham Island.

7.3.7.2   Operational requirements and activities relevant to the forecasting process

- *Rothera* is the centre for British flying operations in Antarctica and during the summer four Twin Otter and one Dash–7 aircraft are based at the location. The Twin Otters are used to deploy and recover field parties within the Peninsula area. The Dash–7 has the primary function of providing an air bridge between the Falkland Islands and Rothera, but is also used to carry fuel south to the Sky Hi/Sky Blu location (see Section 7.3.9 below). Aviation forecasts are required each day for the Twin Otters and for the Dash–7 as necessary. The British Antarctic Survey has two ships that operate around the Peninsula and Weddell Sea on re–supply activities and on research cruises. Marine forecasts are provided for the two vessels on a daily basis by the forecaster at Rothera.
- At *Carvajal* there is a skiway located 1,600 m from the base at an elevation of 302 m (~990 ft). The station is operational from October to March and forecasts are required for Twin Otter air operations here as well as general base activities.
- *St Martin Station* uses Twin Otter aircraft from a sea ice runway 2 km from the base.
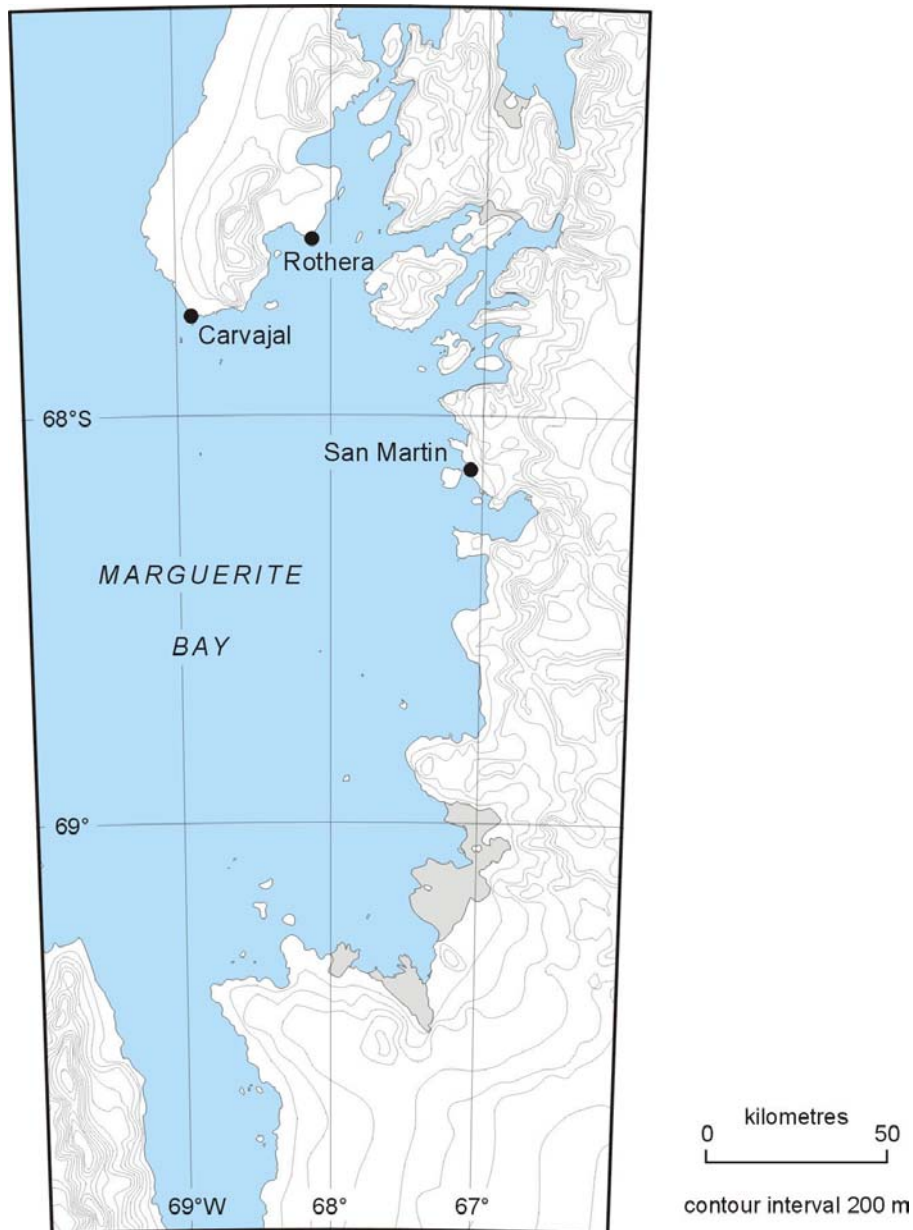
Fig 7.3.7.1.1   Map of Marguerite Bay area.

7.3.7.3   Data sources and services provided

- At *Rothera* there is an Inmarsat link to the BAS headquarters in Cambridge and analyses/forecast charts from the UK Met. Office model are transferred twice a day. The link is also used to obtain observations from the GTS. An HRPT satellite receiver is located at Rothera providing about 13 passes of AVHRR imagery each day. Reports from AWSs around the Peninsula are also extracted from the HRPT data stream. Surface analyses are prepared manually for 0000 and 1200 UTC each day and occasionally for 0600 and 1800 UTC as required. These cover the Peninsula, the Weddell Sea and the eastern Bellingshausen Sea.
- Weather forecasts for *Carvajal* are obtained from the Meteorological Antarctic Center at Frei Station. Satellite imagery is available as well as wind, synoptic and significant weather charts. A forecaster is available on site from October to March and forecasts are available on request. The surface meteorological observations from

Carvajal are not put on the GTS.

- *St Martin* operates a surface meteorological programme and the observations are put on the GTS.

7.3.7.4   <u>Important weather phenomena and forecasting techniques used at the location</u>

General overview

Because of the prevailing northerly wind the area has a relatively mild climate and in summer daytime temperatures usually rise a few degrees above freezing. Winter temperatures can be very variable with rain even occurring during periods when mild maritime airmasses cover the area.

Marguerite Bay is frequently affected by lows moving eastwards from the Bellingshausen Sea with the systems becoming slow–moving as they come up against the barrier of the Antarctic Peninsula. Large synoptic–scale weather systems are generally handled well by the models, although the orography of the Peninsula is not well represented in the model. However, it does recognise it as a barrier and is reluctant to move depressions across the Peninsula but will instead develop a new system on the Weddell Sea side. Depressions over the Bellingshausen Sea will often move east–southeast to become slow–moving near Alexander Island where they steadily fill, although areas of snow/showers can still be generated by these old lows, even when in their death throes and leave a lot of cloud to the west of the Peninsula.

Mesoscale lows are not a frequent occurrence in the area but some lows may approach in a re–curved continental airmass arriving from the northwest. However, some of the heaviest and most persistent precipitation in summer has come from mesoscale systems, which on more than one occasion produced significant snowfall at Rothera such that runway clearance was necessary. Obviously the global model cannot pick up or develop these small scale systems but the model has often hinted at the areas where these systems may develop by producing locally increased thickness gradients poleward of the main polar front and small thermal troughs, which at first may appear to be almost random drawing of the thickness lines, particularly in the area around the southern Peninsula. Experience would suggest that these small thermal troughs should not be ignored as several mesoscale systems have developed in association with them. Once the likely area of development has been identified then confidence in a forecast can increase if cloud development is seen on satellite imagery. Without these hints from the model it is almost impossible to say which cloud on the satellite images will produce precipitation.

Most large–scale fronts are relatively weak but sometimes move with surprising speed as they approach from the west. Some large–scale fronts do give enough precipitation to reduce visibility and cloud base enough to affect aircraft operations. Although fronts will move across the Peninsula, they have, on several occasions, left a band of cloud on the western side which has prolonged the precipitation and delayed frontal clearance by several hours. The delayed frontal clearance can sometimes allow the next front to reach the Peninsula before the previous one has cleared. On the other hand, some fronts do clear readily. Further research needs to be done to determine which fronts are likely to clear quickly and which will leave a residual band of cloud and precipitation on the west side of the Peninsula. The fronts that are likely to leave a residual band of cloud and precipitation on the western side of the Peninsula are probably those cold fronts that are immediately followed by anticyclonic development.

Surface wind and the pressure field

At Rothera winds of any significant speed tend to be generally northerly or southerly, with northerly (340–040º) being the most frequent direction. The wind speed is often stronger with northerlies than the pressure gradient as drawn on the charts might suggest. There may be two reasons for this. Firstly, funneling through the Gullet, or secondly, with pressure falling from the west and the Peninsula orography acting as a barrier to air movement, the pressure gradient between the mountains of the Peninsula and Adelaide Island may become stronger than indicated by the large–scale pressure field. This latter factor seems to be a frequent occurrence when the pressure gradient suggests a west or northwesterly wind the wind direction can often be directly from the north.

Even with a south–westerly wind suggested by the pressure gradient, the surface wind might well be north or north–easterly. On occasions cloud at 300 m (~ 1,000 ft) has been observed to move from the north–east, in the opposite direction to the gradient wind. On other occasions the wind has been observed to increase inexplicably from the north north–west to 10–15 m s^{-1} (~20–30 kt) with gusts 15–20 m s^{-1} (~30–40 kt) and persist for some hours. On these occasions the gradient was very light with aircraft confirming only 5 m s^{-1} (~10 kt) from the north west at 2,000ft. The local orography does not seem conducive to a katabatic wind and at the present time no satisfactory explanation can be offered for this phenomena. North to north–east winds often spring up unexpectedly when the gradient would not merit the actual wind speed. The wind can die again just as suddenly. This is probably due to subtle changes in the wind direction causing funnelling due to the local orography. Strong easterly winds can occur at Rothera, but are not common. On one occasion the wind was light and variable but picked up from the east to 12–15 m s^{-1} (~25–30 kt), gusting 19 m s^{-1} (~8 kt) in the afternoon. This may have been a Foehn wind that developed as the result of warm air being advected south down the eastern side of the Peninsula by a slow–moving depression to the north. On the second occasion a small low was centred immediately to the north north–west of Rothera.

The wind speed and direction at Rothera is largely dependent of the synoptic–scale circulation, although in some areas it can be heavily influenced by orography, even with quite strong pressure gradients. At Rothera, strong winds come mainly from the north, although the pressure field usually indicates a northwesterly or a westerly wind direction. With easterlies or westerlies, moderate turbulence can be experienced over the south of the runway.

During the preparation of the surface pressure analyses the frontal positions and low centres are determined from satellite imagery but due to the complete lack of synoptic data to the west a great reliance is placed on the model's analysis of the pressure field in that area. As in temperate latitudes, the model will pick up most of the major synoptic systems and handle them quite well but systems on the mesoscale are often missed but can be identified and their movement and development/decay followed on satellite imagery. The model also smoothes out troughs and occasionally even misses quite large systems because of the lack of data in these latitudes. It seems to perform better in slow–moving situations. In summer the model's forecast pressures for Rothera are often, on average, too high. Some fast–moving depressions seem to be moved too slowly by the model. The model wind fields are mainly reliable, but south of 70º S they have to be used with care.

Care needs to be taken in the preparation of the surface analysis with regard to reported winds, as in a number of cases they may be affected significantly by local orography and may not be representative of the large–scale flow produced by the synoptic pressure field.

Generally speaking northerly winds bring mild, moist air southwards whereas southerly winds tend to bring dry, cold air northwards. However, a lookout needs to be kept for returning maritime air on a southerly or returning continental air on a northerly.

Needless to say, winds are heavily influenced by the local orography and it is almost impossible to accurately forecast winds for a particular locality without the detailed local knowledge and experience. Hence in field party forecasts only general winds can be given, based on the synoptic flow. Indeed for deep field parties, no attempt is made to predict winds over the continent, not only because of the orography but also because of the great uncertainty surrounding the likely pressure field in these areas. However, careful analysis of the high resolution satellite images for these areas may reveal wave effects in the cloud sheets and also cloud movement which will give an indication of the current wind.

Katabatic winds are common, particularly down the numerous glaciers. Foehn winds are less common but do occur. Normally the cold air on the eastern side of the Peninsula is prevented from reaching the west due to the orography of the Peninsula. However, Schwerdtfeger suggests that even in these conditions a Foehn wind can develop down western slopes, provided that the pressure difference across the Peninsula is at least 8 hPa and this having been maintained for 12 hours. One Foehn wind has been observed under different circumstances i.e. a depression became slow–moving near the tip of the Peninsula, in itself an uncommon event as the flow at that latitude is usually zonal, advecting warm and less dense air southwards down the eastern side of the Peninsula, resulting in a quite strong wind developing down the western slopes, helped by the general easterly gradient across the Peninsula.

Upper wind, temperature and humidity

For forecasting at Rothera these fields are usually taken directly from the UK Met. Office model fields and used to predict the winds at the aircraft flight levels. Adjustments to the winds are made in the light of the satellite imagery.

Clouds

The Rothera airfield is generally well protected from very low cloud by the high mountains on all sides. When major frontal systems cross the airfield a combination of high winds and the shelter effect generally keeps the cloud base above a level where it would affect aircraft operations. Pilots have often reported heavy precipitation/worse visibility and lower cloud base in Marguerite Bay than at Rothera.

Orography plays a major part in the generation of cloud. The only way detailed cloud forecasts can be provided is by study of the high resolution imagery available from the HRPT satellite system and using a nowcasting approach combined with knowledge of the larger scale synoptic developments. This becomes particularly important when aircraft are flying to areas where no one is on the ground and decisions of go or wait have to be made based on satellite imagery interpretation.

The wave pattern apparent in cloud sheets indicates lenticular clouds, which can be a very valuable guide to where turbulence is present.

Cloud top heights are derived from the cloud top temperature facility on the HRPT satellite system. The technique used is to compute the temperature difference (T) between the surface and the cloud top and divide this by a mean lapse rate of 0.6ºC per 100 m e.g. with a temperature difference of 12ºC the height is taken to be 2,000 m (~6,500 ft). The pilots confirm that heights computed by this method are generally correct.

Visibility: snow and fog

Visibility in the central Peninsula area is usually good because of the lack of pollution sources, but mist and fog do occur when the wind velocity is low and a moist maritime air mass stagnates over the area. Visibility is most often reduced by precipitation. Moderate to heavy precipitation tends to reduce the visibility. Advection fog has been observed to form over the sea near to Rothera and drift over the runway from the south and west.

Because of the extremely good visibility, the judging of distance is very difficult with mountains and islands appearing much nearer than they actually are.

In this central part of the Peninsula fog will form during periods of light winds and clear skies when maritime air has been advected from the north and then stagnates. Fog can also occur in a returning maritime airmass from the south (unlike a true southerly continental).

Visibility is predicted for the ships in very much the same way as for any other ocean area, taking into account the sea surface and air temperatures, wind speed and continuity.

Visibility can be reduced markedly by blowing snow at the beginning and end of the season, but falling precipitation is the main reason for reduced visibility when the snow around the station melts. The worst visibility and cloud base problems seem to be in light airs. Once the sea ice melts, there is available moisture from the surrounding water to modify the air in stagnant conditions. Sometimes there can be a day of sunshine in a col or a ridge, before low cloud or fog drifts across the airfield. The low cloud or fog can sometimes be detected on the satellite imagery in Marguerite Bay before it reaches the Rothera airfield, although you need to look carefully at the channel 3 imagery with the sun up. Fog is not uncommon over the sea when maritime/returning maritime air stagnates under clear skies, however it does seem reluctant to advect onto the runway, even with a southerly breeze, although this cannot be relied upon. When the runway direction is 180° on these occasions the met tower wind was often westerly.

Surface contrast including white–out

Surface contrast is usually good at Rothera due to the presence of a crushed rock runway.

Horizontal definition

Horizontal definition is generally good due to a backdrop of mountainous orography.

Precipitation

Much of the precipitation brought to the Peninsula by large synoptic–scale features is light as a result of the frontal systems being weak and the cloud relatively thin. In some seasons most of the heaviest precipitation events at Rothera have been associated with mesoscale features, some of which were local to Adelaide Island. However, in other summer seasons there have been very few mesoscale disturbances over the station. Major frontal systems can bring moderate or heavy precipitation, although heavy precipitation is rare. Precipitation can often take the form of rain during the summer months. Precipitation in the form of showers is relatively common. In unstable airmasses convection is often triggered by orographic lifting

rather than surface heating. At Rothera the frequency of convective activity can be seen by the relatively frequent occurrence of cumulus and stratocumulus cloud.

Precipitation over the Antarctic Peninsula is most frequent in the spring and autumn, while summer and winter are relatively drier. Rain can occasionally occur in winter in this area. The only real guide to precipitation type is the 1000-500–hPa thickness field. Values as high as 540 dm were predicted by the model for Marguerite Bay on one occasion and although that value cannot be verified, continuous moderate rain did occur and hence it is likely that thickness values were abnormally high.

Most solid precipitation is in the form of snow flakes although on the odd occasion precipitation has been in the form of snow grains. Light snow can fall out of cloud as thin as 300 m (~1,000 ft). This seems to mainly occur in light wind situations.

Temperature and chill factor

Temperature is the least important parameter as far as operations are concerned, but it is an element which can fluctuate by a surprising amount. Diurnal variations at Rothera in mid–summer, in sunny conditions, are of the order of 4–5ºC. Advection, of course, also contributes to temperature change and most of the temperature forecasting is done subjectively based on airmass type.

Icing

The cloud below cirrus levels is composed of water droplets (often supercooled) and ice crystals. Hence airframe icing is common, but because of the low temperatures and hence generally low water content of the cloud most icing seems to be light. However, moderate icing is not uncommon. Although the –20º C isotherm is often used in temperate latitudes as the limit for moderate icing, anything colder being regarded as producing only a light icing risk, it has been suggested that –30º C may be more appropriate in the Antarctic. Nevertheless, limited observational data would suggest that significant icing conditions can occur in conditions not normally associated with moderate or severe icing in temperate latitudes.

Turbulence

Turbulence is predicted using the model upper level winds and from noting the locations of the jet streams.

Hydraulic jumps

Hydraulic jumps do not occur in the vicinity of Marguerite Bay.

Sea ice

The occurrence of sea ice in Marguerite Bay is very variable on a year–to–year basis, making the initial access date via ship at the start of the Antarctic season difficult to predict. A lack of storms at the start of the season can delay the break up of sea ice.

Wind waves and swell

Wind waves are computed from the model surface wind speed, and fetch or duration. Swell has to be estimated using a knowledge of wind and wave conditions over the previous few days and the few available swell observations.
        Large swell can be experienced at Carvajal because of the station's exposed position and this can make access by ship difficult.

7.3.8   Fossil Bluff, King George VI Sound

7.3.8.1   Orography and the local environment

The northern part of King George VI sound lies between the high orography of the Antarctic Peninsula and that of the mountains of Alexander Island. It is therefore in a relatively sheltered position with winds being predominantly from the north or south. The southern end of the Sound curves round to the west and is more exposed to weather systems arriving from the west. The Sound is largely ice–covered with the ice shelf being up to 200 m (~ 650 ft) thick. However, there are some ice–free areas and pools of open water on the ice surface during the summer.

7.3.8.2   Operational requirements and activities relevant to the forecasting process

The British Antarctic Survey maintains a summer only forward field station and fuel depot at Fossil Bluff (71.3º S, 68.3º W) as an aid to the southward transport of fuel and field parties into the interior of the continent. During the summer there are always at least two staff on the station including, whenever possible, a meteorological observer who maintains the surface observing programme.
        Forecasts for Fossil Bluff are provided by the forecaster at Rothera when aircraft are passing through the station.

7.3.8.3   Data sources and services provided

The Fossil Bluff surface meteorological observations taken at 12, 18 and 00 UTC are sent by HF radio to Rothera for use in the analysis and forecasting process. No forecasts are available from Fossil Bluff.

7.3.8.4   Important weather phenomena and forecasting techniques used at the location

General overview

With its location on the western side of the Antarctic Peninsula, King George VI Sound/Fossil Bluff has a relatively mild climate and comes under the influence of the many synoptic–scale lows in the circumpolar trough. Often depressions to the west of Rothera will move east–southeast to become slow–moving near Alexander Island where they fill steadily, although areas of snow/showers can still be generated by these old lows, even when in their death throes and leave a lot of cloud to the west of the Peninsula. On occasions lows can move southwards down the western side of the Peninsula, producing 25–30 m s^{-1} (~50–60 kt) winds at Fossil Bluff, but these events are rare and the relatively sheltered position of Fossil Bluff to the east of the mountains of Alexander Island means that few low–pressure centres actually move over the station itself.

With the large amount of water present during the summer, fog can be a problem for the flying operations.

The narrow sound is not well represented in the current generation of NWP models so model output needs to be used with care and satellite imagery is an important tool in the analysis/forecasting process.

Surface wind and the pressure field

Because of the effects of orography, the winds at Fossil Bluff tend to be from the north or south and are therefore not representative of the large–scale flow produced by the synoptic–scale pressure field.

The prevailing northerly winds usually bring mild, moist air southwards, with southerly winds tending to bring dry, cold air northwards. However, returning maritime air on a southerly or returning continental air on a northerly can occur. Returning continental air from the north can bring improving conditions southwards down the western side of the Peninsula to Fossil Bluff.

The wind speed as measured at the accommodation hut may be different to that at the skiway. The wind is often a north north–westerly at the hut (where most of the observations are made) due to the flow down the Eros glacier. The direction is often more northerly and stronger at the skiway.

Upper wind, temperature and humidity

With no radiosonde data available for the region, upper–air conditions are predicted at Rothera using the fields from the UKMO model. These tend to be reasonable, although errors can occur in the strength and position of the jets.

Clouds

The distribution of low cloud is very variable due to the complex orography, with areas of quite low stratus 60–150 m (~200–500 ft) in some places whilst it may be completely clear in

others. Sometimes with extensive stratus over the Sound the skiway may be in the clear as it is approximately 200 ft above the Sound. Stratus seems to be more extensive in the middle to late summer, which is probably due to the formation of melt pools in the Sound. When the Sound is frozen there is less available moisture, so stratus has to be advect in, rather than form *in situ.*

Fronts arriving from the north can cause a deterioration of conditions in terms of cloud lowering to the surface and visibility falling to fog limits.

Channel 3 (3.7 μm) imagery is particularly valuable during the summer for the detection and tracking of low cloud/fog in the Sound.

Visibility: blowing snow and fog

As in the rest of the Peninsula, visibility in the Sound is usually good, although fog does occur and can be a problem for flying activities. The formation of fog is aided by the large areas of water on the ice shelf, coupled with the areas of exposed ice. Fog over the Sound tends to be rather reluctant to clear in light winds, particularly if temperatures are around zero or above and melt pools have developed.

Surface contrast including white–out

Surface contrast is important at Fossil Bluff because of the large amount of flying activity in the area. During the summer, observations of contrast are available for the skiway and the flags at its edge help during landing. Contrast often improves as the summer progresses with the development of large melt pools which take on a blue or turquoise colour.

Horizontal definition

Since the Sound is a floating ice shelf horizontal definition can be problem when aircraft are attempting to land. However, the observers at Fossil Bluff provide frequent reports of horizontal definition to the aircraft, especially when conditions are changing rapidly.

Precipitation

The Bluff is usually well protected from precipitation, and snow stake data suggests that the Sound generally has low precipitation. Large depressions near western Alexander Island often fail to produce any precipitation at the Bluff, although the northern half of the Sound may receive precipitation and low cloud. Some of the heaviest and most prolonged precipitation events have been associated with mesoscale features. Slow–moving fronts can also produce precipitation. A spell of northerlies with a slow–moving front to the west will advect low cloud and precipitation into Fossil Bluff. Precipitation is usually in the form of snow or sleet, although rain has been reported.

Although large depressions west of Alexander Island often do not produce any significant precipitation at the Bluff, snow often occurs when the depression is filling and a

relatively light pressure gradient develops with snow falling from shallow stratocumulus cloud.

Temperature and chill factor

Temperatures at Fossil Bluff are usually several degrees colder than at Rothera, but nevertheless get a few degrees above freezing on a number of days during the summer. The exposed rock surfaces on the sides of the Sound absorb a lot of radiation during the summer, resulting in extensive melting of the snow and 'rivers' running down many of the glaciers.

Icing

With the large amounts of water droplet cloud in the Sound, icing of airframes can be a problem, although when it occurs it is usually light. However, moderate or even heavy icing can occur on occasions. One severe icing event occurred between Sky–Hi and Fossil Bluff in the 1996/97 season when a Twin Otter reported quickly picking up 4–5 cm of clear ice as it descended towards the Fossil Bluff Skiway. The thickness chart showed a cold air mass (514 dm) over the Peninsula and there was a surface temperature of –14ºC. The thickness chart for 12 UTC 11 February 1997 indicated the invasion of a warm air mass from the northwest. This air mass moved over the colder and denser air in the lower levels introduced multi–layered clouds with precipitation. This precipitation formed in the warm air and fell as liquid droplets through the colder air below, so becoming supercooled. When these droplets collided with the aircraft (or surface) they turned immediately to clear ice.

Turbulence

As in other parts of the Peninsula, turbulence is predicted by analysis of the model upper level winds and especially from the locations of the jet streams. However, it is questionable whether we get true jet streams in this area and most turbulence can be regarded as being orographically driven. Mountain waves are not unusual in this area.

Hydraulic jumps

Hydraulic jumps have not been reported in the Sound.

Sea ice

Sea ice is only found at the two ends of the Sound and its location is determined from the HRPT imagery available at Rothera.

Wind waves and swell

Not relevant at this location.

7.3.9   Ski Hi/Ski Blu

7.3.9.1   Orography and the local environment

Sky–Blu and Sky–Hi are depots located near the Sky–Hi Nunataks. During the summer season a British forward field camp is set up to make use of the blue ice runway situated at Sky–Blu. The Sky–Hi depot is located some distance from the Nunataks and has been little used in recent years as operations have moved to Sky–Blu, using wheeled aircraft on the blue ice runway.

        The Sky–Blu blue ice runway (74º 51.14′ S, 71º 33.6′ W) is located very close to the Sky–Hi Nunataks, which are to the north of the runway (Figure 7.3.9.1.1). The area of blue ice is probably caused by the precipitation shadow of the high ground to the north and the scouring effect of winds enhanced by the local orography. The ground to the south of the runway drops away towards the Merrick mountains.

7.3.9.2   Operational requirements and activities relevant to the forecasting process

The British Antarctic Survey maintains a summer only forward field camp and depot at Sky–Blu to assist with transport of fuel and scientists into the deep field. A previous depot, called Sky–Hi, some 12 km away is now no longer used operationally. The blue ice runway at Sky–Blu is used, during the summer season, by wheeled aircraft, however, the diversion options available for a wheeled aircraft operating this far south are very limited.

        The blue ice runway has different operating criteria from the normal skiway used in Antarctica. On the blue ice wheeled aircraft can only handle quite low cross winds while taking off and landing and wind from any direction can make taxiing difficult. However, low contrast is less important when the blue ice is exposed. During the flying season drifting snow often covers the blue ice runway and this has to be cleared by hand and using light machinery before the runway can be used.

        A ski–way, for use by ski–equipped planes, is located some distance from the blue ice runway for use when the blue ice runway cannot be used.

        A small hut is located near the blue ice runway and is occupied by two or three staff during the summer. Staff with only basic training make basic meteorological observations in support of air operations here.
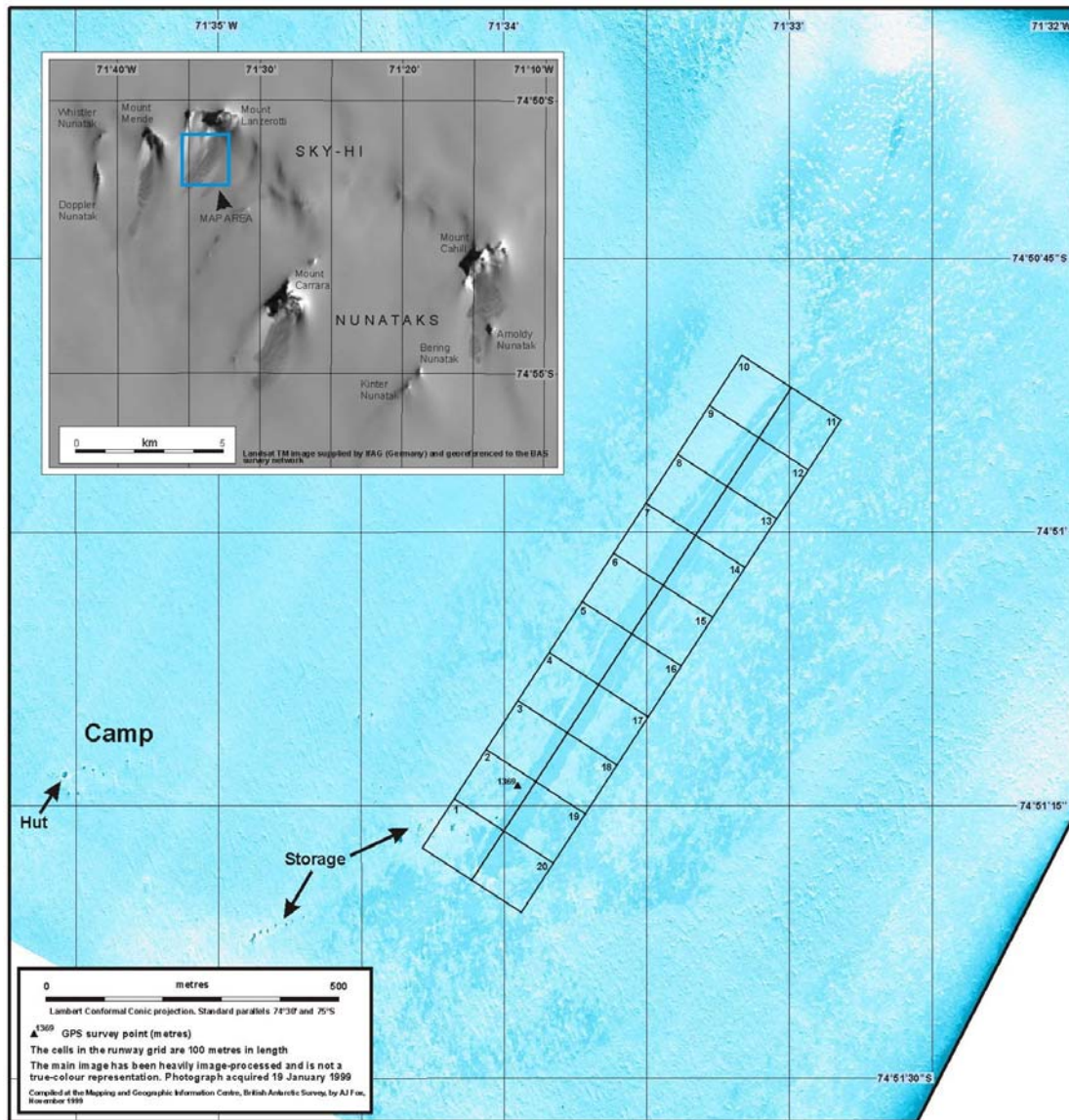
Figure 7.3.9.1.1 Map of the Sky–Blu blue ice runway and camp.

7.3.9.3   Data sources and services provided

Meteorological observations are only made at Sky–Blu in support of air operations. These are either passed to Rothera or to aircraft on route to Sky–Blu. An AWS, which feeds data into the GTS via ARGOS, is situated near the runway. No forecasts are available from Sky–Blu, although Rothera Station will issue forecasts for this area during the summer season.

7.3.9.4   Important weather phenomena and forecasting techniques used at the location

General overview

Sky–Hi nunataks are located at the base of the Antarctic Peninsula some 200 km from the coast. This means that synoptic–scale lows associated with the circumpolar trough are less

important at this site than at sites further north on the Peninsula. However, occasionally frontal system associated with slow–moving low–pressure systems near Alexander Island can give periods of low visibility and blowing snow.

These notes on weather phenomena and forecasting techniques are written for the Sky–Blu depot and the blue ice runway and are only applicable to the Ski–Hi depot in a general way. The Ski–Hi depot is further from steep orography, being about 1 km from the nearest nunataks.

Surface wind and the pressure field

Quite often orographic effects will dominate the weather experienced at Sky–Blu. The general surface wind is often defined by katabatic flow from the high ground to the north, while the local wind is controlled by the presence of the steep orography of the Ski–Hi Nunataks.

Forecasting the occurrence of a katabatic flow can be difficult in this location with so little *in situ* data available. In general katabatic flow is enhanced when the large–scale geostrophic flow is northerly. Also the katabatic flow tends to vary diurnally, being at a maximum during the morning and slackening slightly during the afternoon. Unfortunately, the katabatic wind often disregards even these simple rules.

The close proximity of the Ski–Hi nunataks means that the local wind is extremely difficult to forecast. The accommodation hut is some distance from and higher than the blue ice runway and the wind speed and direction may be different between the two sites.

Upper wind, temperature and humidity.

No radiosonde data are available for this region and so upper–air condition are predicted at Rothera using UKMO model fields. These tend to be reasonable although need to be used with caution this far south.

Clouds

The distribution of clouds at Sky–Blu is strongly controlled by the orography. Clouds are mostly stratiform and normally at least 300 m (~1,000 ft) above the station. Cloud is most prevalent during northerly winds when moisture is advected south from the coast. The high orography just to north of the blue ice runway tends to prevent the formation of lower cloud.

Low lying stratus does sometimes form in the low–lying areas to the south of the runway some 5 km away. The base, and sometimes the tops, of this stratus are often below the height of the blue ice runway.

Visibility: blowing snow and fog

Fog is rare at Sky–Blu as it is too far south and distant from the coast for there to be sufficient moisture for fog to form. Low cloud to the south of the runway can reduce the visibility to a few kilometres in that direction.

The major cause of reduced visibility at Sky–Blu is blowing snow. This can occur when the wind is greater than 7–10 m s^{-1} (~15–20 kt) although the exact threshold and the total flux

of blowing snow will depend on the state of the snow surface. Blowing snow can reduce the visibility to less than 100 m. Blowing snow can also effect flying operations by causing snowdrifts to form across the blue ice runway.

Surface contrast, including white–out

The presence of the blue–ice runway means that surface contrast is less critical at Ski–Blu for air operations, than at other sites in Antarctica. When the blue ice runway is clear of surface snow, wheeled aircraft can land in conditions that would normally be described as poor contrast. Wheeled aircraft can use the blue–ice runway if there is a thin (<50 mm) uniform layer of snow covering it. When the runway is in this condition it necessary for the contrast to be moderate to good before aircraft can land.

Horizontal definition

The presence of the nearby nunataks and the blue–ice runway means that horizontal definition is less important at this site than at other sites on uniform featureless ice sheets.

Precipitation

The precipitation at this site is very low as the site is in the precipitation shadow of higher ground to the north. What little snow that does fall blows away and the net accumulation is zero or negative which allows the blue–ice areas to form. Even a few kilometres further south, away from the direct effect of the nunataks, stake measurements show that the annual accumulation is only a few centimetres. Sky–Blu is too far south for rain ever to have been recorded.

Temperature and chill factor

The temperature at Sky–Blu is normally below −10ºC during the summer, although occasionally warm air pushing south will raise the temperature towards, but not above, zero.

Icing

The clouds found at Sky–Blu tend to be thinner and contain less liquid water than at sites further north on the Peninsula. Therefore airframe icing at Sky–Blu itself is not a great problem, although light icing may occur in some conditions. However, further to the north, closer to the coast, cloud liquid water is likely to be higher and icing could become moderate to heavy and this could affect flights to and from Sky–Blu.

Turbulence

As Sky–Blu is well south of the track of the jet streams most turbulence in this area will be driven by orography. The northern end of the blue ice runway is very close to a nunatak and turbulence can affect both take off and landing. This turbulence is very difficult to forecast, although observations of blowing snow flowing around the nunatak may give some idea of the presence of turbulence.

Hydraulic jumps

Hydraulic jumps have not been reported at Sky–Blu.

Sea ice

Not relevant at this location

Wind and swell

Not relevant at this location.

7.3.10   The Larsen Ice Shelf

7.3.10.1   Orography and the local environment

The Larsen Ice Shelf is on the eastern side of the Antarctic Peninsula and is an extensive area of floating ice.. Since the Peninsula extends to more than 2 km in height for much of its length the ice shelf is well sheltered from the many depressions to the west of the barrier. During the 1990s there has been a disintegration of the northernmost parts of the shelf with the Larsen–A and part of the Larsen–B sections collapsing (see Section 2.7.3.2 above).

7.3.10.2   Operational requirements and activities relevant to the forecasting process

There are no staffed stations on the Larsen Ice Shelf so the only forecasting requirement is for flights to the area in connection with research activities or those for maintenance of the AWS at 66º 58´ S, 60º 33´ W. With the AWS providing the only *in situ* observations for the area forecasts are made based on NWP fields and satellite imagery.

7.3.10.3   Data sources and services provided

As noted above, the only *in situ* observations for the Larsen Ice Shelf are from the AWS at 66º 58´ S, 60º 33´ W. The provision of good forecasts is therefore reliant on NWP output and satellite imagery.

7.3.10.4   <u>Important weather phenomena and forecasting techniques used at the location</u>

General overview

The climate of the Larsen Ice Shelf is much more continental than that on the western side of the Peninsula with temperatures several degrees colder than comparable latitudes to the west. The lower temperatures are partly a result of the frequent southerly, barrier winds which occur because of the blocking effect of the Peninsula.

Since many of the depressions approaching the Peninsula are blocked by this substantial barrier there are fewer depressions found here than on the western side. However, some lows do cross the Peninsula and a number of lee cyclogenesis events take place on the Larsen and over the ocean area to the east. Although few depressions cross the Peninsula, the fronts associated with many of the lows that become quasi–stationary on the western side do pass down the Peninsula and affect the Larsen.

Surface wind and the pressure field

The barrier winds are an important phenomena affecting the eastern side of the Peninsula (Schwerdtfeger, 1984). The barrier winds arise as a result of the piling up of cold low–level air, created over the Ronne and Filchner Ice Shelves and its advection towards the Peninsula on the climatological easterly winds which affect Antarctic coastal areas. The resulting thermal and pressure gradients create a surface wind parallel, in a generally southerly sense, to the mountain barrier of the Peninsula. Since the NWP models do not currently have a very good representation of the Peninsula the model pressure and wind fields should be used with care in this area. The surface wind direction in the area can often be determined from the cloud motion observed in sequences of satellite images if low clouds can be seen.

Upper wind, temperature and humidity

These fields are usually taken directly from the model fields and used to predict the winds at the aircraft flight levels if required. Adjustments to the winds can be made in the light of the satellite imagery.

Clouds

Climatologically there is less cloud over the Larsen than to the west of the orographic barrier, however, there can often be extensive high level cloud streaming off the top of the Peninsula, which can obscure the surface. The channel 3 images are particularly useful over the ice shelf in detecting water cloud over ice surfaces and can at times detect lower cloud beneath cirrus. There is often a coastal lead along the edge of the ice shelf which can be covered in cloud.

Visibility: snow and fog

Visibility is usually very good on the ice shelf but fog can occur, especially close to the coastal lead which can provide a source of moisture. As elsewhere across the Peninsula, precipitation is a major factor in reducing visibility, although moderate or heavy precipitation events are fairly rare in this area..

Surface contrast including white–out

The surface contrast on the ice shelf is usually better than in other parts of the Peninsula because of the smaller amount of cloud occurring. However, contrast can be poor if extensive low cloud cover is present. Contrast is predicted using satellite imagery.

Horizontal definition

Horizontal definition is very important on the ice shelf because of the featureless nature of the surface, causing problems to aircraft operations at times. Since the horizontal definition is affected strongly by the cloud cover satellite imagery is extremely important in predicting this quantity. The presence of clear water leads off the ice shelf can be an important element in enhancing the horizontal definition in these areas.

Precipitation

Mean annual precipitation on the Larsen ice shelf is about 0.5 m water equivalent per year, roughly half that found on the western side of the Peninsula. Virtually all the precipitation falls in the form of snow, with rain being very rare indeed. The frequent southerly barrier winds bring little precipitation and the heaviest snowfalls occur when relatively mild, moist air masses approach from the north or northwest. Such conditions can arise when a depression becomes quasi–stationary in the Drake Passage or north of the Weddell Sea.

Temperature and chill factor

Temperatures on the eastern side of the Peninsula are much colder than those on the western side since the area is effectively isolated from the maritime air masses brought southwards by the climatological low–pressure system over the Amundsen/Bellingshausen Sea. However, warmer air can reach the region when a low becomes slow–moving north of the Weddell Sea and air is advected around this system. Temperatures are predicted using the AWS observations and a knowledge of the air mass origins.

Icing

Satellite imagery indicates that cloud composed of water droplets (often supercooled) is quite common on the Larsen Ice Shelf so airframe icing can be expected fairly frequently. However, because of the low temperatures and hence generally low water content of the cloud most icing will be light.

316

Turbulence

Turbulence can be predicted using the model upper level winds and from noting the locations of the jet streams.

Hydraulic jumps

Hydraulic jumps do not occur on the bulk Larsen Ice Shelf but may take place at the western side, close to the mountains down the spine of the Peninsula.

Sea ice

The western Weddell Sea is the largest area of multi–year sea ice in the Antarctic and presents problems in navigation for even the most powerful ships. As discussed earlier, a lead is often present along the edge of the ice shelf because of the prevailing westerly flow. The location and movement of the sea ice is usually predicted from sequences of high resolution satellite imagery.

Wind waves and swell

Not relevant for this area.

7.4   **Ronne and Filchner Ice Shelves**

This section deals with the Ronne and Filchner Ice Shelves and, excluding the Antarctic Peninsula covers the area between about 85º W and 35º W. From west to east, some of the features and bases referred to in this section include:

- *The Haag Nunataks* near (77º S, 78º W);
- *The Ronne Shelf Depot* near (75.30º S, 57.41º W);
- *Berkner Island* near (80º S, 50 º W)

The above places are shown in Figure 7.4.1.
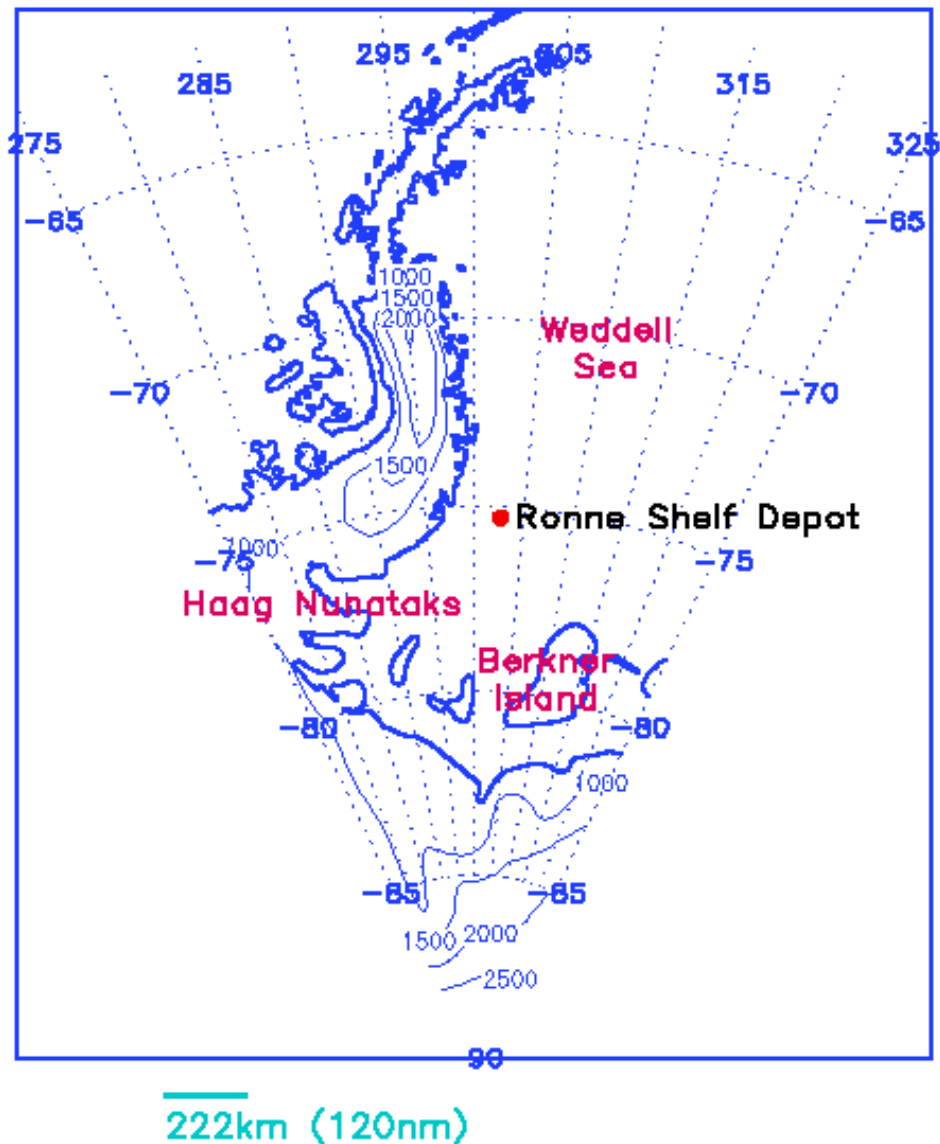
Figure 7.4.1   Sketch map showing some locations on and around the Ronne and Filchner Ice Shelves (contours in metres; the area is bounded by: 85º S, 65º S, 85º W and 35º W).

7.4.1   Berkner Island

7.4.1.1   Orography and the local environment

Berkner Island is located on the eastern side of the Ronne Ice Shelf and consists of an ice–covered island with two domes. South Dome (Thyssenhohe) has an elevation of 850 m (~2,800 ft), while North Dome (Reinwarthhohe) is lower at 700 m (~2,300 ft) elevation.

7.4.1.2   Operational requirements and activities relevant to the forecasting process

There are no staffed stations on Berkner Island itself. However, the area is important since there are major ice core drilling projects taking place on the domes of the island and accurate forecasts are required for the flights to deploy and collect the drilling parties at this location.

7.4.1.3   Data sources and services provided

No *in situ* observations are available for Berkner Island so forecasts are prepared based on NWP output and satellite imagery.

7.4.1.4   Important weather phenomena and forecasting techniques used at the location

General overview

Berkner Island is located close to the edge of the Ronne/Filchner Ice Shelf at the southern end of the Weddell Sea. Generally the area is sheltered from most of the major storms in the circumpolar trough by the high orographic barrier of the Antarctic Peninsula. However, a number of lows develop as lee cyclones to the east of the Peninsula and these can move southeastwards towards Berkner Island. In addition, when the upper level steering flow is from the north moisture–laden lows can move over the area from the South Atlantic giving some of the largest precipitation events experienced at this location.
        With the convergent, low level flow experienced on the shelf, because of the katabatic winds from the surrounding higher ground, a number of synoptic and mesoscale lows develop around Berkner Island. Many of the mesoscale systems tend to be found on the ice shelf and not on the island itself.

Surface wind and the pressure field

Climatologically the edge of the ice shelf is within the easterly flow regime that is found around much of the continent. However, offshore flow is common on many occasions, as can be seen via the coastal polynya that is often present over the southern Weddell Sea. During the winter months in particular there is a strong surface inversion on the shelf and there will be katabatic flow down from the top of Berkner Island onto the ice shelf.
        The many low–pressure systems around the island make the surface wind field more variable than on the high interior plateau.

Upper wind, temperature and humidity

These fields are usually taken directly from the model fields and used to predict the winds at the aircraft flight levels if required. Adjustments to the winds can be made in the light of the satellite imagery.

Clouds

Satellite imagery shows that cloud cover is rather variable around Berkner Island with periods of extensive, non–frontal cloud or cloud associated with low–pressure systems, alternating with cloud–free interludes. Throughout the year there is more cloud over the northern part of the island compared to the southern end. This is particularly true during the summer months when there is a plentiful supply of moisture from the coastal polynya at the edge of the ice shelf. Climatologically, the International Satellite Cloud Climatology Project suggests that there is about 25% (45%) cloud cover over the southern (northern) part of the island during the summer and 45% (60%) in winter. Satellite imagery indicates that the high, central part of the island is often cloud–free when there is extensive low cloud on the ice shelf.

Visibility: snow and fog

Visibility is generally good on the ice shelf but fog can occur, especially close to the coastal lead during periods of southerly flow. However, as indicated above, the fog/low cloud can often ring the island with the top being clear. As elsewhere, precipitation is a major factor in reducing visibility, although moderate or heavy precipitation events are fairly rare in this area.

Surface contrast including white–out

The surface contrast is rather variable around Berkner Island and, as with other locations depends on the amount of cloud present. Contrast will usually be better on the top of the island because of the tendency for this area to be cloud–free. Contrast is predicted using satellite imagery.

Horizontal definition

Horizontal definition is again very dependent on the amount of cloud present and will generally be better on the top of the island. Just north of the island the coastal lead can be very useful in finding a good horizon.

Precipitation

Ice core data indicates that the mean annual accumulation on Berkner Island is 15 cm water equivalent per year over South Dome and 21 cm on North Dome. All the precipitation falls as snow. The island receives some clear sky precipitation as well as precipitation from low–pressure systems and non–frontal cloud. Precipitation is forecast using a combination of model output and satellite imagery.

Temperature and chill factor

Annual mean surface temperatures on Berkner Island, deduced from 10 m snow temperatures, are –26.1ºC on South Dome and –24.1ºC on North Dome. The near surface temperatures are strongly dependent on the cloud cover, which can be predicted in the short term by the use of satellite imagery. When quasi–stationary deep lows are present in the Weddell Sea warm air can be drawn down the eastern side of the Weddell Sea affecting Berkner Island. The warmest temperatures are found when such a synoptic pattern persists for several days.

Icing

Icing can be a problem around Berkner Island because of the occurrence of cloud with supercooled water droplets. Icing is forecast using satellite imagery (especially channel 3 of AVHRR) and a knowledge of air temperatures determined from a model. When relatively warm air intrudes into the area icing can be moderate or severe because of the higher water content of the cloud.

Turbulence

Turbulence is predicted using the model upper level winds and from noting the locations of the jet streams.

Hydraulic jumps

Hydraulic jumps have not been reported around Berkner Island.

Sea ice

Not relevant for Berkner Island itself. However, the sea ice off the Ronne Ice Shelf and especially the presence of a coastal lead can have an impact on the weather over the island, as described above.

Wind waves and swell

Not relevant for this area.

7.4.2   Shelf Depot

7.4.2.1   Orography and the local environment

The Ronne Shelf Depot is an unstaffed British fuel depot on the edge of the Ronne Ice Shelf at 75.30º S, 57.41º W . British aircraft do not visit the shelf very often, but it is a useful depot and lay–up location for aircraft flying to/from Halley and Berkner Island in case they encounter severe weather.

7.4.2.2   Operational requirements and activities relevant to the forecasting process

Forecasts are required for the Shelf Depot area when aircraft are flying past on the way to/from Berkner Island and Halley.

7.4.2.3   Data sources and services provided

There are no staffed stations anywhere in the vicinity of shelf depot, although there is an AWS called 'Limbert' currently (January 2000) located on the edge of the shelf at 60º W, which can provide some *in situ* data. Otherwise forecasts are prepared based on NWP output and satellite imagery.

7.4.2.4   Important weather phenomena and forecasting techniques used at the location

General overview

Shelf Depot is located well south of the circumpolar trough and is therefore affected be few major depressions. However, some lows can track across the base of the Antarctic Peninsula and affect the area. In addition, a number of synoptic and mesoscale lows can develop on the shelf because of the general convergent nature of the low level wind field on the shelf, coupled with the baroclinicity that exists between continental air and more maritime air masses over the Weddell Sea.

Surface wind and the pressure field

As described above, the katabatic flow down from the plateau onto the ice shelf gives general convergent conditions with an outflow into the Weddell Sea. There is therefore generally southerly surface flow at Shelf Depot. This is also consistent with the veering of the wind in this general location from a coastal easterly to a southerly barrier wind up the eastern side of the Peninsula.

Upper wind, temperature and humidity

Since no *in situ* upper–air measurements are available on the Ronne Ice Shelf the main upper level parameters are estimated and forecast using model fields, adjusted in the light of satellite imagery.

Clouds

The Ronne Ice Shelf is often clear of low cloud, but large areas of shallow low stratus or fog are not uncommon. This cloud/fog is usually composed of water droplets and hence can be picked up on the AVHRR channel 3 imagery quite readily.

Visibility: fog

When a gap of ice–free ocean opens up between the edge of the ice shelf and the sea ice, sea smoke may occur and even develop into cumulus cloud. This is also an area for the development of fog if winds are light.

Surface contrast including white–out

Surface contrast can be poor on the featureless ice shelf when there is extensive cloud.

Horizontal definition

The lack of orographic features can make the determination of a horizon very difficult if stratiform cloud is present. Although the coastal lead just off the edge of the shelf can be very useful in finding a good horizon.

Precipitation

Moderate of heavy precipitation is very rare at the shelf depot because of the small number of deep, active depressions that cross the location. However, slight precipitation occurs on many occasions either as clear sky precipitation or from non–frontal cloud. All the precipitation falls as snow. About 30 cm water equivalent of precipitation falls at this location each year. Precipitation is forecast using a combination of model output and satellite imagery.

Temperature and chill factor

Annual mean surface temperature at Shelf Depot, deduced from 10 m snow temperatures, is about –20ºC . During the winter temperatures can be very low on the shelf as cold air drains from higher ground.

Icing

Severe airframe icing has occurred in low cloud/fog over the Ronne in the past, with a pilot reporting severe ice build up on descent through the cloud in just 3 minutes with temperatures of –20ºC .

Turbulence

Turbulence is predicted using the model upper level winds and from noting the locations of the jet streams.

Hydraulic jumps

Hydraulic jumps have not been reported near Shelf Depot.

Sea ice

A coast lead near the edge of the ice shelf is a common occurrence throughout the year. As discussed above this can have implications for the weather at Shelf Depot.

Wind waves and swell

Not relevant for this area.

7.4.3   Haag Nunataks

7.4.3.1   <u>Orography and the local environment</u>

Haag Nunataks are located on the Fowler Peninsula at the base of the Antarctic Peninsula and have an elevation in excess of 1,000 m. The British Antarctic Survey maintains a small unstaffed fuel depot here at approximately 77º S, 78º W . The area is also visited by glaciological field parties, who can be input by aircraft at this location.

7.4.3.2   <u>Operational requirements and activities relevant to the forecasting process</u>

Forecasts are required for occasional summer visits by aircraft to collect/input field parties.

7.4.3.3   <u>Data sources and services provided</u>

There are no staffed stations or AWSs anywhere near Haag. So all analyses and forecasts are prepared using satellite data and model output.

7.4.3.4   <u>Important weather phenomena and forecasting techniques used at the location</u>

General overview

Haag is located well south of the circumpolar trough so few very deep lows affect the area, although a number of less active systems cross the base of the Antarctic Peninsula from the Bellingshausen Sea. A number of old fronts with persistent cloud have been observed to affect the area.

Surface wind and the pressure field

The predominant wind direction is southwest to southeast, based on limited field party reports. Field reports also indicate that periods of up to two weeks of extensive cloud and high winds can occur at this location.

Upper wind, temperature and humidity

Since no *in situ* upper–air measurements are available anywhere near Haag the main upper level parameters are estimated and forecast using model fields, adjusted in the light of satellite imagery.

Clouds

Cloud associated with old fronts will often penetrate as far south as Haag and may be quite persistent. There are reports that extensive low cloud may develop over the Evans Ice Stream, but it does not always affect Haag.

Visibility: fog

Little is known about the frequency of fog at this location.

Surface contrast including white–out

The usual conditions for the occurrence of poor surface contrast over an interior site apply here.

Horizontal definition

During periods of good visibility the Ellsworth Mountains are visible on the horizon from Haag Nunataks, but with extensive cloud cover the featureless nature of the top of the nunatak can make detection of a horizon difficult.

Precipitation

There is not a great deal of information available about the types of precipitation that occur at Haag but moderate of heavy precipitation is probably rare because of the low temperatures and the lack of active weather systems. Climatologically it is thought that about 30 cm water equivalent of precipitation falls at this location each year. Precipitation is forecast using a combination of model output and satellite imagery.

Temperature and chill factor

Annual mean surface temperature at Haag, deduced from 10 m snow temperatures, is about -30ºC.

Icing

Severe airframe icing has been reported on the Ronne Ice Shelf so moderate to severe icing can probably also occur in exceptional circumstances at Haag. The AVHRR channel 3 imagery can indicate when clouds composed of supercooled water droplets are present.

Turbulence

Turbulence is predicted using the model upper level winds and from noting the locations of the jet streams.

Hydraulic jumps

Hydraulic jumps have not been reported near Haag Nunataks.

Sea ice

Not relevant for this area.

Horizontal definition

Wind waves and swell

Not relevant for this area.

7.5   Coats Land and Dronning Maud Land

The Coats Land–Dronning Maud Land area extends approximately between meridians 35º W to 45º E. From west to east, the stations/bases covered in this section include:

- *Belgrano II*   (77º 52´ 29″ S, 34º 37' 37″ W, 50 m AMSL);
- *Halley*   (75º 35´ S, 26º 27´ W, on shelf ice);
- *Aboa*   (73° 03´ S, 13° 25´ W);
- *Wasa*   (73° 03´ S , 13° 25´ W);
- *Neumayer*   (70° 39´ S , 08° 15´ W, 42 m AMSL);
- *SANAE IV*   (71º 40´ S, 02º 50´ W, 846 m AMSL);
- *Troll*   (72° 0´ 07″ S, 02° 32´ 2″ E, 1298 m AMSL);
- *Tor*   (71° 53´ 20″ S, 05° 9´ 30″ E)
- *Maitri*   (70º 45´ 52″ S, 11º 44´ 03″ E, 117 m AMSL);
- *Novolazarevskaya*   (70° 46´ 04″ S, 11° 50´ 54″ E, 102 m AMSL)
- *Dakshin Gangotri*   (69° 59´ 23″ S , 11º 56´ 26″ E, shelf ice);
- *Asuka*   (71º 31´ S, 24º, 07´ E, 931 m, AMSL);
- *Syowa*   (69º 00´ S, 39º 35´ E);
- *Dome Fuji*   (77º 19´ S, 39º 42´ E, 3810 m AMSL);
- *Mizuho*   (70º 42´ S, 44º 20´ E , 2230 m AMSL).

The above places are shown in Figure 7.5.1.

7.5.1   Belgrano II Station

7.5.1.1   <u>Orography and the local environment</u>

The Argentine Belgrano II Station is located at 77º 52' 29" S, 34º 37' 37" W on the Bertrab Nunatak in Coats Land. The station is built on rock and is at an elevation of 50 m ASL and is located next to the Filchner Ice Shelf. It is about 120 km from the southern coast of the Weddell Sea and about 400 km away from the British Halley Station.

The station is surrounded by a huge white plateau consisting of glaciers, featureless ice and many deep crevasses. The area is subject to extreme temperatures and the region is very hostile.

7.5.1.2   Operational requirements and activities relevant to the forecasting process

Belgrano II is the most southerly Argentine Station and is the successor to the Belgrano I Station that was established in 1955. The station is re–supplied by air so forecasts are required for flights to and from the glacier airstrip.
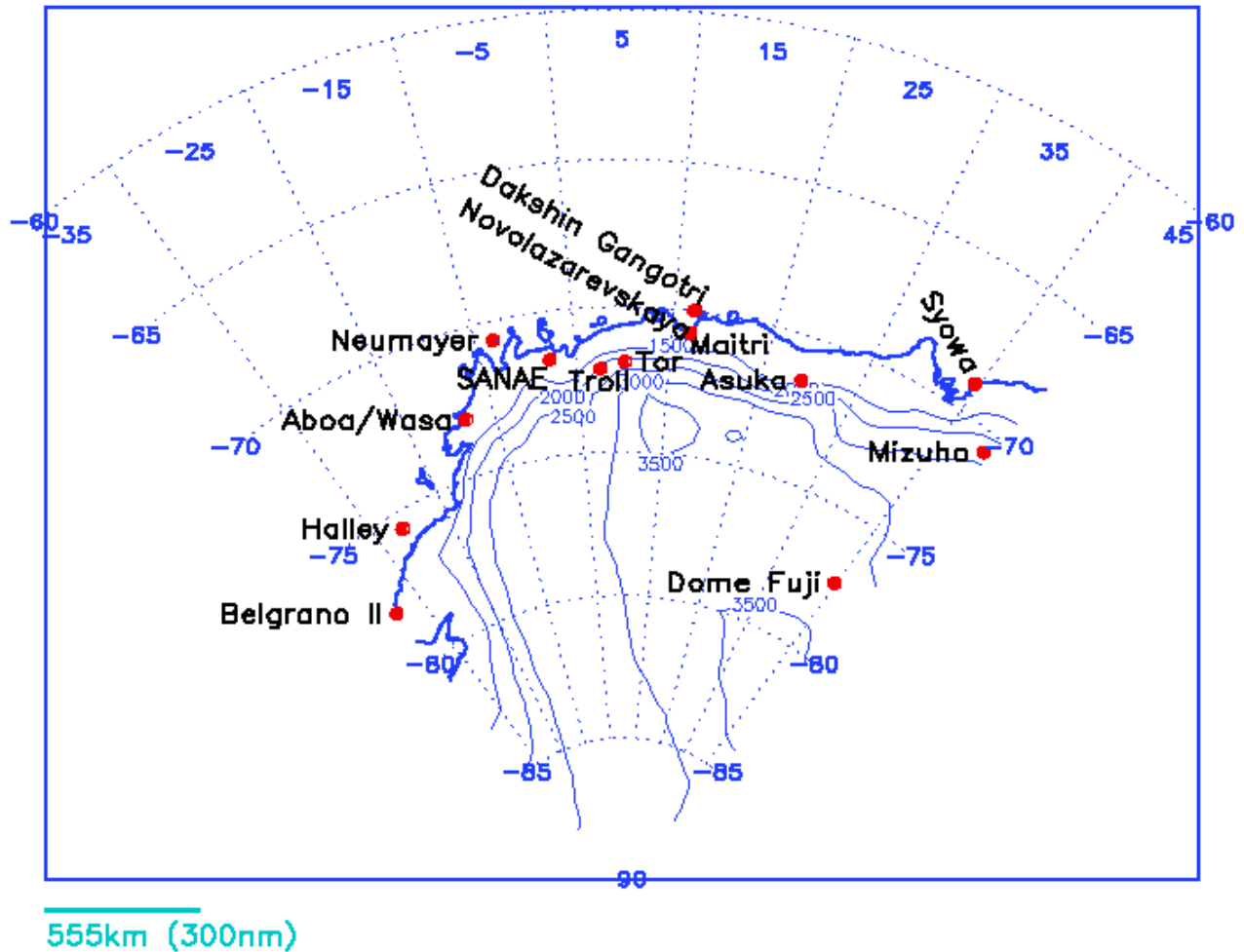

555km (300nm)

Figure 7.5.1   Sketch map showing some locations in Coats and Dronning Maud Lands (contours in metres; the area is bounded by: 85º S, 60º S, 30º W and 40º E).

7.5.1.3   Data sources and services provided

There is a full surface meteorological observing programme on the station and a resident meteorologist.

7.5.1.4   Important weather phenomena and forecasting techniques used at the location

General overview

The area is affected by the low–pressure systems that are found in the Weddell Sea, which can either have formed as lee lows to the east of the Antarctic Peninsula or moved into the area from the South Atlantic. When the long waves are amplified and there is a steering flow from the north then lows can move down to the coast of the southern Weddell Sea and over Belgrano. Occasionally lows can cross the base of the Peninsula from the Bellingshausen Sea and onto the Ronne Ice Shelf.

Surface wind and the pressure field

Climatologically the edge of Coats Land is within the easterly flow regime that is found around much of the continent. However, offshore flow is common on many occasions, as can be seen via the coastal polynya that is often present over the southern Weddell Sea. Deep lows in the Weddell Sea can enhance the easterly flow giving gale or occasionally storm force winds.

Upper wind, temperature and humidity

These fields are usually taken directly from the model fields and used to predict the winds at the aircraft flight levels if required. Adjustments to the winds can be made in the light of the satellite imagery. Because of the lack of *in situ* data in the area (the nearest upper–air station is Halley) the upper winds from the model should be used with care.

Clouds

Satellite imagery shows that cloud cover is rather variable around Belgrano Station with periods of extensive, non–frontal cloud or cloud associated with low–pressure systems, alternating with cloud–free interludes. During the summer months there is a plentiful supply of moisture from the coastal polynya at the edge of the ice shelf so cloud is more extensive than in winter. Cloud is monitored and predicted using satellite imagery.

Visibility: blowing snow and fog

Visibility is generally good in this area but fog can occur, especially close to the coastal lead during periods of southerly flow. Fog/low cloud can be monitored using channel 3 data from AVHRR. As elsewhere in the Antarctic, precipitation is a major factor in reducing visibility, although moderate or heavy precipitation events are fairly rare in this area.

Surface contrast including white–out

The surface contrast is rather variable around Belgrano and as with other locations depends on the amount of cloud present. Contrast is predicted using satellite imagery.

Horizontal definition

Horizontal definition is again very dependent on the amount of cloud present and can be poor because of the lack of snow–free areas and the general featureless nature of the terrain.

Precipitation

At Belgrano all the precipitation falls as snow. The area receives some clear sky precipitation as well as precipitation from low–pressure systems and non–frontal cloud. Precipitation is forecast using a combination of model output and satellite imagery.

Temperature and chill factor

At Belgrano the January mean temperatures range from about -4°C to -10°C, while in July they are of the order -30°C to -40°C. The extreme temperatures recorded are -2°C and -54°C. The near surface temperatures are strongly dependent on the cloud cover, which can be predicted in the short term by the use of satellite imagery. When quasi–stationary deep lows are present in the Weddell Sea warm air can be drawn down the eastern side of the Weddell Sea affecting Belgrano. The warmest temperatures are found when such a synoptic pattern persists for several days and there is a long fetch for the warm air.

Icing

Icing can be a problem around Belgrano because of the occurrence of cloud with supercooled water droplets. Icing is forecast using satellite imagery (especially channel 3 of AVHRR) and a knowledge of air temperatures determined from a model. When relatively warm air intrudes into the area icing can be moderate or severe because of the higher water content of the cloud.

Turbulence

There is little information available. However, as in the rest of the Antarctic, turbulence can be predicted using the model upper level winds and from noting the locations of the jet streams.

Hydraulic jumps

No specific information on forecasting has been obtained.

Sea ice

Not relevant for Belgrano itself. However, the sea ice off the Filchner Ice Shelf and the presence of a coast polynya can have an impact on the weather of the region as a whole. The sea ice is monitored via satellite imagery.

Wind waves and swell

No relevant for this area.

7.5.2   Halley Station

7.5.2.1   Orography and the local environment

Halley Station is situated at 75º 35′ S , 26º 27′ W on the Brunt Ice Shelf. The ice shelf is flat and the base is situated about 25 km from the seaward edge of the shelf and about 90 km from the grounding line of the shelf where the ground begins to rise rapidly to the polar plateau. Near the base the seaward edge of the shelf is too high to allow the unloading of a ship directly onto the shelf but several indentation (locally know as creeks or bays) fill with sea ice and ships can be unloaded onto this and then the cargo can be pulled up wind tails onto the ice shelf.

7.5.2.2   Operational requirements and activities relevant to the forecasting process

Halley Station is primarily a station for the study of meteorology and the upper atmosphere. The base is normally visited twice during the summer by a ship bringing stores and personnel. The unloading of the ship at the edge of the ice shelf is dependent on the weather and the state of the sea ice. If good sea ice is present in the creeks close to the base the journey from the ship to the base is relatively short and so less dependant on good weather. Often, however, it is necessary for the ship to moor some 60 km away at the low shelf and then the trip from the ship to the base for heavily loaded cargo sledges can take up to 12 h and is heavily weather dependent.

      The station also acts as a base for British Antarctic Survey field activities in Dronning Maud Land and the eastern half of the Ronne Ice Shelf and towards the pole. The level of activity can vary a lot from year to year but always includes some flying to support the servicing of several Automatic Geophysical Observatories. It is normal for up to two twin otter aircraft to be stationed at Halley for a period during the summer season.

7.5.2.3   Data sources and services provided

Forecasts for Halley are normally issued by the forecaster at Rothera, who has responsibility for all forecasts issued for British Antarctic Survey activities. These forecasts are only

available during the summer months and are normally issued in the morning, although this varies from year to year with operational requirements. An HRPT receiver is located at Halley and high resolution AVHRR imagery is available.

UK Met Office forecast model fields and surface observations from the GTS are sent to Halley via an Inmarsat link. The UK Met. Office model is quite good at representing synoptic scale systems over the ocean and coastal regions but has more difficulty with mesoscale systems that can develop near to Halley (see below). Inland, over the high Antarctic plateau, the model has more difficulty and output must be used with more care. In all cases satellite imagery should be used to identify systems missed by the model. The surface wind on the Brunt Ice Shelf is dominated by drainage flow down the slope from the high plateau and so the surface gradient shown in the model fields is often in error.

7.5.2.4   Important weather phenomena and forecasting techniques used at the location

General overview

Because of Halley Station's position on the edge of the Weddell Sea the climate is largely dependent on the amount of sea ice in the Weddell Sea. During the summer, when there is little sea ice in the eastern Weddell Sea, temperatures tend to hover around freezing, but during the winter when there is little open water present temperatures can drop to −50ºC during clear calm conditions. At these times a strong surface inversion forms and the temperature just a few hundred meters above the surface can be 20–30 ºC higher. When the wind strengthens the stable boundary layer tends to break down and the temperature can rise 20–30ºC in an hour or two.

In general the weather at Halley is controlled by large synoptic scale systems that form in the circumpolar trough and track south into the Weddell Sea or lee lows that form on the east side of the Peninsula and then move slowly across the Weddell Sea.

Surface wind and the pressure field

The local orography of the plateau near to the ice shelf has a large controlling effect on the surface wind, which is predominately easterly with the strongest winds always coming from that direction. Northeasterly and southwesterly are the next favoured directions but the wind is usually weaker from these directions.

Large–scale synoptic depressions are capable of producing strong easterly winds at Halley with mean speeds of around 15 m s^{-1} (~30 kt) or more. Several occasions have been reported of occlusions moving around a low in the Weddell Sea became slow–moving as they approached Halley. This gives stronger easterly winds than the gradient suggested, probably because of squeezing against the plateau to the south. This can give prolonged periods of gales and blowing and falling snow.

Strong easterly winds at Halley are often preceded by a light westerly flow, induced by the surface pressure field. This flow will advect mild air over the area, consequently the temperature difference between the Halley area and the upsloping ice sheet to the south will increase significantly. After a few days the temperature gradient becomes very tight resulting in the initiation of a katabatic wind from the east.

The eastern coast of the Weddell sea is favoured for the formation of mesocyclones, particularly when strong thermal gradients build up along the coast due to mild air being advected into the area from further north. Mesocyclones developing off the coast have been

known to produce severe weather (eg Christmas 1995) at Halley and are very difficult to forecast. Fortunately, although mesocyclones are a relatively common occurrence, the severe weather is quite rare.

During periods with relatively light winds and clear skies a strong surface inversion can develop on the Brunt ice shelf. This means that the boundary layer is extremely stable and internal gravity waves can form – although these do not tend to cause operational problems for aircraft.

Upper winds, temperature and humidity

These upper level fields are well represented by the UK Met office model and present no special forecasting problem, although adjustments may have to be made occasionally after comparison with satellite imagery.

Clouds

Clouds are generally layer in form and it is not uncommon to have stratus with a base as low as 150–300 m (~500–1,000 ft). When the cloud is uniform surface contrast tends to be poor and this can made operations very difficult. When open water is present close to the coast "water sky" (the dark sea reflected in the clouds) is often seen.

Visibility: blowing snow and fog

Fog can sometimes develop over the leads in the sea ice and is occasionally advected into Halley on a light westerly or northerly wind and most fog occurs when the wind is from this direction.

The main cause of a reduction in visibility and surface contrast at Halley is blowing snow. It is normal to stop all but essential outdoor activity during heavy blowing snow

Surface contrast

No specific information on forecasting has been obtained.

Horizontal definition

No specific information on forecasting has been obtained.

Precipitation

During the summer the precipitation is almost always in the form of snow, rain being very rare. As convective clouds are relatively rare this far south most precipitation comes from layer clouds and these can be as thin as 300 m (~1,000 ft). During the winter some of the

precipitation falls as "precipitation from a clear sky" (diamond dust) although this does not add appreciable to the total yearly accumulation.

Temperature and wind chill

No specific information on forecasting has been obtained.

Icing

No specific information on forecasting has been obtained.

Turbulence

No specific information on forecasting has been obtained.

Hydraulic jumps.

It is thought that hydraulic jumps can form in the stable boundary layer in the zone where the katabatic airflow down the grounded continental ice meets the flat ice shelf. This can show up in infra–red satellite imagery as a dark (warm) band along the junction between the continental and shelf ice.

Sea ice

No specific information on forecasting has been obtained.

Wind waves and swell.

The ice in the Weddell Sea damps out most swell long before it reaches the Brunt Ice Shelf. It is rare for there to be an area of open water large enough for wind waves to get to any significant height. However, knowledge of the wind and fetch can be used to estimate the significant wave height in any area of open water that does form if this is needed.

7.5.3   Aboa and Wasa Bases

7.5.3.1   Orography and the local environment

The Swedish research station Wasa was built on Vestfjella, Queen Maud Land during the 1988/89 Antarctica expedition. It is situated at 73 ^{o} 03′ S, 13 ^{o} 25′ W on the Basen nunatak. Nearby is the Finnish Station Aboa (established in 1988) which, together with Wasa, makes up the so called Nordenskiöld base. The site is 120 km inland from the marine edge of the Riiser–Larsen Ice Shelf and is at an elevation of 467 m (~1531 ft) AMSL. Wasa is operated by the Swedish Polar Research Secretariat.

7.5.3.2   Operational requirements and activities relevant to the forecasting process

Wasa is a summer–only station, which has a helicopter landing area and forecasts are required for helicopter operations. Aboa is occupied from December to February.

7.5.3.3   Data sources and services provided

There is no meteorological service at the station for air traffic. A Milos–type AWS is located at the station.

7.5.3.4   Important weather phenomena and forecasting techniques used at the location

General overview

This site is just inland of the coast at an elevation of 400 m so is affected by weather systems in the Antarctic coastal region.

Surface wind and the pressure field

No specific information on forecasting has been obtained.

Upper wind, temperature and humidity.

No specific information on forecasting has been obtained.

Clouds

No specific information on forecasting has been obtained.

Visibility: blowing snow and fog

No specific information on forecasting has been obtained.

Surface contrast including white–out

No specific information on forecasting has been obtained.

Horizontal definition

No specific information on forecasting has been obtained.

Precipitation

No specific information on forecasting has been obtained.

Temperature and chill factor

No specific information on forecasting has been obtained.

Icing

Icing is potentially a problem in this area since there will be a plentiful supply of supercooled water droplets

Turbulence

No specific information on forecasting has been obtained.

Hydraulic jumps

There are no reports of hydraulic jumps in this area.

Sea ice

Not relevant at this location.

Wind and swell

Not relevant at this location.

7.5.4   Atka Bay– Neumayer Station– Cape Norwegia

7.5.4.1   <u>Orography and local environment</u>

Neumayer (70° 39´ S, 008° 15´ W) is situated on the Ekström Ice Shelf at about 5 km distance from the southeastern part of Atka Bay, 42 m above sea level. The Ekström Ice Shelf has a homogenous flat surface sloping gently upwards to the south. Except for some nunataks about 100 km south of Neumayer no ice–free land or mountains exist. The orographic conditions around the area of Cape Norwegia are nearly the same.

7.5.4.2   <u>Operational requirements and activities relevant to the forecasting process</u>

The most intensive research activities here take place in the summer season. During this time two Dornier 224 aircraft are frequently based at Neumayer. They are used to deploy field parties; for traverses; and for logistic operations. More than 30 scientists live on the station in addition to the station crew at Neumayer and the neighbouring region during summer. The Alfred Wegener Institute for Polar Research in Bremerhaven operates one research vessel ("*Polarstern*", DBLK) that operates in the southern summer near Neumayer, Cape Norwegia, in the Weddell Sea and near the Peninsula. Two helicopters are stationed on board *Polarstern*.

7.5.4.3   <u>Data sources and services provided</u>

At Neumayer Station there is a permanent satellite communication link to receive observations from the GTS and forecast charts up to 48 h from the ECMWF model once a day. Synoptic observations are made every three hours and transferred directly into the GTS by e–mail and into the Internet address at:
     http:// www.awi–bremerhaven.de/MET/Neumayer/latest_obse.html.
     Once a day (at about 0100 UTC) a radiosonde is launched to measure the vertical profiles of air pressure, temperature, humidity and wind vector. The resulting TEMP–CODE is available without delay at http://www.awi–bremerhaven.de/MET/Neumayer/nrt–temp and via the GTS. By using a satellite image receiver (Sea Space) up to six passes of NOAA and DMSP satellite data are processed daily (AVHRR, SSMI), see http://www.awi–bremerhaven.de/MET/Neumayer/satpics/. The station meteorologist at Neumayer provides actual synoptic surface observations (METAR) and descriptions of the lower atmosphere's structure and satellite images on demand.
     Polarstern's meteorological office is staffed with one meteorologist (forecaster) and one Information Technology (IT) assistant. Synoptic observations are made every three hours and transferred directly onto the GTS by a DCP. Once a day the ship–meteorological office receives via E–mail, or satellite communication, analyses and forecast charts of surface pressure, 500–hPa, and sea state, up to 144 h ahead based of the ECMWF and the DWD–

models (German Weather Service). Observations from the GTS are also available via E–mail/Inmarsat. The data base is complemented with synoptic data received by short wave exchange, because of poor satellite communications at higher latitudes. One radiosonde is launched every day at noon while for flight operations other radiosondes are launched if required. The meteorologist on board is responsible for provision of all forecasts for *Polarstern*, Neumayer Station, and for all ship, flight, and ground operations and for field parties in the vicinity.

7.5.4.4   <u>Important weather phenomena and forecasting techniques used in the location</u>

General overview

During the summer season the weather is dominated by low–pressure systems moving across the northern Weddell Sea from the Antarctic Peninsula in an easterly direction with periods of two to seven days. Ahead of the low–pressure systems relative warm air with high humidity streams in from a northeasterly direction mostly accompanied by moderate to strong snowfall. Sometimes fog develops due to the high dew–points in relation to the cold water.

Moderate to strong southerly winds with cold, dry air and good visibility are found to the rear of the low–pressure systems with cloudy to fair sky. It can often be observed that eastward moving lows lose their speed if they move to a position under an upper low–pressure system. One of the most frequent positions where lows become stationary is situated east of Neumayer, near Novolazarevskaya: this gives mostly clear weather with katabatic flows over the Neumayer region.

The meteorologist on *Polarstern* produces surface pressure analyses at 0000 and 1200 UTC, and occasionally at 0600 UTC. The analyses cover the operational area of *Polarstern* usually including the Antarctic Peninsula, the Weddell Sea and Neumayer regions. The analysis of frontal systems is supported by satellite imagery in combination with surface observations.

Synoptic scale weather systems are quite well forecast by using the DWD and ECMWF models. Difficulties often occur when a low–pressure system is moving up against the barrier of the Antarctic Peninsula. Low–pressure developments leeward are sometimes not predicted by the model but they can be analysed well by satellite imagery. Model forecasts often produce speeds of movement of these lows that are too fast, with phase differences of more than 24 h.

The development of polar lows is hardly ever observed during anticyclonic conditions, at the ice edge north and northwest of Neumayer region. Analysis and forecast of these systems is only possible using HRPT satellite imagery and *in situ* data. Especially in the summer season, the forecasting of polar lows near Neumayer is very important for flight operations, field parties or other logistic work. In polar lows, visibilities can change rapidly to poor conditions due to drifting snow and precipitation accompanied by a low cloud base.

Surface wind speed and pressure field

The most frequent wind directions observed are northeast to east caused by eastward moving low–pressure systems north of the Neumayer region but also by the local orography. There are two secondary maxima observed around the directions south and west–southwest, as may be seen in Figure 7.5.4.4.1 in Appendix 2 below. The maximum around west–southwest is

caused by high–pressure ridges swinging east from the northern Weddell Sea, while the southerly maximum is forced by katabatic flows.

Synoptic disturbances are responsible for the maximum around 90° and a wind speed about 13 m s^{-1} (~25 kt). The katabatic flows tend to give a direction of around 180° and a speed of 5 m s^{-1} (~10 kt). Wind speeds above 20 m s^{-1} (~40 kt) are restricted to easterlies. Moderate winds between 8 and 18 m s^{-1} (~16 and 35 kt) may also occur from west to southwest. Southerly winds always stay below 10 m s^{-1} (~20 kt).

Wind direction and wind speed can be forecast using the hand drawn analysis of surface pressure and the model data (wind vectors or surface pressure gradients) with corrections due to local orography. In anticyclonic situations with light synoptic pressure gradients katabatic flows tend to dominate.

For the area around Cape Norwegia the easterly geostrophic wind is enhanced by katabatic winds. The increase in wind speed reaches 5 to 10 m s^{-1} (~10 to 20 kt). Thus wind speeds up to 28 m s^{-1} (~55 kt) are measured near the Cape. The katabatic winds can be calculated and forecast in combination with the ground temperature (sea surface temperature), the temperature on the mountain plateau and slope of the ice sheet. This katabatic effect is shown in Figure 7.5.4.4.2 and Figure 7.5.4.4.3. Figure 7.5.4.4.2 shows the frequency distribution of the measured wind forces between 24 January and 2 February 1998 on *Polarstern* near Cape Norwegia. The frequency distribution of wind direction for wind speeds greater or equal 14 m s^{-1} (~28 kt) is shown in Figure 7.5.4.4.3. It is evident that the highest values correspond to easterly and northeasterly directions. While cruising near Cape Norwegia it is important to know that a high wind speed is generated due to the katabatic effect.
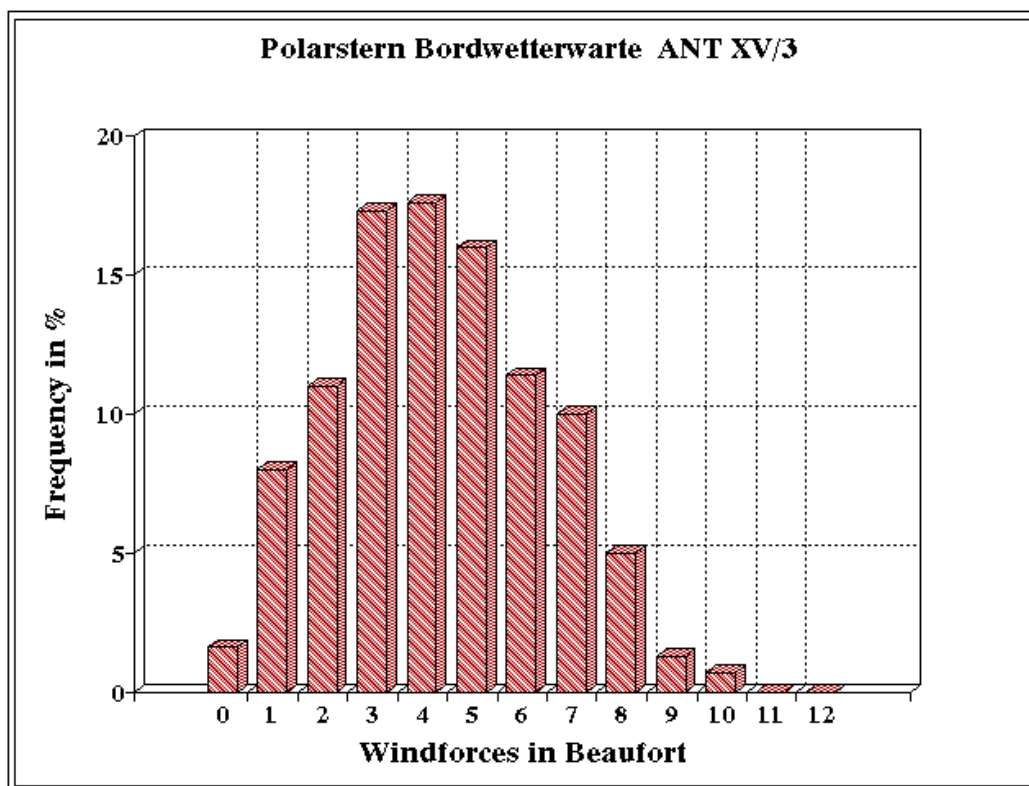

Figure 7.5.4.4.2 Frequency distribution of Beaufort scale wind force measurements taken between 24 January 1998 and 02 February 1998 on board of *Polarstern.*
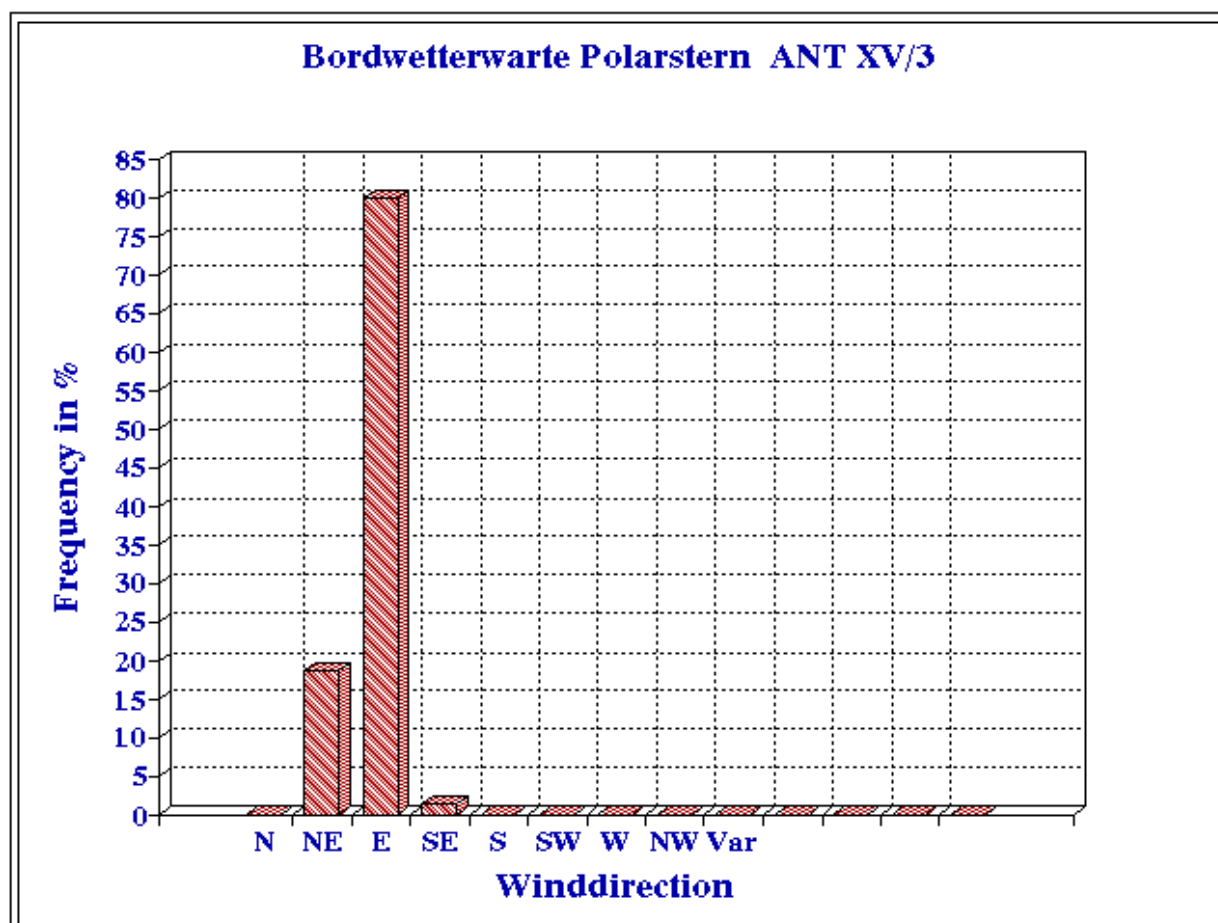
Figure 7.5.4.4.3 Frequency of wind directions for speeds greater than 14 m s^{-1} (28 kt) measured on board *Polarstern* between 24 January 1998 and 02 February 1998.

Upper wind, temperature and humidity

These fields are predicted using the model forecasts in combination with the daily radiosonde data from Neumayer and *Polarstern*. Usually the circumpolar vortex, with increasing westerly winds with height, prevails while an easterly wind is observed mostly in the lowest two kilometres of the troposphere. Only between November and February do easterly winds exist in levels above two kilometres.

Clouds

The cloud cover and type are mainly related to frontal systems. The height of cloud bases are determined by a laser ceiliometer. Cloud bases and tops are also calculated by analysing the latest radiosonde ascent. Cloud forecasts can be made by studying the high resolution satellite imagery in combination with measured cloud tops and bases with consideration of the general synoptic situation.

A special effect is often observed near Neumayer Station in relation to cloud cover. On the southern flank of low–pressure systems the sky becomes suddenly filled with scattered cloud, or the sky clears in correlation with wind direction veering from 90° to 110°. This

happens while mild north–northeasterly origin airmasses are replaced by cold and dry airmasses due to katabatic flows.

Another typical situation is often observed when frontal systems approach Neumayer Station. The start of precipitation with a descending cloud base occurs just before frontal systems reach Neumayer Station with winds backing from east to north–northeast. This is an effect caused by strong ageostrophic components in front of the low–pressure system due to the orography.

Visibility: blowing snow and fog

Visibility is an important parameter in the Antarctic region normally estimated by visual observations with sight marks but also measured on *Polarstern* by using a Videograph III. Fog sometimes develops near the Neumayer region on the forward side of low–pressure systems due to the high dew–point of the air over the cold water or the shelf ice. Also sea smoke exists when cold air due to katabatic flow moves over warm open water. For prediction of visibility, including fog, satellite imagery, *in situ* observations and radiosonde data processed with special software are used.

At Neumayer Station poor visibility conditions are mainly associated with drifting or blowing snow starting at wind speeds of more than 7 m s^{-1} (15 kt). About 40 % of all visual observations report these kinds of significant weather, mostly in combination with white–out. Blowing snow at Neumayer makes any air operations impossible. Even land operations are then restricted to the closest neighbourhood. Thus visibilities have to be forecast carefully.

Surface contrast including white–out

Even in summer poor surface contrast or white–out is observed in the vicinity of Neumayer. These situations are mostly accompanied by precipitation and an opaque cloud layer on the forward side of low–pressure systems. But also under high pressure poor surface contrast is possible in overcast conditions of low stratus or stratocumulus layers. On the ice shelf the surface contrast is additionally influenced by blowing snow.

A forecast of surface contrast can be done by using satellite imagery bearing in mind the general synoptic situation as well as using a regression formula (Equation 7.5.4.4.1) developed during several expeditions with *Polarstern*.

$$\text{CON} = 0.00002*\text{VIS} + 0.0634*\text{RH} + 0.0014*\text{SUN} - 0.135*\text{ICE} - 0.9462*\text{COV} + 4.092656 \qquad \text{Equation 7.5.4.4.1}$$

where VIS is the horizontal visibility in km; RH is the relative humidity in percent; SUN is the relative azimuth angle in degrees between observer and sun position; ICE and COV are cover of ice and cloud in oktas.

Surface contrast is poor for CON <= 2 and very good for CON 9 to 10. Poor surface conditions over the sea, known as "glassy sea", are sometimes observed on *Polarstern* in light air with sea state like a "mirror".

Horizontal definition

No specific information on forecasting has been obtained.

Precipitation

Precipitation is possible during all seasons of the year. Most of the precipitation is slight to moderate with snow brought by frontal systems. Drifting or blowing snow make the quantification very difficult. During summer drizzle and rainfall occur rarely. Even with high pressure, snow, rainfall and showers are possible in combination with low stratus.

Temperature and chill factor

Surface inversions can be detected by analysing radiosonde data. The inversions are normally created by radiative cooling in light air or by descending airmasses in anticyclonic situations. The thickness of the inversions extends during wintertime approximately two kilometres while in summer it is typically less than one kilometre. Inversions caused by radiative cooling become unstable near noon. In anticyclonic situations inversions become well established and assist in maintaining cloud cover.

　　　Forecasting of temperature during the summer season is mostly tied to the synoptic situation. In summer the temperature can be above freezing with values up to 5°C ahead of low–pressure systems or in sky clear conditions without wind. Behind lows, in combination with katabatic winds, temperatures down to –25°C are observed. With wind speeds from 5 to 7 m s^{-1} (~10 to 15 kt) windchill temperatures below –50°C can be calculated using the formula of Schwerdtfeger (1984). The distribution of mean temperature as well as maximum– and minimum–temperature for every month is shown in Appendix 2 below as Figure 7.5.4.4.4.

Icing

Icing is normally tied to frontal systems. Light, moderate and severe icing is observed in the vicinity of Neumayer. Supercooled droplets are observed only occasionally at Neumayer Station. Analysis and forecasting of this parameter is prepared by using the radiosonde data processed by special software and by use of the so called "–8D–curve" (see Section 6.6.9.1 above)

Turbulence

Turbulence is correlated to the general synoptic situation and the local orography. Forecasts of turbulence are provided using radiosonde data and by calculating the vertical wind profile.

Hydraulic jumps

Hydraulic jumps have not yet been investigated near Neumayer region.

Sea ice

Atka Bay is mostly covered with close fast ice (first–year and some parts multi–year–ice) with some icebergs of medium size. Only from January to March does Atka Bay experience open ice conditions, or is free of ice. Pack ice is located about 15 km north of Neumayer. Sometimes, strong southwesterly to westerly winds open a coastal polynya. The sea ice state can be well analysed with AVHRR satellite images. For example, in Figure 7.5.4.4.5 the coastal region around Neumayer can be seen. Forecasts in relation to sea ice cover in Atka Bay are done using model surface winds in combination with satellite imagery.

Wind waves and swell

In summer wave heights between one to four metres are observed in the outer Atka Bay and at the northern edge of the pack ice due to eastward moving lows north of Neumayer region. But mostly in the inner Atka Bay the sea is subdued by fast ice. Waves and swell forecasts are needed for logistic work if *Polarstern* is alongside the ice shelf edge. Predictions of sea state are done using model surface wind with the WMO standard wave prediction algorithm. Model sea state forecasts can be used if no fast ice exists windward. The quality of wave forecasts from models in Antarctic waters such as in the Weddell Sea, around the Antarctic Peninsula, and in regions with sparse meteorological data, are relatively poor. Forecasts for four to six hours ahead can be produced using the techniques presented in the WMO (1988) handbook of wave analysis and forecasting.
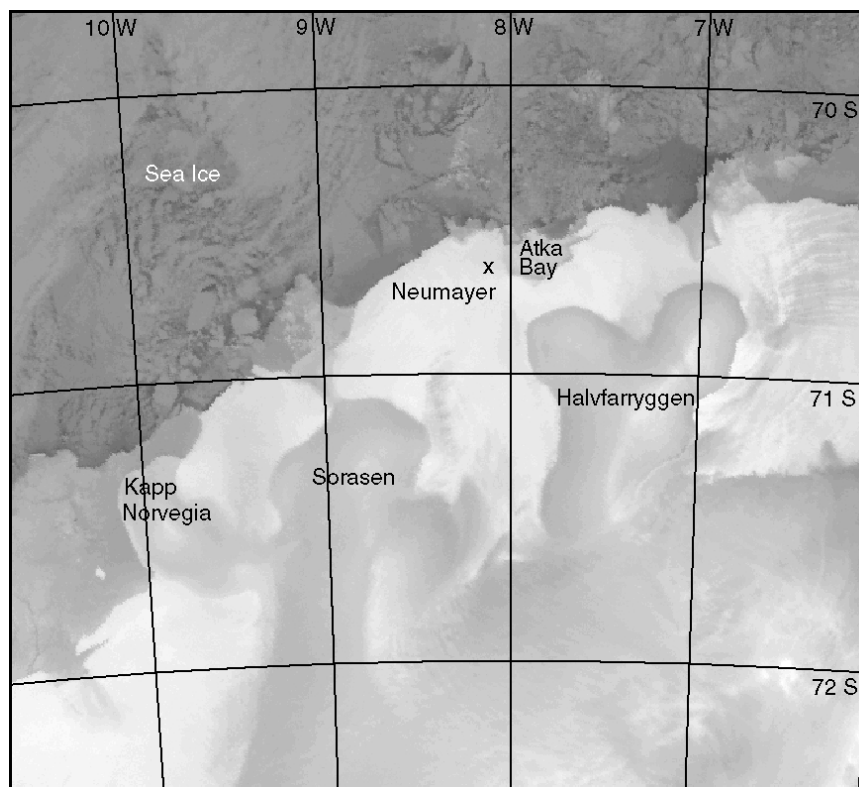

Figure 7.5.4.4.5 An example of AVHRR imagery showing the sea ice in the coastal region around Neumayer.

7.5.5   **SANAE Station**

The South African National Antarctic Expedition (SANAE) Station is situated near the northeast extremity of a Peninsula which separates Jelbut Ice Shelf from Finibul Ice Shelf about 32 km to the east. The station, which is now maintained by the South African Government, was formerly located at 70º 30′ S, 2º 38′ W, and was originally established in 1957 by the Norwegian government.

7.5.5.1   Orography and Local Environment

In this section we discuss the weather regimes for two stations, the old SANAE III, and the new SANAE IV base at Vesleskarvet. SANAE III (70º 18' S, 2º 21' W, 62 m AMSL) is located on the Fimbulisen ice shelf and has been abandoned since1996. Its emergency base (known as E–Base) is now used as a logistics centre and forwarding point for cargo (to SANAE IV) during the austral summer.

    SANAE IV is situated on the southern buttress of a nunatak (71º 40' S, 2º 50' W, 846 m AMSL) and has been occupied permanently since the summer of 1997/1998. Apart from some exposed rock, the southern buttress is covered by a smooth snow surface sloping towards the east. The buttress terminates in a 200 m (~260 ft) high cliff (running approximately north to south) some 50 m west of the station.

    All climate data provided in this section were obtained from the South African Weather Bureau (SAWB) climate archives. Owing to its distance from the barrier edge and altitude, certain meteorological parameters observed at SANAE IV may differ significantly from those at SANAE III and these differences are discussed where relevant.

7.5.5.2   Operational Requirements

A relief vessel brings fresh supplies to the base once a year (from December to February). In years when the lack of sea ice precludes building a ramp down to the bay ice, helicopters are used extensively to cargo sling supplies to the ice shelf. The helicopters also make regular flights between the ship and SANAE IV to transfer personnel and/or equipment. The annual supply of polar diesel is pumped directly from the ship into fuel bladders located on sleds. All the aforementioned tasks are highly dependent on the weather and sea conditions in the vicinity of the ice shelf.

7.5.5.3   Data Sources and Services Provided

All upper–air measurements at SANAE stopped with the shifting of the base. The upper–air programme on the vessel SA *Agulhas* followed suit a few years later. From the beginning of 2000 manual surface weather observations were restarted at SANAE IV from the same location as the AWS (which reports via Argos).

    Dedicated forecasts (valid up to 4 days ahead) are provided to assist with the logistics and are issued during take–over and voyages to and from the ice shelf. When compiling a good forecast, an accurate surface analysis is crucial and surface charts for the Southern Atlantic are analysed at 6–hour intervals. The surface pressure field is analysed using observations from land, ships and drifting weather buoys, as well as the UKMO "first guess"

pressure field and METEOSAT images. The METEOSAT imagery is particularly useful when determining the position of depressions and their corresponding frontal systems. These images have proven to be a very useful analysis and nowcasting tool, but south of 60º S, distortion makes interpretation of the images difficult.

Surface winds are forecast using the gradient winds inferred from the European Centre for Medium Range Weather Forecasting prognostic surface pressure fields. Other forecast parameters include the expected weather and visibility. *In situ* surface and upper–air data (when available) are available on the GTS and are taken into consideration when issuing short–term forecasts. A very recent development in the SAWB has been the ability to display a vast array of parameters at 6–hour intervals (in plan view or the vertical) using PCGRIDDS (a PC based Gridded Information Display and Diagnostic System). World Area Forecast System data (1.25º by 1.25º horizontal resolution) is now available for the forecast area and in the future (depending on the model's accuracy), and these could assist in improving forecasts of cloud cover, precipitation probability and winds for various flight levels.

Sea conditions (swell period and height, as well as total sea) are forecast up to four days ahead using the UKMO swell model data available every 12 h. No swell data are currently available south of 57.5º S and no forecasts for swell or wind waves are issued south of this latitude.

7.5.5.4   <u>Important Weather Phenomena and Forecasting Techniques</u>

General overview

Deep synoptic–scale depressions embedded within the circumpolar trough can cause blizzards lasting up to four days and severely hamper relief operations. Generally, unsettled weather and strong winds (typically easterly) can be expected prior to and during the passage of a depression north of the station, with clearing skies and moderating winds (typically south–easterly) observed in its lee. Mesoscale low–pressure systems are not handled well by the global model, but can also have a significant impact the weather. Satellite imagery is currently the only means the SAWB has of detecting mesoscale lows and monitoring their movement.

An AWS has been operational at SANAE IV since 1997, but no climate analysis of the data has yet been undertaken. However, a subjective analysis of temperature and wind data from June 1997 through August 1999 has been made by the authors and the results are discussed where relevant. Two authors (J. Brimelow and de Broy Brooks) conducted a detailed evaluation of the ECMWF prognostic surface pressure fields and gradient winds (compared with observations made at SANAE III and IV) during February and March 1998. Some of these results, together with observations made during other relief seasons are also presented in the following sections.

Surface Winds and the pressure field

When issuing forecasts for the ice shelf, accurately forecasting the wind speed and direction is perhaps most important. This is due to their impact on the movement and break–up of the sea ice, visibility, helicopter flights, crane operation and wind–chill. During storms, sustained wind speeds as high as 28 m s^{-1} (~55 kt) (with gusts exceeding 50 m s^{-1} (~100 kt) are possible.

The wind speed statistics for SANAE III are summarized in Appendix 2 below in Table 7.5.5.4.1. Similarly the direction statistics are shown in Table 7.5.5.4.2 in Appendix 2 below.

The air–flow displays a strong easterly component, with 47.7% of the winds blowing from the southeast quadrant. The most frequent and strongest winds are typically easterly, with a mean annual frequency of 16.6% and mean speed of about 24 knots. Winds from the northwest and northeast quadrant have the lowest frequency at 5.3% and 11.2% respectively. Winds from the northwest quadrant are generally the weakest, with a mean speed of approximately 6 m s^{-1} (11 kt).

May is typically the windiest month, with a mean speed of 9.8 m s^{-1} (~19.1 kt). The lowest mean wind speed (5.5 m s^{-1} (~10.7 kt)) is observed in January. Calms occur most frequently in January and are observed an average of 14.5% days per month.

During storms, the wind speeds observed at SANAE IV are noticeably stronger than those at the coast. For the period 1997 to 1999, sustained winds greater than 33 m s^{-1} (64 kt) (hurricane force) have been observed every month of the year at SANAE IV during storms associated with depressions.

Forecasting the onset and duration of strong winds is critical for relief operations and safety. The following guidelines have been determined when considering issuing a gale warning for the ice shelf:

- Gale–force east–northeast/east–southeast winds can be expected when a deep depression (central pressure typically lower than 980 hPa) is located between 15º W and 05º E and tracks south of 65º S.
- Issuing wind forecasts for the ice shelf is difficult at the best of times and this is compounded by the inferior performance of the numerical models south of 60º S. Experience and case studies have shown that with the passage of a deep low south of 65º S , the ECMWF model underestimates the wind speed at the ice shelf by 20–50% and under extreme conditions by as much as 100%. The reason for the model underestimating the speed is believed to be threefold.
  –First, the model tends to place the centre of the depressions too far north.
  –Second, the model underestimates the intensity of the continental high and rather than concentrating the pressure gradient along the ice/sea interface, spreads the gradient across the coastal zone.
  –Third, it is possible that the katabatic wind (which has an easterly component) can be superimposed on the synoptic flow, thereby further increasing the wind speed.
- However, although the model does not display much skill in accurately forecasting the wind speeds during storms, it is useful for determining trends and provides valuable guidance regarding the onset and cessation of strong winds.
- Katabatic Winds (i): SANAE IV frequently experiences strong to gale–force south–easterly katabatic winds following the passage of depressions. Katabatic winds reaching the coast are generally weaker and of shorter duration. The following criteria have been used with a fair degree of success when determining the likelihood of a strong (> 15 m s^{-1} (> ~30 kt) katabatic wind event at SANAE IV and/or the coast within 24 h following the passage of a depression:
  –Passage of a slow–moving deep depression south of 65º S, followed by the formation of a ridge of high pressure west of Greenwich;
  –Rapid clearance in the lee of the depression;
  –Formation of a relatively deep surface inversion (at least 1,000 ft deep).
- Katabatic winds (ii): Another forecast sequence which has some success involves cyclogenesis just east of Greenwich with the Polar High extending a ridge northwards of 70º S and west of Greenwich. During weakly forced synoptic conditions, i.e. weak synoptic–scale pressure gradients, a low–level temperature inversion develops over the ice shelf. Under such conditions, highly directionally

consistent inversion winds are observed at SANAE IV. Preliminary analysis of the data indicates that these winds are typically 120º at 8 m s^{-1} (~15 kt) during the summer months.

Upper wind, temperature and humidity

No specific information on forecasting has been obtained.

Clouds

Cloud cover is greatest in mid–summer (December to January) with a mean of 5.8 oktas. This can be attributed to the lack of pack ice and resultant increase in moisture content of the air. Cloud cover is a minimum in mid–winter (July to August), with a mean of 4.2 oktas. No climate data of cloud type or base height are currently available. During the relief period cloud base heights are estimated from the latest upper–air sounding made from the ship.

Experience has shown that the cloud cover is less at SANAE IV and the weather is likely to clear more rapidly after a storm than at the coast. This is most likely due to its distance from the coast and in turn open water.

Visibility

The most common factors responsible for reducing visibility on the ice shelf are falling snow, blowing snow and to a lesser extent fog.

Fog is rare and limited to the summer months. Conditions conducive to the formation of fog are a prolonged period (several days) of light winds having a northerly component, and the absence of sea ice. No statistics are available for the mean monthly occurrence of fog at SANAE III. Fog is not expected to be a problem at SANAE IV, due to its altitude and distance from the coast.

Strong katabatic winds, although generally associated with clear skies, can significantly reduce the visibility due to blowing snow.

Surface contrast

Blowing snow can significantly reduce the contrast and horizontal visibility near the surface. The extent of blowing snow depends on many factors, for example the composition or texture of snow and even the amount of loose snow. As a rule of thumb, winds of around 10 m s^{-1} (~20 kt) cause drifting snow and those around 15 m s^{-1} (~30 kt) create blowing snow; this usually reduces the visibility sufficiently to suspend helicopter flights. Increasing cloud cover also decreases the amount of contrast, especially when the cloud cover is in the form of a uniform deck or layer.

Horizontal definition

Cloud can be responsible for obliterating the horizon, even for aircraft flying several thousand feet above the surface.

Precipitation

At SANAE III, precipitation is almost exclusively in the form of snow, with liquid precipitation very rarely observed during the summer months. The most significant precipitation events are associated with the passage of deep depressions near the station. Mesolows can also be responsible for heavy falls of snow, but their dynamics and characteristics have not yet been studied in detail at this location.

Temperature

The temperature statistics for SANAE III are displayed in Table 7.5.5.4.3 in Appendix 2 below. Temperatures display a marked seasonal variation, with temperatures ranging from as high as +7ºC in the summer to as low as –50ºC in the winter. The mean annual temperature is –16.9ºC. The warmest month is January (mean temperature of –3.6ºC), with July and August the coldest months (mean temperature of about –28ºC). Temperature forecasts are currently not issued during relief operations.

During the summer months, temperatures at SANAE IV tend to be a couple of degrees cooler than SANAE III, with a mean temperature of approximately –7ºC and –10ºC in January and February respectively. Temperatures have been observed to briefly go above freezing in mid–summer. A rather puzzling observation from the preliminary data analysis, is that since 1997, the lowest temperature recorded at SANAE IV is only –37ºC.

Icing

No specific information on forecasting has been obtained.

Turbulence

No specific information on forecasting has been obtained.

Hydraulic jumps

No specific information on forecasting has been obtained.

Sea ice

No specific information on forecasting has been obtained.

Wind waves and swell

No specific information on forecasting has been obtained.

7.5.6   Troll and Tor Stations

7.5.6.1   Orography and the local environment

Troll (72° 0' 7" S, 2° 32' 2" E) and Tor (71° 53' 20" S, 5° 9' 30" E) are two Norwegian summer–only stations located in Dronning Maud Land at elevations of 1298 and 1625 m above mean sea level respectively. Troll is built on a solid rock surface and is 250 km from the coast. Tor is located in an area called Svarthamaren while Troll is in Jutulsessen.

7.5.6.2   Operational requirements and activities relevant to the forecasting process

Troll was opened in February 1990 and surface meteorological observations are made at the site. Tor was established in January 1993, but no information is available about the meteorological activities.

7.5.6.3   Data sources and services provided

Surface meteorological observations are made at Troll. No weather forecasting is carried out at either station.

7.5.6.4   Important weather phenomena and forecasting techniques used at the location

General overview

These stations are in the transition zone between the more maritime climate in the coastal sector and the cold, continental regime of the high plateau. Major weather systems can affect the area, especially when the long waves are amplified, but the diamond dust precipitation characteristic of the interior is also experienced.

Surface wind and the pressure field

No specific information on forecasting has been obtained.

Upper wind, temperature and humidity

No radiosonde data are available for the region but upper–air conditions can be predicted using numerical weather prediction model output.

Clouds

No specific information on forecasting has been obtained.

Visibility: blowing snow and fog

No specific information on forecasting has been obtained.

Surface contrast including white–out

No specific information on forecasting has been obtained.

Horizontal definition

No specific information on forecasting has been obtained.

Precipitation

No specific information on forecasting has been obtained.

Temperature and chill factor

No specific information on forecasting has been obtained.

Icing

No specific information on forecasting has been obtained.

Turbulence

No specific information on forecasting has been obtained.

Hydraulic jumps

No specific information on forecasting has been obtained.

Sea ice

Not relevant at this location.

Wind waves and swell

Not relevant at this location.

7.5.7   **Maitri and Dakshin Gangotri**

The Indian Scientific Expedition to Antarctica has operated since 1981. For the first two years of operation, Indian scientists took surface meteorological observations during the summer period only, housed in temporary shelters on the Prince Astrid coast a few kilometres away from the open sea. During the third expedition in 1983 India established the "permanent" scientific Dakshin Gangotri (69º 59´ 23″ S , 11º 56´ 26″ E) on an ice shelf. However, as this station began sinking in the ice, a second permanent station, Maitri (70º 45´ 52″ S, 11º 44´ 03″ E, 117 m) was set up in the Schirmacher Range during the eighth Indian Expedition in 1988–89. Since 1990, all the scientific activities/observations have been carried out at Maitri, although the Dakshin Gangotri site is still used as a summer camp.

The information in this section is mostly about Maitri, however, comparisons with Dakshin Gangotri, or information about the latter station, are provided where relevant.

7.5.7.1   Orography and local environment of Maitri

Maitri is located in the central part of Schirmacher Range, Queen Maud Land, East Antarctica (Figure 7.5.7.1.1). This oasis is about 16 km long stretching in an east–west direction between 70º 44´ 30″ S to 70º 46´ 30″ S and 11º 22´ 40″ E to 11º 54´ 00″ E with a maximum width of about 2.7 km in the central part. The altitude of Maitri is 117 m above sea level. There is a big glacial lake (Priyadarshini Lake) in front of the station which provides water for all domestic purposes throughout the year.

The Schirmacher oasis forms a group of low lying hills about 50 to 200 m (160 to 650 ft) high. One such small hill is located in the vicinity of Maitri by the side of Priyadarshini Lake. It is about 500 m away from the station. There is a small hillock of conical shape popularly known as SHIVA–LING surrounded by continental ice located west of Maitri at a distance of about 2.5 km. A wall of glacier ice (snout) about 6 to 7.5 m high is located towards the south at a distance of about 500 m approximately in the east – west direction. During the summer months the melt from the northern periphery of the continental ice sheet cascades gently down over the exposed bed rock.

The scientific station of Novolazarevskaya is situated towards the southwest about 4 km from Maitri while "Gorge Foster", the German scientific station, is located 5 km away from Maitri towards the south–southwest. The Schirmacher Range lies in between the Wolthat Mountains about 80 km to the south and the tip of the shelf ice which is about 100 km to the north. The northern boundary of the Schirmacher oasis has an abrupt and steep fall towards the shelf ice.

Figure 7.5.7.1.1 Location of Maitri

7.5.7.2   Operational requirements and activities relevant to the forecasting process

The main objectives of the meteorological programme are as follows:

- to build up a data set for climatology of the Antarctic;
- to conduct research on various aspects of weather at Antarctica and it's influence on global weather in general and weather over the Indian sub–continent in particular;
- to organize an observational programme for the study of radiation budget, ozone hole phenomenon etc;
- to arrange real–time transmission of main hours (6 hourly) synoptic observations on the Global Telecommunication System.

Meteorological Observations

Along with synoptic observations, the meteorological programme also includes the study of radiation, surface ozone, atmospheric turbidity etc. Regular reception of gridded APT satellite pictures in the infra–red and visible channels from polar orbiting satellites (NOAA) and analyzed weather charts from Pretoria (South Africa) help in monitoring and forecasting of weather systems approaching and affecting the station.

The facsimile equipment on board the ship (MV *Polar Bird*) is also of great help in monitoring the weather charts transmitted from India and Pretoria (South Africa) during the route from India (Goa) to Antarctica. The autorecorder data of temperature, wind speed, wind direction, pressure, global solar radiation, surface ozone is regularly tabulated and computed. The continuous record of surface meteorological observations at Maitri indicates that the weather over Antarctica experiences large seasonal variations.

Upper–air Observations

The upper–air programme presently consists of Radiometer Sonde ascents (RMS) and ozonesonde ascents

Weather Sensitive Activities at the Station

The main weather sensitive activities at the station are helicopter operations during the summer period and convoy activity between station and ice shelf, almost throughout the year.

Weather in Antarctica is subjected to frequent and sudden changes. The fast deterioration of fair weather is common here. Drifting and blowing of snow and high wind gusts are typical of Antarctic conditions during blizzards. In severe cases it leads to zero visibility conditions. Helicopter operations are carried out for transportation of equipment and scientists for scientific activities. Before every helicopter flight from ship to the station and back, prevailing weather conditions are communicated to the pilot. Pilots are generally most interested in wind speed/wind direction, visibility, cloudiness etc. over the station.

Snowfall is observed mostly during the summer period but it's intensity is very light and it is in the form of snow flakes (generally star shaped). As such snowfalls may not affect the field activities of the station.

From April to September the number of bad weather days increases and most of them are either due to blowing or drifting of snow. Under these conditions, working outside the laboratory is restricted depending upon the intensity of the bad weather. But during such periods, various in–house activities are arranged.

Local weather forecasts/outlooks for 24–48 h are being provided regularly for day to day planning and execution of station maintenance, scientific and other logistic activities. The day's weather summary is also displayed at the station for general awareness of weather to expedition members.

7.5.7.3   Data sources and services provided

A meteorological observatory at Maitri was established in January 1990. A Stevenson screen and two wind masts were installed in front of the station. A view of the meteorological observatory is shown in Figure 7.5.7.3.1. Self recording instruments for continuous recording of pressure, temperature, wind speed and direction, surface ozone and global solar radiation are kept inside the lab and the sensors installed outside. An APT recorder, radiosonde ground equipment, fax recorder are also kept in the laboratory. The APT omni–directional antenna and helical antenna for ozonesonde/radiometer–sonde are erected on the top of the main building.
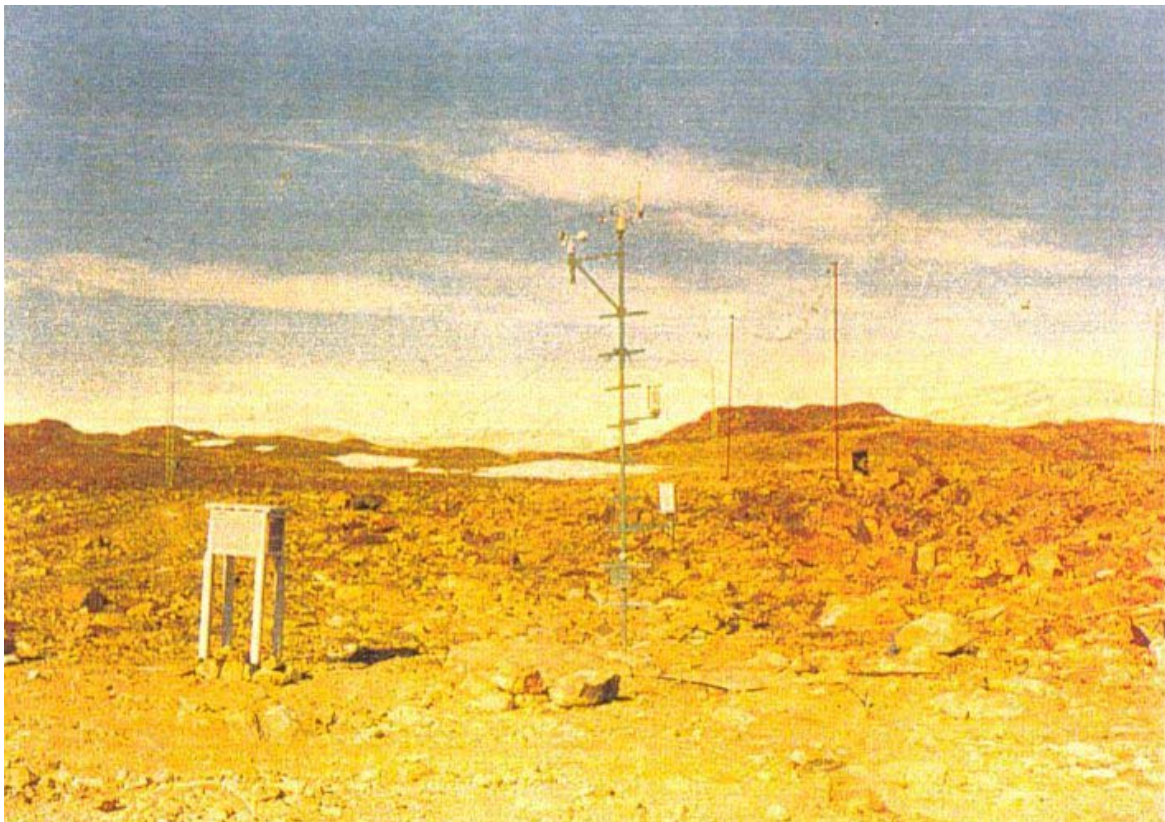

Figure 7.5.7.3.1   A view of the meteorological instrument array at Maitri

The main source of Maitri surface data, such as temperature, pressure, wind speed and wind direction, weather (past and present), visibility, cloud type and amount etc. is the routine three hourly synoptic observation. In addition to manual observations every three hours, continuous

recording of wind speed and direction, atmospheric pressure, air temperature, diffuse and direct solar radiation, is being carried out with the help of self recording instruments. Hourly measurement of atmospheric turbidity during the summer period and for the available sunshine period during winter is done through sun–photometer. During periods of significant weather such as blizzards, hourly observations are also recorded.

For upper–air data such as temperature, pressure, humidity, vertical ozone distribution etc. the upper–air ascents from radiosondes, ozonesondes, radiometer–sondes etc. are taken weekly, fortnightly, or more frequent, as required.

Maitri is in a valley between continental ice and shelf ice, located on a narrow hill range which is 17 km long and 4 km wide, east–west oriented. Due to its location and magnetic field disturbances disabling HF communication during winter, it becomes almost impossible to receive the analysed weather charts transmitted from the Pretoria weather service. These weather charts are mainly aimed at catering to the needs of ships in southern waters: there is no analysis of systems over the Antarctic continent.

7.5.7.4   <u>Important weather phenomena and forecasting techniques used at the location</u>

General overview

Maitri and Dakshin Gangotri are affected by the eastward moving depressions which are synoptic scale frontal systems. These systems move in the circumpolar trough zone which lies between 60 and 66º S meandering north and south between seasons. The large amplitude cloud bands in association with these systems move across the station, producing dramatic variation in cloud cover. The cyclonic circulation associated with these low–pressure systems is frequently also seen on the 500–hPa chart. These systems bring warm and moist air to the coastal areas of the Antarctic continent from northern latitudes. Therefore, when a depression approaches the station, pressure starts falling continuously and temperature starts rising. The rise in temperature, which can be of the order of 10ºC, during a blizzard is also due to the fact that the low level inversion is broken due to turbulence caused by increase in wind speed.

The pressure gradient in the field of the system is very steep and consequently produces very strong winds. There may or may not be precipitation. It is very difficult to judge whether there is precipitation or not due to drifting snow. After the system moves away, the opposite sequence of changes occur: pressure increases (often steeply); temperature falls; wind becomes light or calm; and the sky clears.

On some occasions when small lows move at relatively higher latitudes, the skies are overcast with stratus and calm or light wind prevails. Such situations result in heavy snowfall at the station.

It has been observed that the intensity of blizzards is greater and their duration longer at Dakshin Gangotri than at Maitri, for the simple reason that the former location is closer to the coast.

There is little mesoscale activity affecting the station.

Surface wind and the pressure field

Maitri and Dakshin Gangotri Stations lie between the high–pressure region centred around the South Pole and the circumpolar trough of low pressure roughly along 63º S. Therefore atmospheric pressure at the stations is influenced by the relative position and strength of these features.

At Maitri the seasonal variation in pressure shows a trend of alternate rise and fall with highest values in summer and winter and lowest values in autumn and spring (See Figure 7.5.7.4.1 in Appendix 2 below). Day to day variation in pressure can be very dramatic.

The surface wind regime at Maitri is characterized by alternating spells of strong wind and light wind or calm. The duration of these spells varies considerably from a few hours to several days. The mean daily wind speed varies between 5 and 10 m s^{-1} (~10 and 20 kt). The wind maximum recorded in each month varies between 28 and 41 m s^{-1} (~55 and 80 kt).

A study of wind data collected at Dakshin Gangotri, during 1987, revealed that on 65% of the days average wind speed exceeded 5 m s^{-1} (~10 kt) and on 30% of the days the mean daily wind speed exceeded 10 m s^{-1} (~20 kt); 15% of the daily maximum wind speed exceeded 20 m s^{-1} (~40 kt). At this station strong wind is invariably from the east–southeast direction whereas at Maitri strong wind is from the southeast. Figure 7.5.7.4.2 in Appendix 2 below shows the monthly mean wind speed at Maitri while Figure 7.5.7.4.3 in Appendix 2 below shows the mean monthly days of blizzard.

Wind direction is a significant feature of weather both at Dakshin Gangotri and Maitri. It serves as a sure indication of the type of ensuing weather. A wind rose for Maitri based on 1992 data is shown in Appendix 2 below as Figure 7.5.7.4.4.

The most predominant direction at Dakshin Gangotri is east (52%) while at Maitri it is southeast (28.5%). Sector–wise it is the east–southeast sector (090 –135º) that accounts for 80% of wind directions at Dakshin Gangotri and 56% at Maitri. The next important sector is the south (160 – 200º).

Based on the synoptic situations that give rise to different wind directions at Maitri, five different groupings can be made which are explained in terms of synoptic influences as follows:

- *East to south winds* (56.0% of occasions) result from approaching depressions from the west. As long as the station is under the influence of these systems the wind direction remains constant in this sector.
- If the depression recurves to northeast after crossing the station's longitude the station experiences *north–northeast to east–northeast or easterly* winds (1.6% of occasions).
- Wind directions from the *southwest or west* occur (2.3% of occasions) when a low–pressure system crosses the continent radially and move over the continent to the south of the station's location.
- *Southerly* winds (28.6% of occasions) are due to katabatic winds driven by the polar anticyclone.
- Winds from the *northwest or north* (2.4% of occasions) are due to the passage of a high–pressure ridge across the station.

As discussed above there exists a close relation between the wind direction, speed and the synoptic situation. Hence it is not too difficult to predict the local winds at Maitri Station. If analysed weather charts are available, one may attempt to predict the wind speed. As a rule of thumb it is noted that in the case of depressions 4 to 5 m s^{-1} (~8 to 10 kt) can be counted for every closed isobar.

Katabatic winds are characterized by high directional constancy but show large variations in speed: their direction at Maitri is invariably southerly, since the elevation increases in that direction.

Katabatic winds are more frequently experienced at Maitri than at Dakshin Gangotri as it is located about 80 km south of Dakshin Gangotri at the margin of the polar ice cap. While the frequency of katabatic winds at Maitri is about 28%, at Dakshin Gangotri the frequency is

about 10%. Although katabatic winds occur throughout the year; their frequency is a maximum during winter season from April to August, followed by spring and autumn. Their frequency is least in summer (November–January). During autumn and spring katabatic winds set in by late evening (1800 hrs) and continue to morning (0600 hrs). But during winter these winds occur at any time of the day. The speed of katabatic winds may vary from 3 to 15 m s^{-1} (~6 to 30 kt), and shows large variations frequently over short time intervals. Sudden onsets with the wind speed jumping from almost calm to 12 to 15 m s^{-1} (~25 to 30 kt) and equally sudden cessation (lull) are common.

Upper wind, temperature and humidity

No specific information on forecasting has been obtained.

Clouds

Most cloud forms are a variation of stratus, although strato cumulus is often seen in summer. Cumulus cloud is very rare but cirrus cloud is often widespread and forms at much lower levels than in temperate regions. Reliable cloud observations are very difficult during blizzard conditions since the sky invariably remains obscured.

Visual cloud observations made during 1987 at Dakshin Gangotri showed that mean daily cloud cover was maximum in autumn followed by summer. It was significantly less in spring and winter. The sky was overcast on 13% of the days, cloudy (4 to 7 oktas) on 26% of the days and partly cloudy (1 to 4 oktas) on 46% of the days. Seven percent of the days were absolutely free from cloud when fine weather prevailed. The sky was obscured on 7% of the days mostly due to blizzards. In the peripheral regions of Antarctica it frequently happens that the sky is clear for most of the days but gets " engulfed" by clouds in a short time or vice versa. This is because of the frontal nature of the weather systems and associated cloud bands.

The cloud types most commonly observed are stratus (stratus fractus), altostratus (Altostratus translucidus and Altostratus opacus), Altocumulus (Altocumulus translucidus and Altostratus duplicatus) and Cirrostratus (Cirrostratus fibratus and Cirrostratus nebulosus).

There are several forecasting approaches to cloud forecasting which may be taken:

- *Uses of Satellite Imagery and other data*: At Maitri Station satellite cloud imagery transmitted by NOAA satellites are received. These images, in conjunction with ground observations of cloud cover and type, are used for prediction of local weather. As mentioned earlier, cloud coverage over the station is determined by the movement of cloud–bands, which often originate in mid–latitudes and are present for some time. Hence satellite cloud imageries are of great help in monitoring the cloud coverage.
- *Clear sky compared to overcast conditions:* Irrespective of the season, clear sky can exist over Antarctica. From Table 7.5.7.4.1 in Appendix 2 below it may be seen that about 30% of days in year, winter or summer will be clear or near clear at Maitri. Generally speaking periods of clear sky are associated with calm or light winds, although even during blizzards the sky may be clear above the blowing snow.
- *Prediction of clear sky conditions* : A general understanding of the weather systems at Maitri, will greatly help in predicting a clear sky at Maitri. A ridge, a col region or a region without any significant pressure variations and gaps between the

cloud bands of low–pressure systems, and long distance between two pressure systems gives us scope to predict predominantly clear skies.

Visibility: blowing snow and fog

- *Blowing snow*: Blowing snow is quite a common occurrence and is encountered in all the months. It is associated with blizzards or snow storms and often reduces horizontal visibility considerably. In common with other areas of Antarctica, drifting snow and blowing snow occur in the Maitri and Dakshin Gangotri area in a sequence controlled by the wind speed and other antecedent factors, such as snowfall and temperature. Usually surface snowdrift is initiated at a wind speed of about 10 m s^{-1} (~20 kt). As the wind speed increases intensity of drift increases and at a speed of about 18 m s^{-1} (~35 kt) blowing snow is initiated. The intensity of blowing snow increases with further increase in wind speed. The visibility progressively decreases and becomes zero at a wind speed of about 36 m s^{-1} (~70 kt). However, these threshold wind speeds may be reached earlier if there is recently fallen snow. During winter, due to very low temperature initiation of drift and blowing of snow may occur at relatively higher wind speeds as compared to other seasons given the same surface snow condition.
- *Fog*: Fog is not common at Dakshin Gangotri. During 1987, there were 13 days with fog; out of which 6 days were in the summer months of December and January. The remaining fog days occurred in the other seasons. Advection fog is the most common, although shallow radiation (ground) fog occurs in the evening (1600–1800 hours local time) in the summer months. Advection fog is generally thick, reducing the visibility to zero on some occasions and lasting for 3 to 6 h. The occurrence of fog at Maitri is even rarer (about 3 days in a year) and is mostly in the summer month of December.

Surface contrast including white–out

No specific information on forecasting has been obtained.

Horizontal definition

Maitri enjoys good horizontal definition as it has shelf ice in the north, a gradually rising valley in the east, an east–west oriented and steeply rising glacier front in the south, and a three peaked hill in the west, defining the horizon. If a person regularly moves around on fair weather days it becomes difficult for him to be lost in blizzards as he/she will be familiar with the environmental objects and their bearing to the station.

During calm days, with intense temperature inversions over the continental ice, or over the shelf ice, the surface appears lighted causing mirages and extending the general horizon, when compared to that normally seen on other days. During December and January one can see ice bergs in the sea (north of station) which is about 100 km away. There are reports of sighting anchored ships from the glacier near the station. On a late evening during December 1993 one could see the illusion of the northern ice shelf getting lifted like a wall when viewed from the glacier. Helicopter pilots have not reported any difficulty in flying due to mirage effect or temperature inversions.

Precipitation

Precipitation is usually in the form of snow, although a shower was reported once during February in 1996. During December 1997 there was an occasion when the snow particles turned into water drops on touching the ground and evaporated. Such precipitation is called snowfall of solid precipitation, irrespective of their structural differences and are classified as "snow" for meteorological recording purposes.

Snowfall occurs in two typical forms:

- associated with polar depressions;
- as more conventional snowfall with calm or light winds.

Snowfall associated with polar depressions generally cause blizzards due to high winds associated with the low–pressure systems. The snowfall will be generally horizontal (almost), relatively warm, and visibility falls below 10 metres. Blizzards also occur due to heavy blowing snow even without normal snowfall. Hence it becomes difficult sometimes to say whether there is snowfall associated with a particular blizzard or not. Hence snowfall associated with blizzards are not treated as conventional snowfall for meteorological accounting.

Conventional snowfall can be easily identified due to its occurrence and nature. Calm or light wind, snowfall accumulation, no significant temperature change, vertical precipitation are some of the salient properties associated with a conventional snowfall. Under a simple microscope, one can observe the crystalline structure of the snow grains. The fresh snow will be generally soft and loosely packed with very low density (snowfall density of accumulated snow during a blizzard will be almost 5 to 10 times that of fresh snow due to light packing by wind).

During summer months the low–pressure systems move far north of Maitri causing a good number of clear days. During winter cols, ridges and high–pressure zones residing over or near the station give a fair indication of light/calm winds. Micro–barograph data help to locate these systems in a broad patch of featureless cloud, generally detached or very far away from a low–pressure system. When such a system is seen approaching the station, snowfall can be predicted. By experience one should assess the type of cloud (low/medium/high) using the "colour" with reference to sea or ice surface. If the temperature is "warmer", it indicates the capacity of the cloud to give precipitation. Continuous observation of the clouds also gives the observer an idea of what types of cloud gives precipitation.

In summer ragged cumulus clouds are seen, but they rarely give snowfall. Very fast moving stratus and stratocumulus have given "passing showers of snow" some times. Thick altostratus covering a large area have produced large amounts of heavy snowfall during winters. Such clouds generally resulted when the cloud organisation got disturbed and disorganised when they crossed the "cold land" of Antarctica during spring and autumn months.

Snowfall prediction is of importance for stations on the shelf ice where there is a chance that items like food dumps, fuel dumps or scientific instruments installed on ice, small vehicles and tools etc. are likely to be lost after intense snowfall. At Maitri such problems are never experienced except that open servicing of vehicles and construction activities need to be suitably warned to enable them to take precautionary measures. Though there were days when the accumulated snowfall lasted for a week at Maitri after snowfall, most snowfall accumulation either evaporated or was absorbed by land in about 2 days. A snow gauge/rain gauge was installed in the summer of 1997 at Maitri.

Temperature and chill factor

The temperature gradually falls from January to July, but rapidly rises up to December. July is generally the coldest month. Annual average temperature is around −10ºC at Maitri though highest temperature goes up to +10ºC and lowest up to −35ºC.

Icing

No specific information on forecasting has been obtained.

Turbulence

No specific information on forecasting has been obtained.

Hydraulic jumps

Hydraulic jumps have not been reported at Maitri.

Sea ice

No information provided for Dakshin Gangotri – not relevant for Maitri.

Wind waves and swell

No information provided for Dakshin Gangotri – not relevant for Maitri.

7.5.8   Novolazarevskaya

7.5.8.1   <u>Orography and the local environment</u>

The Novolazarevskaya Station (70°46'04" S, 11°50'54" E, 102 m) above sea level is located at the extreme southeastern tip of the Schirmacher oasis approximately 80 km from the Lazarev Sea coast. An ice shelf with a slightly undulating surface resting against an ice cap extending north of the station in the vicinity of Leningradsky Bay. From the south, there is a continental ice sheet slope.
        The oasis presents a bedrock area elongated in a narrow strip around 17 km long and 3 km wide in the direction from west–northwest to east–southeast. Its relief is typically hillocky with the highest hills up to 228 m in elevation. There are up to 180 lakes in the Oasis. The ice cover on the lakes typically persists in summer melting, however, occurs on some lakes.

The oasis climate has predominantly continental characteristics. It is mainly formed depending on the intensity of solar radiation. Much of the oasis area is characterized by the absence of continuous ice cover not only in summer but also in winter. Moraines outcrop to the surface of glaciers surrounding the oasis. In winter, moraines and hillocky relief are partly snow–covered.

7.5.8.2   Operational requirements and activities relevant to the forecasting process

The station was opened on January 18, 1961. There is a runway for ski– and wheeled– aircraft located some 15 km south of the station on the ice sheet surface at 500 m above sea level. The runway has dimensions of 1,200 m by 60 m and the landing direction of 114º.

A station re–supply visit occurs once per season (in January – March) with the re–supply vessel anchored some75 km from the station.

7.5.8.3   Data sources and services provided

No specific information has been obtained.

7.5.8.4   Important weather phenomena and forecasting techniques used at the location

General overview

The atmospheric circulation pattern over Queen Maud Land is in general as follows. In the west and east of the Queen Maud Land, two high–pressure ridges of low mobility extend in the meridional direction with the axes along 8–9° W and 50° E. These ridges probably combine above the inland plateau. A quasi–stationary depression in the coastal zone between the ridges (4 to 37° E) is maintained by oceanic depressions intruding from the north around 20–25° E. Two branches of the meridional cyclone trajectories almost converge here, the eastern branch of the Falkland and the western branch of the South–African trajectories. The cyclones of the eastern branch of the Falkland trajectory move along the coast influencing the weather in the oasis to a smaller extent, whereas along the western branch of the South– African trajectory, the cyclones move almost along a meridian southward. They are deeper and produce a significant influence on the weather character in the coastal areas of the Queen Maud Land.

The Schirmacher oasis is also subjected to the influence of the peripheral area of the Antarctic High that gives clear frosty weather with dominating katabatic winds. Winter (April–September) is relatively "mild" in general but with strong winds, frequent storms and snowstorms with snowfall. More than 70% of annual precipitation falls out. During the anticyclonic situation, frosty weather sets in, winds attenuate and the air temperature drops and air dryness increases. The atmospheric pressure is high and the absolute humidity is the least for the year. The frequency of occurrence of middle clouds and clear weather is high.

In spring (October–November), the atmospheric pressure sharply decreases, winds attenuate and the air temperature and humidity increase considerably although the amount of lower clouds decreases. The frequency of occurrence of upper clouds increases. Precipitation is still abundant. Active evaporation and melting of winter snow begins. In mid–October, the above zero temperatures on the snow–free soil surface are recorded.

In summer (December–January), the atmospheric pressure is the highest. There is relatively high temperatures and air humidity. Cloudiness (especially low clouds) increases and the frequency of clear weather decreases, the winds are comparatively weak. Snowfall is rare and precipitation is insignificant. There is rapid snow and ice melting and intense drainage of melt water from the oasis to the ice shelf.

Autumn (February–March) is characterized by decreasing air temperature and humidity and increasing total cloudiness with dominating middle clouds. Winds become stronger although snowfall is still rare and precipitation amounts are small. The atmospheric pressure slightly decreases, but remains high. Melt water in the oasis freezes and ice cover forms on the lakes.

In view of the remoteness of the Novolazarevskaya Station from the coast, the probability of occurrence of meso–vortices is very small, especially in winter when the mesoscale cyclogenesis area moves northward to the drifting ice edge.

Surface wind and the pressure field

The average annual station–level air pressure is very low being 975.5 hPa. This is the lowest atmospheric pressure for all coastal Antarctic stations. Annual variations of atmospheric pressure, similar to the other Antarctic stations have two maximums (in June and February) and two minimums (in April and October).

The inter–annual amplitude of atmospheric pressure in the station area varied between 11 to 28 hPa with the absolute amplitude changing from 62 to 73 hPa.

At the coastal Antarctic stations exposed to the action of katabatic winds, the atmospheric pressure is poorly related to other meteorological elements. The wind speed typically increases with decreasing pressure, but at its maximum values, the wind also increases.

Winds in the Schirmacher oasis are naturally weaker than at the coast. The average annual wind speed at Novolazarevskaya Station is 10.2 m s^{-1} (~20 kt). The maximum wind speed is observed in winter with the minimum in summer. June is distinguished by the largest average wind speed (12.8 m s^{-1} (~25 kt)). There are 196 days with strong winds on average, for a year. December and January are characterized by the lowest average wind speeds, with the wind speed in January being 2–5 m s^{-1} (~ 4–10 kt) in more than 45% of all cases.

One maximum (in the morning and at night during the intermediate seasons) and one minimum (in the evening) are observed in daily wind speed variations.

An analysis of the frequency of occurrence of wind directions revealed that cyclonic easterly–southeasterly winds had the largest intensity (with the frequency of occurrence of 34% and a speed of 12.8 m s^{-1} (~25 kt)), then the southeasterly winds followed (with a frequency of occurrence of 20% and the speed of 12.8 m s^{-1}) and the katabatic south–southeasterly to south–southwesterly winds (with a frequency of occurrence of 26% and a speed of 10.3 m s^{-1} (~20kt)) were third most common. The frequency of occurrence of winds of other 11 directions was 13% and the average speed 3.3 m s^{-1} (~ 6.5 kt). The main wind types corresponding to the main weather types as identified. Cyclonic weather is accompanied by cyclonic easterly–southeasterly winds while the anticyclonic weather is characterized by katabatic south–southeasterly to south–southwesterly winds. In winter, the atmospheric pressure decreases with changing wind type and the difference in weather conditions is more pronounced with cyclonic and katabatic winds.

Upper wind, temperature and humidity

No specific information on forecasting has been obtained.

Clouds

Total cloudiness is equal on average to 4.6 oktas for the year. The highest cloudiness occurs in summer (4.9 oktas). The least total cloudiness was recorded in winter (4.5 oktas) with the minimum monthly mean observed in September 1965 (2.2 oktas). The lower–level clouds are insignificant comprising 0.8 oktas on average for a year. The least values are observed in summer (1.1 oktas). The minimum values of lower clouds occur in spring (0.5 oktas).

The middle–level clouds prevail above the station. These are alto cumulus and alto stratus (with the frequency of occurrence of 42%), their largest frequency observed in autumn and the least in winter. The high–level clouds are mainly cirrus, being observed in 26% of all observation cases. In the annual variations, the frequency of occurrence of these clouds is minimum in autumn and winter and a maximum in spring and summer.

The lower–level clouds are predominantly nimbostratus clouds and stratocumulus were rare above the stations. Their frequency of occurrence for the year comprising 9%. Clear weather prevails in winter and in general over the year, the frequency of occurrence comprises 21%.

Visibility: blowing snow and fog

No specific information on forecasting has been obtained.

Surface contrast including white–out

No specific information on forecasting has been obtained.

Horizontal definition

No specific information on forecasting has been obtained.

Precipitation

Precipitation at the Novolazarevskaya Station is mostly in the form of snow. Rime and hoarfrost, tapioca snow or wet snow were rarely recorded. The annual amount of precipitation is 309 mm.

Precipitation is almost exclusively brought by cyclones and accompanies a typically cyclonic pattern with low atmospheric pressure, elevated air temperature and humidity, strong wind and almost continuous and significant low clouds. Snow falls mainly from stratus clouds whose frequency of precipitation is 45%, or from high stratus clouds (with the frequency of precipitation of 39%).

In the overwhelming majority of the cases, the cyclonic easterly–southeasterly winds or transient southeasterly winds (with the frequency of occurrence of 75 and 20%, respectively) were observed when this occurs. Precipitation was most often recorded during snowstorms

with strong winds. For example, in 67 cases of snowfalls in July–September the average wind speed was 18–23 m s^{-1} (~35–45 kt) (at the average monthly wind speed of 11–14 m s^{-1} (~20–27 kt)) while the air temperature was 3–5ºC higher than monthly means. On average for a year, there are 72 days with snowfalls in the station area. The largest amount of precipitation falls out in winter and spring with the lowest precipitation in summer and autumn.

Temperature and chill factor

The warming influence of the oasis is expressed in a relatively higher air temperature. The average annual temperature is equal to –11.0ºC i.e. higher than at the nearest coastal stations. The average temperature oscillations from year–to–year are insignificant, within 1ºC.

The winter air temperatures are observed already in April and persist around –14 to -15ºC during the following months. By the temperature regime, the winter season continues for 6 months. July is the coldest month. Summer in the oasis is relatively warm and continues for two months – December and January. The maximum temperatures and the highest minimum temperatures during the year are typically observed in the summer months. The highest temperatures are recorded between the second 10–day period of December and the second 10–day period of January, i.e. during the summer solstice. Usually at this time in the oasis, rapid snow and ice melting occurs, numerous relief depressions are filled with melt water and there is intense discharge from the lakes to the ice shelf.

Based on the temperature regime the duration of intermediate seasons is two months: October–November (spring) and February–March (autumn). Average temperatures in spring are –10.2ºC and in autumn –6.4ºC.

Daily air temperature variations at the station are typical, with the maximum at midday and the minimum at night. The non–periodic air temperature oscillations are related to changes in the synoptic conditions. Dramatic cooling events in winter occur with the onset of anticyclonic weather and very light winds.

The absolute air humidity partial pressure, on average for a year, is 1.6 hPa, its values from year–to–year varying only by 0.1 hPa. The largest air humidity partial pressure is in summer (3.2 hPa) and the smallest in winter (1.0 hPa). The extreme humidity values at the observation times reach almost 5 hPa in summer and 0.2 hPa in winter. Relative humidity on average for the station was 52%. The changes of its average annual values ranged between 48 to 56%. The largest relative humidity is observed in summer (58%) while in the other seasons it is lower being 50–51%. Complete air saturation with moisture (100%) was recorded comparatively frequently with passing cyclones bringing moist warm air typically with snowfall from the ocean. The driest air is transported by katabatic winds.

Icing

No specific information on forecasting has been obtained.

Turbulence

No specific information on forecasting has been obtained.

Hydraulic jumps

364

No specific information on forecasting has been obtained.

Sea ice

The recurring polynya in Leningradsky Bay between 10–14º E is the most remarkable and important feature of ice conditions in the coastal area of the Novolazarevskaya Station. This is one of the most stable Antarctic polynyas persisting in most years almost throughout the year.

The development of polynyas typically begins in September being due to the breakup of the marginal land–fast ice zone whose maximum width in this area comprises 40 km. At first, the polynya is mainly localized under the northwestern tip of the protruding Lazarev Ice Shelf. Then with land–fast ice decay, following the breakup "wave", it extends in the general west–southwest direction and by March typically covers the entire Bay with an area of up to 5,000 km^2.

However, the inter–annual variability of the final decay of local land–fast ice and the corresponding maximum polynya dimensions of approximately 150 by 35 km is around 4 months from January to April.

North of the polynya there is a belt of close drifting ice that decreases by the end of summer in February up to 55 to 110 km (~30–60 nm), on average, disappearing completely in some years.

Autumn ice formation begins in the polynya area in late February–early March, but its intensity is weak up to mid–March. In addition, new ice produced in the polynya in March–April is completely exported from the Bay northward by the dominating offshore winds towards the southern edge of the belt of residual drifting ice.

The formation of new land–fast ice begins on average only in late April–early May being interrupted by frequent breaks at its margins. As a result, the final freeze–up of Leningradsky Bay signifying establishment of land–fast ice up to 40 km wide and disappearance of the polynya is mainly observed only during August. The average land–fast ice width at the time of the spring–summer breakup is about 1.5 m with prevailing snow cover depth of 30 cm. The land–fast ice thickness increases from 1 m near the edge to more than 2 m near the glacier barrier in connection with the intense frazil ice formation here.

Wind waves and swell

No specific information on forecasting has been obtained.

7.5.9   Inland of Syowa (Asuka, Mizuho, Dome Fuji)

Three stations, Asuka (71° 32´ S, 24° 08´ E), Dome Fuji (77° 19´ S, 39° 42´ E) and Mizuho (70° 42´ S, 44° 20´ E), are located inland of Syowa Station (see the map in Figure 7.5.9.1). These stations have been used for over–wintering, but at present, are used as summer–only or temporary stations. Over–wintering has taken place during February 1987 to November 1991 at Asuka, during January 1995 to January 1998 at Dome Fuji, and from June 1976 to October 1986 at Mizuho.
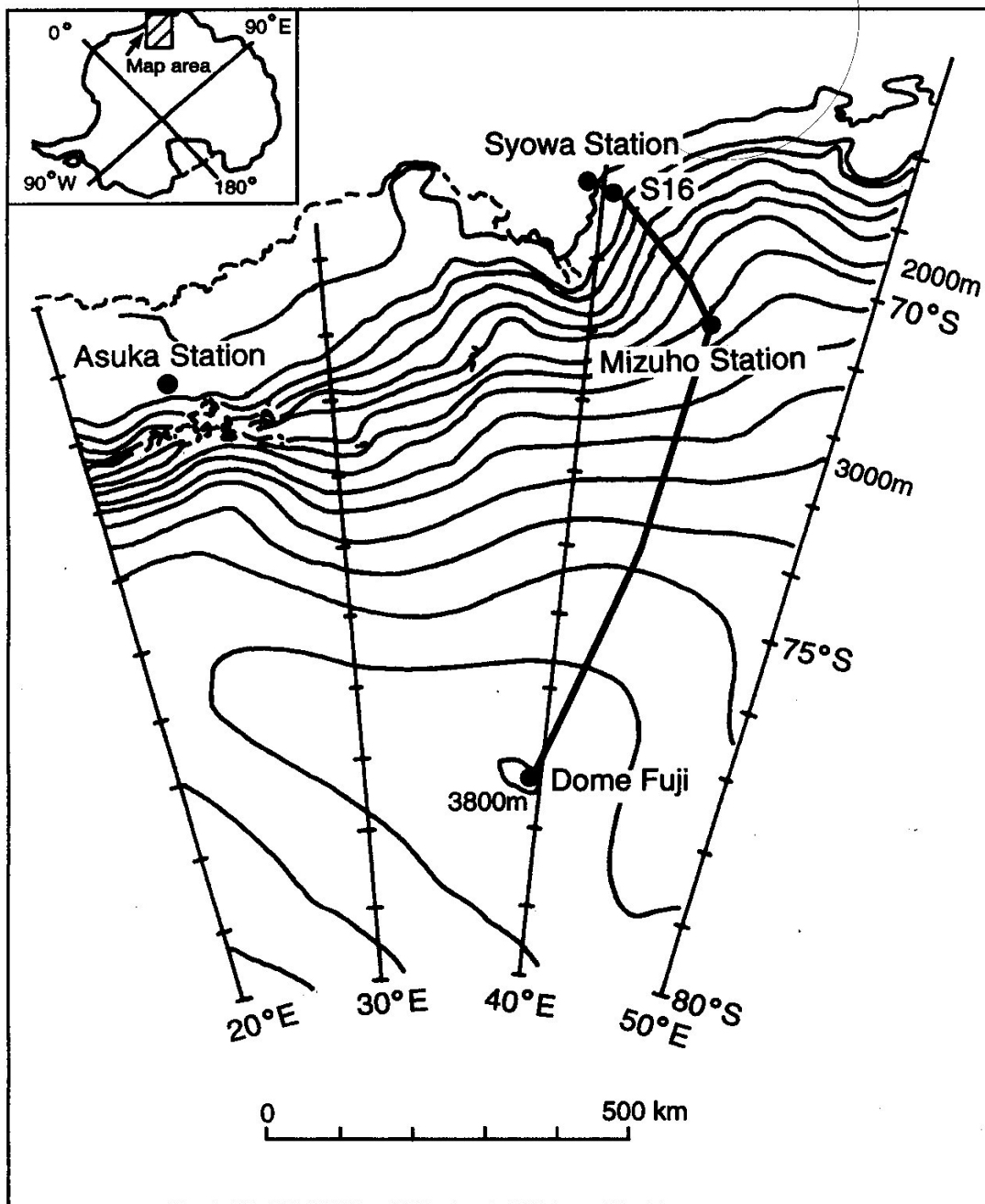
Figure 7.5.9.1   Map of the area inland of Syowa showing the locations of the stations.

7.5.9.1   Orography and the local environment

- *Asuka Station* is located in East Queen Maud Land, close to the Sor Rondane Mountains, at a height of 930 m AMSL. It is about 120 km from Breid Bay, Princess Ragnhild Coast. The former Belgian and Dutch station, Roi Baudouin was located in this area near the coast on an ice shelf. (Although noticeably west of Syowa, Asuka is included in the group of Japanese operated stations).

- *Mizuho Station* is located at a height of 2,230 m AMSL.

- *Dome Fuji* Station is located 1,000 km from the coast at an altitude of 3,810 m AMSL – the highest station in the Antarctic – and is used mainly for deep ice core drilling.

7.5.9.2   <u>Operational requirements and activities relevant to the forecasting process</u>

The stations are operated on a summer–only basis as required.

7.5.9.3   <u>Data sources and services provided</u>

During wintering at each station synoptic meteorological observations have been collected. However, all observations were made when the stations were operating as research bases, except for 1990 and 1991 at Asuka Station, when the Japan Meteorological Agency (JMA) conducted the routine base observation programme. In addition to these synoptic observations, aerological observations were also collected sporadically at the stations in some years. Measurements of temperature and wind profiles using a 30 m tower were made at Mizuho Station during the Polar Experiment (POLEX) South project. Those data were reported in publications from JMA and the Japanese National Institute of Polar Research (NIPR) (see http://www.nipr.ac.jp/). The POLEX South project took place during 1979 and 1981 and included extensive observations of the surface radiation budget, surface boundary layer profiles and conditions in the katabatic wind zone.
     Extensive field observations for geology and geomorphology were made at Asuka Station during five summer seasons.
     At Dome F, extensive atmospheric observation programmes were carried out under the project "Atmospheric circulation and material transfer in the Antarctic" in 1997.

7.5.9.4   <u>Important weather phenomena and forecasting techniques used at the location</u>

General overview

As discussed below, Mizuho and Asuka are located on or close to the steep continental slope and their climates are dominated by katabatic winds. Dome F on the other hand has a climate typical of the inland high plateau.
     Monthly summaries of conditions at each station are given as follows:

- *Asuka Station* – in Table 7.5.9.4.1 in Appendix 2 below;
- *Dome Fuji* – in Table 7.5.9.4.2 in Appendix 2 below;
- *Mizuho Station* – in Table 7.5.9.4.3 in Appendix 2 below.

Surface wind and the pressure field

- *Asuka Station*. Since the station is located in the katabatic wind zone and close to the mountains, its meteorological conditions are strongly affected by downslope winds. The annual mean wind speed is more than 12 m s^{-1} (~23 kt) and even the monthly mean exceeded 15m s^{-1} (30 kt) for 6 months during 5 years of observation. This high frequency of strong winds often gives deep blowing snow and poor visibility.
- *Dome Fuji.* Since the station is on the "dome" of a high plateau on the ice sheet, there is no predominant surface wind direction, as is found in the katabatic wind zone. However, the wind speed is stronger than expected, with an annual mean

of 5.8 m s⁻¹ (~11 kt).

- *Mizuho Station.* The station is located on the slope of the continental ice sheet and the climate is characterised by strong katabatic winds. The average wind speed in winter exceeds 12 m s⁻¹ (~23 kt) and the annual average is 11 m s⁻¹ (~21 kt) and is predominantly easterly (more than 90 % of the wind directions reported are from between east–southeast and east–northeast.

Upper wind, temperature and humidity

No specific information on forecasting has been obtained.

Clouds

Cloud amounts at Dome Fuji are low, especially during winter and only a few synoptic disturbances intrude into the inland area. However, pronounced blocking high episodes occur approximately once a month in winter, accompanied by abrupt increases of temperature, with a rise of more than 40ºC being recorded on one occasion. More than one third of days during the year are clear.

Visibility: blowing snow and fog

No specific information on forecasting has been obtained.

Surface contrast including white–out

No specific information on forecasting has been obtained.

Horizontal definition

No specific information on forecasting has been obtained.

Precipitation

At Dome Fuji there are more than 300 days a year with precipitation (clear sky precipitation or diamond dust).

Temperature and chill factor

- *Dome Fuji:* Here temperatures are very low with the annual mean temperature

for three years being –54.3ºC. At this location a typical coreless winter is seen with monthly mean temperatures of less than –60ºC being found from April to September. At Dome F, due to the location on the dome, the air temperature at the surface is higher than that at Vostok Station, although Dome F is at a higher elevation than Vostok.

- *Mizuho Station*. There is a strong surface inversion, especially in winter. However, normally, the lowest layer up to a few tens of meters above the surface is well mixed and the inversion is reduced in this layer owing to the strong wind.

Icing

No specific information on forecasting has been obtained.

Turbulence

No specific information on forecasting has been obtained.

Hydraulic jumps

No specific information on forecasting has been obtained.

Sea ice

Not relevant at these locations.

Wind waves and swell

Not relevant at these locations.

7.5.10   Syowa Station

7.5.10.1   <u>Orography and the local environment</u>

Syowa Station (69º 00' S, 39º 35' E) is located on the East Ongul Island, 5 km from the Soya Coast in the eastern side of Lutzow–Holm Bay. The sea around the island is normally covered with fast sea ice and it is possible to travel around by over–snow vehicles. However, in some years, especially in summer to autumn, the sea ice around the station melts at the surface, breaks up and is blown out.

Shirase Glacier exists at the bottom of the Lutzow–Holm Bay, about 100 km from the station. This glacier is famous for its high rate of flow of about 2.5 km/a.

7.5.10.2   Operational requirements and activities relevant to the forecasting process

Syowa Station is the centre for all the activities of the Japanese Antarctic Research Expedition (JARE). Inland traverses to Mizuho Station (70º 42' S, 44º 20' E, 2230 m), Dome Fuji Station (77º 19' S, 39º 42' E, 3810 m AMSL), the Yamato Mountains, and the surrounding area, start from Syowa Station, or the S16 point which is a nearby depot on the ice sheet. Research expeditions to the coastal bare rock area and also sea ice traverses are made from Syowa. Weather forecasts are necessary for each of these operations.
     The JARE operates two single engine aircraft, a Pilatus Porter PC 6, and a Cessna 185A Sky wagon, at Syowa Station. Aviation forecasts are required for these aircraft operations during summer and winter.
     The research vessel Shirase, equipped with three helicopters, supplies Syowa with personnel, fuel and goods, once a year during December to February. The Shirase has its own forecaster on board; however, this person needs additional information from Syowa's meteorological office.

7.5.10.3   Data sources and services provided

Routine meteorological observations are conducted at Syowa Station by the JARE, with five members from Japan Meteorological Agency. Surface synoptic observations are conducted using an automatic meteorological system together with manual observations of present weather, visibility and atmospheric phenomena. Aerological observations are conducted with balloon launches twice a day at 0000 and 1200 UTC. Other special observations are also carried out on ozone and radiation.
     At Syowa Station there is an Inmarsat link to Japan, to the National Institute of Polar Research and to the Japan Meteorological Agency (JMA). Analyses/forecast products from Tokyo Global Data Processing System Centre (GDPS, JMA) are transferred once a day. Observational data, SYNOP, TEMP CLIMAT and CLIMAT TEMP, are sent to the GTS through Meteosat DCP (Data Collection Platform), and those from other stations including AWSs are acquired from the GTS through Meteosat MDD (Meteorological Data Distribution). The latter system also provides orbit parameters of NOAA series satellite, ECMWF charts, and satellite imagery from Meteosat.
     An APT satellite receiver is located at Syowa Station providing about 14 passes of AVHRR visible and infra–red imagery each day, and also an HRPT receiver providing about 4 to 5 AVHRR data and imagery passes each day. Information from the AWS at S16 is also used.

7.5.10.4   Important weather phenomena and forecasting techniques used at the station

General overview

Because of the location of the station, the climate of Syowa Station is rather mild and maritime. Table 7.5.10.4.1 in Appendix 2 below provides a monthly summary of some of the key parameters. Katabatic winds, common to the continental slopes, are not necessary common to the station. Occasionally, blowing snow on the continental slope, due to the katabatic wind, is visible from the station but the katabatic wind does not itself affect the station. However, every now and then, the katabatic wind will reach Syowa, producing an

easterly surface wind of about 7 to 10 m s^{-1} (~ 15 to 20 kt). On the other hand, the eastward passage of low–pressure systems is rather common near the station: and the weather at the station is affected each time. When a low stops near the station, or moves southward and the inland over the continent, blizzards often occur at Syowa.

Summer conditions may be summarised as follows. In December and January, the possibility of clear or fair weather is more than 50%. Blizzards rarely occur at the station in these two months, but are more common in February. The inter–annual variation of meteorological parameters is large in this season. Monthly mean cloud amount during December and February was less than 4.8 oktas before 1987; however, it became more than 5.6 oktas during 1989 to 1993.

In autumn the likelihood of cloudy conditions or snow is more than 60% in March and April. Blizzards tend to occur in this season. The variation of the weather is periodic, with a frequency of about 7 to 10 days. The sea ice extent is a minimum in this season and open water is closest to the station. Sometimes, all the sea ice moves out and Ongul Islands, where the station is located, is surrounded by open water. Atmospheric circulation in the stratosphere also change to a winter pattern.

In winter the variations of weather become relatively less and the possibility of clear days become higher. However, strong blizzards also occur in this season. The possibility of snowfall is highest and a drastic variation between clear weather and snow events occurs in July. The relative humidity is lowest in July and vapour pressure or absolute amount of water vapor is lowest in August: so much so that care is needed by staff to combat the dryness.

In spring, daylight hours become longer and the possibility of clear weather is higher in September: however, the possibility of major blizzards is also high in this month. The possibility of snowfalls is high in October, second only to July, and cloud amount is also high in this season. The loss of stratospheric ozone, (the ozone hole), is most pronounced in this season, and a decreasing trend of stratospheric temperature is clear from the last 20 years of record. The time of occurrence of warming of the stratosphere also shows a delaying trend in these years of record.

Surface synoptic observations are indispensable for forecasting, especially during periods when there are no new analyses or satellite imagery. Most of the surface observational data are from continuous recorders and can be used to interpolate between the analyses and prognoses. The local observations also reflect the local conditions directly, bearing in mind that the analyses or imagery are more on the synoptic scale. The observations are also used at Syowa to assess how well the numerical prognoses are performing.

Surface wind and the pressure field

When examining the surface pressure field from charts available at Syowa it should be noted that only a coarse distribution of pressure pattern is expressed in the Southern Hemisphere charts. Sometimes, there is no low analysed on the weather chart, even though a cyclonic vortex is seen in the cloud imagery. Also no frontal systems are depicted in numerical weather charts. The Southern Hemisphere analyses and prognoses show only the general fields, and it is necessary to use the cloud imagery to determine the actual weather conditions.

When there is a stationary low–pressure system to the north west of the station cloud systems arrive one after another, from the north or north east of the station as seen in the cloud imagery. However, large–scale blizzards are accompanied by low–pressure systems moving to the southeast to south–southeast. In other words, care should be taken when a low-pressure system moves toward the station from the north–west and north–westerly winds strengthen at the 500–hPa level.

In summer, the extent of anticyclonic conditions over the continent dominates the weather condition at Syowa Station, with cloud cover, if any, caused by coastal lows. One needs to estimate the strength of anticyclone from the MSL prognosis to determine the relative effects.

Surface pressure decreases of 3 to 5 hPa hr^{-1} or more might be accompanied by the development of blizzards. When the general pressure field is a high (high–pressure system dominates), blizzards tend to be minor. However, when the dominant pressure system is a low then a major blizzard will develop. When the low–pressure systems pass north of the station, the wind speed grows to the maximum when the surface pressure starts to increase.

In terms of wind direction, blizzards will occur with the surface wind direction *only* from the northeast or east–northeast. An easterly direction is also the normal katabatic wind direction. However, if the wind is forced by a low–pressure system, then the wind direction will usually change to the northeast.

Two types of increase in wind speed are seen when blizzards occur. Firstly, an approaching synoptic scale low will usually cause the wind speed to gradually increase. On the otherhand, typically the wind speed will increase from light to strong, in a short time scale, such as thirty minutes, when a mesoscale cyclone approaches. This type of system occasionally approaches from the south–east.

With respect to katabatic winds, while these are not a major feature they can reach speeds of 10 m s^{-1} (~20 kt) or more in the morning, but will invariably cease in the afternoon.

Upper wind, temperature and humidity

The twice daily aerological observations programme is indispensable for the forecasting process at Syowa. For wind speeds of 10 m s^{-1} (~20 kt) or more, upper northerly winds bring bad weather to Syowa while southerlies bring good weather. So when the latter case has been observed and then a change occurs in the wind direction in the upper layers to northerlies then warm air is being advected southwards. The weather will change for the worse.

An increase of wind speed often suggests the approach of a low–pressure system: in particular with an increase of the 500–hPa wind in the direction of 300º one needs to be cautious. On the other hand it is difficult to say anything solely from the height of 500–hPa surface: one needs to monitor the variations in trends.

Looking at the value of the 500–hPa field in more detail it has been noted that, east of the 500–hPa trough there is generally a region of bad weather and east of a 500–hPa ridge is a region of fair weather. Generally speaking, when the trough at 500 hPa moves past Syowa, phenomena such as a blizzard will terminate.

Whereas in the mid–latitudes, low–pressure systems at the surface generally precede the 500 hPa by about 10 degrees in longitude when the low–pressure system approaches the Antarctic continent, the vertical slope of the vortex normally decreases. Usually, the surface pressure changes almost at the same time as the heights of pressure surfaces change up to 100 hPa, indicating that the vortex tube is standing nearly vertical.

There are two typical patterns in the 500–hPa height field affecting Syowa, *viz,* a "zonal pattern" and a "meandering or meridional pattern". In the case of a zonal pattern the strength of the continental high determines the weather conditions. If the high–pressure system over the continent extends to the coast near Syowa Station, fair weather occurs at the station. If the high does not extend to the coast, the weather will be worse, but not so as to be very severe. In the case of large amplitude meandering in the 500–hPa height field, the relative positions of the ridges and troughs is a key factor. Under these situation, sometimes a low moves southwards from lower latitudes, near the east coast of Africa, and the weather becomes

suddenly bad at Syowa. Periodic variations in the weather pattern are common; however, sometimes, a trough cannot move eastward due to blocking.

Clouds

Satellite imagery is indispensable for forecasting in the Antarctic, where surface observations are limited. It is helpful to analyze the cloud imagery together with the 500–hPa weather chart.

Vortex patterns of clouds with radii between 100 to 1000 km need to be watched. If the wind direction at the 500–hPa level is northeasterly, lows within 15º longitude east of the station may be steered southwest towards the station. If the wind direction at 500 hPa is northwesterly, lows to the west will approach the station, deepen and a major blizzard may develop. Normally, as the lows approach the upper clouds increase rapidly. If the 500–hPa wind direction is westerly, lows will approach from the west.

If there is a strong ridge west of the station, cloud systems from the northwest will be stopped by the ridge, and are liable to approach the station with the movement of the ridge and a blizzard may develop. There is a "graveyard" of lows west of the station: many lows approaching the continent lose their energy in this area and disappear within a few days.

Low level clouds (Sc or St) are liable to stay at the coast for more than a few days in some situations. Blizzards need not occur, but cloudy weather continues with precipitation, that affects aircraft operations. Aerological data show a moist layer confined below the low inversion. If the edge of a cloud layer moves northward, then the weather improves at once.

Sometimes cloud regions intrude inland, and bring a blizzard not only to Syowa Station but also to the inland Dome Fuji Station.

Visibility: blowing snow and fog

Strong wind may create drifting and blowing snow with low visibility. Blowing snow may be visible on the continental slope and suggests the existence of strong wind. While these winds may normally not reach Syowa itself great care should be taken, since, if they do, the visibility at the station can decrease from 1 km to 100 m within five minutes.

Surface contrast including white–out

No specific information on forecasting has been obtained.

Horizontal definition

No specific information on forecasting has been obtained.

Precipitation

No specific information on forecasting has been obtained.

Temperature and chill factor

Temperature is strongly related to wind direction. Northerly wind brings higher temperatures and southerly wind lower temperatures. Large temperature inversions may appear at the surface in light wind situations. It is not uncommon to have a sudden increase of air temperature of about 10ºC within three to four hours. This sudden increase of temperature is caused by the destruction of the surface inversion and might be accompanied by the development of a blizzard.

      The dew point depression (T − Td) is smaller in situations involving falling snow compared to drifting snow events.

Icing

No specific information on forecasting has been obtained.

Turbulence

No specific information on forecasting has been obtained.

Hydraulic jumps

No specific information on forecasting has been obtained.

Sea ice

No specific information on forecasting has been obtained.

Wind waves and swell

No specific information on forecasting has been obtained.

7.6   Enderby Land and Kemp Land

Enderby Land extends from 45º to 55º E while Kemp Land extends from 55º to 60º E. From west to east, key stations covered in this section are:

-     *Molodezhnaya*   (67º 40´ S, 45º 50´ E, 42 m AMSL);
-     *Mount King*   (67º 06´ S, 52º 30´ E, 112.5 m AMSL).

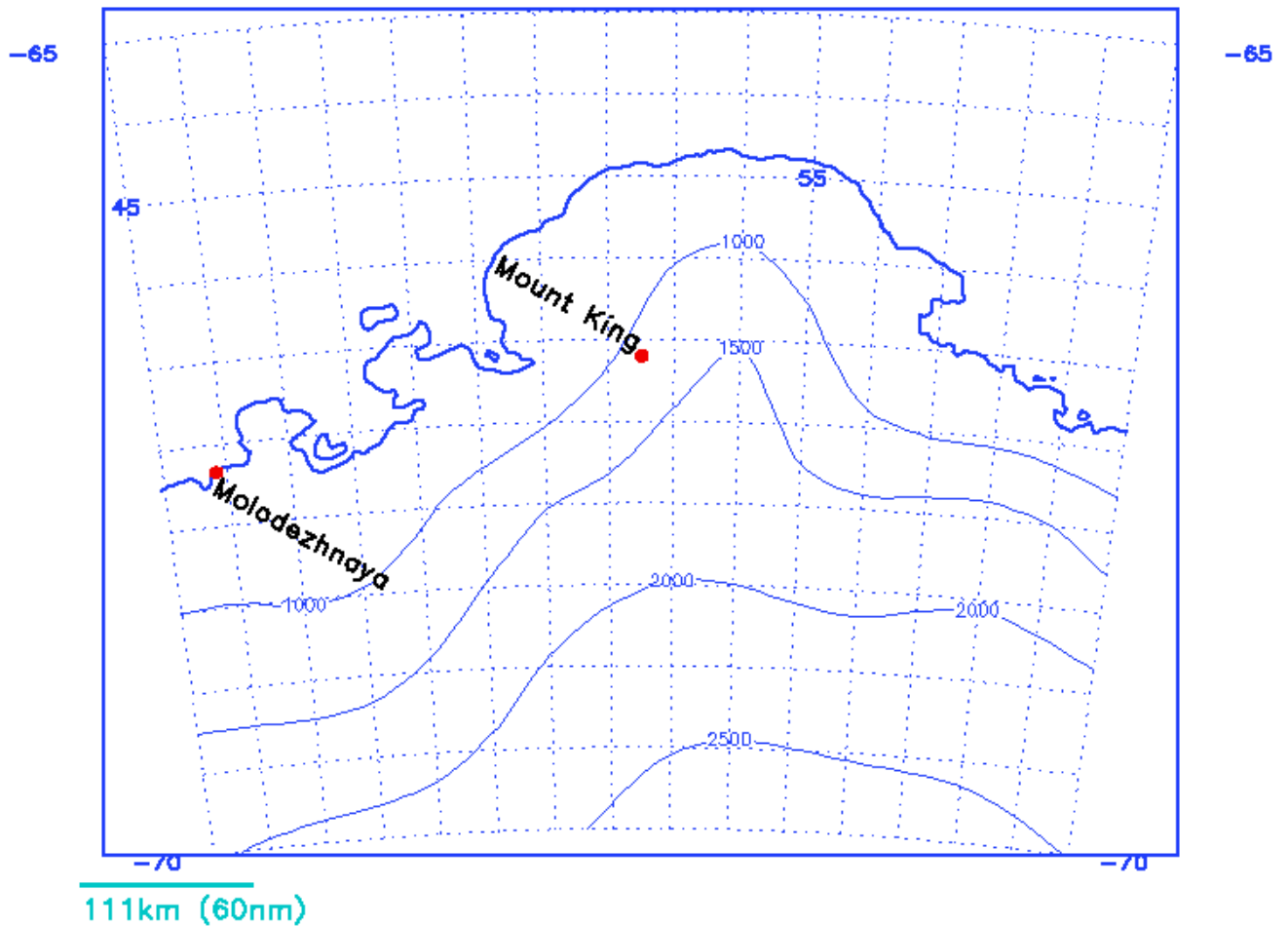The above places are shown in Figure 7.6.1.

Figure 7.6.1   Sketch map for Enderby and Kemp Lands (contours in metres; the area is bounded by: 70º S, 65º S, 45º E and 60º E).

7.6.1   Molodezhnaya

7.6.1.1   Orography and the local environment

Molodezhnaya Station opened in February 1962 and is located on the southern shore of Alasheyev Bay. The settlement is located in a small coastal oasis in the Thala Hills and is 500–600 m from the coast. The station area presents a hillocky locality with rocky ridges separated by snow–covered depressions and lakes. The Cosmonauts Sea in the station area is ice–covered much of the year. There are many icebergs. The land–fast ice width by the end of winter reaches almost 100 km. The rise to the Antarctic ice dome begins about 1.5–2.0 km from the coast. An outlet Kheis Glacier is located 15 km eastward from the station and the outlet Campbell Glacier at the same distance southwestward.

7.6.1.2   Operational requirements and activities relevant to the forecasting process

The settlement numbers more than 70 structures including: living and office buildings; a mess–room; upper–air sounding station; aerological building; power station; radio centre: and a warehouse. West of the settlement there is a runway for aircraft and 12 km to the east–southeast of the station a snow–ice airfield was constructed for heavy aircraft. At present Molodezhnaya Station is temporarily decommissioned and the information below outlines what was available before decommissioning.

7.6.1.3   Data sources and services provided

Information was received in the form of synoptic messages. Ship–borne and drifting buoy data allowed compilation of weather maps as well as pressure orography maps at 500 for 00 and 12 UTC. If necessary, the maps for 06 and 18 UTC were also prepared. The archive of synoptic maps and satellite images for all operational years is stored in St. Petersburg at the Russian Federal Service for Hydrometeorology and Environmental Monitoring's Arctic and Antarctic Research Institute (AARI). These maps provide a possibility to review the atmospheric processes near the Earth's surface and in the tropospheric layer in East Antarctica, as well as in the Weddell Sea and in the east of the Bellingshausen Sea. In previous years, radio communication could be interrupted completely during geomagnetic perturbations in the upper atmospheric layers (magnetic storms) that were mainly observed in winter. About one or two cases of interrupted radio communication for this reason were usually observed every month from May to October. In these cases the analyst had to analyze the atmospheric processes using only meteorological satellite data received on a daily basis at Molodezhnaya.

ECMWF charts were also received. This information included surface and upper–air (500–hPa) analyses, as well as the pressure field forecasts for 24 and 72 h. A synoptic analysis GRID code was used for processing the synoptic maps for the Southern Hemisphere while the prognostic information was invaluable for issuing short and medium–range weather forecasts.

The surface analysis maps for 00 UTC from the Australian WMC Melbourne (via HF transmitters in Canberra, Australia) were received via facsimile communication on a regular basis. In addition, a synoptic map covering the Australian continent and the adjoining oceanic area was received. A surface analysis from the South African Regional Meteorological Centre (RMC) in Pretoria for 0600 UTC over the southern areas of the Indian and the Atlantic Oceans was received by facsimile on a daily basis.

Based on all aero–meteorological and satellite data received, the Molodezhnaya Weather Section prepared and disseminated the following information among the users:

- daily synoptic surface and upper–air charts for 0000 UTC,
- nephanalysis charts and "Meteosat" bulletins based on satellite data,
- semi–diurnal and daily weather forecasts for the regions of the Russian Antarctic stations and sea areas,
- three–day weather forecasts on requests for ships and stations,
- weekly and monthly reviews of synoptic processes and weather conditions for the regions of the Antarctic,
- large–scale ice charts with application by ships,
- 10–day and monthly reviews of ice conditions for the Antarctic Seas,
- ice consultations on requests,

- atmospheric circulation forms for the Southern Hemisphere and types of synoptic processes on a monthly basis.

The main goals addressed by weather forecasters at Molodezhnaya were hydro–meteorological information support of activities for different scientific teams, sledge–tractor traverses, aircraft flights, navigation of ships and loading–unloading at the stations also during helicopter operations. At present, due to decommissioning of the Molodezhnaya Station, preparation is underway for organizing a new Weather Forecasting Section at the Progress Base (Prydz Bay) based on new technologies for synoptic data acquisition and processing.

7.6.1.4   Important weather phenomena and forecasting techniques used at the location

General overview

The main factor determining weather processes in the Molodezhnaya area is cyclonic activity, with cyclones passing along both zonal and meridional trajectories. During the cold half of the year the number of days with moving cyclonic eddies in the Cosmonauts Sea reaches 24 a month, on average. More than half of this number are comprised of cyclones with zonal trajectories moving along the Antarctic front. The remaining group of cyclones (8–10 cases a month, on average,) is related to the meridional tracks.

The zonal tracks are characterized in all cases by a steady western movement in the troposphere and lower stratosphere and hence by a rapid movement of surface cyclones and anticyclones from west to east. With respect to the meridional tracks, surface pressure features move with significant northerly and southerly components, resulting in the inter–latitudinal air mass exchange in different coastal zones of the Cosmonauts Sea.

Typically, this air exchange occurs as a result of merging of the Antarctic High ridges in the troposphere with the anticyclones of the subtropical belt. Near the Earth's surface, this relationship is expressed in the form of the blocking ridge. The locations of this ridge and of the trajectories of low–pressure systems determine the weather character in the coastal region connected with different types of meridional processes.

The influence of different meridional circulation types, which are in turn governed by the development of warm West Atlantic and East Atlantic ridges, on the weather in Molodezhnaya, is significant. In the first case, the cyclonic activity in the Falkland branch is strongly developed. However, at Molodezhnaya the weather is mainly governed by the influence of the eastern branch of the West Atlantic ridge and is distinguished by certain stability. In the second case, the branch of low motion is developed. The movement of warm and humid cyclones with intense storm activity along this trajectory also gives unstable weather in Molodezhnaya with alternating strong easterly and southeasterly (katabatic) winds with snowfall and blizzards and significant air temperature oscillations in the wintertime.

With respect to the zonal type of processes, shallow occluded cyclones with small moisture content move along the Antarctic front. They rarely approach the coast and frequently stable weather is established at Molodezhnaya without snowfall and a wind increase.

During the warm half of the year, the frequency of the movement of lows on or near to the coast, and the activity of cyclonic eddies, significantly decreases with corresponding increase of stability of weather conditions. However, extreme conditions do sometimes occur in summer and the forecasting of these events is connected with certain problems. The corresponding example will be given below. It has to be noted that global model predictions

for the area of the Cosmonauts Sea and to its north, in the absence of significant orographic effects, yield quite satisfactory results in respect of the development of large–scale cyclones and blocking ridges not only for 1–2 days, but also for an extended period. These forecasts are obviously taken into account by weather forecasters and sometimes provide the only basis for forecasting for the area. On the other hand, the mesoscale systems are identified in this region with difficulty, and only from cloud images. In general, the study of these mesoscale features, which although comparatively rare in frequency, do result sometimes in significant weather deterioration, is still not well developed.

Surface wind and the pressure field

Easterly and southeasterly winds are the most prevalent winds at Molodezhnaya: on an annual basis these winds comprise 85% of all observations at the synoptic times. From historical averages, easterly winds prevail in the summer months, and the southeasterly winds are most frequent in the other months of the year. During the period March to July the frequency of occurrence of the latter comprises around 50% with increasing southerly direction (the third by frequency of occurrence) up to 18–20%.

The main factor controlling the wind direction is the surface pressure distribution. As indicated on mean surface pressure analyses, the zone of north to south surface pressure gradient (easterly geostrophic wind) covers the coastal region of the Cosmonauts Sea up to latitude 65° S. In the winter months, the climatic circumpolar trough axis is located slightly more to the south and in the summer months slightly north of this latitude.

Thus the main wind types for the coastal Antarctic regions (cyclonic, katabatic and transient) have quite a steady direction in Molodezhnaya, but the wind speeds change sharply and over a wide range. Particularly intense and persistent cyclonic winds are observed as maritime lows move to the coast. Thaws and heavy snowfalls accompany them. The katabatic wind following the cyclonic wind can have hurricane force lifting enormous amounts of freshly fallen snow into the air.

The katabatic (gravitational) wind occurs above the steep slope of the dome whose height reaches 2,500 m some 350 km distant from Molodezhnaya. The conditions for consistently gusty winds in the night-time with a gust speed range from 0 to 25–30 m s^{-1} (0 to ~50–60 kt) are created at the beginning of autumn. At this time, the ocean produces a warming effect and the cold katabatic flow penetrates far over the sea. In winter, in connection with air cooling in the coastal area above the sea ice, the katabatic wind becomes irregular. Sometimes katabatic winds decrease only at the dome foot and calm weather persists at the station. Continuous katabatic wind at the station is observed in the presence of relatively warm air masses near the coast.

The development of katabatic winds at the station is related to cyclonic activity near the coast. The highest wind speeds are observed in the rear part of the cyclones when the katabatic and cyclonic wind vectors coincide. Strong katabatic winds are formed above Molodezhnaya with appearance of strong southerly jet currents in the troposphere above the dome. These jets form strong lower level flows that merge with the surface katabatic flow at the northwestern slope of the ice sheet ridge, which is directed from the centre of East Antarctic towards Enderby Land. The surface relief features induce separate jets depending on the slope forms and relative positions. Note that appearance of snow eddies above Mount Vechernyaya in the Hays Glacier outlet area is one of the direct signs of the beginning of subsidence and downslope flow at Molodezhnaya. Typically, if the direction of the downslope flow at Molodezhnaya is 140°, then it is 160° at the airfield near Mount Vechernyaya.

The subsiding downslope flow becomes especially gusty at the end of winter. Its strong jets can interact with the relief irregularities contributing to the occurrence of eddies. The

378

southeasterly wind speed reaches 40 and even 50 m s^{-1} (~80–100 kt) with an almost complete loss of visibility. In summer, the katabatic wind can also be significant (with individual gusts up to 25–30 m s^{-1} (~50–60 kt) but this is rare and typically occurs in the night–time (between 1 and 5 AM local time.). The diurnal heating of the dome slope induces a pressure decrease and air advection from the sea towards the dome. Only with the passage of an east–southeasterly jet current in the troposphere can the katabatic wind persist in the daytime, but it is less intense.

The number of days with storm force winds at Molodezhnaya has been as great as 221 a year with as many as 174 blizzards. The largest average monthly speed occurs in May and is 14.5 m s^{-1} (~28 kt). The maximum speeds are about 40 m s^{-1} (~80 kt) and occur from April to October: the maximum gust reported (54 m s^{-1} (~105 kt)) being in May.

The presence of wind data from permanent stations, ships, buoys and automated weather stations is necessary for the synoptic analysis of the surface pressure field and 850-hPa field. It is also important to take into account the influence of the orography of the area, as the observations do not necessarily reflect the general character of the air mass transfer in the given area. This should also be taken into account in updating the model pressure forecasts that should be used with caution south of 70º S.

Upper wind, temperature and humidity

No specific information on forecasting has been obtained.

Clouds

The amount of total cloud, on average, for a year in the Molodezhnaya area is 5.5 oktas. The months with high cloud amount are April and March when the average cloud amount is 6.2 oktas. The largest frequency of occurrence of overcast conditions (6 to 8 oktas) is 72% and is observed during the same period. This statistic does not decrease significantly in the other months of the year. In other words, gloomy weather predominates at Molodezhnaya. However, the frequency of occurrence of clear sky is observed in 20 to 30% of observations at standard times in all months of the year, except for March and April. Active cyclonic activity in the Antarctic coast zone is a cause of constantly significant cloud cover. Upper and low clouds typically prevail. However, as deep cyclones leave the ice–free sea, multi–layered cloud systems accompany the passage of the main and secondary frontal zones, including low stratus and cumulus clouds with precipitation in the form of snow.

Visibility: blowing snow and fog

Good visibility conditions generally prevail at Molodezhnaya. The frequency of occurrence of visibility greater than 10 km comprises 85–88% of all observation times in the summer months notably decreasing in winter. Blizzards are the main factor restricting visibility, hence to predict deteriorating visibility means to correctly predict the wind increase accompanied with snowfall or snow–drift. The latter occurs in the presence of non–compact snow cover and wind speeds greater than 7–9 m s^{-1} (~ 14–17 kt). Since strong winds predominate in many Antarctic coastal regions, the number of days with blizzards is more than 170 days a year. In winter, they comprise 18–22 days a month but in summer they typically do not exceed 1–2 days per month.

The presence of a cyclone is the most dangerous synoptic situation connected with occurrence of strong blizzards. When the station is influenced by the rear sector of a low, the storm force winds can persist for a long time. Drifting snow is obviously a less dangerous phenomenon than blizzards, but they are quite frequent in winter. In summer, their frequency of occurrence notably decreases as non–compact snow cover is quite seldom observed at this time of the year.

Advective sea fogs at Molodezhnaya are very rare, occurring during periods of light wind speed. These are purely local phenomena and are of short duration.

Ice fog is even a rarer phenomenon compared to sea fog in summer. After a strong blizzard, a fine snow dust remains in the air at the station and especially in the vicinity of the station at the dome slope at low wind speeds. This snow dust remains in the suspended state for many hours and may result in the snow haze phenomenon with visibility reducing to 4 km. A successful forecast of such a phenomenon by an experienced forecaster is quite possible.

Surface contrast including white–out

White–out presents a significant danger for aviation flights under Antarctic conditions. In sunny weather, with discontinuous and thin stratus clouds over a uniform snow surface, there is no contrast and the horizon is not discernible. An example of a dangerous synoptic situation is a period when a subtropical high–pressure ridge in the Cosmonauts Sea area merges with the Polar High ridge. This leads to the formation of a southerly jet at the eastern periphery of the high–pressure ridge typically at the tropopause height. A zone of continuous mainly stratocumulus cloud is formed on the dome at the contact of warm and cold air masses. Some times the southeasterly winds can increase and the horizontal visibilities reduce in the snowfall. Orientation in space above the dome is very difficult under these conditions since the horizon blends with the snow surface. Then when the wind decreases, and visibility improves and the sun is at a sufficient height, a no less dangerous situation can appear – the white–out. There is a rule, according to which the flights above the dome, especially inland, are better undertaken with a cloud–free forecast.

Horizontal definition

See the section on surface contrast above.

Precipitation

In accordance with the features of the development of cyclonic activity, the maximum precipitation is observed at Molodezhnaya in autumn, during March and April. A secondary maximum is observed at the end of winter and at the beginning of spring, namely, in August and September. The minimum precipitation occurs in the summer months – December and January. Typically, less than 350 mm of precipitation falls in solid form except for rare cases in the summer months.

One usually pays attention to the similar physical–geographical conditions and atmospheric circulation conditions of Mirny and Molodezhnaya. This similarity is manifested in the characteristics of clouds and precipitation. In addition, both stations, similar to the entire coast of East Antarctica, are characterised by significant air dryness and comparatively low relative humidity values. The yearly average comprises 65% for Molodezhnaya and 71%

for Mirny. For the ice–covered coastal areas, the low humidity values are connected with air drying at discharges. The annual humidity variations as well as water vapor elasticity at Molodezhnaya is very weakly pronounced.

The forecast of cloud and precipitation depends typically on the correct forecasting of the development of the synoptic situation provided upper–air synoptic data and satellite data are available.

Temperature and chill factor

The temperature regime at Molodezhnaya, similar to other Antarctic areas is influenced by solar radiation, the underlying surface character and atmospheric circulation. According to the "Atlas of the Antarctic" this region belongs to the coastal climatic zone in the form of a narrow coastal strip including outlet glaciers, land–fast ice, oases and areas with snow–free hills and rocks.

The albedo value at Molodezhnaya is quite significant, but much less than at Mirny. From the middle of spring and up to the beginning of autumn, the value of absorbed radiation flux and the full balance in bare areas become much greater compared to the surrounding snow surface. The annual balance, unlike Mirny, is positive: around 7 months positive at Molodezhnaya but 4 months at Mirny. A comparatively large radiation heat flux to the underlying surface in summer is compensated by the heat lost in warming the near surface air layer. The summer at Molodezhnaya is warmer and the winter is colder than at Mirny, but the air temperature multiyear averages at both stations are negative in all months.

The maximum monthly average temperature is in January (–0.40ºC) with the record maximum of +9.0ºC. August is the most severe month (–18.8ºC mean temperature) with a record minimum of –42.0ºC. Air temperature variations from day–to–day are related to the atmospheric circulations, primarily to the track of cyclones from the northern oceanic regions to the coast. The pattern of development of such systems is sometimes quite complicated being connected with the study of large–scale circulation modification over extensive areas. For example, such phenomenon as the formation of significant air temperature increases (several degrees higher than the multi–year norm) at Molodezhnaya in summer can be connected to the variant of the process beginning 1–2 weeks earlier in the Australian sector at the development of the meridional Ma circulation form. According to this variant a sharp large–scale warming in the tropospheric layer begins with the formation of a strong blocking ridge and the surface high south of Tasmania. A steady southward warm air transport is established at the ridge southern periphery with cyclones developing at the West Australian branch. This contributes to an intensified coastal high and its displacement south–westward to the near–pole area resulting in a sharp air temperature increase along its pathway, for example up to above zero values at Vostok Station then changing its direction the high moves towards the Cosmonauts Sea. A significant air temperature increase at Molodezhnaya and at Syowa occurs with increasing southeasterly flows. Warm air flowing from the high down the ice dome slopes from a height of more than 3,000 m, warms additionally as a result of the Foehn effect and an almost daily incoming solar radiation. Some times the air temperature in the coastal oases can rise to 8–12ºC .

The forecasters at Molodezhnaya developed in this way many variants of typical processes leading to the anomalous weather conditions in different seasons.

Icing

No specific information on forecasting has been obtained.

Turbulence

In weather forecasting for the coastal Antarctic regions, it is necessary to constantly make observations of turbulence occurring both at a height in the jet streams and near the surface especially at the ice slopes. Typically, a westerly and southwesterly jet occurs above the region of a low that has moved from temperate latitudes along the meridional trajectory 12–18 h beforehand. Strong heat advection from the north in the frontal sector leads to the development of continuous low clouds, snowfall and precipitation in the form of drizzle. Under such conditions clouds and warm air extends to the plateau over 400–500 km away where the strongest turbulence is observed at the contact with cold air, which is often accompanied with icing of aircraft.

During the sinking flow in winter the largest eddy formation occurs when a mass of very cold air forms near the coast above the fast ice while the katabatic wind mixed with the upper layer air has a higher temperature. In these cases strong jets occur at the contact of cold air and interact with it. The irregular relief contributes to eddy formation. Occasionally, tornado–like eddies with a 10–150 m diameter are observed with the wind speeds of 50 m s^{-1} (~100 kt).

The winter and spring flow is sometimes manifested in occurrences of eddy waves with a horizontal axis descending from the ice slopes. In the rear part of the eddy a strong downward flow is felt while at the frontal wave there a sudden deterioration of visibility due to rising snow dust.

The effect of the aforementioned and similar phenomena on the landing aircraft can be very dangerous. There is a large gap of detailed observations of turbulence and a need for projects investigating these phenomena using modern instruments and equipment, as well as experience of investigating the dynamic and thermodynamic processes in the boundary atmospheric layer, for example, during the international winter expedition to the Weddell Sea in 1989.

Hydraulic jumps

No specific information on forecasting has been obtained.

Sea ice

The drifting ice zone in the Cosmonauts Sea is mainly formed during winter with maximum intensity in October-November, when under average climatic conditions the ice edge reaches 58^0 S. In the summer season the drifting ice zone decreases and the ice decays rapidly. It is due to location of the eastern part of Cosmonauts Sea that is in the western peripheral area of a vast current system with prevailing conditions for the outflow drift.

The most favorable conditions for mooring at Molodezhnaya usually occur from the third 10-day period of February till the second 10-day period of March. During this time it is

often possible for ships to access the shore through clear water, or by leads where the ice concentration is not greater than 3/10.

The thickness of the fast ice in Alasheev's Bay does not usually exceed 100-140 cm. The width of fast ice is significant during pre-spring months, about 70 km on average, therefore the most reasonable period for mooring the station for disembarkation on the ice moorage is after the break-up of fast ice. From the second half of February till the end of March fast ice is destroyed in 70 % of all cases, and if it remains, then its width does not exceed 20-30 km and its strength characteristics are strongly reduced.

In the station area there are deltas of outlet glaciers, which are responsible for higher concentration of icebergs in Alasheev's Bay. From the station it is possible to observe up to several tens of icebergs along the horizon, mostly drifting very slowly in winter.

Wind waves and swell

No specific information on forecasting has been obtained.

7.6.2   Mt King

7.6.2.1   Orography and the local environment

That part of the coastline which bounds eastern Enderby and western Kemp Lands, protrudes like a mushroom–shaped knob some 100 km, beyond the general line of the coast. This gives a more maritime climate on this part of the coast, especially once the sea ice on the northern coast breaks up (the second week in January has been noted on one occasion).

Another factor influencing local weather patterns is the basically north–south ridge line running east of Knuckey Peaks down to the 1,500 m contour into a saddle shaped landform and then rising to a dome bounded by the 2,000 m contour through which rises Mt Elkins. Mt King sits on the western side of this saddle. Another spur of the ridge from the plateau extends northwest towards Perov Nunataks.

Other notable features are the large valley formed by the Robert and Wilma Glaciers to the east, the Seaton and Rippon Glaciers north of these and all running into the King Edward Ice Shelf, the Beaver Glacier to the west of Mt King and the Napier Mountains running northwest from Mt Elkins. The modifications these terrain features make to weather produced by synoptic scale systems are significant. Dramatic changes can occur over short distances and in short time intervals.

7.6.2.2   Operational requirements and activities relevant to the forecasting process

A temporary summer camp was operated by Australia at Mount King from 1975 to 1980 inclusive after a similar camp was sited at the much worse weather location of Knuckey Peaks. (These peaks are just visible in Figure 6.6.4.1 above that was taken from the Mount King camp looking south).

7.6.2.3   <u>Data sources and services provided</u>

The Mount King camp is closed. If there was a forecast service required it would most probably be provided by forecasters located at Davis Station.

7.6.2.4   <u>Important weather phenomena and forecasting techniques used at the location</u>

General overview

The descriptions of weather reported here come mostly from four reports from operational forecasters charged with forecasting for ANARE expeditions in 1975/76, 1976/77, 1977/78, and 1979/80. A summary of the conditions experienced during these summers is given in Table 7.6.2.4.1 in Appendix 2 below.

It appears that the weather experienced in Enderby Land in the 1976–77 summer was more clement than in other years, this is supported by the number of flying days lost due to weather (15% compared to 20% in 1975–76): moreover, above average geopotential heights, temperatures and pressures were recorded over the Antarctic during the 1976–77 summer. By way of contrast the weather experienced in Enderby Land in the summer of 1977/78 was worse than the previous two seasons and there was a 31% loss of flying time. In 1976–77 the upper trough persisted in the Molodezhnaya area giving an east to northeasterly trajectory to upper winds over Enderby Land. For the 1977/78 summer a closed upper circulation (very evident at 500 hPa) persisted to the west of Syowa, giving a mainly upper northwest flow over Enderby Land. The surface winds remained their normal easterly. As in previous years, coastal lows stagnated in Lutzow–Holm Bay, but this year instead of dissipating they eventually moved eastwards around the Enderby Land coast, often splitting into two centres when near Proclamation Island. The three blizzards that occurred at Mt King during the 1977/78 summer formed when these coastal lows deepened suddenly between Sheelagh Island and Proclamation Island.

The upper low west of Syowa kept the relatively moist northwest flow over Enderby Land and probably helped the progression of the coastal lows. It was significant that the only substantial period of nil cloud occurred when there was no northerly component in the upper winds at Mt King and Molodezhnaya.

Most deteriorations in weather at Mt King in 1977/78 moved in from the northwest quadrant. On only two occasions was the previously (1976/77) common "cloud band and snow showers from the east" observed. Most often middle level cloud thickened from the west as a coastal low moved eastwards past Molodezhnaya. The cloud base then gradually lowered and snow would begin falling in the Tula Mountains. This low cloud and snow would then gradually build up towards Mt King.

During the December of 1979/80, in response to the long wave pattern, the lows moved over the ocean well to the north with the main cyclonic activity being along 50º S. This suddenly changed in early January and for the remainder of this season the cyclones tracked along the coast and even south of Mt King on one occasion. It is interesting to note that this change in cyclone paths coincided with the final break–out of the sea ice from Amundsen and Casey Bays, which increased the moisture available over Enderby Land.

Mt King is fairly sheltered from north and north–easterly airstreams, slightly more exposed to easterly and south–easterly airflows and quite open to westerlies. The Robert and Wilma Glaciers form an area of pronounced cloudiness in easterly airstreams because moist air both converges and rises up the valley. If the stream is sufficiently developed and moist,

this cloud follows a natural channel off to the west–southwest to encompass Knuckey Peaks and McLeod Nunataks. If cloud in the King Edward Ice Shelf area is more extensive in an easterly air–stream, low cloud north of Wilma Glacier moves east to the vicinity of Bird ridge, but middle cloud from this area usually extends as far as Mt King, and produces white–out.

South–easterly airstreams are usually drier and the above effect is less noticeable. These streams produced good weather at Knuckey Peaks which otherwise had very poor weather overall compared to Mt King. One problem with some moist southeasterly airstreams is cloud formation northwest of Seaton and Rippon Glaciers which produces white–out looking inland of Rippon Depot.

Northeasterly airstreams are almost invariably very moist and produce extensive low cloud on the windward side of the Napier Mountains. Mt King's protected position delays the cloud build–up some six to ten hours but eventually a good cover of stratocumulus drifts across. Mt King does however seem to have less precipitation and wind than a more exposed position.

The most frequent path followed by the lows that produce poor weather in Enderby Land is from a point usually near 50º S latitude and west of Marion Island to a pronounced stagnation point north of Prydz Bay. These lows sometimes amalgamate with pre–existing weak lows in the Antarctic coastal trough to produce a fair sized blow at Mawson and strong winds right along the coast, probably as far as Cape Ann. The effect at Mt King depends on how close to the coast the lows come, their strength and local effects but will at least bring increasing cloud, wind and snowdrift.

Extended periods of fine weather occur when a strong ridge from the polar high extends northwards over Enderby Land to the coast.

Surface wind and the pressure field

The predominant surface wind direction is easterly. It would seem from the earlier discussion that most weather comes from the east when the long wave pattern is conducive to an upper east to northeast air flow over Enderby Land. On the other hand a persistent upper northwesterly to westerly flow over Enderby Land is also associated with weather arriving from those directions, even if the surface airflow was easterly

Early in the 1979/80 season a high correlation was noted between the value of Mawson's MSL pressure minus Molodezhnaya's MSL pressure and the velocity of the surface wind at Mt King. High positive values (i.e. northerly gradient) were associated with the strongest easterly winds at Mt King. Negative values were associated with light easterly or even westerly winds. The reason for this correlation appears to be the barrier the continental ice dome presents to a northerly flow. The barrier deflects the flow westwards. The wind increase appears to lag the Mawson–Molodezhnaya pressure difference value by approximately six hours.

Upper wind, temperature and humidity

NWP would be used to forecast upper–air information along with radiosonde date from Mawson and Molodezhnaya.

Clouds

Apart from blizzards, the main cause of deteriorating weather at Mt King appears to be broad bands of cloud moving westward accompanied by light snow or virga and snowdrift (usually slight). Only occasionally do these bands make the camp inoperative for helicopter operations and then at most for about six hours as the band moves through. Possibly a diurnal effect operates because the improvements often happen in the evening. Usually the degree of effect can be judged from the nature of the cloud. If there are several cloud layers to the east, or the depth of cloud appreciable, then it is likely that the cloud will eventually move over most of Enderby Land with some deterioration at Mt King.

This location, being west of the ice ridge joining the ice dome near Mt Elkins to the main ice plateau enjoys some protection from adverse conditions: to reach the camp the easterly airflow undergoes subsidence, the resulting warming being sufficient to evaporate much of the cloud.

On some occasions front–like cloud bands associated with maritime lows passed through Mawson with a north–south orientation and headed westwards to subsequently affect eastern Enderby Land. On other occasions, these lows themselves became stationary or moved westwards.

The early identification of major lows coming in from the northwest is straight forward provided observations from Marion Island and satellite imagery are available, but the accurate timing of weather deterioration at the coast is difficult because of the lack of data to the immediate north. The rate of movement of east to west moving cloud bands can usually be fairly accurately assessed.

The other interesting synoptic scale feature of the area is the pronounced stagnation area for low–pressure systems near Lutzow–Holm Bay. These lows produce onshore winds and cloud in the Molodezhnaya coastal region with occasional snow but rarely do they move further eastwards to produce significant blows for eastern Enderby Land.

A feature of all these systems, particularly those moving in from around 50º S, is the advection of relatively warm air over the relatively warm sea. This southward airflow is cooled by contact with progressively colder sea water and eventually the continent itself. Moreover, a general upslide occurs as the maritime air becomes relatively more buoyant with respect to This mechanism is a significant cloud producer with associated white–out problems. So whenever an approaching low turns the basic wind flow on the coast from Mawson to Enderby Land (from southeasterly, easterly, to northeasterly), increasing cloud can be expected.

Visibility: fog

An infrequent but interesting airstream direction at Mt King is from the west. On infrequent occasions a weak low may move inland near Molodezhnaya producing a light onshore airflow over the coast further to the east. Low cloud formed in this way may move up the valleys between mountains. On Beaver Glacier the cloud will generally move as far as Mt Reed with the wind at Mt King calm or a light easterly during the day. On one reported occasion in late January, the wind at Mt King swung to a very light westerly in the late afternoon. Within two hours the low cloud had drifted up towards Mt King and enveloped the camp in fog. On other occasions distant fog was observed to the northwest of the camp in the morning.

On two occasions in 1976–77 fog enveloped the Mt King camp following a set pattern: stratus formed about the mountains to the north and north–west during the late afternoon. At about 2100 h (local) the low stratus/fog appeared to form just west of the camp and when the

surface wind gave way to a light westerly at about 2200, the fog moved over. For the next few hours it would fluctuate, usually going when the easterly wind sprung up. By about 0200 local the fog retreated west of the camp but was still to be seen in the distance until around 0700 local time.

Fog at Mt King was more common in the 1977–78 season. Usually it formed on relatively clear afternoons in the Beaver Glacier and drifted eastwards to envelop Mt King by mid–evening. In this sequence, a light easterly wind often persisted at the camp until the fog was within one or two miles. When the surface wind at Mt King turned westerly by mid–afternoon, fog on two occasions actually formed over the camp, rather than drifting in.

Surface contrast including white–out

White–out conditions were most commonly created by an overcast of cloud causing the ice surface to appear to blend in with the cloud. At Mount King, a chain of mountains runs approximately westward to the coast, and, provided cloud did not cover the peaks, these rock formations did provide some visual reference in white–out conditions and a relatively safe path for the aircraft. However, there is no such relief in other directions and cloud will readily cause white–out problems.

Horizontal definition

No specific information on forecasting has been obtained.

Precipitation

NWP and satellite imagery would be used.

Temperature and chill factor

No specific information except see Table 7.6.2.4.1 in Appendix 2 below for an appreciation of summer temperatures.

Icing

Rime icing is possible in summer when the moisture content is high in a maritime airflow.

Turbulence

Mechanical turbulence is probable around nunataks and rock outcrops in strong low level wind conditions.

Hydraulic jumps

Hydraulic jumps have not been reported in the area of Mt King.

Sea ice

Not applicable at Mt King.

Wind waves and swell

Not applicable at Mt King.

7.7   MacRobertson Land

MacRobertson Land spans 60º to 73º E. From west to east, key features or stations/bases referred to in this section include:

- *Mawson*   (67° 36′ S, 62° 53′ E, 16 m AMSL);
- *The Prince Charles Mountains*;
- *Soyuz*   (70° 35′ S, 68° 47′ E, 336 m AMSL);
- *The Amery Ice Shelf*;
- *The Lambert Glacier*.

The above places are shown in Figure 7.7.1 and in Figure 7.8.2 below.

7.7.1   Mawson

7.7.1.1   Orography and the local environment

Mawson is near 67° 36′ S, 62° 53′ E. Although the coastline is generally oriented east/west near Mawson, the station itself is on a northwest–facing section of coastline on the Mawson coast. It is situated at the foot of the continental ice plateau, with mountain ranges to the south.
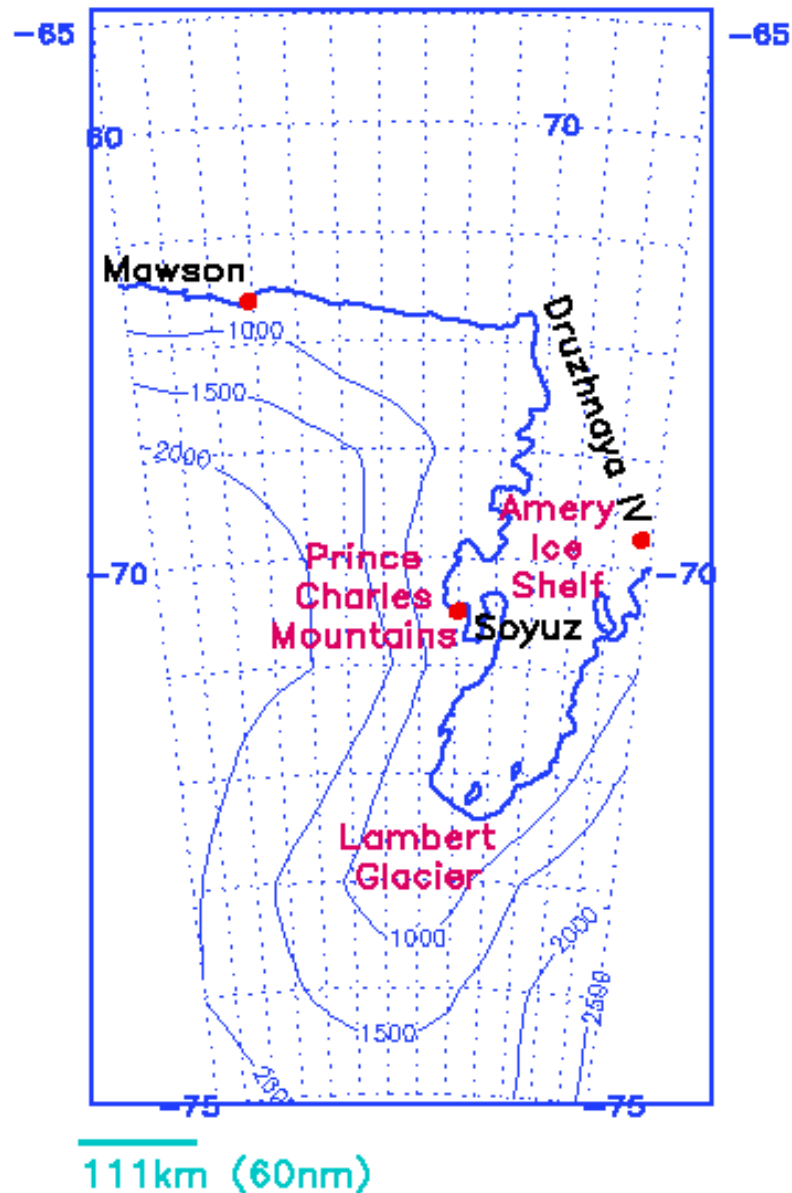
Figure 7.7.1   Sketch map for MacRobertson Land
(contours in metres; the area is bounded by: 75º S, 65º S, 60º E and 73º E) .

7.7.1.2   Operational requirements and activities relevant to the forecasting process

At present, S76 helicopters are used to ferry personnel to Mawson from Davis and return during the Austral summer. Operations at Mawson are currently supported from Davis (see Section 7.8.4 below). As in the past, should fix–winged aircraft operate into Mawson then a blue ice airstrip at the nearby Rumdoodle site (67º 48′ S, 62º 50′ E, 498 m AMSL) may be used.

7.7.1.3   Data sources and services provided

The only service available at Mawson at present is APT satellite reception, although grid point data from some global models can easily be sent to a forecaster at Mawson via e–mail. Access to the World Wide Web allows the forecaster to browse a wide set of products from various forecasting centres.

7.7.1.4   Important weather phenomena and forecasting techniques used at the location

General overview

Table 7.7.1.4.1 in Appendix 2 below gives a summary of mean monthly values of certain weather elements at Mawson.
        Mawson is affected by katabatic winds from the ice slopes to the south. These katabatic winds are associated with a strong diurnal variation of wind speed, with a morning maximum. Temperatures above zero are common in summer, often leading to the break–out of fast ice from along the Mawson coast in January. Winter temperatures are more typically near –15 to –25°C. Mawson is affected by mobile depressions, and, while many depressions appear to form to the north near the Antarctic convergence south of Kerguelen Island, intense depressions often reach the base.
        Frontal precipitation is generally in the form of snow generated by warm fronts, occasionally travelling westwards along the Antarctic coastline as the parent depression moves slowly eastwards. Snow commonly falls from stratocumulus or nimbostratus.
        Table 7.7.1.4.2 in Appendix 2 below is taken from work by D. Shepherd (personal communication) and summarises the suitability of Mawson as an aircraft landing site based on the incidence of adverse cross–wind, cloud, white–out and adverse visibility. While these parameters are discussed in more detail below it may be seen from the table that potential white–out aside, Mawson enjoys a relatively low percentage of weather which might be adverse to aviation. December (only 6 % adverse conditions (excluding white–out)) is the best month and the July–August period the worst (17 % adverse conditions).

Surface wind and the pressure field

Figure 7.7.1.4.1 in Appendix 2 below shows wind roses for Mawson for each season. It may be seen from this figure that for Mawson the prevailing winds are from the southeast. About 15% of Mawson's winds are over 15 m s^{-1} (~30 kt) for summer, rising to around 27% for winter. The mean wind speed is 11 m s^{-1} (~22 kt) or more for most months and still around 9 m s^{-1} (18 kt) for December and January. There is little diurnal variation in mean speed through late autumn and winter, but for other months there is a maximum near 0000 UTC and a minimum near 1200 UTC. The January range is from about 11.9 m s^{-1} (~23 kt) to 6.7 m s^{-1} (~l3 kt) for those times.
        Significant winds at Mawson are also mostly southeasterly in the case of katabatic flows or easterly when strong to gale–force synoptically forced winds occur. (Gale–force winds rarely have westerly components at Mawson, with a strong preference for easterlies.) Katabatic flows may be nearly southerly, but rarely have a westerly component. Sea breezes occur during summer, generally northwesterly. Strong northwesterlies or westerlies are very

rare, although moderate sea breeze westerly to southwesterly flow is common on summer afternoons.

Winds stronger than gale–force are generally associated with synoptic scale low–pressuresystems moving southwards or eastwards towards or along the Mawson coast. The northward deviation of the Antarctic convergence towards Kerguelen Island may be responsible for the tendency of most low–pressuresystems to pass well north of Mawson. It is observed (Phillpot 1997, p 98) that gale–force winds at Mawson are associated with 500–hPa ridges crossing the coast between Mawson and Davis, especially when the ridge causes north to northeast flow at 500 hPa over Mawson (see Phillpot's Figure 4.24d – Phillpot's composite for gales at Mawson). It appears the northerlies are needed in order to 'steer' the synoptic scale lows close to the coastline, however short blizzards have been caused by low–pressure systems moving eastwards. (As the Antarctic convergence moves closer to the coast near Casey, it would be expected that synoptic scale depressions would more frequently affect the coast.)

Considerable variation is found over the Mawson coast in wind speed. Field party reports suggest that the strong katabatics of Mawson Station are not commonly experienced to the west near the Stillwell Hills, even in exposed areas. However, to the east the strong katabatic zone extends beyond Scullin Monolith.

In terms of aircraft operations it is useful to not only consider the potential absolute wind strength but the cross–wind component may also be of concern. Cross–wind component thresholds for safe landing/takeoffs are aircraft dependent. Table 7.7.1.4.3 in Appendix 2 below shows the percentage frequency of occasions when the wind normal to the prevailing 130º mean wind direction at Mawson exceeds 7.7 m s^{-1} (~15 kt). Such occurrences are not common at Mawson, ranging from 8% in August to 3% in December.

The above data relate to Mawson itself where perhaps only rotary–winged aircraft could land. However, there is an area of blue ice at the nearby Rumdoodle site where fixed–winged aircraft can, and have, landed. Observations made in February and March 1960 indicate that average winds at this site are about one half those at Mawson, there being shelter from the south and east due to the Masson range. Targett (personal communication) has processed approximately three months of wind data collected during the period 6 September 1993 to 11 Dec 1993 at the "Rumdoodle Turn Off" (RTO) site located at 67º 47′ S, 62º 42′ E, which is somewhat closer to Mawson than Rumdoodle itself. Targett has compared the Mawson winds for the same period and reports that the average 10 m elevation wind speed for Mawson was 8.9 m s^{-1} for the period, compared to the RTO anemograph recording, at 3 metres, of 11.1 m s^{-1}. Advice from Allison (personal communication) suggests that the RTO data could be increased by between about 1.1 (for snow surface) and 1.3 times (for blue ice) to adjust from 3 m to 10 m elevation.

So, using a height adjustment factor of 1.2 (assuming a part blue ice/part snow surface), for the approximate three month period the winds at RTO were about (11.1*1.2)/8.9=1.5 times greater than at Mawson. This is in contrast to Streten's (1961) finding for the more inland Rumdoodle site. This ratio compares with the 1.89 factor reported by Shaw (1960) at Mt Henderson, however, Mather and Miller (1966) state that the Mt Henderson site was at a "high rock nunatak, and the winds sweeping over the ridge could well be much stronger than those on the adjacent plateau". It should also be noted that the RTO site is between the Massom and David Ranges and so may be protected from the general southeast katabatic flow to some extent.

To assess the likely risk to aircraft it should be noted that Targett's 1993 data indicated a 10 m mean wind speed at the RTO site of around 13.3 m s^{-1} (~26 kt) for spring/early summer. The strongest 10 minute averaged 10 m wind inferred from Targett's data set was 36 m s^{-1} (70 kt) on 10 and 20 October. An inference regarding the likely strongest gust at RTO was made as follows, taking the month of December as an example. The strongest gust on record at

Mawson for December is 53 m s^{-1} (~103 kt) in 1966. A "guesstimate" as to the ratio of gust to mean speed at Mawson would be about 1.2 to 1.3. Taking a factor of 1.25 gives a mean speed at Mawson at the time of the gust as 42 m s^{-1} (~82 kt). Scaling this by 1.5 gives an estimated mean wind speed at RTO of 64 m s^{-1} (~124 kt). RTO is slightly smoother than Mawson so the gustiness factor should be less, let us say, 1.2. Thus the extreme gust at RTO in December is likely to be in the order of 64*1.2=81 m s^{-1} (~148 kt). (A second way of estimating the peak gust might be to simply scale the gusts according to the ratio of mean wind speeds, thus the 53 m s^{-1} scaled by 1.5 would give 79 m s^{-1} (153 kt). It should be stressed that this would likely be an extreme event, perhaps a one in 30 to 50 year event. On the other hand, from Targett's 1993 data, peak gusts of around 28 to 42 m s^{-1} (~50 to 75 kt) might be expected at RTO at least once per month during spring and early summer.

Upper wind, temperature and humidity

These fields are usually taken from GASP numerical products, with cross checking of satellite images.

Clouds

As with most continental areas, stratocumulus or stratus are the most common low clouds, with cirrostratus the most common high cloud. As may be seen from Table 7.7.1.4.4 in Appendix 2 below low cloud of major significance to aircraft landing/takeoff at Mawson has a very low frequency of occurrence. As discussed in the section on white–out below, the total cloud amount could lead to white–out problems if it were not for the relief afforded by the rocky terrain.

Stratocumulus is most commonly brought over the base by maritime streams, but satellite pictures need careful analysis to detect the occasions when low to mid level stratiform clouds, especially upper level deformation clouds, are swept along the coast by depressions to the north along the coast near Mawson. Satellite imagery, especially when looped between pictures with the same projection, is the major tool for detecting and forecasting cloud, as no land–based observations are available close to Mawson.

During summer, cumulonimbus clouds may form on rare occasions, leading to short term reductions in visibility in heavy snow showers.

Visibility: blowing snow and fog

Visibility is generally good, at least during summer, other than with snow. Tables 7.7.1.4.5 and 7.7.1.4.6 in Appendix 2 below show, for example, frequencies of occurrence of poor visibility and of adverse weather types (all of which affect the visibility) respectively. It may be seen that over the summer months, and in December and January in particular, the visibility and related weather types have frequencies of occurrence which are less than about ten per cent.

Fogs are rare during summer, but may occur with light northerly winds in transition seasons and winter, especially in moist maritime air masses that pass over tidal cracks in the sea ice. As daytime temperatures fall below –25°C, ice crystal haze is common, extending to 1,000 m or more and reducing visibility to a few kilometres at times.

Surface contrast including white–out

White–out is significant for aviation along the Mawson coast, however, it is often possible to navigate eastwards towards Cape Darnley by reference to the coastline, due to the frequent occurrence of open water about 100 km east of Mawson. Flight to the west probably requires fairly clear skies unless the fast ice breaks out. Flight to the south obviously requires clear skies as it passes over the plateau.

For Mawson itself, the local rocky terrain, if substantially ice or snow free during the summer melt, affords some relief. However, as may be seen from Table 7.7.1.4.7 in Appendix 2 below the potential for white–out at Mawson, at least in some sectors, is greater than 50 per cent for much of the year.

Horizontal definition

The presence of extensive ice and snow make the loss of both horizon and surface definition common near Mawson, especially at any blue ice airstrip inland, mainly due to overcast cloud at any level and falling snow reducing visibility.

Precipitation

Nearly all precipitation is in the form of snow, with rare occurrences of rain during the summer months. Ice crystals reach the surface on colder days of autumn on occasion. Snowfalls can be heavy as warm frontal cloud bands pass over Mawson, often followed by strong winds. Snow falls most frequently from stratocumulus or stratus if it is at least 200 m thick.

Temperature and chill factor

Temperature is not particularly important in this area, provided that wind speeds are minimal. Chill factor is significant for field work, as although rain is unlikely workers may be wet if undertaking work in small boats. Wind chill is significant, especially under gale–force winds, and needs to be considered by all field workers.

Very low temperatures can lead to difficulties for helicopter operations, with certain aircraft being hard to start below –30°C. In such conditions, interior aircraft temperatures may also be too low for aircrew to function.

Very low temperatures can also lead to higher fuel consumption on base as electricity requirements soar.

Icing

Generally, the low water content of cloud over Mawson leads to only light icing. There is little experience of icing amongst pilots because helicopter operations through cloud have not been approved in the past. It is possible for icing to occur in clear air when the air is close to saturation and air temperature is near zero, although this is not common.

Turbulence

Severe mechanical turbulence is common in the lee of elevated terrain to the south of Mawson.

Hydraulic jumps

Hydraulic jumps have been reported near Mawson on occasions both published and anecdotal. Presumably the steep terrain to the south of the station is conducive to their formation, however a study of their frequency and climatology is not available.

Sea ice

Sea ice commonly forms during April between Mawson and the offshore islands becoming thick enough to support vehicular travel in May, although routine checks of thickness are made before using the ice. The ice extends some 50 to 100 km offshore by September, with shipping usually unable to reach Mawson in that month. Grounded icebergs stabilise the fast ice northeast of Mawson, while an indentation usually forms in the fast ice to the northwest, with a polynya allowing shipping to approach within approximately 50 km of Mawson – if able to penetrate the sea ice further north. In most years, this fast ice breaks out in January, however occasionally it remains for the full summer, causing breeding failures amongst penguins on the islands near Mawson. In the years when the sea ice breaks out, small boating activities become possible for the period January to mid March.

Wind waves and swell

The tendency towards southeasterly flow, especially in strong winds, means that fetch is rarely long enough for significant wave development, however rough seas can obviously be generated under storm force wind conditions. During the presence of extensive pack ice to the north, little swell reaches Mawson.

7.7.2   Prince Charles Mountains (Soyuz)

7.7.2.1   Orography and the local environment

The Prince Charles Mountains (PCMs) consist of a number of massifs aligned along the Lambert Glacier, extending from the Athos, Porthos and Aramis Ranges in the northwest, to Mount Mather in the southwest to Mt Borland in the south and along the Mawson Escarpment. Most of the mountains are submerged below continental ice, with glaciers flowing between them, tributaries to the Lambert Glacier. The prevailing winds exhibit a drainage pattern, with east to northeasterlies on the eastern side of the Lambert and southwesterlies on the western side, although near the larger mountains themselves more

complex flows may occur. Being such a significant feature is likely that the Lambert basin would have a significant effect on winds throughout the lower troposphere.

7.7.2.2   <u>Operational requirements and activities relevant to the forecasting process</u>

The Russian Soyuz Station (70° 35′ S, 68° 47′ E, elev. 336 m) was opened in December, 1982 and closed in February 1989 and was located on the eastern shore of Beaver Lake, 260 km away from the coastline of Prydz Bay. The purpose of the base was to support geological work

For Australian science too geological and glaciological work has predominated in the Prince Charles Mountains. Thus the main requirement to date has been support of scientific parties travelling to and within the PCMs. Because of the extensive ice and snow cover, travel between massifs is mostly limited to visual flight rules to avoid white–out conditions. Fuel is often placed into depots in the PCMs/Amery Ice shelf at Sansom Island, Beaver Lake and near the northern end of the Mawson Escarpment. Shelters are also in place at Sansom Island and Beaver Lake, hence operations in the past have tended to focus on these locations.

7.7.2.3   <u>Data sources and services provided</u>

Forecasters are no longer positioned in the field in this location but are based at Davis. Satellite observations are the main source of information for this area, although upstream AWS observations are becoming available surrounding the Lambert/Amery. No regular surface observations are available.

7.7.2.4   <u>Important weather phenomena and forecasting techniques used at the location</u>

General overview

The PCMs are frequently affected by mesoscale low–pressure systems moving southwards into the Lambert Basin. Such features do not appear to be intense, however snowfall often accompanies them and the cloud systems tend to persist over several days. Surface winds are strongly affected by the drainage flow about the basin. Synoptic systems also affect wind speed, especially in the northern PCMs but not wind direction.

Activities during 1994–95 and 1995–96 ANARE summer operations demonstrated that mid–November to mid–February is the optimal season for field parties and helicopter operations as high winds and low temperatures hindered operations in the earlier and later months, especially in elevated areas. During late February to early March 1996 very little work could be achieved at Mt Kirkby (elevation 1,500m) due to wind, blowing snow, low temperatures or poor visibility. In early and late parts of the 1994/5 season helicopters suffered mechanically from the low temperatures (–25°C or lower).

Data are available for the 1997–98 summer parties visiting the Mawson escarpment and Mt Menzies. These parties consisted of field training officers and geologists, who stayed for about a month in the two locations. Their observations were made generally near 00 UTC and 15 UTC near their camps. Although untrained in meteorology, they were professionals in their respective fields and their observations represent the best data available, so the following comments draw upon their observations.

At the Soyuz base the climate was found to be favorable for work in summer. The mean temperature of the warmest month (January) was -3.1^0C, although the extreme temperatures can vary from +3.5^{0}C in January to -23^0C in March during the summer. The monthly mean wind speed varied from 5 m s^{-1} (~ 10 kt) in December to 9 m s^{-1} (~18 kt) in February and in March. The maximum wind speed reached 20–25 m s^{-1} (~40 to 50kt) with gust up to 30 m s^{-1} (~60 kt). December and January had the clearest summer weather and the minimum of snow–storm days.

Surface wind and the pressure field

The main influence on wind is the continental Antarctic drainage flow, often experienced as a katabatic outflow. This is probably strongest during autumn, winter and spring, however few records are available to support that suggestion. There are anecdotal reports of gale to storm force katabatics in both the northern and southern PCMs in April (observed by aircrew in 1998). AWSs located at higher elevations about the Lambert Basin show highly persistent winds, representing a cyclonic circulation about the basin at near–surface levels dominated by the slope of the ice.

The 1997–98 Mawson Escarpment party reported winds averaging about 4 m s^{-1} (8 kt), mostly easterly. These winds were probably affected by choice of camp site (for many of the observations (26 over 22 days) the direction 110º was reported). Wind speeds (estimated with a hand held anemometer) were not over about 13 m s^{-1} (25 kt). Surface pressure was fairly constant, averaging 984 hPa with a standard deviation of 5 hPa, however variation of site elevations make this figure unreliable.

The 1997–98 Mt Menzies party reported winds of no more than 5 m s^{-1} (~10 kt), however their reports were strongly site–dependent. They were camped on the northern side of the mountain and sheltered from the prevailing winds, thought to be southerly.

Observations at Beaver Lake (October/November 1995 and February/March 1996)) and Mt Kirkby (February/March 1996) did not show the diurnal variation typical of summer–katabatic flow, that is, pronounced winds in the morning then an easing in wind strength in the afternoon. The strongest wind usually occurred with strong synoptic pressure gradients. At Beaver Lake the wind direction is south to southwesterly due to the orientation of Pagodrama Gorge, just upstream. There was no useful correlation between wind speed at Mt Kirkby and Beaver Lake. From February 1996 the six AWSs around the Lambert Basin could be used to approximate Mt Kirkby and Beaver Lake winds. Overcast low cloud, snow and fog depressed wind speed by 5 to 10 knots on average compared with no cloud or cirrus only. Gusts at Mt Kirkby were of the order of 1.5 to 2 times the average wind, with severe mechanical turbulence and rotors being common in strong winds. Winds at both sites and the AWS strengthened (but maintained direction) when the notional inland high on mean sea level charts intensified, or pressure gradients increased due to synoptic systems, or significant fronts approached from the east.

Upper wind, temperature and humidity

These fields are usually taken from GASP numerical products, with cross checking of satellite images. No local observations are currently available, although it is believed that upper winds were recorded from Dovers in the northern PCMS during the late 1980s. In the absence of data, numerical products are the only guide.

Clouds

Cirrus can be advected over the PCMs from inland, most likely associated with synoptic systems outside the field of the locally available satellite imagery. It has also been observed in association with oceanic lows near longitude 55° E. Altostratus can also form inland near the PCMs, probably from upper troughs over the area. Banner cloud, lee waves and rotor cloud all form due to the mountains. Banners and wave clouds can be quite extensive and persistent. Convective cumulus occurs in summer over bare rock. Layers of low or mid–level cloud may reduce or clear during summer days then reform in the evening.

Moisture, once inserted into the PCMs by northerly airflows, tends to persist for several days. There appears to be a slight correlation between 500–hPa northerlies (suggested by ECMWF composite 500–hPa gradients) and subsequent cloud increases. Total cloud averaged over the observations taken by both the 1997–98 Mawson Escarpment and Mt Menzies parties was about 3 to 4 oktas. There was poor correlation between pressure and cloud. Accordingly, an attempt is made to nowcast cloud movement from satellite pictures using image loops. Prediction of cloud formation and dissipation is difficult, and relies on numerical products and the slender correlation between northerly gradients in the upper levels and moisture advection into the continent.

Cloud can be exceedingly difficult to detect especially in winter. Extensive stratus at very low level may be impossible to detect. The forecaster can use low sun angles in visual images to detect cloud, however stratus may cast no shadow.

The reader is also referred to relevant comments in Section 7.8.1.4 below.

Visibility: snow and fog

Fog has been reported on numerous occasions during the summer over the Amery Ice Shelf and occasionally in the southern PCMs. The summer maximum appears to be associated with extensive melt pools over the Lambert/Amery system providing a source of moisture for steam fog, often advected by light afternoon winds into the northern and southern PCMs.

Little experience exists of conditions during the spring, autumn or winter, so it would seem prudent to assume that ice crystal hazes are likely during those seasons as temperatures fall below –20ºC, however strong katabatics may prevent them from forming.

Surface contrast including white–out

White–out is highly significant for aviation within the PCMs. Most of the mountains are separated by extensive ice sheets and of course the glacier is fairly featureless from an aircraft. Flight from the northern to the southern PCMs and to the more isolated peaks usually requires fairly clear skies. Operations within the various massifs can usually continue under an overcast, however. The Mawson Escarpment party in January 1998 reported poor surface definition on three occasions during the month, associated with overcast, while the Mt Menzies part reported poor surface definition on five occasions.

Careful notice must be taken of all cloud types. Even apparently thin stratocumulus (difficult to detect on satellite pictures unless AVHRR channel 3 images are available) can cause white–out in this region. The coastline or mountains in the interior are often clearly visible through cloud that produces very poor surface definition and white–out. Provided there are breaks in the stratocumulus cloud, however, or a layer of altocumulus cloud is

sufficiently high, a setting sun can generate shadows from sastrugi to provide acceptable surface definition.

Horizon definition

As with most Antarctic locations, horizon definition is easily lost under falling snow. The Mawson Escarpment reported poor horizon in at least one direction on nine occasions in January 1998. The Mt Menzies party reported poor horizon on four occasions. Generally, horizon definition was poor in only part of the horizon.

Precipitation

Nearly all precipitation is in the form of snow. It is possible that rain may occur at times during summer, as temperatures can reach well above 0°C.

Temperature

Average temperatures for the month of January reported by the two field parties are shown in Table 7.7.2.4.1 in Appendix 2 below.

Icing

No reports have been reported, however it would be expected that with temperatures near zero during summer icing would be an occasional hazard.

Turbulence

Mechanical turbulence has been anecdotally reported, associated with terrain, as expected.

Hydraulic jumps

Under clear sky conditions it is often observed that surface temperatures (as evidenced by satellite images) are lower along the eastern side of the Lambert Glacier/Amery Ice shelf than to the immediate east on the continental ice sheets or to the west over the western Lambert/Amery. This may be due to the formation of a hydraulic/katabatic 'jump' on the sloping ice sheets to the east, allowing very light winds in the lee of the jump and associated radiational cooling of the eastern side of the glacier.

Sea ice

Not relevant to this area.

7.8　　　　Princess Elizabeth Land and Wilhelm II Land

Princess Elizabeth Land extends from 73º to 86º E and Wilhelm II Land spans 86º E to 91º E. From approximately west to east, key features or stations/bases referred to in this section include:

- *Prydz Bay*;
- *The Amery Ice Shelf*;
- *Progress*　　　　(69º 22′ 50″ S, 76º 23 ′22″ E; .15.5 m AMSL);
- *Druzhnaya IV*　　(69° 44′ S, 72° 42′ E) (See Figure 7.7.1 above)
- *Zhongshan*　　　(69º 22′ S, 76º 22′ E; 14.9 m AMSL);
- *Law Base*　　　　(~ 69º 23′ 24″ S, 76º 23′ E, 65 m AMSL);
- *Davis*　　　　　(68.6º S, 78.0º E, 22 m AMSL);
- *The Vestfold Hills*.

The above places are shown in Figures 7.8.1 and 7.8.2. Although Zhongshan, Progress 2 and Law Base are less than 3 km apart they are included separately due to the complementary information provided for each station and due to the relatively limited amount of information available to be synthesised due to the relatively recent permanence of activities in the area. These three sites are located in the eastern part of the Larsemann Hills, the general features of which are described in the section on Law Base, for convenience only.
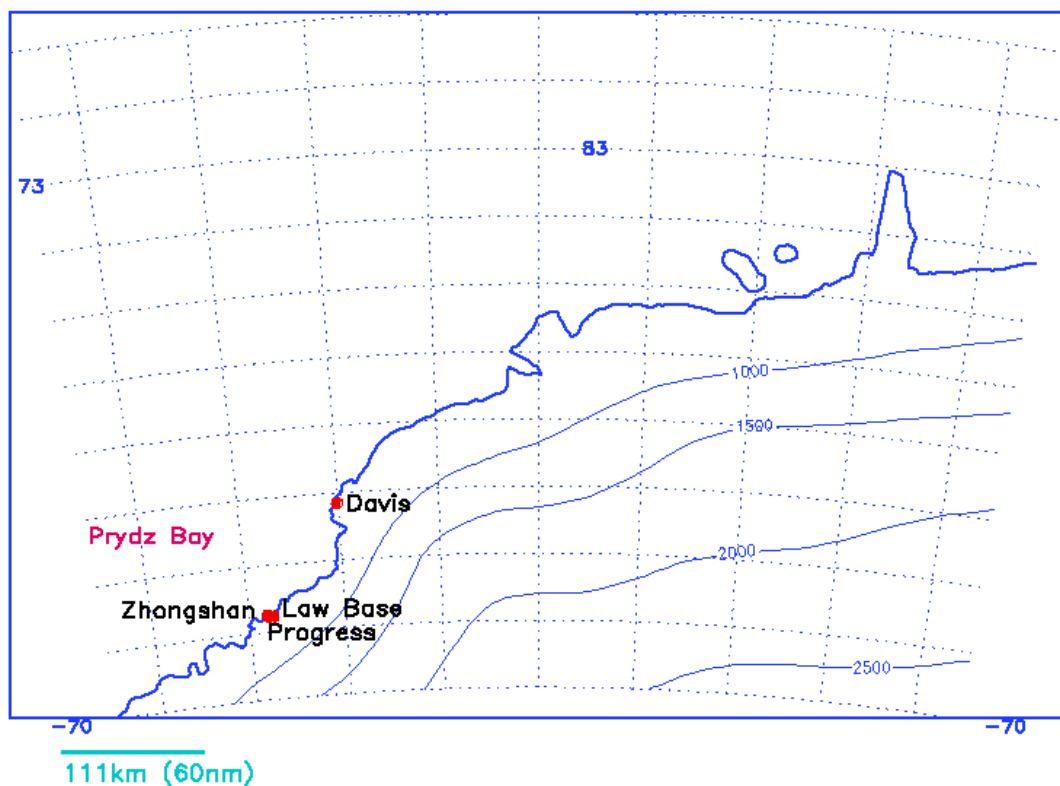
Figure 7.8.1　　　Sketch map for Princess Elizabeth and Wilhelm II Lands (contours in metres; the area is bounded by: 70º S, 65º S, 73º E and 93º E).
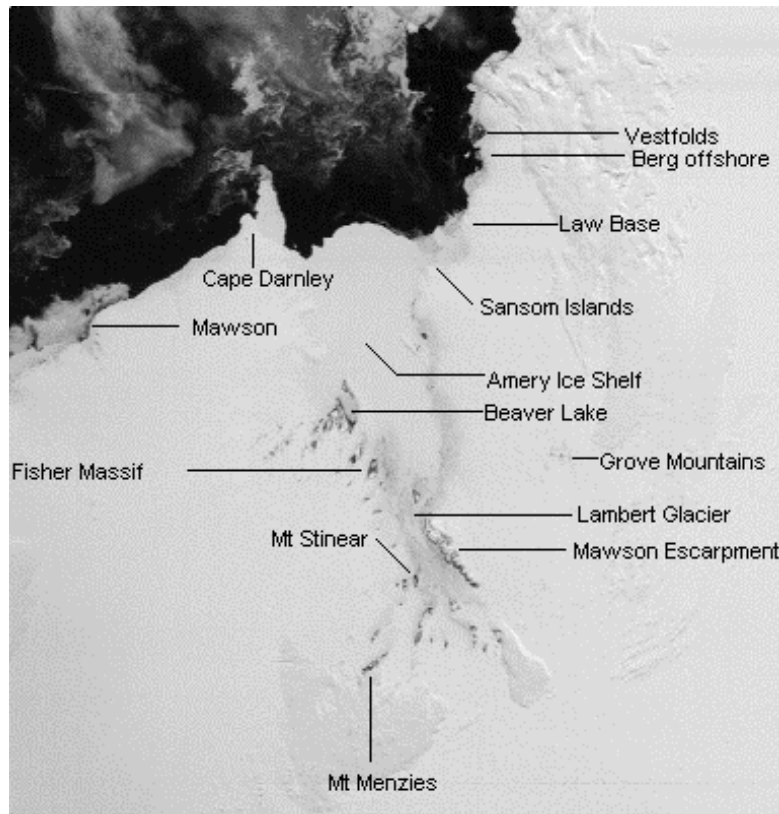
Figure 7.8.2   Satellite image showing the relative locations of some sites in the MacRobertson–Princess Elizabeth area

7.8.1   The Larsemann Hills and Law Base

7.8.1.1   Orography and the local environment

The Larsemann Hills are located on the east of Prydz Bay and consist of four large peninsulas and more than 130 small islands (of heights up to about 60 m) with a seasonal ice–free area of approximately 200 km^2. The area became free of the Antarctic ice sheet about 100,000 years ago, and became a oasis on the edge of the ice sheet. The local coastline has many indentations with fjords forming deep inlets.

7.8.1.2   Operational requirements and activities relevant to the forecasting process

Law Base (~ 69º 23′ 24″ S, 76º 23′ E, 65 m) has been and is still visited intermittently, and was occupied by the ANARE in the summers of 1986–87 and 1987–88. It is from the reports (Nairn, 1987, McCarthy, 1991) of the forecasters for these summers that the information below is provided. The general method of transportation to and from the area is by helicopter and so aviation forecasts are the main requirement.

7.8.1.3   Data sources and services provided

Forecasts for Law Base would now be provide from forecasters located at Davis, or in their absence, at Casey, or Hobart, Australia.

7.8.1.4   Important weather phenomena and forecasting techniques used at the location

General overview

The summer weather at Law Base seems to vary from year to year depending on how the atmospheric long–wave trough–ridge system is arranged. In 1987–87, for example, only one day in forty–one days of flying was lost due to inclement weather. However, in 1987–88, when the down–stream long–wave ridge was further east of the base the low–level air–flow was more commonly onshore. Limited meteorological data are shown in Table 7.8.1.4.1 in Appendix 2 below.

    It is probably useful to briefly describe the two contrasting summer seasons noted above. In 1986–87 days were noted to be sunny until about the end of the first week in February when the skies remained overcast, the lakes froze, and snow fell several times. As noted, only one day saw flying halted and this was when the wind averaged 25 m s^{-1} (~50 kt) and dense snow fell all day.

    In 1987–88, one out of three days of flying operations was lost due to inclement weather. There were three major poor weather situations in that particular season:

- *Frontal passage*: on one occasion a deep low–pressuresystem was north of Mawson and moved slowly in a south–southeast direction and an associated front moved over the base. Large flaked snow from nimbostratus occurred ahead of the front, with calm winds. After the frontal passage cumuliform clouds with hail, granular snow and rapidly strengthening east to northeast winds occurred. Conditions improved after about 24 hr to allow a resumption in flying.
- *Westward moving troughs*: westward moving troughs and associated snow bearing cloud bands (usually middle level at Law base) originated from major depressions in the vicinity of Casey. These cloud bands in many ways resembled those described by Callaghan and Betts (1987) but lacked the associated sharp pressure minima. The cloud bands were relatively easy to track on satellite images, and their passage over Davis gave a good indication of arrival time at, and duration over Law Base.
- *Light northerly airflow*: with the mean position of the 500hPa trough just to the west of Mawson, the resulting light northerly airstream, being maritime in origin, advected moisture over Prydz Bay. Within this moist airmass, small troughs and at times low–level mesocyclonic circulations formed just off the coast. Often these minor perturbations in the air–stream remained a few kilometres off the coast, but periodically they drifted onto the coast producing moderate snowfalls and disrupted flying operations. Pressure changes were only slight and the cloudy conditions dampened down the morning katabatic wind.
- It should be noted that both the westward moving and moist northerly troughs reached the Prince Charles Mountains on several occasions and would have had a serious effect if flying operations had been taking place there. Closed circulations

were evident over the PCMs at least twice during the summer.

Surface wind and the pressure field

Indications are that on about three days out of four during the 1986–87 and 1987–88 seasons a katabatic wind of around 9–10 m s^{-1} (~17–20 kt) peaked in the morning (local time) after about 0200 UTC (~7 AM local) with the time of onset varying between 1500 and 2200 UTC. The katabatic occasionally was strong enough to delay flying for a few hours. Afternoons were almost always calm (in the absence of major maritime lows) and an occasional northwesterly sea–breeze was noted. Table 7.8.1.4.2 in Appendix 2 below shows the wind frequency distribution for the 1996–87 summer.

Upper wind, temperature and humidity

Forecasters would now use upper–air observations from Davis to assist in nowcasting upper–air elements and would use NWP output for longer term trends.

Clouds

Satellite imagery and NWP output would be used in the forecasting of clouds. Even in 1987–88 when the position of the long–waves allowed frequent on–shore flow low cloud was seldom a problem in the area of the Larsemann Hills, Bolingen Islands and Amanda Bay. Aircraft travelling northeast to the Rauer Islands then onto the Vestfold Hills tended to encounter significantly lowering cloud bases.

Visibility: snow

During the 1995–96 summer season westward moving fronts were more likely to produce snowfall over the Larsemann Hills than at Davis, and drifting snow was more common also. Reduced visibility in falling snow was the main deterrent to flying during the 1987–88 summer season.

Surface contrast including white–out

In the area of the Larsemann Hills, Bolingen Islands and Amanda Bay white–out does not seem to be a problem due to the exposed nature of the rock terrain. However, white–out was a more serious consideration when flights occurred over the continental ice or over the Amery Ice Shelf.

Horizontal definition

No specific information on forecasting has been obtained.

Precipitation

No specific information on forecasting has been obtained.

Temperature and chill factor

No specific information on forecasting has been obtained.

Icing

No specific information on forecasting has been obtained.

Turbulence

Turbulence does not appear to have affected helicopter operations in the Larsemann Hills in surface wind speeds below about 10 m s^{-1} (~20 kt).

Hydraulic jumps

No specific information on forecasting has been obtained except that in the summer of 1987–88, during the passage to the west of a relatively narrow cloud band event, helicopters flying from Davis to Law Base at about 300 m (~1,000ft) reported an hydraulic jump just west of the Sørsdal Glacier. The pilots described a distinct shear line, rotor–like clouds, a pressure surge and a sharply delineated falling snow edge. The phenomena were orientated almost east–west and appeared to extend seawards towards the Rauer Islands.

Sea ice

No specific information on forecasting has been obtained except the points noted in the relevant Section 7.8.3 on Zhongshan below should be relevant.

Wind waves and swell

Although not relevant at the stations of Law Base, Zhongshan or Progress, themselves, re–supply and research vessels may moor relatively near to the sites. However, no specific information on forecasting marine conditions has been obtained.

7.8.2   Progress Station and Druzhnaya–4 Base

7.8.2.1   <u>Orography and the local environment</u>

The Druzhnaya–4 field base (69° 44′ S, 72° 42′ E; elev. 250–300 m) was opened on January 1, 1987 and closed on April 18, 1995 and was located on the edge of the Amery Ice Shelf on a nunatak called Landing Bluff overlooking Sandefjord Bay. This bay is effectively the southern–most portion of the much larger and adjacent Prydz Bay. The main functions of activities at the Druzhnaya–4 summer base were the logistical support of the field station Soyuz, which was situated in the Prince Charles Mountains (see Section 7.7.2 above), and the assistance in the development of the all–year Progress Station. The Ingrid Christensen shore in the vicinity of Druzhnaya–4 base is an area with irregular glacier relief. Southward the orography rises gradually, turning into continental ice–slopes.

Progress Station has had a couple of locations and was operating as a summer base at least as early as the summer of 1986–87. The station moved to Progress 2 (69^0 22′ 50″ S, 76^0 23′ 22″ E, elev. 15.5 M AMSL) on February 26, 1989 and is located at the eastern end of the Larsemann Hills on a rocky–sandy plateau with a relatively smooth surface.

7.8.2.2   <u>Operational requirements and activities relevant to the forecasting process</u>

The Druzhnaya–4 Station functioned continuously during five summer seasons (1987–91), then it was temporarily closed on March 24, 1991, put into operation on February 6, 1994, and it functioned in summer seasons of 1994–95 then closed again.

The Progress Airstrip is situated 5.8 km to the south–southwest of Progress Station on continental ice.

7.8.2.3   <u>Data sources and services provided</u>

At Progress the standard meteorological measurements at the station were carried out in 1988–89, 1991, and also from April 1998 to April 1999. The relocation of the station to the coastline by 2.5 km has had insignificant influence on the meteorological observations.

7.8.2.4 <u>Important weather phenomena and forecasting techniques used at the location</u>

General overview

At the Druzhnaya – 4 field base the climatic conditions are favorable for out–door activity. For the spring– summer period (the middle of November – the middle of March) the temperature varies from 0^0C to – 25^0C, but at the beginning and at the end of the period the temperature can fall to –30^0 and even lower, especially at night. Clear and cloudless weather takes place about 10 – 12 days a month.

Similarly at Progress, due to orographic features, the climatic conditions are less severe in comparison with the nearest coastal stations. The mean annual air temperature is –9.8^0 C, the absolute maximum of +9.3^0C was registered in December 1989, the absolute minimum of –38^0C took place in April 1998. December is the warmest month, July is the coldest. The mean annual wind speed is 6.7 m s^{-1} (~13 kt) and the prevailing wind direction is easterly.

The weather conditions at Progress and at the aerodrome site are very different.

Surface wind and the pressure field

At Progress the number of days with wind speed of 15 m s^{-1} (~30 kt) or stronger is near 50 days per year. The maximum wind gust of 53 m s^{-1} (~103 kt) was registered in July, 1998.

In summer a diurnal variation of wind direction and wind speed is typical. As a rule, at night, an easterly wind is registered with speeds up to 10 m s^{-1} (~20 kt) and stronger. In the afternoon the wind drops significantly and wind the direction can change to west or southwest.

Upper wind, temperature and humidity

No specific information on forecasting has been obtained.

Clouds

No specific information on forecasting has been obtained.

Visibility and fog

No specific information on forecasting has been obtained.

Surface contrast including white–out

No specific information on forecasting has been obtained.

Horizontal definition

No specific information on forecasting has been obtained.

Precipitation

No specific information on forecasting has been obtained except at Progress it is noted that snow is the typical precipitation type. In summer the precipitation is ice grains, although sometimes there is rain. The number of snow–storm days is about 60 per year.

Temperature and chill factor

No specific information on forecasting has been obtained, although see the general overview above

Icing

No specific information on forecasting has been obtained.

Turbulence

No specific information on forecasting has been obtained.

Hydraulic jumps

No specific information on forecasting has been obtained.

Sea ice

With respect to Druzhnaya base, the coastline of Sandefjord Bay has the following characteristics: the altitude of the Amery Ice Shelf does not exceed 6 m in this area; the sea depth does not exceed 100 m, and the thickness of the coastal fast ice is not more than 160–

180 cm. The land–fast ice breakup takes place usually from the end of January to the first days of February.

The sea ice conditions in the area of Prydz Bay near Progress is controlled by the presence of Dalk Glacier, situated immediately to the east of the Larsemann Hills. This glacier produces large icebergs. There are a lot of icebergs: these and their fragments are found near the coast from this source and from further east. The sea ice situation is improved with westerly winds, but the frequency of westerly wind events is very insignificant in the area of the station. During the summer period the Bay is clear of ice except in the fjords where ice breakout does not occur in some seasons. According to observations in 1998 the beginning of ice formation was registered on March 14 with fast ice developing very soon thereafter.

The relevant part of Section 7.8.3 on Zhongshan should be also be consulted.

Wind waves and swell

No specific information on forecasting has been obtained.

7.8.3   Zhongshan

7.8.3.1   Orography and the local environment

Zhongshan Station (69º 22´ S, 76º 22´ E, 14.9 m AMSL). was established by the Chinese National Antarctic Research Expeditions (CHINARE) in February 1989. The position of the station is located on Mirror Peninsula in the Larsemann Hills

Located at a relatively high latitude for stations on the Antarctic coast, Zhongshan Station is influenced by Antarctic continental highs as well as intense polar depressions. The forecasting of gales is thus the principal task of the station's weather forecasters. On the other hand precipitation is relatively weak in intensity, and generally has little or no impact on scientific activities of the station.

7.8.3.2   Operational requirements and activities relevant to the forecasting process

Routine meteorological observations have been made continuously since March 1989. The visibility, clouds and weather phenomena are observed visually according to the WMO standards.

7.8.3.3   Data sources and services provided

A weather service has been provided for the safety and effectiveness of voyages and Chinese research scientists at Zhongshan Station since 1989. The operational weather service consists of forecasts, which are prepared on site, for the station and its vicinity, and for the research ships *Polar* and *Snowdragon*. The Zhongshan weather forecasts are based on information from Antarctic Meteorological Centres, e.g. the AMC at Casey, and from Southern

Hemisphere surface, upper–air and NWP products issued by the World Meteorological Centre, Melbourne, Australia. Other data include high–resolution imagery from polar orbiting weather satellites and analysis of station elements. Meteorological information for the operation of the research vessels is processes by ship–board meteorologists with the aid of facsimile synoptic charts, satellite data, marine and meteorological observations, and weather related ship routing data sent from Beijing for consideration. This section outlines the meteorology of the Zhongshan area, with technical support provided by China Meteorological Administration.

7.8.3.4   <u>Important weather phenomena and forecasting techniques used at the station.</u>

General overview

Situated to the south of the Antarctic circumpolar low–pressurebelt and to the north of the Antarctic continental high, the Larsemann Hills is under the effect of prevailing easterly flow all the year round, and influenced by the two systems in a systematic manner. In the presence of high pressure, clear weather with light winds and low temperature appears in sharp contrast to the low–pressuretrough related weather that is markedly windy and snowy. Figure 7.8.3.4.1 in Appendix 2 below shows that the frequency of snowfall days is higher in winter than in summer; the percentage of sunshine days is 50% in summer while overcast and cloudy days are dominant in winter, suggesting that severe winter days are more common than in summer.

Surface wind and the pressure field

It may be seen from Figure 7.8.3.4.2 in Appendix 2 below that the monthly mean pressure at Zhongshan and the monthly mean pressure in the 70–80° E sector of the circumpolar trough axis exhibit an oscillation with a half–year period. The trough is always centreed to the north of the Larsemann Hills and is southward of its average position in February–March and August–September, and northward in other months, with its northernmost locality in June – July, a conclusion that was obtained by Streten (1986) in the context of the Davis Station dataset.

Severe weather is often observed in the Larsemann Hills, where gales and snowstorms can last a few days, the duration and intensity depending on the position of a low–pressurecentre and the strength of pressure gradients. Related to the orographical role of Prydz Bay, a low may steered in its eastward course to the north of the Larsemann Hills, then turns westward at low speed of movement, during which Zhongshan Station will experience a drop in air pressure; an air temperature and humidity rise; with these trends accompanied by a snowstorm. The intensity of some lows exceeds that of a tropical cyclone/hurricane with central pressures as low as 930 hPa and maximum winds of 50 m s^{-1} (~100 kt). Synoptic processes, controlling the weather over Prydz Bay are so intricate that some have not been understood completely.

A site close to the ice cap is more affected by katabatic winds than a site more seaward of the continental ice. To determine whether or not the station is influenced by katabatic winds Figure 7.8.3.4.3 in Appendix 2 below was prepared to show the daily variation in wind speed for Zhongshan versus Mawson. It may be seen that an almost identical pattern occurs at the two stations except there is a difference in mean wind strength. By inference, at Zhongshan katabatic winds are dominant in January (summer) and October (spring), with few, if any, occurring in winter and autumn.

Zhongshan shows annual mean wind of 7 m s^{-1} (~14 kt), larger (smaller) when compared to Davis (Mawson) but its extreme maximum winds are larger than the other two, a phenomenon that is obviously attributed to the joint effects of the orography of Prydz Bay and weather systems. Inspection of the Zhongshan hourly winds on an annual basis shows that winds of greater than force 5 (on the order of 8 m s^{-1} (~16 kt)) constitute 42% (see Figure 7.8.3.4.4 in Appendix 2 below); they are enhanced from summer to autumn and weakened from spring to summer; winds of less than force 5 make up 80% of occasions. Winds greater than force 6 occur on 32 % of occasions in winter, suggesting that gales are frequent in that season.

Figure 7.8.3.4.5 in Appendix 2 below is a plot of monthly variation in the frequency of calm and strong winds/gales (>14 m s^{-1} (~27 kt)) at the Zhongshan Station, indicating that calm conditions often occur between 1800 to 2400 hr (local time) and gales between 0700 and 1200 hr (local) in summer and autumn, which is typical of katabatic winds. The gale frequency is considerably higher in winter than in other seasons, with no diurnal variation. The frequency of gales and calm conditions is smaller in spring.

At Zhongshan Station easterly winds prevail all the year round (see Figure 7.8.3.4.6 in Appendix 2 below). As seen from the hourly wind direction record on an annual basis, east–northeast to east–southeast wind directions (67.5 – 112.3°) have a frequency of 72%, of which 31% is for the due east wind and 27% for east–southeast winds. Owing to the seasonal transition in intensity between polar depressions and anticyclones, the northerly (southerly) component of the winds is diminished (enhanced) from summer to autumn and *vice versa* from spring to summer.

Table 7.8.3.4.1 in Appendix 2 below presents the means of the elements investigated at the station. One can see that the number of gale days are 171 (47% of the year) on an annual mean basis and exceeds 10 (days) on a monthly basis except January; easterly winds prevail all the year round, with maxima of >40 m s^{-1} (~78 kt) observed from March – October.

For Zhongshan, gales result dominantly from polar cyclones and Antarctic continental highs and from the effects of subtropical highs. The weather patterns may be separated into the following classes: (1) a single polar depression (2) a single frontal surface; (3) subtropical high blocking; and (4) katabatic wind These classes are outlined below:

- *Gales from a single polar depression*: This type of gale at Zhongshan results from a single low moving eastward past the station. Typically a well developed and deep depression travels north of the station on an eastward path at around latitude 65° S. The locality of the subtropical high is normal and there is no evidence of an outbreak of continental air due to the building of an Antarctic high. These single depressions can be classified into two kinds: lows which develop in longitudes 20–30° E and mature as they travel eastwards; and, secondly, lows which develop closer to the station between latitudes 45–50° S. Gales develop as the low approaches the station and are strongest when the cyclone is nearby. The gales diminish after the passage of the low–pressurecentre.
- *Gales related to a single frontal surface*: The weather in question owes its origin to a depression, travelling along the fringe of the continent, with the associated cloud system moving faster than the low and detaching from it. Gales develop as the frontal cloud band approaches the station. At this time, the continental high is weak, small–sized; and generally ill defined (see Figure 7.8.3.4.7 in Appendix 2 below). This type of event with a weak gale occurs at intervals of 2–3 days, on average, lasting 1–24 h per event.
- *Gales from a blocking situation*: This type of gale situation is characterized by northward displacement of an Antarctic continental ridge, often generating a high–pressureblock by connecting with the ridge of a southward extending Indian Ocean

subtropical high. The ridge blocks depressions on its western flank. The lows stay almost stationary, and deepen so that the pressure gradients increase giving rise to gales.

- *Gales related to katabatic winds*: The outbreak of cold air from an Antarctic continental high–pressure system is another cause of gales in the Zhongshan area. There are two typical scenarios. Firstly, a low–pressuresystem may be well north of high–pressure ridging over the station. Local weather conditions will be typically cloudless with a steady east–southeast wind. In this case the pressure gradient between the low and the ridge may increase sufficiently to cause gales at the station. Secondly, purely gravity driven winds are believed to affect the station. The Antarctic plateau air (cold and dense) moves northward at increased speed over the ice cap and is deflected eastward under the influence of the Coriolis force. East to southeasterly gales occur as the cold air arrives at the station. Gales from the two cases do not differ greatly from each in character and as such they are considered to be of a "katabatic" wind type. For Zhongshan, katabatic winds occur frequently in summer (January) and spring (October) and but are not common in winter and autumn.

Gale forecasting is more difficult at Zhongshan when compared to the other CHINARE station at Great Wall. Generally, the success rate is higher in forecasting the first three gale types based on the circulation features identified through the use of satellite imagery and synoptic charts. Using weather charts from the Antarctic Meteorological Centre at Casey and the World Meteorological Centre at Melbourne, then quite a good success rate is achieved in forecasting these types of gales.

The forecasting of strong gully–channelled katabatic winds is more difficult. They usually occur in stable conditions and with wind speeds often being in the range 17–25 m s^{-1} (~33–48 kt), the characteristics of this type of wind is worthy further research.

Upper wind, temperature and humidity

No specific information on forecasting has been obtained.

Clouds

Prydz Bay and the surrounding area is a region of high–frequency genesis of mesoscale polar lows. On reaching Prydz Bay a frontal cloud–band may exhibit a variety of behaviours. At times the local orography might cause the band to become stationary or even retrogress. The cloud band might also slow down due to the blocking action of a south Indian Ocean subtropical ridge. Often, as soon as a disturbance occurs in the cloud system, a new low will form, detach from its parent, and develop rapidly, causing pressure gradients to strengthen sufficiently over Zhongshan for gales to develop. Upon the low leaving Prydz Bay, the gale reduces its severity swiftly. As seen from satellite imagery the new low is shown first as an enhanced cloud feature, which becomes inhomogeneously white, looking like a thick–wall cell. Cirrus filosus is shown in a divergent form, indicative of suitable upper–air conditions for development. This is followed by the development of the cloud system typical of depressions.

However, caution must be exercised in deciding on the potential for gales at Zhongshan from a single front. In some cases a few hours after the cyclone's frontal cloud–band moves

south of Zhongshan (that is south of 67° S), the band will move back over the station and gales redevelop. This is attributed to the station locality and southeast flow from the Antarctic high.

If the cloud band far away from the main low experiences a small perturbation a new low will be generated over Prydz Bay, leading to gales from a single front. When a blocking high is east of the station and a low is to the west, gales are normally intense: the gale duration depending on the duration of the blocking. Once the blocking situation collapses, the low moves quickly away and the gale diminishes in severity rapidly. Sometimes blocking may persist for a few days so that the parent cyclone is stagnant, followed by steady genesis of new lows, or by complement or replacement of eastward travelling cyclones, thus bringing the station under the effect of gales for a number of days.

Visibility: blowing snow and fog

No specific information on forecasting has been obtained.

Surface contrast including white–out

No specific information on forecasting has been obtained.

Horizontal definition

No specific information on forecasting has been obtained.

Precipitation

From Table 7.8.3.4.1 in Appendix 2 below it may be seen that the number of days per year of precipitation is 150 (41%) on average. However, because measurement of the amount of snowfall is impossible in southeast Antarctica, the Zhongshan Station, like others in that area, has no such data available.

It is also relevant to note that that the relative humidity is 57% on a yearly basis for the station while it is higher in the Larsemann Hills only when is the temperature above 0ºC, leading to a higher content of water in air in mid–summer. Additionally, during a snowstorm or blowing snow, the relative humidity is higher, too, sometimes in excess of 90% but absolute humidity remains low.

Temperature and chill factor

Figure 7.8.3.4.8 in Appendix 2 below shows the annual variations of 1989–95 monthly mean temperature at stations Zhongshan, Davis and Mawson, which, though differing in latitude and distance from the ice cap, show a roughly similar trend except individual months in winter. This indicates that the climate in the Larsemann Hills is similar to that of stations to the east and west, suggesting that they are under the effect of the same large–scale climate

process. As shown in Streten (1986), oases along the coasts of southeast Antarctic have very few effects on the monthly mean temperature.

Zhongshan has a mean annual temperature of –10ºC and a range of 16ºC in the monthly means, with January's mean temperature above 0ºC and the coldest month, September's mean temperature of –16.3ºC (see Table 7.8.3.4.1 in Appendix 2 below). Its temperature record shows a great drop from summer to autumn and fast rise from spring to summer, and quite steady variation between May to August, a pattern analogous to that of a "coreless" winter and a "brief" summer. In view of the fact that the station is frequently affected by warm and moist air from the north and, conversely, cold and dry air from the south, it has an extreme maximum of 10ºC and an extreme minimum of –40ºC.

The temperature displays remarkable diurnal variation in summer and its daily temperature range is 3ºC, on average. The maximum temperature occurs in the afternoon when the winds are lightest. In contrast, little or no diurnal variation occurs during winter.

Icing

No specific information on forecasting has been obtained.

Turbulence

No specific information on forecasting has been obtained.

Hydraulic jumps

No specific information on forecasting has been obtained.

Sea ice

Figure 7.8.3.4.9 in Appendix 2 below delineates the annual variation of the northern limit of sea ice between 70–80° E. Similar to other sea areas around Antarctica, the sea ice grows steadily in March – September, with maximum growth in April – June, reaching maximum area in September – October; it experiences steady melting in November – December, and a minimum in extent in February. Based on 1973–92 observations, the ice extends as far north as 57°S (60°S) as its northernmost limit in the year with maximum (minimum) growth.

Details of the concentrations of summertime sea ice distribution along the coast north of the Larsemann Hills are poorly understood because the observations are of low resolution and even the microwave data have the resolution only of 25 km × 25 km. The Chinese Antarctic research ships have discovered through their voyages in the sea ice regions that ice–free sectors often emerge on the west side of the Prydz Bay and an ice dam occurs on the east side in December – January, and the ice is nearly disintegrated in February. In contrast, ice along the Larsemann Hills shore is always present in some of the years and moves away only when westerly winds are persistent. However, the westerlies have low frequency of occurrence which is indicative that the ice distribution bears a close relation to wind direction and orography on a local basis.

The ice thickness is another parameter of great operational (and climatic) importance. Chinese meteorologists at Zhongshan Station made drilling measurement of ice depth at three sites 3–5 km distant from the coast in 1989–93. Figure 7.8.3.4.10 in Appendix 2 below depicts the annual variation in the depth averaged over the sites, with a maximum depth of 1.5 m in October − November, showing no great difference as compared to the same latitude. Investigation of the inter–annual variation requires monitoring over a long period.

Wind waves and swell

No specific information on forecasting has been obtained.

7.8.4   Davis

7.8.4.1   Orography and the local environment

Davis is one of four stations supported by the Australian Antarctic Division. It is near 68.6º S, 78.0º E, on a westward facing section of coastline on the shores of Prydz Bay. It is situated on the seaward side of the Vestfold hills, a roughly triangular area of ice free islands and peninsulas (see Fig 7.8.2).

7.8.4.2   Operational requirements and activities relevant to the forecasting process

Davis is currently the hub for Australian flying operations into the Prince Charles Mountains, Mawson and Casey. S76 helicopters are used for most operations at present (2000) but it is possible that a landing strip will be constructed in the coming years, although no final location has yet been selected. Currently, the forecaster(s) at Davis support(s) fly–off activities from ships supplying Davis and Mawson Stations, scientific expeditions into the Lambert Glacier/Prince Charles Mountains areas, along the Mawson coast and into the ice plateau to the east and southeast of Davis, including Mt Brown. Aviation forecasts are required on most days for possible long range flights and a watch is kept on weather to support activities within the Vestfold hills. Outlooks are supplied to personnel on base and in the field for planning purposes.
        The forecaster is also available for consultation by tourist operators, who are increasingly visiting Davis and its environs.

7.8.4.3   Data sources and services provided

Analyses of MSLP and 500–hPa height are currently supplied by Australia's Antarctic Meteorological Centre (AMC) at Casey, via digital facsimile transmission relayed by satellite. The AMC also provides diagnostic graphics based on Australian numerical models such as GASP and the US aviation products. GTS observations are also available and once–daily ECMWF MSLP and 500–hPa analyses and prognoses are received. There is also a facility to

receive GASP MSLP and 500–hPa grid point data from Casey. Charts may be analysed at the forecaster's discretion, but Davis is not a primary analysis centre.

A basic APT facility is also present, supplemented by HRPT images processed by Casey into JPG format for limited areas.

The meteorological office at Davis also performs twice daily radiosonde flights.

7.8.4.4   Important weather phenomena and forecasting techniques used at the location

General overview

Table 7.8.4.4.1 in Appendix 2 below gives a summary of mean monthly values of certain weather elements at Davis.

The influence of katabatic winds at Davis is limited by the presence of the Vestfold Hills to the east. Wind speeds are thus generally light when compared, for example, to Mawson or Zhongshan. Temperatures above zero are common during the summer, with extrema as high as 10°C, while winter temperatures are typically near –25°C, ranging down to extrema near –40°C. Davis is commonly affected by depressions passing north of the station during autumn, winter and spring, although gales are less common than at Mawson. Mesoscale lows commonly form in Prydz Bay, leading to near–gales and showers of snow. While synoptic scale depressions are well handled by numerical models, the mesoscale lows are rarely predicted.

Frontal precipitation is generally in the form of snow generated by warm fronts, often travelling westwards along the Antarctic coastline as the parent depression moves slowly eastwards. Snow showers are possible during summer as convection over the Vestfold hills occasionally produces large cumulus, however snow more commonly falls from stratocumulus.

Table 7.8.4.4.2 in Appendix 2 below is taken from work by Shepherd (personal communication) and summarises the suitability of Davis as an aircraft landing site based on the incidence of adverse cross–wind, cloud, white–out and adverse visibility. While these parameters are discussed in more detail below it may be seen from the table that potential white–out aside, Davis enjoys a relatively low percentage of weather which might be adverse to aviation. December and January (only 4 % adverse conditions (excluding possible white–out)) are the best months while the period March through to September experience uniformly around 13 to 14 % adverse conditions.

During the summer of 1996 a field party worked on Hop Island in the Rauer Group, just to the south of the Sørsdal Glacier. Their measurements of wind speed and observations of clouds and precipitation indicated similar conditions as to those experienced at Davis. Temperatures tended to be up to 2°C warmer than at Davis, but no reason for this is suggested.

Surface wind and the pressure field

Significant winds at Davis are mostly northeasterly, as can be seen from the many semi–permanent snowdrifts within the hills and from the wind rose shown in Figure 7.8.4.4.1 in Appendix 2 below. Gale–force southerlies or southeasterlies are rare but can be caused by continental outflows during winter. Strong northwesterlies or westerlies are very rare, although moderate seabreeze westerly to southwesterly flow is common on summer afternoons.

Winds stronger than gale–force are generally associated with synoptic scale low–pressuresystems moving southwards towards the coast. The northward deviation of the Antarctic convergence towards Kerguelen Island may be responsible for the tendency of most low–pressuresystems to pass well north of Davis. Phillpot used composite 500–hPa data to suggest that gale–force winds at Davis are associated with 500–hPa ridges crossing the coast between Davis and Mirny, especially when the ridge caused north to northeast flow at 500 hPa over Davis (Phillpot, 1997, his figure 4.24c).

Considerable variation is found over the Vestfold hills in wind speed. Pilot reports suggest gale–force winds near the eastern border of the hills, where permanent ice fields rise into the Antarctic interior, while field reports suggest that these gales often extend well into the fjords near the plateau. These gales often occur with light winds observed at Davis. Evidence has been provided for the propagation of hydraulic jumps (Targett, 1998) from the plateau towards Davis as synoptic scale depressions pass north of Davis.

In terms of cross–wind component effects on aircraft, Table 7.8.4.4.3 in Appendix 2 below shows the percentage frequency of occurrence of wind components normal to the mean wind direction of 050º at Davis greater than 7.7 m s^{-1} (~15 kt). It may be seen that the frequencies are all very low.

Upper wind, temperature and humidity

Forecast upper winds, temperatures and humidity are extracted where needed from numerical model data, with cross checking of satellite images.

Clouds

As with most continental areas, stratocumulus or stratus are the most common low clouds, with cirrostratus the most common high cloud. Stratocumulus is most commonly brought over the base by maritime streams, but satellite pictures need careful analysis to detect the occasions when low to mid level stratiform clouds are swept inland by depressions to the northeast, persisting to cross the coast near Davis. Southwesterlies often bring extensive low stratus (cloud base about 250 m (~800 ft)) in summer, moistened by convection over large ice free sea areas, but this is usually shallow – in which case helicopters are able to fly underneath without difficulty. Satellite images, especially when looped between pictures with the same projection, is the major tool for detecting and forecasting cloud, as very few land–based observations are available.

During summer, cumulonimbus clouds form on rare occasions, leading to short term reductions in visibility under heavy snow showers.

Extensive low stratus was observed on a flight from Davis towards Mirny Station to the northeast, just after sunrise in April 1998. On the return leg, it was not seen although the route was very similar, suggesting that night time cooling of the near–surface layer may have produced fog or low. On this occasion, no cloud was detectable from satellite imagery, as would be expected for low cloud over the ice plateau. Obviously, the forecaster must bear in mind the difficulty of detecting low cloud or fog over ice at all times.

As may be seen from Table 7.8.4.4.4 in Appendix 2 below low cloud of major significance to aircraft landing/takeoff at Davis has a very low frequency of occurrence. As discussed in the section on white–out below, the total cloud amount could lead to white–out problems if it were not for the relief afforded by the rocky terrain.

Visibility: blowing snow and dust; and fog

Visibility is generally good, at least during summer, other than with snow. Tables 7.8.5.4.5 and 7.8.4.4.6 in Appendix 2 below show, for example, frequencies of occurrence of poor visibility and of adverse weather types (all of which affect the visibility) respectively. It may be seen that over the summer months, and in December and January in particular, the visibility and related weather types have frequencies of occurrence which are less than about ten per cent.

Good horizons prevail over the Vestfold hills because of the areas of rock. Fogs are rare during summer, but may occur in transition seasons and winter, especially in moist maritime air masses that pass over tidal cracks in the sea ice. As daytime temperatures fall below –25°C, ice crystal haze is common, extending to 1000 m or more and reducing visibility to a few kilometres at times. It is wise to examine channel 3 AVHRR imagery for fogs

Visibility reduction by blowing snow is rare during summer because of the absence of snow upstream of Davis and over much of the Vestfold hills and adjacent plateau area (due to melting in summer temperatures, extending some distance inland from the edge of the plateau). Gales do, however, cause considerable blowing dust and sand at times, especially in summer. In fact, in the absence of snow cover, even only "strong" winds may allow flying grit or pebbles to cause considerable damage to vehicles, parked aircraft, and windows etc.

Near the ice plateau, blowing snow is still possible during summer in very strong wind events. After snow falls, of course, gales are able to cause blowing snow or even blizzards in any season.

Surface contrast including white–out

White–out is not usually significant for aviation in the Vestfolds, given the presence of areas of rock, however persons on foot, on skis or on motor vehicles travelling under extensive overcast do become disoriented because of their shorter distance focus.

And at Davis itself, the local rocky terrain, if substantially ice or snow free during the summer melt, also affords relief. However, as may be seen from Table 7.8.4.4.7 in Appendix 2 below the potential for white–out at Davis, at least in some sectors, is 60 per cent or greater throughout the year.

Horizontal definition

Horizon is more likely to be lost than surface definition in the Vestfolds, as areas of plateau to the northeast and southeast and sea ice to the west can merge with cloud to make the horizon indistinguishable. This is a fairly common event, especially in spring and autumn, although pilots can often continue flight along the coast with some difficulty by reference to rock areas.

Precipitation

Nearly all precipitation is in the form of snow, with rare occurrences of rain during the summer months. Ice crystals reach the surface on colder days of autumn on occasion. Snowfalls can be heavy as warm frontal cloud bands pass over Davis, often followed by strong winds. Snow falls most frequently from stratocumulus or stratus if it is at least 200 m

thick. Coastal convergence, presumably associated with variation of friction has occasionally led to a maximum of precipitation near the coast, with lighter falls inland over the Vestfolds. Mesoscale lows and lines of stratocumulus clouds forming over the water west of Davis may produce snowfall.

More commonly favoured areas for snowfalls appear to be the Sørsdal Glacier to the south, the ice edge to the west when it exists and, during summer, over the Vestfolds where convection may play a part. The forecaster must be careful not to confuse "ice blink" (whiteness of ice reflecting against the lower surface of low clouds) or "water sky" (darkness of water shown up as lack of brightness on the under–surface of low clouds) with precipitation, however, especially during summer.

Heavy convective showers are rare, but can occur in summer or with strong southwesterly flows off the Lambert Glacier in autumn.

Temperature and chill factor

Temperature is not particularly important, provided that wind speeds are minimal. Little success has been achieved in forecasting maxima using forecast thickness variations, however very low values of 1000–500–hPa thickness were associated with record low temperatures experienced at Davis in April 1998. Chill factor is significant for field work, as although rain is unlikely workers may be wet if undertaking work in small boats. Wind chill is far more significant, especially under gale–force winds, and needs to be considered by all field workers.

Very low temperatures can lead to difficulties for helicopter operations, with certain aircraft being hard to start below –30°C. In such conditions, interior aircraft temperatures may also be too low for aircrew to function effectively. Very low temperatures can also lead to higher fuel consumption on base as electricity requirements soar.

Icing

Generally, the low water content of cloud over Davis leads to only light icing, although it appears likely that the occasional large cumulus could lead to moderate icing. There is a variation of experience of icing amongst pilots because helicopter operations through cloud have not been approved in the past. It is certainly possible for icing to occur in clear air when the air is close to saturation and air temperature is near zero.

Turbulence

Severe turbulence is common over the portions of the Vestfolds near the plateau during the mornings when katabatic flow is strongest. Moderate thermal turbulence is also common during summer when a large area of bare rock is exposed. CAT at high levels has not been reported due to the lack of aircraft in transit.

Hydraulic jumps

Hydraulic jumps are common to the east of Davis during the autumn, winter and spring (Lied 1964). On occasion (either the passage of a deep depression to the north of Davis or strong ridging over the Mawson coast) a katabatic jump may propagate as far as Davis.

Sea ice

Sea ice commonly forms during April between Davis and the offshore islands becoming thick enough to support vehicular travel in May, although careful checks of thickness are made before using the ice. The ice extends some 20 to 30 km offshore by September, with some difficulty being experienced by shipping in getting within 4 km of Davis. In Prydz Bay to the west, ice is generally a metre or so in thickness with up to 10/10 coverage during the winter as far as 64º S although by January it tends to reduce to about 3/10. The sea ice between Davis and the offshore islands becomes unsafe for mechanised travel by early December and by the end of December the ice is usually closed to human access. Small boating activities become possible for the period January to mid March.

Wind waves and swell

The tendency towards northeasterly flow, especially in strong winds, means that fetch is rarely long enough for significant wave development. Swell rarely penetrates the sea ice deeply enough to cause more than half a metre of swell at Davis. Standing on the sea ice, however it is clear that a small swell is present occasionally, causing movement of adjacent ice slabs. Tidal effects are much more significant in cracking the ice near islands or submerged rocks.

7.9   Queen Mary Land

Queen Mary Land extends between meridians of 91º E to 102º E. From west to east, key features or stations/bases referred to in this section include:

- *The Davis Sea*;
- *Mirny Station*   (66º 33' S, 93º 01' E,35 m AMSL);
- *The Shackleton Ice Shelf*;
- *Edgeworth–David Base*   (66º 15' S, 100º 36' E, 6 m AMSL)
- *"Oasis"/Dobrowolsky*   (66º 16' S, 100º 45' E, 28 m AMSL
- *The Bunger Hills*.

The above places are shown in Figure 7.9.1.

7.9.1   Mirny

7.9.1.1   <u>Orography and the local environment</u>

Mirny (opened on February 15, 1956) is situated on the coast of Cape Davis at a small protrusion of Mirny Peninsula at a point with coordinates of 66º 33′ S, 93º 01′ E and elevation of 35 m AMSL. The shore in the vicinity of the station is called Pravda shore. The station structures are located at four rock outcrops. The mainland shore presents a snow–ice barrier of about 15–20 m above sea level. The ice surface south of the station rises to a height of 1.5 km at a distance of 100 km. A 10 m isobath passes in 15–20 m from the coastline. Offshore there is a group of rocky islands known as the Haswell Islands. Land–fast ice near the station is observed much of the year reaching 30–40 km in width by the end of the winter.
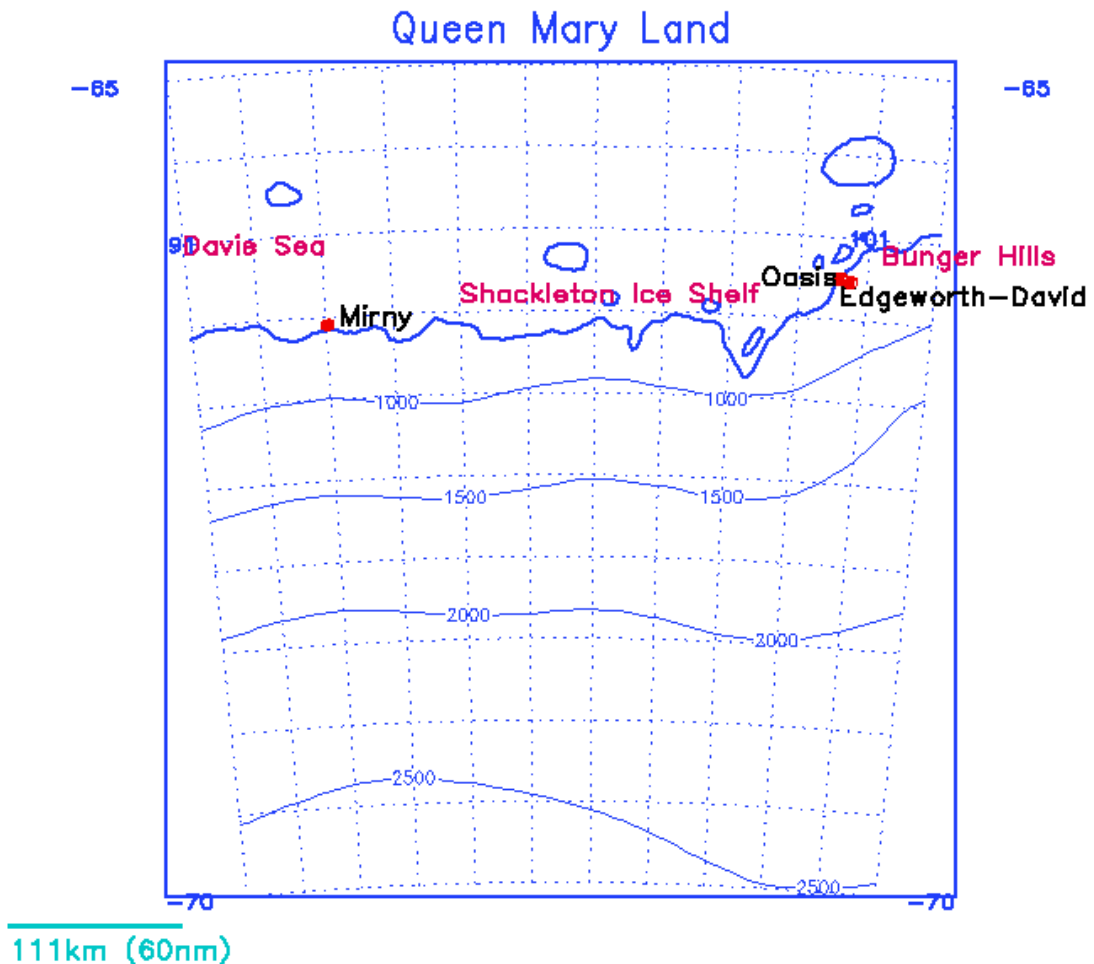
Figure 7.9.1   Sketch map for Queen Mary Land
(contours in metres; the area is bounded by: 70º S, 65º S, 91º E and 102º E).

7.9.1.2   Operational requirements

Mirny is the main base of Russian studies in the Antarctic. One of the main functions of the station is to provide support for activities at Vostok Station. For the last few years, the supplies were delivered to Vostok from Mirny by transport vehicles. A permanent synoptic group at the station provides forecasts for transportation traverses along the Mirny–Vostok–Mirny route, cargo operations near the land–fast ice and at the approaches during the navigation period, as well as for other operations.

7.9.1.3   Data sources and services provided

Information received in the form of synoptic messages, ship–borne observation and drifting buoy data allows a synoptic group to compile weather and air pressure orography charts for 00 UTC for the coast areas, the Cosmonauts, Sodruzhestvo and Davis Seas. Up to five IR or visible images from meteorological satellites are received on a daily basis. A restricted portion of upper–air–synoptic information from the European Centre for Medium–Range Weather Forecasting for the Southern Hemisphere is received via INMARSAT in GRID code. Synoptic information is also received from the Melbourne RMC via HF facsimile. Based on this information weather forecasts are provided for marine, ground, and air operations.

7.9.1.4   Important weather phenomena and forecasting techniques

General overview

The station is located in the climatic area at the ice slope foot. The weather character is governed by frequent blizzards especially in winter and by strong katabatic winds. The yearly air temperature average is –11.3ºC with the maximum temperature of +6.8ºC and the minimum of –40.3ºC. The average wind speed is 11.2 m s^{-1} (~ 22 kt) with a maximum of 56 m s^{-1} (~ 109 kt). East–southeasterly winds predominate. During a year, there are 204 days on average with the wind speed in the station area greater than 15 m s^{-1} (~ 29 kt).

The polar day lasts about a month (from December 10 to January 10), the polar night is almost absent. Cyclonic activity is the prevailing component of the circulation climate–forming factor for the study area. The influence of the Antarctic high on climate formation is less significant here and is explicitly manifested in the absence of cyclonic depressions near the Pravda Shore. An especially active cyclogenesis forms high–pressure ridges connecting the Antarctic High with the subtropical High. In these cases, the maximum atmospheric pressure values are recorded at the coastal stations.

The cyclonic eddies forming the weather at Mirny Station move to this region both along zonal and meridional trajectories. Weak lows of the Antarctic front moving along the coast rarely result in significant weather deterioration in the vicinity of Mirny. Active polar frontal depressions from temperate oceanic latitudes are mainly generated in the areas of cyclogenesis near South Africa and between Crozet and Kerguelen Islands. These depressions are blocked by the high Antarctic continent from the south and longitudinal ridges from the east allowing repeated regeneration of deep depressions which persist near the coast. A high frequency of mobile active cyclonic eddies is typical of the cold season, such processes being less frequent in summer. The especially dangerous weather phenomena for the station activities are caused by active lows.

Surface wind and atmospheric pressure field

Three main winds are identified in the Mirny Station area:

- The cyclonic winds connected with cyclones moving over to the Pravda Shore have northeast–east or east–south–west directions. They are quite stable in speed and direction and their speed increases with height. The characteristics of these winds that are typically accompanied with snowfall and warming are determined by the direction of motion and evolution of the cyclonic eddies. Meridional movement of lows, particularly when they persist near the coast due to blocking, cause the cyclonic winds to be more persistent and stable than with zonally mobile depressions.

- The katabatic winds depend on a number of factors (slope and coast orography, thermal conditions, gravitation and gradient wind) are accompanied by below zero temperatures, high air dryness and predominantly clear weather. In summer and during the transient seasons with diurnal temperature variations, the katabatic flows arise or intensify in the evening reaching their maximum around 5–8 hr local time attenuating by 15–18 hr and then increasing again. In the wintertime the katabatic wind speeds increase and their attenuation or increase depend on the change of the pressure gradient with approaching cyclones. The katabatic wind in the coastal area completely decreases at a distance of 10–15 km from the slope foot and here the influence of the pressure systems is manifested to a full extent.

- Transient winds that have simultaneously the characteristics of the katabatic and cyclonic winds have an east–southeast direction and strongly depend (as do the cyclonic winds) on the direction of motion and evolution of the cyclonic eddies.

Each of these three wind types is characterized by specific weather conditions and by changes in the profile and the temperature with height. Forecasters have to take into account the vector directions of the katabatic flow and the pressure gradient wind. The wind will be weaker if these components opposes each other and will be stronger if they coincide. In reality, it means that the wind in the sink zone may attenuate with cyclones approaching from the west. The highest wind speeds are observed to the rear of cyclones with the coincident vectors of the katabatic and synoptic pressure gradient winds.

The maximum number of days in a year when storm force winds were recorded at Mirny was 247. Storm force winds are strictly from a southeasterly direction which is highly constant. The average speeds of storm force winds with the passage of cyclones are higher than those due solely to katabatic influences. Around 20–25 days with hurricane force occur per year. The maximum wind speed of 56 m s^{-1} (~ 109 kt) recorded at the station, was an easterly cyclonic wind. The maximum frequency of occurrence of storm and hurricane force winds occurs in winter.

Storms may last from several hours to several weeks. A case was recorded in Mirny where the katabatic storm wind persisted continuously for 220 h. Calm weather and weak winds comprise only about 3% of all cases observed.

A semi–annual component in the seasonal variability of the atmospheric pressure at sea level is typical of the Mirny Station with the amplitudes of the semi–annual oscillations greater than those of the annual oscillations. The maximum of the semi–annual wave is observed in winter with the minimum in the transient seasons.

Clouds and precipitation

The amount of total cloud in the Mirny area comprises 5.1 oktas, on average throughout a year. The frequency of occurrence of low cloud producing precipitation is insignificant being 10–15%.

Active cyclonic activity in the Antarctic coastal zone contributes to the development of all cloud forms excluding strong cumulus clouds. Cloud–free sky is frequently observed under the effect of the Antarctic high especially in winter.

Typically in summer high and middle clouds prevail. Low stratocumulus clouds 600–1000 m (~2000–3300 ft) high move to the coast from the sea. Cloud height below 300 m (~1000 ft) is rare. However, with deep cyclones moving over the Pravda Shore along meridional trajectories at any time of the year, strong advection of warm and moist air occurs from the north in the frontal zone. The passage of the fronts are accompanied by continuous low cumulus. In such situations, the snowfall can last continuously for 5–7 days.

Corresponding to the cyclonic activity, the maximum precipitation in Mirny is observed in wintertime and the minimum in December and January. Around 400 mm of precipitation falls over the year, the number of days with precipitation being 146. Precipitation is mainly solid except for infrequent cases in the summer months.

The quality of cloud forecasting and correspondingly, precipitation forecasting, depends on the availability of frequent satellite information. Cloud forecasting can be based in general on the dependence revealed for the Mirny area between clear or overcast sky and the wind direction in the troposphere. The largest number of days with clear weather during a year is related to southwesterly and southeasterly winds. The southwesterlies are associated with the southeastern periphery of a ridge or sub–polar high while the southeasterlies are governed by the influence of the rear part of the southern half of lows. Typically, katabatic wind is observed at the station under such conditions.

Gloomy weather, often with snowfalls is predominantly connected with northeasterly and northwesterly winds, which characterize the cyclonic circulation in the vicinity of Mirny. In summary, clear weather dominates with offshore air–flow and gloomy weather with onshore air–flow.

Visibility: blowing snow and fog

High transparency and an almost absolute air purity, which provide good visibility conditions are typical of Antarctica. However, the Mirny area is characterized by weather phenomena that significantly deteriorate visibility. A reduced visibility forecast is primarily connected here with forecasting strong wind and snowfall.

Blizzards significantly reducing the visibility are frequently typically due to active cyclones moving towards the coast along a meridional trajectory. The strongest blizzards are observed in the cold half of the year and in the rear sector of passing cyclones where the wind speeds may be greater than 50 m s^{-1} (~100 kt). Blizzards in combination with low air temperatures create extremely severe weather conditions. In the summer months, however, three to four cases of persistent (up to three days) strong blizzards are also possible with visibility reduced to 50 m or less and wind speed up to 30 m s^{-1} (~60 kt).

The success of predicting blizzards depends on the capability of correctly defining development and duration of depressions with which the occurrence of this phenomenon is connected. The duration of blizzards in rapidly moving cyclones is short comprising around half a day. The onset of a blizzard is determined by the visibility reduced to several tens of metres. This typically takes place during a heavy snowfall in a northerly wind of more than 10

m s^{-1} (~19 kt) and during a less heavy snowfall in a southerly wind of more than 13 m s^{-1} (~25 kt). Obviously, the end of a blizzard is to be expected as the wind decreases below the criteria indicated.

Snow-storm events that decrease visibility (without the snowfall) are also predicted from the wind increasing to 10–13 m s^{-1} (~20–25 kt). In predicting a snow-storm event the cases with a pressure gradient and a katabatic wind should be differentiated. The katabatic winds do not spread more than 10–15 km from the coast notwithstanding their intensity in the station area. Snow-storm events due to the pressure gradient wind can be observed over the entire area. In late spring and up to late summer, approximately from November to February, snow-storms are rare at the coast and on the continent near the coast during wind increases due to the changed snow surface structure under the influence of direct solar radiation. Their occurrence is predicted only in the presence of freshly fallen snow.

The highest frequency of occurrence of snow-storm is observed in winter up to 26 days with snow-storm per month and in summer up to 10 days per month. The overall duration of snow-storm events in Mirny averages 3.5 months throughout a year.

Advective maritime fog at Mirny is observed once in two years, on average, in summer. Such event arise typically with weak northerly or westerly winds and do not seriously hamper the operation of ground transport vehicles and aviation due to their short duration and insignificant spreading inland.

In the case of such fogs, landing of light aircraft is possible at the dome. Fogs of this type are not typically envisaged in forecasts due to their exceptionally low frequency of occurrence and correspondingly due to the lack of experience of their prediction.

Frost or ice fogs and haze resulting from the process of sublimation and condensation of atmospheric moisture in the form of ice crystals or rime, are also extremely rare in the Mirny area. They are however, common for the inland areas where they hamper the operation of ground vehicles. Forecasting of these phenomena should be based on the favorable conditions for accumulation of ice crystals in the surface layer, which occurs in calm weather in the central parts of highs or ridges when clear weather or thin cirrus clouds are observed. The maximum frequency of occurrence of frost or ice haze and fog is observed in winter and the minimum in summer.

The phenomenon of snow haze at wind speeds of 3–5 m s^{-1} (~6–10 kt) can be observed in Mirny and more frequently over the inland regions. It is caused by fine snow dust in the suspended state after snow storms. This phenomenon is mainly typical of the cold season if there is reduced density of snow cover. The visibility is not greatly affected being 6–4 km. A snow haze forecast can be issued as a forecast of the phenomenon following drifting snow when wind is expected to decrease to 5–3 m s^{-1} (~6 to 10 kt).

The frequency of occurrence of good visibility (10 km and more) in the Mirny area in summer is around 80% decreasing to 50–60% in the winter months.

White–out

The optical phenomenon 'white out' can be observed both in the vicinity of the station and at the ice dome. Forecasting should take into account that 'white out" occurs more often near midday (due higher sun elevations) in the frontal part of deep depressions with dispersed upper fronts.

Temperature and chill factor

The Mirny area is characterized by below zero monthly temperature averages throughout the year and the absence of a pronounced winter minimum. The maximum monthly temperature average is observed in January. The absolute maximum recorded for 25 observation years is +6.8ºC. Significant air temperature oscillations from day–to–day during a year are always connected with deep lows passing the coast from the northern oceanic regions. The temperature increase at the station is typically observed at the east wind change. The success of air temperature forecasts is determined by forecasting the motion and evolution of cyclonic features. The temperature anomalies within a year have positive values with meridional circulation and negative values with zonal flow.

Low air temperatures and the wind are the major factors restricting outdoor activities. A combined effect of these factors governs the intensity of chilling of that part of the human body that is unprotected by clothing. Experimental studies, using special instruments, were performed over one year in Mirny to determine the intensity of cooling. The results have shown that on 48% of occasions the weather was suitable for work in the open air; on 49% of occasions there was a risk of frostbite; and only on 3% of the time (10 days) the weather was so severe that even a short stay in the open without special face protection was impossible.

Icing

Ice deposition on objects in the form of rime and glaze at Mirny is quite rare. The total duration of rime phenomenon is about three days, on average for a year. Glaze forms predominantly at air temperature between 0 to –3ºC being found for 20–30 hr a month from November to January and for several hours and less than an hour in the other months.

Sea ice

First indications of ice formation in the Davis Sea appear in early March, however due to strong autumn winds stable ice formation does not begin until the second 10–day period of March, on average. The duration of the onset of stable ice formation before the establishment of land–fast ice comprises about a month for the Mirny area. Land–fast ice is established at ice thicknesses of about 20–40 cm. Land–fast ice thickness reaches its maximum values in the second 10–day period of November at the end of the ice growth. The maximum land–fast ice width in the Davis Sea in September–October reaches 30–40 km. The dates of land–fast ice breakup in the vicinity of Mirny vary between January 27 to March 9 (with February 13 as an average date). East of Mirny a significant concentration of icebergs forms resulting from a slower drift of icebergs produced by the outlet Helen glacier. Similar aggregations of icebergs in the central and northwestern Davis Sea are due to shallow water depths resulting in their grounding.

7.9.2   Edgworth David (Bunger Hills)

7.9.2.1   <u>Orography and the local environment</u>

Edgeworth David is a camp site located on the south western perimeter of the Bunger Hills, adjacent to Transkriptsii Gulf, adjoining the glacial ice sheets extending into the Shackleton Ice Shelf (see Figure 7.9.2.1.1).

     The Bunger Hills are on the Antarctic coast, about 75 km (~40 nm) inshore of Mill Island and the attached Shackleton Ice Shelf at an approximate location of 66º S, 101º E (see Figure 7.9.2.1.2). The Bunger Hills cover an approximate area of 37 km by 28 km (~20 nm by 15 nm), with the long axis abutting the continental ice sheet to the south east. Moraine and glacial rubble cover most of the exposed rock, which is otherwise bare or sparingly covered in snow. The area is made up of islands and isthmuses dotted with fresh water cairns. Much of the area is near sea level with frequent steep sided hills rising less than 150 m (~500 ft). Edgeworth David's site on the western flank of the hills provides significant shelter from the prevailing east to southeasterly winds.

7.9.2.2   <u>Operational requirements and activities relevant to the forecasting process</u>

Edgeworth David was used as a summer camp supported by ship and helicopters operations in the summer of 1985/86. A coastal depot was established on the Shackleton Ice Shelf to the west of Mill Island, from where helicopters sling loaded equipment and ferried expeditioners approximately 75 km (~40 nm) to the camp across the ice shelf. Re–supply by air remains the most probable method even now, due to the heavy and frequent crevasses evident in the ice shelf.

     In the summer of 1985/86 Edgeworth David supported the operation of two Hughes 500s and one Bell Jet Ranger helicopter. Equipment and fuel dumped at the coast was ferried to camp when over–ice flying operations were possible. Otherwise, the aircraft were used to deploy and recover field parties within the Bunger Hills, and for expeditionary investigations to the west, which encompassed the Obruchev Hills, the Denman Glacier and surrounding mountains and coast. The Jet Ranger was also used for aerial photography.

     Aviation forecasts were required each day for the helicopters as necessary. These forecasts would frequently dictate aircraft activity for the day, dependant principally upon the extent of white–out.

     Under the emergency evacuation plan, the helicopters would hop to either Mirny or Casey utilizing fuel dumps at coastal midway points to either location. A route forecast would be required to help select the appropriate destination. Future operations may seek to use the permanently frozen Transkriptsii Gulf for fixed wing operations. The multi–year ice is about two metres thick and only shows weakness at the edges where tide cracks follow the contour of the shore.
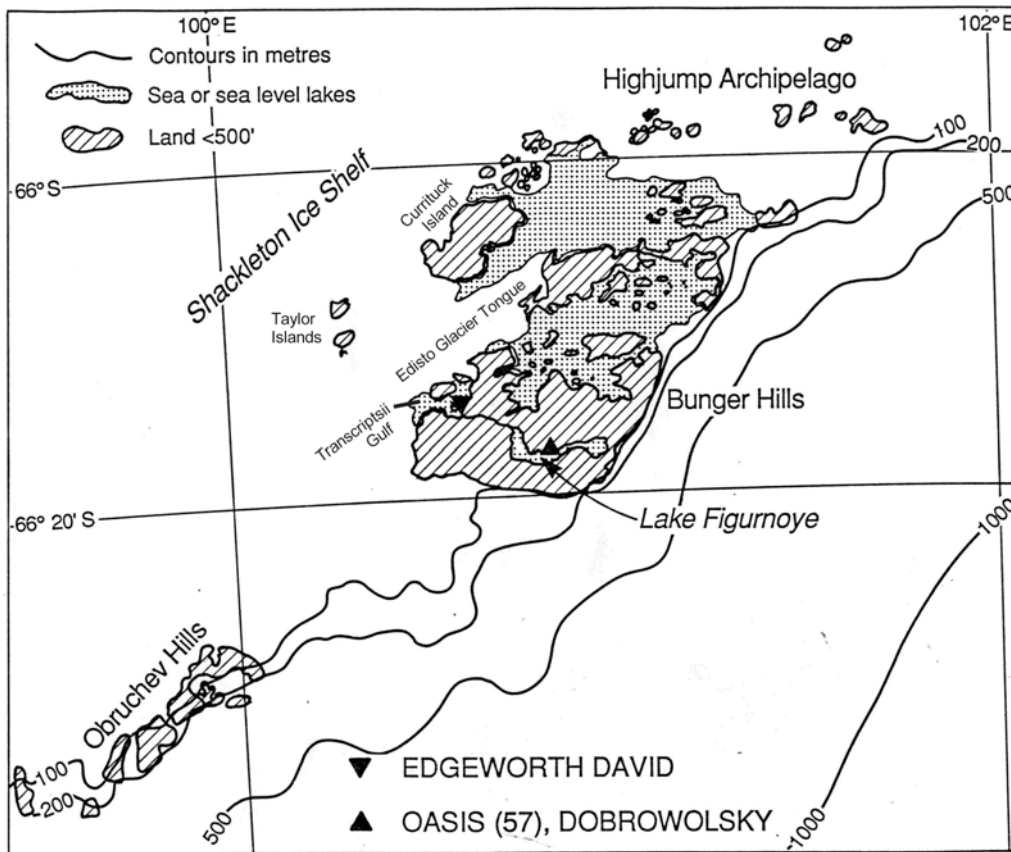
Figure 7.9.2.1.1   Location map for the Bunger Hills area.
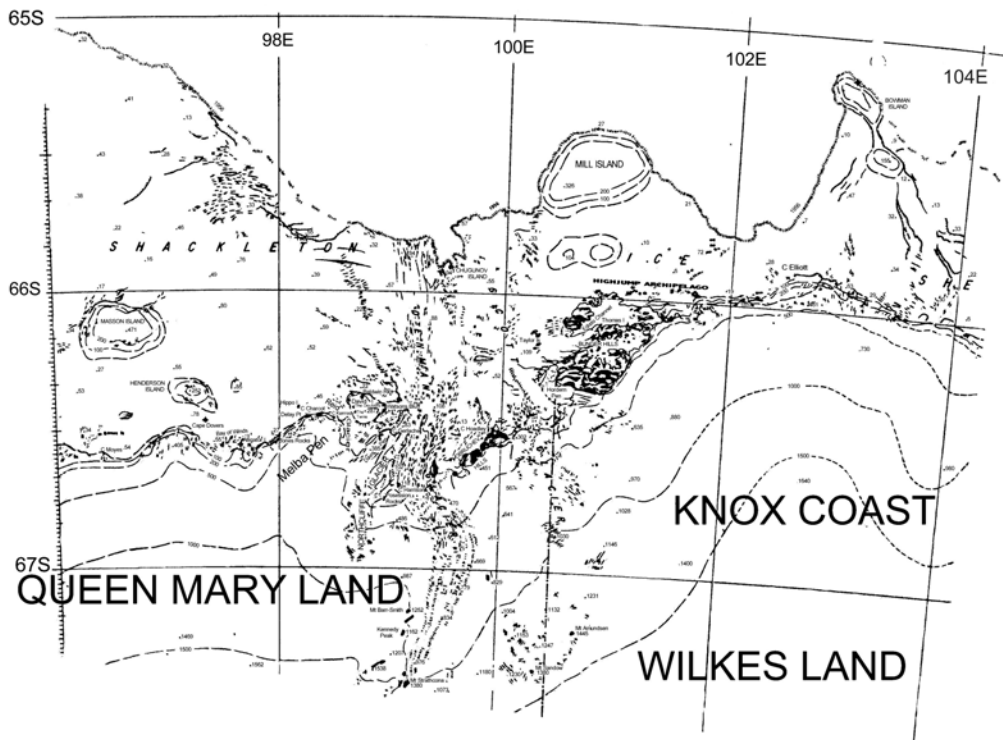
Fig 7.9.2.1.2   Detailed map of Queen Mary Land.

7.9.2.3   <u>Data sources and services provided</u>

A forecaster at Edgeworth David is dependent upon equipment ferried in from the coast, which must be able to run on intermittent generator power. This would normally produce APT satellite reception, HF AXM chart reception, scheduled data broadcasts from Casey Station and local data, including pilot balloons, barograph and screen based observations.

7.9.2.4   <u>Important weather phenomena and forecasting techniques used at the location</u>

General overview

Table 7.9.2.4.1 in Appendix 2 below is a summary of the means of a few of the elements observed during the 1986 summer at Edgeworth David, while Table 7.9.2.4.2 in Appendix 2 below is a similar summary of data observed at the nearby Oasis base in the 1958 summer.
In general, during the operation of the summer camp in 1985/86 marginal conditions were mainly encountered in the prevailing easterlies. Weather patterns delivered complex and difficult forecasting problems. If weather patterns moved slowly, it was not uncommon for a low or extensive frontal band to move inland, resulting in extensive penetration of moisture inland with very strong easterly winds (> 35 m s^{-1} ($\sim$ 70kt) in the low levels up to 3600 m ($\sim$ 12,000 ft)). If weather patterns moved rapidly gales could onset rapidly, with low cloud following quickly from the west.

Prevailing strong south easterly winds across the Bunger Hills frequently produced strong turbulence adjacent to the continental ice sheet, with winds grading to light at Edgeworth David. The summer camp temperature generally rose a few degrees above freezing during the day, reaching above 10ºC on a few occasions (see Table 7.9.2.4.1 in Appendix 2 below). Precipitation was infrequent and on one notable occasion fell as rain.
     The Bunger Hills are frequently affected by deep slow–moving lows to the north. On average, a stable long wave trough is found in the longitude of the Shackleton Ice Shelf during summer. Consequently, lows are often rapidly advected in from the northwest, and may recurve to the west after becoming embedded in the circumpolar trough. These large synoptic scale weather systems are well handled by the models, and have resulted in multiple day gales at Edgeworth David.
     Satellite imagery is an important forecasting tool for verification of numerical model predictions and short term development. Frequently, deep depressions over the Southern Ocean are made up of multiple centres, or have well defined centres of cyclonic vorticity advection (CVA) which explain short term increases in wind velocity. Broad scale advection of moisture into the continent to the east of the Bunger Hills must also be monitored, as easterly return flow to the coast would result in white out and possible precipitation. Visible imagery is an important tool for detection of cloud over the inland ice sheet, particularly as the similar surface temperature of cloud and ice reduces the effectiveness of infra–red imagery.
     Significant mesoscale lows are rarely detected in this part of the coast due to the lack of significant orography. The area around the Denman Glacier was noted for its interesting weather phenomena. Most notable was the recurrent hydraulic jump. This phenomenon's scale was reported on the scale of the width of the glacier. A more broad scale hydraulic jump may have been present as evidenced by the severe weather conditions experienced in the

Bunger Hills. It was not possible to determine if broad scale hydraulic jumps were active during severe wind events due to restricted transport.

Surface wind and the pressure field

The wind direction is equally determined by the prevailing easterly pressure gradient and the broad–scalesoutheasterly katabatic flow generated by the interior continental ice slope across the eastern shield.

Wind speed is determined mainly by the oceanic pressure gradient and on occasions by the strength of the katabatic flow, which appears to strengthen when easterly gradients reinforce continental outflow to the south east of the Shackleton Ice Shelf. In the event of gradient–reinforced katabatic flow, severe turbulence occurs along the coast. It is particularly evident over the hills, where a semi–permanent layer of low to mid–level cloud forms parallel to the continental ice sheet, with the cloud lowering as the turbulence increases. Mammatus and turbulent billows were observed on occasion.

During weak pressure events, winds became light and variable over the hills, although moderate south easterly flow continued diurnally along the eastern flank of the hills. This wind usually eased significantly during the morning, resuming during the night. It was during these lulls in the pressure field that conditions permitted operations extending to the Denman Glacier and the exposed coast and interior ranges at the head of this glacier.

Upper wind, temperature and humidity

These fields were taken directly from the model fields available on the HF AXM and were augmented by local observations to 3000 m (~10,000 ft) using pilot balloon. Adjustments to the chart patterns were also made in the light of the satellite imagery.

Clouds

A semi–permanent bank of stratocumulus and sometimes altocumulus would develop over the Bunger Hills when strong south easterly winds occurred. This cloud bank was a good indicator of strong turbulence along the continental ice sheet edge.

Middle level cloud frequently resulted in white–out, particularly for flights to the coast over the unrelieved ice shelf. An unreliable aide in these events was the use of 'water cloud' signatures, where open sea or ice leads would show as a darkened underside of the cloud. This water cloud would assist pilots to break up some of the white out, particularly when determining the horizon. This tool was unreliable due to the frequent presence of blowing snow across the ice shelf. It is also important to remember that it was only useful with the sun behind the pilot, flying to the coast. Return flight was significantly more difficult, unless the pilot could gain significant altitude to sight the Bunger Hills.

Visibility: blowing snow and fog

Visibility across the region was generally very good due to the lack of pollution sources. White out, however occurred regularly, as significant middle level cloud masses passed over the region in association with the frequent passage of deep lows.

Reduced visibility due to mist or fog was not reported in the hills nor the coast. In the Bunger Hills the lack of significant exposed water areas and the distance from the coast guaranteed the absence of these phenomena. There may have been some events on the coast, but during this camp there were few light wind events and no reports from flight crews. Blowing snow was not a problem in the hills due to the lack of snowfall.

Mill Island was frequently obscured by drifting snow. North and west of the High Jump Archipelago the winds appeared to funnel against rising orography, increasing by 5–10 m s^{-1} (~10–20 kt). This drift was often a determining no–flight factor when combined with marginal white out conditions.

Surface contrast including white–out

White–out did not affect field parties as their movement was confined to the hills. Aircraft activities were confined to the hills during white–out.

Horizontal definition

Edgeworth David camp was enclosed by hills on it's eastern flank and the Edisto Glacier, across permanent sea ice on it's western flank. Hills ranged from 100 m to 500 m, whilst features of the Edisto Glacier ranged approximately 1 to 2 km. Ranges below 2 km did not offer any useful indication for visibility reduction, particularly given the lack of weather impact on the south western sector of the Bunger Hills.

Precipitation

Precipitation only occurs as a significant broad scale low brings warm conveyor belt moisture over the coast. In one event where strong northerly advection occurred, rain developed. The other two events produced snow when a westward moving front brought warm sector cloud south of the low, along the coast and moving west–northwest back to the coast from the continent. Forecasts of precipitation are heavily dependent upon reliable satellite imagery interpretation.

Temperature and chill factor

Temperature ranges are modest due to the normally windy conditions. Colder conditions affected field parties more as night redeveloped and the hours of dark lengthened. The principal difference in the temperature range in Tables 7.9.2.4.1 and 7.9.2.4.2 in Appendix 2 below (Edgeworth David and Oasis), can be attributed to the Oasis record extending to the end of March, whereas Edgeworth David was evacuated at the start of March. The lower

maximum and minimum temperatures would have posed a significant restriction upon Edgeworth David camp activities given the camp was equipped for warmer conditions.

Icing

No icing was reported during the 1985/86 summer camp.

Turbulence

Severe turbulence was frequent across the Bunger Hills and in the vicinity of the base of the continental ice slope. Some site specific turbulent characteristics of the area which have been noted are:

- *Bunger Hills*: The Edgeworth David base is extremely well protected from prevailing east and south easterly winds. Hence observations at Edgeworth David are not representative for flight conditions elsewhere. Field parties indicated that in easterly air flows, strong winds extended within 9 km (~5 nm) of the base of the ice plateau on the northern, eastern and southern margins of the hills. For example if a pilot balloon measured easterlies at 23 m s^{-1} (~45 kt) above 600 m (~2000 ft) then surface to 300m (~1000 ft) winds channelled in northeast to southwest oriented valleys were greatly strengthened and gusty. These winds would consistently average 25 m s^{-1} (~50 kt) gusting greater than 35 m s^{-1} (~70 kt) and pilots would report moderate to severe turbulence within 9 km (~5 nm) of the edge of plateau. It is supposed that the katabatic or gravity winds combined with gradient winds to produce the high surface winds and severe turbulence. Pilots reported blowing snow on the plateau reaching as high as the cloud base (around 900 m (~3000 ft)). In these strong easterlies, Edgeworth David was relatively warm (+4 to 7ºC), with 10 to 15 m s^{-1} (~20 to 30 kt) winds, gusting to greater than 20 m s^{-1} (~40 kt) by late morning or early afternoon. A guide to turbulence in these moist air streams is a semi–permanent roll cloud sitting inside the eastern margin of the hills.
- *Denman Glacier*: This glacier is west of Bunger Hills. It was noted that even in a light pressure gradient wind, strong winds would not allow helicopters to land on rock pinnacles at the base of the Glacier, while another party was able to land on the nearby Watson's Bluff in light and variable winds. Now, Watson's Bluff is elevated and the contrast in wind behaviour would seem to indicate that a shallow katabatic–drainage wind was occurring at the base of the Denman Glacier. On other occasions with easterly flow present this area was unflyable. It was generally found that drainage winds could add up to 20 m s^{-1} (~40 kt) to winds recorded on pilot balloon flights, for example, the Edgeworth David pilot balloon flight at 1500 m (~5000 ft) would show 20 m s^{-1} (~40 kt) easterly while the wind at 1500 m over the surface of Denman Glacier (pilot observation) was 40 m s^{-1} (~80 kt) southeasterly, with very severe turbulence. Moreover, very severe turbulence was also encountered near hydraulic jump phenomena. These jumps developed very rapidly (pilot observations) with recorded aircraft vertical displacements of +/– 450 m (~1500 ft).
- *Obruchev Hills*: The steep fall of the plateau to the south east of these hills supplies a consistent strong katabatic. In an easterly wind regime (23 m s^{-1} (~45 kt) synoptic flow) southeasterly surface winds have been recorded in excess of 40 m s^{-1} (~ 80 kt). Pilots have also recorded severe down drafts to the south east of the hills

(that is, up wind). In one case even with full power a Hughes 500 helicopter could not climb.

Hydraulic jumps

Pilots frequently reported the rapid development of hydraulic jumps moving down (and confined to) the Denman Glacier. On one occasion an aircraft nearly came to grief when landing to the west of a range adjoining the Denman Glacier. It appears that the stable stratified south easterly flow developed a stable rotor in the lee of the range, reversing the easterly wind. Without visual clues to detect the new wind direction the pilot nearly stalled on landing with a tail wind
    Short trails of fair weather cumulus which could be seen in the vicinity of the base of the Denman Glacier were also thought to indicate the presence of hydraulic jumps. Such cumulus is thought to have developed from the top of the hydraulic jump wall, where evaporation of the vertically blown snow and recondensation leave tell tale cloud. Under these circumstance this cloud would be quickly dispersed in the surrounding dry air, which fits with the short trail of cloud.

Sea ice

Sea ice off the Shackleton Ice Shelf forms as fast and pack ice during winter. Its break up can be unreliable due to a very large semi–permanent iceberg which grounds on a bank well off shore. During the 1985/86 camp, little pack ice was encountered until the Shackleton Ice Shelf. In the subsequent year the ship became beset in pressure pack ice, which was packing against a very large iceberg to the west of the ship. Satellite imagery failed to find this iceberg the year before, yet the iceberg was easily found on imagery in the summer of 1986/87, and matched Russian maps which noted its location. It appears that a section of ice shelf broke away and then drifted to the same bank.

Wind waves and swell

Wind waves are computed from model surface wind speed, and fetch or duration. Swell has to be estimated using a knowledge of wind and wave conditions over the previous few days and the few available swell observations. NWP is used where available.

7.10   **Wilkes Land**

Wilkes Land spans meridians 102º to 136º E . From west to east, key features or stations/bases referred to in this section include:

- *Casey Station*   (66.28º S, 110.52º E, 42 m AMSL);
- *Law Dome*   near(66.7 º S , 112.7 º E , 1395 m AMSL)
- *Vostok Station*   (78º 28´ S, 106º 48´ E, 3488 m AMSL);

- *Concordia Station (Dome C)*   (74° 30´ S, 123° 00´ E, 3280 m AMSL).

The above places are shown in Figure 7.10.1.

7.10.1   Casey Station including Law Dome Summit

7.10.1.1   Orography and the local environment

Casey Station is situated at 66.28º S, 110.52º E on the Antarctic coast in an area known as the Windmill Islands. The station is very near sea level on a section of coast oriented north/south, with the plateau rising to the southeast of the station onto Law Dome. The Dome rises to a height of 1395 m some 120 km from the station. The Vanderford Glacier, situated 25 km south of Casey, and the Adams Glacier immediately west of the Vanderford, empty into Vincennes Bay and act as a drainage basin for the trench south of Law Dome, as does the Totten Glacier to the east of Law Dome. The Dome has a significant effect on the weather in the Casey area.

The Law Dome drilling site is at the summit of Law Dome. At the time of writing there was no active drilling programme on Law Dome and the only visits to the site are to maintain entrances, measure strain grids and maintain cane lines. Forecasting for the site is *ad hoc* and mostly based on the synoptic features forecast. Being at the top of a significant orographical feature the site is not dominated by katabatic flow so the wind regime is assumed to be dominated by the gradient flow predicted by the models.
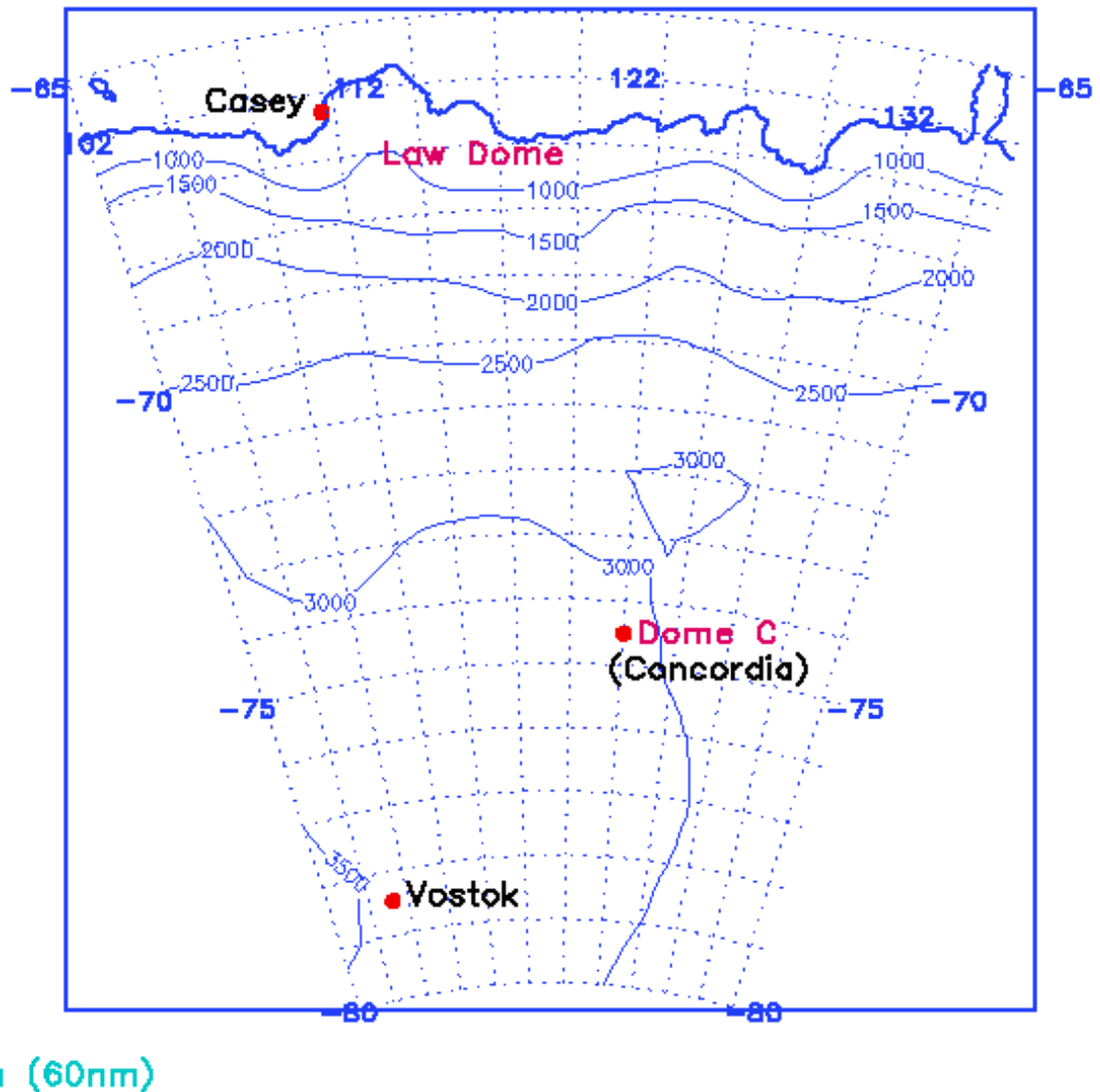
Figure 7.10.1   Sketch map for Wilkes Land (contours in metres; the area is bounded by: 80º S, 65º S, 102º E and 135º E).

7.10.1.2   Operational requirements and activities relevant to the forecasting process

Casey houses the Antarctic Meteorological Centre (AMC) which acts as the primary forecasting centre for all Australian activities in East Antarctica. During the summer three meteorologists provide an analysis and forecasting service to both personnel at Casey and users anywhere in East Antarctica or the southern Ocean south of 50º S, from 0º E to 180º E. Local activities include field parties working in the surrounding Windmill Islands and coastal areas and glaciologists working on Law Dome. Other forecasting duties include flight forecasts for helicopters operating either locally or transiting between Casey and Davis, some 1400 km to the west. High–seas forecasts are provided for shipping operating between 60º E and 160º E, south of 50º S, and ocean route forecasts are also provided, on request, for ships operating south of 50º S.

Australia has the research vessel *Aurora Australis* providing marine science capabilities and providing the resupply for the Australian stations, Mawson, Davis, Casey and Macquarie Island. Australia relies on helicopter support for field work around Davis and the Prince

433

Charles Mountains with Casey providing data and scientific support for the meteorologist based at Davis.

7.10.1.3   Data sources and services provided

The AMC is connected to the Australian Bureau of Meteorology network (and to the internet) via a 64 Kbps satellite link. Routine data downloaded to Casey from Melbourne, Australia includes 3 hourly GMS IR, water vapour and visual images, three hourly IR METEOSAT images, twice daily low resolution 4–D numerical data from the Australian GASP model and very low resolution MSLP gridded data from the ECMWF model. As well as the data provided by the Bureau, high resolution NCEP Aviation model data are downloaded to Casey twice a day. Casey has an HRPT system ingesting NOAA–12, NOAA–14 and NOAA–15 data. These passes are processed locally providing high resolution satellite coverage of the East Antarctic region. Reduced resolution (4 km) mosaics of the band 4 AVHRR data are prepared locally and sent back to Australia every 6 h, along with the TIP data from every pass.

The AMC has an HF metfax system for transmitting products to end users with locally prepared products being broadcast during the summer months and Australian derived charts being broadcast over the winter months when no meteorologists are on base. The primary frequency used is 7468.1 kHz with the secondary frequency being 11453.1 kHz.

Routine products prepared by the meteorologists for transmission via HF metfax (and subsequently being available on the world wide web) include :

- Surface analyses (MSLP over the ocean and streamline analysis over the continent) at 1800 UTC, 0000 UTC, 0600 UTC and 1200 UTC).
- Manual surface prognoses for +12 h (valid at 1200 UTC the same day) and +36 h valid 1200 UTC the next day.
- High–seas products for +12 h, +24 Hours and +36 hours valid from 1200 UTC the same day through to 1200 UTC the following day. These products are a combination of a streamline analysis and isotach analysis. The prognoses are put out for two regions with the western high–seas area covering 60º E to 115º E, south of 50º S and the eastern area covering from 105º E to 160º E, south of 50º S. The overlap is to assist in navigation around the Casey area. Synoptic situations for both areas are also transmitted.
- Weekly sea ice analyses for the Casey area and for the Mawson/Davis area are also prepared.

7.10.1.4   Important weather phenomena and forecasting techniques used at the location

General overview

Table 7.10.1.4.1 in Appendix 2 below gives a summary of mean monthly values of certain weather elements at Casey while Table 7.10.1.4.2 in Appendix 2 below is taken from work by Shepherd (personal communication) and summarises the suitability of Casey as an aircraft landing site based on the incidence of adverse cross–wind, cloud, white–out and adverse visibility. While these parameters are discussed in more detail below it may be seen from the table that potential white–out aside, Casey enjoys a relatively low percentage of weather

which might be adverse to aviation. December and January (only 15 % adverse conditions (excluding possible white–out)) are the best months while the period March through to September experience uniformly around 25 to 345% adverse conditions.

The wind and weather regimes at Casey are strongly modified by the close proximity of Law Dome. Rather than a general katabatic outflow from the plateau giving rise to strong southeasterly flow, as experienced at other coastal stations on the plateau verge Casey has, in general a light wind regime and only a weak katabatic signature. The wind is most commonly from the southeast, although on occasions a weak northeasterly outflow is experienced. Strong wind events at the station are generally associated with deep synoptic scale cyclones moving north of the station. On a few occasions mesoscale lows forming in Vincennes Bay give rise to gale to occasionally storm force wind events and on rare occasions the strong cold outflow typical of the Vanderford Glacier area makes it far enough north to encompass Casey. These southerly gales are typically in sunny conditions with just low ground drift.

Mesoscale low–pressuresystems forming in Vincennes Bay are almost impossible to forecast as they are typically of a scale well under the resolution of the available numerical models. The only way the systems may be detected is by the AVHRR imagery available. The dynamics of formation of these systems is not well understood but it appears that under some circumstances the strong southerly outflow from the Vanderford Glacier interacts with the weak, moister northeasterly gradient to spin up a small scale low–pressuresystem. The systems are capable of accelerating the incipient northeasterly flow from a light to moderate breeze up to gale to storm force and typically have a life time of the order of 12 hours.

The gale to storm force katabatic events at Casey are infrequent and not well forecast. The dynamics behind why the katabatic makes it up the coast to Casey on some occasions is not known. However, it would appear that the situations in which these events occur are just after the passage of a synoptic scale low–pressuresystem where the gradient flow becomes southerly. Perhaps the weak southerly flow assists the downslope flow of a pool of cold air up on the plateau inland of Casey. However, it is more common that after the passage of low–pressuresystems the wind remains only light from the southeast.

Casey is renowned for the strength of the blizzards that strike with the passage of deep cyclonic systems. The wind speed experienced at Casey is typically near double that of the gradient level flow. As low–pressuresystems approach Casey, generally from the northwest, and the gradient level flow (easterly or northeasterly) increases the wind at Casey becomes extremely variable with the direction swinging through all directions, with stronger gusts likely from the east. At some critical point the wind direction becomes stable at 090º and the wind speed dramatically increases to somewhere near twice the gradient level wind. Once the gale to storm force wind has become established the direction is very stable with only about a 5º fluctuation either side of the mean position (normally 090º). The storms typically last from around 12 hours through to 3 or 4 days. Once the low–pressuresystem begins to move away and the gradient level wind shifts from being easterly the wind at Casey drops dramatically with strong fluctuations in direction as observed at the commencement of the strong wind event. The storm force wind events are very much direction dependent and any wind shift of more than about 10º from 090º generally results in a dramatic drop in wind speed.

The difficulty in forecasting these storm events at Casey lies in ascertaining whether an approaching low has the right characteristics to develop a suitable gradient level flow for the wind to accelerate in the Casey area. Over the years several forecasting aids have been developed to assist in the forecast process. These rules are listed out below.

In the medium term, look for :

- a well–developed synoptic scale low visible on the satellite imagery approaching Casey with the centre of the low moving to be south of 60º S;
- and a strong upper level westerly jet forming over Casey.

In the very short term (anywhere between about 20 minutes and several hours warning) look for:

- strongly fluctuating surface wind at Casey with the wind direction changing between westerly and easterly on a time scale measured in minutes.
- very obvious drift tails of snow above the moraine line some two kilometres east of the station.

All of the above signs may become obvious at the station but unfortunately do not necessarily lead to a 100% reliable forecast of a storm. There appears to be a definite critical point (see, for example, Section 6.6.1.5 above) that has to be reached for the storm to move down off the plateau and over the station. On occasions there can be visible signs of strong wind on the plateau some five kilometres away from the station and a deep low just to the north yet the strong wind never reaches down to the station. Deciding whether a storm event is going to reach the station remains one of the challenges at Casey.

Possible landing sites for fixed–winged aircraft located near Casey are at a site known locally as the "Casey Airstrip" and at Lanyon Junction:

- *Casey Airstrip and Casey*: A comparison of available conditions for these sites is provided in Table 7.10.1.4.3 in Appendix 2 below. Overall, the mean temperature at Casey Airstrip is about 2°C colder than at Casey, but during summer months the difference is closer to 3°C. The mean wind speed is slightly stronger at Casey Airstrip than at Casey. It is likely that if more data were available the mean wind speed for Casey Airstrip would be similar to that for Lanyon Junction, given their elevated locations, and that the mean speed for Casey would be less as a result of the rotor effects experienced there at times. The percentage occurrence of adverse cross–wind is similar for the two sites. In the absence of visual observations at Casey Airstrip, it is difficult to compare other aspects. However, given the higher elevation of Casey Airstrip compared to Casey, and bearing in mind the data for Lanyon Junction, one would expect a higher frequency of adverse low cloud and visibility conditions at Casey Airstrip than at Casey.
- *Lanyon Junction and Casey*: A comparison of conditions for these two sites is given in Table 7.10.1.4.4 in Appendix 2 below. The mean temperature at Lanyon Junction is about 4°C colder than at Casey, largely a result of the elevation difference between the sites. The overall mean wind speed at Lanyon Junction is nearly 40% stronger than that at Casey. This would seem to reflect the times when wind speeds are much less at Casey as a result of rotor effects that affect Casey but not Lanyon Junction. However, it should be noted that at other times the winds at both places are similar, or indeed stronger at Casey. The frequency of adverse cross–wind is higher at Lanyon Junction than at Casey. This may just be the result of limited data, but it would appear that the generally more consistent wind direction of Lanyon Junction is offset by the stronger wind speeds involved. The frequency of both adverse low cloud and poor visibility at Lanyon Junction is about three times those at Casey. The occurrence of adverse weather type is about twice as much at Lanyon Junction. The percentage occurrence of at least four oktas of total cloud is slightly higher at Casey, as is the occurrence of times when adverse criteria were met for at least one of all the elements considered. The frequency of occasions when adverse conditions were met for at least one of cross–wind, low cloud or visibility is nearly three times higher for Lanyon Junction than it is for Casey.

Surface wind and pressure field

As mentioned above the wind at Casey is generally light (less than 7 m s^{-1} (~15 kt) and from the easterly sector, either southeasterly or northeasterly (seethe wind rose for shown in Figure 7.10.14.1 in Appendix 2 below). Flying operations and field work at Casey itself are typically not effected by wind. For example, in terms of cross–wind component effects on aircraft, Table 7.10.1.4.5 in Appendix 2 below shows the percentage frequency of occurrence of wind components normal to the mean wind direction of 090º at Casey greater than 7.7 m s^{-1} (~15 kt). It may be seen that the frequencies are all less than 10 per cent.

However, to the south and the north of the station, significantly different wind regimes exist. At an old AWS site 40 km (~21 nm) north at the Balaena Islands the predominant wind is a northeasterly and it is typically much stronger than at Casey with a significant strong outflow signature. Similarly, to the south of Casey the predominant wind is a south to southeasterly outflow from the Vanderford Glacier. On many occasions this outflow makes it up the coast to Ardery Island (site of ornothological studies), some 10 km (~5 nm) south of Casey yet not to the station itself.

The wind events affecting Casey are the less common southerly gales that make it up from the Vanderford, mesoscale low–pressuresystems forming in Vincennes Bay giving rise to gale–force northeasterly flow and synoptic scale low–pressuresystems resulting in full storm force wind (typically averaging anywhere from 25 m s^{-1} (~50 kt) through to 45 m s^{-1} (~90 kt) with gusts recorded in excess of 60 m s^{-1} (~120 kt).

The preparation of surface analyses and the accompanying study of both GMS and NOAA AVHRR imagery certainly is most beneficial in the forecasting of the synoptic scale events and in some cases may even assist in picking the formation of the cloud signatures associated with mesoscale lows forming in Vincennes Bay. However, such analyses do not appear to be at all useful in picking strong southerly wind events.

The numerical models available to the forecasters are all global in scale and so of relatively low resolution. The best model available to the forecaster is the NCEP aviation run with 1.0 degree data available on pressure levels and the first sigma level. However, as with the ECMWF and GASP models the orography around Casey, and in particular Law Dome, are not represented at all well. In fact Law Dome appears as little more than a ridge pushing slightly out into the ocean. Because of the poor representation the surface wind fields from the model need to be treated with care. One of the main problems arising from the poor model orography is the tendency for the NCEP model to over estimate the southeasterly outflow at Casey – quite often by as much as 100%, and not pick those occasions when Casey experiences a northeasterly outflow from around Law Dome. Storm force easterly wind at Casey is also not well handled with the models not picking the accelerations experienced at Casey. These model shortfalls are fairly consistent and can be accounted for when interpreting the model data.

Upper wind, temperature and humidity.

These fields are taken directly from the model for flight forecasting or cloud prediction. Aerological diagrams may be generated from any model time–step for the GASP and NCEP for assistance in cloud prediction and upper flow.

Clouds

The location of Casey makes for interesting wind effects but unfortunately the location also acts as a cloud trap. Once the weather begins to warm during the summer months and the sea ice breaks up, allowing large fluxes of heat and moisture from Vincennes Bay a bank of low cloud (typical base anywhere between 1000 and 6000 ft) forms over Casey.

As may be seen from Table 7.10.1.4.6 in Appendix 2 below low cloud of major significance to aircraft landing/takeoff at Casey has a frequency of occurrence below 10 per cent in all months. The extent of the lower level cloud in "cloud trap" situations is generally not large, with sunshine visible on the horizon from the south, through west to the north. On the AVHRR imagery the cloud bank can be picked up hugging the western sector of Law Dome. The signature is warm with the cloud tops quite low. The Vanderford and Adams Glaciers are typically cloud–free as is much of the Peterson Bank. The cloud is typically thin but significant enough to reduce the visibility to the east and on occasions produce very light falls of snow. This phenomena does not typically upset flying as the locations the helicopters are normally heading for are cloud–free and there is only a short hop of some 20 to 30 km to clear the cloud bank. During summer months when a lot of rock is exposed surface definition remains fair under the cloud even with the poor horizon definition.

More significant cloud events are associated with the synoptic scale low–pressuresystems where warm and moist northeasterly flow produces large amounts of middle and low level cloud over Casey, often with good falls of snow. During storm events wave, or banner cloud, is quite predominant over the station with a stationary lenticular cloud positioned just to the southwest of the station with significant rotoring observable underneath.

Visibility: blowing snow and fog

Visibility at Casey is normally very good, particularly in summer as may be seen from Tables 7.10.1.4.7 and 7.10.1.4.8 in Appendix 2 below. These tables show, respectively, frequencies of occurrence of poor visibility and of adverse weather types (all of which affect the visibility). It may be seen that over the summer months, and in December and January in particular, the visibility and related weather types have frequencies of occurrence which are less than about 10 to 14 per cent. Moreover, during the summer months a lot of rock is exposed to assist in surface definition. Visibility is generally only ever lost in falling or blowing snow associated with storm events. During the summer months of November to February the chances of a synoptic scale low inducing a blizzard are very low so visibility is normally only reduced in falling snow events and these are not very common at all during summer.

Fog is a rare event at Casey with perhaps two to three fog days a year, at most. The fog formations observed have all occurred during the height of summer and under the same regime. A light afternoon northwesterly flow has prevailed for a few days (quite possibly a weak sea breeze circulation) advecting moisture in from Vincennes Bay over Casey. This moisture packs in against the steeply sloping terrain above the moraine forming a thin deck of stratus. As the evening progresses the weak northwesterly is replaced by a weak southerly flow and the stratus moves back towards the station, sinking as it does so and enveloping the station in a misty fog. Visibility typically reduces to around 200 to 300 m.

Surface contrast including white–out

Typically the surface contrast around Casey remains good due to the amount of exposed rock. However, as may be seen from Table 7.10.1.4.9 in Appendix 2 below the potential for white–out at Casey, should the rock be covered with ice or snow, at least in some sectors, is 66 per cent or greater throughout the year. Furthermore, surface definition inland from the nearby moraine line, where there are no obvious ground features, does pose a problem on a number of occasions. The band of stratiform cloud that typically forms in the Casey area during summer does lead to white–out conditions on the plateau necessitating the use of GPS and radar for navigation. Flying inland on these occasions does not take place

Horizon Definition

Horizon definition in the Casey area is typically very good due to the visible land marks up and down the coast and with the icebergs off the coast. The stratiform cloud formation typical in summer only really reduces the horizon definition to the east.

Precipitation

Most of the precipitation falling at Casey is as a result of synoptic scale low–pressuresystems moving close to the coast. These systems are capable of producing sizeable amounts of snow in a short period of time. These falls can cause a significant reduction in visibility and stop flying operations. Such events are not common during the summer months and typically only effect flying operations during March and April when the helicopters are being used to expatriate the summer personnel. These large falls of snow have another adverse effect in that the loose snow is easily picked up by the wind and any subsequent strong wind event will almost certainly result in blizzard conditions.
     The more typical weather patterns at Casey generally do not produce much snow at all and when precipitation does occur it is most typically observed falling out to sea over the icebergs or further south over the Mitchell Peninsula, leaving Casey relatively fine.
     On a very few occasions over the summer months, when the temperatures are high enough, drizzle or very light rain may be observed. This may cause problems with riming on vehicles or helicopters but is uncommon.

Temperature and chill factor

The forecasters at Casey do not carry out any temperature forecasting as the parameter is not considered important.

Icing

Forecasting airframe icing in Antarctica is quite difficult as an assessment needs to be made of whether the clouds are fully glaciated or whether some supercooled liquid may still be present. Certainly helicopters operating in the Australian sector of the Antarctic have experienced icing on numerous occasions so the forecaster needs to be aware. As a matter of

course if there is any cloud present where the temperatures are above –20ºC then icing is mentioned. Severe icing is considered a possibility in pre–frontal cloud near the coast where it is possible that the airflow has been strong enough to carry supercooled liquid to the Antarctic coast.

Turbulence

Turbulence is forecast at Casey using the wind profile from the twice daily radiosonde ascents and the profiles from the numerical models. One of the output parameters from each radiosonde flight is a profile of Richardson's number. This may assist in picking those levels where turbulence is most likely, however, strong shear is most commonly used to deduce turbulence.

Hydraulic jumps

Hydraulic jumps have been observed at Casey but they are not a common event. The commencement or cessation of strong wind at Casey is most commonly linked with synoptic scale lows and a critical Froude number were the flow shifts from being separated (light wind at the station) to a downslope flow (strong wind at Casey). Forecasting a hydraulic jump is not an issue.

Sea ice

Sea ice at Casey is quite variable. The regularity of strong wind events during winter (typically every 8 to 10 days and lasting for 2 to 3 days at a time) keeps a semi–permanent polynya in the eastern part of Vincennes Bay near Casey. At a smaller scale the blizzards quite often clear out the ice in Newcombe Bay north of a line between Kilby Island and the tip site at Wilkes with the inner part of the bay holding ice until early summer.

Wind waves and swell

Casey does not do any wind or swell forecasting for the local area. It is quite rare to get much of a swell into the Casey area. Extended periods of westerly wind to the west of Casey have generated swells that have penetrated into Casey but they are typically of very long wave length with amplitudes less than one metre. Boating around the Windmill Islands is only allowed when the wind speed is under 7 m s^{-1} (~5 kt) and wind waves are quite low.

7.10.2   Vostok Station

7.10.2.1   Orography and the local environment

Vostok Station (78º 28´ S, 106º 48´ E, 3488 m AMSL) was opened on December 16, 957. It is located on the snow surface of the ice plateau of Central Antarctica 1410 km distant from Mirny Station and 1260 km from the nearest sea coast. The ice sheet thickness in this area is 3700 m.

The highest part of the ice plateau is at a distance of 450 km to the west–southwest of the station at a height of more than 4000 m above sea level. The station is located on the snow plane which has a generally insignificant slope to the main ice divide of the continent.

Snow sastrugi and naduvy (blown snow fields) are typical micro–relief features of the snow surface in the station vicinity forming a slightly undulated surface. The height of sastrugi typically varies between 20–40 cm and that of naduvy is not greater than 50 cm.

7.10.2.2   Operational requirements and activities relevant to the forecasting process

The inland research station Vostok is one of the major Russian in Antarctica. The following year–round observations at Vostok are undertaken:

- Meteorological and actinometric observations, snow line measurements;
- Total ozone content measurements and observations of the anomalous phenomena in the atmosphere;
- Geomagnetic observations, including ionosphere studies and observations of atmospheric electrical field variations;
- Upper–air sounding of the atmosphere;
- Deep drilling of the Antarctic ice sheet. Based on the deep–drilling results, a sub–glacial lake was discovered whose study continues;
- Study of the influence of environmental factors and micro–social conditions on the health of staff.

7.10.2.3   Data sources and services provided

A surface meteorological programme continues although the upper–air programme has ceased.

7.10.2.4   Important weather phenomena and forecasting techniques used at the location

General overview

The geographical location of the station, features of the underlying surface, solar radiation and atmospheric circulation regime give a severe climate. The ice sheet is perennially covered by snow that never melts. High transparency and dryness as well as a smaller atmosphere mass above the ice surface of Antarctica (compared to the coastal stations) result in relatively large

quantities of total incident radiation to the ice surface. Intense cooling occurs above the Antarctic plateau and strong surface inversions develops throughout the year. Here the air temperatures are unusually low during the entire year. Mean annual air temperature at the station is −55.4ºC with the absolute minimum of −89.2ºC recorded at Vostok on July 21, 1983, which is the absolute minimum surface air temperature record on the globe. The absolute maximum recorded at Vostok is −13.6ºC.

Surface wind and the pressure field

Winds in central Antarctica are much weaker than at the coast. The wind regime at Vostok Station is characterized by weak katabatic southerly–southwesterly winds with a mean annual speed of 5.0 m s^{-1} (~10 kt). Annual wind speed variations have two pronounced maxima (March and September) and one sharp minimum (January). The highest mean monthly wind speed is observed in September (5.5 m s^{-1} (~10.7 kt)).

The maximum wind speeds are low, in the order of 13–14 m s^{-1} (~26 kt) and sometimes 16–18 m s^{-1} (~33 kt). They can in individual cases reach 20–25 m s^{-1} (~40–50 kt). The maximum wind speeds are observed in all seasons of the year being due to the most active cyclones moving from the Antarctic coast over the continent.

The probability of storm winds throughout the year is small (only 0.1%). The probability of calms and of strong winds of around 11–15 m s^{-1} (~ 20–30 kt) is also small comprising 2.7% and 1.3%, respectively. Weak winds (0–5 m s^{-1} (less than about 10 kt) are predominantly observed in summer and autumn whereas stronger winds (6–15 m s^{-1} (~12–30 kt) occur in winter and spring.

Vostok Station is located near the eastern foot of a giant spur extending northward from the central dome of the ice sheet of East Antarctica. The prevailing weak southwesterly winds here are determined by downward cold air sinking along the ice spur slope. The persistent wind directions and speeds and dependence of their direction on the relief indicate their katabatic nature. These winds also possess the features of katabatic winds. Compared to the winds of other directions (gradient and cyclonic), they are colder and total cloud and humidity of these winds are smaller, with a greater frequency of occurrence of clear weather.

However, the main indicator of katabatic winds is absent in these winds, namely, the maximum of daily speed variations is observed in the daytime, rather than at night as with true katabatic winds. Such daily wind speed variations are observed at the station in all months except for April, June and September. This is because of the presence of a strong surface high in central Antarctica in whose system the gradient winds are developed due to the anticyclonic pressure field.

In spite of being significantly remote (about 1300 km) from the shores of the Indian and Pacific Oceans with a high elevation of the station above the ocean level, this area as mentioned above, is subjected to the influence of coastal cyclonic activity. The cyclones penetrating the continent both from the Indian Ocean coast and the Ross Sea, reach the station. The influence of the latter in the form of the frontal zones reaching the station area, is primarily manifested in a sharp deterioration of weather conditions accompanied with increased cloudiness, temperature and westerly and southwesterly wind speeds up to 18–20 m s^{-1} (~40 kt). The cyclones coming occasionally from the Indian Ocean also bring cyclonic weather to the station area but with easterly winds. Their speeds are attenuated by contrary katabatic winds and are hence low (8–10 m s^{-1} (~20 kt), but the other indications of cyclonic features are quite pronounced.

The downslope flow in the station area is screened by a coincidence with the gradient wind and a superposition in some cases of cyclonic winds. These effects are so strong that they distort the daily speed variations typical of katabatic winds. However, the katabatic wind

preserves all its other indications at the Vostok Station. In summer, the frequency of occurrence of cyclonic winds similar to the other Antarctic stations increases and that of katabatic winds decreases while in winter it is vice versa.

Due to a high station elevation above sea level, the atmospheric pressure here is very low being 624.2 hPa on average for a year. It varies little in individual years. The annual variations as in other mountainous areas have one maximum in summer (January) and one minimum in late winter (September).

The variability of mean monthly pressure values has annual variations with a winter maximum and summer minimum. The largest deviations are typical of the entire cold period (autumn–winter) with dominating anticyclonic weather conditions. However, the largest frequency of occurrence of cyclonic activity is also observed at this time governing thus the significant amplitudes of atmospheric pressure reaching 20 hPa.

Upper wind, temperature and humidity

No specific information on forecasting has been obtained.

Clouds

Due to extremely low air temperatures, the clouds present over Vostok consist of ice and only occasionally do clouds comprised of supercooled water droplets occur.

Lower level clouds (stratocumulus) occur very rarely above the high mountainous Antarctic plateau where the station is located. Their frequency of occurrence comprises only 1.2%, which is natural as the plateau surface lies above the boundary of lower–level cloud formation and only occasionally does convection from the surface occur contributing to the appearance of low cloud.

Stratus clouds have the largest frequency of occurrence in summer and in the intermediate seasons (1.3%) and the least (0.4) in winter. With these clouds in summer, the atmospheric pressure (638.6 hPa), air temperature (–30.9ºC) and absolute humidity (0.37 hPa) are greater than in winter, when they comprise 623.1 hPa, –65.0ºC and 0.01 hPa, respectively.

Middle level clouds are recorded more often, their frequency of occurrence comprising 8.5%, on average for a year. The prevailing cloud type over the station area is high–level clouds, whose frequency of occurrence for a year comprises 52.9%. The frequency of occurrence of clear weather comprising 37.4% is likewise high. The highest frequency of occurrence of clear weather throughout the year is in winter (41.6%) with the least in spring (30.8%). In winter during clear sky conditions, the weather is characterized by high wind speed (5.4 m s^{-1} (10.5 kt)), but low pressure (620.0 hPa), temperature (–68.8ºC) and humidity (absolute: 0.00 hPa and relative: 66%). In summer, there is a low wind speed (4.7 m s^{-1} (~9 kt)), but high air pressure (631.0 hPa), temperature (–33.5ºC) and humidity (absolute: 0.30 hPa, relative:74%).

The undulated cloud forms (Ci, Cc, Ac, Sc) have the largest frequency of occurrence in summer when the air above the Antarctic plateau warms noticeably. The largest (39–42%) frequency of occurrence of cirrus clouds is observed not only in the summer, but also during the intermediate seasons. The lowest frequency of occurrence of cirrus and cirrocumulus clouds is recorded in winter while that of high cumulus and stratocumulus in spring.

The frequency of occurrence of stratiform clouds (Cs, As) is characterized by inverse annual variations. Whereas for high stratiform clouds such annual variations are pronounced, the frequency of occurrence of Cirrostratus has two phases during the year: a maximum in

winter and spring (18.4–18.2%) and a minimum in summer and autumn (12.3–12.5%). With stratiform clouds, the atmospheric pressure is lower (624.2 hPa) on average for a year, compared to undulated clouds. The temperature is slightly less (–54.5ºC), but the wind speed (5.5 m s^{-1} (~10.6 kt)) and especially total cloudiness (6.5 oktas) is much higher. The absolute humidity comprises 0.07 hPa with relative humidity of 72%.

Large values of total cloudiness and wind speed with stratiform clouds confirm that this form belongs to frontal system clouds. They result from an interaction between the cooled surface of the Antarctic plateau and a relatively warm air flowing onto it. Their prevailing frequency in winter points to dominance of meridional intrusions of comparatively warm air masses in winter from the ocean to the continent.

Visibility: blowing snow and fog

The atmospheric transparency in the inland region of Antarctica is very pronounced. Except for water vapour and ice crystals, the air is not polluted with anything. But humidity here is less than anywhere else since precipitation is insignificant and snowstorms are rather rare. Therefore, the meteorological visibility in the station area is quite high. The largest frequency of occurrence of good visibility (of more than 10 km) is observed in summer while poor visibility (of up to 1 km) is most prevalent in winter.

Snowstorms in the station area are rare due to the weak winds. Drifting snow occurs more frequently at wind speed of up to 8 m s^{-1} (~15 kt) and snowstorms with winds of more than 9 m s^{-1} (~17 kt). The frequency of occurrence of snowstorms changes depending on the snow surface state by seasons of the year. In spring and in summer, when the snow surface is consolidated, the frequency of occurrence of snowstorms is minimum. The largest frequency of occurrence of snowstorms is recorded in winter when loose surface snow is present.

There are 106 days with drifting snow on average over a year. Blowing snow is less frequent (50 days a year). Snowstorms significantly deteriorate visibility being mainly caused by active cyclones moving along the meridional trajectories and penetrating deep onto the continent giving strong winds at the station. This is related to the situation where the New Zealand high–pressure ridge above the Ross Sea develops and intensifies. The development of this ridge leads to a cyclone near the Balleny Islands moving over the continent. Vostok in this case is located at the southwestern periphery of the depression. The transformed maritime air flows along the western ridge periphery to the continent bringing middle and high–level clouds to the station, causing snowfall, snowstorms, a wind change to stronger southerlies and a visibility deterioration of 2–4 km or less.

Fogs and haze produced by ice crystals are typical of the inland regions of Antarctica. There are 42 days with fog and 166 days with haze on average for a year. In summer, fog is observed one day a month while during the other seasons, fog in the station area is observed 4 days a month. The largest number of days with haze is 16 a month in winter and a minimum of 8 days a month in summer. The mean duration of fog and haze is also largest in winter and the least in summer. Fog and haze form in the Antarctic high during calm and cloudless weather.

The dangerous phenomenon of snow fog is also quite common. It is the formation of very fine (indiscernible to the human eye) snow particles and ice crystals above the snow surface due to water vapor sublimation at strong surface inversions. The horizontal visibility decreases to 1 m. Snow fog, unlike ice fog and the clouds near the snow surface, never produces a halo around the sun.

During calm weather, frost or ice fog and haze occur in the central parts of anticyclones and ridges. At wind speeds of 3 to 5 m s^{-1} (~6–10 kt), the phenomenon of "snow mist" can occur caused by fine snow dust in the air after a snowstorm or with the formation of snow

fog. The visibility during "snow mist" as in the presence of snow fog disappears. The absence of visibility makes the snow mist an especially dangerous phenomenon.

Surface contrast including white–out

No specific information on forecasting has been obtained.

Horizontal definition

No specific information on forecasting has been obtained.

Precipitation

The mean annual total of precipitation is 37.9 mm while that of accumulation on the snow surface is 21.5 mm. The sum of precipitation is non–uniform throughout the year comprising on average 4.7 mm during one month in winter, 2.0 mm in spring, 0.6 mm in summer and 2.2 mm in autumn. The largest amount (75% of the annual sum) falls in winter, being especially intense in September, which is distinguished by increased cyclonic activity. On average over the year, there are 26 days with snow, 247 days with deposition of ice needles and 225 days with deposition of hoarfrost. The duration of precipitation is quite long, its intensity however, being so small that in respect of the total annual precipitation the station area can be compared to the most arid regions on earth.

The meteorological conditions under which it snows differ sharply from the weather accompanying the fallout of ice needles and deposition of hoarfrost. During snowfalls, the air temperature and humidity are much higher (with total cloudiness twice as large) than during other kinds of precipitation throughout the year.

The weather during fallout of ice needles is almost similar to hoarfrost deposition conditions, the only difference being a slightly greater frequency of clear weather and middle clouds (along with lower clouds in winter and spring) and higher air humidity and wind speed. Similar weather conditions for these types of precipitation are understandable as the fallout of ice needles and deposition of hoarfrost occur often simultaneously.

The occurrence of ice needles is determined by maritime air flowing to the inner regions of the cold mainland at elevations of about 500–1000 m (~1600–3200 ft) above the ice sheet surface and its sinking due to downward air flow.

Temperature and chill factor

Low air temperatures are extremely dangerous, the more so if they are accompanied by strong winds. For example, a temperature below –75ºC and wind speeds of up to 11 m s^{-1} (~21 kt) were observed at Vostok in August 1978. Under such conditions, the time that people can stay in the open is significantly limited. The maximum permissible duration of stay outside buildings is the time for which the human body surface temperature will decrease to the value dangerous to health.

The annual temperature variations are typical with the maximum in summer and the minimum in winter. The natural seasons in Antarctica are divided conventionally by the

character of the temperature and illumination changes. A peculiar feature is in the absence of a pronounced minimum in one of the winter months (the 'coreless" winter). The difference of the average temperatures of any two adjacent months is not greater than 2.0ºC. Frequently in the middle of winter, warm periods occur that are also clearly pronounced in the middle troposphere being due to heat advection from the north. Active cyclonic eddies reaching the station area are more often observed during the colder period than at the warmer time of the year.

Similar large–scale warming with record high air temperatures both near the surface and in the troposphere was observed at some stations of East Antarctica at the beginning of January 1974, while at the inland Vostok Station a new record of –13.6ºC was observed on January 5, which exceeded the previous maximum air temperature by 7.3ºC.

This process was preceded in late December 1973 by generation of a strong blocking ridge in the middle troposphere (at 500 hPa) and near the surface south of Tasmania. As a result of meridional cyclonic activity, there was a transfer of warm air masses along its western periphery. This in turn, contributed to the formation of an extensive surface anticyclone above East Antarctica near Dumont d'Urville Station. Intensifying, it slowly moved southwestward towards Vostok Station. At the time when the anticyclone centre was located east of the station, the transfer of warm and moist air masses from the north along its western periphery was most intense. With the anticyclone centre passing over Vostok and the establishment of southerly winds whose speed increased up to 18–22 m s^{-1} (~35–43 kt), the temperature sharply dropped for two days.

The formation of ridges and heat sources in the upper troposphere above Antarctica begins more frequently in the Indian–Australian sector. This is primarily connected with a large frequency of occurrence of cyclones compared to other regions, governing intense meridional air exchange processes in the troposphere and lower stratosphere.

In April, the average monthly temperature at Vostok drops below –65ºC and remains at this level throughout the entire winter. In some years, the mean monthly temperature in June–September can be below –70ºC. August is the coldest winter month (–68.6ºC) when the atmosphere cooling above the mainland achieves its maximum.

Transition from winter to summer is characterized by a steady and significant air temperature increase. The mean temperature of the first spring month (October) is 9.7ºC higher than in the last winter month (September). From September (–65.8ºC) to December (–32.9ºC, mean air temperature increases almost two–fold.

In the middle of summer (December–January) the temperature is highest not dropping below –36ºC on average, for over a month. The highest temperature is observed in late December–early January indicating a direct relation to the sun's elevation. Abundant and uniform incident solar radiation determines not only relatively high temperatures in summer, but also an insignificant difference between mean temperatures of the summer months (0.2ºC)

The beginning of autumn is accompanied with dramatic cooling. The average temperature in February is 11.3ºC lower than January. The lowest mean monthly temperatures in autumn are recorded in March (–61.8ºC) with the highest temperatures (–42.7ºC) in February.

The temperature regime of the transition season is characterized by sharp variations in the middle of each season. Mean monthly temperatures in spring (October to November) increase and in autumn (February to March) decrease by the same value comprising 13.4ºC).

The mean annual air temperature anomalies vary from year–to–year between 2.1ºC to –1.4ºC. The daily temperature variability is small with mean values comprising 4.5ºC in winter, 1.4ºC in summer and 2.6ºC in the intermediate seasons. This indicates the increased activity of inter–latitudinal exchange of air masses in winter and a significant role in these processes of advective heat transfer by cyclonic eddies moving along the meridional trajectories to the inner areas of the continent.

Icing

No specific information on forecasting has been obtained on airframe/ship superstructure icing but see the section on precipitation on hoar frost and ice needle formation.

Turbulence

No specific information on forecasting has been obtained.

Hydraulic jumps

No specific information on forecasting has been obtained.

Sea ice

Not relevant at Vostok.

Wind waves and swell

Not relevant at Vostok.

7.10.3   Concordia (Dome C) Station

The French and Italian Antarctic programmes have agreed to cooperate in developing a research programme that includes the construction and operation of a scientific station named "Concordia" located at Dome C, high on the Antarctic plateau, some 1100 km inland from the French station of Dumont d'Urville and 1200 km inland from the Italian station at Terra Nova Bay (See Section 7.12.2 below). The station at Dome C was originally chosen for a drilling experiment because of the very large ice thickness the needs in paleoclimatology and is open to the worldwide scientific community for conducting scientific research.

   After several exploratory seasons the station was officially opened for summer routine operation in December 1997 and is expected to be open year round from the 2003 Austral summer.

7.10.3.1   <u>Orography and the local environment</u>

Dome C (74° 30′ S, 123° 00′ E, 3280 m elevation AMSL) is located on the Antarctic plateau 1080 km from the coast. (see Figure 7.10.3.1.1).
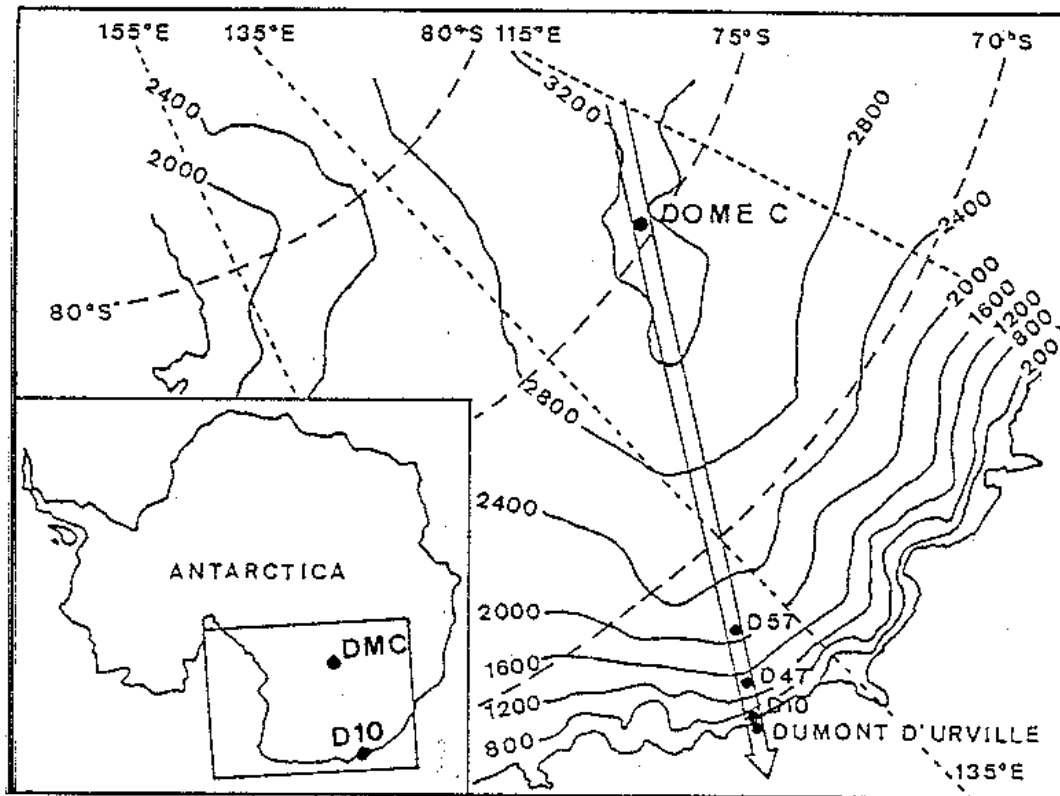
Figure 7.10.3.1.1   Map of the region of Dome C and Dumont d'Urville.

7.10.3.2   <u>Operational requirements and activities relevant to the forecasting process</u>

Concordia can be reached by:
- tractor trains from Dumont d'Urville. About 2,000 tonnes of cargo will have been delivered by tractor trains during the construction phase then about 380 tonnes each year during the operational phase; and
- (ii) ski–equipped planes. Personnel and light, fragile or urgent equipment are delivered by ski–equipped planes from Terra Nova Bay or Dumont d'Urville.

Accommodation at Concordia will be provided for a typical population of 15 expeditioners over winter and 30 over summer.
Six areas of scientific research have been selected by the Concordia steering committee. The station will also carry out programmes in other research areas after the first winter of operation. The six initial research areas selected are: glaciology; atmospheric sciences (including the study of the annual variation of the evolution of the ozone hole in spring; the polar boundary layer; and the triggering of katabatic winds); astronomy and astrophysics; earth sciences; human biology and medicine, and technology.

7.10.3.3   Data sources and services provided

Dome C is in line of sight of geostationary satellites and the future AUSSAT communications satellite, being at the same longitude as Dome C, will cater for fast data transmission needs. Communications are currently only available through the INMARSAT system for parts of the day.

7.10.3.4   Important weather phenomena and forecasting techniques used at the location

General overview

Information not yet provided.

Surface wind and the pressure field

As at Dumont d'Urville the annual course of the atmospheric pressure shows a well–pronounced semi–annual cycle. Minima are observed in autumn and spring, with the spring minimum being larger, while the maxima are observed in summer and winter. The inter–diurnal pressure variation gives an indication of the cyclonic activity. The highest values are found in winter, the lowest in the summer. This is in agreement with the idea that the increased horizontal latitudinal temperature gradient in the Antarctic atmosphere in winter increases cyclonic activity, even though the circumpolar trough is farthest away from the continent in winter.

The wind speeds at Dome C are very light. A comparison with other stations shows that Dome C experiences the lowest wind speeds of any inland station in Antarctica. A mean value of about 3 m s^{-1} (~6 kt) is observed with no pronounced annual cycle. This is unique, as a freely exposed station at a height of 3280 m on any other continent would have higher wind speeds than lower–lying stations. In winter (June), there is no diurnal variation in wind speed at Dome C. The sun is, of course, below the horizon, and no systematic variation in surface heating can occur. However, in summer (December), higher wind speeds are observed in the afternoon. Assuming no gravitational flow for Dome C, the stronger inversions at night hinder the transfer of momentum to the surface, whereas in the afternoon the inversions are weaker.

Upper wind, temperature and humidity

No specific information on forecasting has been obtained.

Clouds

No specific information on forecasting has been obtained.

Visibility: blowing snow and fog

No specific information on forecasting has been obtained.

Surface contrast including white–out

No specific information on forecasting has been obtained.

Horizontal definition

No specific information on forecasting has been obtained.

Precipitation

No specific information on forecasting has been obtained.

Temperature and chill factor

In Table 7.10.3.4.1 in Appendix 2 below the monthly mean, minimum and maximum temperatures are presented. Dome C is very cold; the winter is kernlose or ("coreless"); that is, no systematic changes in temperature are observed during the winter months. An absolute minimum of –84.6°C has been recorded, and the average winter temperature hovers –60°C. Even in summer, Dome C is cold, with the warmest monthly temperature around –30°C. The highest temperature ever measured was well below freezing point. Dome C, of course, lies in the dry snow zone, where melting never occurs. In autumn (March), there is a high degree of diurnal temperature variation with the maximum occurring in the early afternoon. The variation is much larger for Dome C (about 10°C) than for the coastal station D10 (about 2°C). The reason for this is not easy to find because it is the result of the coupled processes of heat exchange at the surface and conditions in the boundary layer. An explanation was first offered by Simpson, the well known meteorologist on Scott's expedition. The larger heat conductivity of snow and ice in the coastal areas suppresses extremes in temperature, while the drier and lower–density snow of inland areas has a poor heat conductivity and capacity, thereby enhancing extremes.

Icing

No specific information on forecasting has been obtained.

Turbulence

No specific information on forecasting has been obtained.

Hydraulic jumps

Do not occur at Dome C

Sea ice

Not relevant at Dome C

Wind waves and swell

Not relevant at Dome C.

7.11   Terre Adélie Land and George V Land

Terre Adélie Land spans meridians 136º to 142º E, while George V Lands extends from 142º E to 155º E. From west to east, key features or stations referred to in this section include:

- *Dumont d'Urville Station* (66° 40' S, 140° 01' E, 0 to 42 m AMSL);
- *Port Martin*   (66° 49'S, 141° 24'E);
- *Cape Denison*   (67° 00'S, 142° 42'E);
- *Commonwealth Bay* near (67 º S 143 º E)

The above places are shown in Figure 7.11.1. (See also Figure 7.10.3.1.1 above)

7.11.1   Dumont d'Urville

7.11.1.1   Orography and the local environment

Dumont d'Urville Station (66° 40' S, 140°01' E, 0 to 42 m elevation AMSL) occupies Île des Pétrels on the Adélie Coast, an ice–free, rocky island some 1 km wide by 1.5 km long with a central plateau of about 40 m altitude. The island, part of the Pointe Géologie archipelago discovered by Frenchman Dumont d'Urville in 1840, is less than 2 km from the coast and 5 km from a good access point to the plateau, Cape Prud'homme.

7.11.1.2   <u>Operational requirements and activities relevant to the forecasting process</u>

The station is serviced by ship from Hobart, Tasmania, 2700km to the north–northeast, a relatively short six day crossing. The closest permanently staffed stations are Casey 1400 km to the west and McMurdo 1500 km to the southeast.

The current, typical population of Dumont d'Urville Station is 26 expeditioners over the eight month winter (14 for general support and 12 staffing the scientific laboratories) and up to 70 expeditioners over the four month summer.

The scientific programmes conducted at Dumont d'Urville include: Earth sciences; atmospheric studies (katabatic winds, ozone, atmospheric chemistry, air–snow interactions); and biology. Most of these programmes are conducted in collaboration with foreign research organizations and are part of formal international programmes.
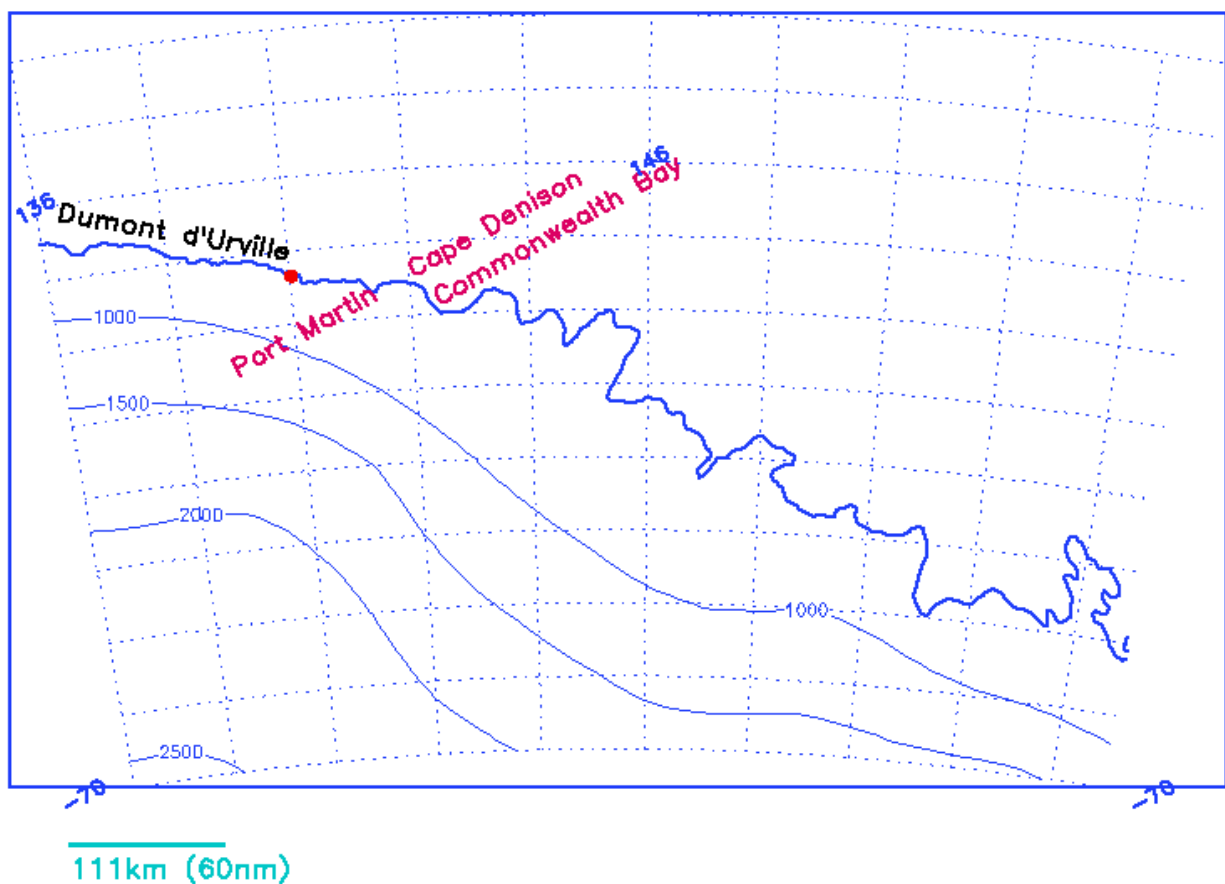
Figure 7.11.1   Sketch map for Terre Adélie and George V Lands (contours in metres; the area is bounded by: 70º S, 65º S, 136º E and 154º E).

7.11.1.3   <u>Data sources and services provided</u>

No specific information on forecasting has been obtained.

7.11.1.4   <u>Important weather phenomena and forecasting techniques used at the location</u>

General overview

Due to local effects, the climate of Dumont d'Urville is relatively temperate and that's why the members of the French polar expeditions call the base the "Antarctic Riviera". That is also probably why many bird colonies have taken up residence in the archipelago. Parish and Wendler (1991) have shown, using a three–dimensional model, that the extreme katabatic wind regime as observed at Cape Denison and Port Martin is due to the confluence of cold air flow from the interior when approaching these zones of the Adélie Land coast. As Dumont d'Urville is not downwind of a confluence zone but rather a divergence one, an intense katabatic wind regime would not be expected there.

The meteorological station at Dumont d'Urville has been operating since 1956 and a long climatological data series is available to establish a reliable climatology of the region of Dumont d'Urville. Table 7.11.1.4.1 in Appendix 2 below shows the mean and standard deviation by month of pressure, temperature, wind speed and day temperature range for Dumont d'Urville, while Table 7.11.1.4.2, also in Appendix 2 below, shows the maximum and minimum values of air pressure, air temperature and wind–speed at the station. Table 7.11.1.4.3 in Appendix 2 below shows the mean and standard deviation of pressure, temperature, wind speed and diurnal temperature range.

Surface wind and the pressure field

The surface wind is the major climatic Adélie coast phenomenon. The meteorological station of Dumont d'Urville holds the record for the windiest month and the record for the highest surface wind speed (90 m s^{-1} (~175 kt).

The wind speed is strong all the year, varying from 8 to 12 m s^{-1} (~16–23 kt), but one observes an annual cycle with two maxima during the transition seasons and two minima, one in summer and one in winter. This cycle results from the reinforcement of the depressions which force the katabatic wind during the inter–seasons. As for the temperature or the pressure, in relation to the semi–annual oscillation, the variability of the wind is stronger during the winter and the transition months. The rapid reduction in the average and the variability of the wind at the beginning of October indicates the beginning of the summer. There are several interesting aspects of the wind at Dumont d'Urville:

- *Occurrence of strong katabatic winds*: Since the local climate depends largely on the katabatic winds, it is interesting to study the katabatic duration and the frequency of the events. For this study episodes were counted during which the wind speed remained higher than 20 m s^{-1} (~40 kt). The results confirm the annual cycle of the katabatic winds with two maximum relative during the transition seasons, a minimum from October to January and a reduction relating to the middle of the winter in July.
- *The diurnal cycle of wind*: The formation of a layer of cold air on the surface due to outgoing longwave radiation is an essential element so that a katabatic wind occurs. It is interesting to study the dependence of the force of the wind compared to the diurnal cycle of the radiation by separating the cases in which the fraction of insolation was higher than 70%. The result suggests that the force of the wind depends on the diurnal cycle of the radiation during all the year but with a strong

reduction in the middle of the winter when the solar radiation is a minimum.

- *Wind direction*: The rose wind (not presented) of Dumont d'Urville shows the dominant direction of the katabatic winds which blow with a remarkable persistence in a limited sector from 120 to 140 degrees. One notes some cases, however, where the wind blows in an opposite direction of 300 degrees, i.e. from ocean towards the continent. These cases, which occur mainly in spring and in summer, correspond to situations of sea breezes (Pettré et al, 1993). Indeed, in spring and especially in summer, the ocean is free of ice but remains relatively cold while the continent can be heated by solar radiation creating the gradient of temperature at the origin of the breeze. One could also think that these winds directed towards the continent result from the passage of depressions in the area. Passing lows can also be responsible for initiating katabatic winds which are always directed towards the ocean.

As mentioned the Adélie coast is well known to be one of the areas of the Antarctic where katabatic winds blow most extremely, most frequently, and with the most persistence and so the forecasting of strong katabatic events is important. Because of their force and their very rapid onset, katabatic winds constitute a permanent danger for all the human activities which are performed far from the base, in particular the flying or marine activities. For several years, great efforts have been expended to understand the physical mechanisms at the origin of these winds and to improve their forecasting.

The forcing of the katabatic winds on a local scale, analyzed for the area of Dumont d' Urville and modelled at the mesoscale for area of Terra Nova Bay, is now well known. On the other hand, although the effect of the synoptic field is undeniable, it remains difficult to quantify. Bromwich (1989) obtained contradictory results in the area of Terra Nova Bay. Parish *et al.*(1993) showed that the external atmospheric conditions modulate the intensity of the katabatic winds in the area of Dumont d' Urville and that the strong katabatic winds were associated with a flow at the top of the katabatic layer implying a south–north pressure gradient. In a study of two cases, Phillpot (1991) showed that the wind at the surface, in particular in Dumont d' Urville and Dôme C, was consistent with the contour pattern at 500 hPa.

Observations showed that the principal triggering factor for katabatic storms is the passage of a depression in the area. The depressions generally move from the west around the Antarctic creating in the coastal area a pressure gradient which induces the katabatic wind. The greatest frequency of cases of strong wind during the inter–seasons can be explained by the greatest number of stronger depressions for these periods. However, it will be noted that, because of the katabatic effect, the direction of the wind is relatively independent of the position of the depression.

The katabatic storms can persist several days. Taking into account the volume of air transported northwards towards the periphery of the Antarctic this supposes the formation of an important cold air reservoir and/or a meridional circulation ensuring a supply of air from above the ice surface.

A recent study had the goal of attempting to forecast the Adélie coast katabatic winds by using the data available in real at Dumont d'Urville, that is to say the data from the AWS of Dome C and D–10 and of the daily analysis at 00 UTC. The construction of an index was based on the combination of three factors relating to the forcing of the winds:

- the slope of the 500–hPa surface;
- the quantity of cold air available on the plateau to supply the katabatic flow;
- the force of the wind at Dome C like indicator of the penetration of oceanic disturbances inside the continent.

The results of trialling the forecast method over two years showed that the technique is able to predict the changes of situation, but not capture all cases of strong wind. The forecaster has thus to use other information, especially satellite imagery to precisely locate the lows, in conjunction with the index to improve his/her forecast.

A study on the external gradient of pressure evaluated according to the slope of the 500 hPa suggests that the cases of strong wind are associated with a parallel increase in the zonal pressure gradient and a reduction of the meridional gradient. One can thus suppose that the forecast would be improved if one had the data from an analysis or prognostic chart to evaluate the slope of the 500–hPa surface in the zonal direction. The comparative study of the monthly averages of wind and temperature at Dumont d' Urville and Dome C from 1993 to 1995 showed that the wind at Dome C was a good indicator.

Upper wind, temperature and humidity

No specific information on forecasting has been obtained.

Clouds

No specific information on forecasting has been obtained.

Visibility: blowing snow and fog

No specific information on forecasting has been obtained.

Surface contrast including white–out

No specific information on forecasting has been obtained.

Horizontal definition

No specific information on forecasting has been obtained.

Precipitation

No specific information on forecasting has been obtained.

Temperature and chill factor

The average temperature (Table 7.11.1.4.1 in Appendix 2 below) over the year shows three quite distinct phases, that is to say a cooling from –0.5°C to –15°C in autumn from February to May, a weak cooling from –15°C to –17°C during the long winter from June to September,

then a very fast warming from –15°C to –5°C in spring over October and November. During the short summer in December and January the average temperatures do not exceed 0°C. One can make the following observations:

- *the spring warming is faster than the autumnal cooling*. This can be explained by the formation of the sea ice which takes longer than the melt. Indeed for sea water to freeze it must decrease to a temperature of –1.9°C (depending on the salinity), but the water cooled on the surface has its density increase and sinks and is replaced on the surface by warmer water which lengthens the time necessary for the formation of the sea ice.
- *the end of the winter is colder than the beginning*. The continent cools earlier than mid–latitude areas and consequently the sea ice reaches its maximum extent at the end of the winter when the mid–latitudes are coldest. At the same time, the circumpolar trough whose depressions bring the warm air towards the Antarctic, moves away from the coasts, from where cooling takes place.
- *one observes light warming in the middle of the winter*. This phenomenon, called "coreless winter" (van Loon, 1967). At Dumont d'Urville this phenomenon generally occurs in a clear way.
- *the variability of the temperature is much stronger in winter*. In the Antarctic warm air can come only from mid–latitudes with the depressions of the circumpolar vortex. But the depressions force the katabatic winds which transport very cold air from the centre of the Antarctic towards its periphery. The winter variability of temperature thus represents the equinoctial reinforcement of the polar vortex and its katabatic feedback;
- *in summer, at the beginning of the autumn and the end of spring variability is lower*. At these periods the cyclonic activity is weak since the meridian variation in temperature in the middle troposphere is reduced. On the other hand the katabatic winds, even if they are less frequent, continue bring cold air, which explains the variability observed.
- *the annual average temperature shows a tendency for a statistically significant warming* of 0.025 °C over 37 years of record (1960–96) which is less than the result obtained by Jones (1990) who evaluated the tendency for warming of the Antarctic as 1°C over the century.

Icing

No specific information on forecasting has been obtained.

Turbulence

No specific information on forecasting has been obtained.

Hydraulic jumps

Apart from the severe downslope wind common to Adélie Land, the most spectacular phenomenon occurring during the katabatic periods is the "Loewe's phenomenon". This type of phenomenon has been described by Valtat (1960) for Dumont d'Urville.

As mentioned in Section 6.6.13 above the IAGO (Interaction–Atmosphère–Glace–Océan) experiment aimed at producing detailed documentation of the vertical structure of the katabatic layer, and of its evolution along the slope. Two French and one American team took simultaneous measurements of vertical profiles of atmospheric properties at three points (D57, D47 and D10) distributed over 200 km along the slope from the plateau, at about 2000 m height, toward the coast near the Dumont d'Urville Station.

During the IAGO–experiment several Loewe's phenomena were observed as the terminal phase of several katabatic events. On 3 December 1985, a surprisingly large surface–pressure change (almost 6 hPa) through a jump was measured, differing very strongly from the predicted value (about 2 hPa) derived from the hydraulic theory.

Sea ice

No specific information on forecasting has been obtained.

Wind waves and swell

No specific information on forecasting has been obtained.

7.11.2   Port Martin, Commonwealth and Cape Denison

George V Land was discovered and explored by the Australasian Antarctic expedition, under Sir Douglas Mawson, in 1911–14. More recently couples have been wintering over in the Commonwealth Bay area: the first being Don and Margie McIntyre in 1995. Although there is only a limited, albeit famous, record of the meteorology of the Commonwealth Bay area the section is included due to its historical significance and the renewed activity in the area.

7.11.2.1   Orography and the local environment

The name Commonwealth Bay may be used in a wide sense to denote the bay entered between Point Alden and Cape Grey (66º 52´ S, 143º 20´ E), ~55 km to the east, but the Australian Antarctic expedition used the name in a more restricted application to denote that part of the bay between Cape Hunter and Mackellar Islands. Cape Denison (67 00'S, 142 40'E, 2m) is the rocky outcrop where the Australasian Antarctic expedition established its main base (Figure 7.11.2.1.1).
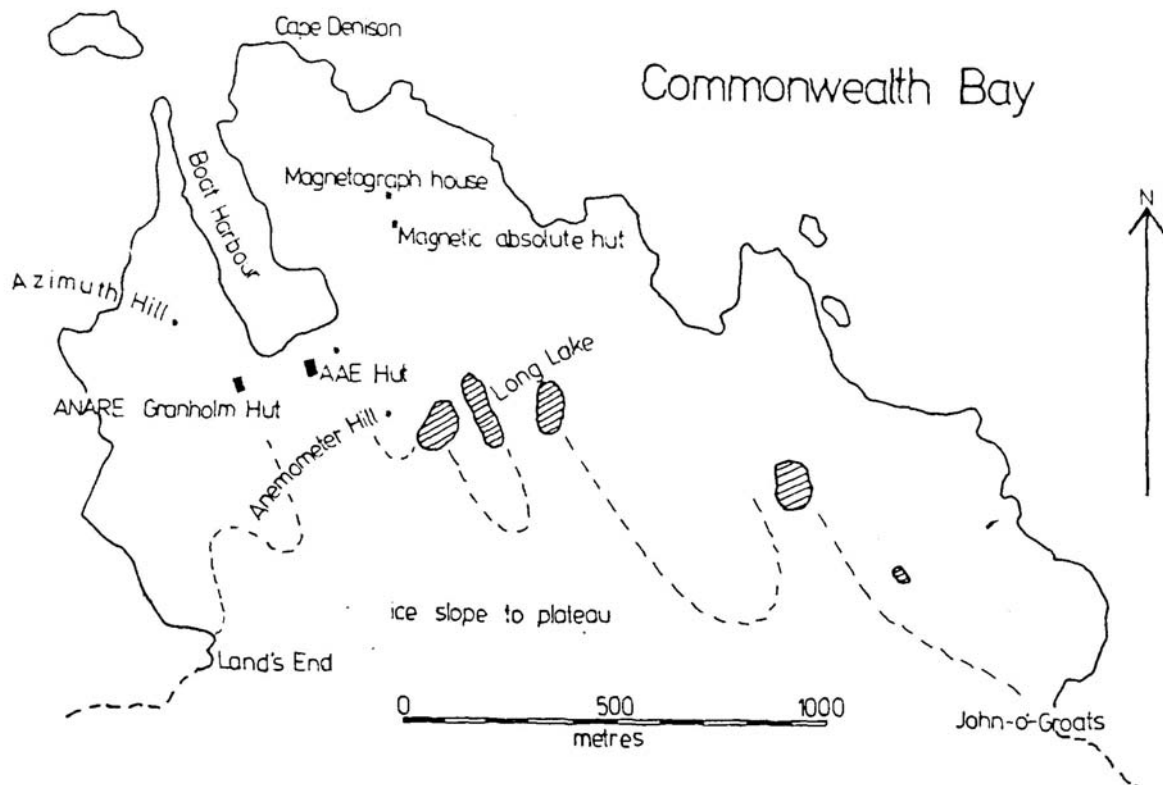
Figure 7.11.2.1.1   Sketch map the Cape Denison area. Mawson's Hut is shown as the AAE hut.

About 1 km within the cape the land, which is very broken, rises to an elevation of about 600 m about 22 km inland. At the western end an inlet 200 m long forms a useful boat harbour for shallow draft vessels. Being very windy and an ablation area the ice is sparsely covered by occasional drift patches. A small number of melt pools form on Cape Denison during the summer. The largest, Long Lake, is about 50 m long. About 2 km offshore at the head of this inlet lie the Mackellar Islands which are covered by 20 m thick caps of frozen spray.

Further east the Mertz and Ninnis Glaciers are major features of the coast and discharge an immense volume of ice into the sea from the inland plateau. The seaward extension of the Ninnis glacier is known as Ninnis Glacier Tongue. Near the inner end of the tongue there is a large rocky mass named Dixson Island, which is embedded in the ice and obstructs the outflow of the Ninnis glacier.

From the east edge of Ninnis Glacier Tongue the coast trends east about 63 km to Cape Wild (65° 15′ S, 149° 05′ E). The bight formed between this stretch of coast and the east side of Ninnis Glacier is named Buckley Bay.

7.11.2.2   Operational requirements and activities relevant to the forecasting process

The hut built at Commonwealth Bay in 1912 by Sir Douglas Mawson's Australasian Antarctic Expedition of 1911–14 was the main base of the expedition. Although recent interest in preserving Mawson's Hut has increased activity in the area the demand for forecasting services remains more in the area of potential rather than actual services. This is probably due to the being no aircraft involved in recent expeditions.

458

7.11.2.3   <u>Data sources and services provided</u>

The USA has several AWS located in the area (see Table 7.1.1 in Appendix 1 below)

7.11.2.4   <u>Important weather phenomena and forecasting techniques used at the location</u>

General overview

As mentioned above the first long duration stay in the region of Adélie Land and west of King George V Land was that by members of the Australian Antarctic Expedition 1911–14, directed by Douglas Mawson. During the winters 1912 and 1913 at Cape Denison, Mawson's expedition measured wind blowing from the Antarctic plateau with a strength and a regularity not observed in other parts of the globe. Thus, Mawson (1915) entitled the report of the expedition: "The home of the blizzard". He described the violence of the storms and their influence over the life and the work of the explorers.

About forty years later, the Expéditions Polaires Françaises maintained a meteorological station at Port Martin, located ~62 km west of Cape Denison from February 1950 to January 1952. The climate of the two stations proved quite similar. At Port Martin the mean wind speed for March 1951 was 29.1 m s^{-1} (~56.5 kt), while 48 days experienced mean wind speeds larger than 30 m s^{-1} (~60 kt) and 10 occurrences of winds of around 40 m s^{-1} (~80 kt) over four days in succession were observed during 1951.

After the destruction of the meteorological station of Port Martin by fire in 1952, the French explorers established a permanent station at Dumont d'Urville (see Section 7.11.1 above).

Surface wind and the pressure field

H. Phillpot (Australian Bureau of Meteorology, 1991) examined a short series of observations from Commonwealth Bay taken during the period 22 January to 25 February 1978. 72 % of the winds were from directions 160º to 185º and a marked diurnal speed variation was noted with a maximum evident between 0000 and 0300 local (UTC + 10 hrs) and a minimum between 1200 and 2000 local. These data indicate a katabatic wind influence.

The following is believed to come from a 1947 account by E Kidson regarding the 1911–14 expedition. "At Commonwealth Bay the south or south–southeast katabatic wind was blowing almost constantly, was nearly always strong, usually of gale–force, and frequently of hurricane force for considerable periods. The stronger the wind the greater, in general, was the turbulence and the mixing of the lower layers of the atmosphere. The smaller, consequently, was the surface inversion and the higher the surface air temperature. This effect on the surface temperature was so large relatively to the changes due to the advent of different air masses that it is practically impossible to isolate the latter at any time. With the approach of a depression the blizzard almost always increased while at varying intervals, usually a few hours, after what according to the analysis was the time of advent overhead of the cold air there would be a decrease. The increase in the wind during the approach of a depression the writer believes to be due to the arrival of warmer air over the ocean to the north and also above the katabatic wind, over the land. The contrast between the radiation

equilibrium temperature of the inland ice and the temperature of the free air is thereby increased. This would tend to cause an increase in the katabatic wind. The warm air, also, would be more stable so that the katabatic wind would probably be shallower. It is true that the warm air would have a component of motion from the north which would oppose the blizzard but apparently at Shackleton this effect was entirely masked by that described above. The sea was practically always free of ice at Commonwealth Bay so that the horizontal temperature gradient on the coast always tended to be steep."

Upper wind, temperature and humidity

No specific information on forecasting has been obtained.

Clouds

No specific information on forecasting has been obtained.

Visibility and fog

No specific information on forecasting has been obtained.

Surface contrast including white–out

No specific information on forecasting has been obtained.

Horizontal definition

No specific information on forecasting has been obtained.

Precipitation

No specific information on forecasting has been obtained.

Temperature and chill factor

No specific information on forecasting has been obtained, however, it may be inferred from Table 7.11.2.4.1 in Appendix 2 below that mid–summer temperatures at Cape Denison are close to zero while mid–winter temperatures are often around –20ºC.

Icing

No specific information on forecasting has been obtained.

Turbulence

No specific information on forecasting has been obtained, however it is likely that with the persistently strong surface winds low level mechanical turbulence would occur.

Hydraulic jumps

No specific information on forecasting has been obtained.

Sea ice

From observations made by the Australasian Antarctic Expedition, it would appear that the Buckley Bay ice does not break out of this bay until late summer. There is a continually thick and highly concentrated pack ice zone east of ~150º E understood to be associated with an ocean current system influenced by two large submarine banks above 500 m depth near 150º E and 153º E and which reach north of 67º S. The chain of islets extending north of Cape Denison staves off ice bergs and the pressure of pack ice coming down with the wind and current from the east.

Wind waves and swell

No specific information on forecasting has been obtained.

7.12   Oates Land, Victoria Land, the Transantarctic Mountains, the Ross Ice Shelf, and the South Pole area

This section covers Victoria Land, the Ross Ice Shelf, the Transantarctic Mountains, and the South Pole area: the total region covered by these areas spans approximately the longitudes 150º E to 150º W. From west to east, key features or stations referred to in this section include:

- *Leningradskaya* (69º 30′ S, 159º 23′ E, 304 m AMSL);
- *Terra* Nova Bay Station (74º 41′ 42″ S, 164º 7′ 23″ E, 17 m AMSL);
- *McMurdo Station* (77.86º S, 166.67º E , 24 m AMSL);

- *The Transantarctic Mountains*;
- *The Ross Ice Shelf*;
- *The Ross Sea*;
- *Amundsen–Scott (South Pole) Station* (90º S, 2800 m AMSL).

The above places are shown in Figure 7.12.1. (The New Zealand operated Scott Base (77.86 º S, 166.75 º E , elev. 14 m AMSL) is only a few kilometres distant from McMurdo Station. As Scott Base experiences similar conditions to McMurdo Station and the base operations rely on forecasting from McMurdo, Scott Base is not explicitly covered).

7.12.1   Leningradskaya Station

7.12.1.1   Orography and the local environment

Leningradskaya (69º 30′ S, 159º 23′ E, 304 m elevation AMSL) opened in February 1971 with operations ceasing in 1991. The station is situated on the coast of Oates Land. The station buildings are located in the ice–free area near the top of the Leningradsky nunatak.

Leningradsky nunatak is a rocky feature. Its ridge comprises alternating leucocratic granites and grey biotite gneiss extending from east to west for over 1 km with a width of 100–150 m. Snow covers two thirds of the nunatak area. The station is located on the western part of the nunatak at a distance of 600 m from its top (330 m AMSL). The nunatak height is 100–230 m above the surrounding glaciers. The ice edge in this area has a height of 15–20 m.

The station has not been extensively studied with respect to synoptic influences. However, the local weather is characterized by a close proximity to the area of cyclone activity that is usually located over the Ross Sea, as well as by unique local conditions influencing the weather processes. The station's weather is characterised by its persistent and frequent storms that occur due to its considerable elevation above sea level.

7.12.1.2   Operational requirements and activities relevant to the forecasting process.

The station structures consist of several houses with living space, a radio–station, a power station, a meteorological station, an upper–air sounding complex, a garage and a warehouse.. The station territory is restricted being only 200–250 m in length and not more than 50 m in width. The station was re–supplied by vessels that stop far from the station in drifting ice or near land–fast ice. The personnel and cargo were delivered to the station by helicopters.

7.12.1.3   Data sources and services provided
The station is not operational at present.
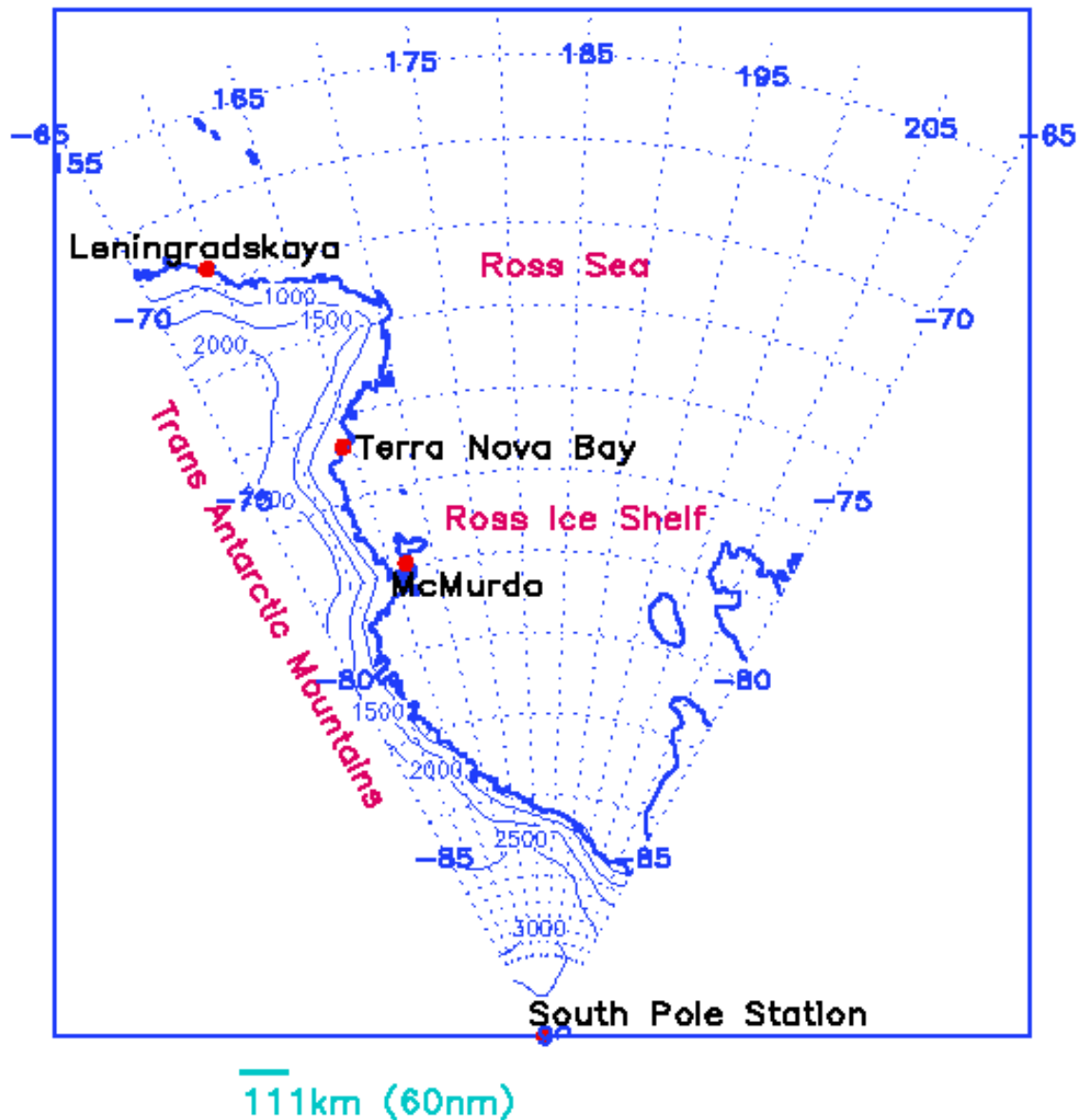
Figure 7.12.1   Sketch map for Oates Land, Victoria Land, the Transantarctic Mountains, the Ross Ice Shelf, and the South Pole area (contours in metres; the area is bounded by: 90º S, 65º S, 155º E and 155º W).

7.12.1.4   Important weather phenomena and forecasting techniques used at the location

General overview

It is known that at high latitudes of the Southern Hemisphere, cyclonic pressure features prevail. However, large high–pressure ridges are quite frequent, developing from north to south and sometimes combine with the Antarctic high creating a blocking effect and causing the displacement of cyclones in the meridional direction. One of the areas where the southerly displacement of cyclones is most frequently observed is the Australian–New Zealand sector. In the area between 140 to 170º E, there is a change in the direction of displacement of cyclones that persist then in the Ross Sea. Note that the cyclones of the Australian–New Zealand sector have large energy supplies as the warm air outflow from the north and cold air

sinking from Antarctica contribute to their regeneration. As to the Oates Coast and the George V Coast, the cyclones mainly pass over the oceanic regions in the zonal direction. However, from May to August up to two to four cyclones a month move along meridional trajectories from temperate and sub–tropical latitudes in the southeastern Indian Ocean.

Surface wind and air pressure field

The main feature of the pressure fields of the Australian–New Zealand sector of the Antarctic is the presence in all seasons of climatic cyclonic centres over the Ross and Mawson Seas. The average monthly pressure fields suggest the existence of either an increased pressure ridge or an isthmus between two cyclones in the Oates Coast area during much of the year. In winter and spring, the climatic centre from the east is located close to the Leningradskaya area whereas in summer and autumn, the direct influence of cyclones from the Mawson and d'Urville Seas increases.

Leningradskaya Station is located in the Antarctic maritime zone with rapidly changing of weather conditions. The main wind types in the coastal regions – cyclonic, katabatic and transient, are quite pronounced here, but they have their peculiarities, primarily in respect of the prevailing directions. Southeasterly winds in all months of the year are most common. Their frequency of occurrence is around 50% decreasing only in May and June to 40–43%. The southerly winds are the second most common, occurring on 13 to 18 % of occasions, increasing to 20–22% in autumn from March to April. Westerlies are the third most frequent wind direction (8–12% in all months of the year) and together with northwesterly winds are close to the frequency of occurrence to the southerly winds. The pronounced easterly winds at the coastal stations of East Antarctica (for example, 34% on average for a year at Mirny and 30% at Molodezhnaya) only occur 6% of the time at Leningradskaya. The wind rose for Leningradskaya reflects the features more typical of stations at much lower latitudes, for example, Bellingshausen.

The increased frequency of occurrence of westerly winds at Leningradskaya is related to three factors:

- Firstly, cyclones developing over the Ross Sea in certain instances, especially in summer, attain an easterly component, cross the Scott Coast and in rare cases reach Victoria Land, an extensive plateau at 1500–2200 m height.
- Secondly, some cyclones move from the east Indian Ocean–Western Australian area to the George V Coast, at a sufficiently large angle to the coastline to also sometimes appear above Victoria Land. In both cases, the Leningradskaya Station area becomes for some time at the northern periphery of the cyclone, i.e. in the zone of westerly winds.
- Finally, westerly winds can be observed in the event of a high–pressure ridge moving to the Oates Coast from the north.

Strong winds, storms and snowstorms come to the station from the southeast. Average speeds in the colder time of the year are 8–9 m s^{-1} (~17 kt). In summer, this decreases insignificantly, only by tenths. The number of days of strong winds (wind speeds of 15 m s^{-1} (~ 30 kt) or more) in autumn and winter months is 18–20 and in summer up to 14–16 days a month. Strong wind events are especially frequent and long from June to September. The maximum ten minute average wind speed for the 1971–79 period was 48 m s^{-1} (~93 kt) with a maximum gust of 60 m s^{-1} (~117 kt). The largest wind gust was recorded on July 9, 1989 when under conditions of persistent (several hours) storm force winds, the instrument recorded twice the

maximum gust of 78.3 m s^{-1} (~152 kt). Between these readings, there was an instrument failure and there is no certainty that the wind gusts were not greater.

At Leningradskaya there is no strict difference between the katabatic and cyclonic wind. It is difficult to determine the end of one type of wind and the beginning of the other. This comment does not obviously refer to the case where the cyclonic wind is expressed in the form of westerly flows.

Mesoscale vortices deserve a special comment with respect to the Leningradskaya area. In most cases, cloud meso–vortices in East Antarctica occur to the rear (in the southwest) of extensive polar front depressions when a cold polar front is displaced far to the north and the cold Antarctic air moves with the southern flows onto a comparatively warm water surface. In some cases, the conditions that are sufficient for the development of a mesoscale cyclogenesis are created above the ocean areas. The clockwise turning of the wind with height to the rear of depressions contribute to increased cyclonic circulation in the lower atmosphere which probably also influences the formation of meso–vortices. The frequency of occurrence of meso–vortices is probably lower near the Oates Coast, than in the Ross or Mawson Seas, but obviously they are generated with the development of the most active cyclonic features that move here along the meridional trajectories from the northern oceanic areas.

During the warm period of the year, the sub–synoptic cloud vortices can in some cases develop near the coast and influence the weather in the vicinity of Leningradskaya Station. Typically, this is manifested in a wind increase to 10–15 m s^{-1} (~20–30 kt), low stratus forming and solid precipitation with deterioration of visibility. With satellite observations received on a daily basis, a forecaster does not always notice such perturbations. As a rule, these phenomena are not long lived, but due to their sudden occurrence they can adversely influence aircraft operations. The dimensions of these meso–vortices formed typically of stratiform clouds comprise 200–300 km with duration of not greater than two days.

During the colder period, the area of mesoscale cyclogenesis is displaced northward and cloud meso–vortices more frequently form near the northern boundary of drifting ice. At this time of the year, they appear more active as viewed on satellite imagery, being in some cases similar to polar lows typical of Arctic ocean areas. These vortices do not usually reach the coast, quickly decaying when moving above sea ice.

Upper wind, temperature and humidity

No specific information on forecasting has been obtained.

Clouds

A high frequency of occurrence of overcast sky (7–8 oktas) is observed at all stations of East Antarctica, comprising 63% on average for a year for Leningradskaya. In the summer months, more than 70% of all observations report a complete sky coverage while in the winter months this percentage decreases to 55–50%. However, the low cloud frequency is much less being not greater than 20%.

Clear sky frequency in winter and in early spring (including October) is 30% decreasing in the summer months and reaching only 15% in January and February.

Middle and high clouds of undulated forms typically predominate in summer. In winter, the fraction of stratus cloud forms increases. With deep cyclones reaching the coast along meridional trajectories, the passage of fronts is accompanied by continuous multi–layer clouds, which often sink to the level of Leningradskaya and is recorded as fog in some cases.

The number of stratus–rain and high stratus clouds in the observation results is probably slightly underestimated since it is impossible to accurately assess the cloud form and height during precipitation and in snowstorms.

Visibility: blowing snow and fog

There are good conditions for observations of visibility at Leningradskaya as there is a sufficient number of orientation marks both at the station, near the station (for example, a island within 2 km) and at some distance (for example the mountain tops in the southwestern direction are located between 8 and 19 km). The farthest object that is seen at very good visibility (Governor Mountain) is located at a distance of 38 km. The frequency of occurrence of visibility of more than 10 km is 86–93% of all observation times in the spring and autumn months decreasing in winter and summer. The worst visibility over the period 1971 to 1979 was observed in December when the frequency of occurrence of good visibility was 75% and that of poor (less than about 2 km (~ 1nm) visibility was 22%. The main factor restricting visibility is snowstorms. The number of days per season, with snowstorms obviously increases in winter reaching 15 whereas in summer it is about 10.

Note a peculiarity of determining the meteorological visibility range at Leningradskaya relates to the high elevation (304 m) of the station. In the presence of clouds below the station and in the absence of other meteorological phenomena, visibility is reduced to 2–4 km whereas with blowing snow (slight and even moderate), visibility of up to 15–20 km is often preserved. The average number of days with snowstorms is more than 140 a year. In 1989, there were 149 days with snowstorms, 41 day of them with general snowstorms. An example of a quiet year was 1974 when the number of days with snowstorms was only 62.

Frost fogs are rare at the station (on average 1–2 cases for a winter month). They occur under low wind conditions when the amount of cloud is small and significant air temperature decreases occur. In summer, the number of fogs increases due to advective sea fogs as well as low stratus clouds covering the station area. Typically in December and January up to 10 cases a month are recorded. In January 1972 17 days with fog and in January 1974 14 days were recorded.

Surface contrast including white–out

No specific information on forecasting has been obtained.

Horizontal definition

No specific information on forecasting has been obtained.

Precipitation

Around 150 days with precipitation are recorded on average at the station during a year. This number includes all days with snowfall, tapioca snow and granular snow regardless of their amount. Total precipitation amount is about 600 mm per year. The 1989 year was the most snowy year when precipitation comprised 830 mm. The maximum precipitation is observed in

the summer and autumn months (specifically January to April) when 70–80 mm of precipitation falls on average for a month. The fact that precipitation in July 1989 comprised 154 mm against a 50 mm norm for the month indicates a large inter–annual variability. This is due to the anomalous high frequency of occurrence and intensity of the meridional flow in the Australian–New–Zealand sector in the indicated month. On the other hand, it is necessary to remember that with blowing snow and during snow storms, snow is both blown in and out of the snow gauge bucket.

Note that during storm wind events and in snowstorms generally, abundant deposition of granular rime is observed, which is probably connected with a cloud passing across the station. The number of days with rime is about 100 a year reaching in some months especially in summer and autumn 10–15 days and more.

Temperature and chill factor

The temperature regime of Leningradskaya is influenced significantly by local conditions, its elevation above sea level, as well as the synoptic processes which contribute cloud amount, particularly overcast or clear sky conditions. The main factor is a large frequency of occurrence of southerly and southeasterly winds from the cold mainland. The mean annual temperature is –14.6ºC. By way of comparison, this is much lower than the temperature at Molodezhnaya and Novolazarevska Stations, for example, but slightly higher than the mean temperature at Mirny. Compared to stations close by, the temperature at Leningradskaya is closer to Hallett Station than to Dumont d'Urville .

The mean monthly temperatures for the period of observation (~1971–91) are characterized by minimum value of –21.7ºC in August and maximum value of –3.9ºC in January. The extreme values have a large spread between –0.5ºC to –37.4ºC in August and 8.9ºC to –13.0ºC in January. A successful temperature forecast depends on correctly taking into account the aforementioned features and factors.

Low air temperature and wind speed are the main factors influencing the time people can work outside. A complex assessment of weather severity is typically expressed in points and is calculated by Bodman's formula (Equation 7.12.4.1.1).

$$S = (I + 0.272\ V)\ (I - 0.04\ T) \qquad\qquad \text{Equation 7.12.4.1.1}$$

where V and T are the wind speed (m s^{-1}) and air temperature (ºC), respectively.

The calculation of the severity coefficient (S) was performed using data at the meteorological observation times for Leningradskaya and for other Antarctic and Arctic stations over a number of years. The most significant S values are observed from May to September. The average severity values for the indicated period comprised 6.5 points for Leningradskaya, 7.4 for Mirny and 9.3 for the Vostok Station. Note that the S coefficient at the North Pole in winter (5.3 points) is almost the same as at the Vostok Station in summer (5.5 points).

Icing

No specific information on forecasting has been obtained.

Turbulence

No specific information on forecasting has been obtained.

Hydraulic jumps

No specific information on forecasting has been obtained.

Sea ice

The sea ice regime of the coastal area of the Somov Sea within a radius of about 60 km from the Leningradskaya is unique. One of its typical features is a very early onset of ice formation. In most years, it occurs as early as mid–February and in some years even during the second half of January. This is primarily attributed to the limited summer heating of the surface sea layer due to a constant preservation here of the Balleny ice massif.

Thus, during the entire 20–year operation of the station (1971–91) no complete ice clearance of the area in question was recorded. Moreover, on average up to 60% of its area was typically occupied by residual drifting ice off the southern periphery of the massif and often by land–fast ice that was preserved over 20% of the area east of the station near the barrier of the Gillett Ice Shelf.

However, in January–February, a mostly continuous polynya with a total area of up to 1500 km^2 exists directly along the glacial–land–fast ice coast between 158–160º E. The polynya has a wedge–like form with its width being 30 km on average in the west behind the outlet Tomilin glacier, around 10 km opposite the station and decreasing to zero near the land–fast ice edge in the vicinity of 160º E.

An unusually early (even for the Antarctic) intense ice formation develops in the polynya, occurring at first only at night hours due to radiation cooling. It can also be suggested that strong local freshening of the shelf zone contributes to this due to the discharge of a large volume of sub–glacial melt water along the channels of numerous outlet glaciers in this region.

In contrast, the formation of new land–fast ice begins quite late in mid–April, approximately two months after the onset of ice formation. The land–fast ice expansion is interrupted with frequent breaks at its marginal area. As a result, the land–fast ice often reaches its maximum dimensions only in late July, when the last area of the aforementioned summer recurring polynya west of the Tomilin glacier finally freezes. The width of the stabilized continuous land–fast ice band varies during August within 50–60 km. Continuous drifting ice with 100% concentrations is located behind the land–fast ice.

However, sometimes irreversible land–fast ice edge breakup begins as early as September and in late October–early November a complete decay of its westernmost segment behind the Tomilin glacier usually occurs. Here, a recurring near–glacier polynya with average dimensions of 20 by 15 km appears again at the place of broken and exported land–fast ice. Offshore katabatic winds keep its surface ice–free.

The breakup of the main land–fast ice belt east of the station combined with expansion of the polynya typically extends up to late March of the next year.

During the 1971–79 period, the breakup process never ended with the final land–fast ice breakup. A land–fast ice segment directly under the station and east of it with a length up to 70 km and a width of 10–20 km was preserved by a concentration of icebergs grounded in

coastal shallow water. Multiyear land–fast ice was predominantly comprised of ice more than 10 m thick whose age in 1971 was estimated as 10–12 years old.

In 1980–87, the land–fast ice was completely destroyed every year. From 1988, a tendency for formation of multiyear land–fast ice in this region was again observed.

Although there are little data, first–year ice seemed to form in the vicinity of Leningradskaya in April (see above), grew by early December on average up to 1.5 m, and had about 50 cm of snow on the surface.

The period of its melting is obviously restricted to only one month – approximately from mid–December to mid–January. The decrease of land–fast ice thickness for this time comprises not more than 10 cm.

The growth of unbroken land–fast ice is already observed in mid–January. Probably, it grows both from the top due to freezing of the lower wet snow layer at night hours and from the bottom due to frazil ice formation.

In the case of land–fast ice preservation, it reaches a thickness of not less than 2 m at the second year of its existence and is probably not subjected to melting at all.

Wind waves and swell

No specific information on forecasting has been obtained.

7.12.2   Terra Nova Bay Station

7.12.2.1   Orography and the local environment

Terra Nova Bay (TNB) Station is located at 74° 41' 42"S, 164° 7' 23"E, 17 m ASL on a promontory extending out into the Gerlache Inlet sector of Terra Nova Bay (Figure 7.12.2.1.1), on the western side of the Ross Sea. The Northern Foothills shield the base on the west against the katabatic flow sloping down along the Priestley and Reeves Glacier (Figure 7.12.2.1.2). A very extensive and persistent polynya is sustained by such a flow at the confluence of these two glacial valleys in the area known as Nansen Ice Sheet which is only a few miles south apart from the station. The Priestley Glacier flows from the Antarctic Plateau into a narrow canyon 8 km wide and 90 km long aligned along a northwest–southeast direction before joining with the steeper and wider Reeves Glacier which falls in and east–west direction from the same elevation to the sea level in a distance of only 45 km.

Shelter for the Gerlache Inlet is offered by the Campbell Ice Tongue to the east and by the huge Drygalski Ice tongue to the south (Figure 7.12.2.1.2). which prevents the sea swell driven by the easterlies and the southerlies reaching the station in January and February when the sea ice has drifted away from Terra Nova Bay itself.
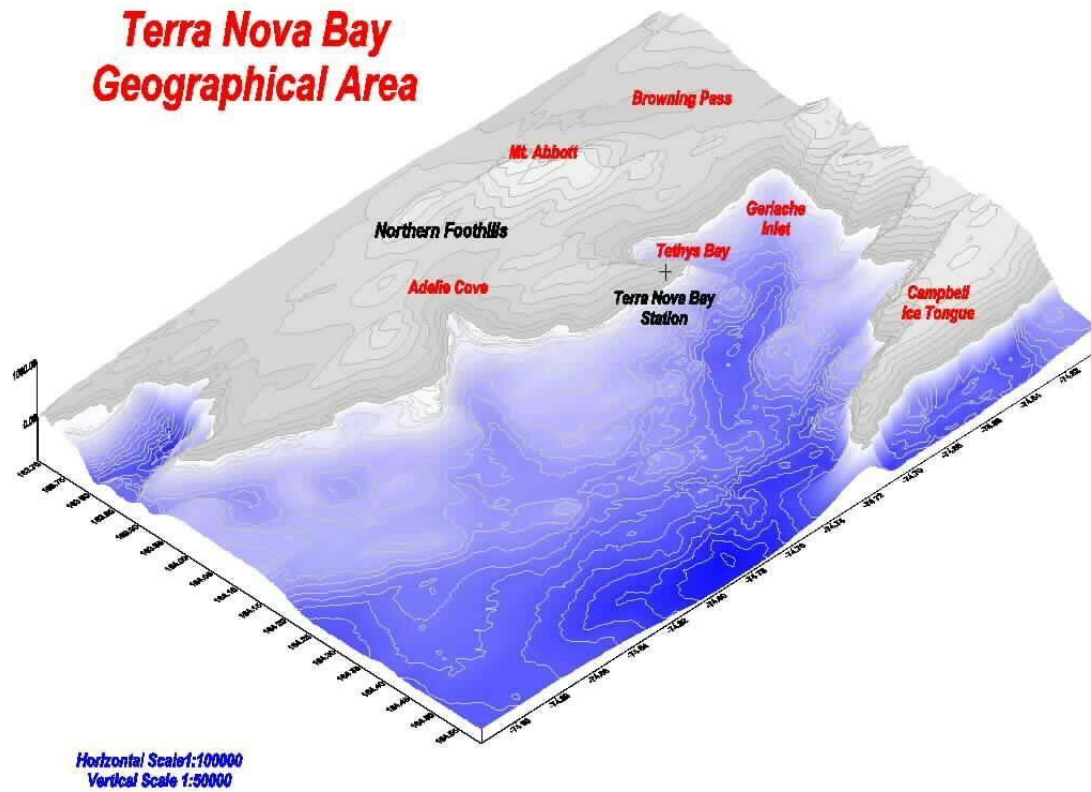
Figure 7.12.2.1.1   Sketch map of the Terra Nova Bay local area.
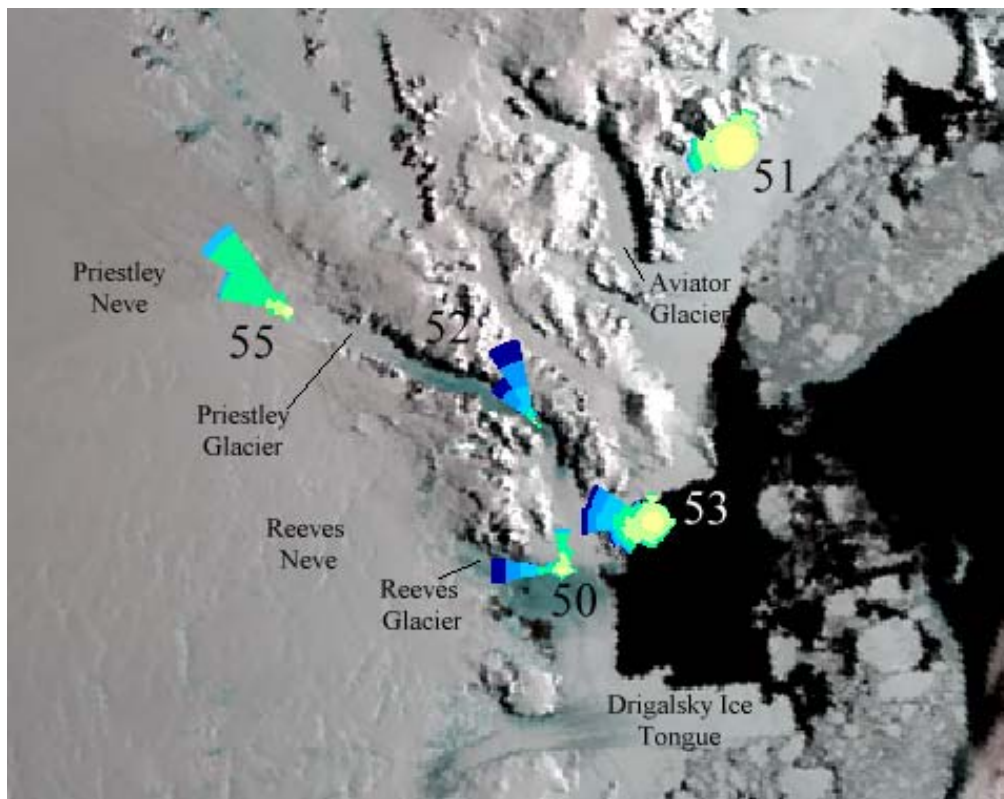
Figure 7.12.2.1.2   Satellite image showing glacial valleys around the location of TNB which is shown as the yellow dot at 53. The coloured icons are wind roses from the local AWS network. See Section 7.12.2.4.

7.12.2.2   Operational requirements and activities relevant to the forecasting process

TNB Station was established in 1985 by the Italian Antarctic Research Programme (PNRA) and is currently open from late October to mid–February only. However, during the summer season the base is very active and both fixed–wing and rotating–wing aircraft are used. From October to December a sea icerunway in the Tethys Bay, the inner part of the Gerlache Inlet, is operational for Italian wheeled C–130 aircraft operating the intercontinental flights to and from New Zealand and is an alternate airstrip for the US Air National Guard ski–equipped LC–130 and Royal New Zealand Air Force (RNZAF) C–130 aircraft heading to McMurdo. Due to the local orography such a runway offers a single direction of approach (Figures 7.12.2.2.1 and 7.12.2.2.2) and the great incidence of katabatic winds (for which this area is famous), makes the glide/take off path very sensitive to turbulence, vertical and horizontal wind shear. For these reasons the wind behaviour is continuously monitored by a set of two anemometers on the runway and other two complete automatic weather stations located at different heights on the surrounding hills. The data gathered are processed to provide real time turbulence and vertical and horizontal wind–shear factors.

     The same airstrip is used by Twin Otter aircraft involved in the continental flights to Dome C and Dumont d'Urville and when in January the air–strip breaks up due to temperature and to mechanical stress induced by wind and sea swell, these operations are diverted to a "white ice" ski–way in Browning Pass (Figure 7.12.2.1.1). a glacial valley adjacent to the Northern Foothills.

     In addition every season two to four single–engine Squirrel helicopters are used for the operations in the Transantarctic Mountains between Cape Adare and the McMurdo Sound and are also tasked for Search and Rescue during the take–off and landing of fixed–wing aircraft or in case of emergency along the coastal region of the Victoria Land.

     There is frequent HF and telephone communications with the Weather Office at McMurdo Station and within the framework of this cooperation the exchange of TAF, METAR and SPECI messages is included. A similar agreement has been reached with the Dumont D'Urville and Dome C weather stations for the provision of METAR and SPECI messages before and during the Twin Otter flights heading to Concordia Station and to Adelie Land of which TNB Weather Office is responsible for weather support.

     Moreover. the sea operations in which the Research Vessel *Italica* is involved are of significant importance from the scientific and logistic point of view. Every season such an "ice–class" ship carries on an oceanographic campaign all around the Ross Sea and provides the valuable service of resupplying fuel and goods to the station. Detailed weather assistance is required both when the ship plies the Ross Sea, providing real time weather and sea iceconcentration maps, and when it is moored on the ice for the load/unload operations and a meticulous monitoring of wind essential.
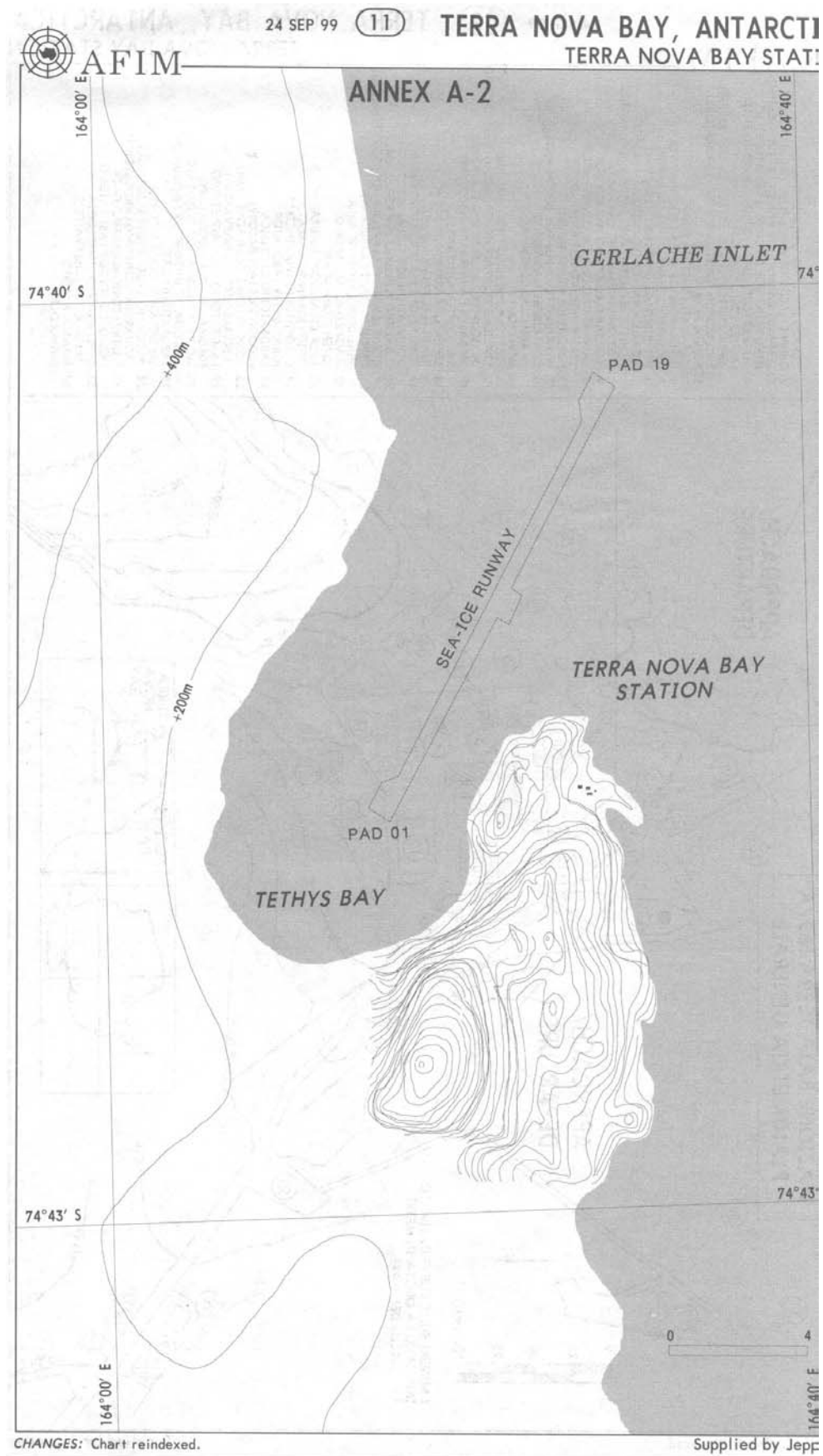
Figure 7.12.2.2.1   Map of Terra Nova Bay Station, Tethys Bay, showing in particular the location of the sea ice runway.
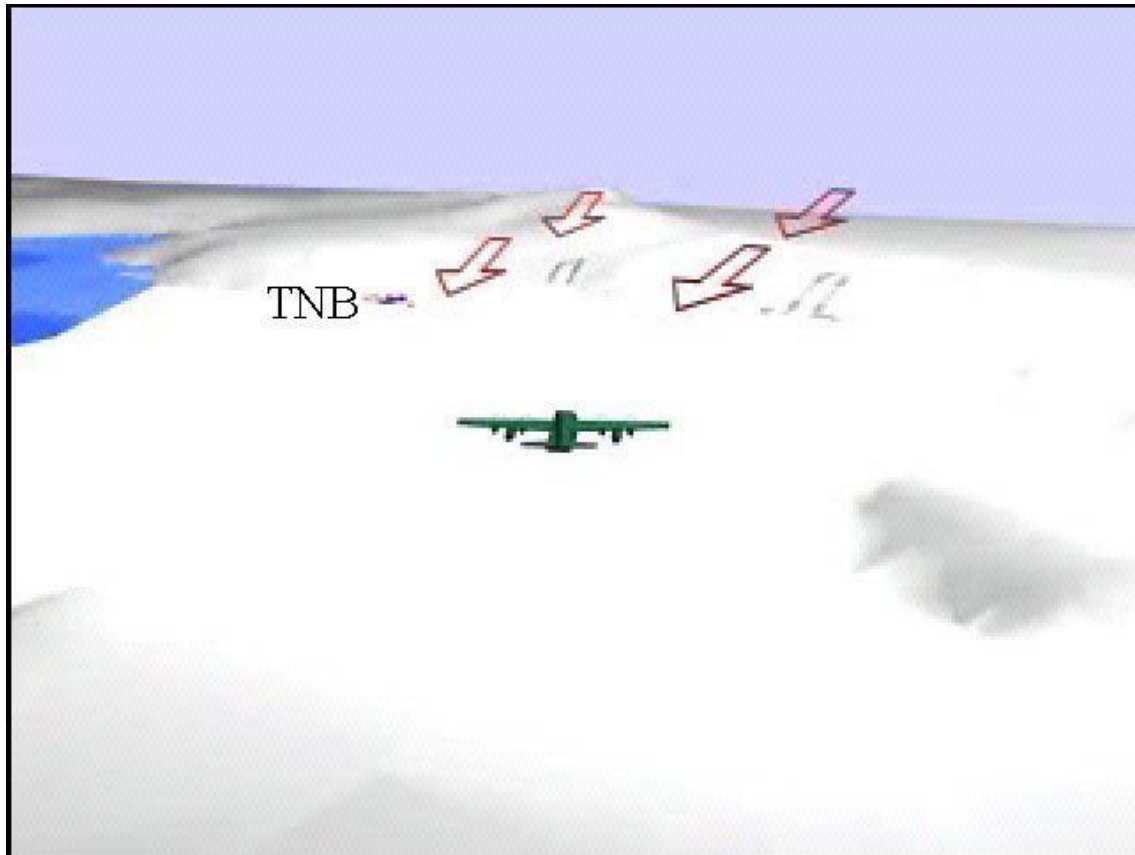
Figure 7.12.2.2.2   Schematic of a C–130 aircraft approaching the TNB sea ice runway. TNB Station is indicated by "TNB" while the runway is approximately abeam TNB at centre of the graphic. The red arrows indicate the direction of prevailing katabatics.

7.12.2.3   Data sources and services provided

Two forecasters work at the Terra Nova Bay Weather Office and their duty time is normally from 1700 UTC until 1200 UTC but it can be extended to cover the 24 hours when required. A full six hourly surface observing programme is in operation at the station and there are radiosondes launched every 12 hours at 0000 and 1200 UTC. When air operations are in progress, hourly and special aeronautical observations are carried out and coded in METAR and SPECI codes. Nine and twenty–four hours aeronautical forecasts (TAF) are issued as well. Surface and upper–air data are put in real time onto the GTS through the Italian Air Force Weather Service.

The network (Figure 7.12.2.3.1.) of AWSs deployed along the Victoria Land between Cape Phillips and Cape Ross and in the interior of the Antarctic Plateau consists of 13 installations (see Table 7.12.2.3.1 in Appendix 1 below) aimed on one hand to collect data to enrich the climatological archive and on the other hand to provide valuable observations for aeronautical use and in forecasting on the mesoscale. All the "climatological" AWSs deliver the information they gather through to the ARGOS system, while the AWSs installed in crucial sites for air operations can also transmit back to the base via HF radio–modem their measurements to reduce the time between observations down to the proper scale. At Dome C in the period of camp activity, from November to February, a very advanced AWS has been operational since 1997. Beyond the conventional sensors, it includes also a ceilometer and an RVR sensor and all the data are set up for the issue of METAR and SPECI messages on a

Personal Computer controlled by a weather observer. Any aircraft flying within the range of 75 km (~40 nm) from the station can receive on demand such observations by triple–clicking on the VHF radio and get the messages through a vocal sythesizer.
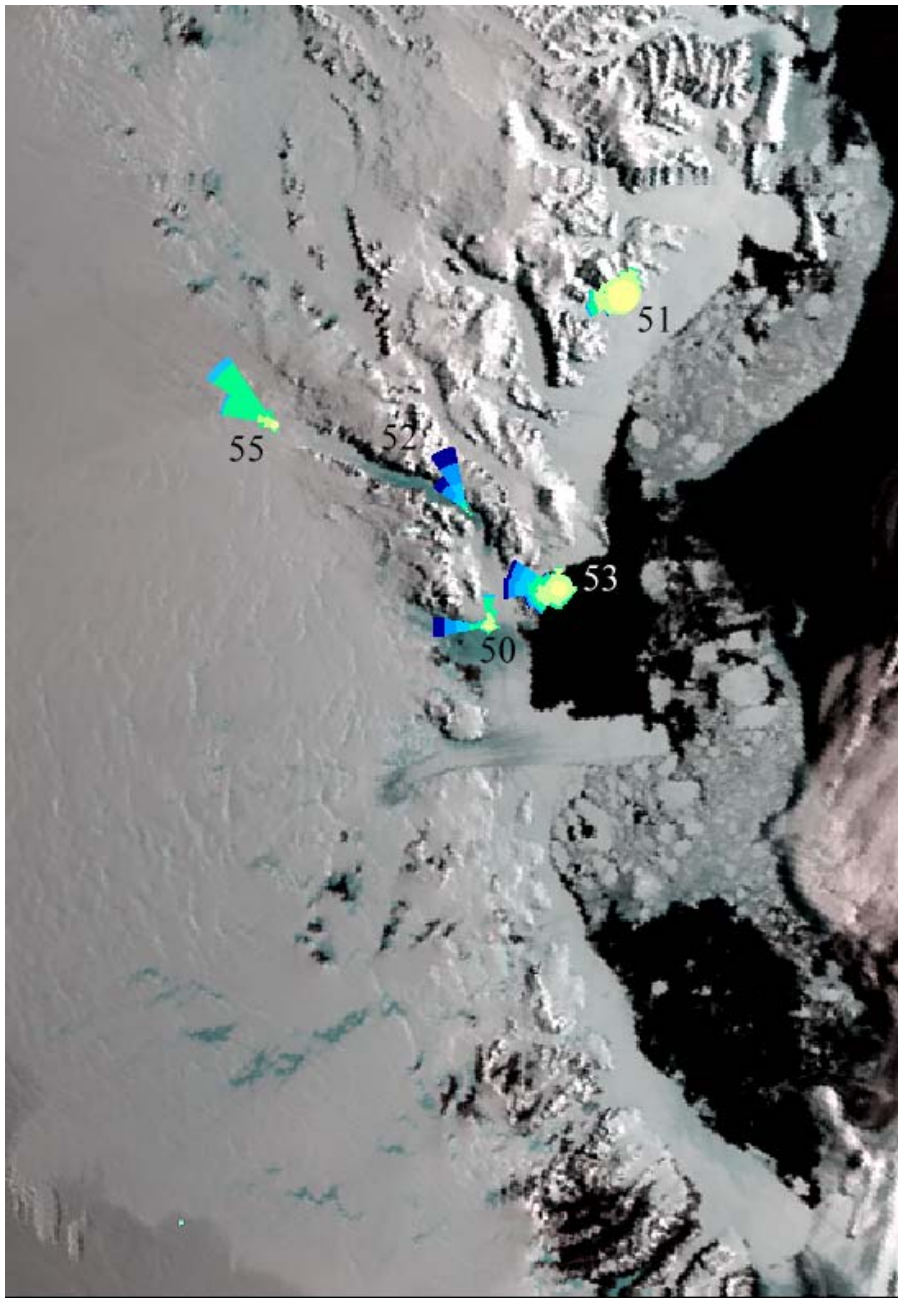
Figure 7.12.2.3.1   Satellite image showing coloured wind roses from part of the AWS network in Victoria Land. (This is an expanded view of Figure 7.12.2.1.2)

From 1985 to 1996 a NOAA satellite receiver has been in operation at the base providing high resolution imagery for the forecaster. In 1997 the old receiver was replaced in favour of a dual system able to receive both NOAA and DMSP satellite data. This new implementation has thus increased the imagery availability up to 35–40 passages per day not only for the augmented number of transmitting platforms, but also for a better noise/signal ratio of the receiver. The AVHRR and OLS sensors are extensively used and also the 85 GHz microwave

data from SSM/I are processed almost in real time to produce colour sea iceconcentration maps (Figure 7.12.2.3.2) according to the Svendsen, Matzler and Grenfell algorithm.

The fields produced by the ECMWF models[1] for atmosphere and sea swell are used for forecasting and are routinely received in GRIB code once a day via INMARSAT. The production of weather maps is then carried on "*in situ*" and the fields refer to two different frames; a wide coarse grained area (2.0° grid spacing) (see for example Figure 7.12.2.3.3 in which the Southern Ocean is included to emphasize the synoptic signals and a fine resolution area (0.5° grid spacing) (not shown) focussed on the Victoria Land and on the sites of operational interest in the Antarctic Plateau, Adelie Land and Ross Ice Shelf. The atmospheric cross section examined in the forecasting process ranges from the surface up to 100 hPa to monitor the evolution of warm air intrusions in the upper levels over the Antarctic Plateau. The same products are used to prepare the documentation for continental and intercontinental flights or sea–cruises and are available on demand for any aircraft or ship also in transit.
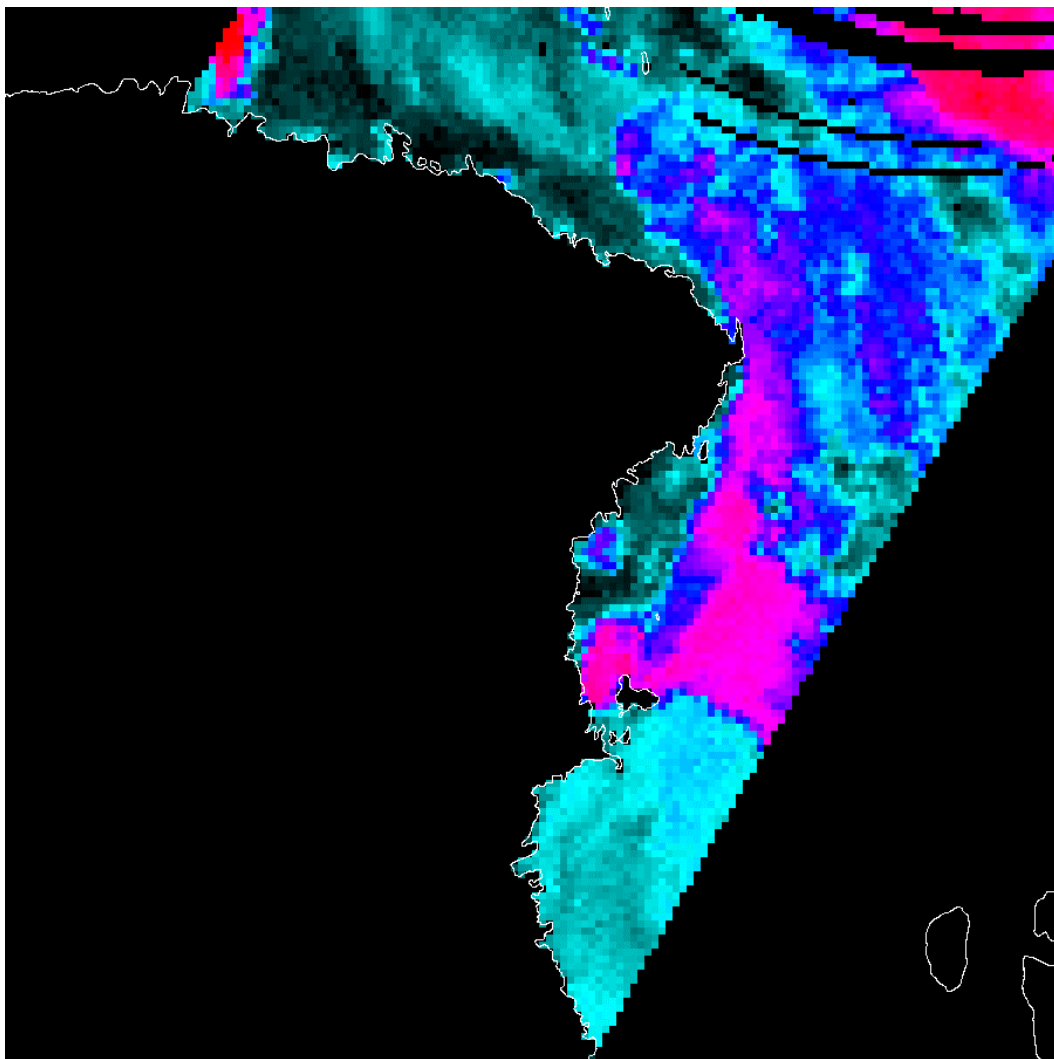
Figure 7.12.2.3.2   An example of a sea ice classification scheme output.

---

[1] ECMWF T319L60 is currently used for the atmosphere and the ECMWF WAM model for the sea swell.
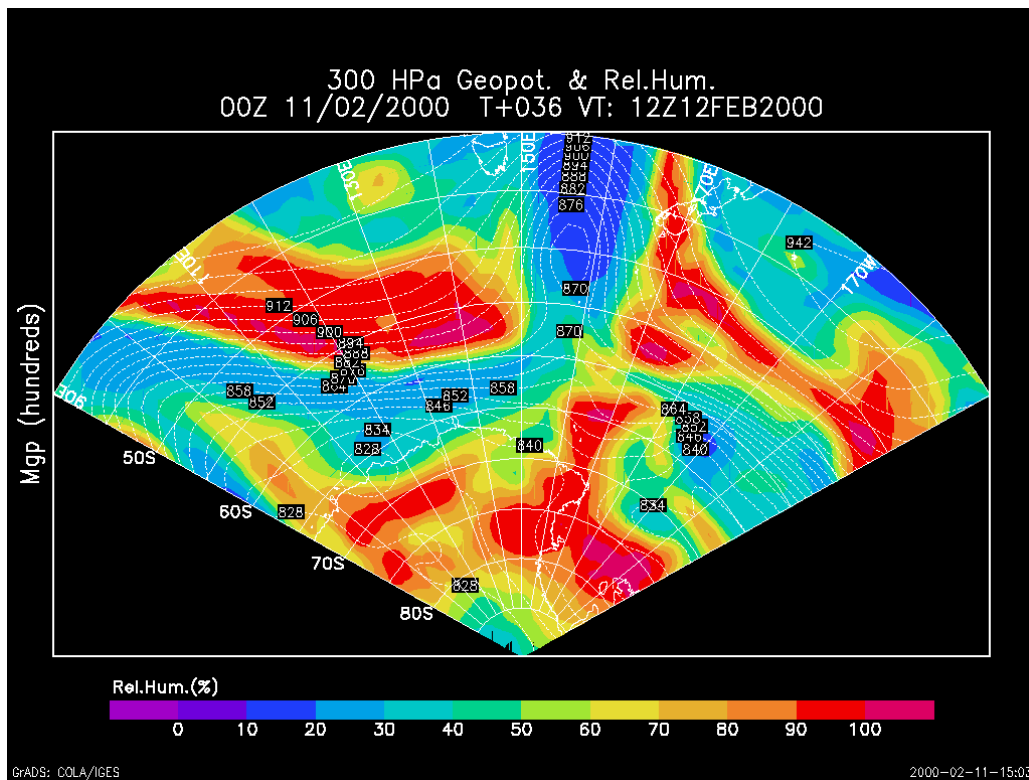
Figure 7.12.2.3.3   An example of the "coarse" (2.0 º) horizontal NWP output from the ECMWF model. The graphic shows 300–hPa geopotential heights and relative humidities for an area 40º S to the South Pole and from 90º E to 150º W.

7.12.2.4   <u>Important weather phenomena and forecasting techniques used at the location</u>

General overview

The monthly mean temperature for TNB (see Figure 7.12.2.4.1 in Appendix 2 below) shows the typical behaviour of the Antarctic coastal regions with a short summer from late November to January and a coreless winter and very short transition seasons (spring and autumn) interposed. In July a reversal cooling trend is evident for all the sites in which the AWSs are installed and the simultaneous relative humidity increase (see Figure 7.12.2.4.2 in Appendix 2 below) and pressure fall (see Figure 7.12.2.4.2 in Appendix 2 below) is coherent with the assumption that moister air masses are more frequent in July than in other winter months. An increase of cyclonic activity in this period is also confirmed by the occurrence of stronger katabatic winds (see Figure 7.12.2.4.4 in Appendix 2 below)
     The climate of TNB is heavily influenced by the circulation of the Ross Sea and the strong orographic influence of the Transantarctic Mountains to the west of the station. The Ross Sea is often occupied by decaying depressions that have moved south from the Southern Ocean, with there being climatological easterlies over the southern Ross Sea and a southerly barrier wind along the coast of Victoria land (see below). The ECMWF model shows a good skill for large–scale synoptic weather systems and large–scale fronts and even if it does not provide a fully detailed description for the smaller mesoscale weather systems (<50–60 km), in several cases some useful hints about where and when they form and develop are given to

some extent. The partial failure of the model on the mesoscale can be traced back to the following two elements:

- The complex orography of the several glacial valleys cutting the Transantarctic Mountains is not highly resolved and such a smoothing leads to a systematic underestimate of the katabatic outflow from the high Plateau. The same phenomenon in the gentler–sloping area nearby Dumont d'Urville is in fact fairly better represented by the model.
- The sea ice cover dynamics included in the model is incomplete in that no freezing of the water or melting of the ice is allowed and the sea ice distribution is kept constant during the forecast neglecting the energy involved in these processes which is crucial especially during the austral summer.

Satellite imagery has shown that TNB has many cyclogenesis events on the mesoscale at the boundary of the cold, dry airmasses from the interior and the maritime air over the Ross Sea. There is a substantial body of literature on TNB mesoscale cyclogenesis e.g. see Carrasco and Bromwich (1996).

Surface wind and the pressure field

The surface wind field is one of the most important factors to forecast correctly at TNB as winds can be very strong and highly variable over short distances. An examination of TNB AWS measured synoptic wind observations for between 1988 and 1997 inclusive has shown that there were 97 occasions during the colder (March to October) part of the year when the maximum wind gust on the synoptic hour was 52 m s^{-1} (~ 01 kt) or more. On 31 occasions the mean wind was 41 m s^{-1} (~80 kt) or more. The highest gust recorded was 64.9 m s^{-1} (~126 kt) and the highest average speed was 51.5 m s^{-1} (~100 kt). The gust ratio (10 minute mean to gust) was varied considerably, for example from 1.18 at 2000 on 6 June 1997 when the average 10 min wind was 51.5 m s^{-1} (~100 kt) and the gust 60.8 m s^{-1} (~118 kt); to 1.88 at 2100 on 23 August 1989 when the mean wind was 34.5 m s^{-1} (~67 kt) and the gust 64.9 m s^{-1} (~126 kt) to 2.32 at 1800 26 June 1991 when the mean wind was a mere 22.7 m s^{-1} (~ 44 kt) but the gust 52.5 m s^{-1} (~102 kt). In all of the 97 observations the wind direction was between 240 and 300 degrees true, with most observations being almost due westerly
Two important types of wind flow which occur in the TNB area are:

(i) Katabatic winds:

The terrain slopes sharply at a number of sites in this area increasing towards the coast, and several glacier valleys channel the flow: the combined effect of channelling and increased slope greatly increases the wind speed. There is therefore a strong wind shear, both horizontal (due to the presence of glacier valleys) and vertical (due to the fact that the layer affected by the wind follows the orography and does not extend to higher levels), which is a severe limitation to aircraft operations. The Tethys Bay airstrip can be affected by both the Reeves and Priestley katabatic flow even if the Northern Foothills offer in general a better shelter for the latter. In the ECMWF model the direction of the two flows is well represented in direction but the wind speed is normally underestimated. Since a downslope wind along the two glacial valleys is quite common and being unable to predict the speed, the ECMWF model in most

cases provides a more valuable information in the reversal case when an upslope wind is predicted which is a severe warning for an incoming weather system. In any case the extent of the area involved in the katabatics, which is also directly related to the strength of the phenomenon, is well outlined through the airmass vertical velocity (ω) near the intersection between the 700–hPa surface and the terrain which is located just above the Antarctic Plateau escarpment and that exhibits down–welling values for katabatic flows.

The wind along the Priestley Glacier is monitored by two AWSs, 7955 (see Figure 7.12.2.4.5 in Appendix 2 below) and 7952 (see Figure 7.12.2.4.6 in Appendix 2 below), installed respectively on the top and at the middle–length of the glacier. A speed measurement higher than 18 m s^{-1} (~35 kt) on the latter provides a sufficient alert condition for the wind to reach the station and the Tethys Bay airstrip. In fact if the cold flow has enough kinetic energy to climb over Black Ridge and the Northern Foothills, that is to say that the Froude number for these barriers is greater than 1, it will also have an impact on the air operations in the Gerlache Inlet where the coupling with the local orography generates characteristic turbulence, wind–shear patterns and cross–wind along the glide path. The occurrence of strong katabatic events along the Priestley Glacier is also remarked by high wind speed recorded by the AWS 7956 (see Figure 7.12.2.4.7 in Appendix 2 below) which dominates the AWS 7952 from the height of 1700 m on the steep northern side of the valley.

At TNB Station (AWS 7953) (see Figure 7.12.2.4.4 in Appendix 2 below) the Priestley steady flow condition is in general preceded by short peaks of strong wind followed by long lulls and its distinctive signature is the flow direction ranging between 290° and 340° with the higher average wind–speed occurring for greater western components.

The highest wind–speeds ever recorded at TNB are in the range 45 to 50 m s^{-1} (90–100 kt) and are related to the Reeves katabatics since the Northern Foothills gentle relieves offer on this side an easier access into the bay. Due to its orographical deployment, the Reeves Valley channels the katabatic flow along the east–west direction and this is well represented on the wind–rose of the AWS 7350 (see Figure 7.12.2.4.8 in Appendix 2 below) installed down–wind of the glacier on the Nansen Ice Sheet. Since the weather station has been positioned a few km away from the glacier, the measured wind–speed represents an under–estimate of the effective value that the sensor would feel just along the axis of the glacier. On the other hand the AWS in that position is able to monitor also the northerly barrier wind (see below) generated by the Priestley katabatic flow against the Northern Foothills and Black Ridge.

Other indirect evidence provides the forecaster with a good guidance for katabatic wind prediction on the nowcasting time scale:

- The clear skies that normally accompany strong katabatic flows favour the detection of blowing snow in the imagery from the AVHRR band–3 sensor from the infra–red channel of the OLS.
- Similarly the wind–induced ruffling of the surface of the open water in the polynya determines an abrupt change in reflectivity and emissivity compared to the surrounding calm water. Such a difference is easily detected respectively in the VIS channels of AVHRR and OLS and in the micro–wave channels of the SSM/I.
- If the ground level flow is coupled with northwesterly large–scale winds, typical orographic (lenticular) clouds can be observed downwind of orographic obstacles: these clouds can be stationary on the same site for several days. Wind peaks are always preceded by blowing snow above the surrounding mountains.

(ii) Barrier winds:

During summer, a cyclonic circulation is semi–permanent over the Ross Sea and when the easterly flow along the southern Ross Sea approaches the Transantarctic Mountains it follows the orographic barrier as a southerly. There is a clear evidence of this behaviour in the wind–rose of the AWS 7357 (see Figure 7.12.2.4.9 in Appendix 2 below) installed at Cape Ross which exhibits a characteristic predominance of southerlies which are normally considered as a first warning of low–pressuresystems developing in the south–eastern part of the Ross Sea. Since there is a break in the Transantarctic Mountains in the central part of the Victoria Land corresponding to the Drigalsky Ice Tongue and Nansen Ice Sheet, the barrier winds mix their southerly character with a not negligible easterly component which can let them penetrate well inland and also ascend the glaciers. In fact a 8 m s^{-1} (~15 kt) upslope wind at the Medium Priestley AWS 7352 (see Figure 7.12.2.4.6 in Appendix 2 below) is not unusual and is normally associated with low clouds and quite often with precipitation. A similar behaviour is less evident in the Nansen Ice Sheet AWS 7350 (see Figure 7.12.2.4.8 in Appendix 2 below) data because of its slantwise position with respect to the axis of the glacier.

  In the region between Mt. Melbourne and Cape Adare, the Transantarctic Mountains bend towards the 170° E meridian and induce southwesterly barrier winds that can be easily identified in the wind–roses of the AWSs installed at Cape King (7351) (see Figure 7.12.2.4.10 in Appendix 2 below) and Cape Philips (7379) (see Figure 7.12.2.4.11 in Appendix 2 below) where the channelling effect determined by the parallel deployment of Coulman Island orography, makes them stronger than anywhere else along the coasts of the Victoria Land.

  The barrier winds are generally well forecast by the ECMWF model while the wind reversal in the glaciers is predicted only when the larger and well developed weather systems affect the Eastern part of the Ross Sea.

Upper wind, temperature and humidity.

Upper conditions are predicted using the ECMWF model fields, modified in light of the radiosonde data (see Figure 7.12.2.4.12 in Appendix 2 below). Moreover the upper atmospheric evolution envisaged by the ECMWF model is cross–checked with the TOVS data which are processed according the Wisconsin University algorithm retrieval. Valuable information on the wind field, such as the position of jet–streams, orographic clouds etc., are also inferred from the satellite imagery.

Clouds

Cloud can be associated with the synoptic–scale weather systems in the Ross Sea or the more local mesoscale lows. In addition, the barrier wind moving northwards along the coast can cause stratified cloud cover on the coast and for tens of kilometres inland. In the area around TNB an increasing cloud cover extending also inland is always associated with an easing of the katabatic flow in the glacial valleys. Clouds are more likely to develop at the interface between the ice and the open water especially during the summer season when an equilibrium condition between the sea breeze and a weak katabatic flow is reached quite often and low clouds follow the coastline of the Victoria Land. This condition is quite critical for air operations because a local sudden break of the dry and cold katabatic wind may lead to a foggy condition for the airstrips in Tethys Bay and in Browning Pass. For the same reason, in

December and January when the ice edge gets closer to the Transantarctic Mountains in northern Victoria Land, that coastal region has a lower 'degree of accessibility' with respect to the beginning of the season in October or November especially for single–engine helicopters which require a constant visual contact with the ground.

Since the clouds coverage has a direct influence on the surface and horizon definitions particularly where there is no orographical reference, a correct forecast for this parameter has a strong impact on air operations in Antarctica. The cloud coverage fields produced by the ECMWF model to initialize the internal radiation and precipitation computation provide the forecaster with an approximate guidance. Particular care needs to be taken when using such for operational forecasting due to the above mentioned underestimate of the dry katabatic flow action particularly on low and medium clouds.

More precise information can be inferred from satellite imagery on the nowcasting time–scale; the top height can be deduced by the top cloud temperature provided by the AVHRR applying the dry or moist lapse rate to the surface temperature. When the cloud edge and its shadow on the surface are clearly discernible an estimate of the top height can be calculated using elementary trigonometry based on the sun elevation at that time and the terrain altitude. The stratiform feature of the Antarctic clouds makes the results of this simple computation considerably realistic.

Visibility: snow and fog

For the most part of the summer period the visibility at Terra Nova Bay Station is good but sometimes it may be reduced by blowing snow and precipitation, and only infrequently by mist and fog. There are plenty of orographical references in the area, such as rocks and peaks, that are helpful even in low visibility conditions.

Katabatic winds stronger than 20 m s^{-1} (~40 kt) may induce drifting or blowing snow that may lead the visibility to go down to 6–7 km during which the rocky coasts of the Tethys Bay are always clearly discernible. Only with the occurrence of extraordinary katabatic winds may the visibility be reduced below 3 km. These events are more frequent in winter months and during the short transition seasons. The most dramatic decrease of visibility is caused by moderate to heavy precipitation that can reduce the horizontal visibility to 50–100 m. and determine a white–out condition.

The occurrence of mist and fog during the summer in the area between the Nansen Ice Sheet and Mt Melbourne is related to the above mentioned equilibrium between the katabatic flow and sea breeze in which advection fog forms over the sea and drifts towards the coast by light marine winds when the equilibrium area for short periods is pushed inland. Such a rare phenomenon normally happens during the hottest days in December and January when the majority of the sea ice in the Bay has melted so that the transfer of moisture from the open water to the surrounding air is favoured.

Low clouds and fog may also be driven into the Gerlache Inlet by a low–pressuresystem developing nearby, but in this case the main limitation for the visibility is determined by the precipitation. The detection and the evolution of fog patches can be investigated through AVHRR channel–3 coupled with the analysis of the fine resolution wind field predicted by the ECMWF model and observed in satellite imagery.

Surface contrast including white–out

Beyond the usual lines of drums or poles used to mark the airstrip location, the variegated orography of the Gerlache Inlet provides plenty of reference elements for the pilots on final approach to the Tethys Bay airstrip even in situations involving extensive featureless clouds or fog. The local orography greatly enhances the surface and horizontal contrast. In fact the relationship between cloud coverage and contrast is relative to the local environment: a low cloud overcast sky provides different conditions over the featureless Antarctic plateau compared to the better referenced Tethys Bay. It may also happen that if all the geographical references are not well distributed in all the directions, the contrast can be different depending on the direction you are looking at. In the Dumont d'Urville area, for instance, there are a lot of islands but no distinguishing features over the plateau where the airstrip used by Twin Otters has been set up.

In Tethys Bay, when marginal weather conditions prevail, the contrast between the sea ice and open water is normally used to recognize the obstacles–free entrance of the bay, while the contrast of the rock–sides during the "short–final" approach provides an helpful reference during the landing. In summer the katabatic winds generally determine a fair to poor surface contrast, but never reaching white–out conditions which on the contrary may be reached in case of moderate or heavy precipitation.

Horizontal definition

There are many geographical references are well distributed all around TNB Station. As for the surface contrast in summer, the katabatic wind is never responsible for white–out condition, while mist, fog and precipitation can determine a featureless boundary between the ground and the sky. For aeronautical use the horizontal definition is provided in all the directions relevant for air operations.

Precipitation

Both synoptic scale and mesoscale lows can give precipitation in this region. In addition, the coastal cloud band associated with the barrier wind can give precipitation in the form of snow with up to 60–80 cm in a few hours being reported. Since the Italian Base has been established in 1985, no reports have been made of liquid precipitation during the summer season, while cumulus and stratocumulus clouds are frequently reported in December and January as indication of limited convective activity. The convection is mostly induced by heating from the sea rather than by the orography which for air masses coming from the ocean has a negligible relevance. The solid precipitation is mostly in the form of snow flakes, but snow grains and snow pellets reports are not unusual.

Cumulated 12 hr total precipitation fields are drawn from the ECMWF model and provide valuable information about the amount and about when and where it may occur. The precipitation is indicated in $kg.m^{-2}$ of equivalent water and no information is inferred about the snow depth due to its highly variable density. A somewhat qualitative validation of these fields is regularly performed on the satellite imagery through the estimates of form, texture, and top temperatures of clouds.

Temperature and chill factor

During the period of station activity the temperature has no impact on operations. In October and February the combined effect of wind and temperature may determine extreme chill factors that may go beyond –50°C particularly when the sun is below the horizon. In this period the diurnal temperature variation may also be of the order of 15°C in clear sky condition. From November to January the maximum daily temperature can be well above 0°C reaching as high as 7–9°C and the daily variation decreases to 4–8°C.

A recent verification has shown the 2 m summer temperature derived from the ECMWF provides a considerably accurate description of the data measured by the AWS 7353 for forecasts up to 72 hr. The data at all the prognoses times show a negative bias from the second half of October to the first decade of December, while the bias is positive from December to February. This behaviour corresponds to the two different regimes determined before and after the sea ice melting near TNB Station.

Icing

The low temperatures commonly found at latitudes south of 70°S generally allow for only a very low cloud water content and consequently a very low risk of airframe icing. Nevertheless moderate icing being reported by the pilots is not unusual particularly when descending in unstable airmasses near the ocean. For this reason during the scientific experiments requiring the installation of external devices on the airframe, the in–cloud flight is prohibited by the operating companies.

The radiosonde data and the forecast sounding drawn by the ECMWF model are used to issue ice warnings and the –23°C isotherm is the threshold under which the icing risk is negligible. Such a choice is determined by the parameterisation of the hydrological cycle performed in the model which does not allow any liquid water below this temperature. This criterion which, according to the pilots is applicable to the central and southern Victoria Land, has been contradicted many times by crews flying to Dumont d'Urville, that experienced in January and February moderate icing and reported temperature as low as –28°C. For this reason before each flight, Dumont d'Urville radiosonde data are required and –30°C is used as threshold for warnings issued during these two months.

Turbulence

Turbulence warnings included in the flight documentation produced for fixed–wing aircraft are drawn from the ECMWF model. Also the position and strength of jet–streams are specifically outlined in the upper level maps provided for the cruise flight.

Moreover, a diagnostic model containing a fully detailed orography of the area close to Terra Nova Bay Station is used to infer the wind field at various levels up to 600 m (~ 2000 ft) from spot measurements. AWS data, upper soundings, and possibly SODAR measurements are assimilated by the model which performs the Richardson Index computation between each pair of levels. Since the information drawn by aircraft pilots operating in the area has shown a good agreement with the model output, the AWS measured wind have been clustered and associated with turbulence patterns which nowadays are considered as the basic rules for flying in this area. The model is generally run close to the radiosonde launch hours to have a closer relationship between the evolution of the surface and of the upper–air parameters.

Hydraulic jumps

The glacial valleys around TNB have the characteristics required for hydraulic (or katabatic) jumps, i.e. strong katabatic flow and rapid changes in orographic gradients. This phenomenon is very common on the edges of the confluence areas just before channelling along the Reeves and Priestley Glacier. In the period of the station activity the highest probability for the occurrence of hydraulic jumps is in October and in the first days of November when the still strong katabatic flow makes them grow up and persist. In most cases the high–resolution OLS imagery provides a quite impressive description of these events for which no routine prediction is carried out.

Sea ice

The most part of the success of the scientific season of the Italian Programme depends on the seasonal behaviour of the sea ice in the Gerlache Inlet and in the Tethys Bay. From April to October, all the area between Cape Washington, the Campbell Ice Tongue and Adelie Cove is fully covered with first–year sea ice. The first drillings taken in October, indicate an increasing sea icethickness along the Tethys Bay airstrip ranging from 3.5m under the eastern threshold to 4.5m at the opposite side. The temperature measured 2 meters below the surface fluctuate in this period around –10°C. Hence on the sea ice cover undergoes a lot mechanical, chemical and thermodynamical processes that will lead to the final breaking. The mechanical action is partly produced by the wind and partly by the sea swell induced by the tide and storms crossing the region.

The katabatic flow on one hand falls against the ice surface and contributes to crack it and on the other hand is primarily responsible of drifting the floes away. The tide induces a low frequency sea swell which greatly enhances the ice frailty, while the higher frequency primary and wind swell raised by storms mainly crumble the ice edge.

The periodical check performed along the airstrip shows that from October to December the ice temperature (T_{-2m}) increases up to –2°C/–3°C and the ice thickness undergoes a 1–1.5m reduction. These may be considered the macroscopic effects of the seasonal increase of temperature, but also other effects occur in the microscopical structure of the sea ice. The incorporation of air and brine determines a dramatic change in the physical properties of the sea icethat weakens the structure of the ice–crystals.

An accurate prediction of the sea icebreaking period is considerably important because sometimes it takes only 2 or 3 hours for the cracks to percolate in the Tethys Bay and in the Gerlache Inlet. Since this phenomenon is determined by the concurrence of the above mentioned elements they all must be taken into account; a good guidance for the prediction is the periodic check of the detachment of the sea iceedge from the rocks delimiting the bay. When only a weak constraint is applied at the boundaries, the ice sheet may be easily and quickly broken by the tidal and/or the primary swell. After that, a katabatic event may sweep away all the floes in less than 4/5 hours. This generally happens in January with highest probability in the 3rd or 4th week, but the fraction of the sea icethat will be drifted away is difficult to predict and varies considerably season by season. At this stage many floes may be re–pushed in by southerlies winds and swell, but the evidence that no iceberg has ever been found in the Bay in October at the beginning of the season, suggests that the refreezing phase, which at the end of February is already on the way, is preceded by strong katabatic winds.

Wind and swell

For ocean wave forecasting the ECMWF WAM model on 2.0° by 2.0° grid is used. On this basis forecasts up to 72 hours of significant height and direction of primary and wind swell forecasts are issued for the Italica Research Vessel and on demand for any ship in transit in the region. Such predictions have been also tailored to the route to and from Lyttelton (New Zealand) for which specific weather maps are produced.

In the Ross Sea the underestimate of the katabatic forcing requires some corrections which are computed from the speed, fetch and duration of the observed wind. A good estimate of the wind forcing on open water surfaces is provided by the SSM/I imagery which in turn permits to validate the model indications.

7.12.3   McMurdo Station

7.12.3.1   <u>Orography and the local environment</u>

McMurdo Station (77.86 ° S, 166.67 ° E , elev. 24 m AMSL) is located at the tip of Hut Point Peninsula on Ross Island. The peninsula extends about 13 km (~ 7 nm) southwest off the lower slopes of Mt. Erebus, an active volcano with a summit of 3794 m. Mounts Terra Nova (2130 m), Terror (3250 m) and Byrd (1800 m) make up the remainder of Ross Island. The McMurdo Sound lies directly west of McMurdo and is the southern most extension of open water in the late summer. The Royal Society Mountains, and its backdrop of the ice plateau, provide intrusions of Antarctic air mass within the region. Each environment is contrasting in terms of temperature and moisture profiles with modification and mixing of these air masses in the near proximity to McMurdo. Extremes of this contrast are at a maximum during the height of the summer season when open water is present, allowing for greater capabilities of cloud enhancement or fog development.

7.12.3.2   <u>Operational requirements and activities relevant to the forecasting process</u>

McMurdo provides weather data, observations, and forecasts for all United States Antarctic Program (USAP) operations. Typical weather facility operations include:

- Area observations and forecasts for safety for McMurdo and all operating camps to include the South Pole Station.
- Climatic information.
- Transoceanic flights from Christchurch, New Zealand to McMurdo:
    - –Air Force C–5
    - –Air Force C141
    - –Air National Guard and US Navy LC130 Hercules
    - –NZRAF and Italian C130 Hercules
- Continental Flights from any point to any point by USAP Aircraft (normally originating from McMurdo Station):
    - –Air National Guard and US Navy LC130 Hercules
    - –Twin Otter

–PHI Helicopter
- Information for Safety of Flight purposes is provided to any requesting aircraft within the McMurdo Area of Responsibility.
- Ship forecasting is provided for USAP vessels within the McMurdo Area of Responsibility.

7.12.3.3   Data sources and services provided

McMurdo predominately utilizes U.S. Navy Fleet Numerical computer products available via the Internet. The global model is updated twice daily. Real time data from AWSs, composite satellite imagery, and computer products are available and frequently down–loaded from the University of Wisconsin web site.

NOAA, DMSP, and Meteor satellite data are received and processed providing McMurdo Station and the Ross Ice Shelf with nearly continuous coverage. The TeraScan processor enables overlay, and still animation for the DMSP and NOAA images. Co–operation with other existing TeraScan sites periodically assist with images outside of the receiver's swath.

Products and satellite images are normally distributed by the McMurdo or Christchurch Office. Requests are made periodically to fax or e–mail computer information to various sites to support USAP related programmes.

7.12.3.4   Important weather phenomena and forecasting techniques for McMurdo

General overview

McMurdo is normally within the boundaries of the barrier winds set up as a thermal contrast between the plateau and Ross Ice Shelf. The barrier winds move north along the Transantarctic Mountains and are forced around Ross Island providing McMurdo Station with a northeast wind. The plateau high frequently extends across the McMurdo Sound into the Ross Island and the western portion of the Ross Ice Shelf. This situation provides for generally fair conditions at McMurdo. Because of this pattern, low–pressuresystems located on the Ross Ice Shelf cause a large pressure, temperature, and moisture contrast along the barrier winds. With a breakdown or over–running of the barrier winds, the low and associated weather is allowed to move into the Transantarctic Mountains and McMurdo Sound.

Several general synoptic patterns effect the weather at McMurdo and are the product of the zonal or meridional upper–level flow between Antarctica and the mid–latitudes. The synoptic flows in the McMurdo area are enhanced or hindered from normal progression due to large geographic obstructions and wide variations within the local environment. Synoptic scale highs and lows may directly effect the area's weather but more often it is the indirect relationship of mesoscale systems or the initiation of tertiary winds that cause temperature and humidity variations around McMurdo.

The upper–level pattern frequently referred to as the Ross Sea Low provides perhaps the best indications of the movement of synoptic scale highs and lows within the Ross Sea area. The upper level low is normally produced from a continuation of decaying waves within the region. From this origin it contains many characteristics of the wintertime Aleutian Low.

When the low is within about 600 km (~300nm) of McMurdo, high humidity is expected from the surface to 3000m (~10,000 ft). This increase in humidity will relate to

layers of stratified clouds, and frequent fog patches over most of the Ross Ice Shelf and Ross Sea. Results from this pattern would drive an occluded low, migrating from the Indian Ocean into the Ross Sea, in a more northern direction. This would make a direct hit on Ross Island highly unlikely since the surface low would be directed away from Victoria Land. It would also disfavour initiation of katabatic winds allowing the plateau high to spread but not build in intensity. This system may advect additional moisture into McMurdo if the warm air advection side of the low extends into the Ross Sea as it moves north of Cape Adare.

A Ross Sea low within about 600 km (~300 nm) of McMurdo generally equates to long periods of stable conditions, light winds, and low stratus ceilings. Occasionally an easterly wind pattern will force a piling of moisture into the Royal Society Range, which develops nimbostratus clouds and light snow progressing back across the McMurdo Sound. The best forecasting tools are:

- Do not expect any long term clearing while a 400–hPa low is within this range.
- Minor ridges may provide a southwest wind from 1500 to 4500 m (~5,000 to 15,000 ft). This will provide the best possible weather pattern, normally working the moisture away from McMurdo Sound. This flow would be abnormal and should not be expected to last for any length of time considering the location of the Ross Sea low.
- Surface to 3000 m (~10,000 ft) winds from the southeast push moisture from the Ross Sea into the McMurdo Sound. Gathering of the moisture and additional lifting is provided with the Royal Society Range west of McMurdo. This will develop the clouds from the bases downward in a nimbostratus cloud formation. The clouds will develop across the sound and light snow can be expected.

With a Ross Sea low 600 to 1100 km (~300 to 600 nm) from McMurdo wide variations can be expected within the weather patterns. With wide spacing between McMurdo and this steering low centre, synoptic scale systems may affect the area.

Polar highs will split off the Antarctic air mass over Victoria Land to separate migratory lows. In this situation the McMurdo area is indirectly affected by the expansion of the plateau high, providing clear skies with normal northeast winds. A strong upper level ridge west of McMurdo will indicate the set up of this situation. The 500–hPa vorticity chart will normally pick up an associated channel jet over Victoria Land into the Ross Sea up to 48 hours in advance of the formation.

When the Ross Sea low drifts eastward, occluded lows may migrate into Victoria Land prior to entering into its steering flow. This will normally provide enough upper level cyclonic support to develop a triple point low which will proceed around the Ross Sea low dragging the existing occluded front west to east across the Ross Sea. In this situation high pressure is developed over McMurdo and fair conditions prevail. Moisture and warm air is limited to the flow around the newly formed low well to the north keeping cold dry air in the region.

When the Ross Sea low is in this location mesoscale lows may develop near the transition from the Ross Sea to the continent's coast near 150º W. This is normally initiated by a short wave progressing around the eastside of the low. With a natural trough and warmer temperatures in the Ross Ice Shelf as opposed to the surrounding continent, lows can further develop as they move around the south end of the Ross Sea low. Based on the steering level the low may move into the McMurdo area causing increasing clouds and snow if they can break the protective barrier wind pattern. If the upper level flow forces the low into the Royal Society Ranges, the low may stall near McMurdo and heavy snowfall can be expected for an

extended period. One such system in December 1997 deposited over 350 mm of snow during a 27–hour period.

The absence of a Ross Sea low will produce normally the best weather for extended periods. The plateau high is allowed to naturally flow off the continent allowing for cold dry air to dominate over the Ross Ice Shelf and into the Ross Sea. This is the normal flow of the winter months as expected. It may also be seen in many seasons during the early summer months when there is a gradual disparity between the plateau temperatures and warmer Ross Sea temperatures and absence of any upper level cyclonic behaviour preventing surface low development.

Katabatic winds are widely studied around the McMurdo area. They are known to cause clearing weather patterns as dry air descends into the region. The katabatic flow can be divided into two categories of weather–related phenomena and two separate categories noted in forecasting the onset and intensities.

The building of the plateau high over Victoria Land will normally produce a glacier flow in the Ross Ice Shelf or Ross Sea affecting McMurdo on a regular basis. The katabatic winds are produced from an imbalance of the horizontal pressures between the plateau and the Ross Sea or Ross Ice Shelf. An increase in subsidence resulting in higher surface pressure over the eastern plateau will normally promote the onset of this wind pattern. As the pressure increases the flow around the anticyclone builds and forces the air outward. When the high builds to the west of the Transantarctic Mountains (eastern ice plateau) the air flows down the glacial passes spilling onto the ice shelf to the south, or Ross Sea to the north. A number of factors can cause the increase in the subsidence from low level cooling to upper level convergence.

The most noted and easiest forecasting event is the increase of upper level ridging to the west of the Transantarctic Mountain Range. The upper level confluent area will exert pressure on the underlying layers forcing downward vertical motion. With its decreased compressibility from cold air properties it has a more immediate reaction to subsidence. Surface air over the plateau will move anticyclonically and outward. When the outflow extends across the Transantarctic Mountains the wind will be forced down the glaciers, warming adiabatically as it descends. Stronger flow is noted when the ridging creates a perpendicular component to the mountain ranges promoting an aligned upper level force with the surface wind direction. When this situation occurs over the Ross Ice Shelf, McMurdo will have an initial strong northeast wind and may be accompanied by reductions to visibility for one to three hours in blowing snow. This reduction is normal except during the mid– to late–summer when the snow is too moist and heavy to be carried. Due to the orientation of Ross Island to the wind flow the availability of loose snow is depleted within this limited time frame.

The second situation is the onset of katabatic winds north of McMurdo. This can have varying effects on McMurdo's weather. The dependent variables are low–level winds and availability of open water in the Ross Sea. A dry katabatic wind pattern flowing into a low–level cyclonic circulation with open water can result in an explosive low formation. The dry relatively cold air over relatively warm water creates this situation. Care is always taken in this situation to determine whether the low–level circulation will engulf Ross Island. When the pattern develops with outflow at Tera Nova Bay and moves cyclonically around Ross Island, heavy snow and light east to southeast winds can be expected. This situation has been commonly referred to as a Tera Nova Bay low. This weather will persist as long as the upper level flow supports the glacier winds at Tera Nova Bay and upper level support is provided to support the surface low.

More difficult to forecast is the effects of cyclones in the Ross Sea or Ross Ice Shelf. The low can equally cause the horizontal pressure disparity required for the onset of glacier winds. In this situation the low must be broad enough to encompass most of the Ross Ice

Shelf or Ross Sea. It must redirect the barrier winds into its centre to replace ascending air. As this occurs the Barrier Wind pattern away from the Transantarctic Mountains are replaced by a light glacier flow.

The katabatic winds will provide a drying effect on the lower cloud masses either preventing them from entering McMurdo Sound or delaying them for several hours. This situation provides difficulties in forecasting the motion of weather producing low clouds. When this situation arises with a low to the south, McMurdo commonly will stay under a blanket of altostratus with cloud base near 2400 m (~8,000 ft). McMurdo's wind may change from northeast to light and variable, then swinging to the northwest towards 5 m s^{-1} (~10 kt) as the barrier winds are redirected into the low. Temperature disparities commonly exist between the low and the drier air boarding McMurdo and the foot of the Transantarctic Mountains. When the temperatures become modified closer to that of the low the katabatic winds may be subsiding. This could be in part from the entrainment of the barrier winds filling the low–pressuresystem and eliminating the horizontal pressure contrast that created the katabatic flow. At this point the low clouds will meet no resistance and if the low–level flow supports it they will move into McMurdo area.

When the same situation is presented with a low to the north the dynamics of the low change. This low will be moist and warmer than its ice shelf counter part. The relatively cold dry katabatic air will become cold and moist as it modifies over the Ross Sea. This will induce new instability into a decaying wave, or rapidly modify a mesoscale cyclone (see Tera Nova Bay low above). The concave curvature of the Transantarctic Mountains within the region will also assist in confining the cyclonic motion in the lower levels. In this situation it is required to know what the upper–level wind pattern is doing. If this system is directed into the McMurdo area around the Ross Sea low, or if it is vertically stacked under a Ross Sea low within the proximity of McMurdo, heavy snow and gusty winds can be expected. The onset of severe weather is marked by the transition of the upper level ridge moving across Ross Island. This can be easily identified in the accompanied cirrus shield in all observed decaying wave situations.

Surface wind and the pressure field

Prevailing wind over the eastern Ross Ice Shelf is southerly due to the barrier wind as discussed. Although Ross Island is located in this band of southerly winds, the predominant McMurdo winds are easterly as the cold and more dense air flows around the orography of Ross Island rather than over it. With a strong increase in the pressure gradient the flow will begin to scale over rather than around Ross Island causing a shift of the wind direction toward the south.

Low level jet winds can develop if winds below 500 hPa shift to southerly and strengthen to above 20 m s^{-1} (~40kt). This southerly jet can cause surface winds above 25 m s^{-1} (~50kt) producing severe low level turbulence. This condition will frequently be accompanied by extensive cloudiness. The onset of the strong surface winds usually will be within 12 hours of the development of this jet.

McMurdo's wind direction may also be affected by high and low–pressuresystems within the region. These systems can modify or eliminate the prevailing wind flow.

Upper wind, temperature and humidity

Ross Island normally falls within a westerly upper–level wind pattern. This pattern follows the normal polar vortex wind direction. The formation of the Ross Sea low and its position frequently disrupt the flow, and intensity of the Ross Sea low will drive low–level features.

Temperature and humidity fluctuations are common. Dry cold wind from the continent normally will dominate the region. During the summer months large areas of open water exist on the north side of Ross Island introducing a ready source of humidity for the cold dry air. Low–level wind patterns, surface inversions, and wind speeds dictate the results which normally equate to low clouds or fog when the moisture is advected over the cold surface of the Ross Ice Shelf.

Clouds

Clouds within the region are generally limited to stratiform at various levels. Cap clouds are common over Minna Bluff, Ross Island, and Mount Discovery indicting increasing winds at those altitudes.

Visibility: blowing snow and fog

Visibility normally exceeds 50 km (~27 nm) with limits by land obstructions and the earth's curvature. Fata Morgana (a shimmering inverted and elevated mirage) is common and on occasion Superior Morgana can be observed. The most common obstruction is light snow and blowing snow. The snowfall is generally light enough that under calm winds the visibility will remain above 4800 m (~2.5 nm). Since the snow is so light and dry it is easily displaced by the wind. Winds above 5 m s^{-1} (~10 kt) will cause the visibility to lower to less than 1600 m (~0.9 nm) for hours after the snowfall has ended. Wind directions from any southerly component provide the worse reductions.

During the summer months snowfall becomes moist, the flakes grow in size and adhere to the surface easier and faster. Winds in excess of 15 m s^{-1} (~30 kt) are normally required out of the south to provide any prolong reductions in the visibility from blowing snow alone. With the increase in flake size reductions to less than 3200 m (1.7 nm) will be observed even in calm winds.

Fog has been noted in all months of the year but most frequent occurrences are during the peak summer months. The cold surface of the Ross Ice Shelf provides the temperatures to condense moisture advected from the Ross Sea. The Windless Bight with its natural divergent wind pattern is a common area for fog to form and rapidly expand. Wind directions pushing moisture into this area are cause for forecasting fog in McMurdo. Fog most frequently occurs during the middle to late morning hours. Although diurnal effects are minimal it tends to assist fog development in these situations.

Fog normally develops when McMurdo falls on the fringe of any mesoscale high that promotes moisture advection into the windless bight. Fog has also been observed in advance of mesoscale lows moving from the Ross Sea into the Ross Ice Shelf. This situation pushes low–level moisture around Ross Island into the Windless Bight. The latter of these situations causes only a short term fog condition that is quickly removed as the low skirts just east of Ross Island and then switches the wind direction as it passes.

Surface contrast including white–out

McMurdo has an established runway with markers, TACAN, approach lights, and strobes. Even with all the amenities surface definitions are used and transmitted on all hourly METAR observations. Because of the runway markers and large non–snow covered landmasses within the area white–out conditions from optics alone is not a factor.

Horizontal definition

Contrast in the horizon definitions is easily discernible against the numerous landmarks within the region. Snow, blowing snow, and fog can frequently obscure it. Horizon definitions are used and transmitted on all hourly METAR observations.

Precipitation

Snowfall occurs all year with a maximum from December to March associated with the availability of moisture and the warmer air temperatures. Snowfall is normal with any meso or synoptic–scale low within the region. Heaviest snowfall accompanies decaying waves that retrograde across the Ross Sea and move toward Ross Island from the southwest. Terra Nova Bay lows (formation discussed earlier) will provide a continuous snowfall for extended periods.

 Liquid precipitation is uncommon but has been observed. To forecast the occurrence parameters for forecasting a cold rain process should be used.

 Ice needles, snow grains, and ice crystals have all been observed at McMurdo during the coldest months.

Temperature and chill factor

McMurdo's diurnal effects are limited to the sun angle and obstructions of mountainous terrain. Large temperature variations are attributed to temperature advection. Extreme maximum temperatures have been noted when warm air is advected from the Ross Sea to the Ross Ice Shelf, when the air rises moist adiabatically over the Transantarctic Range and then falls dry adiabatically into the McMurdo Sound. Wind chill is monitored during all months and special weather warnings are in place to limit exposure under harsh wind chill conditions. Extreme temperatures for each month for McMurdo are given in Table 7.12.3.4.1 below in Appendix 2 below.

Icing

Aircraft icing is normally restricted to the summer months with nimbostratus cloud formations. When suitable conditions exist light occasional moderate rime icing can be seen and on rare occasions moderate mixed icing has been observed.

Turbulence

Gusty surface winds can provide light to severe turbulence normally from the surface to near 1500 m (~5,000 ft). Funnelling of air between Ross Island and the continent provides gusty winds in excess of what the pressure gradient would suggest.

Hydraulic jumps

McMurdo experiences periods of sudden pressure changes, squall line type weather patterns, and changes of inversion heights. This may be the attributes of atmospheric hydraulic jumps and correlation is being studied at this time.

Sea ice

Sea ice in McMurdo Sound normally allows for shipping to be practical by late December. The sea ice naturally breaks by this time to south of Cape Royds. Coast Guard cutter operations begin near the first of the year breaking southward into McMurdo Station. McMurdo Sound will completely refreeze by early April, with the exceptions of open areas driven by strong off shore winds.

Wind waves and swell

Wind waves within the McMurdo Sound are normally slight to nil due to limited fetch. Sea ice concentrations and land–mass restrict the wave development.

7.12.4   Transantarctic Mountains

7.12.4.1   <u>Orography and the local environment</u>

The Transantarctic Mountains provide a primary glacier source and western barrier for the Ross Ice Shelf. This formidable barrier extends from the continent's edge at Cape Adare southward dipping below 87º S. Individual mountains average nearly 3,000 m (~11400 ft) with the ice plateau covering the western slopes dropping to sea level on the eastern side. The Antarctic air mass is the predominate weather feature of the Transantarctic range. The dense characteristic of this mass only requires the slightest of external forces to begin the katabatic flow from the ice plateau into the Ross Ice Shelf. The Ross Sea to the north provides frequent intrusions of maritime air over the Ross Ice Shelf and may extend into various levels over the Transantarctic range. This will normally set up a density imbalance increasing cyclonic behaviour over the ice shelf and frequently forces the air with modified maritime properties into the Transantarctic region.

7.12.4.2   Operational requirements and activities relevant to the forecasting process

The United States Antarctic Program (USAP) will frequently establish camps within the Transantarctic range south of McMurdo. Various fixed and rotor wing air support is directed from McMurdo Station.

Tourists flights (Boeing 747–400 aircraft) originating from Sydney or Melbourne, Australia during the summer season aim to over–fly the Transantarctic Mountains as far south as about 75 º S. (see http://www.anzac.com/at/ant/antdd.htm and Figure 7.12.4.2.1). The forecasts for these flights are provided by the Antarctic Meteorological Centre at Casey (when staffed) or by the Australian Bureau of Meteorology Regional Forecasting Centre in Hobart, Tasmania, Australia.

Figure 7.12.4.2.1 The Transantarctic Mountains as seen from a Boeing 747–400 Tourist flight. The Ross Sea (covered in sea ice) is visible on the right hand side of the photo adjacent the second engine cowling. See Section 6.6.2 above for an example of the route taken and forecast service. (Photo courtesy Mike Ball).

7.12.4.3   Data sources and services provided

USAP weather operations are limited to camp personnel providing basic weather observations upon request to the McMurdo weather facility via HF radio. Camp personnel will transport portable weather sensors to provide temperature, winds, and pressure.

7.12.4.4   <u>Important weather phenomena and forecasting techniques for the
Transantarctic Mountains south of McMurdo Station.</u>

General overview

The variation in altitude and orography makes this a complex weather area: the complexity
ameliorated to some extent by the remoteness of the area from moisture sources.

Surface wind and the pressure field

The eastern slopes are normally within the boundaries of the barrier winds set up as a thermal
contrast between the plateau and Ross Ice Shelf. These higher elevations fall within the
established cold and dry Antarctic air mass with a normal light to moderate downslope wind
feeding into the barrier wind flow. The predominant wind direction for unsheltered locations
is typically a pattern of funnelling to the closest glacier.

Extreme elevations of this region and modification of advected maritime air into the
Ross Ice Shelf limited the duration of clouds and snowfall. Only deep pooled moisture
patterns when coupled with a strong up slope wind field produce ample energy to overcome
the massive terrain feature. These wind patterns can be attributed to a decaying wave in the
Ross Sea or along the Hobbs Coast. The influence of such a system can produce enough
horizontal temperature contrast to sustain jet level winds and vorticity lobes far into Marie
Byrd Land. This wind will support and often enhance low level cyclonic features in the
southern Ross Ice Shelf. With the proper wind field the moisture can be driven into any
portion of the Transantarctic Mountains spreading stratus clouds, light snow, and strong
surface winds far into the Ice Plateau.

Upper wind, temperature and humidity

The 500 to 400–hPa winds provide a good source for forecasting progression of low level
moisture over the Transantarctic Mountains onto the plateau. A Ross Ice Shelf depression in a
tight easterly 400–hPa flow that extends over the plateau provides the perfect means to push
the mass over the area.

Clouds

Mesoscale lows migrating northward along the eastern slopes of the Transantarctic Mountains
will frequently drive low cloud or fog up the glaciers as the low moves north. Any katabatic
outflow will restrict this cloud movement or force the depression and associated clouds
eastward into the central ice shelf continuing fair skies over the much of the region.

Clouds are dependent on specific location and elevation. The primary moisture source is
the Ross Sea. Cap clouds and lenticular cloud formations are the norm for advancing systems.
Note the direction of the lenticular or cap clouds to assist in forecasting whether low level
stratus will be forced into a particular location. The more easterly the clouds extend the
greater the threat of advancing low clouds becomes..

Visibility: blowing snow and fog

Snowfall will normally be light and fog will exist in higher elevations. With many protected areas it is not unusual for the low stratus or fog to stall over the region for extended periods. The onset of any katabatic wind flow is the normal means to decrease the cloud cover.

Surface contrast including white–out

No specific information on forecasting has been obtained.

Horizontal definition

No specific information on forecasting has been obtained.

Precipitation

No specific information on forecasting has been obtained.

Temperature and chill factor

Temperature ranges are dependent on the elevation and latitude. In such a large region with these two items are too vast to be specific.

Icing

No specific information on forecasting has been obtained.

Turbulence

Turbulence is rare and normally only exists in the presents of cap clouds or jet cirrus. When these items are present, light and on occasions, moderate turbulence has been observed.

Hydraulic jumps

No specific information on forecasting has been obtained.

Sea ice

Not relevant to this location.

Wind waves and swell

Not relevant to this location.

7.12.5   Amundsen–Scott (South Pole) Station

7.12.5.1   Orography and the local environment

Amundsen–Scott (South Pole) Station is located within the proximity of the geographical South Pole. At an elevation of 2,800 m (~9,000 ft) and near 1300 km (~700 nm) from the closest water source, commonly only a single air mass effects the local area. Periodical influences of modified maritime polar air can migrate into the region on occasion bringing some snow, increased wind velocity and a gradual increase in temperatures. With all cardinal points directing north, a grid system of navigation is used. All referenced directions will be in the grid system, using prime meridian as north and the date line (180° longitude) as south. The area to the west of South Pole, typical of western Antarctica, provides a gentle slope to sea level. The Ronne Ice Shelf and Weddell Sea lie just past the Pensacola Mountains to the grid northwest, providing the closest moisture source. The slope continues to rise in nearly all directions to the east. The Transantarctic Mountains extend to the south, dropping to lower elevations over either Marie Byrd Land or the Ross Ice Shelf.

   Elevation and seclusion nearly eliminate intrusive air masses at this location. The polar high dominates the continent with common high–pressure centres situated over the extreme elevations of Eastern and Western Antarctica. The high over the greater plateau to the east normally extends over Amundsen–Scott (South Pole)providing cold dry conditions throughout the year. The most common intrusion of moisture is accompanied by a decaying wave in the Weddell Sea. This locale is the most direct route for a maritime flow and will normally only progress over the extended distance and scaling the elevation barrier when ample jet winds and dense multiple layered cloud cover are still associated with the depression.

7.12.5.2   Operational requirements and activities relevant to the forecasting process

Amundsen–Scott (South Pole) provides surface synoptic observations every 6 hours and upper–air observations every 12 hours during the normal operating summer season. Hourly metar and special weather observations are taken as needed during flight operations. Amundsen–Scott (South Pole)synoptic and upper–air data transmitted via McMurdo Weather to MET New Zealand over AFTN. Data are also available for climatic purposes by accessing the National Science Foundation Web Page. Forecasting facilities are located at McMurdo Station. South Pole weather operations include:

- Area observations for safety at South Pole Station.
- Climatic information.
- Continental Flights from McMurdo Station:
    –Air National Guard and US Navy LC130 Hercules;
    –Twin Otter.

- Information for Safety of Flight purposes is provided to any requesting aircraft via HF broadcast.

South Pole monthly climatological data are also placed on the ATSVAX in Miami in the anonymous.polewx directory, and can be retrieved by anyone that has the ability to FTP. Users wishing to download the files should log on ATSVAX.RSMAS.MIAMI.EDU using the password "anonymous". After changing to the [polewx] directory, the desired file can then be retrieved. Typically the files are kept on the ATS VAX for a period of one month. In addition to the files which are stored on the ATS VAX in Miami, various research groups will occasionally make direct requests to this department for climatological data dating back to 1957.

7.12.5.3   Data sources and services provided

Amundsen–Scott (South Pole)provides observational information for operational use and climatology. McMurdo Station provides all forecasting support using numerical products and satellite imagery. Communications with McMurdo exists on a 24–hour basis via HF communications and periodical windows of e–mail service.

7.12.5.4   Important weather phenomena and forecasting techniques for South Pole Station

General overview

Amundsen–Scott (South Pole)is dominated by the plateau high with periodical influences of modified maritime air from the Bellingshausen Sea, the Weddell Sea, and on rare occasions, residual moisture from the Atlantic Ocean via Queen Maud Land. The most typical and intense systems are those from the Weddell Sea due to the proximity and gradual slope.
    The predominating plateau high extending from Eastern Antarctica produces a light northeast wind normally less than 5 m s^{-1} (~ 10 kt). With a compressed upper–air pattern following the polar vortex, clouds in the region will lack the basic dynamics to develop providing mostly clear skies and unrestricted visibility as the norm.
    The normal northeast wind, clear skies and cold temperatures can abruptly end when a jet finger propagating around a decaying wave moves over the South Pole transporting moisture from the expanded decaying system. The upper–air sounding may herald poor weather by showing slight low level wind shifts in the direction of the advancing system, warm air advection indicted by height rises, and increased moisture patterns. More frequently is the lack of telegraphing signatures in the upper level due the extreme barotropic nature of the air masses. Poor weather normally accompanies or is in advance of all changes to the upper level pattern.
    Residual stratified clouds may become trapped in inversion layers over the plateau and meander with the lower level winds. The stratified cloud masses frequently move slowly and may produce snow grains or ice needles reducing both ceiling and visibility at the station. The slow nature its motion will allow a small cloud mass to hinder flight operations for several hours.
    Forecasts from McMurdo Station are typically developed using satellite imagery and computer model output. Look for an upper level ridging pattern and associated cloudiness

intruding from a coastal location. The low–level wind directions are monitored for shifts from the norm (Figure 7.12.5.4.1). When all the above are present an expected shift is forecast normally to the grid northwest. The thickness of the cloud pattern, forecasted wind fields from computer charts and IR temperature patterns off the satellite provide guidelines to the intensity of poor weather. Frequently a thick smooth arching cloud pattern will equate to visibility dropping under 1mile for the duration of the cloud pattern. Overcast to broken clouds will persist throughout the period of reduced visibility with a slow rise in heights above 300 m (~1,000 ft) as the cloud pattern thins from precipitation and air mass modification.

Surface wind and the pressure field

Prevailing winds over the South Pole migrate around the plateau high centred over Eastern Antarctica with a downslope influence into Western Antarctica. This produces a grid northeast wind, which may vary from 010º grid to 080º grid depending on the potential temperature difference from west to east Antarctica.

Winds from the northwest are typically influenced by the remnants of a decaying low advancing or spreading out from the Weddell Sea. The degree of wind shift truer to the moisture source normally equates to the intensity of the weather. A depression moving or expanding in such a manor producing a wind direction that would provide the maximum amount of moisture with the least amount of modification with near equal dependency on the wind speed.
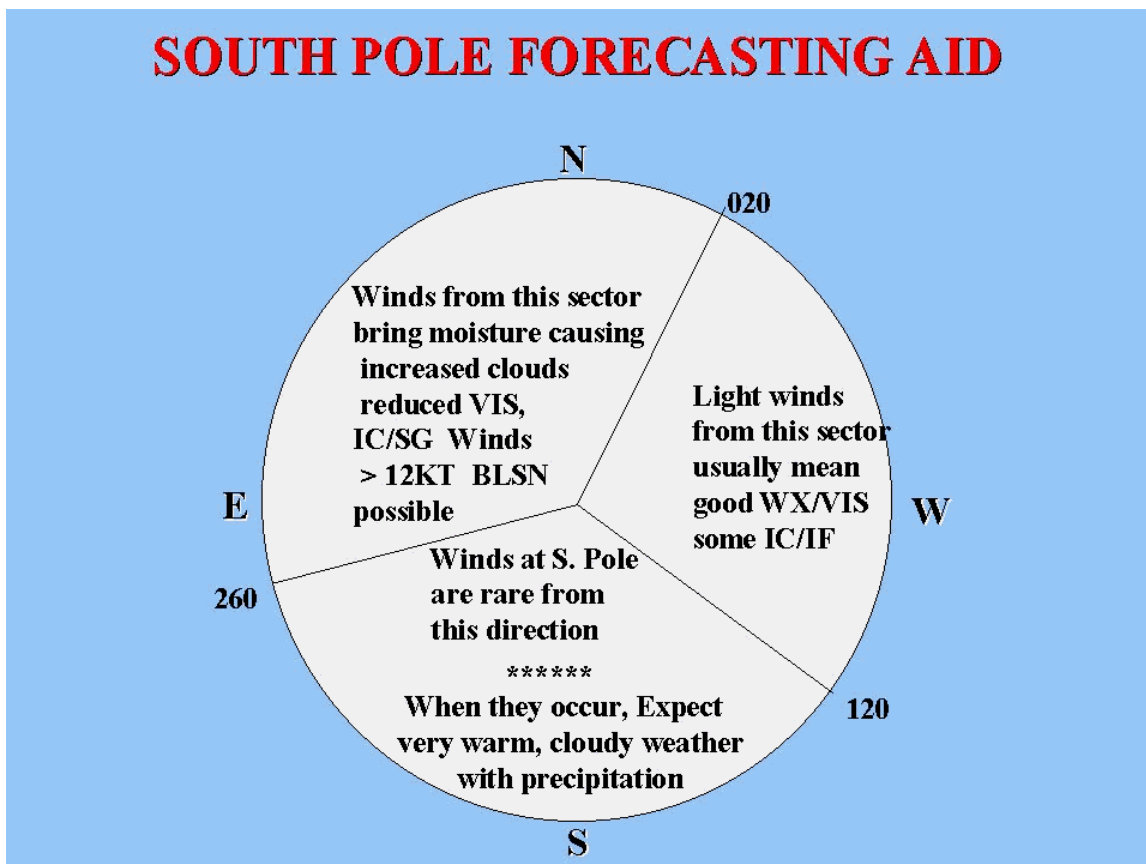
Figure 7.12.5.4.1   Forecast aid for Amundsen–Scott (South Pole)

Wind directions from the south are rare as stated in Figure 7.12.5.4.1 but may occur if a depression is forced inland over Marie Byrd Land. This may occur from blocking highs extending into Ellsworth Land. These systems are intense over the southern portion of the Transantarctic Mountain Range as indicated by satellite depicting turbulent wave clouds with identifiable directions toward the Pole. With sufficient force and strong reinforced temperature advection over Marie Byrd Land the system can scale the geographic incline and move into the South Pole. Winds will slowly progress to the grid southeast. These systems can produce snow grains and even snow over the area. The effects of the system are normally short lived with rapid modification as the flow typically redirects northward toward McMurdo

Upper wind, temperature and humidity

Amundsen–Scott (South Pole) upper level winds are typically a reflection of plateau high in the lower levels changing to a influenced direction from coastal lows in the mid levels, and changing to the polar vortex pattern in the extreme upper levels. The mid level 500 to 300 hPa drive the majority of changes within the surface weather features as discussed in the general weather description

Temperature fluctuations are subtle and they are normally preceded by poor weather. Surface humidity is not reported at the site but influences of maritime air are consistent with obscuring weather phenomena. The most common are ice crystals, and ice needles, followed by snow grains, which are present when an intense system migrates into the pole.

The data from the radiosonde programme provides information on conditions at upper levels. In addition, these observations are assimilated into the numerical analyses for the model fields around the station should be fairly reliable.

Clouds

The surface observations indicate that the annual average cloud amount is close to 45%. However, there are problems for the observers in deciding how to report the semi–permanent veil of thin cirrus that is found over the area. This can either be reported at zero oktas or eight oktas of cloud, depending on the thickness of the cloud. Intrusions of lower latitude air associated with synoptic disturbances obviously introduce thicker cloud to the area. The most frequently reported cloud at the station are altostratus and cirrus.

Visibility: ice crystals and fog

Ice fog and ice crystals are the only conditions that produce "instrument flight rules weather" at the South Pole. Otherwise the visibility is excellent. The forecaster needs to watch closely the effects of surface temperature, wind speed, and direction and inversion strength on the formation and dissipation of ice fog and ice crystals. Cloud cover is normally cirrus (above the saturation layer) but altostratus is occasionally present during ice crystal formation. Small ice crystals from the cirrus fall into the saturated layers, serving to nucleate columnar ice crystals which then precipitates.

Winds from GRID 260 to 020 at greater than 6 m s^{-1} (~ 12 kt) will normally accompany a storm from the Weddell Sea and produce ice crystals followed by blowing snow. Winds in excess of 10 m s^{-1} (~ 20 kt) are normally restricted to this sector. With this wind speed and direction the weather conditions will lower to less than 150 m (~ 500 ft) ceilings and/or less

than 900 m (~ 0.5 nm) visibility restricting flying conditions. When the winds are between 6 and 10 m s^{-1} (~12 and 19 kt), slant range visibility may allow a distinction of runway markers. Winds within this speed range will vary in effects based on the direction from which it is coming, and on the availability of newly fallen snow.

Another common obstruction to visibility at the South Pole is fog. Ice fog or freezing fog can develop from a flux in moisture most commonly found after a wind change to the southeast to south. After a 6 to 18 hr period of this wind component freezing fog is likely to occur provided the winds remain under 3 m s^{-1} (~6 kt). A second common occurrence is the production of fog from ample moisture, extremely cold temperatures and the availability of nuclei from combustion engines, otherwise known as "camp fog". Combustion and aircraft engines will produce similar conditions to those that produce contrails. Amundsen–Scott (South Pole)can become IFR due to the landing of an aircraft.

Surface contrast including white–out

Contrast in the surface definitions is observed and incorporated in the remarks column of the METAR observation. Cloud cover over the uniform surface will make frequent and major changes to the surface contrast. Overcast skies, snow, blowing snow, and fog will typically cause poor to nil contrasts.

Horizontal definition

Contrast in the horizon definitions is observed and incorporated in the remarks column of the METAR observation. As all plateau locations the region offers little assistance in discerning the white surface against a white sky when any cloud cover is present. Snow, blowing snow, and fog will typically obscure the horizon causing poor definitions at the surface and at aircraft approach altitudes.

Precipitation

Precipitation over the interior of Antarctica is extremely light, and is difficult to measure due to the nearly constant drifting of snow across the plateau. Ice crystals, or diamond dust, are the most common form of precipitation and are observed on the majority of days. Unlike other forms of precipitation, ice crystals often precipitate out of a clear sky, glittering in the sunshine or moonlight, sometimes creating spectacular halos and arcs. Snow grains are commonly observed during strong upper level storms, while actual snowflakes (branched crystals) are much less common, usually only occurring in the summer months. The intensity of precipitation, almost without exception, is light. Snow accumulation in the vicinity of station, which is comprised of both fallen and deposited drifting snow, averages about 280 mm annually.

Temperature and chill factor

During the summer months of November–February, temperatures usually remain above –50ºC/–58ºF, and may even approach –18ºC/0ºF during the warmest weeks of late December and early January. With the loss of incident solar radiation in March, temperatures cool rapidly, usually dipping below –73ºC/–100ºF at least once during the austral winter. The coldest temperature ever recorded at South Pole is –82.8ºC /–117.0 ºF, while the warmest is –13.6ºC/+7.5ºF. The average annual temperature is –49.4ºC/–56.9ºF. Temperatures begin to climb rapidly after sunrise in late September. Apart from the elevation of the sun, the largest factor affecting surface temperatures is cloud cover. Cloud cover immediately changes the surface radiation balance, and therefore can have a rapid and significant effect on the observed temperature.

One of the most pronounced features of the vertical temperature structure is a strong low–level inversion that is especially prominent during the winter months. The temperature often increases by over 20ºC in the lowest few hundred meters of the atmosphere, then steadily declines again to a well–defined tropopause at 7,000 through 10,000 m above sea level. The stratospheric temperatures also exhibit a strong annual cycle, with the minimum slightly below –90ºC during July and August.

Icing

Aircraft icing is rare but has been observed during intense influxes of maritime air over the region. A low cloud deck may provide a warm inversion falling within the prescribed temperature regime to promote rime icing. During summer months the upper–air temperatures must be monitored closely to determine the capabilities to form rime icing in a low cloud deck.

Turbulence

Turbulence in this region has historically been restricted to the areas near the Queen Maud Mountains.

Hydraulic jumps

Do not effect the region around the South Pole.

Sea ice

Not relevant at this location.

Wind waves and swell

Not relevant at this location.

7.12.6   Ross Ice Shelf camps

7.12.6.1   Orography and the local environment

Siple Dome camp is the most widely used base during recent years. Siple Dome is located near 81.7º S, 148.8º W on the Siple Coast. The camp has an elevation of approximately 620 m (~ 2030 ft). At this increased altitude, Siple Dome receives cloud bases at a much lower level than surrounding camps. A cloud base passing over Roosevelt Island at 600 m (~ 2,000 ft) will be fog when it moves over Siple Dome. A lower stratus cloud or fog over the ice shelf may not reach Siple Dome or be prolonged in its advance due to the increased elevation. The gradual increased slope normally does not preclude any cloud formations from moving over the Dome, unlike the Transantarctic camps. Climatology shows a mean wind from any GRID southerly component will produce snow, fog or extremely low cloud bases. This wind direction is a direct result of a low–pressuresystem being within close proximity to the camp.
          Down Stream Bravo is another camp commonly used, and is located near 84º S, 155º W, on the Gould Coast. This location is near the Transantarctic Mountains to the south and Siple Dome to the north. The elevation is approximately 110m (360 ft). At this lower elevation and with higher land masses on three sides, it provides some protection from advecting moisture off the Ross Sea. The glacial winds from the Transantarctic Mountains and the barrier wind flow provide favorable weather conditions at this location. When low–pressurecentres find their way onto the southern ice shelf, it normally is only a matter of time before all of these protecting factors give way, and flight restricting weather moves over the camp.

7.12.6.2   Operational requirements and activities relevant to the forecasting process

No specific information on forecasting requirements has been obtained.

7.12.6.3   Data sources and services provided

No specific information on data or services has been obtained.

7.12.6.4   Important weather phenomena and forecasting techniques used at the location

General overview

Low centres that migrate east of Cape Colbeck and take a track toward the southern portion of the Ross Ice Shelf will produce a moderate grid north wind, turning westerly as the low passes. Snow and blowing snow may accompany the system, but the ceiling and visibility remain predominately above 300 m (~ 1,000 ft) and 5,500 m (~ 3 nm), due to the higher elevation and colder surface the system had to pass over before moving onto the Ross Ice Shelf. If the low is large enough, it may engulf existing low cloud cover or pre–existing fog, providing a temporary reduction to ceilings and visibility.
          Low centres that move over or to the west of Cape Colbeck have a direct impact on the southern ice shelf. Large amounts of moisture up to 3000 m (~ 10,000 ft) will be advected

over the cold, dry surface causing condensation at a multitude of levels, which may include the surface. Camps such as Roosevelt Island and Ford Range will be immediately affected with low ceilings, reduced visibility and increasing southerly winds. As the low moves onto the ice shelf, the cloud cover will advance over the remainder of the ice shelf to the south, and then circle up the west side of the low along the Transantarctic Mountains toward McMurdo. Cloud bases can range from the surface to 600 m (2,000 ft) and stay over the ice shelf until a new synoptic pattern pushes the clouds out to sea.

Surface wind and the pressure field

No specific information on forecasting has been obtained.

Upper wind, temperature and humidity

No specific information on forecasting has been obtained.

Clouds

No specific information on forecasting has been obtained.

Visibility: blowing snow and fog

Schematic forecasting rules are shown in Figures 7.12.6.4.1 and 7.12.6.4.2 for Siple Dome and Downstream Bravo respectively. In summary the guidelines are:

- Wind directions from west–northwest to north and speeds between 3 to 7 m s^{-1} (~ 6 to 14 kt) are the best case for good visibility. But when the wind exceeds 8 m s^{-1} (~ 15 kt) and loose snow is available, visibility becomes poor due to blowing snow.
- Wind directions from north–northeast to east produce both light snow and light fog, with visibility normally not reducing below 3,700 m (~ 2 nm).
- Wind directions from east–southeast to south produces heavy snow and dense fog with visibility normally below 3,700 m (~ 2 nm).
- Wind directions from south–southwest to west produce the greatest chance of fog development with very low visibility, especially when the wind speed is between 3 to 6 m s^{-1} (~ 6 to 12 kt) (fog onset is approximately 3 to 6 hr). This area also produces blowing snow when speeds exceed 8 m s^{-1} (15 kt) and will last until the wind either dies or shifts direction.
- Fog can develop at Siple Dome with light wind from any direction.

Surface contrast including white–out

No specific information on forecasting has been obtained.

Horizontal definition

No specific information on forecasting has been obtained.

Precipitation

No specific information on forecasting has been obtained.

Temperature and chill factor

No specific information on forecasting has been obtained.
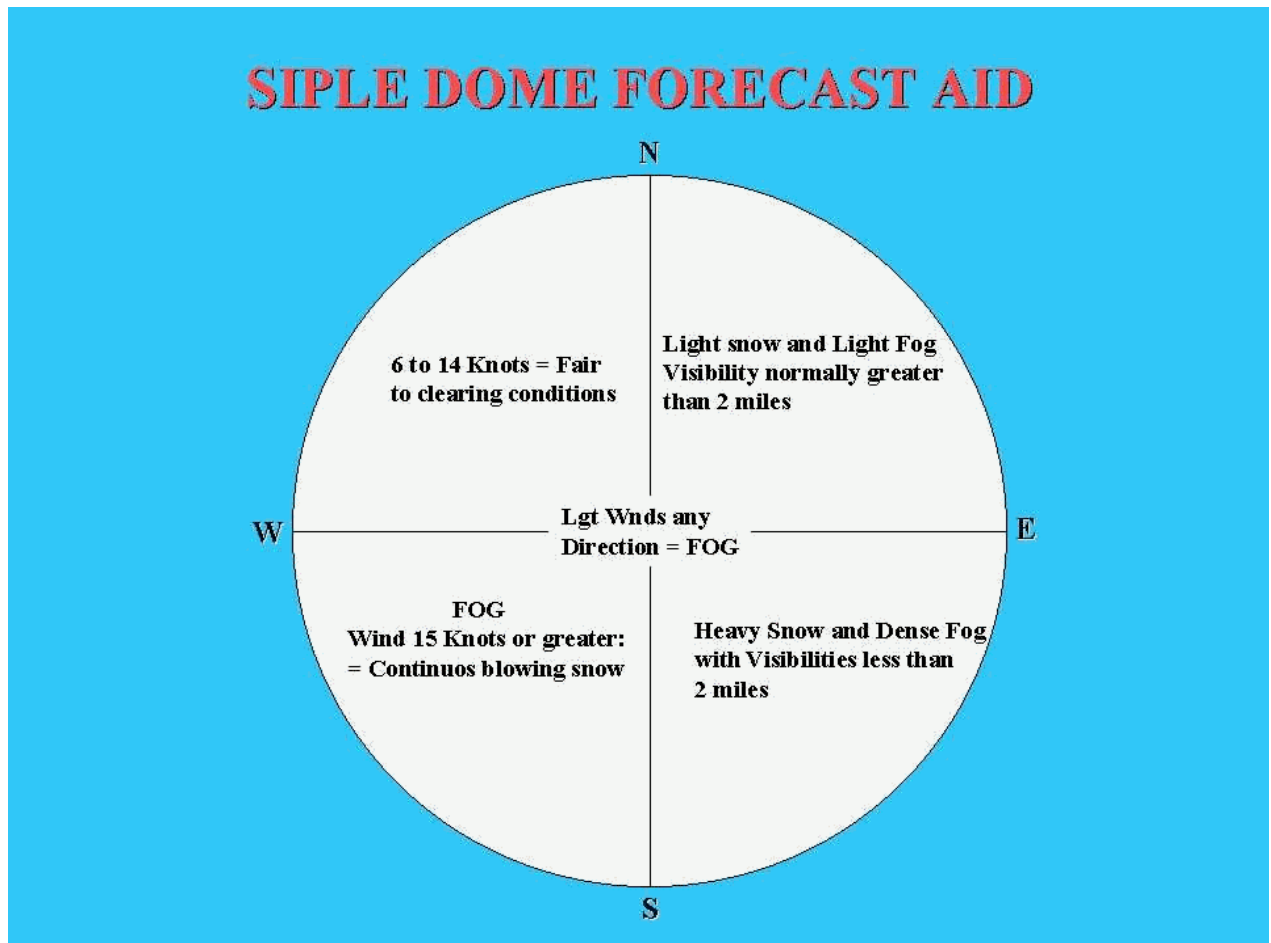
Figure 7.12.6.4.1   Forecasting aid for Siple Dome
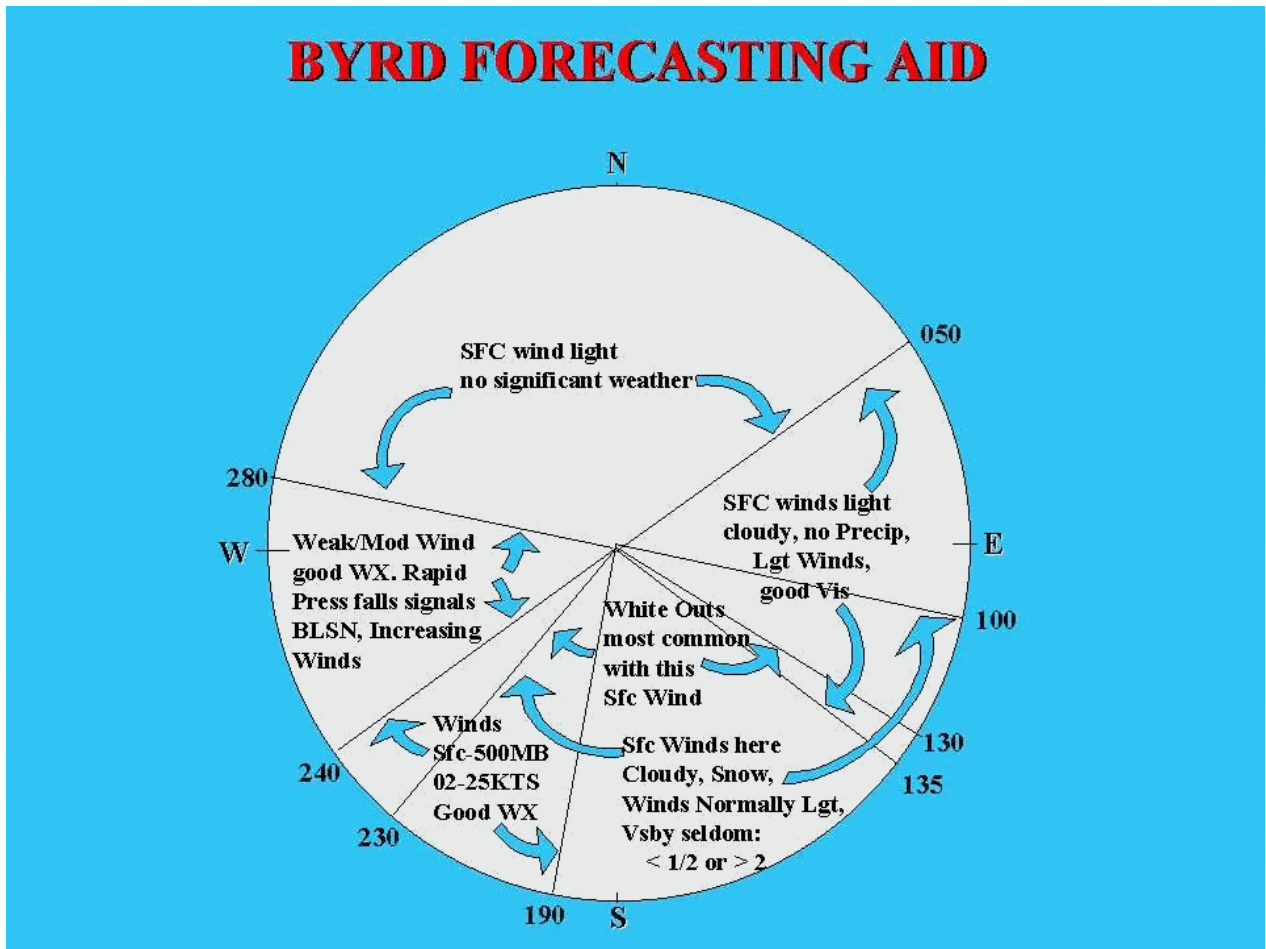
Figure 7.12.6.4.2   Forecasting aid for Downstream Bravo

Icing

No specific information on forecasting has been obtained.

Turbulence

No specific information on forecasting has been obtained.

Hydraulic jumps

No specific information on forecasting has been obtained.

Sea ice

Not relevant at this location.

Wind waves and swell

Not relevant at this location.

7.13   Edward VII Land, Marie Byrd Land, and Ellsworth Land

Edward VII Land, Marie Byrd Land, and Ellsworth Land together span approximately longitudes 160º W to 80º W. From west to east, the stations/features specifically referred to in this section include:

- *Russkaya Station* (74° 46´ S, 136° 52´ W, elev. 124 m AMSL);
- *Mount Sidley* near (77º S, 126º W , peak elev. 4181 m AMSL);
- *Byrd Station* (79º, 59´ S, 120º 00´ W, elev. 1528 m AMSL);
- *Amundsen Sea*;
- *Mount Seelig* near (82º S, 103 º W, peak elev. 3022 m AMSL);
- *Patriot Hills Base* (80º 19´ S, 81º 16´ W, 1,000 m AMSL);
- *Teniente Parodi* (80º 08´ S, 81º 16´ W, 855 m AMSL);
- *Ellsworth Mountains* (peak elev. (Vinson Massif) 4897 m AMSL);
- *Siple Station* (75.90º S, 83.92º W, 1054 m AMSL).

Most of the above places are shown in Figure 7.13.1.

West Antarctica appears to have held meteorological interest in so far as the higher ground might affect the weather at lower altitudes, over for example, the Ross Ice Shelf (see for example Bromwich *et al.*,1994). However, there are no stations currently operating year round and very few summer stations. And so, while some of the information presented below is of a limited nature it seems important to record what data are available.

Although not covered in detail here the US Antarctic Programme operated Siple Station for some years (see for example, Foster (1985), and Heide (1990)) but closed the station in the early nineties. According to A. Cayette (personal communication) Siple Station appears to be in an area where decaying waves and associated occlusions stagnate. With a frequent flow off the ocean from these large–scale systems, an upslope of ice orography, and a continually cooling of the surface air layer as the airmass migrates inland it is understandable why the operation at Siple might close. Climatically Siple Station would appear to be in a location which is windy, with frequent low cloud/fog, and considerable blowing snow.

A. Cayette goes on to advise that the forecasting programme at McMurdo Station currently includes coverage of western Marie Byrd Land. However, for this area the McMurdo office has limited experience and the recent records are restricted to two seasons in the late nineties. The McMurdo office has come up with some conclusions, some limited forecasting tools, and lots of questions which they hope to answer in the near future.

The information supplied below on Byrd Station (now closed) is also of a limited nature but is included to at least give a first impression of the area and is included due to the dearth of available meteorological information on this part of Antarctica.
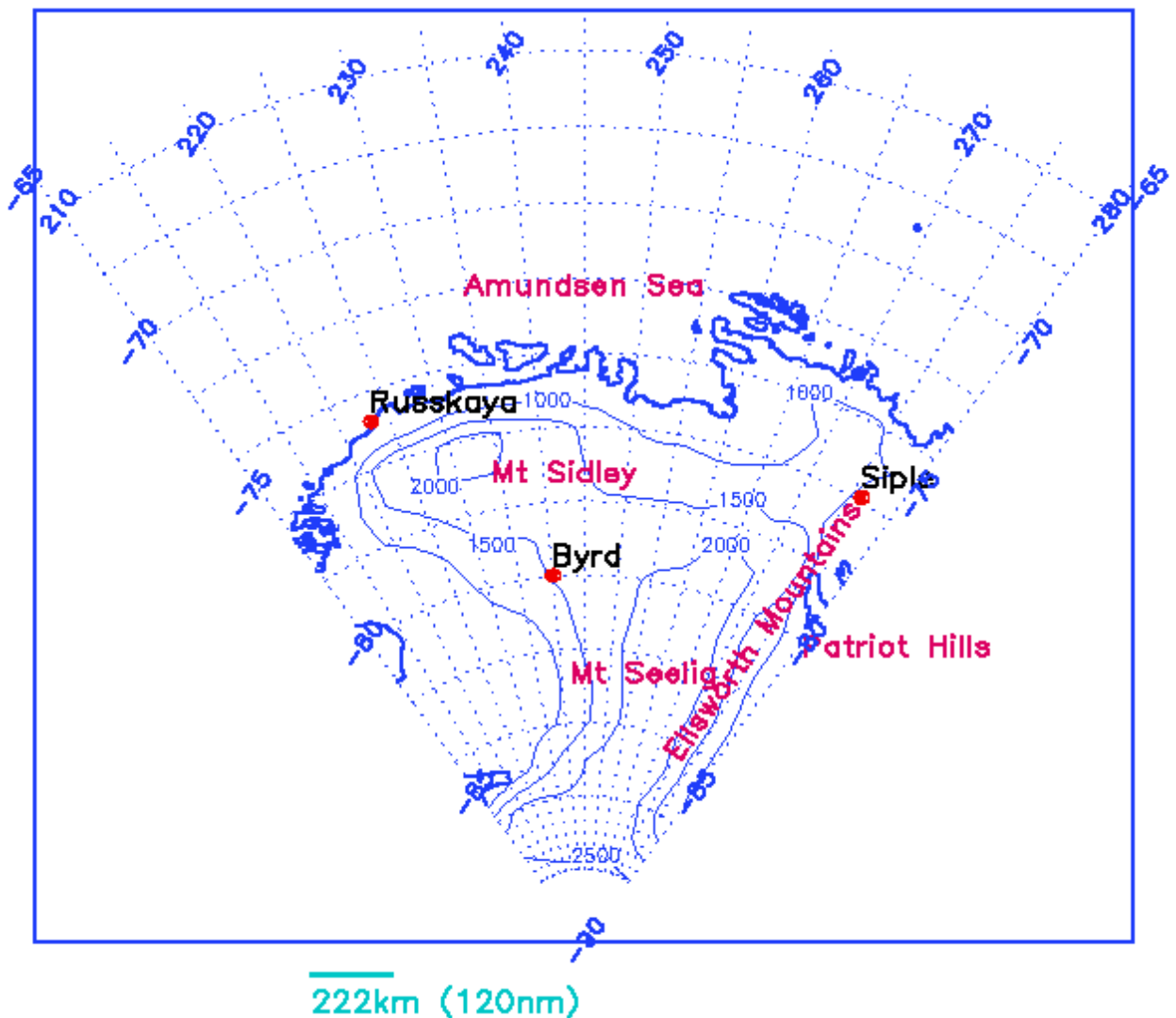
Figure 7.13.1   Sketch map for Edward VII, Marie Byrd and Ellsworth Lands area (contours in metres; the area is bounded by: 90º S, 66º S, 150º W and 80º W).

7.13.1   Russkaya Station

7.13.1.1   <u>Orography and the local environment</u>

Russkaya Station (opened on March 9, 1980, closed on March 12, 1990) was situated Cape Berks (Hobs shore) at 74° 46′ S, 136° 52′ W at an altitude of 124 m above sea level. The coast in the station area is a snow–glacial barrier with a height of 2 to 40 m. From the western side of Cape Berks the coastline turns sharply southward. In this sector of the Ruppert shore the slope of the continental glacial cover towards the pole is 300 m per 10 km. The 100 m contour is 3 km away from the coastline. In the vicinity of the station along the coastline there

is a row of hills with heights of 125–145 m. The orographic features intensify the eastern winds in the surface layer.

The sea bottom in the area of the station has a sharp declination away from the station. The 50 m isobath is at a distance of 200 m from the shore, and the 20 m isobath is at a distance of 100 m from the shore. The ocean bed is of rocky type.

7.13.1.2   Operational requirements and activities relevant to the forecasting process

During its 10 years of operation Russkaya Station was the only scientific base in the immense coastal area between the Ross Sea and Antarctic Peninsula. Therefore the scientific observations carried out there are of great importance. In addition, Russkaya Station is remarkable amongst the coastal Antarctic stations due to the extraordinary values of some meteorological characteristics.

During its period of operation a wide variety of hydro–meteorological, geophysical, astronomical medico – physiological and others observations were carried out at the station. The weather forecast information for crucial activities at the station was provided by the forecasting group at Molodezhnaya Station.

7.13.1.3   Data sources and services provided

Russkaya Station is currently closed.

7.13.1.4   Important weather phenomena and forecasting techniques used at the location

General overview

Typically for a station in this area, extremely severe weather conditions occur because of a combination of low temperatures and very strong winds. The mean annual air temperature recorded over the 10 year period of station occupation was -12.4^0C. The warmest month was January, the coldest was August. The absolute temperature minimum recorded during the occupation of the station was -46.4^0C, and the absolute maximum was $+7.4^0$ C. In the station area blizzards were often observed (about 150 days a year) accompanying by snowfall and by restriction of visibility. Due to orographic factors, easterly winds prevail.

The atmospheric circulation in the Pacific sector of Antarctic is characterized by high variability. Cyclogenesis is more prevalent in the cold period of the year and less common in November – January. The maximal frequency of mobile cyclonic eddies occurs in the area of $60–70^0$ S, and the area of intensive cyclogenesis is located south of Tasmania and New Zealand in the area of $50–60^0$ S. Most cyclonic eddies move along a zonal trajectory, but some systems move along a meridional trajectories from the above mentioned areas toward the Hobs shore. Such tracks are associated with the development of blocking tropospheric highs, orientating north of the Amundsen Sea. The high frequency of depressions north of the station leads to a climatological low north of the Hobs Shore, especially for cold period of the year. In contrast, there is a climatological high pressure area over Marie Byrd Land.

Surface wind and the pressure field

At Russkaya Station the mean annual pressure at sea level (980.9 hPa) is the lowest pressure registered at any Antarctic coastal station. The annual pressure variation is characterized by a maximum value in January and minimum in October. The absolute pressure maximum was 1019.1 hPa. The absolute pressure minimum of 923.4 hPa was lower than any absolute pressure minimum values previously registered at a coastal station. The annual pressure variation amplitude of monthly mean data at Russkaya Station is much higher also, than at other Antarctic station.

The severity of the wind regime is a peculiarity of the climate of the Russkaya Station region. The mean annual wind speed experienced was 12.9 m s^{-1} (~25 kt). The monthly mean wind speed maximum of 18.1 m s^{-1} (~35 kt) was registered in March, the minimum of 9.6 m s^{-1} (~19 kt) in January. The wind speed maximum (excluding January and February) fluctuated between 46–61 m s^{-1} (~89–118 kt). The highest registered wind gust was 77 m s^{-1} (~150 kt) – it was impossible to register stronger wind gusts due to the destruction of the wind anemometer. There was one situation when the wind had speeds of 50–60 m s^{-1} (~97–116 kt) blowing continuously for 16 days. On an average during the year the number of days with wind speed exceeding 15 m s^{-1} (~30 kt) was 264 days and there were 136 days a year with wind speed exceeding 30 m s^{-1} (~60 kt). All the hurricane force winds registered at the station were of cyclonic origin with directions in the range 75–85^0. The downslope south–easterly winds, which are typical for other areas of Antarctic coastline with sharp glacial are not found here. To the west of cyclonic disturbances the wind direction has a west–south–westerly direction, because of the orientation of the shore

All cases of hurricane force winds were associated with the approach of a very active cyclones moving from the northwest to the Marie Byrd Land coastline. Their trajectory was dictated by a blocking high over the Amundsen sea. In such a situation the centres of the lows were located over the ocean west of Russkaya Station and fronts were orientated along the coastline. Hurricane force winds occur because of the above synoptic situation and the particular orography along the coastline.

For successful forecasting of such situations it is necessary to have satellite imagery not less than twice a day. This allows the estimation of the movement of lows. The synoptic maps can give additional information, but they may be poor here due to lack of meteorological data.

It is possible also to predict the wind speed increases up to hurricane force with the help of meteorological observations carried out at the station. The approach of an active cyclone towards the coast is accompanied usually by cirrostratus and altostratus cloud 6–12 hours before the wind speed increase. At the same time a fall of pressure and an increase in temperature of 5–10^0 are registered. The subsequent wind turn towards 75–85^0 precedes the wind speed increase if the wind direction was different earlier. The turn of wind towards the northeast accompanied by a wind speed decrease does not always indicate the end of a storm, because it can be connected with the passage of a front, followed by another cyclone. Sometimes, there is the possibility of two and more cyclonic disturbances passing within a period of about a day, which is the reason for long periods of stormy conditions. Usually the wind drops fully with a turn to the southwest.

Upper wind, temperature and humidity

No specific information on forecasting has been obtained.

Clouds

No specific information on forecasting has been obtained.

Visibility: blowing snow and fog

No specific information on forecasting has been obtained.

Surface contrast including white–out

No specific information on forecasting has been obtained.

Horizontal definition

No specific information on forecasting has been obtained.

Precipitation

No specific information on forecasting has been obtained.

Temperature and chill factor

No specific information on forecasting has been obtained.

Icing

No specific information on forecasting has been obtained.

Turbulence

No specific information on forecasting has been obtained.

Hydraulic jumps

No specific information on forecasting has been obtained.

Sea ice

The main feature of the ice regime in the area of Russkaya Station is the annual wide, solid strip of fast ice and chain of stationary polynyas, formed along the coastline in the summer period. The typical feature of fast ice is its increased stability. Each year it achieves the same maximum size of about 100 km, bounded by shelf area. In the spring–summer period about half of the fast ice is destroyed. In the station area the fast ice breaks down once every 3–4 years. In the case of breakdown of multiyear fast ice the frequent hurricane force winds block (prevent) the formation of stable ice for a long time.

Due to heavy ice conditions the disembarkation at Russkaya Station was carried out by helicopters only.

Wind waves and swell

No specific information on forecasting has been obtained.

7.13.2   Byrd Station

7.13.2.1   <u>Orography and the local environment</u>

Byrd Surface Camp is located at 80º S, 120º W, at an elevation of 1,530m (5,020ft) on the lower plateau of West Antarctica. The camp is some 350 km distant from the Executive Committee Mountain Range (high point being Mount Sidley at 4181 m AMSL) and 400 km away from the Whitmore Mountains located to the southeast of the station, (the highest point being Mount Seelig, 3022 m AMSL). Byrd Station is thus southwest of the ridge line which links these two mountain ranges. The station is also approximately 600 km east–northeast of the Ross Ice Shelf; and some 800 km south–southwest of the Amundsen Sea.

7.13.2.2   <u>Operational requirements and activities relevant to the forecasting process</u>

No specific information on requirements has been obtained.

7.13.2.3   <u>Data sources and services provided</u>

Forecast services are available from McMurdo Station.

7.13.2.4   Important weather phenomena and forecasting techniques used at the location

General overview

At a relatively low altitude (1530 m), Byrd Station (and all camps within the general area) are greatly affected by the intrusion of migratory mid–latitude cyclones. Climatology shows a mean wind from GRID west at 5 m s^{-1} (10 kt), making blowing snow a major flight restriction. Winds are from the sector GRID235 to GRID275 nearly 63 % of the time, and strong winds have essentially the same direction as the mean winds. Mean sky cover is near 4.8 oktas. This high degree of cloudiness is due to the ease with which cyclones can penetrate into the area. Fog banks and blowing snow often move into Marie Byrd Land with little or no warning, due to the poor surface and horizon definition and lack of visual markers to highlight their approach.
        Table 7.13.2.4.1 (from Phillpot, 1967) in Appendix 2 below provides limited monthly mean temperature, station level pressure and cloud data for Byrd Station while Table 7.13.2.4.2, also in Appendix 2 below presents wind frequency data (also from Phillpot, 1967). Figure 7.13.2.4.1 provides a schematic of weather types that may be associated with wind direction.
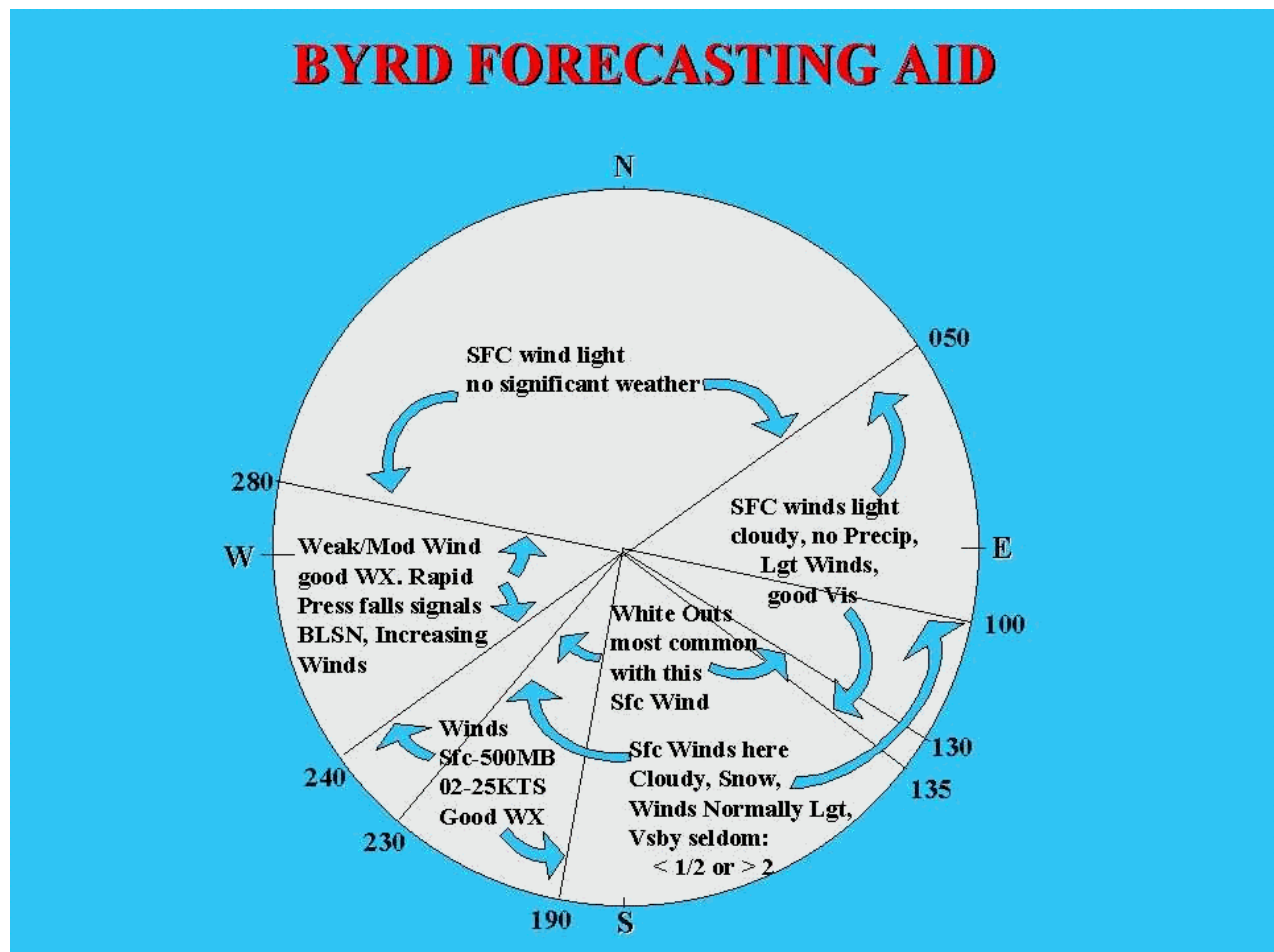
Figure 7.13.2.4.1   Schematic of weather and surface wind associations.

Surface wind and the pressure field

Table 7.13.2.4.2 in Appendix 2 below is a limited record of surface winds at Byrd. It is evident that orography has a controlling influence of the surface wind at Byrd. Low–pressurecentres of 976 hPa or higher in the vicinity or west of Cape Colbeck give Byrd Station good weather, as moisture is drawn off Marie Byrd Land and toward the Ross Ice Shelf. Deeper lows, however, will advect moist air over Marie Byrd Land on the eastern edge of the low, and produce moderately bad weather for Byrd Station and vicinity. Deep lows between Cape Colbeck and Byrd Station produce the worst weather, as significant moisture is advected over West Antarctica. These synoptic patterns can be related to wind directions and speeds as follows:

- Weak or moderate surface winds from GRID235 to GRID275 bring good weather unless the barometer begins a marked drop (in which case expect gusts exceeding 20 m s^{-1} ($\sim$ 40 kt).
- Surface winds from GRID130 to GRID225 are accompanied by cloudiness, fog and/or snow. Winds from GRID215 to GRID225 may be frequently strong. Winds from other directions in this group are normally light. Visibility is seldom less than 900 m ($\sim$ 0.5 nm) or over 3,700 m ($\sim$ 2 nm).
- Surface winds between GRID275 to GRID045 are usually light and of short duration with no significant weather.
- Winds aloft from GRID north produce excellent weather.
- When winds from the surface to 500hPa are from GRID southwest to west and above 13m s^{-1} ($\sim$ 25 kt), look for blowing snow.
- If winds aloft between surface and 500hPa are light/ variable and suddenly all line up from GRID southwest, expect storm conditions.
- Prolonged clear weather with low sun angles produces increasing downslope wind. High sun angles, strong winds, and thick clouds weaken the surface inversion, allowing the gradient winds aloft to have more influence on the surface.

Upper wind, temperature and humidity

No specific information on forecasting has been obtained.

Clouds

With the intrusion of mid–latitude migratory cyclones over Marie Byrd Land, Byrd Station can experience a wide variety of sky conditions. Stratus, altostratus, cirrus, cirrostratus, and altocumulus are all seen at Byrd Station.

Visibility: blowing snow and fog

Very few visibility markers exist at Byrd Station. Although visibility is generally good, obstructions to vision can move into the area virtually undetected due to poor horizon definitions.

Blowing snow is the primary flight restriction at Byrd Station. When the sun is high and no fresh snow has fallen, wind speeds above 13 m s^{-1} (~ 25kt) are required to reduce visibility rapidly. With fresh snow, however, the critical speed for significant blowing snow drops to about 9 m s^{-1} (~ 18 kt). When satellite imagery shows clouds streaking off the tops of the mountains to the GRID south and GRID west of Byrd Station, blowing snow can be forecast at Byrd Station with reasonable confidence.

The other restriction to visibility at Byrd Station is fog. During the summer, fog is most prevalent during the early morning when low sun angles strengthen the surface inversion. "Camp Fog", as at South Pole Station, can create IFR conditions at Byrd Station when temperatures are below –20°C (–4°F).

Surface contrast including white–out

No specific information on forecasting has been obtained except see Figure 7.13.2.4.1

Horizontal definition

No specific information on forecasting has been obtained.

Precipitation

Precipitation occurs with migratory cyclones. The primary form of precipitation at Byrd Station is snow.

Temperature and chill factor

With light winds, a sudden clearing of the skies will result in a temperature drop of 7°C to 12°C (10°F to 20°F) within an hour. Likewise, a sudden clouding over raises the temperature 7°C to 12°C (10°F to 20°F) within an hour. The temperature changes decrease as wind speed increases.

Icing

No specific information on forecasting has been obtained.

Turbulence

No specific information on forecasting has been obtained.

Hydraulic jumps

No specific information on forecasting has been obtained.

Sea ice

Not relevant at this location.

Wind waves and swell

Not relevant at this location.

7.13.3   The Patriot Hills – Teniente Parodi

7.13.3.1   <u>Orography and the local environment</u>

The Patriot Hills are in the Heritage Range at the southernmost end of the Ellsworth Mountains, to the west of the Ronne Ice Shelf. From 1987, Adventure Network International (ANI) has operated a blue ice runway during the summer season of November to February at their Patriot Hills Camp (also known as Base Camp) (80° 19' S, 81° 16' W, 1,000 m (~3280 ft) elevation). In 1995 the Chilean Antarctic Institute and the Chilean Air Force established a field camp named Teniente Parodi at 80° 08′ S, 81° 16′ W, (855 m AMSL) which is close to the ANI site. The Teniente Parodi field camp is deployed about 1000 m to the north of a blue ice area located along the northern side of Patriot Hills, and which is used as runway for large wheeled aircraft.

7.13.3.2   <u>Operational requirements and activities relevant to the forecasting process</u>

ANI use Hercules C–130 aircraft to fly to the Patriot Hills runway from Punta Arenas, Chile. They often have a meteorological observer at the station during the summer. Hourly METARs are available, although no forecasts are available. The Chilean Air Force require weather forecasts for their air operations.

7.13.3.3   <u>Data sources and services provided</u>

The Chilean Air Force obtain forecasts from the (Frei) Antarctic Meteorological Center on King George Island. Their Patriot Hills Station is occupied from early October to late January with there being a forecaster and an observer located at the station. The meteorological office prepares forecasts for the local area and for other areas of aviation interest. Forecasts for up to 24 hours ahead are prepared. TAFs are available from Patriot Hills by HF radio. Satellite

imagery is available along with various meteorological charts. The ANI operation make surface meteorological observations at the camp and have a satellite imagery receiver.

7.13.3.4   <u>Important weather phenomena and forecasting techniques used at the location</u>

General overview

The Patriot Hills are well south of the circumpolar trough so there is not the constant passage of depressions that is found at more northerly stations. However, the area is often on the edge of depressions and some systems do reach the area. Depressions seem to arrive via two means. Firstly, a system passes from the Bellingshausen Sea across the base of the Antarctic Peninsula and onto the Ronne Ice Shelf. These systems give moderate winds, overcasts skies and some snow. Secondly, a more rare event involves a low tracking westwards from the eastern Weddell Sea, over the Ronne Ice Shelf towards the Patriot Hills. When this happens the system can stay in the Patriot Hills area until it fills, usually giving large quantities of snow.

As well as synoptic–scale depressions, the area can be affected by mesoscale lows that are a common feature on the Ronne Ice Shelf.

Surface wind and the pressure field

The Patriot Hills is a very windy area with the presence of blue ice indicating the strength and persistence of the surface winds. However, the area is also characterised by the highly variable nature of the wind, with some very marked local wind speed variations. At the ANI site there are reports of 17–18 m s^{-1} (~34 kt) winds on the ice runway and less than 5 m s^{-1} (~10 kt) at the camp, about 1 km directly downwind of the runway. This appears to be a very common occurrence. Moreover, katabatic winds can gust up to 50 m s^{-1} (~100 kt) but more generally blow at a steady 5–8 m s^{-1} (~10–15 kt).

After the passage of a weather system observers at the ANI camp report that there would be a short period (half a day or so) of calm, clear weather. During this period snow could be observed blowing through the cols and off the peaks of the mountain ranges to the south and southwest. It would become apparent that strong winds were approaching and within a few hours the winds would pick up on the runway and then at the Patriot Hills camp itself. These winds could last for several days and clear skies were not uncommon.

Based on three years of record from Teniente Parodi the average wind direction at this camp prevails most of the time from the south-southwest (constancy above 0.85) with a mean speed about 5.3 m s^{-1} (~10 kt). However, stronger wind events above 10 m s^{-1} (~20 kt) were frequently observed at the camp (30% of the total time). On average, the wind speed decreases as the summer season becomes established.

The smoothed pressure behavior (four-day running mean) indicates a synoptic-scale oscillation between maximum and minimum values on a five to six day cycle. Analysis of meteorological charts reveals that this behavior is, in fact, associated with passing synoptic-scale cyclones (troughs) and ridges to the north of Patriot Hills, which affect the Bellinghausen and Weddell seas and surrounding areas.

Upper wind, temperature and humidity

No specific information on forecasting has been obtained.

Clouds

Cloud is highly variable in this area. Depressions can bring extensive cloud cover, but there are also long periods of cloud–free conditions. In addition, satellite imagery reveals non–frontal cloud can linger for long periods in the area.

Visibility: blowing snow and fog

Fog has been reported on a number of occasions. On one of these a large fog bank moved in from the south (and nearly forced an incoming flight to turn back). On occasions Patriot Hills camp would be clear but surrounded by fog, sheltered in the lee of the hills.

Surface contrast including white–out

Poor contrast is a regular feature of the Patriot Hills, particularly when under the influence of low–pressuresystems.

Horizontal definition

No specific information on forecasting has been obtained.

Precipitation

Depressions can bring long periods of moderate or heavy snowfall to the area.

Temperature and chill factor

During the summer season temperatures are typically around -15°C, but there are reports that temperatures can be as low as -30°C in October and as high as -5°C in December. Although no one has over–wintered in this area, winter temperatures are estimated to be around -40°C.

Based on three years of record from Teniente Parodi the overall behavior of the air temperature at the camp behaves as expected in that the temperature increases as direct solar radiation increases, in other words, as the summer approaches. The average daily oscillation in temperature at the camp is around 2ºC while the average linear increase of the temperature from the beginning of November to mid-December is around 0.5ºC per day.

Icing

No specific information on forecasting has been obtained.

Turbulence

Mechanical and lee turbulence can be experienced along the length of the blue ice runway.

Hydraulic jumps

No specific information on forecasting has been obtained.

Sea ice

Not relevant at this location.

Wind waves and swell

Not relevant at this location.

8   REFERENCES

Adams, N. (1996), The detection and analysis of a gravity wave observed over Casey in East Antarctica using radiosonde data, *Aust. Met. Mag.* **45**, 219–32.

Adams, N. (1997), Model prediction performance over the Southern Ocean and coastal region around East Antarctica, *Aust. Met. Mag.* **46**, 287–96.

Adams, N., H. Hutchinson and T. Hart (1999), An analysis of TOVS data during the FROST Special Observing Periods, *Aust. Met. Mag.* **50,** 12–42.

Alishouse, J., S. Snyder, J. Vongsathorn and R. Ferraro (1990), Determination of oceanic total precipitable water from the SSM/I, *IEEE Trans. Geosci. Remote Sens*ing, **28**, 811–16.

Allison, I. (1986), *SCAR Antarctic Climate Research Newsletter No. 1*, I. Allison, editor, Scott Polar Research Center, Cambridge.

Allsion, I. (1989), Pack–ice drift off east Antarctica and some implications, *Ann. Glaciol.* **12**, 1–8.

Alpert, P. and J. Neumann (1983), Simulation of Lake Michigan's winter land breeze on 7 November 1978, *Mon. Wea. Rev.* **111,** 1873–81.

Anderson, R. K. and collaborators (1969), Application of meteorological satellite data in analysis and forecasting, *ESSA Technical Report NESC 51.* NOAA, Washington DC, USA.

Astapenko, P. D. (1964), Atmospheric processes in the high latitudes of the Southern Hemisphere, *Israel Program for Scientific Translations*, Jerusalem, 286 pp.

Australian Bureau of Meteorology (1973), Internal memo: Services Circular 40/1538 of 16 May 1973.

Australian Bureau of Meteorology (1981), *Manual of meteorology part 2: aviation meteorology*, Australian Gov. Publishing Service, pp131.

Australian Bureau of Meteorology (1984), *Short–term forecasting manual*, Australian Bureau of Meteorology, Melbourne, 200 pp.

Australian Bureau of Meteorology (1991), *Australian Antarctic Forecasters' Handbook*. Version 2, Tasmania and Antarctica Regional Office, Australian Bureau of Meteorology.

Baba, K. (1993), Relationship between position of long wave upper–air westerly trough and weather condition of geological survey area in the Antarctic Ocean. In: *Proc. of the NIPR Symposium on Polar Meteorology and Glaciology*. **45**, 3–118.

Bacci, G. and A. Pelligrini (1996), Operational meteorology at Terra Nova Bay. In*: Italian Geophysical Observatories in Antarctica*. A. Meloni and A. Morelli, editors, Instituto Nazionale di Geofisica, Rome, pp. 151–62.

Bader, M. J., G. S. Forbes, J. R.Grant, R. B. E. Lilley and A. J.Waters (1995), *Images in Weather Forecasting: A practical Guide for Interpreting Satellite and Radar Imagery,* Cambridge University Press. 498pp.

Ball, F. K. (1956), The theory of strong katabatic winds, *Aust. J. Phys*, **9**, 373–86.

Ball, F. K. (1960), Winds on the ice slopes of Antarctica. In: *Antarctic Meteorology: proceedings of the symposium held in Melbourne, February 1959,* Pergamon Press, 483 pp.

Ballish, B., X. Cao, E. Kalnay and M. Kanamitsu (1992), Incremental nonlinear normal mode initialisation, *Mon. Wea. Rev*. **120**, 1723–34.

Beckwith, W. B. (1976), Early days of airline meteorology, *Bull Amer. Met. Soc*. **57**, 1327–29

Bell, I. D., J. Wilson and N. Weston (1988), Satellite *Cloud Imagery Interpretation Guide* Bureau of Meteorology Training School.

Bergeron, T. (1959) *Methods in scientific weather analysis and forecasting. The Atmosphere and Sea in Motion*, Rockefeller Institute Press, New York , pp.440–74.

Bernstein, B. C., T. A. Omeron, F. McDonough and M. K. Politovich (1997), The relationship between aircraft icing and synoptic–scale weather conditions, *Wea. and For*. **12**, 742–762.

Berry, F. A., E. Bollay and N. R. Beers(1945), *Handbook of Meteorology*, McGraw–Hill. 1068 pp.

Blakers, A. (1983), *Internal Report to Bureau of Meteorology Australia on an attachment as meteorologist to the ANARE summer expedition, December 1982 to February 1983*.

Bjerknes, J. and H. Solberg (1922), Life cycle of cyclones and the polar front theory of atmospheric circulation, *Geofys. Publ., Norske Videnskaps–Akad, Oslo* **3**, pp.1–18.

Bluestein, H. B. (1993a), *Synoptic–Dynamic Meteorology in Midlatitudes. Volume I. Principles of kinematics and dynamics*, Oxford University Press, 431 pp.

Bluestein, H. B. (1993b), *Synoptic–Dynamic Meteorology in Mid–latitudes. Volume II: Observations and theory of weather systems*, Oxford University Press, 594 pp.

Bourke, W., R. Seaman, G. Embery, B. McAvaney, M. Naughton, T. Hart and L. Rikus (1990), *The BMRC Global Assimilation and Prediction System*, ECMWF Seminar Series.

Bradbury, T. A. N. (1977), The use of wet–bulb potential temperature charts, *Met. Mag. Lond*. **106**, 233–50.

Brighton, P. W. M. (1978), Strongly stratified flow past three–dimensional obstacles, *Quart. J. Roy. Met. Soc*. **104**, 289–300.

British Antarctic Survey (1997), *Weather Forecasting Manual*. Edited By J. Turner, T. A. Lachlan–Cope and R. Ladkin, Version 2.0, September 1997, Cambridge.

Bromwich, D. H. (1988), Snowfall in high southern latitudes, *Rev. of Geophys*. **26**, 149–68.

Bromwich, D. H. (1989), An extraordinary katabatic wind regime at Terra Nova Bay, Antarctica, *Mon. Wea. Rev*. **117**, 688–95.

Bromwich, D. H., and T. R. Parish (1998), Meteorology of the Antarctic. In: *Meteorology of the Southern Hemisphere*, D. J. Karoly and D. G. Vincent, editors, American Meteorological Society, Boston, pp. 175–200.

Bromwich, D. H., Yang, Du and T. R. Parish (1994), Numerical simulation of winter katabatic winds from west Antarctica crossing the Siple Coast and the Ross Ice Shelf, *Mon. Wea. Rev*. **122**, 1417–35.

Brown, R. 1973, New indices to locate clear–air turbulence, *The Met. Mag*. **102**, 347–61.

Browning, K. A. and T. W. Harrold (1970), Air motion and precipitation growth at a cold front, *Quart. J. Roy. Met. Soc.* **96**, 369–89.

Budd, W. F., D. Jenssen, E. Mavrakis and B. Coutts (1994), Modelling the Antarctic ice–sheet changes through time, *Ann. Glaciol*. **20,** 291–7.

Bureau of Meteorology (1983), *Analysis Techniques and Synoptic meteorology*, (Internal training document.)

Businger, S. and R. J. Reed (1989), Cyclogenesis in cold air masses, *Wea. and For*. **4**, 133–55.

Byers, H.R. (1959), *General Meteorology*, McGraw–Hill. 540 pp.

Callaghan, J. (1984), Internal Report to Bureau of Meteorology Australia on the 1983/84 summer aviation weather forecasting support at Davis Station Antarctica.

Callaghan, J .J. and M. S. Betts. (1987), Some cases of westward moving disturbances in the Mawson–Davis area, Antarctica, *Aust. Met. Mag*. **35**, 79–85.

Carleton, A. M. (1979), A synoptic climatology of satellite–observed extratropical cyclone activity for the Southern Hemisphere winter, *Arch. Met. Geophys. and Biocl. B* **27**, 265–79.

Carleton, A. M. (1983), Variations in Antarctic sea ice conditions and relationships with Southern Hemisphere cyclonic activity, winters 1973–77, *Arch. Met. Geophys. and Biocl. **B.** **32***, 1–22.

Carleton, A. M. and D. A. Carpenter (1990), Satellite climatology of "polar lows" and broadscale climatic associations for the Southern Hemisphere, *Int. J. Climat. 10,* 219–46.

Carleton, A. M., L. A. McMurdie, H. Zhao, K. B. Katsaros, N. Mognard, and C. Claud (1993), Satellite microwave sensing of Antarctic ocean mesocyclones. In: *Proceedings of the Fourth International Conference on Southern Hemisphere Meteorology and Oceanography*, March 29–April 2, 1993, Hobart, Australia, AMS, Boston. pp. 497–98.

Carleton, A. M., L. A. McMurdie, K. B. Katsaros, H. Zhao, N. M. Mognard, and C. Claud (1995), *The Global Atmosphere and Ocean System* **3**, 209–48.

Carlson, T. N. (1980), Airflow through mid–latitude cyclones and the comma cloud pattern, *Mon. Wea. Rev.* **108**, 1498–1509.

Carrasco, J. F. and D. H. Bromwich (1996), Mesoscale cyclone activity near Terra Nova Bay and Byrd Glacier, Antarctica during 1991, *The Global Atmosphere and Ocean System*, **5**, 43–72.

Clapperton, C. M. (1990), Quaternary glaciations in the Southern Ocean and Antarctic Peninsula area. *Quart. Sci. Rev.* **9,** 229–52.

Claud, C., K. B. Katsaros, G. W. Petty, A. Chedin, and N. A. Scott (1992), A cold air outbreak over the Norwegian Sea observed with the TIROS–N Operational Vertical Sounder (TOVS) and the Special Sensor Microwave Imager (SSM/I), *Tellus* **44a**, 100–18.

Comiso, J. C., D .J. Cavalieri, C. L. Parkinson, P. Gloersen (1997) Passive Microwave Algorithms for Sea Ice Concentration: A comparison of two techniques, *RemoteSens. Environ.* **60**, 357–84.

Crapper, G. D. (1984), *Introduction to Water Waves*, Ellis Harwood, 224 pp.

Crisp, C. A. (1979), Training Guide for Severe Weather Forecasters, **AFGWC/TN–79/002**, Air Weather Service (MAC), US Air Force, 74 pp.

Cullather, R. I., D. H. Bromwich and R. W. (1997), Validation of operational numerical analyses in Antarctic latitudes, *J. Geophys. Res.* **102**,13761–84.

Daley, R. (1991), *Atmospheric Data Analysis*, Cambridge University Press, 457 pp.

Dalu, G., C. Prabhakara and J. Nuccarione. (1993), Optimization of an algorithm for the estimation of rainfall from the SSM/I data, *J. Met. Soc. Jap.* **71**, 419–24.

Dalrymple, P.C. (1966), A physical climatology of the Antarctic Plateau. In*: Studies in Antarctic Meteorology (Antarctic Research Series, Vol. 9)*, M. J. Rubin, Ed., AGU, 231 pp.

Davidson, N. E. and K. Puri (1992), Tropical prediction using dynamical nudging, satellite defined convective heating, and a cyclone bogus, *Mon. Wea. Rev*. **120**, 2501–22.

Derber, J. (1989), A variational continuous assimilation technique, *Mon. Wea. Rev*. **117**, 2437–46.

Doake, C. S. M. and D. G. Vaughn (1991), Rapid disintegration of the Wordie ice shelf in response to atmospheric warming, *Nature,* **350,** 328–30.

Domack, E. W., S. E. Ishman, A. B. Stein, C. E. McClennen and A .J. T. Jull (1995), Late Holocene advance of the Müller ice shelf, Antarctic Peninsula, sedimentological, geochemical, and palaeontological evidence, *Antarctic Sci*. **7**, 159–170.

Ebert, E. E. and J. L. McBride (1997), *Methods for verifying quantitative precipitation forecasts: application to the LAPS model 24–hour precipitation forecasts*, Bureau of Meteorology Research Centre Techniques Development Report No.2, 87pp.

Ellrod, G. P. (1989), Decision tree approach to clear air turbulence analysis using satellite and upper–air data, In: *United States. National Oceanic and Atmospheric Administration, National Environmental Satellite, Data, and Information Services, Wash., D.C., Technical Memorandum (NOAA TM NESDIS 23),* 20 p.

Ellrod, G. P. and D. I. Knapp (1992), An objective clear–air turbulence forecasting technique: verification and operational use, *Wea. and For*. **7**, 150–65.

Facquet, R. A. (1982), *A synoptic/statistical analysis of summer season circulation patterns over eastern Antarctica during moist air intrusions*, M. Sc. thesis, Naval Postgraduate School, 84 pp.

Ferraro, R. R., S. J. Kusselson and M. Colton (1998), An introduction to passive microwave remote sensing and its applications to meteorological analysis and forecasting. In: *National Weather Digest*, **22**, pp.11–23.

Förchtgott, J. (1969), Evidence for mountain–sized lee eddies, *Wea.,* 255–60

Foster, M. S. (1985), Aviation support of the US Antarctic program, *Ant. J. of the US*, **17**, 265–66.

Fraedrich, K. and Leslie, L. (1991), Predictability studies of the Antarctic atmosphere, *Aust. Met. Mag.*, **39**, 1–9.

Francis, J. A. (1994), Improvements to TOVS retrievals over sea ice and applications to estimating Arctic energy fluxes, *J. Geophys. Res*., **99**, 10,395–408.

Fritts, D. C., T. L. Palmer, O. Andreassen and I. Lie, I. (1996), Evolution and breakdown of Kelvin–Helmholtz billows in stratified compressible flows. Part I: Comparison of two– and three dimensional flows, *J. Atmos. Sci* **53**, 3173–91.

Fujita, T. (1963), Analytical Meso–meteorology: A Review, *Met. Monographs* **5**, (27), Amer. Met. Soc. 77–125.

Gallée, H., P. Pettré and G Schayes (1996), Sudden cessation of katabatic winds in Adélie Land, Antarctica, *J. App Met*. **35**, 1142–52.

Gallée, H. and P. Pettré (1998), Dynamical constraints on katabatic wind cessation in Adélie Land, Antarctica, *J. Atmos*. Sci. **55**, 1755–70.

Gibson, J. K., A. Hernandez, P. Kållberg, A. Nomura, E. Serrano, and S. Uppala (1996), Current status of the ECMWF re–analysis project. In: *Proceedings of the Seventh Conference on Global Change Studies*, American Meteorological Society, Boston. pp. 112–15.

Gibson, T. T. (1989), A Climatology of mid–tropospheric wind maxima over the coast of East Antarctica. In: *Extended abstracts of ASAC Conference and Workshop on Antarctic Weather and Climate, Adelaide, July1989*, pp. 48–51.

Golden, J. H. C. F. Chapell, C. G. Little, A. H. Murphy, E. B. Burton and E. W. Pearl (1978), What should the NWS be doing to improve short–range weather forecasting? – a panel discussion with audience participation 12 April 1978, Boulder, Colo., *Bull. Amer. Met. Soc.* **59**, 1334–42.

Goodberlet, M. A., C. T. Swift and J. C. Wilkerson (1989), Remote sensing of ocean surface winds with the Special Sensor Microwave/Imager, J. *Geophys. Res*. **94**, 14547–55.

Grace, W. and I. Holton (1988), A mechanism for downslope winds with special reference to the Adelaide Gully wind, *Met. Note 179*, Bureau of Meteorology, Melbourne.

Green, J. S. A., F .H. Ludlam and J. F .R. McIlveen (1966), Isentropic relative flow and parcel theory, *Quart. J. Roy. Meteor. Soc.* **92**, 210–19.

Greenpeace (1997), Polar Meltdown. http://www.greenpeace.org/meltdown. (Editor's Note, March, 2000: This file is no longer available at the Greenpeace Web site.)

Grigioni P., L. De Silvestri, A. Pellegrini, R.Sarao (1991), Some climatological aspects in the Terra Nova Bay Area, Antarctica, In: *Proceedings of the 4th Workshop Italian Research on Antarctic Atomosphere,* pp.97–121.

Grody, N. C. (1993), Remote sensing of the atmosphere from satellites using microwave radiometry. In: *Atmospheric Remote Sensing by Microwave Radiometry*, M. A. Janssen editor, John Wiley, New York, pp. 259–334

Groen, P. and R. Dorrestein (1976), Zeegolven. KNMI Opstellen op Oceanografisch en Maritiem Meteorologisch Gebied, 11.

Guymer, L. B. (1978), *Operational application of satellite imagery to synoptic analysis in the Southern Hemisphere*, Australian Bureau of Meteorology Technical Report 29, 87 pp.

Haltiner, G. J. and R. T. Williams (1980), *Numerical prediction and dynamic meteorology*, Wiley, 477 pp.

Hasselman, K.,T. P. Barnettt, E. Bouws, H. Carlson, D. E. Cartwright, K. Enke, J. A. Ewing, H. Gienapp, D. E. Hasselman, P. Kruseman, A. Meerburg, P. Muller, D. J. Olbers, K. Richter, W. Sell, W. and H. Walden (1973), Measurements of wind–wave growth and swell decay during the joint North Sea wave project (JONSWAP), *Deut. Hydrogr. Z.* **A8.**

Hasselman, S., K. Hassleman, E. Bauer, P. A. E. M. Janssen, G. J. Komen. G.J., L. Bertotti, P. Lionello, A. Guillaume, V. C. Cardone, J. A. Greenwood, M. Reistad, L. Zambresky and J. A. Ewing (1988), The WAM model – A Third Generation Wave Prediction Model, *J. Phys. Oceanogr.* **18**, 1775–810.

Heide, G. H. (1990), US weather observations in Antarctica, *Ant. J. of the US.* **22**, 309–10.

Heinemann, G. (1990), Mesoscale vortices in the Weddell Sea region (Antarctica), *Mon. Wea. Rev.* **118**, 779–93.

Heinemann, G. and C. Claud (1997), Report of a workshop on 'Theoretical and observational studies of polar lows' of the European Geophysical Society Polar Lows Working Group, *Bull. Amer. Met. Soc.* **78**, 2643–58.

Hines, K. M., D. H. Bromwich and T. R. Parish (1995), A mesoscale modelling study of the atmospheric circulation of high southern latitudes, *Mon. Wea. Rev.* **123**, 1146–65.

Hirschberg, P. A., M. C. Parke, C. H. Wash, M. Mickelinc, R. W. Spencer and E. Tahaler, (1997), The usefulness of MSU3 analyses as a forecasting aid: a statistical study, *Wea. and For.* **12**, 324–46.

Holmes, R. E., C. R. Stearns, G. A. Weidner, and L. M. Keller (2000), Utilization of automatic weather station data for forecasting high wind speeds at Pegasus Runway, Antarctica, *Wea. and For.* **15**, pp. 137–51.

Hoskins, B. J., M. E. McIntyre and A. W. Robinson (1985), On the use and significance of isentropic potential vorticity charts, *Quart. J. Roy. Meteor. Soc.* **111**, 877–946.

Hulbe, C. L. (unpublished), Stability of the new (1995) Northern Larsen Ice Shelf.

Hutchinson, H. A., S. Dixon, L. Marsh, L. H. Cowled, S. F. Pendlebury, H. R. Phillpot, M. J. Pook and J. Turner (1999), Re–analysis of weather data for Antarctica and the Southern Oceans during the FROST Project. *Wea. and For.* **14,** 909–19.

Huybrechts, P. and J. Oerlemans 1990, Response of the Antarctic ice sheet to future Greenhouse warming, *Clim. Dynamics* **5**, 93–102.

Jacka, K. J. (1997), Impact of ERS–1 Scatterometer Wind Data in the Australian Bureau of Meteorology Global Data Assimilation and Prediction System, In: *Proceedings of the Fifth International Conference on Southern Hemisphere Meteorology and Oceanography, Pretoria, South Africa, 7–11 April 1997*, American Meteorological Society, Boston, pp. 41–42.

Janssen, M. A. (1993), An introduction to the passive microwave remote sensing of atmospheres. In: *Atmospheric Remote Sensing by Microwave Radiometry*, M. A. Janssen editor, John Wiley, New York, pp. 1–34.

Johnson, R. H. (1984), Mesoscale weather effects of variable snow cover over northeast Colorado*, Mon. Wea. Rev*. **112**, 1141–52.

Joly, A., D. Jorgensen, M. A. Shapiro, A. Thorpe, P. Bessemoulin, K. A. Browning, J. P. Cammas, J. P. Chalon, S. A. Clough, K. A. Emanuel, L. Eymard, R. Gall, P. H. Hildebrand, R. H. Langland, Y. Lemaître, P. Lynch, J. A. Moore, P. O. G. Persson, C. Snyder and R. M. Wakimoto (1997), The Fronts and Atlantic Storm–Track Experiment (FASTEX): Scientific objectives and experimental design, *Bull. Amer. Met. Soc.* **78**, 1917–40.

Jones, D. A. and I. Simmonds (1993a), A climatology of Southern Hemisphere extratropical cyclones, *Climate Dynamics* **9**, 131–45.

Jones, D. A. and I. Simmonds (1993b), Time and space spectral analyses of Southern Hemisphere sea level pressure variability, *Mon. Wea. Rev*. **121**, 661–72.

Jones, P. D. and D. W. Limbert (1987), *A data bank of Antarctic surface temperature and pressure data. Office of energy research, report no. TR038*, United States Dept. of Energy, Washington, DC, 52 pp.

Jones, P. D. (1990), Antarctic temperatures over the present century – A study of the early expedition record, *J. Climate* **3**, 1193–203.

Junker, N. W. (1977), Estimation of surface pressure from satellite cloud patterns, In: *Mariners Log*, London.

Kalnay, E., M. Kanamitsu, R. Kistler, W. Collins, D. Deaven, L. Gandin, M. Iredell, S. Saha, G. White, J. Woollen, Y. Zhu, M. Chelliah, W. Ebisuzaki, W. Higgins, J. Janowiak, K. C. Mo, C. Ropelewski, J. Wang, A. Leetmaa, R. Reynolds, R. Jenne and D. Joseph (1996), The NCEP/NCAR 40–year reanalysis project, *Bull. Amer. Met. Soc.* **77**, 437–71.

Kaneto, S. (1982), Billow clouds observed at the Mizuho Plateau, East Antarctica. In: *Memoirs, Special Issue No. 24*, National Institute of Polar Research, Tokyo, pp. 65–69.

Karoly, D. J. (1989), Southern Hemisphere circulation features associated with El Niño–Southern Oscillation events, *J. Climate*. **2**, 1239–52.

Kep, S. L. (1984), *A climatology of cyclogenesis, cyclone tracks and cyclolysis in the Southern Hemisphere for the period 1972–81*, Publication No. 25, Department of Meteorology, University of Melbourne.

Keys, H. J. R., S. S. Jacobs, and D. Barnett (1990), The calving and drift of iceberg B–9 in the Ross Sea, Antarctica, *Ant. Sci*., Oxford, **2**, 243–57.

Keys, H. J. R., S. S. Jacobs, and L. W. Brigham (1998), Continued northward expansion of the Ross Ice Shelf, Antarctica, *Annals of Glaciol.* 27, 93–8.

Keyser, D., and M .A. Shapiro (1986), A review of the structure and dynamics of upper–level frontal zones, *Mon. Wea. Rev.* **114**, 452–99.

Kidder, S. Q. and T. H. Vonder Haar (1995), *Satellite Meteorology: An Introduction*, Academic Press, San Diego, 466 pp.

King, J. C. (1994), Recent climate variability in the vicinity of the Antarctic Peninsula, *Int. J. Climatol.* **14**, 357–69.

King, J. C. and J. Turner (1997), *Antarctic meteorology and climatology*, Cambridge University Press. 409 pp.

Knox, J. A. (1997), Possible mechanisms of clear–air turbulence in strongly anticyclonic flows, *Mon. Wea. Rev.* **125**, 1251–59.

Kobayashi, S. (1982), Observations of an atmospheric gravity wave by shear instability in katabatic wind at Mizuho Station, East Antarctica. In: *Memoirs, Special Issue No. 24*, National Institute of Polar Research, Tokyo, pp. 46–56.

Komen, G. J. and N. R. Smith (1999), Wave and Sea Level Monitoring and Prediction in the Service Module of the Global Ocean Observing System (GOOS), *J. Mar. Sys.* **19**,235–50.

Kozo, T. L. (1982a), Observational study of sea breezes along the Alaskan Beaufort Sea coast, Part 1*, J. of App. Met.* **21**, 891–905.

Kozo, T. L. (1982b), Mathematical model of sea breezes along the Alaskan Beaufort Sea coast, Part 2*, J. of App. Met.* **21**: 906–24.

Lachlan–Cope, T. A. (1992), The use of a simultaneous physical retrieval scheme for satellite derived atmospheric temperatures: Weddell Sea, Antarctica, *Int. J. Remote Sensing*, **13**, 141–54.

Lamb, H. H. and G. P. Britton (1955), General atmospheric circulation and weather variations in Antarctic, *The Geographical Journal*, **121**, 334–49.

Launiainen, J. and T.Vihma (1994), On the surface heat fluxes in the Weddell Sea. In: *The Polar Oceans and Their Role in Shaping the Global Environment*, O. M. Johannessen, R. D. Muench and J. E. Overland, editors, American Geophysical Union, Washington, DC, pp. 399–419.

Leighton, R. M. (1992), Monthly anticyclonicity and cyclonicity in the Southern Hemisphere: Averages for March and September, *Wea. and Clim.* **12**, 76–82.

Leighton, R.M. (1997), Variations in annual cyclonicity across the Australasian region during the 29 year period 1965–1993. In: *Proceedings of the Fifth International Conference on Southern Hemisphere Meteorology and Oceanography*, Pretoria, South Africa, 7–11 April 1997, Boston, American Meteorological Society, 362–63.

Leighton, R.M. and R. Deslandes (1991), Monthly anticyclonicity and cyclonicity in the Australasian region: Averages for January, April, July and October. *Aust. Met. Mag. 39,* 149–54.

Leighton, R. M., K. Keay and I. Simmonds (1997), Variations in annual cyclonicity across the Australian region for the 29–year period 1965–1993 and relationships with annual Australian rainfall. In: *Climate Prediction for Agricultural and Resource Management.* R. K. Munro, and L. M. Leslie, Eds., Bureau of Resource Sciences, Australia, 257–67.

Le Marshall, J. F., G. A. M. Kelly and D. J. Karoly (1985), An atmospheric climatology of The Southern Hemisphere based on ten years of daily numerical analyses (1972–82), an overview, *Aust. Met. Mag*. **33**, 65–85.

Leonard, S., J. Turner and S. Milton (1997), An assessment of UK Meteorological Office numerical weather prediction analyses and forecasts for the Antarctic, *Antarctic Sci*., **9**, 100–09.

Lied, N. T. (1964), Stationary hydraulic jump in a katabatic flow near Davis, Antarctica 1961, *Aust. Met. Mag*. **47**, 40–51.

Lied, N. T. (1968), A note on limitations imposed by weather on the use of helicopters and light fixed wing aircraft in Antarctica, some forecasting considerations, *Met. Note 14*, Bureau of Meteorology, Melbourne, 24 pp.

Lin, C. A. and R. E. Stewart (1986), Mesoscale circulations initiated by melting snow*, J. Geophys. Res*. **91,** 13299–302.

Liou, K–N. (1980), *Introduction to Atmospheric Radiation,* Academic Press, 392 pp.

Lorenc, A. C. (1981), A global three–dimensional statistical interpolation scheme, *Mon. Wea. Rev*. **109**, 701–21.

Loewe F. and U. Radok (1955), A wave cloud at Heard Island, Wea. **10**, 78–80.

Loewe, F. (1972), The land of storms, *Weathe*r **27**, 10–121.

Lutz, H. J., W. L. Smith and E. Raschke (1990), A note on the improvement of TOVS temperature retrievals above the Antarctic snow and ice fields, *J. Geophys. Res*. **95**, 11,747–754.

Lynch, P. and X–Y. Huang (1992), Initialisation of the HIRLAM model using a digital filter. *Mon. Wea. Rev*. **120**, 1019–34.

Maarouf, A. and M. Bitzos (2000), Windchill indices: A review of science, current applications and future directions for Canada. *A background document for the Windchill Workshop (April 3–7, 2000) – hosted on the Internet (http://windchill.ec.gc.ca/) by the Meteorological Service of Canada*, Environment Canada, 4905 Dufferin Street, Downsview, Ontario M3h 5t4

MacAyeal, D. R., Rignot, E., Hulbe, C. L. (1998), Ice shelf dynamics near the front of the Filchner–Ronne Ice Shelf, Antarctica, revealed by SAR interferometry: model/interferogram comparison, *J. of Glaciol.* 44, 419–28.

MacAyeal, D. R., S. Shabtaie, C. R. Bentley and S. D. King (1986), Formulation of ice shelf dynamic boundary conditions in terms of a Coulomb rheology, *J. Geophys. Res.* **91(B8),** 8177–91.

Madigan C.T. (1929), Meteorology of the *Cape Denison Station. In: Australian* Antarctic Expedition 1911–14 Science Report Series B 4, 286 pp.

Malone, T.F.(editor) (1951), *Compendium of Meteorology.* American Meteorological Society, 1334 pp.

Manins, P. C. and B. L. Sawford (1979), A model of katabatic winds*, J. Atmos. Sci.* **36**, 619–30.

Mansfield, D. (1994), The use of potential vorticity in forecasting cyclones: operational aspects. In: *the proceedings of the international symposium on the life cycles of extratropical cyclones Vol. III, Bergen, Norway, 27 June–1 July 1994.* University of Bergen, pp. 326–31.

Martin, D. W. (1968), Satellite studies of cyclonic developments over the Southern Ocean, *IAMRC Tech. Report No. 9.* Australian Bureau of Meteorology, 57 pp.

Mass, C. F. (1991), Synoptic frontal analysis: Time for a reassessment?, *Bull. Amer. Met. Soc* **72**, 348–363.

Matley, W. R. (1981), *Meteorological analysis and the LFM. They work together.* AF GWC/FM–81/001. Airforce Weather Service (MAC) US Air Force, 23 pp.

Mawson, D. (1915), *The Home of the Blizzard*, Heinemann, 2 v.

McCarthy, I (1991), Law Base summer 1987–88. *In: the Australian Antarctic Forecaster's Handbook, Version 2,* pp. 17–7.

Mercer, J. H. *1978, West Antarctic Ice Sheet and CO2 greenhouse effect: a threat of disaster, Nature* **271**, 321–25.

Meteorological Office (1971), *Handbook of aviation meteorology,* HMSO, London. 404 pp.

Meteorological Office (1991), *Meteorological glossary (sixth ed*), HMSO, London, 335 pp.

Meteorological Office (1993), Forecasters' reference manual (second ed.), HMSO, London, 191 pp.

Miller, P. P. and D. R. Durran (1991), On the sensitivity of downslope windstorms to the asymmetry of the mountain profile, *J. Atmos. Sci.* **48**, 1457–73.

Miller, R. C. (1972), Notes on analysis and severe storm forecasting procedures of the Air Force Global Weather Central, *Technical Report 200 (Revised), Air Weather Service (MAC), US Air Force*, 190 pp.

Mills, G. A. and I. Russell (1992), The April 1990 floods over eastern Australia : synoptic description and assessment of regional NWP guidance, *Wea. and For*. **7**, 636–68.

Mills, G. A. (1997), Studies of cva maxima south of Australia. Part 1: a long–lived enhanced cumulus signature and induced cyclogenesis, *Aust. Met. Mag*. **46**, 87–107.

Mosely–Thompson, E. (1992), Paleoenvironmental conditions in Antarctica since A.D. 1500: ice core evidence. In: *Climate since A.D. 1500*. R. S. Bradley and P. D. Jones Eds, Rutlidge, New York, pp. 572–91.

Murphy, B. F. and I. Simmonds (1993), An analysis of strong wind events simulated in a GCM near Casey in the Antarctic, *Mon. Wea. Rev*. **121**, 522–34.

NACA (1954), Manual of the ICAO standard atmosphere calculations by the NACA, *Technical Note 3182*, (*International Civil Aviation Organisation, Montreal, Canada, and Langley Aeronautical Laboratory, Langley Field, Va., USA),* National Advisory Committee for Aeronautics, Washington.

Nairn, J. (1987), *Internal Report to Bureau of Meteorology Australia on Antarctic summer forecasting in Law Base 1987*.

National Geographic Society (1981), *Atlas of the World, Antarctica*, 1:10,230,000., Washington, D.C., National Geographic Society.

O'Connor, W. P. and D. H. Bromwich (1988), Surface airflow around Windless Bight, Ross Island, Antarctica. *Quart. J. Roy. Met. Soc*. **114**, 917–38.

O'Connor, W, P., D. H. Bromwich and J. F. Carrasco (1994), Cyclonically forced barrier winds along the Transantarctic Mountains near Ross Island, *Mon. Wea. Rev* **122**, 137–50.

Ohata, T., S. Kobayashi, N. Ishikawa and S. Kawaguchi (1985), Structure of the katabatic winds at Mizuho Station, East Antarctica, *J. Geophy. Res*. **90**, 10651–658

Oliver, V. J. and M. B. Oliver (1945), Weather analysis from single station data. In*: Handbook of Meteorolog*y. F. A. Berry, E. Bollay and N. R. Beers, editors, McGraw–Hill, pp. 858–79.

Overland J. E., C. H. Pease and R. W. Preisendorfer (1986), Prediction of Vessel Icing,

   J. Clim. & Appl. Met. **25**, 1793–852.

Palmer, T. L., D. C. Fritts and O. Andreassen (1996), Evolution and breakdown of Kelvin–Helmholtz billows in stratified compressible flows. Part II: Instability structure, evolution, and energetics, *J. Atmos. Sci*. **53**, 3192–212.

Parish, T. R. (1984), Numerical study of strong katabatic winds over Antarctica, *Mon. Wea. Rev.* **112**, 545–54.

Parish, T. R. and D. H. Bromwich (1986), The inversion wind pattern over West Antarctica, *Mon. Wea. Rev.* **114**, 849–60.

Parish, T. R. and D. H. Bromwich (1987), The surface wind field over the Antarctic ice sheets, *Nature* **328**, 51–54.

Parish, T. R. and *K. T. Waight III (1987),* The forcing of Antarctic katabatic winds, *Mon. Wea. Rev.* **115**, 2214–26.

Parish, T. R. (1988), Surface winds over the Antarctic continent, *Reviews of Geophys.* **26**, 169–80.

Parish, T. R. and G. Wendler (1991), The katabatic wind regime at Adélie Land, Antarctica., *Int. J. Climatol.* **11**, 97–107.

Parish, T. R., D. H. Bromwich and Ren–Yow Tzeng (1994), On the role of the Antarctic continent in forcing large–scale circulations in the high southern latitudes, *J. Atmos. Sci.* **51**(24): 3566–79.

Parish,T. R. and D. H. Bromwich (1998), A case study Antarctic katabatic wind interaction with large–scale forcing, *Mon. Wea. Rev.* **126**, 199–209.

Peixoto, J. P. and A. H. Oort (1992), *Physics of Climate*, American Institute of Physics, 520 pp.

Peltier, W. R. and J. F. Scinocca (1990), The origin of severe downslope windstorm pulses. J. Atmos. Sci. **47**, 2853–70.

Pendlebury, S. F., I. C. McCarthy and I. R. Andersen (1981), A note on forecasting "in the field" for recent ANARE summer expeditions to Enderby Land, Antarctica. *In: preprints of Antarctica: weather and climate, Melbourne, 11–13 May 1981.* N. W. Young editor (the then) Royal Meteorological Society, Australian Branch, section 20.

Pendlebury, S. and G. Reader (1993), Case study of numerical prediction of an extreme wind event in Antarctica. In: *Proceedings Fourth International Conference on Southern Hemisphere Meteorology and Oceanography. March 29–April 2, 1993. Hobart, Australia,* Boston, American Meteorological Society, pp. 124–125.

Petterssen, S. (1941), *Introduction to Meteorology*, McGraw–Hill. 263 pp.

Petterssen, S. (1956), *Weather analysis and forecasting*. McGraw–Hill. 266 pp.

Pettré, P. and J. C. André (1991), Surface–pressure change through Loewe's phenomena and katabatic flow jumps: Study of two cases in Adélie Land, Antarctica, *J. Atmos. Sci.* **48**, 557–71.

Pettré, P., C. Payan, and T.R. Parish (1993), Interaction of katabatic flow with local thermal effect in a coastal region of Adélie Land, East Antarctica, *J. Geophys. Res*. **98**, 10,429–440.

Phillpot, H. R. (1967), *Selected surface climatic data for Antarctic stations*, Meteorological Summary, Australian Bureau of Meteorology**,** Melbourne, 113 pp.

Phillpot, H. R. (1991), The derivation of 500 hPa height from automatic weather station surface observations in the Antarctic continental interior, *Aust. Met. Mag*. **39,** 79–86.

Phillpot, H. R. (1997), Some observationally–identified meteorological features of East Antarctica, *Meteorological Study No. 42. Bureau of Meteorology, Australia.*

Pierson, W. J. and L. Moskowitz (1964), A proposed spectral form for fully–developed wind–seas based on the similarity theory of S. A. Kitaigorodskii, *J. Geophys. Res*. **69**(24), 5181–90.

Pook, M. J. (1992), A note on the variability of the mid–tropospheric flow over the Southern Ocean in the Australian region, *Aust. Met. Mag*. **40**, 169–77.

Pook, M. J. and L.H. Cowled (1997), Detection of lows over the East Antarctic plateau in the FROST analysis set. In: *Proceedings of the Fifth International Conference on Southern Hemisphere Meteorology and Oceanography, Pretoria, South Africa, 7–11 April 1997*, Boston, American Meteorological Society, pp. 61–62.

Pook, M. J. and L. H. Cowled (1999), A note on the detection of weather systems over the Antarctic interior in the FROST analyses, *Wea. and For*. **14**, 920–29.

Puri, K., G. S. Dietachmeyer, G. A. Mills, N. E. Davidson, R. A. Bowen and L. W. Logan, (1998), The new BMRC Limited Area Prediction System, LAPS, *Aust. Met. Mag*. **47**, 203–23.

Rabier, F., E. Klinker, P. Courtier and A. Hollingsworth (1996), Sensitivity of forecast errors to initial conditions, *Quart. J. Roy. Met. Soc*. **122**, 121–50.

Rabier, F., J–N. Thepaut, and P. Courtier (1998), Extended assimilation and forecast experiments with a four–dimensional variational assimilation system, *Quart. J. Roy. Met. Soc*. **124**, 1861–87.

Radok U, and T. J. Brown (1996), Antarctic 500 hPa heights and surface temperatures, *Aust. Met. Mag*. **45**, 55–58.

Raper, S. C., T. M. Wigley, P. D. Jones and M. J. Salinger (1984), Variations in surface air temperatures: Part 3. The Antarctic, 1957–1982, *Mon. Wea. Rev*. **112**, 1341–53.

Reece, F. D. (1979), Severe low–level turbulence near Cross Fell (England), *Met. Mag*., 108, 27–32.

Reed, R. J. (1977), The development and status of modern weather prediction, *Bull. Am. Met. Soc*. **58**, 390–400.

Rees, J. M. and S. D. Mobbs (1987), Studies of internal gravity waves at Halley Base, Antarctica, using wind observations, *Quart. J. Roy. Met. Soc*. **114**, 939–66.

Rees, J.M. (1987), Propagation of internal gravity waves in the stably stratified atmospheric boundary layer, *Ann. Geophys*. **5B** , 421–32.

Rogers, C. W. and P. E. Sherr (1965), The identification and interpretation of cloud vortices using TIROS infra–red observation, *Final report, U.S. Weather Bureau (NWSC),Contract Nr. CWB–10812, ARACON Geophys. Company*.

Romanov, A A. (1996), Ice Navigation Conditions in the Southern Ocean. World Meteorological Organisation *WMO/TD–No. 783*.

Romeiser, R. (1993), Global validation of the wave model WAM over a one year period using Geosat wave weight data, *J. Geophys. Res*. **C98**, 4713–26.

Rott, H., P. Skvarca and T. Nagler (1996), Rapid collapse of the Northern Larsen Ice Shelf, *Antarct. Sci*. 271, 788–92.

Ryabkov, G.E. (1999), The consideration of troposphere-stratosphere interactions in method of long-range meteorological forecasts in Antarctic. In: *Proceedings of AARI, 1999*, vol. 441, pp. 52-58.

Ryzhakov, L. Yu. (1983), The application of macrocirculation method in preparing of long-range weather forecasts for spring – summer period in the Antarctic. In: *Proceedings of Soviet Antarctic Expedition. 1983*, vol. 76, pp. 76-83.

Ryzhakov L. Yu., G.B. Savitsky, and G.E. Ryabkov (1990), Seasonal features of baric formations movement in the Southern Hemisphere under typical large scale atmospheric processes. In: *Proceedings of Soviet Antarctic Expedition. 1990*, vol. 87, p. 70-75.

Saucier, W. J. (1955), *Principles of meteorological analysis*, University of Chicago Press, 438 pp.

Scambos, T. A. and C. L. Hulbe (1996), Recent events in the Northern Larsen Ice Shelf and their importance, URL: http://www–nsidc.colorado.edu/NSIDC/LARSEN

Schultz, D. M., D. Keyser and L. F. Bosart (1998), The effect of large–scale flow on low–level frontal structure and evolution in mid–latitude cyclones, *Mon. Wea. Rev*. **126**, 1767–91.

Schwalb, A. (1979), The TIROS–N/NOAA A–G Satellite Series, *NOAA Technical Memorandum NESS* **5**, NOAA/NESDIS, World Weather Building, Washington, DC 20233, 75 pp.

Schwalb, A. (1982), *NOAA Technical Memorandum*, NESS 95: *The TIROS–N/NOAA A–G Satellite Series*, NOAA, Washington DC.

Schwerdtfeger, W. (1970), The climate of the Antarctic. In: *Climates of the Polar Regions, World Survey of Climatology, Vol. 14.*, S. Orvig, editor, Elsevier, New York, pp. 253–355.

Schwerdtfeger, W. (1975), The effect of the Antarctic Peninsula on the Temperature Regime of the Weddell Sea, *Mo. Wea. Rev*. **103**, 45–51.

Schwerdtfeger, W. (1984), *Weather and Climate of the Antarctic, Developments in Atmospheric Sciences*, Elsevier Science Publishing Company Inc., New York. 261 pp.

Scinocca, J. F. and W. R. Peltier (1989) Pulsating downslope windstorms, *J. Atmos. Sci*. **46**, 2885–914.

Scofield, R. A. and C. E. Weiss (1972), A report on the Chesapeake Bay Region Nowcasting Experiment. *NOAA Tech. Man*, **NESS 94**, 52 pp.

Seaman, R. S. (1994), Impact of observations on a data assimilation system, *Aust. Met. Mag.* **43,** 41–8.

Seaman, R. S. and L. M. Leslie (1977), Numerical analysis and prognosis of fronts. In: *Two day workshop on fronts, Roy. Met. Soc., Melbourne, 26–27 May 1977.*

Segal, M., and R. W. Arritt (1992), Nonclassical mesoscale circulations caused by surface sensible heat–flux gradients, *Bull. Amer. Met. Soc.* **73**, 1593–1604.

Shapiro M. A. and D. Keyser (1990), Fronts, jet streams and the tropopause. In: *Extra–tropical cyclones, The Erik Palmen Memorial Volume*, C. W. Newton and E. O. Holopainen, editors, American Meteorological. Society, pp.167–91.

Shapiro, M. A. (1981), Frontogenesis and geostrophically forced secondary circulations in the vicinity of jet stream–frontal zone systems, *J. Atmos. Sci*, **38**, 954–73.

Shaw, P. R. J. (1955), Some effects of orography on weather observations at Heard Island *Aust. Met. Mag*. **10**, 34–60.

Simmonds, I. (1998), The Climate of the Antarctic Region. In: *Climates of the Southern Continents,* J. E. Hobbs, J. A. Lindesay and H. A. Bridgman, editors, John Wiley and Sons, pp. 137–60.

Simmonds, I. and D. A. Jones (1998), The mean structure and temporal variability of the semiannual oscillation in the southern extratropics, *Int. J. Climatol*. **18**, 473–504.

Simmonds, I., D. A. Jones and D. J. Walland (1998), Multi–decadal climate variability in the Antarctic region and global change, *Ann. of Glaciol*. **28**, 617–22.

Simmonds, I. and R. J. Murray (1999), Southern extratropical cyclone behavior in ECMWF analyses during the FROST Special Observing Periods, *Wea. and For*. **14**, 878–91.

Simmonds, I., R. J. Murray and R. M. Leighton (1999), A refinement of cyclone tracking methods with data from FROST, *Aust. Met. Mag.* **Special Edition**, 35–49.

Simmonds, I. and K. Keay (2000a), Variability of Southern Hemisphere extratropical cyclone behavior 1958–1997, *J. Climate* **13**, 550–61.

Simmonds, I. and K. Keay (2000b), Mean Southern Hemisphere extratropical cyclone behavior in the 40–year NCEP reanalysis, *J. Climate* **13**, 873–85.

Sinclair, M. R. (1981), Record high–temperatures in the Antarctic – A synoptic case study. *Mon. Wea. Rev*. **109**, 2234–42.

Sinclair, M. R. (1994), An objective cyclone climatology for the Southern Hemisphere, *Mon. Wea. Rev*. **122**, 2239–56.

Sinclair, M. R. (1995), A climatology of cyclogenesis for the Southern Hemisphere, *Mon. Wea. Rev*. **123**, 1601–19.

Sinclair, M. R. (1997), Objective identification of cyclones and their circulation intensity, and climatology, *Wea. and For*. **12**, 595–612.

Sivillo, J. K., J. E. Ahlquist and Z. Toth (1997), An ensemble forecasting primer, *Wea. and For*. **12**, 809–18.

Smith, W.L., H. M. Woolf, C. M. Hayden, D. Q. Wark and L. M. McMillin (1979), The TIROS–N Operational Vertical Sounder, *Bull. Amer. Met. Soc. 60,* 1177–87.

Snellman, L. W. (1982), Impact of AFOS on operational forecasting. In: *Preprints, 9th Conf. on weather forecasting and analysis*, American Meteorological Society, pp. 13–16.

Steadman, R. G. (1971), Indices of windchill of clothed persons, *Jl. of Appl. Met. 10,*: 674–83.

Steadman, R. G. (1979), The assessment of sultriness, *Jl. of Appl. Met.* **18**, 861–85.

Steadman, R. G.(1984), A universal scale of apparent temperature, *Jl. of Climate and Appl. Meteorology*, **23,** 1674–87.

Steadman, R.G. (1994), Norms of apparent temperature in Australia, *Aust. Met. Mag*. **43,** 1–16.

Stearns, C. R. and G. Wendler (1988), Research results from Antarctic automatic weather stations, *Rev. Geophys*. **26**, 45–61.

Streten, N. (1968), Some characteristics of strong wind periods in coastal East Antarctica, *J. Appl. Met.* **7**, 46–52.

Streten, N. A. and W. R. Kellas (1973), Aspects of cloud pattern signatures of depressions in maturity and decay, *J. Appl. Met*. **12**, 23–27.

Streten, N. A. and A. J. Troup (1973), A synoptic climatology of satellite observed cloud vortices over the Southern Hemisphere, *Quart. J. Roy. Met. Soc.* **99**, 56–72.

Streten, N. A. and J. W. Zillman (1984), Climate of the South Pacific Ocean. In: *World Survey of Climatolog*y, *Vol. 15,* H. van Loon, editor, pp. 263–429.

Svendsen, E, C. Matzler, T. C. Grenfell. (1987), A model for retrieving total ice concentration from a spaceborne dual polarized passive microwave instrument operating near 90 GHz, *Int. J. Rem. Sens*. **8**,1479–87.

Swithinbank, C. (1988), Satellite image atlas of glaciers of the world, Antarctica, *US Geological Survey Professional Paper* **1386–B**, 1–278.

Sykes, R. I. and W. S. Lewellen (1982), Numerical study of breaking Kelvin–Helmholtz billows using a Reynolds–stress turbulence closure model, *J. Atmos. Sci*. **39**, 1506–20.

Taljaard, J. J., H. van Loon, H. L. Crutcher and R. L. Jenne (1969), *Climate of the upper–air: Southern Hemisphere, Vol. 1, temperatures, dew points and heights at selected pressure levels,* NAVAIR 50–IC–55, Chief Naval Operations, Washington, DC. 135 pp.

Taljaard, J. J. (1972), Synoptic meteorology of the Southern Hemisphere. In: Meteorology of the Southern Hemisphere, *Met. Monogr*. **13**, 139–213

Targett, P. S. (1998), Katabatic winds, hydraulic jumps and wind flow over the Vestfold Hills, East Antarctica, *Ant. Sci.* **10**, 502–06.

Tremblay, A., A. Glazer, W. Szyrmer, G. Isaac, I. Zawadzki (1995), Forecasting of supercooled clouds, *Mon. Wea. Rev.* **123**, 2098–113.

Tremblay, A., S. G. Cober, G. Glazer, G. Isaac, J. Mailhot (1996), An intercomparison of mesoscale forecasts of aircraft icing using SSM/I retrievals, *Wea. and For.* **11,** 66–77.

Trenberth, K. E. (1979), Interannual Variability of the 500 mb Zonal Mean Flow in the Southern Hemisphere, *Mon. Wea. Rev.* **107**, 1515–24.

Troup, A. J. and N. A. Streten (1972), Satellite observed Southern Hemisphere cloud vortices in relation to conventional observations, *J. Appl. Met.* **11**, 909–17.

Taljaard, J. J. (1967), Development, distribution, and movement of cyclones and anticyclones in the Southern Hemisphere during the IGY, *J. Appl. Met.* **6**, 973–87.

Turner, J. and M. Row (1989), Mesoscale vortices in the British Antarctic Territory. *In: Polar and Arctic Lows.* P. F. Twitchell, E. A. Rasmussen and K. L. Davidson, editors, Deepak Publishing, pp. 347–56.

Turner, J., T. Lachlan–Cope and E. A. Rasmussen, (1991), Polar lows, *Weather* **46**, 107–14.

Turner, J. and H. Ellrott (1992), High latitude moisture structure determined from HIRS water vapour imagery, *Int. J. Rem. Sens*. **13**, 81–95.

Turner, J., T. A. Lachlan–Cope and J. P. Thomas (1993), A comparison of Arctic and Antarctic mesoscale vortices, *J. Geophys. Res*. **98**, 13019–34.

Turner, J., T. A. Lachlan–Cope, D. E. Warren and C. N. Duncan (1993), A mesoscale vortex over Halley Station, Antarctica, *Mon. Wea. Rev.* **121**, 1317–36.

Turner, J. and J. P. Thomas (1994), Summer–season mesoscale cyclones in the Bellingshausen–Weddell region of the Antarctic and links with the synoptic–scale environment, *Int. J. Climatol.* **14**, 871–94.

Turner, J. and M. Row (1995), Polar phenomena. images in weather forecasting. In: *A practical guide for interpreting satellite and radar imager*y, M. J. Bader, G. S. Forbes, J. R. Grant, R. B. E. Lilley and A. J. Waters, editors, Cambridge University Press, pp. 484–90.

Turner, J., D. Bromwich, S. Colwell, S. Dixon, T. Gibson, T. Hart, G. Heinemann, H. Hutchinson, K. Jacka, S. Leonard, M. Lieder, L. Marsh, S. Pendlebury, H. Phillpot, M. Pook, and I. Simmonds (1996a), The Antarctic First Regional Observing Study of the Troposphere (FROST) Project, *Bull. Amer. Met. Soc.* **77**, 2007–32.

Turner, J., G. Corcoran, S. Cummins, T. Lachlan–Cope, and S. Leonard (1996b), Seasonal variability of mesocyclone activity in the Bellingshausen/Weddell region of Antarctica, *Global Atmos. Ocean Sys.* **5**, 73–97.

Turner, J., S. R. Colwell, and S. A. Harangozo (1997), Variability of precipitation over the coastal western Antarctic Peninsula from synoptic observations, *J. Geophys. Res.* **102**, 13999–4007.

Turner, J., G.J. Marshall and T. A. Lachlan–Cope (1998), Analysis of synoptic–scale low pressure systems within the Antarctic Peninsula sector of the circumpolar trough, *Int. J. Climatol.* **18**, 253–280.

Turner, J., S. Pendlebury, L. Cowled, M. Jones and P. Targett (2000a), Report on the first international symposium on operational weather forecasting in Antarctica, *Bull. Amer. Met. Soc.* **81**, 75–94.

Turner, J, S. Pendlebury, N. Adams, S. Leonard, T. A. Lachlan–Cope and G. Marshall (in press with *J. Geophys. Rev*), An Extreme Wind Event in the Antarctic Coastal Region.

Twitchell, P. F., E. A. Rasmussen and K. L. Davidson (1989), *Polar and arctic lows*, A Deepak Publishing, Hampton, Virginia, 421 pp.

Twomey, S. (1977), *Introduction to the Mathematics of Inversion in Remote Sensing and Indirect Measurements,* Elsevier Scientific Publishing Company, 243 pp.

US Navy (1970), *Antarctic forecasters handbook*, Antarctic Support Activities, Detachment Charlie.

US Air Weather Service (1978), Lecture notes and daily weather map practical exercises. In: *Probability Forecasting Seminar*, HQ AWS/DNTS April 1978.

Vaughan, D. G., J. L. Bamber, M. Giovinetto, J. Russell, A. P. R. Cooper (1999), Reassessment of net surface mass balance in Antarctica, *J. Climate,* **12,** 933–46.

Vaughan, D. G. and C. S. M. Doake (1996), Recent atmospheric warming and retreat of ice shelves on the Antarctic Peninsula, *Nature* **379**, 328–30.

Valtat, B. (1960), Loewe's phenomenon. *In: Antarctic Meteorology, Proceedings of the symposium held in Melbourne February 1959*, Pergamon Press, pp. 67–71.

van der Veen, C. J. 1991, State of balance of the cryosphere, *Rev. Geophys*. **29,** 433–56.

van Loon, H. (1967), The half–yearly oscillations in middle and high southern latitudes and the coreless winter*, J. Atmos. Sci*. **24**, 472–486.

van Loon, H. (1979), The association between latitudinal temperature gradient and eddy transport. Part I: Transport of sensible heat in winter, *Mon. Wea. Rev* 107, 525–34.

van Loon, H. and D. J. Shea (1988), A survey of the atmospheric elements at the ocean's surface south of 40° S. In: *Antarctic Ocean and Resources Variability*, D. Sahrhage, editor, Springer–Verlag, Berlin, Heidelberg, pp. 3–19.

van Loon, H. and J. J. Taljaard, T. Sasamori, J. London, D. V. Hoyt, K. Labitzke, and C. W. Newton (1972), Meteorology of the Southern Hemisphere, *Meteor. Mongr*. **35**, C. W. Newton, editor, American Meteorological Society, Boston, 263 pp.

Velden, C. S. and G. A. Mills (1990), Diagnosis of upper–level processes influencing an unusually intense extratropical cyclone over southeast Australia, *Wea. and For*. **5**, 449–82.

Warren, S. G., C. J. Hahn, J. London, R. M. Shervin, and R. L. Jenne, (1986), *Global distribution of total cloud and cloud type amounts over land,* Vol. NCAR Technical Note TN–273+STR/DOE Technical Report ER/60085–HI, NCAR, Boulder, 29 pp.

Weertman, J. 1957, Deformation of floating ice shelves. *J. Glaciol*. **3**(21), 38–42.

Weldon, R. (1977), *Satellite training course notes*. US National Weather Service.

Weldon, R .B., and S. J. Holmes (1991), Water vapour imagery. Interpretation and applications to weather analysis and forecasting, *NOAA Technical Report NESDIS 57*. National Oceanic and Atmospheric Administration, Washington, DC. 213 pp.

Whitehead., J. B. (1972) The sea–breeze at Hobart Airport, *Meteorological Note ; 60*. Australian Bureau of Meteorology

Wickham, P G. (1970), *The practice of weather forecasting*, HMSO London. 187 pp.

Williams, D. T. (1963), *Analysis methods for small–scale surface networks*. Nat. Sev. Storms Proj. Rep. No. 17. US Dept of Commerce, Washington DC. 20 pp.

Wilson, J. C. (1992), *Wind flow around Law Dome, East Antarctica*, Minor MSc Thesis, Dept. of Mathematics, Monash University, 171 pp.

WMO (1998), *Guide to Wave Analysis and Forecasting* (2nd ed.), (Editor – A.K. Laing), WMO–No 702, Secretariat of the World Meteorological Organization, Geneva.

WMO (2000), *Sea ice Information Services in the World*, WMO–No 702, Secretariat of the World Meteorological Organization, Geneva.

Worby, A. P. (1999), *Observing Antarctic sea ice. A practical guide for conducting sea ice observations from vessels in the Antarctic pack ice*. A CD–ROM produced for the Antarctic Sea Ice Processes and Climate (ASPeCt) programme of the Scientific Committee for Antarctic Research (SCAR) Global Change and the Antarctic (GLOCHANT) programme, Hobart Australia.

Zillman, J. W. and P. G. Price (1972), On the thermal structure of mature southern ocean cyclones, *Aust. Met. Mag.* **20**, 34–48.

Zillman, J. W. (1969), Interpretation of satellite data over the Southern Ocean using the technique of Martin (1968). *In: Proceedings of the inter–regional seminar on interpretation of meteorological satellite data, Melbourne. 43–47.*

APPENDIX 1   TABLES OF METEOROLOGICAL STATIONS AND AWS

There are three groupings of tables in this appendix. Tables 4.1.2.1 to 4.1.2.5 are referred to in Section 4.1.2 and relate specifically to the known AWS network in Antarctica. Table 7.1.1 is a (thought to be) complete list of every staffed station, AWS, and upper–air sounding station in the Antarctic and on some of the sub–Antarctic islands. Many of these observations sites are referred to in the various station–focussed sections of Chapter 7. Table 7.12.2.3.1 refers to the Italian AWS network and is referred to in Section 7.12.3. The reader will note some duplication among these tables, and there may well be some inconsistencies, as the data have come from different sources: where possible it is intended to address these issues in version 2 of this handbook.

Table 4.1.2.1 The 2000 Antarctic automatic weather station site name, ARGOS identification number, latitude, longitude, altitude above sea level, site start date and WMO number for the Global Telecommunications System. Sites with three digits after the decimal point in the latitude and longitude were located using the ARGOS positions for a three day period, aircraft GPS, or hand held GPS. (For more information email chucks@ssec.wisc.edu (Additional sources of Antarctic data are: The British Antarctic Survey, http://www.nerc–bas.ac.uk/public/icd/metdbusr.metadata.climat.html)).

Site	ARGOS ID	Lat.	Long.	Alt. (m)	Date Start	WMO#
			Adelie Coast			
D–10	8914	66.71°S	139.83°E	243	Jan 80	89832
D–47	8986	67.397°S	138.726°E	1560	Nov 82	89834
D–57		68.199°S	137.538°E	2105	Jan 96	
D–80		70.040°S	134.878°E	2500	Jan 83	89836
Dome C II	8989	75.121°S	123.374°E	3250	Dec 95	89828
Port Martin	#8909	66.82°S	141.40°E	39	Jan 90	
Cape Denison	#8988	67.009°S	142.664°E	31	Jan 90	
Penguin Point	8910	67.617°S	146.180°E	30	Dec 93	89847
Sutton	8939	67.08°S	141.37°E	871	Dec 94	
Cape Webb		67.943°S	146.812°E	60?	Dec 94	

West Antarctica

Name	Number	Latitude	Longitude	Elevation	Date	WMO
Byrd Station	8903	80.007°S	119.404°W	1530	Feb 80	89324
Brianna	21362	83.889°S	134.150°W	@526	Nov 94	
Elizabeth	21361	82.607°S	137.078°W	@519	Nov 94	89332
J.C.		85.070°S	135.516°W	549	Nov 94	
Erin	21363	84.904°S	128.828°W	@990	Nov 94	
Harry	8900	83.003°S	121.393°W	945	Nov 94	
Theresa	21358	84.599°S	115.811°W	1463	Nov 94	89314
Doug	8922	82.315°S	113.240°W	1433	Nov 94	
Mount Siple	8981	73.198°S	127.052°W	230	Feb 92	89327
Siple Dome	8938	81.656°S	148.773°W	@668	Jan 97	89345
Swithinbank	21356	81.200°S	126.174°W	945	Jan 97	
Noel/ITASE*	#8936	79.334°S	111.077°W	@1833	Jan 00	

Ross Island Region

Name	Number	Latitude	Longitude	Elevation	Date	WMO
Marble Point	8906	77.439°S	163.754°E	@108	Feb 80	89866
Ferrell	#21355	77.910°S	170.817°E	45	Dec 80	89872
Pegasus North	#21357	77.952°S	166.500°E	@8	Jan 90	89667
Pegasus South	8937	77.990°S	166.576°E	10	Jan 91	
Minna Bluff	8935	78.554°S	166.656°E	920	Jan 91	89768
Linda	8919	78.464°S	168.382°E	@47	Jan 91	89769
Willie Field	8929	77.865°S	167.017°E	40	Jan 92	
Windless Bight	8927	77.728°S	167.703°E	61	Nov 98	
Cape Spencer*	#8697	77.97°S	167.55°E	30?	Jan 99	
Herbie Alley*	#8722	78.10°S	166.67°E	30?	Jan 99	
Cape Bird	8901	77.224°S	166.440°E	@42	Jan 99	
Laurie II*	#21364	77.549°S	170.817°E	30	Jan 00	

Ocean Islands

Whitlock	8921	76.144^{o}S	168.392^{o}E	274	Jan 82	89865
Scott Island		67.37^{o}S	179.97^{o}W	30	Dec 87	89371
Young Island		66.229^{o}S	162.275^{o}E	30	Jan 91	89660
Possession Is.	8984	71.891^{o}S	171.210^{o}E	30	Dec 92	89879
Manuela	8905	74.946^{o}S	163.687^{o}E	80	Feb 84	89864

Ross Ice Shelf

Marilyn	8931	79.954^{o}S	165.130^{o}E	75	Jan 84	89869
Schwerdtfeger	8913	79.904^{o}S	169.973^{o}E	60	Jan 85	89868
Gill	8911	79.985^{o}S	178.611^{o}W	55	Jan 85	89376
Elaine	8915	83.134^{o}S	174.169^{o}E	60	Jan 86	89873
Lettau	8908	82.518^{o}S	174.452^{o}W	55	Jan 86	89377

Antarctic Peninsula

Larsen Ice	8926	66.949^{o}S	60.897^{o}W	17	Oct 85	89262
Butler Island	8902	72.207^{o}S	60.160^{o}W	91	Mar 86	89266
Uranus	8920	71.43^{o}S	68.93^{o}W	780	Mar 86	89264
Limbert	8925	75.422^{o}S	59.851^{o}W	40	Dec 95	89257
Racer Rock	8947	64.067^{o}S	61.613^{o}W	17	Nov 89	89261
Bonaparte Point	8923	64.778^{o}S	64.067^{o}W	8	Jan 92	89269
Ski–Hi	8917	74.792^{o}S	70.488^{o}W	1395	Feb 94	89272
Santa Claus I	#8933	64.964^{o}S	65.670^{o}W	25	Dec 94	

High Polar Plateau

Clean Air	8987	90.00^{o}S		2835	Jan 86	89208
Henry	8985	89.011^{o}S	1.025^{o}W	2755	Jan 93	89108
Nico	8924	89.000^{o}S	89.669^{o}E	2935	Jan 93	89799
Relay Station	8918	74.017^{o}S	43.062^{o}E	3353	Feb 95	89744
Dome Fuji	#8904	77.31^{o}S	39.70^{o}E	3810	Feb 95	89734

New site for 2000: # New ARGOS ID at the site for 2000: @ UNAVCO GPS Location: and Elevation: CRS, 16 MARCH 2000

Table 4.1.2.2 Australian National Antarctic Research Expedition automatic weather stations as of 1999. The table is based on records that have not been checked with ANARE and may not be up to date. One should email with Ian Allison, I.Allison@utas.edu.au for the latest site information and the availability of the data.

Site	ARGOS ID	Lat.	Long.	Alt. (m)	WMO#
LGB00	3114	68.66°S	61.11°E	1830	89762
LGB10	3110	71.29°S	59.21°E	2620	89758
LGB20	1178	73.83°S	55.67°E	2741	89757
LGB35	3111	76.03°S	65.02°E	2342	89568
Rumdoodle Airfield		67.715°S	62.80°E	430	89565
LGB46	3112	75.85°S	71.50°E	2352	89577
LGB59	3113	73.45°S	76.78°E	2537	89774
Amery Ice Shelf	1180	70.89°S	69.87°E	84	89767
Rauer Plateau Airfield		68.87°S	78.04°E	363	89572
Mt Brown	8561	69.11°S	87.00°E	2078	89586
Bunger Hills Airfield		66.34°S	100.81°E	150	89602
Casey Airfield	1170	66.27°S	110.80°E	390	89612
Law Dome (LD)	1174	66.73°S	112.73°E	1366	89811
LDSummit South	1181	66.76°S	112.81°E	1376	89816
A028	1179	68.41°S	112.21°E	1622	89812
GC41	1171	71.60°S	111.25°E	2761	89813
GC46	1172	74.13°S	109.83°E	3096	89805
GF08	1173	68.50°S	102.18°E	2123	89803
Stillwell Island.	3627	67.95°S	143.93°E	52	89644

Table 4.1.2.3 Antartide (Italian) AWS sites in the vicinity of Terra Nova Bay, Antarctica. Additional information on Antartide can be obtained from"www2.pnra.it".

Site	ARGOS ID	Lat.	Long.	Alt. (m)	WMO#
Tourmaline Plat.	7356	74.10°S	163.49°E	1700	
Priestley Neve.	7355	73.63°S	160.65°E	1900	
Priestley Gl.	7352	74.25°S	163.20°E	640	
Nansen Ice Sheet	7350	74.80°S	163.32°E	40	
Terra Nova Bay	7353	74.70°S	164.10°E	90	
Enigma Lake	7354	74.70°S	164.04°E	210	89910
Cape King	7351	73.58°S	166.62°E	160	
Cape Phillip	7379	73.07°S	169.12°E	`550	
Cape Ross	7357	76.73°S	163.60°E	150	89666
Mid Point	1627	74.62°S	145.64°E	400	

Table 4.1.2.4 AWS sites installed by the Alfred Wegener Institute, Germany as of 1998. (Unconfirmed).

Site	ARGOS ID	Lat.	Long.	Alt. (m)	WMO#
Filchner	3310	77.12°S	51.22°W	20	89258
Drescher	3312	72.87°S	19.04°W	20	89214

Table 4.1.2 5 USAP automatic geophysical observatory (AGO) sites.
The AGOs record meteorological variables every minute and store the data
on tape for recover during the next site visit. The sites have WMO numbers
and do transmit to the ARGOS System.

Site	ARGOS ID	Lat.	Long.	Alt. (m)	WMO#
AGO–1	73131	83.87^{o}S	29.12^{o}E	2865	89628
AGO–2	71061	85.67^{o}S	46.38^{o}W	1860	89049
AGO–3	74301	82.77^{o}S	28.96^{o}E	2912	89528
AGO–4	73132	82.02^{o}S	96.77^{o}E	3565	89598
AGO–5	73133	77.23^{o}S	123.52^{o}E	3084	89627
AGO–6	73134	69.85^{o}S	130.02^{o}E	2560	89637

Table 7.1.1 A list of meteorological stations and AWS in the Antarctic and on some of the sub–Antarctic Islands

The table below lists stations and AWSs in the Antarctic and on some of the sub–Antarctic Islands The data have been entered in the approximate order of mention in Chapter 7. Not all the places listed are explicitly mentioned in Chapter 7 but the list is intended to present a summary of the meteorological observing network in the Antarctic and surrounding areas. Figure A1 to A3 below shows the relative locations of the places listed in the table (except for the sub–Antarctic Island stations). The map number refers to the location of the station or AWS in these figures. Elevations are AMSL.

Map No.	WMO/ ARGOS No.	Latitude	Longitude	Elev. – (m)	Name of station or AWS	Country responsible (GTS = AWS data on GTS) (W = staffed in winter) (S = staffed summer only)	Upper– air prog. times (if any) (*summ –er only)	Satellite Recept. & type (if any)	Sub–Section in Chapter 7 (Forecasting for specific locations) above. Click on the word "above" in each case to go to the relevant section
	88889	51º49´S	58º27´W	74	Mount Pleasant	UK (W)	00/12	APT/geost	Section 7.2.1 above
		54ºS	37ºW		South Georgia	UK (W)			Section 7.2.2 above
	88986	59º27´S	27º18´W	18	South Thule	S African AWS (GTS)			Section 7.2.2 above
	68906	40º21´ S	9º53´W	54	Gough Island	South Africa (W)	00/12	Meteosat	Section 7.2.3 above
	98992	54º24' S	3º25'E	28	Bouvetoya	Norway			Section 7.2.4 above
	68994	46º53' S	37º52'E	22	Marion Island	South Africa (W)	00/12		Section 7.2.5 above
	61997	46.43 º S	51.87ºE	143	Crozet Island	France (W)			Section 7.2.6 above
	61998	49.35º S	70.25ºE	29	Kerguelen Island	France (W)			Section 7.2.7 above
	95997	53º01´12″S	73º23´24″E	3	Heard Island (Atlas Cove)	Australian AWS (GTS)			Section 7.2.8 above
	94997	53º06´24″S	73º43´15″E	12	Heard Is. (The Spit)	Australian AWS (GTS)			Section 7.2.8 above
		53º3'S	72º35'E		McDonald Island	Australia			Section 7.2.8 above

	94998	54º25'S	158º58'E	6	Macquarie Island	Australia (W)	00/12		Section 7.2.9 above
104	89042	60º43'S	45º36'W	6	Signy	UK (W)			Section 7.3.1 above
105	88968	60º45'S	44º43'W	6	Orcadas	Argentina (W)			Section 7.3.1 above
91	89064	62º40'S	60º23'W		Juan Carlos	Spain (S)			Section 7.3.2 above
96	89050	62º12'S	58º56'W	16	Bellingshausen	Russia (S)	00*		Section 7.3.2 above
97	89251	62º13'S	58º45'W	10	King Sejong	Korea (W)			Section 7.3.2 above
98	89054	62º10'S	58º50'W	10	Dinamet	Uruguay (W)			
93	89056	62º25'S	58º53'W	10	Frei	Chile (W)		HRPT	Section 7.3.2 above
94	89058	62º13'S	58º58'W	10	Great Wall	China (W)		HRPT	Section 7.3.2 above
95	89053	62º14'S	58º38'W	4	Jubany	Argentina (W)			Section 7.3.2 above
92	89057	62º30'S	59º41'W	5	Arturo Prat	Chile (W)			Section 7.3.3 above
101	89059	63º19'S	57º54'W	10	O'Higgins	Chile (W)			Section 7.3.5 above
102	88963	63º25'S	56º59'W	13	Esperanza	Argentina (W)			Section 7.3.5 above
103	89055	64º14'S	56º43'W	198	Marambio	Argentina (W)	12		Section 7.3.5 above
85	8910	64º58'S	65º40'W	25	Santa Claus Island	USA AWS			
86	89061	64º46'S	64º05'W	8	Palmer	USA (W)		HRPT/DMSP	Section 7.3.6 above
87	89063	65º15'S	64º16'W	11	Vernadasky	UK (W)			Section 7.3.6 above
88	89269	64º47'S	64º04'W	8	Bonaparte Point	USA AWS (GTS)			
89	89261	64º16'S	61º54'W	17	Racer Rock	USA AWS (GTS)			
90	88970			32	Matienso	Argentina (S)			Section 7.3.6 above
83	89062	67º34'S	68º08'W	16	Rothera	UK (W)		HRPT	Section 7.3.7 above
84	89066	68º08'S	67º08'W	4	San Martin	Argentina (W)			Section 7.3.7 above

81	89264	71º26'S	68º56'W	780	Uranus Glacier	USA AWS (GTS)			
82	89065	71º20'S	68º17'W	55	Fossil Bluff	UK (S)			Section 7.3.8 above
80	8917	74º58'S	70º46'W	1395	Ski–Hi	USA AWS			Section 7.3.9 above
99	89262	66º58'S	60º33'W	17	Larsen Ice Shelf	USA AWS (GTS)			Section 7.3.10 above
100	89266	72º13'S	60º20'W	91	Butler Island	USA AWS (GTS)			
106	89258	77º05'S	51º13'W	20		German AWS (GTS)			Section 7.4.1 above
107	89967	77º52'S	34º37'W	32	Belgrano II	Argentina (W)			Section 7.5.1 above
108	89022	75º35'S	26º22'W	39	Halley	UK (W)	11	HRPT	Section 7.5.2 above
112	8932	80º49'S	22º16'W	1220	Recovery Glacier	USA AWS (GTS)			
109	89214	72º52'S	19º02'W	20		German AWS (GTS)			
110	89014	73º03'S	13º23'W		Nordenskiold/Milos	Finish AWS (GTS)			Section 7.5.3 above
111	89002	70º40'S	8º15'W	50	Neumayer	Germany (W)	10	HRPT/DMSP	Section 7.5.4 above
	89004	71º40'S	2º 50'W	846	(SANAE IV)	South African AWS			Section 7.5.5 above
		72°0'7"S	2°32'2"E	1298	Troll	Norway (S)			Section 7.5.6 above
2	89514	70º46'S	11º45'E	117	Maitri	India (W)			Section 7.5.7 above
3	89512	70º46'S	11º50'E	102	Novolazarevskaya	Russia (W)	00		Section 7.5.8 above
4	89524	71º32'S	24º08'E	931	Asuka	Japan (S)			Section 7.5.9 above
6	8982	77º19'S	39º42'E	3810	Dome Fuji	USA AWS Also Japanese (S)			Section 7.5.9 above
5	89532	69º00'S	39º35'E	21	Syowa	Japan (W)	00/12	HRPT/APT	Section 7.5. 10 above
6a	8918	74º00'S	43º00'E	3353	Relay Station	USA AWS			
7	89542	67º40'S	45º51'E	40	Molodezhnaya	Russia (closed)			Section 7.6.1 above

8	89757	73º49'58″S	55º40'18″E	2741	LGB20	Australian AWS (GTS)			
9	89762	68º39'19″S	61º06'46″E	1830	LGB00	Australian AWS (GTS)			
10	89564	67º36'S	62º52'E	16	Mawson	Australia (W)	00/12	APT	Section 7.7.1 above
11	89758	71º17'15'S	59º12'37″E	2620	LGB10	Australian AWS (GTS)			
	89565	67º42´54″S	62º48´18″S	430	Rumdoodle Airfield	Australian AWS (GTS)			
12	89568	76º02'34″S	65º00'E	2342	LGB35	Australian AWS (GTS)			
	89767	70º53'31″S	69º52'21″E	84	Amery	Australian AWS (GTS)			
12a	89577	75º51'S	71º30'E	2352	LGB46	Australian AWS			
12b	89774	73º27'06″S	76º47'21″E	2537	LGB59	Australian AWS (GTS)			
13	89573	69º22'S	76º22'E	18	Zhongshan	China (W)			Section 7.8.3 above
	89572	68º51´22″S	78º02´21″S	363	Rauer Plateau Airfield	Australian AWS (GTS)			
	89586	69º07´52″S	85º59´57″S	2078	Mount Brown	Australian AWS (GTS)			
14	89571	68º34'S	77º57'E	22	Davis	Australia (W)	00/12	APT	Section 7.8.4 above
15	89592	66º33'S	93º01'E	30	Mirny	Russia (W)			Section 7.9.1 above
	89602	66º20´40″S	100º48´50″S	150	Bunger Hills Airfield	Australia AWS (GTS)			
16	89803	68º29'36″S	102º10'32″E	2123	GF08	Australian AWS (GTS)			
17	89611	66º17'S	110º32'E	42	Casey	Australia (W)	00/12	HRPT/APT	Section 7.10.1 above
18	89612	66º16'42″S	110º47'48″E	390	Casey Airfield	Australian AWS (GTS)			Section 7.10.1 above
19	89812	68º24'28″S	112º13'03″E	1622	A028	Australian AWS (GTS)			
20	89813	71º36'10″S	111º15'46″E	2761	GC41	Australian AWS (GTS)			
21	89805	74º08'15″S	109º50'23″E	3096	GC46	Australian AWS (GTS)			
23	89816	66º43'50″S	112º48'38″E	1376	Law Dome Summit	Australian AWS (GTS)			Section 7.10.1 above

					South				
22	89606	78º27'S	106º52'E	3420	Vostok	Russia (W)			Section 7.10.2 above
24	89828	74º30'S	123º00'E	3280	Dome C	USA AWS (GTS)			Section 7.10.3 above
25	89836	70º01'S	134º43'E	2500	D–80	USA AWS (GTS)			
26	89834	67º23'S	138º43'E	1560	D–47	USA AWS (GTS)			
27	89832	66º42'S	139º43'E	240	D–10	USA AWS (GTS)			
28	89642	66º40'S	140º01'E	43	Dumont d'Urville	France (W)	UA 00	Yes	Section 7.11.1 above
29	8930	66º49'S	141º23'E	39	Port Martin	USA AWS			Section 7.11.2 above
29a	8939	67º05'S	141º22'E	871	Sutton	USA AWS			
30		67º01'S	142º41'E	31	Cape Denison	USA AWS			Section 7.11.2 above
	89644	66º57'30″S	143º56'24″E	52	Stillwell Islands	Australian AWS (GTS)			
31	89847	67º37'S	146º00'E	30	Penguin Point	USA AWS (GTS)			
31a	8933	67º56'S	146º49'E	37	Cape Webb	USA AWS			
32	89660	66º17'S	162º20'E	30	Young Island	USA AWS (GTS)			
33	89371	67º22'S	179º58'W	30	Scott Island	USA AWS (GTS)			
34	7356	74º41'S	163º29'E	1700	Tourmaline Plateau	Italian AWS			
35	7355	73º38'S	160º39'E	1983	High Priestley Gl.	Italian AWS			
36	89860	74º14'S	160º17'E	1772	Lynn	USA AWS (GTS)			
37	89861	74º29'S	160º29'E	1525	Sandra	USA AWS (GTS)			
38	7352	74º15'S	163º09'E	87	Priestley Glacier	Italian AWS			
39	89862	74º42´S	161º29´E	1200	Shistri	USA AWS (GTS			
40	7350	74º48'S	163º19'E	85	Nansen Ice Sheet	Italian AWS			
41	7353	74º42'S	164º06'E	88	Tethys Bay	Italian AWS			

42	89864	74º55'S	163º36'E	80	Manuela	USA AWS (GTS)			
43	89662	74º42'S	164º06'E	80	Terra Nova Bay	Italy (S)	00*/12*	HRPT/DMSP	Section 7.12.2 above
44	7351	73º35'S	166º37'E	163	Cape King	Italian AWS			
45	7379	73º04'S	169º07'E	200	Cape Phillips	Italian AWS			
46	89879	71º54'S	171º08'E	30	Possession Island	USA AWS (GTS)			
47	89865	76º14'S	168º42'E	275	Whitlock	USA AWS (GTS)			
48	7357	76º44'S	163º01'E	200	Cape Ross	Italian AWS			
49	89866	77º26'S	163º45'E	120	Marble Point	USA AWS (GTS)			
50	8901	77º51'S	167º05'E	40	Willie Field	USA AWS			
51	8937	78º02'S	166º36'E	10	Pegasus South	USA AWS			
52	89664	77º51'S	166º40'E	24	McMurdo	USA (W)	00/12*	HRPT/DMSP	Section 7.12.3 above
53	89667	77º57'S	166º31'E	10	Pegasus North	USA AWS (GTS)			
54	89674	77º52'S	166º58'E	8	Williams Field	USA (S)			Section 7.12.3 above
55	89872	78º01'S	170º48'E	45	Ferrell	USA AWS (GTS)			
55a	89768	78º33'S	166º41'E	920	Minna Bluff	USA AWS			
55b	89768	78º30'S	168º21'E	50	Linda	USA AWS			
56	89869	79º57'S	164º58'E	75	Marilyn	USA AWS (GTS)			
57	89868	79º56'S	169º50'E	60	Schwerdtfeger	USA AWS (GTS)			
58	89873	83º09'S	174º28'E	60	Elaine	USA AWS (GTS)			
59	89863	80º02'S	178º38'W	55	Gill	USA AWS (GTS)			
60	89377	82º35'S	174º16'W	55	Lettau	USA AWS (GTS)			
62	89799	89º00'S	90º08'E	3065	Nico	USA AWS (GTS)			
64	89208	89º57'S	0º01'W	2835	Clean Air	USA AWS (GTS)			

65	89009	90º00'S	0º00'W	2800	Amundsen–Scott	USA (W)	00/12*		Section 7.12.5 above
66	89108	89º00'S	0º18'W	2877	Henry	USA AWS (GTS)			
68	89349	87º19´S	149º33´W	2400	Mount Howe	USA AWS (GTS)			
69	21357	85º03'S	135º03'W	549	J.C.	USA AWS			
70	21361	84º54'S	128º42'W	1006	Erin	USA AWS			
71	21362	83º54'S	134º12'W	549	Brianna	USA AWS			
72	21358	84º36'S	115º36'W	1463	Theresa	USA AWS			
73	21356	82º36'S	137º00'W	549	Elizabeth	USA AWS			
74	21355	83º00'S	121º24'W	945	Harry	USA AWS			
75		81º12'S	126º06'W	1000		Planned AWS			
76	21359	82º12'S	113º24'W	1433	Doug	USA AWS			
77	89324	80º00'S	120º00'W	1530	Byrd Station	USA AWS (GTS) (S)?			Section 7.13.2 above
78	89125	80º01'S	119º32'W	1515	Byrd	USA			Section 7.13.2 above
79	89327	73º12'S	127º03'W	30	Mount Siple	USA AWS (GTS)			

Table 7.12.2.3.1　　　**Italian Automatic Weather Stations Network.**

Name	Geographical Site	AWS/WMO Id.	Latitude	Longitude	Elevation	Sensors Installed	Dissemination	Period of Operation
SOFIA 10 m. mast. [1987–1999] 3 m. mast [1999–]	Nansen Ice Sheet	7350	74° 48' S	163° 19' E	40 m.	2m. Press. 2m. Temp. 2m. Rel. Hum. 3 m. Wind	ARGOS service	1987– 10m. Wind [1987–2000] 3m. Wind [2000–].
ALESSANDRA (10 m. mast)	Cape King	7351	73° 35' S	166° 37' E	160 m.	2m. Press. 2m. Temp. 2m. Rel. Hum. 10m. Wind 2m. Solar Rad.	ARGOS service.	1987– Solar Radiation [Feb 1989–].
ZORAIDA 10 m. mast. [1987–1997] 3 m. mast [1997–]	Medium Priestley	7352	74° 15' S	164° 10' E	640 m.	2m. Press. 2m. Temp. 10 m. Rel. Hum. 3m. Wind	ARGOS service	1987– 10m. Wind [1987–1997] 3m. Wind [1997–].
ENEIDE (10 m. mast)	Terra Nova Bay Station	7353/89662	74° 42' S	164° 06' E	88 m.	2m. Press. 2m. Temp. 2m. Rel. Hum. 10m. Wind 2m. Solar Rad.	ARGOS service. GTS	1986– Solar Radiation [Feb 1988–Feb 1989]

RITA (10 m. mast)	Enigma Lake	7354	74° 43' S	164° 02' E	210 m.	2m. Press. 2m. Temp. 2m. Rel. Hum. 10m. Wind	ARGOS service	1993–
MODESTA (10 m. mast)	Priestley Neveé	7355	73° 39' S	160° 39' E	1900 m.	2m. Press. 2m. Temp. 2m. Rel. Hum. 10 m. Wind	ARGOS service	1989–
LOLA (10 m. mast)	Sarao Point [Tourmaline Plateau]	7356	74° 08' S	163° 26' E	1700 m.	2m. Press. 2m. Temp. 2m. Rel. Hum. 10m. Wind	ARGOS service	1989–

Table 7.12.2.3.1 continued (Italian Automatic Weather Stations Network)

ARELIS (10 m. mast)	Cape Ross	7357	76° 43' S	162° 58' E	150 m.	2m. Press. 2m. Temp. 2m. Rel. Hum. 10m. Wind	ARGOS service. GTS.	1989–
SILVIA (10 m. mast)	Cape Philips	7379	73° 03' S	169° 36' E	550 m.	2m. Press. 2m. Temp. 2m. Rel. Hum. 10m. Wind	ARGOS service.	1990–
GIULIA (3 m. mast)	Mid Point	1627	75° 33' S	145° 50' S	2500 m.	2m. Press. 2m. Temp. 2m. Rel. Hum. 10m. Wind Snow Depth T–2m Temp. T–5m Temp. T–10m Temp.	ARGOS service.	1997–

ALPHA (6 m. mast)	Thethys Bay airstrip	–			0 m.	10m Wind	MODEM HF.	1993– Seasonal service Oct–Jan
BRAVO (6 m. mast)	Thethys Bay airstrip	–			0 m.	10m Wind	MODEM HF.	1993– Seasonal service Oct–Jan
MARIA (10 m. mast)	POINT CHARLIE [Browning Pass]	–	74° 37' S	164° 00' E	400 m.	2m. Press. 2m. Temp. 2m. Rel. Hum. 10m. Wind	MODEM HF.	1997–
ITALICA (10 m. mast)	Italica Research Vessel	1626	–	–	–	2m. Press. 2m. Temp. 2m. Rel. Hum. 10m. Wind	ARGOS service.	1997–
JENNICA (10 m. mast)	Terra Nova Bay Station	1218	74° 42' S	164° 06' E	20 m.	2m. Press. 2m. Temp. 2m. Rel. Hum. 10m. Wind 10m. Wind (Heated sensor) Precipitation	ARGOS service.	2000–

Table 7.12.2.3.1 continued   (Italian Automatic Weather Stations Network)

DOME C (10 m. mast)	Concordia Station	–	75°	123° 23' E	3223 m.	2m. Press.	HF–VHF.	1997– Seasonal service Nov–Feb
						2m. Temp.		
						2m. Rel. Hum.		
						10m. Wind		
						Clouds Cover		
						Ceiling		
						Visibility		
PENGUIN (3 m. mast)	Edmonson Point	–				2m. Press.	–	1997–
						2m. Temp.		
						2m. Rel. Hum.		
						3m. Wind		

Locations of all meteorological bases and AWS sites in the Antarctic as of 1/1/98
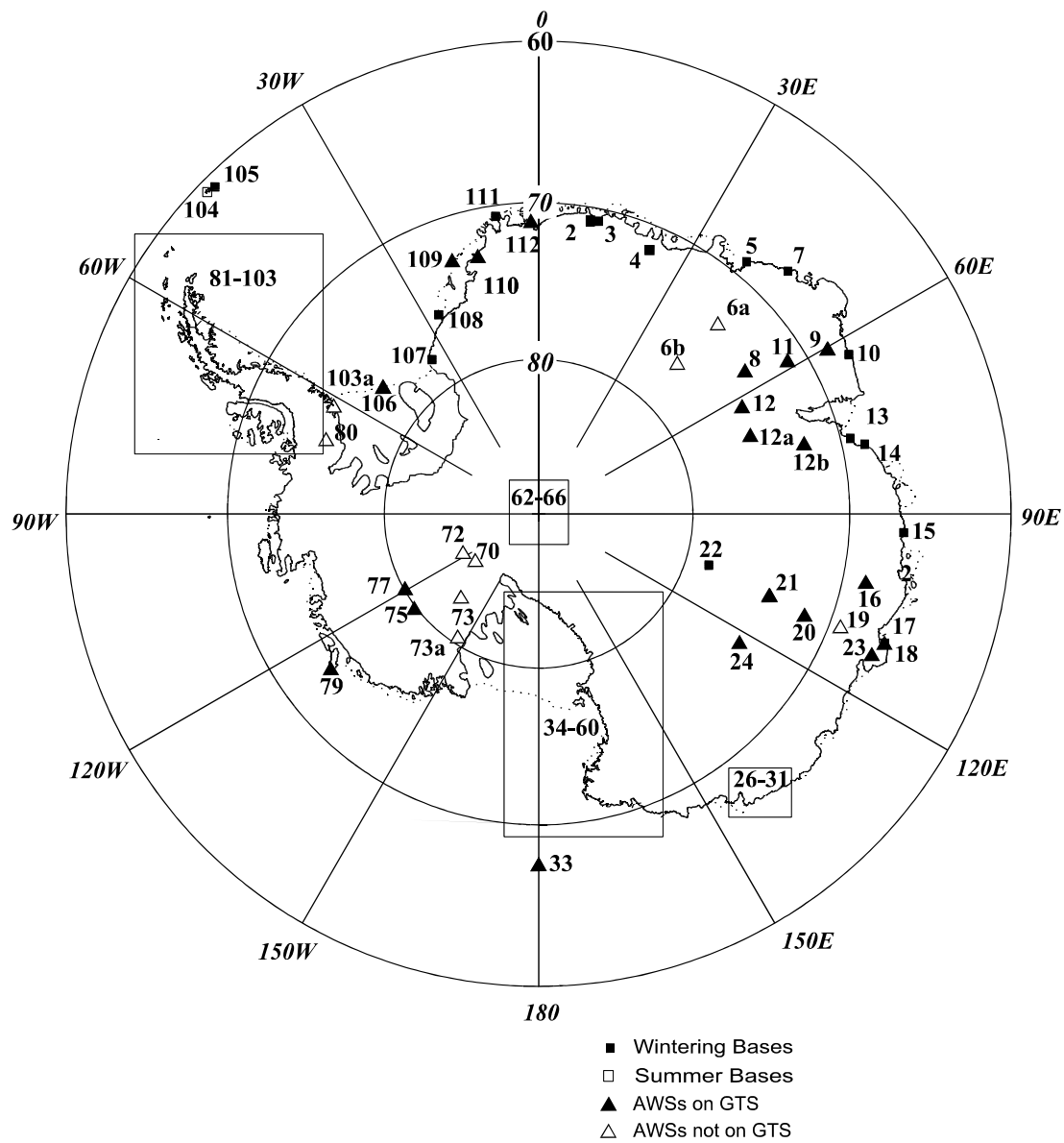
Figure A1–1　　　Location of meteorological stations and AWS as of 1 January 1998
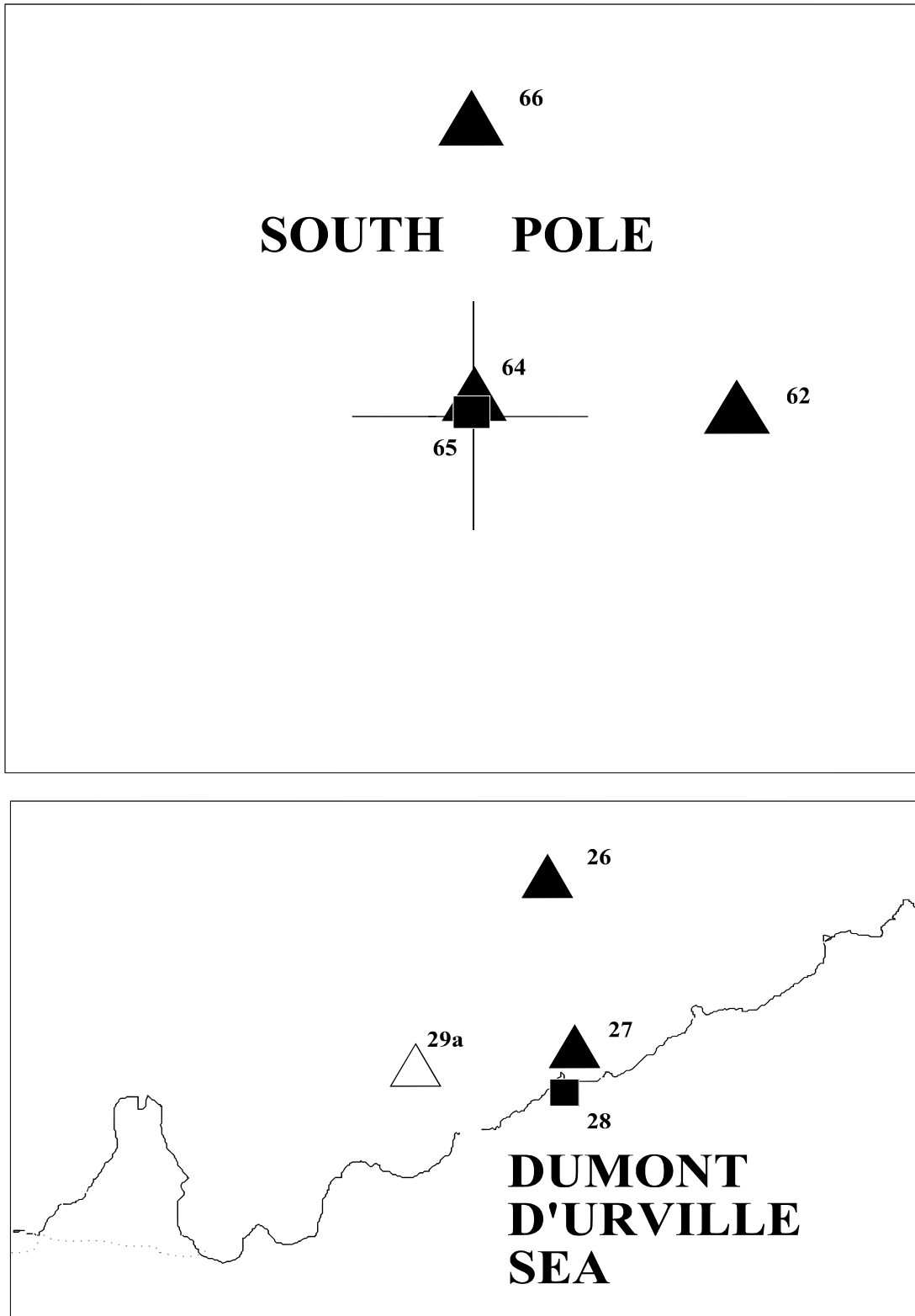
Figure A1–2   Top panel–location of AWSs about Admundsen–Scott (65); bottom panel–locations of AWSs about Dumont d'Urville (28).
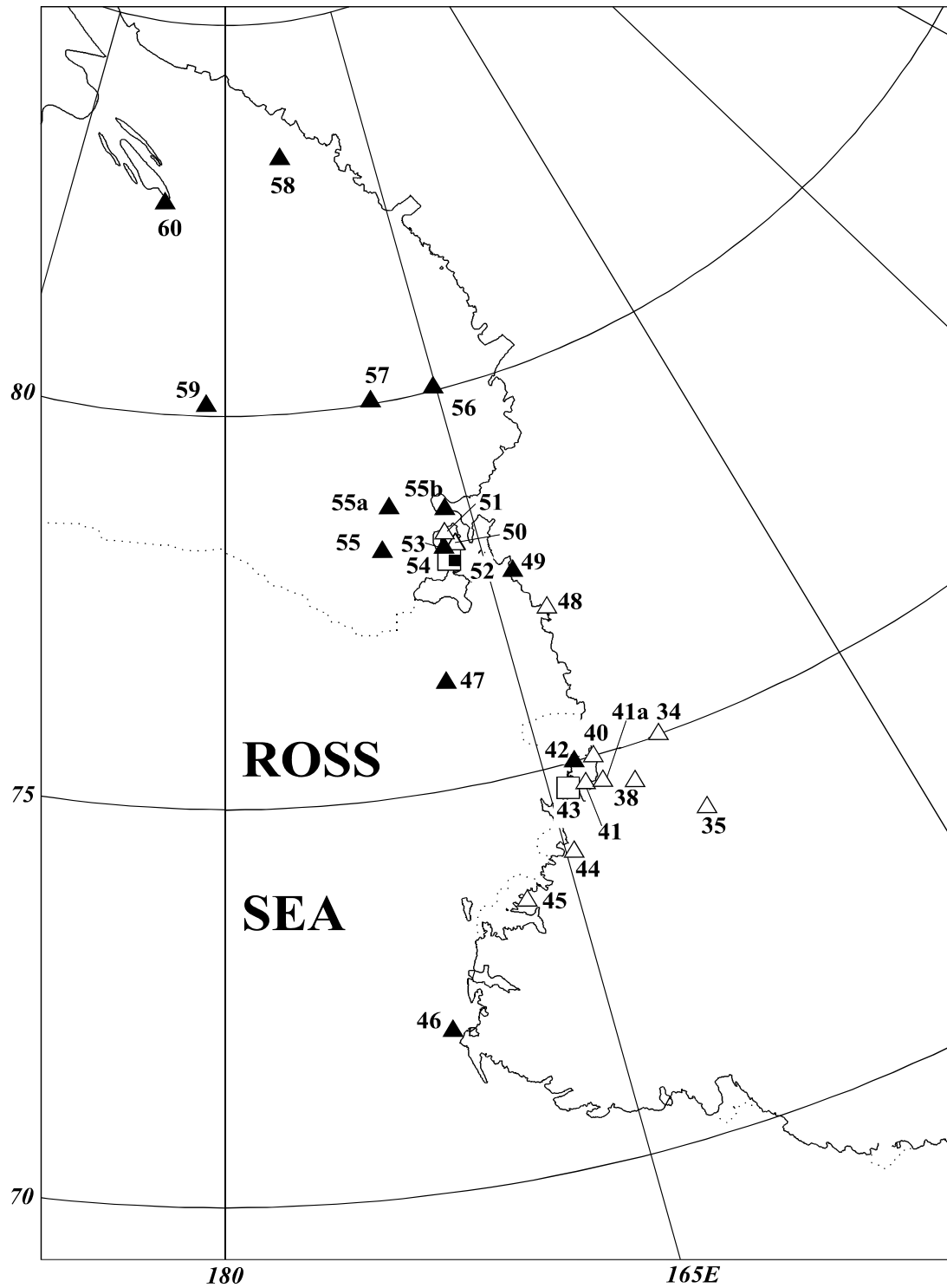
Figure A1–3   Locations of stations and AWSs in the Ross Ice Shelf–Transantarctic Mountains sector.

 APPENDIX 2.   CLIMATOLOGICAL DATA (Tables and Figures) FOR VARIOUS LOCATIONS IN THE ANTARCTIC

Transvaal Bay, Gough Island (refer Section 7.2.3 above)

Month	Jan	Feb	Mar	Apr	May	Jun	Jul	Aug	Sept	Oct	Nov	Dec	Year
Ave. no. fog days	2.7	1.9	3.3	2.6	1.4	1.7	1.2	1.8	1.5	1.4	1.7	1.9	23

Table 7.2.3.4.1   Average numbers of days with fog in Transvaal Bay, Gough Island.

Month	Ave. total (mm)	Ave. no days > 0.1 mm	Ave. no. thunder days	Ave. no. days with hail or ice pellets	Ave. no. days with snow
January	207	22.5	0.1	0.0	0.0
February	178	19.3	0.1	0.0	0.0
March	256	23.8	0.0	0.9	0.0
April	277	23.4	0.3	0.3	0.1
May	289	26.7	0.7	0.9	0.6
June	318	27.7	0.4	1.1	0.9
July	266	28.4	0.2	2.2	2.0
August	299	27.1	0.3	1.8	1.9
September	267	25.3	0.2	1.9	1.9
October	296	24.8	0.1	0.7	0.5
November	261	21.4	0.2	0.6	0.2
December	240	22.5	0.2	0.1	0.1
Total for year	3154	293	3	11	8

Table 7.2.3.4.2   Monthly mean precipitation statistics for Transvaal Bay, Gough Island.

Month	Mean (ºC)	Mean Maximum (ºC)	Mean Minimum (ºC)	Record Maximum (ºC)	Record Minimum (ºC)
January	14.2	17.2	11.2	26.4	4.2
February	14.5	17.4	11.7	26.7	5.1
March	14.0	16.8	11.3	25.9	4.8
April	12.9	15.3	10.4	22.6	2.6
May	11.3	13.6	8.9	20.5	1.4
June	10.1	12.5	7.7	19.0	0.8
July	9.1	11.6	6.6	19.3	−0.9
August	8.9	11.3	6.5	18.6	−2.7
September	9.1	11.6	6.7	19.3	0.2
October	10.4	12.9	7.9	21.4	0.5
November	12.1	14.9	9.4	23.9	2.4
December	13.2	16.2	10.3	25.1	4.1
Year	11.7				

Table 7.2.3.4.3   Temperature statistics for Transvaal Bay, Gough Island.

Crozet Islands (refer Section 7.2.6 above)

Month	Jan	Feb	Mar	Apr	May	Jun	Jul	Aug	Sept	Oct	Nov	Dec	Year
Ave. wind speed (m s^{-1})	10.2	9.5	9.9	10.2	10.8	11.5	11.6	11.5	11.5	10.7	10.3	10.5	10.8

Table 7.2.6.4.1 Average wind speed at Crozet (1966–90)

Month	Jan	Feb	Mar	Apr	May	Jun	Jul	Aug	Sept	Oct	Nov	Dec	Year
Pressure (hPa)	1005.9	1012.4	1012.3	1009.7	1009.1	1006.1	1009.9	1008.3	1008.5	1005.4	1002.3	1004.2	1007.8

Table 7.2.6.4.2 Average mean sea level pressure at Crozet (1973–82)

Month	Jan	Feb	Mar	Apr	May	Jun	Jul	Aug	Sept	Oct	Nov	Dec	Year
Rain amount (mm)	178	162	204	222	214	201	203	236	208	199	186	200	2413

Table 7.2.6.4.3 Mean precipitation measurements for Crozet (1966–90)

Month	Jan	Feb	Mar	Apr	May	Jun	Jul	Aug	Sept	Oct	Nov	Dec	Year
Temperature (ºC)	7.2	7.8	7.5	6.1	4.7	3.9	3.4	3.0	2.9	3.5	4.6	6.0	5 .0

(The all time extreme daily values are +23 .1°C and –5.4°C).

Table 7.2.6.4.4 Mean monthly temperature at Crozet (1966–90).

Kerguelen Islands (refer Section 7.2.7 above)

Month	Jan	Feb	Mar	Apr	May	Jun	Jul	Aug	Sept	Oct	Nov	Dec	Year
Ave. wind speed (m s^{-1})	9.5	9.0	9.4	9.4	9.2	9.7	10.1	10.7	10.7	10.5	10.0	9.7	9.8

Table 7.2.7.4.1　Average wind speed at Kerguelen (period 1951-1990).

Month	Jan	Feb	Mar	Apr	May	Jun	Jul	Aug	Sept	Oct	Nov	Dec	Year
Ave. surf. Press. (hPa)	1000.9	1005.9	1007.1	1004.6	1001.4	998.9	1001.2	1001.2	1000.2	1001.4	999.2	999.0	1001.7

Table 7.2.7.4.2　Average surface air pressure at Kerguelen (period 1951-1990).

Month	Jan	Feb	Mar	Apr	May	Jun	Jul	Aug	Sept	Oct	Nov	Dec	Year
Ave. precip' (mm)	55.5	46.6	61.1	72.7	83.9	71.7	77.2	75.3	75.6	62.3	62.6	66.5	811.1

Table 7.2.7.4.3　Average precipitation totals at Kerguelen (period 1951-1990).

Month	Jan	Feb	Mar	Apr	May	Jun	Jul	Aug	Sept	Oct	Nov	Dec	Year
Ave. temp' (ºC)	7.2	7.6	7.0	5.7	3.7	2.3	2.0	2.0	2.2	3.3	4.6	6.2	4.5

Table 7.2.7.4.4　Average temperature at Kerguelen (period 1951-1990).

Heard Island (refer Section 7.2.8 above)

Month	Jan	Feb	Mar	Apr	May	Jun	Jul	Aug	Sept	Oct	Nov	Dec	Year
Mean maximum temperature (ºC)	5.2	5.1	4.6	4.1	3.1	1.5	1.3	1.3	1.0	1.5	2.5	4.2	3.4
Extreme maximum temperature (ºC)	12.8	14.4	13.3	13.3	10.6	7.2	8.9	11.7	5.0	6.7	6.1	11.7	14.4
Mean minimum temperature (ºC)	1.6	1.7	1.2	0.7	−0.3	−2.0	−2.6	−2.5	−3.1	−1.9	−0.7	0.7	
Extreme minimum temperature (ºC)	−1.1	−1.1	−1.7	−4.4	−5.0	−8.9	−7.8	−8.9	−8.9	−8.3	−4.4	−1.1	−8.9
Mean rain amount (mm)	128	149	144	155	146	84	84	54	72	99	100	138	1353
Day of precipitation	28	25	27	27	24	21	20	20	18	21	20	23	274
Maximum wind gust & direction (kt)	W/85	E/85	W/90	SW/86	W/83	SW/93	SW/93	SW/113	W/96	W/90	WNW103	E/88	
Mean cloud amount (oktas)	8	8	8	7	7	7	7	7	7	7	8	8	

Table 7.2.8.4.1   Climate Statistics for Heard Island – Atlas Cove site (1948–54).

Macquarie Island (refer Section 7.2.9 above)

Month	Jan	Feb	Mar	Apr	May	Jun	Jul	Aug	Sept	Oct	Nov	Dec	Year
Mean daily maximum temperatures (º C)	8.7	8.6	8.0	6.9	5.8	5.0	4.9	5.1	5.4	5.7	6.5	7.9	6.5
Mean daily minimum temperatures (º C)	5.3	5.3	4.6	3.5	2.4	1.6	1.6	1.6	1.5	2.0	2.7	4.3	2.9
Highest daily maximum temp. (º C)	13.6	12.3	12.6	10.2	9.6	8.7	8.3	8.5	8.6	10.3	10.7	14.4	
Lowest daily minimum temp. (º C)	0.6	–0.6	–2.3	–4.5	–6.8	–7.0	–8.9	–8.9	–8.7	–4.6	–3.3	–1.7	
Mean 9am relative humidity (%)	88	87	88	88	89	89	89	89	87	85	86	87	88
Mean 3pm relative humidity (%)	86	86	87	89	89	88	89	88	86	85	85	85	87
Mean 9am cloud amount (oktas)	7	7	7	7	7	7	7	7	7	7	7	7	7
Mean 3pm cloud amount (oktas)	7	7	7	7	7	7	7	7	7	7	7	7	7
Maximum wind gust – Dir–Speed (m s^{-1})	W 46.9	W 40.2	WNW 50	W 47.4	W 45.8	W 46.9	W 49.4	SW 43.8	W 51.5	W 44.8	W 39.1	WNW 44.3	W 51.5
Mean MSL Pressure 9am (hPa)	999.4	1000.2	1001.6	1000.7	1001.3	1003.1	1004.0	1001.9	997.1	996.6	997.8	999.2	1000.2
Mean MSL Pressure 3pm (hPa)	998.9	100.0	1001.1	1000.1	1000.7	1002.5	1003.2	1001.4	996.5	996.2	997.4	998.9	999.7
Mean Daily Sunshine Duration (hours)	3.3	3.5	2.6	1.8	1.0	0.6	0.8	1.4	2.2	2.9	3.5	3.4	2.3
Mean monthly rainfall (mm)	85	82	90	89	75	71	65	65	74	72	68	73	916

Table 7.2.9.4.1   Climate statistics for Macquarie Island

Great Wall Station (refer Section 7.3.2 above)

Element/Month	Jan	Feb	Mar	Apr	May	Jun	Jul	Aug	Sept	Oct	Nov	Dec	Year
Mean daily temperatures (º C)	1.8	1.9	0.4	–2.2	–4.7	–6.0	–7.0	–5.9	–4.2	–2.9	–1.0	0.5	–2.5
Highest daily maximum temp. (º C)	11.7	8.4	8.4	4.3	6.8	5.7	2.6	3.3	3.8	3.6	5.5	8.3	11.7
Lowest daily minimum temp. (º C)	–3.1	–5.5	–10.3	–17.2	–24.0	–22.4	–26.6	–26.6	–23.5	–16.3	–12.4	–8.2	–26.6
Mean relative humidity (%)	88	89	88	88	87	87	90	90	90	89	90	88	89
Mean cloud amount (oktas)	7.4	7.0	7.0	7.1	6.6	6.6	6.7	6.9	7.0	6.9	7.1	7.4	7.0
Mean wind direction	ESE	WNW	ESE	ESE	ESE	ESE	ESE	WNW	WNW	WNE	WNW	WNW	ESE
Mean wind speed (m s^{-1})	6.3	6.6	7.3	7.3	7.6	7.7	7.7	7.6	8.4	8.5	7.3	6.4	7.4
Maximum wind gust – (m s^{-1})	26.0	29.0	30.0	29.8	28.0	37.7	34.5	28.0	34.2	37.2	27.0	30.8	37.7
No. days of gales	6	6	11	11	14	12	15	14	16	15	8	5	133
Mean MSL pressure (hPa)	990.0	994.2	987.4	989.5	994.0	991.7	991.4	990.2	988.1	988.1	984.8	986.7	989.8
Mean monthly rainfall (mm)	48.5	61.9	68.2	54.7	38.5	48.7	51.9	35.5	42.0	38.7	41.9	36.1	566.6
No. of rain days	19	19	23	22	20	22	23	22	23	22	20	19	254

Table 7.3.2.4.1　　Annual weather/climate characteristics over 1985–95, from measurements at Great Wall Station.

Direction	JAN	FEB	MAR	APR	MAY	JUN	JUL	AUG	SEP	OCT	NOV	DEC
360	10.9	10.6	10.1	8	8.8	10.4	8.3	12.2	13.9	12.4	13.6	12.9
30	7.1	7.6	6.4	6.3	6.5	6.5	6	5.8	7.5	5	5.9	5.9
60	2.4	2	2.5	2.1	2.4	2.4	1.5	1.1	0.5	0.8	2	1.8
90	12.2	7.4	8.6	9.3	7.5	8.9	5.6	8.2	5	4.3	6.4	9
120	17.8	16.5	13.3	14.6	15	14.9	13.7	12	9.7	7.5	10.6	15.9
150	5.1	3.6	3.3	3.9	5.9	7.1	4.8	6.8	5.2	1.5	2.5	4.1
180	1.2	1	0.9	1.5	2.7	2.1	2.4	1.9	1	1.1	0.9	0.8
210	1.5	1.6	1.5	2.6	3.5	1.8	2.1	3.5	2.4	2.5	1.8	1
240	3.7	5.5	4.4	6	9.2	6.2	8.1	7	8.3	8.1	5.7	4.3
270	11.7	14.5	17.1	13.6	9.7	10.8	10.9	9.7	12.7	17.9	16.2	12.6
300	9.6	10.8	12.5	9.7	7.1	7	8	9	9.7	13.4	11	3.4
330	11.5	14.4	14.9	16.6	12.2	10	12.1	12.3	16.8	19.8	16.9	13.6
CALM	5.4	4.4	4.5	5.8	9.6	12	16.5	10.6	7.4	5.7	6.5	4.8

Table 7.3.2.4.2   Monthly distribution (%) of wind directions at Frei Station.
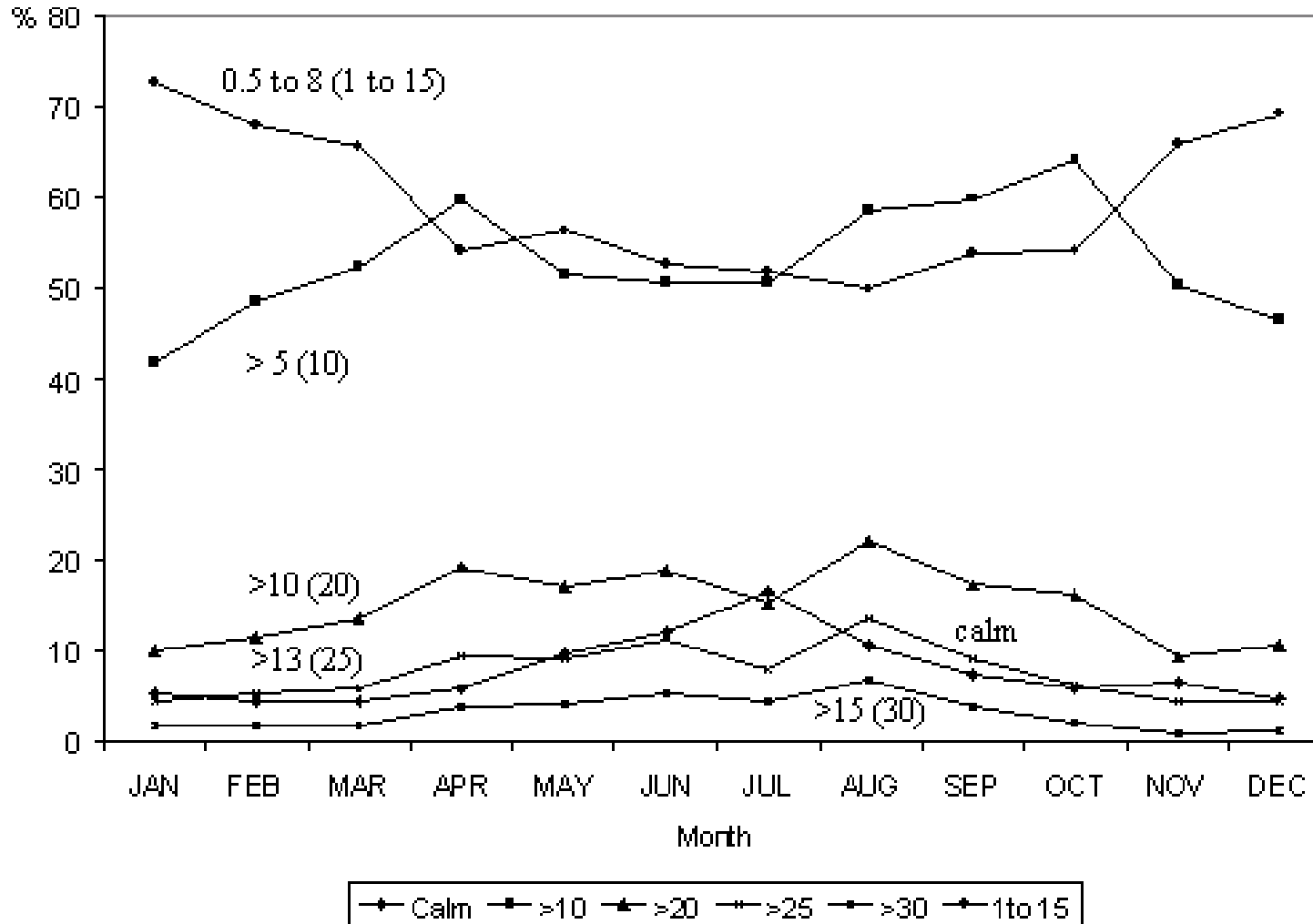
Figure 7.3.2.4.1 Frequency of occurrence of wind speeds higher than certain specified values at Frei Station.
(The key shows the units in kt while the figure shows m s^{-1} (kt)).
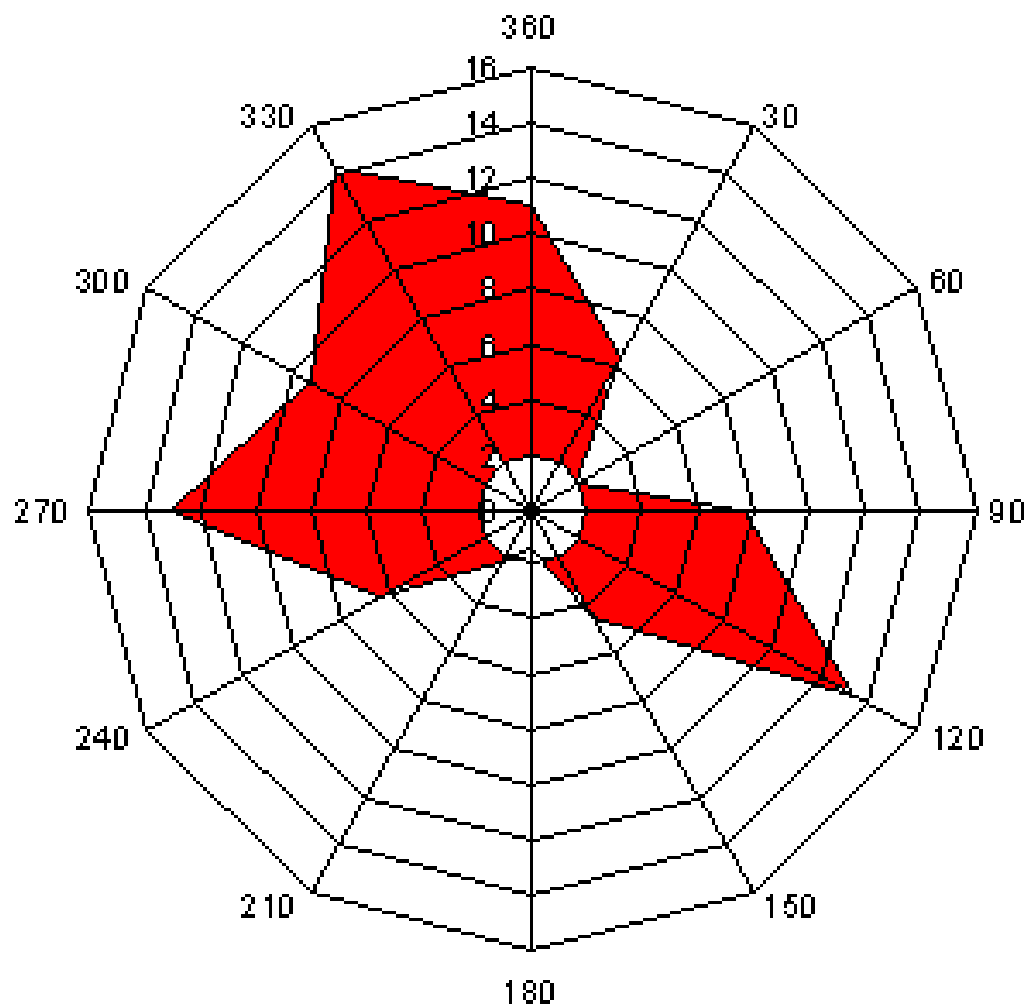
Figure 7.3.2.4.2   Annual mean wind direction at Frei Station.
(The red area shows the envelope of wind directions at Frei).
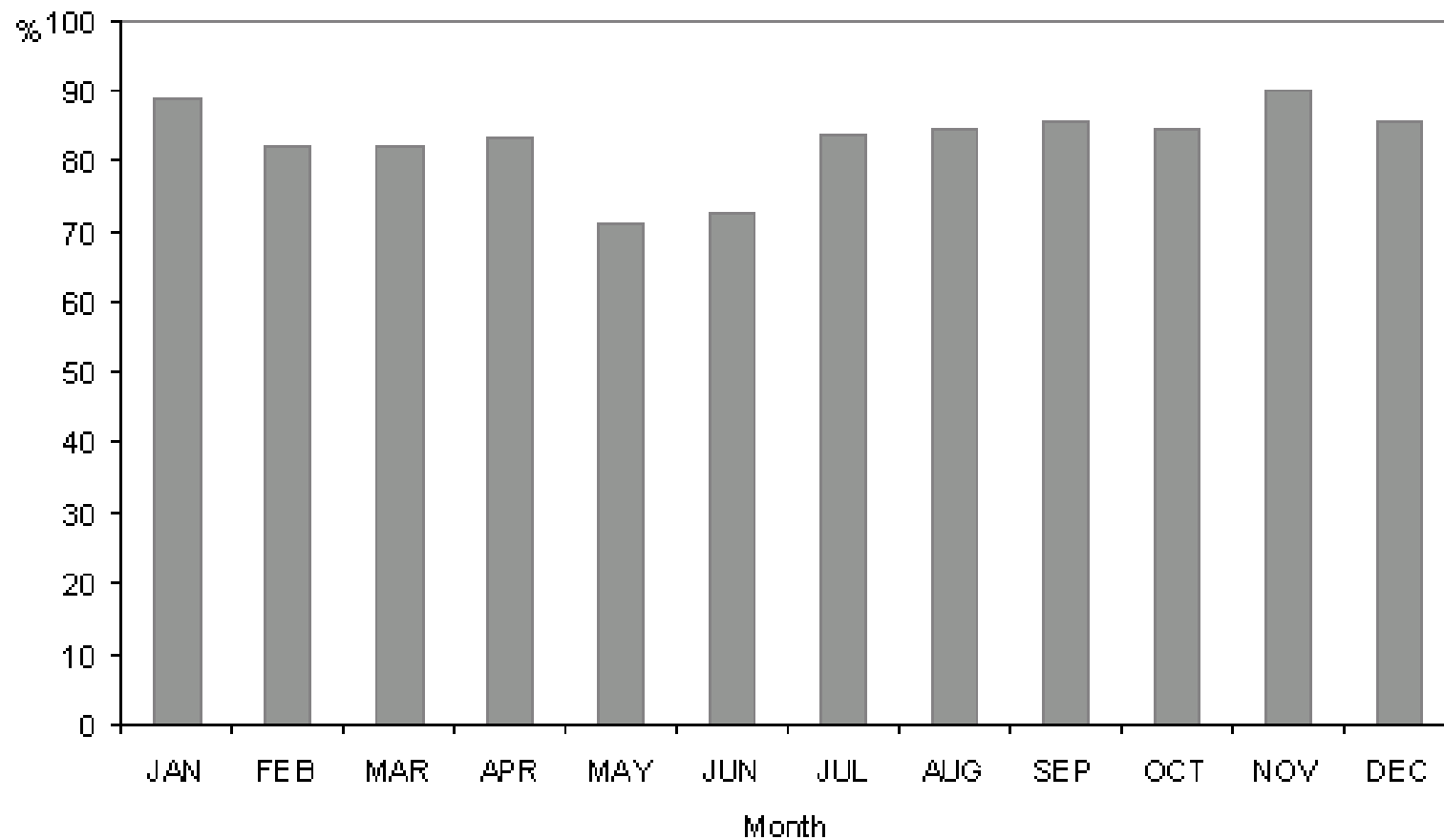
Figure 7.3.2.4.3   Percentage of days at Frei with 6 or more oktas of cloud.
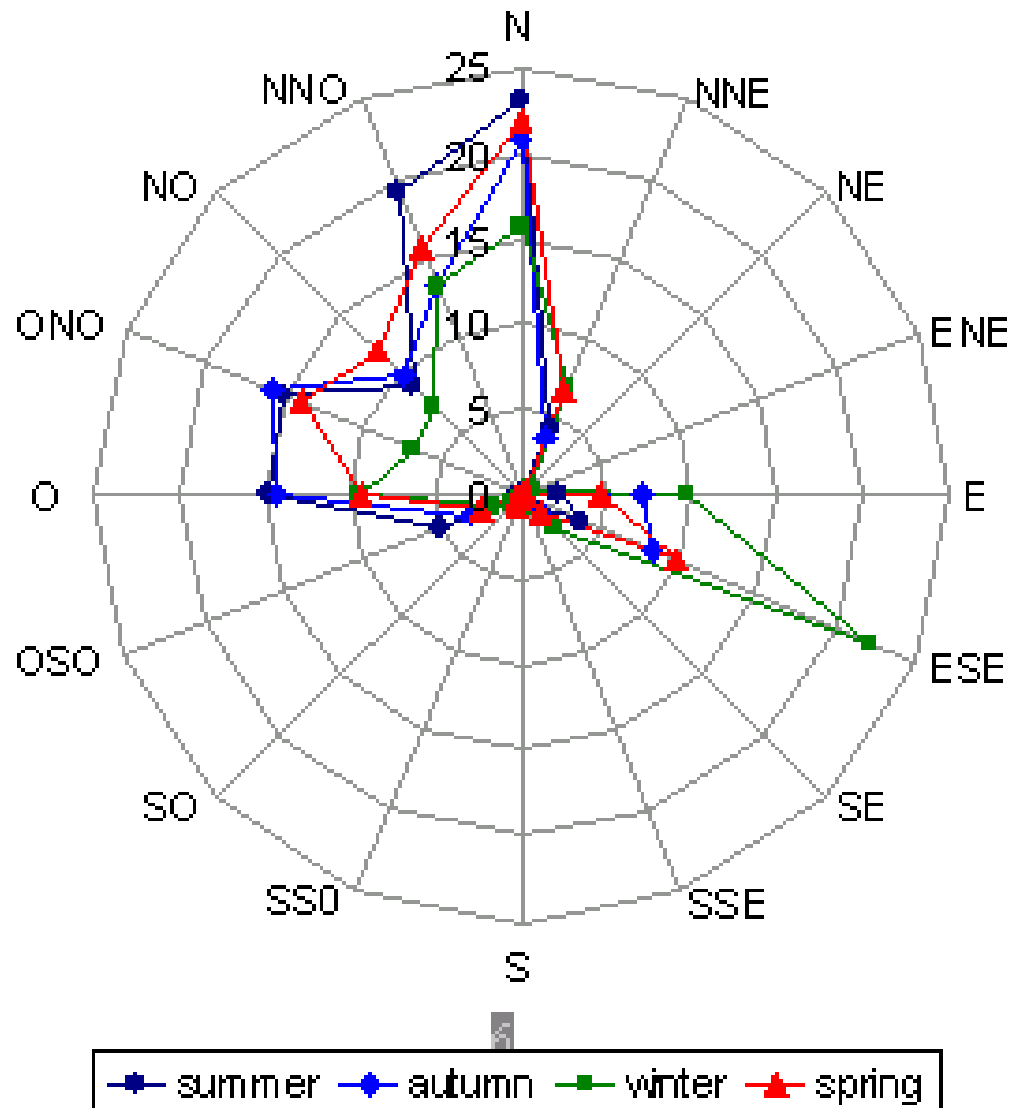
Figure 7.3.2.4.4   % frequency of wind directions at Frei Station when the visibility is less than 1600m for the various seasons.
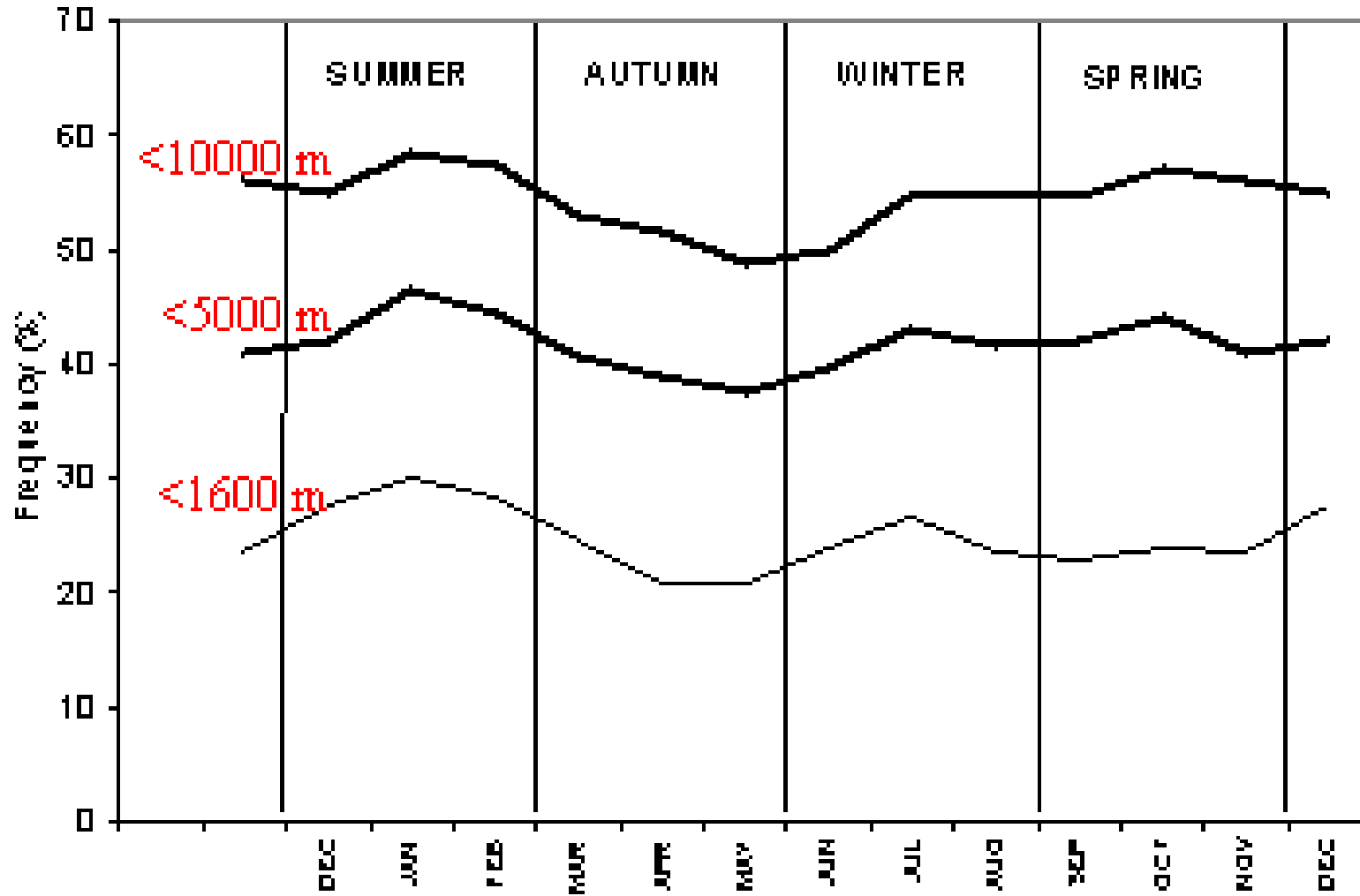
Figure 7.3.2.4.5   Percentage frequency of reduced visibility at Frei Station when the visibility is less than 1600m, 5000m and 10000 m for the various seasons.
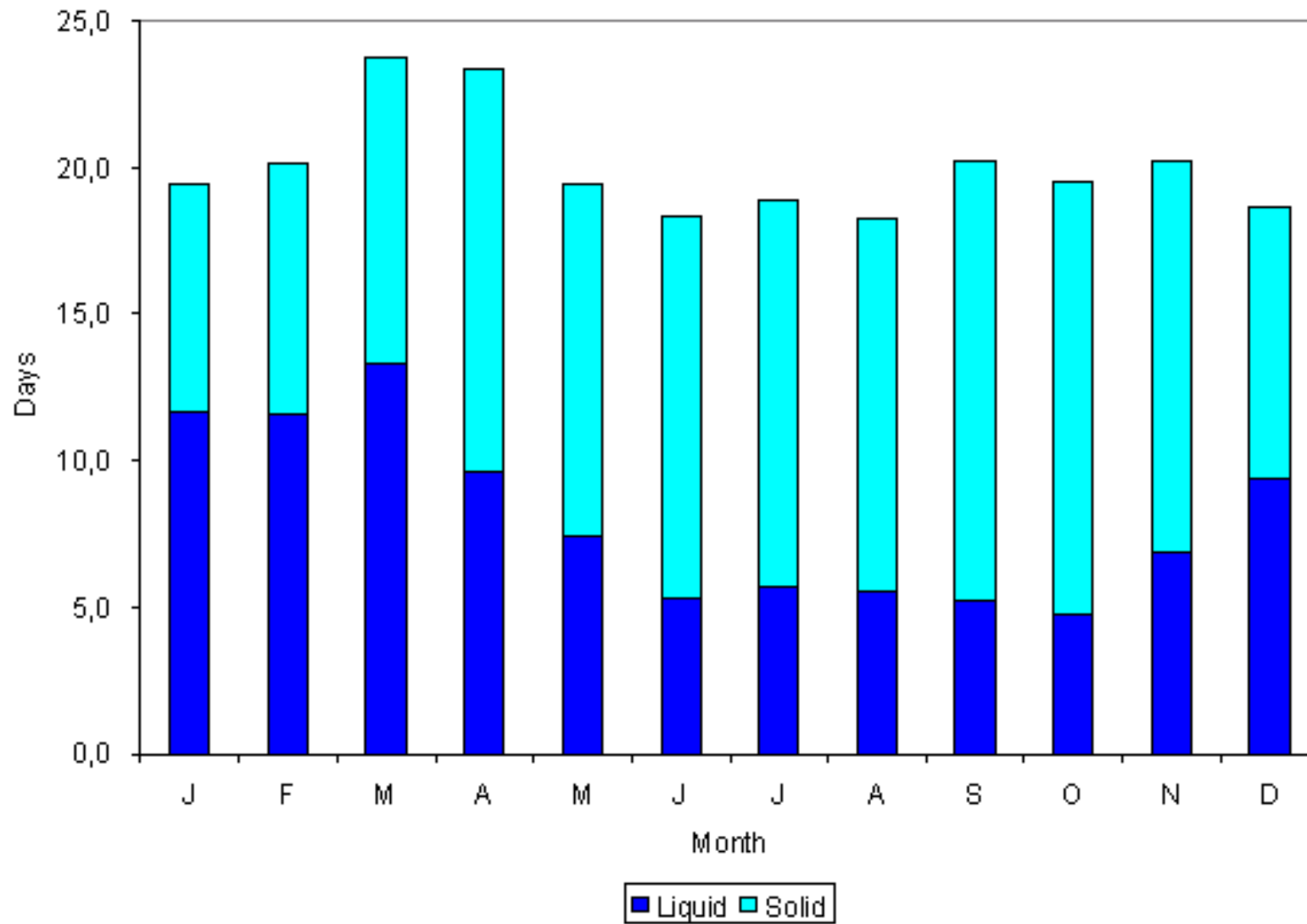
Figure 7.3.2.4.6 Average numbers of days per month of liquid or solid precipitation at Frei Station.
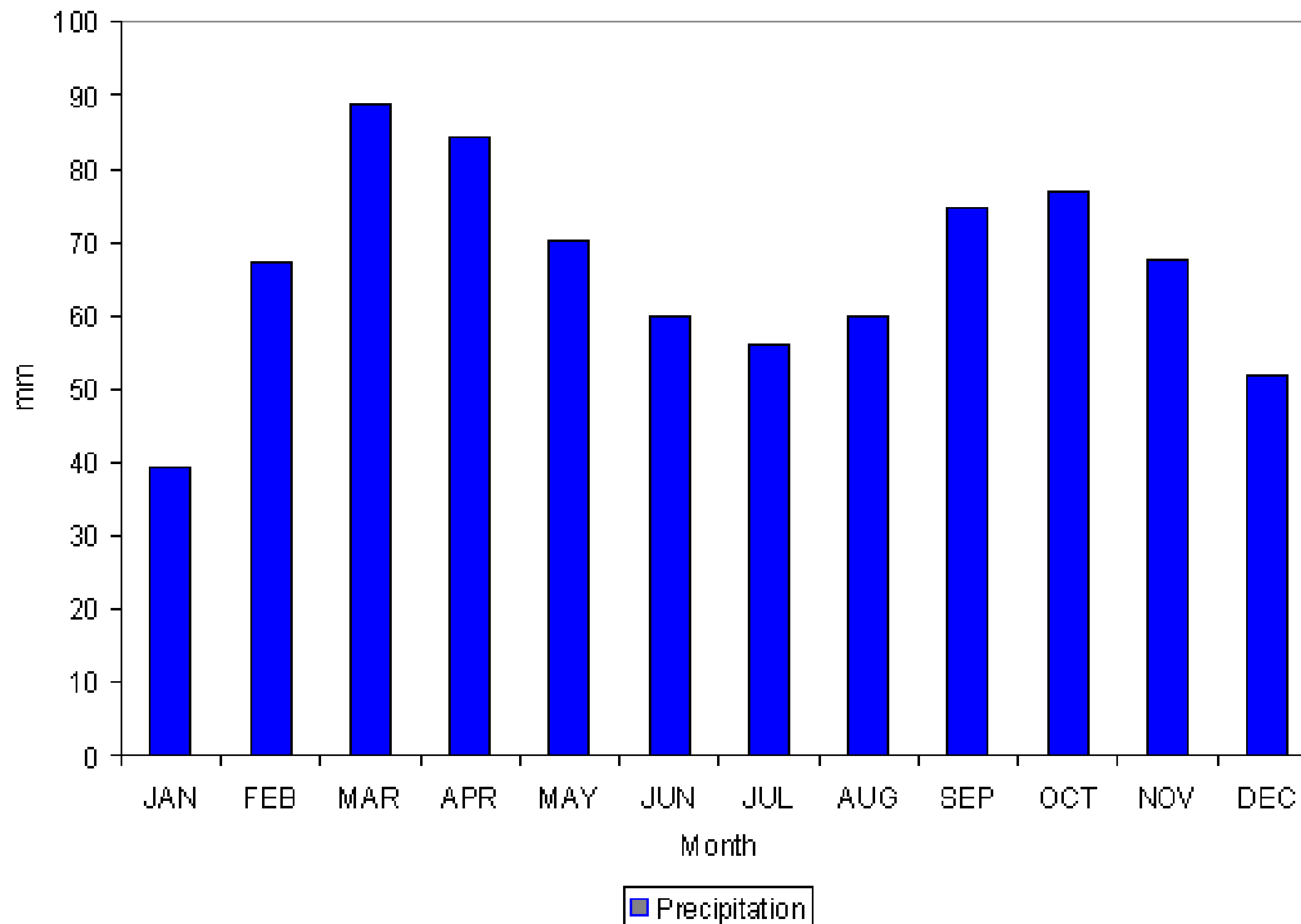
Figure 7.3.2.4.7 Average numbers of days per month of liquid or solid precipitation at Frei Station.
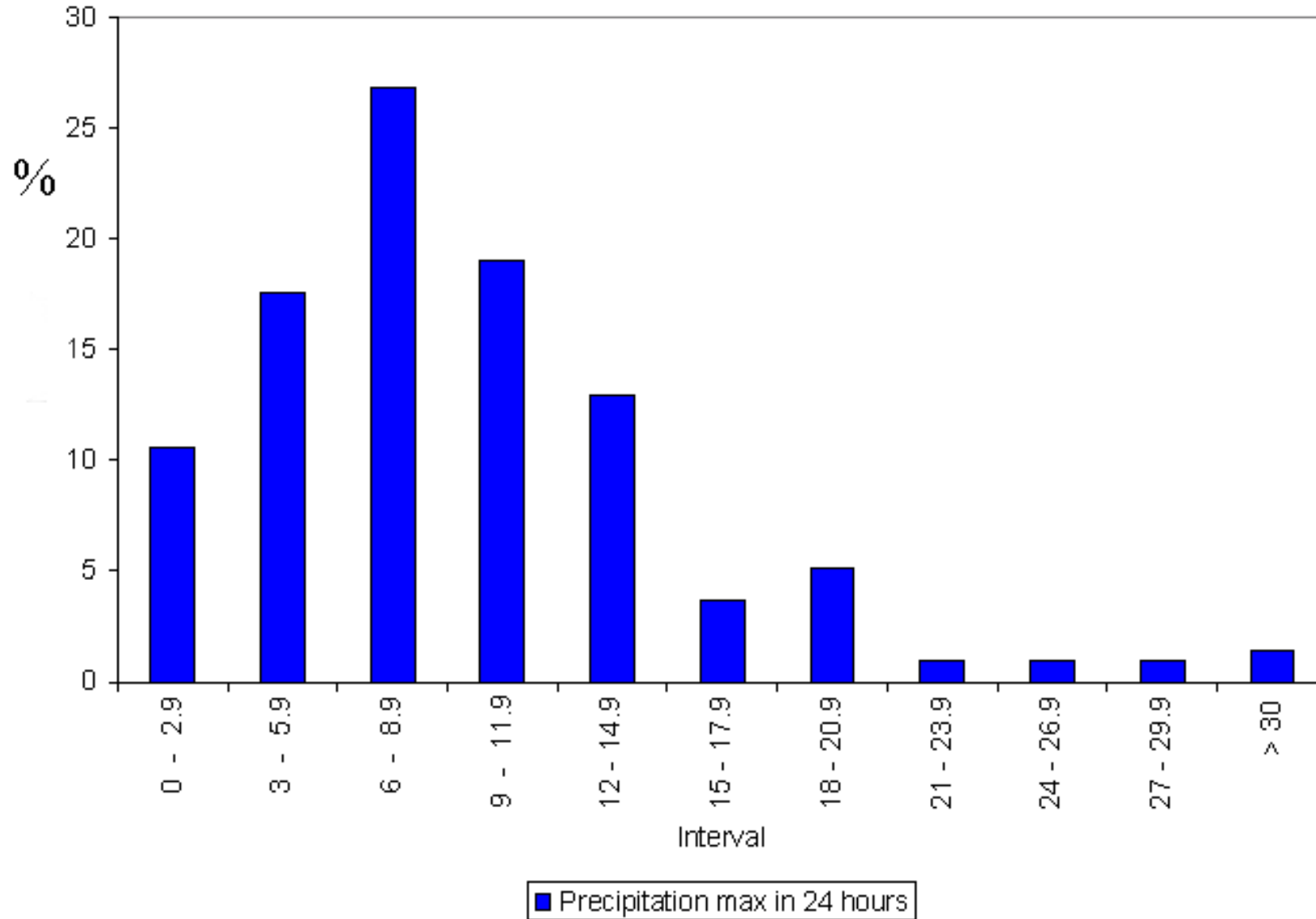
Figure 7.3.2.4.8   Percentage occurrence of rainfall amounts falling in 24 hr at Frei Station.
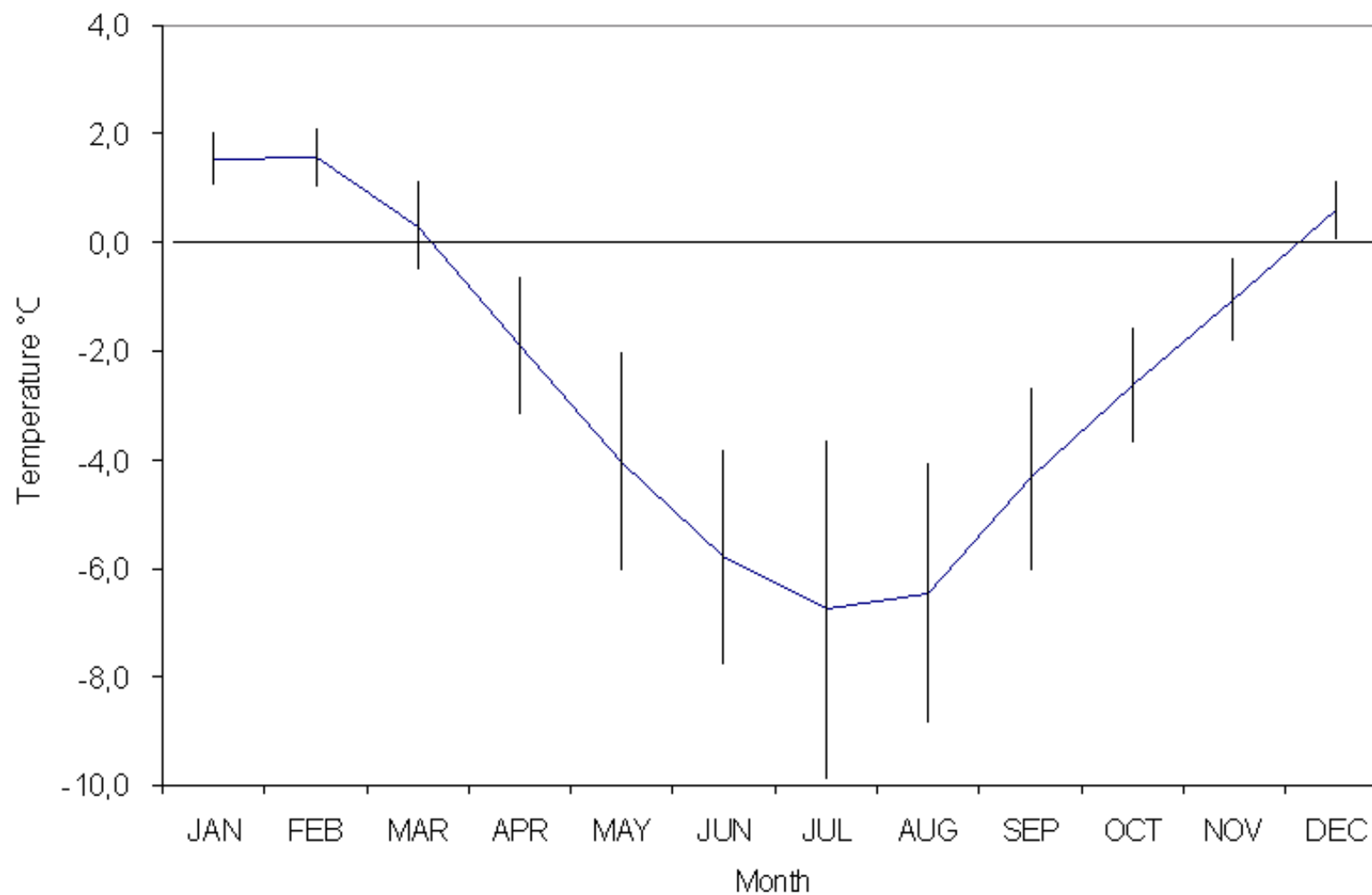
Figure 7.3.2.4.9 Mean monthly temperature (solid line) and standard deviations (vertical bars) of the monthly mean temperatures at Frei Station.
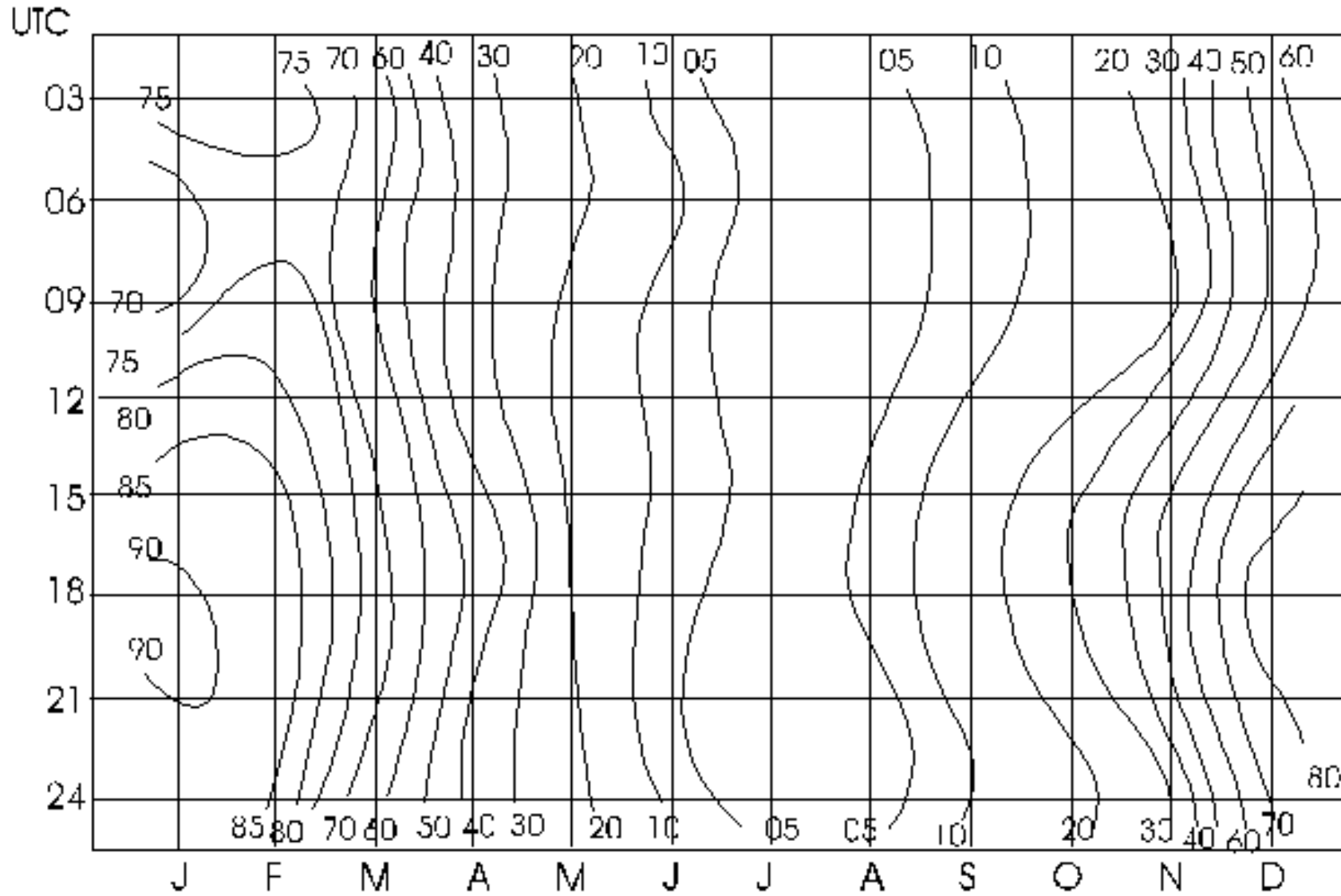
Figure 7.3.2.4.10   Hourly and monthly percentage distribution of above freezing temperatures (T>0ºC) at Frei Station.
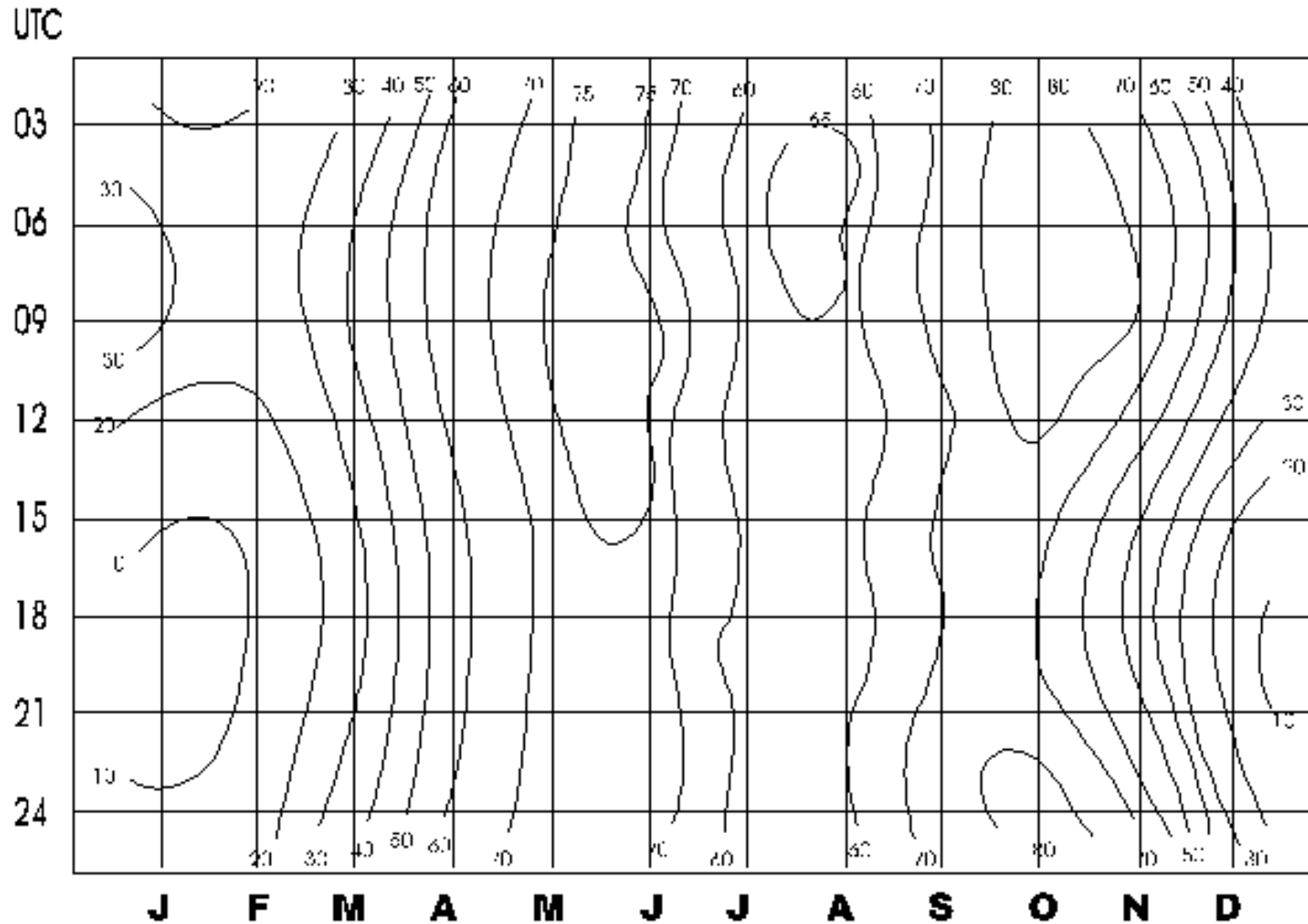
Figure 7.3.2.4.11   Hourly and monthly percentage distribution of above freezing temperatures (T>0ºC) at Frei Station.

Marambio (refer Section 7.3.5 above)
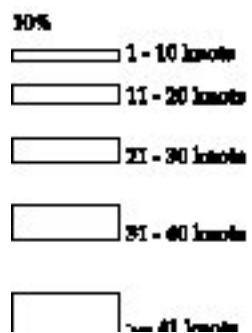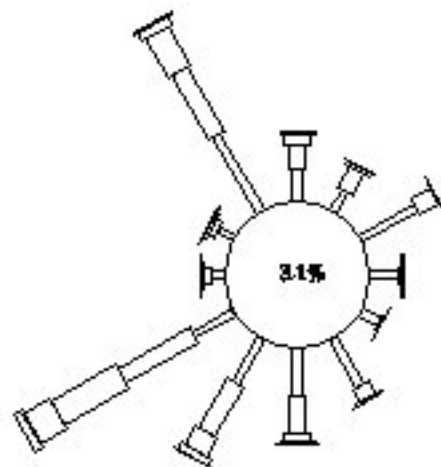
Figure 7.3.5.4.1   A summer season (November to March) wind rose for Marambio.
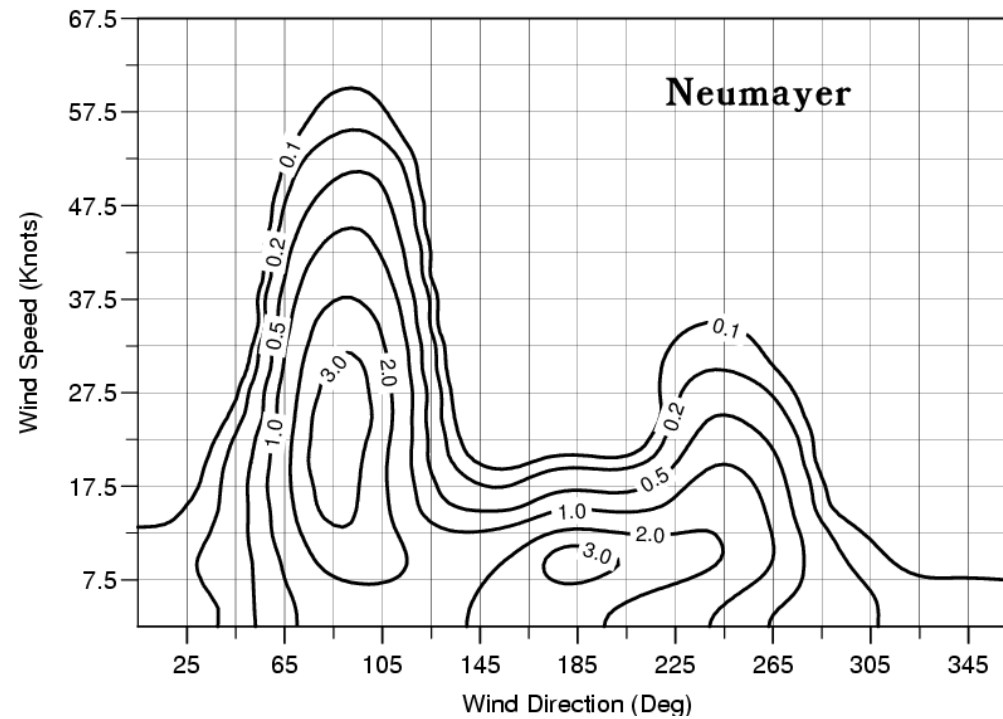
Figure 7.5.4.4.1   Frequency distribution of wind speed vs wind direction at Neumayer in percent of all observations with a wind speed exceeding 2.5 kt (1.3 m s^{-1}). The class widths are 5 kt (2.6 m s^{-1}) and 20°, respectively.
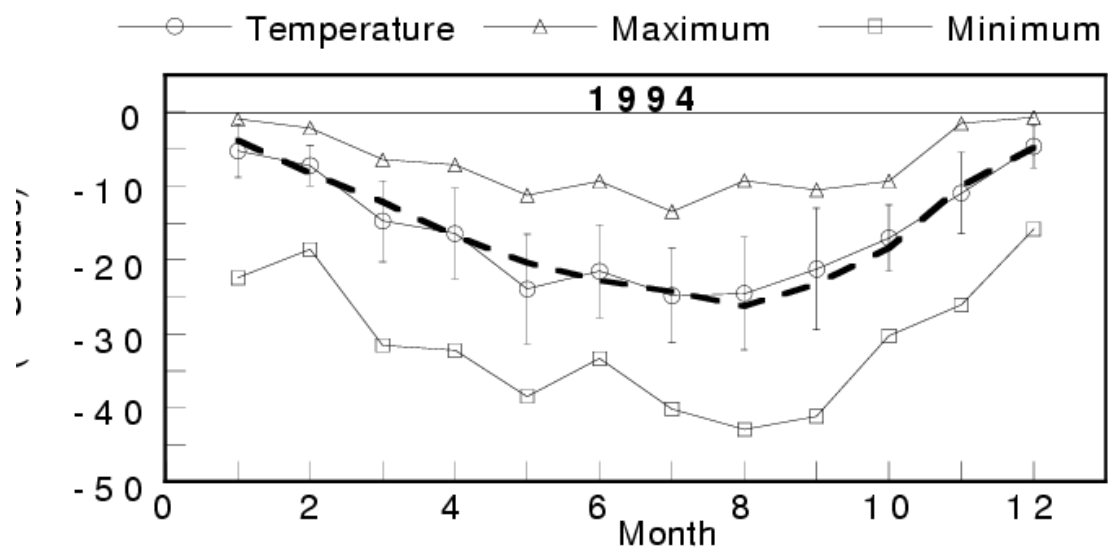
Figure 7.5.4.4.4 Mean monthly maximum and minimum temperature for Neumayer

SANAE (refer Section 7.5.5 above)

	N	NNE	NE	ENE	E	ESE	SE	SSE	S	SSW	SW	WSW	W	WNW	NW	NNW	Year
Jan	6.9	8.0	14.3	16.7	17.8	11.7	10.7	9.3	8.5	8.0	8.3	9.3	9.8	8.7	7.6	6.1	10.7
Feb	9.4	8.5	18.3	25.4	19.8	15.7	13.3	9.8	9.6	8.7	8.9	12.8	13.5	10.4	7.8	6.5	13.9
Mar	8.1	10.2	15.9	20.4	25.0	19.6	15.9	13.9	12.6	12.2	12.0	14.4	14.8	10.0	13.1	4.6	16.9
Apr	15.	23.3	23.9	29.6	25.2	20.9	16.7	13.9	12.6	11.1	11.1	10.0	10.6	12.8	11.3	8.7	17.2
May	11.	12.6	22.2	29.4	29.6	21.3	18.3	15.0	11.9	11.1	11.1	12.6	12.4	12.8	12.2	12.6	19.1
Jun	9.8	11.1	26.1	16.5	28.5	21.5	14.6	12.4	11.5	25.6	25.6	22.8	13.1	12.8	15.4	14.8	16.3
Jul	12.	19.4	20.7	25.0	25.4	22.4	14.4	12.6	11.5	11.3	11.3	15.4	13.7	15.2	11.3	10.2	15.7
Aug	13.	12.8	20.6	28.0	28.5	19.1	15.6	12.4	11.5	15.2	15.2	14.4	13.1	11.7	11.3	9.1	16.1
Sep	13.	11.5	25.2	24.1	27.0	19.1	14.6	12.6	11.5	12.6	12.6	12.0	12.6	13.3	12.0	11.1	16.1
Oct	10.9	10.2	23.5	25.9	27.0	19.1	15.4	11.3	10.4	12.2	12.2	12.8	12.2	13.3	11.7	8.5	16.5
Nov	9.4	12.0	16.7	22.2	21.9	22.4	14.6	10.6	11.1	9.8	9.8	11.9	11.5	10.0	8.9	9.4	14.4
Dec	6.3	9.4	15.9	20.6	19.6	18.0	12.4	9.4	8.0	7.8	7.8	7.8	10.9	9.1	7.8	7.8	13.0
Year	11.1	14.3	18.1	23.5	24.1	15.7	15.0	12.2	10.7	12.4	12.4	13.0	12.2	11.5	10.6	9.3	15.6

Table 7.5.5.4.1   Mean wind speed (kt) for SANAE III, 1960–83.

	N	NNE	NE	ENE	E	ESE	SE	SSE	S	SSW	SW	WSW	W	WNW	NW	NNW	Calms (%)
Jan	0.9	0.9	4.3	8.3	20.1	10.7	10.8	5.8	5.5	3.7	2.7	1.9	4.3	3.1	1.9	0.6	14.5
Feb	0.2	0.4	1.3	6.7	20.5	16.3	16.3	9.1	8.5	4.3	2.5	1.7	2.3	1.5	0.6	0.2	7.6
Mar	0.2	0.4	2.0	6.0	19.2	15.5	19.1	12.5	8.3	4.6	2.9	1.1	1.7	0.8	0.7	0.3	4.7
Apr	0.5	1.6	3.2	8.9	12.4	13.2	16.7	12.0	10.8	6.1	3.9	1.6	1.4	0.9	0.6	0.3	5.9
May	0.7	0.9	3.7	9.4	18.3	14.5	15.5	10.7	8.5	5.1	1.6	1.4	1.2	1.3	0.7	0.5	6.0
Jun	0.2	0.3	2.5	9.3	14.2	15.3	13.9	10.2	9.2	5.0	2.7	1.8	1.1	1.6	1.1	0.4	11.2
Jul	1.2	1.1	3.8	6.2	11.9	15.6	15.3	12.3	11.0	4.4	1.9	1.4	2.0	1.7	0.7	0.3	9.2
Aug	0.6	0.3	1.2	5.2	13.0	13.2	18.6	12.7	11.2	5.3	3.7	2.7	2.8	1.5	0.7	0.2	7.1
Sep	0.6	0.2	2.4	6.5	15.4	15.6	15.3	9.8	9.8	5.2	3.2	1.8	2.7	2.1	1.2	0.5	7.7
Oct	0.3	0.4	2.2	6.7	16.1	16.2	14.4	10.0	9.8	4.8	3.3	1.9	2.3	1.8	1.2	0.4	8.2
Nov	0.5	0.7	2.5	6.0	16.7	18.0	16.5	9.5	7.2	4.2	2.7	1.8	1.8	1.8	1.4	0.6	8.1
Dec	0.3	0.7	3.8	8.6	21.3	17.2	11.0	7.0	5.2	4.1	2.4	1.7	2.4	2.0	1.1	0.6	10.6
Year	0.5	0.7	2.7	7.3	16.6	15.1	15.3	10.1	8.8	4.7	2.8	1.7	2.2	1.7	1.0	0.4	8.4

Table 7.5.4.4.2   Mean wind direction frequency (%) and Calms for SANAE III, 1963–80

Month	Mean (ºC)	Mean Max. (ºC)	Mean Min. (ºC)	Record Max. (ºC)	Record Min. (ºC)
January	−3.6	−0.5	−7.9	7.3	−19.9
February	−8.7	−4.9	−13.9	3.7	−29.3
March	−13.0	−9.3	−17.5	2.0	−35.5
April	−18.9	−14.5	−24.0	−0.1	−42.8
May	−21.2	−16.7	−25.7	3.6	−51.0
June	−23.5	−18.8	−28.3	−1.2	−47.9
July	−27.7	−22.6	−32.8	−5.5	−50.0
August	−27.6	−22.7	−32.4	−3.8	−50.0
September	−25.0	−20.4	−30.5	−1.9	−48.3
October	−18.7	−14.4	−24.3	−1.3	−41.7
November	−10.7	−6.7	−16.4	3.1	−33.0
December	−4.6	−1.2	−9.2	7.0	−21.2
Year	−16.9	−12.7	−21.9		

Table 7.5.5.4.3   Temperature statistics for SANAE III, 1963–80

Maitri and Dakshin Gangotri (refer Section 7.5.7 above)
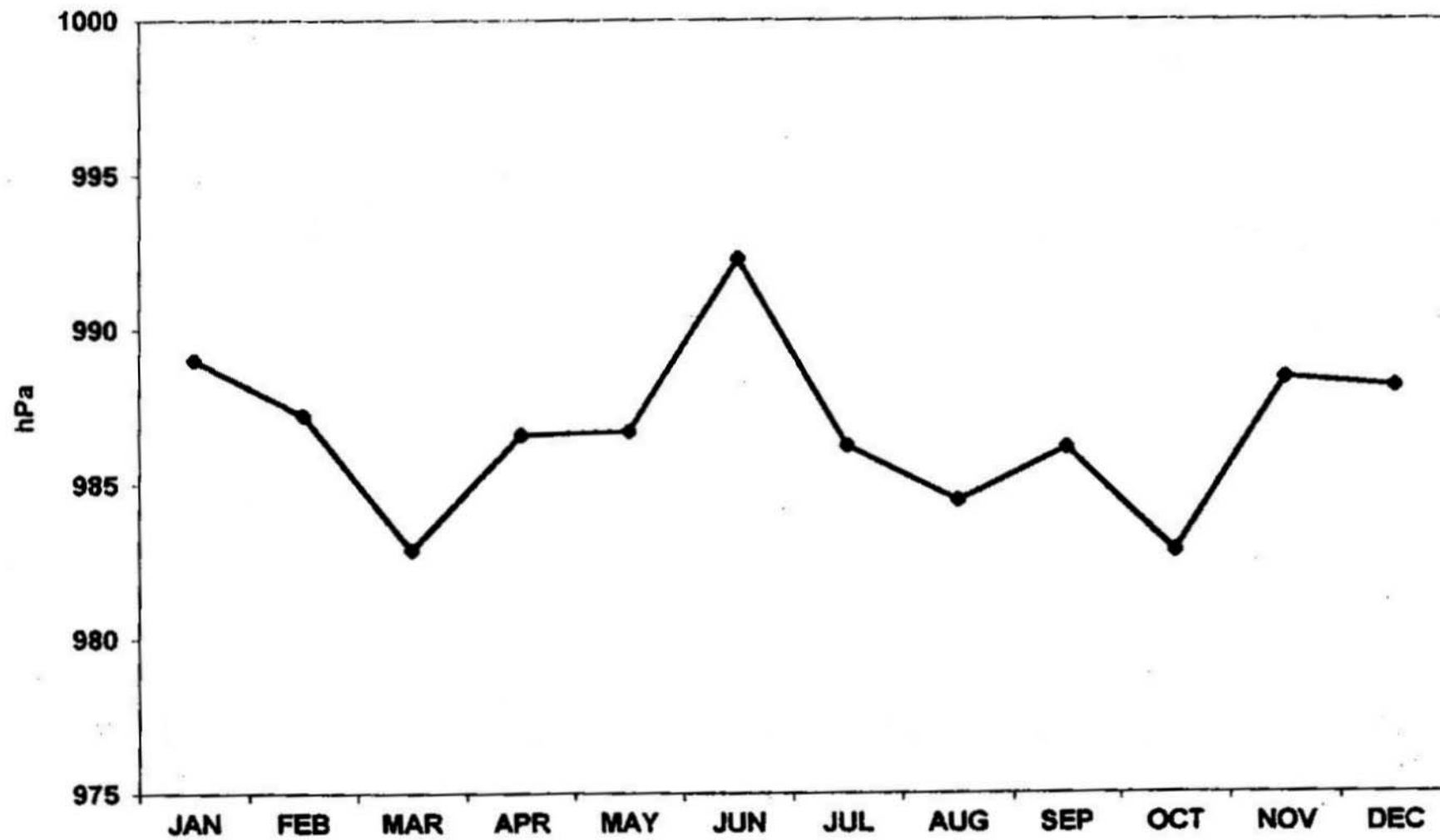
Figure 7.5.7.4.1 Mean monthly pressure recorded at Maitri for the period 1990–97
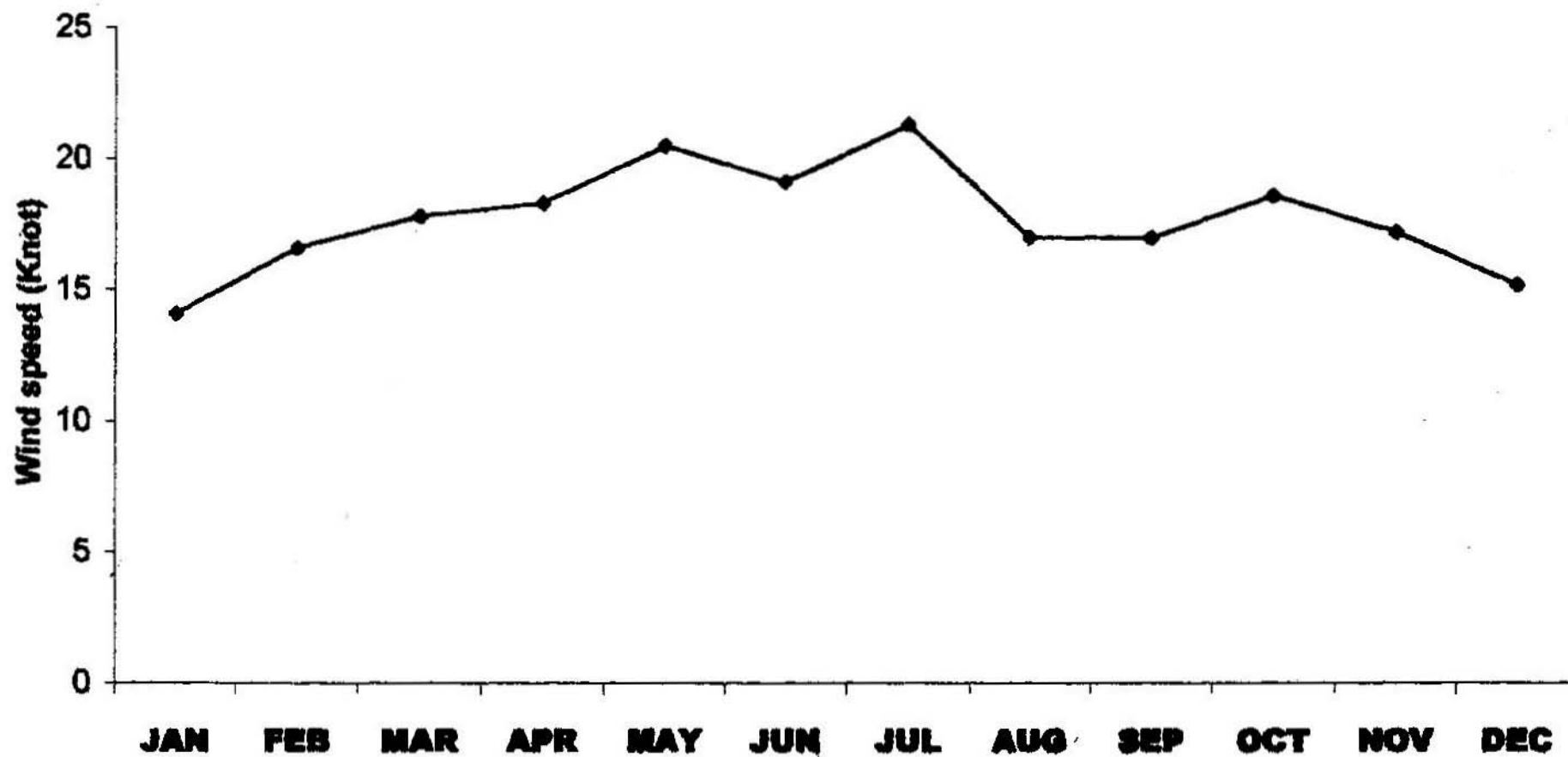
Figure 7.5.7.4.2 Mean monthly wind speed at Maitri (1990–97)
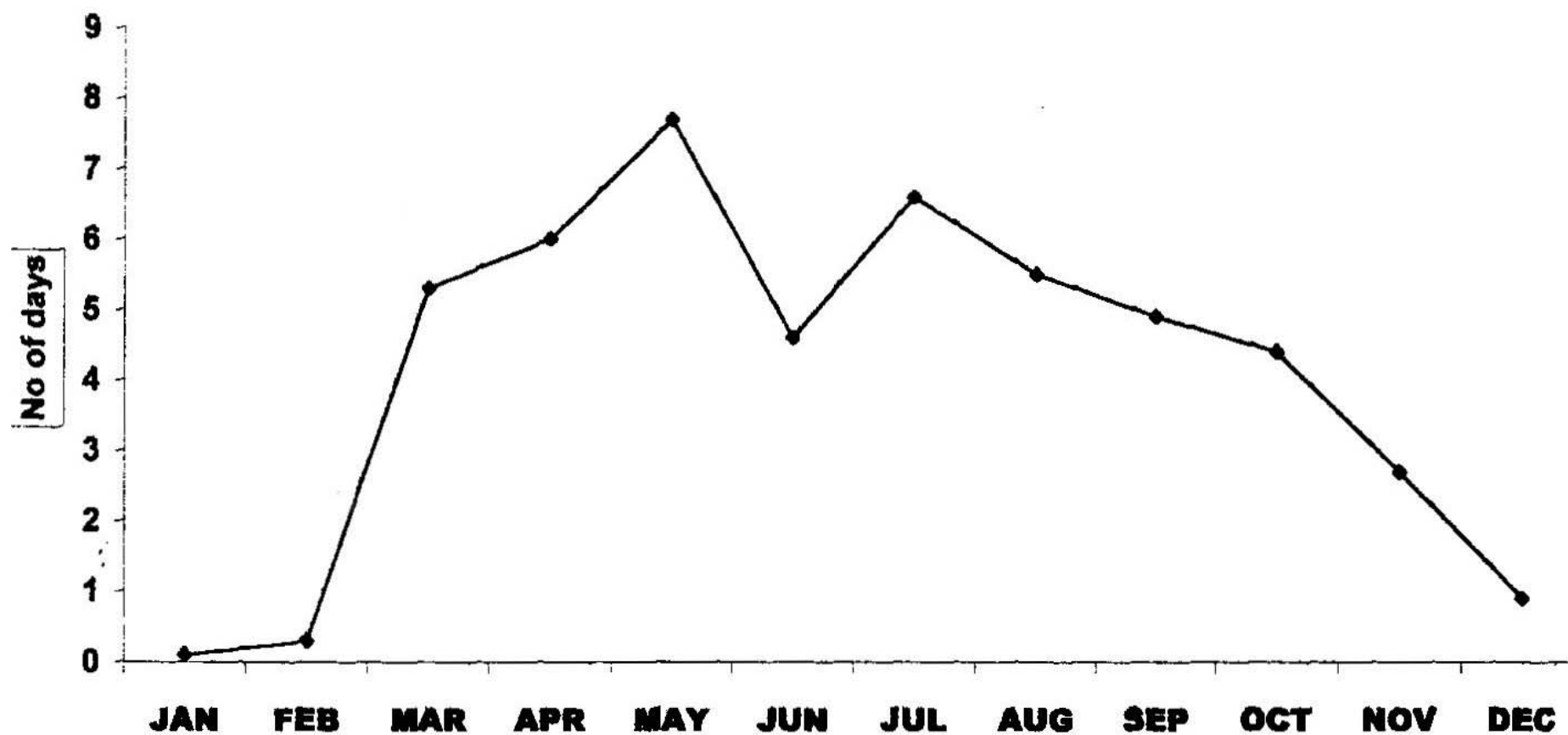
Figure 7.5.7.4.3 Mean monthly days of blizzard at Maitri (1990–97)

CALM 8·2 % VARIABLE 1·0 %
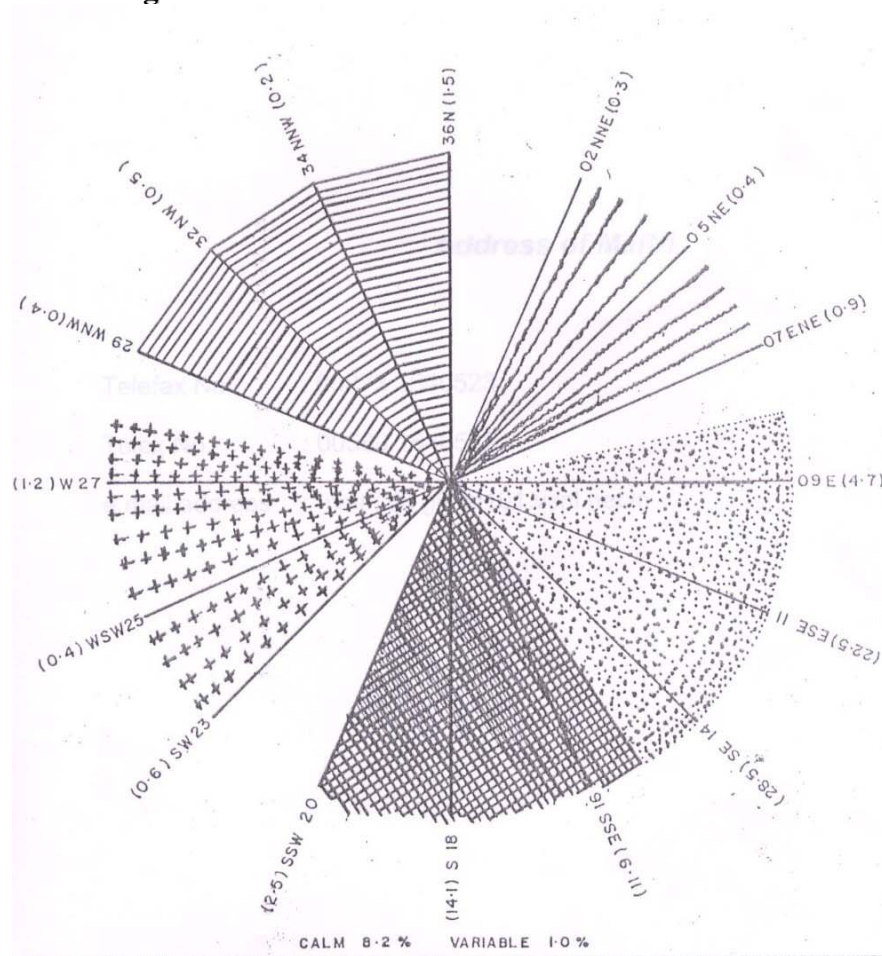
Fig 4.1   MAITRI WIND ROSE (1992 DATA)

▨ ALMOST ALWAYS DUE TO EASTWARD MOVING DEPRESSIONS ALONG THE COAST.

▨ INVARIABLY DUE TO KATABATIC / POLAR ANTICYCLONIC FLOW

▨ DUE TO SYSTEMS PENETRATING SOUTH OF 70° S

▭ GENERALLY DUE TO PENETRATION OF HIGH PRESSURE RIDGE OVER STATION LONGITUDE

▭ GENERALLY DUE TO RECURVING OF SYSTEMS TOWARDS 'NE' AFTER THEY CROSS
THE STATION LONGITUDE.

(FIGURES IN BRACKET INDICATE PERCENT OCCASIONS OF WIND BLOWING FROM THE
INDICATED DIRECTION.)

Figure 7.5.7.4.4   Wind rose for Maitri based on 1992 data

	% occurrence in 1993		% occurrence in 1997	
	Annual	**"Winter"**	**Annual**	**"Winter"**
		(Mar–Aug)		(Mar–Aug)
Clear sky	30	26	30	28
Obscured sky	5	–	15	7
Overcast sky	45	39	25	25

Table 7.5.7.4.1　Percentage of overcast/sky clear/sky obscured conditions from 1993 and 1997 data at Maitri.

Inland of Syowa (Asuka, Mizuho, Dome Fuji) (refer Section 7.5.9 above)

Parameter/Month	Jan	Feb	Mar	Apr	May	Jun	Jul	Aug	Sept	Oct	Nov	Dec	Year
Mean temperatures (º C)	−8.3	−11.9	−16.1	−20.6	−23.7	−22.3	−23.3	−25.6	−25.7	−20.2	−14.0	−8.5	−18.3
Highest daily maximum temp. (º C)	0.5	0.0	−1.7	−8.8	−7.0	−7.8	−9.2	−12.9	−12.3	−6.6	−2.8	0.3	0.5
Lowest daily minimum temp. (º C)	−18.8	−24.4	−33.8	−38.1	−42.9	−44.6	−42.0	−48.7	−45.7	−37.0	−32.9	−19.0	−48.7
Mean cloud amount (oktas)	4.5	5.1	4.5	3.9	4.1	4.2	4.1	4.0	3.6	3.8	3.7	3.4	4.1
Global radiation (mJ m^{-2})	29.7	19.1	9.1	2.3	0.1	0.0	0.0	1.1	6.3	16.3	28.2	34.8	12.2
Mean wind speed (m s^{-1})	10.8	13.4	13.7	12.1	11.4	13.9	14.4	13.7	12.9	12.7	12.5	9.4	12.6
Maximum wind gust – Dir–Speed (m s^{-1})	ESE 27.8	ESE 32.0	ESE 30.9	ESE 27.2	SE 29.9	ESE 34.3	E 29.1	ESE 30.8	SE 30.5	SE 33.0	E 26.5	ESE 23.8	ESE 34.3
Mean station level pressure (hPa)	876.2	872.5	871.3	873.1	872.2	874.1	869.1	865.5	868.3	868.1	871.2	875.8	871.5

Table 7.5.9.4.1   Climate statistics for Asuka Station (averages (5 yr) and extremes from 1987–91)

Parameter/Month	Jan	Feb	Mar	Apr	May	Jun	Jul	Aug	Sept	Oct	Nov	Dec	Year
Mean temperatures (º C)	−35.4	−43.8	−56.4	−60.9	−66.5	−64.0	−61.2	−65.5	−63.6	−57.2	−43.8	−33.0	−54.3
Highest daily maximum temp. (º C)	−18.6	−18.9	−37.4	−36.9	−49.4	−29.2	−38.2	−41.5	−44.1	−38.4	−25.0	−21.1	−18.6
Lowest daily minimum temp. (º C)	−48.9	−60.9	−67.9	−75.0	−79.7	−79.6	−79.7	−79.6	−78.3	−72.3	−64.8	−47.2	−79.7
Mean cloud amount (oktas)	3.6	2.9	2.0	2.6	2.0	1.8	3.2	2.2	2.6	2.3	2.7	3.7	2.6
Global radiation (mJ m^{-2})	35.3	22.1	9.7	1.2	0.0	0.0	0.0	0.2	5.1	17.3	32.2	39.1	13.5
Mean wind speed (m s^{-1})	4.4	5.0	5.6	6.5	6.0	6.2	6.6	6.5	6.1	5.9	5.6	4.8	5.8
Maximum wind gust – Dir–Speed (m s^{-1})	NE 11.1	NE 11.3	ESE 9.4	WSW 12.0	S 11.8	N 16.5	NE 18.4	E 13.0	NE 13.5	NE 14.5	NE 13.5	NE 13.3	NE 18.4
Mean station level pressure (hPa)	607.0	605.7	596.8	596.2	592.4	597.1	596.1	593.8	591.7	593.3	606.1	608.0	598.7

Table 7.5.9.4.2   Climate statistics for Dome Fuji Station (averages (3yr) and extremes from 1995–97).

Parameter/Month	Jan	Feb	Mar	Apr	May	Jun	Jul	Aug	Sept	Oct	Nov	Dec	Year
Mean temperatures (º C)	−18.1	−24.0	−31.3	−36.9	−38.6	−40.3	−40.1	−40.6	−38.8	−35.2	−25.6	−18.2	−32.3
Highest daily maximum temp. (º C)	−2.7	−9.6	−14.4	−18.2	−16.2	−21.2	−16.9	−18.0	−19.4	−17.1	−6.8	−4.2	−2.7
Lowest daily minimum temp. (º C)	−33.5	−39.9	−48.4	−52.8	−55.0	−58.1	−61.9	−58.4	−57.7	−53.6	−45.9	−36.0	−61.9
Mean cloud amount (oktas)	3.0	3.9	4.5	4.1	3.2	3.8	3.1	3.7	3.6	3.8	4.1	3.8	3.8
Mean wind speed (m s^{-1})	8.9	9.5	10.7	12.1	12.9	12.0	12.5	12.4	12.1	10.7	9.7	8.8	11.0
Maximum wind gust – Dir–Speed (m s^{-1})	E 24.8	E 23.3	E 24.3	E 23.8	SE 25.9	E 26.6	ENE 26.0	ESE 28.0	E 28.0	E 24.0	E 24.0	ENE 24.5	ESE 28.0
Mean station level pressure (hPa)	741.9	737.9	733.8	732.3	733.0	731.2	728.2	727.9	723.8	725.7	733.5	741.8	732.5

Table 7.5.9.4.3 Climate statistics for Mizuho Station (averages (15 yr)and extremes from 1972–86).

Syowa (refer Section 7.5.10 above)

Parameter/Month	Jan	Feb	Mar	Apr	May	Jun	Jul	Aug	Sept	Oct	Nov	Dec	Year
Mean temperatures (º C)	−0.6	−3.1	−6.3	−9.9	−13.3	−15.8	−17.8	−19.7	−17.9	−13.4	−6.4	−1.5	−10.4
Highest daily maximum temp. (º C)	10.0	8.0	3.6	0.4	2.8	−0.7	−2.5	−2.8	−3.0	−0.6	5.5	9.4	10.0
Lowest daily minimum temp. (º C)	−12.6	−18.2	−24.7	−35.9	−38.5	−38.3	−42.7	−42.2	−45.3	−34.7	−23.9	−12.3	−45.3
Mean cloud amount (oktas)	4.7	5.8	6.2	6.0	5.3	5.3	5.2	5.2	5.0	5.4	5.3	4.6	5.4
Mean wind speed (m s^{-1})	3.9	6.1	7.9	8.7	7.8	6.7	6.7	6.0	6.0	6.2	6.2	4.5	6.4
Maximum wind gust – Dir–Speed (m s^{-1})	NE 38.3	NE 41.6	NE 36.3	ENE 41.2	ENE 47.2	ENE 42.7	NE 40.0	ENE 43.5	ENE 44.6	NE 37.3	NE 37.8	NE 38.9	NE 47.2
Mean sea level pressure (hPa)	991.4	998.4	985.8	986.1	989.1	989.3	986.1	984.5	982.7	983.0	985.6	989.8	986.8

Table 7.5.10.4.1–   Climate statistics for Syowa Station (averages (30 yr) from 19961–90 and extremes from 1957–97).

Mount King (refer Section 7.6.2 above)

Meteorological element/periods	26/12/75 to 09/02/76	27/12/76 to 12/02/77	25/12/77 to 15/02/78	29/11/79 to 01/03/80
Mean maximum temperature.(ºC)	−6.7	−6.4	−7.8	N/A
Mean minimum temperature(ºC)	−14.3	N/A	−15.6	N/A
Highest maximum temperature (0 C)	−3.3 (29 Dec)	−3.3 (06 Jan)	−0.8 (08 Jan)	−1.0 (13 Jan)
Lowest minimum temperature(ºC)	−21.4 (08 Feb)	−22.5 (11 Feb)	−23.2 (03 Feb)	−28.1 (13 Feb)
Maximum wind gust (approx) (m s^{-1})	N/A	33	33	38
Mean wind direction	E	E	E	N/A
Number of days of strong wind	20	19	20	N/A
Number of days of gales	6	5	7	N/A
Number of days of slight drift snow	16	23	17	N/A
Number of days of moderate drift snow	10	1	6	N/A
Number of days of blizzard	3	5	6	17 (9 in Jan)
Number of days of falling snow	8	14	14	N/A
Number of days of fog	N/A	3	8	N/A
Mean cloud amount (oktas)	N/A	4	5	N/A
Number of days of white–out	20	24	30	N/A

Table 7.6.2.4.1   Summary of Mount King's weather during the 1975/76, 1976/77 and 1977/78 and 1979/80 summers.

Mawson (refer Section 7.7.1 above)

Element/Month	Jan	Feb	Mar	Apr	May	Jun	Jul	Aug	Sept	Oct	Nov	Dec	Year
Mean daily maximum temperatures (º C)	2.6	–1.3	–7.2	–11.8	–13.7	–13.7	–15.0	–15.6	–14.5	–9.9	–2.6	2.2	–8.4
Highest daily maximum temp. (º C)	10.6	8.0	4.0	0.0	–1.8	0.7	5.0	6.7	–0.1	0.0	9.7	9.3	10.6
Mean daily minimum temperatures (º C)	–2.6	–7.3	–13.3	–17.3	–19.3	–19.6	–20.8	–21.6	–20.7	–16.4	–8.8	–3.2	–14.2
Lowest daily minimum temp. (º C)	–10.0	–17.3	–25.0	–33.3	–34.4	–34.0	–36.0	–35.9	–35.8	–29.0	–20.0	–10.5	–36.0
Mean of 9am & 3pm rel. humidities (%)	56	53	49	47	52	56	50	54	52	51	52	56	52.6
Mean 9am cloud amount (oktas)	5.1	4.8	4.7	4.5	3.8	3.6	3.8	4.2	4.4	4.6	4.8	5.0	4.4
Mean 3pm cloud amount (oktas)	5.1	4.9	4.9	4.7	4.5	4.7	4.9	4.7	4.8	4.8	4.9	5.0	4.8
Mean no. of clear days	4.8	5.4	6.4	7.6	9.6	8.6	8.3	7.9	7.2	7.3	6.1	5.3	84.5
Max. wind gust (m s^{-1})	55.0	53.0	51.4	65.0	57.8	61.4	61.4	68.4	61.7	56.7	56.7	50.3	68.9
Mean no. days with strong winds	24.3	25.7	28.5	26.4	27.3	26.3	27.3	28.0	26.8	27.5	27.2	23.9	319.1
Mean no. days with gales	8.0	9.8	13.1	12.2	13.9	15.0	15.1	15.3	14.1	12.9	12.3	8.5	150.3
Mean of 9am & 3 pm MSL Pressure (hPa)	990.5	989.5	988.4	990.3	991.8	992.1	989.0	986.7	984.7	984.1	986.4	989.2	988.5

Table 7.7.1.4.1   Climate statistics for Mawson for the period 1954–98 (except humidity data only over 11 years of record).

	Jan	Feb	Mar	Apr	May	Jun	Jul	Aug	Sep	Oct	Nov	Dec	Year
*Percentage occurrence of combined adverse conditions for all elements	68	62	62	60	55	57	62	62	62	62	63	66	62
**Percentage occurrence of combined adverse conditions for cross–wind, low cloud and/or visibility	7	7	11	13	12	14	17	17	13	11	9	6	11

Table 7.7.1.4.2   Percentage occurrence of weather adverse to aviation at Mawson based on synoptic observations taken during the period 1969–97. (% to the nearest integer) (*The first row ("combined") refers to observations in which one or more of the following occurred: the cross–wind component (normal to 130º) was 7.7 m s^{-1} (~15 kt), or more; 5 oktas or more of cloud was present below 460 m (~1500 ft) (taken to be the low cloud height at which aircraft might seek an alternate landing site); visibility was below 8000 m (taken to be the visibility threshold at which aircraft might seek an alternate landing site); adverse weather such as mist, fog, falling snow or blowing snow was present; or there was potential for white–out in at least one sector–assumed to exist when there was at least 4 oktas of total cloud cover. **The second row is the same as the first except only the cross–wind; low cloud; and visibility criteria were used).

Jan	Feb	Mar	Apr	May	Jun	Jul	Aug	Sep	Oct	Nov	Dec	Year
4	4	5	6	6	7	7	8	6	5	4	3	5

Table 7.7.1.4.3   The percentage frequency of occasions when the wind normal to the 130 º mean wind direction (ie the cross–wind) at Mawson equalled or exceeded 7.7 m s^{-1} (~15 kt) during the period 1969–97 (% to the nearest integer).

Jan	Feb	Mar	Apr	May	Jun	Jul	Aug	Sep	Oct	Nov	Dec	Year
1	1	1	0	1	0	0	0	0	0	0	1	0

Table 7.7.1.4.4   The percentage of occasions when low cloud at Mawson had heights <= 460 m (1500 ft) and amounts >= 5 okta during the period 1969–97 (% to the nearest integer).

Jan	Feb	Mar	Apr	May	Jun	Jul	Aug	Sep	Oct	Nov	Dec	Year
4	7	9	12	12	13	17	19	15	12	9	4	11

Table 7.7.1.4.5   The percentage frequency of occasions when the visibility at Mawson was <= 8000m during the period 1969–97 (% to the nearest integer).

Jan	Feb	Mar	Apr	May	Jun	Jul	Aug	Sep	Oct	Nov	Dec	Year
7	11	16	23	23	24	30	34	28	20	15	8	20

Table 7.7.1.4.6   The percentage frequency of occasions when the weather at Mawson during the period 1969–97 was of a type considered to be adverse, for example: mist, fog, falling snow; and blowing snow (% to the nearest integer).

Jan	Feb	Mar	Apr	May	Jun	Jul	Aug	Sep	Oct	Nov	Dec	Year
66	59	57	52	45	47	51	52	54	57	60	65	56

Table 7.7.1.4.7   The percentage frequency of occasions when there was potential for white–out at Mawson during the period 1969–97 based on there being a total cloud cover of >= 4 oktas (% to the nearest integer).
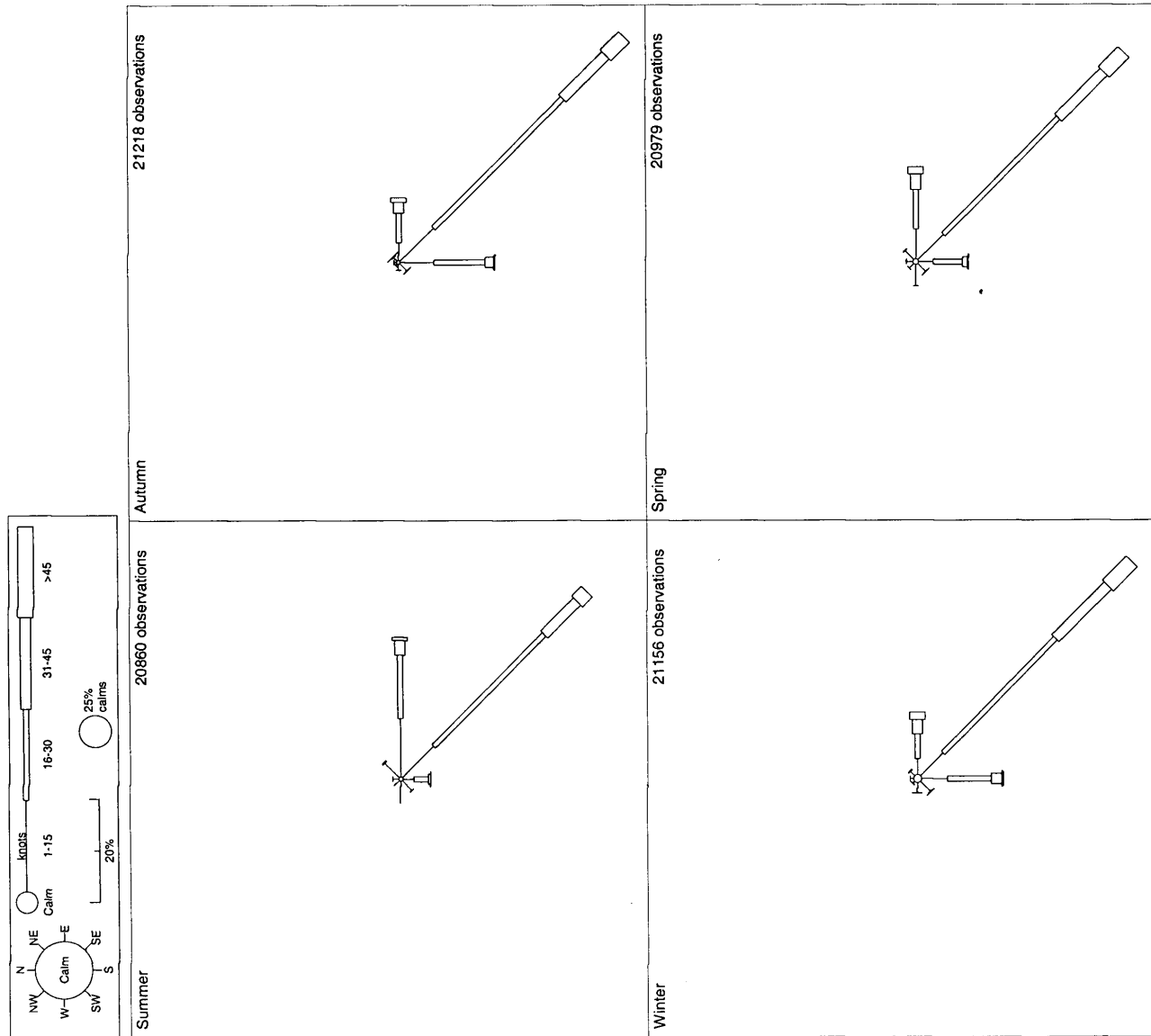
Figure 7.7.1.4.1 Seasonal wind roses for Mawson (1969–97 data). (North is on the left hand side).

	Mawson Escarpment	Mt Menzies
Average temperature (all observations) (ºC)	−3	−15.7
Average Maximum (ºC)	3.2	−5.7
Standard Deviation (ºC)	3.9	3.2
Average Minimum (ºC)	−6	−19.9
Standard Deviation (ºC)	2.7	2.4
Highest maximum (ºC)	12.0	−0.8
Lowest minimum (ºC)	−12.0	−23.4

Table 7.7.2.4.1   Average temperatures for the month of January reported by two field parties in the Prince Charles Mountains during the summer of 1998.

Law Base (refer Section 7.8.1 above)

Element/Month	Jan 87	Feb 87	Jan 88	Feb 88
Mean daily temperatures (º C)	−0.1	−3.0	1.0	−3.1
Highest daily maximum temp. (º C)	9.0	4.7	7.5	2.7
Lowest daily minimum temp. (º C)	−5.2	−9.0	−5.2	−6.6
Mean dew–point temperature (ºC)	−10.8	−10.7	−13.4	−9.3
Mean MSL level pressure (hPa)	996	988	996	988

Table 7.8.1.4.1   Limited climate statistics for Law Base
for the periods 19 January to 26 February 1987 and 9 January to 12 February 1988.

Speed (m s^{-1})/(kt))	WSW	SW	SSW	S	SSE	SE	ESE	E	ENE	NE	NNE	N	NNW	NW	WNW	W
0–2.5 (0–5)	0	3	1	3	0	4	4	6	11	20	8	2	1	1	0	1
2.6–5 (6–10)	0	1	0	1	2	2	2	6	13	31	6	1	2	1	2	0
5.7–7.3 (11–15)	0	0	0	0	0	0	0	7	20	13	2	0	0	0	0	0
8.2–10.3 (16–20)	0	0	0	0	0	1	0	5	37	4	3	0	0	0	0	0
>10.3 (>20)	0	0	0	0	0	0	0	2	13	2	0	0	0	0	0	0

Table 7.8.1.4.2   Percentage wind frequency table for Law Base for the period 19 January to 26 February 1987.

Zhongshan (refer Section 7.8.3 above)
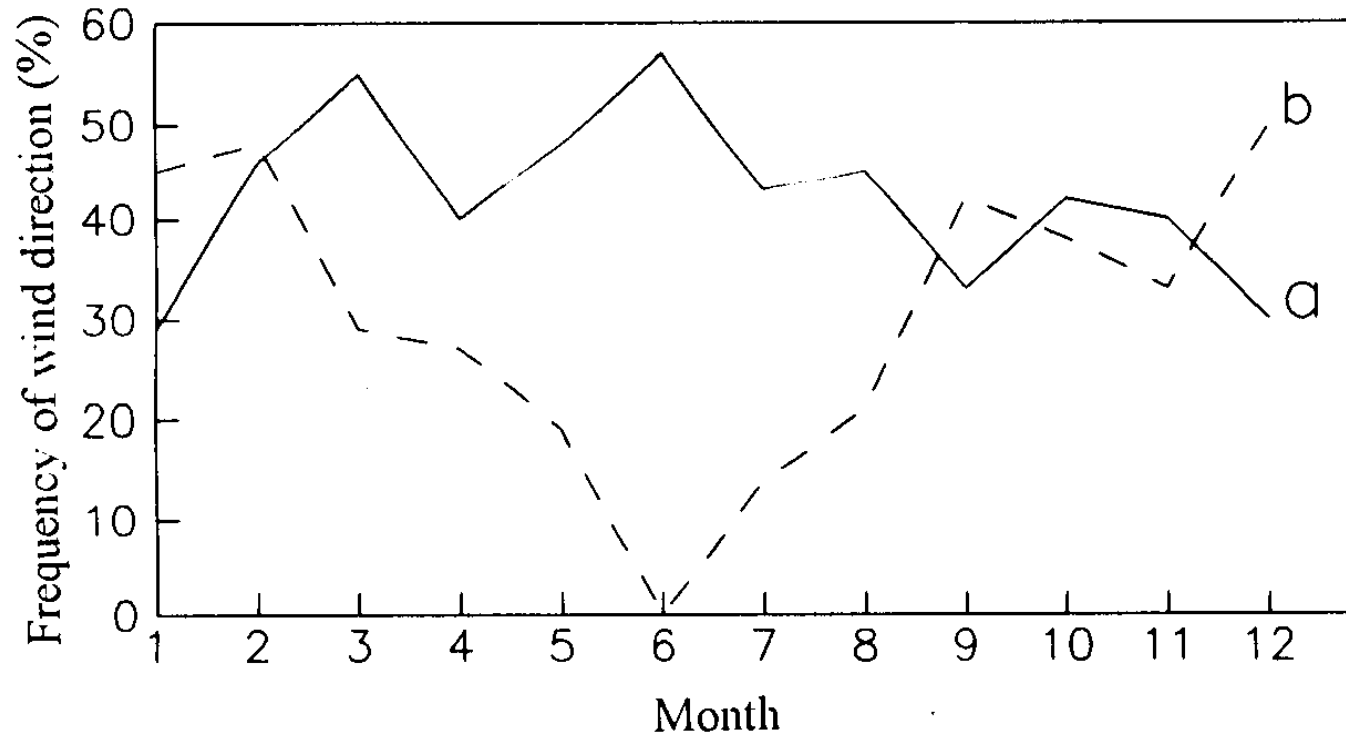
Figure 7.8.3.4.1 Percentage frequency of snowdays (solid line) and percentage frequency of sunny days (dashed line) based on long term data from Zhongshan.
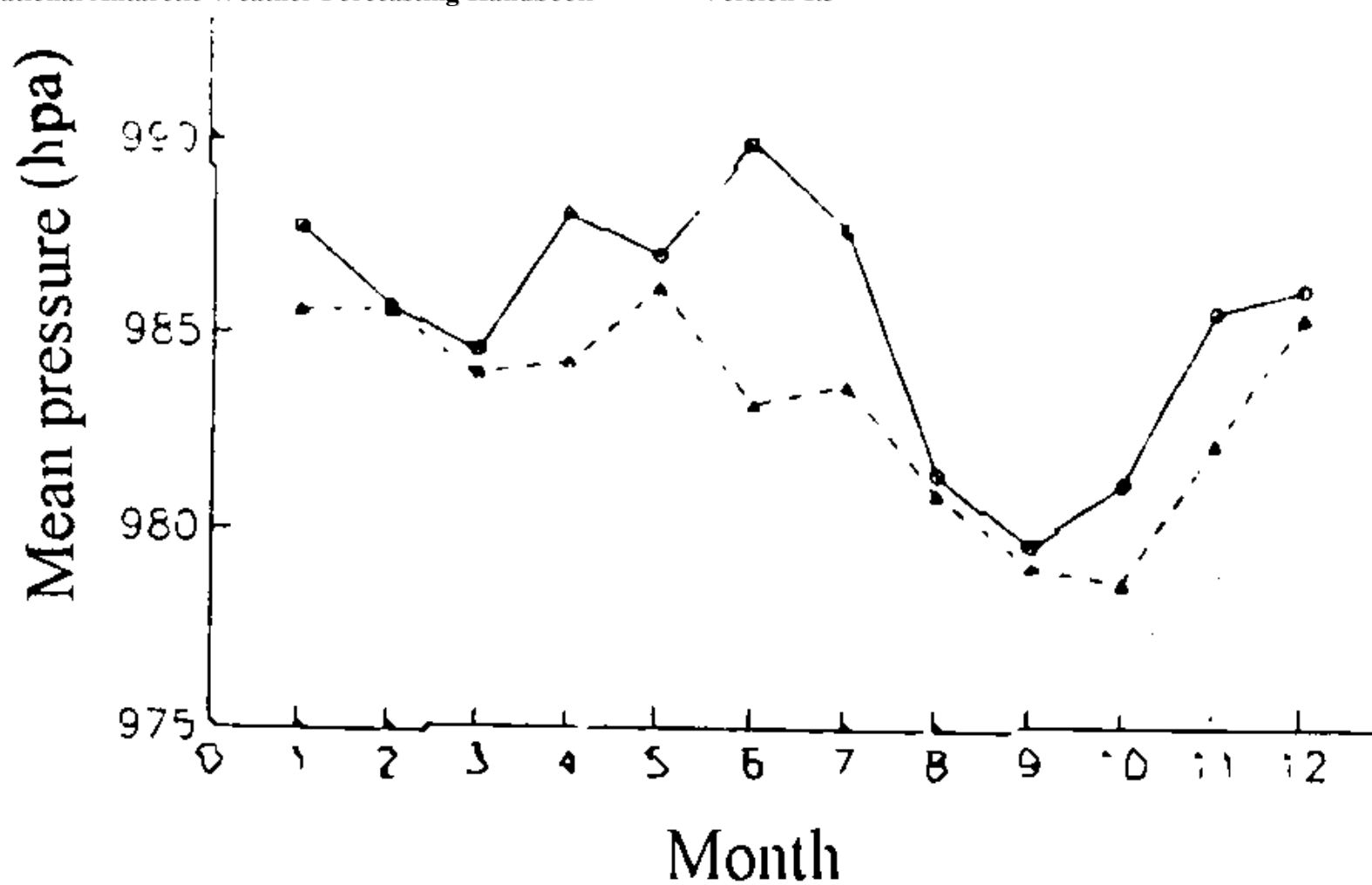
Figure 7.8.3.4.2 Annual variation of monthly mean pressure at Zhongshan (solid line) and annual variation of the monthly mean pressure of the Antarctic circumpolar trough between 70 and 80º E (dashed line – derived from Antarctic sea–level gridded data complied by the National Meteorological Office of China).
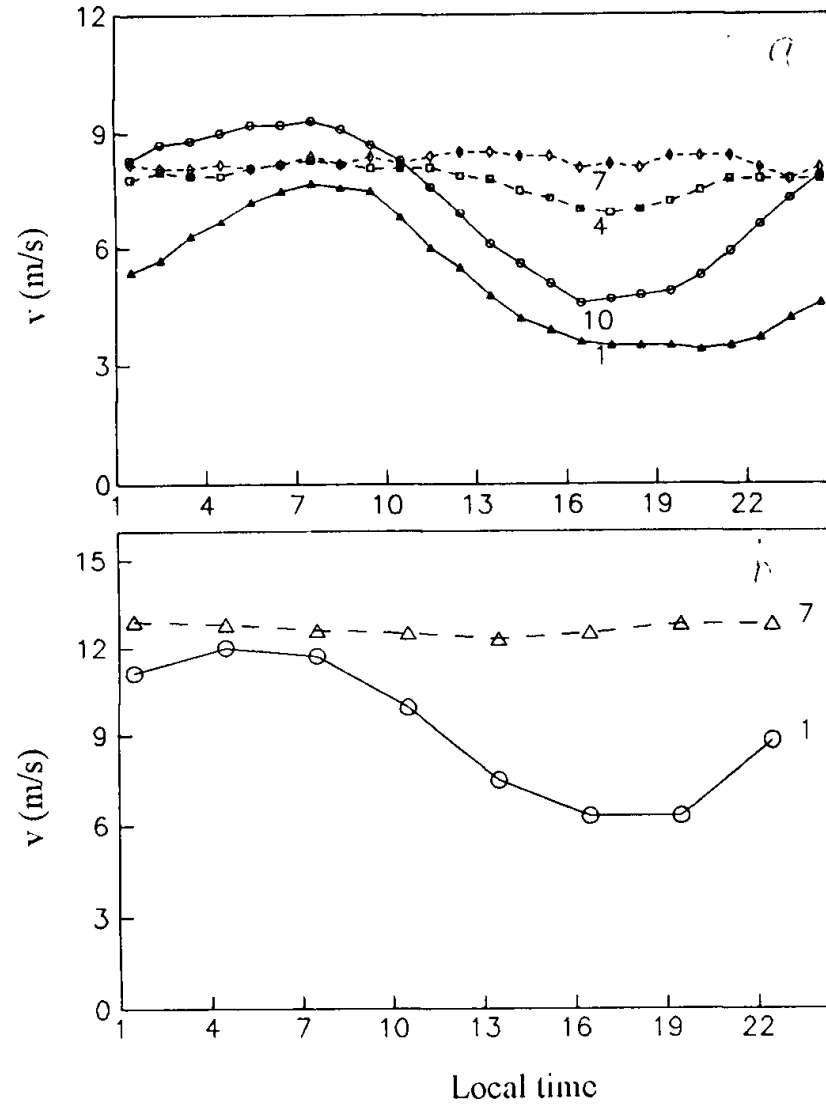
Figure 7.8.3.4.3 Top panel: daily variation of wind speed (m s^{-1}) against local time (hr) at Zhongshan for January (1); April (4); July (7); and October (10), taken from daily records between 1989–96. Bottom panel: Similar data for Mawson for January (1) and July (7).
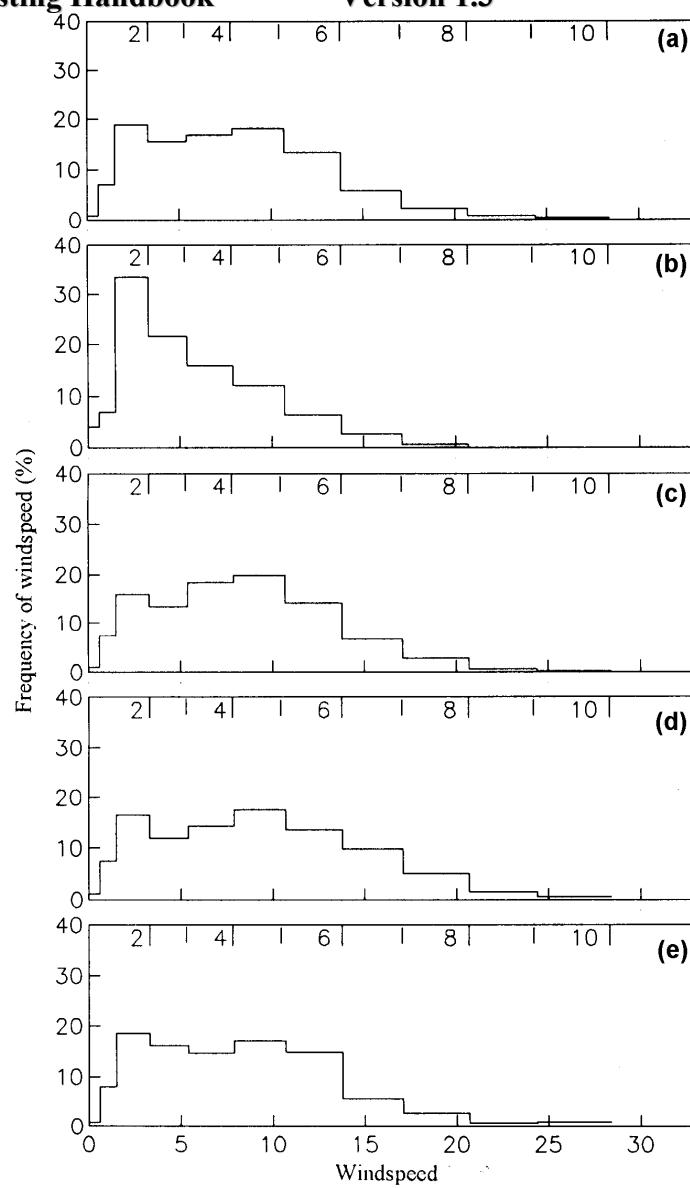
Figure 7.8.3.4.4 Percentage frequency of wind speed (m s$^{-1)}$ for Zhongshan for:(a) annual average; (b) summer; (c) autumn; (d) spring; (e) spring.
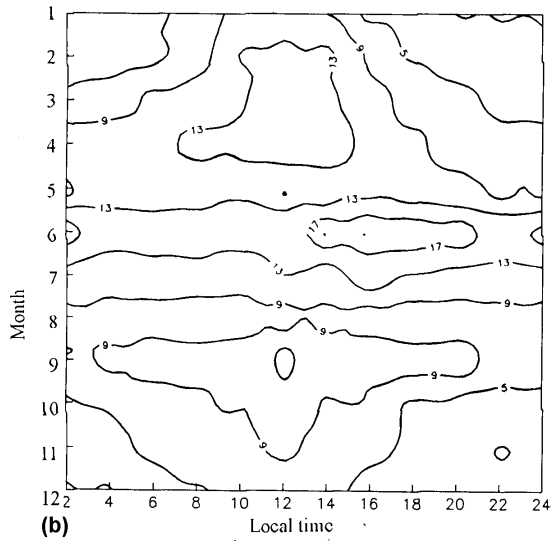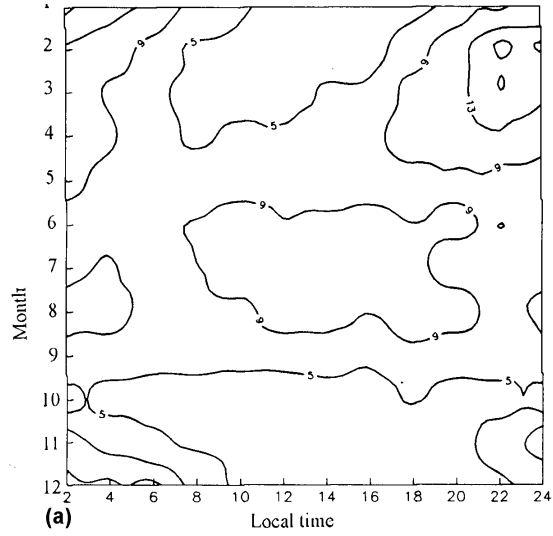
Figure 7.8.3.4.5 Percentage frequency of calms and (b) strong winds–gales at Zhongshan on a monthly (1=January, 12=December) versus local time (hr).
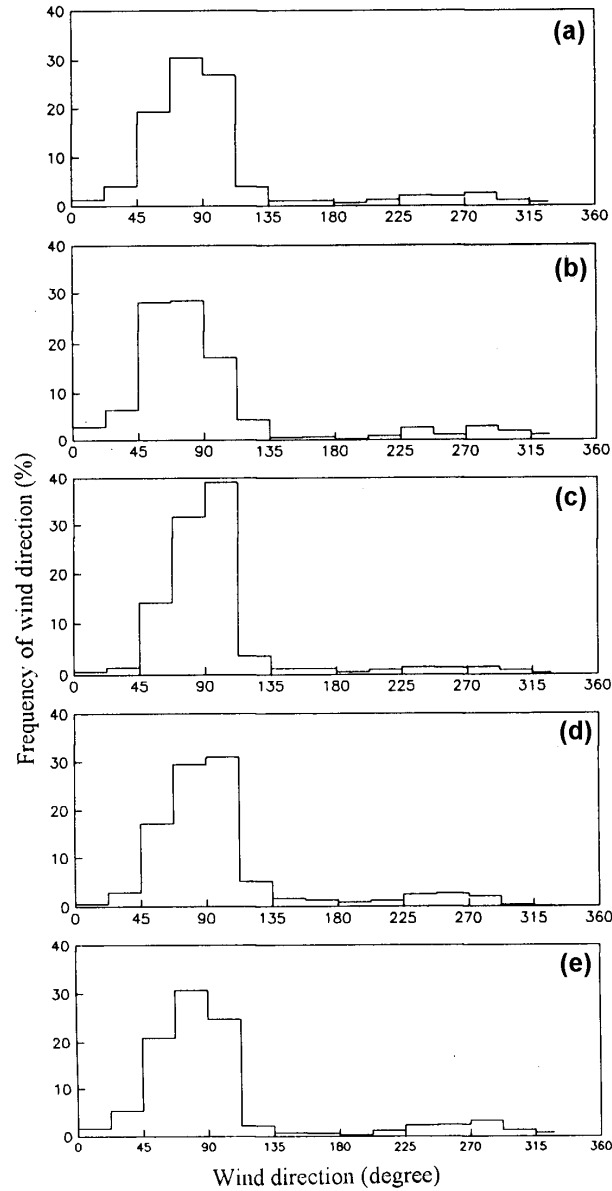
Figure 7.8.3.4.6   Percentage frequency of wind direction
for Zhongshan for:(a) annual average; (b) summer; (c) autumn; (d) spring; (e) spring.
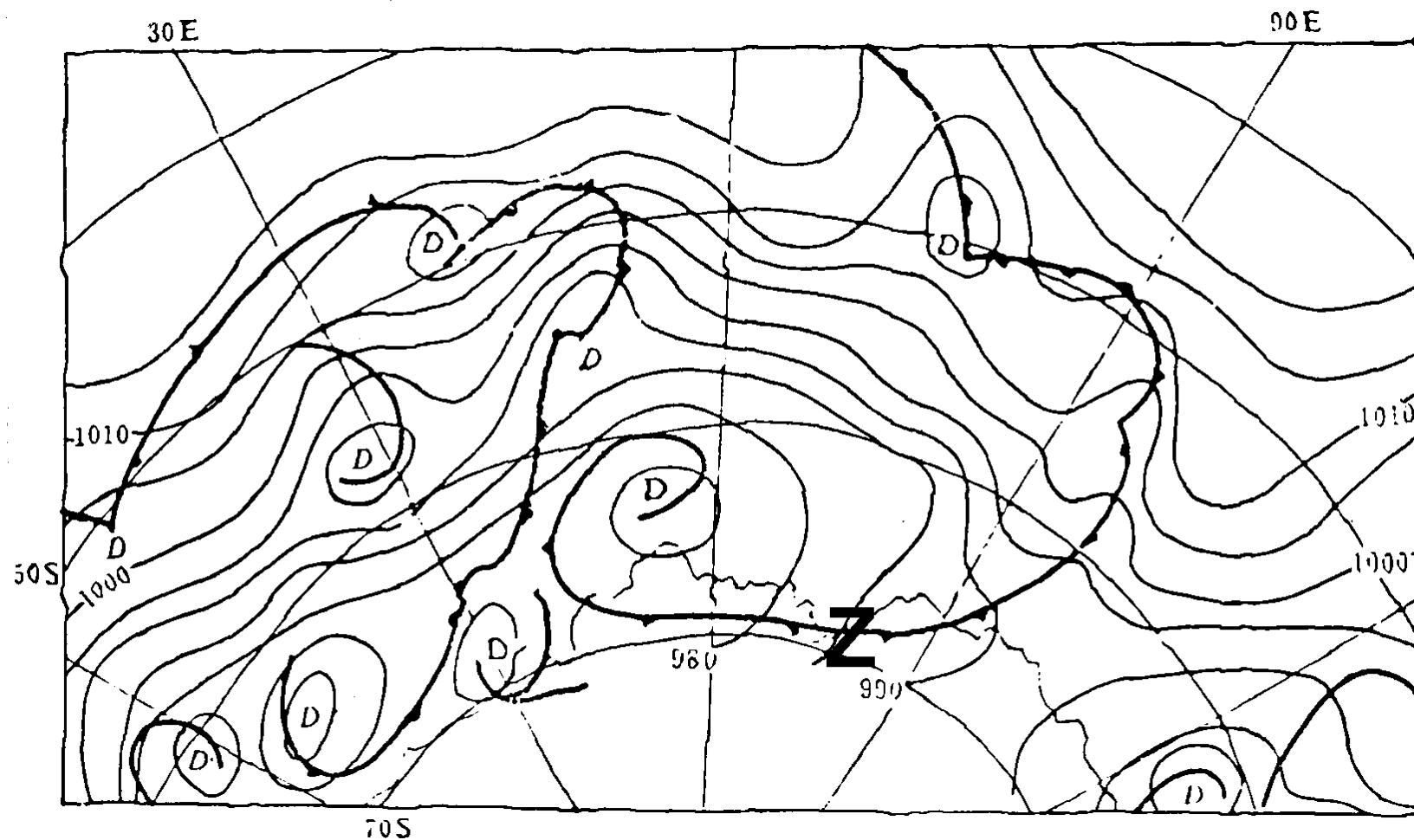
Figure 7.8.3.4.7 A sketch showing a typical pattern in which a frontal cloud band brings gales to Zhongshan (Z).
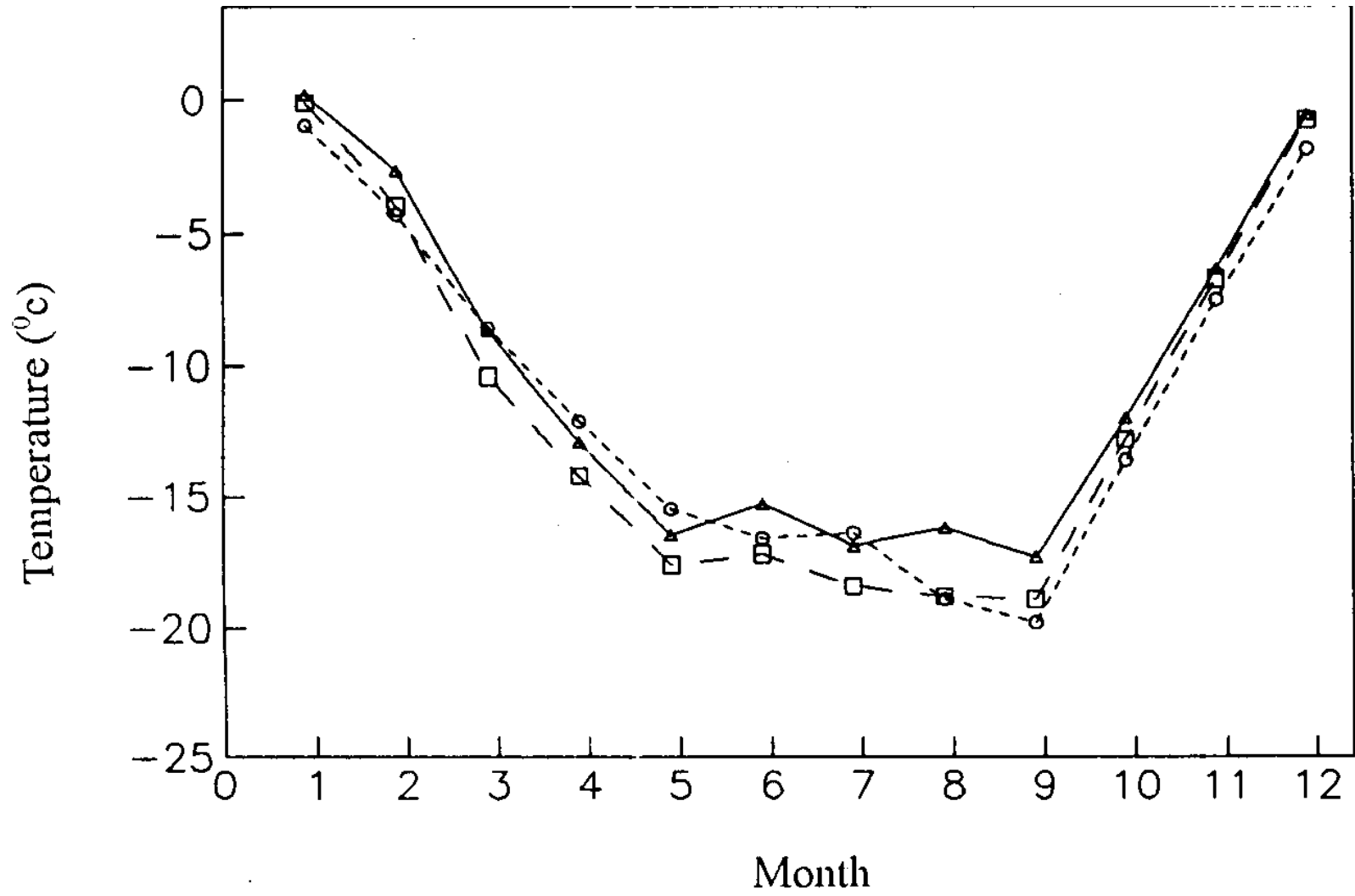
Figure 7.8.3.4.8 Monthly mean temperature for Zhongshan (circles); Davis (squares) and Mawson (triangles) for the period 1989–95.
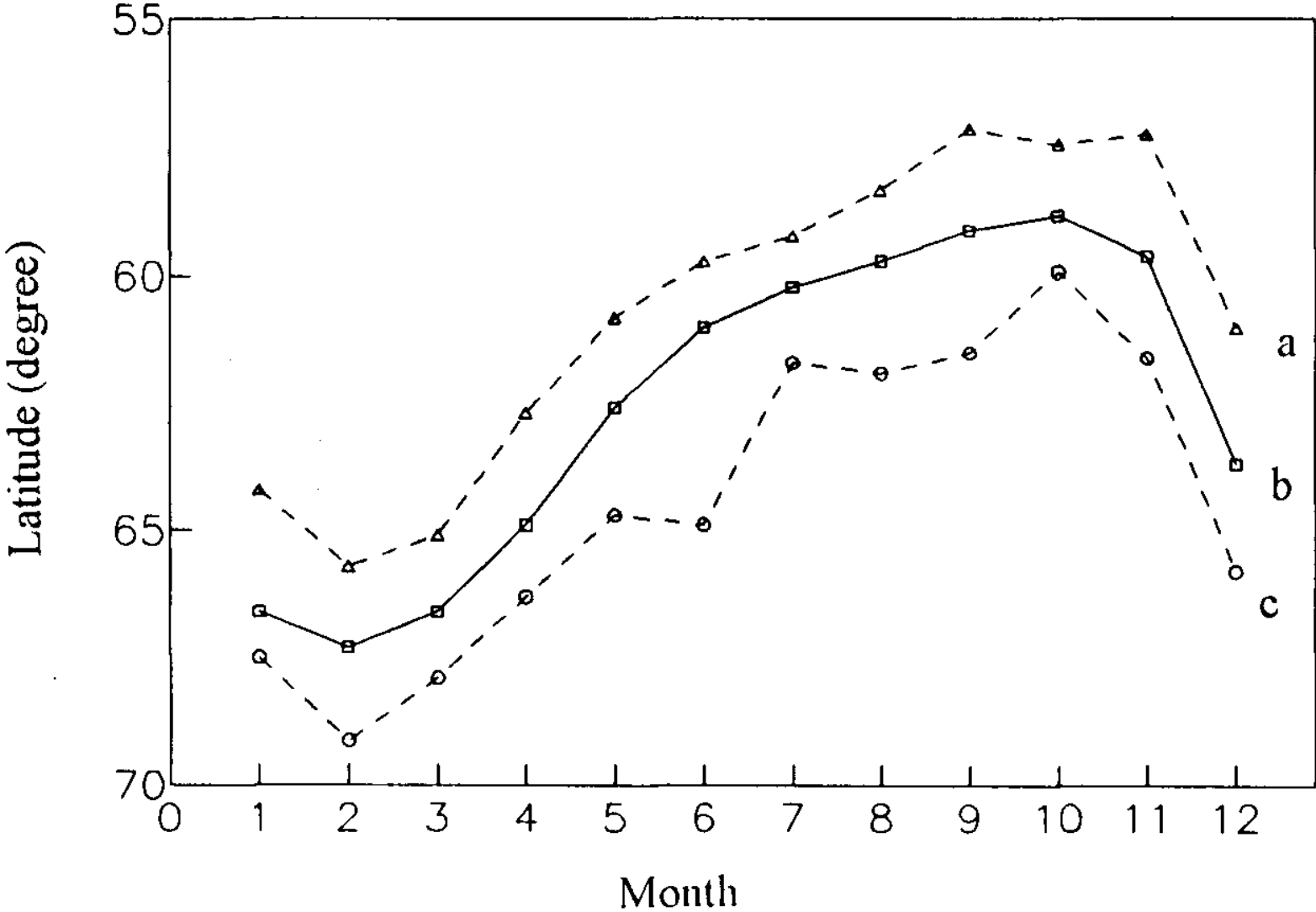
Figure 7.8.3.4.9 Annual variation of the mean northern latitude limit of Antarctic sea ice between 70–80° E: (a) northern limit of maximum growth; (b) average northern limit; (c) northern limit of minimum growth.
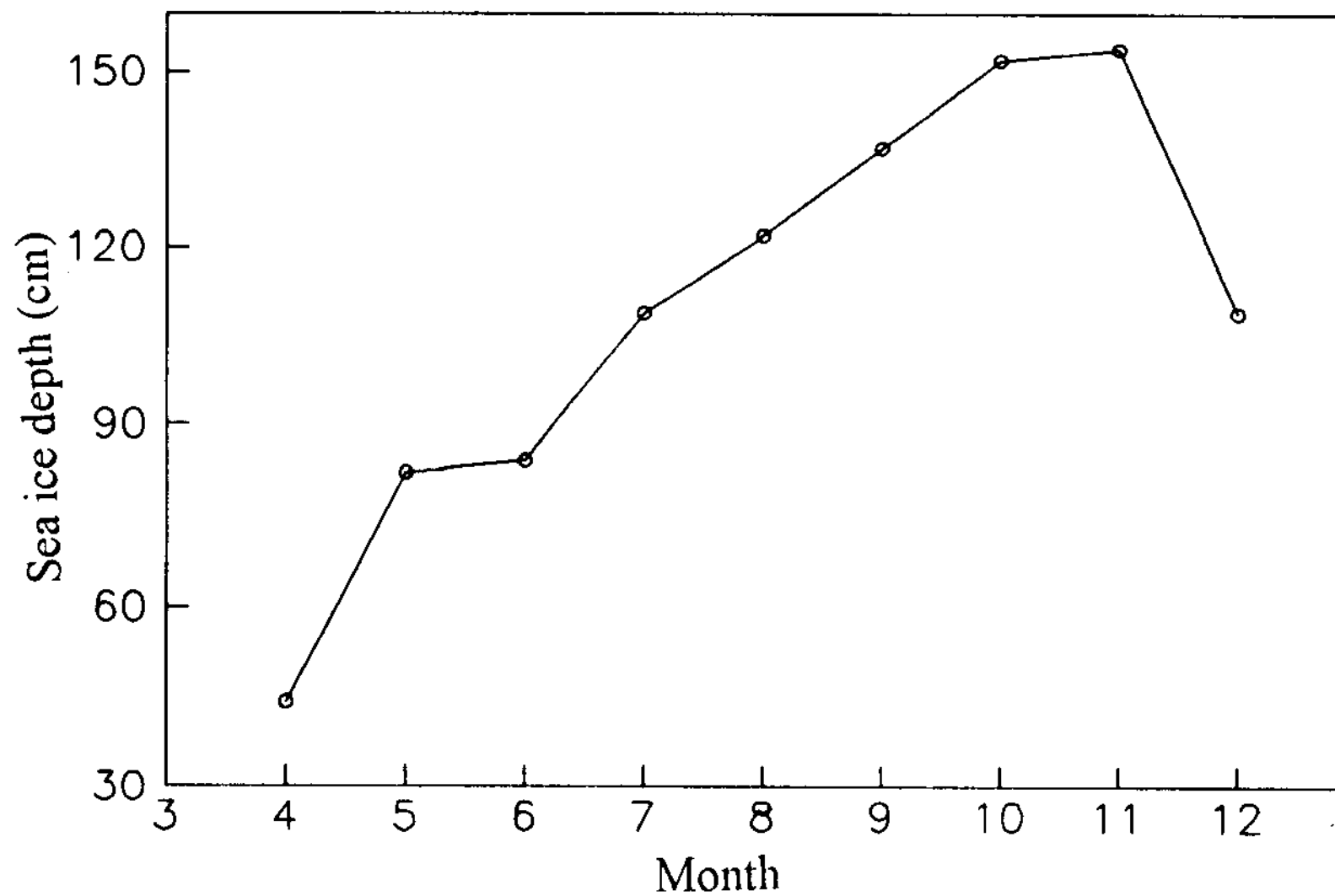
Figure 7.8.3.4.10   Annual variation of sea ice thickness around Zhongshan.

Month	Jan	Feb	Mar	Apr	May	Jun	Jul	Aug	Sept	Oct	Nov	Dec	Year
Mean daily temperatures (º C)	0.4	–2.7	–8.3	–12.4	–16.0	–14.4	–15.0	–15.6	–16.3	–11.6	–5.7	–0.2	–9.8
Highest daily maximum temp. (º C)	8.1	7.4	2.3	4.8	1.9	1.2	2.2	0.9	0.9	1.7	5.1	9.6	9.6
Lowest daily minimum temp. (º C)	–6.8	–10.6	21.9	–29.4	–35.0	–36.3	–36.7	–39.0	–34.2	–28.3	–19.5	–11.5	–39.0
Mean relative humidity (%)	61	56	56	49	57	58	56	53	52	54	56	53	55
Mean cloud amount (oktas)	5.0	5.0	5.5	4.9	4.6	4.8	4.4	5.0	4.6	4.9	5.2	4.5	4.9
Mean wind direction	E	E	E	ESE	ESE	ESE	E	ESE	ESE	ESE	ESE	ESE	ESE
Mean wind speed (m s^{-1})	5.3	7.1	7.7	8.0	6.9	8.0	7.9	8.4	7.8	7.4	6.4	5.9	7.2
Maximum wind gust – (m s^{-1})	33.0	33.8	44.1	46.2	46.0	48.1	47.2	36.6	47.5	48.3	35.6	38.6	48.3
No. days of gales	9	13	14	14	11	17	18	18	15	16	13	13	171
Mean MSL pressure (hPa)	987.9	985.4	985.1	988.0	987.5	989.9	987.6	981.4	980.0	981.4	985.4	985.1	985.6

Table 7.8.4.1   Annual weather/climate characteristics over 1989–95, from measurements at the Zhongshan Station.

Davis (refer Section 7.8.4 above)

Element/Month	Jan	Feb	Mar	Apr	May	Jun	Jul	Aug	Sept	Oct	Nov	Dec	Year
Mean daily maximum temperatures (º C)	3.0	–0.4	–5.8	–10.4	–12.8	–12.4	–14.3	–14.2	–13.2	–9.1	–2.5	2.3	–7.5
Highest daily maximum temp. (º C)	13.0	10.0	4.1	11.8	2.0	2.0	0.8	1.0	0.3	6.4	8.0	11.0	13.0
Mean daily minimum temperatures (º C)	–1.2	–4.6	–11.0	–16.1	–19.0	–18.7	–20.5	–20.6	–20.2	–15.4	–7.7	–2.1	–13.1
Lowest daily minimum temp. (º C)	–8.3	–15.0	–26.7	–41.8	–38.3	–40.1	–39.0	–38.4	–36.2	–31.0	–19.8	–10.0	–41.8
Mean of 9am & 3pm rel. humidities (%)	55	52	56	57	70	65	66	66	60	61	53	56	59.8
Mean 9am cloud amount (oktas)	5.2	5.6	6.0	5.7	5.4	4.9	4.9	5.4	5.3	5.7	5.4	5.1	5.4
Mean 3pm cloud amount (oktas)	5.1	5.5	5.9	5.8	5.6	5.6	5.3	5.6	5.3	5.5	5.2	5.1	5.4
Mean no. of clear days	5.1	3.8	3.4	4.2	5.8	6.1	6.7	5.3	6.0	4.8	5.5	6.2	62.9
Max. wind gust (m s^{-1})	45.3	52.5	45.7	57.2	51.9	51.4	54.2	55.0	48.9	49.4	46.7	46.7	57.2
Mean no. days with strong winds	5.3	5.7	6.8	6.1	6.1	7.4	7.3	7.1	5.9	7.7	9.0	7.4	81.9
Mean no. days with gales	1.1	1.4	2.3	2.6	2.6	3.2	3.6	3.6	3.1	2.9	3.0	1.7	31.2
Mean of 9am & 3 pm MSL Pressure (hPa)	990.4	988.1	986.2	988.2	989.2	990.7	987.1	984.9	983.4	983.0	985.9	989.1	987.0

Table 7.8.4.4.1   Climate statistics for Davis for 38 years of record during the period 1957–2000 (except humidity data only over 9 years of record).

	Jan	Feb	Mar	Apr	May	Jun	Jul	Aug	Sep	Oct	Nov	Dec	Year
*Percentage occurrence of combined adverse conditions for all elements	66	70	74	70	67	65	62	64	66	71	68	64	67
**Percentage occurrence of combined adverse conditions for cross–wind, low cloud and/or visibility	4	7	14	14	14	13	14	13	13	11	7	4	11

Table 7.8.4.4.2   Percentage occurrence of weather adverse to aviation at Davis based on synoptic observations taken during the period 1969–97. (% to the nearest integer). (*The first row ("combined") refers to observations in which one or more of the following occurred: the cross–wind component (normal to 130º) was 7.7 m s^{-1} (~15 kt), or more; 5 oktas or more of cloud was present below 460 m (~1500 ft) (taken to be the low cloud height at which aircraft might seek an alternate landing site); visibility was below 8000 m (taken to be the visibility threshold at which aircraft might seek an alternate landing site); adverse weather such as mist, fog, falling snow or blowing snow was present; or there was potential for white–out in at least one sector–assumed to exist when there was at least 4 oktas of total cloud cover. **The second row is the same as the first except only the cross–wind; low cloud; and visibility criteria were used).

Jan	Feb	Mar	Apr	May	Jun	Jul	Aug	Sep	Oct	Nov	Dec	Year
0	0	1	1	1	2	2	2	2	1	1	0	1

Table 7.8.2.4.3   The percentage frequency of occasions when the wind normal to the 050 º mean wind direction (ie the cross–wind) at Davis equalled or exceeded 7.7 m s^{-1} (~15 kt) during the period 1969–97. (% to the nearest integer)

Jan	Feb	Mar	Apr	May	Jun	Jul	Aug	Sep	Oct	Nov	Dec	Year
1	2	4	3	4	3	3	3	2	2	1	2	2

Table 7.8.4.4.4   The percentage of occasions when low cloud at Davis had heights <= 460 m (1500 ft) and amounts >= 5 okta during the period 1969–97. (% to the nearest integer)

Jan	Feb	Mar	Apr	May	Jun	Jul	Aug	Sep	Oct	Nov	Dec	Year
3	7	13	14	13	12	13	14	13	11	6	3	10

Table 7.8.4.4.5   The percentage frequency of occasions when the visibility at Davis was <= 8000m during the period 1969–97. (% to the nearest integer).

Jan	Feb	Mar	Apr	May	Jun	Jul	Aug	Sep	Oct	Nov	Dec	Year
6	12	23	24	26	22	23	23	22	20	11	7	18

Table 7.8.4.4.6   The percentage frequency of occasions when the weather at Davis during the period 1969–97 was of a type considered to be adverse, for example: mist, fog, falling snow; and blowing snow. (% to the nearest integer).

Jan	Feb	Mar	Apr	May	Jun	Jul	Aug	Sep	Oct	Nov	Dec	Year
65	70	73	69	66	63	60	62	64	71	68	65	66

Table 7.8.4.4.7   The percentage frequency of occasions when there was potential for white–out at Davis during the period 1969–97 based on there being a total cloud cover of >= 4 oktas. (% to the nearest integer).
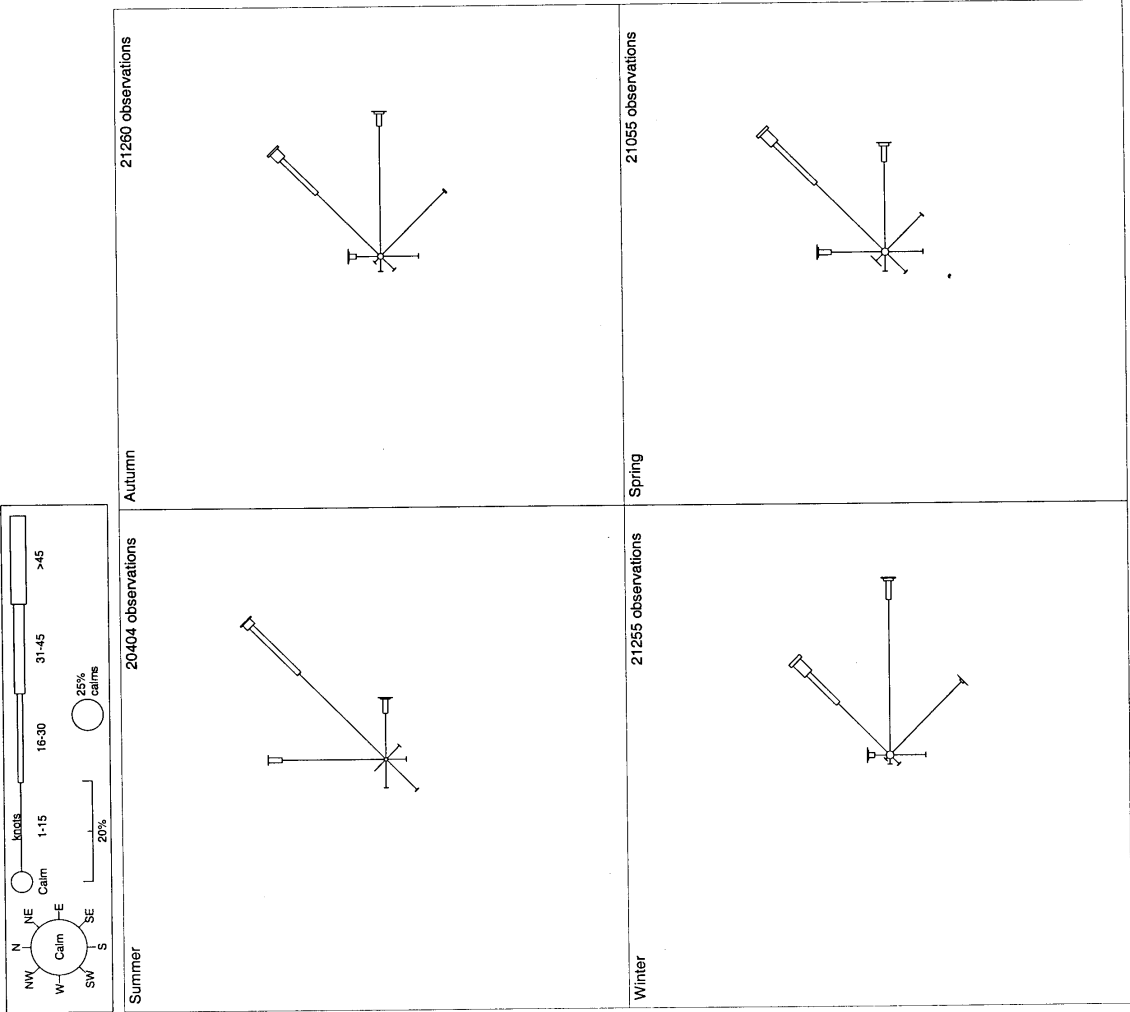
Figure 7.8.4.4.1 Seasonal wind roses for Davis (1969–97 data). (North is on the left hand side).

Edgworth David (Bunger Hills) (refer Section 7.9.2 above

	Max daily speed (kt)	Min daily speed (kt)	Max T (ºC)	Min T (ºC)	Ave T (ºC)	Ave Pressure (hPa)
Max	50	25	10.5	4.6	7.1	1008.5
Min	2	0	−2.2	−7.1	−4.4	976.4
Average	19.3	3.5	3.7	−0.3	1.9	990.0

Table 7.9.2.4.1   Edgeworth David observations, for the period 24 January to 3 March 1986

	Max daily speed (kt)	Min daily speed (kt)	Max T (ºC)	Min T (ºC)	Ave T (ºC)	Ave Pressure (hPa)
Max	34	28	9	3	5.5	1016.3
Min	2	0	−10	−15	−12.8	969.2
Average	7.6	1.7	−0.6	−4.6	−2.5	997.8

Table 7.9.2.4.2   Oasis observations, for the period 1 January to 31 March 1958.

Casey (refer Section 7.10.1 above)

Element/Month	Jan	Feb	Mar	Apr	May	Jun	Jul	Aug	Sept	Oct	Nov	Dec	Year
Mean daily maximum temperatures (º C)	2.1	0.0	−4.3	−8.0	−12.0	−10.2	−10.5	−10.3	−10.4	−8.2	−2.4	1.6	−6.0
Highest daily maximum temp. (º C)	9.2	6.6	3.6	3.0	3.4	4.2	7.5	1.3	3.9	0.8	4.9	7.4	9.2
Mean daily minimum temperatures (º C)	−2.6	−4.9	−10.2	−15.4	−19.5	−18.1	−18.8	−18.0	−17.8	−15.0	−8.9	−3.6	−12.7
Lowest daily minimum temp. (º C)	−8.9	−15.8	−22.3	−31.3	−34.4	−34.1	−33.2	−32.9	−30.7	−31.2	−23.4	−13.0	−34.4
Mean of 9am & 3pm rel. humidities (%)	70	71	74	74	73	74	73	73	71	70	67	68	71.5
Mean 9am cloud amount (oktas)	5.9	6.1	6.1	5.9	5.6	5.9	5.5	5.5	5.7	5.9	5.2	5.6	5.7
Mean 3pm cloud amount (oktas)	5.6	6.0	6.2	5.7	5.5	5.5	5.3	5.9	5.6	5.7	5.3	5.5	5.7
Mean no. of clear days	4.6	3.3	3.4	4.4	4.4	4.6	6.4	5.4	4.5	4.0	7.6	5.7	58.2
Max. wind gust (m s^{-1})	42.2	48.9	66.9	61.7	59.7	66.3	66.9	56.7	63.3	59.2	51.1	50.3	66.9
Mean no. days with strong winds	8.5	9.5	11.0	14.6	13.3	14.3	16.1	16.0	16.0	12.0	11.9	11.2	154.5
Mean no. days with gales	6.0	6.6	6.1	10.3	8.1	10.6	12.2	12.5	11.5	8.5	7.6	6.4	106.4
Mean of 9am & 3 pm MSL Pressure (hPa)	987.7	985.3	982.6	983.2	983.6	989.4	984.8	980.2	979.6	979.7	985.5	986.4	984.0

Table 7.10.1.4.1 Climate statistics for Casey for 11 years of record during the period 1989–2000. (These data are from the latest Casey site: other data may be obtained from the older "Tunnel" site and from the nearby Wilkes site).

	Jan	Feb	Mar	Apr	May	Jun	Jul	Aug	Sep	Oct	Nov	Dec	Year
*Percentage occurrence of combined adverse conditions for all elements	78	81	81	78	76	74	77	75	75	77	71	76	76
**Percentage occurrence of combined adverse conditions for cross–wind, low cloud and/or visibility	15	17	25	27	28	34	33	30	28	22	18	15	24

Table 7.8.5.4.2   Percentage occurrence of weather adverse to aviation at Casey based on synoptic observations taken during the period 1969–97. (% to the nearest integer) (*The first row ("combined") refers to observations in which one or more of the following occurred: the cross–wind component (normal to 130º) was 7.7 m s^{-1} (~15 kt), or more; 5 oktas or more of cloud was present below 460 m (~1500 ft) (taken to be the low cloud height at which aircraft might seek an alternate landing site); visibility was below 8000 m (taken to be the visibility threshold at which aircraft might seek an alternate landing site); adverse weather such as mist, fog, falling snow or blowing snow was present; or there was potential for white–out in at least one sector–assumed to exist when there was at least 4 oktas of total cloud cover. **The second row is the same as the first except only the cross–wind; low cloud; and visibility criteria were used).

Mean temperature (°C).

	Jan	Feb	Mar	Apr	May	Jun	Jul	Aug	Sep	Oct	Nov	Dec	Year
Casey Airstrip	–4.9	–8.1	–11.7	–14.0	–20.0	–13.9	–13.7	–16.9	–13.4	–13.1	–8.4	–5.1	–12.3
Casey	–2.1	–4.8	–8.1	–12.0	–18.7	–12.4	–11.4	–14.8	–11.0	–10.6	–5.4	–2.3	–10.0
No. obs	*156*	*114*	*151*	*200*	*138*	*260*	*263*	*284*	*132*	*147*	*166*	*184*	*2195*

Mean wind speed (knots).

	Jan	Feb	Mar	Apr	May	Jun	Jul	Aug	Sep	Oct	Nov	Dec	Year
Casey Airstrip	11.8	8.1	13.3	12.5	11.5	19.0	20.8	14.4	20.0	13.6	10.1	14.1	14.7
Casey	11.3	6.2	11.8	11.7	9.5	17.4	20.8	13.7	20.7	15.5	8.4	13.2	13.9
No. obs	*159*	*116*	*154*	*202*	*139*	*257*	*263*	*284*	*126*	*150*	*165*	*188*	*2203*

Percentage occurrence of cross–wind >= 15 knots (to nearest integer).

	Jan	Feb	Mar	Apr	May	Jun	Jul	Aug	Sep	Oct	Nov	Dec	Year
Casey Airstrip	3	1	3	6	1	5	7	7	14	10	2	4	5
Casey	3	2	2	9	4	10	6	7	9	6	2	3	6
No. obs	*156*	*114*	*150*	*199*	*137*	*257*	*243*	*252*	*123*	*145*	*160*	*185*	*2121*

Table 7.10.1.4.3 Comparison of conditions for Casey Airstrip and Casey

Mean temperature (°C).

	Jan	Feb	Dec	All
Lanyon Junction	−3.1	−7.1	−2.7	−4.4
Casey	0.7	−2.3	0.5	−0.4
No. obs	*174*	*188*	*147*	*509*

Mean wind speed (kt).

	Jan	Feb	Dec	All
Lanyon Junction	14.9	10.5	12.3	12.6
Casey	11.7	7.1	8.6	9.1
No. obs	*134*	*133*	*147*	*414*

Percentage occurrence of cross–wind >= 15 kt (to nearest integer).

	Jan	Feb	Dec	All
Lanyon Junction	5	4	2	4
Casey	0	2	0	0
No. obs	*134*	*133*	*147*	*414*

Percentage occurrence of low cloud >= 5/8 <=1500ft (to nearest integer).

	Jan	Feb	Dec	All
Lanyon Junction	14	11	6	10
Casey	6	2	3	3
No. obs	*120*	*126*	*133*	*379*

Percentage occurrence of visibility <= 8000m (to nearest integer).

	Jan	Feb	Dec	All
Lanyon Junction	19	13	20	17
Casey	5	4	13	7
No. obs	*127*	*126*	*140*	*393*

Percentage occurrence of adverse weather type (to nearest integer).

	Jan	Feb	Dec	All
Lanyon Junction	36	27	35	33
Casey	6	11	26	15
No. obs	*127*	*126*	*140*	*393*

Table 7.10.1.4.4 Comparison of conditions for Lanyon Junction and Casey....continued (next page).

616

Percentage occurrence of potential white–out, ie total cloud >= 4/8 (to nearest integer).

	Jan	Feb	Dec	All
Lanyon Junction	73	75	73	74
Casey	76	81	79	79
No. obs	*124*	*126*	*133*	*383*

Percentage occurrence of times when adverse criteria were met for at least one of cross–wind, low cloud, visibility, weather type or potential white–out (to nearest integer).

	Jan	Feb	Dec	All
Lanyon Junction	73	75	74	74
Casey	75	81	79	78
No. obs	*120*	*126*	*133*	*379*

Percentage occurrence of times when adverse criteria were met for at least one of cross–wind, low cloud or visibility (to nearest integer).

	Jan	Feb	Dec	All
Lanyon Junction	26	21	20	22
Casey	7	6	11	8
No. obs	*120*	*126*	*133*	*379*

Table 7.10.1.4.4 Comparison of conditions for Lanyon Junction and Casey (continued from previous page)

Jan	Feb	Mar	Apr	May	Jun	Jul	Aug	Sep	Oct	Nov	Dec	Year
3	4	6	8	7	9	8	8	9	5	4	2	6

Table 7.8.5.4.5   The percentage frequency of occasions when the wind normal to the 090º mean wind direction (ie the cross–wind) at Casey equalled or exceeded 7.7 m s^{-1} (~15 kt) during the period 1969–97. (% to the nearest integer)

Jan	Feb	Mar	Apr	May	Jun	Jul	Aug	Sep	Oct	Nov	Dec	Year
7	6	9	8	8	8	6	6	6	5	5	7	7

Table 7.8.5.4.6   The percentage of occasions when low cloud at Casey had heights <= 460 m (1500 ft) and amounts >= 5 okta during the period 1969–97. (% to the nearest integer)

Jan	Feb	Mar	Apr	May	Jun	Jul	Aug	Sep	Oct	Nov	Dec	Year
9	11	17	21	23	31	30	29	25	19	13	8	20

Table 7.8.5.4.7   The percentage frequency of occasions when the visibility at Casey was <= 8000m during the period 1969–97. (% to the nearest integer)

Jan	Feb	Mar	Apr	May	Jun	Jul	Aug	Sep	Oct	Nov	Dec	Year
14	20	30	35	37	40	41	39	36	32	21	14	30

Table 7.8.5.4.8   The percentage frequency of occasions when the weather at Casey during the period 1969–97 was of a type considered to be adverse, for example: mist, fog, falling snow; and blowing snow. (% to the nearest integer)

Jan	Feb	Mar	Apr	May	Jun	Jul	Aug	Sep	Oct	Nov	Dec	Year
75	77	76	70	68	66	71	68	69	72	69	75	71

Table 7.8.5.4.9   The percentage frequency of occasions when there was potential for white–out at Casey during the period 1969–97 based on there being a total cloud cover of >= 4 oktas. (% to the nearest integer).
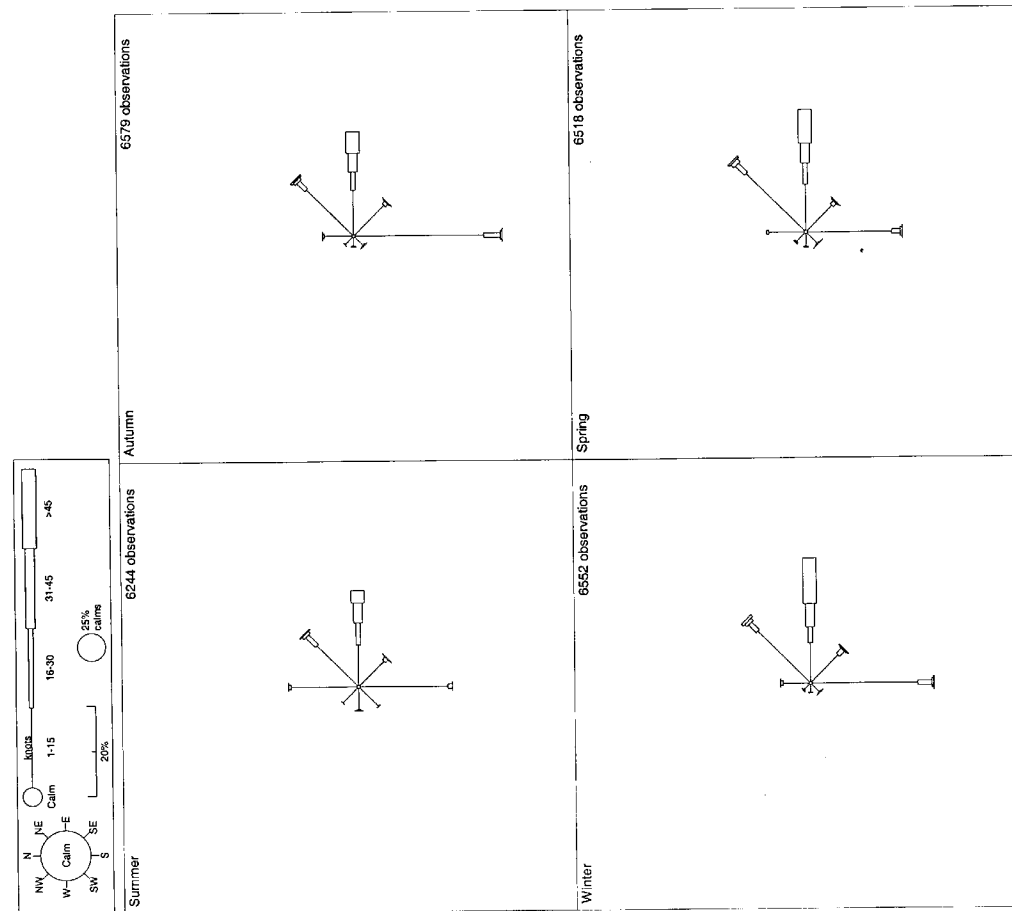
Figure 7.10.1.4.1　　　Seasonal wind roses for Casey (1969–97 data). (North is on the left hand side).

Concordia (Dome C) (refer Section 7.10.3 above)

Months	Mean	Maximum	Minimum
February to April	−48.3	−13.1	−79.7
May–June	−57.9	−13.5	−82.2
August to October	−54.2	−17.6	−84.6
November to January	−29.8	−15.0	−67.4
Annual	−47.5	−13.1	−84.6

Table 7.10.3.4.1 Temperatures (ºC) Celsius (Mean, Maximum and Minimum) at Dome C.

Dumont d'Urville (refer Section 7.11.1 above)

Month	Pressure (hPa)		Temperature (ºC)		Wind Speed (m s⁻¹)		D.T.R. (ºC)
	Mean	*Std dev*	*Mean*	*Std dev*	*Mean*	*Std dev*	
January	991.2	8.6	−.7	2.2	8.2	5.8	3.7
February	988.8	8.7	−4.1	3.1	10.4	6.3	4.1
March	986.2	10.1	−8.7	3.8	10.9	6.8	4.1
April	987.6	10.6	−12.9	4.3	10.5	6.6	3.9
May	989.9	11.9	−15.2	5.2	10.0	7.0	4.0
June	992.5	12.0	−15.9	5.3	9.8	7.6	4.3
July	991.0	12.7	−16.2	5.8	9.4	7.2	4.5
August	987.9	13.1	−16.4	5.4	10.0	7.4	4.4
September	983.6	12.4	−15.5	5.2	10.4	7.8	4.4
October	982.9	10.5	−13.2	4.7	8.8	6.7	5.0
November	986.3	8. 9	−7.0	3.8	9.0	6.1	5.2
December	989.6	8. 5	−1.7	2.5	8.1	5.8	4.3

Table 7.11.1.4.1 Mean and standard deviation by month of pressure, temperature, wind speed and day temperature range (DTR) at Dumont d'Urville.

Month	Pressure (hPa)				Temperature (ºC)				Wind speed (m s⁻¹)	
	Maximum	Year	Minimum	Year	Maximum	Year	Minimum	Year	Maximum	Year
January	1018.9	96	961.2	78	8.0	91	−9.9	86	34.1	69
February	1017.0	86	948.8	78	6.5	93	−15.9	95	37.0	87
March	1019.4	68	933.2	82	3.1	93	−23.3	94	40.8	67
April	1028.9	90	936.2	92	−0.3	68	−28.4	76	41.4	63
May	1033.0	77	940.8	69	1.7	68	−32.0	64	47.0	76
June	1030.2	64	948.8	71	0.2	83	−32.0	89	50.0	72
July	1033.5	82	946.5	79	2.8	61	−35.2	76	42.0	82
August	1027.7	95	9431	75	0.3	92	−37.4	90	49.0	75
September	1026.0	67	943.9	68	−0.8	83	−36.2	92	44.2	69
October	1012.8	89	946.0	80	0.0	67	−31.0	72	46.2	67
November	1016.2	96	954.5	78	4.0	92	−20.2	86	42.7	67
December	1019.7	74	952.8	83	8.0	84	−12.0	85	38.2	64

Table 7.11.1.4.2 Maximum and minimum by month of pressure, temperature and wind speed, and year of occurrence for Dumont d'Urville.

Years	Pressure (hPa)		Temperature (ºC)		Wind Speed (m s⁻¹)		D.T.R. (ºC)
	Mean	Std dev	Mean	Std dev	Mean	Std dev	
1960–96	988.1	11.2	−10.6	7.2	9.6	6.8	4.3

Table 7.11.1.4.3 Yearly average and standard deviation of pressure, temperature, wind speed and day temperature range (DTR) at Dumont d'Urville from 1960 to 1996.

Element/Month	Jan	Feb	Mar	Apr	May	Jun	Jul	Aug	Sept	Oct	Nov	Dec	Year
Mean daily maximum temperatures (º C)	1	−2	−8	−15	−12	−16	−17	−16	−16	−12	−5	−1	−10
Mean daily minimum temperatures (º C)	−3	−7	−13	−18	−17	−20	−23	−21	−21	−18	−12	−6	−15
Mean wind direction	S	S	S	S	S	S	S	S	S	SE	S	S	S
Mean wind speed (m s^{-1})	12.9	12.4	21.6	21.1	23.2	22.1	24.2	21.6	19.1	21.6	17.0	16.5	~29
Mean MSL Pressure (hPa)	992	989	990	991	987	991	986	988	991	983	990	992	989

Table 7.11.2.4.1   Climate statistics for Cape Denison (1912 to 1913) (Believed to be from Madigan (1929).

Terra Nova Bay (refer Section 7.12.2 above)
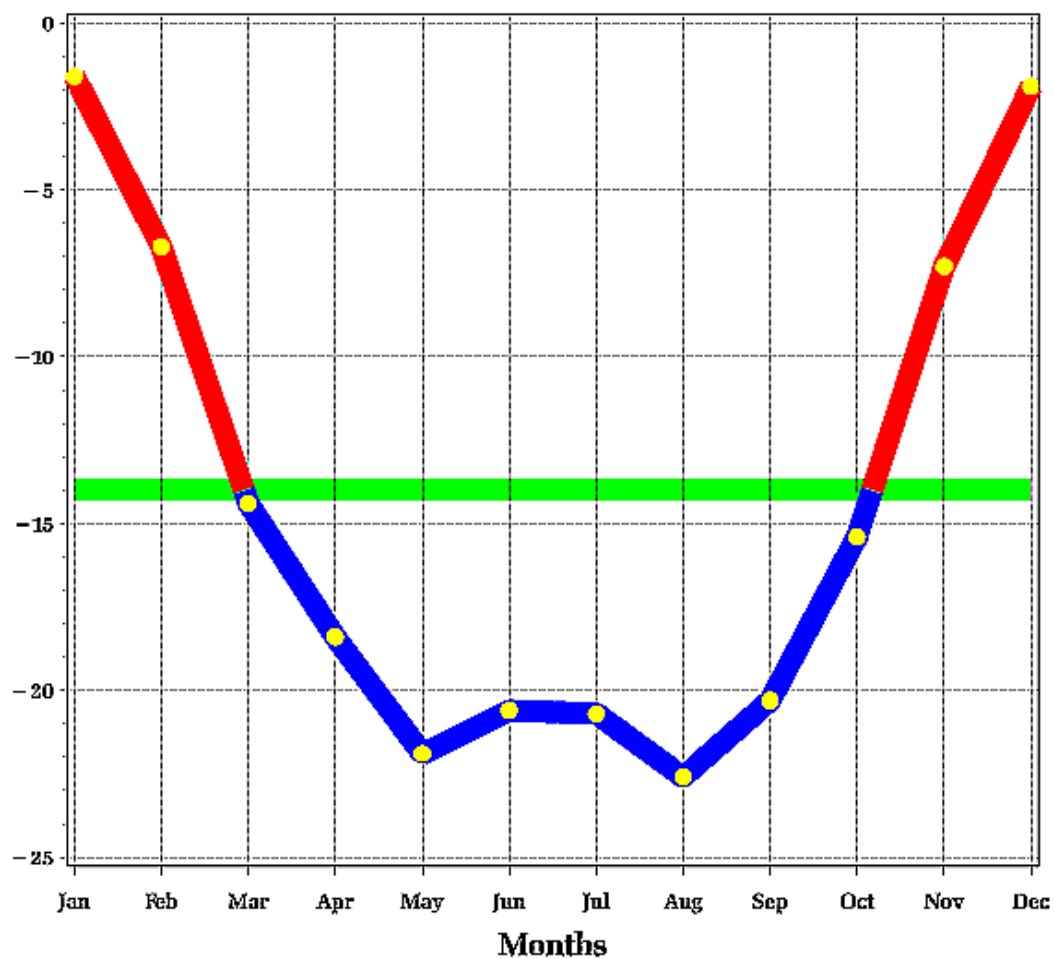
Figure 7.12.2.4.1   Monthly mean temperature (ºC) for Terra Nova Bay.
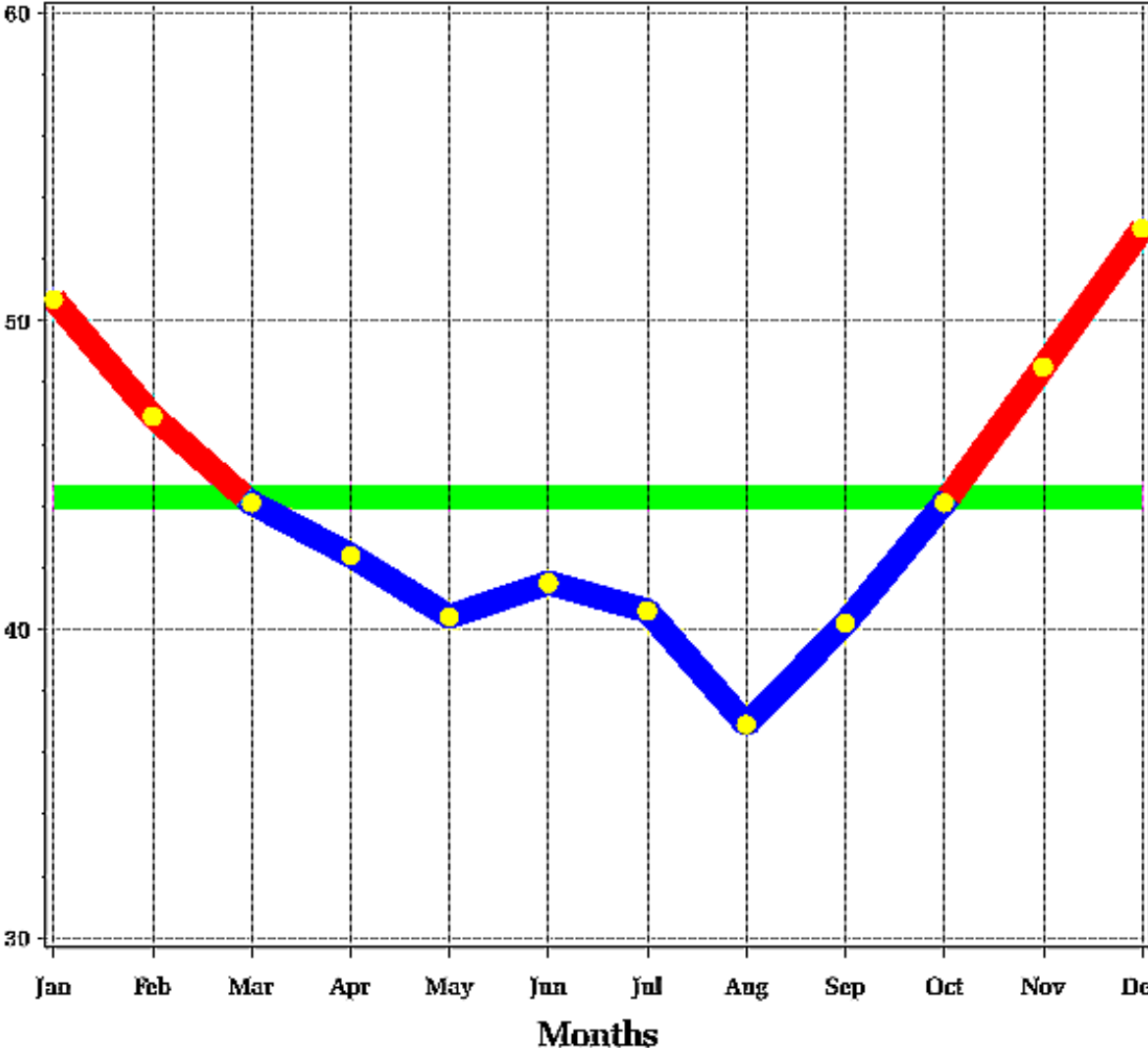
Figure 7.12.2.4.2   Monthly mean relative humidity (%) for Terra Nova Bay.
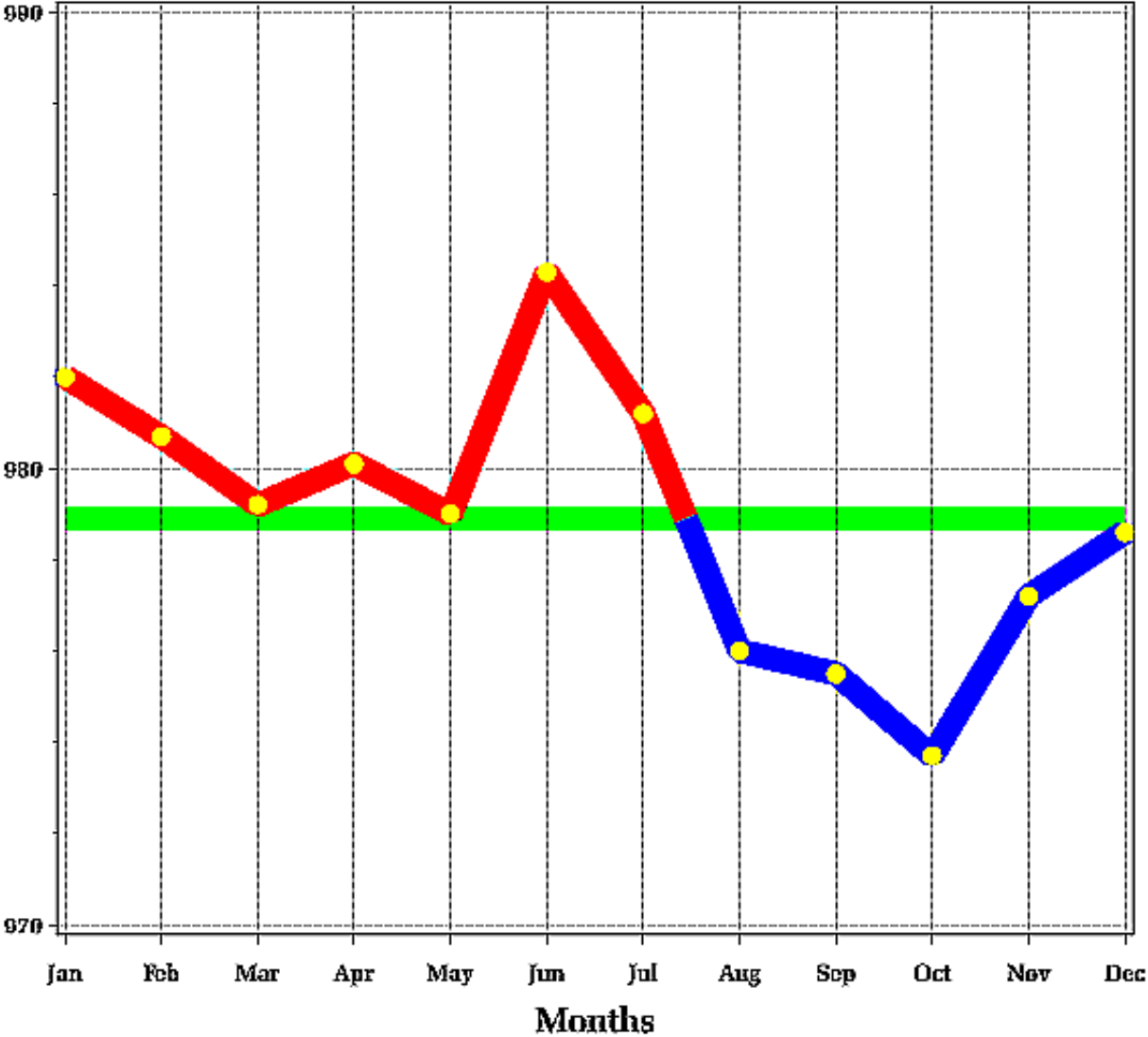
Figure 7.12.2.4.3   Monthly mean pressure (hPa) for Terra Nova Bay.
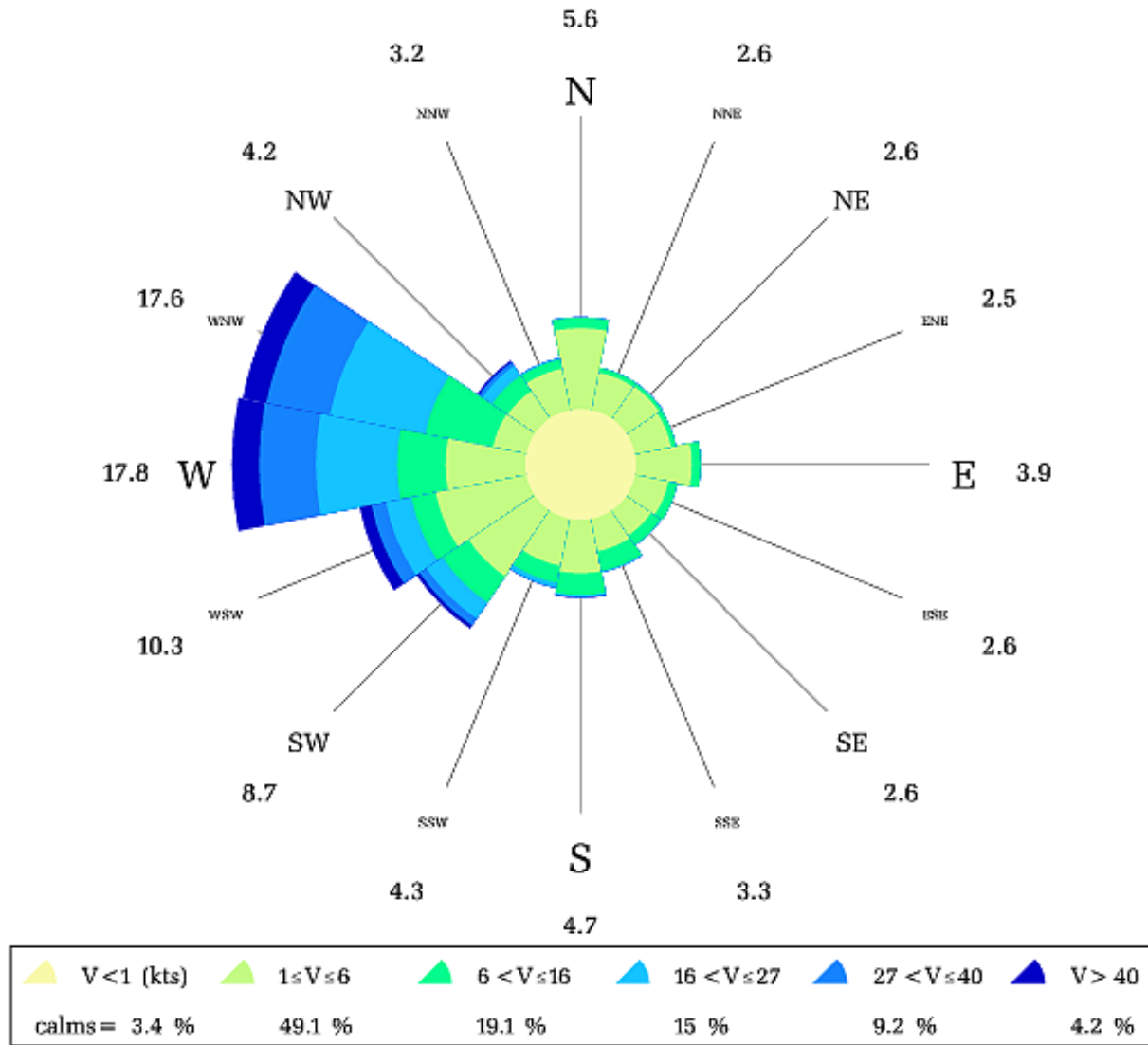
Figure 7.12.2.4.4   Annual mean wind rose for Terra Nova Bay.
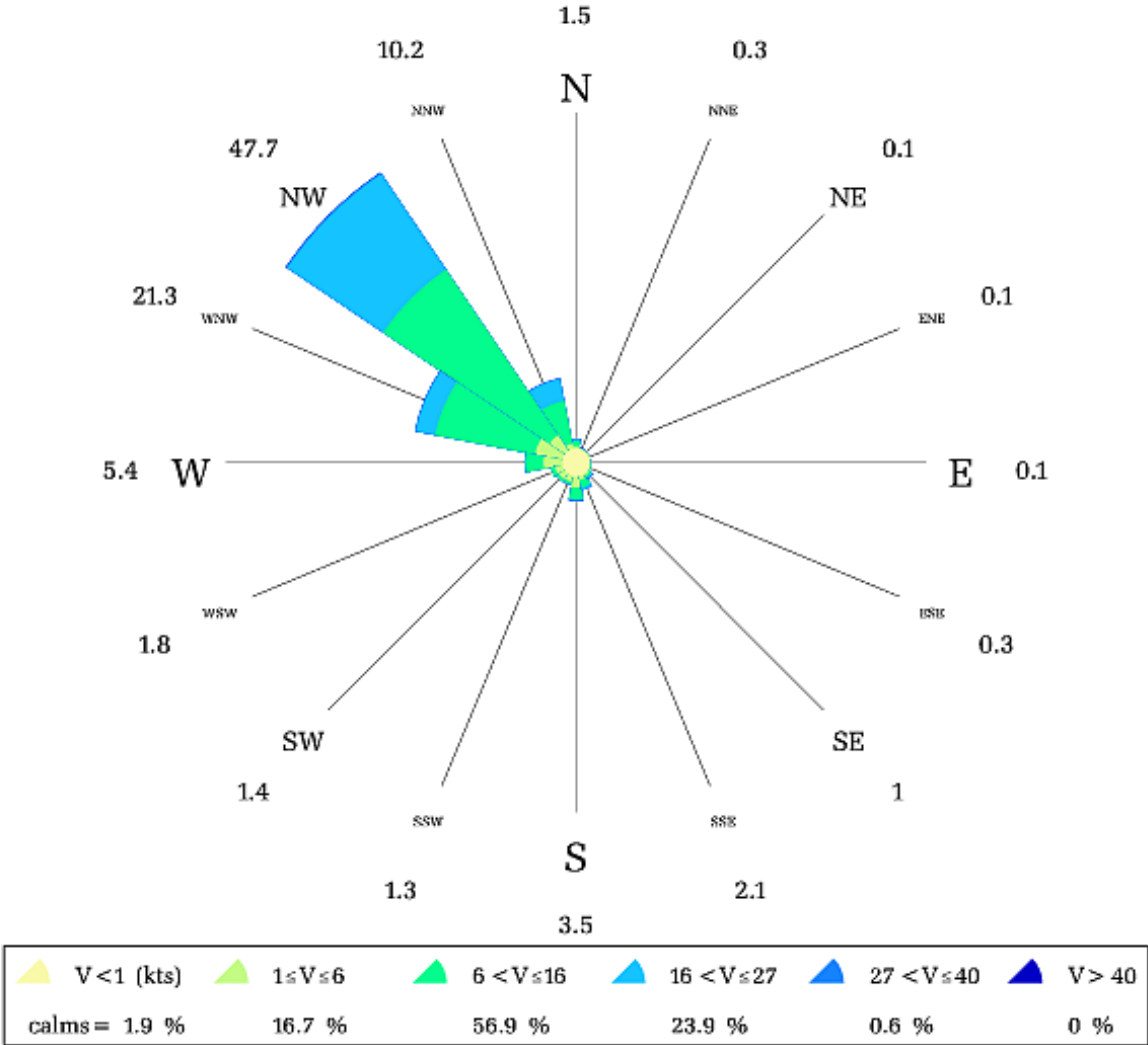
Figure 7.12.2.4.5   Annual mean wind rose AWS 7955.
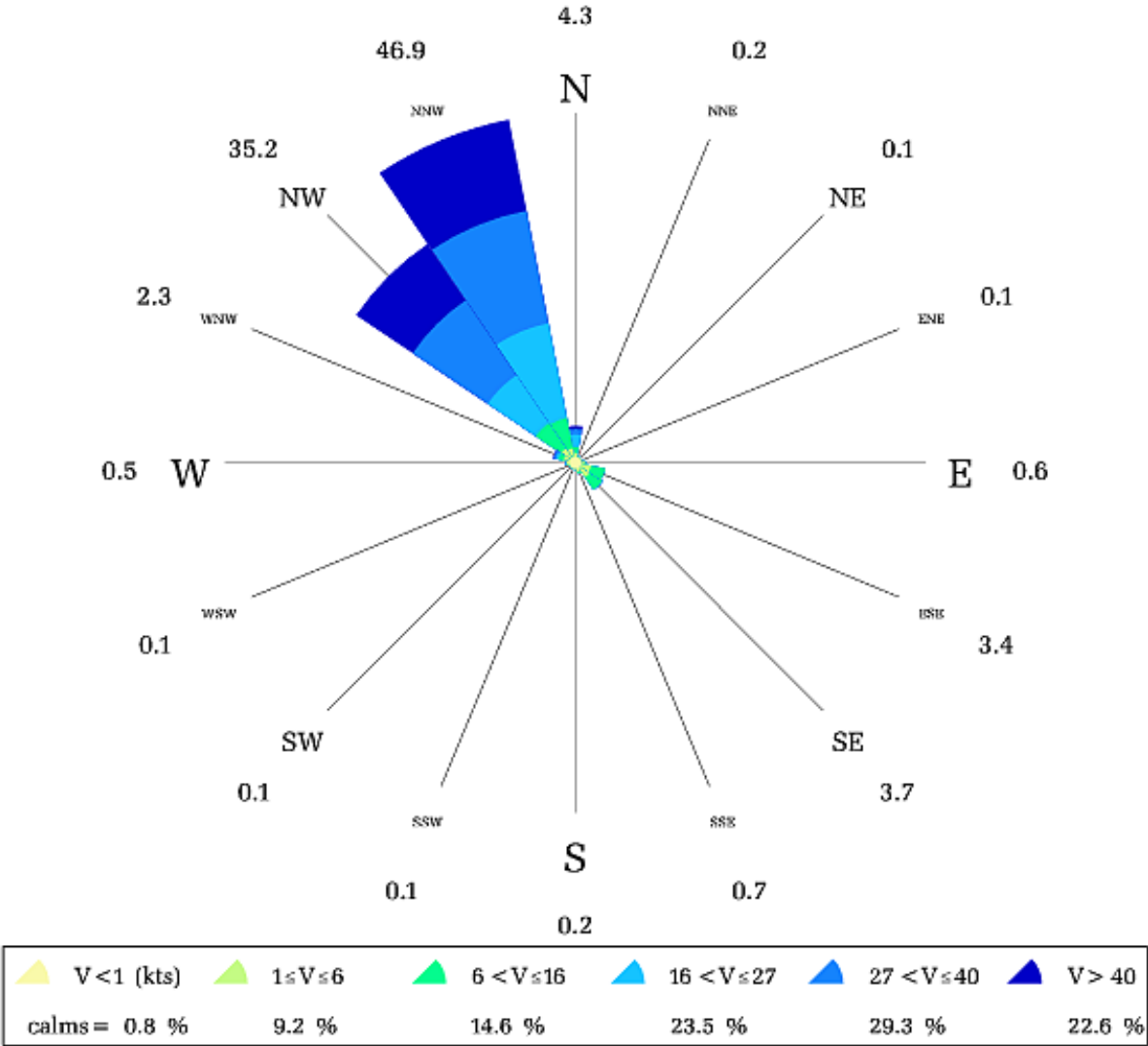
Figure 7.12.2.4.6   Annual mean wind rose AWS 7952.
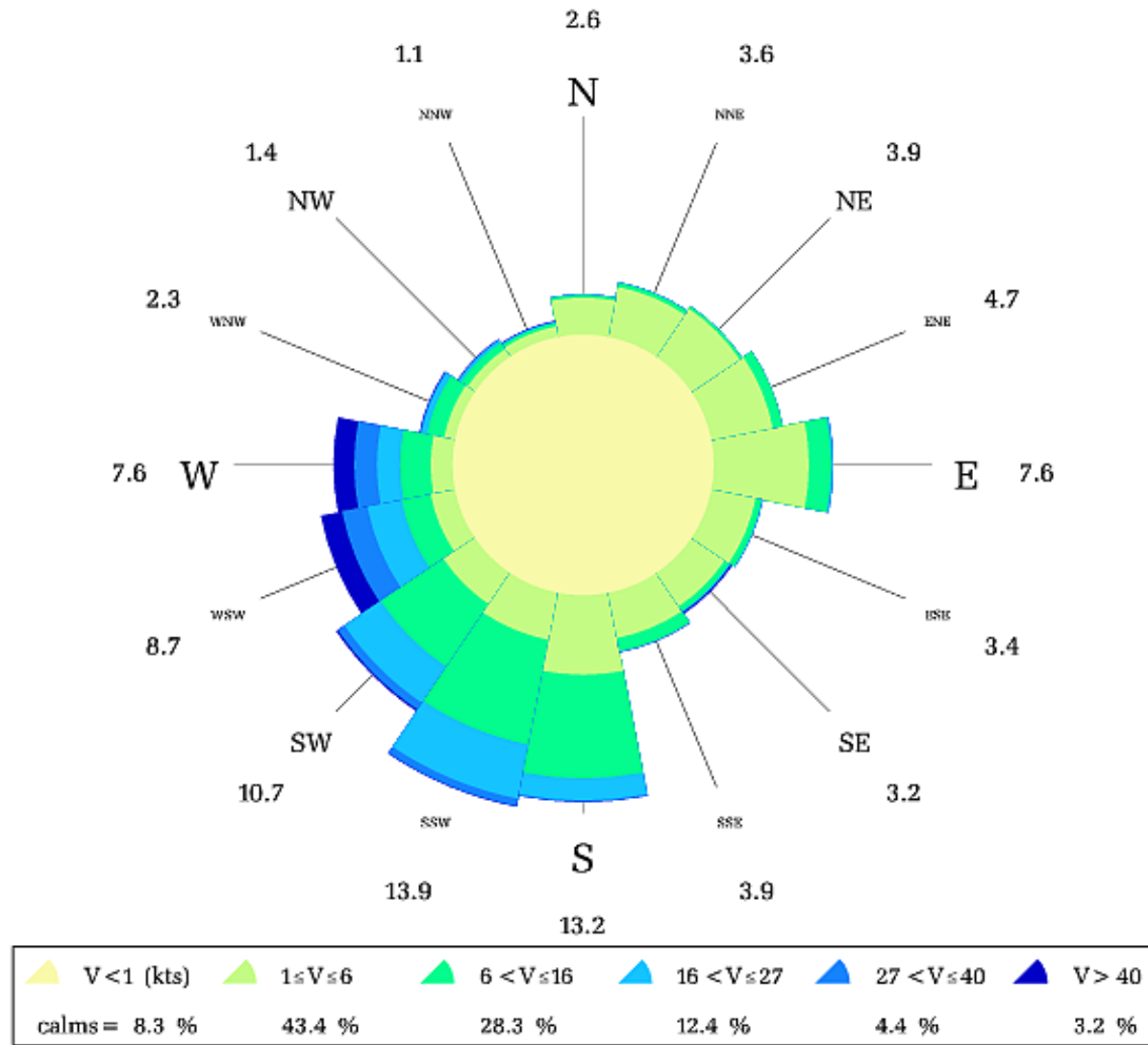
Figure 7.12.2.4.7   Annual mean wind rose AWS 7956.
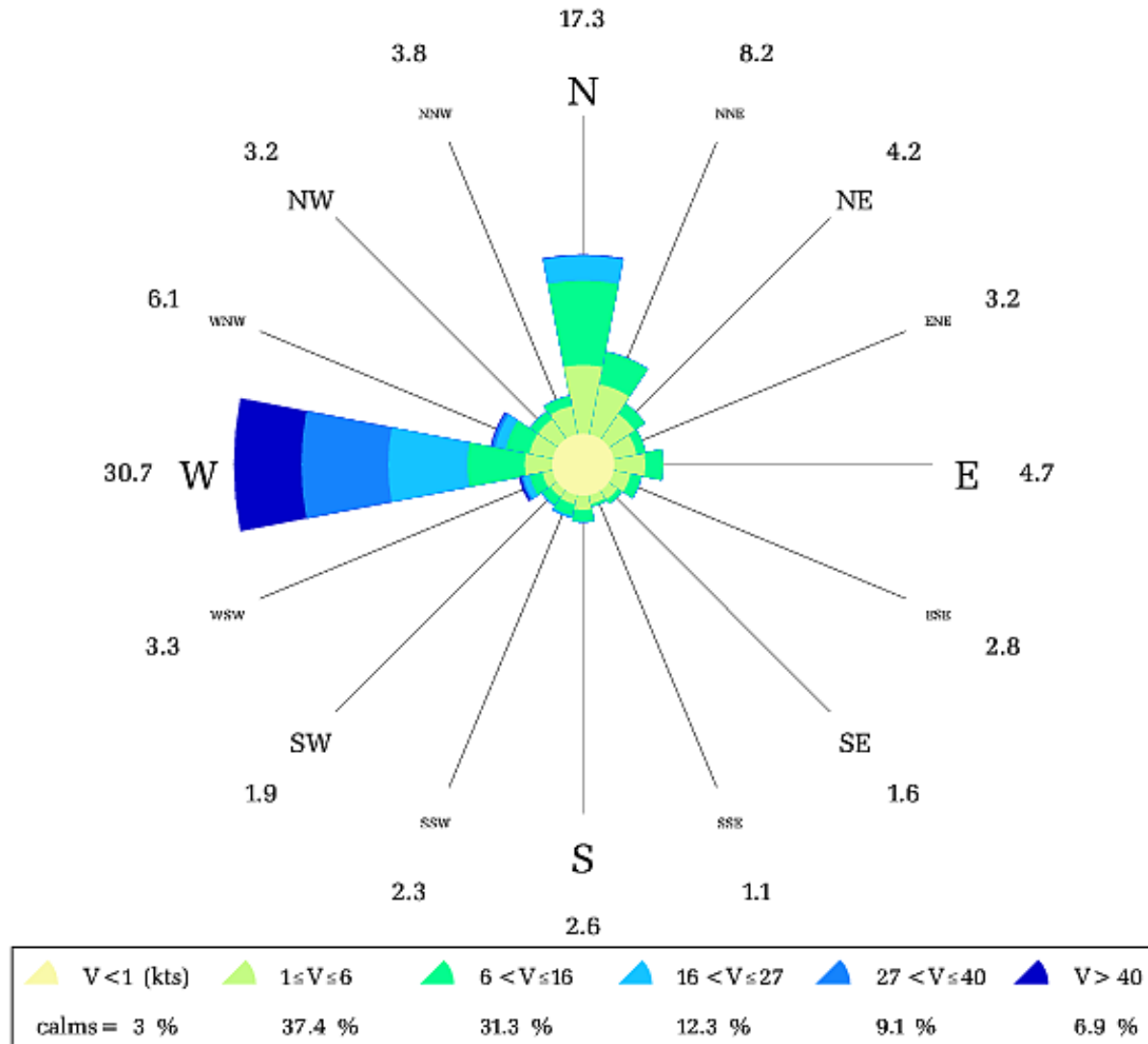
Figure 7.12.2.4.8   Annual mean wind rose AWS 7950.
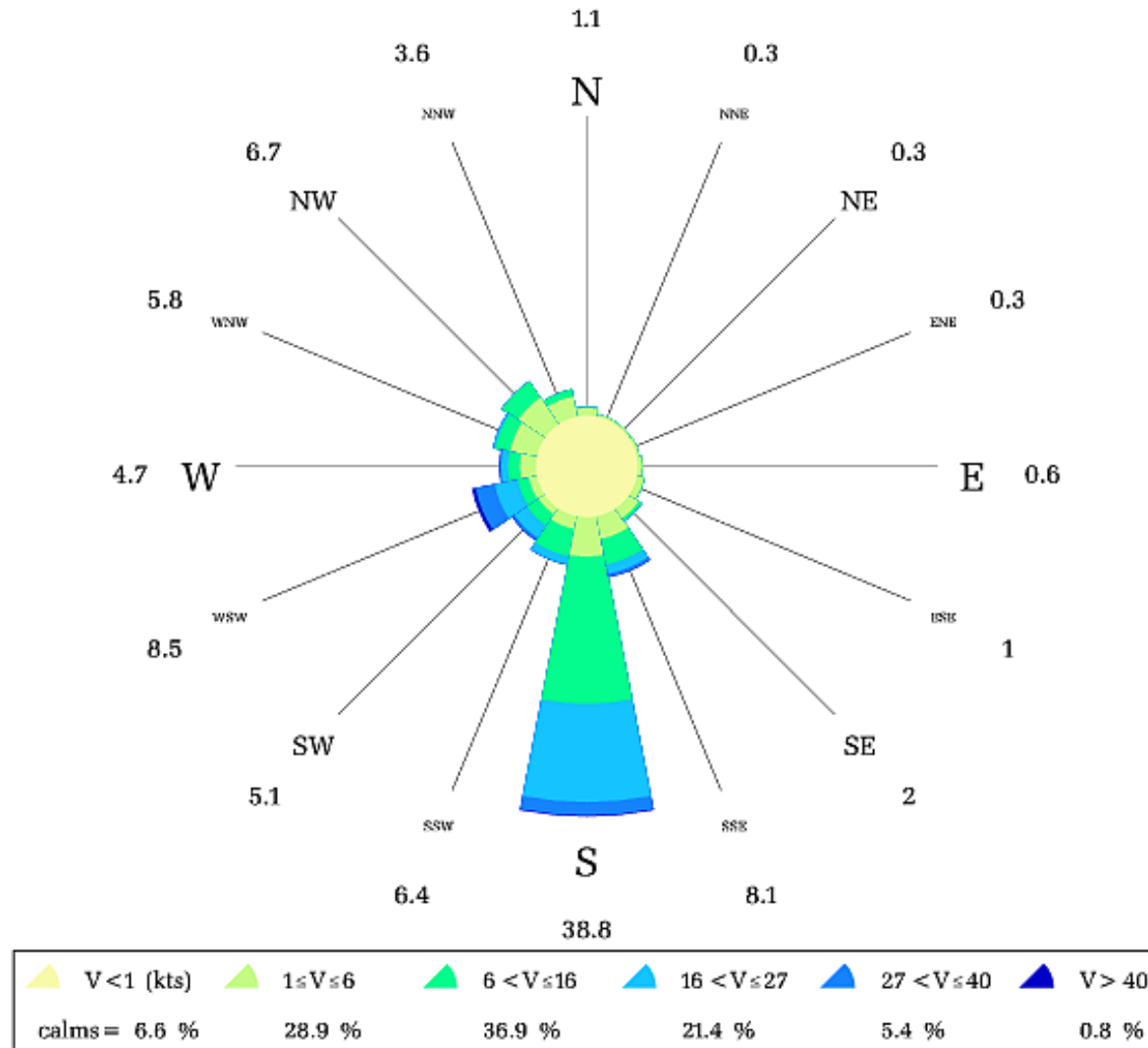
Figure 7.12.2.4.9   Annual mean wind rose AWS 7957.
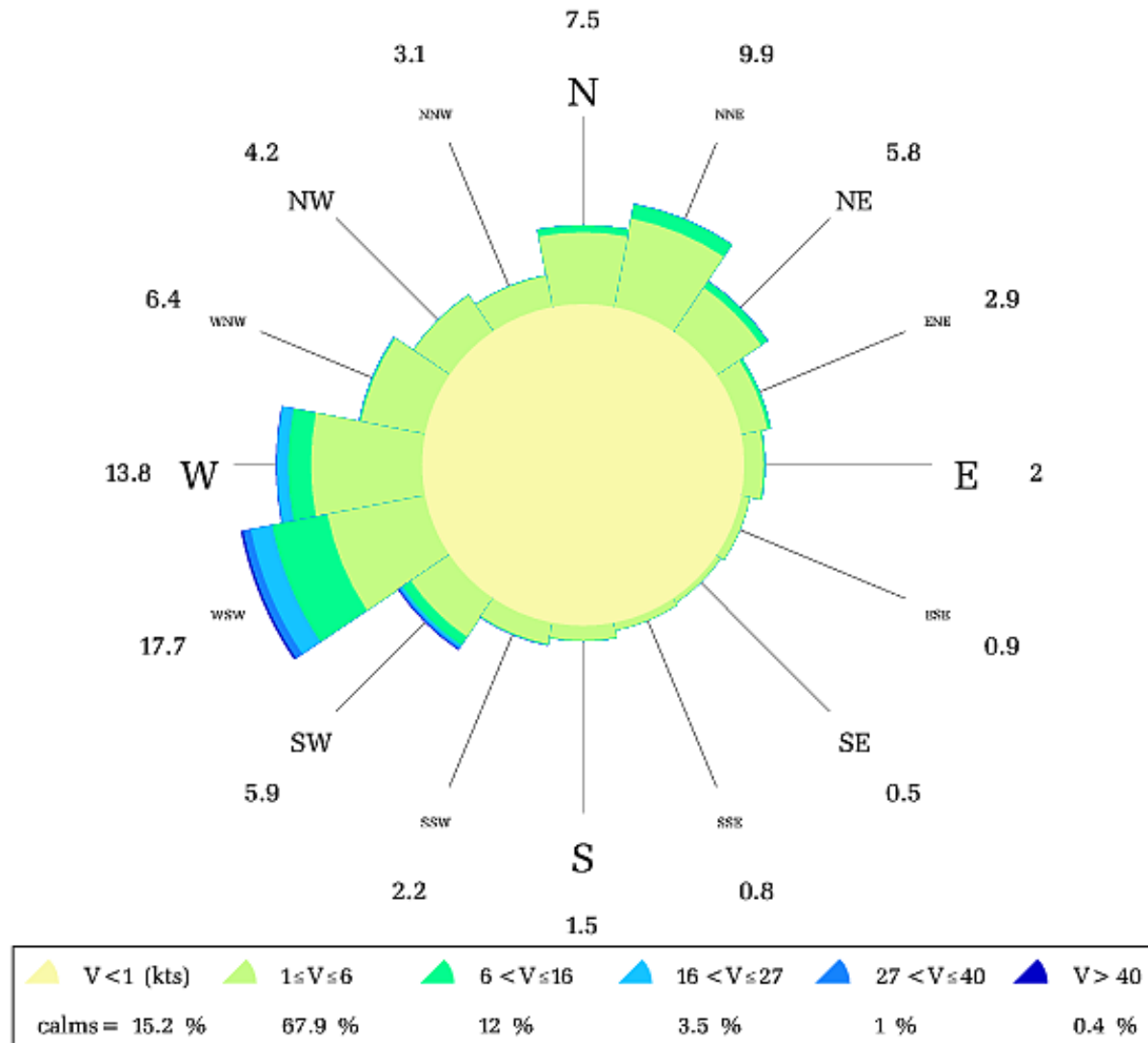
Figure 7.12.2.4.10   Annual mean wind rose AWS 7951.
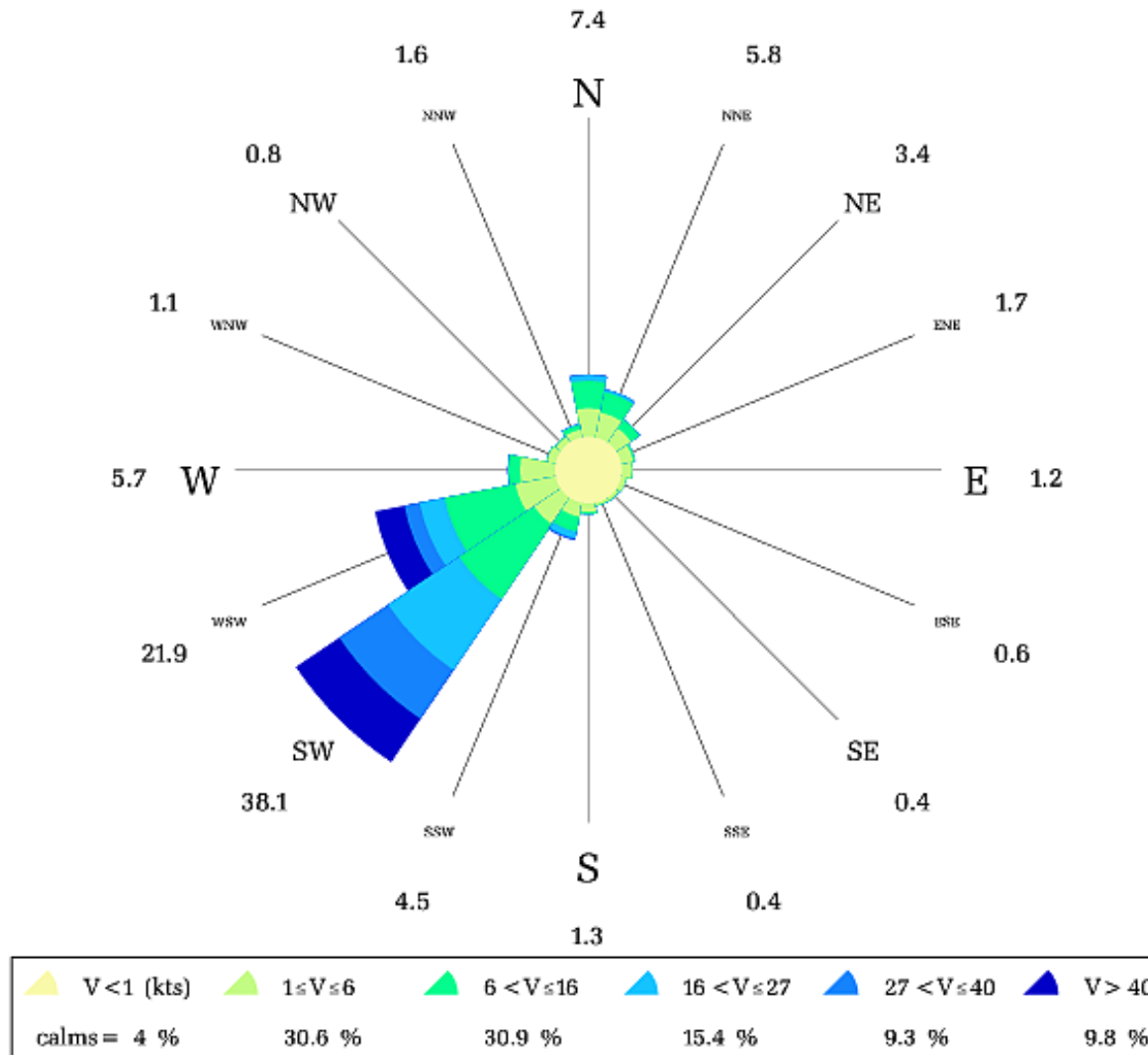
Figure 7.12.2.4.11   Annual mean wind rose AWS 7958.
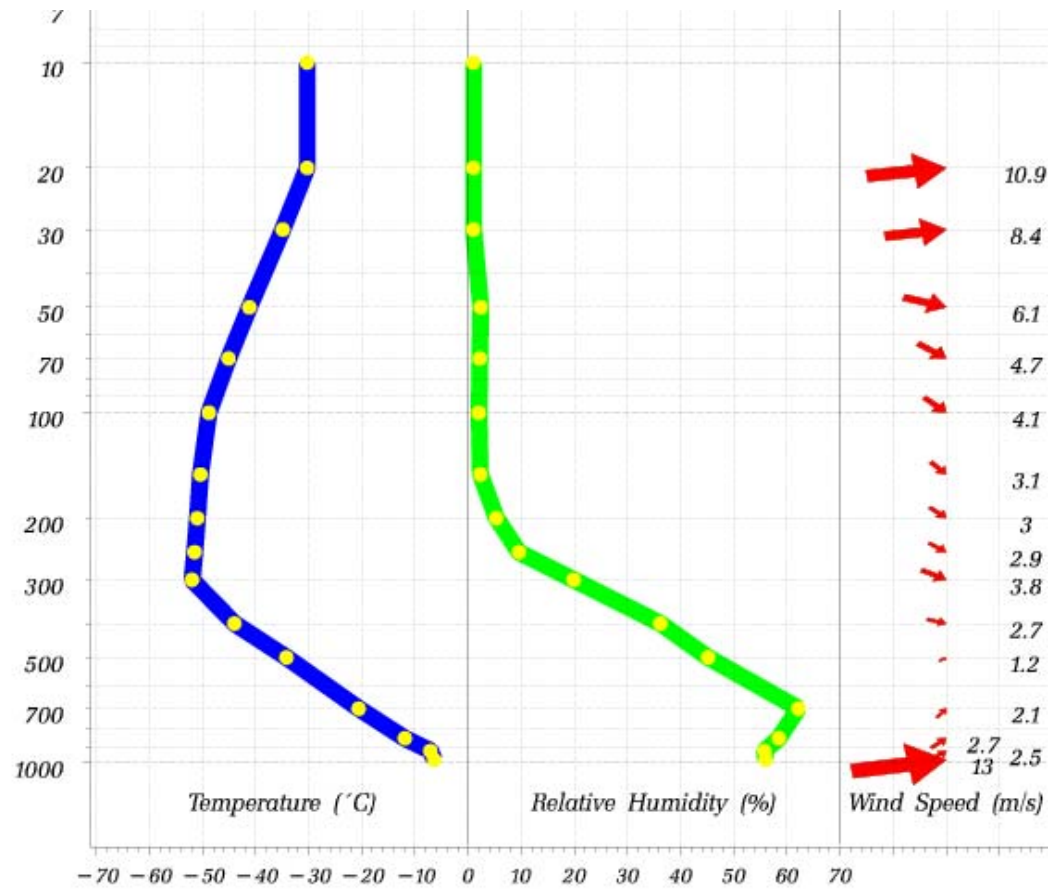
Figure 7.12.2.4.12   Annual mean lapse rate of temperature and relative humidity at Terra Nova Bay.

McMurdo (refer Section 7.12.3above)

Month	Temperature (ºC)	
	Maximum	*Minimum*
January	8	−16
February	4	−25
March	−2	−43
April	−4	−42
May	−3	−44
June	−5	−41
July	−5	−48
August	−6	−40
September	−2	−44
October	1	−39
November	4	−29
December	9	−17

Table 7.12.3.4.1 Extreme temperatures for McMurdo

Byrd Station (refer Section 7.13.2 above)

Month	Jan	Feb	Mar	Apr	May	Jun	Jul	Aug	Sept	Oct	Nov	Dec	Year
Mean daily maximum temperatures (º C)	−13.1	−16.5	−24.7	−25.7	−27.9	−30.0	−32.9	−33.5	−31.6	−25.0	−18.9	−12.1	−24.4
Highest daily maximum temp. (º C)	−5.0	−7.2	−12.8	−8.3	−7.2	−16.1	−14.4	−15.0	−16.7	−11.1	−6.7	−2.8	−2.8*
Mean daily minimum temperatures (º C)	−18.8	−22.9	−32.7	−34.9	−36.9	−39.1	−41.8	−41.7	−38.8	−33.9	−26.0	−17.6	−32.2
Lowest daily minimum temp. (º C)	−29.4	−38.9	−52.8	−58.9	−54.4	−59.4	−62.8	−62.2	−53.0	−50.0	−41.1	−29.4	−62.8*
Mean total cloud amount (oktas)	5.1	5.7	5.4	4.8	3.9	3.8	4.2	4.2	4.8	5.5	4.5	5.4	4.7
Maximum wind gust – Dir–Speed (m s^{-1})	NE 21.1	NNE 26.8	N& NNE 25.2	N 25.8	NE 31.9	ENE 29.9	NW 37.1	NE 36.1	ENE 39.7	NE 29.9	NNE 25.8	NE 27.8	ENE* 39.7
Mean station level (hPa)	813	812	805	811	808	809	802	803	796	801	805	815	807

Table 7.13.2.4.1   Mean monthly and extreme* data for Byrd Station for the period 1957–60. (Based on data from Phillpot (1967).

		N	NNE	NE	ENE	E	ESE	SE	SSE	S	SSW	SW	WSW	W	WNW	NW	NNW	Calms
Jan	(a)	20.9	26	17.1	2.3	2.8	1.2	3.5	2.3	3.2	2.2	4.6	2	5.1	1.8	5.7	3.5	3.6
	(b)	7.9	7.7	6.7	5.3	3.8	3.1	3.6	4.6	5.5	5.1	5.9	5.3	4.6	4.2	4.7	5.5	0
Feb	(a)	29.7	24.8	18.9	2.4	1.6	0	0.8	0.6	1.8	0.6	1	1.2	3.1	2.9	9	6.8	2.2
	(b)	8.4	9.3	8.8	8.2	6.5		2	1.5	4.2	4.6	4.7	4.9	7.2	6.1	5.1	5.8	0
Mar	(a)	20.6	32.8	26.6	2.7	1	0	0.6	0	0.8	1	2.7	2.2	2.2	2.1	4.9	5.6	1.4
	(b)	8.6	9.9	9.7	8.6	7.7		5.6		3.7	5	4.9	4.5	5.4	5.5	5.3	6.3	0
Apr	(a)	24.5	33.6	17.8	2	0.6	0	0	0	0.8	1.1	1.5	1.1	3.1	3	8.7	7.3	1.4
	(b)	7.7	9.4	9.6	8	8.7				4.9	4.9	6.8	4	8.4	7	6	6.4	0
May	(a)	17.2	25.6	27.6	4.5	1	0.8	0.9	0.6	1.3	0.9	1.9	1.4	3.1	4.7	9.6	6.2	0.9
	(b)	8.7	10.6	11.1	12	8.2	4.6	4.5	3	4.1	4.2	8.1	4.9	8.7	9.4	7.5	7.7	0
Jun	(a)	25.5	30	21.1	3.2	1.1	0.7	0.7	0.7	0	1	1.7	1.2	4.4	2.8	6.5	5.8	1
	(b)	8.5	10.1	10.8	12.3	10	8.9	5.3	4.3		6.3	6.4	6.4	6.4	5.5	5.2	5.8	0
Jul	(a)	28.5	26.8	16.7	5.5	2.4	1	0.9	0	0	0	1.2	1.7	2.4	3.2	7.1	7.6	1.6
	(b)	8.6	10.2	13.3	11.4	11.1	10.5	6.3				6.7	6	6.3	5.5	7.2	7.9	0
Aug	(a)	19.2	31.9	27.8	8.1	1.5	0.6	0.8	0.7	0.6	0	0.9	1	3.1	1.9	3	5.5	1.1
	(b)	9.7	10.5	11	11.1	6.8	6.6	5.8	4.6	6.6		5.2	8	7.7	5	6.5	6.9	0
Sep	(a)	11.3	32	42.6	10.7	2	1.1	0.6	0.7	0.6	0	0.6	0.6	0.9	0.6	0.9	1.7	0.7
	(b)	8.7	10.1	12.2	12.3	7.6	5.2	9.7	5.3	4.6		4.6	7.1	5.7	7.7	5.7	7.1	0
Oct	(a)	15.9	25.8	33.3	5.5	1.3	0.6	0.7	0.6	1.2	0.9	2.3	1.6	2.7	1.9	7.6	5.1	1.2
	(b)	7.7	9.4	11.2	10.4	7.2	5.6	5.1	2.5	3.7	4.6	6.5	8	6.5	5.9	6.5	6.9	0
Nov	(a)	12.5	35.8	33.3	6.7	2.6	1	1	0.7	0.8	0	0.9	1	0.9	1.8	2.6	2.8	2.8
	(b)	7.5	9.5	8.8	8.3	7.3	5.3	2.4	4.1	2.5		4.3	4.3	4.9	2.5	6.2	5.1	0
Dec	(a)	18.6	24.4	20.9	3.7	1.2	0.8	1.1	1.1	2.8	1.8	3.9	2.6	3.9	3.6	5.6	8.7	3.3
	(b)	7	7.9	8.9	7.5	4.3	2.8	3.3	3.5	6.2	6.4	5.4	4.7	5.4	5.5	4.7	6.8	0

Table 7.13.2.4.2   Wind frequency table for Byrd Station for the period 1957–60 (~ 950 synoptic observations). (Based on data from Phillpot (1967). For each month line (a) is the % frequency and line (b) the mean wind speed in m s^{-1}

APPENDIX 3:   ANTARCTIC "REPRESENTATIVE" ATMOSPHERES

On Standard Atmospheres

A "standard" atmosphere serves as a reference for the relation between pressure, height, and temperature in the vertical. There have been several such atmospheres adopted in the past, for example: the US National Advisory Committee for Aeronautics (NACA) Atmosphere; the International Commission for Air Navigation Atmosphere; and the International Civil Aviation Authority (ICAO) standard atmosphere. Each of these is similar in many respects. (Saucier, 1955, p.53). The ICAO standard atmosphere is now generally in use and its chief specifications are:

- Mean sea level pressure: 1013.25 hPa;
- Mean sea level temperature:15°C;
- Temperature (virtual) lapse rate 6.5°C up to 11 km (where T = –56.5°C);
- Isothermal lower stratosphere above 11 km (to at least 20 km).

NACA (1954, p.2) indicates that the ICAO standard atmosphere is in "fairly good agreement" with the annual average values of pressure, temperature and density for the North American atmosphere near 40º N up to an altitude of about 20,000 m (~65,000 ft). Being an hypothetical approximation to the "real" atmosphere found in mid–latitudes of the Northern Hemisphere, the ICAO (or any of the others mentioned above) is likely to be a poor representation of the Antarctic atmosphere. The practical implication of this is that while the ICAO atmosphere is used, among other purposes, for the calibration of altimeters allowance needs to be made for the cold Antarctic environment. As mentioned in Section 3.4.2.7 above to adjust for the real atmosphere's departure from 15 °C the following equation may be used:

$$Z = Z_{ind}(1 + (T_s - 15)/288)$$ Equation A3–1

It may be seen that when the surface air temperature (T_s) is *below* 15 °C the altimeter readings (Z_{ind}) will be *higher* than the estimated "true" height Z. For example, if the surface air temperature is –20 °C the indicated height (Z_{ind}) has to be multiplied by 0.88 to give a more accurate (lower) estimate of altitude.

Suggested "Representative" Antarctic Atmospheres

It is evident from the discussion above that ideally a "standard atmosphere" might usefully be derived for the Antarctic. While a rigorous derivation of such a model atmosphere is beyond the scope of this handbook the following describes related work steered by the editors but with I. Barnes–Keoghan and D. Shepherd of the Australian Bureau of Meteorology and S. Colwell and S. Harangozo of the British Antarctic Survey performing most of the data manipulation and processing and data display work. The aim of this work is to suggest "Representative Antarctic Atmosphere" (RAA) which might more closely reflect the vertical atmospheric profile of high southern latitudes than does the ICAO standard atmosphere. As will be seen there appears to be merit in defining at least two "RAAs": one for summer and one for winter, and, RAAs for the various latitude–based geographical regions of the Antarctic and sub–Antarctic.

Data

In deriving the ideas for the suggested RAAs the mean January and July vertical temperature traces (along with extreme daily and standard deviations of daily temperature values) were constructed for:

- Mt Pleasant Airport, (Tables A3–1 (a) and (b) and Figures A3–1 (a) and (b));
- Bellingshausen, (Tables A3–2 (a) and (b) and Figures A3–2 (a) and (b));
- Halley, (Tables A3–3 (a) and (b) and Figures A3–3 (a) and (b));
- South Pole, (Tables A3–4 (a) and (b) and Figures A3–4 (a) and (b));
- Vostok, (Tables A3–5 (a) and (b) and Figures A3–5 (a) and (b));
- Casey, (Tables A3–6 (a) and (b) and Figures A3–6 (a) and (b));
- Macquarie Island, (Tables A3–7 (a) and (b) and Figures A3–7 (a) and (b)).

The data used to compile these figures and tables were from available standard pressure level data from all radiosonde flights during the period 1980 to 1999 inclusive. The surface data, however, were from other available long term means and are shown in Tables A3–8 (a) and (b).

The seven stations used were chosen because not only do they provide good sectional data across the Antarctic ((Mount Pleasant Airport and Bellingshausen are almost on the 60°W longitude, and Vostok/Casey are approximately on the 110° E longitude, and being south of 75° S, Halley is physically not far from this transect) but because they are believed to represent various regions of the Antarctic. Mount Pleasant Airport would be representative of the sub–Antarctic climate with Macquarie Island also being used to average out any local bias, due, for example to the proximity of the South American orography. Bellingshausen is representative of the Antarctic maritime climate being at the tip of the Antarctic Peninsula; South Pole Station and Vostok represent continental stations, while Halley and Casey are considered to be typical of coastal Antarctic stations more exposed to low level easterlies than the more frequent westerlies that, for example, Bellingshausen experiences.

Rationale behind suggested separate summer and winter and latitudinal RAAs

The mean January and July temperature profiles for each of the above stations are displayed in Figure A3–8 (a) and (b) respectively. Given that the data used to compile these figures, apart from the surface data, were from all available flights during the period 1980 to 1999 inclusive, it is considered valid to compare the traces one with the other. Features to note are:

- (a) the trend below about 250 hPa, summer and winter, for the temperature to be colder as one moves further south;
- (b) this trend reverses in summer above about 250 hPa, at which level all the traces and the ICAO standard atmosphere apparently have about the same temperature;
- (c) the traces all depart further (become colder) from the ICAO standard in July;
- (d) the Mount Pleasant Airport and Macquarie Island traces are, apart from the lower levels in summer, almost co–incident with each other;
- (e) the South Pole and Vostok traces are almost co–incident with each other in both January and July (to the extent that both are sampling the same pressure levels;
- (f) Casey and Halley have similar profiles in January (apart from the lowest levels) although in July these profiles separate a little;
- (g) below 250 hPa the trace for Bellingshausen remains intermediate between the sub–Antarctic traces (Mount Pleasant Airport and Macquarie Island) and the coastal stations of Halley and Casey;
- (h) the traces do not adequately show the radiation induced surface inversions as only standard pressure level and surface data were used.

There may well be many reasons for the above characteristics however, *prima facie,* it seems reasonable to assert that:

- Most of the observations ((a), to (g)) are a consequence of the seasonality which comes from the Antarctic being mostly shaded from the sun in winter. Point (b), for example, probably reflects that in summer, the lower level Antarctic environment causes tropopause heights to be lower the further one goes south, whereas in winter, being in darkness, the whole atmosphere above the Antarctic cools, with the destruction of ozone is a major factor in the cooling aloft.
- There is sufficient shift (cooling) between January and July for there to be separate RAAs for each of these months.
- With Casey and Halley, being almost ten degrees of latitude apart in location relative to the South Pole, the separation of their profiles in July is probably due to the effective increased "continentality" of Halley as the sea –ice zone increases, and Halley being more completely in the Earth's shadow.
- However, given the closeness of the profiles for these two stations in summer it seems pragmatic to average their profiles even in the July case;
- A sensible characterisation of the high southern latitude atmosphere might be to have January and July atmospheres constructed according to Table A3–9

Region	Approx. latitude band	Typical Stations
Sub–Antarctic	50º S to 60º S	Mount Pleasant Airport & Macquarie Island
Intermediate	60º S to 65º S	Bellingshausen
Coastal Antarctic	65º S to 75 º S	Halley and Casey
Continental Antarctic	South of 75º S	Vostok and South Pole

Table A3–9   A suggested geographical distribution for the characterisation of the vertical structure of the high Southern Hemisphere atmosphere.

Mean upper winds

Upper wind conditions, while generally not considered to be part of the specifications of a representative atmosphere are, however, useful in depicting the average state of an atmosphere. Figures A3-9A and A3-9B are, respectively, wind roses for January and July for the above stations for which the mean temperature profiles have been calculated. The periods of record for each wind rose were:

- Mount Pleasant   1988 to 1999
- Bellingshausen   1980 to 1998
- Halley   1957 to 1999
- South Pole   1980 to 1999
- Vostok   1980 to 1991
- Casey   1959 to 1998
- Macquarie   1994 to 1999

Features such as the polar vortex in winter and the variable nature of the upper winds over the pole are quite evident.

An application of the Representative Antarctic Atmosphere

Quite apart from altimeter settings another practical application to which a "standard" atmosphere may be put is the "correlation" between height (Z) and pressure in order to gain an appreciation of the pressure altitude at which certain cloud types might be usually present. In practice, in the absence of other objective guidance (for example, NWP) a forecaster might construct a "pressure height line" on the latest radiosonde trace in order to ascertain the geopotential heights of clouds or moisture band/temperature inversions which may be present to assist with a "nowcast". According to the WMO International Cloud Atlas cloud ètages (ranges of levels at which clouds of certain genera occur most frequently) vary from the tropics (highest upper limits) to the polar regions (lowest upper limits) according to Table A3–10.

Ètage	Polar regions	Temperate regions	Equatorial regions
High	3–8 km	5–13 km	6–18 km
Middle	2–4 km	2–7 km	2–8 km
Low	From the earth's surface to 2 km	From the earth's surface to 2 km	From the earth's surface to 2 km

Table A3–10   Ètage of low, middle and high cloud for various temperature regimes.

Using the Halley July data (Figure A3–3(b) and Table A3–3(b) and Table A3–8(b)) (perhaps as a proxy for a "Representative **Coastal** Antarctic Atmosphere" for the purposes of this discussion) leads to the pressure boundaries corresponding to the Polar ètages given in Table A3–10. For comparison, the pressure levels for an ICAO Atmosphere are also given assuming the ètages for polar regions and it may be seen that the ICAO values overestimate the pressure both the upper and lower boundaries of the ètage.

Polar Ètage	Halley pressure limits of Ètage (hPa)	ICAO standard atmosphere pressure limits of Ètage (hPa)
High (3–8 km)	660 – 310	700 – 370
Middle (2–4 km)	760 – 580	800 – 620
Low (0 to 2 km)	987.7 – 760	1013.25 – 800

Table A3–11   Pressure limits of Polar Ètages of low, middle and high cloud assuming an ICAO standard atmosphere (right hand column) and a Halley July mean temperature profile (left hand column).

Concluding remarks

The authors have not, in fact constructed actual "RAAs" as described above for two reasons: firstly, it may be prudent to process all available radiosonde data for all stations before averages are made; and secondly, given the latitudinal and seasonal effects evident in the profiles presented there may be scope for a model which had latitude and season as input parameters. Obviously, on a day to day basis, NWP could provide these types of output, but for the purposes of characterisation of the "average" atmosphere a Representative Antarctic Atmosphere seems to have merit. This is work perhaps worthy of version 2 of the handbook.
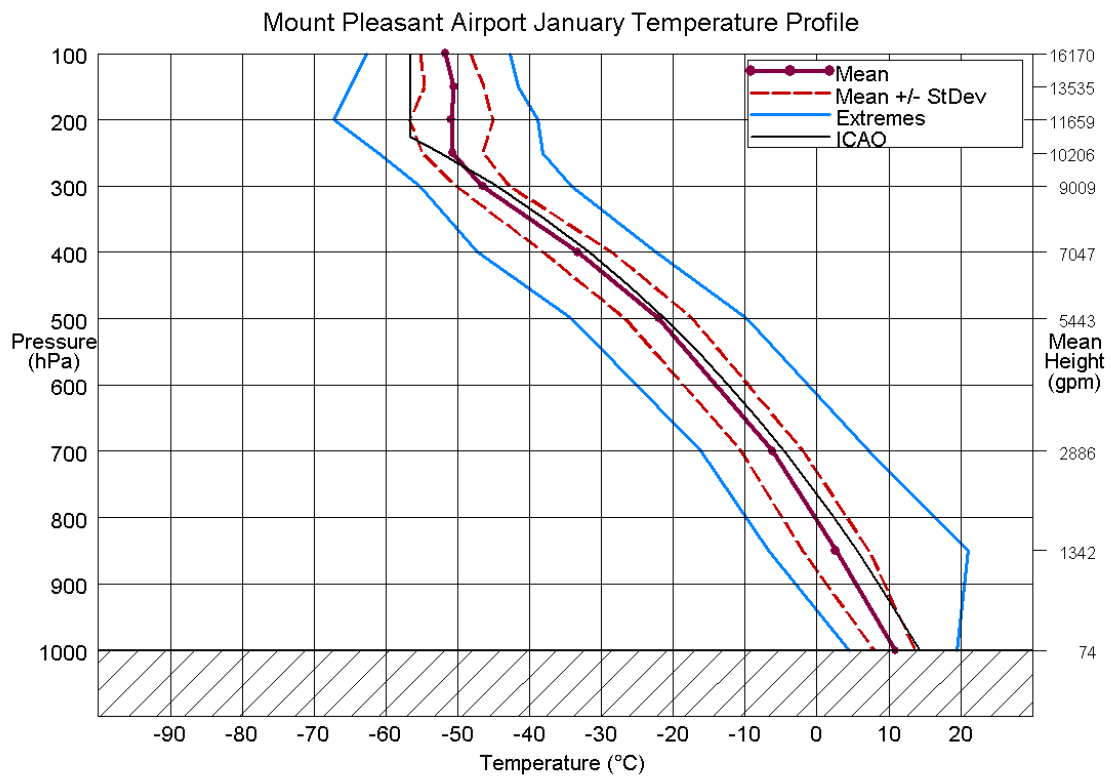
Figure A3–1 (a)   Mean temperature profile for Mt Pleasant Airport for January.
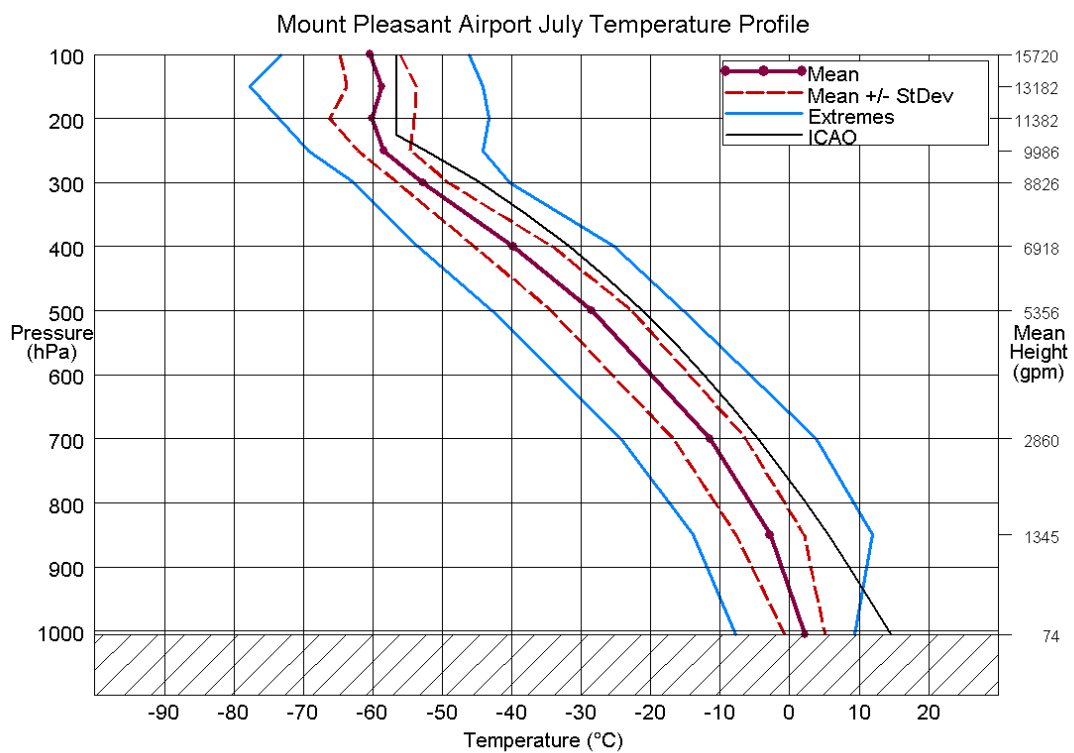
Figure A3–1 (b)   Mean temperature profile for Mt Pleasant Airport for July.
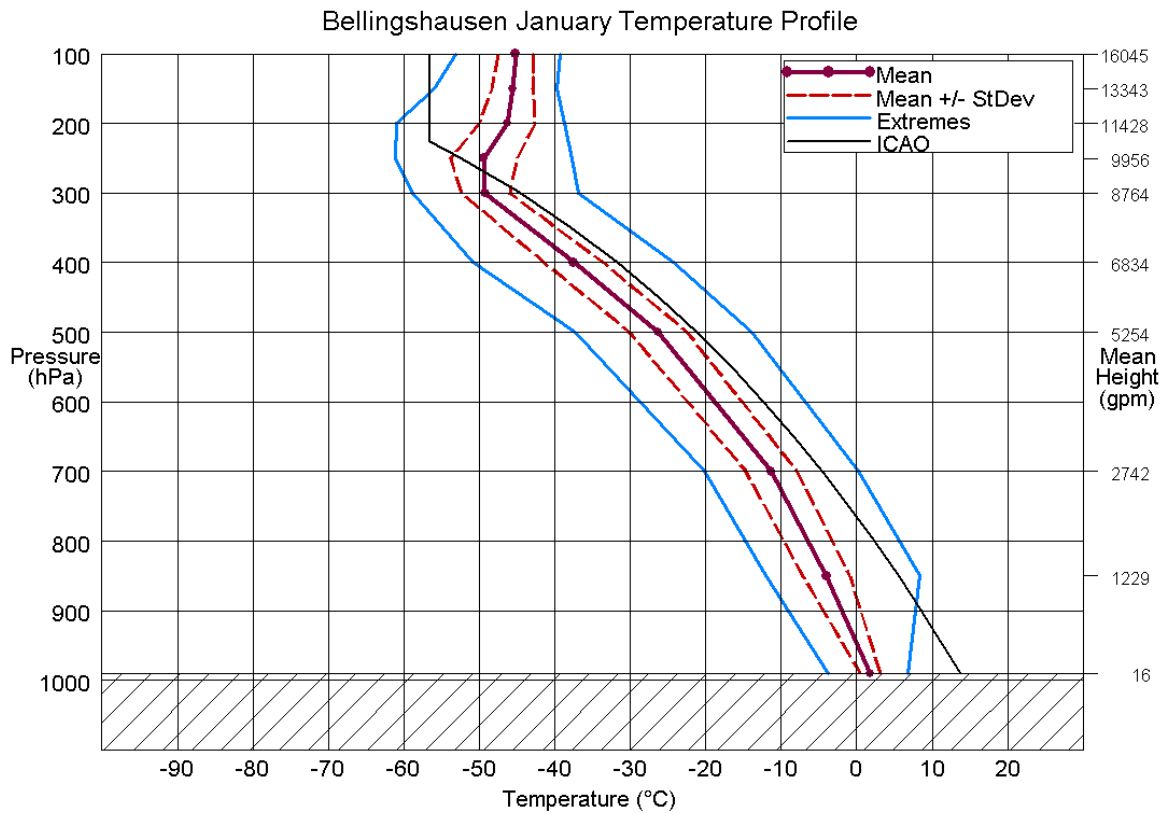
Figure A3–2 (a)   Mean temperature profile for Bellingshausen for January.
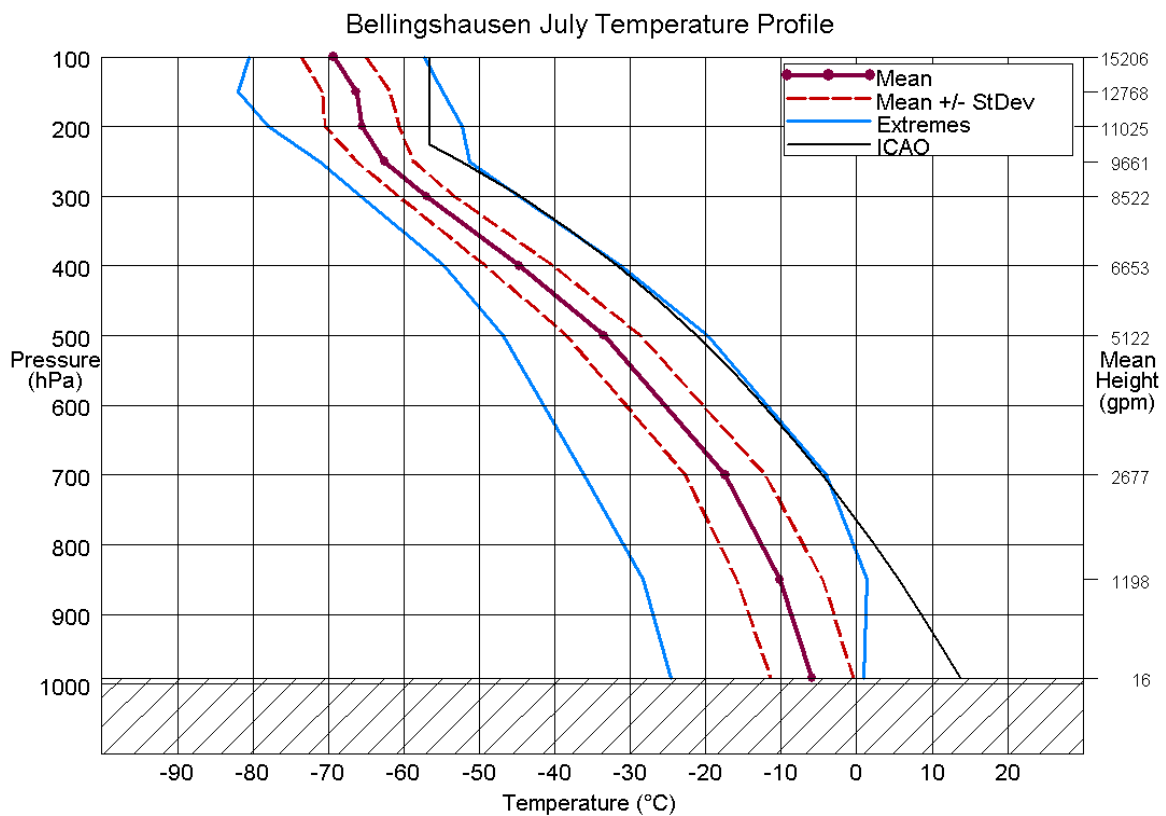
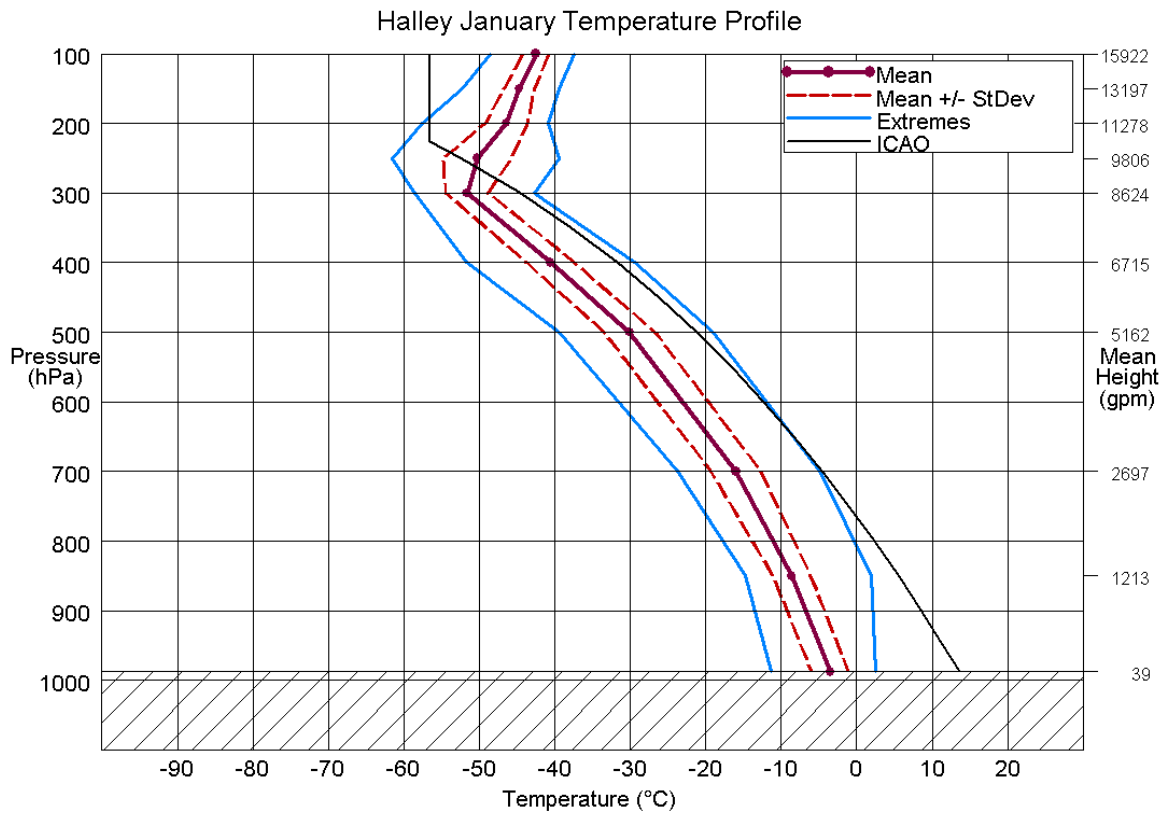**Figure A3–2 (b)**   Mean temperature profile for Bellingshausen for July.

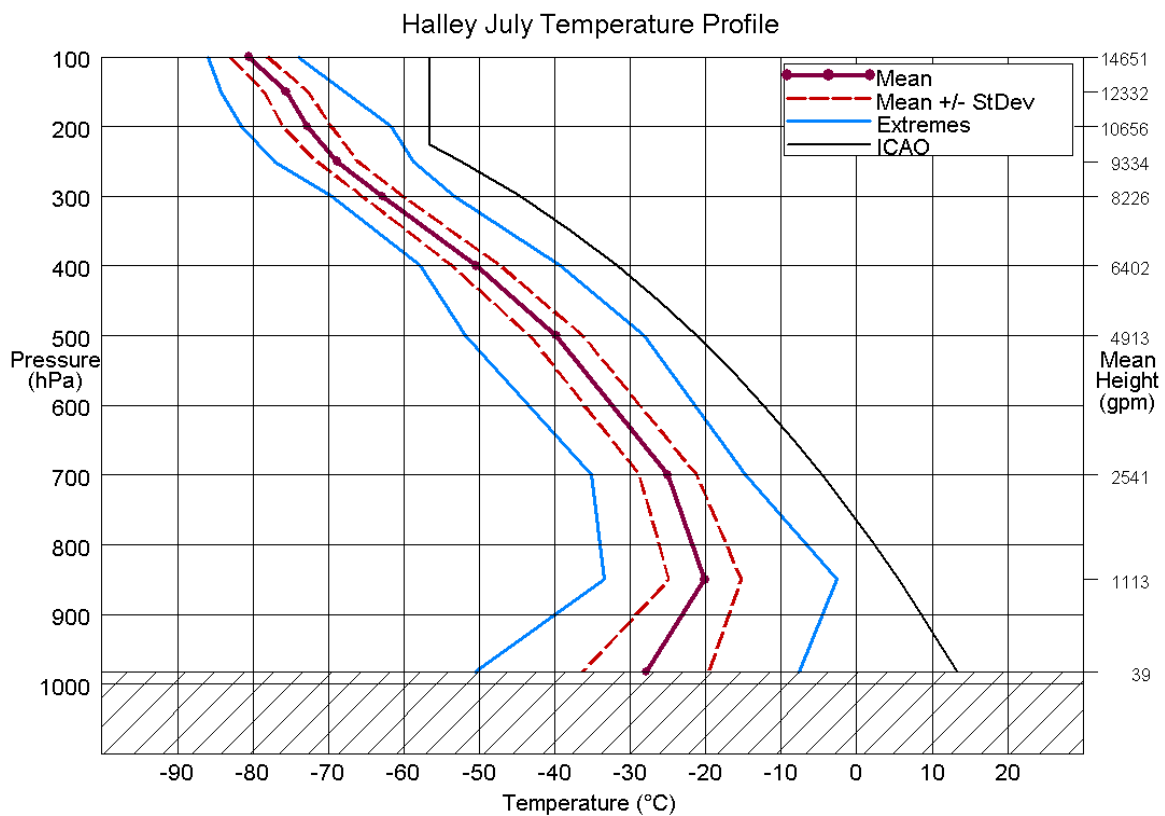**Figure A3–3 (a)**   Mean temperature profile for Halley for January.

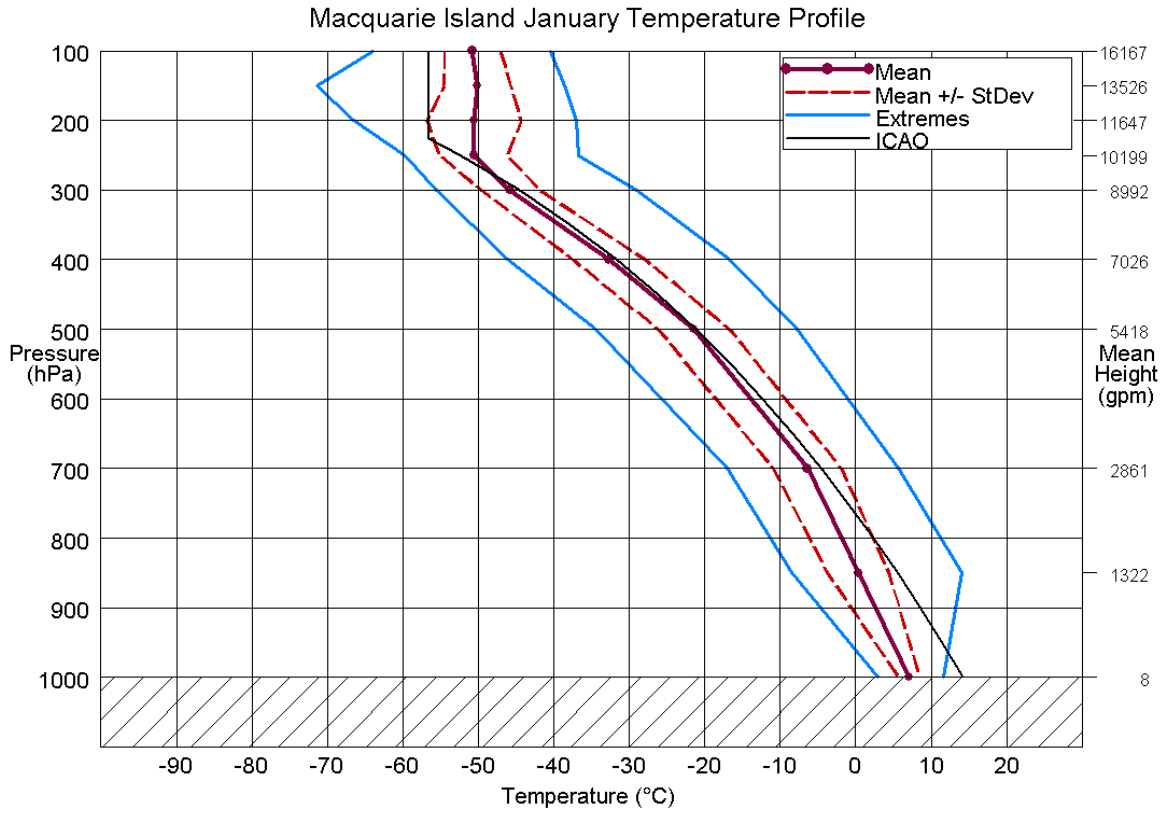**Figure A3–3 (b)**   Mean temperature profile for Halley for July.
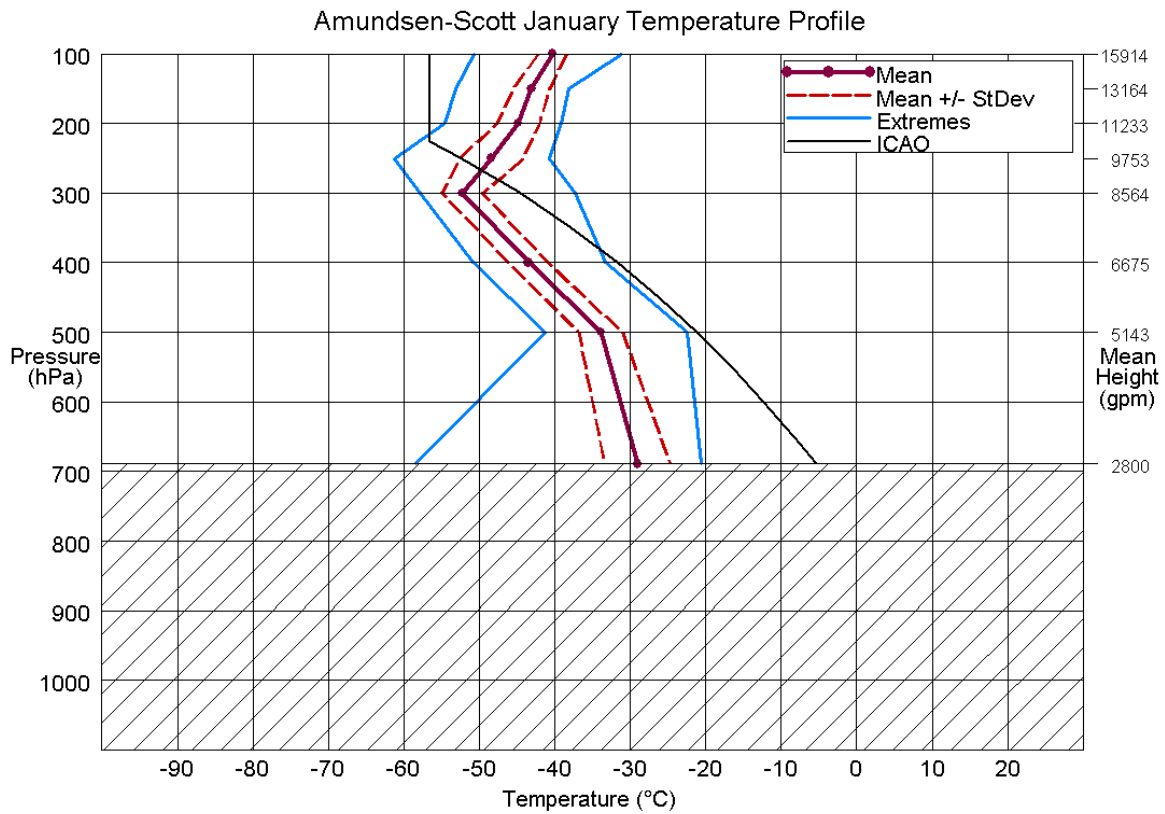
Figure A3–4 (a)   Mean temperature profile for Amundsen–Scott for January.
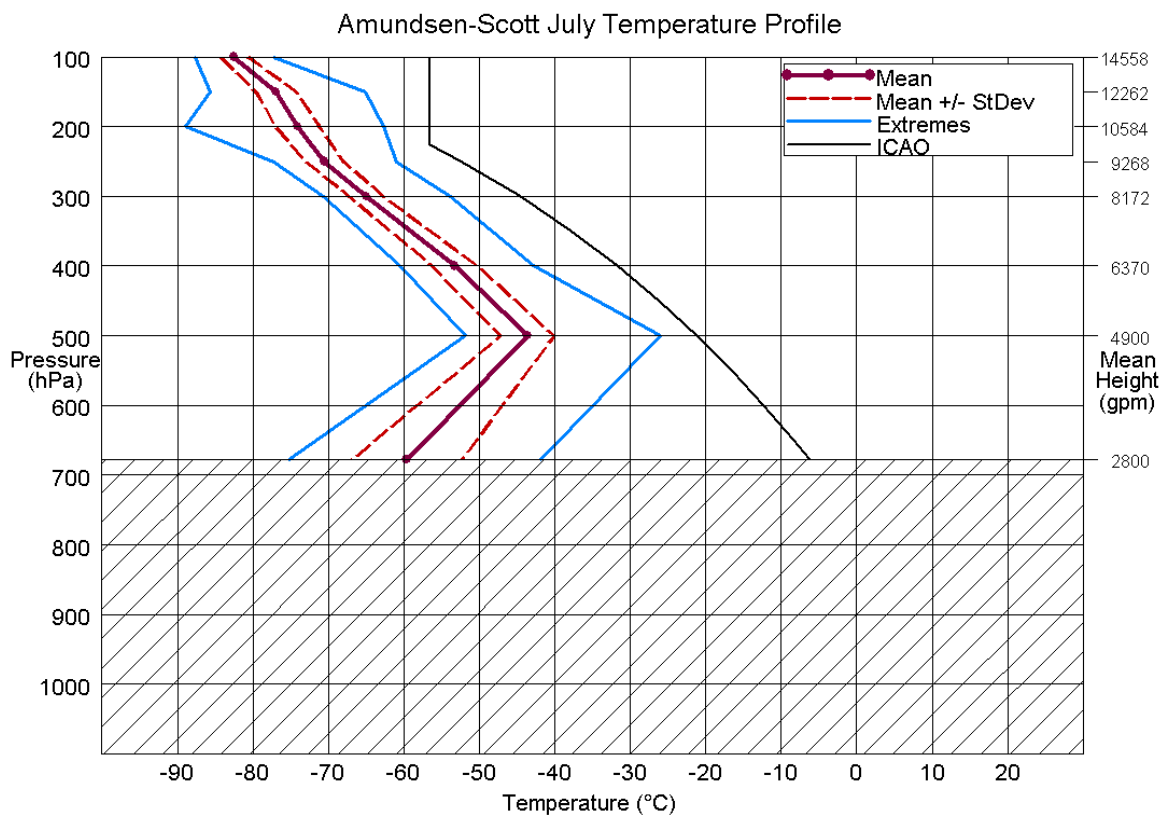
Figure A3–4 (b)   Mean temperature profile for Amundsen–Scott for July.
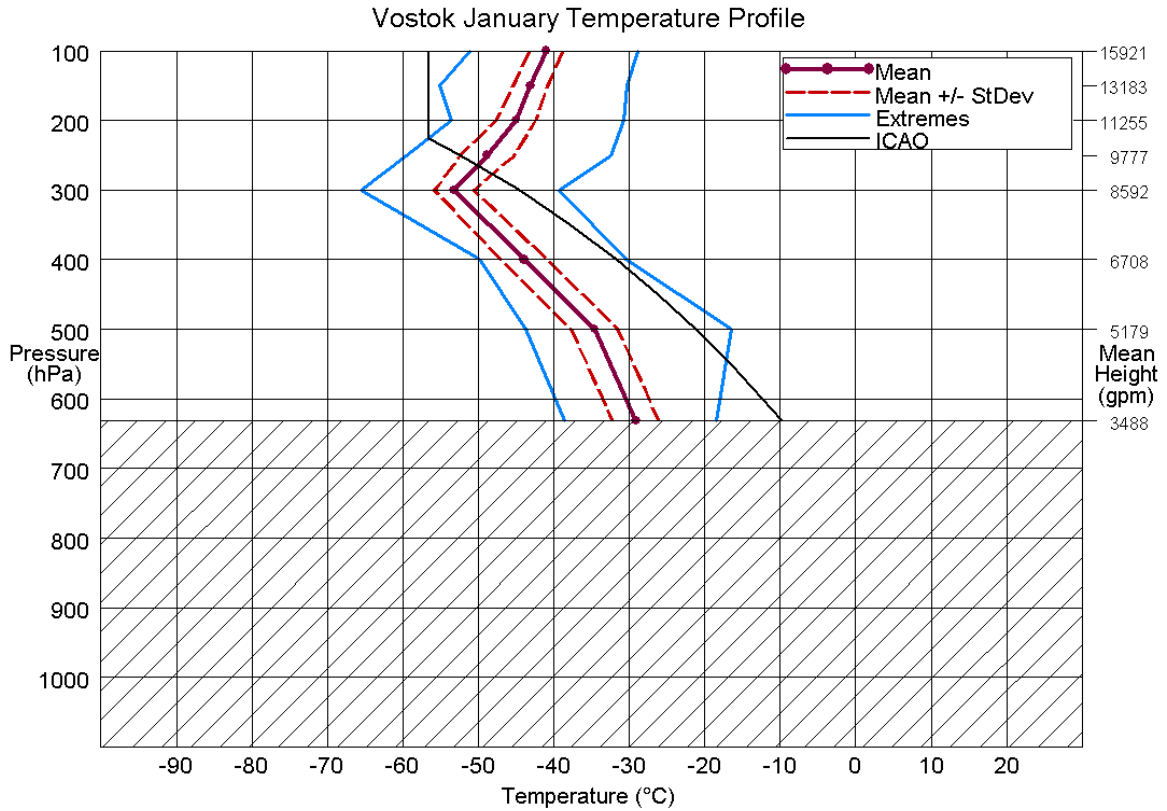
Figure A3–5 (a)   Mean temperature profile for Vostok for January.
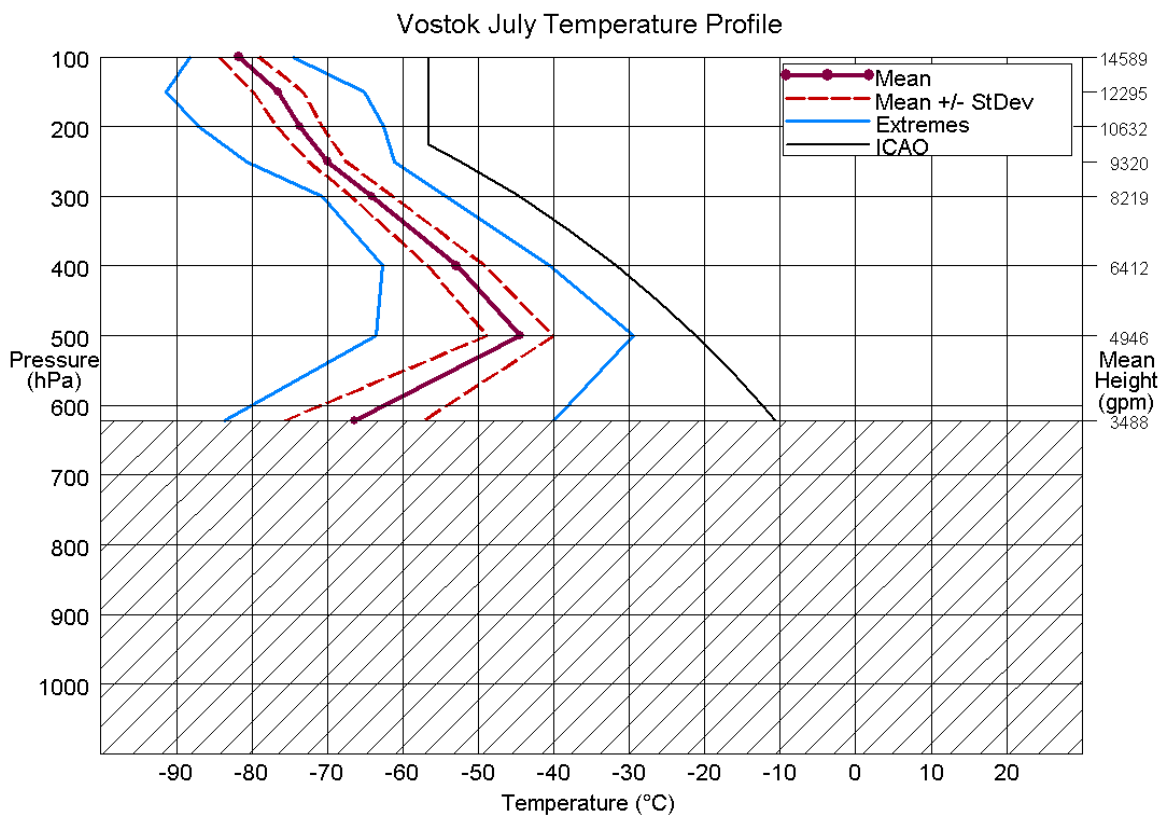
Figure A3–5 (b)   Mean temperature profile for Vostok for July.

648
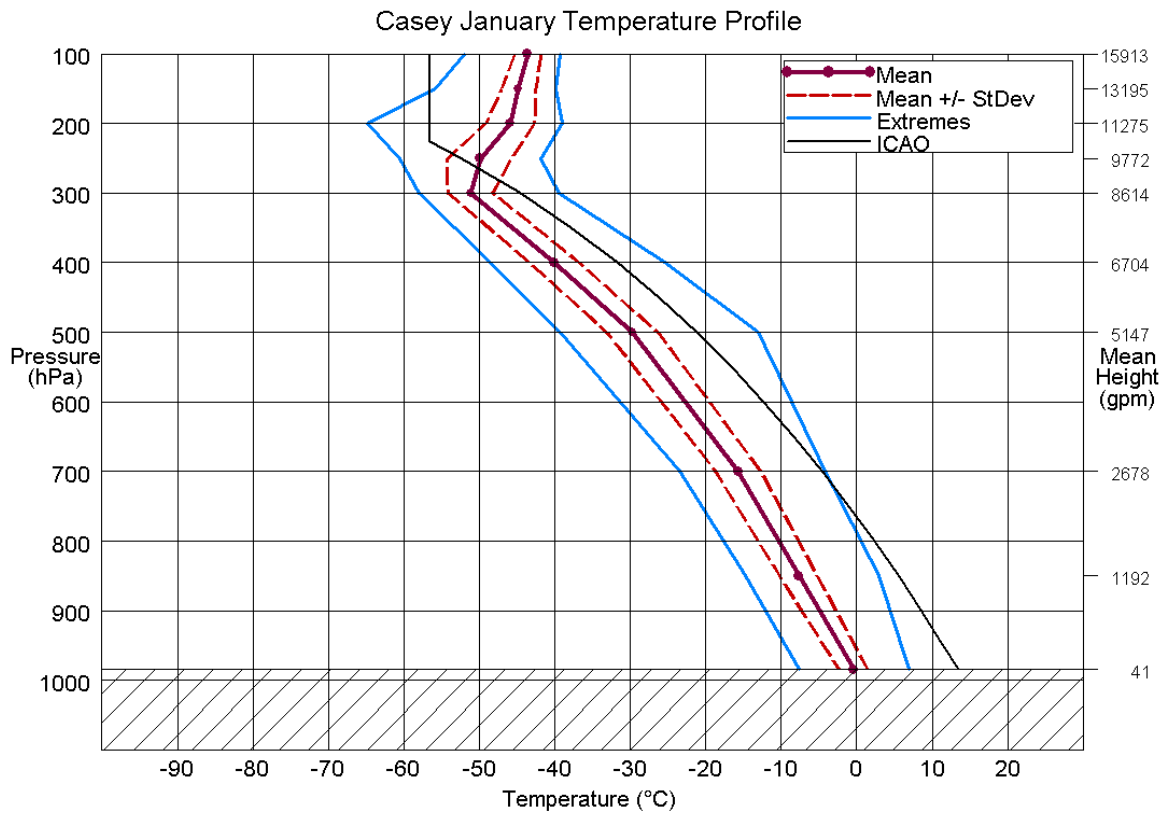
Figure A3–6 (a)   Mean temperature profile for Casey for January.
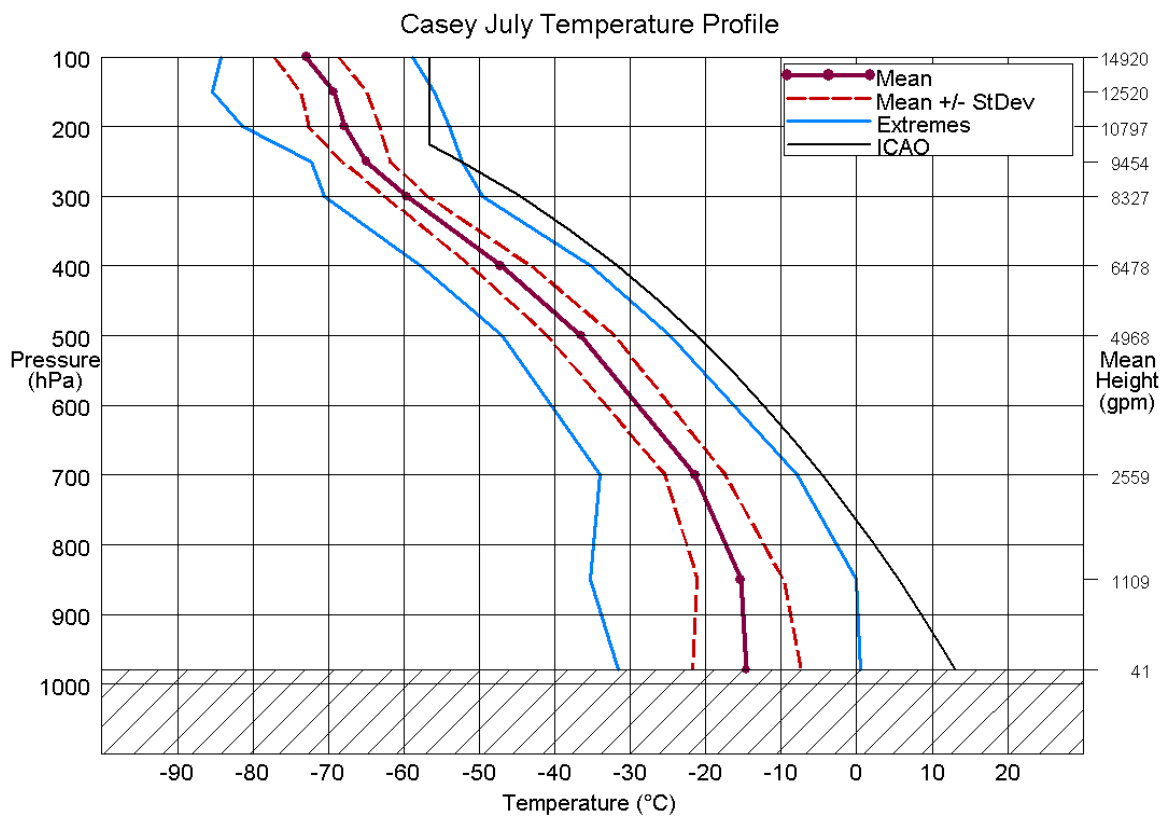
Figure A3–6 (b)   Mean temperature profile for Casey for July.

Macquarie Island January Temperature Profile

Figure A3–7 (a)   Mean temperature profile for Macquarie Island for January.

Macquarie Island July Temperature Profile
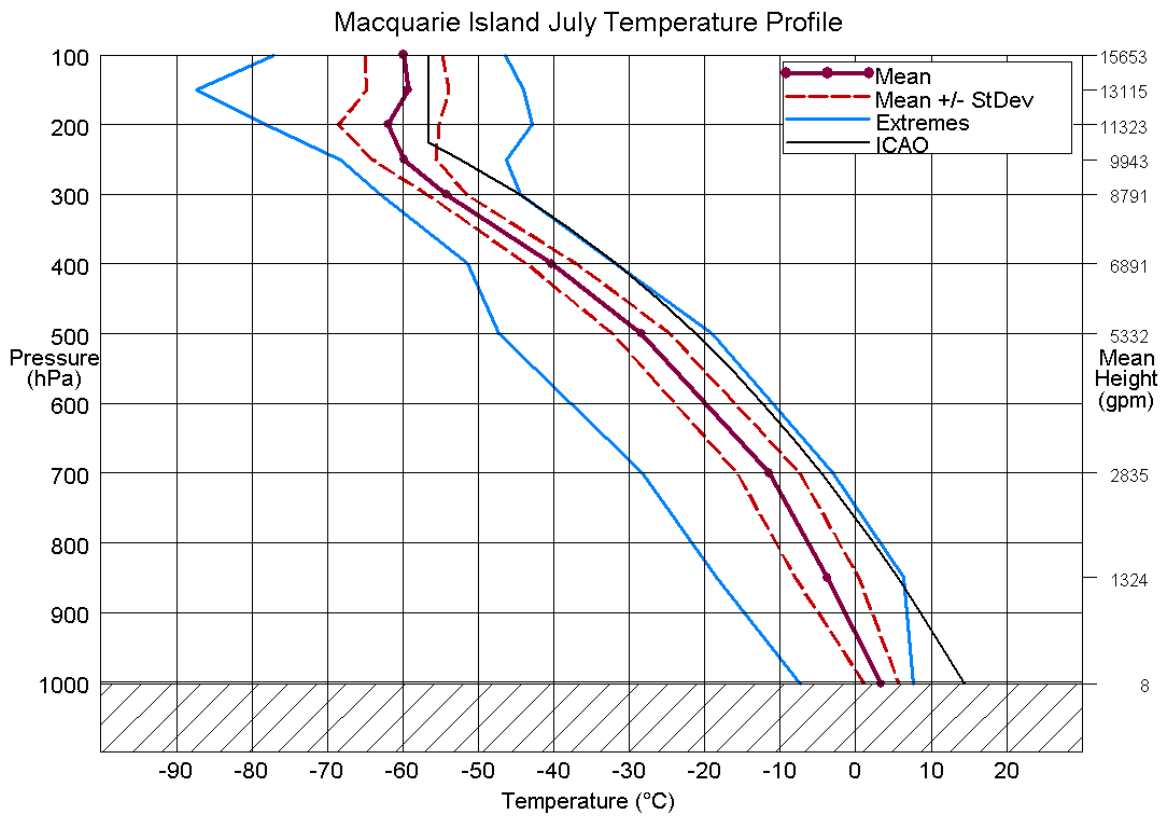
Figure A3–7 (b)   Mean temperature profile for Macquarie Island for July.

January Temperature Profile
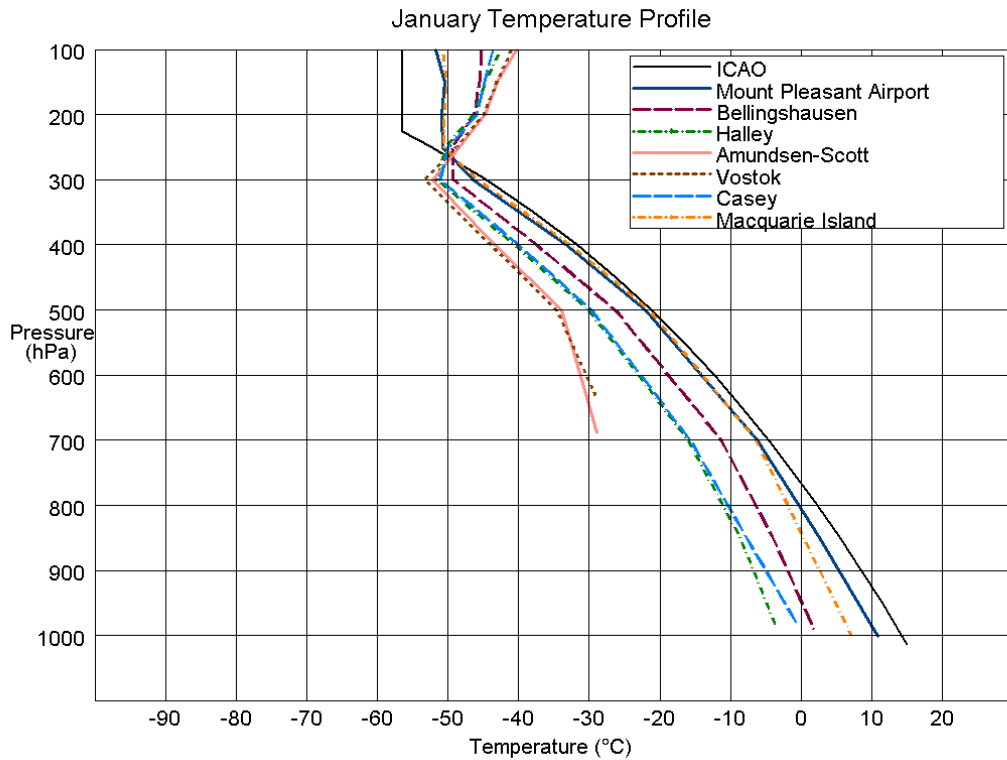
Figure A3–8 (a) Mean temperature profiles for seven stations for January

July Temperature Profile
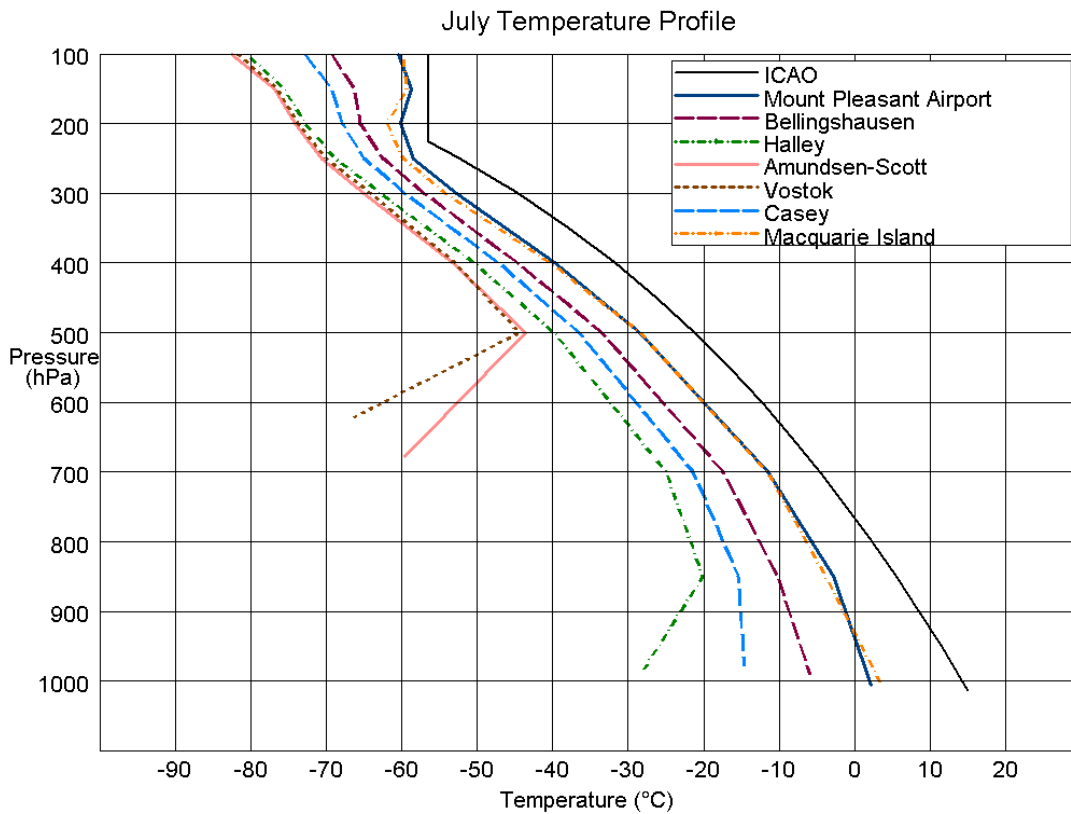
Figure A3–8 (b)   Mean temperature profiles for seven stations for July.

Pressure level (hPa)	Mean monthly height (m)	Standard deviation of daily heights (m)	Highest observed daily height (m)	Lowest observed daily height (m)	Mean monthly temp. (ºC)	Standard deviation of daily temp. (ºC)	Highest observed daily temp. (ºC)	Lowest observed daily temp. (ºC)
100	16170	96	16590	15870	−51.7	3.5	−42.7	−62.7
150	13535	124	13990	13200	−50.5	4.1	−41.5	−64.9
200	11659	152	12120	11310	−50.9	5.8	−38.9	−67.3
250	10206	174	10680	9820	−50.7	4.2	−38.1	−60.9
300	9009	172	9460	8620	−46.5	3.7	−34.1	−55.3
400	7047	141	7440	6700	−33.3	4.8	−22.5	−47.3
500	5443	115	5790	5150	−22.0	4.7	−9.7	−34.1
700	2886	81	3176	2636	−6.2	4.3	7.2	−16.1
850	1342	69	1600	1095	2.6	4.6	21.0	−6.7

Table A3–1(a) Upper–air data for Mount Pleasant Airport (WMO: 88889) for January. Based on data for the period 1980–99.

Pressure level (hPa)	Mean monthly height (m)	Standard deviation of daily heights (m)	Highest observed daily height (m)	Lowest observed daily height (m)	Mean monthly temp. (ºC)	Standard deviation of daily temp. (ºC)	Highest observed daily temp. (ºC)	Lowest observed daily temp. (ºC)
100	15720	197	16200	15170	−60.4	4.3	−46.1	−73.3
150	13182	191	13650	12700	−58.7	5.0	−44.1	−77.7
200	11382	206	11920	10880	−60.1	6.1	−43.3	−73.5
250	9986	218	10520	9460	−58.4	3.8	−44.1	−69.3
300	8826	212	9330	8310	−52.8	3.7	−40.3	−62.7
400	6918	181	7350	6460	−39.8	5.6	−25.3	−53.5
500	5356	149	5720	4970	−28.5	5.8	−15.3	−42.9
700	2860	110	3097	2546	−11.5	5.2	3.8	−24.3
850	1345	98	1552	1045	−2.8	4.9	12.0	−13.9

Table A3–1(b) Upper–air data for Mount Pleasant Airport (WMO: 88889) for July. Based on data for the period 1980–99.

Pressure level (hPa)	Mean monthly height (m)	Standard deviation of daily heights (m)	Highest observed daily height (m)	Lowest observed daily height (m)	Mean monthly temp. (ºC)	Standard deviation of daily temp. (ºC)	Highest observed daily temp. (ºC)	Lowest observed daily temp. (ºC)
100	16045	91	16440	15760	–45.2	2.3	–39.3	–53.1
150	13343	100	13790	13110	–45.6	2.7	–39.7	–55.9
200	11428	114	11960	11180	–46.3	3.7	–38.7	–60.9
250	9956	127	10520	9680	–49.4	4.4	–37.7	–61.1
300	8764	132	9280	8470	–49.2	3.2	–36.9	–58.9
400	6834	115	7360	6550	–37.5	3.9	–24.3	–50.9
500	5254	94	5570	5020	–26.3	3.8	–13.9	–37.3
700	2742	73	2960	2550	–11.3	3.4	0.2	–20.1
850	1229	69	1410	1041	–4.0	3.1	8.4	–12.1

Table A3–2(a) Upper–air data for Bellingshausen (WMO: 89050) for January. Based on data for the period 1980–99.

Pressure level (hPa)	Mean monthly height (m)	Standard deviation of daily heights (m)	Highest observed daily height (m)	Lowest observed daily height (m)	Mean monthly temp. (ºC)	Standard deviation of daily temp. (ºC)	Highest observed daily temp. (ºC)	Lowest observed daily temp. (ºC)
100	15206	203	15650	14700	–69.3	4.3	–57.3	–80.5
150	12768	188	13280	12290	–66.3	4.5	–54.9	–81.9
200	11025	190	11580	10540	–65.5	4.9	–52.3	–77.9
250	9661	193	10200	9160	–62.5	3.8	–51.3	–71.1
300	8522	187	9030	8010	–57.0	3.7	–44.7	–65.7
400	6653	166	7060	6170	–44.7	4.5	–31.3	–54.7
500	5122	145	5460	4690	–33.5	4.9	–19.7	–46.9
700	2677	115	2964	2353	–17.4	5.3	–4.1	–36.1
850	1198	106	1468	928	–10.2	5.7	1.4	–28.3

Table A3–2(b) Upper–air data for Bellingshausen (WMO: 89050) for July. Based on data for the period 1980–99.

Pressure level (hPa)	Mean monthly height (m)	Standard deviation of daily heights (m)	Highest observed daily height (m)	Lowest observed daily height (m)	Mean monthly temp. (°C)	Standard deviation of daily temp. (°C)	Highest observed daily temp. (°C)	Lowest observed daily temp. (°C)
100	15922	82	16150	15550	–42.5	1.7	–37.5	–48.5
150	13197	81	13580	12940	–44.7	2.0	–39.5	–52.3
200	11278	81	11510	11060	–46.4	2.8	–40.9	–57.5
250	9806	91	10100	9560	–50.3	4.5	–39.5	–61.5
300	8624	100	8910	8330	–51.6	2.8	–42.7	–58.5
400	6715	87	6940	6430	–40.6	3.2	–29.5	–51.7
500	5162	73	5330	4910	–30.1	3.4	–19.1	–39.5
700	2697	58	2854	2501	–16.0	3.3	–4.9	–23.7
850	1213	55	1381	1044	–8.6	2.5	2.0	–14.7

Table A3–3(a) Upper–air data for Halley (WMO: 89022) for January. Based on data for the period 1980–99.

Pressure level (hPa)	Mean monthly height (m)	Standard deviation of daily heights (m)	Highest observed daily height (m)	Lowest observed daily height (m)	Mean monthly temp. (°C)	Standard deviation of daily temp. (°C)	Highest observed daily temp. (°C)	Lowest observed daily temp. (°C)
100	14651	125	15000	14250	–80.5	2.4	–73.9	–85.9
150	12332	119	12690	11940	–75.6	2.9	–67.9	–84.3
200	10656	123	11040	10260	–72.8	3.2	–61.7	–81.5
250	9334	131	9730	8860	–68.8	2.7	–58.7	–77.1
300	8226	132	8610	7630	–62.8	2.7	–53.3	–69.5
400	6402	123	6740	5830	–50.4	3.2	–39.3	–57.9
500	4913	114	5500	4450	–39.8	3.5	–28.1	–51.9
700	2541	90	2842	2271	–25.0	3.8	–14.7	–35.1
850	1113	85	1486	828	–20.1	4.8	–2.7	–33.5

Table A3–3(b) Upper–air data for Halley (WMO: 89022) for July. Based on data for the period 1980–99.

Pressure level (hPa)	Mean monthly height (m)	Standard deviation of daily heights (m)	Highest observed daily height (m)	Lowest observed daily height (m)	Mean monthly temp. (ºC)	Standard deviation of daily temp. (ºC)	Highest observed daily temp. (ºC)	Lowest observed daily temp. (ºC)
100	15914	81	16220	15610	–40.3	1.9	–31.1	–50.7
150	13164	77	13430	12820	–43.1	2.4	–38.1	–53.1
200	11233	78	11540	10970	–44.8	2.8	–39.1	–54.5
250	9753	85	10150	9570	–48.4	4.2	–40.7	–61.3
300	8564	94	8970	8350	–52.2	2.7	–37.3	–57.9
400	6675	83	7010	6470	–43.5	2.6	–33.3	–50.9
500	5143	71	5400	4950	–33.9	2.9	–22.5	–41.3
700	–	–	–	–	–	–	–	–
850	–	–	–	–	–	–	–	–

Table A3–4(a) Upper–air data for Amundsen–Scott (South Pole) (WMO: 89009) for January. Based on data for the period 1980–99.

Pressure level (hPa)	Mean monthly height (m)	Standard deviation of daily heights (m)	Highest observed daily height (m)	Lowest observed daily height (m)	Mean monthly temp. (ºC)	Standard deviation of daily temp. (ºC)	Highest observed daily temp. (ºC)	Lowest observed daily temp. (ºC)
100	14558	137	14910	14260	–82.5	1.8	–77.3	–87.7
150	12262	141	12890	11850	–76.9	2.7	–65.1	–85.7
200	10584	136	11110	10180	–74.1	2.9	–62.7	–88.9
250	9268	137	9810	8870	–70.5	2.5	–60.9	–77.3
300	8172	134	8690	7780	–65.0	2.3	–53.9	–70.7
400	6370	123	6830	6020	–53.3	3.0	–42.9	–60.5
500	4900	113	5300	4600	–43.6	3.5	–26.0	–51.9
700	–	–	–	–	–	–	–	–
850	–	–	–	–	–	–	–	–

Table A3–4(b) Upper–air data for Amundsen–Scott (South Pole) (WMO: 89009) for July. Based on data for the period 1980–99.

Pressure level (hPa)	Mean monthly height (m)	Standard deviation of daily heights (m)	Highest observed daily height (m)	Lowest observed daily height (m)	Mean monthly temp. (ºC)	Standard deviation of daily temp. (ºC)	Highest observed daily temp. (ºC)	Lowest observed daily temp. (ºC)
100	15921	105	16640	15680	–41.0	2.2	–28.9	–51.1
150	13183	112	13740	12970	–43.1	2.3	–30.3	–55.1
200	11255	110	11710	11050	–45.0	2.6	–30.7	–53.5
250	9777	117	10390	9560	–48.8	3.6	–32.5	–59.5
300	8592	119	9100	8350	–53.2	2.6	–39.3	–65.5
400	6708	102	7120	6500	–43.9	3.1	–30.5	–49.9
500	5179	87	5480	4990	–34.6	3.1	–16.5	–43.7
700	–	–	–	–	–	–	–	–
850	–	–	–	–	–	–	–	–

Table A3–5(a) Upper–air data for Vostok (WMO: 89606) for January. Based on data for the period 1980–99.

Pressure level (hPa)	Mean monthly height (m)	Standard deviation of daily heights (m)	Highest observed daily height (m)	Lowest observed daily height (m)	Mean monthly temp. (ºC)	Standard deviation of daily temp. (ºC)	Highest observed daily temp. (ºC)	Lowest observed daily temp. (ºC)
100	14589	186	15250	14090	–81.7	2.6	–74.5	–88.3
150	12295	177	12880	11890	–76.5	3.3	–65.1	–91.3
200	10632	184	11270	10241	–73.7	3.0	–62.5	–87.1
250	9320	185	9940	8930	–70.0	2.5	–61.1	–80.7
300	8219	178	8800	7840	–64.1	2.8	–54.3	–70.7
400	6412	159	6920	6050	–52.9	3.8	–40.5	–62.7
500	4946	139	5370	4600	–44.4	4.4	–29.5	–63.5
700	–	–	–	–	–	–	–	–
850	–	–	–	–	–	–	–	–

Table A3–5(b) Upper–air data for Vostok (WMO: 89606) for July. Based on data for the period 1980–99.

Pressure level (hPa)	Mean monthly height (m)	Standard deviation of daily heights (m)	Highest observed daily height (m)	Lowest observed daily height (m)	Mean monthly temp. (ºC)	Standard deviation of daily temp. (ºC)	Highest observed daily temp. (ºC)	Lowest observed daily temp. (ºC)
100	15913	98	16200	15620	–43.6	1.8	–39.3	–52.0
150	13195	99	13540	12930	–44.8	2.3	–39.8	–55.8
200	11275	101	11720	11036	–45.9	3.2	–39.0	–64.8
250	9772	104	10136	9560	–49.9	4.3	–41.8	–60.5
300	8614	114	9070	8349	–51.1	3.0	–39.5	–58.0
400	6704	100	7060	6449	–40.1	3.3	–25.5	–48.5
500	5147	85	5440	4917	–29.7	3.4	–13.0	–39.3
700	2678	66	2908	2402	–15.7	3.0	–4.2	–23.5
850	1192	62	1396	903	–7.7	2.5	3.0	–14.8

Table A3–6(a) Upper–air data for Casey (WMO: 89611) for January. Based on data for the period 1980–99.

Pressure level (hPa)	Mean monthly height (m)	Standard deviation of daily heights (m)	Highest observed daily height (m)	Lowest observed daily height (m)	Mean monthly temp. (ºC)	Standard deviation of daily temp. (ºC)	Highest observed daily temp. (ºC)	Lowest observed daily temp. (ºC)
100	14920	191	15610	14410	–72.9	4.2	–58.9	–84.2
150	12520	176	13158	12060	–69.3	4.4	–56.0	–85.3
200	10797	181	11437	10360	–67.9	4.7	–54.0	–81.4
250	9454	195	10100	9092	–65.0	3.2	–52.3	–72.3
300	8327	185	8952	7910	–59.6	2.9	–49.5	–70.6
400	6478	167	7039	6100	–47.2	4.0	–35.3	–57.8
500	4968	147	5465	4630	–36.5	4.4	–24.8	–47.0
700	2559	119	2945	2220	–21.4	4.0	–7.9	–34.0
850	1109	106	1454	810	–15.4	5.7	–0.1	–35.3

Table A3–6(b) Upper–air data for Casey (WMO: 89611) for July. Based on data for the period 1980–99.

Pressure level (hPa)	Mean monthly height (m)	Standard deviation of daily heights (m)	Highest observed daily height (m)	Lowest observed daily height (m)	Mean monthly temp. (°C)	Standard deviation of daily temp. (°C)	Highest observed daily temp. (°C)	Lowest observed daily temp. (°C)
100	16167	107	16470	15884	−50.8	3.6	−40.4	−64.0
150	13526	139	13910	13183	−50.1	4.4	−38.6	−71.4
200	11647	170	12110	11260	−50.6	6.3	−37.0	−66.6
250	10199	192	10630	9785	−50.6	4.5	−36.7	−59.7
300	8992	196	9470	8510	−45.8	3.8	−29.0	−55.5
400	7026	169	7720	6610	−32.7	4.8	−16.8	−46.2
500	5418	142	5783	5060	−21.5	4.7	−7.8	−34.4
700	2861	109	3160	2536	−6.4	4.5	5.7	−17.0
850	1322	96	1576	989	0.4	4.0	14.0	−8.5

Table A3–7(a) Upper–air data for Macquarie Island (WMO: 94998) for January. Based on data for the period 1980–99.

Pressure level (hPa)	Mean monthly height (m)	Standard deviation of daily heights (m)	Highest observed daily height (m)	Lowest observed daily height (m)	Mean monthly temp. (°C)	Standard deviation of daily temp. (°C)	Highest observed daily temp. (°C)	Lowest observed daily temp. (°C)
100	15653	156	16051	14890	−59.9	5.1	−46.4	−77.1
150	13115	143	13480	12480	−59.3	5.4	−44.0	−87.4
200	11323	157	11708	10713	−61.9	6.7	−42.9	−78.3
250	9943	189	10352	9300	−59.8	4.2	−46.3	−68.3
300	8791	178	9194	8137	−54.2	2.6	−44.4	−63.0
400	6891	164	7268	6276	−40.3	3.3	−31.8	−51.4
500	5332	146	5681	4809	−28.4	3.8	−19.0	−47.3
700	2835	118	3123	2410	−11.5	4.2	−3.0	−28.3
850	1324	105	1571	910	−3.8	4.2	6.3	−18.5

Table A3–7(b) Upper–air data for Macquarie Island (WMO: 94998) for July. Based on data for the period 1980–99.

658

Station	Station height (m)	Mean monthly pressure (hPa)	Standard deviation of daily pressure (hPa)	Highest observed daily pressure (hPa)	Lowest observed daily pressure (hPa)	Mean monthly temp. (ºC)	Standard deviation of daily temp. (ºC)	Highest observed daily temp. (ºC)	Lowest observed daily temp. (ºC)
Mount Pleasant Airport*	74	1001.0	8.67	1022.6	976.4	10.9	2.86	19.5	4.5
Bellingshausen*	16	990.3	8.55	1016.8	971.2	1.8	1.31	6.8	−3.8
Halley*	39	992.5	7.12	1016.0	966.9	−3.54	2.42	2.5	−11.3
Amundsen–Scott**	2800	689.1	6.05	707.9	660.8	−29.	4.35	−20.6	−58.4
Vostok**	3488	631.6	5.59	651.5	618.9	−29.1	3.06	−18.4	−38.6
Casey*	42	987.9	7.82	1012.4	951.2	−0.4	2.12	8.4	−8.4
Macquarie Island*	8	1001.1	11.21	1030.8	950.1	6.9	1.46	12.2	1.6

Table A3–8(a)   Surface data for January for the stations shown. Based on data for the period 1988–99. (* indicates that for these coastal stations sea level pressure values are given whereas for those elevated stations (marked **) station level pressure is given).
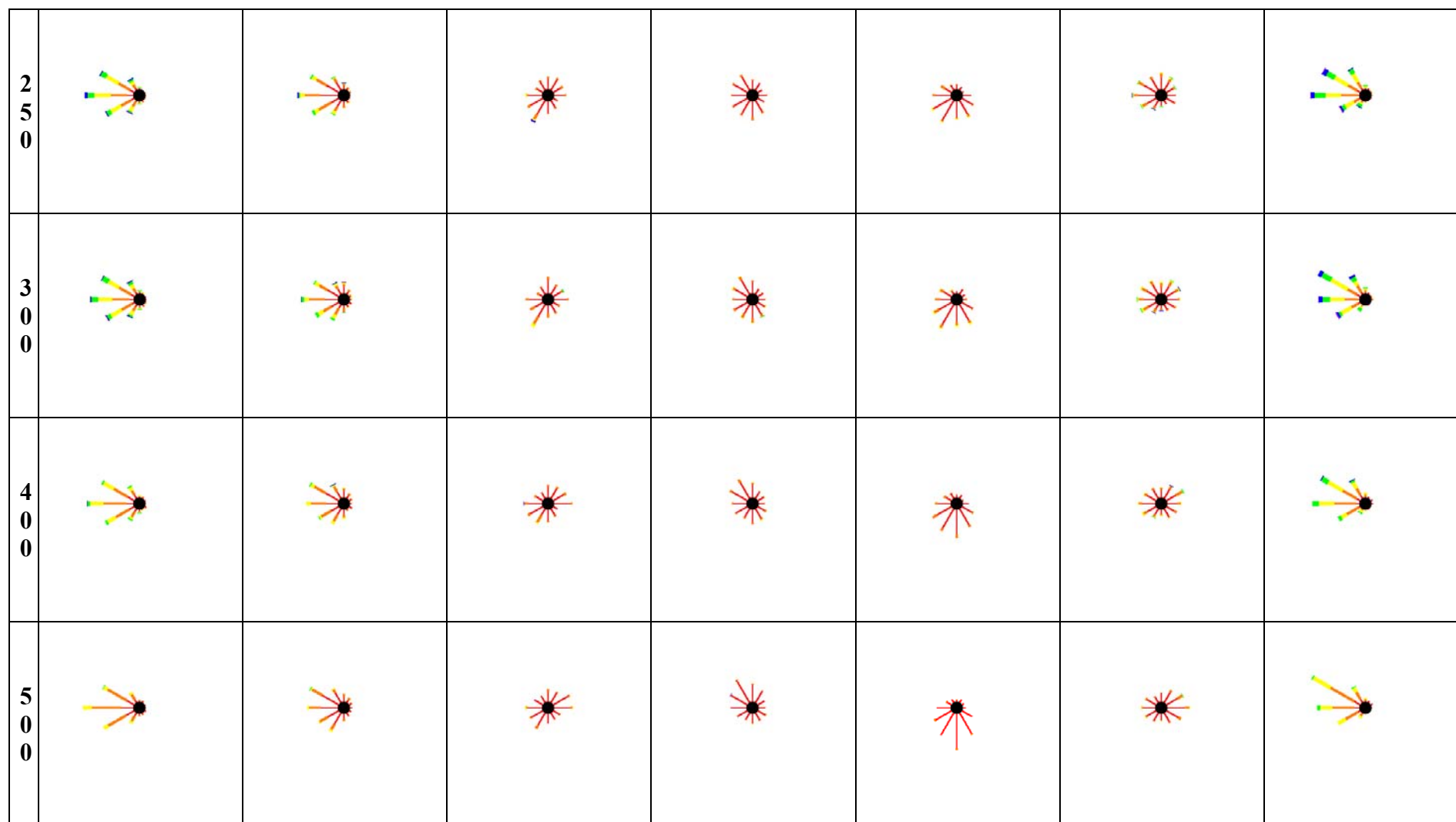
Station	Station height (m)	Mean monthly pressure (hPa)	Standard deviation of daily pressure (hPa)	Highest observed daily pressure (hPa)	Lowest observed daily pressure (hPa)	Mean monthly temp. (ºC)	Standard deviation of daily temp. (ºC)	Highest observed daily temp. (ºC)	Lowest observed daily temp. (ºC)
Mount Pleasant Airport*	74	1005.3	11.35	1028.6	973.7	2.2	2.92	9.4	−7.8
Bellingshausen*	16	991.2	12.91	1017.7	952.8	−5.9	5.52	1.0	−24.6
Halley*	39	987.7	11.13	1017.4	946.6	−27.9	8.32	−7.8	−50.6
Amundsen–Scott**	2800	677.8	9.83	704.8	655.3	−59.6	7.28	−41.8	−75.2
Vostok**	3488	621.6	10.25	651.2	596.1	−66.4	9.20	−40.0	−83.7
Casey*	42	983.9	13.91	1024.5	943.0	−14.8	6.95	0.0	−32.0
Macquarie Island*	8	1002.3	13.61	1031.9	958.8	3.3	2.27	7.4	−7.8

Table A3–8(b)   Surface data for July for the stations shown. Based on data for the period 1988–99. (* indicates that for these coastal stations sea level pressure values are given whereas for those elevated stations (marked **) station level pressure is given).

	Mount Pleasant 51.82°S	Bellingshausen 62.20°S	Halley 75.5°S	Amundsen-Scott 90.00°S	Vostok 78.45°S	Casey 66.28°S	Macquarie Island 54.48°S
50							
100							
150							
200							

10 % frequency scale   **Speed colour code**

Figure A3-9A   Long-term January wind roses for various levels for the
                     stations shown. (Calms are not represented but are
                     generally less 5 % and often around 1%).

662

	Mount Pleasant 51.82°S	Bellingshausen 62.20°S	Halley 75.5°S	Amundsen-Scott 90.00°S	Vostok 78.45°S	Casey 66.28°S	Macquarie Island 54.48°S
5 0							
1 0 0 0							
1 5 0							
2 0 0							

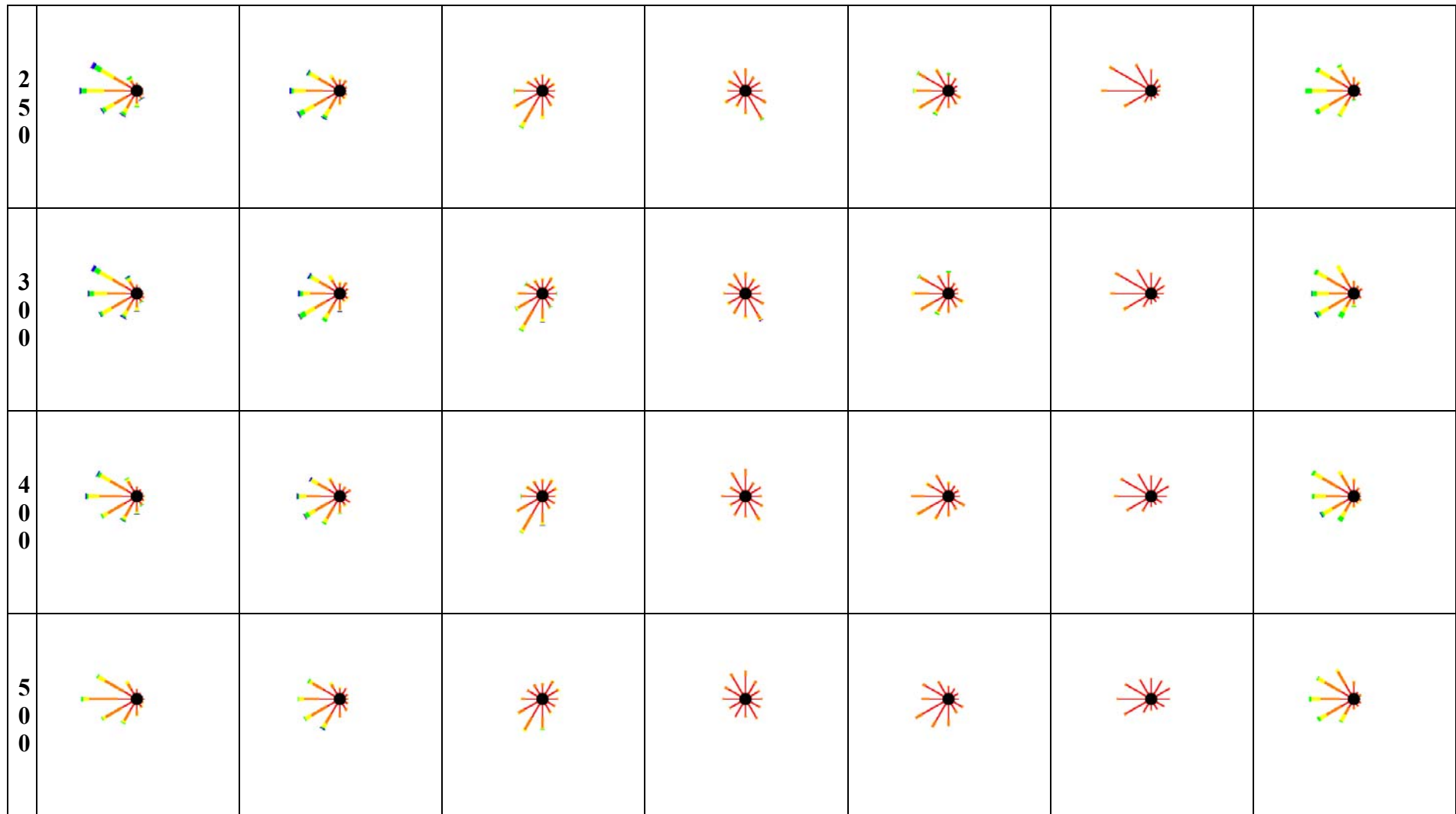|						
2 5 0							
3 0 0							
4 0 0							
5 0 0							

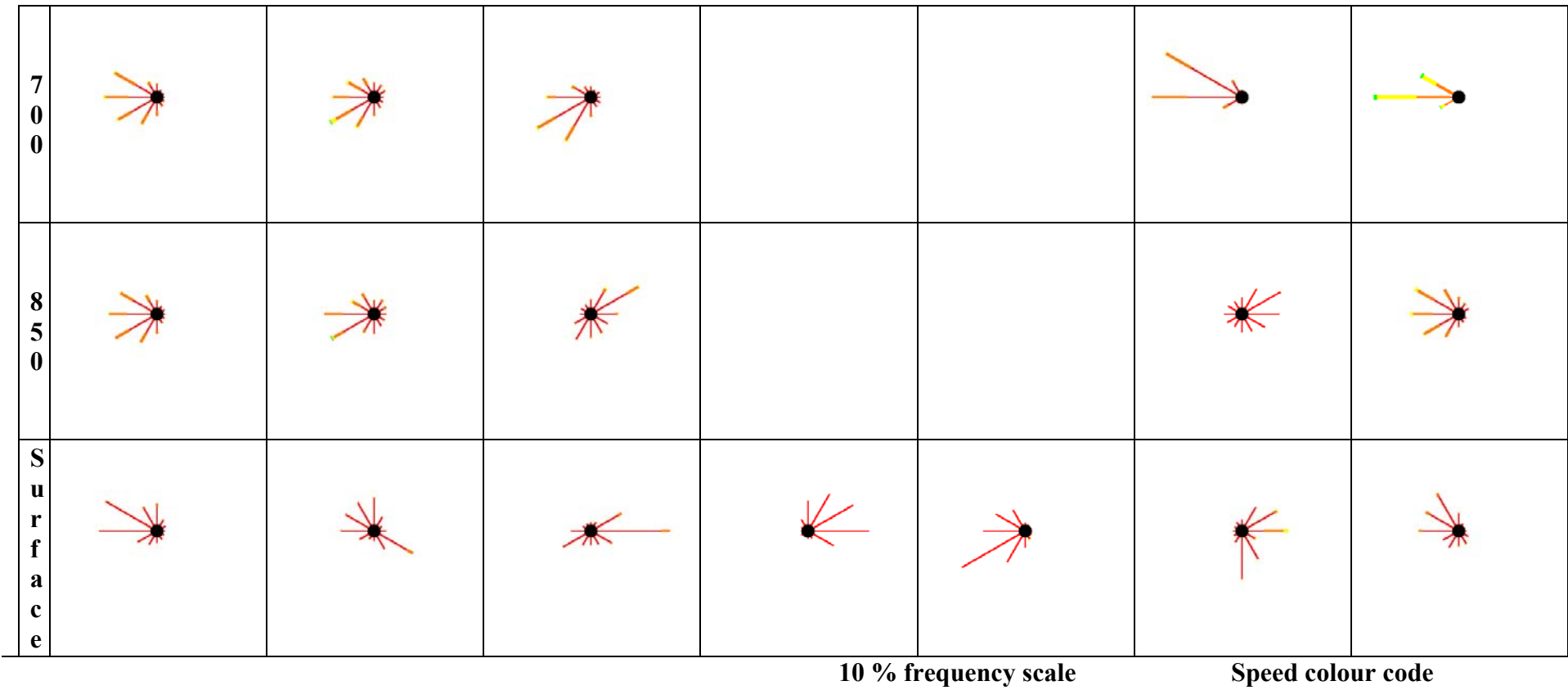**10 % frequency scale**   **Speed colour code**

Figure A3-9B   Long- term July wind roses for various levels for the
stations shown. (Calms are not represented but are
generally less 5 % and often around 1%).

APPENDIX 4:   A SUGGESTED TRAINING PROGRAMME FOR ANTARCTIC WEATHER FORECASTERS

Each weather service/agency will approach the training of Antarctic weather forecasters in its own way taking into account the policies, priorities and resources which pertain to the individual weather service/agency. There are no doubt several or more excellent Antarctic forecaster training programmes in existence. The pre–departure training programme outlined below is, therefore, presented as a suggestion only for those forecasting services which might appreciate some lead in this area, or which are seeking alternative training ideas. *Following a personal communication from J. Wilson (Australian Bureau of Meteorology Training Centre it is intended that this appendix be rewritten for version 2 of the handbook to focus more on the core competencies required of weather forecasting for Antarctic conditions, and less on specific detail.*

In the meantime the training programme example outlined below assumes that the forecaster will have to provide forecasting for ship operations en route to and from the Antarctic and will have to provide forecasts for aviation operations whilst in the Antarctic. The infrastructure assumed to be available to the forecaster on–station includes: AVHRR; APT; access to FTP/internet; access to numerical model data and to conventional surface and upper–air observations. Moreover, access to a data visualisation–display system is assumed: for the purposes of this suggested training programme the display systems assumed are the "Man computer Interactive Data System" (McIDAS) see, for example, http://ftp.ssec.wisc.edu/software/McIDAS.html and the Grid Analysis and Display System (GrADS) – see, for example, http://grads.iges.org/grads/head.html). The training programme would obviously need to be modified to accommodate systems which are different to those listed and modified if different forecast functions are required.

Training Programme Map

The suggested training programme covers four streams (or proxy core competencies): data availability; numerical tools; satellite image acquisition and interpretation; and Antarctic forecasting. It is assumed that through the prerequisite Diploma of Meteorology, or equivalent, the participants will have a good grounding in general forecast methodology.

Each stream is divided into learning modules and each module is divided into content parts. Learning outcomes for each module and content part are described so that participants have a clear guide as to what is expected to be learnt. The Assessment criteria; conditions under which the learning physically takes place; assessment method; resources; and references, are all indicative only and will vary depending on the actual training requirements.

Stream–module layout

Stream A   Data availability

- Module 1   Antarctic communications networks.
- Module 2   Codes.

Stream B   Numerical Tools

- Module 1   UNIX procedures.
- Module 2   Display of numerical products (McIDAS and GRADS).
- Module 3   Use and assessment of numerical products.

Stream C   Satellite image acquisition and interpretation

- Module 1   Orbital elements.
- Module 2   AVHRR image acquisition and analysis.
- Module 3   APT image acquisition and analysis.
- Module 4   Identification of cloud and ice features
- Module 5   Assessment of cyclogenesis potential.

Stream D   Antarctic Forecasting

- Module 1   Climatology (micro and synoptic scale).
- Module 2   Significant weather event characteristics.
- Module 3   Helicopter operation requirements.
- Module 4   Airline operation requirements.
- Module 5   Conditions at sea.
- Module 6   Chart preparation and analysis.
- Module 7   User profiles.
- Module 8   High profile scientific issues.

Training Outcomes

The highest level of prerequisite education assumed is that of Bachelor of Science (BSc.) with a post graduate Diploma in Meteorology (Dip. Met.) or equivalent. No doubt such qualifications will vary from nation to nation. Where additional skills are required these are mentioned as "additional prerequisites". There has been no detailed attempt in the suggested training programme to prescribe *how* the topics might be

taught, rather the emphasis has been *what* might be taught. The overall learning outcome for the programme is the acquisition and standardisation of skills facilitating the provision of high quality forecasts immediately following departure from the participants' home ports

Stream A Data availability

Purpose

To equip participants with the skills necessary to extract data from the Antarctic communications networks and decode it as necessary.

List of Modules

- 1: Antarctic communications networks
- 2: Codes.

Details of Module 1

Description: Antarctic communications networks.

Duration: 1 hour

Module purpose: to provide participants with knowledge of the network necessary to extract data for routine purposes and the appropriate actions to carry out in the event of communications system failures.

Summary of Content:
- 1: Structure of the communications system.
- 2: Limitations on data availability.
- 3: Data extraction procedures.

This module should be amenable to tutorial style teaching via example with a personal computer (PC).

Learning Outcome from Contents 1, 2, and 3 (comms. system structure, limitations; extraction) of Module 1 (Antarctic comms. network): participants will be able to

verify that communications are operational using simple tests and to send messages in all formats required.

Teaching overview:
- Assessment criteria:
  - 1.1 demonstrate steps required to test systems.
  - 1.2 send samples of each type of message to be sent during the season in test mode.
- *Conditions*: learning will take place in a tutorial type situation.
- *Assessment method*: performance in task.
- *Resources*: PC running Eudora or similar E–mail front end; fax transmitter.

Details of Module 2

Description: Codes.

Duration: Up to 1 hour.

Module Purpose: To equip participants with knowledge and skills necessary to decode such coded messages as are likely to be received and require manual decoding, e.g. TTAA, TTBB, AAXX.

Summary of Content:
- 1: Decoding upper–air temperature/wind messages.
- 2: Decoding surface synoptic messages.
- 3: Decoding ship/drifting buoy observations.

This module requires face to face learning and practice with sample messages.

Learning Outcome from Contents 1, 2, and 3 (decoding upper, surface, ship/buoy observations) of Module 2 (Codes): Participants will be able to extract upper winds and temperatures from TTAA and TTBB messages, avoiding common errors and verifying that messages contain the correct dates and times and identifying the correct station identifiers. Participants will be able to decode the other observation types.

Teaching overview:
- Assessment criteria:
  - 1.1:decoded observations are correct.
- *Conditions*: learning will take place in a tutorial type situation.
- *Assessment method*: performance in task.
- *Resources*: code templates, decoding documents, sample messages.

Stream B   Numerical Tools

Purpose

To equip participants with the skills and understanding necessary to maximise the utility of system software and take remedial action when minor failures occur. Participants should also be able to choose the appropriate data types for given forecast contexts.

List of Modules:

- Module 1: UNIX procedures.
- Module 2: Display of numerical products (McIDAS, GrADS).
- Module 3: Use and assessment of numerical products.

Details of Module 1

Description: UNIX Procedures.

Duration: 1 hour

Module Purpose: to equip participants with the skills and knowledge necessary to perform basic UNIX tasks necessary for the operation of the forecast office.

Summary of Content:
- 1: Overview of the most commonly used UNIX commands, including: pwd, cd, ls, whereis, ps, kill, df, more, grep, man, apropos, xedit.

Learning Outcome from Content 1 (overview of Unix) of Module 1 (UNIX): at the end of instruction the participant will be able to demonstrate an understanding of basic UNIX commands.

Teaching overview:
- Assessment criteria:
  1: Participant can choose the correct command(s) to achieve specified outcomes in the UNIX environment and employs them efficiently.
  2: Participant can describe any risks inherent in a nominated procedure.
  3: Participant can carry out recovery procedures from common errors.

4: Participant can modify schedules or batches to achieve specified outcomes.

- *Conditions*: teaching will be conducted by a suitably qualified person at a suitable venue: out–sourced if necessary.
- *Assessment Methods*: Participant will demonstrate the required skills to his/her instructor in a classroom context.
- *Resources*: SGI UNIX system.

Details of Module 2

Description: Display of numerical products

Duration: 2 hours

Module Purpose: To equip participants with the skills and knowledge necessary to utilise fully the data display systems used in the forecast office for the visualisation of observational and numerical model data, including surface observations, upper–air data and satellite imagery.

Additional prerequisites: basic PC and UNIX skills (eg: Module 1 above).

Summary of Content:
- 1: Overview of the forecast office data structures and data flow.
- 2: Introduction to GrADS/McIDAS if needed.
- 3: Model output display system.
- 4: Surface synoptic data display system.
- 5: Upper–air data display system (real and numerical).

Learning Outcome from Content 1, 2, 3, and 4 (overview of Unix) of Module 2 (display of products): At the end of instruction the participant will be able to demonstrate the ability to use the GrADS and McIDAS systems to display all meteorological data available at the forecast office.

Teaching overview:
- Assessment criteria:
  1. Participant can choose the correct command(s) to achieve specified outcomes using GRADS and McIDAS and employs them efficiently.
  2. Participant can describe any risks inherent in a nominated procedure.
  3. Participant can carry out recovery procedures from common errors.
  4. Participant can modify McIDAS schedules or batches to achieve specified outcomes

- *Condition*s: teaching will be conducted by a suitably qualified person at a suitable venue: out–sourced if necessary.
- *Assessment Methods*: Participant will demonstrate the required skills to his/her instructor in a classroom context.
- *Resources*: SGI UNIX system with McIDAS/X, GrADS and a functioning AMC look–a–like system.

Details of Module 3

Description: Use and assessment of numerical products.

Duration: 4 hours

Module Purpose: to equip participants with the skills and knowledge necessary to assess the value of numerical products.

Summary of Content:
- 1: Introduction to products available.
- 2: General evaluation of the strengths and weaknesses of the various products.

Learning Outcome from Contents 1 and 2 (products and their evaluation) of Module 3 (assessment of numerical products): At the end of instruction the participant will have a knowledge of the available numerical products, the contexts under which they are useful and an appreciation of the relative strengths of the models.

Teaching overview:
- *Assessment criteria*: Participant can describe the limitations and the relative strengths and weaknesses of numerical products where such information is available and relevant.
- *Conditions*: learning will be undertaken in a tutorial type situation.
- *Assessment Methods*: Participant will either describe numerical model strengths and weaknesses to his/her instructor in a classroom context or complete a multi–choice examination of approximately 10 questions on the subject.
- *Resources*: case study materials, overhead projector, and UNIX terminal to display satellite imagery, McIDAS and GrADS output.

Stream C Satellite image acquisition and interpretation

<u>Purpose</u>

Equip participants with the skills and understanding necessary to maximise the utility of satellite data in high latitude oceanic and Antarctic regions.

<u>List of Modules</u>

- 1: Orbital elements.
- 2: AVHRR image acquisition and analysis.
- 3: APT image acquisition and analysis.
- 4: Identification of cloud and ice features
- 5: Assessment of cyclogenesis potential.

<u>Details of Module 1</u>

Description: Orbital Elements

Duration: 15 min.

Module Purpose: to equip participants with the skills and knowledge necessary to programme and operate satellite equipment with all necessary orbital elements.

Summary of Content:
- 1: Orbital description.
- 2: Sources of orbital elements.
- 3: Utilisation of elements in TBUS and NASA two–line element messages in orbital prediction software.

    This module requires face to face learning which must be accomplished mainly by theory presentation. The extraction of orbital elements can be postponed to after this module if samples are available.

Learning Outcome from Contents , 2, and 3 (orbital description, sources and utilisation) of Module1 (orbital elements): at the end of this instruction, the participant will be able to load orbital elements into prediction software and make rough checks as to accuracy.

Teaching overview:
- Assessment criteria:
    - 1.1: Use templates or manuals to identify all required elements of

> the messages, with the correct units and magnitude for groups with assumed digits.
>> 2.1: Confirm that all derived elements are plausible values.
- *Conditions*: learning will be conducted in a classroom situation.
- *Assessment method*: all required elements must be correctly extracted, either verbally or transcribed to paper within a period of 5 minutes.
- *Resources*: TBUS and NASA two line element decoding publications and templates.

Details of Module 2

Description: AVHRR image acquisition and analysis.

Duration: 4 hours

Module Purpose: to equip participants with the skills and knowledge necessary to operate the HRPT system at the forecast office and understand the data flow from the HRPT system to the AVHRR area files produced for the satellite data display system (eg: McIDAS). Also provide additional skills for the inclusion of GMS data in polar regions.

Additional prerequisites: experience with McIDAS; and UNIX.

Summary of Content
- 1: System Hardware and software.
- 2: Data flow, including automated downloading of GMS imagery from a suitable source and user initiated retrieval of external data sources.
- 3: McIDAS processing of data.
- 4: Relevant McIDAS & UNIX operations.

This module requires some face to face learning that must be accomplished mainly by theory presentation. Most procedures may be demonstrated and practiced at the national or regional forecast centre. It may be necessary for certain HRPT training to be conducted at a suitable HRPT station.

Learning Outcome from Contents 1, 2, 3, and 4 (orbital description, sources and utilisation) of Module 2 (AVHRR image acquisition): at the end of instruction the participant will be able to demonstrate the basic operations of the HRPT system and the McIDAS area files available to the forecaster and be able to manually request satellite data from a remote source.

Teaching overview:
- Assessment criteria:
  1. Given access to relevant equipment, participant can put it in the required state for ingestion of normally required satellite data within

the time normally allowed for setup.

2. Participant is able to diagnose common error conditions that have occurred, recover data that may be retrievable and make changes to the system which will allow correct future ingestion.

3. Given a request for satellite imagery for a specified area south of 50S, participant can access readily available data within a reasonable period (to be determined by the assessor in consultation with experienced forecasters).

- *Conditions:* Learning will best undertaken in a tutorial situation with access to real time data or to relevant simulated data (case study).

- *Assessment methods*: Given access to relevant equipment, participant will demonstrate the required skills to his/her instructor in a classroom context. If equipment is not available, participant will describe the steps necessary to achieve the required outcome.

- *Resources*: McIDAS system with Exabyte drive. UNIX system with McIDAS/X function.

Details of Module 3

Description: APT image acquisition and analysis.

Duration: 4 hours.

Module Purpose: to equip participants with the skills and knowledge necessary to operate APT equipment.

Additional prerequisites: experience in the use of MS–DOS and Windows 95 operating systems, or relevant other operating systems assuming that the APT output is displayed on a PC.

Summary of Content
- 1: Use of an APT PC to acquire, navigate, analyse and save satellite data.
- 2: Use of DOS software to maintain the APT PC.
- 3: Use of Windows software to manipulate, display and transmit images.
- 4: Use of a ship–based satellite receiver to receive, analyse and print images.

This module requires a small amount of face–to–face learning but mainly requires practice with an APT PC and any dedicated ship–based system. It will be necessary to schedule learning sessions when suitable satellite passes are available and when access to the relevant re–supply/research vessel is available.

Learning Outcome from Contents 1, 2, 3, and 4 (APT functions) of Module 3 (APT image acquisition): at the end of this instruction the participant will be able to:

- adjust all APT PC parameters for NOAA or METEOR satellite
- reception,
- programme automatic reception of desired passes,
- display passes received,
- renavigate images,
- enhance images,
- save images in GIF format,
- transfer images to other PC's transfer images to other stations and
- maintain the APT PC hard disk for optimum efficiency.

Teaching overview:

- Assessment criteria:

  1.1: Satellite images are correctly aligned and can be gridded such that the outline of Antarctica (or home nation if using live reception) matches the visible coastal outline.

  1.2: Orbital elements are correctly updated for current passes.

  1.3: Satellite images are correctly enhanced.

  1.4: The PC is left in a state in which the next satellite pass is automatically received.

  1.4: Satellite images are transferred to other computers via the communications network without assistance from the receiving end.

- *Conditions*: learning will be conducted using operational equipment.
- *Assessment method*: competency in performing tasks.
- *Resources*: PC APT receiver, correctly aligned and connected to a working APT antenna with preamplifier.
- *References:* PC APT manual and other relevant operating instructions.

Details of Module 4

Description: Identification of cloud and ice features

Duration: 2 hours

Module Purpose: to equip participants with the skills and knowledge necessary to identify and distinguish cloud and ice features on satellite pictures.

Additional prerequisites: Stream C, Module 2: use of McIDAS (or similar satellite image display system).

Summary of Content:

- 1: Detection of ice features.
- 2: Detection of cloud features.

- 3: The use of multi–channel data in cloud/ice discrimination.
- 4: Ice edge detection techniques.
- 5: Preparation of ice edge maps.

This module requires a small amount of face–to–face learning but mainly requires supervised hands–on practice with McIDAS and real data (not necessarily real time).

Learning Outcome from Contents 1, 2, 3, 4, and 5 (ice–cloud detection) of Module 4 (identification of ice–cloud features): at the end of this instruction the participant will be able to use multi–channel AVHRR imagery to distinguish ice and cloud.

Teaching overview:
- Assessment criteria:
    1.1: The differences in appearance between ice and cloud in various channels is understood and can be utilized to distinguish ice from cloud.
    1.2: The ice edge can be detected.
    1.3: Ice concentration can be estimated.
- *Conditions*: Learning will be conducted using operational equipment and archived imagery.
- *Assessment Method*: Competency in performing tasks.
- *Resources*: McIDAS terminals, imagery.
- *References*: Badger *et al*. (1995).

Details of Module 5

Description: Assessment of cyclogenesis potential

Duration: 2 hours

Module Purpose: to equip participants with the skills and knowledge necessary to assess the likelihood of cyclogenesis, especially explosive cyclogenesis.

Additional prerequisites: Stream C, Module 2: use of McIDAS or other suitable satellite image display system.

Summary of Content
- 1: Summary of high latitude cyclogenesis models.
- 2: Dynamical support required for cyclogenesis.
- 3: Favoured locations for cyclogenesis.
- 4: Detection of significant cloud features.

This module requires a small amount of face–to–face learning but mainly requires supervised hands–on practice with McIDAS and real data (not necessarily real time), mostly in case study mode.

Learning Outcome from Contents of Module 5 (Assessment of cyclogenesis potential:
at the end of this instruction the participant will be able to list the most likely types of cyclogenesis experienced in the Antarctic region, distinguishing types by reference to the dynamical environment. Participants will be assisted in this by knowledge of favoured locations for cyclogenesis.

Teaching overview:
- Assessment criteria:
  1.1: Participants can list the most likely regions for cyclogenesis, the likely types of cyclogenesis and describe the distinguishing features.
  1.2: Participants can employ available numerical diagnostics to assess cyclogenesis on the basis of expected cyclogenesis type.
- *Conditions*: Learning will be conducted using overhead slides summarizing the significant types.
- *Assessment method*: Competency in performing tasks.
- *Resources*: Overhead projector, prepared slides, handouts, case study material. Whiteboard, pens.
- *References:* Badger *et al.* (1995); Bussing and Reed (1989).

Learning Outcome from Contents of Module 5 (Assessment of cyclogenesis potential:
at the end of this instruction the participant will be able to identify regions on satellite images showing evidence of either potential for cyclogenesis or cyclogenesis in progress.

Teaching overview:
- Assessment criteria:
  2.1: Participants can classify cyclogenesis situations in terms of likely development types and defend the classification in terms of available numerical guidance.
  2.2: The evolutionary model for any specific cyclogenesis type can be used to assess the numerical model output.
  2.3: Explosive cyclogenesis case study images are all correctly identified.
- *Conditions:* Learning will be conducted using case study charts.
- *Assessment Method*: Competency in performing tasks.
- *Resources*: Case study charts and imagery.
- *References:* Badger *et al.* (1995); Bussing and Reed (1989); Twitched *et al.* (1989). Previous Antarctic seasonal reports by forecasters.

Stream D   Antarctic Forecasting

Purpose

To equip participants with the skills and understanding necessary to make accurate forecasts in high latitude oceanic and Antarctic regions.

List of Modules

- 1: Climatology (micro and synoptic scale).
- 2: Significant weather event characteristics.
- 3: Helicopter operation requirements.
- 4: Airline operation requirements.
- 5: Conditions at sea.
- 6: Chart preparation and analysis.
- 7: User profiles.
- 8: High profile scientific issues.

Details of Module 1

Description: Climatology (micro and synoptic scale)

Duration: 2 hours

Module Purpose: to equip participants with knowledge of the basic Antarctic climate, with special reference to locations of relevance to current operations, and an understanding of the processes which result in the observed climatology.

Summary of Content:
- 1: Antarctic climatology – the basic circulation and dynamics.
- 2: Climate of the main Antarctic stations/bases in forecast area.
- 3: Climate of special locations.

This module requires face to face learning that must be accomplished mainly by theory presentation.

Learning Outcome from Content 1(basic circulation) of Module 1 (climatology):
Participants should be able to describe the basic Antarctic circulation, recognise the component parts as represented on daily charts and be able to indicate the significant regions for cyclogenesis and blocking.

Teaching overview:
- Assessment criteria:
  1.1 Given a seasonal average chart, identify the significant features and describe their significance to daily forecasting.
  1.2 Given a satellite picture, identify the major circulation features with relevance to Antarctic forecasting.
- *Conditions*: learning will take place in a tutorial type situation.
- *Assessment method*: participants will demonstrate knowledge of climatology by indicating relevant features on charts or satellite pictures supplied.
- *References*: Schwerdtfeger (1984); van Loon *et al.* (1972); Schwerdtfeger (1970, pp. 253–55).

Learning Outcome from Content 2 & 3 (climate main stations/sites) of Module 1 (climatology): Participants should be able to discuss briefly the common phenomena affecting each of the bases and areas of special interest (field party locations or helicopter way–points).

Teaching overview:
- Assessment criteria:
  2.1 All phenomena significant to safety at each location can be listed.
- *Conditions*: learning will take place in a tutorial type situation.
- *Assessment method*: participants will indicate locations of areas of significant interest and list significant phenomena.
- *Resources*: Previous season reports.

Details of Module 2

Description: Significant Weather Event Characteristics.

Duration: 2 hours

Module Purpose: to give the participants the knowledge and skills required for the prediction of significant weather events in the Antarctic region.

Additional prerequisites: Stream C, Module 4 – Identification of cloud and ice features, and Stream C, Module 5 – Assessment of cyclogenesis potential.

Summary of Content:
- 1: Blizzards at main stations/operational sites
- 2: White–out events over the plateau.
- 3: Calm wind events.

- •   4: Snowfall events.
- •   5: Blowing snow events.

This module requires face to face learning that must be accomplished mainly by theory presentation. Ideally this should include extensive case studies.

Learning Outcome from Content 1(blizzards at main sites) of Module 2 (significant weather): Participants will be able to define the term 'blizzard'. Participants will be able to recognise the synoptic scale environments conducive to blizzards at the relevant stations and operational sites, assess the potential for blizzard conditions given satellite imagery prognostic charts and estimate the likely time of arrival of wind speeds over 17.5 m s^{-1} (34 kt).

Teaching overview:
- •   Assessment criteria:
  - 1.1 Conditions matching specified criteria can be recognised.
  - 1.2 Onset times can be specified with confidence limits nominated.
- •   *Conditions*: learning should be conducted in a tutorial situation, with case studies for each station.
- •   *Assessment method*: given charts for a given case, a forecast is made and can be defended on the basis of recognised forecast techniques.
- •   *Resources*: charts and satellite imagery for specific situations, for which the outcome is known. Practical forecasting workshops.

Learning Outcome from Content 2 (white–out events) of Module 2 (significant weather): White–out events *can be forecast within confidence limits, given appropriate.*

Teaching overview:
- •   Assessment criteria:
  - 2.1 Conditions matching specified criteria can be recognised.
  - 2.2 Onset times can be specified with confidence limits nominated.
- •   *Conditions*: learning will be conducted in a tutorial situation, with case studies for each station.
- •   *Assessment method*: given charts for a given case, a forecast is made and can be defended on the basis of recognised forecast techniques.
- •   *Resources*: satellite images and charts for specific situations, for which the outcome is known. Practice forecasting workshops.

Learning Outcome from Content 3 (calm winds) of Module 2 (significant weather): Participants can recognise and predict conditions leading to the onset and cessation of prolonged low wind speed events.

Teaching overview:
- •   Assessment criteria:
  - 3.1: Conditions matching specified criteria can be recognised.

3.2: Onset times can be specified with confidence limits nominated.
3.3: Cessation times can be specified with confidence limits nominated.

- *Conditions*: learning will be conducted in a tutorial situation, with case studies for each station.
- *Assessment method*: given charts for a given case, a forecast is made and can be defended on the basis of recognised forecast techniques. Of the *Assessment criteria* above, 3.3 is the most important and performance in this is regarded as crucial to the success of the forecaster.
- *Resources*: satellite images and charts for specific situations, for which the outcome is known. Practical forecasting workshops.

Learning Outcome from Content 4 (snow events) of Module 2 (significant weather):
Participants can recognise and predict conditions leading to the onset and cessation of heavy snowfall events.

Teaching overview:
- Assessment criteria:
  4.1 Conditions matching specified criteria can be recognised.
  4.2 Onset times can be specified with confidence limits nominated.
  4.3 Cessation times can be specified with confidence limits nominated.
- *Conditions*: learning will be conducted in a tutorial situation, with case studies for each station.
- *Assessment method*: given charts for a given case, a forecast is made and can be defended on the basis of recognised forecast techniques. Of the *Assessment criteria* above, 4.2 is the most important.
- *Resources*: satellite images and charts for specific situations, for which the outcome is known. Practical forecasting workshops.

Learning Outcome from Content 5 (blowing snow) of Module 2 (significant weather):
Participants can recognise and predict conditions leading to the onset of blowing snow above eye level.

Teaching overview:
- Assessment criteria:
  5.1: Conditions matching specified criteria can be recognised.
  5.2: Onset times can be specified with confidence limits nominated.
  5.3: Cessation times can be specified with confidence limits nominated.
- *Conditions*: learning will be conducted in a tutorial situation, with case studies for each station.
- *Assessment method*: given charts for a given case, a forecast is made and can be defended on the basis of recognised forecast techniques. Of the *Assessment criteria* above, 5.2 is the most important.
- *Resources*: satellite images and charts for specific situations, for which

the outcome is known. Practical forecasting workshops.

Details of Module 3

Description: Helicopter Operation Requirements.

Duration: 30 min.

Module Purpose: to give the participants an understanding of the requirements of helicopter operations in order to facilitate the focusing of forecasting effort on the most relevant weather elements.

Summary of Content:
- 1: Visual flight requirements.
- 2: Effects of Icing.
- 3: Effects of Turbulence.
- 4: Effects of Wind.
- 5: Effects of snow.
- 6: Other problems.

This module requires face to face learning that must be accomplished mainly by theory presentation. Ideally, a helicopter pilot or representative of the company providing helicopter operations for the season should present it. It is acceptable for this module to be presented on the ship after departure if time is short.

Learning Outcome from Content 1 (visual flight requirements) of Module 3 (helicopter requirements): Participants will know the limitations on Antarctic helicopter operations imposed by the requirement for flight under visual flight rules. Participants will be able to define terms to be used in helicopter support operations, specifically 'horizon', 'surface definition' and 'white–out'.

Teaching overview:
- Assessment criteria:
    1.1: The conditions under which visual flight becomes difficult can be listed.
    1.2:Conditions under which pilots can continue to fly under adverse visual conditions can be described.
- *Conditions*: learning will be conducted in a tutorial situation.
- *Assessment method*: discussion with participants.
- *Resources:* any available operations manuals.

Learning Outcome from Contents 2, 3, 4, & 5 (effects of icing etc) of Module 3 (helicopter requirements): Participants will know the limitations on Antarctic helicopter operations imposed by icing, turbulence, strong wind, and snow.

Teaching overview:
-      Assessment criteria:
  2.1: The effects of strong winds, turbulence, icing and snow can be listed.
  2.2: Conditions conducive to icing can be listed.
-      *Conditions*: learning will be conducted in a tutorial situation.
-      *Assessment method*: discussion with participants.
-      *Resources*: any available helicopter operations manuals.

Details of Module 4

Description: Airline operational requirements.

Duration: 4 hours

Module Purpose: to give the participants an overview of the format of flight forecasts produced for scenic flights over the Antarctic coastline.

Summary of Content
-      1: Preparation of typical forecast.
-      2: Method of dissemination.

This module requires face to face learning that must be accomplished mainly by theory presentation and also by practical preparation of a forecast.

Learning Outcome from Contents 1 (forecast preparation) of Module 4 (airline operational requirements): Participants will be able to prepare and send a sample forecast to the customer.

Teaching overview:
-      Assessment criteria:
  1.1: The forecast is received within the nominated time frame.
  1.2: The customer regards the forecast as suitable.
-      *Conditions*: learning will be conducted in a tutorial situation.
  Assessment method: discussion with participants.
-      *Resources*: sample forecast, PC, satellite imagery, GRADS model output, real–time high resolution image FTP'd from Antarctic station.

Details of Module 5

Description: Conditions at Sea.

Duration: 4 hours

Module Purpose: to give the participants the knowledge and skills necessary to produce forecasts for ships at sea within the southern ocean.

Summary of Content
- •   1: Use of the HF radiofax aboard vessels.
- •   2: Typical conditions at sea.
- •   3: Preparation of sample forecast.

     This module requires face to face learning that must be accomplished mainly by theory presentation.

Learning Outcome from Contents 1 (use of HF radio fax) of Module 5 (conditions at sea): Participants will be able to operate and programme the HF facsimile receiver aboard a re–supply/research vessel.

Teaching overview:
- •   Assessment criteria:
        1.1: Forecast products are received as programmed.
- •   *Conditions*: learning will be conducted in a tutorial situation aboard ship while in harbour before departure.
- •   *Assessment Method:*   discussion with participants.
- •   Resources:

Learning Outcome from Contents 2 & 3 (typical conditions at sea translated into a forecast) of Module 5 (conditions at sea): Participants will have the knowledge and skills necessary to prepare a forecast for use aboard re–supply/research ships.
- •   Assessment criteria:
        2.1: The forecast is assessed as likely to be suitable for the customer.
- •   *Conditions*: learning will be conducted in a tutorial situation.
- •   *Assessment method*: discussion with participants.
- •   *Resources*: sample forecast, PC, satellite imagery, DIFACS charts available on HF fax.

Details of Module 6

Description: Chart Preparation and analysis.

Duration: 2 days.

Module Purpose: to give the participants the knowledge and skills necessary to prepare chart for forecasting and dissemination to external users.

Additional prerequisites: Stream C (Satellite image acquisition and interpretation).

Summary of Content
- •   1: Plotting charts.
- •   2: Analysis of charts.
- •   3: Dissemination of charts.

This module requires practical tutorial sessions with real data.

Learning Outcome from Contents 1 (plotting charts) of Module 6 (chart preparation and analysis): Participants will be able to prepare charts for analysis.

Teaching overview:
- •   Assessment criteria:
     1.1: Charts are suitable for analysis.
- •   *Conditions*: learning will be conducted in a tutorial situation.
- •   *Assessment method*: discussion with participants.
- •   *Resources*: appropriate plotting equipment.

Learning Outcome from Contents 2 (analysis of charts) of Module 6 (chart preparation and analysis): Participants will have the knowledge and skills to analyse MSL and 500–hPa charts to a standard suitable for dissemination to external users.

Teaching overview:
- •   Assessment criteria:
     2.1:Charts are suitable for dissemination.
- •   *Conditions*: learning will be conducted in a tutorial situation.
- •   *Assessment method*: discussion with participants.
- •   *Resources:* Pencils, rubbers.
- •   *References:* Bader *et al*. (1995); Guymer (1978).

Learning Outcome from Contents 3 (dissemination of charts) of Module 6 (chart preparation and analysis): Participants will have the knowledge and skills to prepare sea ice analyses for transmission over HF.

Teaching overview:
- •   Assessment criteria:
     3.1: Charts are suitable for dissemination.
- •   *Conditions*: learning could be conducted in a tutorial situation before departure or be postponed to arrival at the Antarctic forecasting office.
- •   *Assessment method*: discussion with participants.
- •   *Resources:* Pencils; erasers; light table for tracing; blank sea ice analysis charts; sample images; graphics design software (eg: NeoPaint) ; PC scanner to convert the chart to a GIF image.

Details of Module 7

Description: User Profiles.

Duration: 30 min.

Module Purpose: to give the participants knowledge of external users in Antarctica.

Summary of Content
- 1: Introduction to the Expeditioners.
This module requires a short discussion only.

Learning Outcome from Contents 1 (introduction to expeditioners) of Module 7 (user profiles): Participants will have an understanding of the requirements of typical Antarctic users.

Teaching overview:
- Assessment criteria:
    1.1   N/A.
- *Conditions:* learning will be conducted in a tutorial situation.
- *Assessment method*: discussion with participants.
- Resources: N/A

Details of Module 8

Description: High profile scientific issues.

Duration: Optional: 30 minutes to 1 hour.

Module Purpose: to give the participants a familiarity with scientific priorities for the current season, including the agency's own corporate objectives.

Summary of Content
- 1: Publicly recognised issues such as, for example, global warming and ozone, and their relation to the meteorology of Antarctica.
- 2: The agency's corporate objectives in Antarctica.
This module might include a visit to or a talk by a prominent scientist or a high level officer in the agency.

Learning Outcome from Contents 1 (greenhouse etc) of Module 8 (high profile scientific issues): Participants will be able to address their efforts, where possible to

the agency's corporate outcomes in particular but also with an eye to national priorities in Antarctic research. They will be aware of the context of relevant current national scientific research in Antarctica.

Teaching overview:
- Assessment criteria:
  - 1.1   N/A
- *Conditions*: learning will be conducted in a discussion or tutorial situation.
- *Assessment method*: discussion with participants.
- *Resources*: lecturer's preferences, possibly overhead projector, video player.

APPENDIX 5   DETAILED LIST OF CONTRIBUTORS

Sections		Description of Section	Contributors
1.0	to 1.0	Introduction	J. Turner
2.0	to 2.3	An overview of the meteorology & climatology etc.	W. Budd
2.4	to 2.4.6	Synoptic–scale weather systems etc	I. Simmonds R. Leighton M. Pook
2.5	to 2.5	Mesocyclones	J. Turner
2.6	to 2.6	Mean values of the main met. elements	Various as follows:
2.6.1	to 2.6.1	Pressure at Mean Sea Level	J. Turner
2.6.2	to 2.6.2	The upper–air height field	J. Turner
2.6.3	to 2.6.3	Surface air temperature	H. Hutchinson S. Pendlebury
2.6.4	to 2.6.4	The continental surface temperature inversion	H. Hutchinson
2.6.5	to 2.6.5	Cloud, white–out and surface and horizon definition	S. Pendlebury H. Hutchinson
2.6.6	to 2.6.6	Precipitation/Accumulation	J. Turner
2.6.7	to 2.6.7	The wind field	J. Turner H. Hutchinson S. Pendlebury
2.6.8	to 2.6.8	Visibility including blizzards/blowing snow	S. Pendlebury; M. De Keyser
2.7	to 2.7.1	Recent change in the Antarctic etc	J. Turner
2.7.2	to 2.7.2	Ozone over Antarctica	J. Shanklin
2.7.3	to 2.7.3	Recent changes to Antarctic ice shelves	S. Pendlebury
2.8	to 2.8	Some aspects of Antarctic ice	S. Pendlebury using Aust. BoM (1991)
3.0	to 3.5.2	The forecasting requirement	S. Pendlebury
4.0	to 4.1.	Data availablity etc	J. Shanklin
4.1.2	to 4.1.2	AWS	C. Stearns G. Weidner
4.1.2	to 4.1.3	Drifting buoys	J. Turner S. Pendlebury
4.2	to 4.2.6	Model fields	G. Mills J. Turner
4.3	to 4.3.1	Visible and infra-red imagery.	J. Turner
4.3.2	to 4.3.2	Synthetic Aperture Radar imagery	S Pendlebury
4.3.3	to 4.3.3	Antarctic Composite Satellite Images	M. Lazzara
4.3.4	to 4.3.4	Scatterometer winds	K. Jacka S. Pendlebury
4.3.5	to 4.3.5	Passive microwave products	R. Massom J. Turner
4.3.6	to 4.3.6	Temperature sounding instruments	T. Hart J. Turner

4.3.7 to 4.3.7	Some aspects of future satellite systems	M. Lazzara R. (Buzz) Bernstein D. Lubin G. Weidner J. Cassano
5.0 to 5.1.6	Analysis techniques etc	S. Pendlebury using Aust. BoM (1984)
5.2 to 5.2	Conventional surface/frontal analysis	S. Pendlebury
5.3.1 to 5.3.	Techniques for estimating MSLP	R. Brauner G. König–Langlo W. Seifert
5.3.2 to 5.3.2	Techniques for upper–air analysis	M. Pook
5.4 to 5.4.3	Analysis over the interior	As follows
5.4.1 to 5.4.2	Streamline analysis etc	N. Adams
5.4.3 to5.4.3	Estimating 500 hPa etc	L. Cowled
6.0 to 6.2	The forecasting process etc	S. Pendlebury using Aust. BoM (1984)
6.3 to 6.3	Long waves	J. Callaghan
6.4 to 6.4	Synoptic scale system and fronts	S. Pendlebury
6.5 to 6.5	Mesoscale systems etc	J. Turner A. Yates S. Pendlebury
6.6 to 6.6.13	Forecasting the main met. elements	As follows
6.6.1 to 6.6.2	Surface and upper winds	S. Pendlebury
6.6.3 to 6.6.3	Clouds	N. Adams
6.6.4 to 6.6.4	Visibility and fog	M. De Keyser S. Pendlebury
6.6.5 to 6.6.7	Surface contrast/horizon def/precipitation	J. Turner
6.6.8 to 6.6.8	Temperature and wind chill factor	S. Wattam S. Pendlebury
6.6.9 to 6.6.9	Airframe icing	S. Pendlebury S. Wattam R. Brauner G. König–Langlo W. Seifert
6.6.10 to 6.6.10	Turbulence	S. Pendlebury
6.6.11 to 6.6.11	Sea ice	S. Pendlebury
6.6.12 to 6.6.12	Waves and swell	B. Southern
6.6.13 to 6.6.13	Hydraulic jumps	P. Pettré
7.0 to 7.0	Forecasting at specific locations	As follows
7.1 to7.1	Introductory remarks	S. Pendlebury
7.2 to 7.2.9	Representative sub–Antarctic Islands	As follows
7.2.1 to 7.2.2	The Falkland Islands/ South Georgia	P. Salter
7.2.3 to 7.2.3	Gough Island	J. Brimelow de Broy Brooks I. Hunter
7.2.4 to 7.2.5	Bouvetoya & Marion Islands	S. Pendlebury I. Hunter
7.2.6 to 7.2.6	Crozet Island	B. Clavier
7.2.7 to 7.2.7	Kerguleun Island	B. Clavier

7.2.8 to 7.2.8	Heard and Mc Donald Islands	S. Pendlebury
7.2.9 to 7.2.9	Macquarie Island	S. Pendlebury
7.3 to 7.3	Antarctic Peninsula (summary)	S. Pendlebury
7.3.1 to 7.3.1	South Orkney Islands (Signy &Orcadas	T. Lachlan–Cope
7.3.2 to 7.3.2	King George Island	J. Turner J. Carrasco L. (Lingen) Bian L. Ryzhakov V. Lagun
7.3.2 to 7.3.3	Greenwich, Robert and Media Luna Is	J. Turner
7.3.4 to 7.3.4	Decepcion Island	T. Lachlan–Cope
7.3.5 to 7.3.5	Trinity Peninsula	J. Turner M. Romain
7.3.6 to 7.3.6	West–Central Section	J. Turner S. Krakovaskaja
7.3.7 to 7.3.7	Marguerite Bay/Adelaide Island	J. Turner
7.3.8 to 7.3.8	Fossil Bluff, King George Sound	J. Turner
7.3.9 to 7.3.9	Ski Hi/Ski Blu	T. Lachlan–Cope
7.3.10 to 7.3.10	The Larsen Ice Shelf	J. Turner
7.4 to 7.4.3	Ronne and Filchner Ice Shelves/ Berkner Island/ Shelf Depot/ Haag Nunataks	J. Turner
7.5 to 7.5.10	Coats Land/Dronning Maud Land	As follows
7.5.1 to 7.5.1	Belgrano II	J. Turner
7.5.2 to 7.5.2	Halley	T. Lachlan–Cope
7.5.3 to 7.5.3	Aboa and Wasa	J. Turner
7.5.4 to 7.5.4	Atka Bay–Neumeyer Cape Norwegia	R. Brauner G. König–Langlo W. Seifert
7.5.5 to 7.5.5	SANAE	J. Brimelow De Broy Brooks
7.5.6 to 7.5.6	Troll and Tor	J. Turner
7.5.7 to 7.5.7	Maitri and Dakshin Gangotri	Lakshmanaswamy
7.5.8 to 7.5.8	Novolazarevskaya	V. Belyazo A. Korotkov
7.5.9 to 7.5.9	Inland of Syowa (Asuka, Mizuho, Dome Fuji)	T. Yamanouchi
7.5.10 to 7.5.10	Syowa Station	T. Yamanouchi T. Takao
7.6 to 7.6.2	Enderby and Kemp Lands	As follows
7.6.1 to 7.6.1	Molodezhnaya	L. Ryzhakov
7.6.2 to 7.6.2	Mt King	S. Pendlebury
7.7 to 7.7.2	MacRobertson Land	As follows
7.7.1 to 7.7.1	Mawson	L. Cowled
7.7.2 to 7.7.2	Prince Charles Mountains (inc. Soyuz)	L. Cowled V. Lagun M. Jones
7.8 to 7.8.4	Princess Elizabeth and Wilhelm II Lands	As follows
7.8.1 to 7.8.1	Larsemann Hills/Law Base	S. Pendlebury M. Jones
7.8.2 to 7.8.2	Soyuz/Progress/Druzhnay–4	E. Loutsenko V. Lagun

7.8.3 to 7.8.3	Zhongshan	L. (Lingen) Bian
7.8.4 to 7.8.4	Davis	L. Cowled
7.9 to 7.9.2	Queen Mary Land	As follows
7.9.1 to 7.9.1	Mirny	E. Loutsenko
7.9.2 to 7.9.2	Edgworth David (Bunger Hills	J. Nairn
7.10 to 7.10.3	Wilkes Land	As follows
7.10.1 to 7.10.1	Casey (inc. Law Dome)	N. Adams
7.10.2 to 7.10.2	Vostok	A. Kuznetsov
7.10.3 to 7.10.3	Concordia (Dome C)	P. Pettré
7.11 to 7.11.2	Terre Adélie and George V Lands	As follows
7.11.1 to 7.11.1	Dumont d'Urville	P. Pettré
7.11.2 to 7.11.2	Port Martin/Commonwealth Bay/Cape Denison	S. Pendlebury
7.12 to 7.12.6	Oates Land, Victoria Land, the Transantarctic Mountains, the Ross Ice Shelf, and the South Pole area	As follows
7.12.1 to 7.12.1	Leningradskaya	L. Ryzhakov E. Loutsenko V. Lagun A. Korotkov
7.12.2 to 7.12.2	Terra Nova Bay Station	F. Coppola J. Turner
7.12.3 to 7.12.3	McMurdo (inc. Scott Station)	A. Cayette
7.12.4 to 7.12.4	Transantarctic Mountains	A. Cayette
7.12.5 to 7.12.5	South Pole area	A. Cayette M. Moyher
7.12.6 to 7.12.6	Ross Ice Shelf Camps	J. Kramer
7.13 to 7.13.3	Edward VII, Marie Byrd and Ellsworth Lands	As follows
7.13.1 to 7.13.1	Russkaya	E. Loutsenko
7.13.2 to 7.13.2	Byrd Station	J. Kramer
7.13.3 to 7.13.3	Patriot Hills – Teniente Parodi	J. Evans J. Carrasco
Appendix 1	Lists of stations and AWS in the Antarctic	J. Turner S. Colwell B. Stearns G.Weidner F. Coppola H. Hutchinson
Appendix 2	Climatological data for various locations in the Antarctic	Various from above
Appendix 3	A Representative Antarctic Atmosphere	S. Pendlebury J. Turner I. Barnes–Keoghan S. Colwell D. Shepherd S. Harangozo
Appendix 4	A suggested Antarctic Training Programme	L. Cowled N. Adams R. Jardine
Appendix 5	Detailed list of contributors	S. Pendlebury